ARCHITECTURAL
ACOUSTICS

MARSHALL LONG

ARCHITECTURAL ACOUSTICS

This page intentionally left blank

ARCHITECTURAL ACOUSTICS

by Marshall Long

from the
Applications of Modern Acoustics Series
Edited by Moises Levy and Richard Stern

ELSEVIER
ACADEMIC
PRESS

Amsterdam • Boston • Heidelberg • London • New York • Oxford
Paris • San Diego San Francisco • Singapore • Sydney • Tokyo

This book is printed on acid-free paper. ∞

Cover image: The cover shows Grosser Musikvereinssaal in Vienna, Austria. The photograph
was provided by AKG Acoustics, U.S., and is reproduced with permission.

For all information on all Elsevier Academic Press publications visit our
Web site at www.books.elsevier.com

This page intentionally left blank

CONTENTS

This page intentionally left blank

Architectural acoustics has been described as something of a black art or perhaps more charitably, an arcane science. While not purely an art, at its best it results in structures that are beautiful as well as functional. To produce art, however, the practitioner must first master the science of the craft before useful creativity is possible, just as a potter must learn clay or a painter his oils.

Prior to Sabine's work at the beginning of the 20th century there was little to go on. Jean Louis Charles Garnier (1825-1898), designer of the Paris Opera House, expressed his frustration at the time,

> "*I gave myself pains to master this bizarre science [of acoustics] but . . . nowhere did I find a positive rule to guide me; on the contrary, nothing but contradictory statements . . . I must explain that I have adopted no principle, that my plan has been based on no theory, and that I leave success or failure to chance alone . . . like an acrobat who closes his eyes and clings to the ropes of an ascending balloon.*"
> (Garnier, 1880).

Since Sabine's contributions in the early 1900's, there has been a century of technical advances. Studies funded by the EPA and HUD in the 1970's were particularly productive. Work in Canada, Europe, and Japan has also contributed greatly to the advancement of the field.

When Dick Stern first suggested this work, like Garnier one-hundred years earlier, I found, at first, few guides. There were many fine books for architects that graphically illustrate acoustic principles. There were also excellent books on noise and vibration control, theoretical acoustics, and others that are more narrowly focused on concert halls, room acoustics, and sound transmission. Many of these go deeper into aspects of the field than there is room for here, and many have been useful in the preparation of this material. Several good books are, unfortunately, out of print so where possible I have tried to include examples from them.

The goal is to present a technical overview of architectural acoustics at a level suitable for an upper division undergraduate or an introductory graduate course. The book is organized as a step-by-step progression through acoustic interactions. I have tried to include practical applications where it seemed appropriate. The algorithms are useful not only for problem solving, but also for understanding the fundamentals. I have included treatments of certain areas of audio engineering that are encountered in real-life design problems, which are not

normally found in texts on acoustics. There is also some material on computer modeling of loudspeakers and ray tracing. Too often designers accept the conclusions obtained from software models without knowing the underlying basis of the computations. Above all I hope the book will provide a intellectual framework for thinking about the subject in a logical way and be helpful to those working in the field.

ACKNOWLEDGMENTS

Although I have tried to purge the document of errors, there are undoubtedly some that I have missed. I hope that these are few and do not cause undue confusion.

This page intentionally left blank

1 HISTORICAL INTRODUCTION

The arts of music, drama, and public discourse have both influenced and been influenced by the acoustics and architecture of their presentation environments. It is theorized that African music and dance evolved a highly complex rhythmic character rather than the melodic line of early European music due, in part, to its being performed outdoors. Wallace Clement Sabine (1868–1919), an early pioneer in architectural acoustics, felt that the development of a tonal scale in Europe rather than in Africa could be ascribed to the differences in living environment. In Europe, prehistoric tribes sought shelter in caves and later constructed increasingly large and reverberant temples and churches. Gregorian chant grew out of the acoustical characteristics of the Gothic cathedrals, and subsequently baroque music was written to accommodate the churches of the time. In the latter half of the twentieth century both theater design and performing arts became technology-driven, particularly with the invention of the electronic systems that made the film and television industries possible. With the development of computer programs capable of creating the look and sound of any environment, a work of art can now not only influence, but also define the space it occupies.

1.1   GREEK AND ROMAN PERIOD (650 BC - AD 400)

Early Cultures

The origin of music, beginning with some primeval song around an ancient campfire, is impossible to date. There is evidence (Sandars, 1968) to suggest that instruments existed as early as 13,000 BC. The understanding of music and consonance dates back at least to 3000 BC, when the Chinese philosopher Fohi wrote two monographs on the subject (Skudrzyk, 1954).

The earliest meeting places were probably no more than conveniently situated open areas. Their form was whatever existed in nature and their suitability to purpose was haphazard. As the need arose to address large groups for entertainment, military, or political purposes, it became apparent that concentric circles brought the greatest number of people close to the central area. Since the human voice is directional and intelligibility decreases as the listener moves off axis, seating arrangements were defined by the vocal polar pattern and developed naturally, as people sought locations yielding the best audibility. This led to the construction of earthen or stone steps, arranging the audience into a semicircle in

front of the speaker. The need to improve circulation and permanence evolved in time to the construction of dedicated amphitheaters on hillsides based on the same vocal patterns.

Greeks

The Greeks, perhaps due to their democratic form of government, built some of the earliest outdoor amphitheaters. The seating plan was in the shape of a segment of a circle, slightly more than 180°, often on the side of a hill facing the sea. One of the best-preserved examples of the Greco-Hellenistic theater is that built at Epidaurus in the northeastern Peloponnese in 330 BC, about the time of Aristotle. A sketch of the plan is shown in Fig. 1.1. The seating was steeply sloped in these structures, typically 2:1, which afforded good sight lines and reduced grazing attenuation. Even with these techniques, it is remarkable that this theater, which seated as many as 17,000 people, actually functioned.

FIGURE 1.1   Ancient Theater at Epidaurus, Greece (Izenour, 1977)
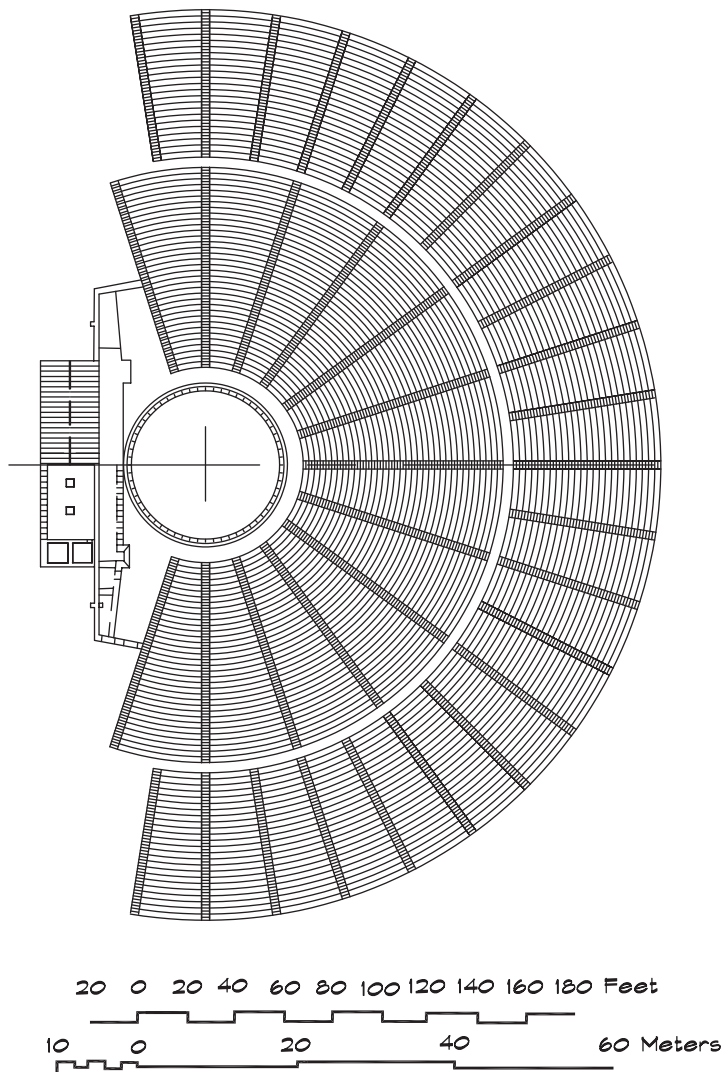
The ancient Greeks were aware of other acoustical principles, at least empirically. Chariot wheels in Asia Minor were heavy, whereas those of the Greeks were light since they had to operate on rocky ground. To achieve high speed, the older Asian design was modified, so that the four-spoke wheels were smaller and the wooden rims were highly stressed and made to be very flexible. They were so light that if left overnight under the weight of the chariot they would undergo deformation due to creep. Telemachus, in Homer's story of the Odyssey, tipped his vehicle vertically against a wall, while others removed their wheels in the evening (Gordon, 1978) to prevent warping. The wheels were mounted on light cantilevered shafts and the vehicle itself was very flexible, which helped isolate the rider from ground-induced vibrations.

Greek music and dance were also highly developed arts. In 250 BC at a festival to Apollo, a band of several hundred musicians played a five-movement piece celebrating Apollo's victory over Python (Rolland et al., 1948). There is strong evidence that the actors wore masks that were fitted out with small megaphones to assist in increasing the directivity of the voices. It is not surprising that the Greek orator Demosthenes (c 384–322 BC) was reputed to have practiced his diction and volume along the seashore by placing pebbles in his mouth. Intelligibility was enhanced, not only by the steeply raked seating, but also by the naturally low background noise of a preindustrial society.

The chorus in Greek plays served both as a musical ensemble, as we use the term today, and as a group to chant the spoken word. They told the story and explained the action, particularly in the earlier plays by Aeschylus (Izenour, 1977). They may have had a practical as well as a dramatic purpose, which was to increase the loudness of the spoken word through the use of multiple voices.

Our knowledge of the science of acoustics also dates from the Greeks. Although there was a general use of geometry and other branches of mathematics during the second and third millennia BC, there was no attempt to deduce these rules from first principles in a rigorous way (Dimarogonas, 1990). The origination of the scientific method of inquiry seems to have begun with the Ionian School of natural philosophy, whose leader was Thales of Miletos (640–546 BC), the first of the seven wise men of antiquity. While he is better known for his discovery of the electrical properties of amber (*electron* in Greek), he also introduced the logical proof for abstract propositions (Hunt, 1978), which led in time to the formal mathematics of geometry, based on the theorem-proof methods of Euclid (330–275 BC).

Pythagoras of Samos (c 570–497 BC), a contemporary of Buddha, Confucius, and Lao-Tse, can be considered a student of the Ionian School. He traveled to Babylon, Egypt, and probably India before establishing his own school at Crotone in southern Italy. Pythagoras is best known for the theorem that bears his name, but it was discovered much earlier in Mesopotamia. He and his followers made important contributions to number theory and to the theory of music and harmony. The word *theorii* appeared in the time of Pythagoras meaning "the beauty of knowledge" (Herodotos, c 484–425 BC). Boethius (AD 480–524), a Roman scholar writing a thousand years later, reports that Pythagoras discovered the relationship between the weights of hammers and the consonance of their natural frequencies of vibration. He is also reported to have experimented with the relationship between consonance and the natural frequencies of vibration of stretched strings, pipes, shells, and filled vessels. The Pythagorean School began the scientific exploration of harmony and acoustics through these studies. They understood the mechanisms of generation, propagation, and perception of sound (Dimarogonas, 1990). Boethius describes their knowledge of sound in terms of waves generated by a stone falling into a pool of water. They probably realized that sound was a

wave propagating through the air and may have had a notion of the compressibility of air during sound propagation.

Aristotle (384–322 BC) recognized the need for a conducting medium and stated that the means of propagation depended on the properties of the material. There was some confusion concerning the relationship between sound velocity and frequency, which was clarified by Theophrastos of Eresos (370–285 BC): "The high note does not differ in speed, for if it did it would reach the hearing sooner, and there would be no concord. If there is concord, both notes must have the same speed." The first monograph on the subject, *On Acoustics*, is attributed to Aristotle, although it may have been written by his followers. Whoever wrote it, the author had a clear understanding of the relationship between vibration and sound: "bodies that are capable of vibrating produce sounds . . . strings are examples of such bodies."

Romans

The Roman and the late Hellenistic amphitheaters followed the earlier Greek seating pattern, but limited the seating arc to 180°. They also added a stagehouse (*skene*) behind the actors, a raised acting area (*proskenion*), and hung awnings (*valeria*) overhead to shade the patrons. The chorus spoke from a hard-surfaced circle (*orchestra*) at the center of the audience. A rendering of the Roman theater at Aspendius, Turkey is shown in Fig. 1.2. The Romans were better engineers than the early Greeks and, due to their development of the arch and the vault, were not limited to building these structures on the natural hillsides.

The most impressive of the Roman amphitheaters, the Flavian amphitheater was built between AD 70 and 81, and was later called the Colosseum, due to its proximity to a colossal statue of Nero. With a total seating capacity of about 40,000 it is, except for the Circus Maximus and the Hippodrome (both racecourses), the largest structure for audience seating of the ancient world (Izenour, 1977). Its architect is unknown, but his work was superb. The sightlines are excellent from any seat and the circulation design is still used in modern stadia. The floor of the arena was covered with sand and the featured events were generally combats between humans, or between humans and animals. This type of spectacle was one of the few that did not require a high degree of speech intelligibility for its appreciation by the audience. The floor was sometimes caulked and filled with water to a depth of about a meter for mock sea battles.

Smaller indoor theaters also became a part of the Greek and Roman culture. These more intimate theaters, called *odea*, date from the age of Pericles (450 BC) in Greece. Few remain, perhaps due to their wood roof construction. The later Greek playwrights, particularly Sophocles and Euripides, depended less on the chorus and more on the dialogue between actors to carry the meaning of the play, particularly in the late comedies. These dramatic forms developed either because of the smaller venues or to accommodate the changing styles.

In the Roman theater the chorus only came out at intermission so the *orchestra* shrunk to a semicircle with seats around it for the magistrates and senators. The front wall or *scaena* extended out to the edges of the semicircle of seats and was the same height as the back of the seating area. It formed a permanent backdrop for the actors with a palace decor. The *proskenium* had a curtain, which was lowered at the beginning of the performance and raised at the end. (Breton, 1989)

The Odeon of Agrippa, a structure built in Athens in Roman times (12 BC), was a remarkable building. Shown in Fig. 1.3, it had a wood-trussed clear span of over 25 meters (83 feet). It finally collapsed in the middle of the second century. Izenour (1977) points out

FIGURE 1.2   Roman Theater at Aspendus, Turkey (Izenour, 1977)

SECTION

PLAN

```
0    20   40   60   80   100        Feet

0              20             40    Meters
```
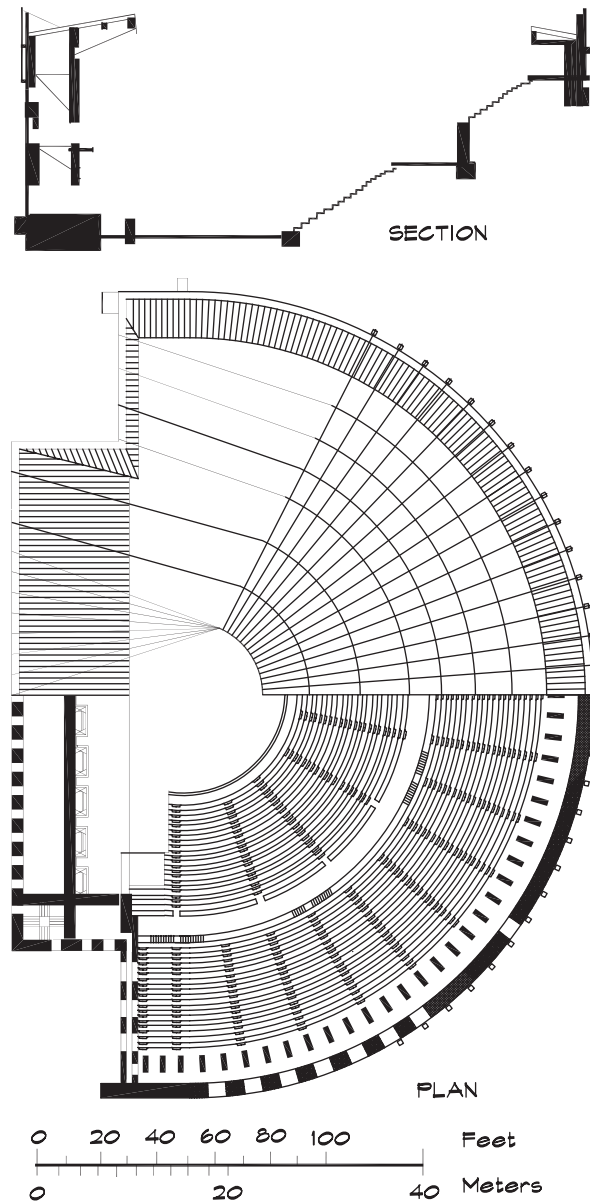
that these structures, which ranged in size from 200 to 1500 seats, are found in many of the ancient Greek cities. He speculates that, "during the decline of the Empire these roofed theaters, like the small noncommercial theaters of our time, became the final bastion of the performing arts, where the more subtle and refined stage pieces—classical tragedy and comedy, ode and epoch—were performed, the latter to the accompaniment of music (lyre, harp, double flute and oboe) hence the name odeum, 'place of the ode'."

Vitruvius Pollio

Much of our knowledge of Roman architecture comes from the writings of Vitruvius Pollio, a working architect of the time, who authored *De Architectura*. Dating from around 27 BC,

Figure 1.3 Odeon of Agrippa at Athens, Greece (Izenour, 1977)

SECTION

PLAN

```
o    20  40  60  80  100        Feet
├──┴──┴──┴──┴──┴──┤
o                 20            40  Meters
```
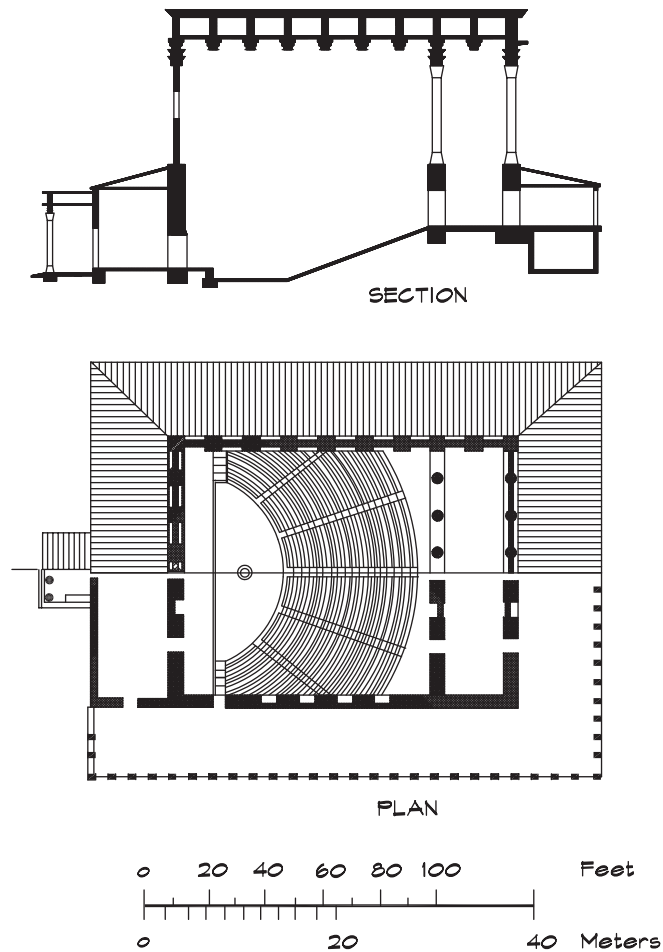
this book describes his views on many aspects of architecture, including theater design and acoustics. Some of his ideas were quite practical—such as his admonition to locate theaters on a "healthy" site with adequate ventilation (away from swamps and marshes). Seating should not face south, causing the audience to look into the sun. Unrestricted sightlines were considered particularly important, and he recommended that the edge of each row should fall on a straight line from the first to the last seat. His purpose was to assure good speech intelligibility as well as good sightlines.

Vitruvius also added one of the great historical mysteries to the acoustical literature. He wrote that theaters should have large overturned amphora or sounding vases placed at regular intervals around the space to improve the acoustics. These were to be centered in cavities on small, 150 mm (6") high wedges so that the open mouth of the vase was exposed to the stage, as shown in a conjectural restoration by Izenour in Fig. 1.4, based on an excavation of a Roman theater at Beth Shean in Israel. The purpose, and indeed the existence of these vases, remains unclear. Even Vitruvius could not cite an example of their use, though he assures us that they existed in the provinces.

FIGURE 1.4   Hypothetical Sounding Vases (Izenour, 1977)

A conjectural restoration in section of sounding vases in a cavity found at a Roman theater at Beth Shean, Israel.
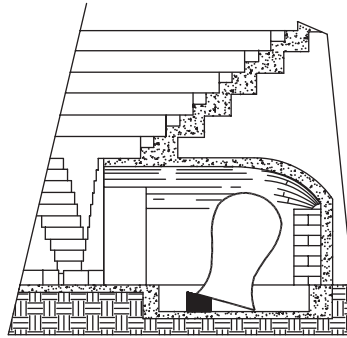
1.2   EARLY CHRISTIAN PERIOD (AD 400–800)

Rome and the West

The early Christian period is dated from the Roman emperor Constantine to the coronation of Charlemagne in 800. Following the official sanction of Christianity by Constantine in 326 and his relocation from Rome to Byzantium in 330, later renamed Constantinople, the age was increasingly dominated by the church, which provided the structural framework of everyday life as the Roman and then the Byzantine empires slowly decayed. Incursions by the Huns in 376 were followed by other serious invasions. On the last day of December in the winter of 406, the Rhine river froze solid, forming a bridge between Roman-controlled Gaul and the land of the Germanic tribes to the east (Cahill, 1995). Across the ice came hundreds of thousands of hungry Germans, who poured out of the eastern forests onto the fertile plains of Gaul. Within a few years, after various barbarian armies had taken North Africa and large parts of Spain and Gaul, Rome itself was sacked by Alaric in 410.

In these difficult times, monasteries became places of refuge, which housed small self-sustaining communities—repositories of knowledge, where farming, husbandry, and scholarship were developed and preserved. These were generally left unmolested by their rough neighbors, who seemed to hold them in religious awe (Palmer, 1961). In time, the ablest inhabitants of the Empire became servants of the Church rather than the state and "gave their loyalty to their faith rather than their government" (Strayer, 1955). "Religious conviction did not reinforce patriotism and men who would have died rather than renounce Christianity accepted the rule of conquering barbarian kings without protest." Under the new rulers a Romano-Teutonic civilization arose in the west, which eventually led to a division of the land into the states and nationalities that exist today.

After the acceptance of Christianity, church construction began almost immediately in Rome, with the basilican church of St. Peter in 330 initiated by Constantine himself. The style, shown in Fig. 1.5, was an amalgam of the Roman basilica (hall of justice) and the Romanesque style that was to follow. The basic design became quite popular—there were 31 basilican churches in Rome alone. It consisted of a high central nave with two parallel aisles on either side separated by colonnades supporting the upper walls and low-pitched roof, culminating in an apse and preceded by an atrium or forecourt (Fletcher, 1963). The builders generally scavenged columns from older Roman buildings that they could not

FIGURE 1.5   Basilican Church of St. Peter, Rome, Italy (Fletcher, 1963)

SCALE FOR SECTION

100   0   100 Feet

30   20   10   0   20   Meters

NAVE   ATRIUM

SCALE FOR PLAN

100   0   100   200   300   Feet

20 10 0   20   40   60   80   100 Meters
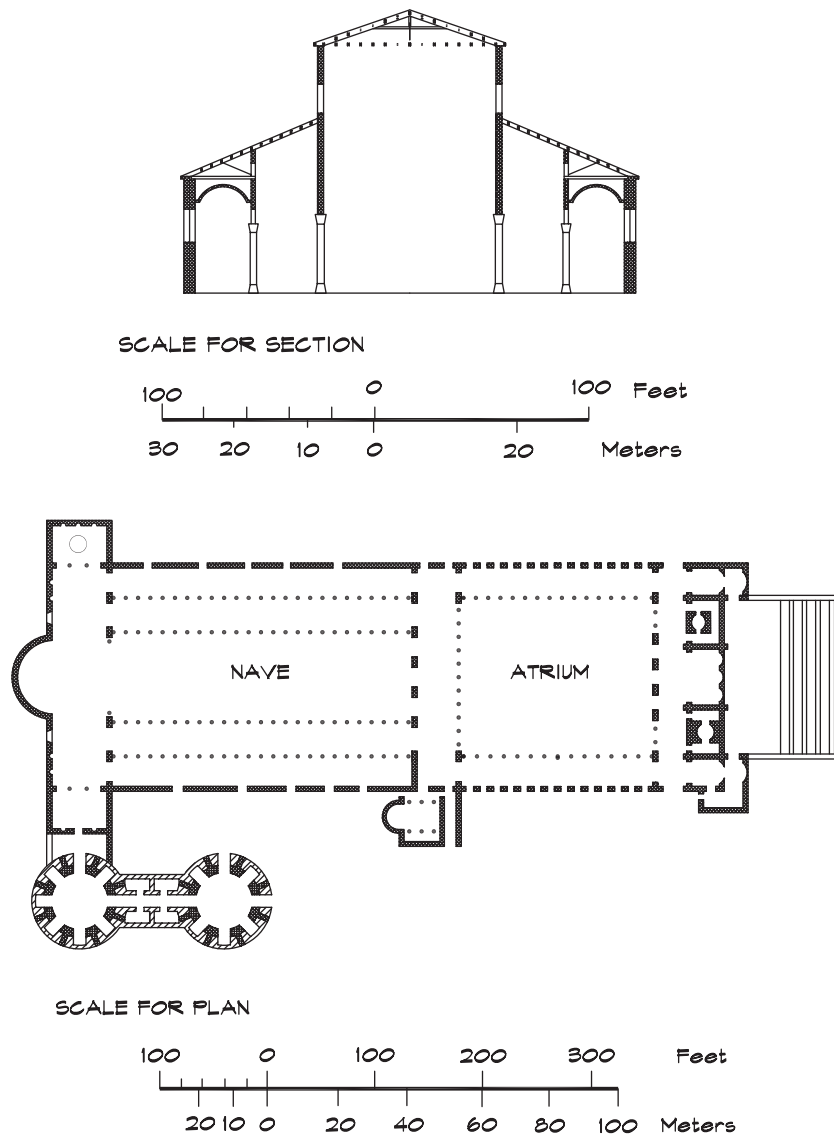
match or maintain, and which had therefore fallen into decay. The basilica style became a model for later church construction throughout Western Europe, eventually leading to the Gothic cathedrals.

Eastern Roman Empire

In the Eastern Roman Empire the defining architectural feature was the domed roof, used to cover square or polygonal floor plans. This form was combined with classical Greek columns supporting the upper walls with a series of round arches. The primary construction material was a flat brick, although marble was used as a decorative facade. The best known building of the time was St. Sophia (532–537) (*Hagia Sophia*, or divine wisdom) in Constantinople. This massive church, still one of the largest religious structures in the world, was built for

FIGURE 1.6   St. Sophia, Constantinople, Turkey (Fletcher, 1963)

SECTION

PLAN

100   0   100   200   300   Feet

20   0   20   40   60   80   Meters
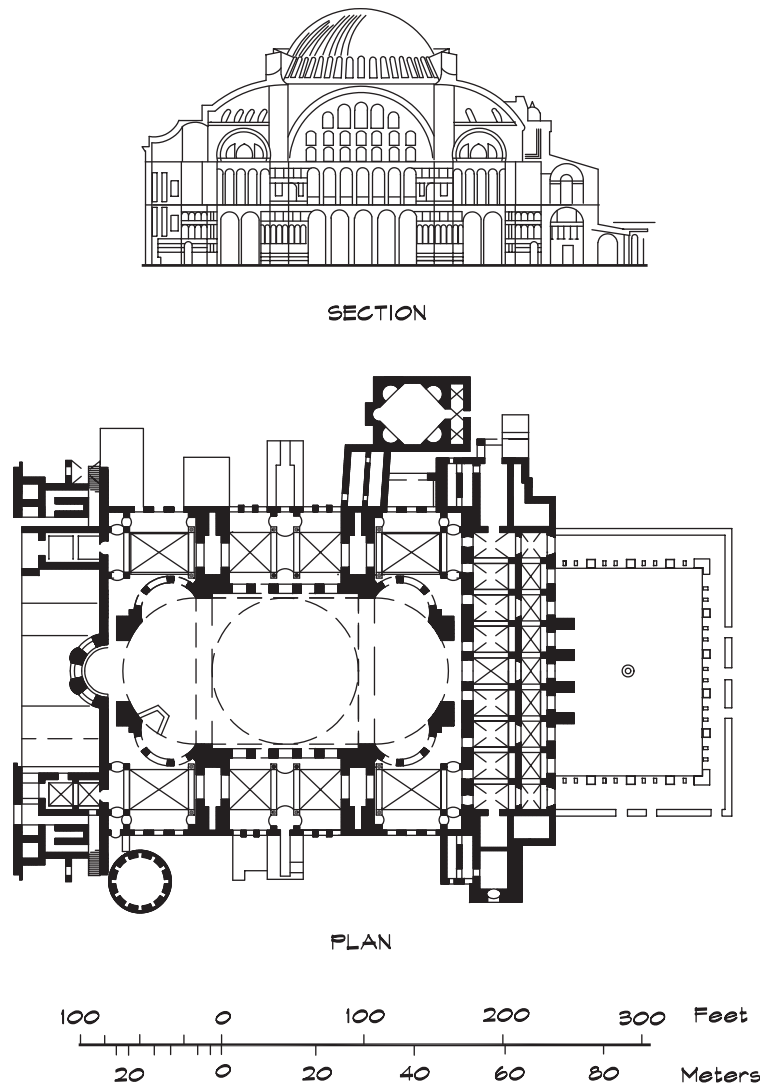
Emperor Justinian by the architects Anthemius of Tralles and Isodorus of Miletus between 532 and 537. Its enormous dome, spanning 33 meters (107 feet) in diameter, is set in the center of a 76 meter (250 foot) long central nave. St. Sophia, shown in Fig. 1.6, was the masterpiece of Byzantine architecture and later, following the Turkish capture of the city in 1453, became the model for many of the great mosques.

In the sixth century the territory of the former Roman Empire continued to divide. The Mediterranean world during this period was separated into three general regions: 1) the Byzantine empire centered in Asia minor, which controlled the Balkans, Greece, and eventually expanded into Russia; 2) the Arab world of Syria, Egypt, and North Africa, which under the leadership of Mohammed (570–632) swept across Africa and into southern Italy, Sicily, and Spain; and 3) the poorest of the three, Western Europe, an agricultural backwater with basically a subsistence economy. Holding the old empire together proved to be more than the Byzantine emperors could afford. Even the reign of the cautious Justinian (527–565),

whose generals temporarily recaptured Italy from the Ostrogoths, North Africa from the Vandals, and southeastern Spain from the Visigoths, did so on the backs of heavy taxation and loss of eastern provinces. The Lombards soon recaptured much of Italy, but the Byzantine representatives managed to hang onto Rome and the neighboring areas. The troubled sixth century closed with the successful pontificate of Pope Gregory I, who strove to standardize the liturgy and is traditionally regarded as the formulator of the liturgical chant, which bears his name.

Gregorian chant or plainsong, which became part of the liturgy in the Western Church, had antecedents in the rich tradition of cantillation in the Jewish synagogues, as well as the practices in the Eastern Church. Plain chant combined the simple melody and rhythm that dominated church music for several centuries.

Until a common system of musical notation was developed in the ninth century, there was little uniformity or record of the music. The early basilican churches were highly reverberant, even with open windows, and the pace and form of church music had to adjust to the architecture to be understood. Even with a simple monodic line, the blending of sounds from chants in these reverberant spaces is hauntingly beautiful.

The eastern and western branches of the Christian church became divided by ideological differences that had been suppressed when the church was clandestine. An iconoclastic movement resulted from a decree from the eastern emperor, Leo III (717–741), forbidding any representation of human or animal form in the church. Subsequently many Greek artisans left Constantinople for Italy, where they could continue their professions under Pope Gregory II. This artistic diaspora caused Leo to relent somewhat and he allowed painted figures on the walls of eastern churches but continued the prohibition of sculpture. His decrees led, in part, to the Byzantine style—devoid of statuary, and unchanging in doctrine and ritual. In contrast, the western church embraced statuary and sculpture, which in time begot the highly ornamented forms of the Baroque period and the music that followed. The split between the eastern and western branches, which had begun in the ninth century with a theological argument over the nature of the divine spirit, finally ended with a formal schism in 1054 when the two churches solemnly excommunicated each other.

1.3   ROMANESQUE PERIOD (800–1100)

The Romanesque period roughly falls between the reign of Charlemagne and the era of the Gothic cathedrals of the twelfth century. In the year 800 it was rare to find an educated layman outside of Italy (Strayer, 1955). The use of Latin decreased and languages fragmented according to region as the influence of a central authority waned. The feudal system developed in its place, not as a formal structure based on an abstract theory of government, but as an improvisation to meet the incessant demands of the common defense against raiders.

The influence of both Roman and Byzantine traditions is evident in the architecture of the Romanesque period. From the Roman style, structures retained much of the form of the basilica; however, the floor plans began to take on the cruciform shape. The eastern influence entered the west primarily through the great trading cities of Venice, Ravenna, and Marseilles and appeared in these cities first. Romanesque style is characterized by rounded arches and domed ceilings that developed from the spherical shape of the east into vaulted structures in the west. The narrow upper windows, used in Italy to limit sunlight, lead to larger openings in the north to allow in the light, and the flat roofs of the south were sharpened in the north to throw off rain and snow. Romanesque structures remained massive until the

introduction of buttresses, which allowed the walls to be lightened. Construction materials were brick and stone and pottery, as well as materials scavenged from the Roman ruins. The exquisite marble craftsmanship characteristic of the finest Greek and Roman buildings had been lost and these medieval brick structures seemed rough and plain compared with the highly ornamented earlier work.

One notable exception was St. Mark's Cathedral in Venice. It was built on the site of the basilica church, originally constructed to house the remains of St. Mark in 864. The first church burned in 976 and was rebuilt between 1042 and 1085. It was modeled after the Church of the Apostles in Constantinople as a classic Romanesque structure in a nearly square cruciform shape, with rounded domes reminiscent of later Russian orthodox churches. St. Mark's, illustrated in Fig. 1.7, was later home to a series of brilliant composers including Willaert (1480–1562), Gabrielli (1557–1612), and Monteverdi (1567–1643).

The music, which we now associate with Gregorian chant, developed as part of the worship in the eighth and ninth centuries. The *organum*, a chant of two parts, grew slowly from the earlier monodic music. At first this form consisted of a melody that was sung (held) by a tenor (*tenere*, to hold) while another singer had the same melodic line at an interval a forth above. True polyphony did not develop until the eleventh century.

1.4   GOTHIC PERIOD (1100–1400)

Gothic Cathedrals

Beginning in the late middle ages, around 1100, there was a burst in the construction of very large churches, the Gothic cathedrals, first in northern France and later spreading throughout Europe. These massive structures served as focal points for worship and repositories for the religious relics that, following the return of the crusaders from the holy lands, became important centers of the valuable pilgrim trade. The cathedrals were by and large a product of the laity, who had developed from a populace that once had only observed the religious forms, to one that held beliefs as a matter of personal conviction. Successful cities had grown prosperous with trade and during the relatively peaceful period of the late middle ages the citizens enthusiastically supported their construction. The first was built by Abbot Suger at St. Denis near Paris between 1137 and 1144 and was made possible by the hundreds of experiments in the building of fortified towns and churches, which had produced a skilled and knowledgeable work force. Suger was a gifted administrator and diplomat who also had the good fortune to attend school and become best friends with the young prince who became King Louis VI. When the king left on the Second Crusade he appointed Suger regent and left him in charge of the government. Following the success of St. Denis, other cathedrals were soon begun at Notre Dame (1163–c1250), Bourges (1192–1275), Chartes (1194–1260), and Rheims (1211–1290). These spectacular structures (see Fig. 1.8) carried the art and engineering of working in stone to its highest level. The vaulted naves, over 30 meters (100 feet) high, were lightened with windows and open colonnades and supported from the exterior with spidery flying buttresses, which gave the inside an ethereal beauty. Plain chant was the music of the religious orders and was suited perfectly to the cathedral. Singing was something that angels did, a way of growing closer to God. It was part of the every day religious life, done for the participants rather than for an outside listener.

In the second half of the twelfth century the beginnings of polyphony developed in the School of Notre Dame in Paris from its antecedents in the great abbey of St. Martial in Limoges. The transition began with the two-part *organum* of Leonin, and continued with the

FIGURE 1.7   St. Mark's Cathedral, Venice, Italy (Fletcher, 1963)

SECTION

PLAN

| 40 | 0 | 40 | 80 | 120 | Feet |
| 20 | 0 | 20 | 40 | Meters |
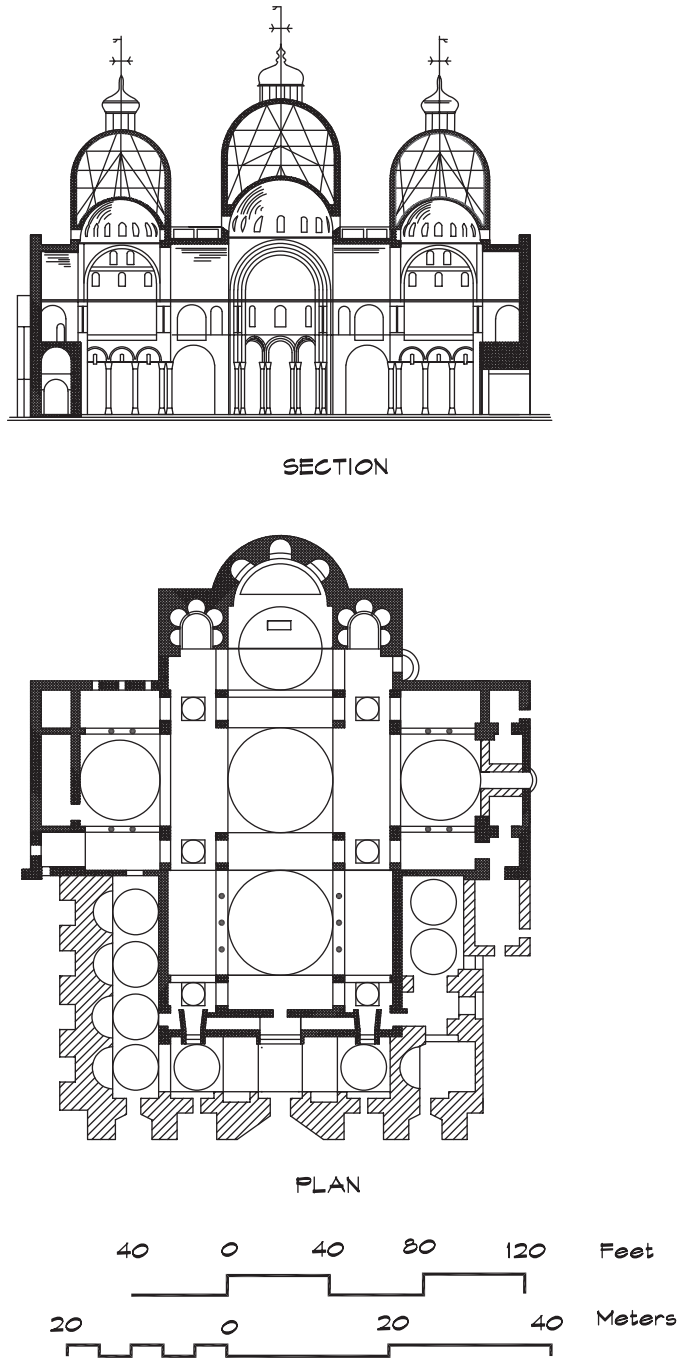
three and four-part *organum* of his successor Perotin. The compositions were appropriate for the large reverberant cathedrals under construction. A slowly changing plainsong pedal note was elaborated by upper voices, which did not follow the main melody note for note as before. This eventually led, in the thirteenth and fourteenth centuries, to the polyphonic motets in which different parts might also have differing rhythms. Progress in the development of

FIGURE 1.8   Notre Dame Cathedral, Paris, France (Fletcher, 1963)

SCALE FOR SECTION

Feet Meters

TRANSVERSE SECTION

PLAN SHOWING ARCHES ABOVE

50   0   50   100   150   200 Feet

15   0   15   30   45 Meters
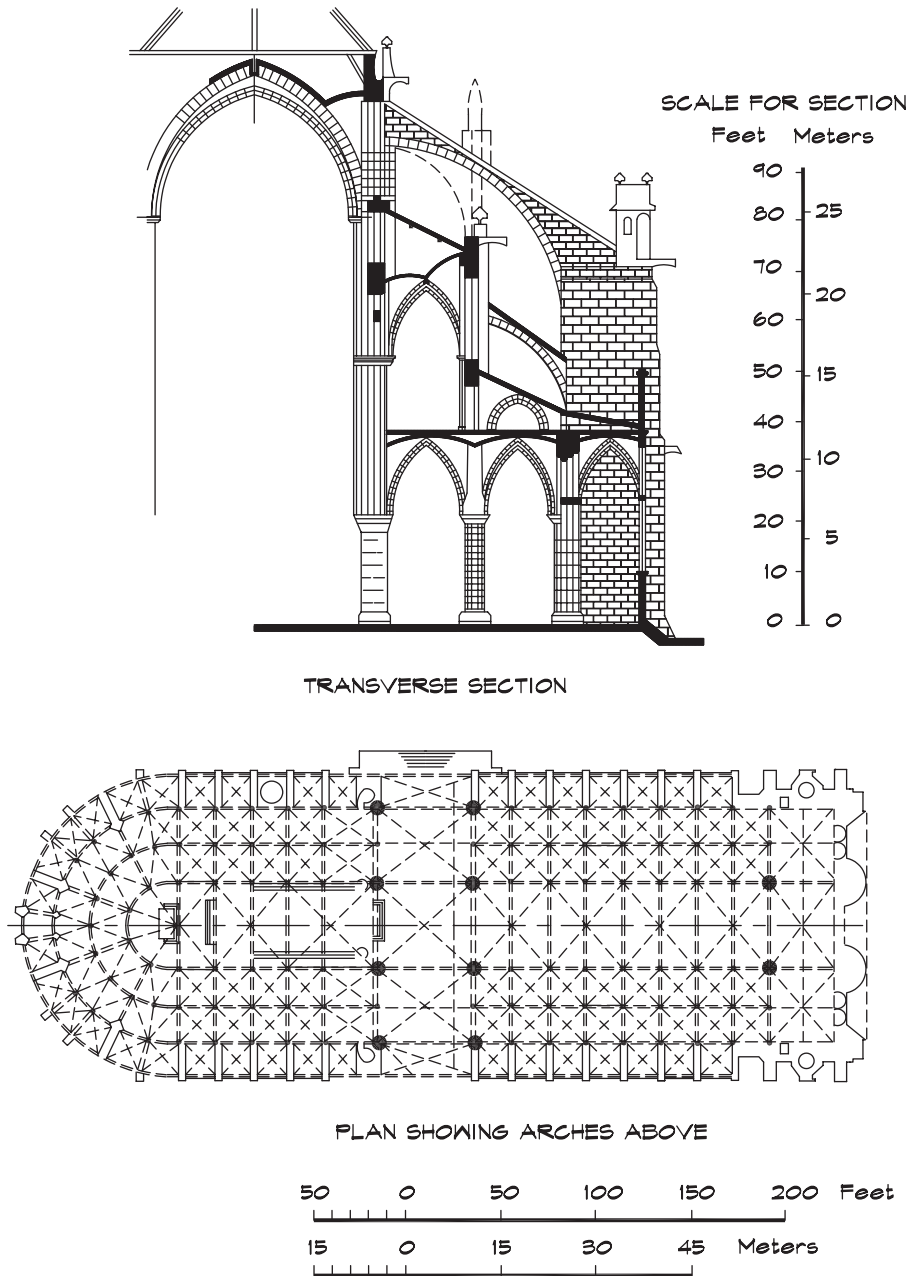
serious music was laborious and slow. Outside the structured confines of church music, the secular troubadours of Provence, the trouveres of northern France and southern England, the story-telling jongleurs among the peasantry, and the minnesingers in Germany also made valuable contributions to the art.

The influence of the Church stood at its zenith in the thirteenth century. The crusades, of marginal significance militarily, had served to unite Western Europe into a single religious community. An army had pushed the Muslims nearly out of the Iberian peninsula.

Beginning in the fourteenth century, however, much of the civilized world was beset by the ravages of the bubonic plague. Between the years 1347 and 1350 it wiped out at least one third of the population. The Church was hit harder than the general populace, losing more than half its members. Many men, largely illiterate, had lost their wives to the plague and sought to join the religious orders. Lured by offers of money from villages that had no priest, others came to the church for financial security. Money flowed into Rome and supported a growing bureaucracy and opulence, which ultimately led to the Reformation. This worsened a problem already confronting the religious leadership, "the danger of believing that the institution exists for the benefit of those who conduct its affairs." (Palmer, 1961)

With the rise of towns and commerce, public entertainment became more secular and less religious in its focus. Theater in the late middle ages was tolerated by the Church largely because it had been co-opted as a religious teaching aid. Early plays, dating from the tenth century, were little more than skits based on scripture, which were performed in the streets by troupes. These evolved, in the thirteenth and fourteenth centuries, into the miracle and mystery plays that combined singing and spoken dialogue. The language of the early medieval theater was Latin, which few understood. This changed in time to the local vernacular or to a combination of Latin and vernacular. The plays evolved from a strictly pedagogical tool to one that contained more entertainment. As the miracle plays developed, they were performed in rooms that would support the dialogue and make it understandable. By 1400, the pretext of the play remained religious, but the theater was already profane (Hindley, 1965).

1.5   RENAISSANCE PERIOD (1400–1600)

Renaissance Churches

The great outpouring of art, commerce, and discovery that was later described as the Renaissance or rebirth, first started in northern Italy and gradually spread to the rest of Europe. The development of new music during these years was rich and profuse. Thousands of pieces were composed and, while sacred music still dominated, secular music also thrived (Hemming, 1988).

Church construction still continued to flourish in the early years of the Renaissance. St. Peter's Cathedral in Rome, the most important building of the period, was begun in 1506 and was created by many of the finest architects and artists of the day. A competition produced a number of designs, still preserved in the Uffizi Gallery in Florence, from which Bramante (1444–1514) was selected as architect (Fletcher, 1963). After the death of Pope Julius II a number of other architects, including Raphael (1483–1520), worked on the project—the best known being Michelangelo (1475–1564). He began the construction of the dome, which was completed after his death, from his models. Some time later Bernini erected (1655–1667) the immense piazza and the baroque throne of St. Peter.

The construction of this great cathedral in Rome also reached out to touch an obscure professor of religion at the university in Whitenberg. In 1517, a friar named Tetzel was traveling through Germany selling indulgences to help finance it. Martin Luther felt that the people were being deluded by this practice and, in the manner of the day, posted a list of 95 theses on the door of the castle church in protest (Palmer, 1961). By 1560, most of northern Europe including Germany, England, Netherlands, and the Scandinavian countries had officially adopted some form of Protestantism.

Renaissance Theaters

Theater construction began again in Italy in the early Renaissance, more or less where the Romans had left it a thousand years earlier. In 1580, the Olympic Academy in Vicenza engaged Palladio (1518–1580) to build a permanent theater (Fig. 1.9), the first since the Roman Odeons. The seating plan was semi-elliptical, following the classical pattern, and the stage had much the same *orchestra* and *proskenium* configuration that the old Roman theaters had. Around the back of the audience was a portico of columns with statues above. The newly discovered art of perspective captured the imagination of designers and they crafted stages, which incorporated a rising stage floor and single point perspective. The terms upstage and downstage evolved from this early design practice. After the death of Palladio, his pupil Scamozzi added five painted streets in forced perspective angling back from the *scaena*.

In 1588, Scamozzi further modified the Roman plan in a new theater, the Sabbioneta. The semi-elliptical seating plan was pushed back into a U shape, the stage wall was removed, and a single-point perspective backdrop replaced the earlier multiple-point perspectives. This theater is illustrated in Fig. 1.10. Its seating capacity was small and there was little acoustical support from reflections off the beamed ceiling.

In mid-sixteenth century England, traveling companies of players would lay out boards to cover the muddy courtyards of inns, while the audience would stand around them or line the galleries that flanked the main yard (Breton, 1989). Following the first permanent theater built in 1576 by James Burbage, this style became the model for many public theaters, including Shakespeare's Globe. The galleries surrounding the central court were three tiers high with a roofed stage, which looked like a thatched apron at one end. Performances were held during the day without a curtain or painted backdrop. The acoustics of these early theaters was probably adequate. The side walls provided beneficial early reflections and the galleries yielded excellent sightlines. The open-air courtyard reduced reverberation problems and outside noise was shielded by the high walls. It is remarkable that such simple structures sufficed for the work of a genius like Shakespeare. Without good speech intelligibility provided by this type of construction, the complex dialogue in his plays would not only have been lost on the audience, it would probably not have been attempted at all.

FIGURE 1.9   Teatro Olimpico, Vicenza, Italy (Breton, 1989)

SECTION   PLAN
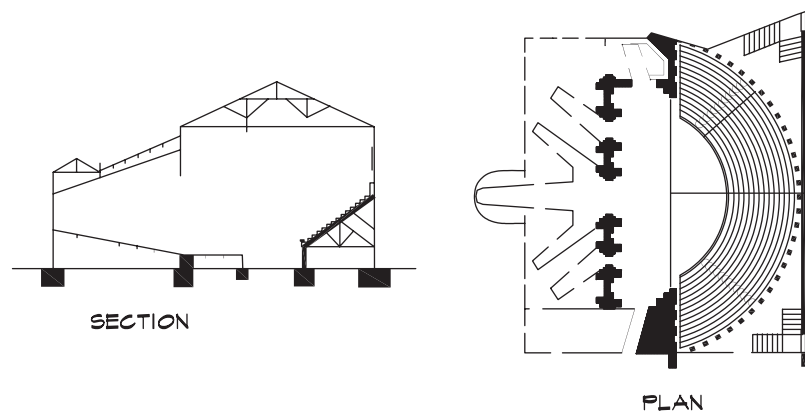
FIGURE 1.10   Sabbioneta Theater, Italy (Breton, 1989)

PLAN

SECTION
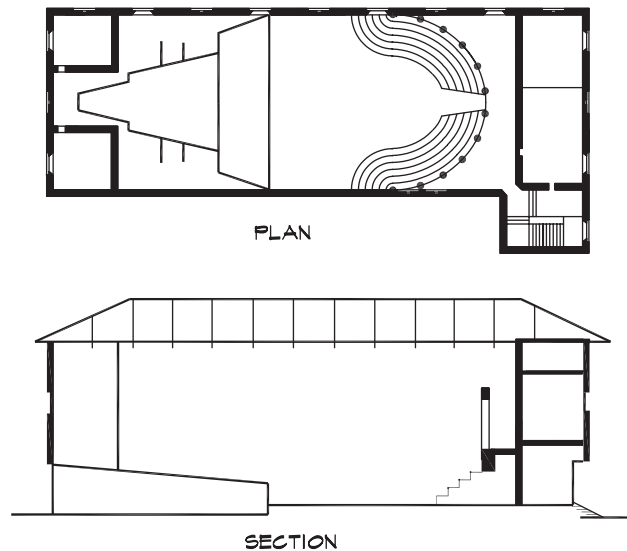
1.6   BAROQUE PERIOD (1600–1750)

Baroque Churches

The first half of the seventeenth century was dominated by the Thirty Years War (1618–1648), which ravaged the lands of Germany and central Europe. This confusing struggle was one of shifting alliances that were formed across religious and political boundaries (Hindley, 1965). The end result was a weakening of the Hapsburg empire and the rise of France as the dominant power in Europe. Italy became a center for art and music during that period, in large part because it was relatively unscathed by these central European wars. In northern Italy a style, which became known as the Baroque (after the Portuguese *barocco*, a term meaning a distorted pearl of irregular shape), grew out of the work of a group of Florentine scholars and musicians known as the *Camerata* (from the Italian *camera*, or chamber). This group abandoned the vocal polyphony of Renaissance sacred music and developed a new style featuring a solo singer with single instrumental accompaniment (the *continuo*) to provide unobtrusive background support for the melodic line. The new music was secular rather than sacred and dramatic, and passionate rather than ceremonial (Hemming, 1988), and allowed for considerably more freedom by the performer.

Both the music and the architecture of the Baroque period was more highly ornamented than that of the Renaissance. Composers began writing in more complicated musical forms such as the fugue, chaconne, passacaglia, toccata, concerto, sonata, and oratorio. Some of the vocal forms, such as the cantata, oratorio, and opera, grew out of the work of the Camerata. Others developed from the architecture and influence of a particular space. St. Mark's Cathedral in Venice was shaped like a nearly square cross with individual domes over each arm and above the center (see Fig. 1.7). These created localized reverberant fields, which supported the widely separated placement of two or three ensembles of voices and instruments that could perform as separate musical bodies. Gabrielli (1557–1612), who was organist there for 27 years, exploited these effects in his compositions, including separate

FIGURE 1.11   Theatro Farnese, Parma, Italy (Breton, 1989)

SECTION

PLAN
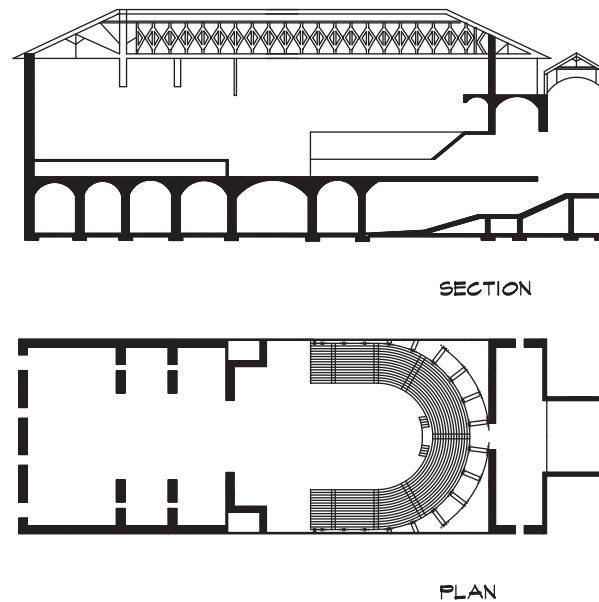
instrument placement, call and response sequences, and echo effects. In less than 100 years this style had been transformed into the concerto grosso (Burkat, 1998).

Baroque Theaters

The progress in theater construction in Northern Italy was also quite rapid. The illusion stages gave way to auditoria with horizontally sliding flats, and subsequently to moveable stage machinery. The *Theatro Farnese* in Parma, constructed between 1618 and 1628 by Giovanni Battista Aleotti, had many features of a modern theater. Shown in Fig. 1.11, it featured horizontal set pieces, which required protruding side walls on either side of the stage opening to conceal them. This allowed set changes to be made and provided entrance spaces on the side wings for the actors to use without appearing out of scale. The U-shaped seating arrangement afforded the patrons a view, not only of the stage, but also of the prince, whose box was located on the centerline.

In Florence at the Medici court, operas were beginning to be written. The first one was *Dafne*, which is now lost, written between 1594 and 1598 by Peri (Forsyth, 1985). The first known opera performance was Peri's *Euridice*, staged at a large theater in the Pitti Palace to celebrate the wedding of Maria de'Medici and King Henri IV of France in 1600. This was followed by Monteverdi's *Orfeo*, first performed in 1607 in Mantua, which transformed opera from a somewhat dry and academic style to a vigorous lyric drama.

Italian Opera Houses

By 1637, when the first public opera house was built in Venice (Fig. 1.12), the operatic theater had become the multistory U-shaped seating arrangement of the Theatro Farnese, with boxes in place of tiers. Later the seating layout further evolved from a U shape into a truncated elliptical shape. The orchestra, which had first been located at the rear of the stage and then in the side balconies, was finally housed beneath the stage as is the practice today

FIGURE 1.12   **Theater of SS. Giovanni e Paolo, Venice, Italy (Forsyth, 1985)**

SECTION

PLAN
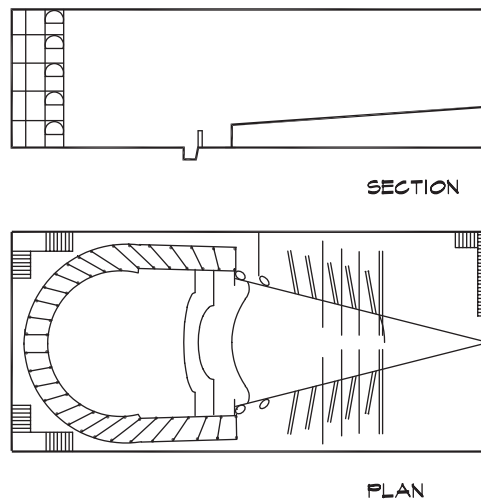
(Breton, 1989). The stage had widened further and now had a flyloft with winches and levers to manipulate the scenery. This became the typical Baroque Italian opera house, which was the standard model replicated throughout Europe with little variation for 200 years.

Italy immediately became the center of opera in Europe. In the years between 1637 and the end of the century, 388 operas were produced in Venice alone. Nine new opera houses were opened during this period, and after 1650, never fewer than four were in simultaneous operation (Grout, 1996). These early opera houses served as public gathering places. For the equivalent of about 50 cents, the public could gain entry to the main floor, occupied by standing patrons who talked and moved about during the performances. The high background noise is documented in many complaints in writings of the time. It led to the practice of loudly sounding a cadential chord to alert the audience of an impending aria. In a forerunner of contemporary films, special effects became particularly popular. As the backstage equipment grew more complicated and the effects more extravagant, the noise of the machines threatened to drown out the singing. Composers would compensate by writing instrumental music to mask the background sounds. The popularity of these operas was so great that the better singers were in considerable demand. Pieces were written to emphasize the lead singer's particular ability with the supporting roles de-emphasized.

Baroque Music

The seventeenth century also saw the rise of the aristocracy and with it, conspicuous consumption. Churches and other public buildings became more ornate with applied decorative elements, which came to symbolize the Baroque style. Music began to be incorporated into church services in the form of the oratorio, a sort of religious opera staged without scenery or costumes. In Rome the Italian courts were opulent enough to embrace opera as a true spectacle. Pope Urban VII commissioned the famous Barberini theater based on a design of Bernini, which held 3000 people and opened in 1632 with a religious opera by Landi.

In the Baroque era instrumental music achieved a status equal to vocal music. Musical instruments became highly sophisticated in the seventeenth and eighteenth centuries and in some cases achieved a degree of perfection in their manufacture that is unmatched today.

The harpsichord and the instruments of the violin family became the basic group for ensemble music. Violins fashioned by craftsmen such as Nicolo Amati (1569–1684), Giuseppi Guarneri (1681–1742) and Antonio Stradivari (1644–1737) are still the best instruments ever made. The lute, which was quite popular at the beginning of the period, was rarely used at the end. Early wind instruments had been mainly shawms (later oboes), curtals (later bassoons), crumhorns, bagpipes, fifes and drums, cornets, and trumpets. New instruments were developed, specifically the recorder, the transverse flute, oboe, and bassoon. The hunting horn having a five-and-one-half-foot tube wound into four or five loops before flaring into a bell, was improved in France by reducing the number of loops and enlarging the bell. When it became known in England, it was given the name French horn. By the early 1600s, the pipe organ had developed into an instrument of considerable technical development.

Antonio Vivaldi (1678–1741), now recognized as one of the foremost Baroque composers, first learned violin from his father, who was a violinist at St. Mark's in Venice. He was a priest and later (1709) music director at a school for foundling girls, the Seminario dell'Ospitale della Pieta. His intricate compositions for the violin and other instruments of the time feature highly detailed passages characteristic of what is now known as chamber music, written for small rooms or salons.

Protestant Music

In Protestant northern Europe the spoken word was more important to the religious service than in the Catholic south. The volume of the northern church buildings was reduced to provide greater clarity of speech. The position of the pulpit was centrally placed and galleries were added to the naves and aisles. Many existing churches, including Thomaskirche in Leipzig, were modified by adding hanging drapes and additional seating closer to the pulpit (Forsyth, 1985). Johann S. Bach (1685–1750) was named cantor there in 1722, to the disappointment of the church governors. He was their second choice behind Georg Philip Telleman (1681–1767). Bach was influenced by the low reverberation time of the church, which has been estimated to have been about 1.6 seconds (Bagenal, 1930). His B-Minor Mass and the St. Matthew Passion were both composed for this space.

Bach wrote music for reverberant spaces as well as for intimate rooms. During his early years in Weimar (1703–1717) he composed mostly religious music including some of his most renowned works for organ, the Passacaglia and double Fugue in C minor and the Toccata and Fugue in D minor. His Brandenberg Concertos, composed for the orchestra at the little court of Anhalt-Cothen, were clearly meant to be played in a chamber setting, as were the famous keyboard exercises known as the *Well Tempered Clavier*, which were written for each of the 24 keys in the system of equal-tempered tuning, completed about the same time.

Baroque music was performed in salons, drawing rooms, and ballrooms, as well as in churches. In general the former were not specifically constructed for music and tended to be small. The orchestras were also on the smallish side, around twenty-five musicians, much like chamber orchestras today. As rooms and audiences grew larger, louder instruments became more popular. The harpsichord gave way to the piano, the viola da gamba to the cello, and the viol to the violin. The problem of distributing the sound evenly to the listener was soon recognized, but there were few useful guidelines. In England Thomas Mace published (1676) suggestions for the designer in his *Musick's Monument or a Rememberancer of the best practical Musick*. He recommended a square room with galleries on all sides surrounding the musicians, much like a theater in the round. Mace advocated piping the sound from the

musicians to the rear seats through tubes beneath the floor, a device that was used extensively in the Italian opera houses of the day, and contemporaneously in loud-speaking trumpets, which were employed as both listening and speaking devices (Forsyth, 1985).

1.7   ORIGINS OF SOUND THEORY

The understanding of the theory of fluids including sound propagation through them made little progress from the Greeks to the Renaissance. Roman engineers did not have a strong theoretical basis for their work in hydraulics (Guillen, 1995). They knew that water flowed downhill and would rise to seek its own level. This knowledge, along with their extraordinary skills in structural engineering, was sufficient for them to construct the massive aqueduct systems including rudimentary siphons. However, due to the difficulty they had in building air-tight pipes it was more effective for them to bridge across valleys than to try to siphon water up from the valley floors. Not until Leonardo da Vinci (1452–1519) studied the motion and behavior of rivers did he notice that, "A river of uniform depth will have more rapid flow at the narrower section than at the wider." This is what we now call the equation of continuity, one of the relationships necessary for the derivation of the wave equation.

   Galileo Galilei (1564–1642) along with others noted the isochronism of the pendulum and was aware, as was the French Franciscan friar Marin Mersenne (1588–1648), of the relationship between the frequency of a stretched string and its length, tension, and density. Earlier Giovanni Battista Benedetti (1530–1590) had related the ratio of pitches to the ratio of the frequencies of vibrating objects. In England Robert Hooke (1635–1703), who had bullied a young Isaac Newton (1642–1727) on his theory of light (Guillen, 1995), published in 1675 the law of elasticity that now bears his name, in the form of a Latin anagram CEII-INOSSSTTUV, which decoded is "ut tensio sic vis" (Lindsay, 1966). It established the direct relationship between stress and strain that is the basis for the formulas of linear acoustics. The first serious attempt to formalize a mathematical theory of sound propagation was set forth by Newton in his second book (1687), *Philosophiae Naturalis Principia Mathematica*. In this work he hypothesized that the velocity of sound is proportional to the square root of the absolute pressure divided by the density. Newton had discovered the isothermal velocity of sound in air. This is a less generally applicable formula than the adiabatic relationship, which was later suggested by Pierre Simon Laplace (1749–1827) in 1816. A fuller understanding of the propagation of sound waves had to wait until more elaborate mathematical techniques were developed.

   Daniel Bernoulli (1700–1782), best known for his work in fluids, set forth the principle of the coexistence of small amplitude oscillations in a string, a theory later known as super-position. Soon after, Leonhard Euler (1707–1783) published a partial differential equation for the vibrational modes in a stretched string. The stretched-string problem is one that every physics major studies, due both to its relative simplicity and its importance in the history of science. The eighteenth century was a time when mathematics was just beginning to be applied to the study of mechanics. Prizes were offered by governments for the solution of important scientific problems of the day and there was vigorous and frequently acrimonious debate among natural philosophers in both private and public correspondence on the most appropriate solutions.

   The behavior of sound in pipes and tubes was also of interest to mathematicians of the time. Both Euler (1727) and later J. L. Lagrange (1736–1830) made studies of the subject. Around 1759 there was much activity and correspondence between the two of them

(Lindsay, 1966). In 1766, Euler published a detailed treatise on fluid mechanics, which included a section entirely devoted to sound waves in tubes.

The tradition of offering prizes for scientific discoveries continued into the nineteenth century. The Emperor Napoleon offered, through the Institute of France, a prize of 3000 francs for a satisfactory theory of the vibration of plates (Lindsay, 1966). The prize was awarded in 1815 to Sophie Germain, a celebrated woman mathematician, who derived the correct fourth-order differential equation. The works of these early pioneers, along with his own insights, ultimately were collected into the monumental two-volume work, *Theory of Sound*, by John W. Strutt, Lord Rayleigh (1842–1919) in 1877. This classic work contains much that is original and insightful even today.

1.8   CLASSICAL PERIOD (1750–1825)

The eighteenth century in Europe was a cosmopolitan time when enlightened despots (often foreign born) were on the throne in many countries, and an intellectual movement known as the Enlightenment held that knowledge should evolve from careful observation and reason. The French *philsophes*, Rousseau, Montesquieu, and Voltaire reacted to the social conditions they saw and sought to establish universal rights of man. In both the visual and performing arts, there was a classic revival, a return to the spirit of ancient Greece and Rome. The paintings of Jacques Louis David, such as the *Oath of the Horatii* (1770), harkened back to Republican Rome and the virtues of nobility, simplicity, and perfection of form. The excavations of Pompeii and Herculeum had created public interest in the history of this earlier era and, with the American Revolution in 1776 and the French revolution in 1789, the interest took on political overtones.

The period referred to as Classical in music occurred during these years, though some historians, such as Grout and Palisca (1996) date it from 1720 to 1800. Classical refers to a time when music was written with careful attention to specific forms. One of these had a particular three-part or ternary pattern attributed to J. S. Bach's son, Carl Philipp Emanuel Bach (1714–1788), which is now called sonata form. Others included the symphony, concerto, and rondo. Compositions were written within the formal structure of each of the types. The best known composers of that time were Franz Joseph Haydn (1732–1809), Wolfgang A. Mozart (1756–1791), and later Ludwig Beethoven (1770–1827). During the Classical period musical pieces were composed for the first time with a formal concert hall performance in mind. Previously rooms that were used for musical concerts were rarely built specifically for that sole purpose.

In England in the middle of the eighteenth century, buildings first were built for the performance of nontheatrical musical works. Two immigrant musicians, Carl Fredrick Abel (1723–1787) and Johann (known as John) Christian Bach (1735–1782), the eighteenth child of J. S. Bach, joined forces with Giovanni Andrea Gallini, who provided the financing, to build between 1773 and 1775 what was to become the best-known concert hall in London for a century, the Hanover Square Rooms. The *Illustrated London News* of 1843 showed an engraving of the main concert hall (Forsyth, 1985) from which Fig. 1.13 was drawn.

When Haydn came to England in 1791–1792 and 1793–1794, he conducted his London Symphonies (numbers 93 to 101), which he had written specifically for this room. The main performance space was rectangular and, according to the London *General Evening Post* of February 25, 1794 (Forsyth, 1985), it measured 79 ft (24.1 m) by 32 ft (9.7 m). The height has been estimated at 22 to 28 ft. (6.7 to 8.5m). In Victorian times, it was lengthened to between 90 and 95 ft (Landon, 1995). It was somewhat small for its intended capacity (800)

FIGURE 1.13   Hanover Square Room, London, England (Forsyth, 1985)

Plan
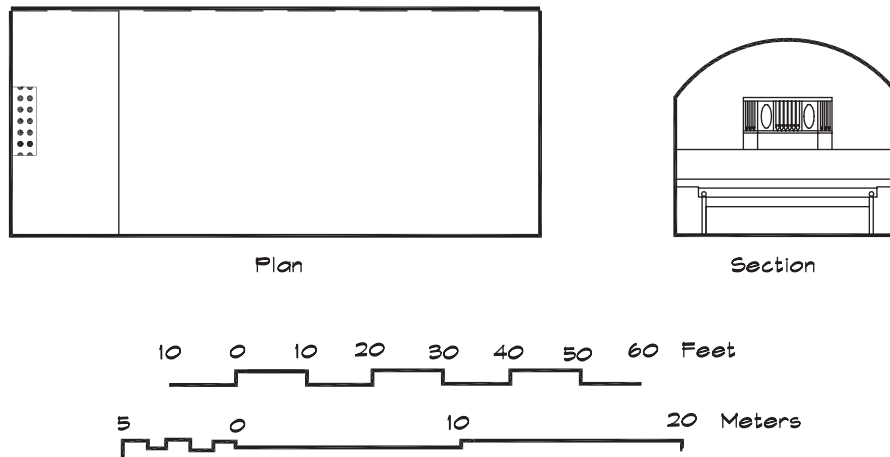
Section

and probably had a reverberation time of less than one second when fully occupied (J. Meyer, 1978). The low volume and narrow width would have provided strong lateral reflections and excellent clarity, albeit a somewhat loud overall level. The room was well received at the time. The *Berlinische Musikalische Zeitung* published a letter on June 29, 1793 describing a concert there by a well-known violinist, Johann Peter Salomon (1745–1815): "The room in which [the concert] is held is perhaps no longer than that in Stadt Paris in Berlin, but broader, better decorated, and with a vaulted ceiling. The music sounds, in the hall, beautiful beyond any description." (Forsyth, 1985)

In the eighteenth century the center of gravity of the music in Europe shifted northward from Italy. Orchestras in London, Paris, Mannheim, Berlin, and Vienna were available to composers of all nationalities. Halls were built in Dublin, Oxford, and Edinburgh, many years before they appeared in cities on the continent. The Holywell Music Room at Oxford, which opened in 1748, still stands today. These halls were relatively small by today's standards with seating capacities ranging from 400 to 600, and reverberation times were generally less than 1.5 seconds (Bagenal and Wood, 1931). Music was also played at public concerts held outdoors in pleasure gardens. In 1749 some 12,000 people paid two shillings sixpence each to hear Handel's 100-piece band rehearse his *Royal Fireworks Music* at Vauxhall Gardens (Forsyth, 1985).

In continental Europe in the mid eighteenth century there was not yet a tradition of public concerts open to all. Concert-goers were, by and large, people of fashion and concerts were usually held in rooms of the nobility, such as Eisenstadt Castle south of Vienna or Eszterhaza Castle in Budapest, which was the home of Haydn during his most productive years. It was not until 1761 that a public hall was built in Germany, the Konzert-Saal auf dem Kamp in Hamberg. In Leipzig, perhaps because it did not have a royal court, the architect Johann Carl Friedrich Dauthe converted a Drapers' Hall or Gewandhaus into a concert hall in 1781. Later known as the Altes Gewandhaus, it seated about 400 with the orchestra located on a raised platform at one end occupying about one quarter of the floor space. It is pictured in Fig. 1.14. The room had a reverberation time of about 1.3 seconds (Bagenal and Wood, 1931) and was lined with wood paneling, which reduced the bass build up. Recognized for its fine acoustics, particularly during Felix Mendelssohn's directorship in the

FIGURE 1.14   Altes Gewandhaus, Leipzig, Germany (Bagenal and Wood, 1931)
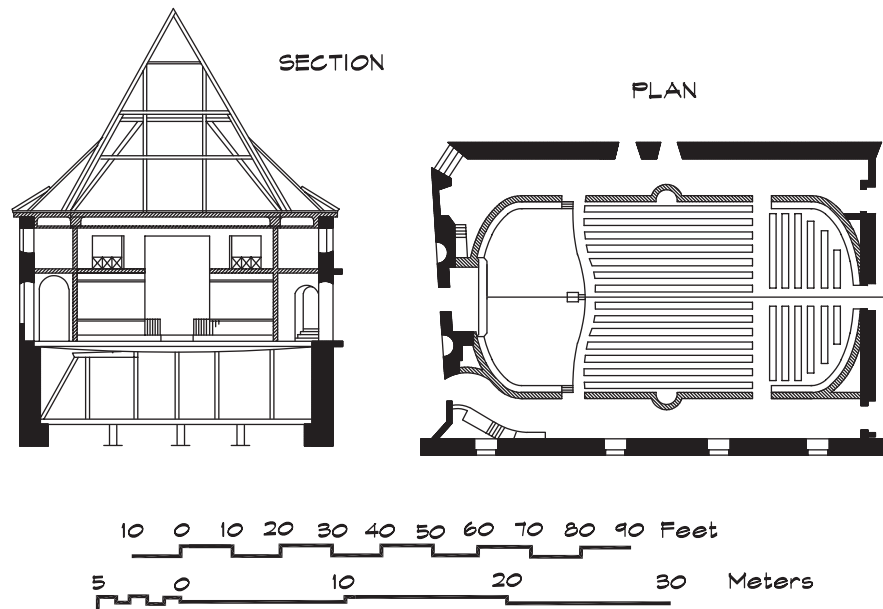
mid-nineteenth century (1835–1847), it was later replaced by the larger Neus Gewandhaus late in the century.

Vienna became an international cultural center where artists and composers from all over Europe came to work and study, including Antonio Salieri (1750–1825), Mozart, and Beethoven. Two principal concert halls in Vienna at the time were the Redoutensaal at Hofburg and the palace of the Hapsburg family. Built in 1740, these two rooms, seating 1500 and 400, respectively, remained in use until 1870. The larger room was rectangular, had a ceiling height of about 30 ft, and side galleries running its full length. The reverberation time was probably slightly less than 1.6 seconds when fully occupied. The rooms had flat floors and were used for balls as well as for concerts. Haydn, Mozart, and Beethoven composed dances for these rooms, and Beethoven's Seventh Symphony was first performed here in 1814 (Forsyth, 1985).

Meanwhile in Italy little had changed. Opera was the center of the cultural world and opera-house design had developed slowly over two centuries. In 1778 La Scalla opened in Milan and has endured, virtually unchanged, for another two centuries. Shown in Fig. 1.15, it has the form of a horseshoe-shaped layer cake with small boxes lining the walls. The sides of the boxes are only about 40% absorptive (Beranek, 1979) so they provide a substantial return of reflected sound back to the room and to the performers. The orchestra seating area is nearly flat, reminiscent of the time when there were no permanent chairs there. The seating arrangement is quite efficient (tight by modern standards), and the relatively low (1.2 sec) reverberation time makes for good intelligibility.

1.9   ROMANTIC PERIOD (1825–1900)

The terms Classic and Romantic are not precisely defined nor do they apply strictly to a given time period. Music written between about 1770 and 1900 lies on a continuum, and every composer of the age employed much the same basic harmonic vocabulary (Grout and

FIGURE 1.15   Theatro Alla Scalla, Milan, Italy (Beranel, 1979)

SECTION

UPPER BALCONY PLAN

ORCHESTRA / FIRST TIER PLAN

| 10 | 0 | 20 | 40 | 60 | 80 | Feet |
| 5 | 0 | 10 | 20 | 30 | Meters |
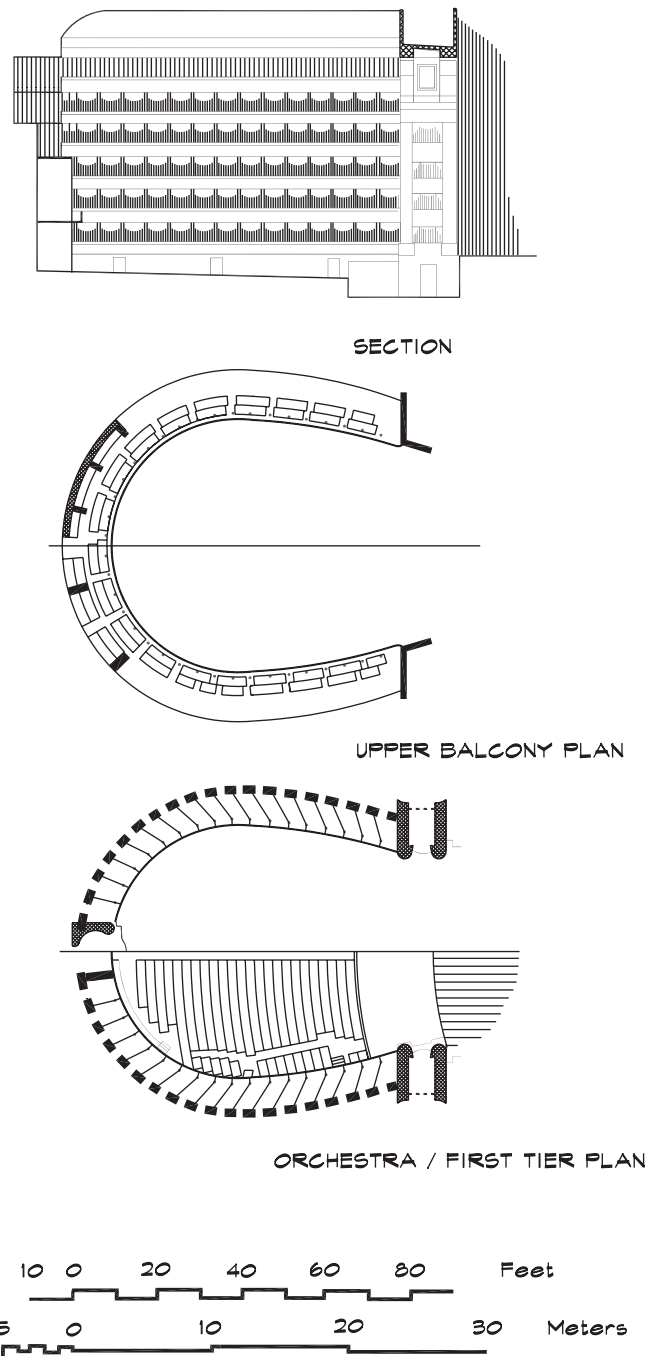
Palisca, 1996). Romantic music is more personal, emotional, and poetic than the Classical and less constrained by a formal style. The Romantic composers wanted to describe thoughts, feelings, and impressions with music, sometimes even writing music as a symphonic poem or other program to tell a story. Although Beethoven lived during the Classical time period, much of his music can be considered Romantic, particularly his sixth and ninth symphonies.

Clearly he bridged the two eras. The best known Romantic composers were all influenced by Beethoven including Franz Schubert (1797–1828), Hector Berlioz (1803–1869), Felix Mendelssohn (1809–1847), Johannes Brahms (1833–1897), and Richard Wagner (1813–1883).

A common characteristic of Classical composers was their familiarity with the piano, which had become the most frequently used instrument. Some Romantic composers were also virtuoso pianists including Franz Liszt (1811–1886), Edvard Grieg (1843–1907), Frederic Chopin (1810–1849), and of course Beethoven. The wide dynamic range of this instrument originally led to its name, the forte (loud) piano (soft), and socially prominent households were expected to have one in the parlor.

As musical instruments increased in loudness they could be heard by larger audiences, which in turn encouraged larger concert halls and the use of full orchestras. As performance spaces grew larger there arose an incentive to begin thinking more about their acoustical behavior. Heretofore room shapes had evolved organically, the Italian opera from the Greek and Roman theaters, and the Northern European concert halls from basilican churches and rectangular ballrooms. Many of these rooms were enormously successful and are still today marvels of empirical acoustical design, although there were also those that were less than wonderful. The larger rooms begat more serious difficulties imposed by excessive reverberation and long delayed reflections.

Concerts were performed in the famous Crystal Palace designed by Joseph Paxton, which had housed the Great Exhibition of 1851 and was later moved from Hyde Park to Sydenham Hill in 1854. This huge structure was built of glass, supported by a cast iron framework, and became a popular place for weekly band concerts. Occasionally mammoth festival concerts were held there, which, for example, in 1882 played to an audience of nearly 88,000 people using 500 instrumentalists and 4000 choir members (Forsyth, 1985).

Knowledge of the acoustical behavior of rooms had not yet been set out in quantitative form. Successful halls were designed using incremental changes from previously constructed rooms. The frustration of many nineteenth-century architects with acoustics is summarized in the words of Jean Louis Charles Garnier (1825–1898), designer of the Paris Opera House, "I gave myself pains to master this bizarre science [of acoustics] but . . . nowhere did I find a positive rule to guide me; on the contrary, nothing but contradictory statements . . . I must explain that I have adopted no principle, that my plan has been based on no theory, and that I leave success or failure to chance alone . . . like an acrobat who closes his eyes and clings to the ropes of an ascending balloon." (Garnier, 1880)

One of the more interesting theatrical structures to be built in the century, Wagner's opera house, the Festspielhaus in Bayreuth, Germany built in 1876, was a close collaboration between the composer and the architect, Otto Brueckwald, and was designed with a clear intent to accomplish certain acoustical and social goals. The auditorium is rectangular but it contains a fan-shaped seating area with the difference being taken up by a series of double columns supported on wing walls. The plan and section are shown in Fig. 1.16. The seating arrangement in itself was an innovation, since it was the first opera house where there was not a differentiation by class between the boxes and the orchestra seating. The horseshoe shape with layered boxes, which had been the traditional form of Italian opera houses for three centuries, was abandoned for a more egalitarian configuration.

Most unusual, however, was the configuration of the pit, which was deepened and partially covered with a radiused shield that directed some of the orchestral sound back toward the actors. This device muted the orchestral sound heard by the audience, while allowing the musicians to play at full volume out of sight of the audience. It also changed the

FIGURE 1.16   Festspielhaus, Bayreuth, Germany (Beranek, 1979)
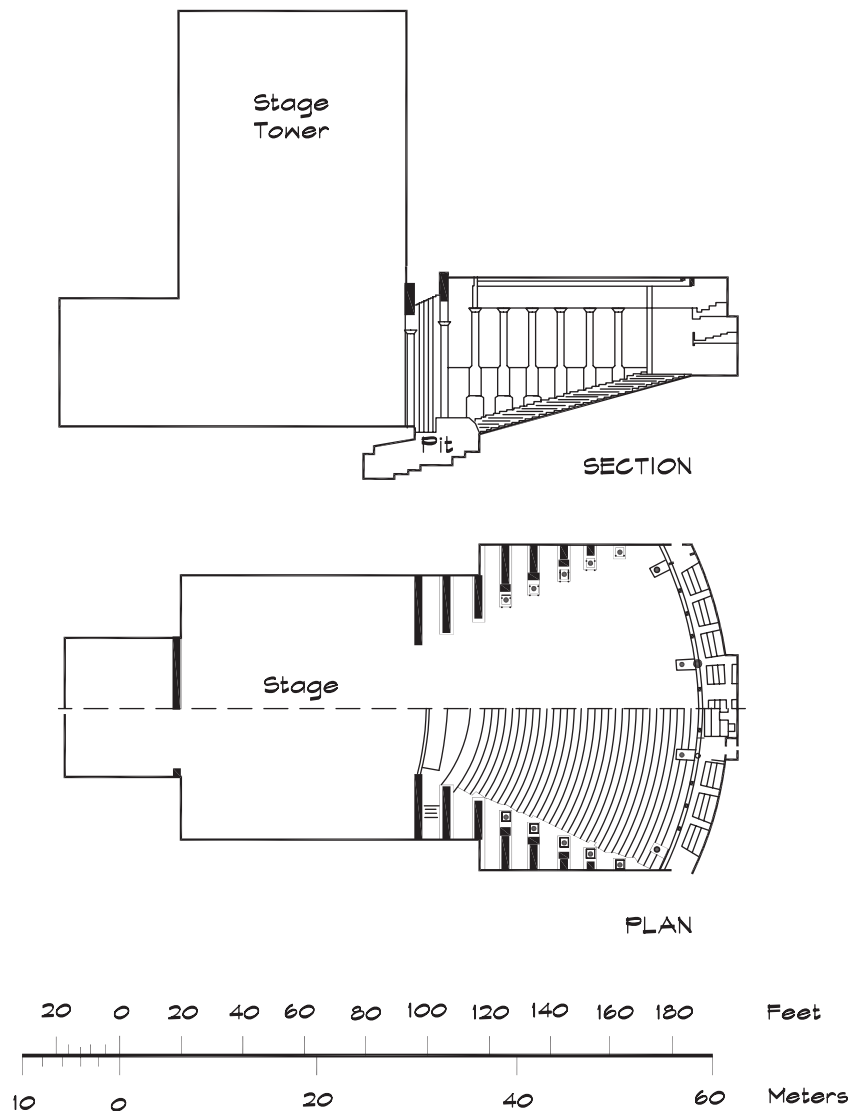
loudness of the strings with respect to the horns, improving the balance between the singers and the orchestra. The reverberation time, at 1.55 seconds (Beranek, 1996), was particularly well suited to Wagner's music, perhaps because he composed pieces to be played here, but the style has not been replicated elsewhere.

Shoebox Halls

Several of the orchestral halls constructed in the late eighteenth and early nineteenth centuries are among the finest ever built. Four of them are particularly noteworthy, both for their fine acoustics and for their influence on later buildings. They are all of the shoebox type with high ceilings, multiple diffusing surfaces, and a relatively low seating capacity. The oldest is the Stadt Casino in Basel, Switzerland, which was completed in 1776. Shown in Fig. 1.17,

FIGURE 1.17   Concert Hall, Stadt Casino, Basel, Switzerland (Beranek, 1979)
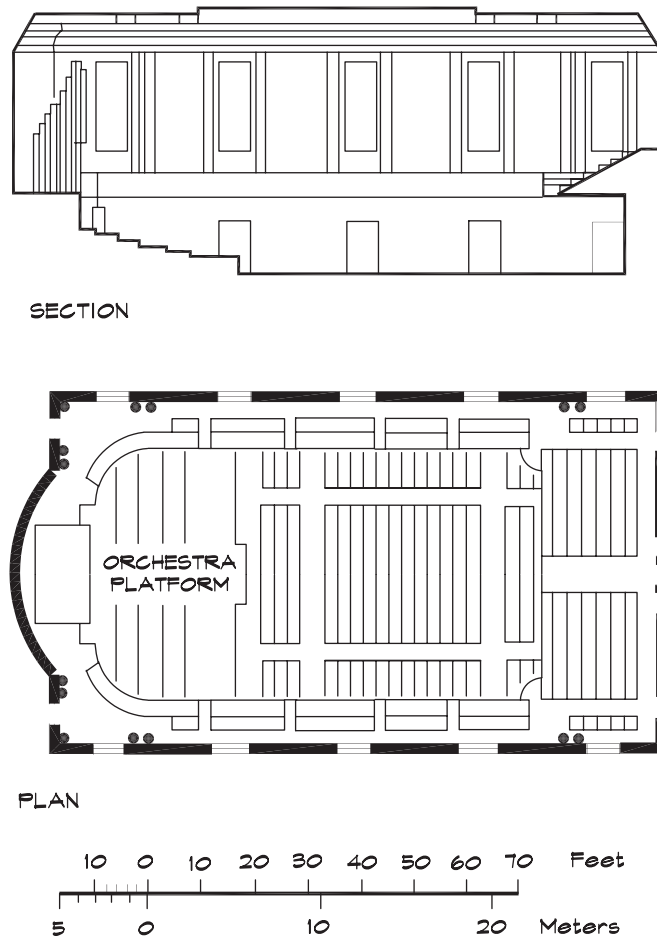
it is very typical of the age with a flat floor reminiscent of the earlier ballrooms, small side and end balconies, and a coffered ceiling. The orchestra was seated on a raised platform with risers extending across its width. Above and to the rear of the orchestra was a large organ. The hall seated 1448 people and had a mid-frequency reverberation time of about 1.8 seconds (Beranek, 1996) making it ideal for Classical and Romantic music.

Ten years later the Neues Gewandhaus was built to provide a larger space for concerts in Leipzig. After it was completed, the old Altes Gewandhaus was torn down. The building was based on a design by the architects Martin K. P. Gropius (1824–1880) and Heinrich Schmieden (1835–1913) and was finally completed in 1882 after Gropius' death, remaining extant until it was destroyed in World War II. A sketch of the hall is shown in Fig. 1.18. Its floor plan is approximately two squares, side by side, measuring 37.8 m (124 ft) by 18.9 m (62 ft) with a 14.9 m (49 ft) high ceiling. The new room housed 1560 in upholstered seats and its reverberation time at 1.55 seconds was less than that of the other three, making it ideal for the works of Bach, Mozart, Haydn, and other Classical chamber music. The upper walls were pierced with arched clerestory windows, looking like the brim of a baseball cap, which let in light and helped to control the bass reverberation. The structural interplay of the

FIGURE 1.18   Neues Gewandhaus, Leipzig, Germany (Beranek, 1979)

SECTION

UPPER BALCONY PLAN

ORCHESTRA, LOWER BALCONY PLAN
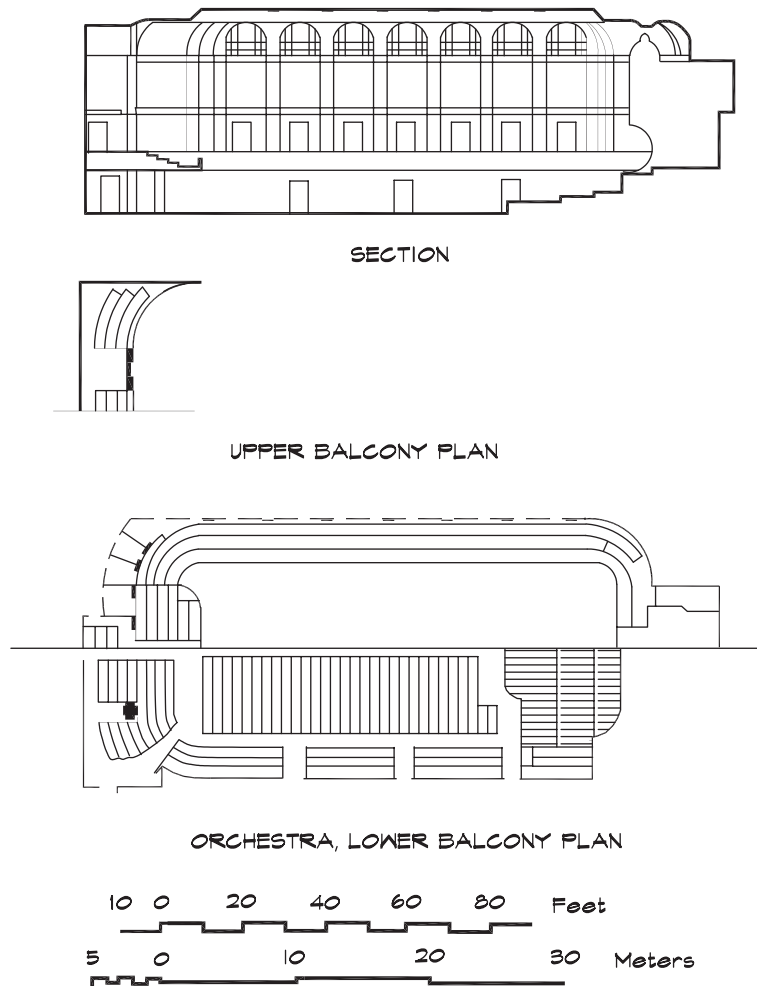
curved transition to the ceiling yielded a highly dramatic form, which, along with three large chandeliers, added diffusion to the space. Like the other halls of this type it had a narrow balcony around its perimeter of about three rows of seating, with a large organ towering over the orchestra.

Grosser Musikvereinssaal (Fig. 1.19) in Vienna, Austria, which is still in use today, is considered one of the top three or four concert halls in the world. It was opened in 1870 and has a long (50.3 m or 185 ft) and narrow (19.8 m or 65 ft) rectangular floor plan with a high (15 m or 50 ft), heavily beamed ceiling. The seating capacity, at 1680 in wooden seats, is relatively small for so long a room.

The single narrow balcony is supported by a row of golden caryatids, much like giant Oscars, around the side of the orchestra seating. Reflections from the underside of the balcony and the statuary are particularly important in offsetting the grazing attenuation due to the audience seated on a flat floor. The high windows above the balcony provided light for afternoon concerts and reduced the bass buildup.

FIGURE 1.19   Grosser Musikvereinssaal, Vienna, Austria (Beranek, 1979)
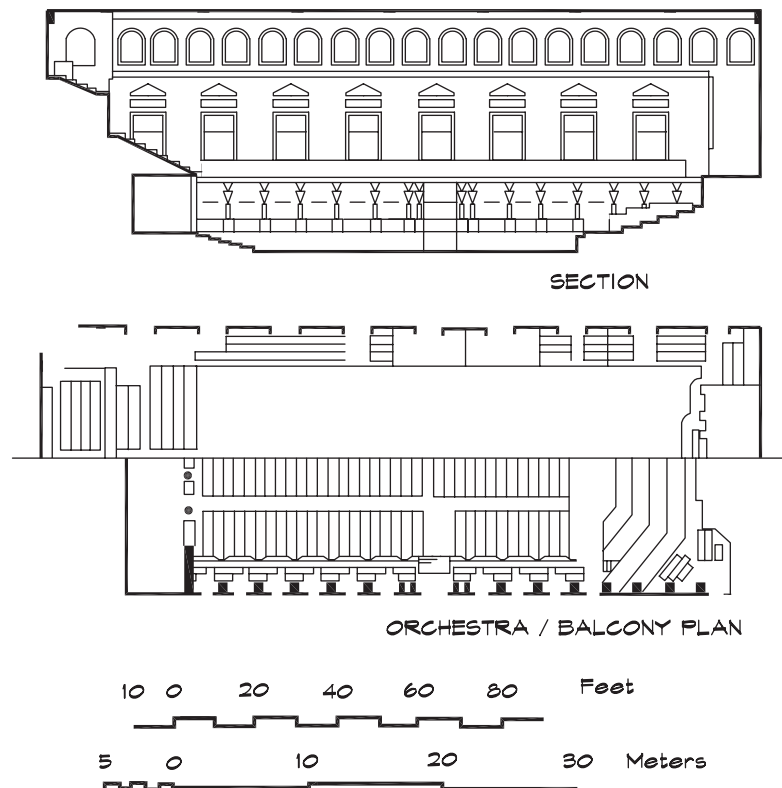
Grosser Musikvereinssaal also was known as the Goldener Saal, since its interior surfaces are covered by meticulously applied paper-thin sheets of gold leaf. The sound in this hall is widely considered ideal for Classical and Romantic music. Its reverberation time is long, just over 2 seconds when fully occupied, and the narrowness of the space provides for strong lateral reflections that surround or envelop the listener in sound. The walls are constructed of thick plaster that supports the bass, and the nearness of the reflecting surfaces and multiple diffusing shapes gives an immediacy and clarity to the high strings. It is this combination of clarity, strong bass, and long reverberation time that is highly prized in concert halls, but rarely achieved.

Concertgebouw in Amsterdam, Netherlands (Fig. 1.20) is the last of the four shoe-box halls. Designed by A. L. Van Gendt, it opened in 1888. Like the others it is rectangular; however, at 29 m (95 ft) it is wider than the other three and seats 2200 people on a flat floor. Consequently it is more reverberant at 2.2 seconds and has somewhat less clarity than Grosser Musikvereinssaal. It is best suited to large-scale Romantic music, providing a live, full, blended tone.

The four halls cited here have similar features that contribute to their excellent acoustics. They are all rectangular and relatively narrow (except in the case of Concertgebouw). The construction is of thick plaster and heavy wood with a deeply coffered ceiling about 15 meters high. The floors are generally flat and the orchestra is seated above the heads of the patrons on a high, raked, wooden platform. The orchestra is located in the same room as the audience rather than being set back into a stage platform. All these rooms are

FIGURE 1.20   Concertgebouw, Amsterdam, Netherlands (Beranek, 1979)
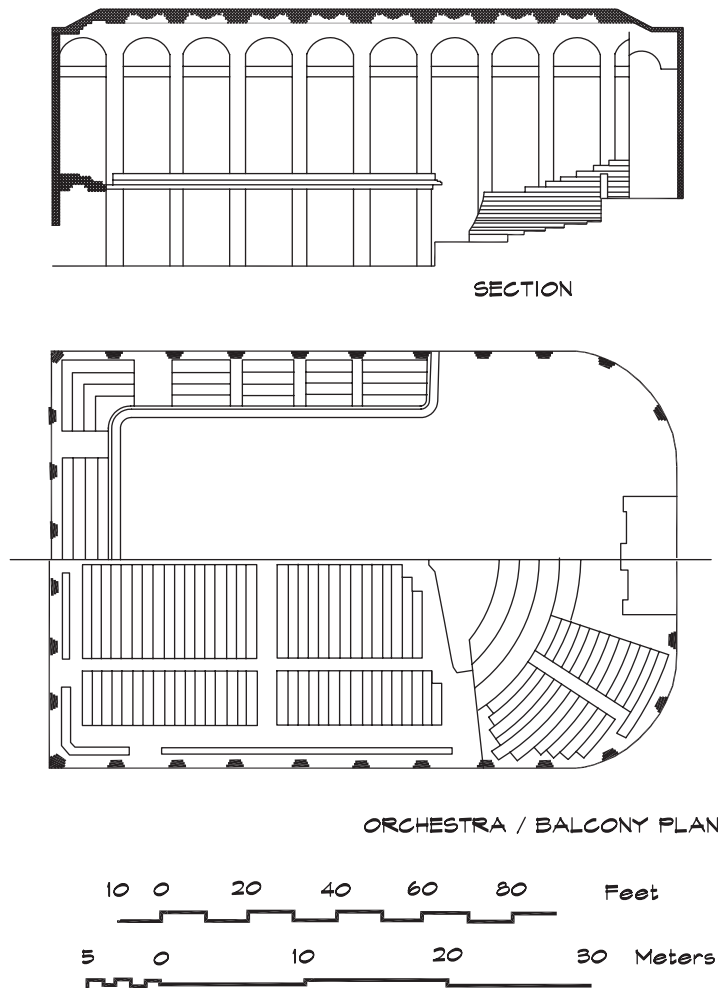
highly ornamented with deep fissures, statuary, recessed windows, organs, and overhanging balconies to help diffuse the sound. They all had highly ornate chandeliers that also scatter the sound.

The capacity of these rooms is not great by modern standards and the seating is tight. No seat is far from a side wall or from the orchestra. The orchestra is backed by a hard reflecting surface to help project the sound, particularly the bass, out to the audience. There is a notable absence of thin wood paneling in these structures. Paneling at one time was considered acoustically desirable in accordance with the hall as a musical instrument theory. These rooms provided excellent acoustics and became the examples to be emulated in the scientific approach to concert hall performance, begun early in the following century.

1.10   BEGINNINGS OF MODERN ACOUSTICS

The nineteenth century produced the beginnings of the study of acoustics as a science and its dissemination in the published literature via technical books and journals. Heretofore scientific ideas had a relatively limited audience and were often distributed through personal

correspondence between leading scholars of the day. Frequently written in Latin they were not generally accessible to the public. In the nineteenth century, books written in English or German, such as Hermann von Helmholtz (1821–1894) *Sensations of Tone* in 1860, established the field as a science where measurement, observation, and a mathematical approach could lead to significant progress. Later in the century (1877) John W. Strutt, Lord Rayleigh published the first of his two-volume set, *Theory of Sound*, followed by the second between 1894 and 1896, which was one of the most important books ever written in the field. In it he pulled together the disparate technical articles of the day and added many valuable contributions of his own. It is remarkable that such a clear presentation of acoustical phenomena was written before careful experimental work was possible. In Rayleigh's time the only practical sound source was a bird whistle (Lindsay, 1966) and the most sensitive detection device (besides the ear) was a gas flame.

About the same time, in the remarkable decade of the 1870s, there was a surge in the development of practical electroacoustic devices. In Germany, Ernst W. Siemens patented in 1874 the moving coil transducer, which eventually led to today's loudspeaker. In 1887 the U.S. Supreme Court held in favor of the patent, originally filed in 1876, and probably the single most valuable patent ever issued, of Alexander Graham Bell (1847–1922) for the telephone. It incorporated the granular carbon microphone, the first practical microphone, and one of the few instruments that is improved by banging it on a table. Within a year (1877), Thomas A. Edison had patented the phonograph and somewhat later, in 1891, motion pictures. Thus within a decade the technical foundation for the telephone, sound recording, music reproduction, and motion-picture industries had been developed.

In the late nineteenth and early twentieth centuries, the theoretical beginnings of architectural acoustics were started by a young physics professor at Harvard College, W. C. Sabine. Sabine's work began inauspiciously enough following a request by president Elliot to "do something" about the acoustical difficulties in the then new Fogg Art Museum auditorium, which had been completed in 1895 (Sabine, 1922). Sabine took a rather broad view of the scope of this mandate and commenced a series of experiments in three Harvard auditoria with the goal of discovering the reasons behind the difficulties in understanding speech. By the time he had completed his work, he had developed the first theory of sound absorption of materials, its relationship to sound decay in rooms, and a formula for the decay (reverberation) time in rooms. His key discovery was that the product of the total absorption and the reverberation time was a constant.

Soon after this discovery in 1898 he helped with the planning of the Boston Music Hall, now called Symphony Hall. He followed the earlier European examples, using a shoebox shape and heavy plaster construction with a modest ceiling height to maintain a reverberation time of 1.8 seconds. Narrow side and rear balconies were used to avoid shadow zones and a shallow stage enclosure, with angled walls and ceiling, directed the orchestra sound out to the audience. The deeply coffered ceiling and wall niches containing classical statuary helped provide excellent diffusion (Hunt, 1964). The auditorium, pictured in Fig. 1.21, opened in 1900 and is still one of the three or four best concert halls in the world.

While the designers of Boston Symphony Hall followed one European design tradition, the designers of New York's Metropolitan Opera House (Fig. 1.22) followed another, that of the Italian opera houses. Opening in 1883 the Met, seating over 3600, is one of the largest opera houses in the world. Despite its size it has reasonably good acoustics in the middle balconies; however, the orchestra seats and the upper balcony seats are less satisfactory (Beranek, 1979). With a volume nearly twice that of La Scalla, it is difficult for singers to sound as loud as in Milan. The hall, with some ceiling and balcony front additions by

FIGURE 1.21   Symphony Hall, Boston, MA, USA (Beranek, 1979)

SECTION

UPPER BALCONY PLAN

ORCHESTRA / LOWER BALCONY PLAN
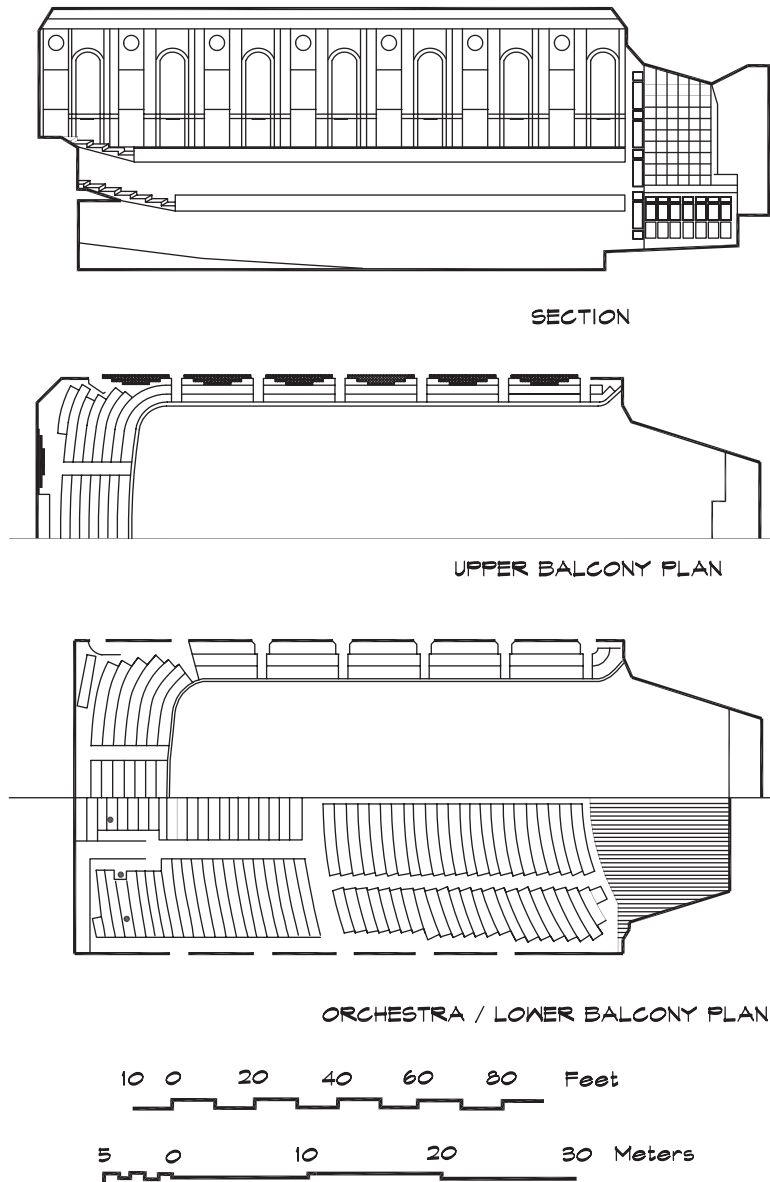
architect Wallace K. Harrison and acousticians Cyril Harris and Vilhelm Jordan to increase diffusion and the sound in the balconies, is in active use today.

Another American hall, constructed around the turn of the century, was Carnegie Hall (Fig. 1.23) in New York. Andrew Carnegie, an entrepreneur and steel baron, was fishing at his vacation home in Scotland with a young American musician, Walter Damrosch, whose father Leopold was director of the New York Symphony Society. The idea to provide a permanent building to house its activities arose while the two were casting in midstream (Forsyth, 1985). The plans were prepared by architect William B. Turnhill and the hall opened in 1891. Carnegie Hall was designed as a shoebox hall but like a theater. The orchestra was

FIGURE 1.22   Metropolitan Opera House, New York, NY, USA (Beranek, 1979)

SECTION

ORCHESTRA / FIRST BALCONY PLAN

| 0 | 20 | 40 | 60 | 80 | Feet |

| 5 | 0 | 10 | 20 | 30 | Meters |
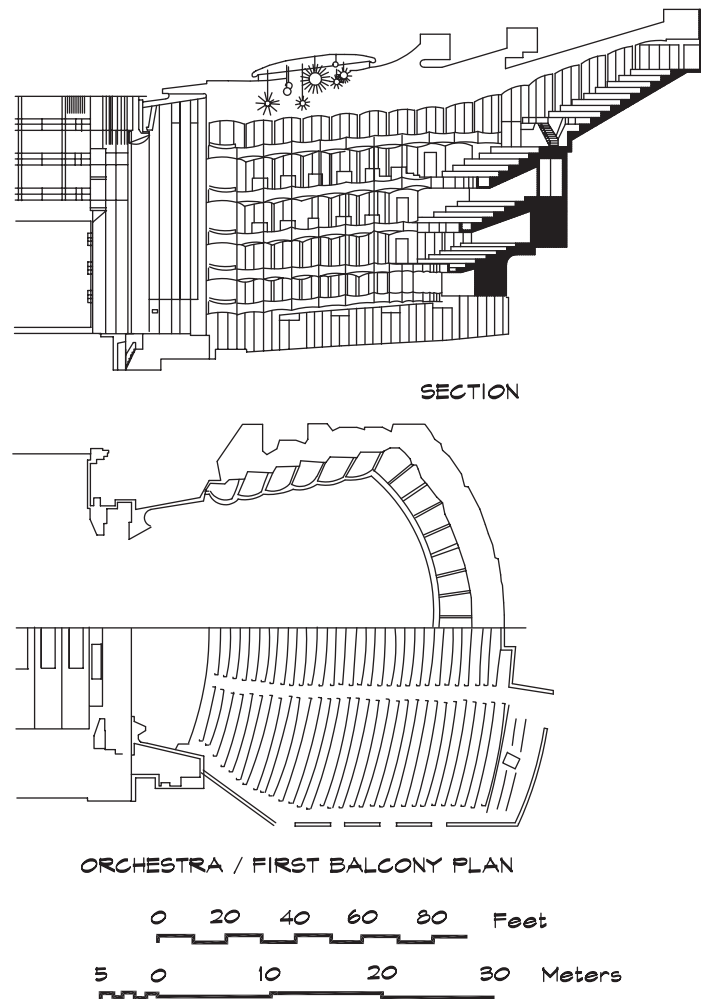
located on stage behind a proscenium arch under a curved orchestra shell. The audience is seated on a nearly flat floor and in four balconies, whose rounded front faces are stacked on an imaginary cylinder. Each balcony flares out into side balconies, which almost reach the stage at the lowest level. Carnegie Hall is known for the clarity of its high frequency sound. At 1.7 seconds it has a slightly dry reverberation with less bass support than in Boston. It was recently refurbished with the stated objective of leaving the acoustical properties unchanged.

1.11   TWENTIETH CENTURY

In the twentieth century, architectural acoustics came to be recognized as a science as well as an art. Although the number and quality of the published works increased, our understanding of many of the principles of acoustical design did not in all cases lead to improvements in concert halls. The more routine aspects of room acoustics, including noise and vibration control and development of effective acoustical materials, experienced marked improvements.

FIGURE 1.23   Carnegie Hall, New York, NY, USA (Beranek, 1979)

SECTION

UPPER BALCONY PLANS

ORCHESTRA / LOWER BALCONY PLAN

10 0   20   40   60   80   Feet

5   0   10   20   30 Meters
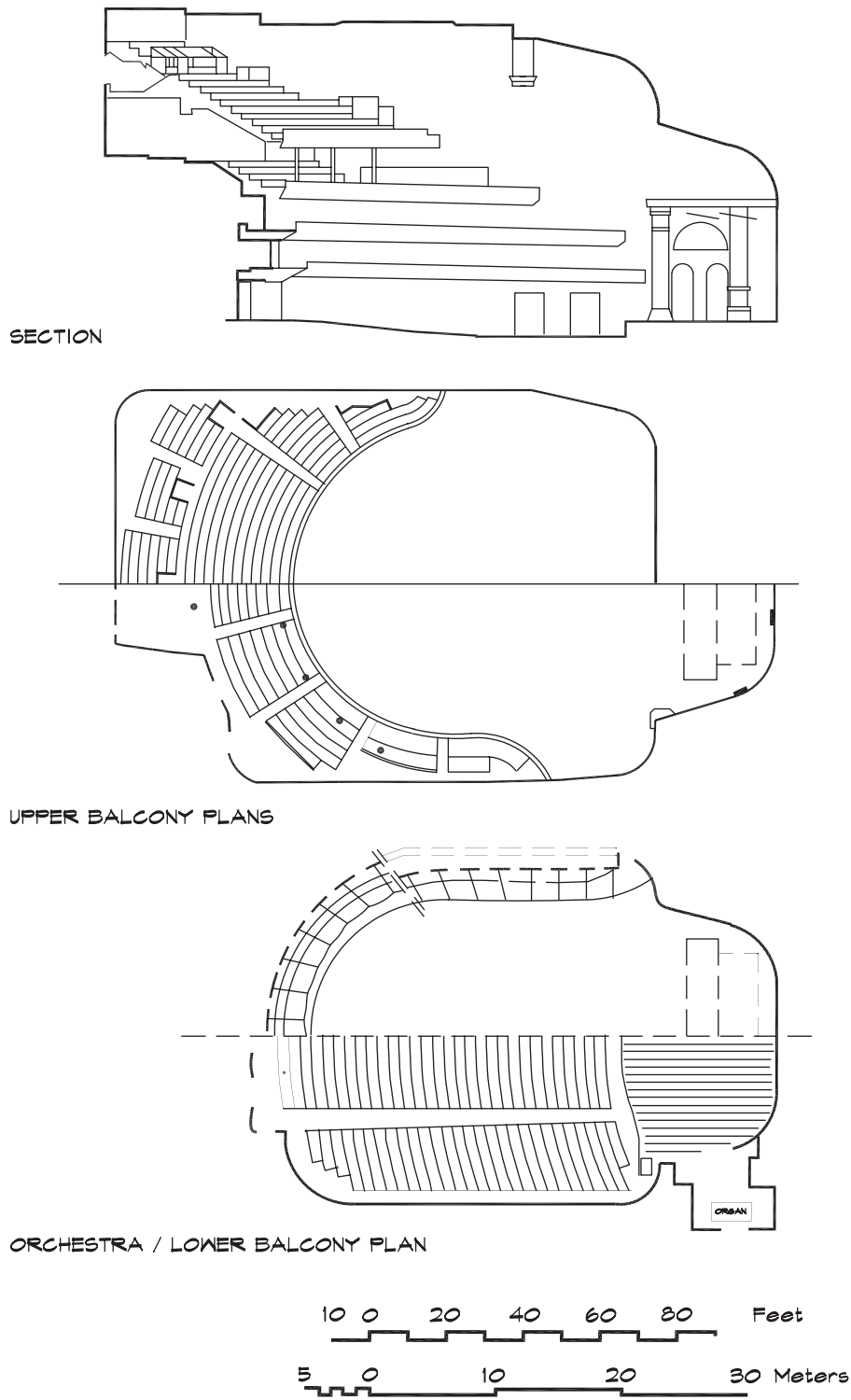
The development of electroacoustic devices including microphones, amplifiers, loudspeakers, and other electronic processing instruments flourished. The precision, which is now available in the ability to record and reproduce sound, has in a sense created an expectation of excellence that is difficult to match in a live performance. The high-frequency response in a hall is never as crisp as in a close-miked recording. The performance space is seldom as quiet as a recording studio. The seats are never as comfortable as in a living room. Ironically, just as we have begun to understand the behavior of concert halls and are able to accurately model their behavior, electroacoustic technology has developed to the point where it may soon provide an equivalent or even superior experience in our homes.

This page intentionally left blank

$$2$$

FUNDAMENTALS
OF
ACOUSTICS

2.1   FREQUENCY AND WAVELENGTH

Frequency

A steady sound is produced by the repeated back and forth movement of an object at regular intervals. The time interval over which the motion recurs is called the *period*. For example if our hearts beat 72 times per minute, the period is the total time (60 seconds) divided by the number of beats (72), which is 0.83 seconds per beat. We can invert the period to obtain the number of complete cycles of motion in one time interval, which is called the *frequency*.

$$f = \frac{1}{T} \tag{2.1}$$

where f = frequency (cycles per second or Hz)
        T = time period per cycle (s)

The frequency is expressed in units of cycles per second, or Hertz (Hz), in honor of the physicist Heinrich Hertz (1857–1894).

Wavelength

Among the earliest sources of musical sounds were instruments made using stretched strings. When a string is plucked it vibrates back and forth and the initial displacement travels in each direction along the string at a given velocity. The time required for the displacement to travel twice the length of the string is

$$T = \frac{2\,L}{c} \tag{2.2}$$

Figure 2.1 Harmonics of a Stretched String (Pierce, 1983)

A

Wavelength = 2L, frequency = f = c/2L

B

Wavelength = L, frequency = 2 f = c/L

C

Wavelength = (2/3)L, frequency = 3 f = 3c/2L

D

Wavelength = (1/2)L, frequency = 4 f = 2c/L
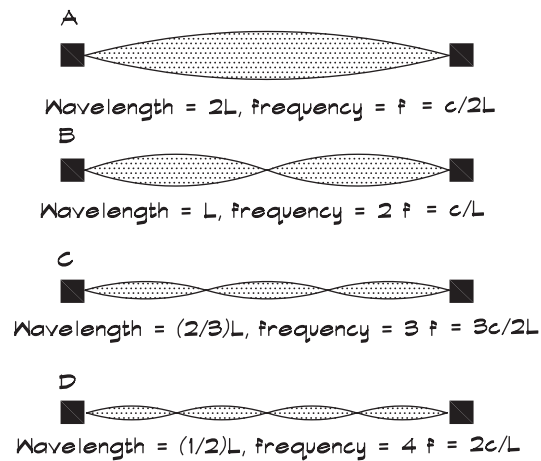
where   T = time period (s)
         L = length of the string (m)
         c = velocity of the wave (m/s)

Since the string is fixed at its end points, the only motion patterns allowed are those that have zero amplitude at the ends. This constraint (called a *boundary condition*) sets the frequencies of vibration that the string will sustain to a fundamental and integer multiples of this frequency, 2f, 3f, 4f, . . . , called *harmonics*. Figure 2.1 shows these vibration patterns.

$$f = \frac{c}{2\,L} \qquad\qquad (2.3)$$

As the string displacement reflects from the terminations, it repeats its motion every two lengths. The distance over which the motion repeats is called the *wavelength*, and is given the Greek symbol lambda, λ, which for the fundamental frequency in a string is 2 L. This leads us to the general relation between the wavelength and the frequency

$$\lambda = \frac{c}{f} \qquad\qquad (2.4)$$

where λ = wavelength (m)
         c = velocity of wave propagation (m/s)
         f = frequency (Hz)

When notes are played on a piano the strings vibrate at specific frequencies, which depend on their length, mass, and tension. Figure 2.2 shows the fundamental frequencies associated with each note. The lowest note has a fundamental frequency of about 27 Hz, while the highest fundamental is 4186 Hz. The frequency ranges spanned by other musical

FIGURE 2.2   Frequency Range of a Piano (Pierce, 1983)
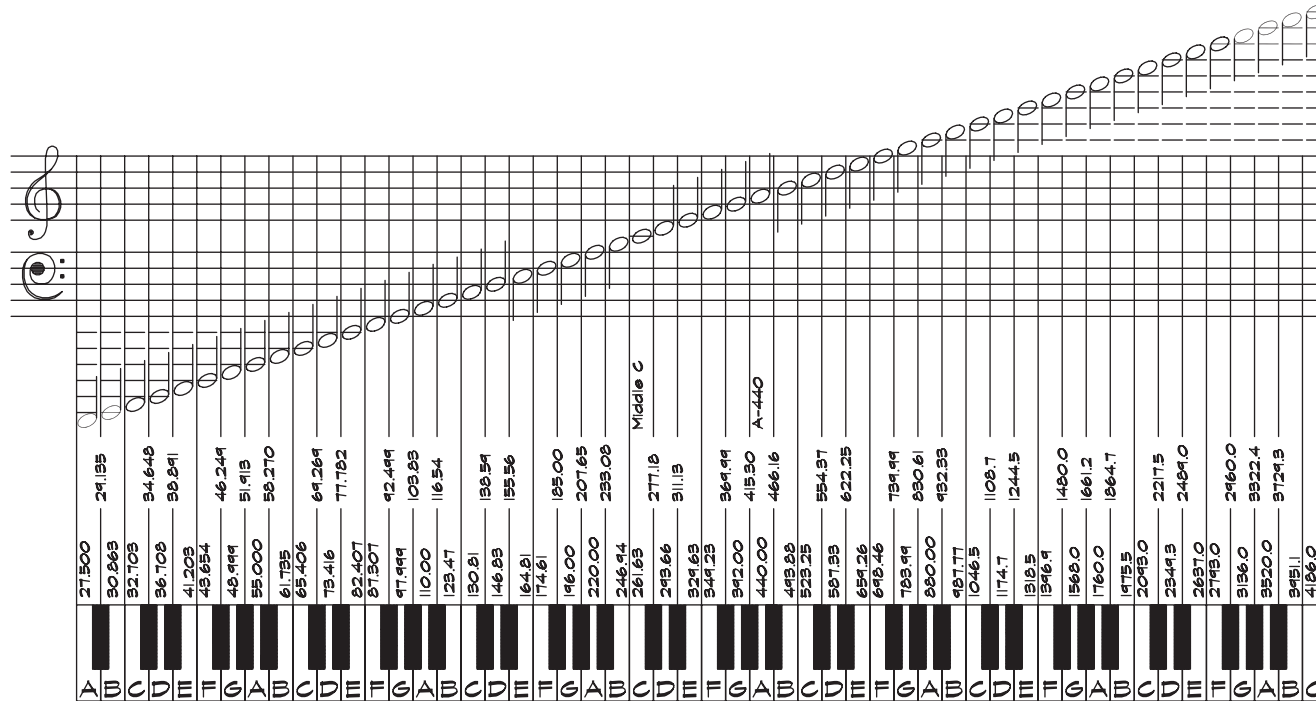
instruments, including the human voice, are given in Fig. 2.3. If a piano string is vibrating at its fundamental mode, the maximum excursion occurs at the middle of the string. When a piano key is played, the hammer does not strike precisely in the center of the string and thus it excites a large number of additional modes. These harmonics contribute to the beauty and complexity of the sound.

Frequency Spectrum

If we were to measure the strength of the sound produced by a particular note and make a plot of sound level versus frequency we would have a graph called a *spectrum*. When the sound has only one frequency, it is called a *pure tone* and its spectrum consists of a single straight line whose height depends on its strength. The spectrum of a piano note, shown in Fig. 2.4, is a line at the fundamental frequency and additional lines at each harmonic frequency. For most notes the fundamental has the highest amplitude, followed by the harmonics in descending order. For piano notes in the lowest octave the second harmonic may have a higher amplitude than the fundamental if the strings are not long enough to sustain the lowest frequency.

Sources such as waterfalls produce sounds at many frequencies, rather than only a few, and yield a flat spectrum. Interestingly an impulsive sound such as a hand clap also yields a flat spectrum. This is so because in order to construct an impulsive sound, we add up a very large number of waves of higher and higher frequencies in such a way that their peaks all occur at one time. At other times they cancel each other out so we are left with just the impulse spike. Since the two forms are equivalent, a sharp impulse generates a large number of waves at different frequencies, which is a flat spectrum. A clap often is used to listen for acoustical defects in rooms.

Electronic signal generators, which produce all frequencies within a given bandwidth, are used as test sources. The most commonly encountered are the pink-noise (equal energy per octave or third octave) or white-noise (equal energy per cycle) generators.

Filters

In analyzing the spectral content of a sound we might use a meter that includes electronic filters to eliminate all signals except those of interest to us. Filters have a center frequency and a bandwidth, which determines the limits of the filter. By international agreement certain standard center frequencies and bandwidths are specified, which are set forth in Table 2.1. The most commonly used filters in architectural acoustics have octave or third-octave bandwidths. Three one-third octaves are contained in each octave, but these do not correspond to any given set of notes. Narrow bandwidth filters, 1/10 octave or even 1 Hz wide, are sometimes used in the study of vibration or the details of reverberant falloff in rooms.

2.2   SIMPLE HARMONIC MOTION

Periodic motions need not be smooth. The beat of a human heart, for example, is periodic but very complicated. It is easiest, however to begin with a simple motion and then to move on to more complicated wave shapes. If we examine the vibration of a stretched string it is quite regular. Such behavior is called simple harmonic motion and can be written in terms of a sinusoidal function.

FIGURE 2.3   Frequency Ranges of Various Musical Instruments (Pierce, 1983)

|HARP|
|ACCORDION|
|GUITAR|
|MARIMBA/XYLOPHONE|
|SOPRANO SAXOPHONE|
|ALTO SAXOPHONE|
|TENOR SAXOPHONE|
|BARITONE SAXOPHONE|
|BASS SAXOPHONE| |PICCOLO|
|SOPRANO CLARINET|
|ALTO CLARINET|
|BASS CLARINET|
|TIMPANI| |OBOE|
|ENGLISH HORN|
|BASSOON|
|CONTRABASS SARRUSOPHONE| |FLUTE|
|CORNET/TRUMPET|
|ALTO MELLOPHONE|
|FRENCH HORN|
|TROMBONE/EUPHONIUM| |CHIMES|
|BASS TUBA|
|VIOLIN|
|VIOLA|
|CELLO|
|BASS| |SOPRANO VOICE|
|ALTO VOICE|
|TENOR VOICE|
|BARITONE VOICE|
|BASS VOICE|

32   63   125   250   500   1 K   2 K   4 K

FREQUENCY, Hz

FIGURE 2.4   Frequency Spectrum of a Piano Note
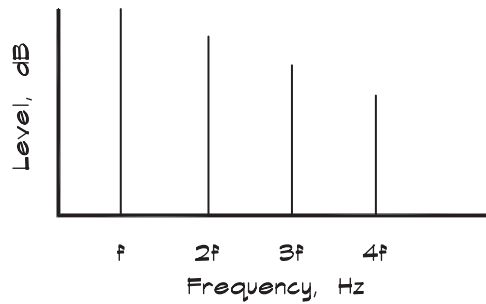
TABLE 2.1   Octave and Third-Octave Band Frequency Limits

Band	Frequency, Hz Octave Lower Limit	Octave Center	Octave Upper Limit	One-third Octave Lower Limit	One-third Octave Center	One-third Octave Upper Limit
12	11	16	22	14.1	16	17.8
13				17.8	20	22.4
14				22.4	25	28.2
15	22	31.5	44	28.2	31.5	35.5
16				35.5	40	44.7
17				44.7	50	56.2
18	44	63	88	56.2	63	70.8
19				70.8	80	89.1
20				89.1	100	112
21	88	125	177	112	125	141
22				141	160	178
23				178	200	224
24	177	250	355	224	250	282
25				282	315	355
26				355	400	447
27	355	500	710	447	500	562
28				562	630	708
29				708	800	891
30	710	1,000	1,420	891	1,000	1,122
31				1,122	1,250	1,413
32				1,413	1,600	1,778
33	1,420	2,000	2,840	1,778	2,000	2,239
34				2,239	2,500	2,818
35				2,818	3,150	3,548
36	2,840	4,000	5,680	3,548	4,000	4,467
37				4,467	5,000	5,623
38				5,623	6,300	7,079
39	5,680	8,000	11,360	7,079	8,000	8,913
40				8,913	10,000	11,220
41				11,220	12,500	14,130
42	11,360	16,000	22,720	14,130	16,000	17,780
43				17,780	20,000	22,390

FIGURE 2.5   Vector Representation of Circular Functions
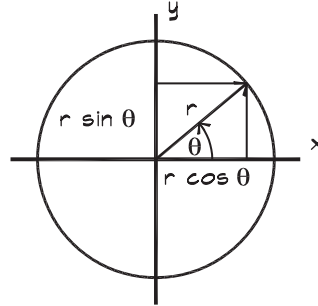
Vector Representation

Sinusoidal waveforms are components of circular motion. In Fig. 2.5 we start with a circle whose center lies at the origin, and draw a radius at some angle θ to the x (horizontal) axis. The angle *theta* can be measured using any convenient fractional part of a circle. One such fraction is 1/360 of the total angle, which defines the unit called a *degree*. Another unit is $1/2\pi$ of the total angle. This quantity is the ratio of the radius to the circumference of a circle and defines the *radian* (about 57.3°). It was one of the Holy Grails of ancient mathematics since it contains the value of π.

In a circle the triangle formed by the radius and its x and y components defines the trigonometric relations for the sine

$$y = r \sin \theta \tag{2.5}$$

and cosine functions

$$x = r \cos \theta \tag{2.6}$$

The cosine is the x-axis projection and the sine the y-axis projection of the radius vector. If we were to rotate the coordinate axes counterclockwise a quarter turn, the x axis would become the y axis. This illustrates the simple relationship between the sine and cosine functions

$$\cos \theta = \sin \left(\theta + \frac{\pi}{2} \right) \tag{2.7}$$

The Complex Plane

We can also express the radius of the circle as a vector that has x and y components by writing

$$\mathbf{r} = \mathbf{i} \, x + \mathbf{j} \, y \tag{2.8}$$

where $\mathbf{i}$ and $\mathbf{j}$ are the unit vectors along the x and y axes. If instead we define x as the displacement along the x axis and j y as the displacement along the y axis, then the vector can be written

$$\mathbf{r} = x + j \, y \tag{2.9}$$

We can drop the formal vector notation and just write the components, with the understanding that they represent displacements along different axes that are differentiated by the

presence or absence of the j term.

$$r = x + j\,y \tag{2.10}$$

The factor j has very interesting properties. To construct the element j y, we measure a distance y along the x axis and rotate it 90° counterclockwise so that it ends up aligned with the y axis. Thus the act of multiplying by j, in this space, is equivalent to a 90° rotation. Since two 90° rotations leave the negative of the original vector

$$j^2 = -1 \tag{2.11}$$

and

$$j = \pm\sqrt{-1} \tag{2.12}$$

which defines j as the fundamental complex number. Traditionally, we use the positive value of j.

The Complex Exponential

The system of complex numbers, although nonintuitive at first, yields enormous benefits by simplifying the mathematics of oscillating functions. The exponential function, where the exponent is imaginary, is the critical component of this process. We can link the sinusoidal and exponential functions through their Taylor series expansions

$$\sin\,\theta = \theta - \frac{\theta^3}{3\,!} + \frac{\theta^5}{5\,!} + \cdots \tag{2.13}$$

and

$$\cos\,\theta = 1 - \frac{\theta^2}{2\,!} + \frac{\theta^4}{4\,!} + \cdots \tag{2.14}$$

and examine the series expansion for the combination $\cos\,\theta + j\,\sin\,\theta$

$$\cos\,\theta + j\,\sin\,\theta = 1 + j\,\theta - \frac{\theta^2}{2\,!} - j\,\frac{\theta^3}{3\,!} + \frac{\theta^4}{4\,!} + \cdots \tag{2.15}$$

which can be rewritten as

$$\cos\,\theta + j\sin\,\theta = 1 + j\,\theta + \frac{(j\,\theta)^2}{2\,!} + \frac{(j\,\theta)^3}{3\,!} + \frac{(j\,\theta)^4}{4\,!} + \cdots \tag{2.16}$$

This sequence is also the series expansion for the exponential function $e^{j\,\theta}$, and thus we obtain the remarkable relationship originally discovered by Leonhard Euler in 1748

$$e^{j\,\theta} = \cos\,\theta + j\sin\,\theta \tag{2.17}$$

Figure 2.6   Rotating Vector Representation of Harmonic Motion
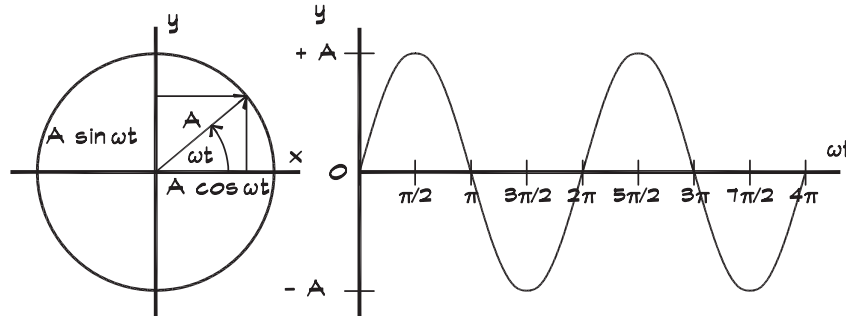
Using the geometry in Fig. 2.6 we see that the exponential function is another way of representing the radius vector in the complex plane. Multiplication by the exponential function generates a rotation of a vector, represented by a complex number, through the angle θ.

Radial Frequency

If the angle θ increases with time at a steady rate, as in Fig. 2.6, according to the relationship

$$\theta = \omega\,t + \phi \tag{2.18}$$

the radius vector spins around counterclockwise from some beginning angular position ϕ (called the *initial phase*). The rate at which it spins is the radial frequency ω, which is the angle θ divided by the time t, starting at $\phi = 0$. Omega (ω) has units of radians per second. As the vector rotates around the circle, it passes through vertical ($\theta = \pi/2$) and then back to the horizontal ($\theta = \pi$) . When it is pointed straight down, θ is $3\,\pi/2$, and when it has made a full circle, then θ is $2\,\pi$ or zero again.

The real part of the vector is a cosine function

$$x = A\cos(\omega\,t + \phi) \tag{2.19}$$

where x, which is the value of the function at any time t, is dependent on the amplitude A, the radial frequency ω, the time t, and the initial phase angle ϕ. Its values vary from $-A$ to $+A$ and repeat every $2\,\pi$ radians.

Since there are $2\,\pi$ radians per complete rotation, the frequency of oscillation is

$$f = \frac{\omega}{2\,\pi} \tag{2.20}$$

where   f = frequency (Hz)
        ω = radial frequency (rad / s)

FIGURE 2.7   Sine Wave in Time and Phase Space
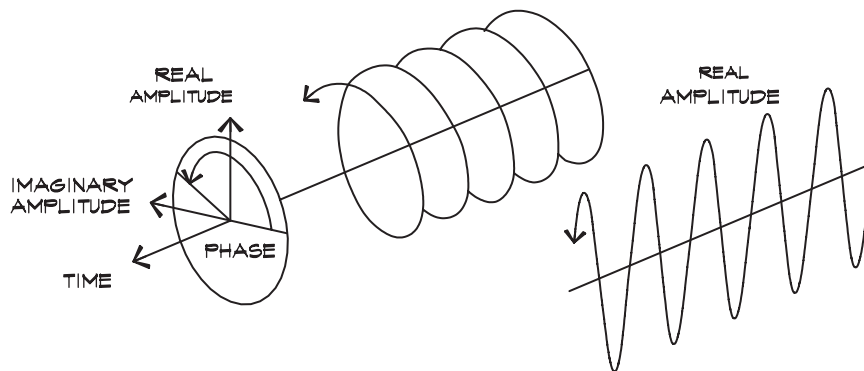
It is good practice to check an equation's units for consistency.

$$\text{frequency} = \text{cycles/sec} = \frac{(\text{radians/sec})}{(\text{radians/cycle})} \tag{2.21}$$

Figure 2.7 shows another way of looking at the time behavior of a rotating vector. It can be thought of as an auger boring its way through phase space. If we look at the auger from the side, we see the sinusoidal trace of the passage of its real amplitude. If we look at it end on, we see the rotation of its radius vector and the circular progression of its phase angle.

Changes in Phase

If a second waveform is drawn on our graph in Fig. 2.8 immediately below the first, we can compare the two by examining their values at any particular time. If they have the same frequency, their peaks and valleys will occur at the same intervals. If, in addition, their peaks occur at the same time, they are said to be in phase, and if not, they are out of phase. A difference in phase is illustrated by a movement of one waveform relative to the other in space or time. For example, a $\pi/2$ radian (90°) phase shift slides the second wave to the right in time, so that its zero crossing is aligned with the peak of the first wave. The second wave is then a sine function, as we found in Eq. 2.6.

2.3   SUPERPOSITION OF WAVES

Linear Superposition

Sometimes a sound is a pure sinusoidal tone, but more often it is a combination of many tones. Even the simple dial tone on a telephone is the sum of two single frequency tones, 350 and 440 Hz. Our daily acoustical environment is quite complicated, with a myriad of sounds striking our ear drums at any one time. One reason we can interpret these sounds is that they add together in a linear way without creating appreciable distortion.

In architectural acoustics, the wave motions we encounter are generally linear; the displacements are small and forces and displacements can be related by a constant. Algebraically it is an equation called Hooke's law, which when plotted yields a straight line—hence the term linear. When several waves occur simultaneously, the total pressure or displacement amplitude is the sum of their values at any one time. This behavior is referred

FIGURE 2.8   Two Sinusoids 90° Out of Phase
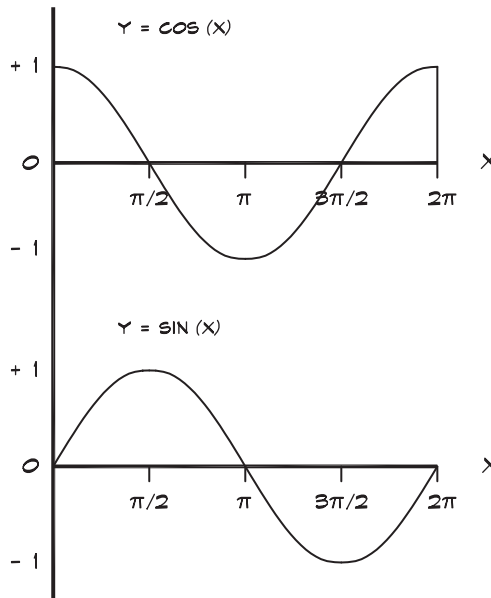
to as a linear superposition of waves and is most useful, since it means that we can construct quite complicated periodic wave shapes by adding up contributions from many different sine and cosine functions.

Figure 2.9 shows an example of the addition of two waves having the same frequency but a different phase. The result is still a simple sinusoidal function, but the amplitude depends on the phase relationship between the two signals. If the two waves are

$$x_1 = A_1 \cos(\omega t + \phi_1) \tag{2.22}$$

and

$$x_2 = A_2 \cos(\omega t + \phi_2) \tag{2.23}$$

FIGURE 2.9   The Resultant of Two Complex Vectors of Equal Frequency
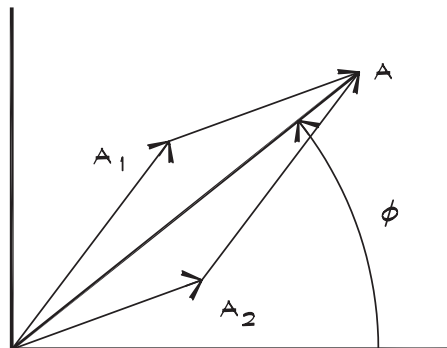
FIGURE 2.10   Sum of Two Sine Waves Having the Same Frequency but Different Phase
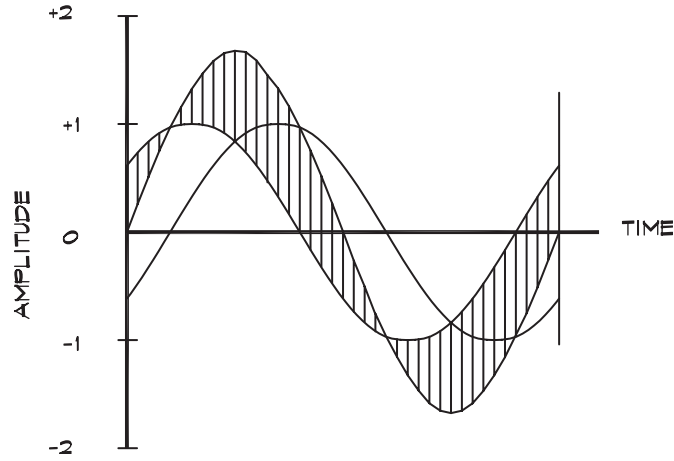
Adding the two together yields

$$x_1 + x_2 = A_1 \cos\left(\omega\, t + \phi_1\right) + A_2 \cos\left(\omega\, t + \phi_2\right) \qquad (2.24)$$

The combination of these two waves can be written as a single wave.

$$x = A \cos\left(\omega\, t + \phi\right) \qquad (2.25)$$

Figure 2.9 shows how the overall amplitude is determined. The first radius vector drawn from the origin and then a second wave is introduced. Its rotation vector is attached to the end of the first vector. If the two are in phase, the composite vector is a single straight line, and the amplitude is the arithmetic sum of $A_1 + A_2$. When there is a phase difference, and the second vector makes an angle ϕ_2 to the horizontal, the resulting amplitude can be calculated using a bit of geometry

$$A = \sqrt{\left(A_1 \cos\phi_1 + A_2 \cos\phi_2\right)^2 + \left(A_1 \sin\phi_1 + A_2 \sin\phi_2\right)^2} \qquad (2.26)$$

and the overall phase angle for the amplitude vector A is

$$\tan\phi = \frac{A_1 \sin\phi_1 + A_2 \sin\phi_2}{A_1 \cos\phi_1 + A_2 \cos\phi_2} \qquad (2.27)$$

Thus superimposed waves combine in a purely additive way. We could have added the wave forms on a point-by-point basis (Fig. 2.10) to obtain the same results, but the mathematical result is much more general and useful.

Beats

When two waves having different frequencies are superimposed, there is no one constant phase difference between them. If they start with some initial phase difference, it quickly becomes meaningless as the radius vectors precess at different rates (Fig. 2.11).

FIGURE 2.11   Two Complex Vectors (Feynman et al., 1989)

The resultant of two complex vectors of unequal frequencies, as seen in the frame of reference of one vector. The composite is shown for positions 1, 5, and 9.
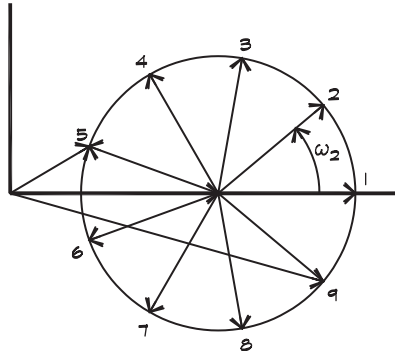
FIGURE 2.12   The Sum of Two Sine Waves with Widely Differing Frequencies
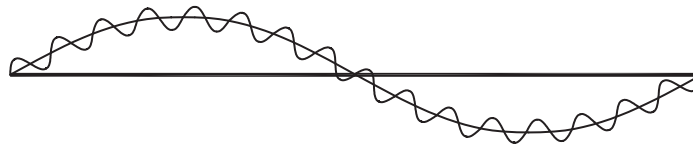
If they both start at zero, then

$$x_1 = A_1 \cos\left(\omega_1\, t\right) \tag{2.28}$$

and

$$x_2 = A_2 \cos\left(\omega_2\, t\right) \tag{2.29}$$

The combination of these two signals is shown in Fig. 2.12. Here the two frequencies are relatively far apart and the higher frequency signal seems to ride on top of the lower frequency. When the amplitudes are the same, the sum of the two waves is[1]

$$x = 2\,A \cos\left[\frac{\left(\omega_1 - \omega_2\right)}{2}\right] \cos\left[\frac{\left(\omega_1 + \omega_2\right)}{2}\right] \tag{2.30}$$

If the two frequencies are close together, a phenomenon known as beats occurs. Since one-half the difference frequency is small, it modulates the amplitude of one-half the sum frequency. Figure 2.13 shows this effect. We hear the increase and decrease in signal strength of sound, which is sometimes more annoying than a continuous sound. In practice, beats

---

[1] The following trigonometric functions were used:
$\cos\left(\theta + \varphi\right) = \cos\theta\cos\varphi - \sin\theta\sin\varphi$
$\cos\left(\theta - \varphi\right) = \cos\theta\cos\varphi + \sin\theta\sin\varphi$

FIGURE 2.13   The Phenomenon of Beats

Beats are created when two sine waves having nearly the same frequency are combined.
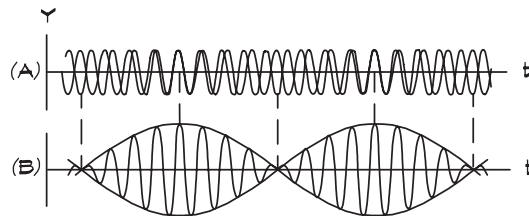
are encountered when two fans or pumps, nominally driven at the same rpm, are located physically close together, sometimes feeding the same duct or pipe in a building. The sound waxes and wanes in a regular pattern. If the two sources have frequencies that vary only slightly, the phenomenon can extend over periods of several minutes or more.

2.4   SOUND WAVES

Pressure Fluctuations

A sound wave is a longitudinal pressure fluctuation that moves through an elastic medium. It is called longitudinal because the particle motion is in the same direction as the wave propagation. If the displacement is at right angles to the direction of propagation, as is the case with a stretched string, the wave is called transverse. The medium can be a gas, liquid, or solid, though in our everyday experience we most frequently hear sounds transmitted through the air. Our ears drums are set into motion by these minute changes in pressure and they in turn help create the electrical impulses in the brain that are interpreted as sound. The ancient conundrum of whether a tree falling in a forest produces a sound, when no one hears it, is really only an etymological problem. A sound is produced because there is a pressure wave, but a noise, which requires a subjective judgment and thus a listener, is not.

Sound Generation

All sound is produced by the motion of a source. When a piston, such as a loudspeaker, moves into a volume of air, it produces a local area of density and pressure that is slightly higher than the average density and pressure. This new condition propagates throughout the surrounding space and can be detected by the ear or by a microphone.

When the piston displacement is very small (less than the mean free path between molecular collisions), the molecules absorb the motion without hitting other molecules or transferring energy to them and there is no sound. Likewise if the source moves very slowly, air flows gently around it, continuously equalizing the pressure, and again no sound is created (Ingard, 1994). However, if the motion of the piston is large and sufficiently rapid that there is not enough time for flow to occur, the movement forces nearby molecules together, locally compressing the air and producing a region of higher pressure. What creates sound is the motion of an object that is large enough and fast enough that it induces a localized compression of the gas.

Air molecules that are compressed by the piston rush away from the high-pressure area and carry this additional momentum to the adjacent molecules. If the piston moves back and forth a wave is propagated by small out-and-back movements of each successive volume

element in the direction of propagation, which transfer energy through alternations of high pressure and low velocity with low pressure and high velocity. It is the material properties of mass and elasticity that ensure the propagation of the wave.

As a wave propagates through a medium such as air, the particles oscillate back and forth when the wave passes. We can write an equation for the functional behavior of the displacement y of a small volume of air away from its equilibrium position, caused by a wave moving along the positive x axis (to the right) at some velocity c.

$$y = f(x - c\,t) \tag{2.31}$$

Implicit in this equation is the notion that the displacement, or any other property of the wave, will be the same for a given value of (x − c t). If the wave is sinusoidal then

$$y = A \sin\left[k\,(x - c\,t)\right] \tag{2.32}$$

where k is called the wave number and has units of radians per length. By comparison to Eq. 2.19 the term (k c) is equal to the *radial frequency* omega.

$$k = \frac{2\,\pi}{\lambda} = \frac{\omega}{c} \tag{2.33}$$

Wavelength of Sound

The wavelength of a sound wave is a particularly important measure. Much of the behavior of a sound wave relates to the wavelength, so that it becomes the scale by which we judge the physical size of objects. For example, sound will scatter (bounce) off a flat object that is several wavelengths long in a specular (mirror-like) manner. If the object is much smaller than a wavelength, the sound will simply flow around it as if it were not there. If we observe the behavior of water waves we can clearly see this behavior. Ocean waves will pass by small rocks in their path with little change, but will reflect off a long breakwater or similar barrier.

Figure 2.14 shows typical values of the wavelength of sound in air at various frequencies. At 1000 Hz, which is in the middle of the speech frequency range, the wavelength is about 0.3 m (1 ft) while for the lowest note on the piano the wavelength is about 13 m (42 ft). The lowest note on a large pipe organ might be produced by a 10 m (32 ft) pipe that is half the wavelength of the note. The highest frequency audible to humans is about 20,000 Hz and has a wavelength of around half an inch. Bats, which use echolocation to find their prey, must transmit frequencies as high as 100,000 Hz to scatter off a 2 mm (0.1 in) mosquito.

Velocity of Sound

The mathematical description of the changes in pressure and density induced by a sound wave, which is called the wave equation, requires that certain assumptions be made about the medium. In general we examine an element of volume (say a cube) small enough to smoothly represent the local changes in pressure and density, but large enough to contain very many molecules. When we mathematically describe physical phenomena created by a sound wave, we are talking about the average properties associated with such a small volume element.

FIGURE 2.14   Wavelength vs Frequency in Air at 20° C (68° F) (Harris, 1991)

WAVELENGTH (FT)

| 100 | 50 | 20 | 10 | 5 | 2 | 1 | 0.5 | 0.2 | 0.1 |

| 10 | 20 | 50 | 100 | 200 | 500 | 1000 | 5000 | 10,000 |

FREQUENCY (HZ)

WAVELENGTH (M)

| 20 | 10 | 5 | 2 | 1 | 0.5 | 0.1 | 0.05 |

| 10 | 20 | 50 | 100 | 200 | 500 | 1000 | 5000 | 10,000 |

FREQUENCY (HZ)
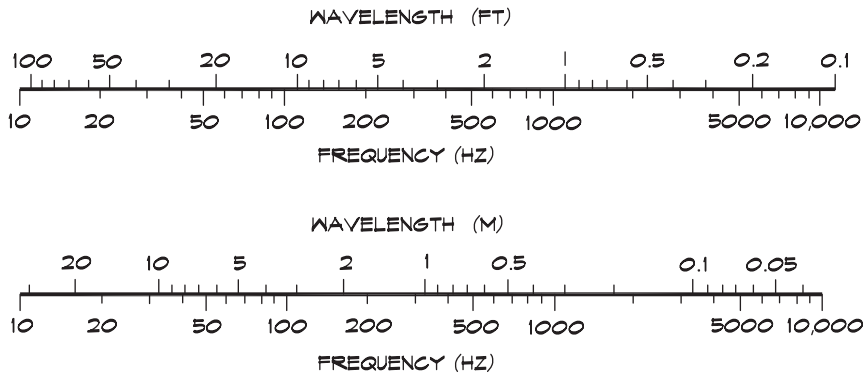
Let us construct (following Halliday and Resnick, 1966), a one-dimensional tube and set a piston into motion with a short stroke that moves to the right and then stops. The compressed area will move away from the piston with a velocity c. In order to study the pulse's behavior it is convenient to ride along with it. Then the fluid appears to be moving to the left at the sound velocity c. As the fluid stream approaches our pulse, it encounters a region of higher pressure and is decelerated to some velocity $c - \Delta c$. At the back (left) end of the pulse, the fluid is accelerated by the pressure differential to its original velocity, c.

If we examine the behavior of a small element (slice) of fluid such as that shown in Fig. 2.15, as it enters the compressed area, it experiences a force

$$F = (P + \Delta P)S - PS \tag{2.34}$$

where S is the area of the tube. The length of the element just before it encountered our pulse was $c \, \Delta t$, where Δt is the time that it takes for the element to pass a point. The volume of the element is $c \, S \, \Delta t$ and it has mass $\rho \, c \, S \, \Delta t$, where ρ is the density of the fluid outside the pulse zone. When the fluid passes into our compressed area, it experiences a deceleration

FIGURE 2.15   Motion of a Pressure Pulse (Halliday and Resnick, 1966)

A high pressure region moving along a tube from left to right. The frame of reference is riding along with the pulse and thus the fluid appears to be moving from right to left. Note that Δc is negative.
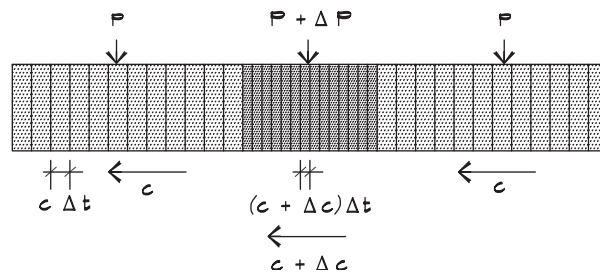
equal to $-\Delta c/\Delta t$. Using Newton's law to relate the force and the acceleration

$$F = m\, a \tag{2.35}$$

which can be written as

$$\Delta P\, S = (\rho\, S\, c\, \Delta t)\, (-\Delta c/\Delta t) \tag{2.36}$$

and rearranged to be

$$\rho\, c^2 = \frac{\Delta P}{(\Delta c/c)} \tag{2.37}$$

Now the fluid that entered the compressed area had a volume $V = S\, c\, \Delta t$ and was compressed by an amount $S\, \Delta c\, \Delta t = \Delta V$. The change in volume divided by the volume is

$$\frac{\Delta V}{V} = \frac{S\, \Delta c\, \Delta t}{S\, c\, \Delta t} = \frac{\Delta c}{c} \tag{2.38}$$

so

$$\rho\, c^2 = -\frac{\Delta P}{(\Delta V/V)} \tag{2.39}$$

Thus, we have related the velocity of sound to the physical properties of a fluid. The right-hand side of Eq. 2.39 is a measurable quantity called the *bulk modulus*, B. Using this symbol the velocity of sound is

$$c = \sqrt{\frac{B}{\rho}} \tag{2.40}$$

where   c = velocity of sound (m /s)
         B = bulk modulus of the medium (Pa)

   ρ = density of the medium (kg/m^3)
         which for air = 1.21 kg/m^3

The bulk modulus can be measured or can be calculated from an equation of state, which relates the behavior of the pressure, density, and temperature in a gas. In a sound wave, changes in pressure and density happen so quickly that there is little time for heat transfer to take place. Processes thus constrained are called *adiabatic*, meaning no heat flow. The appropriate form of the equation of state for air under these conditions is

$$P\, V^\gamma = \text{constant} \tag{2.41}$$

where   P = equilibrium (atmospheric) pressure (Pa)
         V = equilibrium volume (m^3)
         γ = ratio of specific heats (1.4 in air)

Under adiabatic conditions the bulk modulus is γ P, so the speed of sound is

$$c = \sqrt{\gamma \, P / \rho_0} \qquad\qquad (2.42)$$

Using the relationship known as Boyle's Law (P V $=$ μR T where μ is the number of moles of the gas and R $=$ 8.314 joules/mole °K is the gas constant), the velocity of sound in air (which in this text is given the symbol c_0) can be shown to be

$$c_0 = 20.05 \sqrt{T_C + 273.2} \qquad\qquad (2.43)$$

where T_C is the temperature in degrees centigrade. In FP (foot-pound) units the result is

$$c_0 = 49.03 \sqrt{T_F + 459.7} \qquad\qquad (2.44)$$

where T_F is the temperature in degrees Fahrenheit.

Table 2.2 shows the velocity of longitudinal waves for various materials. It turns out that the velocities in gasses are relatively close to the velocity of molecular motion due to thermal excitation. This is a reasonable result since the sound pressure changes are transmitted by the movement of molecules.

TABLE 2.2   Speed of Sound in Various Materials (Beranek and Ver, 1992; Kinsler and Frey, 1962)

Material	Density	Speed of Sound (Longitudinal)	
	(kg/m^3)	(m/s)	(ft/s)
Air @ 0° C	1.293	331	1086
Air @ 20° C	1.21	344	1128
Hydrogen @ 0° C	0.09	1286	4220
Oxygen @ 0° C	1.43	317	1040
Steam @ 100° C	0.6	405	1328
Water @ 15° C	998	1450	4756
Lead	11300	1230	4034
Aluminum	2700	5100	16700
Copper	8900	3560	11700
Iron (Bar)	7700	5130	16800
Steel (Bar)	7700	5050	16600
Glass (Rod)	2500	5200	17000
Oak (Bulk)	720	4000	13100
Pine (Bulk)	450	3500	11500
Fir Timber	550	3800	12500
Concrete (Dense)	2300	3400	11200
Gypsum board (1/2" to 2")	650	6800	22300
Cork	240	500	1640
Granite	—	6000	19700
Vulcanized rubber	1100	54	177

Figure 2.16   Shapes of Various Wave Types

(a) Quasi-longitudinal wave
     (transverse displacements exaggerated)

(b) Transverse shear wave

(c) Flexural (bending) wave

(d) Torsional wave
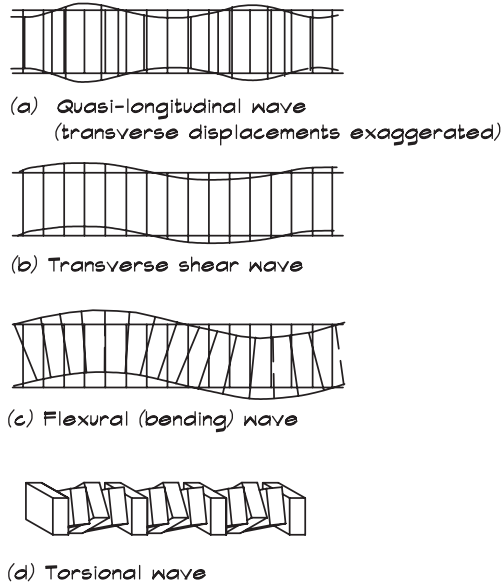
Waves in Other Materials

Sound waves in gasses are only longitudinal, since a gas does not support shear or bending. Solid materials, which are bound tightly together, can support more types of wave motion than can a gas or liquid, including shear, torsion, bending, and Rayleigh waves. Figure 2.16 illustrates these various types of wave motion and Table 2.3 lists the formulas for their velocities of propagation. In a later chapter we will discuss some of the effects of flexural (bending) and shear-wave motions in solid plates. Rayleigh waves are a combination of compression and shear waves, which are formed on the surface of solids. They are most commonly encountered in earthquakes when a compression wave, produced at the center of a fault, propagates to the earth's surface and then travels along the surface of the ground as a Rayleigh wave.

2.5   ACOUSTICAL PROPERTIES

Impedance

The acoustical *impedance*, which is a measure of the resistance to motion at a given point, is one of the most important properties of a material. A substance such as air has a low characteristic impedance, a concrete slab has a high impedance. Although there are several slightly different definitions of impedance, the *specific acoustic impedance*, which is the most frequently encountered in architectural acoustics, is defined as the ratio of the

TABLE 2.3 Types of Vibrational Waves and Their Velocities

Compressional

Gas	Liquid	Infinite Solid	Solid Bar
$\sqrt{\dfrac{\gamma\,P}{\rho}}$	$\sqrt{\dfrac{B}{\rho}}$	$\sqrt{\dfrac{E(1-\nu)}{\rho(1+\nu)(1-2\nu)}}$	$\sqrt{\dfrac{E}{\rho}}$

Shear		**Torsional**

String (Area S)	Solid	Bar
$\sqrt{\dfrac{T}{S\,\rho}}$	$\sqrt{\dfrac{E}{2\,\rho(1+\nu)}}$	$\sqrt{\dfrac{E\,K_B}{2\,\rho I\,(1+\nu)}}$

Bending		**Rayleigh**

Rectangular Bar	Plate (Thickness – h)	Surface of a Solid
$\left[\dfrac{E\,h^2\,\omega^2}{12\,\rho}\right]^{1/4}$	$\left[\dfrac{E\,h^2\,\omega^2}{12\,\rho(1-\nu^2)}\right]^{1/4}$	$0.385\sqrt{\dfrac{E\,(2.6+\nu)}{\rho\,(1+\nu)}}$

where P = equilibrium pressure (Pa)
   atmospheric pressure = 1.01×10^5 Pa
  γ = ratio of specific heats (about 1.4 for gases)
  B = isentropic bulk modulus (Pa)
  K_B = torsional stiffness (m^4)
  I = moment of inertia (m^4)
  ρ = mass density (kg / m^3)
  E = Young's modulus of elasticity (N / m^2)
  ν = Poisson's ratio $\cong$ 0.3 for structural materials
   and $\cong$ 0.5 for rubber-like materials
  T = tension (N)
  ω = angular frequency (rad / s)

sound pressure to the associated *particle velocity* at a point

$$z = \frac{p}{u} \tag{2.45}$$

where   z = specific acoustic impedance (N s / m^3)
     p = sound pressure (Pa)
     u = acoustic particle velocity (m /s)

The specific impedance of a gas can be determined by examining a simple example (Ingard, 1994). We construct a hypothetical one-dimensional tube with a piston in one end, as shown in Fig. 2.17. We push the piston into the tube at some steady velocity, u. After a time Δ t, there will be a region of the fluid in front of the piston that is moving at the piston velocity. The information that the piston is moving is conveyed to the gas in the tube at the speed of sound. The length of the region that is aware of this movement is the velocity of sound, c, times the time Δ t, and beyond this point the fluid is quiescent. The fluid in the tube has acquired a momentum (mass times velocity) of (Sρ c Δ t)(u), where ρ is the mass of density of the fluid, in a time Δ t. Newton's Law tells us that the force is the rate change

FIGURE 2.17   Progression of a Pressure Pulse

A region of high pressure generated by a piston moving to the right at velocity u. The information is transmitted to the fluid at the sound velocity c.

P + p   P

u

c Δt
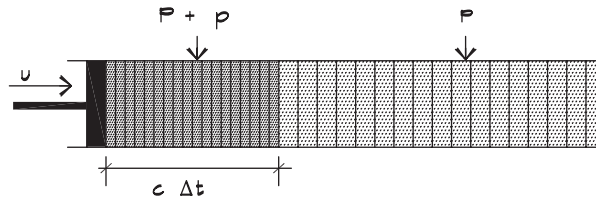
of momentum so

$$p \, S = (S \, \rho \, c) \, u \tag{2.46}$$

The specific acoustic impedance of the fluid is

$$z = \frac{p}{u} = \rho \, c \tag{2.47}$$

where z = specific acoustic impedance (N s / m^3 or mks rayls)
  ρ = bulk density of the medium (kg / m^3)
  c = speed of sound (m / s)

The dimensions of impedance are known as rayls (in mks or cgs units) to honor John William Strutt, Baron Rayleigh. The value of the impedance frequently is used to characterize the conducting medium and is called the characteristic impedance. For air at room temperature it is about 412 mks or 41 cgs rayls.

Intensity

Another important acoustical parameter is the measure of the energy propagating through a given area during a given time. This quantity is the *intensity*, shown in Fig. 2.18. For a plane wave it is defined as the acoustic power passing through an area in the direction of the surface normal

$$I \, (\theta) = \frac{E \, \cos \, (\theta)}{T \, S} = \frac{W \, \cos \, (\theta)}{S} \tag{2.48}$$

FIGURE 2.18   Intensity of a Plane Wave

The intensity, I (θ), of a plane wave is the power, W, passing through an area, S, in a direction normal to the plane of the area.

W

θ

I (θ)

S
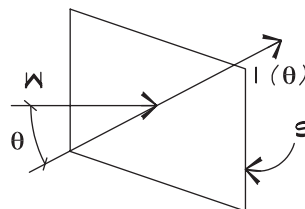
where   E = energy contained in the sound wave (N m / s)
   W = sound power (W)
   I (θ) = intensity (W / m^2) passing through an area in the direction of its normal
   S = measurement area (m^2)
   T = period of the wave (s)
   θ = angle between the direction of propagation and the area normal

The maximum intensity, I, is obtained when the direction of propagation coincides with the normal to the planar surface, when the angle $\theta = 0$.

$$I = \frac{W}{S} \tag{2.49}$$

Plane waves are the most commonly analyzed waveform because the mathematics are simple and the form ubiquitous. A wave is considered planar when its properties do not change in the plane whose normal is the direction of propagation. Intensity is a vector quantity. Its direction is defined by the direction of the normal of the measurement area. When the normal is oriented along the direction of propagation of the sound wave, the intensity has its maximum value, which is not a vector quantity.

Sound power is the sound energy being emitted by a source each cycle. The energy, which is the mechanical work done by a wave, is the force moving through a distance

$$E = p\, S\, dx \tag{2.50}$$

where p is the root-mean-square acoustic pressure, and S is the area. The power, W, is the rate of energy flow so

$$W = \frac{p\, S\, d\, x}{d\, t} = p\, S\, u \tag{2.51}$$

where u is the velocity of a small region of the fluid, and is called the particle velocity. It is not the thermal velocity of individual molecules but rather the velocity of a small volume of fluid caused by the passage of the sound wave. For a plane wave

$$I = p\, u \tag{2.52}$$

where   I = maximum acoustic intensity (W / m^2)
   p = root-mean-square (rms) acoustic pressure (Pa)
   u = acoustic rms particle velocity (m / s)

Using the definition of the specific acoustic impedance from Eq. 2.37

$$z = \frac{p}{u} = \rho\, c \tag{2.53}$$

we can obtain for a plane wave

$$I = \frac{p^2}{\rho\, c} \tag{2.54}$$

where I = maximum acoustic intensity (W / m^2)
        p = rms acoustic pressure (Pa)
        ρ = bulk density (kg / m^3)
        c = velocity of sound (m / s)

The acoustic pressure shown in Eq. 2.44 is the root-mean-square (rms) sound pressure averaged over a cycle

$$p = p_{rms} = \left[\frac{1}{T} \int_0^T P^2 \sin^2 \omega\, t\, dt \right]^{\frac{1}{2}} = \frac{P}{\sqrt{2}} \tag{2.55}$$

which, for a sine wave, is 0.707 times the maximum value. The average acoustic pressure is zero because its value swings an equal amount above and below normal atmospheric pressure. The energy is not zero but must be obtained by averaging the square of the pressure. Interestingly, the rms pressure of the combination of random waveforms is independent of the phase relationship between the waves.

The intensity (generally taken to be the maximum intensity) is a particularly important property. It is directly measurable using a sound level meter and is audible. It is proportional to power so that when waves are combined, their intensities may be added arithmetically. The combined intensity of several sounds is the simple sum of their individual intensities. The lowest intensity that we are likely to experience is the threshold of human hearing, which is about 10^{-12} W/m^2. A normal conversation between two people might take place at about 10^{-6} W/m^2 and a jet aircraft could produce 1 W/m^2. Thus the acoustic intensities encountered in daily life span a very large range, nearly 12 orders of magnitude. Dealing with numbers of this size is cumbersome, and has lead to the adoption of the decibel notation as a convenience.

Energy Density

In certain instances, the *energy density* contained within a region of space is of interest. For a plane wave if a certain power passes through an area in a given time, the volume enclosing the energy is the area times the distance the sound has traveled, or $c\,t$. The energy density is the total energy contained within the volume divided by the volume

$$D = \frac{E}{S\,c\,t} = \frac{W}{S\,c} = \frac{p^2}{\rho\,c^2} \tag{2.56}$$

2.6   LEVELS

Sound Levels — Decibels

Since the range of intensities is so large, the common practice is to express values in terms of *levels*. A level is basically a fraction, expressed as 10 times the logarithm of the ratio of two numbers.

$$\text{Level} = 10\ \log \left[\frac{\text{Number of interest}}{\text{Reference number}} \right] \tag{2.57}$$

Since a logarithm can be taken of any dimensionless number, and all levels are the logarithm of some fraction, it is useful to think of them as simple fractions. Even when the denominator

TABLE 2.4 Reference Quantities for Sound Levels (Beranek and Ver, 1992)

Level (dB)	Formula	Reference (SI)
Sound Intensity	$L_I = 10 \log (I/I_o)$	$I_o = 10^{-12}$ W$/$m^2
Sound Pressure	$L_p = 20 \log (p/p_o)$	$p_o = 20 \ \mu$ Pa $\quad = 2 \times 10^{-5}$ N$/$m^2
Sound Power	$L_W = 10 \log (W/W_o)$	$W_o = 10^{-12}$ W
Sound Exposure	$L_E = 10 \log (E/E_o)$	$E_o = (20 \ \mu$ Pa$)^2$ s $\quad = (2 \times 10^{-5}$ Pa$)^2$ s

Note: Decimal multiples are: 10^{-1} = deci (d), 10^{-2} = centi (c), 10^{-3} = milli (m), 10^{-6} = micro (μ), 10^{-9} = nano (n), and 10^{-12} = pico (p).

has a numeric value of 1, such as 1 second or 1 square meter, there must always be a reference quantity to keep the ratio dimensionless.

The logarithm of a number divided by a reference quantity is given the unit of bels, in honor of Alexander Graham Bell, the inventor of the telephone. The multiplication by 10 has become common practice, in order to achieve numbers that have a convenient size. The quantities thus obtained have units of decibels, which is one tenth of a bel. Typical levels and their reference quantities are shown in Table 2.4. Levels are denoted by a capital L with a subscript that indicates the type of level. For example, the sound power level is shown as L_W, while the sound intensity level would be L_I, and the sound pressure level, L_p.

Recalling that quantities proportional to power or energy can be combined arithmetically we can combine two or more levels by adding their intensities.

$$I_{Total} = I_1 + I_2 + \cdots + I_n \tag{2.58}$$

If we are given the intensity level of a sound, expressed in decibels, then we can find its intensity by using the definition

$$L_I = 10 \ \log \frac{I}{I_{ref}} \tag{2.59}$$

and the definition of the antilogarithm

$$\frac{I}{I_{ref}} = 10^{0.1 \ L_I} \tag{2.60}$$

When the intensities from several signals are combined the total overall intensity ratio is

$$\frac{I_{Total}}{I_{ref}} = \sum_{i=1}^{n} 10^{0.1 \ L_i} \tag{2.61}$$

and the resultant overall level is

$$L_{Total} = 10 \log \frac{I_{Total}}{I_{ref}} = 10 \ \log \sum_{i=1}^{n} 10^{0.1 \ L_i} \tag{2.62}$$

As an example, we can take two sounds, each producing an intensity level of 70 dB, and ask what the level would be if we combined the two sounds. The problem can be formulated as

$$L_1 = L_2 = 70 \text{ dB} \tag{2.63}$$

which, if combined, would yield

$$L_{1+2} = 10 \log \left[(10^7 + 10^7) \right] = 73 \text{ dB} \tag{2.64}$$

Thus when two levels of equal value are combined the resultant level is 3 dB greater than the original level. By doing similar calculations we learn that when two widely varying levels are combined the result is nearly equal to the larger level. For example, if two levels differ by 6 dB, the combination is about 1 dB higher than the larger level. If the two differ by 10 or more the result is essentially the same as the larger level.

When there are a number of equal sources, the combination process can be simplified

$$L_{\text{Total}} = L_i + 10 \log n \tag{2.65}$$

where L_i is the level produced by one source and n is the total number of like sources.

Sound Pressure Level

The *sound pressure level* is the most commonly used indicator of the acoustic wave strength. It correlates well with human perception of loudness and is measured easily with relatively inexpensive instrumentation. A compilation of the sound pressure levels generated by representative sources is given in Table 2.5 at the location or distance indicated.

The reference sound pressure, like that of the intensity, is set to the threshold of human hearing at about 1000 Hz for a young person. When the sound pressure is equal to the reference pressure the resultant level is 0 dB. The sound pressure level is defined as

$$L_p = 10 \log \frac{p^2}{p_{\text{ref}}^2} \tag{2.66}$$

where   p = root-mean-square sound pressure (Pa)
  p_{ref} = reference pressure, 2×10^{-5} Pa

Since the intensity is proportional to the square of the sound pressure as shown in Eq. 2.44 the intensity level and the sound pressure level are almost equal, differing only by a small number due to the actual value versus the reference value of the air's characteristic impedance. This fact is most useful since we both measure and hear the sound pressure, but we use the intensity to do most of our calculations.

It is relatively straightforward (Beranek and Ver, 1992) to work out the relationship between the sound pressure level and the sound intensity level to calculate the actual difference

$$L_p = L_I + 10 \log (\rho_0 c_0 / 400) \tag{2.67}$$

For a typical value of $\rho_0 c_0$ of 412 mks rayls the correction is 0.13 dB, which is ignored in most calculations.

TABLE 2.5   Representative A-Weighted Sound Levels (Peterson and Gross, 1974)

AT A GIVEN DISTANCE	dBA re 20 μN/m²	ENVIRONMENTAL
	140	
50 HP Siren (100')	130	
Jet Takeoff (200')	120	
Riveting Machine	110	Casting Shake-Out Area
Cut Off Saw		Disco
	100	Electric Furnace Area
Textile Weaving Plant		
Subway Train (20')	90	Boiler Room
Jack Hammer (50')		Printing Press Plant
Heavey Truck (50')	80	
Freight Train (100')		
Vacuum Cleaner (10')	70	Near Freeway (Auto Traffic)
Speech (3')		Inside Car (50 MPH)
	60	Large Store
Large Transformer (200')	50	Light Traffic (100')
		Quiet Residence Exterior
	40	Min Levels Residential Areas in Chicago at Night
		Private Business Office
Soft Whisper (5')	30	
		Studio for Sound Pictures
	20	Studio (Voice Over)
	10	
Threshold of Hearing	0	

Sound Power Level

The strength of an acoustic source is characterized by its *sound power*, expressed in Watts. The sound power is much like the power of a light bulb in that it is a direct characterization of the source strength. Like other acoustic quantities, the sound powers vary greatly, and a *sound power level* is used to compress the range of numbers. The reference power for this level is 10^{-12} Watts. Sound power levels for several sources are shown in Table 2.6.

Sound power levels can be measured by using Eq. 2.49.

$$I = \frac{W}{S} \qquad (2.68)$$

TABLE 2.6   Sound Power Levels of Various Sources (Peterson and Gross, 1974)

POWER (Watts)	POWER LEVEL (dB re 10^{-12} Watts)	SOURCE
25 to 40 Million	195	Saturn Rocket
100,000	170	Ram Jet
		Turbo Jet Engine with Afterburner
10,000	160	Turbo Jet Engine, 7000-lb Thrust
1,000	150	
		4-Propellor Aircraft
100	140	
10	130	75-Piece Orchestra } Peak RMS Levels in
		Pipe Organ 1/8 Second Intervals
		Small Aircraft Engine
1	120	Large Chipping Hammer
0	110	Blaring Radio
		Centrifugal Ventillating Fan (13,000 CFM)
0.1	100	Auto on Highway
0.01	90	Vane Axial Ventillating Fan (1500 CFM)
0.001	80	Voice - Shouting (Average Long-Time RMS)
0.000,01	70	Voice - Conversational Level
		(Average Long-Time RMS)
0.000,001	60	
0.000,000,1	50	
0.000,000,01	40	
0.000,000,001	30	Voice - Very Soft Whisper

If we divide this equation by the appropriate reference quantities

$$\frac{I}{I_0} = \frac{\left(W/W_0\right)}{\left(S/S_0\right)} \tag{2.69}$$

and take 10 log of each side we get

$$L_I = L_w - 10 \log S \tag{2.70}$$

where S_0 is equal to 1 square meter. Recalling that the sound intensity level and the sound pressure level are approximately equal,

$$L_p = L_w - 10 \log S + K \tag{2.71}$$

where L_w = sound power level (dB re 10^{-12} W)
   L_p = sound pressure level (dB re 2×10^{-5} Pa)
   S = measurement area (m^2 or ft^2)
   K = $10 \log (\rho_0 c_0 / 400) + 20 \log(r_0)$
     = 0.1 for r in m, or 10.5 for r in ft
   r_0 = 1 m for r in m or 3.28 ft for r in ft

The small correction for the difference between the sound intensity level and the sound pressure level, when the area is in square meters, is ignored. When the area S in Eq. 2.68 is in square feet, a conversion factor is applied, which is equal to 10 log of the number of square feet in a square meter or 10.3. We then add in the small factor, which accounts for the difference between sound intensity and sound pressure level.

These formulas give us a convenient way to measure the sound power level of a source by measuring the average sound pressure level over a surface of known area that bounds the source. Perhaps the simplest example is low-frequency sound traveling down a duct or tube having a cross-sectional area, S. The sound pressure levels are measured by moving a microphone across the open area of the duct and by taking the average intensity calculated from these measurements. The overall average sound intensity level is obtained by taking 10 log of the average intensity divided by the reference intensity. By adding a correction for the area the sound power level can be calculated. This method can be used to measure the sound power level of a fan when it radiates into a duct of constant cross section. Product manufacturers provide sound power level data in octave bands, whose center frequencies range from 63 Hz (called the first band) through 8 kHz (called the eighth band). They are the starting point for most HVAC noise calculations.

If the sound source is not bounded by a solid surface such as a duct, the area shown in Eq. 2.68 varies according to the position of the measurement. Sound power levels are determined by taking sound pressure level data at points on an imaginary surface, called the *measurement surface*, surrounding the source. The most commonly used configurations are a rectangular box shape or a hemispherical-shaped surface above a hard reflecting plane. The distance between the source and the measurement surface is called the *measurement distance*. For small sources the most common measurement distance is 1 meter. The box or hemisphere is divided into areas and the intensity is measured for each segment.

$$W = \sum_{i=1}^{n} I_i S_i \tag{2.72}$$

where W = total sound power (W)
   I_i = average intensity over the i th surface (W / m^2)
   S_i = area of the *i* th surface (m^2)
   n = total number of surfaces

Measurement locations are set by international standards (ISO 7779), which are shown in Fig. 2.19. The minimum number of microphone positions is nine with additional positions

FIGURE 2.19   Sound Power Measurement Positions on a Parallelepiped or Hemisphere (ISO 7779)

a = 0.5 L1 + d
b = 0.5 L2 + d
c = L3 + d
d is normally 1 m

● Primary microphone positions
○ Additional microphone positions

Hemispherical measurement surface
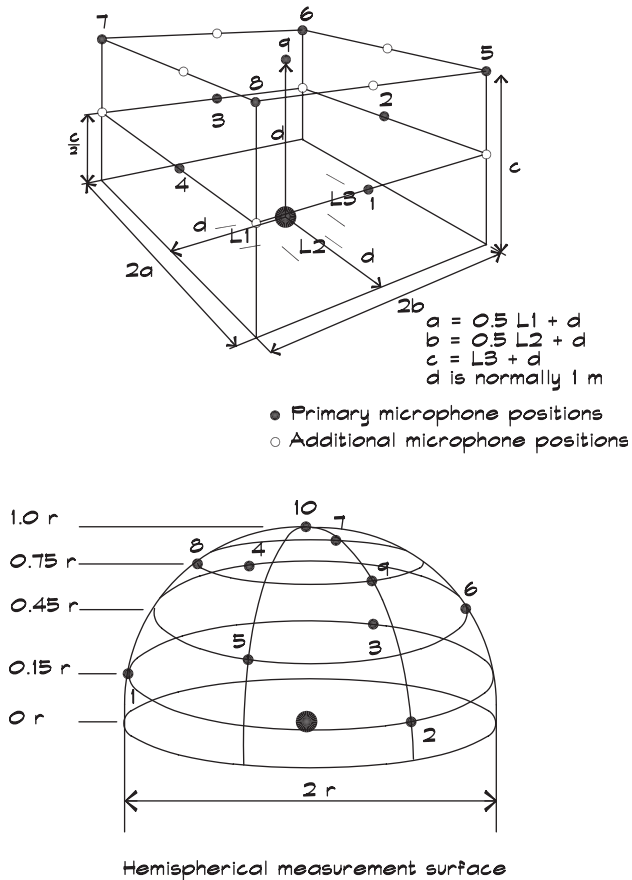
required if the source is long or the noise highly directional. The difference between the highest and lowest measured level must be less than the number of microphone positions. If the source is long enough that the parallelepiped has a side that is more than twice the measurement distance, the additional locations must be used.

2.7   SOURCE CHARACTERIZATION

Point Sources and Spherical Spreading

For most sources the relationship between the sound power level and the sound pressure level is determined by the increase in the area of the measurement surface as a function of distance. Sources that are small compared with the measurement distance are called *point sources*, not because they are so physically small but because at the measurement distance their size does not influence the behavior of the falloff of the sound field. At these distances the measurement surface is a sphere with its center at the center of the source as shown in Fig. 2.20, with a surface area given by

$$S = 4 \pi r^2 \tag{2.73}$$

FIGURE 2.20   Spherical Spreading of a Point Source

The maximum intensity, I , generated by a point source is the power, W, passing through an area, S, equal to the area of a sphere of radius r, centered on the source.
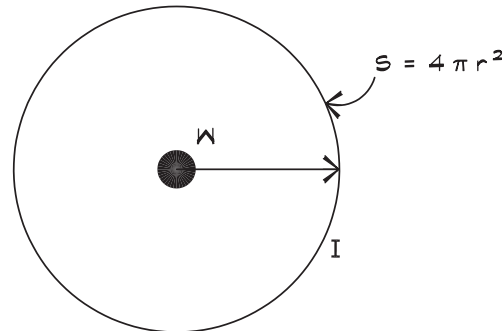
where   S = area of the measurement surface (m^2 or ft^2)
         r = measurement distance (m or ft)

When Eq. 2.73 holds, the falloff is referred to as *free field* behavior and the power-pressure relationship for a nondirectional source is

$$L_p = L_w + 10 \log \left[\frac{1}{4 \pi r^2} \right] + K \qquad (2.74)$$

where L_w = sound power level (dB re 10^{-12} W)
         L_p = sound pressure level (dB re 2×10^{-5} Pa)
         r = measurement distance (m or ft)
         K = $10 \log (\rho_0 c_0 / 400) + 20 \log (r_{ref})$
           = 0.1 for r in m, or 10.5 for r in ft (for standard conditions)
         r_{ref} = 1 m for r in m or 3.28 ft for r in ft

The designation free field means that sound field is free from any reflections or other influences on its behavior, other than the geometry of spherical spreading of the sound energy. For a given sound power level the sound pressure level decreases 6 dB for every doubling of the measurement distance. Free-field falloff is sometimes described as 6 dB per distance doubling falloff.

Figure 2.21 shows the level versus distance behavior for a point source. If the measurement distance is small compared with the size of the source, where this falloff rate does not hold, the measurement position is in the region of space described as the *near field*. In the near field the source size influences the power-pressure relationship. Occasionally there are nonpropagating sound fields that contribute to the sound pressure levels only in the near field.

For a given source, we can calculate the sound pressure level in the free field at any distance, if we know the level at some other distance. One way to carry out this calculation is to compute the sound power level from one sound pressure level measurement and then to use it to calculate the second level at a new distance. By subtracting the two equations used

FIGURE 2.21   Falloff from a Point Source

The decrease in level with distance from a point
source is 6 dB per doubling of distance.
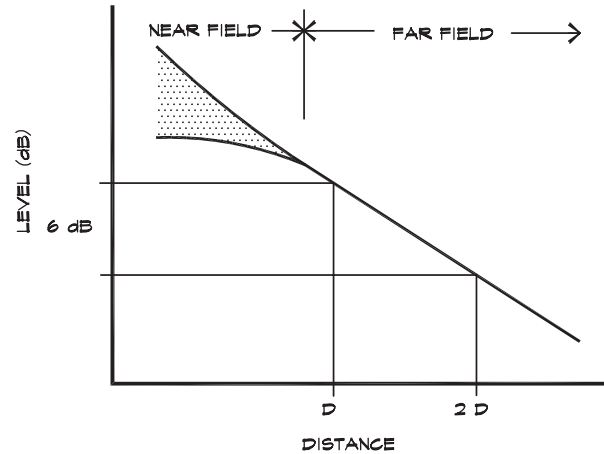
to do this calculation we obtain

$$\Delta L_p = 10 \log \frac{r_2^2}{r_1^2} = 20 \log \frac{r_2}{r_1} \tag{2.75}$$

where ΔL_p = change in sound pressure level ($L_1 - L_2$)
   r_1 = measurement distance 1 (m or ft)
   r_2 = measurement distance 2 (m or ft)

Note that the change in level is positive when $L_1 > L_2$, which occurs when $r_2 > r_1$. As expected, the sound pressure level decreases as the distance from the source increases.

Sensitivity

Although the strength of many sources, particularly mechanical equipment, is characterized by the sound power level, in the audio industry loudspeakers are described by their *sensitivity*. The sensitivity is the sound pressure level measured at a given distance (usually 1 meter) on axis in front of the loudspeaker for an electrical input power of 1 Watt. Sensitivities are measured in octave bands and are published along with the maximum power handling capacity and directivity of the device. The on-axis sound level, expected from a speaker at a given distance, can be calculated from

$$L_p = L_S + 10 \log J - 20 \log \left(\frac{r}{r_{ref}} \right) \tag{2.76}$$

where L_p = measured on axis sound pressure level (dB)
   L_S = loudspeaker sensitivity (dB at 1 m for 1 W electrical input)
   J = electrical power applied to the loudspeaker (W)
   r = measurement distance (m or ft)
   r_{ref} = reference distance (m or ft)

FIGURE 2.22   Source Directivity Shown as a Polar Plot

Directivity data are often shown as horizontal and
vertical polar plots of equal level contours.
Each polar represents a 5 dB difference relative to
the on-axis level.
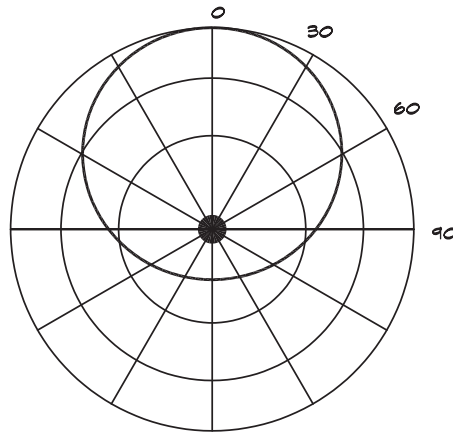
Directionality, Directivity, and Directivity Index

For many sources the sound pressure level at a given distance from its center is not the same in all directions. This property is called *directionality*, and the changes in level with direction of a source are called its *directivity*. The directivity pattern is sometimes illustrated by drawing two- or three-dimensional equal-level contours around it, such as that shown in Fig. 2.22. When these contours are plotted in two planes, a common practice in the description of loudspeakers, they are called horizontal and vertical polar patterns.

The sound power level of a source gives no specific information about the directionality of the source. In determining the sound power level, the sound pressure level is measured at each measurement position, the intensity is calculated, multiplied by the appropriate area weighting, and added to the other data. A highly directional source could have the same sound power level as an omnidirectional source but would produce a very different sound field. The way we account for the difference is by defining a *directivity index*, which is the difference in decibels between the sound pressure level from an omnidirectional source and the measured sound pressure level in a given direction from the real source.

$$D\,(\theta, \phi) = L_p\,(\theta, \phi) - \overline{L}_p \tag{2.77}$$

where $D\,(\theta, \phi)$ = directivity index (gain) for a given direction (dB)
   $L_p\,(\theta, \phi)$ = sound pressure level for a given direction (dB)
      $\overline{L}_p$ = sound pressure level averaged over all angles (dB)
      θ, ϕ = some specified direction

The directivity index can also be specified in terms of a directivity, which is given the symbol Q for a specific direction

$$D\,(\theta, \phi) = 10 \log Q\,(\theta, \phi) \tag{2.78}$$

where $Q\,(\theta, \phi)$ = directivity for a given direction (θ, ϕ)

The directivity can be expressed in terms of the intensity in a given direction compared with the average intensity

$$Q(\theta, \phi) = \frac{I(\theta, \phi)}{I_{Ave}} \tag{2.79}$$

The average intensity is given by

$$I_{Ave} = \frac{W}{4 \pi r^2} \tag{2.80}$$

and the intensity in a particular direction by

$$I(\theta, \phi) = \frac{Q(\theta, \phi)W}{4 \pi r^2} \tag{2.81}$$

When the directivity is included in the relationship between the sound power level and the sound pressure level in a given direction, the result for a point source is

$$L_p(\theta, \phi) = L_w + 10 \log \frac{Q(\theta, \phi)}{4 \pi r^2} + K \tag{2.82}$$

In the audio industry the Q of a loudspeaker is understood to mean the on-axis directivity, $Q(0, 0) = Q_0$.

The sound power level of a loudspeaker can be calculated from its sensitivity and its Q_0 for any input power J

$$L_w = L_S - 10 \log \frac{Q_0}{4 \pi r^2} + 10 \log J - K \tag{2.83}$$

where L_S = loudspeaker sensitivity (dB at 1 m for 1 W input)
       r = standard measurement distance (usually = 1 m)
      J = input electrical power (W)

The sound pressure level emitted by the loudspeaker at a given angle can then be calculated from the sound power level

$$L_p = L_w + 10 \log \frac{Q(\theta, \phi)}{4 \pi r^2} + K \tag{2.84}$$

where $Q(\theta, \phi)$ = loudspeaker directivity for a given direction
      $Q(\theta, \phi) = Q_0 \, Q_{rel}(\theta, \phi)$
         Q_0 = on‑axis directivity
    $Q_{rel}(\theta, \phi)$ = directivity relative to on‑axis
         θ, ϕ = latitude and longitude angles with respect to the aim point direction and the horizontal axis of the loudspeaker

Normally $Q_0 \gg 1$ and $Q_{rel}(\theta, \phi) < 1$. These relationships will be discussed in greater detail in Chap. 18.

FIGURE 2.23   Falloff of a Line Source

The decrease in level with distance from a line
source is 3 dB per doubling of distance since
the measurement surface is a cylinder.
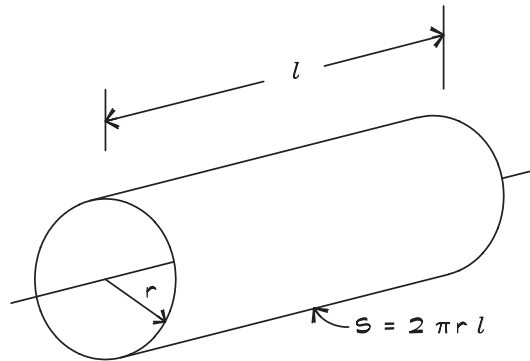
Line Sources

Line sources are one-dimensional sound sources such as roadways, which extend over a distance that is large compared with the measurement distance. With this geometry the measurement surface is not a sphere but rather a cylinder, as illustrated in Fig. 2.23, with its axis coincident with the line source. Since the geometry is that of a cylinder the surface area (ignoring the ends) is given by the equation

$$S = 2 \pi r l \qquad (2.85)$$

where S = surface area of the cylinder (m^2 or ft^2)
r = radius of the cylinder (m or ft)
l = length of the cylinder (m or ft)

   With a line source, the concept of an overall sound power level is not very useful, since all that matters is the portion of the source closest to the observer. Line sources are characterized by a sound pressure level at a given distance. From this information the sound level can be determined at any other distance.

   Assume for a moment that a nondirectional line source of length l emits a given sound power. Then the maximum intensity at a distance r is

$$I = \frac{W}{S} = \frac{W}{2 \pi r l} \qquad (2.86)$$

and the difference in intensity levels at two different distances can be calculated from the ratio of the two intensities

$$\Delta L = L_1 - L_2 = 10 \log \frac{I_1}{I_{ref}} - 10 \log \frac{I_2}{I_{ref}} \qquad (2.87)$$

So for an infinite (very long) line source the change in level with distance is given by

$$\Delta L = 10 \log \frac{I_1}{I_2} = 10 \log \frac{r_2}{r_1} \qquad (2.88)$$

where ΔL = change in level (dB)
L_1 = sound intensity level at distance r_1 (dB re 10^{-12} W/ m^2)
L_2 = sound intensity level at distance r_2 (dB re 10^{-12} W/ m^2)
r_1 = distance 1 (m or ft)
r_2 = distance 2 (m or ft)

If we measure the sound pressure level at a distance, r_1, from an unshielded line source, we can use Eq. 2.88 to calculate the difference in level at some new distance r_2. If $r_2 > r_1$ then the change in level is positive—that is, sound level decreases with increasing distance from the source. The falloff rate is gentler with a line source than it is for a point source—3 dB per distance doubling.

Planar Sources

A *planar source* is a two-dimensional surface that is large compared to the measurement distance and usually, though not always, relatively flat. For purposes of this analysis a planar source is assumed to be incoherent, which is to say that there is no fixed phase relationship among the various points on its surface. From our previous analysis we know that if a surface radiates a certain acoustic power, W, and if that power is uniformly distributed over the surface, then close to the surface the intensity is given by

$$ I = \frac{W}{S} \tag{2.89} $$

where S is the area of the surface. We also know that if we are far enough away from the surface, it is small compared to the measurement distance, and it must behave like a point source; the intensity is given by Eq. 2.82. To model (Long, 1987) the behavior in both regions, it is convenient to imagine the planar source shown in Fig. 2.24 as a portion of a

FIGURE 2.24   Falloff from a Planar Source

Close to a planar source the intensity is determined by the surface area of the source and its sound power. As the measurement distance increases, the falloff behavior approaches that of a point source.

$$ r_s = \sqrt{\frac{S Q}{4 \pi}} $$
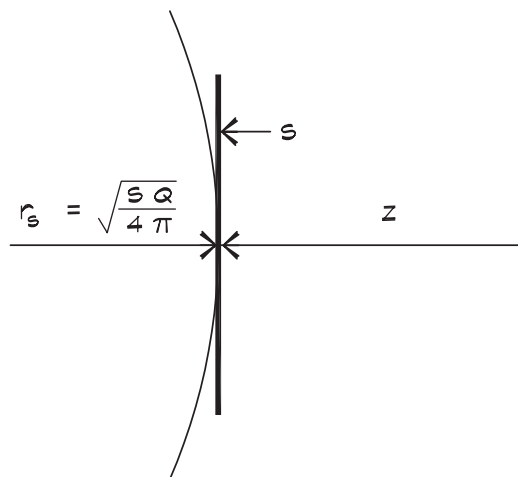
large sphere that has a radius equal to $\sqrt{\frac{S\,Q}{4\,\pi}}$. Since the measurement distance is taken from the surface of the plane, the distance to the center of the sphere from the measurement point is $z + \sqrt{\frac{S\,Q}{4\,\pi}}$. The intensity is then given by

$$I = \frac{W\,Q}{4\,\pi \left[z + \sqrt{\dfrac{S\,Q}{4\,\pi}}\right]^2} \qquad (2.90)$$

When this equation is written as a level by taking 10 log of both sides

$$L_p = L_w + 10 \log \left\{ \frac{Q}{4\,\pi \left[z + \sqrt{\dfrac{S\,Q}{4\,\pi}}\right]^2} \right\} + K \qquad (2.91)$$

where L_p = sound pressure level (dB re 2×10^{-5} Pa)
        L_w = sound power level (dB re 10^{-12} W)
         Q = directivity (dimensionless)
         S = area of the radiating surface (m^2 or ft^2)
         z = measurement distance from the surface (m or ft)
         K = 0.1 (z in m) or 10.5 (z in ft) for standard conditions

Equation 2.91 gives the sound pressure vs sound power relationship for a planar surface at all distances. When a measurement is made close to the surface, the distance z goes to zero, and we obtain Eq. 2.71. When z is large compared to $\sqrt{S\,Q/4\,\pi}$, the behavior approaches Eq. 2.82. Note that the directivity is meaningless when the receiver is very close to the surface since the concept of the direction to the surface is not well defined.

HUMAN PERCEPTION
AND
REACTION TO SOUND

3.1   HUMAN HEARING MECHANISMS

Physiology of the Ear

The human ear is an organ of marvelous sensitivity, complexity, and robustness. For a person with acute hearing, the range of audible sound spans ten octaves, from 20 Hz to 20,000 Hz. The wavelengths corresponding to these frequencies vary from 1.7 centimeters (5/8 inch) to 17 meters (57 feet), a ratio of one thousand. The quietest sound audible to the average human ear, about zero dB at 1000 Hz, corresponds to an acoustic pressure of 20×10^{-6} N/m^2 or Pa. Since atmospheric pressure is about 101,000 Pa (14.7 lb/sq in), it is clear that the ear is responding to extraordinarily small changes in pressure. Even at the threshold of pain, 120 dB, the acoustic pressures are still only about 20 Pa.

The excursion of the ear drum at the threshold of hearing is around 10^{-9} m (4×10^{-7} in) (Kinsler et al., 1982). Most atoms have dimensions of 1 to 2 angstroms (10^{-10} meters) so the ear drum travels a distance of less than 10 atomic diameters at the threshold of hearing. Were our ears only slightly more sensitive, we would hear the constant background noise due to Brownian movement, molecules set into motion by thermal excitation. Indeed, it is thermal motion of the hair cells in the *cochlea* that limits hearing acuity. In very quiet environments the flow of blood in the vessels near the eardrum is plainly audible as a disquieting shushing sound.

The anatomy of the ear, shown in Fig. 3.1, is organized into three parts, termed outer, middle, and inner. The outer and middle ear are air filled, whereas the inner ear is fluid filled. The outer part includes the *pinna*, the fleshy flap of skin that we normally think of as the ear, and a tube known as the *meatus* or auditory canal that conducts sound waves to the *tympanic membrane* or ear drum, separating the outer and middle ear sections. The pinna gathers the sound signals and assists in the localization of the height of a sound source. The 2.7 centimeter (one-inch) long auditory canal acts like a broadband quarter-wavelength tube resonator, whose lowest natural frequency is about 2700 Hz. This helps determine the range of frequencies where the ear is most sensitive—a more or less 3 kHz wide peak centered at about 3400 Hz. The auditory canal resonance increases the sound level at the ear drum around this frequency by about 10 dB above the level at the canal entrance. With the

FIGURE 3.1   A Schematic Representation of the Ear (Flanagan, 1972)
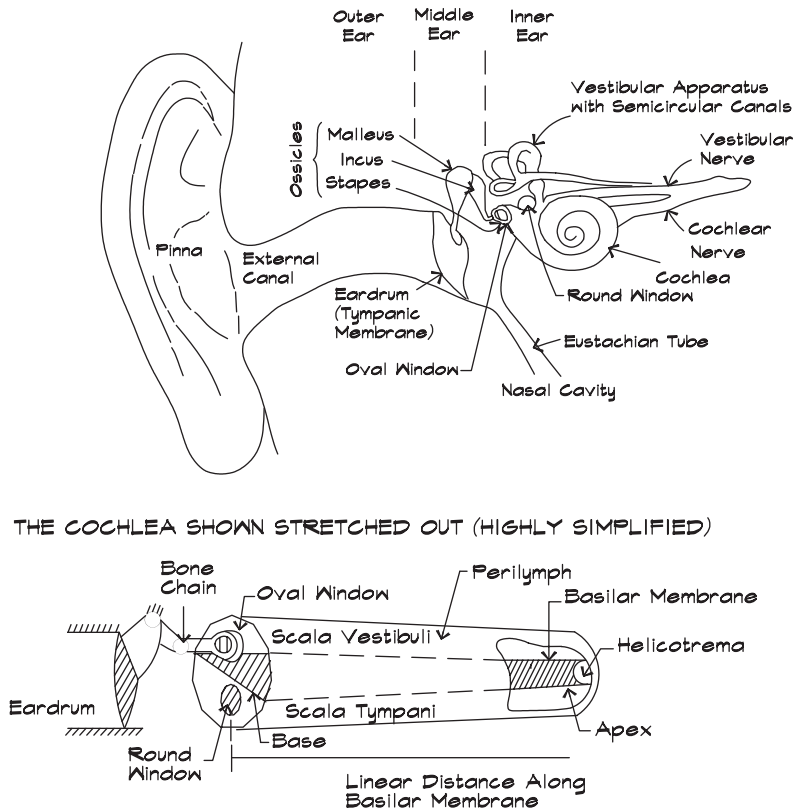
diffraction provided by the pinna and the head, there can be as much as a 15 to 20 dB gain at certain frequencies at the ear drum relative to the free-field level.

The middle ear is an air-filled cavity about 2 cu cm in volume (about the same as a sugar cube), which contains the mechanisms for the transfer of the motion of the eardrum to the cochlea in the inner ear. The ear drum is a thin conical membrane stretched across the end of the auditory canal. It is not a flat drum head, as might be inferred from its name, but rather a tent-like sheath with its peak pointing inward. Near its center, the eardrum is attached to the malleus bone, which is connected in turn to two other small bones. These three, the *malleus* (hammer), *incus* (anvil), and *stapes* (stirrup) act as a mechanical linkage, which couples the eardrum to the fluid-filled cochlea. The stapes resembles a stirrup with its base pressed up against the *oval window*, a membrane that covers the entrance to the cochlea. Because of the area ratio of the eardrum to that of the oval window (about 20 to 1) and the lever action of the ossicles, which produces another factor of 1.5:1, the middle ear acts as an impedance matching transformer, converting the low-pressure, high-displacement motion of the ear drum into a high-pressure, low-displacement motion of the fluid of the cochlea. Atmospheric pressure in the middle ear is equalized behind the eardrum by venting this area to the throat through the *eustation tube*, which opens when we yawn or swallow.

The motion transfer in the middle ear is not linear but depends on amplitude. An *aural reflex* protects the inner ear from loud noises by tightening the muscles holding the stapes to reduce its excursion at high amplitudes, just as the eye protects itself from bright light by

contracting the pupil. The contraction is involuntary in both cases and seldom is noticed by the individual. Pain is produced at high noise levels when the muscles strain to protect nerve cells. Unfortunately the aural reflex is not completely effective. There is a reaction time of about 0.5 msec so it cannot block sounds having a rapid onset, such as gunshots and impact-generated noise. A second reason is that the muscles cannot contract indefinitely. Under a sustained bombardment of loud noise they grow tired and allow more energy to pass.

The inner ear, shown in Fig. 3.2, contains mechanisms that sense balance and acceleration as well as hearing. Housed in the hard bone of the skull, the inner ear contains five

FIGURE 3.2   Structure of the Inner Ear (Hudspeth and Markin, 1994)
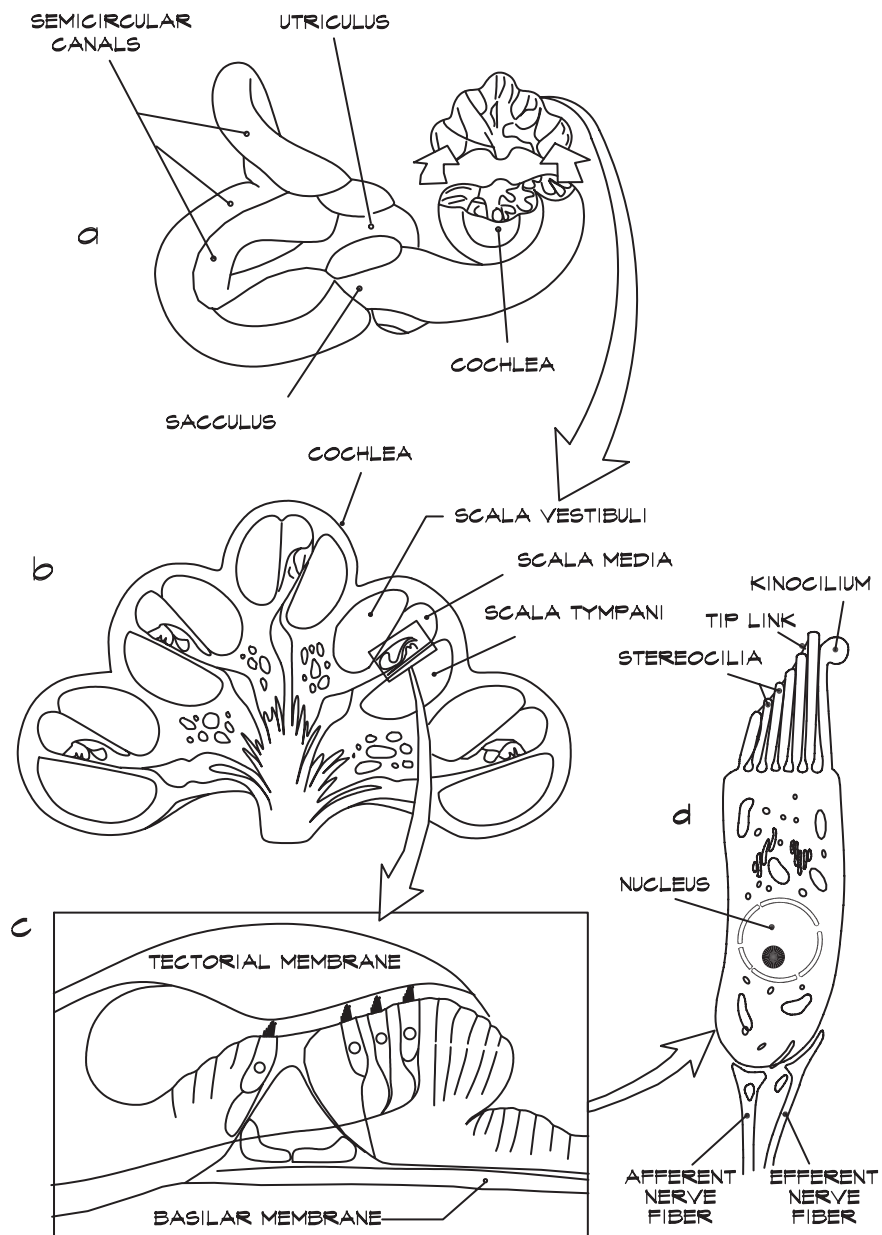
separate receptor organs, each sensitive to a specific type of acceleration, as well as the cochlea, which detects the loudness and frequency content of airborne sound waves. The sacculus and utriculus include about 15,000 and 30,000 hair cells in planar sheets that react to vertical and horizontal linear accelerations respectively. These organs have the capability of encoding a unique signal for an acceleration in any given direction within a plane. Three *semicircular canals* are arranged to sense the orthogonal directions of angular acceleration. Each consists of a fluid-filled tube interrupted by a diaphragm containing about 7000 hair cells. They provide information on the orientation and acceleration of the human head. The bilateral symmetry of the ears gives us not only backup capability but extra information for the decomposition of motions in any direction.

The cochlea is a fluid-filled tube containing the hair cell transducers that sense sound. It is rolled up two and one-half turns like a snail and if we unroll the tube and straighten it out, we would find a narrow cavity 3.5 cm long, about the size and shape of a golf tee scaled down by two-thirds. At its beginning, called the basal end, it is about 0.9 cm in diameter and at the apical end it is about 0.3 cm in diameter. It has two thin membranes running down it near its middle. The thicker membrane is called the *basilar membrane* and divides the cochlea more or less in half, separating the upper gallery (*scala vestibuli*) from the lower gallery (*scala tympani*). Along the membrane lies the *auditory nerve*, which conducts the electrochemical impulses and snakes through a thin sliver of bone called the bony ridge to the brain.

The entrance to the cochlea, in the upper gallery, is the *oval window* at the foot of the stapes. At the upper end of the cochlea near its apex there is a small passageway connecting the upper and lower galleries called the *helicotrema*. At the distal end of the lower gallery near the oval window is another membrane, the *round window*. It acts like the back door to the cochlea, a pressure release surface for fluid impulses traveling along its length and back into the middle ear. The two membranes, the oval window and the round window, seal in the fluid of the cochlea. Otherwise the rest of the cochlea is completely surrounded and protected by bone.

Figure 3.2b shows a cross section of one of the spirals of the cochlea. The upper gallery is separated from a pie-shaped section called the middle gallery (*scala media*) by *Reissner's membrane*. Within this segment and attached to the basilar membrane is the *organ of Corti*, which includes some 16,000 small groups of hair cells (*stereocilia*), arranged in four rows, acting as motion transducers to convert fluid and basilar membrane movement into electrical impulses (Hudspeth and Markin, 1994). The stereocilia are cylindrical rods arranged in a row in order of increasing height and move back and forth as a group in response to pressure waves in the endolymphatic fluid. The hair cells are relatively stiff and only move about a diameter. Through this movement they encode the magnitude and the time passage of the wave as an electrochemical potential, which is sent along to the brain.

Each stereocilia forms a bond between its end and an area on the adjacent higher neighbor much like a spring pulling on a swinging gate (see Fig. 3.2d). When a gate is opened a nerve impulse is triggered and sent to the brain. If the bundle of stereocilia is displaced in the positive direction, toward the high side of the bundle, a greater relative displacement occurs between each stalk and more gates are opened. A negative displacement, towards the short side of the bundle reduces the tension on the biomechanical spring and closes gates. Orthogonal motion results in no change in tension and no change in the signal. The amplitude of the response to sound waves is detected by the number of gate openings and closings and thus the number of impulses sent up the auditory nerve.

FIGURE 3.3 **Longitudinal Distance along the Cochlea Showing the Positions of Response Maxima (Hassall and Zeveri, 1979)**
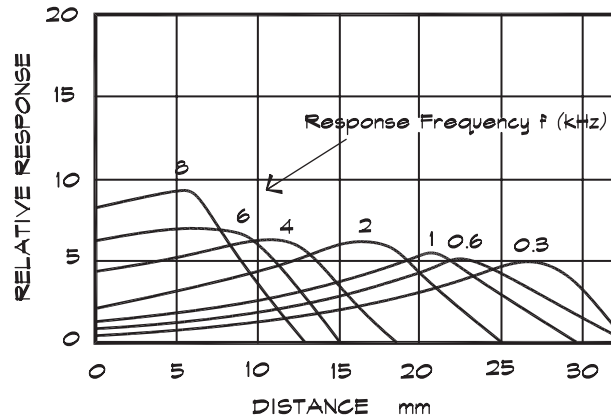
As the stereocilia move back and forth they are sometimes stimulated to a degree that pushes them farther than their normal excursion. In these cases a phenomena known as *adaptation* occurs wherein the hair cells acquire a new resting point that is displaced from their original point. The cells find a new operating position and do a recalibration or reattachment of the spring to a gate at a slightly different point on the neighboring cell. Adaptation also suggests a mechanism for hearing loss when hair cells are displaced beyond the point where they can recover due to exposure to loud sounds over a long time period.

The frequency of the sound is detected by the position of greatest response along the basilar membrane. As a pressure wave moves through the cochlea it induces a ripple motion in the basilar membrane and for each frequency there is a maximum displacement in a certain region. The high frequencies stimulate the area closest to the oval window, while the low frequencies excite the area near the helicotrema. Figure 3.3 illustrates this phenomenon, known as the place theory of pitch detection. It was originated by von Bekesy (1960), and he received a Nobel Prize for his work. The brain can interpret nerve impulses coming from a specific area of the cochlea as a certain sound frequency. There are about 5000 separately detectable pitches over the 10 octaves of audibility.

3.2   PITCH

Critical Bands

Pitch is sensed by the position of maximum excursion along the basilar membrane. This is the ear's spectrum analyzer. There are some 24 discrete areas, each about 1.3 mm long and each contains about 1300 neurons (Scharf, 1970). These act as a set of parallel band-pass filters to separate the incoming sounds into their spectral components. Like electronic filters, the cochlear filters have bandwidths and filter skirts that overlap other bands. When two tones are close enough together that there is significant overlap in their skirts they are said to be within the same *critical band*. The region of influence, which constitutes a critical band, is illustrated in Fig. 3.4. For many phenomena it is about one-third-octave wide. The lower frequencies are sensed by the cochlea at a greater distance from the stapes. The shape of the resonance is not symmetric, having a tail that extends back along the basilar membrane (upward in frequency) from the center frequency of the band. Thus a lower pitched sound

FIGURE 3.4   Critical Bandwidths of the Ear (Kinsler et al., 1982)
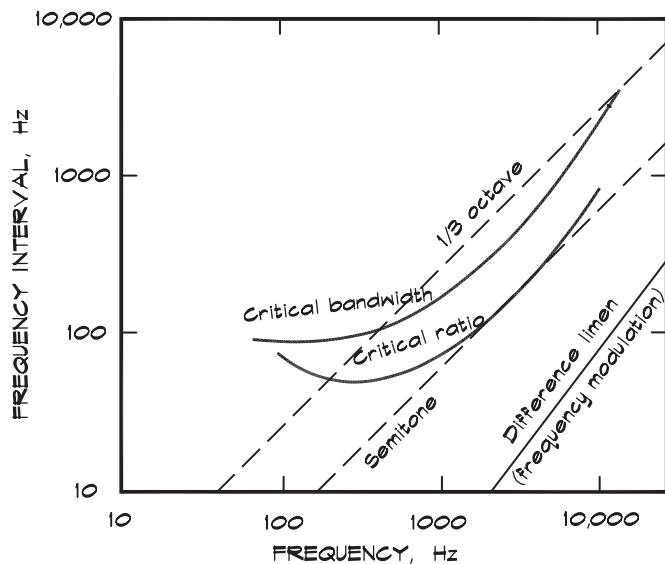
can have a region of influence on a higher pitched sound, but not vice versa unless the sounds are quite close in frequency.

The phenomenon of critical bands is of great significance for many aspects of human hearing. They play a role in music by defining regions of consonance and dissonance. They influence the calculation of loudness by determining the method of combination used for multiple tones. They are critical to the phenomenon of masking, explaining many of the varied masking experiments.

Consonance and Dissonance

When two tones are played together, there is a frequency range over which they sound rough or dissonant (Fig. 3.5). Hermann von Helmholtz in his famous book, *On the Sensations of Tone*, hypothesized that the phenomenon of consonance was closely related to the frequency separation of tones and their harmonics. He thought that when two tones or their partials had a difference frequency of 30 to 40 Hz, this caused unpleasant beats. Subsequent experiments by Plomp and Levelt (1965) added some additional factors to his hypothesis.

Plomp's experiments revealed that the maximum dissonance occurs at about 25% of the critical bandwidth. Figure 3.6 gives a graph of consonance and dissonance as a function

FIGURE 3.5   Auditory Perception within a Critical Band (Pierce,1983)
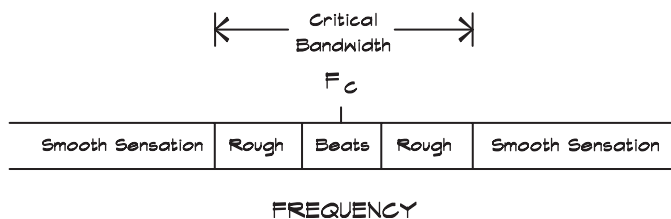
FIGURE 3.6 **Consonance and Dissonance as a Function of the Critical Bandwidth (Pierce, 1983)**
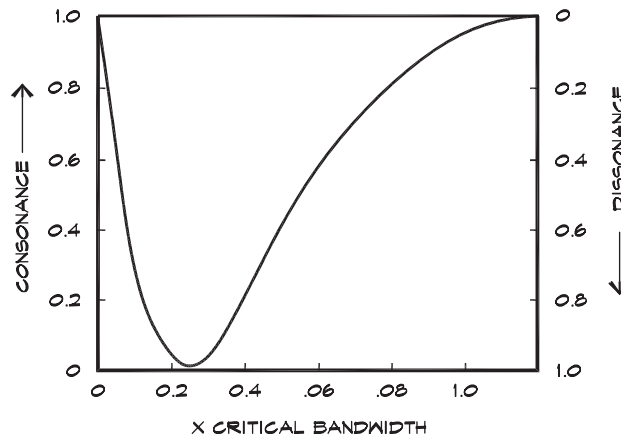
of the difference frequency, shown in terms of the critical bandwidth. When two tones are very close together the difference frequency is too small to be detected as dissonance but is rather a *tremolo*, a rising and falling of level. As they move apart the two tones interfere in such a way as to produce a roughness. When the frequency difference increases still further, the tones begin to be sensed separately and smoothly. For all frequency differences greater than a critical band, separate tones sound consonant.

Tone Scales

One of the traditional problems of music is the establishment of a scale of notes, based on frequency intervals, that sound pleasant when played together. The most fundamental scale division is the octave or doubling of frequency, which is the basis for virtually all music. The octave has been variously divided up into 5 notes (pentatonic scale), 7 notes (diatonic scale), or 12 notes (chromatic scale) by different cultures. Western music uses 12 intervals called *semitones*, but a particular piece usually employs a group of seven selected notes, which are designated as a particular key, bearing the name of the starting note. These scales are called major or minor depending on the order of the single or double steps between the notes selected.

Since many of the early instruments were stringed, not only would the player hear the note's fundamental pitch but also its harmonics, which are integer multiples of the fundamental. Note that the second harmonic frequency is twice the fundamental, the third three times and so forth. The first harmonic is the fundamental. Overtones are sometimes taken to mean the same thing as harmonics. In this work overtones are any significant tonal component of the spectrum of a note whether or not this tone has a harmonic relationship to the note's fundamental. It is not uncommon, particularly in percussion instruments such as chimes, to find nonharmonic overtones, some of which change in frequency as they decay. This group of sounds constitutes a musical instrument's spectrum or timbre, the particular character it has that distinguishes its sound from other similar sounds.

Pythagoras of Samos (sixth century BC) is credited with the discovery that when a string is bridged, with one segment having a certain fractional ratio to the overall length, namely 1/2, 2/3, 3/4, 4/5, and 5/6, the two notes had a pleasing sound. These ratios are called the

FIGURE 3.7   Pythagorean Pitch Intervals (Pierce,1983)

Length	Fundamental Musical Note	Musical Interval Above Original Note	
		Name	Number of Semitones
L	C	–	–
(5/6)L	Eᵇ	Minor Third	3
(4/5)L	E	Major Third	4
(3/4)L	F	Fourth	5
(2/3)L	G	Fifth	7
(1/2)L	C'	Octave	12
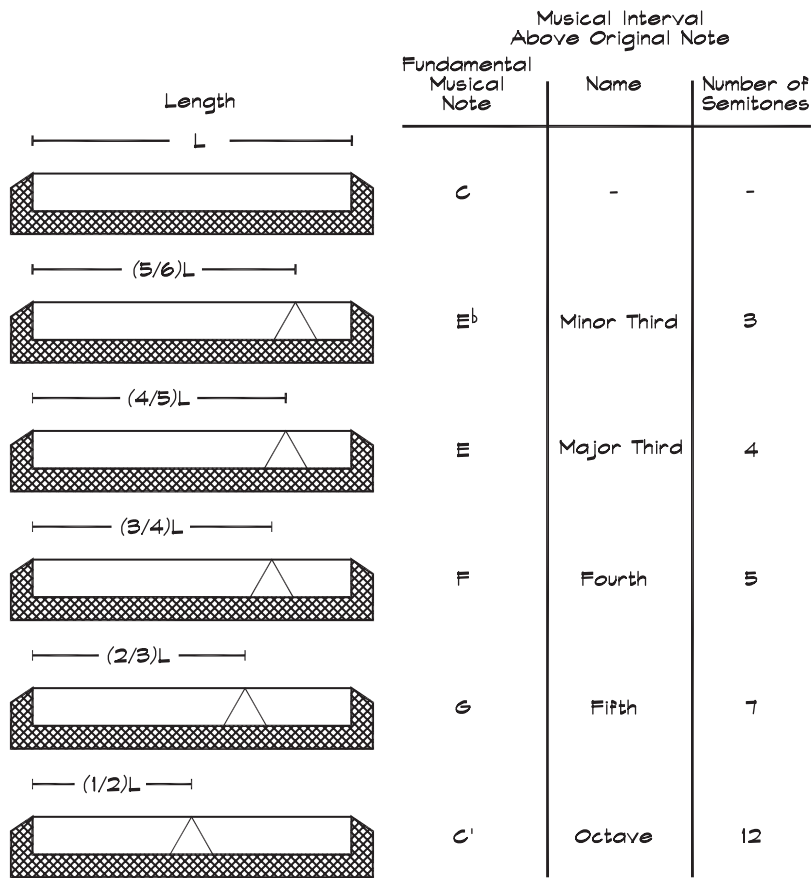
A stretched string held at a constant tension produces different frequencies depending on the length of the string. The whole number ratios and their relation to the pitch were studied by Pythagoras.

perfect intervals in music and traditionally are given special names based on the number of diatonic intervals between them. Figure 3.7 shows the ratios and how they may be obtained from a stretched string and how they relate to the notes we use today. The 2/3 ratio is called a fifth since it has 5 diatonic intervals, the 3/4 ratio is a fourth, 4/5 a major third, and 5/6 a minor third.

Having established the first two consonant intervals, several systems were used to fill in the remaining notes to create a musical scale. One was the just scale, which set all note intervals to small integer ratios. Another was the Pythagorean scale, which sought to produce the most equal whole number ratio intervals. Finally was the *equal-tempered scale*, which set the steps between notes to the same ratio. Each system has some problem. The first two do not transpose well to another key, that is, they do not sound the same since the notes have different relationships. The equal-tempered scale introduced about 300 years ago abandoned adherence to perfect integer ratios but chose intervals that did not differ significantly from those ratios. In this scheme, advocated by J. S. Bach, each note is separated from the following one by a factor of $\sqrt[12]{2} = 1.059463$, called a semitone. Every note interval, is in turn, divided

into 100 cents so that there are 1200 cents in an octave. The frequency ratio between each cent is the 1200th root of 2, or 1.00057779. In this system a scale may begin on any white or black key on the piano and sound alike. Bach wrote his series, *The Well Tempered Clavier*, which contains pieces in all major and minor keys, in part to illustrate this method of tuning.

Once the system of note intervals had been established, there was the problem of choosing where to begin. For many years there were no pitch standards and, according to Helmholtz (1877), pipe organs were built with A's ranging from 374 Hz to 567 Hz. Handel's tuning fork was measured at 422.5 Hz and that became the standard for the classical composers Haydn, Bach, Mozart, and Beethoven. In 1859 the standard A rose to 435 Hz, set by a French government commission, which included Berlioz, Meyerbeer, and Rossini. The so-called "scientific" pitch was introduced in the early twentieth century with the C note frequencies being integer powers of 2, much like the designation of today's computer memory chips. This resulted in an A of 431 Hz. Later, in 1939, an international conference in London adopted the current standard, A equal to 440 Hz at 20° C.

Tunings still vary with individual instruments and musical taste. The natural frequency in woodwinds rises about 3 cents per degree C due to the increase in the velocity of sound. In stringed instruments the fundamental frequency falls slightly with temperature due to the thermal expansion of the strings. Some musicians raise the pitch of their tunings to get additional edge or brightness. This is an unfortunate trend since it stresses older instruments and adds a shrillness to the music, particularly in the strings.

Pitch

Pitch is the human perception of how high or low a tone sounds, based on its relative position on a scale. Musical pitch is defined in terms of notes however, there are psychoacoustical experiments to measure human perception of relative pitch as well. Absolute pitch discrimination is rather rare occurring in only 0.01 percent of the population (Rossing, 1990). Relative pitch discrimination can be measured by asking subjects to respond when one tone sounds twice as high as another. Like loudness experiments, the results are complex, for while they depend primarily on frequency, they also can vary with intensity and waveform. For example if a 100 Hz tone is sounded at 60 dB and then at 80 dB, the louder sound will be perceived as having the lower pitch. This phenomenon is primarily one that occurs at frequencies below 300 Hz. At the mid frequencies (500 Hz to 3000 Hz), pitch is relatively independent of intensity, whereas at frequencies above 4000 Hz, pitch increases with level.

Pitch, as measured in these types of experiments, is different from harmonic relationships found in music. The former is expressed in units of mels, which are similar to sones in that a tone having 2000 mels is judged to be twice as high as one with 1000 mels. The reference frequency for a tone at a given loudness is 1000 Hz, which is defined as 1000 mels. For a given loudness it is possible to define a curve of constant pitch versus frequency as in Fig. 3.8.

3.3   LOUDNESS

Comparative Loudness

Loudness is the human perception of the magnitude of a sound. Early efforts to quantify loudness were undertaken in the field of music. The terms "very loud," "loud," "moderately loud," "soft," and "very soft" were given symbols in musical notation—ff, f, mf, p, and pp, after these words in Italian. But the terms are not sufficiently precise for scientific use,

FIGURE 3.8   Relative Pitch Discrimination vs Frequency (Kinsler et al., 1982)
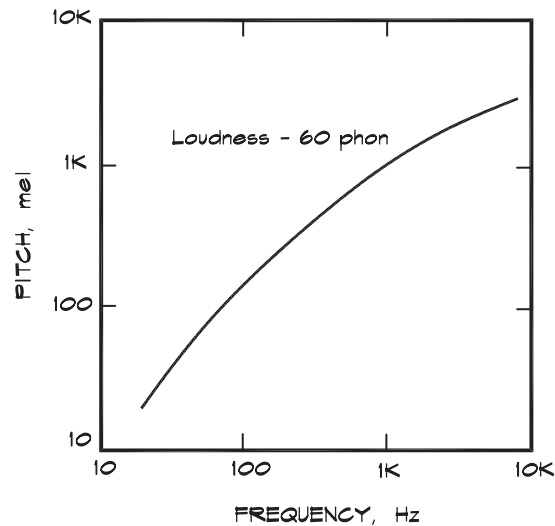
and depend on the hearing acuity and custom of the person using them. It would seem straightforward to use the measured intensity of a sound to determine its loudness, but unfortunately no such simple relationship exists. Loudness is ultimately dependent on the number of nerve impulses reaching the brain in a given time, but since those impulses come from different regions of the cochlea there is also a variation with the frequency content of the sound.

Even when the same sound signal is heard at differing intensities, there will be some variability from listener to listener and indeed even variation with the same listener, depending on his psychological and physiological state. Of general interest is the expected reaction of a listener in a typical environment, which can be determined by testing a number of subjects under controlled conditions. The average of an ensemble of listeners is taken as the result expected from a typical listener, a premise known as the *ergodic* hypothesis in statistics.

Loudness Levels

Comparative loudness measurements were made in the 1920's and 30's by scientists at Bell Laboratories. These tests were done on a group of subjects with acute hearing by presenting them with a controlled set of sounds. Various signals were used, however, in the classic study by Fletcher and Munson, published in 1933, pure tones (sine waves) of short duration were employed. The procedure was to compare the loudness of a tone, presented to the listener at a particular frequency and amplitude, to a fixed reference tone at 1000 Hz having an amplitude that was set in 10 dB intervals to between 0 and 120 dB. Tones were presented to the listeners, by means of headphones, for a one-second duration with a 1.5 second pause in between. Subjects were asked to choose whether a given tone was above, below, or equal to the reference tone, which resulted in a group of loudness-level contours known as the *Fletcher-Munson curves*.

In 1956 Robinson and Dadson repeated the Fletcher-Munson measurements, this time using loudspeakers in an anechoic chamber. The resulting *Robinson-Dadson* curves are shown in Fig. 3.9. The lowest of these curves is the threshold of hearing, which passes through 0 dB at about 2000 Hz and drops below this level at 4000 Hz, where the ear is most sensitive.

FIGURE 3.9   Normal Loudness Contours for Pure Tones (Robinson and Dadson, 1956)
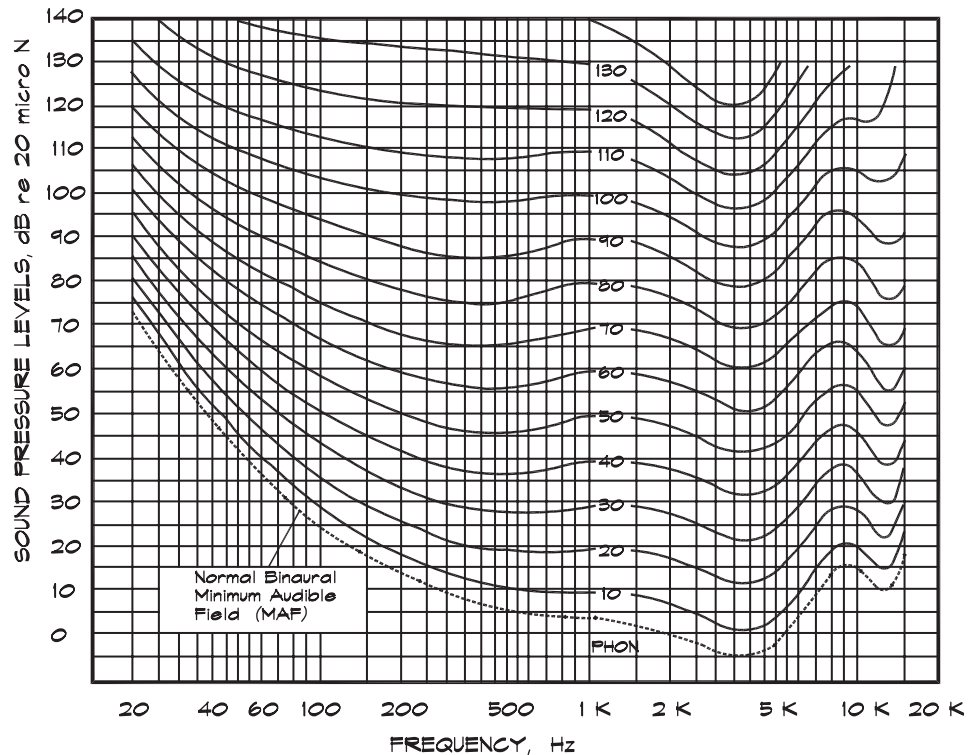
The graph shows that human hearing is significantly less sensitive to low-frequency sounds. At lower frequencies the level rises rapidly as the frequency decreases until, at 30 Hz, the intensity level must be about 65 dB before it is audible. As the intensity of a sound increases, the ear's frequency response becomes flatter. Near 100 dB the ear's response is almost flat except for a small increase in sensitivity around 4000 Hz. These experiments have been repeated many times since the original work was done with various types of signals. They have also been performed on the general population to determine the behavior of hearing acuity with age and other factors.

The curves in Fig. 3.9 are called equal-loudness contours. For any two points along one of these curves the perceived loudness of tones is the same. A loudness level (having units of phons) is assigned to each curve, which is numerically equal to the intensity level of the tone at 1000 Hz. Thus if we follow the 40 phon line we see that a tone having an intensity level of 50 dB at 100 Hz falls on the line and thus has a loudness level of 40 phons. At 1000 Hz the loudness level is equal to the intensity level. At 10,000 Hz the intensity level on the 40 phon line is about 46 dB.

Relative Loudness

The loudness level contours are based on human judgments of absolute loudness. The question asked each subject is whether the tone is louder or quieter than the reference. Another question can be asked, based on a relative comparison, namely, "When is it twice as loud?"

FIGURE 3.10   Loudness vs Loudness Level (Fletcher, 1933)
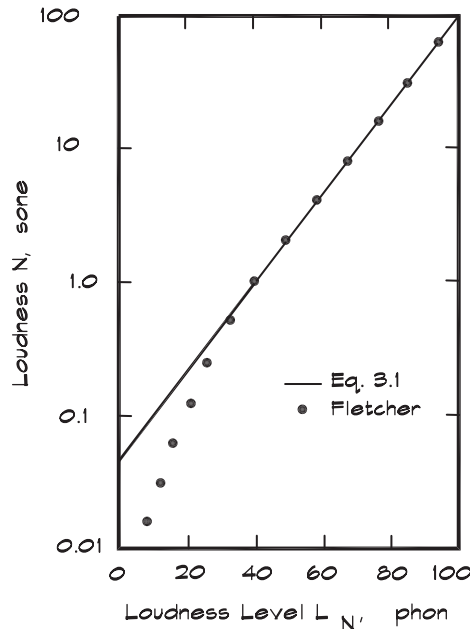
This gives rise to a measure of relative loudness having units of sones. In this scheme the loudness metric is linear; a sound having a relative loudness of 2 sones is twice as loud as a sound of 1 sone and so forth. The baseline is the 40 phon curve that is given the value of 1 sone. Figure 3.10 shows the relationship between (relative) loudness in sones and loudness level in phons. The result of these measurements is that loudness doubles every 9 phons or about 9 dB at the mid frequencies. A general equation can be written for the relationship between loudness and loudness level of pure tones in the linear region of the curve as follows (Kinsler and Frey, 1962)

$$L_N \cong 30 \log N + 40 \tag{3.1}$$

where   N = loudness (sones)
L_N = loudness level (phons)

A determination can also be made of the loudness of sounds, having a spectral content more complicated than pure tones. Starting with measured levels in one-third-octave or full-octave bandwidths, various schemes have been proposed by Kryter, Stevens, and Zwicker for the calculation of both loudness and loudness levels. While these are generally more successful than simple electronic filtering in correlating with the human perception of loudness, their complexity limits their usefulness.

Electrical Weighting Networks

Although the Fletcher Munson curves provided an accurate measure of the relative loudness of tones, their shape was too complicated for use with an analog sound level meter. To overcome this problem, electrical weighting networks or filters were developed, which approximate the Fletcher Munson curves. These frequency weighting schemes were designated by letters of the alphabet, A, B, C, and so forth. The A, B, and C-weighting networks were designed

FIGURE 3.11   Frequency Response Characteristics in the American National Standards Specification for Sound Level Meters (ANSI-S1.4 – 1971)
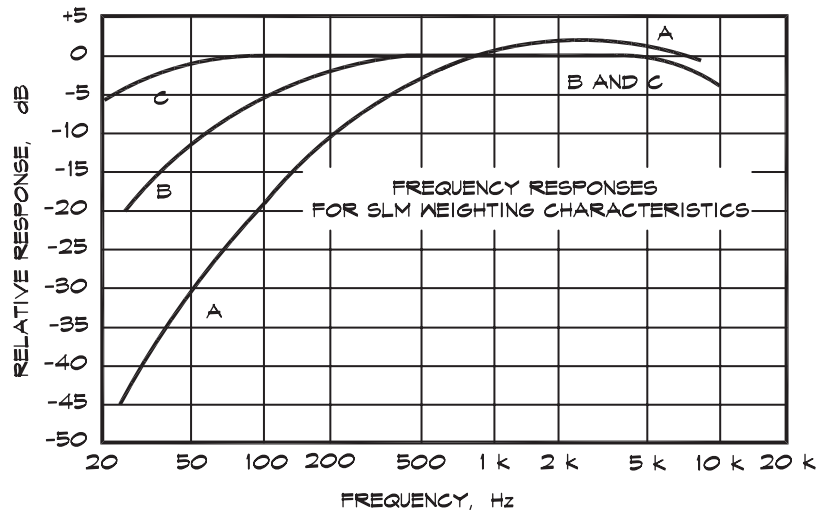
to roughly mirror the 40, 60, and 80 phon lines (turned upside down) shown in Fig. 3.11. The relative weightings in each third-octave band for the A and C filters are set forth in Table 3.1. Since the time of their original development other weighting curves have been suggested. Several D-weighting curves are detailed by Kryter (1970) and an E curve has been suggested, but these systems, along with B-weighting, have not found widespread acceptance.

Only the A and C curves are still in general use. The A-weighted level (dBA) is the most common single number measure of loudness. The C-weighting network is used mainly as a measure of the broadband sound pressure level. Occasionally an ($L_C - L_A$) level is used to describe the relative contribution of low-frequency noise to a spectrum. The weightings can be applied to sound power or sound pressure levels.

Once a weighting is applied it should not be reapplied. For example, if a recording is made of environmental noise using an A-weighting filter (not a recommended practice) it should not be analyzed by playing it back through a meter using the A-weighting network. It is, however, not uncommon to use a C-weighting filter when recording environmental noise, since it limits the low-frequency sounds that can overload the tape recorder. Replaying a tape thus recorded back through an A-weighting filter would be a reasonable practice so long as the main frequencies of interest were those unaffected by the C-weighting.

It is not uncommon to encounter A-weighted octave or third-octave band levels. These levels, if appropriately designated, are understood to have had the weighting already applied. A-weighted octave-band levels can be calculated from third-octave levels using Eq. 2.62 to combine the three levels within a particular octave band. Likewise overall A-weighted levels can be calculated from A-weighted octave-band levels by using the same formula.

Noise Criteria Curves (NC and RC)

Loudness curves based on octave-band sound pressure level measurements are commonly used in buildings to establish standards for various types of activities. The *noise criterion* (NC) curves shown in Fig. 3.12 were developed by Beranek in 1957 to establish satisfactory

TABLE 3.1 Electrical Weighting Networks

Frequency Hz	A-Weighting Relative Response, dB	C-Weighting Relative Response, dB
12.5	−63.4	−11.2
16	**−56.7**	**−8.5**
20	−50.5	−6.2
25	−44.7	−4.4
31.5	**−39.4**	**−3.0**
40	−34.6	−2.0
50	−30.2	−1.3
63	**−26.2**	**−0.8**
80	−22.5	−0.5
100	−19.1	−0.3
125	**−16.1**	**−0.2**
160	−13.4	−0.1
200	−10.9	0
250	**−8.6**	**0**
315	−6.6	0
400	−4.8	0
500	**−3.2**	**0**
630	−1.9	0
800	−0.8	0
1,000	**0**	**0**
1,250	+0.6	0
1,600	+1.0	−0.1
2,000	**+1.2**	**−0.2**
2,500	+1.3	−0.3
3,150	+1.2	−0.5
4,000	**+1.0**	**−0.8**
5,000	+0.5	−1.3
6,300	−0.1	−2.0
8,000	**−1.1**	**−3.0**
10,000	−2.5	−4.4
12,500	−4.3	−6.2
16,000	**−6.6**	**−8.5**
20,000	−9.3	−11.2

conditions for speech intelligibility and general living environments. They are expressed as a series of curves, which are designated NC-30, NC-35, and so on, according to where the curve crossed the 1750 Hz frequency line in an old (now obsolete) octave-band designation. The NC level is determined from the lowest NC curve, which may be drawn such that no point on a measured octave-band spectrum lies above it. Since the NC curves are defined in 5 dB intervals, in between these values the NC level is interpolated.

FIGURE 3.12 Noise Criterion (NC) Curves (Beranek, 1957)
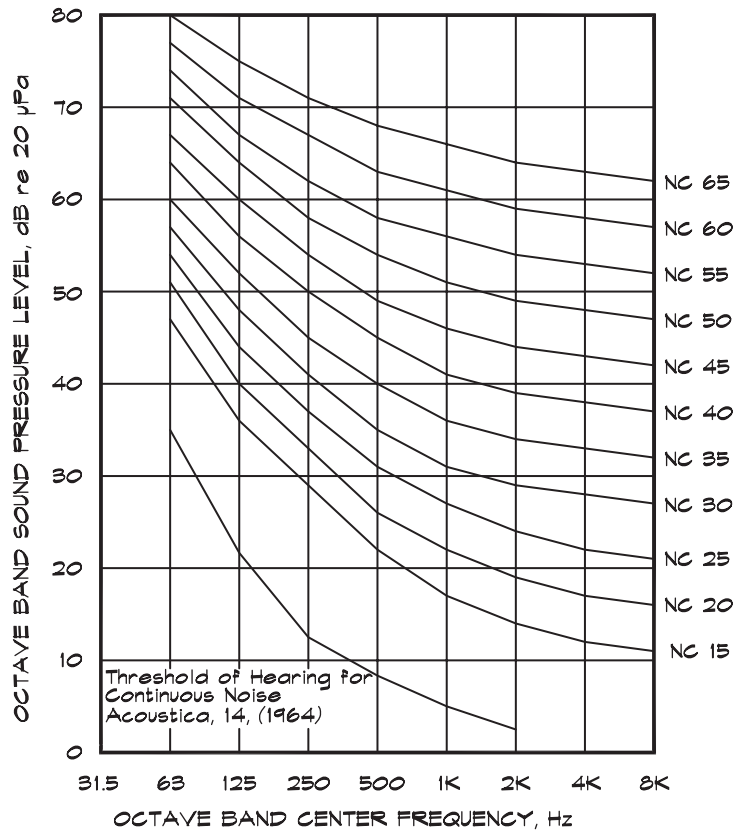
The NC level depends on the actual measured (or calculated) spectrum of the sound but they can be generally related to an overall A-weighted level (Kinsler et al., 1982)

$$NC \cong 1.25 \, (L_A - 13) \tag{3.2}$$

where   NC = NC level, dB

L_A = sound pressure level, dBA

In 1981 Blazier developed the set of curves, shown in Fig. 3.13, called *room criterion* (RC) curves, based on an American Society of Heating, Refrigeration, and Air Conditioning Engineers (ASHRAE) study of heating, ventilating, and air conditioning (HVAC) noise in office environments. Since these curves are straight lines, spaced 5 dB apart, there is no confusion about the level, which can occur sometimes with NC levels. RC curves are more stringent at low frequencies but include 5 dB of leeway in the computation methodology. The RC level is the arithmetic average of the 500, 1000, and 2000 Hz octave-band values taken from the measured spectrum. At frequencies above and below these center bands a second parallel line is drawn. Below 500 Hz the line is 5 dB above the corresponding RC line and above 2000 Hz it is 3 dB above the line. If the measured spectrum exceeds the low-frequency line the RC level is given the designation R for rumble. If it exceeds the high-frequency line the designation is H for hissy. Otherwise the designation is N for normal.

FIGURE 3.13   Room Criterion (RC) Curves (Blazier, 1981)
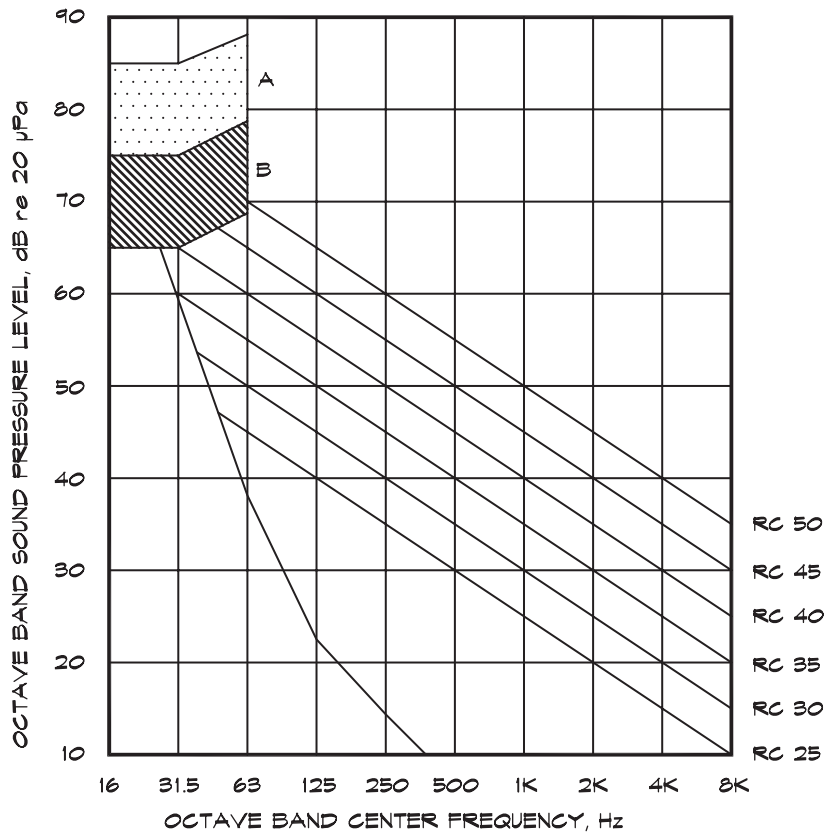
Blazier added two other regions to these curves at the low frequencies where mechanical vibrations can be a nuisance in lightweight structures. In region A there is a high probability of noticeable vibrations accompanying the noise while in region B there is a low probability of that occurring, particularly in the lower portion of the curve.

From time to time ASHRAE publishes a guide to assist in the calculation and treatment of HVAC generated noise levels. As part of this guide they include suggested levels of noise for various classifications of interior space. In general these guidelines are applied to noise generated by equipment associated with a building, such as HVAC systems within a dwelling or office, or noise generated in an adjacent room by HVAC, pumps, fans, or plumbing. The standards are not generally applied to noise generated by appliances, which plug into wall sockets within the same dwelling unit. A portion of the 1987 ASHRAE guidelines are shown in Table 3.2.

Just Noticeable Difference

One of the classic psychoacoustic experiments is the measurement of a *just noticeable difference* (jnd), which is also called a difference limen. In these tests a subject is asked to compare two sounds and to indicate which is higher in level, or in frequency. What is found is that the jnd in level depends on both the intensity and frequency. Table 3.3 shows jnd level values at various sound pressure levels and frequencies. For sound levels exceeding 40 dB and at frequencies above 100 Hz, the jnd is less than 1 dB. At the most sensitive levels

TABLE 3.2 Interior Noise Design Goals (ASHRAE, 1987)

	Type of Area	Recommended NC or RC Criteria Range
1	Private Residences	25 to 30
2	Apartments	25 to 30
3	Hotels/motels	
	a Individual rooms or suites	30 to 35
	b Meeting/banquet rooms	25 to 30
	c Halls, corridors, lobbies	35 to 40
	d Service/support areas	40 to 45
4	Offices	
	a Executive	25 to 30
	b Conference room	25 to 30
	c Private	30 to 35
	d Open plan areas	35 to 40
	e Computer equipment rooms	40 to 45
	f Public circulation	40 to 45
5	Hospitals and clinics	
	a Private rooms	25 to 30
	b Wards	30 to 35
	c Operating rooms	35 to 40
	d Corridors	35 to 40
	e Public areas	35 to 40
6	Churches	25 to 30
7	Schools	
	a Lecture and classrooms	25 to 30
	b Open plan classrooms	30 to 35
8	Libraries	35 to 40
9	Concert halls	5 to 15*
10	Legitimate theaters	20 to 30
11	Recording studios	10 to 20*
12	Movie theaters	30 to 35

*Note: Where ASHRAE has recommended that an acoustical engineer be consulted, the author has supplied the NC or RC levels.

TABLE 3.3 Minimum Detectable Changes (JND) in Level for Sine Waves, dB (Pierce, 1983)

Freq.	Signal Level, dB											
Hz	5	10	20	30	40	50	60	70	80	90	100	110
35	9.3	7.8	4.3	1.8	1.8							
70	5.7	4.2	2.4	1.5	1.0	.75	.61	.57	1.0	1.0		
200	4.7	3.4	1.2	1.2	.86	.68	.53	.45	.41	.41		
1000	3.0	2.3	1.5	1.0	.72	.53	.41	.33	.29	.29	.25	.25
4000	2.5	1.7	.97	.68	.49	.41	.29	.25	.25	.21	.21	
8000	4.0	2.8	1.5	.90	.68	.61	.53	.49	.45	.41		
10,000	4.7	3.3	1.7	1.1	.86	.75	.68	.61	.57			

TABLE **3.4** **Minimum Detectable Changes (JND) in Frequency for Sine Waves, Cents (Pierce, 1983)**

Frequency	Signal Level, dB										
Hz	5	10	15	20	30	40	50	60	70	80	90
31	220	150	120	97	76	70					
62	120	120	94	85	80	74	61	60			
125	100	73	57	52	46	43	48	47			
250	61	37	27	22	19	18	17	17	17	17	
500	28	19	14	12	10	9	7	6	7		
1000	16	11	8	7	6	6	6	6	5	5	4
2000	14	6	5	4	3	3	3	3	3	3	
4000	10	8	7	5	5	4	4	4	4		
8000	11	9	8	7	6	5	4	4			
11,700	12	10	7	6	6	6	5				

(greater than 60 dB) and frequencies (1000–4000 Hz), the jnd is about a quarter of a dB. When the jnd is 0.25 dB it means that we can notice a sound, with the same spectrum, which is 13 dB below the level of the background. This has important implications for both privacy and intelligibility in the design of speech reinforcement systems.

The jnd values in frequency for sine waves are shown in Table 3.4. Like the jnd in level, it is also dependent on both intensity and frequency. At 2000 Hz, where we are most sensitive, the jnd is about 3 cents (0.3% of an octave) or about 0.5% of the pure tone frequency for levels above 30 dB. This is about 10 Hz. Some trained musicians can tell the difference between a perfect fifth (702 cents) and an equal tempered fifth (700 cents), so that greater sensitivity is not uncommon. Note that these comparisons are done by sounding successive tones or by varying the tone, not by comparing simultaneous tones where greater precision is obtainable by listening for beats. Piano tuners who tune by ear use this latter method to achieve precise tuning.

Environmental Impact

Environmental Impact Reports (EIR) in California or Environmental Impact Statements (EIS) for Federal projects are prepared when a proposed project has the potential of creating a significant adverse impact on the environment (California Environmental Quality Act, 1972). Noise is often one of the environmental effects generated by a development, through increases in traffic or fixed noise sources. Impact may be judged either on an absolute scale through comparison with a standard such as a property line ordinance or a Noise Element of a General Plan, or on a relative scale through changes in level. In the exterior environment the sensitivity to changes in noise level is not as great as in the laboratory under controlled conditions. A 1 dB change is the threshold for most people. Since the change in level due to multiple sound sources is equal to $10 \log N$, where N is the ratio of the new to the old number, it takes a 1.26 ratio or a 26% increase in traffic passing by on a street to produce a 1 dB change. Table 3.5 shows a general characterization of human reaction to changes in level.

TABLE 3.5 Human Reaction to Changes in Level

Change in Level (dB)	Reaction
1	Noticeable
3	Very Noticeable
6	Substantial
10	Doubling (or Halving)

The characterizations listed in Table 3.5 are useful in gauging the reaction to changes in environmental noise. If a project increases the overall noise level at a given location by 1 dB or more, it is likely to be noticeable and could potentially constitute an adverse environmental impact. A 3 dB increase is very noticeable and, in the case of traffic flow, represents a doubling in traffic volume.

3.4   INTELLIGIBILITY

Masking

When we listen to two or more tones simultaneously, if their levels are sufficiently different, it becomes difficult to perceive the quieter tone. We say that the quieter sound is *masked* by the louder. Masking can be understood in terms of a threshold shift produced by the louder tone due to its overlap within the critical band on the cochlea. Figure 3.14 illustrates this principle. The figure is helpful in understanding the findings of experiments associated with

FIGURE 3.14   Overlap of Regions of the Cochlea (Rossing, 1990)
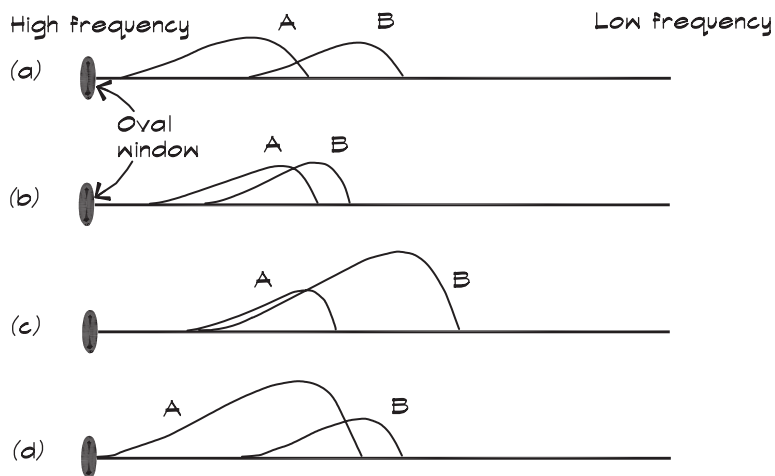
Simplified response of the basilar membrane for two pure tones A and B. (a) The excitations barely overlap; little masking occurs. (b) There is an appreciable overlap; tone B masks tone A and somewhat more than the reverse. (c) The more intense tone B almost completely masks the higher-frequency tone A. (d) The more intense tone A does not completely mask the lower-frequency tone B.

masking. Tones that are close in frequency mask each other more than those that are widely separated.

Tones mask upward in frequency rather than downward. The louder the masking tone the wider the range of frequencies it can mask. Masking by narrow bands of noise mimics that of pure tones and broad bands of noise mask at all frequencies. Early experiments on masking the audibility of tones in the presence of noise were performed by Wegel and Lane (1924) and subsequently published by Fletcher (1953). Two tones are presented to each subject. The first is a constant masking tone at a given level and frequency. A second tone

FIGURE 3.15   Pure Tone Masking Curves (Fletcher, 1953)
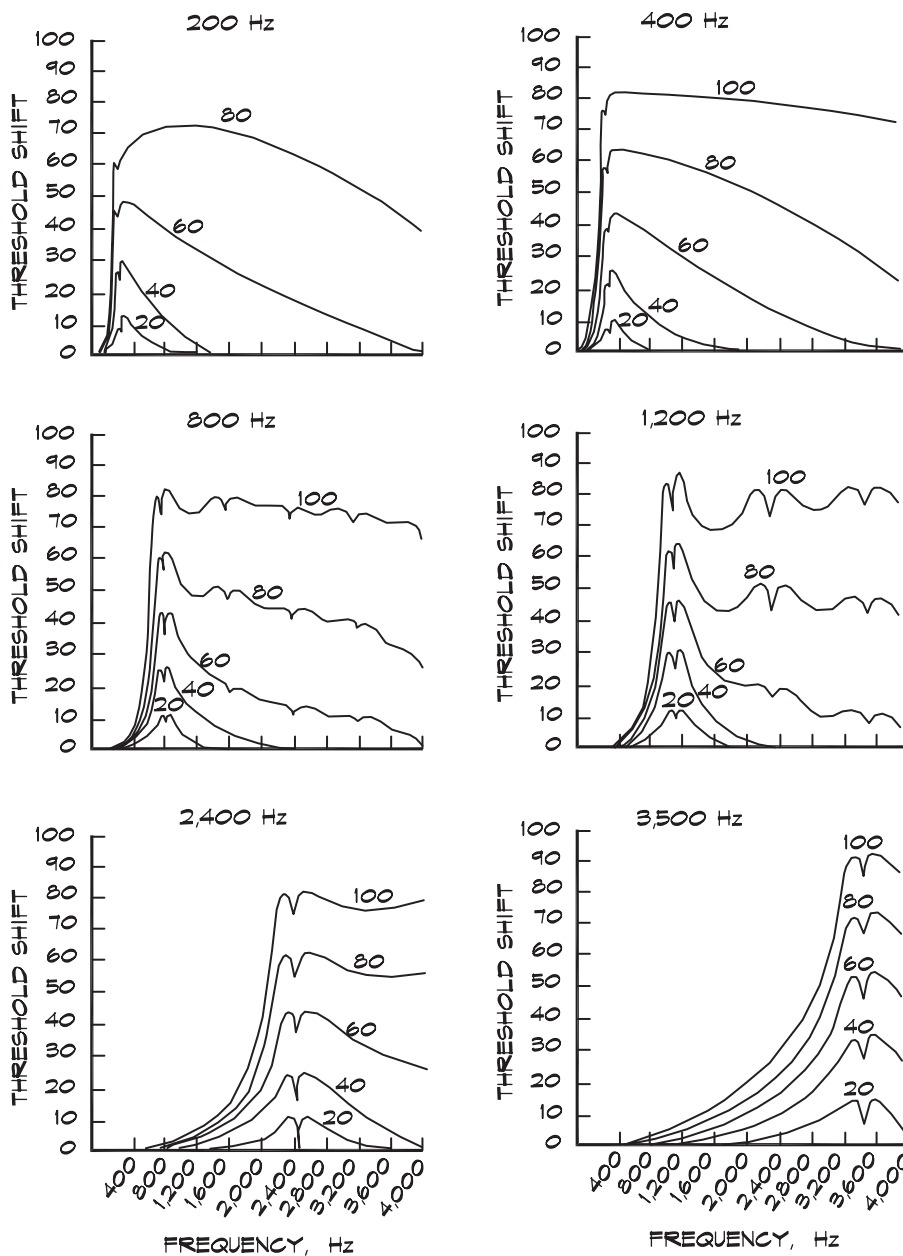
is introduced at a selectable frequency and its level is reduced until it is no longer audible. Based on these types of tests a series of masking curves can be drawn, which are shown in Fig. 3.15. Each curve shows the threshold shift of the masked tone or the difference between its normal threshold of audibility and the new threshold in the presence of the masking tone. For example in the second curve the masking tone is at 400 Hz. At 80 dB it induces a 60 dB threshold shift in an 800 Hz tone. From Fig. 3.9 we can see that the threshold of tonal hearing at 800 Hz is 0 dB, so the level above which the 800 Hz tone is audible is 60 dB. The fine structure on the masking curves is interesting. Around the frequency of the masking tone there are little dips in threshold shift—which is to say the ear becomes more sensitive. These dips repeat at the harmonics of the masking frequency. The reason is that when the two frequencies coincide, beats are generated that alert us to the presence of the masked tone.

As the level of the masking tone is increased, the breadth of its influence increases. A 400 Hz masking tone at 100 dB is effective in swamping the ear's response to 4000 Hz tones, while a 40 or 60 dB masking tone does little at these frequencies. At low levels the bandwidth of masking effectiveness is close to the critical bandwidth. High-frequency masking tones have little or no effect on lower frequency tones. A 2400 Hz masking tone will not mask a 400 Hz tone no matter how loud it is. This graphically illustrates the effect of the shape of the cochlear filter skirts.

Masking experiments also can be used to define critical bands. In the standard masking test a tone is not audible in the presence of masking noise until its level exceeds a certain value. The masking noise can be configured to have an adjustable bandwidth and the tests can be repeated for various noise bandwidths. It has been found (Fletcher and Munson, 1937) that masking is independent of noise bandwidth until the bandwidth is reduced below a certain value. This led to a separate way of measuring critical bandwidths, which gave results similar to those achieved using consonance and dissonance.

Masking is an important consideration in architectural acoustics. It is of particular interest to an acoustician whether speech will be intelligible in the presence of noise. In large indoor facilities, such as air terminals or sports arenas, low-frequency reverberant noise can mask the intelligibility of speech. This can be partially treated by limiting the bandwidth of the sound system or by adding low-frequency absorption to the room. The former is less expensive but limits the range of uses. Multipurpose arenas, which are hockey rinks one day and rock venues the next, should have an acoustical environment that does not limit the uses of the space.

Speech Intelligibility

Speech intelligibility is a direct measure of the fraction of words or sentences understood by a listener. The most direct method of measuring intelligibility is to use sentences containing individual words or nonsense syllables, which are read to listeners who are asked to identify them. These can be presented at various levels in the presence of background noise or reverberation. Both live and recorded voices are used, however recorded voices are more consistent and controllable.

Three types of material are typically used: sentences, one syllable words, and nonsense syllables, with each type being increasingly more difficult to understand in the presence of noise. In sentence tests a passage is read from a text. In a word test individual words are read from a predetermined list, called a closed response word set, and subjects are asked to pick the correct one. A modified rhyme test uses 50 six-word groups of monosyllabic rhyming or similar-sounding English words. Subjects are asked to correctly identify the spoken word

FIGURE 3.16   Results of a Typical Intelligibility Test (Miller et al., 1951)

Intelligibility of different types of test materials in the presence of noise. Speech intelligibility is shown as a function of speech-to-noise ratio for sentences, monosyllabic words, and nonsense syllables.
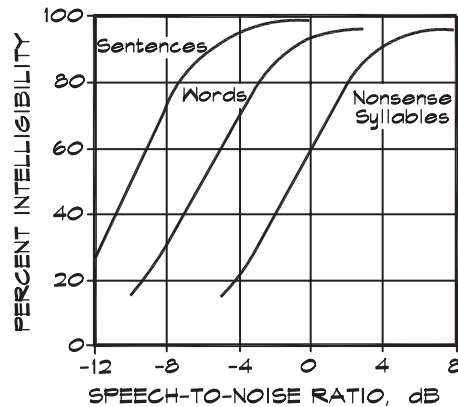
from the list of six possible choices. A group of words might be: sag, sat, sass, sack, sad, and sap. Tests of this type lead to a measure of the fraction, ranging from 0 to 1, of words that are correctly identified. Figure 3.16 shows some typical results.

The degree to which noise inhibits intelligibility is dependent on the *signal-to-noise ratio*, which is simply the signal level minus the noise level in dB. When the noise is higher than the speech level, the signal-to-noise ratio is negative. A signal-to-noise ratio is a commonly used concept in acoustics, audio, and electrical engineering. It is called a ratio since it represents the energy of the signal divided by the energy of the noise, expressed in decibels. For a typical test the noise is broad band steady noise such as that produced by a waterfall.

What is apparent from Fig. 3.16 is that even when the signal-to-noise is negative, speech is still intelligible. This is not surprising since the brain is an impressive computer, which can select useful information and fill in the gaps between the words we understand. For most applications if we can grasp more than 85–90% of the words being spoken we achieve very good comprehension—virtually 100% of the sentences. With an understanding of more than 60% of the words we can still get 90% of the sentences and that is quite good. If we understand fewer than 60% of the words the intelligibility drops off rapidly.

Speech Interference Level

Signal-to-noise ratio is the key to speech intelligibility, and we obtain more precise estimates of the potential interference by studying the background noise in the speech frequency bands. The *speech interference level* (SIL) is a measure of a background noise's potential to mask speech. It is calculated by arithmetically averaging separate background noise levels in the four speech octave bands, namely 500, 1000, 2000, and 4000 Hz. The SIL can then be compared to the expected speech sound pressure level to obtain a relevant speech to noise ratio.

Figure 3.17 shows the expected distance over which just-reliable communications can be maintained for various speech interference level values. The graph accounts for the

FIGURE 3.17   Rating Chart for Determining Speech Communication (Webster, 1969)
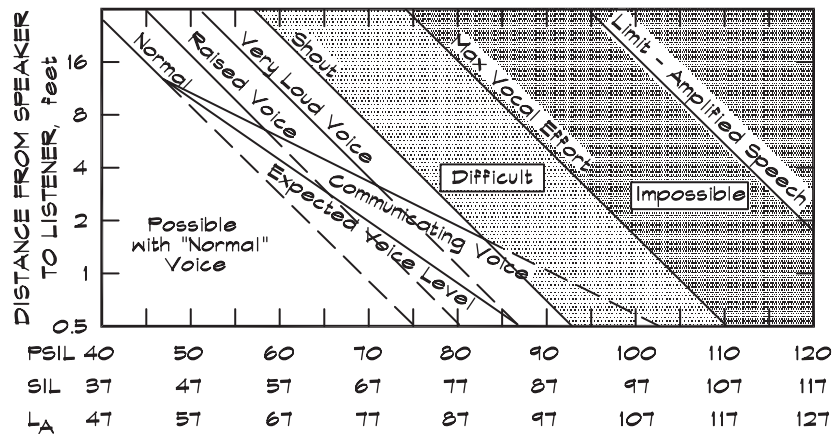
expected rise in voice level, which occurs in the presence of high background noise. Note that these types of analyses assume a flat spectrum of background noise, constant speech levels, and non-reverberant spaces.

The *preferred speech interference level* (PSIL) is another similar metric, calculated from the arithmetic average of background noise levels in the 500, 1000, and 2000 Hz octave bands. The PSIL can also be used to obtain estimates of the intelligibility of speech in the presence of noise.

Articulation Index

The *articulation index* (AI) is a detailed method of measuring and calculating speech intelligibility (French and Steinberg, 1947). To measure the AI, a group of listeners is presented a series of phonemes for identification. Each of the test sounds consists of a logatom, or structured nonsense syllable in the form of *a consonant-vowel-consonant* (CVC) group embedded in a neutral carrier sentence, which cannot be recognized from its context in the sentence. An example might be, "Now try pom." The fraction of syllables understood is the AI.

Developed by researchers at Bell Laboratories in the late 1920s and early 1930s, including Fletcher, French, Steinberg, and others, it also included a method of calculating the expected speech intelligibility by using signal-to-noise ratios in third-octave bands, which are then weighted according to their importance. In this method speech intelligibility is proportional to the long-term rms speech signal plus 12 dB minus the noise in each band. The proportionality holds provided the sum of the terms falls between 0 and 30 dB. Figure 3.18 shows the calculation method along with the weighting factors used in each band. In each of 15 third-octave bands the signal-to-noise ratio is multiplied by a factor and the results are added together.

AI calculations can be made even when the spectrum of the background noise is not flat and is different from that of speech. It also accounts in part for the masking of speech by low-frequency noise. AI uses the peak levels generated by speech as the signal level and the energy average background levels as the noise. Consequently the signal-to-noise ratios are somewhat higher than other methods, such as SIL, which are based on average speech levels for the same conditions.

FIGURE 3.18   An Articulation Index Calculation (Kryter, 1970)
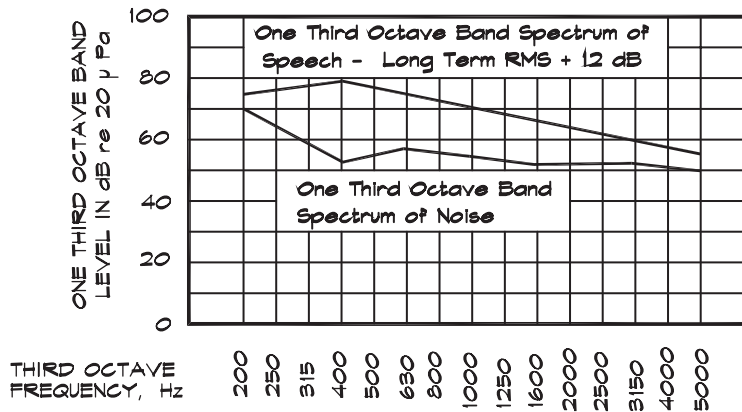
BAND	SPEECH PEAKS MINUS NOISE (dB)	WEIGHT	COLUMN 2 × 3
200	5	0.0004	0.0020
250	12	0.0010	0.0120
315	18	0.0010	0.0180
400	26	0.0014	0.0364
500	23	0.0014	0.0322
630	18	0.0020	0.0360
800	17	0.0020	0.0340
1000	16	0.0024	0.0384
1250	15	0.0030	0.0450
1600	14	0.0037	0.0518
2000	12	0.0037	0.0444
2500	10	0.0034	0.0340
3150	8	0.0034	0.0272
4000	6	0.0024	0.0144
5000	5	0.0020	0.0100
			AI = 0.4358

A typical AI calculation using the data shown in the graph. The one-third octave band spectrum of speech is used plus 12 dB and the noise spectrum is subtracted in each band. The result is multiplied by a weighting factor according to the band and the result is summed to obtain an overall Articulation Index figure.

The result of an AI calculation is a numerical factor, which ranges from 0 to 1, with 1 being 100% word or sentence comprehension. Beranek (1947) suggested that a listening environment with an AI of less than 0.3 will be found to be unsatisfactory or marginally satisfactory, while AI values between 0.3 to 0.5 will generally be acceptable. For AI values of 0.5 to 0.7 intelligibility will be good, and above 0.7 intelligibility will be very good to excellent. Figure 3.19 shows the relation between the AI and other measures of speech intelligibility.

AL_{CONS}

The *articulation loss of consonants* (AL_{CONS}), expressed as a percentage, is another way of characterizing the intelligibility of speech. Similar to the articulation index, it measures the proportion of consonants wrongly understood. V. Peutz also found that the correlation

FIGURE 3.19   Relation between AI and Other Speech Intelligibility Tests (ANSI S3.5, 1969)
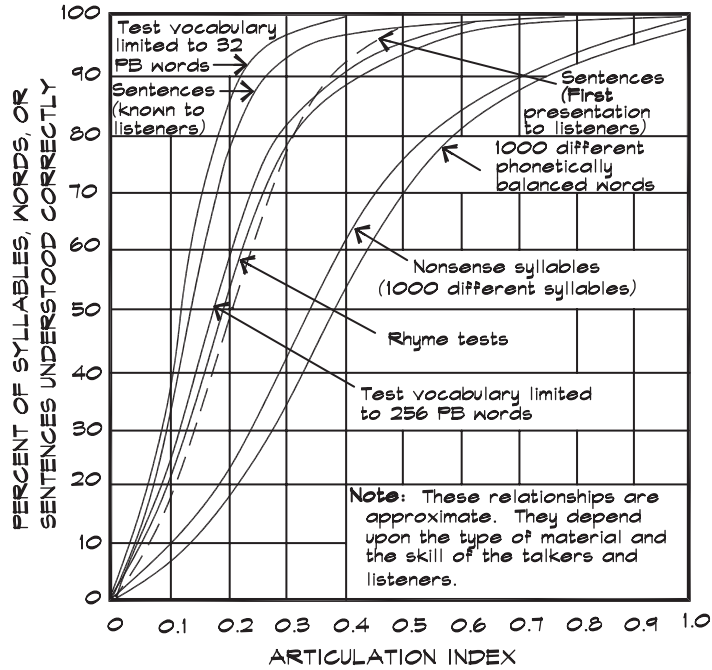
between the loss of consonants (in Dutch) is much more reliable than a similar test with vowels. He published (1971) a relationship to predict intelligibility for unamplified speech in rooms, which had been studied much earlier at Bell Labs.

$$AL_{CONS} = \frac{200 \, r^2 \, T_{60}^2}{V} \tag{3.3}$$

Beyond the limiting distance $r_\ell = 0.21\sqrt{V/T_{60}}$

$$AL_{CONS} = 9 \, T_{60} \tag{3.4}$$

where T_{60} = reverberation time, (s)
$\quad\quad\quad$ V = room volume, (m^3)
$\quad\quad\quad$ r = talker to listener distance, (m)

Privacy

The inverse of intelligibility is *privacy*, and articulation index is equally useful in the calculation of privacy as it was for intelligibility. Both are ultimately dependent on signal-to-noise ratio. Chanaud (1983) defined five levels of privacy, which are shown in Table 3.6, and has related them to AI in Fig. 3.20.

TABLE **3.6 Degrees of Acoustical Privacy (Chanaud, 1983)**

Degree of Privacy	Acoustical Condition	Possible Subjective Response
Confidential Privacy	**Cannot converse with others. Cannot understand speech of others. May not be aware of presence of others. May not hear activity sounds of others. Confidential conversations possible. No distractions.**	**Complete privacy. Sense of isolation. No privacy complaints expected.**
Normal Privacy	**Difficult to converse with others. Occasionally hear the activity sounds of others. Aware of the presence of others. Speech and machines audible but not distracting. Confidential conversations possible only under special conditions.**	**Sense of privacy. Some isolation. No privacy complaints expected.**
Marginal Privacy	**Possible to converse with others by raising voice. Often hear activity sounds and speech of others. Aware of each others presence. Conversations of others occasionally understood.**	**Sense of community. Sense of privacy weakened. Some privacy complaints expected.**
Poor Privacy	**Possible to converse with others at normal voice levels. Activity sounds, speech, and machines will be continually heard. Continually aware of each others presence. Frequent distractions.**	**Sense of community. Loss of privacy. Some loss of territory. Privacy complaints expected.**
No Privacy	**Easy to converse with others. Machine and activity sounds clearly audible. Total distraction from other tasks.**	**Sense of community. Sense of intrusion on territory. No sense of privacy. Many privacy complaints expected.**

3.5   ANNOYANCE

Noisiness

Comparative systems, similar to those used in the judgment of loudness, have been developed to measure *noisiness*. Subjects were asked to compare third-octave bands of noise at differing levels based on a judgment of relative or absolute noisiness. Somewhat surprisingly, the results shown in Fig. 3.21 (Kryter, 1970) differ from a loudness comparison. Relative noisiness is described by a unit called noys, a scale that is linear in noisiness much like the sone is for loudness. It is converted into a decibel-like scale called *perceived noise level* (PNL) with units of PNdB, by requiring the noisiness to double every 10 dB. The perceived noise level scale is used extensively in the evaluation of aircraft noise. The work of other investigators: Ollerhead (1968), Wells (1967), and Stevens (1961) is also shown in the figure.

Noisiness is affected by a number of factors that do not influence loudness (Kryter, 1970). Two that do affect loudness are the spectrum and the level. Others that do not

FIGURE 3.20   Level of Privacy vs Articulation Index (Chanaud, 1983)
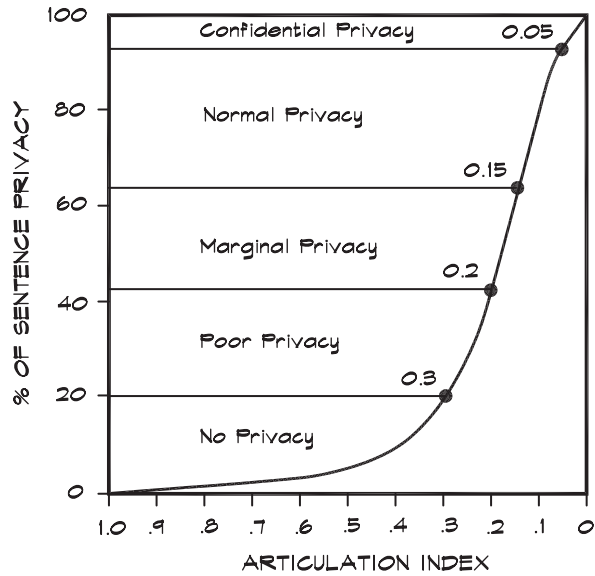
FIGURE 3.21   Equal Noisiness Contours of Various Authors (Kryter, 1970)
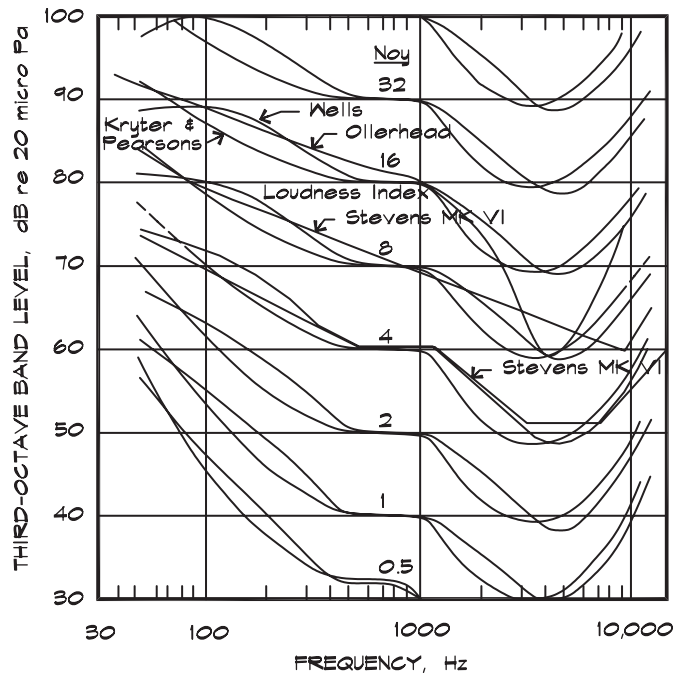
include: 1) spectrum complexity, namely the concentration of energy in pure tone or narrow frequency bands; 2) total duration; 3) in nonimpulsive sounds, the duration of the increase in level prior to the maximum level, called onset time; and 4) in impulsive sounds, the increase in level in a 0.5 second interval. Although these factors normally are not encountered in architectural acoustics, they contribute to various metrics in use in the United States and

in Europe, particularly in the area of aircraft noise evaluation. For further details refer to Kryter (1970).

Time Averaging - L_{eq}

Since the duration of a sound can influence its perceived noisiness, schemes have been developed to account for the tradeoff between level and time. Some of these systems are stated implicitly as part of a particular metric, while others appear in noise standards such as those promulgated by the Occupational Safety and Health Administration (OSHA) or in various noise ordinances.

To a casual observer the simplest averaging scheme would appear to be the arithmetic average of measured levels over a given time period. The advantage of this type of metric is that it is simple to measure and is readily understandable to the layman. Two disadvantages of the arithmetic average are: 1) when there are large variations in level it does not accurately account for human reaction to noise, and 2) for doing prediction calculations on moving sources it is enormously cumbersome.

When a sound level varies in time it is convenient to have a single number descriptor, which accurately represents the effect of the temporal variation. In 1953, Rosenblith and K.N. Stephens suggested that a metric be developed, which included frequency weighting and a summation of noise energy over a 24-hour period. A number of metrics have since evolved that include some form of energy summation or energy averaging. The system most commonly encountered is the equivalent level or L_{eq} (pronounced ell-ee-q), defined as the steady A-weighted level that contains the same amount of energy as the actual time-varying A-weighted level during a given period. The L_{eq} can be thought of as an average sound pressure level, where the averaging is based on energy. To calculate the L_{eq} level from individual sound pressure level readings, an average is taken of the normalized intensity values, and that average is converted back into a level. Mathematically it is written as an integral over a time interval

$$L_{eq} = 10 \, \log \frac{1}{T} \int_{t=0}^{T} 10^{0.1 \, L(t)} \tag{3.5}$$

or as a sum over equal-length periods

$$L_{eq} = 10 \, \log \frac{1}{N \, \Delta t} \sum_{i=1}^{N} 10^{0.1 \, L_i} \Delta t = 10 \, \log \frac{1}{N} \sum_{i=1}^{N} 10^{0.1 \, L_i} \tag{3.6}$$

where　L_{eq} = equivalent sound level during the time period of interest (dB)

　　　$L(t)$ = the continuous sound level as a function of time

　　　　L_i = an individual sample of the sound level, which is representative of the i th time period Δt

It has been found that human reaction to time-varying noise is quite accurately represented by the equivalent level. L_{eq} emphasizes the highest levels that occur during a given time period, even if they are very brief. For example it is clear that for a steady noise level

that does not vary over a time period, the L_{eq} is the same as the average level L_{ave}. However if there is a loud noise, say 90 dBA for one second, and 30 dBA for 59 seconds, then the L_{eq} for the minute time period would be 72.2 dBA. The L_{ave} for the same scenario is 31 dBA. The L_{eq} is much more descriptive of the noise experienced during the period than the L_{ave}. When equivalent levels are used in environmental calculations, they are often based on a one-hour time period. When they begin and end on the hour they are called hourly noise levels, abbreviated HNL.

Twenty - Four Hour Metrics – L_{dn} and CNEL

One metric enjoying widespread acceptance is the L_{dn} or *day-night level*, which was recommended by the U.S. Environmental Protection Agency (EPA) for use in the characterization of environmental noise (von Gierke, 1973). The L_{dn}, or as it is sometimes abbreviated, the DNL, is a 24-hour L_{eq} with the noise occurring between the hours of 10 PM and 7 AM the next day increased by 10 dB before averaging. The L_{dn} is always A-weighted but may be measured using either fast or slow response.

$$L_{dn} = 10 \, \log \left\{ \frac{1}{24} \left[\sum_{i=8}^{22} 10^{0.1 \, HNL_i} + (10) \sum_{i=23}^{7} 10^{0.1 \, HNL_i} \right] \right\} \qquad (3.7)$$

Each of the individual sample levels in Eq. 3.7 is for an hour-long period ending at the military time indicated by the subscript. The multiplier of 10, which is the same as adding 10 dB, accounts for our increased sensitivity to nighttime sounds.

Another system, the Community Noise Equivalent Level (CNEL), is in use in California and predates the day-night level. It is similar to the L_{dn} in that it is an energy average over 24 hours with a 10 dB nighttime penalty; however, it also includes an additional evening period from 7 P.M. to 10 P.M., with a multiplier of 3 (equal to adding 4.8 dB).

$$CNEL = 10 \, \log \left\{ \frac{1}{24} \left[\sum_{i=8}^{19} 10^{0.1 \, HNL_i} + 3 \sum_{i=20}^{22} 10^{0.1 \, HNL_i} + 10 \sum_{i=23}^{7} 10^{0.1 \, HNL_i} \right] \right\} \quad (3.8)$$

Since the CNEL includes the extra evening factor it is always slightly higher than the L_{dn} level over the same time period. For most cases the two are essentially equal. Like the L_{dn}, the CNEL is A-weighted but is defined using the slow response.

Annoyance

The annoyance due to a sound can be highly personal. Any sound that is audible is potentially annoying to a given individual. Studies of annoyance have generally been based on the aggregate response of people exposed to various levels of noise. Much of the work in this field was done in the area of aircraft noise, and much of it is based on exterior noise levels. The U.S. EPA, following the mandate of the Noise Control Act of 1972, undertook a study of both the most appropriate metric to use for environmental noise and also the most appropriate levels. Since aircraft noise varies both from aircraft to aircraft and from day to day, the EPA study (von Gierke, 1973) recommended a 24-hour metric, namely the day-night level. They then developed recommendations on levels appropriate for public health and welfare (EPA Levels Document, 1974). Figure 3.22 shows part of the results of that study, specifically, the community reaction to exterior community noise of various types.

FIGURE 3.22   Community Reaction to Intrusive Noise (EPA Levels Document, 1974)
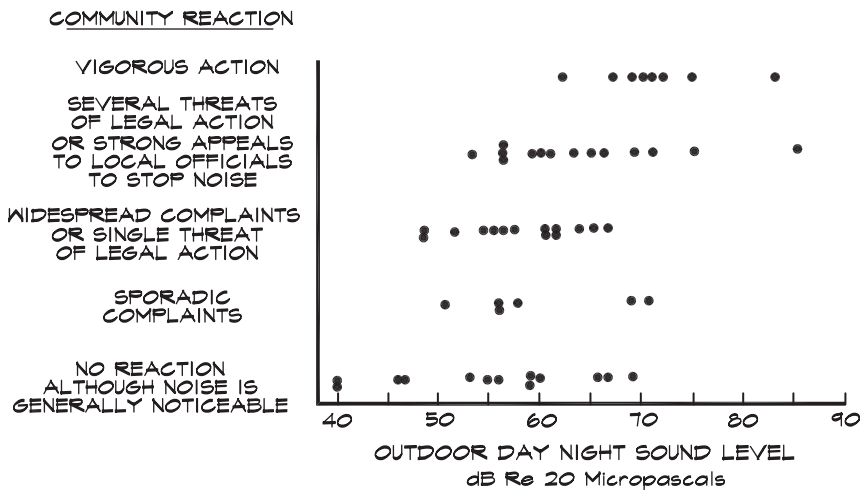
The data were very scattered. As a result of the wide variations in response an attempt was made to include factors other than level, duration, and time of day to normalize the results. A number of corrections were introduced, which were added to the raw day-night levels. These are listed in Table 3.7. Once the corrections had been applied, the data were replotted. The result is shown in Fig. 3.23, and the scatter is considerably reduced.

The final recommendations in the EPA Levels Document, for the levels of noise requisite to protect public health and welfare, are summarized in Table 3.8. It is interesting to note that the recommended exterior noise level of L_{dn} 55 does not guarantee satisfaction, and indeed according to the Levels Document it still leaves 17% of the population highly annoyed. Another interesting finding from this document, shown in Fig. 3.24, is that in one aircraft noise study, which related annoyance and complaints, the number of complaints lag well behind the number of people who are highly annoyed.

Satisfactory levels of interior noise are less well defined. Statutory limits in multifamily dwellings in California (CAC Title 24) are set at a CNEL (L_{dn}) 45 for noise emanating from outside the dwelling unit. It should be emphasized that statutory limits do not imply happiness. Rather they are the limits at which civil penalties are imposed. Many people are not happy with interior noise levels of L_{dn} 45 when the source of that noise is outside of their homes.

The 1987 ASHRAE guide suggests an NC 25 to 30 (30 to 35 dBA) as appropriate for residential and apartment dwellings. The EPA aircraft noise study (von Gierke, 1973) indicates that a nighttime level of 30 dBA in a bedroom would produce no arousal effects. Their recommendation of a maximum exterior L_{dn} of 60 dBA was based, in part, on a maximum interior level of 35 dBA at night with closed windows. The same reasoning, when applied to the Levels Document recommendations of L_{dn} 55 dBA, would yield a maximum nighttime level of 30 dBA with windows closed. Note that most residential structures provide about 20–25 dB of exterior to interior noise reduction with windows closed and about 10–15 dB with windows open. For purposes of this brief analysis maximum levels are taken to be 10 dB greater than the L_{eq} level. Van Houten (Harris, 1994) states that levels of plumbing related noise between 30 and 35 dBA in an adjacent unit can be "a source of

TABLE 3.7   Corrections to Be Added to the Measured Day-Night Sound Level (DNL) to Obtain the Normalized DNL (EPA Levels Document, 1974)

Type of Correction	Description	Correction (dBA)
Seasonal Correction	Summer (or year-round operation).	0
	Winter only (or windows always closed).	− 5
Correction for Outdoor Noise Level Measured in Absence of Intruding Noise	Quiet suburban or rural community (remote from large cities and industrial activities).	+ 10
	Normal suburban community (not located near industrial activities).	+ 5
	Urban residential community (not located adjacent to heavily traveled roads or industrial activities).	0
	Noisy urban residential community (near relatively busy roads or industrial areas).	− 5
	Very noisy urban residential community.	+ 10
Correction for Previous Exposure and Community Attitudes	No prior experience with intruding noise.	+ 5
	Community has had some previous exposure to intruding noise but little effort is being made to control the noise. This correction may also be applied in a situation where the community has not been exposed to the noise previously, but the people are aware that bona fide efforts are being made to control it.	0
	Community has had considerable previous exposure to intruding noise and the noise maker's relations with the community are good.	− 5
	Community is aware that operation causing noise is very necessary and it will not continue indefinitely. This correction can be applied for an operation of limited duration and under emergency circumstances.	− 10
Pure Tone or Impulse	No pure tone or impulsive character.	0
	Pure tone or impulsive character present.	+ 5

FIGURE **3.23** **Community Reaction to Intrusive Noise vs Normalized DNL Levels (EPA Levels Document, 1974)**
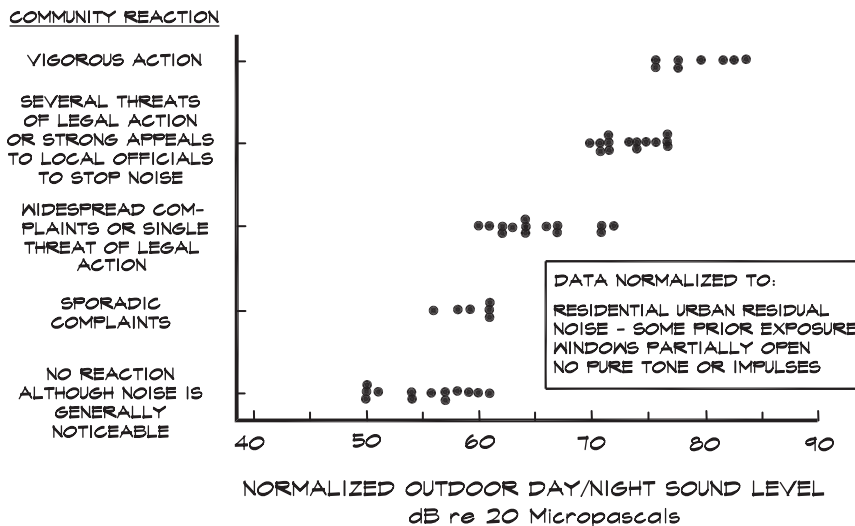
TABLE **3.8** **Summary of Noise Levels Identified as Requisite to Protect Public Health and Welfare with an Adequate Margin of Safety (EPA Levels Document 1974)**

EFFECT	LEVEL	AREA
Hearing loss	$L_{eq(24)}$ < 70 dBA	All areas
Outdoor activity interference and annoyance	L_{dn} < 55 dBA	Outdoors in residential areas and farms and other outdoor areas where people spend widely varying amounts of time and other places in which quiet is a basis for use.
	$L_{eq(24)}$ < 55 dBA	Outdoor areas where people spend limited amounts of time, such as school yards, playgrounds, etc.
Indoor activity interference and annoyance	L_{eq} < 45 dBA	Indoor residential areas.
	$L_{eq(24)}$ < 45 dBA	Other indoor areas with human activities such as schools, etc.

concern and embarrassment." In the author's practice in multifamily residential developments, intrusive levels generated by activities in another unit are rarely a problem below 25 dBA. At 30 dBA they are clearly noticeable and can be a source of annoyance, and above 35 dBA they frequently generate complaints.

FIGURE 3.24   Percentage Highly Annoyed as a Function of Percentage of Complaints (EPA Levels Document, 1974)

% Highly Annoyed = $12.3\sqrt{C}$ + 4.3
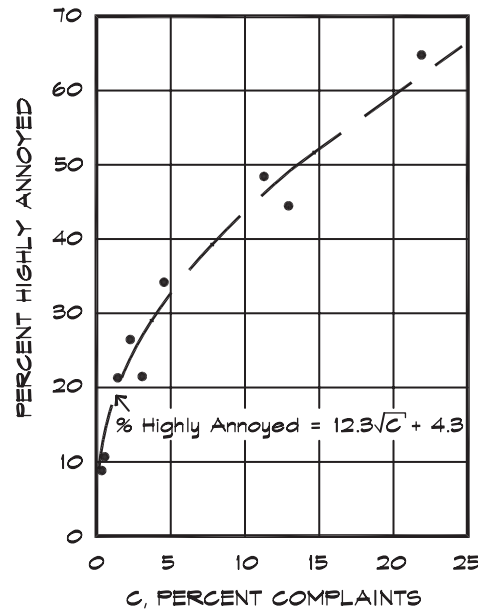
3.6   HEALTH AND SAFETY

Hearing Loss

Noise levels above 120 dB produce physical pain in the human ear. The pain is caused by the ear's unsuccessful attempt to protect itself against sound levels about 80 dB above the auditory threshold by reducing its own sensitivity through use of the aural reflex. Exposure to loud noise damages the cochlear hair cells and a loss of hearing acuity results. If the exposure to noise is brief and is followed by a longer period of quiet, the hearing loss can be temporary. This phenomenon, called *temporary threshold shift* (TTS), is a common experience. The normal sounds we hear seem quieter after exposure to loud noises. If the sound persists for a long time at a high level or if there is repeated exposure over time, the ear does not return to its original threshold level and a condition called *permanent threshold shift* (PTS) occurs. The damage is done to the hair cells in the cochlea and is irreversible. The process is usually a gradual one that occurs at many frequencies, but predominantly at the upper end of the speech band. The loss progressively inhibits the ability to communicate as we age.

Human hearing varies considerably with age, particularly in its frequency response. In young people it is not uncommon to find an upper limit of 20 to 25 kHz, while in a 40 to 50 year old an upper limit of between 10 kHz and 15 kHz is more normal. Most hearing losses with age occur at frequencies above 1000 Hz, with the most typical form being a deepening notch centered around 3500 Hz. Noise induced hearing loss contributes to presbycusis, which is hearing loss with age. Figure 3.25 shows some typical hearing loss curves, one set for workplace noise induced loss, and the other for age-related loss. Scientists do not agree to what extent presbycusis should be considered "natural" and to what extent it is brought on by environmental noise.

A task group was appointed by the EPA to review the research on the levels of noise that cause hearing loss (von Gierke, 1973). It published, as part of its final report, the relationship

FIGURE 3.25   Progressive Hearing Loss Curves (Schneider et al., 1970)
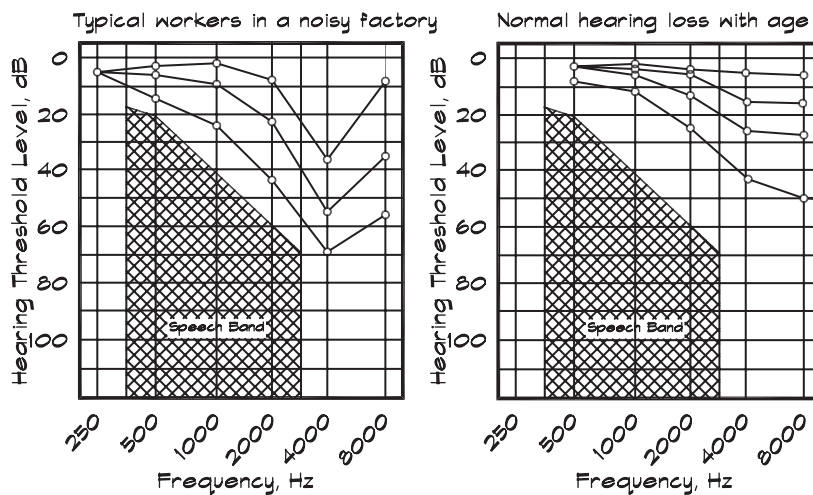
between daily noise exposure and noise induced hearing loss for the most sensitive 10% of the population. Based on this and other data the EPA task force recommended no more than a day-night level of 80 dBA to protect the population from adverse health effects on hearing. The EPA Levels Document (EPA, 1974) went further and recommended an 8-hour L_{eq} level of no more than 75 dBA to protect public health for purposes of hearing conservation alone. These studies found no physiological effects for levels below 70 dBA.

The U.S. Occupational Safety and Health Administration (OSHA) has set legal standards concerning noise exposure of workers in the workplace. The legal limit is 90 dBA (as measured using the slow meter response) for an 8-hour workday with a 5 dBA per time halving tradeoff. This means that a worker may be exposed to no more than 85 dBA for 16 hours, 90 dBA for 8 hours, 95 dBA for 4 hours, 100 dBA for 2 hours, 105 dBA for 2 hours, 110 dBA for 1 hour, or 115 dBA for any time. The OSHA standard exposure is based on a finding by the American Academy of Otolaryngology—Head and Neck Surgery (AAO-HNS) that a hearing loss is significant only when the average hearing threshold at 500, 1000, 2000, and 4000 Hz has increased 25 dB. Clearly OSHA standards are much less restrictive than EPA recommendations, which were established without consideration of cost.

Workplace noise limits are characterized in terms of a noise dose, which is a relative intensity multiplied by a time, expressed as a percentage of an allowable limit. Over a given time period the dose can be calculated from levels, L_i measured in a series of intervals T_i

$$D = (100/T_n) \sum_{i=1}^{N} (T_i) \, 10^{\left[(L_i - L_c)/(10)\,q\right]}$$ (3.9)

where   D = noise dose expressed as a percentage of the allowable daily dose
   T_n = normalization time period, usually 8 hours
   T_i = duration of the ith time period (hours)

L_i = A-weighted, slow meter response, sound pressure level for the ith time interval
lying within the range of 80 to 115 dBA
L_c = criterion noise level, usually 90 dBA
q = nondimensional parameter, which determines the exchange rate over time;
e.g., $q = 5/(\log 2)$ for a 5 dB per time halving exchange rate,
$q = 3/(\log 2)$ for a 3 dB exchange rate
N = total number of intervals

The OSHA standards are expressed in terms of a total allowable level, which is based on 90 dBA over an 8-hour day and the 5 dB exchange rate. In these terms

$$L_{TWA} = 90 + (q) \log(D/100) \tag{3.10}$$

where L_{TWA} = time weighted average level (dBA) normalized to 8 hours
D = noise dose as defined above
q = exchange rate factor = 16.61 for the 5 dB rate

A 3 dB exchange rate assumes that hearing damage is proportional to the total energy of sound impacting the ear over a working lifetime. The 5 dB exchange rate allows more energy to impact the ear based on the understanding that the noise is intermittent and gives the ear some time to recover.

OSHA standards limit the time-weighted-average level to 90 dBA and requires that hearing protection be worn and that administrative and other controls on equipment be initiated. At 85 dBA OSHA requires that periodic hearing tests be performed on workers and that records on these tests be maintained.

3.7   OTHER EFFECTS

Precedence Effect and the Perception of Echoes

When a sound is reflected off a wall or other solid surface, the returning sound wave can be perceived as an echo under certain conditions. If the delay time between the initial sound and a second sound is decreased, the echo eventually disappears. A simple experiment can be carried out by clapping hands 15 meters (50 feet) or more away from a large flat wall and listening for the echo. At about 6 meters from the wall, the echo goes away and we hear a single sound. This is known as the precedence, or Haas effect (Haas, 1951), although its recognition predates Haas. The American scientist, Joseph Henry, demonstrated a similar effect at the Smithsonian in the 1840s (Davis and Davis, 1987). What happened in the hand clapping experiment is that the reflected sound finally fell below the level/delay threshold of perceptibility.

The perceptibility of a single echo is shown in Fig. 3.26 as measured in an anechoic space using speech at 70 dB and a loudspeaker placed in front. Figure 3.27 includes the results of the experiments of Haas, which were performed using a pair of loudspeakers, separated by 90°, placed in front of a listener. The source material was speech at different speaking rates presented at equal levels from each loudspeaker. One loudspeaker was delayed with respect to the other and the subjects were asked whether they felt disturbed by the reflection or echo. When the delay exceeded about 65 msec an annoying echo was perceived. At delay times less than 50 msec, echoes were perceived, which were not annoying even in cases where the reflection was 5 to 10 dB stronger than the primary sound (Blauert, 1983).

FIGURE **3.26**   **Absolute Perceptibility of a Delayed Signal (Kuttruff, 1973)**

Absolute threshold of perceptibility of a delayed signal (reflection) added
to a direct sound signal (speech at 70 dB), as a function of delay time.
Both signals arriving from the front.
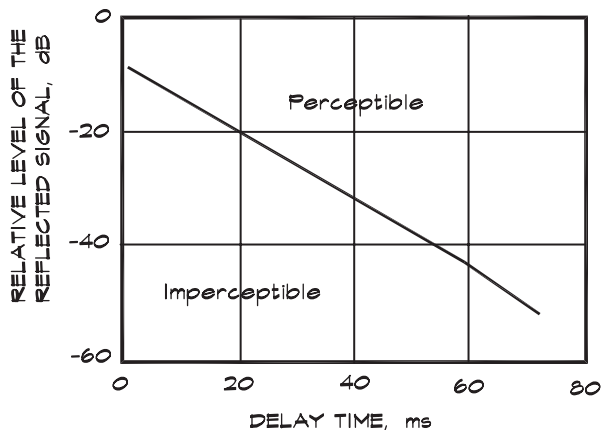
FIGURE **3.27**   **Thresholds for Perception of Reflections (Blauert, 1983)**

A comparison of various thresholds for the perception of reflections.
Standard stereophonic loudspeaker arrangement, base angle = 80 deg.
(Data of Haas 1951, Meyer and Schodder 1952, Burgtorf 1961, Seraphim 1961).
P = Primary sound - D = Delayed sound
Continuous Speech (Normal Speed = 5 Syllables/Sec)
Level of the Primary Sound = 50 dB
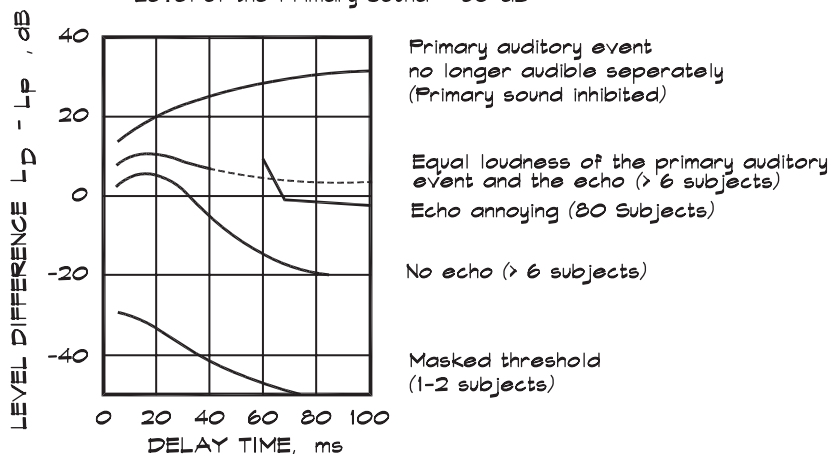
Where the delayed sound was less than 30 msec after the initial event, the two sounds merged and no echo was perceived, even for sounds 5 or more dB above the initial sound.

The precedence effect is of considerable importance in architectural acoustics both for the natural reinforcement of live sounds coming from reflecting surfaces as well as for electronic reinforcement of speech or music. If a sound, originating from a performer on stage, is amplified and projected to an audience from a front loudspeaker, the image will

FIGURE 3.28   Disturbance Due to an Echo (Kuttruff, 1973)
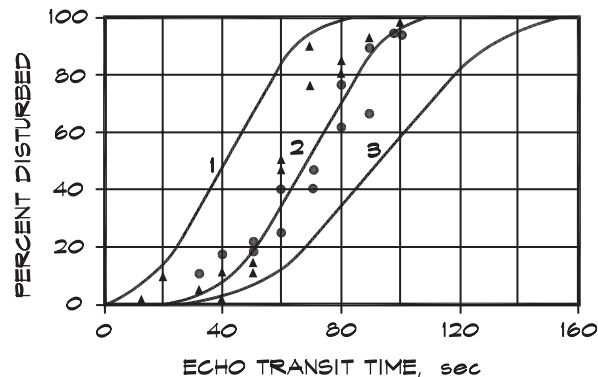
Percentage of listeners disturbed by a delayed signal at the same level as the undelayed sound signal (speech). The abscissa is the delay time.

1. 7.4 syllables per second
2. 5.3 syllables per second
3. 3.5 syllables per second

appear to come from the performer so long as the delay time is sufficiently short. The tradeoff between delay time and level, necessary to preserve the illusion of a single source, depends on the type of sound, i.e. speech or music, and the direction of the loudspeaker or reflector. If a reinforcing sound is within 25 msec of the initial sound, then speech is clearly understood. For music, a delay of 35 msec is normally not a problem even in rapidly played passages. For romantic music, delays as high as 50 msec can be tolerated. The three curves in Fig. 3.28 give the results of different rates of speaking on listener disturbance due to delayed echoes. The experiment is done with two loudspeakers, having the same level, placed in a relatively dead listening room (0.8 s reverberation time). The figure shows the importance of eliminating long-delayed reflections, and indeed even a single reflection, for the intelligibility of speech.

Data taken by Seraphim (1961), which were reproduced by Kuttruff (1973), led to the belief that when a series of delayed reflections arrives at a listener, the so-called Haas zone, where only a single sound is perceived, could be extended in time. Figure 3.29 gives the results of Seraphim's experiments using sounds coming only from the front in an anechoic environment. Here the threshold of perceptibility of the delayed sound is constant with delay time even when delays extend to 70 msec. Olive and Toole (1989) pointed out that this experiment, which was carried out in rather unrealistic conditions with all echoes having the same level, has been misapplied to reflections coming from many directions.

This is not to say that temporal forward masking does not occur for sounds having the same spectral content. Data published by Olive and Toole (1989) in Fig. 3.30 relate the absolute thresholds of perception for single lateral reflections to different types of source signal. In general the perception thresholds for speech and percussive reflections decrease with delay time, while those for music remain flat. The normal perception of a separate reflection, which would occur at a given delay time at much lower levels of reflected sound (Fig. 3.30), is masked. Experiments such as these indicate the importance of the smoothness

FIGURE 3.29   Absolute Perceptibility of a Delayed Signal (Kuttruff, 1973)

Absolute threshold of perceptibility of a delayed (reflection) being added to a sound field consisting of the direct sound plus one, two, three, and four reflections at fixed delay times and relative levels, which are denoted by the vertical lines. The original sound signal is speech. All sound components arriving from the front.
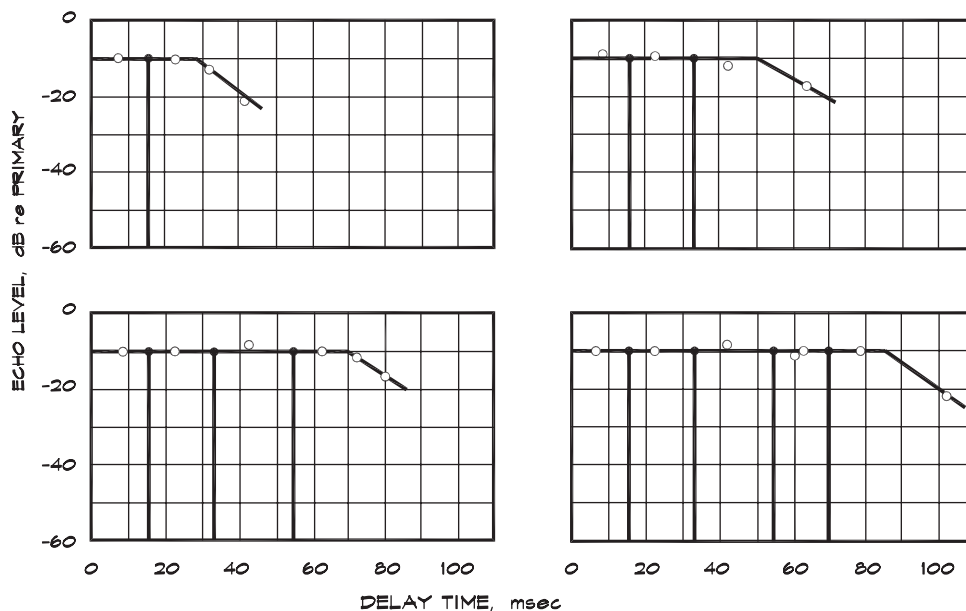
of the series of early reflections, following the arrival of the initial sound, in a critical listening space. These effects will be discussed in more detail in Chapt. 21.

Perception of Direction

The perception of direction is controlled by two factors: 1) the interaural delay time between the ears, and 2) the level difference created by the interaction between the head and the ears. When a sound originates to the left of the head in Fig. 3.31, it arrives at the left ear about a millisecond before the right ear. The high-frequency components are louder for the left ear than the right ear due to the shielding provided by the head itself. The brain uses the combination of level and time differences to decode the sound source direction.

When two sounds arrive at the listener the perceived direction is determined by first sound to arrive, even when the second sound is as much as 10 dB stronger. For equal level sources, delay gaps as low as one millisecond can bias the perceived direction to one side. This is called the precedence effect. Figure 3.32 shows the results of experiments (Madsen, 1970) on the tradeoff between time delay and intensity difference using two loudspeakers. At delay times below 1 msec, the higher level loudspeaker tends to dominate. Between 1 and 30 msec the precedence effect controls the direction, and above this point the two loudspeakers are increasingly perceived as separate sources.

When two sounds arrive at a listener simultaneously, the louder sound determines the direction. The apparent direction of a sound coming from two equidistant loudspeakers can be controlled by adjusting the level (panning) between them. Figure 3.33 contains the results of listening experiments performed by de Boer (1940) and Wendt (1963) by varying the level

FIGURE 3.30 Absolute Thresholds for a Single Lateral Anechoic Reflection (Olive and Toole, 1989)
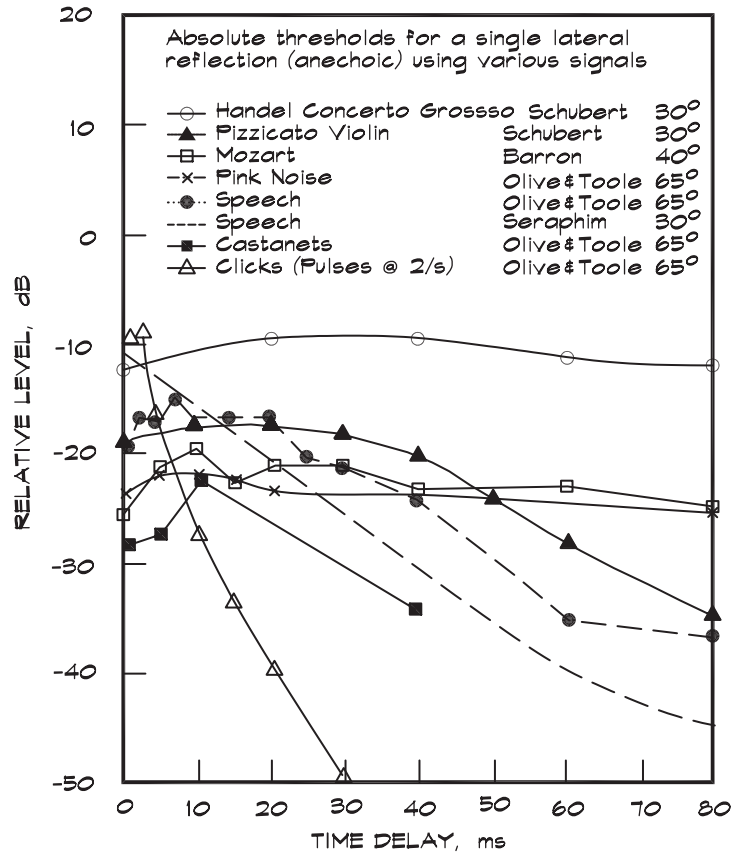
FIGURE 3.31 Head Geometry Relative to a Stereo Source (Blauert, 1983)
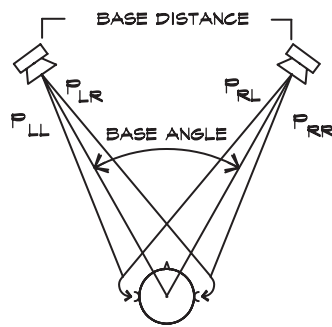
between two loudspeakers positioned 60° apart in the horizontal plane. When loudspeakers were placed 90° apart the error in the perceived direction increased significantly (Long, 1993). In most recording studios and mixdown rooms, loudspeakers spacing has standardized to a 60° spacing. Here the stereo image can be maintained and comfortably manipulated with panning.

In the vertical plane the ability of the brain to interpret time delays is much weaker, since our ears are on the sides of our heads. Results of localization tests in the vertical plane

FIGURE 3.32   **Perception of Source Direction with Delay (Madsen, 1970)**

Range of time delay and intensity over which time/intensity trading takes place, and also the limits of applicability of the precedence effect.
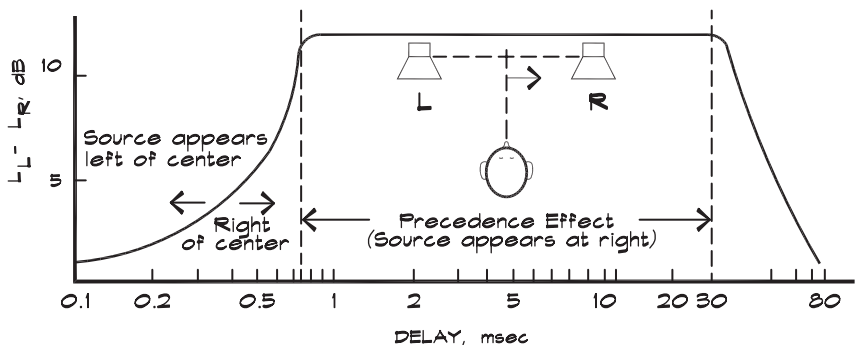
show a greater error and greater tolerance of wide loudspeaker placement. Our inability to precisely locate a vertical source makes realistic sound reinforcement systems possible. A properly designed loudspeaker cluster located above a stage can be used to augment the natural sound of the performers while maintaining the illusion that all the sound is coming from the stage.

The level-delay tradeoff has been carefully studied (Meyer and Schodder, 1952) by asking subjects to indicate the level difference at which the sound seemed to come from midway between a pair of stereo loudspeakers for various delays (Fig. 3.34). Study of this experiment is most helpful in the design of sound systems for it shows how far one can go in raising the loudspeaker level to augment the natural sound. It also shows how the apparent

FIGURE 3.33   **Perception of Source Direction with Level (de Boer, 1940 and Wendt, 1963)**

Included angle between loudspeakers - 60°.

Dashed curves – speech, head free to move.
Solid line – impulses, head immobilized.
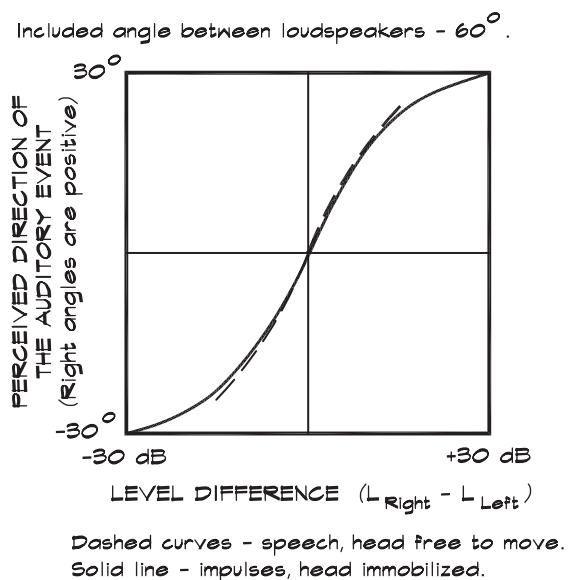
direction of sound can be moved about by using two loudspeakers and adjusting the time delay and level between them.

Clearly a stereo image, where a sound is perceived as originating between two loudspeakers, is difficult to maintain. The center image shifts to one side when one sound arrives only a few milliseconds earlier. Thus true stereo imaging is limited to a relatively small listener region close to the centerline between two carefully balanced loudspeakers. In a large room, such as a church or theater, a true stereo image can seldom be achieved.

Directional cues are best introduced by placing loudspeakers near the location of origin of the sound. For example, in motion picture sound systems, three loudspeaker clusters are arranged behind the screen in a left-center-right configuration, and the sound is panned to the proper level during the mix. In theme park attractions localization loudspeakers are placed in or near animatronic figures to provide a directional cue, even when most of the sound energy may be coming from a separate loudspeaker cluster.

Binaural Sound

It is possible to reproduce many of the three-dimensional spatial attributes we hear in real life by recording sound using a dummy head with microphones in the ears and listening to the sound through stereo headphones, one for each microphone. This recording technique is referred to as dummy head stereophony or binaural reproduction, and is used in the study of concert hall design as well as in highly specialized entertainment venues. The results are startlingly realistic, particularly when the sound sources are located behind and close to the head.

When sounds are recorded binaurally, events that occur on the side or to the rear of our head are clearly localized. Sound sources located in front sound like they originate inside our head, overhead, or even behind. Several explanations for this phenomenon have been offered: 1) the effects of the pinnae are not duplicated when the playback system is a pair of headphones, 2) headphones affect the impedance of the aural canal by closing off the tube, and 3) the cues available from head motion are not present.

FIGURE 3.34   Equal Loudness Curve for Delayed Signals (Kuttruff, 1973)

Critical level difference between a delayed and undelayed signal which results in a perceived equal loudness of both signals (speech). (Meyer and Schodder, 1952)
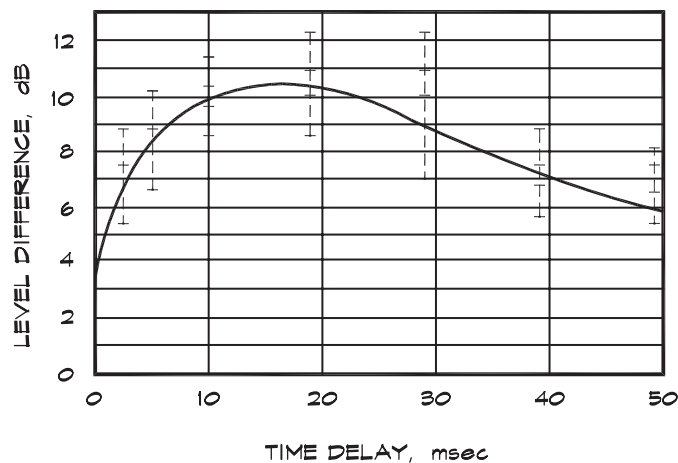
This page intentionally left blank

4

ACOUSTIC
MEASUREMENTS
AND
NOISE METRICS

4.1 MICROPHONES

Both microphones and loudspeakers are transducers—electromechanical devices for converting sound waves into electrical signals and vice versa. Microphones sense small changes in sound pressure through motion of a thin diaphragm. Cone loudspeakers create changes in pressure through the motion of a diaphragm driven by a coil of wire, immersed in a magnetic field. Since both microphones and loudspeakers operate in a similar manner, microphones can be used as loudspeakers and loudspeakers as microphones. Even the human eardrum can act as a loudspeaker.

The most common types of microphones in use are: 1) dynamic, 2) condenser, 3) electret, 4) ceramic, and 5) ribbon. All microphones consist of a diaphragm, which moves back and forth in response to changes in pressure or velocity brought about by a sound wave, and electronic components that convert the movement into an electric signal. Microphones are characterized by a sensitivity, which is the open circuit output voltage produced by a given pressure, expressed in decibels re 1 V/Pa. A one-inch diameter instrumentation microphone might produce 54 mV for an rms pressure of 1 Pa, yielding a sensitivity of $20 \log \left[(54\,\mathrm{mV}) \,/\, (1\,\mathrm{Pa})\right]\left[(1\,\mathrm{Pa}) \,/\, (1\,\mathrm{V})\right] = -\,25\,\mathrm{dB}$. Note that 1 Pa is the sound pressure that corresponds to the 94 dB sound pressure level generated by standard pistonphone calibrators.

A dynamic microphone, illustrated in Fig. 4.1, operates on the same principal as a loudspeaker. A diaphragm moves in response to the changes in sound pressure and is mechanically connected to a coil of wire that is positioned in a magnetic field. The induced current, produced by the motion of the coil, is the microphone's output signal. Both the diaphragm and the coil must be very light to produce adequate high-frequency response. Most dynamic microphones produce a very low output voltage; however, since the electrical output impedance is low, the microphone can be located relatively far away from the preamplifier. Dynamic microphones are rugged and are primarily used in sound reinforcement applications, where low fidelity is good enough. One manufacturer of dynamic microphones used to demonstrate its product's toughness by using the side of it to pound a nail into a block of wood.

A condenser microphone, in Fig. 4.2, consists of a thin stretched stainless-steel diaphragm that is separated from a back plate by a narrow air gap. The two parallel plates

FIGURE 4.1   Dynamic (Moving Coil) Microphone (Rossing, 1990)

Sound pressure on the diaphragm causes
the voice coil to move in a magnetic field.

Voice Coil

Magnet
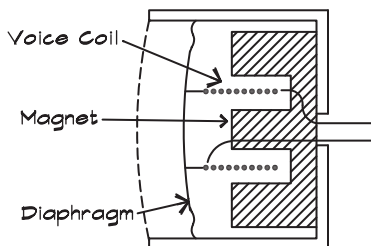
Diaphragm

FIGURE 4.2   Condenser Microphone (Rossing, 1990)

A metal diaphragm is one plate of a capacitor. As it moves the
changing capacitance modulates the voltage at the preamplifier.

Preamplifier

Metal
Diaphragm
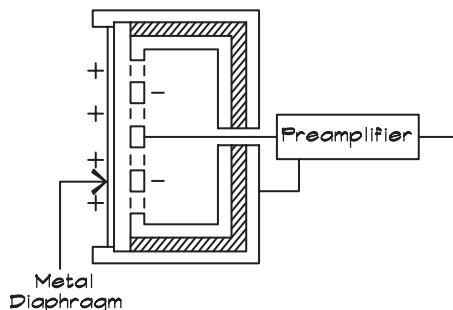
become a capacitor when a DC polarizing voltage, typically 150 to 200 V, is applied. Motion of the diaphragm generates an electrical signal by varying the capacitance and thus the voltage between the plates. These microphones are very sensitive and accurate and have excellent frequency response characteristics. They are less rugged than dynamics and require a source of the polarizing voltage.

An electret microphone, in Fig. 4.3, is another form of condenser, which is sometimes called an electret condenser. It includes a thin polymeric diaphragm, where the polarizing voltage is not externally applied but is built into the polymer so that it is permanent. Otherwise the microphone operates in much the same way as the condenser does.

The ceramic microphone, in Fig. 4.4, has a diaphragm that is mechanically coupled to a piezoelectric material. A piezoelectric generates a voltage when strained. Many such materials exist such as lead zirconate titanate, called PZT, barium titanate, and rochelle salt. These microphones are more rugged than the capacitive types, are less sensitive, and do not require an external polarization voltage.

A ribbon microphone, sometimes referred to as a velocity microphone, works by suspending a thin metallic foil in a magnetic field. Figure 4.5 shows an example. The conducting ribbon is light enough that it responds to the particle velocity rather than the pressure. Since the ribbon is open to the back and shielded on the sides by the magnet, these microphones have a bidirectional polarity pattern. Ribbon microphones are very sensitive to moving air

FIGURE 4.3   Electret Condenser Microphone (Rossing, 1990)

A thin metallized plastic diaphragm is tightly stretched across a perforated backing plate. The holes in the back plate couple to an air cavity.
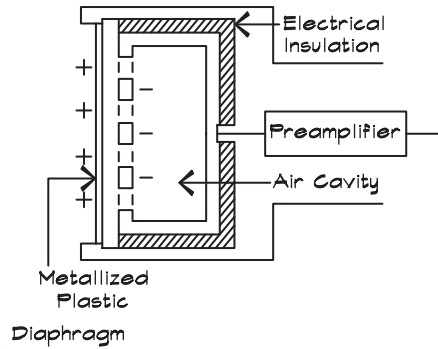
FIGURE 4.4   Ceramic Microphone (Rossing, 1990)

Sound pressure on the diaphragm causes deformation of the crystal, generating an electrical signal.
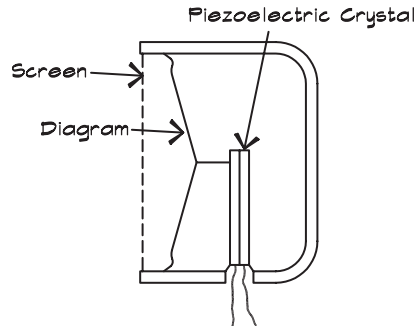
FIGURE 4.5   Ribbon Microphone (Rossing, 1990)

A lightweight ribbon diaphragm moves in a magnetic field, thus generating an electrical signal.
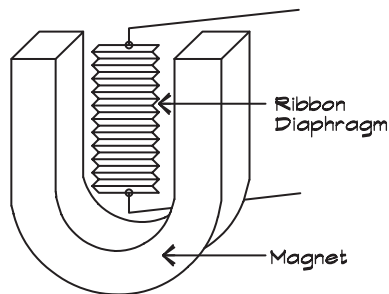
FIGURE 4.6   **Sensitivity of Condenser Microphones (Hassall and Zaveri, 1979)**

Data are shown for normal incidence and B&K mics.
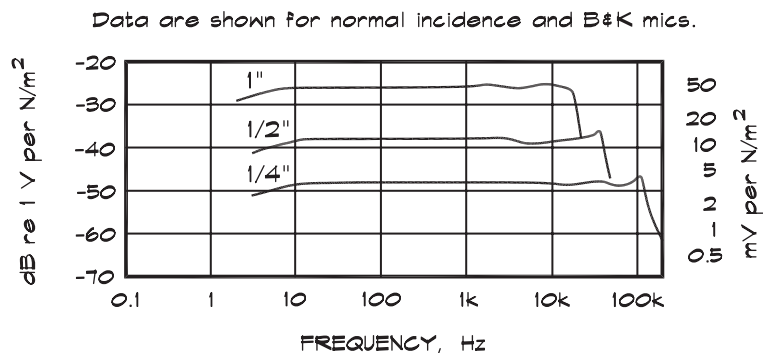
currents as well as high sound pressure levels. An unsuspecting acoustician, seeking to determine the characteristics of a reverberation chamber, once fired a blank pistol in a room full of ribbon microphones, quickly converting them into expensive paperweights. Due to the fragility of this type of microphone, its use is limited to the studio.

Frequency Response

Instrumentation microphones, so called because they can be calibrated using a piston-phone calibrator, are cylindrical and come in nominal sizes: one-inch (actually 0.936 in or 23.8 mm), half-inch (12.7 mm), and quarter-inch (6.5 mm) diameters. The size of a microphone affects its performance. Small microphones can measure sounds at higher frequencies and generally are less directional and less sensitive since they have a lower surface area. A one-inch instrumentation microphone, for example, might be able to measure levels as low as 0 dBA, while having an upper frequency limit of 10 kHz. A half-inch microphone might be good to 10 dBA and 30 kHz, and a quarter-inch microphone typically can measure down to 20 dBA and as high as 70 kHz. Examples of their response curves are given in Fig. 4.6.

Directional Microphones

Microphones, like sound sources, can have a response that varies with angle, which is represented by a polar diagram with angles measured relative to the normal to the diaphragm. Ideally, instrumentation microphones are nondirectional; however, at high frequencies there is some self shielding and loss of sensitivity, which is often greatest at a 120° to 150° angle of incidence. The polar diagrams for several types of microphones are shown in Table 4.1. Directional microphones are not used for precision measurements, but are quite useful for recording and sound-reinforcement systems. When the microphone capsule is smaller than a quarter wavelength, it is not directional; however, directivity can be built in by manipulating the construction of the housing. Figure 4.7 illustrates the design of a cardioid housing. By leaving an opening at the rear, sound coming from the rear arrives at the front and back of the diaphragm at the same time, thus canceling. Sound arriving from the front takes some additional time to reach the rear of the microphone diaphragm. By carefully attenuating selected frequencies traveling along certain paths the sound entering the rear cavities can be delayed so that it arrives close to 180° out of phase and does not cancel out the frontal sound.

TABLE 4.1 Directional Characteristics of Microphones (Shure Inc., 2002)

	Omni-Directional	Bidirectional	Cardioid	Hypercardioid	Super-Cardioid
Polar Response Pattern					
Polar Equation	1	$\cos\theta$	$1/2(1+\cos\theta)$	$1/4(1+\cos\theta)$	$0.37+0.63\cos\theta$
Pickup Arc 3 dB Down	360°	90°	131°	105°	115°
Pickup Arc 6 dB Down	360°	120°	180°	141°	156°
Relative Output At 90° (dB)	0	$-\infty$	-6	-12	-8.6
Relative Output At 180° (dB)	0	0	$-\infty$	-6	-11.7
Angle at Which Output = 0	$--$	90°	180°	110°	126°
Random Energy Efficiency	0 dB	0.333 -4.8 dB	0.333 -4.8 dB	0.250* -6.0 dB	0.268** -5.7 dB
Distance Factor	1	1.7	1.7	2	1.9

  * Minimum random energy efficiency for a first-order cardioid.
** Maximum front to total random energy efficiency for a first-order cardioid.

FIGURE 4.7   Cross-Section of an Electrovoice Variable-D Cardioid (Burroughs, 1974)
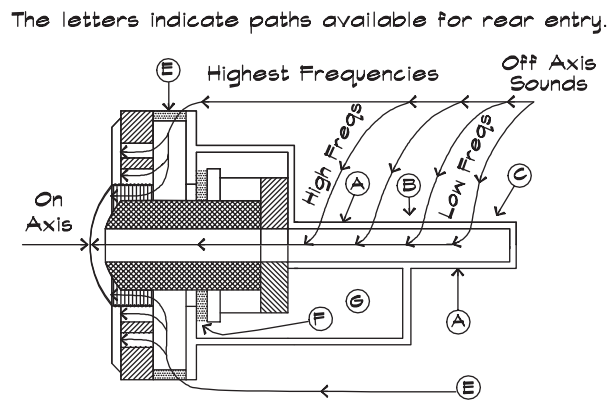
Highly directional microphones can be made using a series of openings in a tube, or a group of different length tubes, leading to the diaphragm. These so-called shotgun microphones work because sounds arriving on axis and entering through the holes combine in the tube in the proper phase relationship. Sounds arriving from the side and traveling down the tube combine with a random phase relationship that attenuates the signal at the diaphragm.

Directional microphones are very important in sound reinforcement systems. They selectively amplify sound coming from one direction, ideally from the user, and attenuate sound from other directions. This reduces feedback and allows a greater system gain. Properly designed directional microphones should have a consistent directivity pattern over a range of frequencies, otherwise they would color the off-axis sound. The more directional a microphone, the greater the coloration and the greater the directional lobing. Sometimes highly directional microphones can generate more system feedback than cardioid microphones, due to the influence of off-axis lobing patterns. In general, the less directional the microphone the more natural sounding it is.

Sound Field Considerations

Microphone directivity sometimes influences the method of making measurements, even with instrumentation microphones. Typical microphones have their greatest sensitivity for sound incident on the diaphragm at 0°, called normal incidence. When the sound is traveling in a direction that is parallel to the plane of the diaphragm, at 90° to the normal, it is called grazing incidence. Most microphones have an angle for which their response is the flattest, usually 0° or 90°, but sometimes it can be another angle.

Microphones are described by their preferred type of sound field; for example, free field, random incidence, or pressure field. All microphones respond to pressure, but their sensitivity can be adjusted to produce the flattest response for a given angle of incidence or type of sound field. A free field is characterized by direct, unimpeded propagation of the wave from the source to the receiver. A diffuse or random field is one where the sound arrives from every direction with equal probability, and in a pressure field the sound pressure has the same magnitude throughout the space.

For a half-inch instrumentation microphone, below 5000 Hz all orientations produce a frequency response that is flat to within 2 dB. If a measurement is being made in a free field above 5000 Hz, the microphone should be oriented so that its flattest response direction is used, but this may vary with frequency, as can be seen in Fig. 4.8. Different standards organizations make different recommendations for proper free-field measurements (Fig. 4.9). IEC standards specify that the meter be switched to frontal mode and be oriented for normal incidence. ANSI standards require the selection of the random mode and an orientation of 70° to 80° to the source. For moving sources the microphone should be oriented for grazing incidence so that the directivity does not change with the motion of the source. This is achieved by angling the microphone upward.

When measurements are being done indoors, the random correction should be selected. Measuring with a free-field microphone in a diffuse field or with a random-incidence microphone in a free field yields only small inaccuracies, usually at high frequencies. The most accurate results will be obtained by using the setting appropriate to the type of sound field, but the differences are generally small.

FIGURE 4.8   Free Field Correction Curves for a Microphone (Bruel and Kjaer, 1986)

Half inch microphone fitted with a protective grid. This response is added to the on-axis response of the microphone as shown in Fig. 4.6.
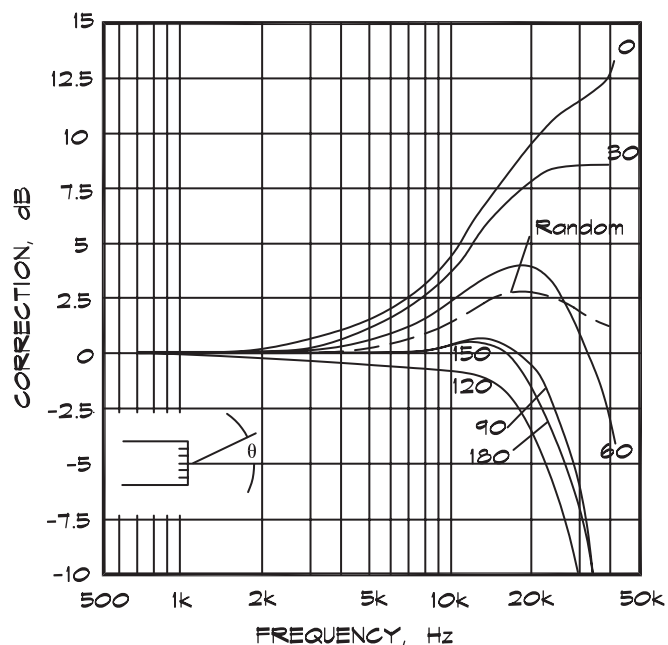
4.2   SOUND LEVEL METERS

The sound level meter, such as that shown in Fig. 4.10, is the fundamental acoustical instrument. Meters are battery powered and have become increasingly sophisticated, frequently containing internal processing, which automates many of the measurement functions. The individual controls vary from meter to meter; however, in general, there is a commonality of features. The basic controls allow for a selection of time weightings—fast, slow, and impulse—each of which represents a different ballistic time constant. Several frequency weightings are available: linear (unweighted), A-weighted, C-weighted, and a band limited linear scale. Frequency bandwidths may be selected from all pass, octave, and third-octave bands. There is a range selection that determines the highest and lowest levels measurable by the meter. Depending on the meter, there may be various types of automatic processing.

The internal parts of a meter include a microphone, preamplifier, various filters, a range control, time averager, and level indicator. The filters sometimes are contained in a separate module that may be attached to the meter, or are an integral part of the meter itself. On most hand-held sound level meters the filter selection is made manually. Where a group of filters operate simultaneously and display a number of levels on a bar graph in real time, the meter is called a spectrum analyzer or real-time analyzer.

Sound level meters are classified into three different groups by accuracy. Each class has a slightly different tolerance allowed in its precision. These standards are defined by the

FIGURE 4.9   Free Field Sound Measurements (Bruel and Kjaer, 1986)

IEC STANDARD

"Frontal" Incidence Correction
Normal Incidence Orientation

ANSI STANDARD

"Random" Incidence Correction
70 to 80° Orientation

70 to 80°
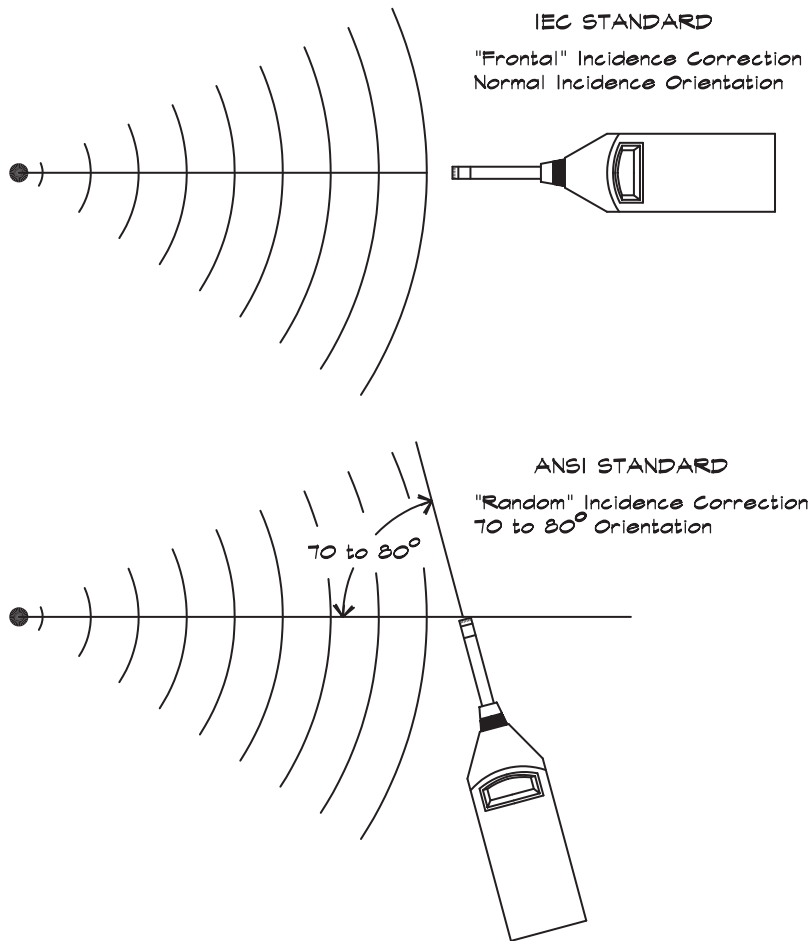
For diffuse field conditions the meter may be oriented in any direction.

MEASUREMENTS NOT REQUIRING IEC OR ANSI STANDARDS

Select "Frontal" sound incidence correction under free field conditions or when the source can be located.

Select "Random" sound incidence correction under diffuse field conditions or when the meter is moved around during L_{eq} measurements.

American National Standard Specification for Sound Level Meters, ANSI S1.4-1983.

Class 0	Laboratory	±0.2 dB 22.4 – 11200 Hz
Class 1	Precision	±0.5 dB 22.4 – 11200 Hz
Class 2	General Purpose	±0.5 dB 63.0 – 2000 Hz
		±1.0 dB 22.4 – 11200 Hz

Meter Calibration

Sound level meters should be calibrated before use, using a pistonphone calibrator placed over the microphone. These calibrators generate a steady tone, usually at 1000 Hz, by means

FIGURE 4.10   Sound Level Meter
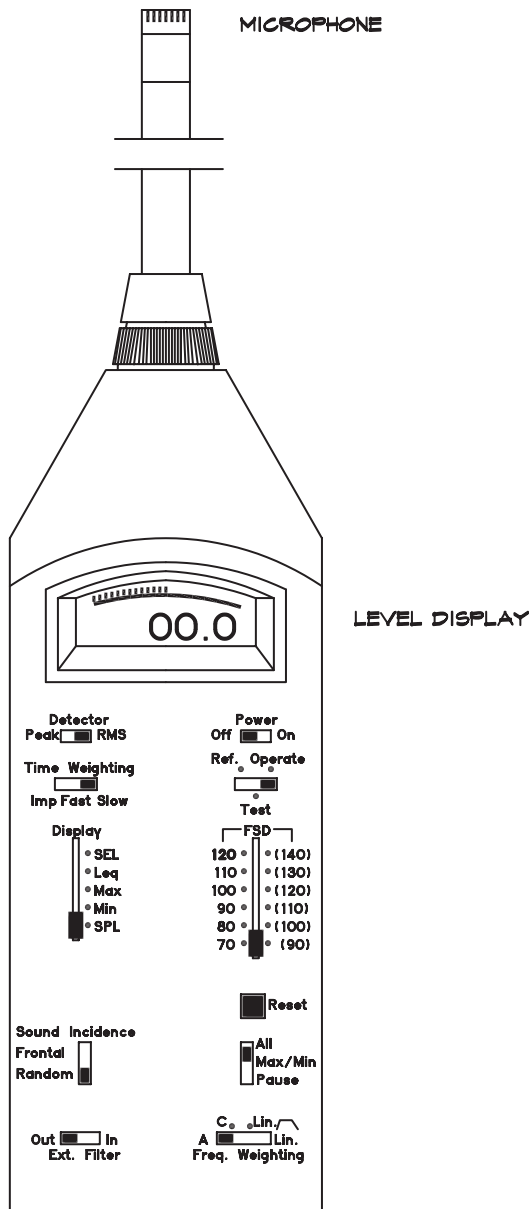
of an oscillating piston in one end of a small cavity. The calibrator produces a nominal 94 dB, or with some calibrators a 114 dB, pure tone signal. The meter is adjusted to the proper level using a screw adjustment.

Pistonphone calibrators produce changes in volume in the cavity, which can be translated into changes in pressure using an equation of state. Most calibrators are set to produce the reference level at normal atmospheric pressure of 1013 millibars (1.01×10^5 Pa). Since atmospheric pressure varies, there is a correction given in Fig. 4.11 that must be applied according to altitude. This is the same correction as the term $10 \, \log(\rho_0 c_0 / 400)$ in Eq. 2.67, including a density that changes with altitude.

FIGURE 4.11   Sound Level Meter Calibration Corrections (Peterson and Gross, 1974)

Corrections for sound pressure level for atmospheric pressure at various altitudes. Correcions are added to the rated output of the calibrator to obtain the actual output of the calibrator.
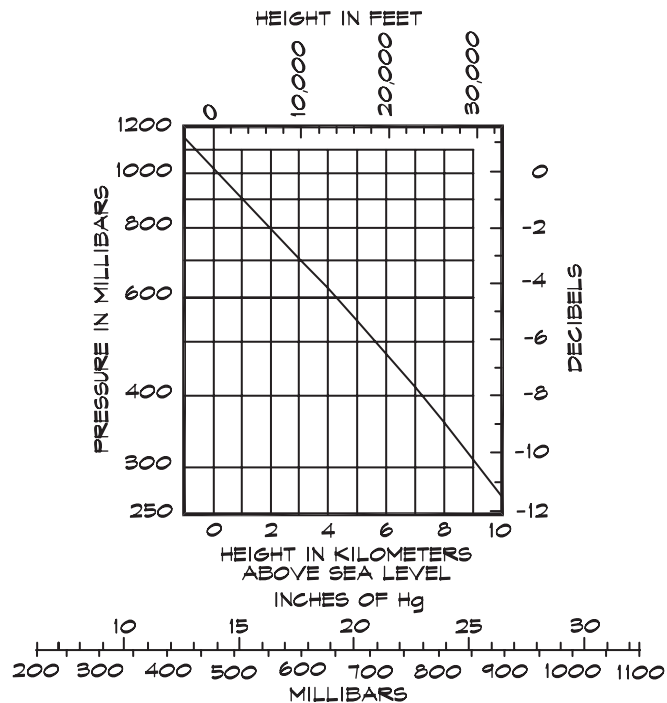
Calibrators themselves should be calibrated periodically against a microphone of known sensitivity. Since microphones are used to calibrate calibrators and vice versa, we encounter a classic chicken and egg conundrum; that is, how do we calibrated the original reference? The original microphone must be calibrated using another microphone in what is called a reciprocity calibration. The microphones used are identical and both transducers are used as loudspeakers and microphones in this technique. Refer to Kinsler et al. (1982) for further details.

Meter Ballistics

Early sound level meters were equipped with a d'Arsinval galvanometer, which responds to a voltage and indicates the sound level with a needle pointer. These early meters were very sensitive and tended to chatter or move back and forth rapidly. Electrical damping was added, which slowed the needle's response and made it more readable. The choice of the damping resistor in the indicator circuit, along with the capacitance of the microphone, set the exponential time constant of the circuit. Three response speeds are now used—*slow, fast*, and *impulse*. The slow setting has a time constant of 1000 ms (1 second), while for fast response it is 125 ms. A time constant has a precise mathematical meaning in engineering. In one time constant the value rises to $(1 - 1/e)$ or falls to $1/e = 1/2.718$ of its steady value. If a sound is instantaneously raised to a certain level the meter will rise to within 2 dB of the actual level in one time constant. Standard practice is to use 200 ms tone bursts at 1000 Hz to test a meter's response, since real sine waves have a finite rise time. The fast meter response

must read within 2 dB of the steady level, and the slow meter response must be between 3 to 5 dB of the steady level (ANSI S4.1).

The rise time for fast and slow response is about the same as the fall time, so for integrating sound level meters, which measure L_{eq} levels, either fast or slow response gives about the same result. Some metrics, such as the CNEL level in California, require a particular response time, in this case, the slow response. For general use, the fast response is preferred. Impulse response is only employed to measure impact noise and other rapidly rising waveforms. The impulse time constant for a rising signal is 35 ms and for a falling signal is 1500 ms. Thus the meter holds the reading near its maximum level.

Meter Range

Sound level meters have an adjustable scale that allows the range of measurable levels to be set. If the range is set too low, then when a high level event occurs the meter will overload and not yield an accurate reading. If the range is too high, the indicated level will not fall below a certain value, and quiet events will not be measured accurately. Most meters have an overload indicator that signals the user to change the range. The range should be set as low as possible without tripping the overload indicator.

Detectors

There are two types of detector circuits found on most meters, peak, and rms (root mean square). Peak circuits sense the maximum amplitude present in the waveform. Mean-square detectors measure the time average of the square of the wave. Since the energy in the wave is proportional to the mean-square value, the rms detector is the most commonly used setting. Peak amplitudes are often of interest in vibration measurements. Peak-hold circuits, which capture the highest level during the measurement period, are utilized in the measurement of special sources such as sonic booms, where the wave shapes are not sinusoidal.

Filters

Sound meters come equipped with various selectable filters. The simplest is the linear filter, which passes sounds within the overall band limits of the instrument, for example 5 Hz to 100 kHz. This is not of particular interest in architectural acoustics, since it includes sounds that are well beyond our hearing capability. A second selection, the band-limited linear setting, includes a bandpass filter between 20 Hz and 20 kHz, and is quite useful for recording, since it blocks out low-frequency sounds that would otherwise overload a tape recorder. The characteristics of this filter along with the A and C weighting networks are shown in Fig. 4.12. Octave and third-octave bandwidth filters are also available. The standard frequency ranges have been given in Table 2.1. Filters may be cascaded, for example both octave band and A-weighting may be applied, yielding an A-weighted octave-band level. It is preferable to use the linear or band-limited linear settings when narrow-band filtering is done. This yields a consistent measurement methodology that does not require undue bookkeeping.

4.3   FIELD MEASUREMENTS

Field measurements are a critical part of architectural and environmental acoustics. Even with the simplest sources, care must be taken to follow proper procedure. A meter appropriate to the task must be selected. For environmental survey work a meter, tripod, calibrator, windscreen

FIGURE 4.12   A, C, and Lin Weighting Characteristics (Bruel and Kjaer, 1979)
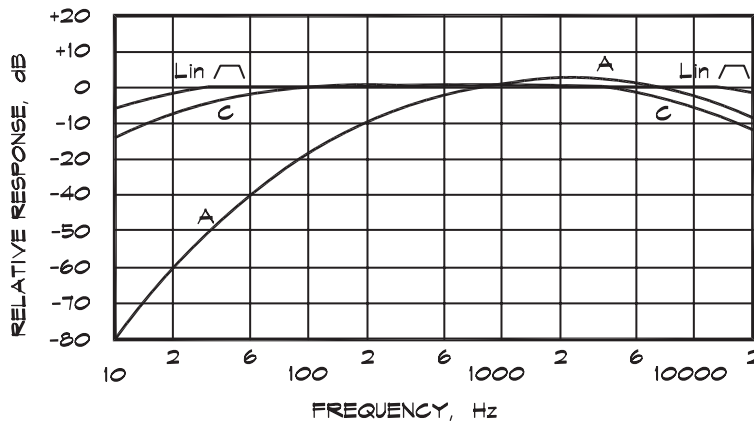
(to reduce wind generated noise), logbook, distance measuring device (tape or rolling ruler), and watch are the standard kit. A small screwdriver is used to set the calibration. Spare batteries are a good idea. If they are left in the original packaging they can be distinguished from used ones. A camera is handy to record any unusual features of the site.

Headphones sometimes are included for listening to the sound being measured through the meter. They are essential for tape recording. Sometimes extraneous noise occurs that is not audible except through headphones. An example is arcing of the microphone, which can be caused by high humidity. Arcing produces a spurious popping sound that affects the data. Thus headphones are recommended when the relative humidity exceeds 90%.

For all measurements a record should be kept, noting the following information where it is relevant:

1) Location

2) Source description

3) Pertinent source details (e.g., manufacturer, model, operating point conditions)

4) Date and time

5) Engineer

6) Source dimensions and the radiating surfaces

7) Distance and direction to the source or a description of the measurement location

8) Meter settings

9) Background noise levels

10) Any unusual conditions

11) Time history

12) Measured data

Sources, which are outdoors and well away from reflecting surfaces, are the most straightforward. If the source is a piece of mechanical equipment the measurement position is selected based on the number of locations necessary to characterize the directivity of the source. For estimation of far-field levels from near-field measurements, data should be taken no closer than the largest dimension of the source, unless the area of the source is taken into account, by using Eq. 2.91.

The measurement distance for source characterization in a free field should be greater than a wavelength. For frequencies of 100 Hz the minimum distance is about 11 ft (3.4 m), while for 50 Hz the distance is about 22 ft (1.7 m). The danger of taking measurements too close is the possibility of including energy from only a portion of the source. If the source includes several separate pieces of equipment, the overall level will not be accurately represented if measurements are made too close to one individual component. Sometimes sound waves close to a source are not planar or are nonpropagating. Low-frequency emissions from large transformers are a good example of this type. Often low-frequency measurements require multiple samples and the microphone locations should be at least $\frac{\lambda}{4}$ apart.

Some sources are simply too large to conveniently get away from them. A good example is a refinery or a power plant. In such cases noise levels should be taken at regular distance intervals around the source and the results logged, according to where they were taken. Measurement locations should be spaced so that there is no more than a few decibels difference from one location to the next.

Measurements that are made to characterize a source rather than a location should be taken well away from reflecting surfaces. A minimum distance of $\frac{\lambda}{4}$ is recommended. If octave-band measurements are being taken and the 63 Hz band is of interest, then a distance of 4 to 5 feet is appropriate. Measurements will include reflections from the ground or other reflecting surfaces. Reflections from the observer can cause high-frequency comb filtering (Fig. 4.13), so the common practice is to hold the meter so that the microphone is extended away from the body or to support the instrument on a tripod.

An accurate measurement for source characterization is also difficult if the source receiver distance is too great. Even if the line-of-sight path is unimpeded, wind, atmospheric turbulence, ground cover, and air attenuation all play an important role in determining the measured noise level given off by a fixed source. At distances greater than 60 m (200 ft), noise level measurements can be dependent on wind velocity and direction. At distances greater than 150 m (500 ft), sound levels can be greatly influenced, even on a calm day, by ground cover, atmospheric turbulence, and air attenuation. At greater distances, thermal inversion layers can also be a major contributor. For all these reasons it is difficult to perform characterization measurements at large distances (say > 60 m or 200 ft) from the source. Such measurements may be representative of a noise environment at a particular location under the measurement conditions, but may not be sufficiently accurate to characterize the source.

Background Noise

If there is a significant background (ambient) level present it should be measured. For a steady background it is best to turn off the source to be measured and note the ambient separately in all frequency bands of interest. The actual source-generated level then can be calculated from

$$L_{Source} = 10 \log \left[10^{0.1 L_{Tot}} - 10^{0.1 L_{Amb}} \right] \tag{4.1}$$

where L_{Source} = source sound pressure level (dB)
L_{Tot} = total combined source + ambient sound pressure level (dB)
L_{Amb} = ambient sound pressure level (dB)

FIGURE 4.13   Effect on Frequency Response as a Result of the Microphone Position (Petersen and Gross, 1974)
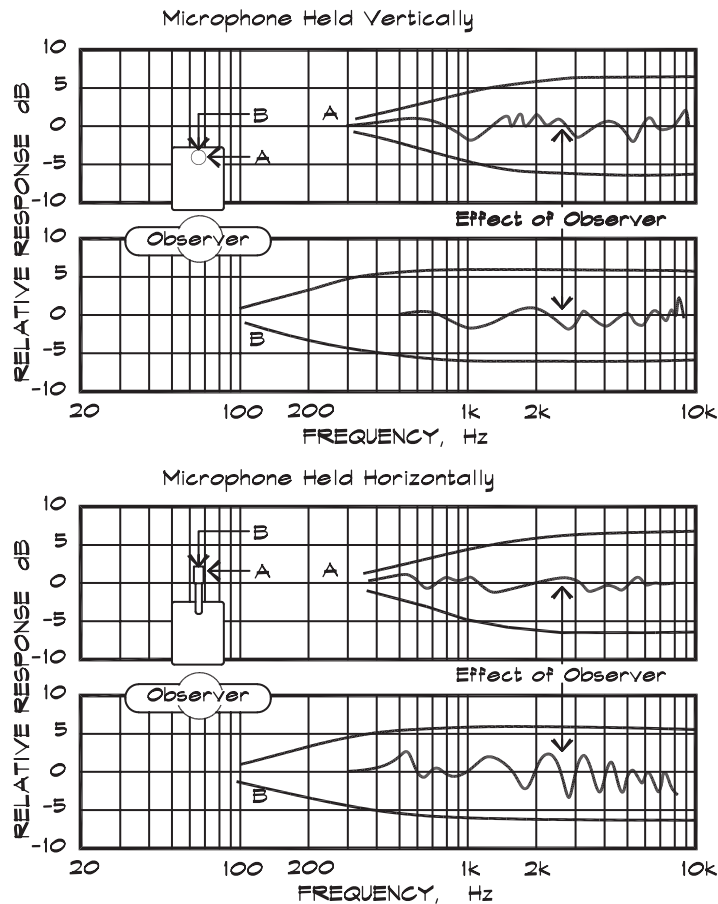
If the sound source cannot be turned off, it may be possible to measure the ambient noise level at a location that is similar to the location of interest but is away from the influence of the source. Locations may be available in shielded areas or, if the ambient noise is due to a roadway, at another site that is the same distance from the roadway.

When the background noise is variable and the source is steady, it is often easiest to measure the minimum combined level at a time when the ambient is quiescent. This gives an accurate source level if the ambient is sufficiently low. When the ambient is quiet, usually 10 dB below the source, its contribution can be ignored. With a varying ambient, if the source can be turned off, the minimum ambient can be recorded and then the minimum combined level measured. This gives a good value for the source level after adjustment using Eq. 4.1 as long as the minimum ambient levels are repeatable.

If the ambient is relatively steady and close to the source level, it can be measured separately using an averaging meter on the L_{eq} setting. The combined level then is measured in the same way and the source level calculated as before. This technique is also useful if the source, or background level, varies periodically, as it might with a pump motor or multiple sources such as fans or pumps, which produce beats. In taking data of this type, it is important to average over several beat cycles so that variations are properly taken into account.

When the source level is less than the ambient, accurate measurements are difficult unless both the source and ambient levels are very steady. Even in these cases long averaging times are required to get good results. If the source is steady and the ambient varies, the minimum level gives the most accurate source level.

Time-Varying Sources

When traffic or other time-varying sources are to be measured, certain additional steps are useful. Although integrating meters are highly accurate, the nature of their output (i.e., one number) is sometimes not ideal, particularly when the data must be presented to a nontechnical audience. In these cases a log sheet such as that shown in Fig. 4.14 is helpful. In taking the data the meter is read at regular intervals, usually 5 or 10 seconds apart, and a notation is made on the log of the level that the meter shows at the interval mark. A representative number of samples are taken as determined either by the metric or the time period. One advantage to this methodology lies in the ability of the user to analyze the sampled data and extract more than one metric from the record. It also allows the engineer to ignore spurious signals such as barking dogs or aircraft flyovers that may not be relevant to the data being collected. Recording data, either on tape or in a recording sound level meter for later analysis, is another way of accomplishing the same goal. Data can be regularly sampled, and average levels calculated over a fixed time period and saved internally on a storage device for later analysis.

When a single moving source is to be measured, data are taken at a standard distance, say 15 m (50 ft), under prescribed conditions of velocity or acceleration. Data may be analyzed internally within the meter, or captured on a digital or analog recording device, or displayed

FIGURE 4.14   Noise Survey Log

graphically on a strip chart. When a recording is made, the calibration should flow through to all devices downstream of the meter. A tone is introduced using a pistonphone calibrator and is recorded along with the data. The meter range may then be adjusted by a known amount to accommodate the actual range of the data. A record should be made in a log or on the strip chart or verbally on tape noting the change in scale.

Both analog and digital recording devices can overload when signal levels exceed their dynamic range. When digital devices run out of headroom the resultant sound is most unpleasant. Analog tape recorders overload by producing a nonlinear or compressed version of the actual signal. If a two-channel device is available, the data may be recorded simultaneously on both channels at different level settings. This technique allows the data having the greater signal-to-noise ratio to be used, while retaining a margin of safety on the attenuated channel in case of overload.

Diurnal (24-Hour) Traffic Measurements

If a diurnal noise metric such as an L_{dn} or CNEL is to be measured, the ideal methodology is to position monitoring equipment at the location of interest for the entire 24-hour period. Often this is not practical due to the security, financial, or technical difficulties involved. In such cases a good estimate of the actual metric can be obtained by short-term monitoring if the hour by hour distribution of traffic is known or can be approximated. Measured distributions (Wyle, 1971) are given for urban traffic in Fig. 4.15 and for highway traffic in Fig. 4.16. The interesting feature about these data is that although they were taken 10 years apart they are almost identical. This implies that average diurnal traffic patterns are relatively stable.

If the reference L_{eq} level is known for the passage of one vehicle then the L_{eq} for N_h identical vehicles over the same time period is

$$L_{eq} = L_{ref} + 10 \log N_h \qquad (4.2)$$

FIGURE 4.15   Typical Hourly Distribution of Total Daily Urban Vehicle Traffic (Wyle Laboratories, 1971)
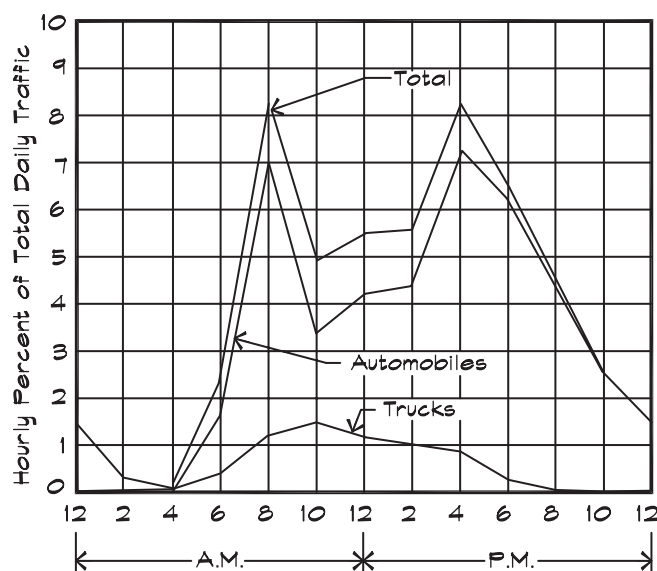
FIGURE 4.16   Hourly and Daily Variations in Intercity Highway Traffic in California (Wyle Laboratories, 1971)
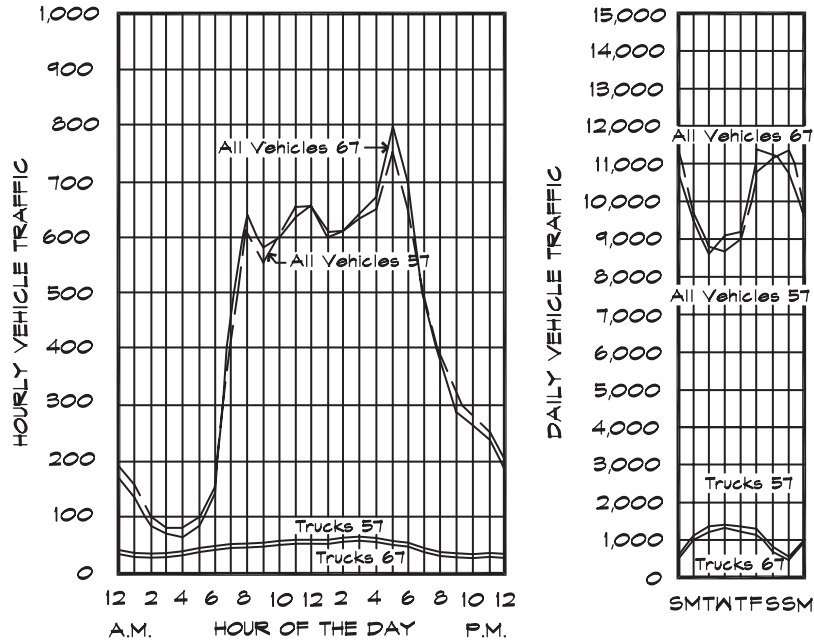
Expressed in terms of vehicles per 10,000 annual daily traffic.
Data shown for 1957 and 1967.

where L_{eq} = equivalent sound level during the time period of interest (dBA)

   L_{ref} = equivalent sound level for one vehicle passage during the time of interest (dBA)

   N_h = number of like vehicles passing the measurement point during the time period of interest (usually one hour)

Assume that we can obtain the L_{eq} level for a given hour by direct measurement at a site. This can be accomplished by measuring over an hour period or by sampling the noise over a shorter time period and by assuming that the sample is representative of the hour period. Once the data have been obtained for the known hour, they can be adjusted for the time of day in which they were measured using standard distributions such as those in Figs. 4.15 and 4.16 or the actual site-specific traffic distribution, if it is known.

A traffic calculation uses a weighted hourly number of vehicles passing a point that yields the L_{dn} or CNEL level if inserted into Eq. 4.2. Thus

$$L_{dn} = L_{ref} + 10 \log N_{dn\,ave} \qquad (4.3)$$

where L_{dn} = day night noise level (dBA)

   L_{ref} = equivalent sound level for one vehicle passing by during an hour period (dBA)

   $N_{dn\,ave}$ = weighted average number of like vehicles passing the measurement point during an equivalent hour

The day-night average number can be calculated from the distributions for urban and highway conditions using Eq. 3.7 for L_{dn} or Eq. 3.8 for CNEL.

$$N_{dn\,ave} = \left\{ \frac{1}{24} \left[\sum_{i=8}^{22} N_i + (10) \sum_{i=23}^{7} N_i \right] \right\} \qquad (4.4)$$

where N_i = number of vehicles passing the measurement
            point during the i th hour

Finally by subtracting Eq. 4.2 and 4.3 we can obtain the difference in decibels between an L_{eq} level in any particular hour and the day-night level over a 24-hour period for a known traffic distribution.

$$L_{dn} \cong L_{eq}(h) + C(h) \qquad (4.5)$$

where L_{dn} = day - night noise level (dBA)
      $L_{eq}(h)$ = equivalent sound level for a given hour, h (dBA)

   $C(h) = 10 \log \dfrac{N_h}{N_{dn\,ave}}$
        = correction (dB) for the hour, h, based on the
          appropriate traffic distribution

The result is given in Table 4.2 for the Wyle urban and highway distributions for L_{dn}. The CNEL for these distributions is about 0.5 dB higher. If the traffic pattern at a particular site differs from those given here and is known, a similar calculation can be done for the specific distribution.

Included in these approximations is the assumption that the traffic speed and other factors that affect traffic noise, such as truck percentage, remain nearly the same over a 24-hour period. On crowded city streets this may not be the case. If traffic is free-flowing during the measurement period this method gives a conservative (high) estimate of the L_{dn} level. If traffic is slowed due to congestion, the noise levels will not be representative of a free-flowing condition.

If readings are taken during congested periods, the method will underestimate the actual 24-hour levels. If traffic slows significantly during rush hour, measurements made during off-peak periods, when traffic is flowing freely, will yield a result that is somewhat higher than the actual L_{dn} value.

The distribution of truck traffic over the day does not exactly track the automobile distribution. A similar calculation can be undertaken that includes truck percentages, with a knowledge of the difference between the reference level for trucks and cars. Naturally this introduces additional complexity. Based on 24-hour measurements, the method has been found to yield levels within one or two dB of the actual values, even without inclusion of a separate truck percentage distribution.

4.4   BROADBAND NOISE METRICS

At first glance the number and variety of acoustic metrics is overwhelming. In no other science are there as many different fundamental ways of measuring and characterizing the

TABLE **4.2   Approximate Conversion from Leq to Ldn or CNEL (Based on the traffic distributions shown in Figs. 4.15 and 4.16)**

Hour	Highway Distribution		Urban Vehicle Distribution	
	$CNEL - L_{eq}$	$L_{dn} - L_{eq}$	$CNEL - L_{eq}$	$L_{dn} - L_{eq}$
	(dB)	(dB)	(dB)	(dB)
1	8.2	7.7	10.9	10.4
2	10.4	9.9	15.1	14.6
3	11.2	10.7	16.9	16.4
4	11.6	11.1	19.9	19.4
5	10.6	10.1	9.5	9.0
6	8.2	7.7	6.5	6.0
7	3.6	3.1	2.6	2.1
8	1.6	1.1	0.8	0.3
9	2.0	1.5	1.7	1.2
10	1.9	1.4	2.9	2.4
11	1.6	1.1	2.7	2.3
12	1.5	1.0	2.6	2.2
13	1.9	1.4	2.5	2.1
14	1.8	1.3	2.4	1.9
15	1.6	1.1	1.5	1.0
16	1.4	0.9	0.8	0.3
17	0.7	0.2	1.3	0.8
18	1.3	0.8	1.8	1.3
19	2.7	2.2	2.7	2.2
20	4.0	3.5	3.6	3.1
21	5.0	4.5	4.3	3.7
22	5.3	4.8	5.6	5.1
23	5.9	5.4	6.9	6.4
24	7.1	6.6	7.8	7.4

basic parameters. In physics the kilogram, meter, and second do not change. In electronics the volt, ohm, and ampere are stable and well defined. In environmental acoustics, however, different countries, states, cities, and counties often use different measurement schemes, which may not be directly convertible from one to another.

Even though the absolute number of metrics is large, the number of types of corrections applied to the measured data is rather modest. For example, a frequency correction for the loudness of a sound is included in most sound metrics but there are a number of ways to account for it, including A-weighting, NC curves, noys, and so on. The fundamental types of corrections include bandwidth, loudness, source number or duration, time of day, variability, onset, and pure tone content. The way each is included in a particular metric varies, but several are usually included in some fashion.

Bandwidth Corrections

The first correction category is the bandwidth of the measurement. Generally this is either wide band (i.e., 20 to 20 kHz) or band limited to octave or third-octave bandwidths. Narrow-band or chirped (swept) filters are also employed but the other corrections are seldom

FIGURE 4.17   Broadband Noise Metrics
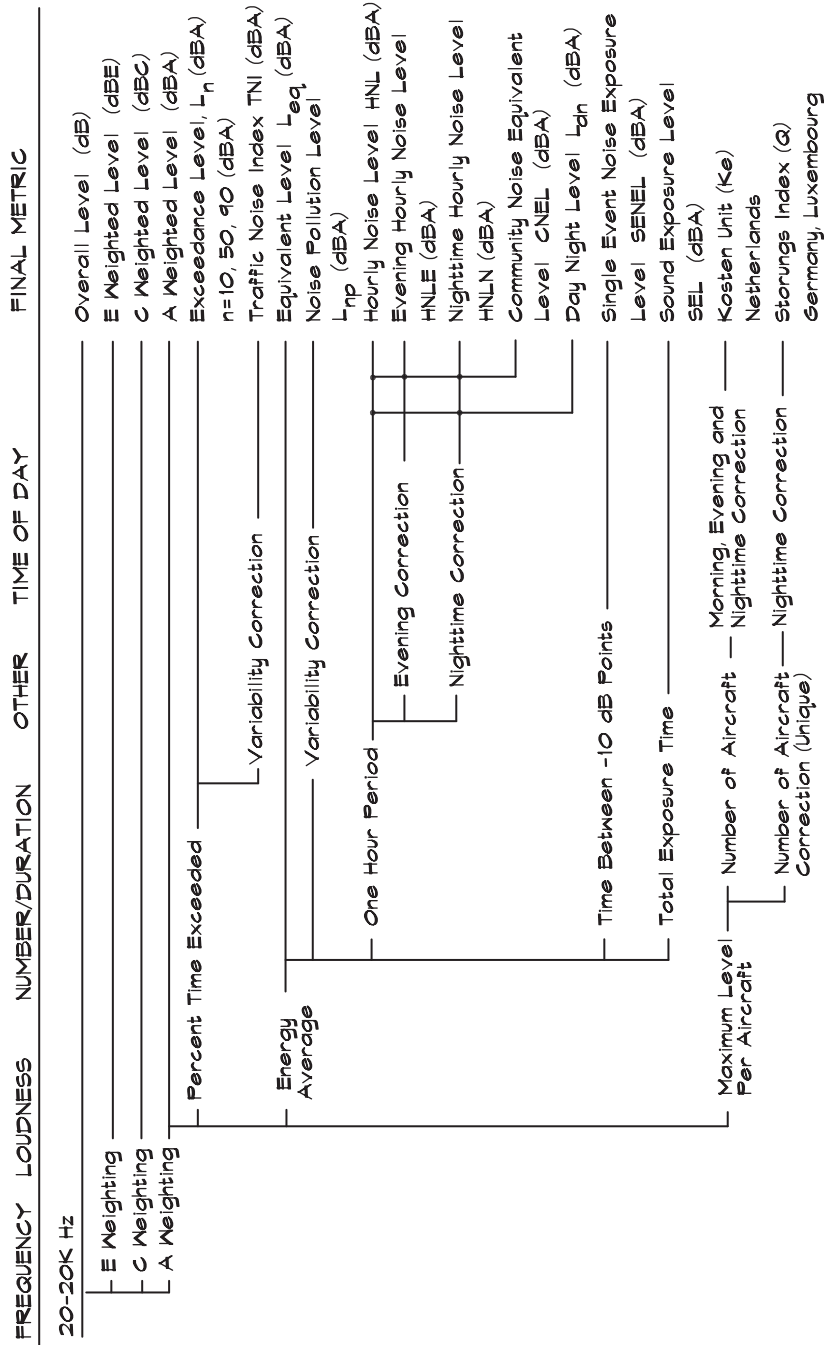
applied to these measurements. Several metrics based on wide-band measurements are shown in Fig. 4.17. The loudness corrections in these measurements are applied by means of electronic filters, such as the A-weighting network, which are included in the meter itself. Subsequent corrections can be applied internally by the meter or can be added by a separate calculation.

Duration Corrections

One of the earliest metrics for describing traffic generated noise was the L_{10} (pronounced *ell-ten*) level. An L_n level is defined as the A-weighted sound level exceeded n % of the time during the measurement period. The L_{10} level is close to the maximum level occurring during a time period and its use reflects the fact that the highest levels are the most annoying. L_{10} levels are measured by using a histogram sampling technique, either manually or internally within the meter. If a histogram of measurements is made and there are 100 total samples, the L_{10} level is determined by counting 10 (10% of the total) measurements down from the highest level.

In a similar fashion the other excedance levels of interest can be determined. The L_{50} level or median is sometimes used. The L_{90} level is frequently used to characterize the residual background. L_n levels are expressed as whole numbers. From the statistical distribution of noise levels that can be characterized as normally distributed, certain relationships can be developed relating excedance levels to L_{eq} levels. For example, the energy average level, expressed in terms of the mean value (Barry and Reagan, 1978), is

$$L_{eq} = L_{50} + 0.115\,\sigma^2 \qquad (4.6)$$

where L_{eq} = equivalent sound level (dB)
$\quad\quad\;\; L_{50}$ = mean value sound level (dB)
$\quad\quad\;\;\; \sigma$ = standard deviation of the sound levels (dB)

For a normal distribution, the L_{50} level and the L_{10} level are related

$$L_{10} = L_{50} + 1.28\,\sigma \qquad (4.7)$$

The relationship between L_{10} and L_{eq} can be obtained

$$L_{eq} = L_{10} - 1.28\,\sigma + 0.115\,\sigma^2 \qquad (4.8)$$

where L_{eq} = equivalent sound level (dB)
$\quad\quad\;\; L_{10}$ = sound level exceeded 10% of the time (dB)
$\quad\quad\;\;\; \sigma$ = standard deviation of the sound levels (dB)

The standard deviation of highway traffic noise is usually 2 to 5 dB, so the L_{10} level is higher than the L_{eq} level. For traffic noise, the L_{eq} level is about equal to the L_{20} level. Not all outdoor noise distributions are normal, so these equations should be used carefully as general estimates of the actual values.

Variability Corrections

Metrics have been developed that include a term for the variability of the sound, the theory being that the more variable the sound distribution, the more annoying it is. The noise pollution level is one of these and is used to characterize community noise impacts. It is defined as

$$L_{NP} = L_{eq} + 2.56\,\sigma \qquad (4.9)$$

where L_{NP} = noise pollution level (dBA)
        L_{eq} = equivalent sound level (dBA)
        σ = standard deviation of the sound levels (dBA)

Note that the noise pollution level uses A-weighting.

The traffic noise index (TNI) is another metric that includes a term for the variability of the noise environment. In this metric the variability is characterized in terms of the difference between the L_{10} and the L_{90} levels. The traffic noise index is given by

$$TNI = 4(L_{10} - L_{90}) + L_{90} - 30 (dBA) \qquad (4.10)$$

where   TNI = traffic noise index (dBA)
        L_{10} = level exceeded 10% of the time (dBA)
        L_{90} = level exceeded 90% of the time (dBA)

Both the noise pollution level and the traffic noise index were developed for use in characterizing traffic noise and are not as accurate in predicting human reaction to other environmental noise sources.

Sound Exposure Levels

Metrics that utilize the format of energy times time are called exposure levels and are expressed in decibels with a reference period time of one second. There is considerable usefulness in such metrics in that they contain all the energy that occurs during a given event packed into a period one second long. The sound exposure level (SEL) is one such metric and is defined as

$$SEL = 10 \log \left[\sum_{i=1}^{N} 10^{0.1 L_i} \right] \qquad (4.11)$$

where   SEL = sound exposure level (dBA)
        L_i = sound level for a given one - second time period (dBA)
        N = number of seconds during the measurement period

The SEL can be measured directly by many sound level meters. The meter can be set to display the SEL, which is internally computed, following the initiation of the measurement, by pushing the meter reset button. The L_{eq} can be calculated from the SEL for a given time period T

$$L_{eq} = SEL - 10 \log(T) \qquad (4.12)$$

where   SEL = sound exposure level (dBA)
        L_{eq} = equivalent sound level for a given time period (dBA)
        T = time (s)

When there are several events, the L_{eq} level can be calculated from the SEL levels for each event. The SEL levels are combined using Eq. 2.62 and the L_{eq} level is calculated using Eq. 4.12. If both the L_{eq} and the SEL are measured simultaneously, the measurement time period can also be calculated using Eq. 4.12.

Single Event Noise Exposure Level

The single event noise exposure level (SENEL) is similar to the SEL in that it sums the energy times the time associated with an event. Originally, it was developed to measure the noise energy of the flyby of a single aircraft. In such measurements it is sometimes difficult to tell when to begin and when to stop the readings. If the data are recorded on a strip chart or tape recorder it is unclear at what point on either side of the peak to stop adding up the energy. To short cut the process the SENEL was developed. This metric is the exposure level contained in the top 10 dB of a single event sound level record. The duration of the event in a SENEL is the time between the two points at which the level falls 10 dB below the maximum. Figure 4.18 shows the L_{eq} for a triangular sound pattern. The SEL or SENEL may be calculated from these L_{eq} levels by using an equation similar to 4.12, where the time period is equal to the pulse duration τ. Once the SENEL is known, the L_{eq} can be calculated for any period of time containing the event.

$$L_{eq} = \text{SENEL} - 10\log(T) \qquad (4.13)$$

where   SENEL = single event noise exposure level (dBA)
           L_{eq} = equivalent sound level for a given time period (dBA)
            T = time period for which the L_{eq} is to be calculated (s)

Note that it is necessary that the time period T in both Eqs. 4.12 and 4.13 be equal to or greater than the time period over which the SEL or SENEL was measured; otherwise, the event is not accurately represented. As with SEL, if several events occur within a given time period, then the individual SENEL levels may be combined using Eq. 2.62. An equivalent level can be calculated using Eq. 4.13 from the combined SENEL level.

4.5   BAND LIMITED NOISE METRICS

Techniques used for measurements employing octave band or other bandwidth filters vary little from those described for measuring broadband levels. Care must be taken in measuring low-frequency sounds so that the appropriate spacing between the source, reflecting surface, and the measurement location is observed. Sufficient sampling time is also a factor with low-frequency measurements because some low-frequency sources produce beat frequencies, which may be on the order of 1 Hz or less and may vary slowly over time.

Figure 4.19 shows a summary of the types of metrics obtained from octave-band measurements. As with the broadband systems there are a number of different metrics; however, the number of correction categories is relatively small. A loudness can be measured using electronic filters such as the A-weighting network. The A-weighted octave-band spectrum is useful as an aid in the determination of the frequency band making the most significant contribution to the overall A-weighted noise level. If most of the A-weighted energy is contained in one frequency band, then noise control efforts should be concentrated there.

A simple unweighted octave-band level is the basis for a number of metrics that determine the loudness by a direct comparison of the measured data to a standard curve of values. Several standards have been developed over the years, having to do principally with heating, ventilating, and air conditioning (HVAC) noise. The NC and RC curves are described in Chapt. 3.

FIGURE 4.18 L_{eq} **Levels for Various Time Patterns (US EPA, 1973)**

For triangular shaped patterns – time period = τ

$$\Delta L = L_{max} - L_b$$

$$L_{eq} = L_b + 10 \log \frac{10}{2.3\,\Delta L}\ (10^{\frac{\Delta L}{10}} - 1)$$
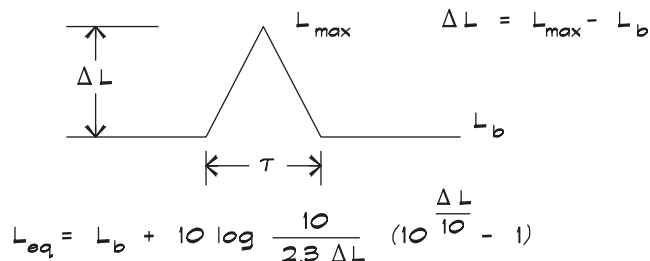
When ΔL is greater than 10 dB the following approximation is accurate.

$$L_{eq} = L_{max} - 10 \log \frac{2.3\,\Delta L}{10}$$

When there are a series of n identical triangular time patterns as shown above occurring within an interval T then

$$L_{eq} = L_b + 10 \log \left[1 + \frac{n\tau}{T} \left\{ \frac{(10^{\frac{\Delta L}{10}} - 1)}{2.3} - \frac{\Delta L}{10} \right\} \right]$$

For trapezoidial shaped patterns – time period = τ
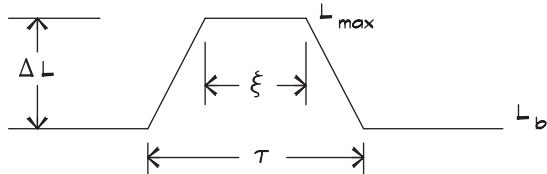
$$L_{eq} = 10 \log \frac{1}{\frac{(\tau - \xi)\Delta L}{10} + \frac{\xi}{2}} \left[10^{\frac{L_b}{10}} \frac{(\tau - \xi)}{2.3} \left(10^{\frac{\Delta L}{10}} - 1 \right) + 10^{\frac{L_{max}}{10}} \frac{\xi}{2} \right]$$

When ΔL is greater than 10 dB and ξ is small compared to τ.

$$L_{eq} = L_{max} - 10 \log \frac{2.3\,\Delta L}{10} + 10 \log \xi$$

When there is a series of n identical trapezodial time patterns as shown above occurring within an interval T then

$$L_{eq} = L_{max} + 10 \log \frac{n\tau}{2.3\,T} + 10 \log n\xi$$

For a series of triangular pulses the last term above can be omitted.

Preferred Noise Criterion (PNC) Curves

PNC curves were introduced by Beranek in 1971 and are a revision of his earlier (1957) NC curves. PNC curves altered the high- and low-frequency octave values somewhat. The difference between the two has not been sufficient to result in the wide acceptance of the PNC version. The PNC curves are shown in Fig. 4.20. The use of the PNC curve is similar to that of the NC curve in that the PNC level is determined using the method of tangency.

FIGURE 4.19   Octave Band Noise Metrics

Column headers: FREQUENCY LOUDNESS NUMBER/DURATION OTHER TIME OF DAY FINAL METRIC

One Octave (Standard Center Frequencies) — Octave Band Level (dB)

E Weighting — E Weighted Octave Level (dBE)

C Weighting — C Weighted Octave Level (dBC)

A Weighting — A Weighted Octave Level (dBA)

Stephens Mark VII (Absolute Loudness) — Loudness Level (OD Phons)

Comparison (Relative Annoyance) — Loudness Index (OD Sones)

1/4 (.5k + 1k + 2k + 4k Bands) — Speech Interference Level SIL (dB)

1/3 (.5k + 1k + 2k Bands) — Preferred Speech Interference Level – PSIL (dB)

NC Curve Comparison — Noise Criterion NC (dB)

PNC Curve Comparison — Preferred Noise Criterion Level PNC (dB)

RC Curve Comparison — Room Criterion Level RC (dB)

NCB Curve Comparison — Rumble and Hiss Test — Balanced Noise Criterion Level NCB (dB)

Balanced Noise Criterion (NCB) Curves (Beranek, 1989)

In 1989, Beranek introduced another version of his 1957 NC curves, which he suggested for application to unoccupied rooms. These NCB levels, given in Fig. 4.21, are similar to the NC curves; however, the frequency range extends to 16 Hz and the metric calls for the calculation of the speech interference level (SIL) from the noise spectrum. This is rounded

FIGURE 4.20   Preferred Noise Criterion (Beranek, 1971)
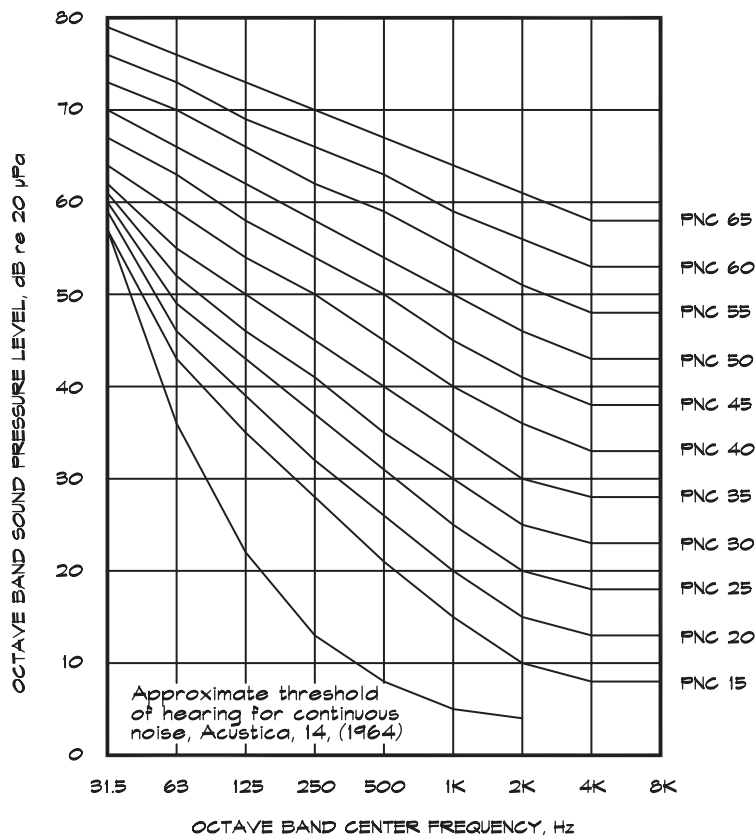
to the nearest dB and compared with the NCB curve designation, which is also characterized by its SIL. If the measured SIL is equal to or below the curve designation, then the noise level meets the NCB criterion for speech interference.

Next comes a test for rumble or low-frequency energy. To check for this condition, 3 dB is added to the measured SIL and the NCB curve corresponding to this level is overlaid on the measured data. Where there are excedances of the new curve in the octave bands below 1 k Hz, they must be reduced to the elevated curve levels to comply with the standard.

Finally there is the NCB test for hiss or high-frequency annoyance. An NCB curve is selected that provides the best fit to the measured data in the 125–500 Hz bands. Then this curve is plotted against the measured data. If the measured data exceed it in any of the three bands above 1 k Hz, then they must be reduced to meet the hiss criterion.

In occupied spaces Beranek calls for the measurement or estimation of noise levels due to normal work activities, which are to be combined with the unoccupied (HVAC) levels before a comparison to the NCB curve is made.

Other Octave-Band Metrics

Other systems exist for the determination of loudness based on measured octave-band data. They are based on empirical tests of relative or absolute comparisons presented to listeners in much the same way that the Fletcher-Munson experiments were done.

FIGURE 4.21   Balanced Noise Criterion Curves (NCB) (Beranek, 1989)

A – Clearly Noticeable Vibrations in Lightweight Structures
B – Moderately Noticeable Vibrations in Lightweight Structures
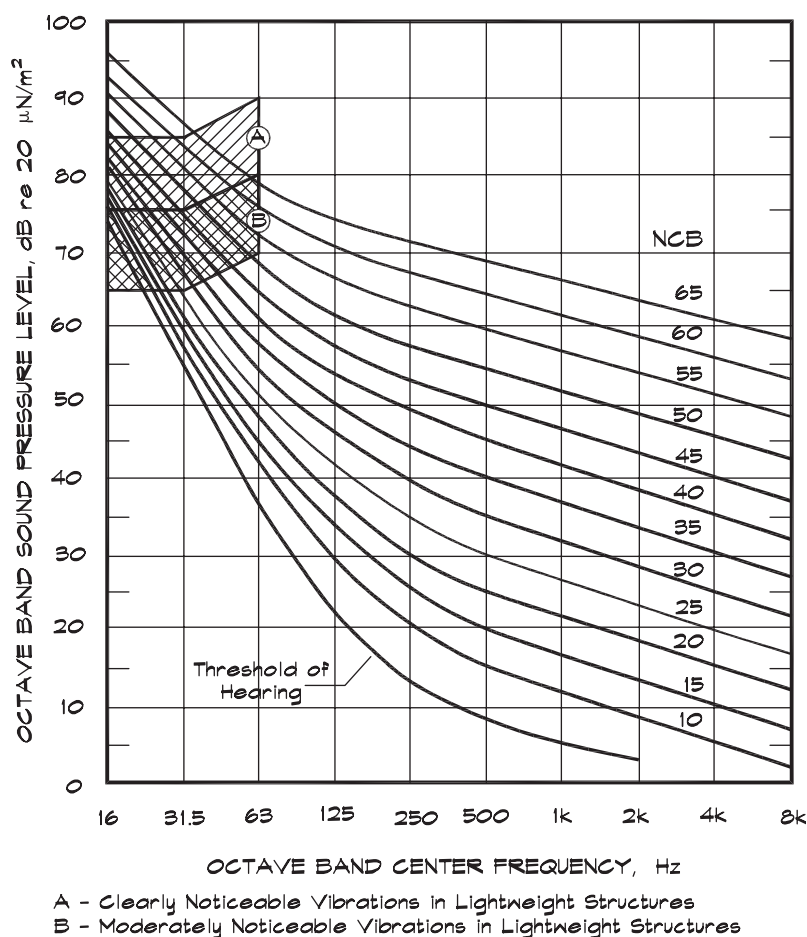
Robinson and Whittle (1962) constructed relative loudness curves in a very similar way. Stevens (1972) developed a series of systems for the calculation of loudness from octave band and other narrower bandwidth data. These systems rarely are encountered in architectural acoustics.

Octave-Band Calculations

It is frequently necessary to obtain an overall A-weighted level from unweighted octave-band data. The calculation is done by first adding the corrections for A-weighting, given in Table 3.1, to the level in each octave, and then by combining the A-weighted octave-band levels together using Eq. 2.62.

Occasionally it is necessary to generate an octave-band spectrum to match a given A-weighted level. This is straightforward if the spectrum shape of the sound source can be obtained. For example, let us assume that it is known that recorded music has a given octave-band spectrum and that this spectrum generates an overall A-weighted sound pressure level of 70 dBA. If we wish to obtain the octave-band spectrum of music that will yield an overall A-weighted level of some other level, for example 80 dBA, it is only necessary to add the difference between 80 and 70 to each octave-band level. It is assumed that the spectrum

shape does not change with level for this source. It is useful to prepare normalized spectra for standard sources, which, when added to the overall A-weighted sound level, will yield an unweighted octave-band level having the same overall value.

If there are two sources present at the same time and we know the octave-band spectrum levels of each source independently, the spectrum for the two sources combined is obtained by applying Eq. 2.62 to the pairs of levels in each octave.

Third-Octave Bandwidth Metrics

Third-octave band metrics are similar to octave-band levels—they are simply a thinner slice of the same pie. They can be combined into groups of three centered around the octave-band center frequencies using Eq. 2.62 to obtain octave-band levels.

A summary of various third-octave and narrow band metrics is shown in Fig. 4.22. As with the octave-band metrics there are different versions of loudness and annoyance comparisons. One of these, the perceived noise level (PNdB) developed by Kryter (1970), has been used as the basis for several of the standard metrics for characterizing aircraft noise.

Aircraft Noise Rating Systems

Aircraft noise ratings vary principally in the methodologies they use for adjusting for the number of aircraft, the addition of pure tone corrections, and the inclusion of nighttime penalties. An excellent review of aircraft metrics was prepared by (Schuller et al., 1995). He summarizes the descriptors using the equation

$$\text{Level} = A \log \left(\sum_{i=1}^{N} n_i \, w_i \, 10^{L_i/B} \right) - C \tag{4.14}$$

where A, B, C = constants
i = aircraft type category index
N = total number of aircraft type categories
n_i = number of noise events for aircraft category i per 24 - hour day
w_i = penalty (or weighting) factor for aircraft operation i
L_i = single event noise level for aircraft category i

The parameters used in Eq. 4.14 for various environmental metrics are given in Table 4.3.

Most of the metrics used for aircraft correlate well with the simpler L_{dn} level, which is the most commonly used system in the United States. For estimation purposes the following formulas may be used:

$$L_{dn} \cong \text{CNEL} \tag{4.15}$$

$$L_{dn} \cong \text{NEF} + 35(\pm 3) \tag{4.16}$$

$$L_{dn} \cong \text{CNR} - 35(\pm 3) \tag{4.17}$$

Similar relationships can be derived for the other metrics currently in use.

FIGURE 4.22   Narrow Band Noise Metrics

Narrow-Band Analysis

The analysis of sound in frequency bands of one-third octave and less is often useful for the detailed analysis of room acoustics and vibration. Instruments used for this type of measurement in real time are called spectrum analyzers or real-time analyzers (RTA). Two types of meters are most frequently encountered, those having a constant percentage bandwidth

TABLE 4.3 Parameters Used in Equation 4.14 (Schuller et al., 1995)

Metric	Constants			Day Interval (Hours)	W_i	Morning, Evening Interval (Hours)	W_i	Night Interval (Hours)	W_i	L_i (dB)
	A	**B**	**C**							
Ke	20	15	105.8	08–18	1	06–08, 18–23	2–8	23–06	10	L_{ASmx}
L_n	10	10	44	06–23	0			23–06	1	L_{AE}
L_d	10	10	47.6[1]	07–23	1			23–07	0	L_{AE}
Q	13.3	13.3	65.7[2]	06–22	1			22–06	5[3]	L_{ASmx}
IP	10	10	49.4	07–22	1			22–07	10	L_{AE}
L_{dn}	10	10	44	06–23	0			23–06	1	L_{AE}
CNEL	10	10	44	07–19	1	19–22	3	22–07	10	L_{AE}
L_{24h}	10	10	44	00–24	1					L_{AE}
NNI	10	10	$80 - 5 \log \sum_{i=1}^{N} n_i w_i$	06–18	1			18–06	0	L_{pnmx}
NEF	10	10	88	07–22	1			22–07	16.7	L_{epn}

Single Event Noise Level Descriptors

L_{AE} = A-weighted sound exposure level
L_{ASmx} = Maximum S (slow) A-weighted sound level
L_{pnmx} = Maximum perceived noise level
L_{epn} = Effective perceived noise level

1) **7 hour night from 00.00 to 06.00 and 23.00 to 24.00 hours on a given day**
2) **16 hour daytime period from 07.00 to 23.00 hours on a given day**
3) **Seperate calculations are specified for day and night. Values shown here are for calculations with emphasis on the contributions from nightime flight operations, Q_n. The weighting penalty includes a multiplication by the duration, in seconds, beween the first and last times that the instantaneous A-weighted sound level is within 10 dB of the maximum A-weighted sound level.**

filter such as octave, third-octave, twelfth-octave, and so on, and those having a constant bandwidth such as 1 Hz. The latter type is used primarily in a laboratory while the former are the more common field instruments.

Instruments have filters of one of two types: analog and digital. An ideal bandpass filter is a device that passes all the electrical signals within its bandwidth and totally rejects all other signals. Analog filters are made of passive (resistors, inductors, and capacitors) or active (operational amplifiers) that approximate this ideal behavior. A meter having a group of such filters, operating in parallel, with each center frequency separated from the next by one-third octave, constitutes a real-time analyzer. These devices are robust and responsive. Some offer internal processing, such as energy averaging, and others feature only a freeze-and-save capability. Internal averaging is preferred since it is difficult to catch a varying signal at a point where all frequencies of interest are simultaneously at an average value.

A second type of system utilizes a mathematical filter, sometimes referred to as a digital filter. Digital filters can be constructed with the same characteristics as their analog counterparts. In these instruments the electrical signal is sampled periodically and the resulting string of numbers analyzed mathematically. One such procedure is the Fourier analysis (Joseph Fourier, 1768–1830), whereby a periodic signal is decomposed into its various harmonic components. Fourier's mathematical theorem states that any periodic waveform can be constructed from the sum of a specific sinusoidal wave called the fundamental, and a series of harmonics of the fundamental, multiplied by suitably selected constants. A graph of the amplitude versus frequency of these components is the spectrum of the original signal. A signal that has been digitally sampled can be sorted into its component frequencies using a mathematical process called the fast Fourier transform (FFT). Using similar techniques, filters can be constructed mathematically and applied to the digital number stream. The advantages of the digital filter are its flexibility, its low-frequency resolution, and its low cost. Disadvantages are its high-frequency limitations (eventually we cannot sample and calculate fast enough) and the features available on a given instrument.

4.6   SPECIALIZED MEASUREMENT TECHNIQUES

Time-Delay Spectrometry

It is desirable to exclude noise intrusions from the measurements of a given signal. Anechoic chambers have been used for this purpose, since they are constructed not only to reduce sound from outside sources, but also to minimize the sound that is reflected off the walls and other surfaces of a room. A measurement technique originally developed by Richard Heyser (1931–1987) called time-delay spectrometry (TDS) can be used to make isolated measurements, even in a reverberant environment. The technique is based on the idea that when a sound source emits a signal it arrives at the receiving microphone after a given time. All the reflected sounds associated with the original signal arrive at some later time since they traveled along longer paths. If the measurement is made during a narrow time interval centered about the arrival time of the direct sound, later sounds are excluded and a nearly anechoic result can be achieved.

This is accomplished by converting the time delay into a frequency change. Figure 4.23 illustrates the principle. A loudspeaker is fed a sinusoidal signal that is chirped, or swept upward in frequency, at a fixed rate. At the receiver a narrow-band filter also is swept upward at the same rate. If the timing is correct the signal at a given frequency will arrive precisely when its filter window arrives. This technique is the same as that used by a quarterback

FIGURE 4.23   Time Delay Spectrometry
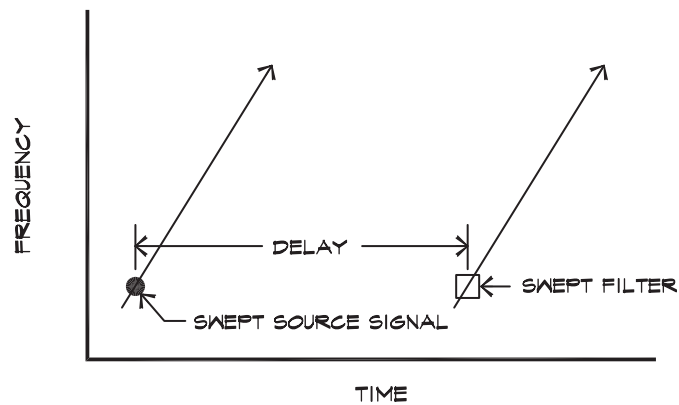
to throw a pass to a moving receiver. The ball (signal) and the receiver (filter window) must arrive at the same point at the same time for a reception. Passes that are delayed by reflections (off the ground or defensive linemen) do not arrive at the proper time and thus are not received.

Time-delay spectrometry can be used to measure the spectral response curve of a loudspeaker. The narrow-band analysis in Fig. 4.24 illustrates the detailed variations found in a typical loudspeaker. To obtain third-octave or octave-band data, the narrow-band energy data must be summed together over the appropriate frequency range. This process tends to smooth out the ripples in the curve and yields a more charitable portrait of the frequency response.

Energy-Time Curves

If a loudspeaker system is excited electronically with an impulsive signal, the signal received by a microphone can be plotted with time. This type of plot is called an energy-time curve (ETC) and contains useful information about the loudspeaker system as well as the room it is in. Turning first to loudspeakers, ETC plots are used to align transducers so that the signals from different components arrive at the listener at the same time. An example is shown in Fig. 4.25. Alignment is critical since a time delay is equivalent to a phase shift, which can produce a cancellation at the crossover frequency between transducers. Note that crossover points can be either electronic or spatial.

When two loudspeakers are misaligned, the ETC plot shows two distinct spikes. If this misalignment is sufficiently large, the result is a lack of clarity. When the two are aligned the overall level increases by 6 dB (due to an in-phase pressure doubling) and the peaks coincide in time. Loudspeaker alignment can be accomplished either by physical arrangement or by electronically delaying the signal transmitted to the forward transducer or both.

ETC plots can also reveal important information about reflections in rooms. A long-delayed reflection from the rear wall of a room, if sufficiently loud, can be disturbing to the perception of speech. Sometimes it is difficult in practice to identify the exact path that is causing the problem, particularly when multiple reflections are involved. An ETC plot can reveal the delay time of a given reflection and aid in the identification of the problem path. Patches of absorption can then be placed on the appropriate surfaces and the ETC measurements repeated for confirmation.

FIGURE 4.24   TDS Loudspeaker Measurements (Community, 1991)

A. Raw Data Without Smoothing

B. 100% (1 Octave) Smoothing
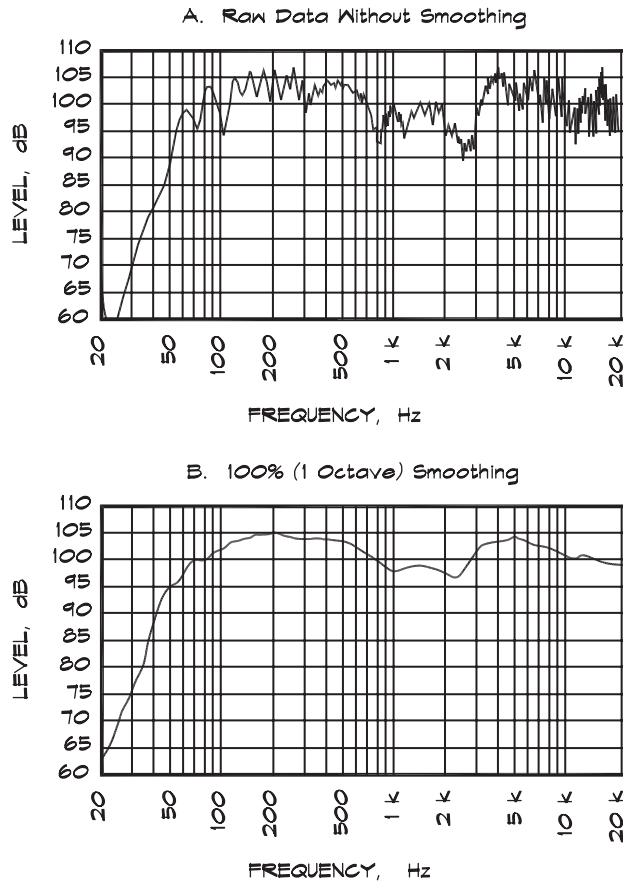
FIGURE 4.25   Energy Time Curves–ETC (Biering and Pedersen, 1983)

Early reflections from a loudspeaker in a normal listening room using TDS narrow band analysis
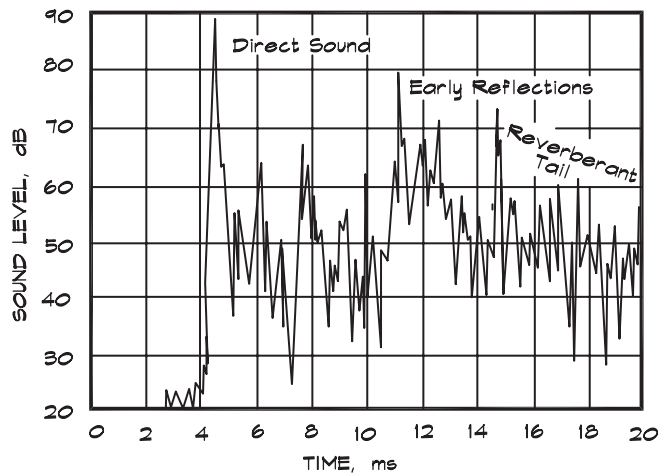
Sound Intensity Measurements

Direct measurement of the sound intensity has become possible through recent developments in commercial instrumentation. The intensity in a plane wave is defined as

$$I = p\,u \tag{4.18}$$

where I = maximum acoustic intensity (W/m^2)
$\quad\quad$ p = acoustic pressure (Pa)
$\quad\quad$ u = acoustic particle velocity (m/s)

The pressure is easily measured; however, direct measurement of the particle velocity is difficult. Instead the pressure can be measured using two closely spaced microphones, shown in Fig. 4.26, from which the change in pressure or pressure gradient can be obtained.

$\quad$ The reasoning is based on Newton's second law ($F = m\,a$) in one direction

$$\frac{d\,p}{d\,x} = -\rho_0\,\frac{d\,u}{d\,t} \tag{4.19}$$

where ρ_0 = density of the bulk fluid (kg/m^3)
$\quad\quad$ $d\,p$ = acoustic pressure change over a small distance $d\,x$ (Pa)
$\quad\quad$ $d\,u$ = acoustic particle velocity change in time $d\,t$ (m/s)

The minus sign is there to indicate in which direction the slice accelerates. This equation is a well-known fluid dynamic relationship called Euler's equation. It relates the difference in pressure across a slice of fluid to an acceleration in the fluid slice that is proportional to its mass. The intensity is calculated by solving Eq. 4.19 for the particle velocity by integration

$$u = -\frac{1}{\rho_0\,\Delta x}\int (p_a - p_b) \tag{4.20}$$

where ρ_0 = density of the bulk fluid (kg/m^3)
$\quad\quad$ p = acoustic pressure measured at two points a and b which are Δx apart (Pa)
$\quad\quad$ u = acoustic particle velocity (m/s)

FIGURE 4.26   **Microphones Used in Intensity Measurements (Gade, 1982)**

Two omnidirectional microphones are configured
face to face at a known separation distance.
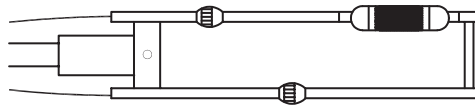
The intensity is then obtained by multiplying the pressure and the particle velocity.

$$I(\theta) = p\, u(\theta) = -\frac{p_a + p_b}{2\, \rho_0\, \Delta x} \int (p_a - p_b) \qquad (4.21)$$

where $I(\theta)$ = acoustic intensity in a given direction (W / m^2)

$\quad\quad\quad$ p = acoustic pressure, which when measured at two points a and b

$\quad\quad\quad\quad$ that are Δ x apart, is designated with a subscript (Pa)

$\quad\quad$ $u(\theta)$ = acoustic particle velocity in a given direction (m / s)

$\quad\quad\quad$ ρ_0 = density of the bulk fluid (kg / m^3)

Since the intensity is a vector, its magnitude depends on the direction in which the microphones are oriented. Using this feature the intensity probe can be used for source location and strength.

Modulation Transfer Function and RASTI

The intelligibility of speech has traditionally been measured by conducting tests, using various word lists, in rooms with human listeners. Although this methodology is the basis of most of our systems for predicting the intelligibility, it is highly desirable to have an electronic method of directly measuring these quantities. Human speech patterns are complex, and simple sinusoidal signals do not accurately mimic their behavior. Two Dutch scientists, Houtgast and Steeneken (1973), developed a measurement system, called the modulation transfer function (MTF), which replicates many of the properties of human speech. The concept is illustrated in Fig. 4.27. The idea behind MTF is that speech consists of modulated bands of noise. Our vocal cords vibrate to produce a band of noise, whereas our mouths modulate it at various frequencies to form words. To recreate this pattern, we start with an octave-wide band of noise and modulate it with a low-frequency tone. Mathematically this means that the carrier is multiplied by a sinusoidal function having a peak-to-peak amplitude of one. The result is a source signal that looks like the one on the left side of Fig. 4.28. For an accurate measurement the test signal level must be set to that of an average speaker and positioned where his mouth would be.

When this signal is transmitted to a listener, it is altered by the environment to some degree and can result in reduced speech intelligibility. The distortion mechanisms include background and reverberant noise, which raise the bottom of the signal above zero, and reflections, which add back a delayed and perhaps distorted copy of the signal. A typical receiver signal, shown on the right side of Fig. 4.28, is less modulated than the original, where the degree of modulation is defined by the depth of the modulation envelope. The reduction in modulation is characterized by a modulation reduction factor, $m(f_m)$, which is a function of the modulation frequency f_m. The modulation reduction factor varies from 0 for no reduction to 1 for 100% modulation reduction. Curves can be measured of the behavior of m versus f_m as shown on the bottom of Fig. 4.28.

When background noise is the principal source of the distortion, the effect on modulation reduction appears in terms of a signal-to-noise ratio, which is independent of modulation frequency. The noise raises all levels at the receiver within the carrier band and thus reduces modulation equally. When the distortion is produced by reverberation, the modulation reduction has the form of a low-pass filter with the faster fluctuations more sensitive to the effects of reverberation. This effect is characterized by the product of the modulation frequency and the

FIGURE 4.27   **Basis of the Modulation Transfer Function (Houtgast and Steeneken, 1985)**

The reduction of the fluctuations in the (octave band specific) envelope of an output signal (A or B) relative to the original signal can be expressed as a Modulation Transfer Function
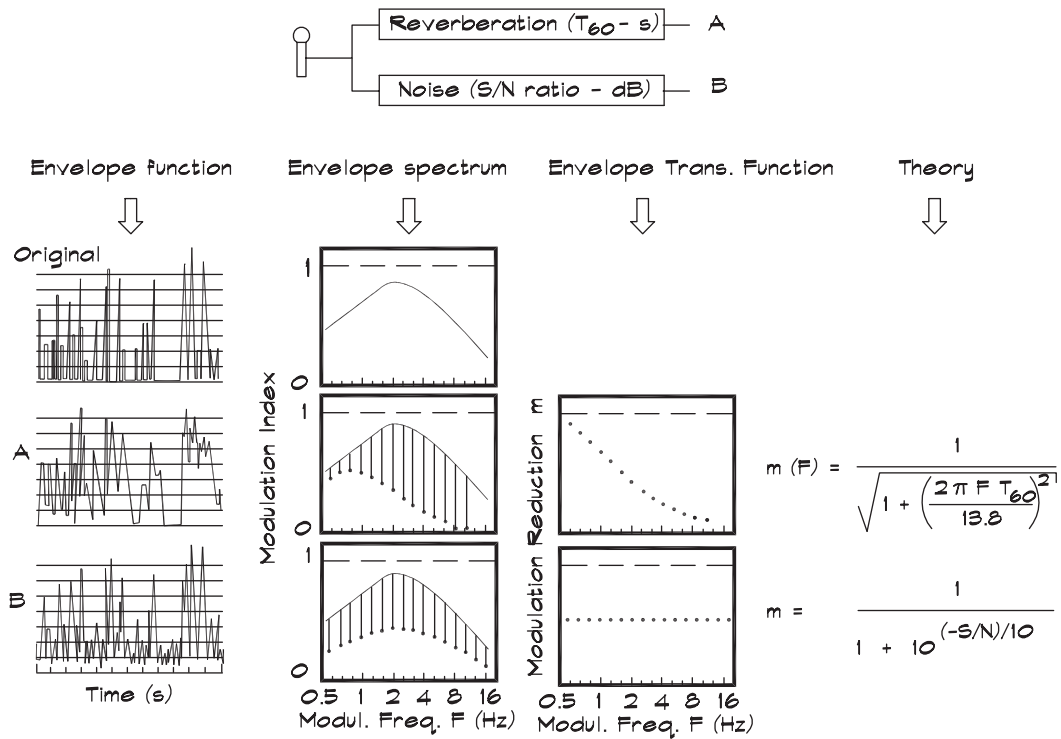
room reverberation time. The overall modulation reduction factor is given mathematically as the product of these two effects for an unamplified signal

$$m(f_m) = \frac{1}{\sqrt{1 + \left[2\pi f_m \dfrac{T_{60}}{13.8}\right]^2}} \frac{1}{1 + 10^{\left(-0.1L_{SN}\right)}} \tag{4.22}$$

where $m(f_m)$ = modulation reduction factor

L_{SN} = signal to noise level (dB)

f_m = modulation frequency (Hz)

T_{60} = room reverberation time (s)

The modulation frequency f_m ranges in value from 0.63 Hz to 12.5 Hz in third-octave intervals. The input-output analysis for a given system is done at 7 octave bands and 14 modulation frequencies, for a total of 98 separate values of m.

FIGURE 4.28   Modulation Transfer Function (Houtgast and Steeneken, 1985)

Original

$I(t) = [1 + \cos 2\pi f\, t]$

Oct. band (Hz)	T60 (s)	S/N (dB)
125	2.0	0
250	2.0	+5
500	2.0	+10
1k	1.4	+10
2k	1.0	+10
4k	0.7	+10
8k	0.5	+10

Transmitted

$I(t) = I[1 + m \cos (2\pi f\, t + \varphi)]$

Time

Carrier: Octave-band Filtered Noise

Time
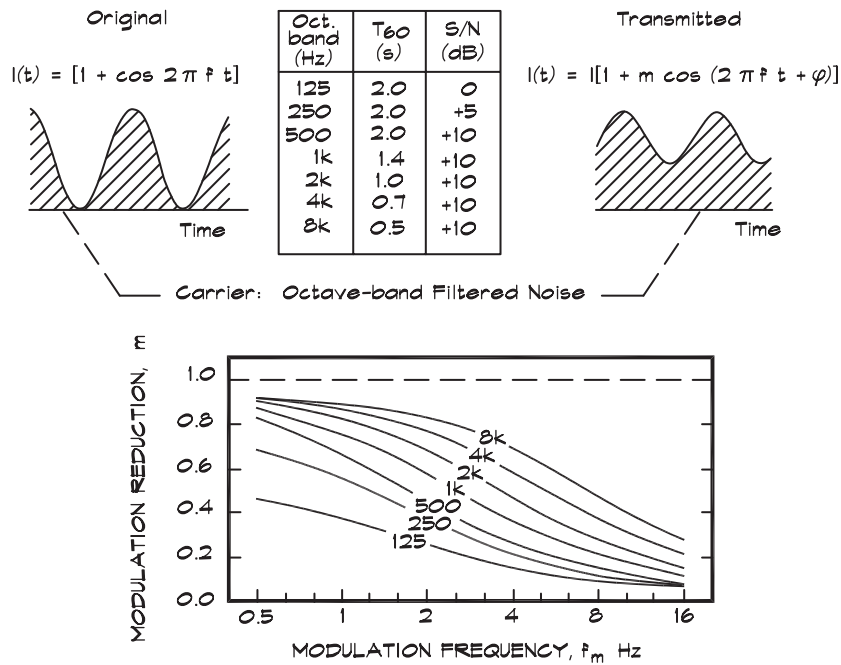
Illustration of how an MTF analysis is performed by using an octave-band filtered noise carrier, 100% intensity modulated, for each modulation frequency sucessively. This leads to a family of MTF curves. Each curve is calculated for the data given in the table.

Speech Transmission Index

With the MTF we have a quantity that mimics the behavior of speech, and can be physically measured with a properly constructed instrument. The missing link is the relationship between MTF and speech intelligibility. This is given in Fig. 4.29 by a speech transmission index (STI), which is similar to an articulation index or a percentage loss of consonants, in that it is a direct measure of speech intelligibility. All three are numerical schemes used to quantify the intelligibility of speech. Fig. 4.30 shows the relation between STI and Alcons, and Fig. 4.31 shows the similarity of STI to AI.

Steeneken and Houtgast (1980, 1985) developed an algorithm for transforming a set of m values into a speech transmission index (STI) by means of an apparent signal-to-noise ratio expressed as a level. This level is the signal-to-noise ratio that would have produced the modulation reduction factor, had all the distortion been caused by noise intrusion, irrespective of the actual cause of the distortion.

$$L_{\text{SNapp}} = 10 \log \frac{m}{1-m} \tag{4.23}$$

where L_{SNapp} = apparent signal to noise ratio (dB)
         m = modulation reduction factor

A weighted average of the 98 apparent signal-to-noise ratios yields the STI after applying a normalization such that

FIGURE 4.29   Typical Relations between the STI and Intelligibility Scores for the Various Types of Tests (Houtgast et al., 1985)
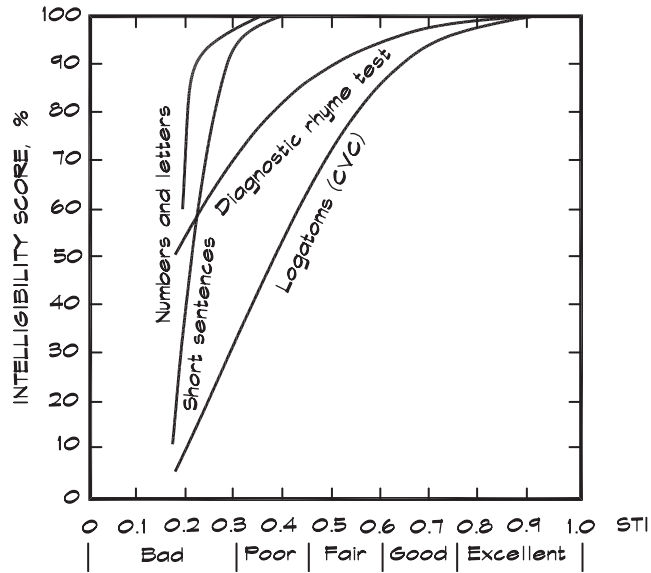
FIGURE 4.30   A Comparison of Articulation Index and Speech Transmission Index (Houtgast et al., 1980)

In this comparison the interference is only due to speech-shaped noise. The intelligibility rating is based on CVC (consonant, vowel, consonant) nonsense syllables embedded in a neutral carrier sentence.
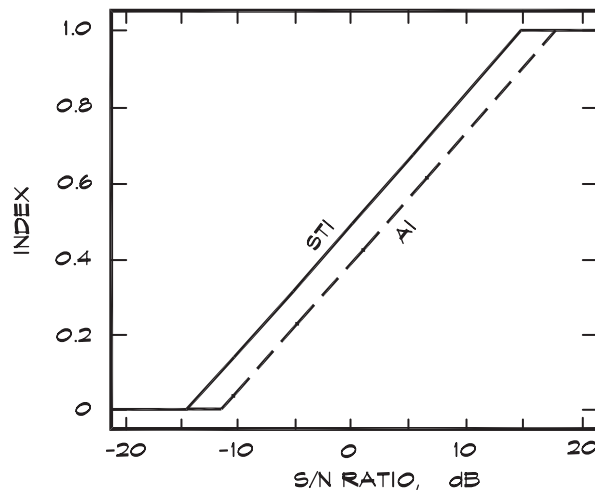
FIGURE 4.31   Relation between STI and Intelligibility Score (Houtgast et al., 1980)

The relation between intelligibility score and STI for a wide variety of conditions comprising many S/N ratios, reverberation times, and echo-delay times.
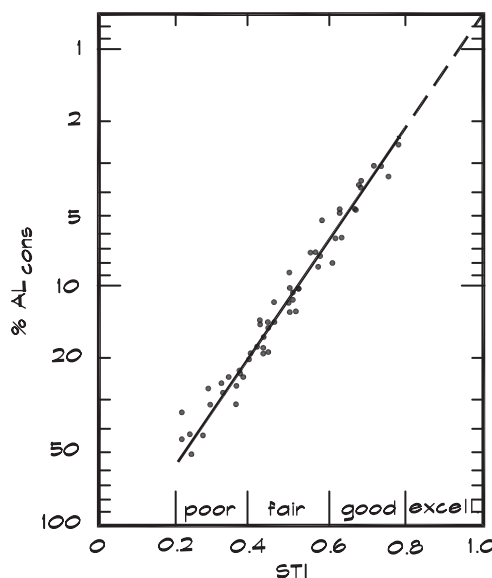
STI = 1.0 when $L_{SNapp} \geq 15$ dB for all 98 data points

STI = 0.0 when $L_{SNapp} \leq -15$ dB for all 98 data points

and

$$\overline{L_{SNapp}} = \sum_{i=1}^{7} w_i \left(L_{SNapp}\right)_i \tag{4.24}$$

where $\overline{L_{SNapp}}$ = average apparent signal-to-noise ratio (dB)

w_i = weighting for octave bands from 125 Hz to 8 k Hz

= 0.13, 0.14, 0.11, 0.12, 0.19, 0.17, and 0.14

then

$$STI = \left[\overline{L_{SNapp}} + 15\right] / 30 \tag{4.25}$$

Figure 4.32 shows the relationship between STI and the signal-to-noise ratio as well as the reverberation time.

The bottom part of Fig. 4.32 represents an alternative way of interpreting the effect of reverberation. The early part of the reverberant tail is considered helpful to the understanding of speech, whereas the end is considered detrimental. The boundary between the two regions occurs in the neighborhood of 70 to 80 ms. Though it may seem that this is rather long, in that a single 65 ms delay can be detected as an echo, it should be remembered that in normal rooms the listener hears a series of reflections and thus the Haas region is extended somewhat (Fig. 3.29).

FIGURE 4.32   **Relationship between Modulation Transfer Function and the Speech Transmission Index (Houtgast and Steeneken, 1985)**

The upper panels represent the theoretical relationships between STI and the S/N ratio, or STI and T_{60}. From this, each T_{60} value may be converted into the equivalent S/N ratio (as shown below).
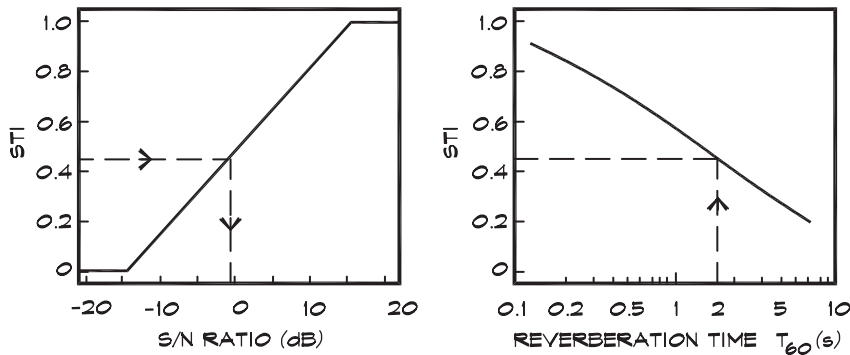
The dashed curves below represent the traditional approach in which the equivalent S/N ratio is defined by the ratio between the early and the late part of the energy time curve.
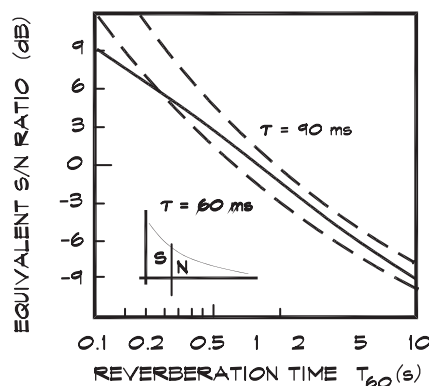
The research done by Houtgast and Steeneken established a way of measuring speech and intelligibility using an electronically generated test signal rather than a group of human subjects. Their calculation method is useful in evaluating rooms for an omnidirectional source, but does not include consideration of loudspeaker directivity, so necessary to the design of reinforcement systems. Once the method has been established as equivalent to other measures of intelligibility without amplification, the measurement system can be used to evaluate installed sound systems.

RASTI

RASTI or RApid STI is an approximation of the full STI taken by doing a measurement of nine of the 98 m values marked on the graph shown in Fig. 4.33. Two octave bands 500 and 2000 Hz are sampled. At 500 Hz, values of m are measured at four modulation frequencies, 1, 2, 4, and 8 Hz. At 2000 Hz, five modulation frequencies are measured, 0.7, 1.4, 2.8, 5.6, and 11.2 Hz. An apparent signal-to-noise ratio is calculated from the measured m values in each band and truncated so as to fall within the range of ±15 dB. The L_{SNapp} values are

FIGURE 4.33   The RASTI Analysis System (Houtgast and Steeneken, 1985)

RASTI only measures 9 of the out of a possible 98 modulation reduction factors as indicated by the hatched rectangles.
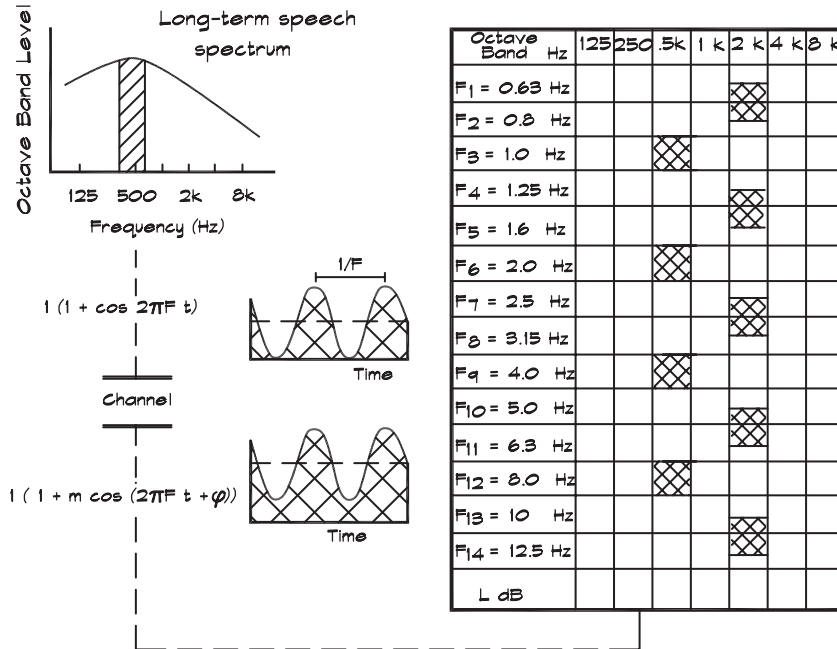
averaged and a RASTI value is calculated

$$\text{RASTI} = \left[\overline{\text{L}_{\text{SNapp}}} + 15\right] / 30 \qquad (4.26)$$

where   RASTI = rapid STI measurement index
$\overline{\text{L}_{\text{SNapp}}}$ = average apparent signal to noise ratio (dB)

In practice RASTI measurements can be made to evaluate the intelligibility of speech both for an unamplified talker as well as for an amplified sound system. The RASTI source is positioned at the talker location. If there is a microphone, the source is set in front of it so that the public address system can be tested. The receiver microphone is located at various points throughout an auditorium to determine the RASTI rating.

This page intentionally left blank

5

ENVIRONMENTAL
NOISE

5.1   NOISE CHARACTERIZATION

Outdoor noise transmission from point to point is discussed in terms of a *source-path-receiver model*, where the source is described by its sound power level and perhaps a directivity, the path is characterized by various attenuation mechanisms such as distance or barriers, and the receiver is a location where a level is to be calculated or a criterion is to be met. When the measurement point is close to the source, attenuation mechanisms, other than distance and directivity, have little effect on the received level. As the source-receiver distance increases, more and more mechanisms come into play until, at large distances, environmental considerations such as air losses, ground attenuation, wind direction, and velocity can be of primary importance.

Fixed Sources

Stationary sources such as pumps, compressors, fans, and emergency generators, which are a fundamental part of buildings, can radiate noise into adjoining properties. In previous chapters various metrics for characterizing the noise from these sources have been discussed. The equivalent sound level L_{eq} will be used here as the primary descriptive metric. It has the advantage of being mathematically efficient for both fixed and moving sources, and correlates well with human reaction. The L_{eq} for a fixed source can be calculated from the steady level emitted over a given time period.

$$L_{eq} = L_s + 10 \log (t / T) \tag{5.1}$$

where L_{eq} = equivalent sound level (dB or dBA)
L_s = steady sound level (dB or dBA)
t = time the source is on (sec)
T = total time $T \geq t$ (sec)

When the on-time is equal to the total time, the L_{eq} is equal to the steady level. Multiple sources may be combined using their individual L_{eq} levels and Eq. 2.62, even if the on-times are not coincident. Twenty-four hour metrics such as L_{dn} can be calculated for fixed sources

in a similar way from a knowledge of the time history. For example, for a constant 24-hour source, the L_{dn} is 6.4 dB higher than the steady level.

Moving Sources

Moving sources such as automobiles, trucks, railroads, and aircraft often dominate fixed sources in the urban environment, but are more transient and difficult to control. When a sound source moves, the measurement distance changes in time as shown in Fig. 5.1.

As the distance increases the sound pressure level decreases by 10 log of the square of the overall source-to-receiver distance. Assuming a source moves at a constant speed, v, along a straight line path a distance, d, away from an observer, the intensity can be written as a function of time

$$I(t) = \frac{I_r \, d_r^2}{d^2 + v^2 \, t^2} \tag{5.2}$$

where
$I(t)$ = sound intensity as a function of time (W / m^2)
I_r = measured sound intensity at distance d_r (W / m^2)
d = distance of closest approach (m)
v = source speed (m / s)
t = time (s)

Equation 5.2 can be converted to levels by dividing by the reference intensity, I_o, and taking 10 log of each side.

$$L(t) = L_r + 10 \log \left[\frac{d_r^2}{d^2 + v^2 \, t^2} \right] \tag{5.3}$$

where
$L(t)$ = sound level as a function of time (dB)
L_r = sound level at distance d_r (dB)

At $t = 0$, which is the point of closest approach, the sound level is dependent only on the ratio of the square of the reference distance to the minimum distance.
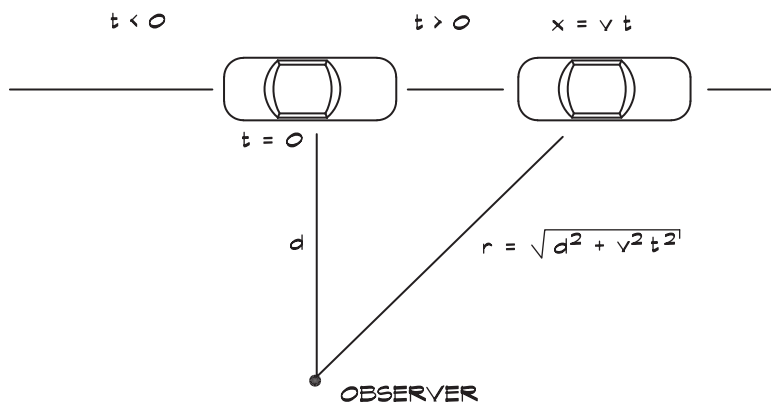
FIGURE 5.1   Geometry of a Moving Source

The L_{eq} for a single vehicle moving along a roadway can be calculated by adding (integrating) the contributions from each point along the source path for the time period under consideration.

$$L_{eq} = L_r + 10 \log \frac{1}{T} \int_{t_1}^{t_2} \frac{d_r^2}{d^2 + v^2 t^2} \, dt \qquad (5.4)$$

The integral is done by letting the limits of integration go to plus and minus infinity, because most of the energy is contributed when the vehicle is close to the receiver.

$$L_{eq} = L_r + 10 \log \frac{\pi d_r}{v \, T} + 10 \log \frac{d_r}{d} \qquad (5.5)$$

This is the equivalent sound level for a single vehicle traveling along a long roadway past a stationary observer in a time T. It is interesting to note that even for a single vehicle the falloff behavior with distance is that of a line source. If N similar vehicles pass a point during time T, a factor of 10 log N is added to Eq. 5.5 to account for them. The vehicle spacing does not matter since the levels combine on an energy basis.

When the noise level emitted by a group of sources varies in a normally distributed (Gaussian) way about a mean value, the L_{eq} level is calculated for the group (Reagan and Barry, 1978) by adding an adjustment that accounts for the variation, based on the standard deviation. The equivalent sound level for a long line of N vehicles passing a point in time T is

$$L_{eq} = \overline{L}_r + 0.115 \, \sigma^2 + 10 \log \frac{N \, \pi d_r}{v \, T} + 10 \log \frac{d_r}{d} \qquad (5.6)$$

where L_{eq} = equivalent sound level (dB or dBA)
       $\overline{L}_r$ = average reference sound level at distance d_r (dB or dBA)
       d = distance of closest approach (m or ft)
       v = source speed (m/s or ft/s)
       T = time (s)
       N = number of vehicles passing the measurement point in time T
       σ = standard deviation of the reference sound level (dB or dBA)

Equation 5.6 is the fundamental relationship for modeling vehicle noise from a long unshielded roadway. When trucks or other classes of vehicles are present, their contributions are calculated separately and the levels combined. Similar calculations can be done to predict noise from other moving sources such as railroads, crawler tractors, earth movers, and construction vehicles simply by using the appropriate reference sound levels.

Partial Line Sources

When a sound source traverses a line segment, or when only part of a straight roadway is to be modeled, the configuration is called a *partial line source*. An example might be a crawler tractor moving back and forth along a fixed path or a segment of roadway such as that shown in Fig. 5.2. The geometry is described in terms of an angular segment, $\Delta \phi = \phi_2 - \phi_1$

FIGURE 5.2   Angular Designation of Partial Line Sources (Barry and Reagan, 1978)
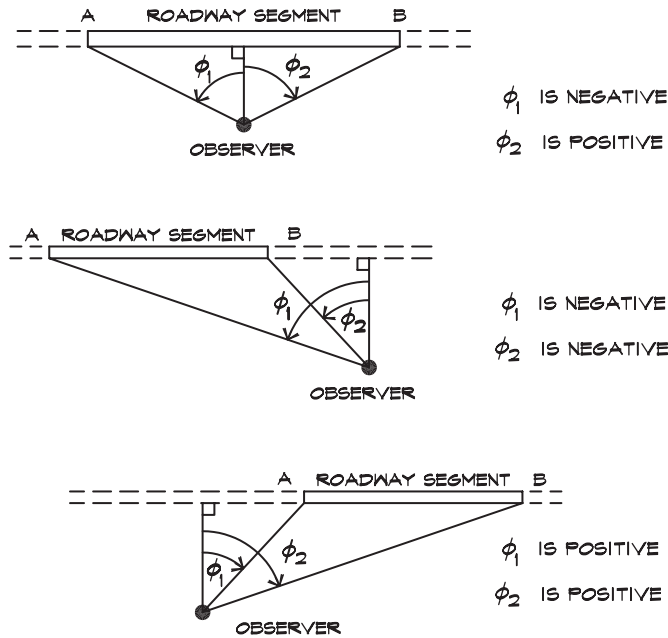
(in radians), which modifies the integration in Eq. 5.4 by changing the time limits to angular limits, and yields the equation for the level generated by a partial line source

$$L_{eq} = \bar{L}_r + 0.115 \, \sigma^2 + 10 \, \log \frac{N \, \pi \, d_r}{v \, T}$$
$$+ 10 \, \log \frac{d_r}{d} + 10 \, \log \frac{\Delta\phi}{\pi} \tag{5.7}$$

If the source is a single vehicle emitting a steady noise level, then $N = 1$ and the standard deviation is set to zero.

Equation 5.7 models the behavior of the noise level from a given segment of roadway. The level varies as the included angle $\Delta\phi$ of the line segment, regardless of whether the segment is near or far away. Note that the distance d is measured perpendicular to the line of travel, from the point on the line closest to the observer, which does not change with the angle under consideration. The formula states that, for a given receiver position, equal noise levels are generated by equal angular segments. This holds as long as the angular segment is not so far away that atmospheric and ground effects come into play and decrease the levels from the more distant sources.

If the measurement point is moved farther away from the line element the change in level can be obtained from the new distance and angle

$$\Delta L_{eq} = 10 \, \log \frac{d_1}{d_2} + 10 \, \log \frac{\Delta\phi_2}{\Delta\phi_1} \tag{5.8}$$

With increasing distance the line element behaves more and more like a point source. Let us take the example of a partial line source, where $\phi_1 = 0$, and use the trigonometric relationship

$\tan \phi = \dfrac{d_s}{d}$, where d_s is the length of the line segment. We then use the approximation for small angles, $\tan \phi \cong \phi$, where ϕ is in radians. The segment length stays the same so that when the measurement distance is large ($d \gg d_s$), the change in level with distance is given by

$$\Delta L_{eq} \cong 10 \, \log \frac{d_1}{d_2} + 10 \, \log \frac{d_1}{d_2} = 10 \, \log \left[\frac{d_1}{d_2} \right]^2 \tag{5.9}$$

Thus we regain the expected point source falloff for the changes in level from distant line source elements.

5.2   BARRIERS

Point Source Barriers

Barriers are the most commonly used way of controlling exterior noise. Figure 5.3 shows a simple barrier geometry. When a plane wave encounters a barrier, the lower portion of it is cut off leaving the rest to propagate over the wall. The high and low-pressure regions of the wave impinge on the quiescent fluid in the shadow zone and propagate into it. In this manner the wave diffracts or is bent into the space behind the barrier. The greater the diffraction angle the greater the attenuation.

Barrier attenuation for a point source is calculated (Maekawa, 1965) using the maximum Fresnel number, which is determined from the difference between the shortest propagation path that touches the edge of the barrier and the direct path through the barrier. The geometry is given in Fig. 5.4. The maximum Fresnel number N is

$$N = \pm \frac{2}{\lambda} \, (A + B - r) \tag{5.10}$$

FIGURE 5.3   Geometry of a Simple Barrier
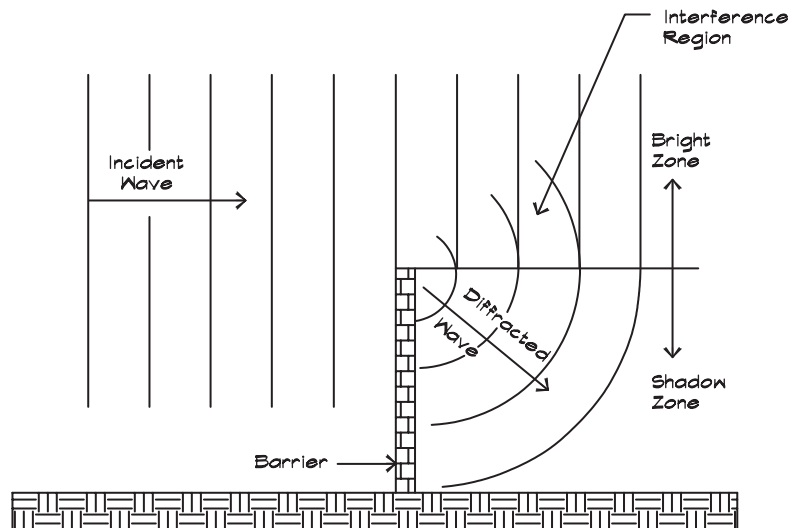
FIGURE 5.4   **Path Length Difference for a Simple Barrier**
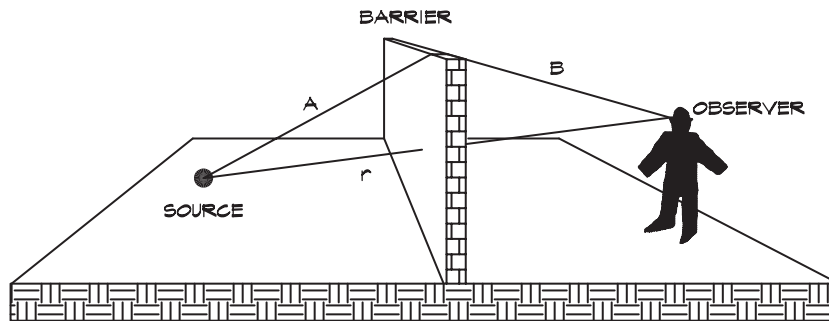
where $(A + B - r)$ is the minimum path length difference. The sign is positive in the shadow zone and negative in the bright zone. For a simple point source the barrier attenuation is

$$\Delta L_b = 20 \; \log \frac{\sqrt{2 \, \pi \, N}}{\tanh \, \sqrt{2 \, \pi \, N}} + K_b \tag{5.11}$$

where ΔL_b = barrier attenuation for a point source (dB)

A, B, r = minimum source to receiver distances over and through the barrier (m or ft)

$\quad$ N = maximum Fresnel number defined by Equation 5.10 $(-0.19 \le N \le 5)$

$\quad$ λ = wavelength of the frequency of interest (m or ft), (usually taken to be 0.63 m or 2 ft as an average value for roadways - equivalent to 550 Hz)

$\quad$ K_b = barrier constant which is 5 dB for a wall and 8 dB for a berm

When N is zero, that is when the line of sight between the source and the receiver is just broken by the top of the barrier, the theoretical attenuation afforded by a wall is 5 dB. For every 0.3 m (1 ft) of barrier above this line the barrier provides about one additional dB of attenuation at 500 Hz. This is a rough rule of thumb, which is useful for estimation purposes. Detailed attenuation calculations should be done for the actual source spectrum and barrier geometry. If the barrier has an unusual shape, such as a truncated triangle in section, the total path length across the top of the barrier must be calculated. For large values of N, the attenuation has a practical limit of 20 dB for walls and 23 dB for berms.

If a receiver, located in the bright zone where the attenuation is zero, is lowered toward the shadow zone the attenuation does not jump instantaneously from zero to 5 dB. Instead, theory predicts a transition zone where sound waves are scattered from the top of the barrier and combine out of phase with the direct path waves, resulting in some attenuation. In the transition zone N is negative (N ranges between -0.19 and 0 for walls and between -0.25 and 0 for berms) and the radical in Eq. 5.11 yields an imaginary number. In this region the hyperbolic tangent becomes a simple tangent function since $\tan(\theta) = \tanh(j\theta)$. In practice, the transition zone is narrow and little attenuation should be expected when the line of sight falls above the top of the barrier.

Practical Barrier Constraints

There are practical limitations to barrier theory. If barriers are not long, the sound can travel around them. Barrier attenuations can be calculated for each of these paths using Eq. 5.11,

FIGURE 5.5   Possible Sound Paths around a Finite Barrier
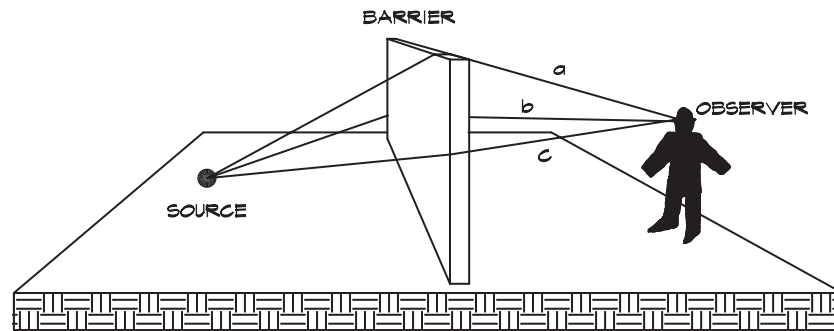
and the resulting levels combined at the receiver location. Reflections from nearby buildings can produce flanking paths where the sound travels around a barrier. Examples can be found in Fig. 5.5.

A high building located behind a barrier can scatter sound back into the shadow zone, particularly where there is an overhanging roof, thereby reducing the barrier's effectiveness. Measured data for these types of conditions are shown in Fig. 5.6. A local reverberant field set up between a barrier and a building can decrease barrier effectiveness, especially at low frequencies. Low-frequency reverberation can also generate an increase in noise level compared with the no-barrier condition.

When a wind is blowing from the source to the receiver and the distance is sufficiently long, the barrier effectiveness is much reduced due to the downward bending of the sound waves. This effect occurs when the barrier is relatively far (say A and B > 100 m) from the source and receiver.

The construction of sound walls on top of berms presents a curious dilemma. Due to the interaction of sound with the top of the berm, an additional attenuation of about 3 dB is achieved over that which would be obtained from a wall. If a 0.3 m (1 ft) wall is built on top of a berm the attenuation would increase about one dB for the extra height and decrease about 3 dB due to its being a wall, yielding a net increase in sound level. Thus walls on top of berms must be sufficiently high to offset the loss of the berm effect. In practice, although berms are more efficient attenuators, they are difficult to build very high. Most berms must be constructed with a 2:1 slope, so they end up being four times wider than they are high, and space constraints limit their use.

Ground attenuation, which occurs when sound waves graze or skim across the ground, is reduced when sound diffracts over a high wall since the barrier changes the angle of approach. Barrier attenuation may be partially offset by the loss of ground attenuation. By doing a few sample barrier calculations one can quickly discover that barriers of a given height are most effective when they are located close to the source or receiver and least effective when they are positioned half-way in between.

Line Source Barriers

When a barrier is constructed along a line source, such as a highway, the geometry and thus the Fresnel number changes for each angle of roadway covered by the barrier. Figure 5.7 illustrates this condition and Fig. 5.2 gives the sign convention for the angle segments.

FIGURE 5.6   Sound Attenuation by a Barrier in Front of a Reflecting Surface (Sharp, 1973)
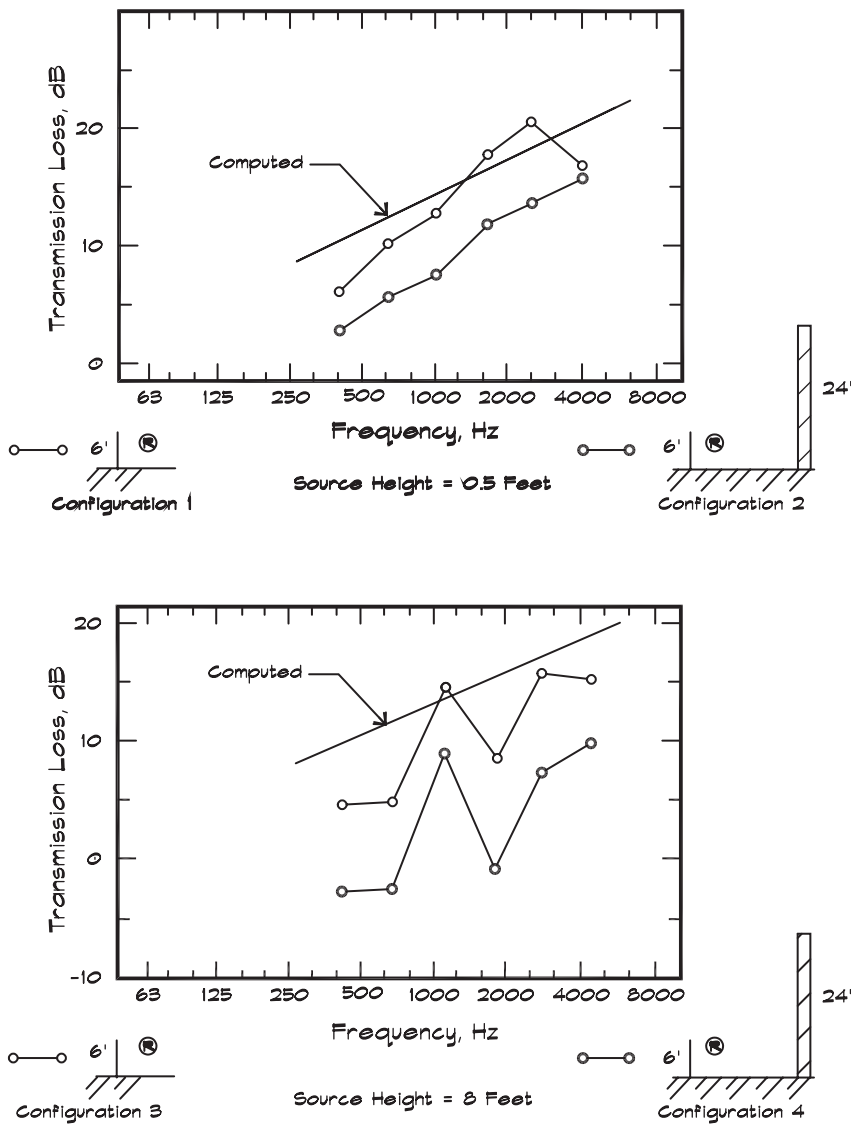
FIGURE 5.7   Finite Roadway/Finite Barrier Geometry
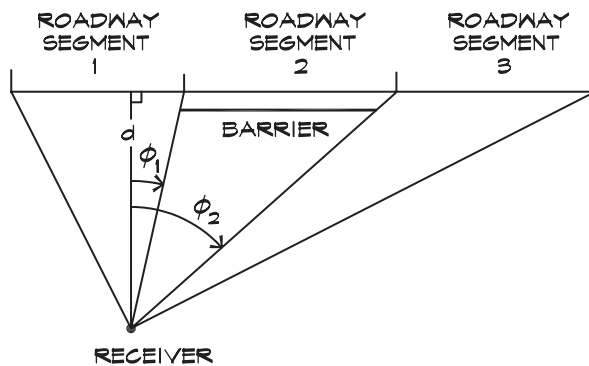
To calculate the barrier shielding for a segment of roadway the attenuation can be integrated over all angles of ϕ that are covered. The formula for the barrier shielding of a partial line source is (Barry and Reagan, 1978)

$$\Delta L_\phi = -10 \, \log \frac{1}{\Delta\phi} \int_{\phi_1}^{\phi_2} 10^{-0.1 \, \Delta L_b(\phi)} \, d\phi \tag{5.12}$$

where ΔL_ϕ = barrier attenuation for a line source element (dB)

$\Delta L_b(\phi)$ = barrier attenuation for a point source located at ϕ (dB)

$\Delta\phi = |\phi_2 - \phi_1|$ = angle of the barrier element (radians)

ϕ_1 = angle from the perpendicular to the left edge of the line element (radians)

ϕ_2 = angle from the perpendicular to the right edge of the line element (radians)

The integral is cumbersome and is done numerically using an approximation for the angular dependence of the Fresnel number, namely

$$N(\phi) \cong N_0 \, \cos \phi \tag{5.13}$$

where $N(\phi)$ = Fresnel number for a small line segment located at ϕ

N_0 = Fresnel number determined along the perpendicular path between the receiver and the line source

ϕ = angle from the perpendicular to the segment (radians)

Barry and Reagan have provided extensive tables showing the results of the integration for barrier segments at various angles. Computer programs for doing the barrier calculations are commercially available and are straightforward to write. When a roadway is divided into angular segments of less than about 25°, the point source barrier attenuation can be applied using the center of each segment and the results combined. For an infinite roadway and an infinite barrier, the integration has been done by Kurze and Anderson (1971) and is shown in Fig. 5.8. Experimental results also are shown in the figure. Note that the barrier attenuation for an infinite line source is about 5 dB less than for a point source at the same perpendicular distance.

Barrier Materials

Many materials are available to the designer; however, there are a few important considerations. First, barriers must be nonporous—that is, they must block the passage of air through them. Second, they must have sufficient mass so that the sound traveling through the barrier is significantly less than the sound diffracting over or around the barrier. This consideration leads to the requirement that barriers be built of a material having a total surface mass density of at least 20 kg/sq m (4 lbs/sq ft). Third, they must be weather resistant and properly designed to withstand wind and other structural loads appropriate for the location.

The mass requirement can be fulfilled using a support structure with one layer of 16 mm (5/8") and one layer of 19 mm (3/4") plywood sandwiched. When the panels are applied to both sides of a stud, 90 mm (3 1/2") wide, they may be less massive, typically 13 mm (1/2") to 16 mm (5/8") plywood. Virtually any thickness of concrete or concrete masonry unit that is self-supporting will meet the mass requirement. A stucco wall is very effective. Stucco is 22 mm (7/8") thick and weighs about 42 kg/sq m (9 lbs/sq ft) at that

FIGURE 5.8   Line Source Barrier Attenuation (Maekawa, 1977)

Sound attenuation by a thin screen in free space versus
the Fresnel zone number N for a point source (solid line) and for
an incoherent line source (dotted and dashed curves). Attenuation
is relative to propagation in free space.

$$N = 2\,\delta/\lambda$$
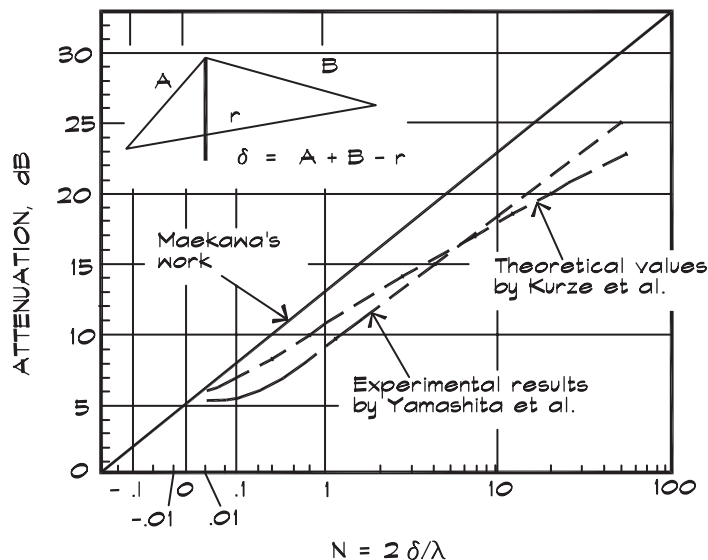
thickness. Precast concrete panels, treated to look like wood or brick and supported by I beam columns, are commercially available. The panels are held in place at their ends by the flange of the I beam.

Corrugated sheet metal panels sometimes are used to construct noise barriers. Commercial barriers with both solid and sound-absorbing perforated skins are available, usually in 18 Ga. steel supported by steel columns. Absorbing materials such as fiberglass can be incorporated behind the perforated panels to reduce barrier reflections. The fiberglass is encased in a plastic bag to protect it from the weather. For very thin layers of plastic there is little reduction in the absorptive properties of the fill.

Noise barriers should be constructed so that there are no openings between the barrier and the ground. Openings allow the sound to pass under the barrier and can reduce its effectiveness. Trees, shrubs, and other foliage are not effective. They are porous and do not meet the mass requirement. Rows of trees, heavy grass, and dense foliage can provide some excess ground attenuation, on the order of 0.1 dB/ m thick (3 dB/100 ft). They are also useful in giving a psychological sense of privacy, or in landscaping a sound barrier to make it more aesthetically acceptable.

Roadway Barriers

Sound barriers constructed along a roadway to protect residential areas have become a common sight in urban areas. Barriers along freeways incorporate a safety shape at their base to protect vehicles from direct impacts. When barriers are located on both sides of a roadway, the multiple reflection of sounds back and forth between them reduces the attenuation that would be expected from calculations using standard formulas. Maekawa (1977), testing scale models, measured the attenuation of parallel walls. The results are shown in Fig. 5.9.

FIGURE 5.9   Measured Sound Attenuation from Reflective Screens (Maekawa, 1977)

Sound attenuation measured by the pulse method with a 1:40 scale model.
The road width W = 20.2 m and the screen height H = 15 m full scale. The plotted
data ○ and ● are for the values obtained at receiving points in zones 1 and 2
respectively. The maximum Fresnel number N is calculated for the near side screen
neglecting the one on the far side, for the center frequency of each one-third
octave band. Attenuation is relative to propagation in free space.

$$N = 2\,\delta/\lambda$$
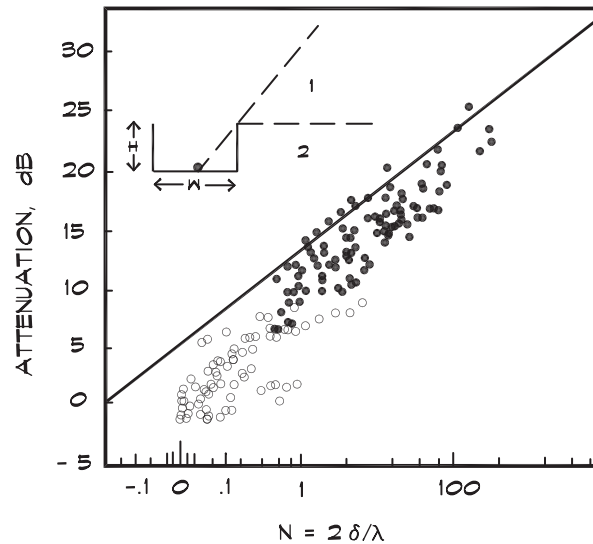
When absorptive materials are applied to the roadway side of these walls, the attenuation values return to their expected levels (Fig. 5.10).

A row of buildings, one story tall, can provide some shielding over and above distance attenuation. The amount depends on the percent of coverage of the line source. For 40% to 65% coverage, about 3 dB is achieved; for 65% to 90% shielding we get about 5 dB. Additional rows of buildings can add about 1.5 dB of extra shielding per row, up to a maximum of 10 dB.

Barrier shielding due to buildings sometimes produces a curious phenomenon. When a receiver is standing behind a row of buildings, not infrequently the sound will be perceived as coming from the side away from the source. This is because the sound is reflected from another building behind the receiver. The sound coming by way of this path is louder than the direct path over the barrier due to the reduced barrier effectiveness at the elevation of the reflection point as in Fig. 5.11.

Figure 5.12 summarizes barrier and ground effects. Where sound propagates over a soft ground cover such as grass, it is common practice to calculate the attenuation by combining the distance and ground effects into a 4.5 dB per distance doubling falloff rate. This is not the most accurate method, but without knowledge of the impedance of the surface it provides a useful estimate.

5.3   ENVIRONMENTAL EFFECTS

Several attenuating mechanisms, over and above those associated with geometrical spreading and barrier losses, influence the propagation of a sound wave. These are grouped in categories

FIGURE **5.10** **Measured Sound Attenuation from Absorptive Screen (Maekawa, 1977)**

The figure is the same as Fig. 5.9 except that the inner surfaces of the screens have been lined with sound-absorbing materials. The normal incidence absorption coefficient α = 0.48 - 0.93 was used for the measurement frequency range.

$$N = 2\delta/\lambda$$
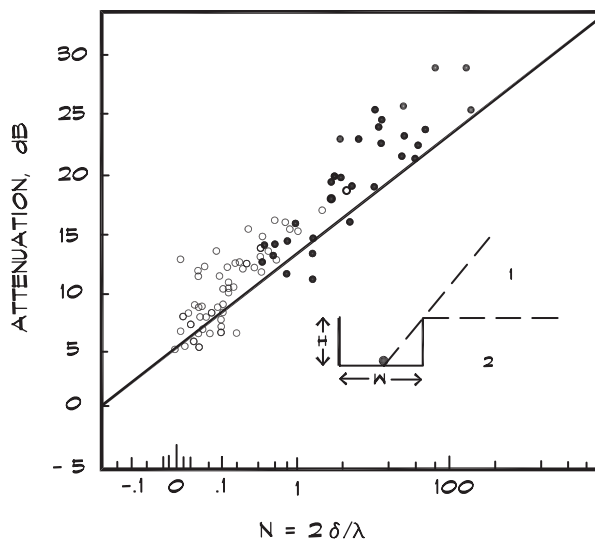
FIGURE **5.11** **Shift in the Perceived Direction Due to Shielding**
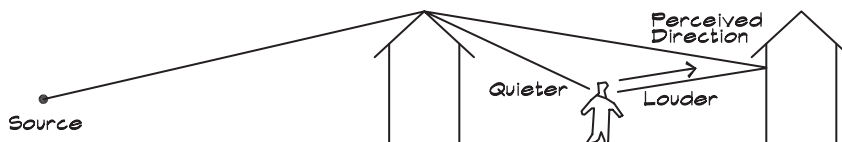
as follows: 1) air attenuation, 2) ground effects, 3) losses due to focusing from wind and thermal gradients, and 4) channeling effects. Air attenuation is always present, even indoors, and contributes to the acoustics of concert halls as well as sound propagation outdoors. Ground effects occur when the sound grazes at a shallow angle over acoustically soft materials such as thick grass, plowed ground, fresh snow, or in theaters, padded opera chairs. Ground effects are not significant unless there is grazing. Wind and thermal focusing are other commonly occurring outdoor phenomena. Channeling effects are more rare, occurring over water, in gullies at night, or in the atmosphere when inversion conditions are present.

Air Attenuation

The theory of sound attenuation, which was discussed in Chapt. 2, was based on the geometrical spreading of acoustical energy due to distance. No internal losses were assumed in that analysis. In a real fluid there are several additional mechanisms that attenuate a sound, including viscous and thermal losses and various relaxation effects. The combination of these

FIGURE 5.12   Attenuation of Highway Noise (Barry and Reagan, 1978)

LINE SOURCE - HARD SITE

3 dB/DD

LINE SOURCE - SOFT SITE

4.5 dB/DD

LINE SOURCE - SOFT SITE WITH HEAVY TREES

5 dB FOR 1st 30 m
5 dB FOR 2nd 30 m
10 dB MAX

LINE SOURCE - HARD SITE WITH BUILDINGS

1st ROW

3 dB FOR 40-65% AREA
5 dB FOR 65-90% AREA

1.5 dB FOR EACH
ADDITIONAL ROW
10 dB MAX

LINE SOURCE - HARD OR SOFT SITE WITH BARRIER

WALL 20 dB MAX
BERM 23 dB MAX
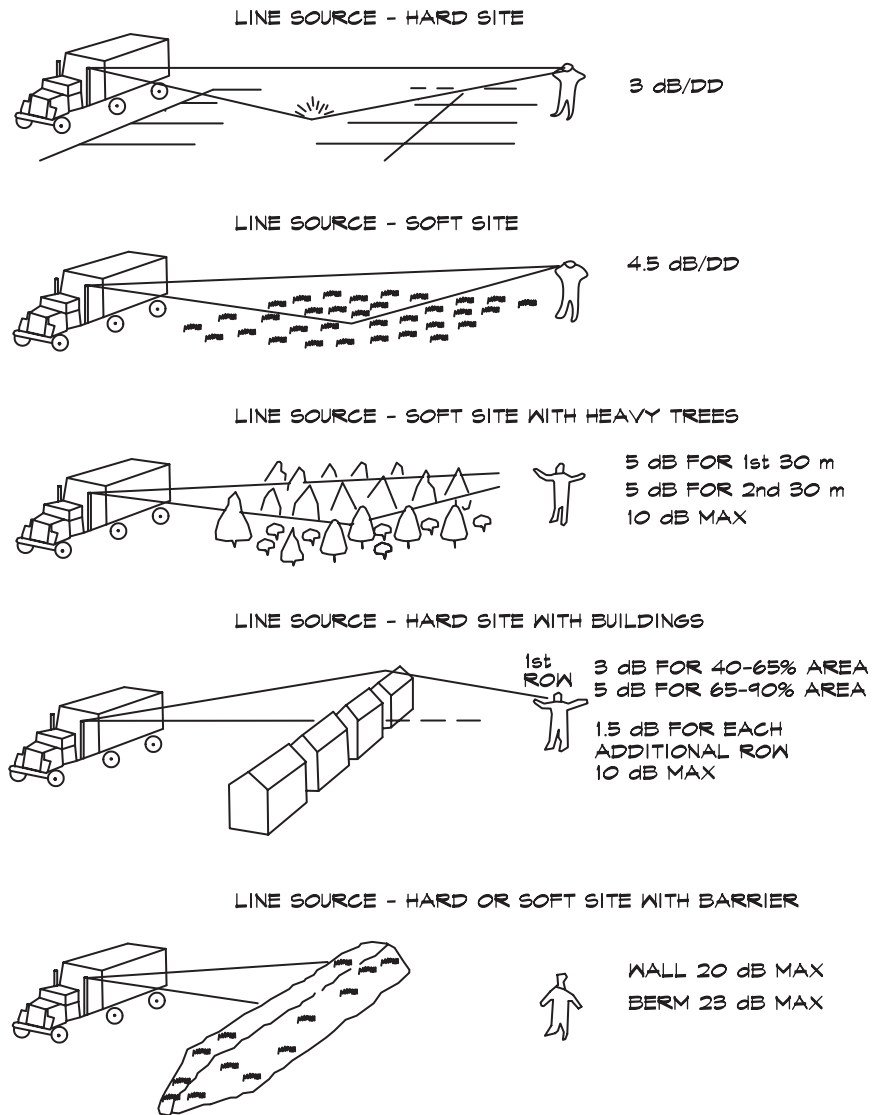
effects is termed atmospheric attenuation and is made up of four components

$$\Delta L_a = \Delta L_{cl} + \Delta L_{rot} + \Delta L_{vib}(O_2) + \Delta L_{vib}(N_2) \qquad (5.14)$$

where ΔL_a = total atmospheric attenuation (dB/km)

ΔL_{cl} = classical losses due to viscosity and thermal effects (dB/km)

ΔL_{rot} = molecular absorption for rotational relaxation of oxygen and nitrogen molecules (dB/km)

$\Delta L_{vib}(O_2)$ = molecular absorption losses for vibrational relaxation of O_2 molecules (dB/km)

$\Delta L_{vib}(N_2)$ = molecular absorption losses for vibrational relaxation of N_2 molecules (dB/km)

All these terms represent different ways in which sound energy is converted into heat or internal energy of the air, thus reducing the strength of the sound wave.

Classical attenuation comes about through the effects of viscosity and thermal conductivity, illustrated in Fig. 5.13. As a wave passes a point, the pressure and thus the temperature increases. Temperature is a measure of the amount of random molecular motion in the fluid. In a region of high temperature, there are more high-speed molecules, which will diffuse into the surrounding cooler regions to equalize the temperature. Once diffused this energy is not available to the sound wave and is lost. Viscosity is also a diffusion effect, the diffusion of particle momentum. A portion of the fluid with a high momentum slides past a region of lower momentum and some of the molecules lose energy due to collisions with the adjacent fluid. Viscosity and heat conductivity make approximately equal contributions to sound attenuation.

When a property of a system, say the temperature of a fluid, is forced away from its equilibrium state and then allowed to relax back to equilibrium, the time it takes to return to the original state is called a *relaxation time*. Relaxation times of natural phenomena can range from microseconds to centuries, depending on the physical process in question (Reif, 1965). Several relaxation effects increase the attenuation of sound propagating through the air. All have to do with the transfer of energy from a translational mode to other molecular energy modes, either rotational or vibrational. Figure 5.14 shows several examples. If a molecule of air (either N_2 or O_2) undergoes an increase in velocity due to the presence of a sound wave, it will, in turn, transfer that energy to other molecules through collisions.

FIGURE 5.13   Classical Air Attenuation Mechanisms

When a sound wave passes a point it creates an area of locally higher momentum and temperature some of which diffuses into the surroundings.

INCIDENT SOUND WAVE

Wavefronts of high pressure and temperature

Diffusion of high velocity particles
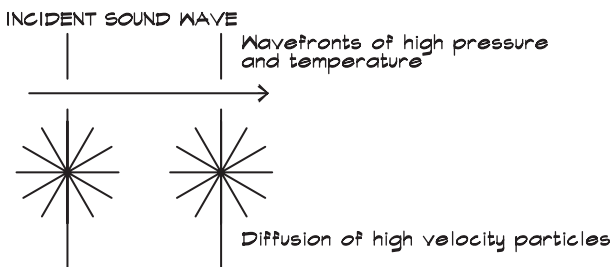
FIGURE 5.14   Energy Transfer to Vibrational Energy States

Energy

First Excited Vibrational Energy State

Ground Energy State

Energy From Collision

Energy Returned By Collision To Another Molecule

Time
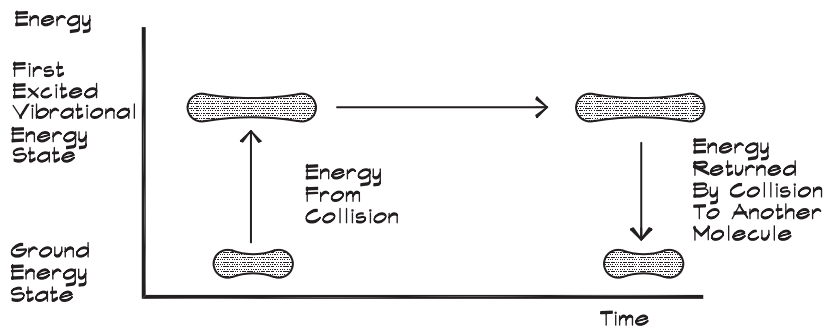
Some energy may be transferred into exciting rotational or vibrational modes of the molecule it impacts and some into creating pure translational motion. When a molecule in an excited state impacts another, some or all of the rotational or vibrational energy may be converted back into particle velocity. The temperatures of translation, rotation, and vibrational motion locally tend toward equilibrium, an effect called the *equipartition of energy*. Each of these equilibrium processes has a different characteristic relaxation time.

If the relaxation time is very long—that is, if it takes a long time to transfer energy back and forth between translation and vibrational motion—then a sound wave, which generates rapid increases or decreases in sound pressure and therefore sound temperature, is unaffected by energy transfer to other modes, which takes place too slowly to influence its passage. The fluid is said to be in a "frozen" condition in so far as this energy transfer mechanism is concerned. Similarly if the relaxation time is very short—that is, much shorter than the time for changes in pressure due to the sound wave to occur—then the energy transfer back and forth between translation and vibration happens so quickly that the fluid is in a state of thermal "equilibrium" between the various energy modes, and again, there is little effect on the passage of the sound wave.

If the relaxation time is just the right value, then when a pressure wave passes by, the increased translational energy is converted into vibration and then back into translation coincident with the arrival of the low pressure region. The wave amplitude is attenuated since the acoustic energy is converted either to random molecular motion (heat) or to pressure that is out of phase. When the acoustic frequency is of the same order of magnitude as the relaxation frequency $(1/2\pi\tau)$ of a particular vibrational mode, air can induce significant sound attenuation. The relaxation frequencies and maximum attenuation amplitudes vary with the type of molecule, the mode of vibration, and the presence of other types of molecules such as water vapor.

Rotational relaxation times are very short and equilibrium conditions can be achieved within a few molecular collisions. Energy losses at normal acoustic frequencies are small and can be combined with classical effects. The expected loss due to both classical and rotational effects is (ISO 9613-1, 1990).

$$\Delta L_{cl} + \Delta L_{rot} = (1.60 \times 10^{-7})\sqrt{\frac{T_k}{T_0}}f^2 / p^* \qquad (5.15)$$

where T_k = absolute temperature in degrees K = temperature in degrees
          Celsius plus 273.15
       T_0 = reference temperature = 293.15 (degrees K)
        f = frequency (Hz)
       p^* = normalized atmospheric pressure in standard atmospheres
          (pressure in k Pa divided by 101.325)

For a mild day

$$T_k = 288°K \ (15°C \ \text{or} \ 59°F)$$

$$p^* = 1$$

and

$$\Delta L_{cl} + \Delta L_{rot} = 1.6 \times 10^{-7} \ f^2 \qquad (5.16)$$

or about 0.6 dB per kilometer at 2000 Hz.

The remaining two absorption terms in Eq. 5.14, which account for most of the air absorption, are due to vibration relaxation mechanisms in nitrogen and oxygen molecules. In this process diatomic molecules are excited by a collision with another molecule into a higher vibrational energy state, and return the energy at a later time through another collision. The process takes many molecular collisions to complete and the attenuation follows the form (ISO 9613-1, 1990)

$$\Delta L_{vib} = 8686\, \mu_{max}\, \frac{f}{c} \left[\frac{2\left(f / f_{r\,i}\right)}{1 + \left(f / f_{r\,i}\right)^2} \right] \tag{5.17}$$

where ΔL_{vib} = vibrational air attenuation (dB/km)

  μ_{max} = maximum loss in nepers for one wavelength (Np)

  $f_{r\,i}$ = frequency of maximum loss per wavelength (Hz)

    where the subscript i refers to oxygen or nitrogen

  f = frequency of sound wave (Hz)

  c = speed of sound (m/s)

Two variables that appear in Eq. 5.17 require some explanation: the maximum loss per wavelength, μ_{max}, and the relaxation frequency, $f_{r\,i}$, at which this maximum loss occurs. The thermodynamic basis for the value of μ_{max} has been given in several texts (Kinsler et al., 1982, or Pierce, 1981). For oxygen and nitrogen, it is dependent on the absolute temperature

$$\mu_{max} = \frac{2\,\pi K}{35} \left(\frac{\theta_i}{T_k} \right)^2 e^{-\theta_i / T_k} \tag{5.18}$$

where θ_i = characteristic temperature corresponding to a particular vibrational mode, (°K) for oxygen, θ_i = 2239.1°K and for nitrogen, θ_i = 3352.0°K

  K = volume concentration of the gas in the air which for oxygen = 0.209 and for nitrogen = 0.781

  T_k = absolute temperature (°K)

At 20°C the predicted values of μ_{max} are 0.00105 for oxygen and 0.00020 for nitrogen, which are quite close to the actual measured values. Since μ_{max} is expressed in terms of a loss per wavelength, the relaxation loss curve has the peak shown in Fig. 5.15. To convert this into a loss per distance we must multiply it by the number of wavelengths per distance, which increases with frequency, to obtain the curves shown in Fig. 5.16. The conversion from nepers to decibels (1 Np = 20 log e = 8.686 dB) is used to obtain Eq. 5.17.

The molecular vibration losses for O_2 and N_2 molecules are strongly influenced by the presence of water vapor in the air, since a vibrational energy transfer is more likely for a collision between H_2O and O_2 or N_2. Thus water vapor catalyzes the transfer of energy between the modes and reduces the vibrational relaxation time. This phenomenon is particularly important in the design of concert halls, where dry air can result in considerable loss of high-frequency energy. The HVAC systems in large halls must be designed to control not only temperature but also humidity.

Having defined μ_{max} there remains the definition of the two relaxation frequencies, $f_{r\,o}$ and $f_{r\,n}$, for the vibrational modes of diatomic oxygen and nitrogen. Both these frequencies are a function of humidity, atmospheric pressure, and temperature. The following equation

FIGURE 5.15   Air Absorption Due to Relaxation Processes (Pierce, 1981)

Frequency dependence of absorption loss for a single relaxation process. Horizontal axis is frequency in units of the relaxation frequency.
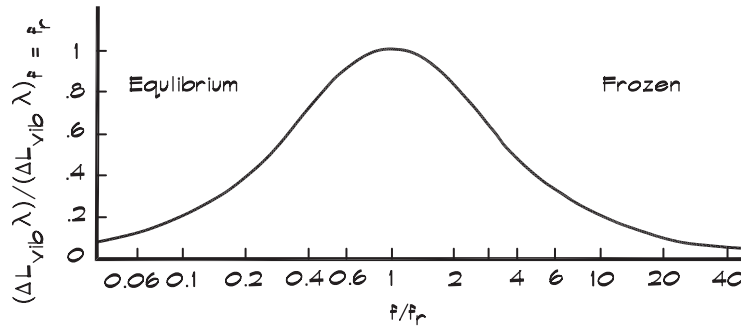
FIGURE 5.16   Components of Atmospheric Absorption Loss
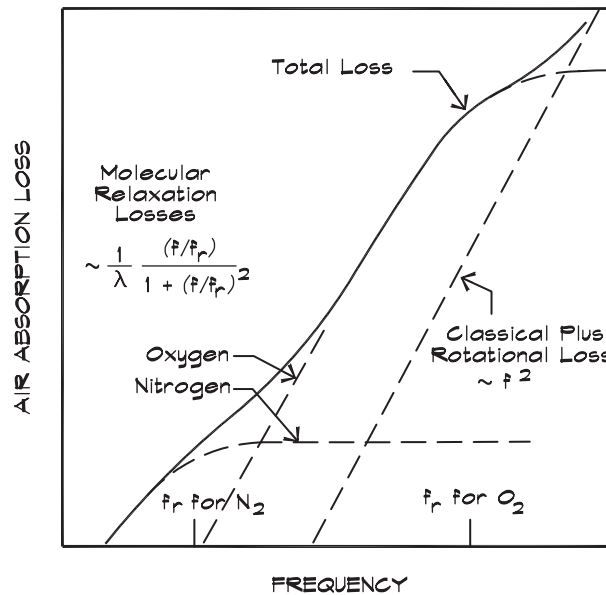
for the relaxation frequency for oxygen was developed by Piercy (1971) and slightly modified in the ISO standard

$$f_{r\,o} = p^* \left\{ 24 + 40\,400\, h \left[\frac{0.02 + h}{0.391 + h} \right] \right\} \tag{5.19}$$

where p^* = absolute pressure in standard atmospheres
h = absolute humidity (% mole ratio)

$$= h_r \frac{10^{\left[-6.8346(T_0/T_k)^{1.261} + 4.6151 \right]}}{p^*}$$

h_r = relative humidity (%)

TABLE 5.1   Air Attenuation at 20° C, dB/km (ISO 9613-1, 1990)

Freq. (Hz) Rel. Hum (%)	10	15	20	30	40	50	60	70	80	90	100
50	2.70 −1	2.14 −1	1.74 −1	1.25 −1	9.65 −2	7.84 −2	6.60 −2	5.70 −2	5.01 −2	4.47 −2	4.03 −2
63	3.70 −1	3.10 −1	2.60 −1	1.92 −1	1.50 −1	1.23 −1	1.04 −1	8.97 −2	7.90 −2	7.05 −2	6.37 −2
80	4.87 −1	4.32 −1	3.77 −1	2.90 −1	2.31 −1	1.91 −1	1.62 −1	1.41 −1	1.24 −1	1.11 −1	1.00 −1
100	6.22 −1	5.79 −1	5.29 −1	4.29 −1	3.51 −1	2.94 −1	2.52 −1	2.20 −1	1.94 −1	1.74 −1	1.58 −1
125	7.76 −1	7.46 −1	7.12 −1	6.15 −1	5.21 −1	4.45 −1	3.86 −1	3.39 −1	3.02 −1	2.72 −1	2.47 −1
160	9.65 −1	9.31 −1	9.19 −1	8.49 −1	7.52 −1	6.60 −1	5.82 −1	5.18 −1	4.65 −1	4.21 −1	3.84 −1
200	1.22 +0	1.14 +0	1.14 +0	1.12 +0	1.05 +0	9.50 −1	8.58 −1	7.76 −1	7.05 −1	6.44 −1	5.91 −1
250	1.58 +0	1.39 +0	1.39 +0	1.42 +0	1.39 +0	1.32 +0	1.23 +0	1.13 +0	1.04 +0	9.66 −1	8.95 −1
315	2.12 +0	1.74 +0	1.69 +0	1.75 +0	1.78 +0	1.75 +0	1.68 +0	1.60 +0	1.50 +0	1.41 +0	1.33 +0
400	2.95 +0	2.23 +0	2.06 +0	2.10 +0	2.19 +0	2.23 +0	2.21 +0	2.16 +0	2.08 +0	2.00 +0	2.90 +0
500	4.25 +0	2.97 +0	2.60 +0	2.52 +0	2.63 +0	2.73 +0	2.79 +0	2.80 +0	2.77 +0	2.71 +0	2.63 +0
630	6.26 +0	4.12 +0	3.39 +0	3.06 +0	3.13 +0	3.27 +0	3.40 +0	3.48 +0	3.52 +0	3.52 +0	3.49 +0
800	9.36 +0	5.92 +0	4.62 +0	3.84 +0	3.77 +0	3.89 +0	4.05 +0	4.19 +0	4.31 +0	4.39 +0	4.43 +0
1 000	1.41 +0	8.72 +0	6.53 +0	5.01 +0	4.65 +0	4.66 +0	4.80 +0	4.98 +0	5.15 +0	5.30 +0	5.42 +0
1 250	2.11 +1	1.31 +1	9.53 +0	6.81 +0	5.97 +0	5.75 +0	5.78 +0	5.92 +0	6.10 +0	6.29 +0	6.48 +0
1 600	3.13 +1	1.98 +1	1.42 +1	9.63 +0	8.00 +0	7.37 +0	7.17 +0	7.18 +0	7.31 +0	7.48 +0	7.68 +0
2 000	4.53 +1	2.99 +1	2.15 +1	1.41 +1	1.12 +1	9.86 +0	9.25 +0	9.02 +0	8.98 +0	9.06 +0	9.21 +0
2 500	6.35 +1	4.48 +1	3.26 +1	2.10 +1	1.61 +1	1.37 +1	1.25 +1	1.18 +1	1.15 +1	1.13 +1	1.13 +1
3 150	8.54 +1	6.62 +1	4.94 +1	3.18 +1	2.39 +1	1.98 +1	1.75 +1	1.61 +1	1.53 +1	1.48 +1	1.45 +1
4 000	1.09 +2	9.51 +1	7.41 +1	4.85 +1	3.61 +1	2.94 +1	2.54 +1	2.29 +1	2.13 +1	2.02 +1	1.94 +1
5 000	1.33 +2	1.32 +2	1.09 +2	7.39 +1	5.51 +1	4.44 +1	3.79 +1	3.36 +1	3.06 +1	2.86 +1	2.71 +1
6 300	1.56 +2	1.75 +2	1.56 +2	1.12 +2	8.42 +1	6.78 +1	5.74 +1	5.04 +1	4.54 +1	4.18 +1	3.91 +1
8 000	1.75 +2	2.21 +2	2.15 +2	1.66 +2	1.28 +2	1.04 +2	8.78 +1	7.66 +1	6.86 +1	6.26 +1	5.81 +1
10 000	1.93 +2	2.67 +2	2.84 +2	2.42 +2	1.94 +2	1.59 +2	1.35 +2	1.18 +2	1.05 +2	9.53 +1	8.79 +1

The relaxation frequency for nitrogen in air is based in part on a compilation of data by Evans (1972)

$$f_{rn} = \frac{p^*}{\sqrt{T_k/T_0}} \left\{ 9 + 280\, h\, e^{-4.17\left[(T_0/T_k)^{1/3} - 1\right]} \right\} \tag{5.20}$$

Even though the equations for air attenuation are somewhat convoluted, the calculations are straightforward. Table 5.1 contains a partial summary of the results. At 4000 Hz, about the highest note on the piano, the air loss at room temperature is 109 dB/km at 10% relative humidity, but only 23 dB/km at 70% relative humidity. In a large concert hall where a 2-second reverberation time is desirable the air loss alone is 36 dB/sec at 10% relative humidity. This forces the reverberation time down to 1.67 s solely due to air losses. Clearly, the humidity must be controlled to limit high-frequency attenuation.

Attenuation Due to Ground Cover

Ground attenuation is caused by several effects including the losses in propagating through dense woods or heavy foliage, and the effect of grazing propagation at shallow angles over an acoustically soft surface such as heavy grass, plowed ground, or new fallen snow. *Grazing attenuation* is also present in concert halls and theaters, where sounds, emanating from a performer on stage, pass over seated patrons or padded opera chairs and induce losses over and above those expected from geometrical spreading and air absorption alone.

The absorption mechanism associated with sound propagation through dense forests and foliage is mostly scattering from the trunks and limbs. Sound absorption by leaves is not a significant contributor (Beranek and Ver, 1992). Hoover (1961) has developed an approximate formula for excess attenuation in forests

$$\Delta L_f \cong 10 \left(\frac{f}{1000} \right)^{1/3} \left(\frac{r}{100} \right) \text{ (dB)} \tag{5.21}$$

which works out to be about 10 dB per 100 m at 1 kHz. Other authors have measured attenuations ranging from 3 dB per 100 m for bare trees, to 18–27 dB per 100 m for heavy Canadian forests. Equation 5.21 represents the average of data compiled for all types of American forests.

Grazing Attenuation

Grazing attenuation is a phenomenon that occurs when an acoustic wave interacts with an absorbing surface at a shallow angle of incidence. When a sound wave reflects off a surface, the reflected wave combines with the original wave and may produce an increase or decrease in overall signal amplitude. A diagram of the geometry is shown in Fig. 5.17. When the reflecting surface is very hard, the reflected wave combines with the incident wave to produce an increase in sound pressure. At low frequencies and short distances this can be as high as 6 dB near the boundary. At very high frequencies the two waves combine incoherently with no particular phase relationship, which can produce a doubling in intensity and a 3 dB increase in level. When the reflecting material is soft the reflected wave is out of phase with the incident wave. Since the two waves are traveling along closely matching paths the combined wave is highly attenuated. This phenomenon and the general theory of reflection from surfaces is discussed in more detail in Chapt. 7.

FIGURE 5.17 **Geometry of Grazing Attenuation**
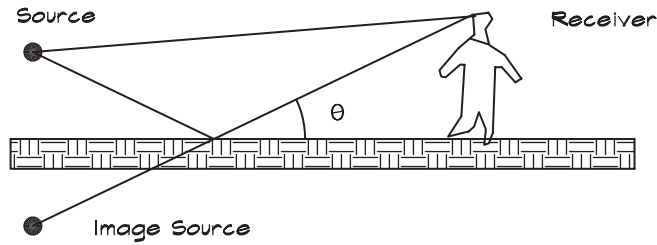
FIGURE 5.18 **Grazing Attenuation Regions**
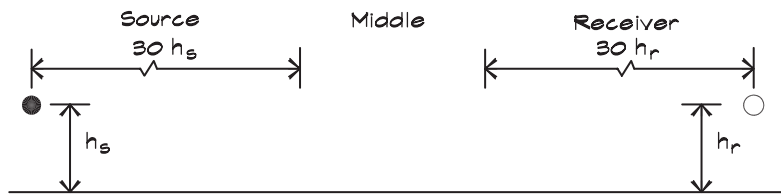
Empirical formulas have been developed (ISO 9613-2.2, 1994) for the prediction of excess grazing attenuation. This method subdivides the ground into three regions, shown in Fig. 5.18: source and receiver regions, no more than 30 times the respective receiver heights from the source or receiver; and a middle region that includes the remainder of the intervening ground. If the overall separation distance is less than $30(h_s + h_r)$, where h_s and h_r are the source and receiver heights, then there is no middle ground and the near and far regions overlap. Each region is rated by a coefficient, ξ ranging from 0 to 1, according to the fraction that is soft (porous). The equations are grouped into the standard octave-band frequencies. Note that negative values indicate an increase in signal level.

$$\Delta L_g = \begin{cases} -3 - 3M & \text{at 63 Hz} \\ -3 + \xi_s A_s + \xi_r A_r - 3M(1 - \xi_m) & \text{at 125 Hz} \\ -3 + \xi_s B_s + \xi_r B_r - 3M(1 - \xi_m) & \text{at 250 Hz} \\ -3 + \xi_s C_s + \xi_r C_r - 3M(1 - \xi_m) & \text{at 500 Hz} \\ -3 + \xi_s D_s + \xi_r D_r - 3M(1 - \xi_m) & \text{at 1 kHz} \\ -1.5(1 - \xi_s) - 1.5(1 - \xi_r) - 3M(1 - \xi_m) & 2k - 8 \text{ kHz} \end{cases} \tag{5.22}$$

The constants A, B, C, D, and M are defined in terms of either h_s or h_r, and the source-receiver separation distance, r (in meters)

$$M = 1 - \frac{30\left(h_s + h_r\right)}{r} \quad \text{when} \quad r > 30\left(h_s + h_r\right)$$

$$M = 0 \quad \text{when} \quad r \le 30\left(h_s + h_r\right)$$

$$A = 1.5 + 3.0\left[1 - e^{-r/50}\right]e^{-0.12(h-5)^2}$$

$$+ 5.7\left[1 - e^{-2.8 \times 10^{-6}r^2}\right]e^{-0.09 h^2}$$

$$B = 1.5 + 8.6 \left[1 - e^{-r/50} \right] e^{-0.09 \ h^2}$$

$$C = 1.5 + 14.0 \left[1 - e^{-r/50} \right] e^{-0.46 \ h^2}$$

$$D = 1.5 + 5.0 \left[1 - e^{-r/50} \right] e^{-0.9 \ h^2}$$

Grazing attenuation is only present at very shallow angles, less than 5°. As the angle increases the ground becomes more reflective. Since grazing waves are highly attenuated the effect has been described as a shadow zone for source and receiver locations close to the ground.

Ground surfaces are grouped according to their acoustical properties as follows:

1. *Hard ground:* Concrete, asphalt, water, ice, or other surfaces having a low porosity such as compacted earth or rock.
2. *Soft ground:* Grass, plowed earth, dense vegetation, soft snow.
3. *Mixed ground:* A mixture of hard and soft areas.

For hard ground the constant ξ is 0; for soft ground it is 1. For a mixture of hard and soft ground the constant is the fraction of soft ground.

Focusing and Refraction Effects

The path taken by a sound wave propagating through a conducting medium such as the air is the one that minimizes the time it takes to get from the source to the receiver. This physical law is called the *principle of least time*, and applies to the motion of objects. Since the velocity of sound varies with the temperature as well as the velocity due to the motion of the medium, the path of least time does not always correspond to the path of minimum distance. If the air itself is moving, its velocity is added vectorially to the sound propagation velocity to obtain an overall velocity. These changes in velocity can affect the path taken by the sound rays and the sound levels at the receiver.

When a wind blows along the ground its velocity increases with height. Thus, if a sound wave propagates in the downwind direction, the upper part, which is at a higher elevation, will travel faster than its lower part. A surface of constant phase connecting the top and bottom parts will bend downward as illustrated in Fig. 5.19. Sound that propagates downwind can travel along a path that is unaffected by grazing and even barrier attenuation. Therefore for long propagation distances the average levels encountered in quiescent conditions, where the effects of shielding and ground effects come into play, can be much lower than levels experienced when the wind blows toward the receiver.

FIGURE 5.19   **Downwind Wave Propagation in a Parabolic Velocity Profile (Scale Exaggerated)**
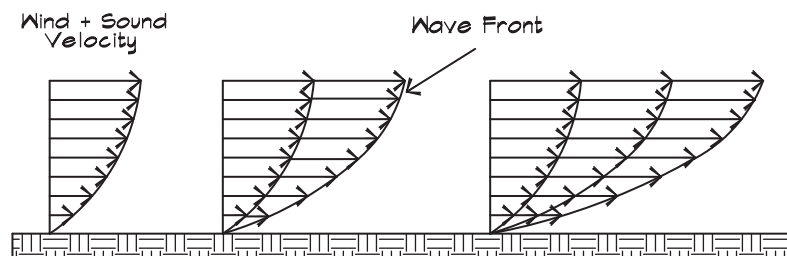
FIGURE 5.20   **Wave Propagation in a Wind Gradient**
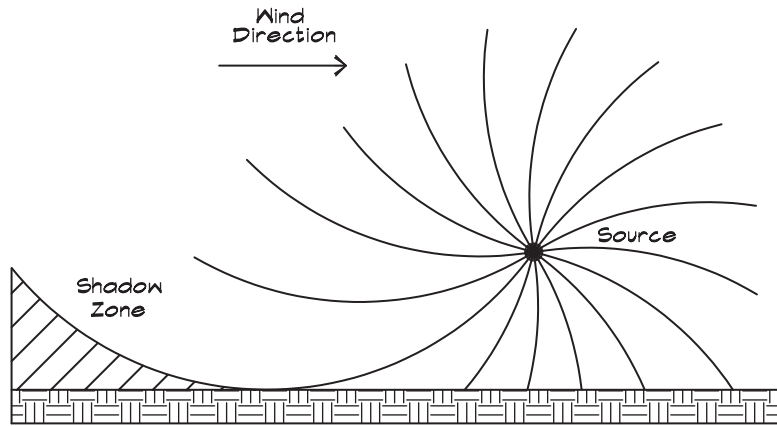
FIGURE 5.21   **Wave Propagation in a Thermal Inversion**
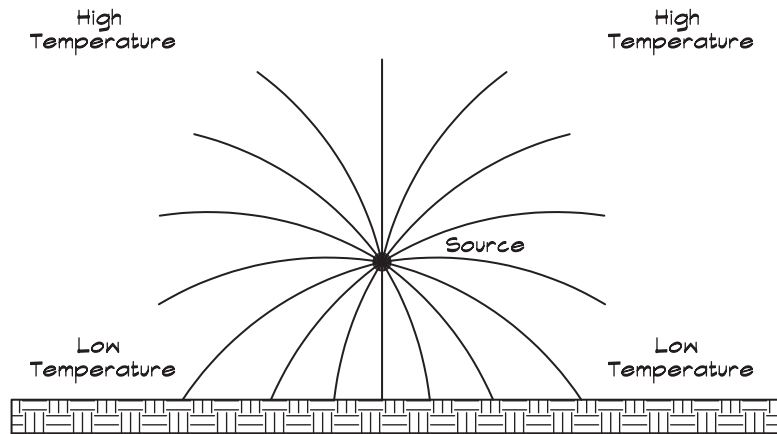
In Fig. 5.20, when a wave travels upwind, and the upper part of the wave is slowed by the higher wind velocity, the propagation path bends upward. In the upwind direction, if a sound emanates from a source at some height above the ground, there will be a curved sound path that just impacts the ground, leaving a shadow zone beyond the impact point, where in theory no sound penetrates. In practice, upwind losses in the shadow zone can be 20 dB or more.

Sound velocities can vary with temperature as well as with wind velocity. Since the velocity is dependent on the square root of the absolute temperature, when the temperature decreases with height the sound rays bend upward in all directions. If an inversion layer is encountered, where temperatures increase with height, sound rays bend down in all directions, much like a fireworks starburst shown in Fig. 5.21.

The change in the sound velocity causes a change in direction of the sound path, a situation illustrated in Fig. 5.22. If two adjacent regions have sound velocities c_1 and c_2, their wavelengths are given by

$$\lambda = \frac{c}{f} \Rightarrow \lambda_1 = \frac{c_1}{f} \Rightarrow \lambda_2 = \frac{c_2}{f} \tag{5.23}$$

FIGURE 5.22   Wave Propagation at a Change in Velocity
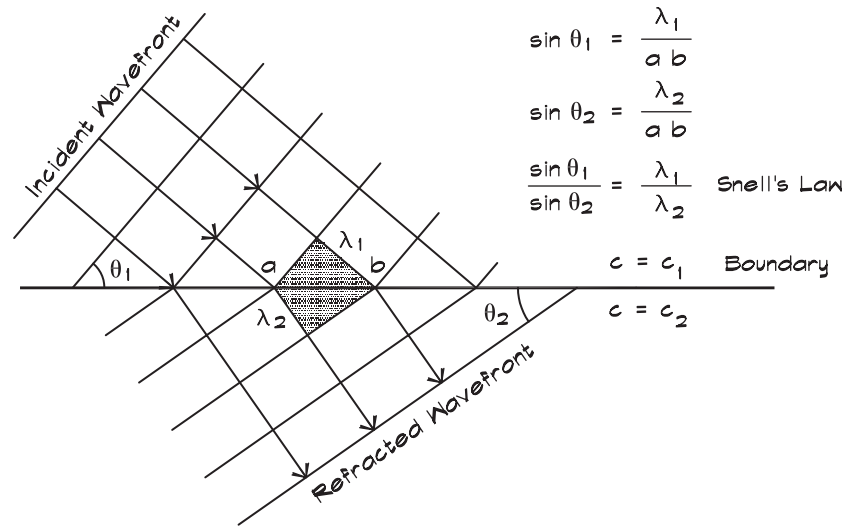
In order for the wavelengths to match at the interface between the two zones there must be a change in direction such that

$$\frac{\sin \theta_1}{\sin \theta_2} = \frac{\lambda_1}{\lambda_2}$$ (5.24)

where θ is the angle between the wavefront and the horizontal. This relationship is known as Snell's law, and the ratio of the sine terms is called the index of refraction, when the waves are light rather than sound. Snell's law can also be expressed in terms of the velocities of sound in the two media as

$$\frac{\sin \theta_1}{c_1} = \frac{\sin \theta_2}{c_2}$$ (5.25)

When the sound velocity is a linear function of the height above the ground we can calculate the shape of the sound path. If we assume sound velocity is a function of height, in Fig. 5.23, which follows the linear relationship, $c(y) = A y + B$, where A and B are constants. A is the slope of the line and B is the y axis intercept, which is taken to be zero at $c(y) = 0$. Substituting into Eq. 5.25 we obtain

$$\cos \phi \, (y) = \frac{y}{r_c} \quad \text{and} \quad c(y) = A y$$ (5.26)

This is the formula for a circle having radius r_c, where at the top of the circle $\cos \phi \, (y) = 1$ and $c(y) = c_0$. At this point we can solve for the radius r_c of curvature of the sound ray

$$r_c = \frac{c_0}{A}$$ (5.27)

FIGURE 5.23 **Relation Between a Velocity Gradient and the Radius of Curvature of a Ray (Kinsler et al., 1982)**
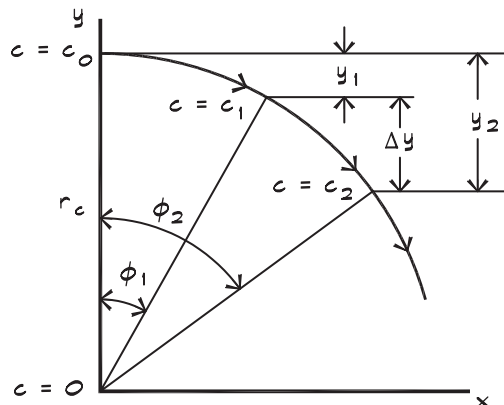
where the origin ($y = 0$) is measured from the point where the sound velocity extrapolates to zero, which is usually below ground level for a positive gradient. Note that the term A in Eq. 5.27 could be due to changes in both wind and thermal gradients. The radius of curvature is (Gutenberg, 1942)

$$r_c = \frac{c_0}{(dc/dy)\cos\phi + dv_x/dy} \qquad (5.28)$$

where r_c = radius of curvature (m)

c_0 = velocity of sound where the ray is horizontal (m/s)

$\dfrac{1}{c_0} = \dfrac{\cos\phi}{c}$ is the velocity at angle ϕ (Snell's Law)

$\dfrac{dc}{dy}$ = rate of change of sound velocity with height (1/s)

$\dfrac{dv_x}{dy}$ = rate of change of wind velocity with height (1/s)

ϕ = angle that the wavefront makes with the y axis (rad)

When r_c is positive (sound velocity increasing with height) the sound ray bends down and when it is negative (sound velocity decreasing with height) it bends up.

If the wind velocity changes from 0 km/hr to 20 km/hr (5.6 m/s) in 5 meters, A would be 4 km/m hr (1.1 s^{-1}). If the velocity at the top of the circle is 40 km/hr (11.2 m/s), then the radius of curvature is the quiescent speed of sound $344 + 11.2 = 355.2$ m/s divided by A, yielding a radius of about 322 m. If we assume that a high school band ($L_w = 100$ dB) is playing and we are located 150 m away, the arc of the sound ray at its highest point is about 10 m above the ground. This path could comfortably clear intervening barriers resulting in a clearly audible sound (45 dB). Without the wind the same source could be inaudible at this distance due to ground effects and shielding. This type of calculation is based on a worst-case scenario without focusing. The most likely scenario would probably include barrier shielding and ground effects if appropriate.

Beranek and Ver (1992) have cited unpublished data by G. S. Anderson giving the approximate attenuations due to refraction over soft ground with and without barrier shielding. Without a barrier the predicted refraction attenuation is

$$\Delta L_r = \begin{cases} -3.0 \log \dfrac{r}{15} & \text{for case 1} \\ 0 & \text{for case 2} \\ (10 - 6.2\,h + 0.03\,h^2) \log \dfrac{r}{15} \geq 0 & \text{for case 3} \\ (14 - 7.9\,h + 0.3\,h^2) \log \dfrac{r}{15} \geq 0 & \text{for case 4} \end{cases} \qquad (5.29)$$

where h is the average unrefracted height over the ground and r is the propagation distance.

Where barriers are present the refraction attenuation can be estimated by

$$\Delta L_r = \begin{cases} -3 & \text{for case 1} \\ 0 & \text{for case 2} \\ +3 & \text{for case 3} \end{cases} \qquad (5.30)$$

The case numbers refer to (1) moderate downward refraction, (2) no refraction, (3) moderate upward refraction, and (4) strong upward refraction. These equations were developed for a wind velocity of about 5 m/s at 3 m above ground. In case 4 it is assumed that both wind and thermal gradients are present.

When wind or thermal gradients are present above a highly reflecting surface, such as the surface of a lake or other large body of water, the sound rays are refracted downward and then reflected off the surface of the water. This process is repeated and the outcome is a channeling of the sound. Since the usual geometric spreading does not occur downwind, levels are considerably higher than normally would be expected. Some channeling can also occur along gullies. In the evening the bottoms of gullies are cooler than the atmosphere above them and are often rocky, providing a highly reflecting surface. Instances of atmospheric focusing have been encountered in which sound is transmitted over distances of a mile or more with localized attenuations much less than geometric falloff would predict (Bronsdon, 1998).

Combined Effects

When calculating the sound pressure levels from a generalized point source out of doors the various loss factors must be combined. The overall level is obtained from the sound power level of the source

$$L_p = L_w + 10 \log \dfrac{Q}{4\,\pi\,r^2} - \Delta L_b - \Delta L_g - \Delta L_f - \Delta L_r - \Delta L_a + 0.5 \qquad (5.31)$$

Appropriate loss terms should be included in accordance with the dictates of the physical situation. For example, air attenuation is always present but it would be inappropriate to include both barrier and refraction losses without modification by a relationship such as

Eq. 5.30. If downward refraction is present then grazing loss would not be included in a calculation but forest attenuation might be, depending on the situation.

Doppler Effect

When a sound source moves, its motion shifts the frequency heard by a stationary observer. A familiar example is a railroad train and the lowering of the frequency of the sound it emits as it passes by. Let us examine in Fig. 5.24 a source located at point a, emitting a square wave that propagates a distance $(c \, \Delta t)$, in time Δt, to reach a point b. If the same source were to move from a to a$'$ with a velocity u, while emitting the same square wave, a compressed signal would result. The front of the first pulse would arrive at b at the same time Δt, but the end of the last pulse would be emitted at the point a$'$. Thus the pulse train would be compressed into a distance that is $(u \, \Delta t)$ less than $\overline{a \, b}$.

$$\overline{a \, b} - \overline{a' \, b} = u \, \Delta t \tag{5.32}$$

The velocity of sound is not affected by the source movement but the apparent wavelength λ' is. The velocity $c = \lambda \, f = \lambda' \, f'$ can be substituted into Eq. 5.32

$$\lambda \, f \, \Delta t - \lambda' \, f \, \Delta t = u \, \Delta t \tag{5.33}$$

and

$$\lambda' = (f \, \lambda - u) \, / \, f \tag{5.34}$$

Hence there is an apparent frequency at the receiver

$$f' = f \, \lambda \, / \, \lambda' = \frac{c}{c - u} \, f \tag{5.35}$$

If we examine the case where the receiver is moving along the same straight line at a velocity v, the apparent frequency is

$$f' = \frac{c - v}{c} \, f \tag{5.36}$$

FIGURE 5.24   Doppler Effect—Frequency Shift Due to Relative Source and Receiver Velocity (Seto, 1971)

A fixed source at point a emits a square wave of frequency f.
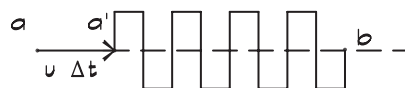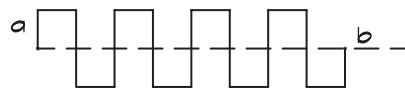
A moving source starting at point a emits a square wave of frequency f.

FIGURE 5.25   Geometry of the Doppler Effect for Planar Motion (Seto, 1971)
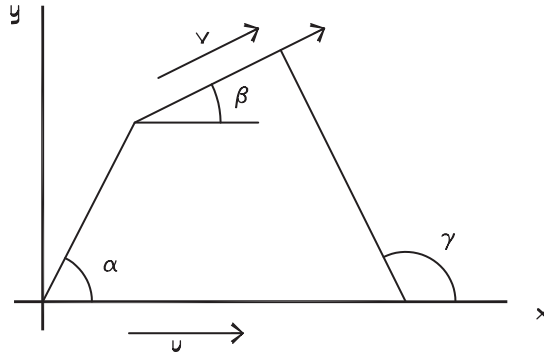
If both the source and receiver are moving along the line between them then the apparent frequency is

$$f' = \frac{c - v}{c - u} f \tag{5.37}$$

In the case of generalized planar motion of both source and receiver, as shown in Fig. 5.25, the observed frequency is

$$f' = \frac{c - v \cos (\gamma - \beta)}{c - u \cos \alpha} f \tag{5.38}$$

When there is a wind present with a velocity w, the frequency becomes

$$f' = \frac{c - v_x + w_x}{c - u_x + w_x} f \tag{5.39}$$

where the velocities are shown in terms of their x components for simplicity. Note that a wind has no effect on the apparent frequency unless there is also motion of the source or receiver.

5.4   TRAFFIC NOISE MODELING

Traffic noise modeling starts with a determination of the radiated sound levels of individual vehicles. For this purpose vehicles are grouped into three categories: automobiles, light trucks, and heavy trucks. Both the measured sound pressure level at a known distance, typically 15 m, and the effective source height are necessary for each category. Vehicle noise is reported as a sound level versus speed.

The vehicle categories for sound prediction purposes are defined as follows (Barry and Reagan, 1978):

1. *Automobiles (A)* - All vehicles having two axles and four wheels designed primarily for the transportation of nine or fewer passengers (automobiles) or the transportation of cargo (light trucks). The gross vehicle weight is less than 4500 kilograms.

FIGURE 5.26   Reference Energy Mean Vehicle Emission Levels (Barry and Reagan, 1978)
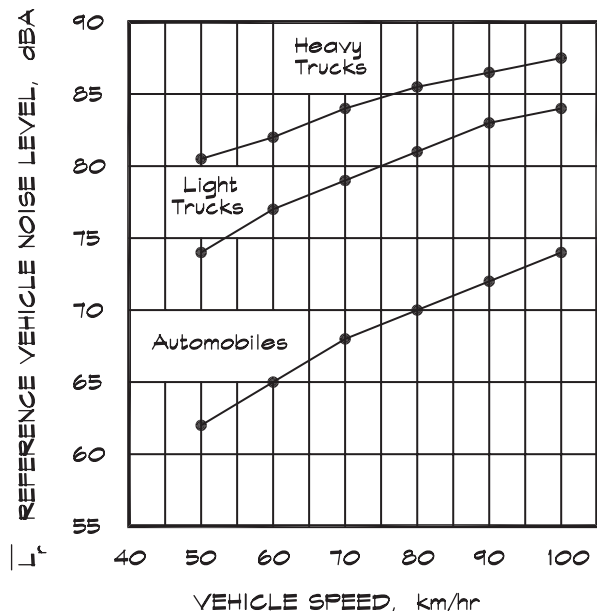
2. *Medium Trucks (MT)* - All vehicles having two axles and six wheels designed for the transportation of cargo. The gross vehicle weight is greater than 4500 kilograms but less than 12,000 kilograms.

3. *Heavy Trucks (HT)* - All vehicles having three or more axles and designed for the transportation of cargo. The gross vehicle weight is greater than 12,000 kilograms.

It is important to determine the vehicle weight definition used by the source of traffic data. Frequently state highway departments include medium trucks in their heavy truck category. When this type of count is used, the calculated noise levels are too high, so the truck count must be adjusted.

The expected noise levels at 15 m are given in Fig. 5.26 and

$$\overline{L_r}(A) = 38.1 \ \log (v_k) - 2.4$$

$$\overline{L_r}(MT) = 33.9 \ \log (v_k) + 16.4 \qquad\qquad (5.40)$$

$$\overline{L_r}(HT) = 24.6 \ \log (v_k) + 38.5$$

for each class of vehicle, where v_k is the vehicle speed in km/hr.

Soft Ground Approximation

When roadway sound propagates over soft ground, such as grass or soft earth, the rate of falloff with distance can be adjusted to approximate the loss due to ground effect. The way this normally is done is to assume a 4.5 dB/distance doubling falloff rate over the soft site

region, rather than the normal 3 dB/dd falloff rate used for hard sites. The 3 dB rate is used 1) in all cases where the source and receiver are located 3 m or more above the ground, 2) whenever there is an intervening barrier 3 m or greater in height, and 3) when the line of sight is less than 3 m above the ground and the ground is hard and there are no intervening structures. The 4.5 dB falloff rate is used when the view of the roadway is interrupted by isolated buildings, clumps of bushes, trees, or the intervening ground is soft or covered with vegetation.

When the soft ground falloff rate is used the adjustment factor for the point source attenuation for a single vehicle moving along a roadway can be written as

$$\Delta L_d = 10 \, \log \left(\frac{d_r}{r} \right)^{\frac{\xi + 4}{2}} \tag{5.41}$$

where ΔL_d = attenuation due to distance (dB)
   r = distance between the source and receiver (m or ft)
   d_r = distance at which the reference level was measured (usually 15 m or 50 ft)
   $\xi = 0$ for a hard site
   $\xi = 1$ for a soft site

The differences in the maximum levels measured at two distances, d and 2 d from the roadway, would be 6 dB for hard sites and 7.5 dB for the soft sites, 6 dB for divergence and 1.5 dB for ground attenuation. The corresponding line source falloff rate is 3 dB/dd for a hard site and 4.5 dB/dd for a soft site.

When calculating levels from roadway segments using the soft-site approximation, the rule of equal noise from equal angle segments no longer holds. The road segment correction, which is given by the last term in Eq. 5.4 for a hard site, must now be integrated over the included angles (Barry and Reagan, 1978)

$$L_{eq} = \overline{L}_r + 0.115 \, \sigma^2 + 10 \, \log \frac{N}{T} + 10 \, \log \int_{t_1}^{t_2} \frac{d_r^{\frac{\xi + 4}{2}}}{\left(\sqrt{d^2 + v^2 \, t^2} \right)^{\frac{\xi + 4}{2}}} \, d \, t \tag{5.42}$$

where L_{eq} = equivalent sound level (dB or dBA)
   $\overline{L}_r$ = average reference sound level at distance d_r (dB or dBA)
   d = distance of closest approach (m or ft)
   v = source speed (m/s or ft/s)
   t = time (s)
   N = number of vehicles passing the measurement point in time T
   σ = standard deviation of the reference sound level (dB or dBA) - usually taken to be 2.5 dBA for automobiles, 3 dBA for medium trucks, and 3.5 dBA for heavy trucks

The integral is done by making the substitution $vt = d \tan \phi$ and $vdt = d \sec^2 \phi \, d\phi$. The result is

$$L_{eq} = \overline{L}_r + 0.115 \, \sigma^2 + 10 \, \log \frac{N \, \pi \, d_r}{T \, v} + 10 \, \log \frac{d_r}{d}$$

$$+ 10 \, \log \left(\frac{d_r}{d} \right)^{\frac{\xi}{2}} + \psi_\xi \, (\phi_1, \phi_2) \tag{5.43}$$

where $\psi_\xi \, (\phi_1, \phi_2) = 10 \log \dfrac{1}{\pi} \displaystyle\int_{\phi_1}^{\phi_2} (\cos \phi)^{\frac{\xi}{2}} \, d\phi$ is the adjustment factor for included angle.

The first line of Eq. 5.43 is the equivalent sound level due to a line of vehicles moving along an infinite roadway. The second line is the adjustment due to distance and the finite roadway segment, which is applied to sites having excess attenuation. When $\xi = 0$, Eq. 5.43 reduces to Eq. 5.7. When $\xi = 1$, the integral can be done numerically and the results are shown in Fig. 5.27. The soft-site approximation is convenient mathematically, but for more accurate calculations it is recommended that the line source be subdivided into segments less than 25° and the ground effects be calculated for each segment using Eq. 5.22. For values of ξ falling between 0 and 1 the segment approach must be used.

Geometrical Mean Distance

Accurate traffic calculations can be done by apportioning the average daily traffic (ADT) on a roadway among the various lanes and calculating the levels for each lane. This technique preserves the geometrical relationship between the lanes and any roadside barriers. Heavy trucks are assumed to be located in the outside lanes. Standard lane spacing in the United States is 12 ft (3.66 m) for traffic lanes and 10 ft (3 m) for parking lanes. In a computer model of traffic noise, a near-lane and a far-lane distance can be used, from which it is straightforward to increment the distances by 12 feet for each lane. This system accounts for any median width.

For rough calculations, when the distance to the roadway is large compared with the road width, the distance to the centerline can be used. For approximate calculations at a closer distance the geometrical mean distance is sometimes used. It is defined as

$$d_{gm} = \sqrt[n]{d_1 \, d_2 \ldots d_n} \tag{5.44}$$

where d_{gm} = geometrical mean distance to the roadway (m or ft)
  n = number of lanes
  d_1 = perpendicular distance to the center of lane 1 (m or ft)
  d_2 = perpendicular distance to the center of lane 2 (m or ft)
  d_n = perpendicular distance to the center of lane n (m or ft)

Barrier Calculations

For barrier calculations a source height is required that depends on the part of the vehicle that creates the noise. For automobiles above about 55 km/hr (35 mph), the road-tire interaction is the predominant noise source so the source height is zero. The actual interaction between vehicle tires and the roadway is quite interesting and is the subject of considerable study.

FIGURE 5.27   **Adjustment Factor for Finite Length Roadways for Absorbing Sites (Barry and Reagan, 1978)**
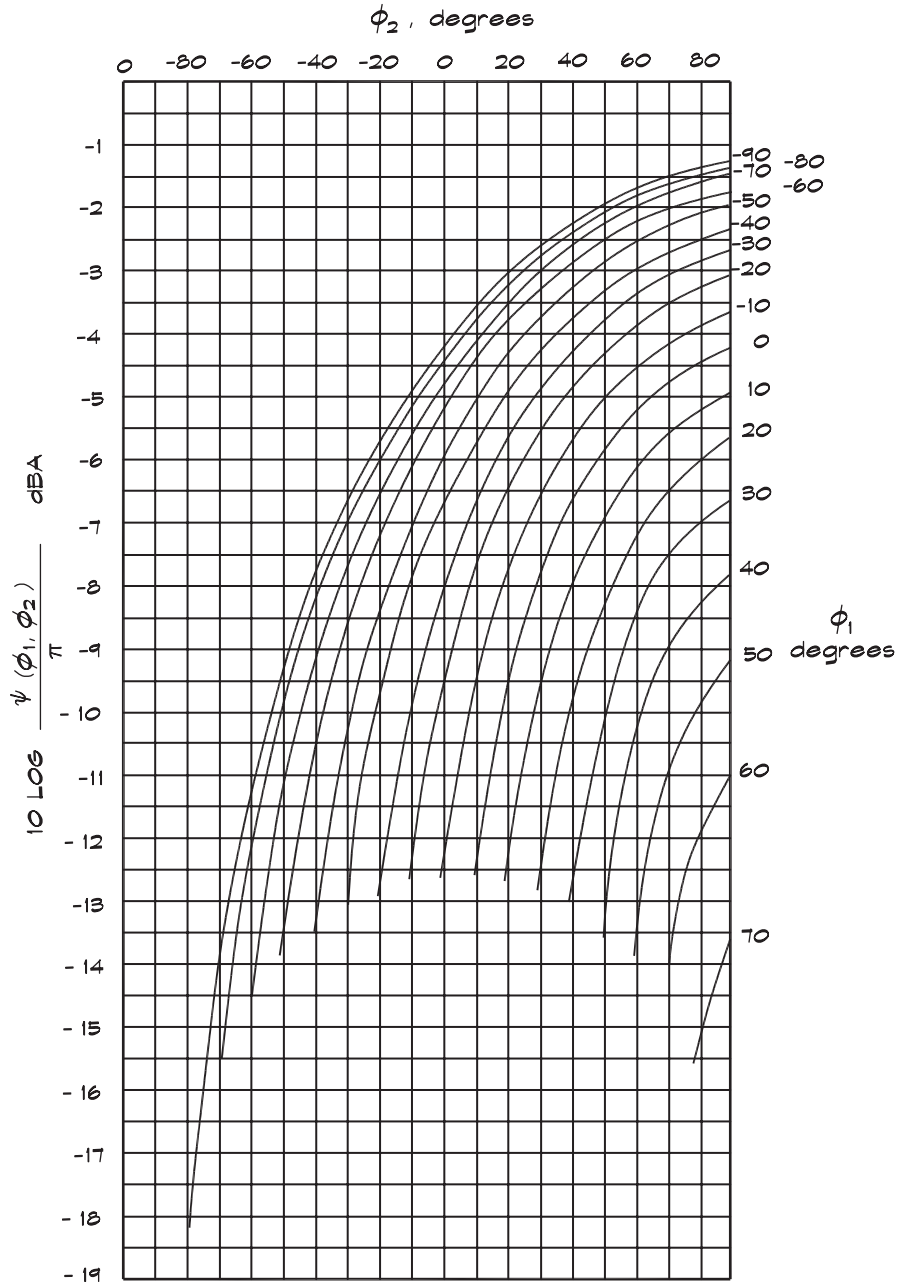
Much progress has been made, principally in Europe, on the development of porous road surfaces, which have been quite effective in reducing traffic-generated noise (Hamet, 1996). For trucks, the noise source is a combination of the truck exhaust, the motor and cooling fan, and the road-tire interaction, with the exhaust stack predominating at highway speeds. The usual height is 2.44 m (8 feet) above the roadway. For medium trucks the source height is 0.7 m (2.3 feet).

When barrier attenuations are calculated, the Fresnel number in Eq. 5.11 requires that the wavelength and thus the frequency of interest be known. Calculations also can be carried out in each octave band and the resultant levels combined in the normal way. In order to reduce the number of calculations, studies were undertaken to determine the frequency that best matched the overall result from the full calculation, based on a traffic spectrum. The result was 550 Hz, which corresponds to a wavelength of about 0.63 m (2 feet). Although the spectra of the various classes vary somewhat, the 550 Hz value is used for all vehicle types.

Roadway Computer Modeling

Where a series of partial barriers shield a roadway, the sound level from the unshielded portion can be calculated and combined with that received from the shielded portion. The calculation of the barrier shielding can be done in increments by assuming that a short line segment is a point source or by integrating the barrier attenuation over the included angles. In practice incremental technique is simpler to use for computer calculations. In both cases simplifying assumptions are made for ease of calculation. In the FHWA hard site model the Fresnel number is approximated using Eq. 5.13 to allow computation of the integral. Where this technique is employed the equation for the equivalent level from an increment of line source is

$$
\begin{aligned}
L_{eq}(\phi) = \overline{L}_r + 0.115\,\sigma^2 + 10\log\frac{N\,\pi\,d_r}{v\,T} \\
+ 10\,\log\frac{d_r}{d} + 10\,\log\frac{\Delta\phi}{\pi} - \Delta L_{bg}(\phi)
\end{aligned}
\tag{5.45}
$$

where $L_{eq}(\phi)$ = equivalent sound level (dB or dBA)
$\overline{L}_r$ = average reference sound level at distance d_r (dB or dBA)
d = distance of closest approach (m or ft)
v = source speed (m/s or ft/s)
t = time (s)
N = number of vehicles passing the measurement point in time T
σ = standard deviation of the reference sound level (dB or dBA)

$\Delta L_{bg}(\phi)$ = barrier or ground attenuation as defined in Eq. 5.11 or Eq. 5.22 for a
point source located at the centerline of travel at angle ϕ (dB)
$\Delta\phi$ = included angle of the barrier element (radians)

Since the geometry of the source-barrier configuration changes with angle, vehicle type, and lane, separate calculations should be carried out for each of these groups, and the results combined. If the source-receiver distance is sufficiently great, air attenuation may also have to be included for each segment. For overall A-weighted levels it is sufficiently accurate to

FIGURE 5.28   Spectral Components of Heavy Truck Noise at 50 Feet at Highway Cruising Speeds (Anderson et al., 1973)
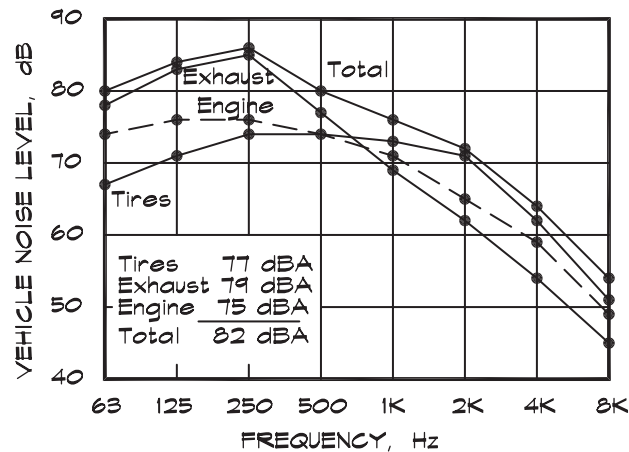
calculate air attenuation for traffic sources at 250 Hz. Software is available from the Federal Highway Administration for doing these computations.

Traffic Noise Spectra

Detailed acoustical analyses such as those required for the transmission of sound from the exterior to the interior of a building are done using the octave-band noise spectrum of a source. For traffic noise a composite spectrum is used that depends on the percentage of heavy trucks present in the vehicle mix. For an individual heavy truck, noise is emitted from the exhaust, engine, cooling system, and tires. The contribution from each source is shown in Fig. 5.28 (Anderson et al., 1973). The overall sound pressure level for these data is 82.4 dBA. By subtracting this number from each octave-band level, a generalized unweighted truck noise spectrum is obtained, normalized to zero dBA. These differences can be added to the desired overall A-weighted truck noise level to obtain the individual octave-band levels.

Figure 5.29 gives normalized heavy truck spectra for various speeds, which when subtracted from an overall A-weighted level results in an A-weighted third-octave band level. For A-weighted octave band levels three adjacent bands must be combined or 4.8 dB added to the center band to approximate the octave-band level. In a similar way A-weighted spectra can be obtained for automobiles from Fig. 5.30, and for medium trucks from Fig. 5.31.

It is frequently necessary to generate a noise spectrum given a certain vehicle mix. For example, we might predict an overall level of 70 dBA from a given roadway for a vehicle mix of 3% heavy trucks and 97% automobiles. To determine the overall spectrum we need to calculate the level generated by each class of vehicle, obtain the spectrum of each vehicle type using the normalized adjustment, and combine the results.

5.5   RAILROAD NOISE

The prediction of railway noise is similar to the calculation of traffic noise. There are two major sources, locomotive engines and rail cars. For purposes of this analysis only line

FIGURE 5.29 **Emission Spectra, Heavy Trucks, Cruise Throttle, Average Pavement (TNM, 1998)**
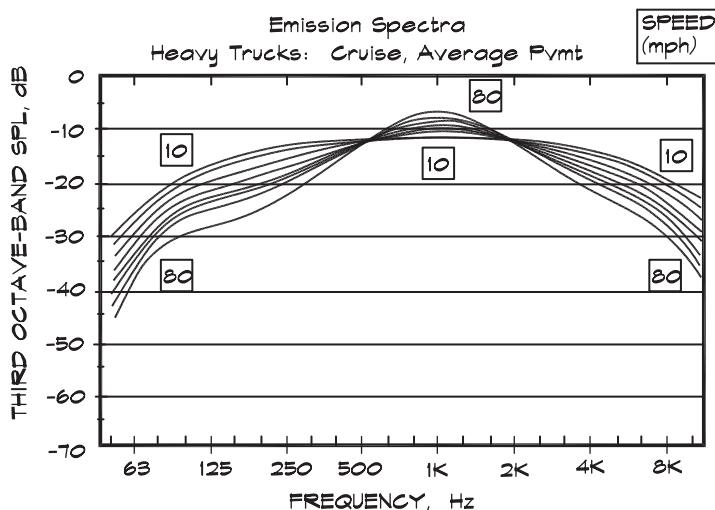
FIGURE 5.30 **Emission Spectra, Automobiles, Average Pavement (TNM, 1998)**
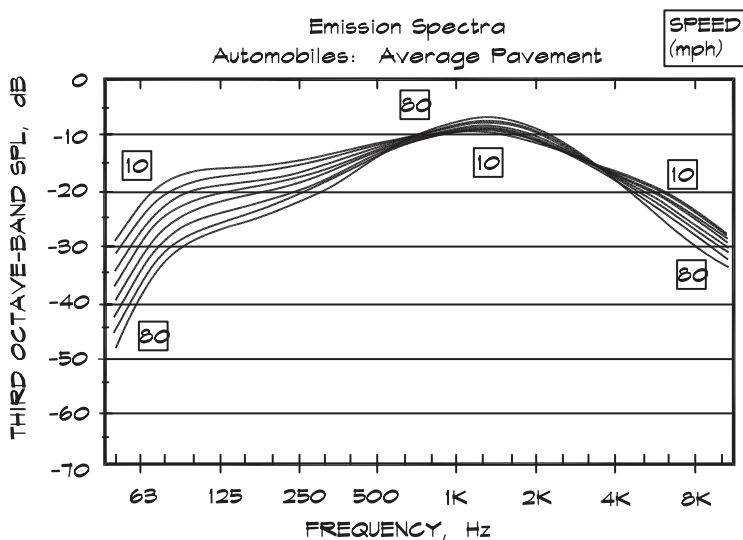
operations will be addressed. Line operations refer to the movements of railroad locomotives and freight or passenger cars over a main line or branch line of tracks. General railroad yard noise and noise due to horns and crossing signals will not be included. For a more detailed analysis of yard noise and other sources associated with general railroad operations, refer to Swing and Pies (1973).

A train noise time history is shown in Fig. 5.32. Locomotive noise is generated by the large diesel-electric engines, typically 2500 to 3000 horsepower (2 mw), which singly or in groups pull the long strings of cars. Locomotive noise depends on the engine throttle setting

FIGURE 5.31   Emission Spectra, Medium Trucks, Cruise Throttle, Average Pavement (TNM, 1998)

Emission Spectra
Medium Trucks: Cruise, Average Pvmt
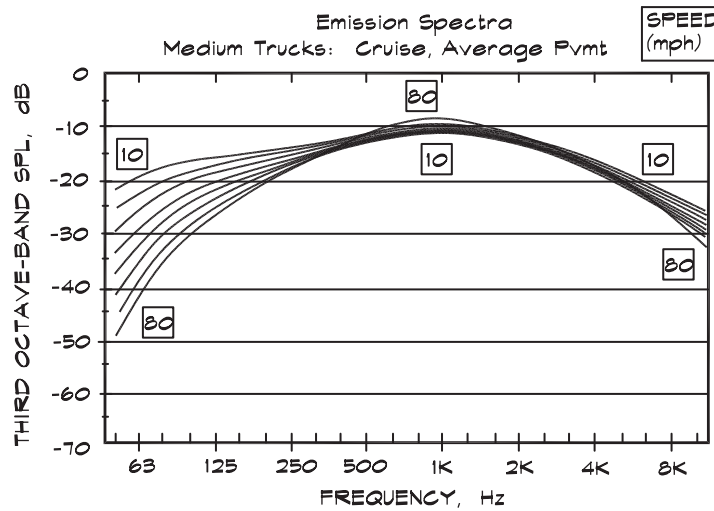
FIGURE 5.32   Typical Time History of a Train Passby (Swing and Pies, 1973)

Measured at 100 feet from track, 32 mph at + 0.6 percent grade.
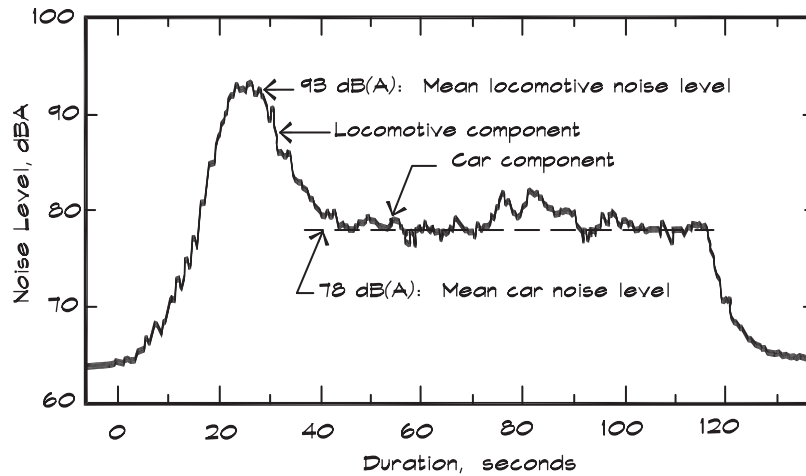
and somewhat on the grade but is relatively independent of velocity. Reference sound levels from a sample of engine passbys are shown in Fig. 5.33. Levels average 91 dBA at 100 ft. Grade adjustments are given in Fig. 5.34.

Rail car noise is produced by wheel-rail interaction and is a strong function of velocity. Rail car noise levels can be estimated using an empirical formula (Swing and Pies, 1973)

$$L_r(cars) = 50 + 20 \, \log \, v_m \qquad (5.47)$$

FIGURE 5.33   Noise Levels of a Locomotive at Level Grade (Swing and Pies, 1973)

Measured at 100 feet from the track.
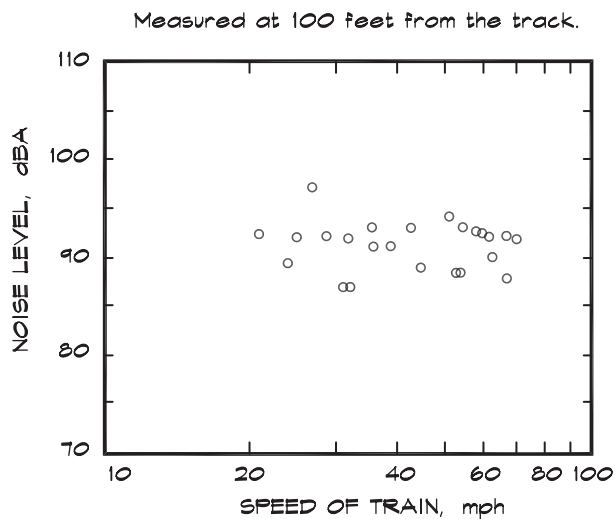
FIGURE 5.34   Grade Dependence of Locomotive Noise (Swing and Pies, 1973)
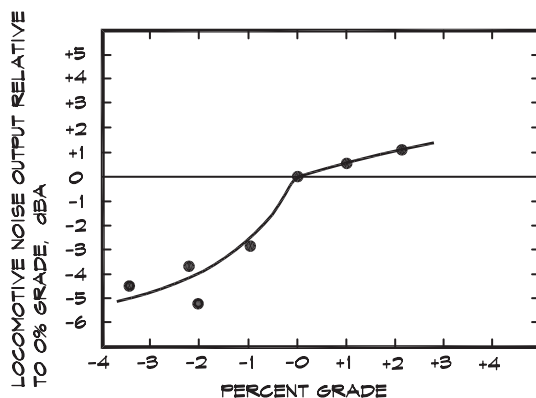
where L_r(cars) = reference rail car level at 30 m (100 ft) (dBA)

v_m = speed of train (mph = 1.61 kph)

Some variations in level are encountered due to different track conditions, which are summarized in Table 5.2. The base level in Eq. 5.47 assumes jointed rails, no crossings, smooth wheels, and no bridgework or short-radius curves.

The normal modeling procedure is to establish a sound exposure level (SEL) for a given train passage and then to adjust the level by the number of like events to determine a day-night level or other metric of interest. Recall that the sound exposure level was defined in Eq. 4.11 and is the energy-time product expressed as a level. Combining this equation with Eq. 5.5 we obtain the SEL value for a locomotive passby

$$SEL_{loc} = L_r(loc) + 10 \, \log \frac{\pi d_r}{v} + 10 \, \log \frac{d_r}{d} \qquad (5.48)$$

TABLE 5.2   Variables Affecting Freight Car Wheel/Rail Noise Emission (Swing and Pies, 1973)

Variable	Increase in Noise Level*	Comments
1. Jointed Rails (vs Welded)	4 to 8 dB(A)	Generally no correction for main line tracks; assign higher value to low speed classified track
2. Presence of Grade Crossings and Frogs	6 to 8 dB(A)	
3. Wheel Irregularities – Flat Spots or Built-up Tread	to 15 dB(A)	
4. Passage Over Bridgework a. Light Steel Structure b. Heavy Steel Structure c. Concrete Structure	 to 30 dB(A) to 15 dB(A) 0 to 12 dB(A)	Use lower range of corrections for heavier structures
5. Short Radius Curves a. Less than 600 ft. Radius b. 600 to 900 ft. Radius	 15 to 25 dB(A) 5 to 15 dB(A)	Random occurrence of wheel squeal

* These factors are assumed to act individually. When in combinations of two or more the net increase will not be equal to the sum of each component, but most likely the largest individual factor.

where L_r (loc) = reference locomotive sound level at d_r (dBA)

   v = speed of train (m/s)

   d = perpendicular distance to the track (m)

When there are multiple locomotives a factor of 10 log N is added in. Figure 5.35 sets forth the modeling scheme. The locomotives are calculated as single passbys. The cars are calculated

FIGURE 5.35   Railroad Noise Modeling Scheme (Swing and Pies, 1973)
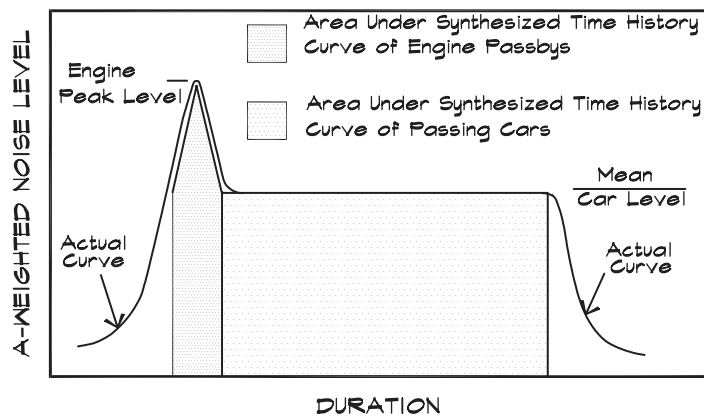
as a steady level having a given duration. For a line of rail cars

$$\text{SEL}_{\text{cars}} = L_r(\text{cars}) + 10 \; \log \; t + 10 \; \log \; \frac{d_r}{d} \tag{5.49}$$

where L_r (cars) = reference rail car sound level at d_r (dBA)

t = time of car passage (s) = .68 l (ft) / v (mph) where l is the length of the train in feet or = 3.6 l (m) / v (kph) where l is in meters

Train lengths and velocities are available from the local railroad dispatch office. In the United States standard train cars are 60 ft (18.3 m) long and stretched cars used for automobile transport are 85 ft (25.9 m) long.

SEL levels from shielded train passbys can be obtained by applying partial line source, barrier, and ground effect adjustments to Eqs. 5.48 and 5.49. The source height of a locomotive engine stack is about 15 ft (4.6 m) and the car source height is zero. The barrier calculation frequency for railroads has not been published. A value of 550 Hz can be used if we assume that locomotive and truck spectra are similar.

Twenty-four hour L_{dn} noise levels can be calculated from SEL values by using the weighted number of trains during an average day

$$N_{dn} = N_d + N_e + 10 \; N_n \tag{5.50}$$

where N_{dn} = weighted number of trains per day

N_d = number of daytime (7 am to 7 pm) trains

N_e = number of evening (7 pm to 10 pm) trains

N_n = number of nightime (10 pm to 7 am) trains

The day-night noise level due to all train events is

$$L_{dn} = 10 \; \log \left[10^{0.1 \; \text{SEL}_{\text{loc}}} + 10^{0.1 \; \text{SEL}_{\text{cars}}} \right] + 10 \; \log N_{dn} - 49.4 \tag{5.51}$$

The constant 49.4 is 10 log (3600 × 24), which normalizes the L_{dn} to the number of seconds in a day.

The spectrum for locomotives is shown in Fig. 5.36, and for cars, in Fig. 5.37. A composite spectrum can be generated by combining a locomotive spectrum adjusted to the SEL for locomotives and a car spectrum adjusted to the SEL for cars. The combined spectrum is then normalized to the L_{dn} level.

5.6   AIRCRAFT NOISE

Jet aircraft noise is generated primarily by the interaction of the high-velocity exhaust gasses with the relatively still atmosphere through which the aircraft passes. As the gasses mix with the surrounding air the resulting turbulence creates large pressure fluctuations, which radiate as sound. The region where most of the sound is formed is 5 to 8 diameters behind the exhaust nozzle. Consequently jet noise is difficult to enclose or otherwise muffle. Jet noise has several distinctive features including a very strong (eighth power) dependence on the velocity (v) of the flow. The frequency spectrum of jet noise is a flat haystack-shaped curve with the maximum scaled to the diameter (d) of the exhaust opening. Figure 5.38 illustrates this behavior. The peak occurs at a frequency $f_o = 0.13 \; \frac{v}{d}$.

**FIGURE 5.36   Spectral Components of Locomotive Noise (Swing and Pies, 1973)
Measurements at 50 feet, 0% grade, and 58 mph**
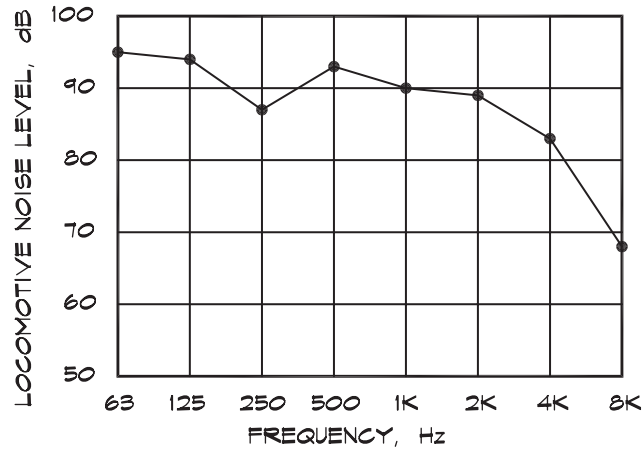
**FIGURE 5.37   Spectral Components of Railroad Car Noise (Swing and Pies, 1973)
Measurements at 100 feet, 0% grade, and 58 mph**
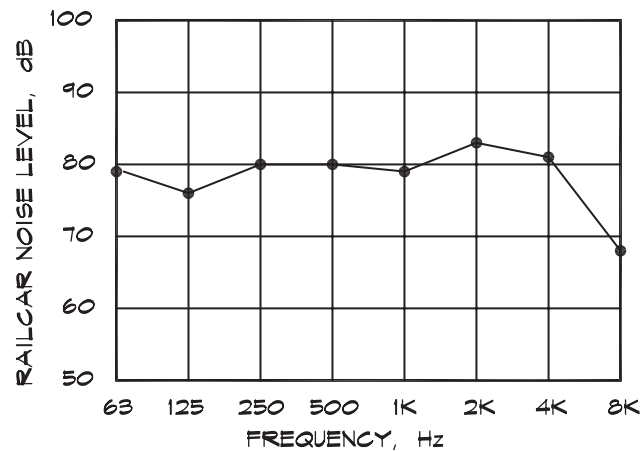
Jet noise is highly directional. The exhaust produces lobes that have their maxima at between 30° and 45° degrees from the axis of the jet. At the front of the engine, high-frequency tonal components of the compressor fans are radiated from the intake. Thus on the approach side of an airport there is a greater high-frequency noise component than on the takeoff side.

Older commercial jet engines and most military aircraft engines are primarily turbojets. In a turbojet, the intake air is compressed by means of a set of rotating and a set of fixed blades. Jet fuel and compressed air are mixed together and burned in the combustion chamber and the hot gas expands and accelerates out the rear of the engine. A rear turbine is driven by the exhaust gasses and provides the power to turn the compressor. The turbojet produces a very high velocity exhaust flow, which dominates other noise sources, particularly at low frequencies. Some high-frequency noise is radiated from the intake compressor toward the front of the aircraft. The spectrum is in Fig. 5.39.

FIGURE 5.38   **Generalized Power Spectrum of Jets (Harris, 1957)**
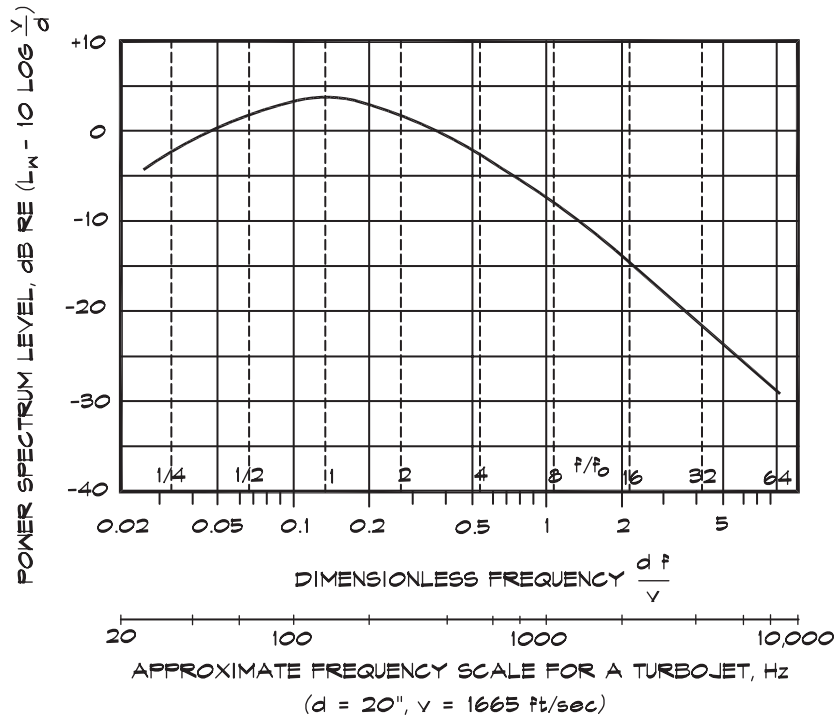
FIGURE 5.39   **Noise Levels and Spectra of 2-3 Engine Low Bypass Ratio Turbofan Aircraft (Wyle Laboratories, 1971)**
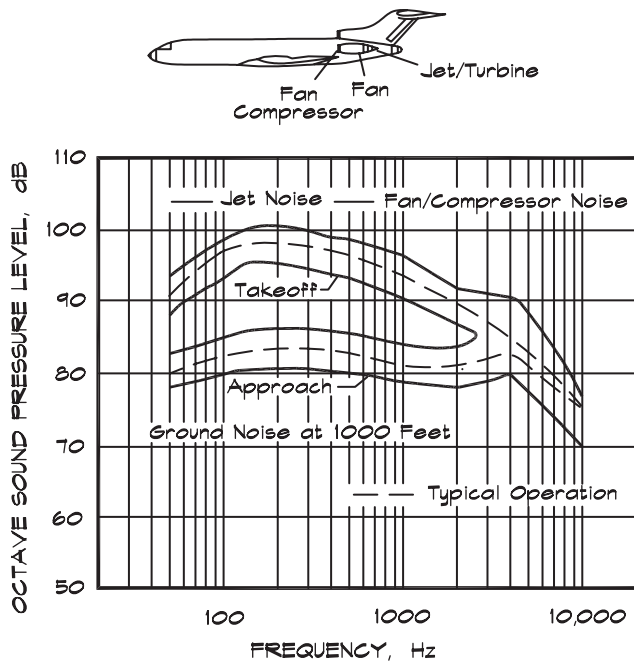
FIGURE 5.40   **Noise Level and Spectra of a 4-Engine High Bypass Ratio Turbofan Aircraft (Wyle Laboratories, 1971)**
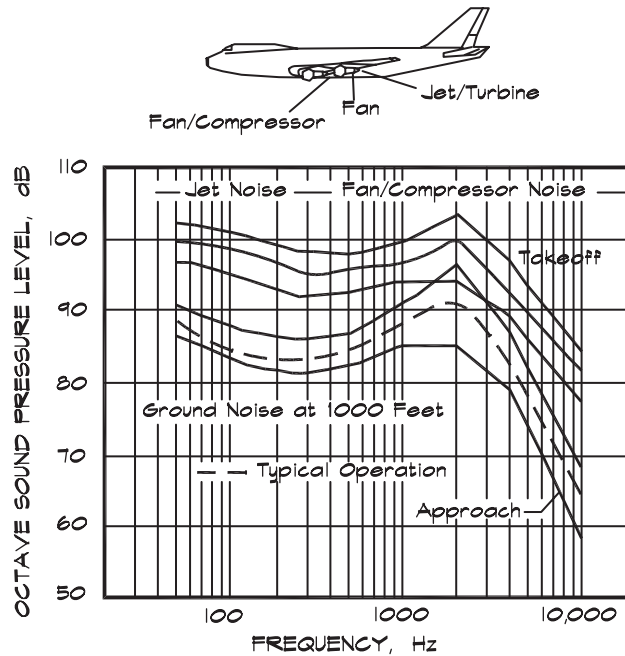
The turbofan engine was developed, in part, as an attempt to reduce turbojet noise. The idea behind a turbofan design is to increase the diameter of the engine and to use the intake compressor as a propeller. Some of the inlet air is bypassed or routed around the combustion chamber and mixed back in with the combustion gas at the rear of the engine. This accomplishes several useful things. First, since the diameter of the intake is large, more air (mass) is forced through the opening. The engine thrust (fluid mass times acceleration) can increase even while the exhaust velocity and the noise level is reduced. Second, the bypassed air eases the transition between the high-velocity jet core and the quiescent atmosphere, so that the turbulent fluctuations due to mixing are less. Again this helps lower the noise levels. The amount of air bypassed divided by the total air passing through the intake is called the bypass ratio. Early turbofan engines such as the Pratt and Whitney JT8D used on the Boeing 707 are characterized as low bypass ratio engines. Engines such as the JT9D used on the Boeing 747 and the General Electric CF6 used on the McDonnell Douglas DC-10 aircraft are termed high bypass ratio engines and have a much lower noise output. A sketch of a turbofan powered aircraft and its spectrum is in Fig. 5.40.

Airport noise is measured at fixed monitoring stations on poles or buildings located around the airfield. In addition, computer models such as the Integrated Noise Model (INM), available from the Federal Aviation Administration (FAA), are used to calculate airport noise contours based on data measured on individual aircraft types. These contours are prepared for most major airports and regularly updated. For military airports Air Installation Compatible Land Use Zone (AICUZ) studies are prepared and are available to the public. Noise levels are shown as contours of equal level in terms of L_{dn}.

FIGURE 5.41   Typical Noise Spectra of Light Piston-Engine Helicopters (Wyle Laboratories, 1971)
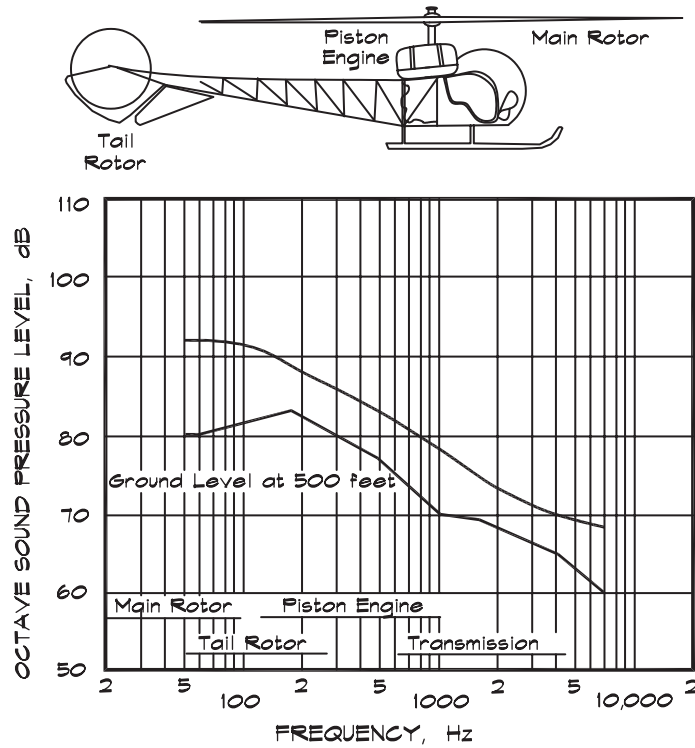
For architectural acoustics calculations of aircraft noise, it is sufficient to obtain the day-night levels from a contour map. If maximum passby levels are of interest then on-site measurements are sometimes necessary. For a major airport such as Los Angeles International, a rough estimate can be obtained by adding 20 dBA to the day-night level. Detailed calculations of interior noise from passing aircraft require a knowledge of the specific spectrum. Where the source is a helicopter a typical noise spectrum is shown in Fig. 5.41.

<div style="text-align: right;">WAVE
ACOUSTICS</div>

Much of architectural acoustics can be addressed without consideration of the wave nature of sound. For example, environmental acoustics and the transmission of outdoor sound, for the most part, can be visualized and modeled as a flow of energy from point to point, although many effects, such as ground and barrier attenuation, are frequency dependent. Nevertheless, for many critical aspects of acoustics, knowledge of wave phenomena is essential. Wave acoustics takes into account fundamental properties that are wavelength and phase dependent, including the scaling of interactions to wavelength, the phenomenon of resonance, and the combination of amplitudes based not only on energy but also on phase.

6.1   RESONANCE

Simple Oscillators

Many mechanical systems have forces that restore a body to its equilibrium position after it has been displaced. Examples include a spring mass, a child's swing, a plucked string, and the floor of a building. When such a system is pulled away from its rest position, it will move back toward equilibrium, transition through it, and go beyond only to return again and repeat the process. All linear oscillators are constrained such that, once displaced, they return to the initial position. The movement repeats at regular intervals, which have a characteristic duration and thus a characteristic frequency, called the natural frequency or resonant frequency of the system.

Although many such systems exist, the simplest mechanical model is the spring and mass shown in Fig. 6.1. A frictionless mass, m, is attached to a linear spring, whose restoring force is proportional to the displacement away from equilibrium, x. This relationship is known as Hooke's law and is usually written as

$$F = -k\,x \tag{6.1}$$

where k is the constant of proportionality or the spring constant.

FIGURE 6.1   A Simple Spring-Mass System
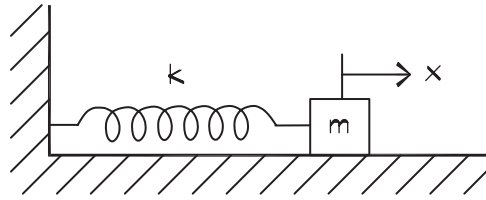
When the body is in motion, inertial forces, due to the mass, counterbalance the spring force, according to Newton's second law

$$F = m\, a = m\, \frac{d^2 x}{d\, t^2} \tag{6.2}$$

where   F = force applied to the mass, (N)

m = mass, (kg)

a = acceleration or the second time derivative of the displacement, (m/s^2)

The forces in a simple spring mass system are: 1) the spring force, which depends on the displacement away from the equilibrium position, and 2) the inertial force of the accelerating mass. The equation of motion is simply a summation of the forces on the body

$$m\, \frac{d^2 x}{d\, t^2} + k\, x = 0 \tag{6.3}$$

If we introduce the quantity

$$\omega_n^2 = \frac{k}{m} \tag{6.4}$$

the equation can be written as

$$\frac{d^2 x}{d\, t^2} + \omega_n^2\, x = 0 \tag{6.5}$$

The solution requires that the second derivative be the negative of itself times a constant. This is a property of the sine and cosine functions, so we can write a general solution as

$$x = A\, \sin \omega_n\, t + B\, \cos \omega_n\, t \tag{6.6}$$

where A and B are arbitrary constants defined by the initial conditions. If the system is started at $t = 0$ from a position x_0 and a velocity v_0, then the constants are defined and the equation becomes

$$x = \frac{v_0}{\omega_n}\, \sin \omega_n\, t + x_0\, \cos \omega_n\, t \tag{6.7}$$

Since we can write the coefficients in Eq. 6.6 in terms of trigonometric functions

$$a\, \sin \omega t + b\, \cos \omega t = \cos \phi\, \cos \omega t - \sin \phi\, \sin \omega t = \cos(\omega t + \phi) \tag{6.8}$$

and we can form a second general solution

$$x = X \cos (\omega_n t + \phi) \tag{6.9}$$

where

$$X = \sqrt{x_0^2 + (v_0 / \omega_n)^2} \quad \text{and} \quad \phi = \tan^{-1} \left[\frac{-v_0}{\omega_n x_0} \right] \tag{6.10}$$

and X = amplitude of the maximum displacement of the system, (m)
   ϕ = initial phase of the system, (rad)

According to Eq. 6.9 the behavior of the spring mass system is harmonic, with the motion repeating every time period $t = T$, where $\omega_n T = 2 \pi$. The period is

$$T = 2 \pi \sqrt{m / k} \tag{6.11}$$

and the natural frequency of vibration is the reciprocal of the period

$$f_n = \frac{1}{2 \pi} \sqrt{\frac{k}{m}} \tag{6.12}$$

The natural frequency of an undamped spring mass system can be specified in terms of the deflection δ of the spring, under the load of the mass since $k \delta$ = force = $m g$, where g is the acceleration due to gravity. Using $g = 386$ in/s^2 = 9.8 m/s^2, the natural frequency can be written as

$$f_n = \frac{3.13}{\sqrt{\delta_i}} = \frac{5}{\sqrt{\delta_{cm}}} \tag{6.13}$$

where f_n = natural frequency of the system,   (Hz)
   δ = deflection of the spring under the weight of the mass $- \delta_i$ in inches
     and δ_{cm} in centimeters

This provides a convenient way of remembering the natural frequency of a spring mass system. A one-inch deflection spring is a 3-Hz oscillator, and a one-centimeter deflection spring is a 5-Hz oscillator. These simple oscillators appear over and over in various forms throughout architectural acoustics.

Air Spring Oscillators

When air is contained in an enclosed space, it can act as the spring in a spring mass system. In the example shown in Fig. 6.2, a frictionless mass is backed by a volume of air. When the mass moves into the volume, the pressure increases, creating a force that opposes the motion. The spring constant of the enclosed air is derived from the equation of state

$$P V^\gamma = \text{constant} \tag{6.14}$$

differentiating

$$\gamma P V^{\gamma - 1} dV + V^\gamma dP = 0 \tag{6.15}$$

FIGURE 6.2   A Frictionless Mass and an Air Spring
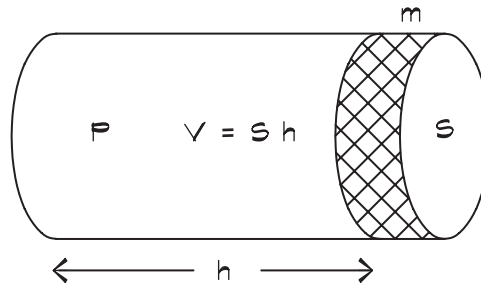
The rate of change of pressure with volume is

$$dP = -\frac{\gamma P}{V}\, dV \qquad (6.16)$$

from which we can obtain the spring constant for a trapped air volume of depth h

$$k = \frac{\gamma\, P\, S}{V}\, \frac{dV}{dh} = \frac{\gamma\, P\, S^2}{V} = \frac{\gamma\, P\, S}{h} \qquad (6.17)$$

and the natural frequency is

$$f_n = \frac{1}{2\,\pi}\, \sqrt{\frac{\gamma\, P_0\, S}{m\, h}} \qquad (6.18)$$

where f_n = resonant frequency of the system, (Hz)
    P_0 = atmospheric pressure, $(1.013 \times 10^5$ Pa)
    m = mass of the piston, (kg)
    γ = ratio of specific heats = 1.4 for air
    S = area of the piston (m^2)
    h = depth of the air cavity (m)

For normal atmospheric pressure, the resonant frequency of an unsupported panel of drywall, 16 mm thick (5/8") weighing 12.2 kg/sq m (2.5 lbs/sq ft) with a 9 cm (3.5") air cavity behind it, is about 18 Hz. If the air gap is reduced to 1.2 cm (about 1/2"), the natural frequency rises to about 50 Hz. If the drywall panel were supported on resilient channel having a deflection due to the weight of the drywall of 1 mm, its spring mass resonant frequency would be about 16 Hz. The presence of the air spring caused by the 1/2" air gap stiffens the connection between the drywall and the support system, which results in poor vibration isolation when resilient channel is applied directly over another panel. A similar condition occurs in the construction of resiliently mounted (floating) floors if the trapped air layer is very shallow.

The air spring was the basis behind the air-suspension loudspeaker system, which was developed in the 1960s. The idea was that a cone loudspeaker could be made lighter and more compliant (less stiff) if the spring constant of the air in the box containing it made up for the lack of suspension stiffness. The lighter cone made the loudspeaker easier to accelerate and thus improved its high-frequency response.

FIGURE 6.3   Geometry of a Helmholtz Resonator
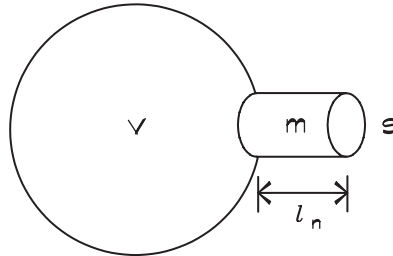
Helmholtz Resonators

A special type of air-spring oscillator is an enclosed volume having a small neck and an opening at one end. It is called a *Helmholtz resonator*, named in honor of the man who first calculated its resonant frequency. Referring to the dimensions in Fig. 6.3, the system mass is the mass of the air in the neck, $m = \rho_0 \, S \, l_n$ and the spring constant k is $\gamma \, P_0 \, S^2 / V$. Using the relationship shown in Eq. 6.12 the natural frequency is given by

$$f_n = \frac{c_0}{2\,\pi} \sqrt{\frac{S}{V\,l_n}} \tag{6.19}$$

Note that the frequency increases with neck area and decreases with enclosed volume and neck length.

Helmholtz resonators are used in bass-reflex or ported loudspeaker cabinets to extend the bass response of loudspeakers by tuning the box so that the port emits energy at low frequencies. The box-cone combination is not a simple Helmholtz resonator, but acts like a high-pass filter. Thiele (1971) and Small (1973) did extensive work on developing equivalent circuit models of the combined system, which is designed so that its resonant frequency is just below the point at which the loudspeaker starts to loose efficiency. An example of a low-frequency loudspeaker response curve is shown in Fig. 6.4. Ported boxes radiate low-frequency sound out the opening, where it combines in phase with the direct cone radiation. Potentially detrimental high-frequency modes, due to resonances within the cavity, are dampened by filling the box with fiberglass.

A similar technique is used to create tuned absorbers in studios and control rooms, where they are called bass traps. Relatively large volumes, filled with absorption, are tucked into ceilings, under platforms, and behind walls to absorb low-frequency sound. To act as a true Helmholtz resonator they must have a volume, a neck, and an opening, whose dimensions are small compared with the wavelength of sound to be absorbed.

Neckless Helmholtz Resonators

When an enclosed volume has an opening in it, it can still oscillate as a Helmholtz resonator even though it does not have an obvious neck. Since the air constricts as it passes through the opening, it forms a virtual tube, illustrated in Fig. 6.5, sometimes called a *vena contrata* in fluid dynamics. This acts like a neck, with an effective length equal to the thickness of the plate l_0 plus an additional "end effect" factor of (0.85 a), where a is the radius of the opening.

FIGURE 6.4   **Frequency Response of a Sealed Cabinet vs a Bass-Reflex Cabinet (Roozen et al., 1998)**
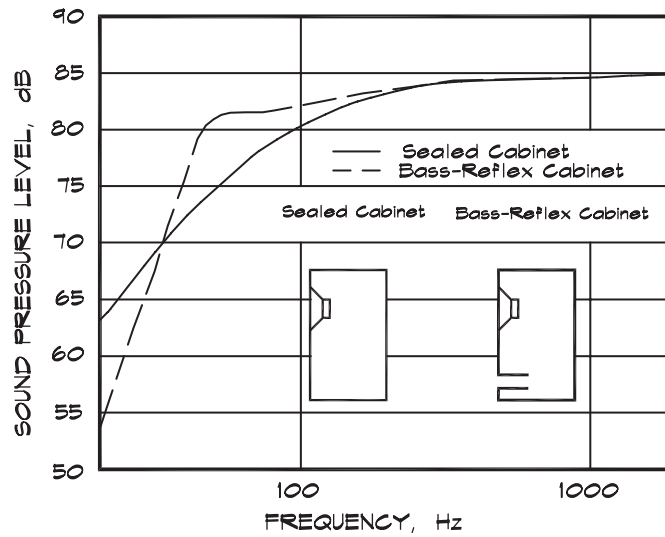
FIGURE 6.5   **Geometry of a Neckless Helmholtz Resonator**
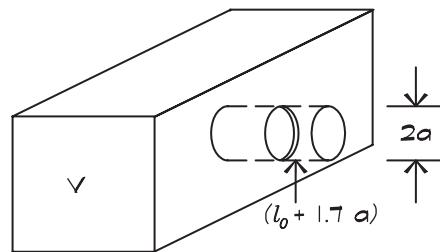
Since there are two open ends of the tube, the natural frequency becomes

$$f_n = \frac{c_0}{2\,\pi}\,\sqrt{\frac{\pi\,a^2}{V\,(l_0 + 1.7\,a)}} \tag{6.20}$$

When there are multiple openings in the side of an enclosure, such as with a perforated plate spaced out from a wall, a Helmholtz resonance effect can still occur. The length of the neck is still the same as that used in Eq. 6.20, but the open area is the area of each hole times the number of holes in the plate.

For a perforated panel located a distance d from a solid wall, the resonant frequency is

$$f_n = \frac{c_0}{2\,\pi}\,\sqrt{\frac{\sigma}{d\,(l_0 + 1.7\,a)}} \tag{6.21}$$

where σ = fraction of open area in the panel which for round holes, staggered
is 0.9 $(2a/b)^2$ and for round holes, straight is 0.785 $(2a/b)^2$,
where b is the hole spacing

  d = depth of the airspace behind the panel in units consistent with
those of l_0, a, and c_0

6.2   WAVE EQUATION

One-Dimensional Wave Equation

The wave equation is a differential equation that formally defines the behavior in space and
time of the pressure, density, and other variables in a sound wave. It is rarely used directly in
architectural acoustics, but its solutions are the basis of wave acoustics, which is important to
the understanding of many phenomena. Its derivation includes several assumptions about the
nature of the medium through which sound passes. It assumes that the conducting medium
follows the equation of continuity (conservation of mass), Newton's second law of motion,
and an equation of state, relating the pressure and density. Refer to Kinsler et al., (1982) for
a more detailed treatment.

To derive the wave equation we examine a small slice of a fluid (such as air), having
thickness dx, shown from one side in Fig. 6.6. As a sound wave passes by, the original
dimensions of the box ABCD move, in one dimension, to some new position A'B'C'D'. If
S is the area of the slice, having its normal along the x axis, then there is a new box volume

$$V + dV = S\,dx \left(1 + \frac{\partial \xi}{\partial x} \right) \qquad (6.22)$$

where ξ is the displacement of the slice. In Chapt. 2, the bulk modulus was defined in
Eq. 2.39 as the ratio of the change in pressure to the fractional change in volume

$$dP = -\,B\ \frac{d\,V}{V} \qquad (6.23)$$

In terms of the volume in Fig. 6.6, the change in the total pressure P is the acoustic pressure
p and the change in volume is S dx. So comparing Eqs. 6.22 and 6.23, we obtain the relation

FIGURE 6.6   The Fluid Displacement during the Passage of a Plane Wave (Rossing and Fletcher, 1995)

The fluid at plane AB is displaced to A'B' and that at CD to C'D'.
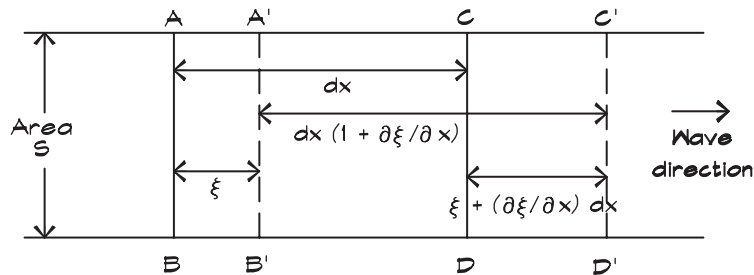
between the acoustic pressure and the change in length. The minus sign means that if the length decreases, the pressure increases.

$$p = -B \ \frac{\partial \xi}{\partial x} \tag{6.24}$$

The motion of the slice is described by Newton's second law, so we set the pressure gradient force equal to the slice mass times its acceleration,

$$-S \left(\frac{\partial p}{\partial x} \ d \ x \right) = \rho_0 \ S \ dx \ \frac{\partial^2 \xi}{\partial \ t^2} \tag{6.25}$$

and simplifying we obtain an expression known as Euler's equation

$$-\frac{\partial p}{\partial x} = \rho_0 \ \frac{\partial^2 \xi}{\partial \ t^2} \tag{6.26}$$

Then using Eqs. 6.24 and 6.26

$$\frac{\partial^2 \xi}{\partial \ t^2} = \frac{B}{\rho_0} \ \frac{\partial^2 \xi}{\partial \ x^2} \tag{6.27}$$

By differentiating Eq. 6.26 once with respect to x, and Eq. 6.24 twice with respect to t, and adding them

$$\frac{\partial^2 p}{\partial \ t^2} = c^2 \ \frac{\partial^2 p}{\partial \ x^2} \tag{6.28}$$

where we have used Eq. 2.40 for the speed of sound. This is the one-dimensional wave equation, expressed in terms of pressure. It relates the spatial and time dependence of the sound pressure within the wave.

Solutions to Eq. 6.28 are not difficult to find; in fact, any pressure wave that is a function of the quantity $(x \pm c \ t)$ will do. This reveals the infinite number of possible waveforms that a sound wave can take. The plus and minus signs indicate the direction of propagation of the wave. Although many functions are solutions to the wave equation, not all are periodic. In architectural acoustics, the periodic solutions are of primary interest to us, although nonperiodic phenomena such as sonic booms are occasionally encountered. A periodic solution, which describes a plane wave traveling in the $+ x$ direction is

$$\mathbf{p} = \mathbf{A} \, e^{-j k x} \, e^{j \omega t} = \mathbf{A} \ \cos \left(-k \ x + \omega \ t \right) \tag{6.29}$$

where $\mathbf{p}$ = acoustic pressure, (Pa)
       $\mathbf{A}$ = maximum pressure amplitude, (Pa)
       $j = \sqrt{-1}$
       ω = radial frequency, (rad / s)
       k = wave number = ω / c, (rad / m)

The right side of Eq. 6.29 is a familiar form, which we derived using heuristic arguments in Eq. 2.32. The terms on the left are another way of expressing periodic motion using exponentials, which are more convenient for many calculations.

Using Eq. 6.26, the particle velocity can be obtained

$$-\frac{\partial p}{\partial x} = \rho_0 \frac{\partial u}{\partial t} \tag{6.30}$$

Assuming that u has the same form as Eq. 6.29, the time derivative can be replaced by $j\,\omega$ or $j\,c\,k$

$$\mathbf{u} = \frac{j}{k\,\rho_0\,c} \frac{\partial \mathbf{p}}{\partial x} \tag{6.31}$$

Three-Dimensional Wave Equation

When dealing with sound waves in three dimensions we have a choice of several coordinate systems. Depending on the nature of the problem, one system may be more appropriate than another. In a rectilinear (x, y, z) system, we can write separate equations in each direction similar to Eq. 6.28 and combine them to obtain

$$\frac{\partial^2 p}{\partial t^2} = c^2 \left[\frac{\partial^2 p}{\partial x^2} + \frac{\partial^2 p}{\partial y^2} + \frac{\partial^2 p}{\partial z^2} \right] = c^2\,\nabla^2 p \tag{6.32}$$

The term in the bracket in Eq. 6.32 is called the Laplace operator and is given the symbol ∇^2.

In the spherical coordinate system in Fig. 6.7, there are two angular coordinates, usually designated θ and ϕ, and one radial coordinate designated r. The Laplace operator in spherical coordinates is

$$\nabla^2 = \frac{1}{r^2} \frac{\partial}{\partial r} \left(r^2 \frac{\partial}{\partial r} \right) + \frac{1}{r^2\,\sin\theta} \frac{\partial}{\partial \theta} \left(\sin\theta \frac{\partial}{\partial \theta} \right) + \frac{1}{r^2\,\sin^2\phi} \frac{\partial^2}{\partial \phi^2} \tag{6.33}$$

For a nondirectional source we can dispense with consideration of the angular coordinates and examine only the dependence on r. This yields the one-dimensional wave equation for a spherical wave

$$\frac{\partial^2 p}{\partial t^2} = c^2 \left[\frac{1}{r^2} \frac{\partial}{\partial r} \left(r^2 \frac{\partial p}{\partial r} \right) \right] \tag{6.34}$$

FIGURE 6.7   The Spherical Coordinate System
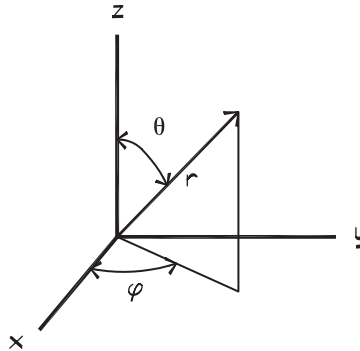
6.3   SIMPLE SOURCES

Monopole Sources

The general solution to Eq. 6.34 for a wave moving in the positive r direction is

$$\mathbf{p} = \frac{A}{r} \, e^{-jkr} \, e^{j\omega t} \tag{6.35}$$

Using Eq. 6.31, we can solve for the particle velocity

$$\mathbf{u} = \frac{A}{r \, \rho_0 \, c_0} \left(1 + \frac{1}{jkr} \right) e^{-jkr} \, e^{j\omega t} \tag{6.36}$$

When we are far away from the source and $k \, r \gg 1$, the particle velocity reverts to its plane wave value, $\mathbf{p} / \rho_0 \, c_0$. Equations 6.35 and 6.36 describe the behavior of a simple point source, sometimes called a monopole.

Doublet Sources

When two point sources are placed at $x = 0$ and $x = d$, they form an acoustic doublet. The sources may be in phase or out of phase. For this analysis, they are assumed to be radiating at the same source strength and frequency. Figure 6.8 shows the geometry for this configuration. When the receiver is close to the source the geometrical relationships are a bit complicated. If the receiver is far away, we can make the approximation that the lines between the sources and the receiver are almost parallel. Under these constraints, the pressure for the two sources combined is

$$\mathbf{p} = \frac{A}{r} \, e^{j\omega t} \, e^{-jkr} \left(1 \pm e^{jkd \sin \theta} \right) \tag{6.37}$$

where the plus sign is for in-phase sources and the minus sign is for out-of-phase sources. The value of the pressure for in-phase sources is

$$p = \frac{2 \, A}{r} \, \cos \left(\frac{1}{2} \, k \, d \, \sin \theta \right) \tag{6.38}$$

and for out-of-phase sources is

$$p = \frac{2 \, A}{r} \, \sin \left(\frac{1}{2} \, k \, d \, \sin \theta \right) \tag{6.39}$$

FIGURE 6.8   The Geometry of a Doublet Source
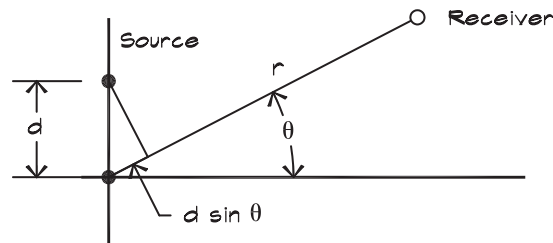
The total power radiated by the doublet can be calculated by integrating the square of the pressure over all angles

$$W = \frac{1}{2} \iint \left(\frac{p^2}{\rho_0 \, c_0} \right) r^2 \sin \theta \; d\theta \; d\phi \qquad (6.40)$$

to obtain

$$W = \frac{A^2}{\rho_0 \, c_0} \left[1 \pm \frac{\sin k \, d}{k \, d} \right] \qquad (6.41)$$

where the plus sign refers to an in-phase doublet and the minus sign to an out-of-phase doublet.

Now there is a great deal of important information in these few equations. Plotting Eq. 6.41 in Fig. 6.9, we can examine the relative power of a doublet compared to a simple source. The top curve shows the power of an in-phase pair as a function of k d. When the two sources are close (compared with a wavelength) together, k d is less than 1.

Recall that the wave number

$$k = \omega/c = 2 \, \pi /\lambda \qquad (6.42)$$

Therefore, when k d is less than 1, the separation distance d between sources is less than a sixth of a wavelength. For this configuration, the acoustic pressure effectively doubles, the combined source power increases by a factor of four, and the sound power level increases by 6 dB.

FIGURE 6.9   **Total Power Radiated from a Doublet Source (Rossing and Fletcher, 1995)**

The total power W of two omnidirectional sources having the same
(+ +) or the opposite (+ -) polarity and separation distance d, as
a function of the frequency parameter kd. The power radiated
by a single source is W_0.
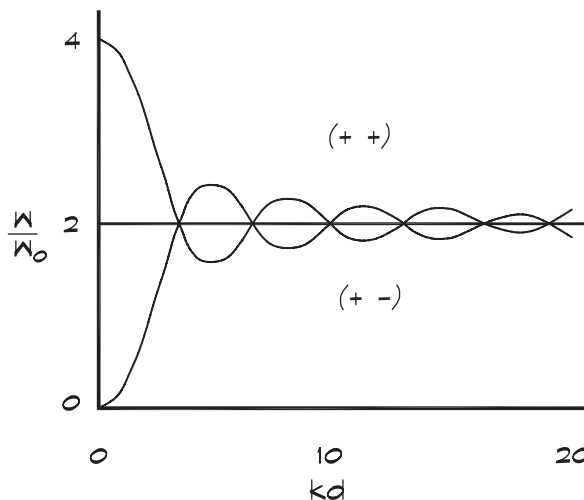
One way this can occur in buildings is when a source is placed close to a hard surface such as a concrete floor or wall. The surface acts like an acoustic mirror and the original source energy is reflected, as if the source were displaced by a distance d/2 behind the surface of the mirror. If the distances are small enough and the frequency low enough, the pressure radiates from the original and reflected source in phase in all directions. When sound level measurements are made very close to a reflecting surface, a 6 dB increase in level can be expected due to pressure doubling.

As the distance d between each source increases, the angular patterns become more complicated. The radiated power for a doublet at higher values of k d, also shown in Fig. 6.9, is about twice the power of a single source whether or not the sources are in phase. This is the same result that we found for incoherent (random phase) sources—a 3 dB (10 log N) increase for two sources combined.

Although the overall power of a doublet has a relatively simple behavior, the directivity pattern is more complicated. Typically, these directivity patterns are displayed in the form of polar plots. The front of the source, which is usually the loudest direction, is shown pointing toward the top of the diagram and the decrease in level with angle is plotted in increments around the source. A uniform directivity pattern is a perfect circle. The *directional characteristic* R_θ is one commonly encountered descriptor. It is the terms in the parentheses in Eq. 6.37 and represents the directional pattern of the sound pressure for a doublet. The directivity is its square and the directivity index is 10 log of that. The directional characteristic pattern produced by an in-phase doublet at various frequencies is shown in Fig. 6.10. Note that the direction of greatest level, when θ is 0, is at right angles to the line between the sources. The directivity patterns vary with frequency. The half-beamwidth angle, which is defined as the angle between on axis and the first zero, occurs when $(k\,d/2)\sin\theta = \pi/2$. The half beamwidth for an in-phase doublet is

$$\psi = \sin^{-1}(\lambda/2\,d) \qquad (6.43)$$

Dipole Sources and Noise Cancellation

If we have a doublet, where the two sources have opposite polarities, the configuration is called a dipole. A practical example of this type of source is an unbaffled loudspeaker. Since sound radiates from the rear of the loudspeaker cone as well as from the front, and the two signals are out of phase, the signal from the rear can combine with the front signal and produce a null pattern at right angles to the axis of the cone.

If the dipole sources are close together, when k d < 1, from Fig. 6.9 we see that the total power radiated approaches zero. This is the basis for the field of active noise cancellation in a three-dimensional acoustic space. Two sources of opposite polarity, when positioned close enough together, radiate a combined null signal. In practice, this can be accomplished by generating a cancellation signal quite close (d less than $\lambda/6$) to the source or to the receiver. A microphone can be used to sense the primary noise signal and by appropriate processing a similar signal having the opposite phase can be produced. Active noise cancellation systems are available in the form of headphones, which suppress sounds having a frequency of less than about 300–400 Hz. Source-cancellation systems for environmental noise control are less common, but have been applied successfully to large transformers and exhaust stacks. Noise cancellation systems have not been applied to the general run of noise problems, due

FIGURE 6.10   **Directional Characteristics in Terms of R_θ of an In-Phase Doublet Source as a Function of the Distance between the Sources and the Wavelength (Olson, 1957)**

The direction corresponding to the angle θ is measured relative to the perpendicular to the line connecting the two sources. The three dimensional polar plots are surfaces of revolution about the line joining the two sources.
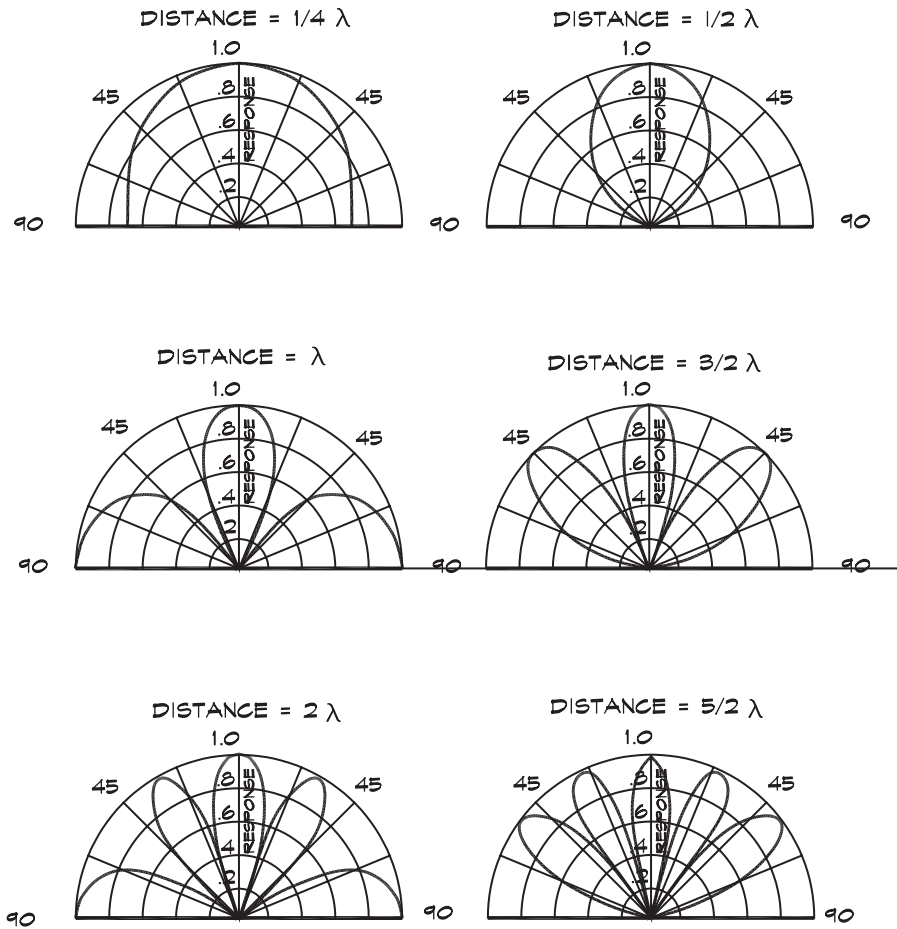
to the distance requirements outlined earlier, although one-dimensional problems such as duct-borne noise have been treated successfully. Due to the one-dimensional nature of ducts at low frequencies, the distance requirements for active noise control are not the same as they are for three-dimensional spaces.

Arrays of Simple Sources

When several simple sources are arrayed in a line, the phase relationship between them increases the directivity of the group along the $\theta = 0$ axis, shown in Fig. 6.11. Loudspeaker systems so configured are called line arrays and are a common arrangement

FIGURE 6.11 **The Geometry of a Line Array**
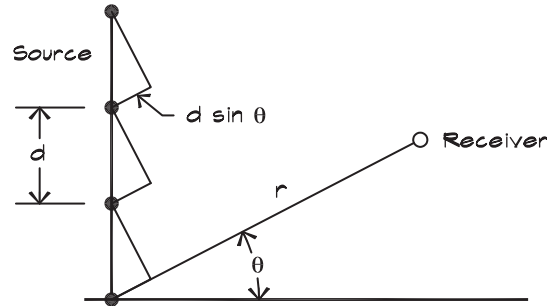
in loudspeaker cluster design. If n in-phase sources are equally spaced along a line, we can calculate the pressure in the far field following the same reasoning we used to derive Eq. 6.37. The pressure is

$$\mathbf{p} = \frac{n \, \mathbf{A} \, e^{j \omega t} \, e^{-j k r}}{r} \left[\frac{1}{n} \sum_{m=0}^{n-1} e^{j k m d \, \sin \theta} \right] \tag{6.44}$$

and the summation can be expressed in terms of trigonometric functions

$$\mathbf{p} = \frac{n \, \mathbf{A} \, e^{j \omega t} \, e^{-j k r}}{r} \left[\frac{\sin \left(\dfrac{n \pi d}{\lambda} \sin \theta \right)}{n \, \sin \left[\dfrac{\pi d}{\lambda} \sin \theta \right]} \right] \tag{6.45}$$

The term on the left of the brackets in Eq. 6.45 is the source strength for all n simple sources. At $\theta = 0$ the bracketed term goes to one so that the overall source strength is the same, as we would expect from a coherent group.

The polar patterns in terms of the directivity index for an array of four omnidirectional sources are shown in Fig. 6.12. The spacing is 2 ft (0.6 m) between sources. The angle to the point where the sound level is down 6 dB from the on-axis value occurs when the bracketed term in Eq. 6.45 equals 1/2, which must be solved numerically.

The half-beamwidth angle is more easily determined

$$\psi = \sin^{-1} \left[\frac{2 \pi}{n k d} \right] = \sin^{-1} \left[\frac{\lambda}{n d} \right] \tag{6.46}$$

so that, when the total length of the line array is about 1.4 wavelengths, the first zero is at about $\pi/4$ radians (45°). Hence, to begin to achieve appreciable control over the beamwidth, line arrays must be at least 1.4 wavelengths long. For narrower coverage angles, the length must be longer. The region of pattern control, without undue lobing, ranges from an overall array length of about 1.4 wavelengths to the point where the spacing between elements approaches a wavelength.

FIGURE 6.12   Directivity Index of Four Point Sources

Sources are arrayed in a line and spaced 2' (0.6 m) apart.
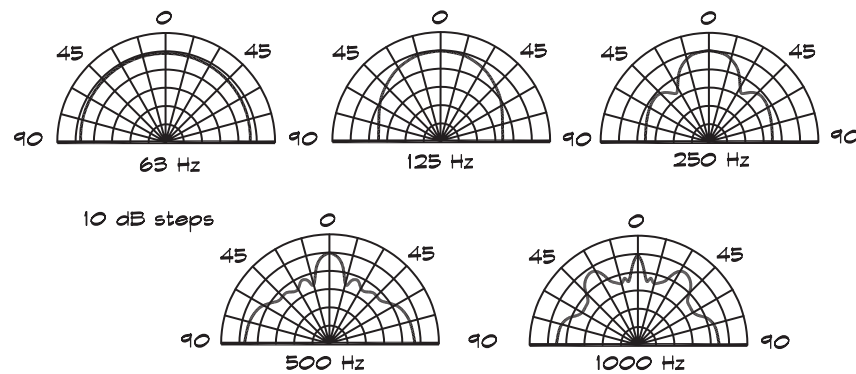
This has profound architectural consequences because it says that loudspeaker systems must be large in the vertical direction to control directivity in a vertical plane. For example, to limit the beamwidth angle to $\pi/3$ radians (60°) at 500 Hz, the array should be about 750 mm (30 inches) high. In cabinet systems the horn, which emits the 500 Hz signal, must be about 30 inches high to achieve a 40° vertical coverage angle. (Note that the coverage angle, which is the angle between −6 dB points, is less than the line array beamwidth.) Architecturally this means that in large rooms such as churches and auditoria, which often require highly directional loudspeaker systems to achieve adequate intelligibility, a space at least 4 feet (1.2 m) high must be provided for a speech reinforcement system. If live music is going to be miked, the directivity should extend down an octave lower to reduce feedback. This requires a line array about 8 feet long, similar to that shown in Fig. 6.12 in a concert venue, or significant loudspeaker displacement or barrier shielding in a permanent installation.

Line source configurations can also be used to control low-frequency directivity in concert systems. When concert loudspeaker systems are arranged by unloading truckloads of multiway cabinets and stacking them up on either side of the stage, there is little control of the low-frequency energy and extremely loud sound levels are generated near the front of the stage and at the performers. If instead, low-frequency cabinets (usually dual 18-inch woofers) are stacked vertically to a height of 20 to 30 feet (6 to 9 m), a line source is constructed that controls bass levels at the stage apron. The front row seats are at an angle of nearly 90° to the midpoint axis of the line source so even coverage is maintained from the front to the back of the seating area.

Continuous Line Arrays

The continuous line array is a convenient mathematical construct for modeling rows of sources that are all radiating in phase. Line arrays have a relatively narrow frequency range over which they maintain a simple directivity pattern. If their length is less than a half-wavelength, they will not provide appreciable directional control. At high frequencies line sources have a very narrow beamwidth, so that off-axis there can be a coloration of the sound.

The directional characteristic of a coherent line source can be obtained (Olson, 1957) by substituting $l \cong n\,d$ into Eq. 6.45. This approximation is true for large n.

$$R_\theta = \frac{\sin\left(\dfrac{\pi l}{\lambda}\sin\theta\right)}{\dfrac{\pi l}{\lambda}\sin\theta} \tag{6.47}$$

where R_θ is the directional characteristic of the sound pressure relative to the on-axis sound pressure, and l is the length of the line source.

The directivity plots are shown in Fig. 6.13. Practical considerations limit the size of a loudspeaker array to an overall length of about λ to 4λ or so. This two-octave span is adequate for many sound source applications, where horns are used on the high end and line arrays are used for the midrange. Directional control is seldom required below the 250 Hz octave band except in concert venues.

As sources are added to a line array, the beamwidth decreases and the number of lobes increases. To compensate for this effect, a line source can be tapered by decreasing the level of the signal fed to loudspeakers farther from the center. The directional characteristic (Olson, 1957) of a tapered line source, whose signal strength varies linearly from the center to zero at the ends is

$$R_\theta = \frac{\sin^2\left(\dfrac{\pi l}{\lambda}\sin\theta\right)}{\left(\dfrac{\pi l}{\lambda}\sin\theta\right)^2} \tag{6.48}$$

As Fig. 6.14 shows, tapering broadens the center lobe of the directivity pattern and decreases the off-axis lobing and the expense of overall sound power.

Curved Arrays

Loudspeakers can be configured in other ways, including convex or concave arcs, twisted line arrays, or helical line sources, which look like a stack of popsicle sticks. For a series of sources arranged in a curve the directivity pattern in the plane of the arc is (Olson, 1957)

$$R_\theta = \frac{1}{2n+1}\left\{\sum_{m=-n}^{m=n}\cos\left[\frac{2\pi r_a}{\lambda}\cos(\theta+m\phi)\right] + j\sum_{m=-n}^{m=n}\sin\left[\frac{2\pi r_a}{\lambda}\cos(\theta+m\phi)\right]\right\} \tag{6.49}$$

where R_θ = directional characteristic of the array sound pressure
relative to the on axis sound pressure
θ = angle between the radius to the center source and the line
to the receiver, (rad)

$2n+1$ = number of sources in the array
$j = \sqrt{-1}$
λ = wavelength, (m)
m = integer variable
ϕ = angle subtended by adjacent sources on the arc, (rad)

FIGURE 6.13   Directional Characteristics of a Coherent Line Source (Olson, 1957)
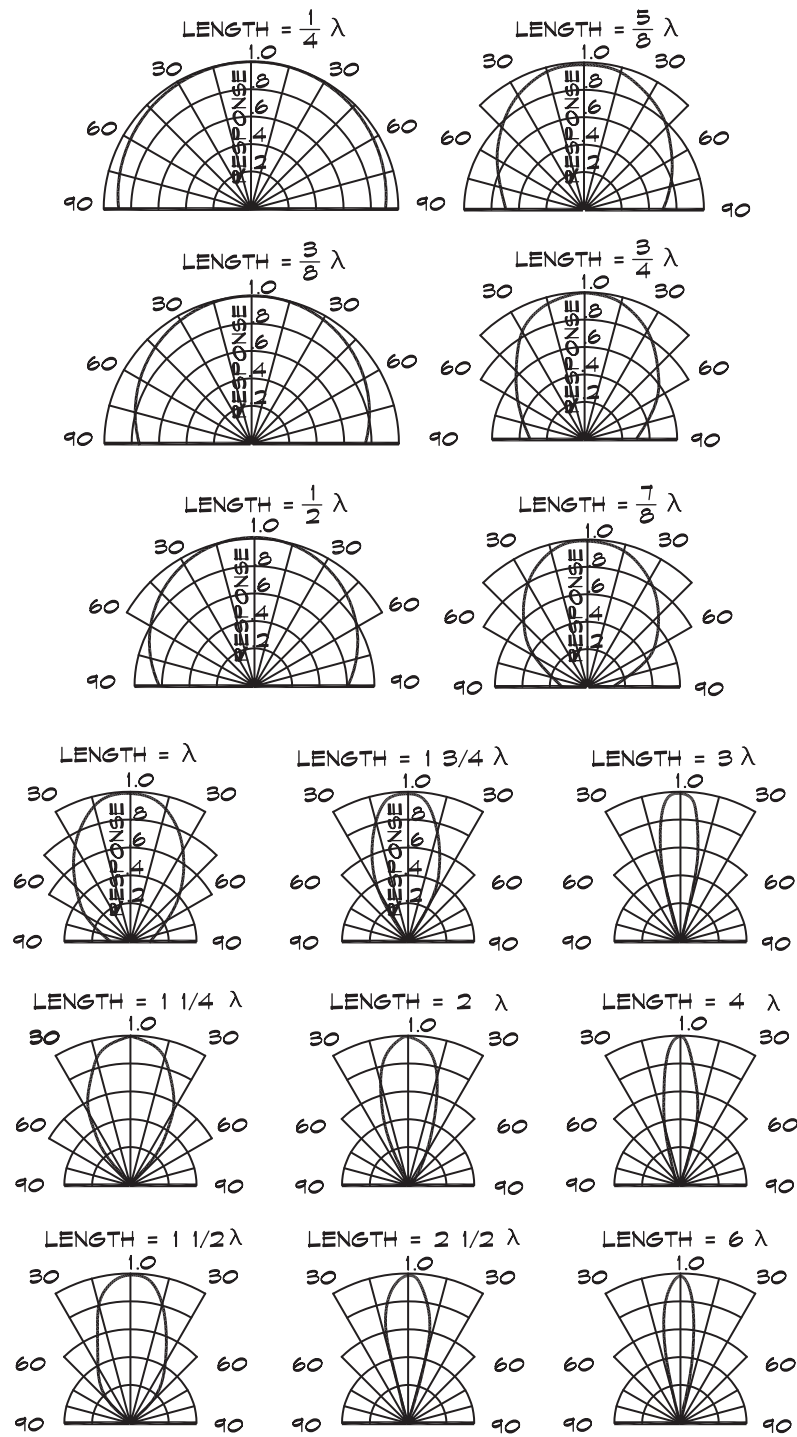
FIGURE 6.14 **Directional Characteristics R_θ of a Tapered Line Source—Linear Taper (Olson, 1957)**
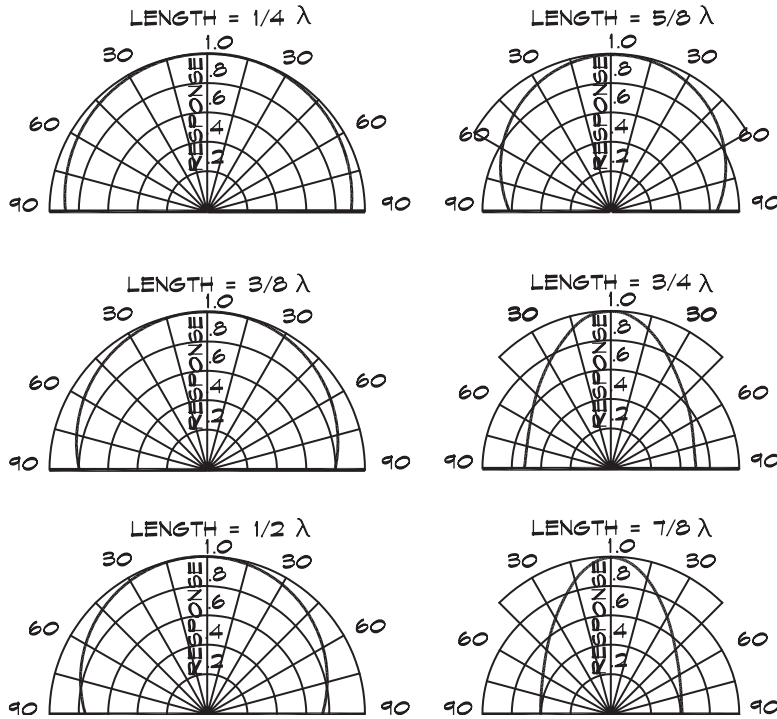
FIGURE 6.15 **Directional Characteristics R_θ of a 60° Segment of Arc (Olson, 1957)**
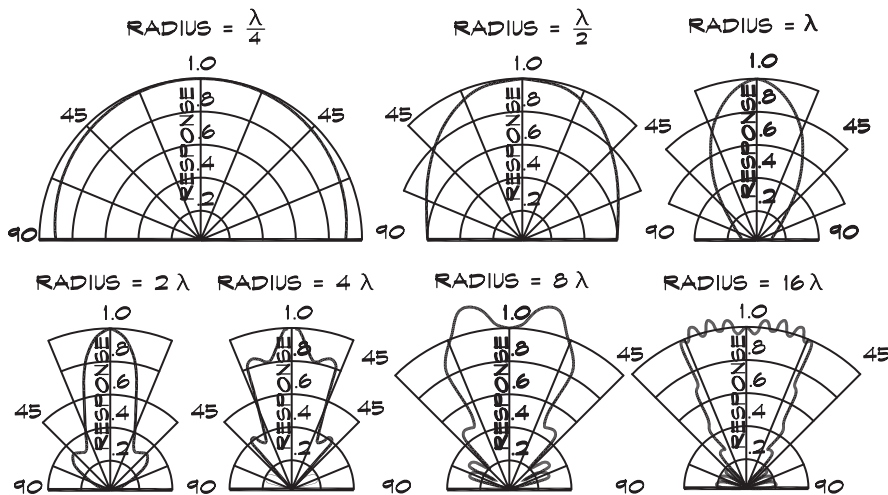
An example of the directivity pattern for a 60° arc is shown in Fig. 6.15. At very high frequencies, the directivity pattern starts to look like a wedge. This behavior was the basis for the design of multicellular horns, which were developed to reduce the high-frequency beaming associated with large horn mouths.

Phased Arrays

A phased array consists of a line or planar group of sound sources, which are fed an electronic signal such that the direction of the emitted wavefront can be steered by controlling the phase or time delay (n τ) to each source. The directional factor becomes (Kinsler et al., 1982)

$$R_\theta = \frac{1}{n} \left[\frac{\sin \left[\frac{n\pi d}{\lambda} \left(\sin \theta - \frac{c\tau}{d} \right) \right]}{\sin \left[\left(\frac{\pi d}{\lambda} \sin \theta - \frac{c\tau}{d} \right) \right]} \right] \tag{6.50}$$

This technique may be used to electronically direct signals radiated from a line or panel of sources. It also can be used to detect the direction of an incoming signal incident on a line of microphones by sensing the time delay between transducers. The major lobe is pointed in a direction given by

$$\sin \theta_0 = \frac{c\tau}{d} \tag{6.51}$$

which is independent of frequency.

Source Alignment and Comb Filtering

When two sources are separated by a distance d, and a receiver lies at an angle θ to their common axis, as shown in Fig. 6.8, there is a difference in distance from each source to the receiver. This difference is d $\sin \theta$ so depending on the frequency of the sound radiating from the doublet the signals may be in or out of phase. If the path length difference is an even multiple of a wavelength then the signals will add and the composite signal will be 6 dB higher. If the path length difference is an odd multiple of a half wavelength then the signals will cancel and the composite signal will be a null. The consequence of this is that as we sweep across a range of frequencies the doublet source will generate a series of filters whose maximum frequencies are given by

$$f_n = \frac{nc}{d \sin \theta} \tag{6.52}$$

where the number n is an integer that ranges from one to infinity, or at least to the upper frequency limit of audibility. The null frequencies are given by

$$f_n = \frac{(2n - 1)c}{2d \sin \theta} \tag{6.53}$$

At $\theta = \pi / 4$ (45°) and a doublet separation distance of 0.5 m (1.6 ft), the null frequencies are 486, 1458, 2430, ... Hz.

If a broadband signal such as speech is transmitted by means of the doublet source, the resultant signal shown in Fig. 6.16 displays a series of dips, which are shaped much like the teeth of a comb (hence the moniker, comb filter). Deep notches at each of these frequencies can have a negative influence on the clarity of the received signal. The extent of the influence depends on the separation between frequencies and the depth of the nulls. The effect can be corrected somewhat by introducing an electronic delay; however, the delay is exact for one direction only. A loudspeaker design strategy, which reduces the time difference between

FIGURE 6.16   The Comb Filter Produced by Two Sound Sources (Everest, 1994)

The axial source separation is approximately 13.5" (340 mm)
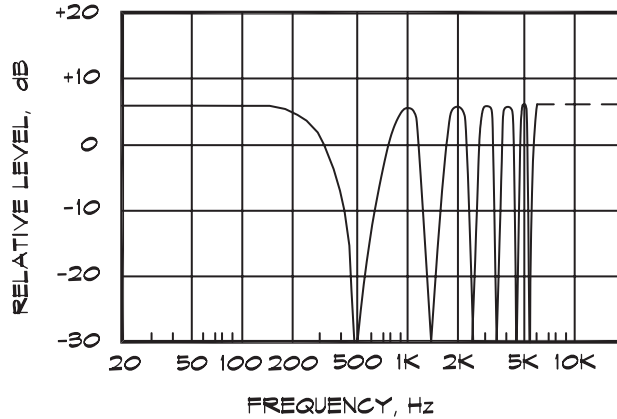
components, reduces the comb filtering effect. It is best to match the time delays at points where the two signals have nearly equal amplitudes. If one source is substantially (6 dB or so) louder than a second, the comb filtering effects are much less.

Comb Filtering and Critical Bands

Everest (1994) provides an interesting analysis of the audibility of comb filtering, which is illustrated in Fig. 6.17. The perceptual importance of comb filtering can be understood in terms of the effective bandwidth of the individual filter, compared to the width of a critical band. When the time delay between sources is small, say 0.5 ms, the range of frequencies between nulls is quite broad—much greater than the width of a critical band at 1000 Hz, which is about 128 Hz. Therefore, the effect of the delay is perceptible. When the time delay is large, say 40 ms, there are many nulls within one critical band, and the effects are integrated by the ear and are not perceptible. This helps explain why comb-filtering effects are not a problem in large auditoria, where reflections off a wall frequently create a delayed

FIGURE 6.17   Audibility of Comb Filtering (Everest, 1994)
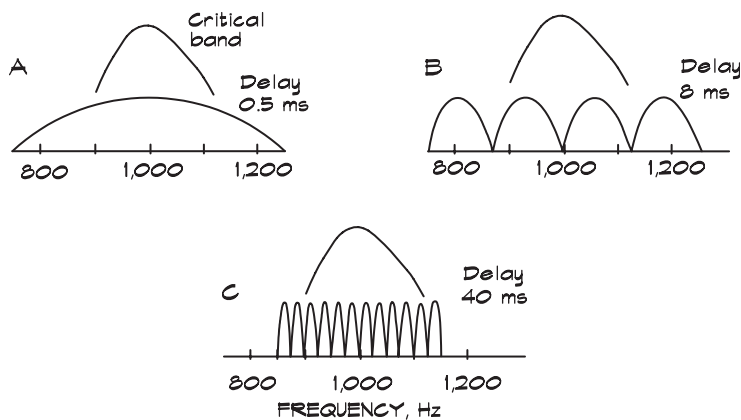
signal of 40 ms or more, without appreciably coloring the sound. In loudspeaker clusters and small studios, small loudspeaker misalignments and reflections from nearby surfaces can be quite noticeable.

6.4   COHERENT PLANAR SOURCES

Piston in a Baffle

The physical effects of sound sources of finite extent are described using a few simple models, which can be applied to a wide range of more complicated objects. The most frequently utilized example is the piston source mounted in a baffle, which was first analyzed by Lord Rayleigh in the nineteenth century. The baffle in this example is an infinite solid wall. The piston may be a loudspeaker or simply a slice of air with all portions of the slice moving in phase at a velocity $\mathbf{u} = u_0\, e^{j\omega t}$. The piston is located at the origin, on the surface of the wall, and pointed along the r axis as shown in Fig. 6.18. The sound pressure at a distance r due to a small element of surface on the piston is

$$\mathbf{p}(r,\,\theta,\,t) = j\,\frac{\rho_0\, c_0\, u_0\, k}{2\,\pi}\, \int_S \frac{e^{j\,(\omega t - k r')}}{r'}\, ds \tag{6.54}$$

If we divide the surface into horizontal slices the incremental pressure due to a slice dx high by $2\,a\,\sin\phi$ wide is

$$d\mathbf{p} = j\,\rho_0\, c_0\, \frac{u_0}{\pi r'}\, k\, a\, \sin\phi\, e^{j\,(\omega t - k\, r')}\, dx \tag{6.55}$$

In the far field where $r \gg a$ we use the approximate value for r'

$$r' \cong r\left(1 - \frac{a}{r}\, \sin\theta\, \cos\phi\right) \tag{6.56}$$

FIGURE 6.18   Geometry of a Piston in a Baffle (Kinsler et al., 1982)
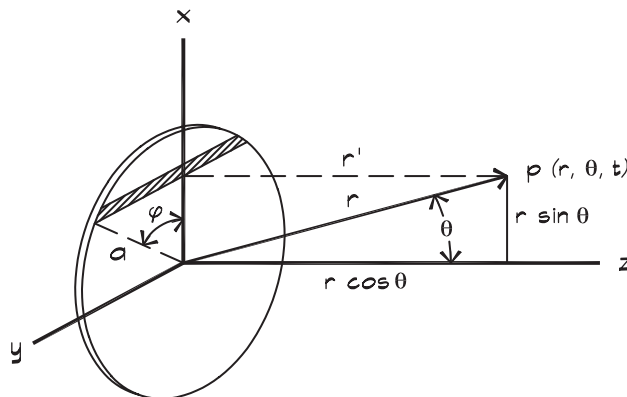
The pressure is then calculated by integrating over the surface of the piston.

$$\mathbf{p} = j \, \rho_0 \, c_0 \, \frac{u_0}{\pi r} \, k \, a \, e^{j \, (\omega t - k r)} \int_{-a}^{a} e^{j k a \sin \theta \cos \phi} \sin \phi \, dx \qquad (6.57)$$

This can be done by making the substitution $x = a \cos \phi$ and integrating over the angle (see Kinsler et al., 1982).

$$\mathbf{p} = \frac{j \, \rho_0 \, c \, u_0 \, k \, a^2}{2 \, r} \, e^{j \, (\omega t - k r)} \left[\frac{2 \, J_1 \, (k \, a \, \sin \theta)}{(k \, a \, \sin \theta)} \right] \qquad (6.58)$$

where θ = angle between the center axis and the line to the receiver, (rad)
   J_1 = Bessel function of the first kind
   $j = \sqrt{-1}$
   λ = wavelength, (m)
   ω = radial frequency, (rad/s)
   t = time, (s)

The Bessel function produces a number, which depends on an argument, similar to a trigonometric function. It is the solution to a particular type of differential equation and can be calculated from an infinite series of terms, which follow the pattern

$$J_1 \, (x) = \frac{x}{2} - \frac{2 \, x^3}{2 \cdot 4^2} + \frac{3 \, x^5}{2 \cdot 4^2 \cdot 6^2} - \cdots \qquad (6.59)$$

The resulting directional characteristic for a piston in a baffle is given in Fig. 6.19. The pattern in the far field depends on the ratio of the circumference of the piston to the wavelength of sound being radiated, which is the term $(k \, a)$.

The directivity relative to the on-axis intensity is

$$Q_{rel} = \left[\frac{2 \, J_1 \, (k \, a \, \sin \theta)}{(k \, a \, \sin \theta)} \right]^2 \qquad (6.60)$$

and the beamwidth as defined by the angle between the -6 dB down points on each side occurs at

$$Q_{rel} = .25 \qquad (6.61)$$

This defines (Long, 1983) the relationship between the coverage angle (between the -6 dB points) and the piston diameter as

$$k \, a \, \sin \theta = 2.2 \qquad (6.62)$$

When the piston diameter, $2 \, a$, is equal to a wavelength the coverage angle $2 \, \theta \cong 90°$. This is a useful rule of thumb in loudspeaker and horn design.

FIGURE 6.19   Directional Characteristics of a Circular Piston in a Baffle (Olson, 1957)
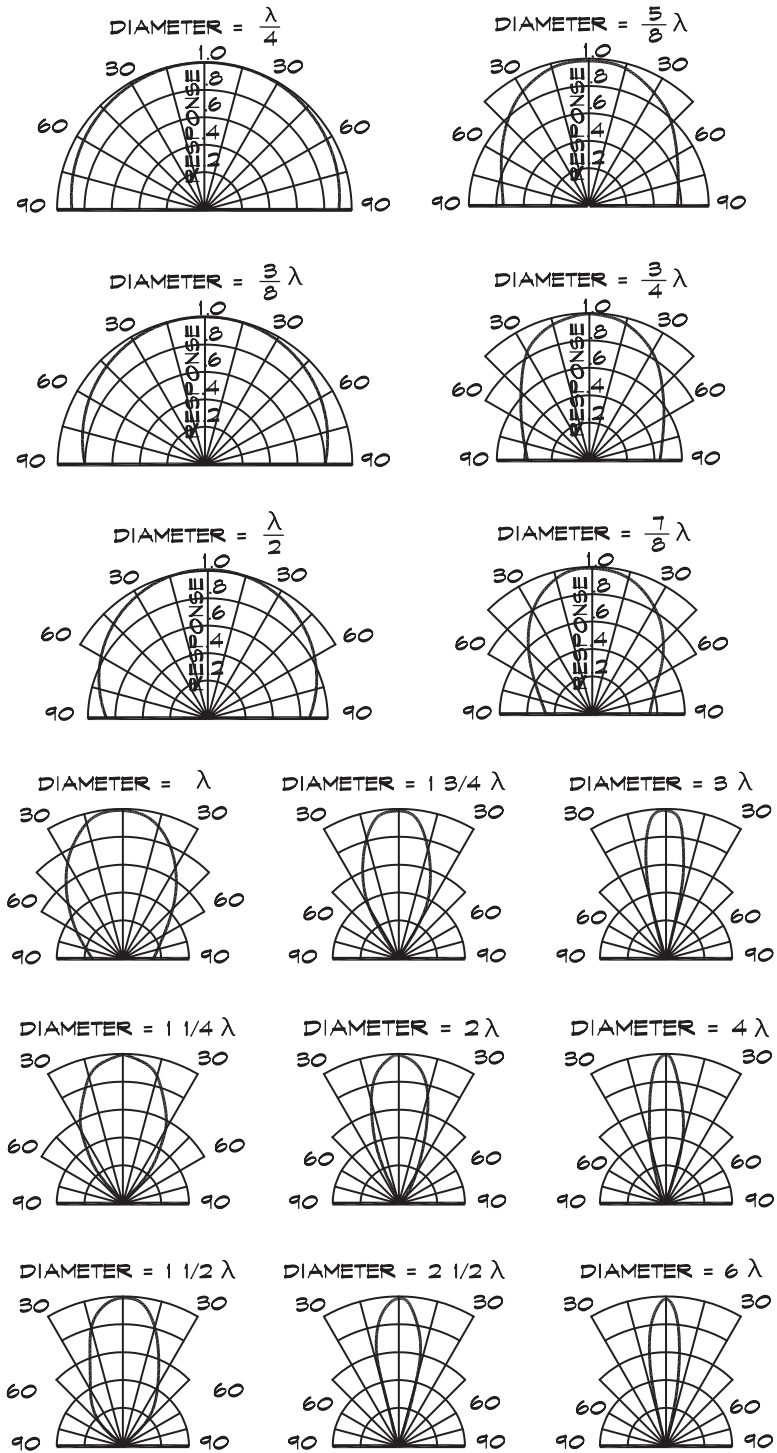
FIGURE 6.20 **Relationship of Directivity Index to −6 dB Angle for Many Different Cone Type Loudspeakers and Baffles (Henricksen, 1980)**
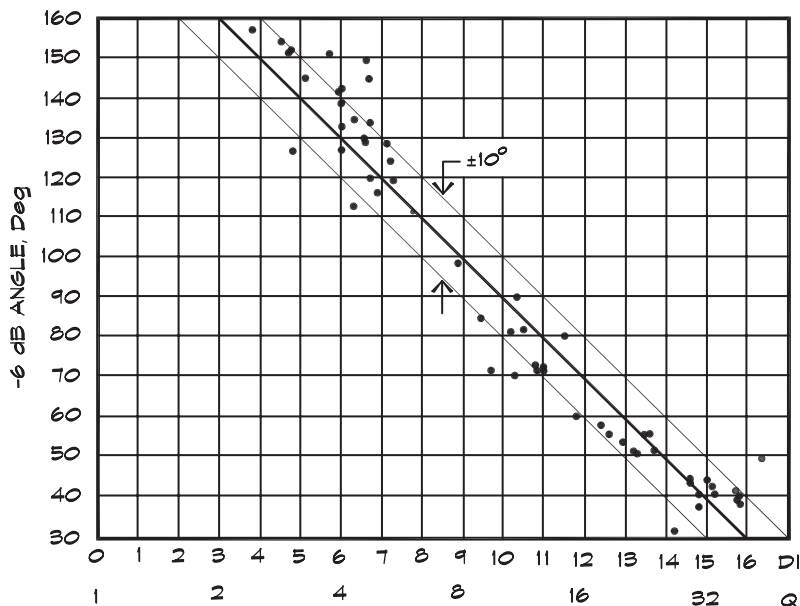
Coverage Angle and Directivity

Henricksen (1980) has compiled a chart of the coverage angle, which is defined as the included angle between the −6 dB down points on a polar plot, versus the source directivity for various sizes of cone loudspeakers. It is reproduced as Fig. 6.20. Referring to this figure, a coverage angle of 90° is equivalent to a Q of about 10. Therefore, if a cone loudspeaker or a horn is to achieve significant directional control, its mouth must be at least a wavelength long in the plane of the coverage angle. Typical directivity patterns for various sizes of cone loudspeakers and baffles are shown in Fig. 6.21 (Henricksen, 1980). The low-frequency directivity is determined by the size of the baffle, which sets the point at which the loudspeaker-baffle combination reverts to a point source with 360° coverage. Henricksen generalized the expected behavior from various loudspeaker and baffle sizes in Fig. 6.22. Here the high-frequency directivity is controlled by cone size, with the smaller cones being less directional. It is interesting to note that in home and near-field monitor loudspeakers, where wide dispersion angles are desired, the crossover to a smaller loudspeaker is made when the wavelength is equal to the cone diameter (k a = π). In sound reinforcement systems, where pattern control is of paramount importance, the crossover is made to a larger format driver when the wavelength is equal to a diameter. This is one reason why monitor loudspeakers are usually not appropriate for commercial sound reinforcement applications and why these systems can be made much smaller than commercial systems.

Loudspeaker Arrays and the Product Theorem

When an array of identical loudspeakers is constructed, the composite directivity pattern is determined by the directional characteristics of the array as well as the inherent directivity of the loudspeakers. The relationship between these directivities is given by the product theorem, which states that the overall directivity of an array of identical sources is the product

FIGURE 6.21   A Chart for Predicting the −6 dB Angle Response for Piston and Box Systems (Henricksen, 1980)
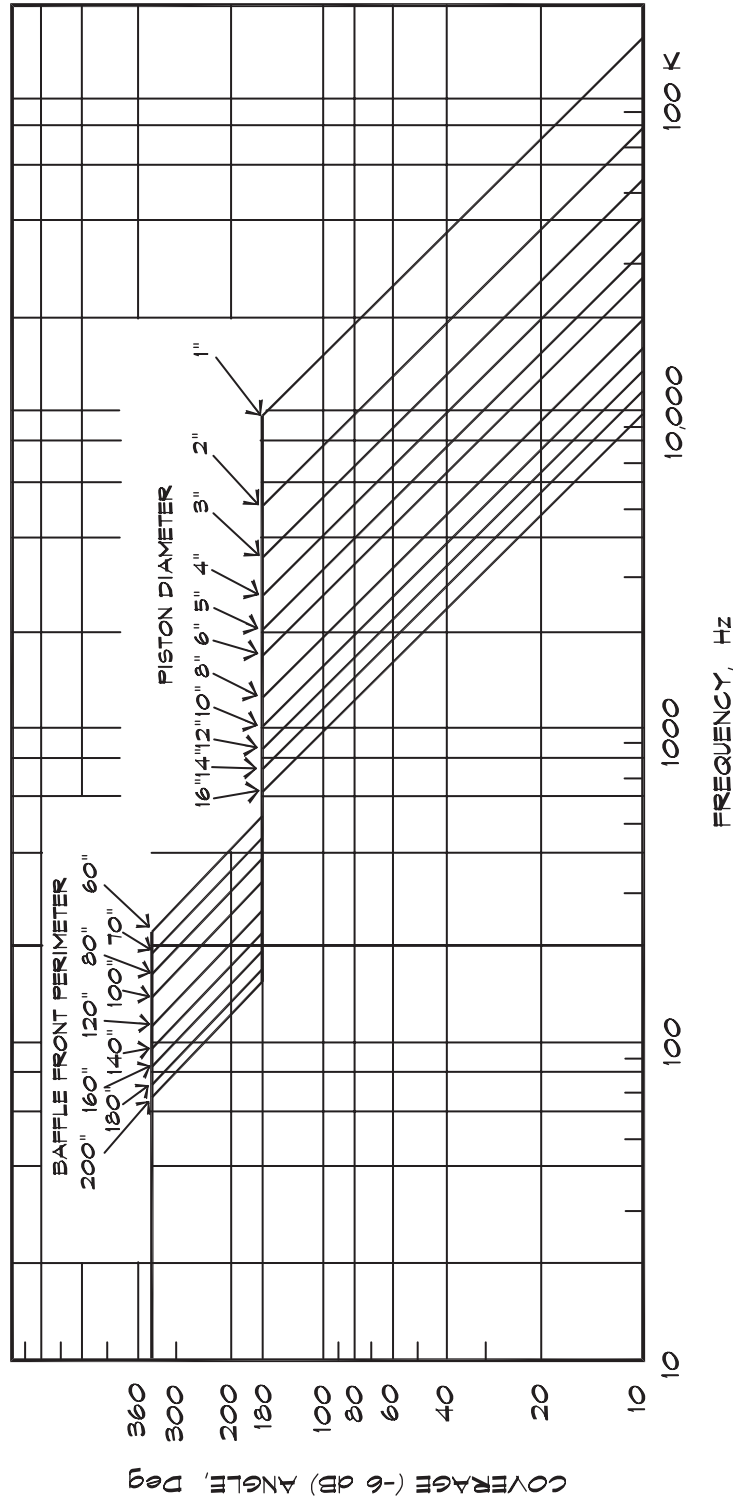
FIGURE 6.22   Directivity Index Response of Direct-Radiator Pistons in Various Configurations (Beranek, 1954)
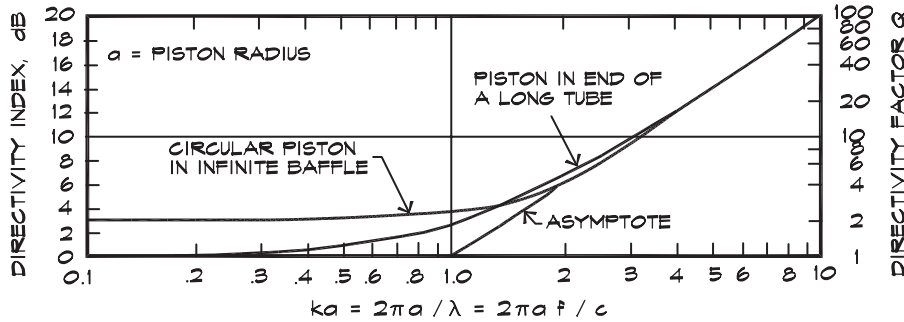
of the directivities of the individual sources and the directivity due to the array.

$$Q_\theta\,(\theta,\,\phi) = Q_0\,Q_{rel}\,(\theta,\,\phi)\,R_\theta^2\,(\theta,\,\phi) \tag{6.63}$$

where $Q_\theta\,(\theta,\,\phi)$ = overall array directivity

Q_0 = on - axis directivity for an individual speakers

$Q_{rel}\,(\theta,\,\phi)$ = off - axis directivity of a given loudspeaker

$R_\theta^2\,(\theta,\,\phi)$ = array directivity relative to the on - axis sound intensity

If the array is composed of different types of loudspeakers or loudspeakers at various levels, for which there is no ready directional characteristic, the directivity must be calculated for each element of the array from its off-axis level and the relative phase due to its position in the array. The off-axis phase behavior for individual loudspeakers may also be important but is seldom available in the data published by loudspeaker manufacturers. Computer programs that perform these calculations are commercially available.

There are theoretical directivity values published for arrays that have a tapered volume level or other more exotic shadings. Olson (1957) has given a general equation for the directivity of a linear array having an arbitrary taper. Davis and Davis (1987) have published a scheme for improving the directivity of an array of loudspeakers in a baffle using a Bessel function weighting. Line arrays have been designed using axially rotated elements to disperse the high frequencies or vertically angled elements to smooth the frequency response. In these arrayed systems, it usually is assumed that each element radiates individually without influence from the others. For this assumption to hold true each transducer should be housed in a separate enclosure so that the loading produced by back radiation into a common cabinet does not influence the other loudspeakers.

Rectangular Pistons

The directional characteristic of a coherent rectangular piston source can be calculated in a similar fashion to that used for the circular piston in a baffle. McLachlan published these calculations in 1934. He showed that a rectangular rigid plate of length 2 a and height 2 b, which vibrates in an infinite rigid baffle, generates a far field directional characteristic

$$R_{\theta,\phi} = \left\{ \left[\frac{\sin\,(k\,a\,\cos\,\phi)}{(k\,a\,\cos\,\phi)} \right] \left[\frac{\sin\,(k\,b\,\cos\,\theta)}{(k\,b\,\cos\,\theta)} \right] \right\} \tag{6.64}$$

The term in the second set of brackets is the same as that found for a line source in Eq. 6.47. In fact, the rectangular piston has the same directional characteristic as the product of two line sources of length 2a and 2b arranged at right angles to one another, whose strength and phase are the same. The rectangular mouth of a horn loudspeaker can be modeled using this equation.

Force on a Piston in a Baffle

The impedance seen by a piston in a baffle can be obtained from Eq. 6.54; in this case the integral is evaluated close to the piston rather than in the far field. The pressure varies across the face of the piston but the quantity of interest is the force on the whole piston. This, along with the piston velocity, yields the mechanical radiation impedance seen by the piston (see Morse, 1948 or Kinsler et al., 1982).

$$\mathbf{z}_r = \int \frac{d\mathbf{F}_S}{\mathbf{u}} = \rho_0 \, c_0 \, S \left[w_r(2ka) + j \, x_r \, (2ka) \right] \tag{6.65}$$

The integration of the force over the face of the piston is complicated and will not be reproduced in detail. The impedance terms include a real part

$$w_r = 1 - \frac{J_1(2k\,a)}{k\,a} = \frac{(k\,a)^2}{2} - \frac{(k\,a)^4}{2^2 \cdot 3} + \frac{(k\,a)^6}{2^2 \cdot 3^2 \cdot 4} - \cdots \tag{6.66}$$

which has limiting values of

$$\begin{aligned} w_r &\to \frac{(k\,a)^2}{2} \quad \text{for } k\,a \ll 1 \\ &\to \quad 1 \qquad \text{for } k\,a \gg 1 \end{aligned} \tag{6.67}$$

and an imaginary part

$$x_r = \frac{1}{\pi(k\,a)^2} \left[\frac{(2k\,a)^3}{3} - \frac{(2k\,a)^5}{3^2 \cdot 5} + \frac{(2k\,a)^7}{3^2 \cdot 5^2 \cdot 7} - \cdots \right] \tag{6.68}$$

with limits

$$\begin{aligned} x_r &\to \frac{8\,k\,a}{3\,\pi} \quad \text{for } k\,a \ll 1 \\ &\to \frac{2}{\pi k\,a} \quad \text{for } k\,a \gg 1 \end{aligned} \tag{6.69}$$

Figure 6.23 shows the resistive (real) and reactive (imaginary) components of the radiation impedance. At low frequencies, the reactive component dominates, whereas at high frequencies, the resistance becomes more important. The impedance at high frequencies approaches the area times $\rho_0 \, c_0$. We will need these results in our later analysis of the absorption due to quarter-wave resonator tubes and quadratic-residue diffusers.

FIGURE 6.23   **Impedance Functions of a Baffled Piston (Kinsler et al., 1982)**
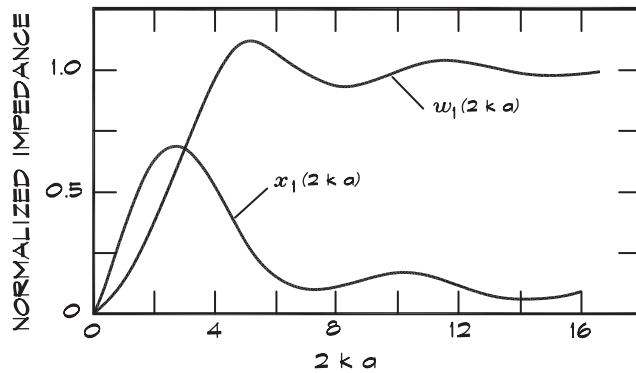
6.5   LOUDSPEAKERS

Cone Loudspeakers

A moving coil or cone loudspeaker, illustrated in Fig. 6.24, is the most commonly used type. It consists of a circular cone of treated paper or other lightweight material, which is attached to a coil of wire suspended in a permanent magnetic field. When a current passes through the wire, the coil is forced out of the magnetic field in one direction or another depending on the direction of the current. A sinusoidal voltage applied to the wire results in sinusoidal motion of the cone. Many broadband cone loudspeakers have a small dome or dust cap at their center, which helps disperse the high frequencies.

FIGURE 6.24   **A Simple Moving Coil Loudspeaker (Kinsler et al., 1982)**

A) Magnet, B) Voice Coil, C) Diaphragm, D) Corrugated Rim,
E) Spider (for stiffness), F) Dome
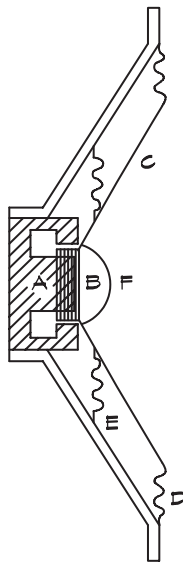
FIGURE 6.25   Input Impedance of a Moving Coil Driver (Colloms, 1980)
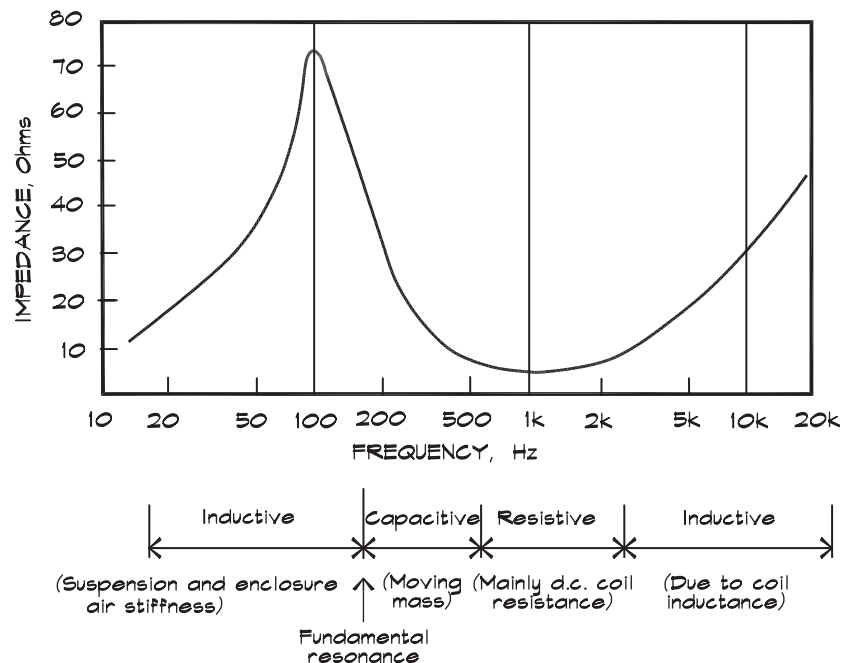
Cone loudspeakers are not particularly efficient sound radiators. Typically, they convert between 0.5 and 2% of the electrical energy to sound. A loudspeaker, driven with 1 electrical Watt, will radiate about 0.01 acoustical Watts of energy, which is equal to a sound power level of 100 dB. At a distance of 1 meter, such a loudspeaker would result in a sound pressure level of about 92 dB assuming a Q of two. This number, that is the on-axis level generated at 1 m for 1 W of power, is the sensitivity of the loudspeaker and was defined in Eq. 2.76.

Loudspeakers are characterized not only by their sensitivity but also by their impedance, frequency response, directivity, and polar pattern or coverage angle. Each of these parameters is useful to the designer. The electrical impedance is like the acoustical impedance in that it represents the electrical resistance of the loudspeaker, which is a complex number. Not all of the resistance is electrical. The mechanical impedance is reflected back as electrical impedance, which is not constant with frequency. Figure 6.25 gives a typical impedance curve for a loudspeaker in a baffle.

The low-frequency peak is at the fundamental resonance of the loudspeaker cone's spring mass system, including the spring effect of the air suspension system. Above the resonant frequency, the impedance drops to a region where it mainly consists of the dc resistance of the coil and reaches a minimum value, which can be measured with an ohmmeter. At the high- and low-frequency extremes, the impedance is mainly inductive, due to the stiffness of the suspension system at low frequencies, and to the coil inductance at high frequencies. Usually the minimum is listed by loudspeaker manufacturers since it is this value that controls the maximum current flow at a given applied voltage.

The frequency response of a loudspeaker is available from the manufacturer, and there is an example in Fig. 6.26. It is measured by sweeping a signal of constant voltage across the frequency range of interest and measuring the sound pressure level of the loudspeaker

FIGURE 6.26   Response of a Moving Coil Driver (Colloms, 1980)
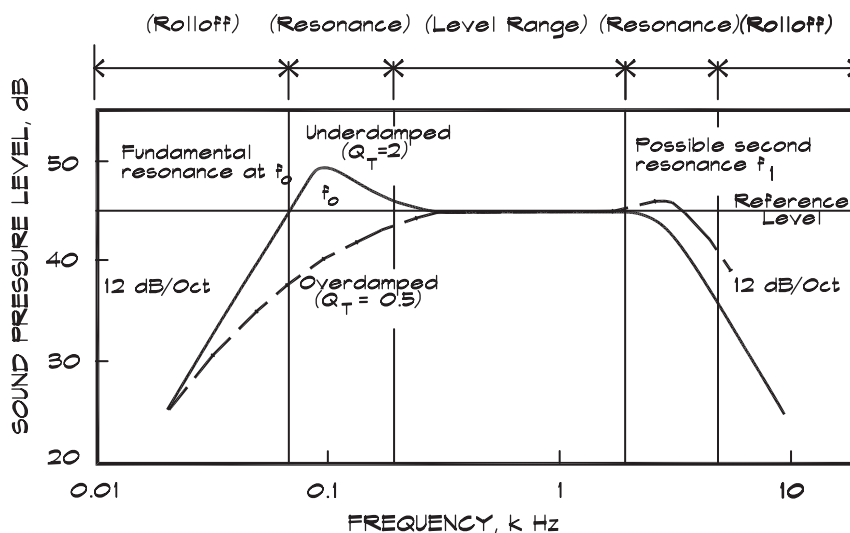
on-axis at a given distance. At both high and low frequencies the response curve rolls off at about 12 dB per octave. In between, it is relatively flat.

The low-frequency portion of the curve is influenced by the configuration of the enclosure. If the loudspeaker is not enclosed the cone radiates as a dipole, with the sound coming from the back canceling out the sound coming from the front. An infinite baffle reduces the dipole effect but is not always convenient to build. An enclosed box helps improve the low-frequency response by eliminating the dipole effect, but the air spring increases the resonant frequency of the cone. A ported enclosure acts as a second loudspeaker at low frequencies, which radiates in phase with the front of the cone. Due to the port resonance, the box emits more energy at low frequencies than the cone does.

Horn Loudspeakers

The use of horns undoubtedly originated with the cupping of the hands around the mouth to increase projected level. The Greeks applied the same idea when they attached conical horns to their theatrical masks to amplify the actors' voices. The development of brass instruments, at least as far back as the Romans, used a flared bell mouth. In the early twentieth century the exponential horn was studied and incorporated by Edison into his phonograph. The exponential horn shape was utilized in one form or another until the early 1980s, when the constant-directivity horn was introduced. Most loudspeaker manufacturers now offer a version of this type of horn.

A horn serves three functions. First, it provides an increased resistive loading for the driver so that it can work against a higher impedance than the air alone would present. Second, it improves the efficiency of the driver by constraining the air that is moved, gradually transitioning the air column into the surrounding space. Third, it controls the coverage pattern of the sound wave by providing side walls, which direct the beam of energy as it radiates away from the driver. Each of these functions may make conflicting demands on the horn designer. The shape that is the most efficient for impedance matching does not always provide the required directivity. The designer has to determine the functions the horn must perform, and trade off the advantages and disadvantages of each to get the best compromise solution.

FIGURE 6.27   Resistive and Reactive Components of the Normalized Acoustic Impedance of Infinite Horns (Olson, 1957)
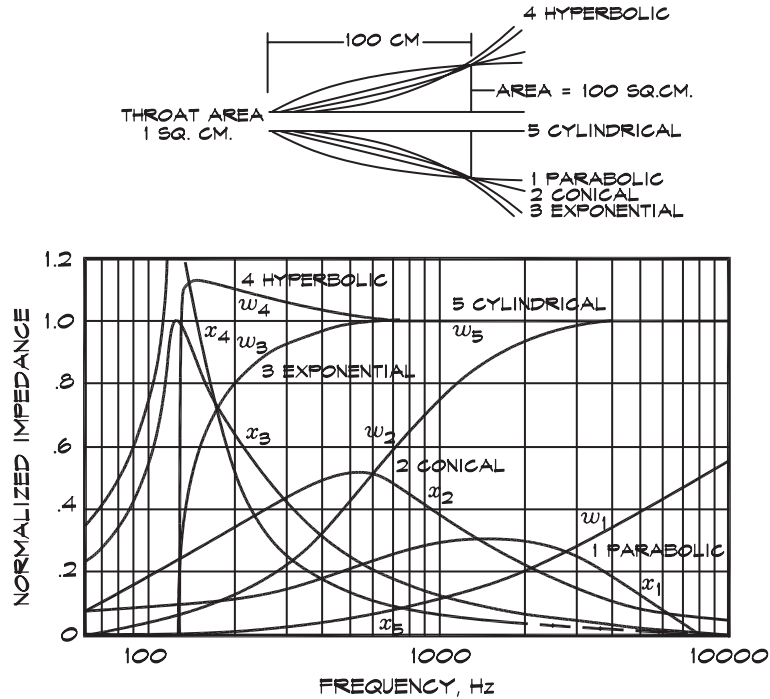
The presence of a horn increases the impedance that is presented to the driver diaphragm. This causes the diaphragm to push against a higher pressure, which, although it makes the driver work harder, also allows more energy to be transmitted to the air. The resistive load placed on the diaphragm is almost totally dependent on the shape of the horn. Figure 6.27 plots the acoustical resistance of an infinitely long horn for five different shapes. As the diagram shows, a conical (straight-sided) horn does not add significant loading to the diaphragm. The cylindrical tube presents an even loading but has no increase in mouth area. The exponential horn, so called because the shape of its sides follows the exponential equation

$$S = S_0\, e^{m\,x} \qquad (6.70)$$

where S = horn area at distance x (m^2)
  S_0 = throat area at x = 0 (m^2)
  m = flare constant (m^{-1})
  x = distance from the throat (m)
provides smooth loading down to a cutoff frequency

$$f_c = \frac{m\,c}{4\,\pi} \qquad (6.71)$$

below which sound does not propagate without loss. Although the loading is constant with frequency for an exponential horn, the shape is not necessarily the best choice. For low-frequency directional control, the horn mouth size has to be relatively large, which leads to high-frequency control problems.

As we have seen from the piston in a baffle analysis, loudspeakers undergo a narrowing in their coverage pattern, called beaming, at high frequencies. To achieve wide coverage, high-frequency drivers must be physically small. Small drivers, however, are inefficient since they neither travel very far, nor push much air. Coupling a small driver to a horn helps solve both the beaming and the efficiency problems. Horn efficiencies as high as 50% can be achieved over a narrow range of frequencies; however, for broadband signals an efficiency of 10% is more likely. The sensitivity of a typical large format horn/driver is about 113 dB, which, with an on-axis Q of 20, represents an efficiency of a little more than 13% or an acoustic power of about 0.13 Watts.

At mid frequencies, where the size of the driver mouth is small with respect to the wavelength, the sound illuminates the side walls and allows them to control the directional pattern emanating from the horn. With constant directivity horns, the side walls are either straight or slightly curved, having different centers of expansion in the horizontal and vertical dimensions. This innovation was introduced by Paul Klipsch in 1951 and has been used in most subsequent horn designs. It allows for a different coverage angle in the horizontal and vertical planes.

Constant-Directivity Horns

Constant-directivity horns are specifically designed to provide an even frequency distribution with direction. A typical example is shown in Fig. 6.28. In the ideal case, the sound spectrum measured at any particular location should be no different from that measured at any other location within the field of the horn's coverage. One result of this type of behavior is that the spectrum at any point is quite close to the actual power spectrum of the driver, since the power is evenly distributed. This feature is critical for successful sound system design and greatly simplifies the design process.

Modern constant directivity horn design started with the work of D. B. (Don) Keele, Jr., John Gilliom, and Ray Newman at Electrovoice in the middle of the 1970s. Their work introduced the features that are the central methods for controlling directivity in all current horn design. Their first design idea was a contraction in the throat immediately following

FIGURE 6.28 Constant Directivity Horn—Nominal 60 × 40 (JBL 2365)
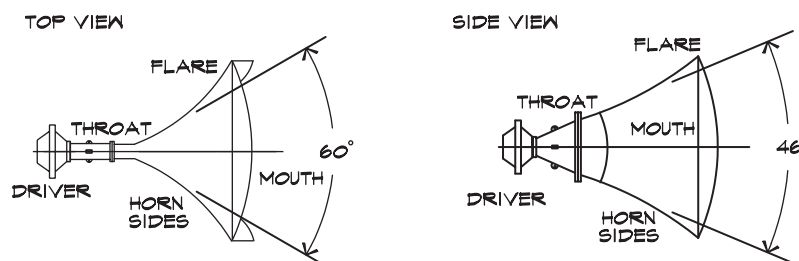
the driver. This detail is emphasized in the White horn series they designed; however, the idea predates this horn (Keele, 1983). The narrow throat allowed the use of a larger driver and improved the directional control by letting the sound illuminate the sides of the horn, without the high-frequency beaming usually associated with larger throat sizes.

The second feature was a conical-exponential (CE) throat shape, which consisted of an exponential throat over a certain distance, after which there was a smooth transition into a conical (straight-sided) shape. The combination of these two curves allowed the control of low-frequency impedance by the use of the quasi-exponential throat expansion, and still maintained excellent directional coverage afforded by the conical shape of the sides.

The third step the group took was to address the problem of mid-range narrowing, present in most horns before this design. Their approach was to flare the mouth of the horn at a point, which was about two-thirds the distance from the beginning of the conical section to the mouth. The flare was added at an angle, which was about twice the angle of the original conical section. The added flare resulted in the high frequencies seeing one mouth size and the lower frequencies seeing another. The flare also allowed the transition between the horn mouth and the surrounding air to be less abrupt. The sound pressure distribution across the mouth of the horn was no longer constant but was higher in the center of the horn. The horn mouth no longer looked like a pure piston in a baffle and as a result the mid-frequency narrowing problems (predicted by the piston model) that were associated with previous designs were no longer present.

The White horn series was highly successful. The design gave good horizontal-directivity control without the mid-frequency beaming that had been associated with most previous horns. The vertical frequency control was not emphasized in the design in favor of a smaller vertical dimension. This shows the design tradeoff that is made between horn mouth height and the capability of controlling the vertical directivity over a wide range of frequencies. Because the vertical dimension of the mouth is relatively small, the frequency at which the vertical control begins is rather high—1.2 kHz. The White horn series was the first commercial product to be a true constant-directivity type.

The next chronological development in horn design was the introduction of the Mantaray horn series by Mark Ureda and Cliff Henricksen at Altec. They wanted to produce a horn with strong directivity control both horizontally and vertically. Ureda and Henricksen decided that if bidirectional control was to be achieved, then the mouth had to be square and relatively large. Once the low-frequency limit was known, the mouth size could be determined from the piston in a baffle formula. With the mouth size fixed, the coverage angles allowed the sides to be drawn back to the driver's mouth. The large vertical mouth dimension resulted in narrow angled top and bottom walls extending back to the throat opening, which controlled length of the horn as well as the loading on the driver. In the horizontal plane the wider coverage angle resulted in the sides converging to a point that was displaced further down the horn from the throat. The throat was connected to this point by an opening having a relatively narrow cross section. The Mantaray design used the flare idea developed by Keele et al., but its flare started further down the horn than the two-third's point.

This horn had some advantages over previous designs. Because the vertical mouth dimension was large, the narrowest side wall angle expanded over a longer distance and was connected directly to the driver. This displaced the driver from the throat of the wide-angle portion of the horn and made it easier for the driver to couple to the horn. This feature is an advantage particularly when using 2-inch drivers, which have a difficult time driving directly into a 90° angle opening without beaming.

The Mantaray horns emphasize the control of directivity in both planes, but do so at the expense of low-frequency loading, which is brought about by an exponential area expansion. The sides of the Mantaray are virtually straight in both the horizontal and vertical planes. The Altec patent claims that the straight-sided walls improve the waistbanding effect (a sideways lobing of the midfrequencies), which is said to have been found in other designs. The Mantaray design yields a directivity that is highly controlled down to 800 Hz and out to 20 kHz. Because of their size, they require more space than other horns. The tradeoffs are good vertical directivity control and excellent high-frequency response against a large physical size and minimal low-frequency loading.

Another horn manufacturer, JBL, subsequently developed its own constant directivity horns, which were also designed by Keele. In these designs, called Bi-Radial horns, Keele used a very general polynomial formula to develop the side shape from the throat to the mouth.

$$y = a + bx + cx^n \tag{6.72}$$

where x = distance along the centerline from the mouth
y = distance perpendicular to the x axis
a = half the throat height
b = $[\tan(0.9 \text{beamwidth})]/2$
c = $[w/2 - bL - a]/L^n$
n = constant between 2 and 8
L = horn length
w = mouth width

The Bi-Radial design, as with all horn designs, is a compromise. The mouth size is selected from the piston in a baffle equation. The throat expansion is quasi-exponential as it is a combination of constant linear taper and an exponential area expansion. The loading is better than the straight-sided Mantaray conical loading, but not as good as the more purely exponential loading used in the Electrovoice designs. The mouth size is large in both dimensions, so that the directivity is controlled to relatively low frequencies. Probably the most interesting design feature is the use of the equation for the flare rate. According to Keele (1983), this curve gives a smooth response both along the horizontal and vertical directions as well as off-axis between the two planes. The line determined by the equation is rotated about a point on two sides and hence the name Bi-Radial. The horn does not have a contraction near the throat so that the horn tends to beam above 10 kHz. The Bi-Radial design is generally a good compromise between loading and directivity. It provides control in both directions and smooth off-axis response.

In Fig 6.29, we can see the various regions of the horn and what controls the directivity in each region. At low frequencies, the size of the mouth is the determinant. It sets the frequency at which the horn begins to control. Above the control point, the angle of the horn sides sets the coverage pattern. At very high frequencies, the diameter of the driver opening controls the beamwidth since the sound no longer interacts with the sides of the horn. Between the side-angle region of control and the low-frequency cutoff point, there is waistbanding or narrowing of the coverage pattern. This is controlled by the horn flare, which prevents the mouth of the horn from acting like a pure piston in a baffle.

FIGURE 6.29   **Beamwidth and Directivity of Constant Directivity Horns (Long, 1983)**

Beamwidth vs Frequency for a JBL 90 x 50 Horn

Directivity vs Frequency
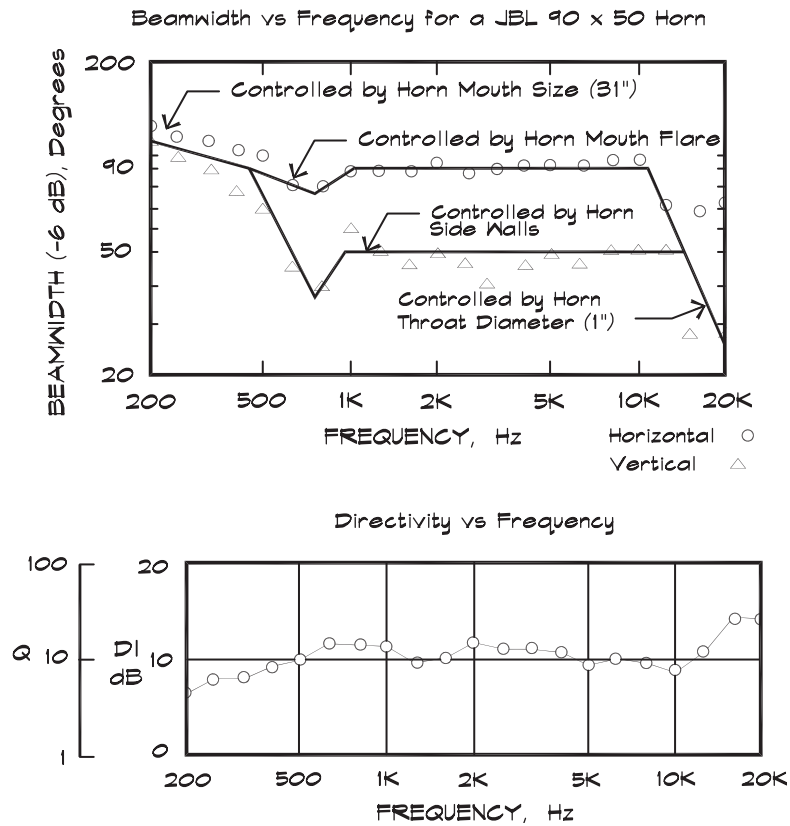
Cabinet Arrays

In recent years, it has become popular for manufacturers to provide two- or three-way cabinets that are trapezoidal-shaped. The idea behind the shape is that the cabinets may be arrayed side by side to provide the appropriate coverage. With the advent of packaged computer design programs, the directivity patterns of these products often are buried in the computer code and not available to the designer. Cabinets are subject to the same physical limitations on directional control imposed by the size of the radiating components as any other device. Arraying cabinets in a line can does not narrow the coverage angle in the plane normal to the line, where directional control may also be needed. At frequencies below the point where the spacing is equal to a wavelength, horizontal stacking will narrow the coverage angle in the horizontal plane, which may or may not be useful. Stacking cabinets in a line can control directivity over a certain frequency range, where the components act as a line array, but is probably not particularly beneficial above that frequency.

Baffled Low-Frequency Systems

The installation of low-frequency cabinets in a baffle wall is a technique that can be used to increase their directivity somewhat. The theoretical result is illustrated in Fig. 6.21. The materials used in constructing these baffles are usually not 100% reflective at the frequencies of interest. For example, a single sheet of drywall is about 30% absorptive at 125 Hz and as much as 40% absorptive at slightly lower frequencies. This significantly reduces the

theoretical effectiveness of a lightweight baffle wall. Double drywall, being about 20% absorptive at 125 Hz and 35% absorptive at 80 Hz, is not significantly better.

Since subwoofer cabinets usually are used below 125 Hz, where the wavelength is about 9 ft (2.8 m) long, it can be helpful to place them on the floor or up against a concrete wall where they would be less than a third of a wavelength away from their image source. From Fig. 6.9 we can see that a power doubling, if not a pressure doubling, would probably be achieved for k d = 2. When there are two reflecting surfaces, the floor and the wall, a 6 dB increase could be achieved.

Baffle walls, if improperly constructed, can sometimes do more harm than good. When an unsealed gap is left around a baffled loudspeaker, it can become the throat of a Helmholtz resonator with the enclosed volume behind the baffle wall acting as the resonator volume. The resulting resonance can significantly color the sound and offset the advantage of a small increase in level at low frequencies provided by the wall.

$$7$$

The interaction of sound with solid surfaces could well be taken as the beginning of architectural acoustics. Sound undergoes three types of fundamental interactions upon encountering an object: reflection, absorption, and transmission. Each of these occurs to some degree when an impact takes place, although usually we are concerned with only one at a time.

7.1 PERFECTLY REFLECTING INFINITE SURFACES

Incoherent Reflections

Up to this point we have considered sound waves to be free to propagate in any direction, unaffected by walls or other surfaces. Now we will examine the effect of reflections, beginning with a perfectly reflecting infinite surface. The simplest model of this interaction occurs with sound sources that can be considered incoherent; that is, where phase is not a consideration. If an omnidirectional source is placed near a perfectly reflecting surface of infinite extent, the surface acts like a mirror for the sound energy emanating from the source. The intensity of the sound in the far field, where the distance is large compared to the separation distance between the source and its mirror image, is twice the intensity of one source. Figure 7.1 shows this geometry. In terms of the relationship between the sound power and sound pressure levels for a point source given in Eq. 2.61,

$$L_p = L_w + 10 \, \log \frac{Q}{4 \, \pi \, r^2} + K \tag{7.1}$$

where L_p = sound pressure level (dB re 20 μN/ m^2)
   L_w = sound power level (dB re 10^{-12} W)
   Q = directivity
   r = measurement distance (m or ft)
   K = constant (0.13 for meters or 10.45 for ft)

When the source is near a perfectly reflecting plane, the sound power radiates into half a sphere. This effectively doubles the Q since the area of half a sphere is $2 \, \pi r^2$. If the source is near two perfectly reflecting planes that are at right angles to one another, such as a floor and a wall, there is just one quarter of a sphere to radiate into, and the effective Q is 4.

FIGURE 7.1   **Construction of an Image Source**
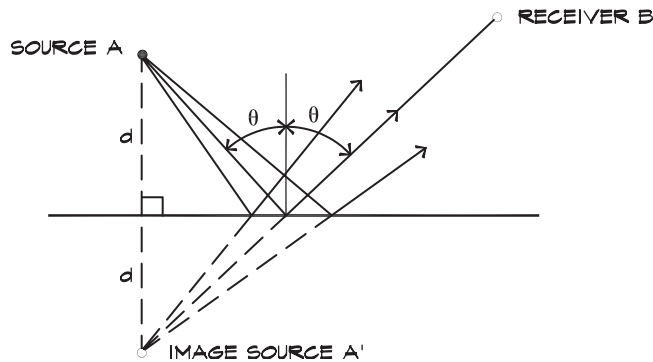
FIGURE 7.2   **Multiple Image Sources**

Acoustic images generated by one-wall, two-wall, and three-wall reflectors when one omnidirectional source is present.

(a)   (b)   (c)

● Source point.   ○ Image point.
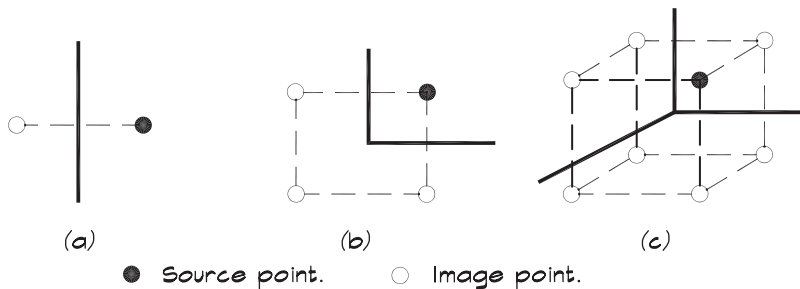
For a source located in a corner bounded by three perpendicular surfaces, the effective Q is 8. Figure 7.2 illustrates these conditions. For a nondirectional source such as a subwoofer, clearly the corner of a room is the most efficient location.

Note that the concept of Q is slightly different here than it is for the inherent directivity associated with a source. The directivity associated with the position of a source must be employed with some discretion. If a directional source such as a horn loudspeaker is placed in the corner of a room pointed outward, then the overall directivity does not increase by a factor of 8, since most of the energy already is focused away from the reflecting surfaces. The mirror image of the horn, pointed away from the corner, also contributes, but only a small amount at high frequencies. Thus changes in Q due to reflecting surfaces must also account for the inherent directivity of the source.

Coherent Reflections—Normal Incidence

When the sound is characterized as a plane wave, moving in the positive x direction, we can write an expression for the behavior of the pressure in space and time

$$\mathbf{p}\,(x) = \mathbf{A}\,e^{\,j\,(\omega\,t - k\,x)} \tag{7.2}$$

If we place an infinite surface at x = 0, with its normal along the x axis, the equation for the combined incident and reflected waves in front of the surface is

$$\mathbf{p}\,(x) = \mathbf{A}\,e^{\,j\,(\omega\,t - k\,x)} + \mathbf{B}\,e^{\,j\,(\omega\,t + k\,x)} \tag{7.3}$$

The particle velocity, **u**, defined in Eq. 6.31 as

$$\mathbf{u}(x) = \frac{j}{k\,\rho_0 c_0}\left(\frac{\partial \mathbf{p}}{\partial x}\right) \tag{7.4}$$

becomes

$$\mathbf{u}(x) = \frac{j}{k\,\rho_0 c_0}\,[-j\,k\,\mathbf{A} + j\,k\,\mathbf{B}]\,e^{j\omega t} \tag{7.5}$$

or

$$\mathbf{u}(x) = \frac{1}{\rho_0 c_0}\,[\mathbf{A} - \mathbf{B}]\,e^{j\omega t} \tag{7.6}$$

When the surface is perfectly reflecting, the amplitude $\mathbf{A} = \mathbf{B}$ and the particle velocity is zero at the boundary. Mathematically the reflected particle velocity cancels out the incident particle velocity at $x = 0$.

The ratio of the incident and reflected-pressure amplitudes can be written as a complex amplitude ratio

$$r = \frac{\mathbf{B}}{\mathbf{A}} \tag{7.7}$$

When $r = 1$, Eq. 7.2 can be written as

$$\mathbf{p}(x) = \mathbf{A}\,e^{j\omega t}\left[e^{j\,k\,x} + e^{-j\,k\,x}\right] = 2\,\mathbf{A}\,\cos(k\,x)\,e^{j\omega t} \tag{7.8}$$

which has a real part

$$p(x) = 2\,A\,\cos(k\,x)\,\cos(\omega t + \varphi) \tag{7.9}$$

The corresponding real part of the particle velocity is

$$u(x) = \frac{2\,A}{\rho_0 c_0}\,\sin(k\,x)\,\cos\left(\omega t + \varphi - \frac{\pi}{2}\right) \tag{7.10}$$

so the velocity lags the pressure by a 90° phase angle.

Equation 7.8 shows that the pressure amplitude, 2 A at the boundary, is twice that of the incident wave alone. Thus the sound pressure level measured there is 6 dB greater than that of the incident wave measured in free space. Figure 7.3 (Waterhouse, 1955) gives a plot of the behavior of a unit-amplitude plane wave incident on a perfectly reflecting surface at various angles of incidence. Note that since both the incident and reflected waves are included, the sound pressure level of the combined waves at the wall is only 3 dB higher than farther away.

The equations illustrated in Fig. 7.3a describe a standing (frozen) wave, whose pressure peaks and valleys are located at regular intervals away from the wall at a spacing that is related to frequency. The velocity in Fig. 7.3b exhibits a similar behavior. As we have seen, the particle velocity goes to zero at a perfectly reflecting wall. There is a maximum in the particle velocity at a distance $(2n + 1)\lambda/4$ away from the wall, where $n = 0, 1, 2$, and so on.

FIGURE 7.3   **Interference Patterns When Sound Is Incident on a Plane Reflector from Various Angles (Waterhouse, 1955)**
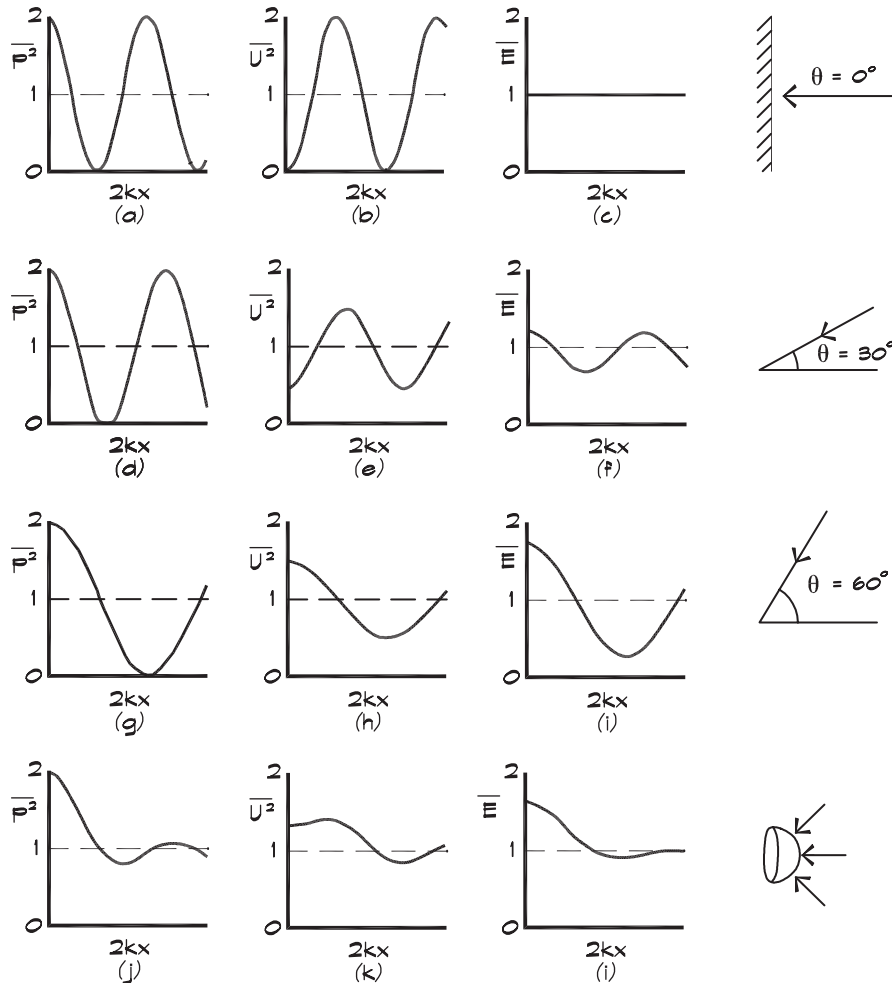
Interference patterns produced when sound is incident on a plane reflector at angles of $0°$, $30°$, $60°$, and from all directions over a hemisphere. P^2 is the normalized mean squared pressure, k the wave number, and x the distance from the reflector. U^2 is the normalized mean square velocity and E is the normalized mean energy density.

Coherent Reflections—Oblique Incidence

When a plane wave moving in the −x direction is incident at an oblique angle as in Fig. 7.4, the incident pressure along the x axis is given by

$$\mathbf{p} = \mathbf{A}\, e^{j\,k\,(x\,\cos\,\theta - y\,\sin\,\theta) + j\,\omega t} \tag{7.11}$$

For a perfectly reflecting surface the combined incident and reflected waves are

$$\mathbf{p} = \mathbf{A}\left[e^{j\,k\,x\cos\,\theta - j\,k\,y\,\sin\,\theta} + e^{-j\,k\,x\,\cos\,\theta - j\,k\,y\,\sin\,\theta} \right] e^{j\,\omega t} \tag{7.12}$$

FIGURE 7.4 Oblique Incidence Reflection
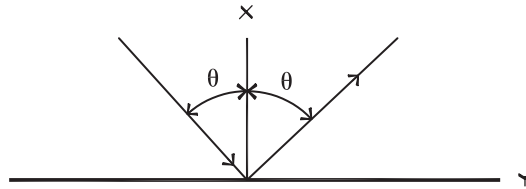
which is

$$\mathbf{p} = 2\,\mathbf{A}\,e^{-j\,k\,y\,\sin\,\theta\,+\,j\,\omega t}\cos\,(k\,x\,\cos\,\theta) \tag{7.13}$$

and the interference is still sinusoidal but has a longer wavelength. Looking along the x axis, the combined incident and reflected waves produce a pattern, which can be written in terms of the mean-square unit-amplitude pressure wave for perfectly reflecting surface given by

$$\langle \mathbf{p}^2 \rangle = [1 + \cos\,(2\,k\,x\,\cos\,\theta)] \tag{7.14}$$

As the angle of incidence θ increases, the wavelength of the pattern also increases. Figures 7.3a, d, and g show the pressure patterns for angles of incidence of 0°, 30°, and 60°.

Coherent Reflections—Random Incidence

When there is a reverberant field, the sound is incident on a boundary from any direction with equal probability, and the expression in Eq. 7.14 is averaged (integrated) over a hemisphere. This yields

$$\langle \mathbf{p}_r^2 \rangle = [1 + \sin\,(2\,k\,x)/\,2\,k\,x] \tag{7.15}$$

which is plotted in Fig. 7.3j.

The velocity plots in this figure are particularly interesting. Porous sound absorbing materials are most effective when they are placed in an area of high particle velocity. For normal incidence this is at a quarter wavelength from the surface. For off-axis and random incidence the maximum velocity is still at a quarter wavelength; however, there is some positive particle velocity even at the boundary surface that has a component perpendicular to the normal. Thus materials can absorb sound energy even when they are placed close to a reflecting boundary; however, they are more effective, particularly at low frequencies, when located away from the boundary.

Coherent Reflections—Random Incidence, Finite Bandwidth

When the sound is not a simple pure tone, there is a smearing of the peaks and valleys in the pressure and velocity standing waves. Both functions must be integrated over the bandwidth of the frequency range of interest.

$$\langle \mathbf{p}_r^2 \rangle = \left[1 + \frac{1}{k_2 - k_1} \int_{k_1}^{k_2} \frac{\sin\,(2\,k\,x)}{2\,k\,x}\,dk \right] \tag{7.16}$$

FIGURE 7.5   Intensity vs Distance from a Reflecting Wall (Waterhouse, 1955)

Normalized intensity or mean square pressure $\overline{p^2}$ versus distance x of the sound reflected from a solid wall in a reverberant sound field for various bandwidths. In the abscissa $k = (k_1 + k_2) / 2$ where k_1 and k_2 are the wave numbers at the extremes of the band.
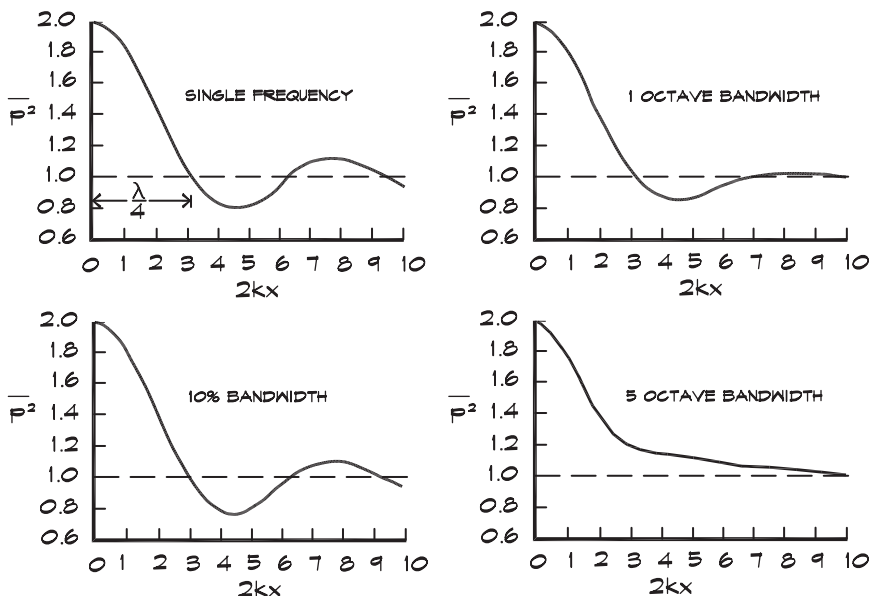
The second term is a well-known tabulated integral. Figure 7.5 shows the result of the integration. Near the wall the mean-square pressure still exhibits a doubling (6 dB increase) and the particle velocity is zero.

7.2   REFLECTIONS FROM FINITE OBJECTS

Scattering from Finite Planes

Reflection from finite planar surfaces is of particular interest in concert hall design, where panels are frequently suspended as "clouds" above the orchestra. Usually these clouds are either flat or slightly convex toward the audience. A convex surface is more forgiving of imperfect alignment since the sound tends to spread out somewhat after reflecting.

If a sound wave is incident on a finite panel, there are several factors that influence the scattered wave. For high frequencies impacting near the center of the panel, the reflection is the same as that which an infinite panel would produce. Near the edge of the panel, diffraction (bending) can occur. Here the reflected amplitude is reduced and the angle of incidence may not be equal to the angle of reflection. At low frequencies, where the wavelength is much larger than the panel, the sound energy simply flows around it like an ocean wave does around a boulder.

Figure 7.6 shows the geometry of a finite reflector having length 2b. When sound impacts the panel at a distance e from the edge, the diffraction attenuation depends on the closeness of the impact point to the edge, compared with the wavelength of sound. The reflected sound field at the receiver is calculated by adding up contributions from all parts of the reflecting surface. The solution of this integral is treated in detail using the

FIGURE 7.6   Geometry of the Reflection from a Finite Panel
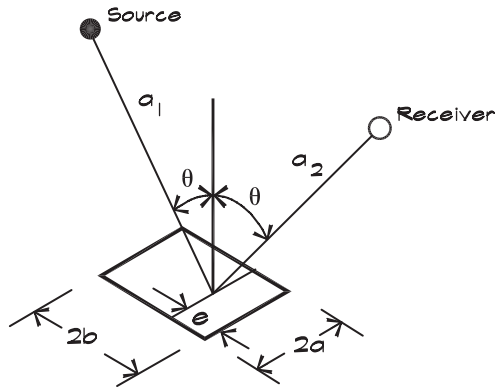
Kirchoff-Fresnel approximation by Leizer (1966) or Ando (1985). The reflected intensity can be expressed as a diffraction coefficient K multiplied times the intensity that would be reflected from a corresponding infinite surface. For a rectangular reflector the attenuation due to diffraction is

$$\Delta L_{dif} = 10 \, \log K = 10 \, \log (K_1 \, K_2) \tag{7.17}$$

where K = diffraction coefficient for a finite panel
   K_1 = diffraction coefficient for the x panel dimension
   K_2 = diffraction coefficient for the y panel dimension

The orthogonal-panel dimensions can be treated independently. Rindel (1986) gives the coefficient for one dimension

$$K_1 = \frac{1}{2} \left\{ \left[C\,(v_1) + C\,(v_2) \right]^2 + \left[S\,(v_1) + S\,(v_2) \right]^2 \right\} \tag{7.18}$$

where

$$v_1 = \sqrt{ \frac{\lambda}{2} \left[\frac{1}{a_1} + \frac{1}{a_2} \right] } \; e \cos \theta \tag{7.19}$$

and

$$v_2 = \sqrt{ \frac{\lambda}{2} \left[\frac{1}{a_1} + \frac{1}{a_2} \right] } \; (2b - e) \cos \theta \tag{7.20}$$

The terms C and S in Eq. 7.18 are the Fresnel integrals

$$C\,(v) = \int_0^v \cos \left(\frac{\pi}{2} \, z^2 \right) dz, \quad S\,(v) = \int_0^v \sin \left(\frac{\pi}{2} \, z^2 \right) dz \tag{7.21}$$

FIGURE 7.7   Attenuation of a Reflection Due to Diffraction (Rindel, 1986)
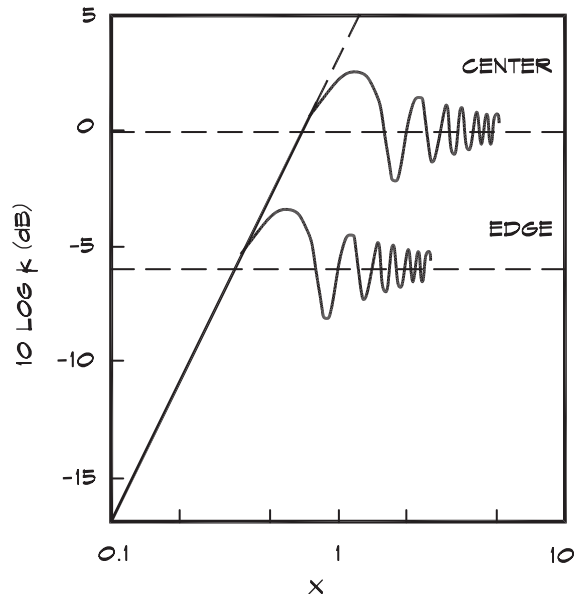
The integration limit v takes on the values of v_1 or v_2 according to the term of interest in Eq. 7.18. For everyday use these calculations are cumbersome. Accordingly we examine approximate solutions appropriate to regions of the reflector.

Rindel (1986) considers the special case of the center of the panel where e = b and $v_1 = v_2 = x$. Then Eq. 7.18 becomes

$$K_{1,\ center} = 2\left\{[C\ (x)]^2 + [S\ (x)]^2\right\} \tag{7.22}$$

where

$$x = 2b\cos\theta/\sqrt{\lambda\ a^*} \tag{7.23}$$

and the characteristic distance a* is

$$a^* = 2\ a_1 a_2\ /\ (a_1 + a_2) \tag{7.24}$$

Figure 7.7 gives the value of the diffraction attenuation. At high frequencies where x > 1, although there are fluctuations due to the Fresnel zones, a panel approaches zero diffraction attenuation as x increases. At low frequencies (x < 0.7) the approximation

$$K_{1,\ center} \cong 2\ x^2 \quad \text{for} \quad x < 0.7 \tag{7.25}$$

yields a good result.

At the edge of the panel where e = 0, $v_1 = 0$, and $v_2 = 2x$ we can solve for the value of the diffraction coefficient (Rindel, 1986)

$$K_{1,\ edge} = \frac{1}{2}\left\{[C\ (2x)]^2 + [S\ (2x)]^2\right\} \tag{7.26}$$

which is also shown in Fig. 7.7. The approximations in this case are

$$K_{1,\,edge} \cong 2\,x^2 \quad \text{for} \quad x \leq 0.35 \tag{7.27}$$

and

$$K_{1,\,edge} \cong 1/4 \quad \text{for} \quad x > 1 \tag{7.28}$$

Based on these special cases Rindel (1986) divides the panel into three zones according to the nearness to the edge of the impact point

a) $x \leq 0.35$: $K_1 \cong 2\,x^2$, independent of the value of e.

b) $0.35 < x \leq 0.7$: $K_1 \cong \dfrac{1}{4} + (e/\,b)\left(2\,x^2 - \dfrac{1}{4}\right)$, is a linear interpolation between the edge and center values.

c) $x > 0.7$: Here the concept of an edge zone is introduced whose width, e_o, is given by

$$e_o = \frac{b}{x\sqrt{2}} = \frac{1}{\cos\theta}\sqrt{\frac{1}{8}\lambda\,a^*} \tag{7.29}$$

If $e \geq e_o$, then we are in the region of specular reflection. When $e < e_o$, then diffraction attenuation must be considered. Rindel (1986) gives

$$K_1 \cong \begin{cases} 1 & \text{for } e \geq e_o \\[2mm] \dfrac{1}{4} + \dfrac{3\,e}{4\,e_o} & \text{for } e < e_o \end{cases} \tag{7.30}$$

Figure 7.8 compares these approximate values to those obtained from a more detailed analysis.

Rindel (1986) also cites results of measurements carried out in an anechoic chamber using gated impulses, which are reproduced in Fig. 7.9. He concludes that for values of

FIGURE 7.8   Calculated Values of K_1 (Rindel, 1986)

Values are given as a function of the distance from the edge to the geometric point of reflection
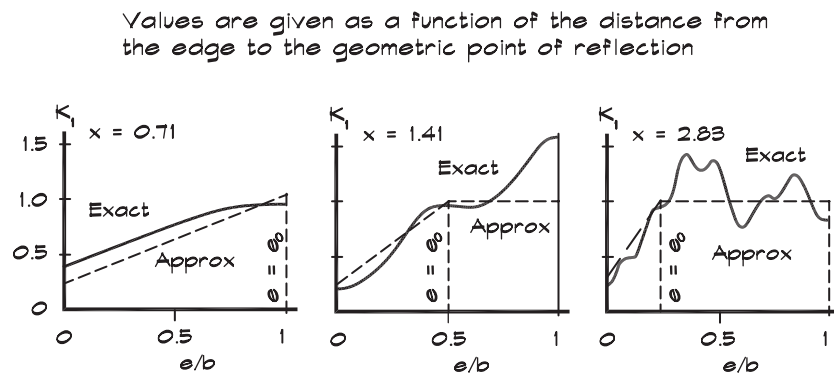
FIGURE 7.9   Measured and Calculated Attenuation of a Sound Reflection from a Square Surface (Rindel, 1986)

Reflection from the center of a 0.6 x 0.6 m plate
a_1 = 6 m, a_2 = 4 m, θ = 60°
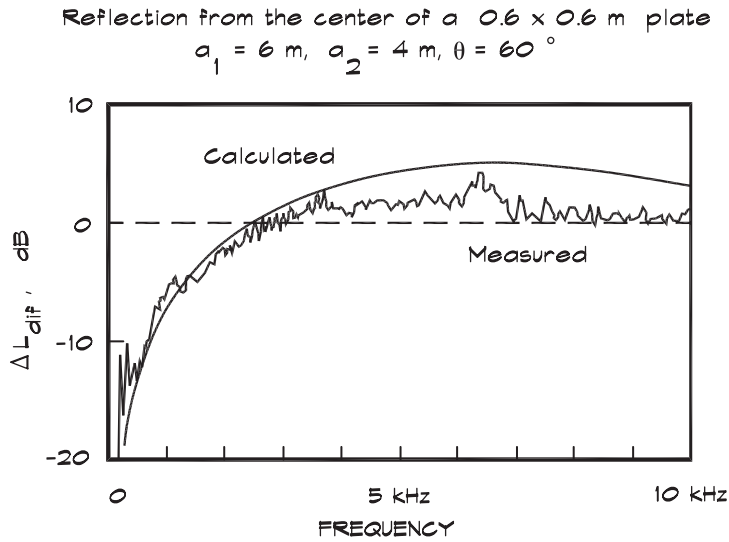
x greater than 0.7, edge diffraction is of minor importance. This corresponds to a limiting frequency

$$f_g > \frac{c\, a^*}{2\, S\, \cos\theta} \tag{7.31}$$

where S is the panel area. For a 2 m square panel the limiting frequency is about 360 Hz for a 45° angle of incidence and a characteristic distance of 6 m, typical of suspended reflectors.

Panel Arrays

When reflecting panels are arrayed as in Fig. 7.10, the diffusion coefficients must account for multipanel scattering. The coefficient in the direction shown is (Finne, 1987 and Rindel, 1990)

$$K_1 = \frac{1}{2}\left\{\sum_{i=1}^{I}\left[C\,(v_{1,i}) - C\,(v_{2,i})\right]^2 + \sum_{i=1}^{I}\left[S\,(v_{1,i}) - S\,(v_{2,i})\right]^2\right\} \tag{7.32}$$

FIGURE 7.10   Section through a Reflector Array with Five Rows of Reflectors (Rindel, 1990)
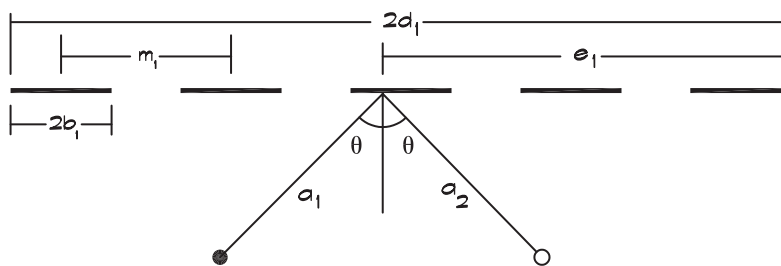
FIGURE 7.11   Simplified Illustration of the Attenuation of Reflections from an Array with Relative Density μ (Rindel, 1990)
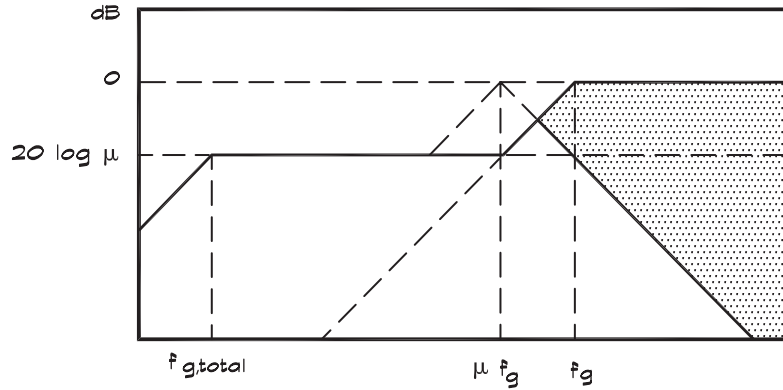
where

$$v_{1,i} = \frac{2}{\sqrt{\lambda\,a^*}}(e_1 - (i-1)\,m_1)\cos\theta \tag{7.33}$$

and

$$v_{2,i} = \frac{2}{\sqrt{\lambda\,a^*}}(e_1 - 2b_1 - (i-1)\,m_1)\cos\theta \tag{7.34}$$

where i is the running row number and I is the total number of rows in the x-direction.

At high frequencies the v values increase and the reflection is dominated by an individual panel. The single-panel limiting frequency from Eq. 7.31 sets the upper limit for this dependence. At low frequencies the v values decrease, but the reflected vectors combine in phase. The diffusion attenuation becomes dependent on the relative panel area density, μ, (the total array area divided by the total panel area), not the size of the individual reflectors. Figure 7.11 shows a design guide.

The K values are approximately

$$K \cong \mu^2 \quad \text{in the frequency range } f_{g,\text{total}} \le f \le \mu f_g \tag{7.35}$$

where the limiting frequency for the total array is given by Eq. 7.31, with the total area of the array used instead of the individual panel area. The shaded area indicates the possible variation depending on whether the sound ray strikes a panel or empty space. Beranek (1992) published relative reflection data based on laboratory tests by Watters et al., (1963), which are shown in Fig. 7.12. In general a large number of small panels is preferable to a few large ones.

Bragg Imaging

Since individual reflectors have to be relatively large to reflect bass frequencies, they are used in groups to improve their low-frequency response (see Leonard, Delsasso, and Knudsen, 1964; or Beranek, 1992). This can be tricky because if they are not arranged in a single plane there can be destructive interference at certain combinations of frequency and angle

FIGURE 7.12 Scattering from Panel Arrays (Beranek, 1992)

FIGURE 7.13 Geometry of Bragg Scattering from Rows of Parallel Reflectors
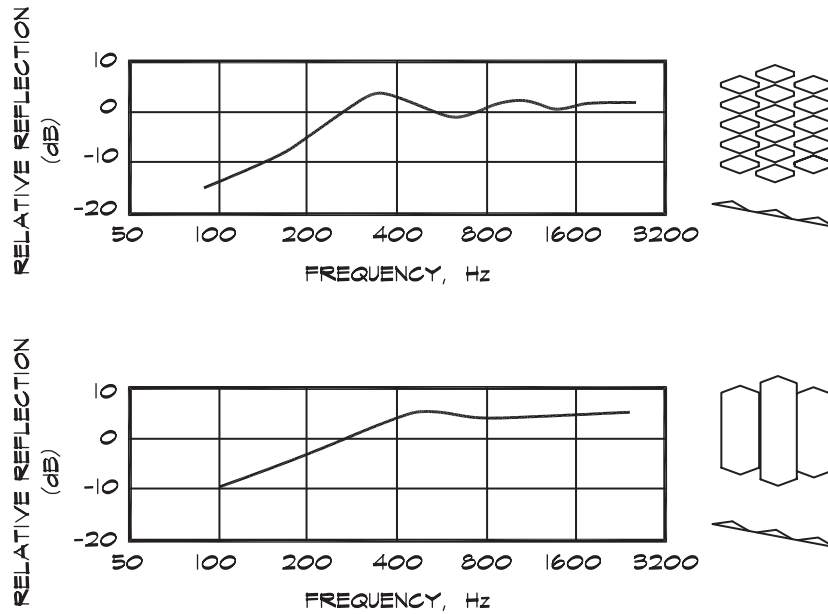
of incidence. When two planes of reflectors are employed, for a given separation distance there is a relationship between the angle of incidence and the frequency of cancellation of the reflected sound. This effect was used by Bragg to study the crystal structure of materials with x-rays. When sound is scattered from two reflecting planes, certain frequencies are missing in the reflected sound. This was one cause of the problems in Philharmonic Hall in New York (Beranek, 1996).

An illustration of this phenomenon, known as Bragg imaging, is shown in Fig. 7.13. When two rows of reflecting panels are placed one above the other, there is destructive interference between reflected sound waves when the combined path-length difference has the relationship

$$2 \, d \, \cos \theta = \frac{(2 \, n - 1) \lambda}{2} \tag{7.36}$$

FIGURE 7.13 Geometry of Bragg Scattering from Rows of Parallel Reflectors

The path length difference between the lower and upper reflectors is $2 \, d \, \cos \theta$.
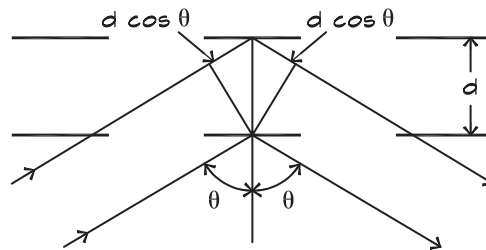
where λ = wavelength of the incident sound (m or ft)
    d = perpendicular spacing between rows of reflectors (m or ft)
    n = positive integer 1, 2, 3, . . . etc.
    θ = angle of incidence and reflection with respect to the normal (rad or deg)

The use of slightly convex reflectors can help diffuse the sound energy and smooth out the interferences; however, stacked planes of reflecting panels can produce a loss of bass energy in localized areas of the audience.

Scattering from Curved Surfaces

When sound is scattered from a curved surface, the curvature induces diffusion of the reflected energy when the surface is convex, or focusing when it is concave. The attenuation associated with the curvature can be calculated using the geometry shown in Fig. 7.14. If we consider a rigid cylinder having a radius R, the loss in intensity is proportional to the ratio of the incident-to-reflected beam areas (Rindel, 1986). At the receiver, M, the sound energy is proportional to the width of the reflected beam tube $(a + a_2)\, d\beta$. If there were no curvature the beam width would be $(a_1 + a_2)\, d\beta_1$ at the image point M_1.

Accordingly the attenuation due to the curvature is

$$\Delta L_{\text{curv}} = -10\,\log\frac{(a + a_2)\,d\beta}{(a_1 + a_2)\,d\beta_1} = -10\,\log\frac{(a + a_2)(d\beta/d\beta_1)}{(a_1 + a_2)} \tag{7.37}$$

Using Fig. 7.14 we see that a $d\beta = a_1\,d\beta_1 = R\,d\phi\,\cos\theta$, and that $d\beta = d\beta_1 + 2\,d\phi$, from which it follows that

$$\frac{d\beta}{d\beta_1} = 1 + \frac{2\,a_1}{R\cos\theta} \tag{7.38}$$

and plugging this into Eq. 7.37 yields

$$\Delta L_{\text{curv}} = -10\log\left|1 + \frac{a^*}{R\cos\theta}\right| \tag{7.39}$$

where a^* is given in Eq. 7.24. For concave surfaces the same equation can be used with a negative value for R. Figure 7.15 shows the results for both convex and concave surfaces.

FIGURE 7.14   Geometry of the Reflection from a Curved Surface (Rindel, 1986)
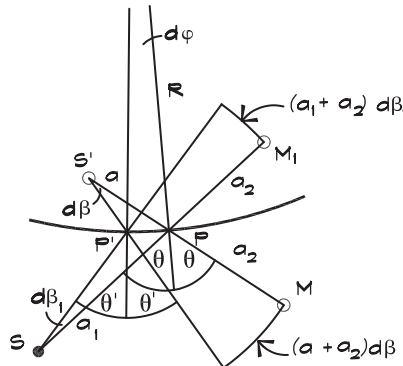
FIGURE 7.15   **Attenuation or Gain Due to Curvature (Rindel, 1985)**
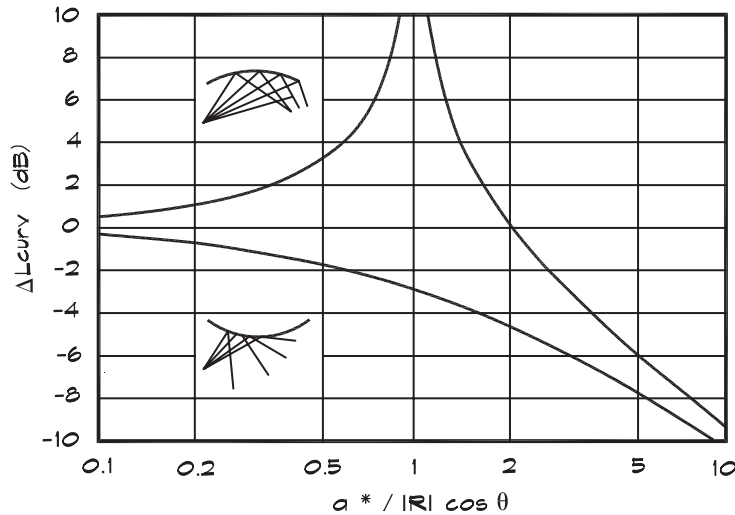
FIGURE 7.16   **Calculated and Measured Values of ΔL_{curv} (Rindel, 1985)**

Sketch				
Radius R	2.0 m	0.5 m	−2.0 m	−0.5 m
$a * / R \cos \theta$	0.5	2.0	0.5	−2.0
ΔL_{curv} (calc.)	−1.8 dB	−4.8 dB	3.0 dB	0.0 dB
ΔL_{curv} (meas.)	−2 ± 0.5 dB	−5 ± 1 dB	3 ± 1 dB	−1 ± 2 dB

This analysis assumes that both the source and the receiver are in a plane whose normal is the axis of the cylinder. If this is not the case, both a* and θ must be deduced from a normal projection onto that plane (Rindel, 1985). Where there is a double-curved surface with two radii of curvature, the attenuation term must be applied twice, using the appropriate projections onto the two normal planes of the surface.

Figure 7.16 gives the results of measurements using TDS on a small (1.4 m × 1.0 m) curved panel at a distance of 1 m for a zero angle of incidence over a frequency range of 3 to 19 kHz. The data also show the variation in the measured values, which Rindel (1985) attributes to diffraction effects.

Combined Effects

When sound is reflected from finite curved panels, the combined effects of distance, absorption, size, and curvature must be included. For an omnidirectional source, the level of the reflected sound relative to the direct sound is

$$L_{refl} - L_{dir} = \Delta L_{dist} + \Delta L_{abs} + \Delta L_{dif} + \Delta L_{curv} \qquad (7.40)$$

where the absorption term will be addressed later in this chapter, and the distance term is

$$\Delta L_{dist} = 20 \log \frac{a_0}{a_1 + a_2} \tag{7.41}$$

The other terms have been treated earlier.

Whispering Galleries

If a source of sound is located in a circular space, very close to the outside wall, some of the sound rays strike the surface at a shallow angle and are reflected again and again, and so propagate within a narrow band completely around the room. A listener located on the opposite side of the space can clearly hear conversations that occur close to the outside wall. This phenomenon, which is called a whispering gallery since even whispered conversations are audible, occurs in circular or domed spaces such as the statuary gallery in the Capital building in Washington, DC.

7.3   ABSORPTION

Reflection and Transmission Coefficients

When sound waves interact with real materials the energy contained in the incident wave is reflected, transmitted through the material, and absorbed within the material. The surfaces treated in this model are generally planar, although some curvature is tolerated as long as the radius of curvature is large when compared to a wavelength. The energy balance is illustrated in Fig. 7.17.

$$E_i = E_r + E_t + E_a \tag{7.42}$$

Since this analysis involves only the interaction at the boundary of the material, the difference between absorption, where energy is converted to heat, and transmission, where energy passes through the material, is not relevant. Both mechanisms are absorptive from the standpoint of the incident side because the energy is not reflected. Because we are only interested in the incident side of the boundary, we can combine the transmitted and

FIGURE 7.17   Interaction of Sound Waves with a Surface
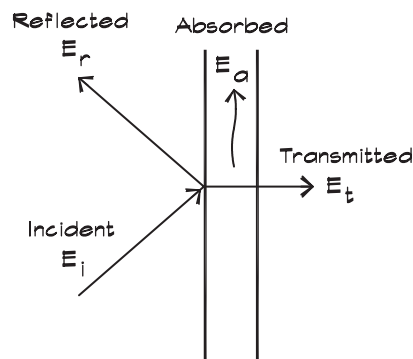
absorbed energies. If we divide Eq. 7.42 by E_i,

$$1 = \frac{E_r}{E_i} + \frac{E_{t+a}}{E_i} \tag{7.43}$$

We can express each energy ratio as a coefficient of reflection or transmission. The fraction of the incident energy that is absorbed (or transmitted) at the surface boundary is the coefficient

$$\alpha_\theta = \frac{E_{t+a}}{E_i} \tag{7.44}$$

and the reflection coefficient is

$$\alpha_r = \frac{E_r}{E_i} \tag{7.45}$$

Substituting these coefficients into Eq. 7.43,

$$1 = \alpha_\theta + \alpha_r \tag{7.46}$$

The reflection coefficient can be expressed in terms of the complex reflection amplitude ratio **r** for pressure that was defined in Eq. 7.7

$$\alpha_r = \mathbf{r}^2 \tag{7.47}$$

and the absorption coefficient is

$$\alpha_\theta = 1 - \mathbf{r}^2 \tag{7.48}$$

The reflected energy is

$$E_r = (1 - \alpha_\theta)E_i \tag{7.49}$$

Impedance Tube Measurements

When a plane wave is normally incident on the boundary between two materials, 1 and 2, we can calculate the strength of the reflected wave from a knowledge of their impedances. (This solution was published by Rayleigh in 1896.) Following the approach taken in Eq. 7.3, the sound pressure from the incident and reflected waves is written as

$$\mathbf{p}(x) = \mathbf{A}\,e^{j\,(\omega t - k\,x)} + \mathbf{B}\,e^{j\,(\omega t + k\,x)} \tag{7.50}$$

If we square and average this equation, we obtain the mean-squared acoustic pressure of a normally incident and reflected wave (Pierce, 1981)

$$\langle \mathbf{p}^2 \rangle = \frac{1}{2}\,\mathbf{A}^2\left[1 + |\,\mathbf{r}^2\,| + 2\,|\,\mathbf{r}\,|\cos\left(2\,k\,x + \delta_r\right)\right] \tag{7.51}$$

where δ_r is the phase of **r**. Equation 7.51 describes a standing wave and gives a method for measuring the normal-incidence absorption coefficient of a material placed in the end of a tube, called an *impedance tube*, pictured in Fig. 7.18.

Figure 7.18   Impedance Tube Measurements of the Absorption Coefficient
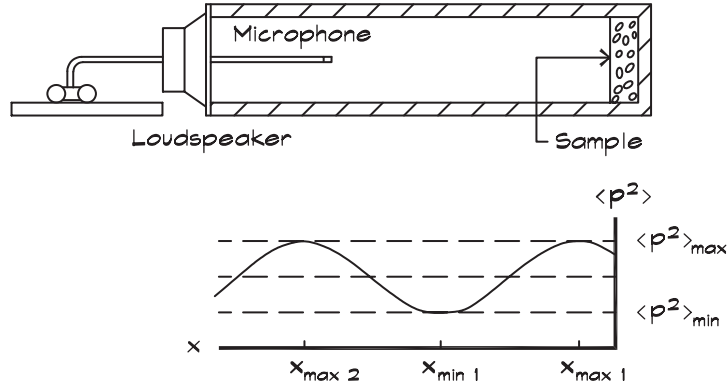
An incident and reflected wave combine to produce a standing wave in a tube. The pressure maximum and minimum are measured and their ratio determines the impedance.

The maximum value of the mean-squared pressure is $\frac{1}{2} A^2 [1 + |r|]^2$, which occurs whenever $2 k x + \delta_r$ is an even multiple of π. The minimum is $\frac{1}{2} A^2 [1 - |r|]^2$, which occurs at odd multiples of π. The ratio of the maximum-to-minimum pressures is an easily measured quantity called the *standing wave ratio*, s, which is usually obtained from its square

$$s^2 = \frac{\langle p^2 \rangle_{\mathrm{max}}}{\langle p^2 \rangle_{\mathrm{min}}} = \left| \frac{A + B}{A - B} \right|^2 = \frac{[1 + |r|]^2}{[1 - |r|]^2} \tag{7.52}$$

The phase angle is

$$\delta_r = -2 k x_{\mathrm{max}\ 1} + 2 m \pi = -2 k x_{\mathrm{min}\ 1} + (2 n + 1) \pi \tag{7.53}$$

where $x_{\mathrm{min}\ 1}$ is the smallest distance to a minimum and $x_{\mathrm{max}\ 1}$ is the smallest distance to a maximum, measured from the surface of the material. The numbers m and n are arbitrary integers, which do not affect the relative phase. Equation 7.52 can be solved for the magnitude and phase of the reflection amplitude ratio

$$r = |r| e^{j \delta_r} \tag{7.54}$$

from which the normal incidence material impedance can be obtained.

$$z_n = \rho_0 c_0 \frac{(1 + r)}{(1 - r)} \tag{7.55}$$

Oblique Incidence Reflections—Finite Impedance

When sound is obliquely incident on a surface having a finite impedance, the pressure of the incident and reflected waves is given by

$$p = A \left[e^{j k (x \cos \theta - y \sin \theta)} + r e^{-j k (x \cos \theta + y \sin \theta)} \right] \tag{7.56}$$

and the velocity in the x direction at the boundary (x = 0) using Eq. 6.31 is

$$\mathbf{u}(x) = \frac{A}{\rho_0 c_0} \left[\cos \theta \, e^{-j k y \sin \theta} - r \cos \theta \, e^{-j k y \sin \theta} \right] \qquad (7.57)$$

The normal specific acoustic impedance, expressed as the ratio of the pressure to the velocity at the surface is

$$\mathbf{z}_n = \left(\frac{\mathbf{p}}{\mathbf{u}_x} \right)_{x=0} = \frac{\rho_0 c_0}{\cos \theta} \frac{(1+r)}{(1-r)} \qquad (7.58)$$

The reflection coefficient can then be written in terms of the boundary's specific acoustic impedance

$$r = \frac{\mathbf{z} - \rho_0 c_0}{\mathbf{z} + \rho_0 c_0} \qquad (7.59)$$

where $\mathbf{z} = \mathbf{z}_n \cos \theta$ and $\mathbf{z}_n = w_n + j\, x_n$
   $\mathbf{z} =$ complex specific acoustic impedance
    $=$ (pressure or force) / (particle or volume velocity)
   $w =$ specific acoustic resistance or real part of the impedance
   $x =$ specific acoustic reactance or the imaginary part of the impedance
      - when positive it is mass like and when negative it is stiffness like
   $\rho_0 c_0 =$ characteristic acoustic resistance of the incident medium
      (about 412 Ns/m^3 - mks rayls in air)
   $j = \sqrt{-1}$

Now these relationships contain a good deal of information about the reflection process. When $|\mathbf{z}| \gg \rho_0 c_0$ the reflection coefficient approaches a value of $+ 1$, there is perfect reflection, and the reflected wave is in phase with the incident wave. If $|\mathbf{z}| \ll \rho_0 c_0$, the boundary is resilient like the open end of a tube, and the value of r approaches -1. Here the reflected wave is 180° out of phase with the incident wave and there is cancellation. When $|\mathbf{z}| = \rho_0 c_0$, no sound is reflected.

For any finite value of $\mathbf{z}_n$, as θ approaches $\pi/2$, the incident wave grazes over the boundary and the value of r approaches $- 1$. Under this condition the incident and reflected waves are out of phase and interfere with one another. This is an explanation of the ground effect, which was discussed previously. Note that in both cases—that is, when r is either ± 1—there is no sound absorption by the surface. The $|r| = -1$ case is rarely encountered in architectural acoustics and only over limited frequency ranges (Kuttruff, 1973).

Reflection and transmission coefficients can also be written in terms of the normal acoustic impedance of a material. The energy reflection coefficient using Eq. 7.59 is

$$\alpha_r = \left| \frac{(\mathbf{z}_n/\rho_0 c_0) \cos \theta - 1}{(\mathbf{z}_n/\rho_0 c_0) \cos \theta + 1} \right|^2 \qquad (7.60)$$

and in terms of the real and imaginary components of the impedance,

$$\alpha_r = \frac{(w_n \cos \theta - \rho_0 c_0)^2 + x_n^2 \cos^2 \theta}{(w_n \cos \theta + \rho_0 c_0)^2 + x_n^2 \cos^2 \theta} \tag{7.61}$$

The absorption coefficient is set equal to the absorption/transmission coefficient given in Eq. 7.44, since it is defined at a surface where it does not matter whether the energy is transmitted through the material or absorbed within the material, as long as it is not reflected back. The specular absorption coefficient is

$$\alpha_\theta = 1 - \left| \frac{(z_n/\rho_0 c_0) \cos \theta - 1}{(z_n/\rho_0 c_0) \cos \theta + 1} \right|^2 \tag{7.62}$$

which in terms of its components is

$$\alpha_\theta = \frac{4 \rho_0 c_0 w_n \cos \theta}{(w_n \cos \theta + \rho_0 c_0)^2 + x_n^2 \cos^2\theta} \tag{7.63}$$

For most architectural situations the incident conducting medium is air; however, it could be any material with a characteristic resistance. Since solid surfaces such as walls or absorptive panels have a resistance $w_n \gg \rho_0 c_0$, the magnitude of the absorption coefficient yields a maximum value when $w_n \cos \theta_i = \rho_0 c_0$. For normal incidence, when $z_n = \rho_0 c_0$, the transmission coefficient is unity as we would expect.

Figure 7.19 shows the behavior of a typical absorption coefficient with angle of incidence. As the angle of incidence increases, the apparent depth of the material increases, thereby increasing the absorption. At very high angles of incidence there is no longer a velocity component into the material so the coefficient drops off rapidly.

FIGURE 7.19   Absorption Coefficient as a Function of Angle of Incidence for a Porous Absorber (Benedetto and Spagnolo, 1985)
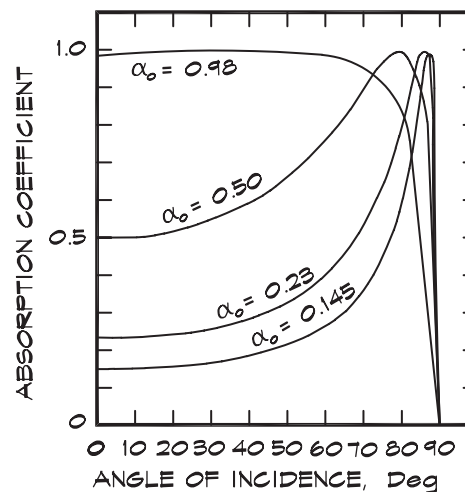
FIGURE 7.20   **Geometry of the Diffuse Field Absorption Coefficient Calculation (Cremer et al., 1982)**
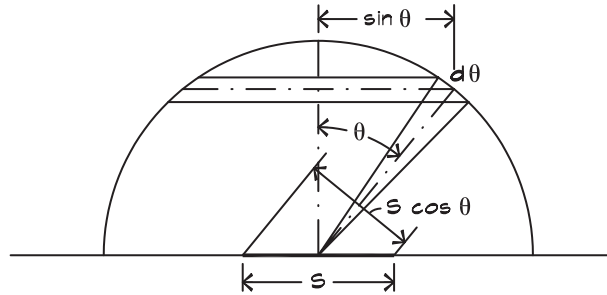
Calculated Diffuse Field Absorption Coefficients

In Eq. 7.63 we saw that we could write the absorption coefficient as a function of the angle of incidence, in terms of the complex impedance. Although direct-field absorption coefficients are useful for gaining an understanding of the physics of the absorption process, for most architectural applications a measurement is made of the diffuse-field absorption coefficient. Recall that a diffuse field implies that incident sound waves come from any direction with equal probability. The diffuse-field absorption coefficient is the average of the coefficient α_θ, taken over all possible angles of incidence. The geometry is shown in Fig. 7.20. The energy from a uniformly radiating hemisphere that is incident on the surface **S** is proportional to the area that lies between the angle $\theta - \Delta\theta/2$ and $\theta + \Delta\theta/2$. The fraction of the total energy coming from this angle is

$$\frac{dE}{E} = \frac{2\,\pi r \sin\theta\,r\,d\theta}{4\,\pi r^2} = \frac{1}{2}\sin\theta\,d\theta \tag{7.64}$$

and the total power sound absorbed by a projected area $S \cos\theta$ is

$$W = E\,c\,S \int_0^{\pi/2} \alpha_\theta \sin\theta\ \cos\theta\,d\theta \tag{7.65}$$

The total incident power from all angles is the value of Eq. 7.65, with a perfectly absorptive material ($\alpha_\theta = 1$). The average absorption coefficient is the ratio of the absorbed to the total power

$$\alpha = \frac{\int_0^{\pi/2} \alpha_\theta \sin\theta\ \cos\theta\,d\theta}{\int_0^{\pi/2} \sin\theta\ \cos\theta\,d\theta} \tag{7.66}$$

which can be simplified to (Paris, 1928)

$$\alpha = 2 \int_0^{\pi/2} \alpha_\theta \sin\theta\ \cos\theta\,d\theta \tag{7.67}$$

Here the sine term is the probability that energy will originate at a given angle and the cosine term is the projection of the receiving area.

Measurement of Diffuse Field Absorption Coefficients

Although diffuse-field absorption coefficients can be calculated from impedance tube data, more often they are measured directly in a reverberant space. Values of α are published for a range of frequencies between 125 Hz and 4 kHz. Each coefficient represents the diffuse-field absorption averaged over a band of frequencies one octave wide. Occasionally absorption data are required for calculations beyond this range. In these cases estimates can be made from impedance tube data, by extrapolation from known data, or by calculating the values from first principles.

Some variability arises in the measurement of the absorption coefficient. The diffuse-field coefficient is, in theory, always less than or equal to a value of one. In practice, when the reverberation time method discussed in Chapt. 8, is employed, values of α greater than 1 are sometimes measured. This normally is attributed to diffraction, the lack of a perfectly diffuse field in the measuring room, and edge conditions. At low frequencies diffraction seems to be the main cause (Beranek, 1971). Since it is easier and more consistent to measure the absorption using the reverberation time method, this is the value that is found in the published literature.

Diffuse-field measurements of the absorption coefficient are carried out in a reverberation chamber, which is a room with little or no absorption. Data are taken with and without the panel under test in the room and the resulting reverberation times are used to calculate the absorptive properties of the material. The test standard, ASTM C423, specifies several mountings as shown in Fig 7.21. Mountings A, B, D, and E are used for most prefabricated products. Mounting F is for duct liners and C is used for specialized applications. When data are reported, the test mounting method must also be included since the airspace behind the material greatly affects the results. The designation E-400, for example, indicates that mounting E was used and there was a 400 mm (16") airspace behind the test sample.

Noise Reduction Coefficient (NRC)

Absorptive materials, such as acoustical ceiling tile, wall panels, and other porous absorbers are often characterized by their noise reduction coefficient, which is the average diffuse field absorption coefficient over the speech frequencies, 250 Hz to 2 kHz, rounded to the nearest 0.05.

$$\text{NRC} = \frac{1}{4}\left(\alpha_{250} + \alpha_{500} + \alpha_{1\,k} + \alpha_{2\,k}\right) \tag{7.68}$$

Although these single-number metrics are useful as a means of getting a general idea of the effectiveness of a particular material, for critical applications calculations should be carried out over the entire frequency range of interest.

Absorption Data

Table 7.1 shows a representative sample of measured absorption data. The list is by no means complete but care has been taken to include a reasonable sample of different types of materials. When layering materials or when using them in a manner that is not representative

FIGURE 7.21   Laboratory Absorption Test Mountings
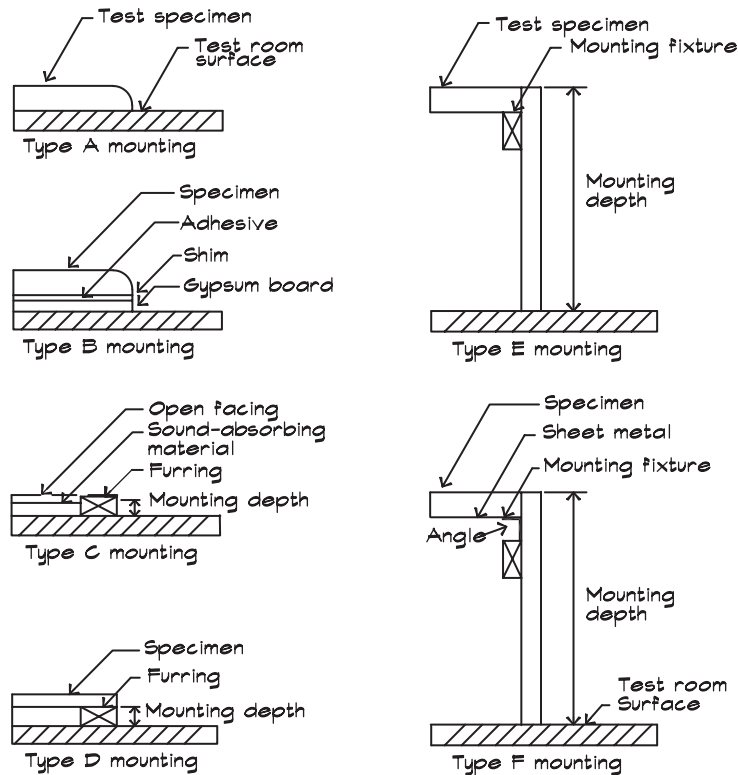
of the measured data, some adjustments may have to be made to account for different air cavity depths or mounting methods.

Occasionally it is necessary to estimate the absorption of materials beyond the range of measured data. Most often this occurs in the 63 Hz octave band, but sometimes occurs at lower frequencies. Data generally are not measured in this frequency range because of the size of reverberant chamber necessary to meet the diffuse field requirements. In these cases it is particularly important to consider the contributions to the absorption of the structural elements behind any porous panels.

Layering Absorptive Materials

It is the rule rather than the exception that acoustical materials are layered in real applications. For example a 25 mm (1 in) thick cloth-wrapped fiberglass material might be applied over a 16 mm (5/8 in) thick gypsum board wall. A detailed mathematical analysis of the impedance of the composite material is beyond the scope of a typical architectural project, and when one seeks the absorption coefficient from tables such as those in Table 7.1, one finds data on the panel, tested in an A-mounting condition, and data on the gypsum board wall, but no data on the combination.

If the panel data were used without consideration of the backing, the listed value at 125 Hz would suggest that there would be a decrease in absorption from the application of the panel relative to the drywall alone. This is due to the lower absorption coefficient that comes about from the test mounting method (on concrete), rather than from the panel itself.

TABLE 7.1 **Absorption Coefficients of Common Materials**

Material	Mount	Frequency, Hz					
		125	250	500	1k	2k	4k
Walls							
Glass, 1/4", heavy plate		0.18	0.06	0.04	0.05	0.02	0.02
Glass, 3/32", ordinary window		0.55	0.25	0.18	0.12	0.07	0.04
Gypsum board, 1/2", on 2×4 studs		0.29	0.10	0.05	0.04	0.07	0.09
Plaster, 7/8", gypsum or lime, on brick		0.013	0.015	0.02	0.03	0.04	0.05
Plaster, on concrete block		0.12	0.09	0.07	0.05	0.05	0.04
Plaster, 7/8", on lath		0.14	0.10	0.06	0.04	0.04	0.05
Plaster, 7/8", lath on studs		0.30	0.15	0.10	0.05	0.04	0.05
Plywood, 1/4", 3" air space, 1" batt,		0.60	0.30	0.10	0.09	0.09	0.09
Soundblox, type B, painted		0.74	0.37	0.45	0.35	0.36	0.34
Wood panel, 3/8", 3-4" air space		0.30	0.25	0.20	0.17	0.15	0.10
Concrete block, unpainted		0.36	0.44	0.51	0.29	0.39	0.25
Concrete block, painted		0.10	0.05	0.06	0.07	0.09	0.08
Concrete poured, unpainted		0.01	0.01	0.02	0.02	0.02	0.03
Brick, unglazed, unpainted		0.03	0.03	0.03	0.04	0.05	0.07
Wood paneling, 1/4", with airspace behind		0.42	0.21	0.10	0.08	0.06	0.06
Wood, 1", paneling with airspace behind		0.19	0.14	0.09	0.06	0.06	0.05
Shredded-wood fiberboard, 2", on concrete	A	0.15	0.26	0.62	0.94	0.64	0.92
Carpet, heavy, on 5/8-in perforated mineral fiberboard		0.37	0.41	0.63	0.85	0.96	0.92
Brick, unglazed, painted	A	0.01	0.01	0.02	0.02	0.02	0.03
Light velour, 10 oz per sq yd, hung straight, in contact with wall		0.03	0.04	0.11	0.17	0.24	0.35
Medium velour, 14 oz per sq yd, draped to half area		0.07	0.31	0.49	0.75	0.70	0.60
Heavy velour, 18 oz per sq yd, draped to half area		0.14	0.35	0.55	0.72	0.70	0.65

TABLE 7.1 Absorption Coefficients of Common Materials, (*Continued*)

Material	Mount	Frequency, Hz					
		125	250	500	1k	2k	4k
Floors							
Floors, concrete or terrazzo	A	0.01	0.01	0.015	0.02	0.02	0.02
Floors, linoleum, vinyl on concrete	A	0.02	0.03	0.03	0.03	0.03	0.02
Floors, linoleum, vinyl on subfloor		0.02	0.04	0.05	0.05	0.10	0.05
Floors, wooden		0.15	0.11	0.10	0.07	0.06	0.07
Floors, wooden platform w/airspace		0.40	0.30	0.20	0.17	0.15	0.10
Carpet, heavy on concrete	A	0.02	0.06	0.14	0.57	0.60	0.65
Carpet, on 40 oz (1.35 kg/sq m) pad	A	0.08	0.24	0.57	0.69	0.71	0.73
Indoor-outdoor carpet	A	0.01	0.05	0.10	0.20	0.45	0.65
Wood parquet in asphalt on concrete	A	0.04	0.04	0.07	0.06	0.06	0.07
Ceilings							
Acoustical coating K-13, 1"	A	0.08	0.29	0.75	0.98	0.93	0.96
1.5"	A	0.16	0.50	0.95	1.06	1.00	0.97
2"	A	0.29	0.67	1.04	1.06	1.00	0.97
Acoustical coating K-13 "fc" 1"	A	0.12	0.38	0.88	1.16	1.15	1.12
Glass-fiber roof fabric, 12 oz/yd		0.65	0.71	0.82	0.86	0.76	0.62
Glass-fiber roof fabric, 37.5 oz/yd		0.38	0.23	0.17	0.15	0.09	0.06
Acoustical Tile							
Standard mineral fiber, 5/8"	E400	0.68	0.76	0.60	0.65	0.82	0.76
Standard mineral fiber, 3/4"	E400	0.72	0.84	0.70	0.79	0.76	0.81
Standard mineral fiber, 1"	E400	0.76	0.84	0.72	0.89	0.85	0.81
Energy mineral fiber, 5/8"	E400	0.70	0.75	0.58	0.63	0.78	0.73
Energy mineral fiber, 3/4"	E400	0.68	0.81	0.68	0.78	0.85	0.80
Energy mineral fiber, 1"	E400	0.74	0.85	0.68	0.86	0.90	0.79
Film faced fiberglass, 1"	E400	0.56	0.63	0.69	0.83	0.71	0.55
Film faced fiberglass, 2"	E400	0.52	0.82	0.88	0.91	0.75	0.55
Film faced fiberglass, 3"	E400	0.64	0.88	1.02	0.91	0.84	0.62

TABLE 7.1 Absorption Coefficients of Common Materials, (*Continued*)

Material	Mount	Frequency, Hz					
		125	250	500	1k	2k	4k
Glass Cloth Acoustical							
Ceiling Panels							
Fiberglass tile, 3/4"	E400	0.74	0.89	0.67	0.89	0.95	1.07
Fiberglass tile, 1"	E400	0.77	0.74	0.75	0.95	1.01	1.02
Fiberglass tile, 1 1/2"	E400	0.78	0.93	0.88	1.01	1.02	1.00
Seats and Audience							
Audience in upholstered seats		0.39	0.57	0.80	0.94	0.92	0.87
Unoccupied well-upholstered seats		0.19	0.37	0.56	0.67	0.61	0.59
Unoccupied leather covered seats		0.19	0.57	0.56	0.67	0.61	0.59
Wooden pews, occupied		0.57	0.44	0.67	0.70	0.80	0.72
Leather-covered upholstered seats, unoccupied		0.44	0.54	0.60	0.62	0.58	0.50
Congregation, seated in wooden pews		0.57	0.61	0.75	0.86	0.91	0.86
Chair, metal or wood seat, unoccupied		0.15	0.19	0.22	0.39	0.38	0.30
Students, informally dressed, seated in tablet-arm chairs		0.30	0.41	0.49	0.84	0.87	0.84
Duct Liners							
1/2"		0.11	0.51	0.48	0.70	0.88	0.98
1"		0.16	0.54	0.67	0.85	0.97	1.01
1 1/2"		0.22	0.73	0.81	0.97	1.03	1.04
2"		0.33	0.90	0.96	1.07	1.07	1.09
Aeroflex Type 150, 1"	F	0.13	0.51	0.46	0.65	0.74	0.95
Aeroflex Type 150, 2"	F	0.25	0.73	0.94	1.03	1.02	1.09
Aeroflex Type 200, 1/2"	F	0.10	0.44	0.29	0.39	0.63	0.81
Aeroflex Type 200, 1"	F	0.15	0.59	0.53	0.78	0.85	1.00
Aeroflex Type 200, 2"	F	0.28	0.81	1.04	1.10	1.06	1.09
Aeroflex Type 300, 1/2"	F	0.09	0.43	0.31	0.43	0.66	0.98
Aeroflex Type 300, 1"	F	0.14	0.56	0.63	0.82	0.99	1.04
Aeroflex Type 150, 1"	A	0.06	0.24	0.47	0.71	0.85	0.97
Aeroflex Type 150, 2"	A	0.20	0.51	0.88	1.02	0.99	1.04
Aeroflex Type 300, 1"	A	0.08	0.28	0.65	0.89	1.01	1.04

TABLE 7.1   Absorption Coefficients of Common Materials, (*Continued*)

Material	Mount	Frequency, Hz					
		125	**250**	**500**	**1k**	**2k**	**4k**
Building Insulation - Fiberglass							
3.5" (R-11) (insulation exposed to sound)	A	0.34	0.85	1.09	0.97	0.97	1.12
6" (R-19) (insulation exposed to sound)	A	0.64	1.14	1.09	0.99	1.00	1.21
3.5" (R11) (FRK facing exposed to sound)	A	0.56	1.11	1.16	0.61	0.40	0.21
6" (R-19) (FRK facing exposed to sound)	A	0.94	1.33	1.02	0.71	0.56	0.39
Fiberglass Board (FB)							
FB, 3lb/ft^3, 1" thick	A	0.03	0.22	0.69	0.91	0.96	0.99
FB, 3 lb/ft^3, 2" thick	A	0.22	0.82	1.21	1.10	1.02	1.05
FB, 3 lb/ft^3, 3" thick	A	0.53	1.19	1.21	1.08	1.01	1.04
FB, 3 lb/ft^3, 4" thick	A	0.84	1.24	1.24	1.08	1.00	0.97
FB, 3 lb/ft^3, 1" thick	E400	0.65	0.94	0.76	0.98	1.00	1.14
FB, 3 lb/ft^3, 2" thick	E400	0.66	0.95	1.06	1.11	1.09	1.18
FB, 3 lb/ft^3, 3" thick	E400	0.66	0.93	1.13	1.10	1.11	1.14
FB, 3 lb/ft^3, 4" thick	E400	0.65	1.01	1.20	1.14	1.10	1.16
FB, 6 lb/ft^3, 1" thick	A	0.08	0.25	0.74	0.95	0.97	1.00
FB, 6 lb/ft^3, 2" thick	A	0.19	0.74	1.17	1.11	1.01	1.01
FB, 6 lb/ft^3, 3" thick	A	0.54	1.12	1.23	1.07	1.01	1.05
FB, 6 lb/ft^3, 4" thick	A	0.75	1.19	1.17	1.05	0.97	0.98
FB, 6 lb/ft^3, 1" thick	E400	0.68	0.91	0.78	0.97	1.05	1.18
FB, 6 lb/ft^3, 2" thick	E400	0.62	0.95	0.98	1.07	1.09	1.22
FB, 6 lb/ft^3, 3" thick	E400	0.66	0.92	1.11	1.12	1.10	1.19
FB, 6 lb/ft^3, 4" thick	E400	0.59	0.91	1.15	1.11	1.11	1.19
FB, FRK faced, 1" thick	A	0.12	0.74	0.72	0.68	0.53	0.24
FB, FRK faced, 2" thick	A	0.51	0.65	0.86	0.71	0.49	0.26
FB, FRK faced, 3" thick	A	0.84	0.88	0.86	0.71	0.52	0.25
FB, FRK faced, 4" thick	A	0.88	0.90	0.84	0.71	0.49	0.23
FB, FRK faced, 1" thick	E400	0.48	0.60	0.80	0.82	0.52	0.35
FB, FRK faced, 2" thick	E400	0.50	0.61	0.99	0.83	0.51	0.35
FB, FRK faced, 3" thick	E400	0.59	0.64	1.09	0.81	0.50	0.33
FB, FRK faced, 4" thick	E400	0.61	0.69	1.08	0.81	0.48	0.34
Miscellaneous							
Musician (per person), with instrument		4.0	8.5	11.5	14.0	15.0	12.0
Air, Sabins per 1000 cubic feet @ 50% RH					0.9	2.3	7.2

In cases where materials are applied in ways that differ from the manner in which they were tested, estimates must be made based on the published absorptive properties of the individual elements. For example, a drywall wall has an absorptive coefficient of 0.29 at 125 Hz since it is acting as a panel absorber, having a resonant frequency of about 55 Hz. A one-inch (25 mm) thick fiberglass panel has an absorption coefficient of 0.03 at 125 Hz since it is measured in the A-mounting position. When a panel is mounted on drywall, the low-frequency sound passes through the fiberglass panel and interacts with the drywall surface. Assuming the porous material does not significantly increase the mass of the wall surface, the absorption at 125 Hz should be at least 0.29, and perhaps a little more due to the added flow resistance of the fiberglass. Consequently when absorptive materials are layered we must consider the combined result, rather than the absorption coefficient of only the surface material alone.

7.4   ABSORPTION MECHANISMS

Absorptive materials used in architectural applications tend to fall into three categories: porous absorbers, panel absorbers, and resonant absorbers. Of these, the porous absorbers are the most frequently encountered and include fiberglass, mineral fiber products, fiberboard, pressed wood shavings, cotton, felt, open-cell neoprene foam, carpet, sintered metal, and many other products. Panel absorbers are nonporous lightweight sheets, solid or perforated, that have an air cavity behind them, which may be filled with an absorptive material such as fiberglass. Resonant absorbers can be lightweight partitions vibrating at their mass-air-mass resonance or they can be Helmholtz resonators or other similar enclosures, which absorb sound in the frequency range around their resonant frequency. They also may be filled with absorbent porous materials.

Porous Absorbers

Several mechanisms contribute to the absorption of sound by porous materials. Air motion induced by the sound wave occurs in the interstices between fibers or particles. The movement of the air through narrow constrictions, as illustrated in Fig. 7.22, produces losses of momentum due to viscous drag (friction) as well as changes in direction. This accounts for most of the high-frequency losses. At low frequencies absorption occurs because fibers are relatively efficient conductors of heat. Fluctuations in pressure and density are isothermal, since thermal equilibrium is restored so rapidly. Temperature increases in the gas cause heat

FIGURE 7.22   Viscous Drag Mechanism of Absorption in Porous Materials

When a sound wave enters a porous material the local flow velocity increases, the direction of flow changes and friction converts sound energy into heat.

INCIDENT SOUND WAVE
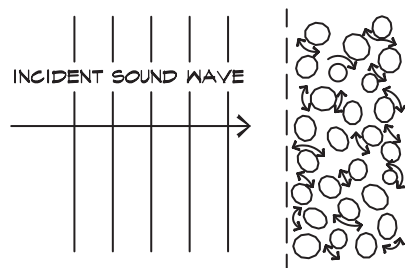
to be transported away from the interaction site to dissipate. Little attenuation seems to occur as a result of induced motion of the fibers (Mechel and Ver, 1992).

A lower (isothermal) sound velocity within a porous material also contributes to absorption. Friction forces and direction changes slow down the passage of the wave, and the isothermal nature of the process leads to a different equation of state. When sound waves travel parallel to the plane of the absorber some of the wave motion occurs within the absorber. Waves near the surface are diffracted, drawn into the material, due to the lower sound velocity.

In general, porous absorbers are too complicated for their precise impedances to be predicted from first principles. Rather, it is customary to measure the flow resistance, r_f, of the bulk material to determine the resistive component of the impedance. The bulk flow resistance is defined as the ratio between the pressure drop ΔP across the absorbing material and the steady velocity u_s of the air passing through the material.

$$r_f = -\frac{\Delta P}{u_s} \qquad (7.69)$$

Since this is dependent on the thickness of the absorber it is not a fundamental property of the material. The material property is the *specific flow resistance*, r_s, which is independent of the thickness.

$$r_s = -\frac{1}{u_s} \frac{\Delta P}{\Delta x} = \frac{r_f}{\Delta x} \qquad (7.70)$$

Flow resistance can be measured (Ingard, 1994) using a weighted piston as in Fig. 7.23. When the piston reaches its steady velocity, the resistance can be determined by measuring the time it takes for the piston to travel a given distance and the mass of the piston. Flow resistance is expressed in terms of the pressure drop in Newtons per square meter divided by the velocity in meters per second and is given in units of mks rayls, the same unit as the specific acoustic impedance. The specific flow resistance has units of mks rayls/m.

Figure 7.23 A Simple Device to Measure the Flow Resistance of a Porous Material (Ingard, 1994)

A weighted piston falls under gravity and forces air through a sample of porous material in the bottom of the tube. When the piston has reached its terminal velocity the flow resistance is calculated from the weight of the piston divided by its area A. The velocity is the distance travelled, l, divided by the time, t. So the flow resistance is $r_f = \Delta P / U_s$ where $U_s = (A / S) U$
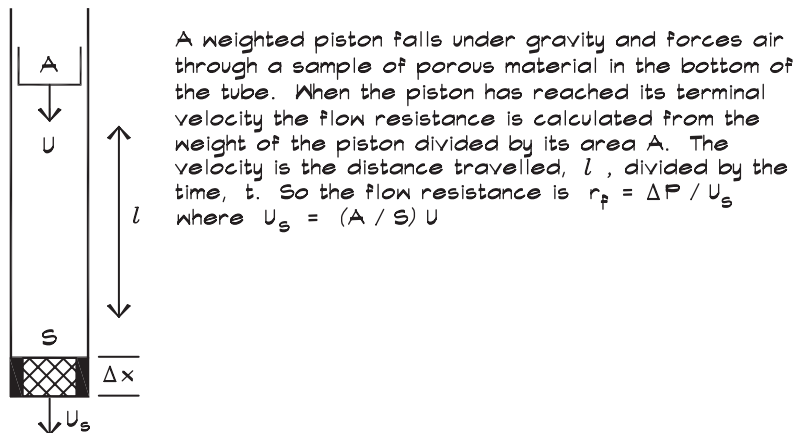
FIGURE 7.24   Geometry of a Spaced Porous Absorber (Kuttruff, 1973)
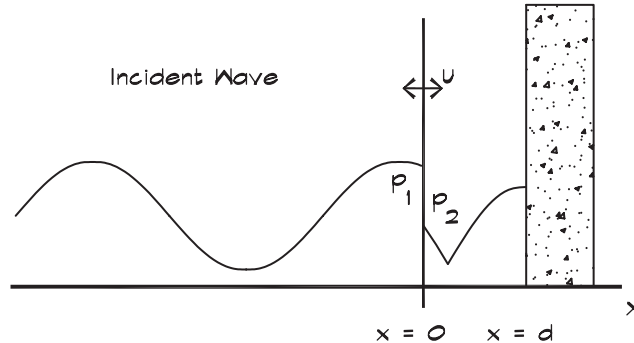
The porous absorber does not move but air flows through it,
creating a standing wave in the cavity behind.

Spaced Porous Absorbers—Normal Incidence, Finite Impedance

If a thin porous absorber is positioned such that it has an airspace behind it, the composite impedance at the surface of the material and thus the absorption coefficient, is influenced by the backing. Figure 7.24 shows a porous absorber located a distance d away from a solid wall. The flow resistance, which is approximately the resistive component of the impedance, is the difference in pressure across the material divided by the velocity through the material.

$$r_f = \frac{\mathbf{p}_1 - \mathbf{p}_2}{\mathbf{u}} \qquad (7.71)$$

where $\mathbf{p}_1$ is the pressure on the left side of the sheet and $\mathbf{p}_2$ is the pressure just to the right of the sheet. In this analysis it is assumed that the resistance is the same for steady and alternating flow. The velocity on either side of the sheet is the same due to conservation of mass. Equation 7.71 can be written in terms of the impedance at the surface of the absorber (at $x = 0$) on either side of the sheet.

$$r_f = \mathbf{z}_1 - \mathbf{z}_2 \qquad (7.72)$$

which implies that the impedance of the composite sheet plus the air backing is the sum of the sheet flow resistance and the impedance of the cavity behind the absorber.

$$\mathbf{z}_1 = r_f + \mathbf{z}_2 \qquad (7.73)$$

To calculate the impedance of the air cavity for a normally incident sound wave we write the equations for a rightward moving wave and the reflected leftward moving wave, assuming perfect reflection from the wall.

$$\begin{aligned}
\mathbf{p}_2(x) &= \mathbf{A}\left[e^{-j\,k(x-d)} + e^{j\,k(x-d)}\right] \\
&= 2\,\mathbf{A}\cos\left[k\,(x-d)\right]
\end{aligned} \qquad (7.74)$$

The velocity in the cavity is

$$
\begin{aligned}
\mathbf{u}_2(x) &= \frac{\mathbf{A}}{\rho_0 c_0} \left[e^{-j\,k\,(x-d)} - e^{j\,k\,(x-d)} \right] \\
&= -\frac{2\,j\,\mathbf{A}}{\rho_0 c_0} \sin\left[k\,(x-d) \right]
\end{aligned}
\tag{7.75}
$$

The ratio of the pressure to the velocity at the sheet surface (x = 0) is the impedance of the cavity

$$
\mathbf{z}_2 = \left(\frac{\mathbf{p}_2}{\mathbf{u}_2} \right)_{x=0} = -j\,\rho_0 c_0 \, \cot\,(k\,d)
\tag{7.76}
$$

The normal impedance of the porous absorber and the air cavity is

$$
\mathbf{z}_n = r_f - j\,\rho_0 c_0 \, \cot\,(k\,d)
\tag{7.77}
$$

By plugging this expression into Eq. 7.63 we get the absorption coefficient for normal incidence (Kuttruff, 1973)

$$
\alpha_n = 4 \left\{ \left[\sqrt{\frac{r_f}{\rho_0 c_0}} + \sqrt{\frac{\rho_0 c_0}{r_f}} \right]^2 + \frac{\rho_0 c_0}{r_f} \cot^2\left(\frac{2\,\pi\,f\,d}{c_0} \right) \right\}^{-1}
\tag{7.78}
$$

Figure 7.25 (Ginn, 1978) shows the behavior of this equation with frequency for a flow resistance $r_f \cong 2\rho_0 c_0$.

FIGURE 7.25   Absorptive Material Near a Hard Surface (Ginn, 1978)
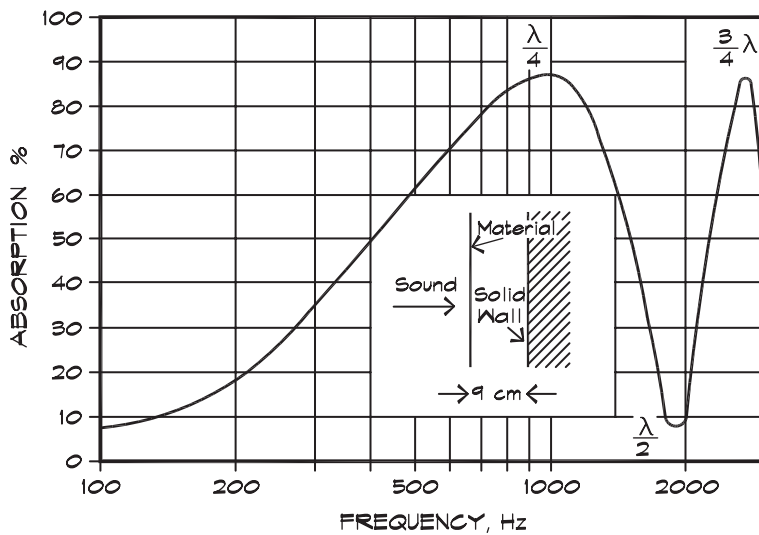
Absorption of freely suspended, thin porous material arranged parallel to a plane hard surface.

A thin porous absorber located at multiples of a quarter wavelength from a reflecting surface is in an optimum position to absorb sound since the particle velocity is at a maximum at this point. An absorber located at multiples of one-half wavelength from a wall is not particularly effective since the particle velocity is low. Thin curtains are not good broadband absorbers unless there is considerable (usually 100%) gather or unless there are several curtains hung one behind another. Note that in real rooms it is rare to encounter a condition of purely normal incidence. For diffuse fields the phase interference patterns are much less pronounced than those shown in Fig. 7.25.

Porous Absorbers with Internal Losses—Normal Incidence

When there are internal losses that attenuate the sound as it passes through a material, the attenuation can be written as an exponentially decaying sinusoid

$$\mathbf{p}\,(x) = \mathbf{A}\,e^{j\,\omega\,t}\,e^{-j\,q\,x} \tag{7.79}$$

where $q = \delta + j\,\beta$ is the complex *propagation constant* within the absorbing material. It is much like the wave number in that its real part, δ, is close to ω/c. However, it has an imaginary part, β, which is the attenuation constant, in nepers/meter, of the sound passing through an absorber. To convert nepers per meter to dB/meter, multiply nepers by 8.69.

For a thick porous absorber with a characteristic wave impedance $\mathbf{z}_w$, we write the equations for a normally incident and reflected plane wave with losses

$$\mathbf{p} = \mathbf{A}\,e^{j\,q\,x} + \mathbf{B}\,e^{-j\,q\,x} \tag{7.80}$$

and the particle velocity is

$$\mathbf{u} = \frac{1}{\mathbf{z}_w}\left[\mathbf{A}\,e^{j\,q\,x} - \mathbf{B}\,e^{-j\,q\,x}\right] \tag{7.81}$$

We use the indices 1 and 2 for the left- and right-hand sides of the material and make the end of the material $x = 0$ and the beginning of the material $x = -d$. The incident wave is moving in the positive x direction. At $x = 0$,

$$\mathbf{p}_2 = \mathbf{A} + \mathbf{B} \tag{7.82}$$

and

$$\mathbf{u}_2 = \frac{1}{\mathbf{z}_w}(\mathbf{A} - \mathbf{B}) \tag{7.83}$$

Solving for the amplitudes A and B,

$$\mathbf{A} = (\mathbf{p}_2 + \mathbf{z}_w\,\mathbf{u}_2)\,/\,2 \tag{7.84}$$

$$\mathbf{B} = (\mathbf{p}_2 - \mathbf{z}_w\,\mathbf{u}_2)\,/\,2 \tag{7.85}$$

Plugging these into Eqs. 7.80 and 7.81 at $x = -d$,

$$\mathbf{p}_1 = \mathbf{p}_2 \cos(q\,d) - j\,\mathbf{z}_w\,\mathbf{u}_2 \sin(q\,d) \tag{7.86}$$

and

$$\mathbf{u}_1 = \left(\frac{-j}{\mathbf{z}_w}\right) \mathbf{p}_2 \sin(q\,d) + \mathbf{u}_2 \cos(q\,d) \tag{7.87}$$

The ratio of these two equations yields the input impedance of the absorbing surface in terms of the characteristic wave impedance of the material and its propagation constant, and the back impedance $\mathbf{z}_2$ of the surface behind the absorber.

$$\mathbf{z}_1 = \mathbf{z}_w \left(\frac{\mathbf{z}_2\,\coth(q\,d) + \mathbf{z}_w}{\mathbf{z}_2 + \mathbf{z}_w\,\coth(q\,d)}\right) \tag{7.88}$$

When the material is backed by a rigid wall ($\mathbf{z}_2 = \infty$), then we obtain

$$\mathbf{z}_1 = \mathbf{z}_w\,\coth(q\,d) \tag{7.89}$$

Empirical Formulas for the Impedance of Porous Materials

It is difficult to predict the complex characteristic impedance of a material from the flow resistance based on theory alone, so empirical formulas have been developed that give good results. Delany and Bazley (1969) published a useful relationship for the wave impedance of a porous material such as fiberglass

$$\mathbf{z}_w = w + j\,x \tag{7.90}$$

$$w = \rho_0\,c_0 \left[1 + 0.0571\left(\rho_0\,f/r_s\right)^{-0.754}\right] \tag{7.91}$$

$$x = -\rho_0\,c_0 \left[0.0870\left(\rho_0\,f/r_s\right)^{-0.732}\right] \tag{7.92}$$

and the propagation constant is

$$q = \delta + j\,\beta \tag{7.93}$$

$$\delta \cong \frac{\omega}{c_0} \left[1 + 0.0978\left(\rho_0\,f/r_s\right)^{-0.700}\right] \tag{7.94}$$

$$\beta = \frac{\omega}{c_0} \left[0.189\left(\rho_0\,f/r_s\right)^{-0.595}\right] \tag{7.95}$$

where $\mathbf{z}_w$ = complex characteristic impedance of the material
        w = resistance or real part of the wave impedance
        x = reactance or imaginary part of the wave impedance
        q = complex propagation constant
        δ = real part of the propagation constant $\cong \omega/c_0$

        β = imaginary part of the propagation constant
           = attenuation (nepers/m)

$\rho_0 c_0 =$ characteristic acoustic resistance of air (about 412 Ns/m^3 $-$ mks rayls)

  $r_s =$ specific flow resistance (mks rayls)
  $d =$ thickness of the material (m)
  $f =$ frequency (Hz)
  $j = \sqrt{-1}$

   Figure 7.26 shows measured absorption data versus frequency compared to calculated data using the relationships just shown for two different flow resistance and thickness values. Note that manufacturers usually give the specific flow resistance in cgs rayls/cm (1 cgs rayl = 10 mks rayls). The shape of the curve is determined by the total flow resistance, and the thickness sets the cutoff point for low-frequency absorption.

   Diffuse-field absorption coefficients show a similar behavior with thickness. For oblique incidence there is a component of the velocity parallel to the surface so there is some absorption, even near the wall. The thickness and spacing of a porous absorber such as a pressed-fiberglass panel, mounted on a concrete wall or other highly reflecting surface, still determines the frequency range of its absorption characteristics. Figure 7.27 shows the measured diffuse-field absorption coefficients of various thicknesses of felt panel.

Thick Porous Materials with an Air Cavity Backing

When a thick porous absorber is backed by an air cavity and then a rigid wall, the back impedance behind the absorber is given in Eq. 7.76. This value can be inserted into Eq. 7.63 to get the overall impedance of the composite. The absorption coefficient is plotted in Fig. 7.28 for several thicknesses. In each case the total depth and total flow resistance are the same. Note that the specific flow resistance has been changed to offset the changes in thickness. When materials are spaced away from the wall, they should have a higher characteristic resistance. It is interesting that, as the material thickness decreases, the effect of the quarter-wave spacing becomes more noticeable since its behavior approaches that of a thin resistive absorber.

FIGURE 7.26   Normal Absorption Coefficient vs Frequency for Pressed Fiberglass Board (Hamet, 1997)
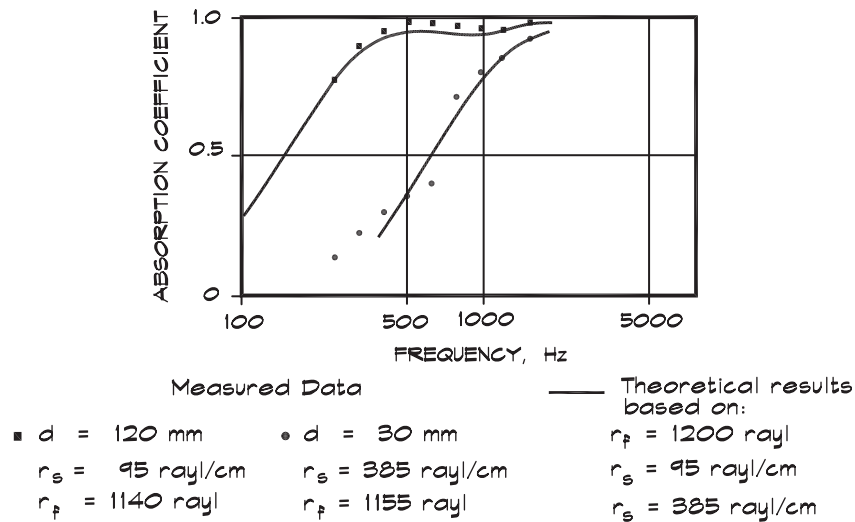
FIGURE 7.27   **Dependence of Absorption on Thickness (Ginn, 1978)**
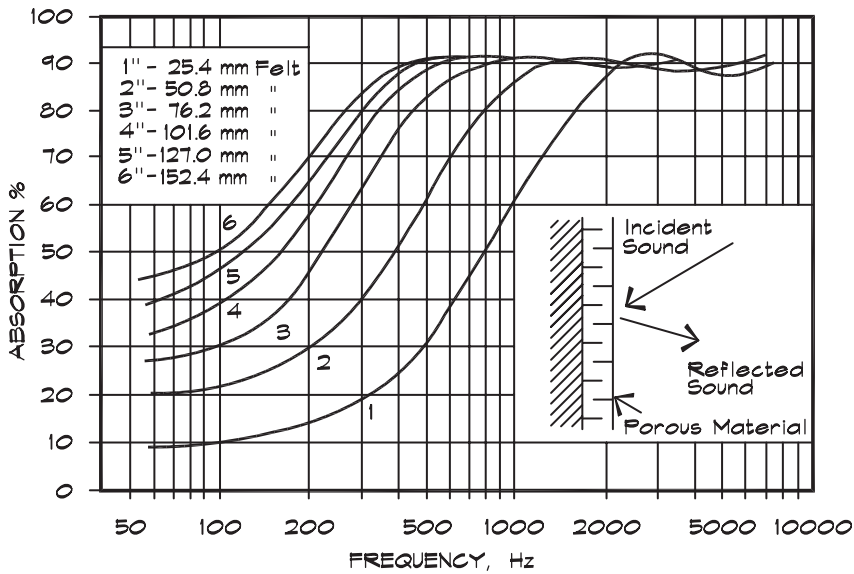
FIGURE 7.28   **Absorption of Thick Materials with Air Backing (Ingard, 1994)**

The absorption coefficient of a nonlocally reacting porous layer backed by an air cavity and a rigid wall. The overall thickness of the layer-cavity combination is 20 cm (8") and the different layer thicknesses are 5 cm (2"), 10 cm (4"), 15 cm (6") and 20 cm (8"). The total flow resistance in each case is $2 \rho_0 c_0$.
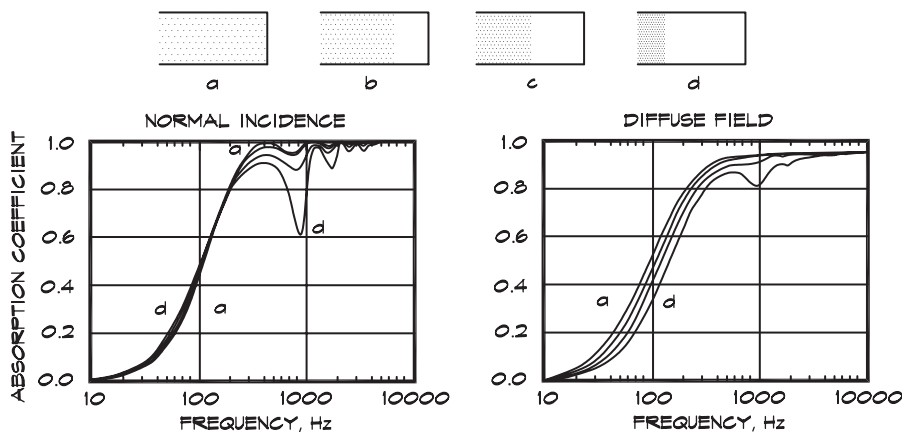
Practical Considerations in Porous Absorbers

For most architectural applications, a 1" (25 mm) thick absorbent fiberglass panel applied over a hard surface is the minimum necessary to control reverberation for speech intelligibility. Some localized effects such as high-frequency flutter echoes can be reduced using thinner materials such as 3/16" (5 mm) wall fabric or 1/4" (6 mm) carpet, but these materials are not thick enough for general applications. If low-frequency energy in the 125 Hz. octave band is of concern, then at least 2" (50 mm) panels are necessary. At even lower frequencies, 63 Hz and below, panel absorbers such as a gypboard wall, or Helmholtz bass traps are required.

FIGURE 7.29   Diffuse Field Absorption Coefficient (Ingard, 1994)

Absorption for various values of the normalized steady flow resistance.
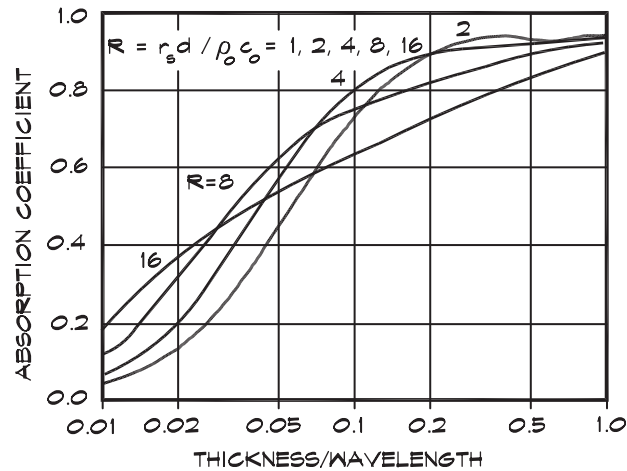
Figure 7.29 shows the absorption of materials of the same thickness but having different flow resistances. Normally a value around $2\rho_0 c_0$ of total flow resistance is optimal at the mid and high frequencies for a wall-mounted absorber (Ingard, 1994). At lower frequencies, or when there is an air cavity backing, higher resistances are better.

When a relatively dense material such as acoustical tile is suspended over an airspace, it can be an effective broadband absorber. Figure 7.30 shows the difference in low-frequency performance for acoustical tiles applied with adhesive directly to a reflecting surface and those supported in a suspension system. The thickness of the material is still important so that the absorption coefficient does not exhibit the high-frequency dependence shown earlier. In general, fiberglass tiles are more effective at high frequencies than mineral-fiber tiles since their characteristic resistance is lower.

Wrapping materials with a porous cloth covering has little effect on the absorption coefficient. The flow resistance of the cloth must be low. If it is easy to blow through it there is little change in the absorption. Paper or vinyl backings raise the resistance and lower the high-frequency absorption. Small perforations made in a vinyl fabric can reduce the flow resistance while delivering a product that is washable.

Screened Porous Absorbers

Absorptive materials can be overlaid by a porous screen with little effect on their properties, so long as the covering is sufficiently open. Slats of wood or metal are commonly used to protect these soft absorbers from wear and to improve their appearance. Perforated metals and wire mesh screens are also employed and can be effective as long as there is sufficient open area and the hole sizes are not so large that the spaces between the holes become reflecting surfaces, or so small that they become clogged with dirt or paint. Figure 7.31 (Doelle, 1972) shows the behavior of a porous absorber covered with a perforated facing. If there is at least 15 to 20% open area, the material works as if it were unfaced. Several examples of spaced facings are shown in Fig. 7.32.

FIGURE 7.30   **Average Absorption of Acoustical Tiles (Doelle, 1972)**

(A) Applied with adhesive, (B) In a suspended grid
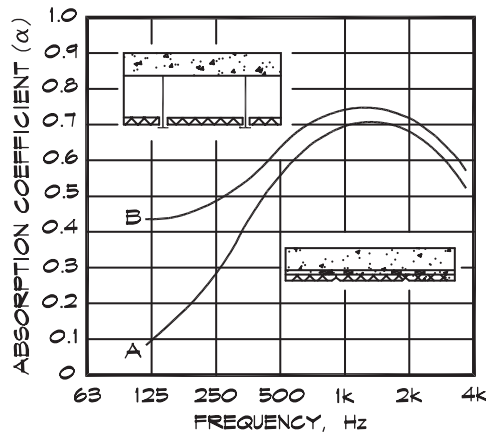
FIGURE 7.31   **Sound Absorption of Perforated Panels (Doelle, 1972)**

Sound absorption of perforated panel resonators with an isolation blanket in the air space. The open area (sound transparency) of the perforated facing has a considerable effect on the absorption.
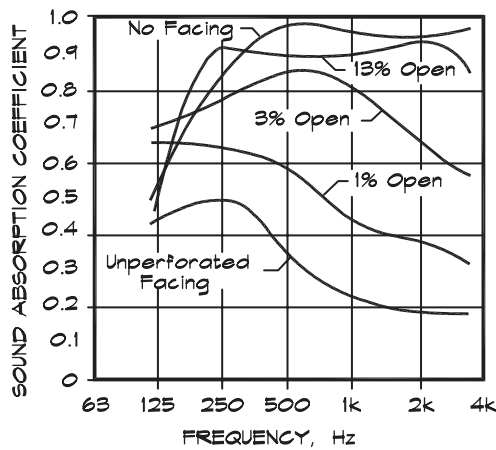
The effects of painting tiles are shown in Fig. 7.33 (Doelle, 1972). When a porous absorber is painted, its effectiveness can drop dramatically if the passage of air through its surface is impeded. This is especially true of acoustical tiles, which rely on holes or perforations to achieve their porosity. Unfaced fiberglass and duct liner boards that have a cloth face can be painted once with a light spray coat of nonbridging (water-base) paint without undue degradation. Multiple coats progressively reduce the high-frequency absorption. Clearly there are marked differences in absorptivity attributable to the thickness and number of coats of paint. Porous materials such as concrete block or certain types of stone need to be coated with paint or sealer to decrease their absorptivity (and increase their transmission loss) when they are used in churches or other spaces where a long reverberation time is desired.

FIGURE 7.32   Various Configurations of Wood Slats (Doelle, 1972)

The spacings shown are wide enough to allow sound passage through without appreciable loss.
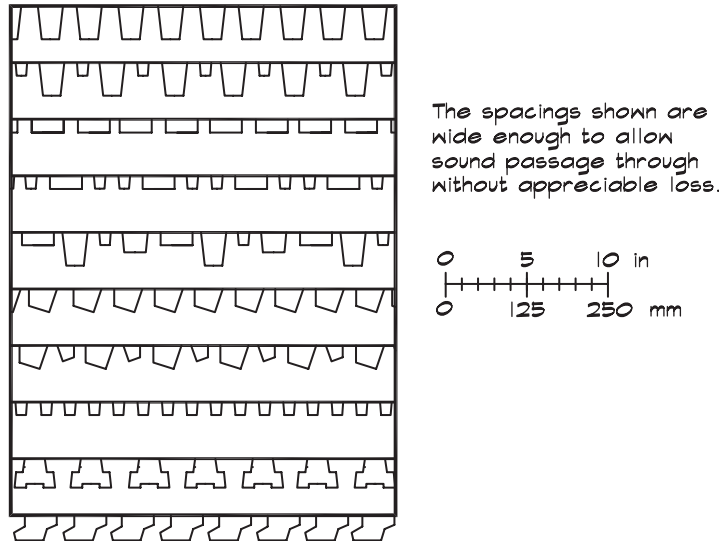
FIGURE 7.33   Effect of Paint on Absorptive Panels (Doelle, 1972)

The effect of paint on porous prefabricated acoustical units: (A) untreated surface (B) one coat of paint applied with a spray gun (C) one coat of paint applied with a brush (D) two coats of paint applied with a brush.
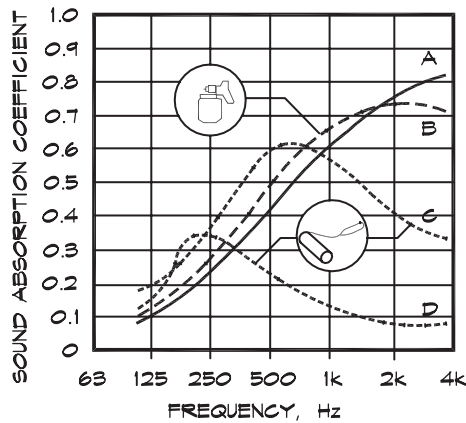
7.5   ABSORPTION BY NONPOROUS ABSORBERS

Unbacked Panel Absorbers

A freely suspended nonporous panel can absorb sound simply due to its mass reactance: that is, its induced motion. For this reason even solid walls provide some residual absorption, which may be only a few percentage points. Figure 7.34 shows the geometry of a normally incident sound wave impacting a solid plate. On the source side we have the incident pressure $\mathbf{p}_1$ and the reflected pressure $\mathbf{p}_3$; on the opposite side we have the transmitted pressure $\mathbf{p}_2$. The total pressure acting on the wall, $\mathbf{p}_1 + \mathbf{p}_3 - \mathbf{p}_2$, induces a motion in the panel according to Newton's law, $\mathbf{p}_1 + \mathbf{p}_2 - \mathbf{p}_3 = j\,\omega\,m\,\mathbf{u}$. Since the sound wave on the right side is radiating

FIGURE 7.34   Geometry of an Unbacked Panel Absorber
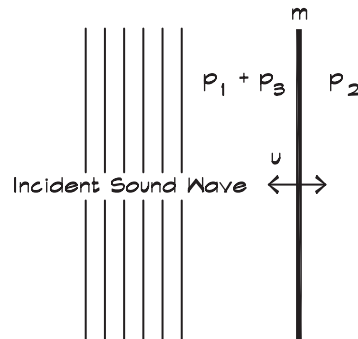
into free space we can write the pressure in terms of the particle velocity $\mathbf{p}_2 = \rho_0\, c_0\, \mathbf{u}$ to obtain the relationship $\mathbf{p}_1 + \mathbf{p}_3 - \rho_0\, c_0\, \mathbf{u} = j\,\omega\,m\,\mathbf{u}$ and from this, the impedance of the panel is (Kuttruff, 1963)

$$\mathbf{z} = j\,\omega\,m + \rho_0\, c_0 \qquad (7.96)$$

Now this expression can be inserted into Eq. 7.63 to calculate the normal incidence absorption coefficient

$$\alpha_n = \left[1 + \left(\frac{\omega\,m}{2\,\rho_0\, c_0} \right)^2 \right]^{-1} \qquad (7.97)$$

From this expression the absorption of windows and solid walls can be calculated; however, their residual absorption is small and only significant at low frequencies.

Air Backed Panel Absorbers

When a nonporous panel, as in Fig. 7.35, is placed in front of a solid surface with no contact between the panel and the surface, the panel can move back and forth, but is resisted by the air spring force.

FIGURE 7.35   Geometry of an Air Backed Panel Absorber
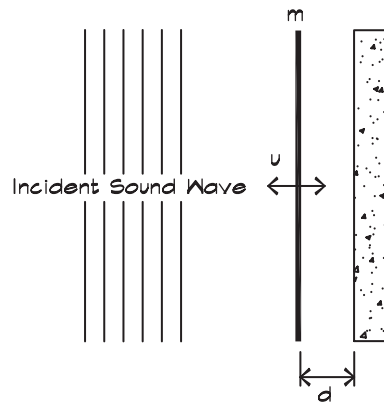
When there is a pressure differential across the panel Newton's law governs the motion

$$\Delta \mathbf{p} = \mathrm{m}\frac{d\,\mathbf{u}}{d\,t} = j\,\omega\,\mathrm{m}\,\mathbf{u} \tag{7.98}$$

where m is the mass of the panel per unit area. Using the same notation as before, with $\mathbf{p}_1 + \mathbf{p}_3$ being the pressure in front of the panel and $\mathbf{p}_2$ the pressure behind the absorber, we obtain

$$\frac{\mathbf{p}_1 + \mathbf{p}_3 - \mathbf{p}_2}{\mathbf{u}} = r_f + j\,\omega\,\mathrm{m} \tag{7.99}$$

and in a similar manner the composite assembly impedance is

$$\mathbf{z} = r_f + j\left[\omega\,\mathrm{m} - \rho_0\,c_0\,\cot{(k\,d)}\right] \tag{7.100}$$

When the depth, d, of the airspace behind the sheet is small compared to a wavelength, we can use the approximation $\cot{(k\,d)} \cong (k\,d)^{-1}$ so that

$$\mathbf{z} \cong r_f + j\left[\omega\,\mathrm{m} - \frac{\rho_0 c_0^2}{\omega\,d}\right] \tag{7.101}$$

As before, we can insert this expression into Eq. 7.63 to obtain the normal-incidence absorption coefficient (Kuttruff, 1973)

$$\alpha_n = \frac{4\,r_f\,\rho_0\,c_0}{\left(r_f + \rho_0 c_0\right)^2 + \left[(\mathrm{m}/\omega)\left(\omega^2 - \omega_0^2\right)\right]^2} \tag{7.102}$$

where we have used the resonant frequency from the bracketed term in Eq. 7.101, whose terms are equal at resonance.

$$\omega_r = \left(\frac{\rho_0\,c_0^2}{\mathrm{m}\,d}\right)^{\frac{1}{2}} \tag{7.103}$$

A simpler version of Eq. 7.103 is

$$f_r = \frac{600}{\sqrt{\mathrm{m}\,d}} \tag{7.104}$$

where m is the panel mass in kg / m^2 and d is the thickness of the airspace in cm. When the airspace is filled with batt insulation the resonant frequency is reduced to

$$f_r = \frac{500}{\sqrt{\mathrm{m}\,d}} \tag{7.105}$$

due to the change in sound velocity.

If the panel is impervious to flow, the flow resistance is infinite, and the absorption is theoretically infinite at resonance. Above and below resonance the absorption coefficient falls

FIGURE 7.36   Sound Absorption of a Suspended Panel (Doelle, 1972)

A 1/4" (6 mm) plywood panel spaced 3 in (75 mm) from the wall (A) with or (B) without a 1" thick fiberglass blanket in the airspace.
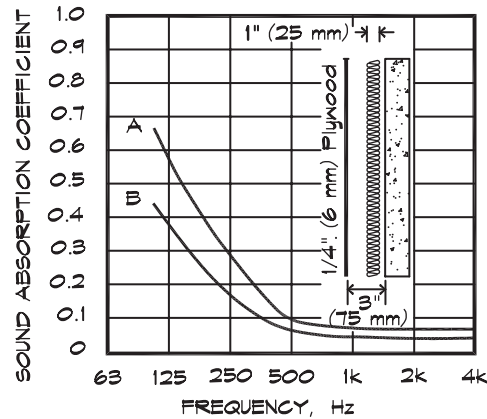
off. In this model the sharpness of the peak is determined by the amount of flow resistance provided by the panel. When damping is added to the cavity the propagation constant in the airspace becomes complex and adds a real part to the impedance, which broadens the resonance. The damping is provided by fiberglass boards or batting suspended in the airspace behind the panel. Figure 7.36 shows the typical behavior of a panel absorber with and without insulation.

Panel absorbers of this type that are tuned to a low resonant frequency are used as bass traps in studios and control rooms. Thin wood panels, mounted over an air cavity, produce considerable low-frequency absorption and, when there is little or no absorptive treatment behind the panel, this absorption is frequently manifest in narrow bands. As a result wood panels are a serious detriment to adequate bass response in concert halls. It is a common misunderstanding, particularly among musicians, that wood, and in particular thin wood panels that vibrate, contribute to good acoustical qualities of the hall. This no doubt arises from the connection in the mind between a musical instrument such as a violin and the hall itself. In fact, vibrating components in a hall tend to remove energy at their natural frequencies and return some of it back to the hall at a later time.

Perforated Panel Absorbers

If a perforated plate is suspended in a sound field, there is absorption due to the mass reactance of the plate itself, the mass of the air moving through the perforations, and the flow resistance of the material. If the perforated plate is mounted over an air cavity, there is also its impedance to be considered. There are quite a number of details in the treatment of this subject, whose consideration extends past the scope of this book. The goal here is to present enough detail to give an understanding of the phenomena without undue mathematical complication.

In a perforated plate the perforations form small tubes of air, which have a mass and thus a mass reactance to the sound wave. Figure 7.37 illustrates the geometry of a perforated plate. The holes in the plate have a radius a, and are spaced a distance e apart. The fluid velocity u_e on the exterior of the plate is raised to a higher interior velocity u_i as the fluid

FIGURE 7.37   Geometry of a Perforated Panel Absorber
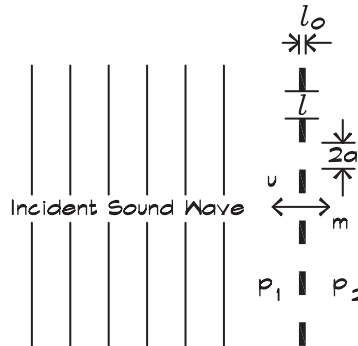
is forced through the holes. The ratio of velocities can be written in terms of the ratio of the areas, which is the porosity

$$\frac{\mathbf{u}_e}{\mathbf{u}_i} = \frac{\pi \, a^2}{e^2} = \sigma \tag{7.106}$$

The impedance due to the inertial mass of the air moving through the pores is

$$\frac{\mathbf{p}_1 - \mathbf{p}_2}{\mathbf{u}_e} = \frac{j \omega \pi \, a^2 \rho_0 \, l}{e^2} = \frac{j \omega \rho_0 \, l}{\sigma} \tag{7.107}$$

so the effective mass per unit area is

$$m = \frac{\rho_0 \, l}{\sigma} \tag{7.108}$$

The effective length of the tube made by the perforated hole in Eq. 7.107 is slightly longer than the actual thickness of the panel. This is because the air in the tube does not instantaneously accelerate from the exterior velocity to the interior velocity. There is an area on either side of the plate that contains a region of higher velocity and thus a slightly longer length. This correction is written in terms of the effective length

$$l = l_0 + 2 \, (0.8 \, a) \tag{7.109}$$

Usually the air mass is very small compared to the mass of the panel itself so that the panel is not affected by the motion of the fluid. If the area of the perforations is large and the panel mass M is small, the combined mass of the air and the panel must be used.

$$m_c = m \, \frac{M}{M + m} \tag{7.110}$$

When M is large compared with the mass of the air, m, then the combined mass is just the air mass.

The absorption coefficient for a perforated panel is obtained from Eq. 7.97, using the combined mass of the air and the panel. In commercially available products, perforated

FIGURE 7.38   Absorption of a Coated Perforated Panel (Wilhelmi Corp. Data, 2000)
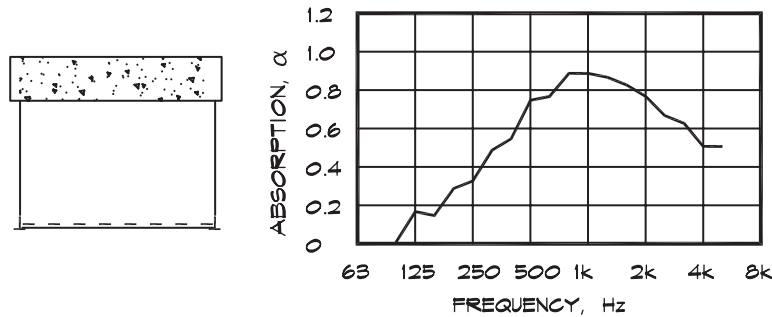
metal sheets are available with an air resistant coating, which adds flow resistance to the mass reactance of the air. These materials can be supported by T-bar systems and are effective absorbers. Absorption data for a typical product are shown in Fig. 7.38.

Perforated Metal Grilles

When a perforated panel is being used as a grille to provide a transparent cover for a porous absorber, it is important that there is sufficient open area that the sound passage is not blocked. In these cases the sound "absorbed" by the panel is actually the sound transmitted through the grille into the space beyond. The normal incidence absorption coefficient in this case is the same as the normal incidence transmissivity. Thus we can set it equal to the expression shown in Eq. 7.97

$$\tau = \left[1 + \left(\frac{\omega \, m_c}{2 \, \rho_0 \, c_0} \right)^2 \right]^{-1} \tag{7.111}$$

If the loss through a perforated panel is to be less than about 0.5 dB, the transmission coefficient should be greater than about 0.9, and the term inside the parenthesis becomes 0.33. At 1000 Hz the combined panel mass should be $0.04 \, \text{kg} / \text{m}^2$. For a 2 mm thick (.079") thick panel with 3 mm (.125") diameter holes, the effective length is about 4 mm and the required porosity calculates out to about 11%. This compares well with the data shown in Fig. 7.38, even though the calculation done here is for normal incidence and the data are for a diffuse-field measurement.

If a perforated panel is to be used as a loudspeaker grille, the open area should be greater, on the order of 30 to 40%. Increasing the porosity preserves more of the off-axis directional character of the loudspeaker's sound. Porosities beyond 40% are difficult to achieve in a perforated panel while still retaining structural integrity.

Air Backed Perforated Panels

When a perforated panel is backed with an airspace of a given depth, the back impedance of the airspace must be considered. The three contributing factors are the mass reactance of the air/panel system, the flow resistance of any filler material, and the stiffness of the air cavity behind the panel. The overall impedance is the sum of these three contributors, which at low

frequencies was given in Eq. 7.102

$$\mathbf{z} = j\,\omega\,m_c \;+\; r_f \;-\; \frac{j\,\rho_0\,c_0^2}{\omega\,d} \tag{7.112}$$

In the case of a perforated panel the combined mass of the panel and the air through the pores is used. We obtain the same result as Eq. 7.102, which we used for the absorption coefficient of a closed panel, and it is expressed in terms of the resonant frequency of the panel-cavity-spring-mass system.

$$\omega_0 = \left(\frac{\rho_0\,c_0^2}{m_c\,d}\right)^{\frac{1}{2}} \tag{7.113}$$

When we substitute the mass of the moving air in terms of the length of the tube and the porosity we get a familiar result—the Helmholtz resonator natural frequency. Here we have assumed that the mass of the air is much smaller than the panel mass

$$m_c = \frac{\rho_0\,l}{\sigma} = \frac{\rho_0\,l\,e^2}{\pi a^2} = \frac{\rho_0\,l\,V}{S\,d} \tag{7.114}$$

and

$$\omega_0 = \left(\frac{\rho_0\,c_0^2}{\rho_0\,l\,V\,/\,S}\right)^{\frac{1}{2}} = c_0\sqrt{\frac{S}{l\,V}} \tag{7.115}$$

It is apparent that a perforated panel with an air backing is acting like a Helmholtz resonator absorber and will exhibit similar characteristics, just as the solid panel did. The major difference is that the moving mass, in this case the air in the holes, is much lighter than the panel and thus the resonant frequency is much higher. These perforated absorbers are mainly utilized where mid-frequency absorption is needed.

The flow resistance of perforated panels can be measured directly or can be calculated from empirical formulas, such as that given by Cremer and Muller (1982)

$$r_f \cong 0.53\,\frac{e^2\,l_0}{a^3}\,\sqrt{f}\cdot 10^{-2}\ \text{mks rayls} \tag{7.116}$$

Figure 7.39 shows the absorption coefficient of a perforated plate in front of an airspace filled with absorptive material.

7.6   ABSORPTION BY RESONANT ABSORBERS

Helmholtz Resonator Absorbers

When a series of Helmholtz resonators is used as an absorbing surface, the absorption coefficient can be calculated in a manner similar to that used for a perforated plate.

FIGURE 7.39   **Absorption of a Perforated Panel (Cremer and Muller, 1982)**
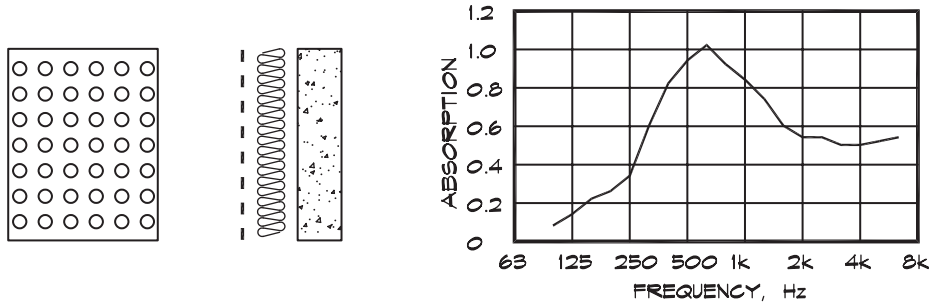
The resonant frequency is given by

$$f_0 = \frac{c_0}{2\pi} \sqrt{\frac{\pi\, a^2}{(l_0 + 1.7\, a)\, V}} \qquad (7.117)$$

where a is the radius of the resonator neck, l_0 is its length, and V its volume. The question then is how to calculate the depth, d, of the cavity. With a perforated plate the volume of the airspace was

$$d = \frac{V}{e^2} \qquad (7.118)$$

where e is the spacing between perforations. Using V as the volume of the Helmholtz resonator the normal-incidence absorption coefficient for a series of resonators is (Cremer and Muller, 1982)

$$\alpha_n = \frac{4\, r_f}{\rho_0\, c_0} \left[\left(1 + \frac{r_f}{\rho_0\, c_0}\right)^2 + \left(\frac{c_0\, e^2}{2\pi\, f_0\, V}\right)^2 \left(\frac{f_0}{f} - \frac{f}{f_0}\right)^2 \right]^{-1} \qquad (7.119)$$

Products based on the Helmholtz resonator principle are commercially available. Some are constructed as concrete masonry units with slotted openings having a fibrous or metallic septum interior fill. Absorption data on typical units are given in Fig. 7.40.

Mass-Air-Mass Resonators

A mass-air-mass resonant system is one in which two free masses are separated by an air cavity that provides the spring force between them. A typical example is a drywall stud wall, which acts much like the resonant panel absorber, except that both sides are free to move. The equation is similar to that used in the single-panel equation (Eq. 7.104) except that both masses are included. The resonant frequency is

$$f_{mam} = 600 \sqrt{\frac{m_1 + m_2}{d\, m_1\, m_2}} \qquad (7.120)$$

where m_1 and m_2 are the surface mass densities of the two surfaces in kg / m^2 and d is the separation distance between the sides in cm. When the cavity is filled with batt insulation,

FIGURE 7.40   Helmholtz Resonator Absorbers (Doelle, 1972)
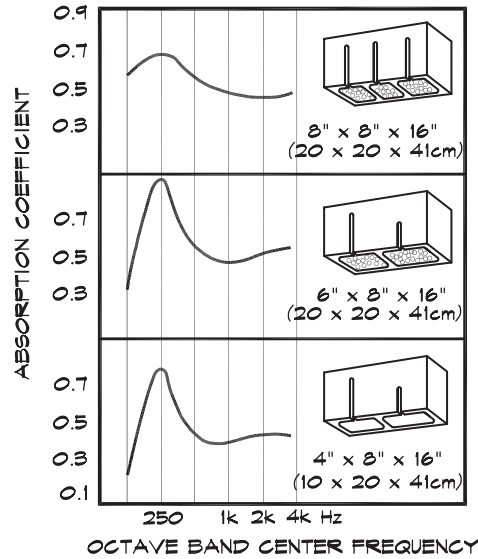
the constant changes from 600 to 500 because the sound velocity goes from adiabatic to isothermal. Away from resonance the absorption coefficient follows the relationship (Bradley, 1997)

$$\alpha(f) = \alpha_{mam} \left(\frac{f_{mam}}{f} \right)^2 + \alpha_s \qquad (7.121)$$

where $\alpha(f)$ = diffuse field absorption coefficient

α_{mam} = maximum absorption coefficient at f_{mam}

α_s = residual surface absorption coefficient at high frequencies

f = frequency (Hz)

f_{mam} = mass-air-mass resonant frequency (Hz)

Figure 7.41 shows the absorption coefficient for a single and double-layer drywall stud wall using $\alpha_{mam} = 0.44$ and $\alpha_s = 0.045$ for the single-layer wall and $\alpha_{mam} = 0.44$ and $\alpha_s = 0.06$ in the double-layer case. The same constants are used for batt-filled stud walls. The agreement shown in the figure between measured and predicted values is quite good.

Quarter-Wave Resonators

A hard surface having a well of depth d and diameter 2 a can provide absorption through reradiation of sound that is out of phase with the incident sound. These wells, shown in Fig. 7.42, are known as quarter-wave resonators because a wave reflected from the bottom returns a half wavelength or 180° out of phase with the wave reflected from the surface. When the length of the tube is an odd-integer multiple of a quarter wavelength it is out of phase with the incident wave and perfectly absorbing. The tube acts as a small resonant radiator, which can have both absorptive and diffusive properties.

As was the case in Eq. 7.89, the interaction impedance of a tube having a depth d is

$$\mathbf{z}_t = -j\,\rho_0\,c_0\,\cot(\boldsymbol{q}\,d) \qquad (7.122)$$

FIGURE 7.41   Resonant Absorption by a Stud Wall (Bradley, 1997)

Gypboard on 90 mm Steel Studs Without Batt Insulation
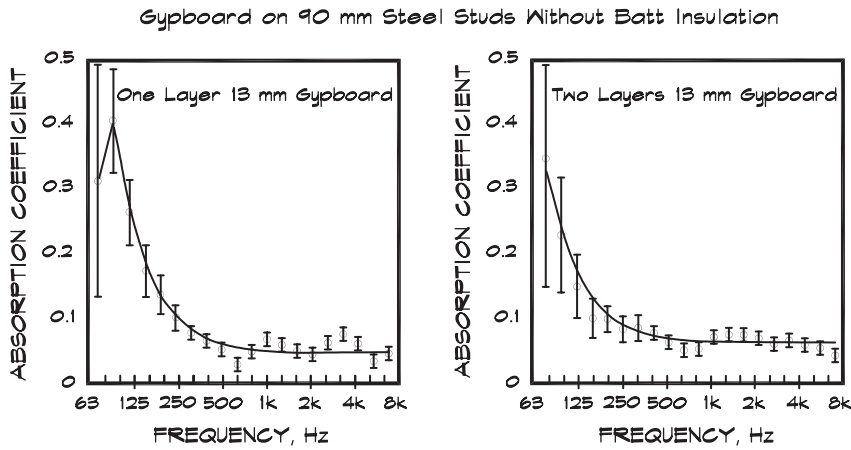
FIGURE 7.42   Quarter Wave Resonator

A quarter wave resonator tube in an infinite baffle.
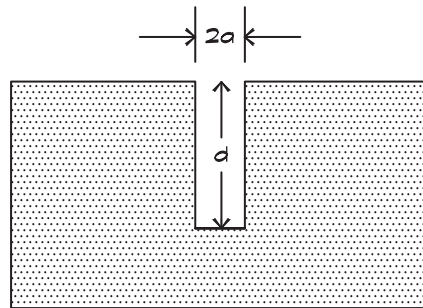
where q is the propagation constant. The tube has small viscous and thermal loss components and the imaginary part of the propagation constant, from an approximation originally due to Kirchoff, can be used to account for them

$$q \cong k \left[1 + \frac{0.31\,j}{2\,a\,\sqrt{f}} \right] \tag{7.123}$$

There are two impedances to be included in the analysis: one having to do with the interaction between the incoming wave and the end of the tube, which was given in Eq. 7.122; and the other having to do with the radiation of sound back out of the tube. The radiation impedance of the tube is that of a piston in a baffle and was examined in Eq. 6.67 and 6.69 in the near field. For low frequencies, where the width of the opening is much smaller than a wavelength, the radiation impedance is approximately (Morse, 1948)

$$\mathbf{z}_r \cong \rho_0 c_0 \left[\frac{1}{2}(k\,a)^2 + \frac{2\,j}{\pi k\,a} \right] \tag{7.124}$$

The pressure just outside the opening to the tube is the pressure radiated by the tube, plus twice the incident pressure, which is doubled due to its reflection off the rest of the hard

FIGURE 7.43   Absorption and Scattering Cross Sections of a Tube Resonator in a Wall (Ingard, 1994)
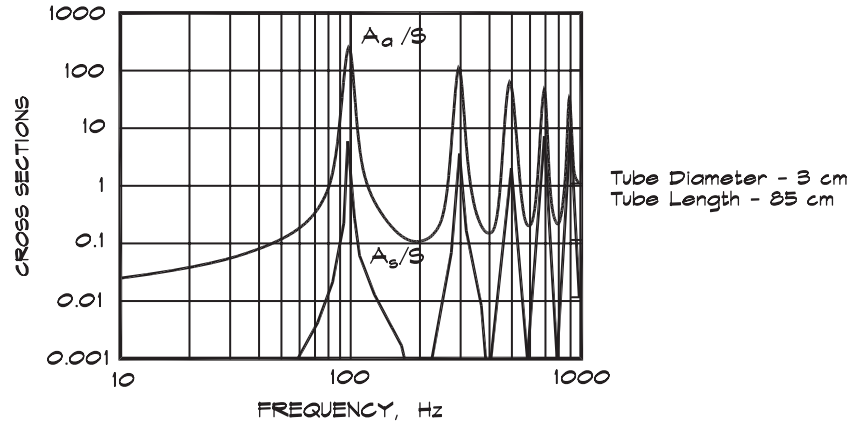
surface, $\mathbf{p}_{outside} = 2\,\mathbf{p}_i + \mathbf{p}_r$ where $\mathbf{p}_r = \mathbf{u}\,\mathbf{z}_r$. The pressure just outside the opening must match the pressure just inside the end of the tube, which is $\mathbf{p}_{inside} = -\mathbf{u}\,\mathbf{z}_t$. At the surface the pressures and the velocities must match, which leads to

$$\mathbf{u} = \frac{2\,\mathbf{p}_i}{\mathbf{z}_t + \mathbf{z}_r} \tag{7.125}$$

The absorption of a well in a surface can be expressed in terms of a cross section, defined (Ingard, 1994) as the power absorbed by the well divided by the intensity of the incident wave. The power absorbed by the resonator tube is

$$W_a = S\,|\,\mathbf{u}\,|^2\,w_t = S\,\frac{|\,\mathbf{p}_i\,|^2}{(\rho_0\,c_0)}\,\frac{4\,\rho_0\,c_0\,w_t}{|\,\mathbf{z}_t + \mathbf{z}_r\,|^2} \tag{7.126}$$

where $\mathbf{z} = w + j\,x$ and $S = \pi a^2$. Since $I_i = |\,\mathbf{p}_i\,|^2 / (\rho_0\,c_0)$ is the intensity of the incident wave, the power absorbed can be expressed as $W_a = A_a\,I_i$, where A_a is the absorption cross section.

$$A_a = S\,\frac{4\,\rho_0\,c_0\,w_t}{|\,\mathbf{z}_t + \mathbf{z}_r\,|^2} \tag{7.127}$$

A typical result, given in Fig. 7.43, shows strong peaks at the minima of the tube impedance. When the cross section is 100, it means that the tube is acting as a perfect absorber equal to 100 times its open area. Note that although a tube can be very effective at a given frequency, its bandwidth is very narrow.

   The same figure shows the cross section of the power scattered back by the tube. The tube behaves like a piston in a baffle when it radiates sound back out. It continues to resonate even after the initial wave has been reflected and emits sound at its resonant frequency for a short period of time. When the tube mouth dimension is small compared with a wavelength, it acts as an omnidirectional source that diffuses sound at that frequency.

FIGURE 7.44   Seat Absorption (Schultz and Watters, 1964)

Anomalous sound attenuation (after correction for spherical divergence)
for the early sound pressure level above the audience seating in a
concert hall, as a function of frequency. —— Various seats on the main
floor. —— First row in the first balcony.
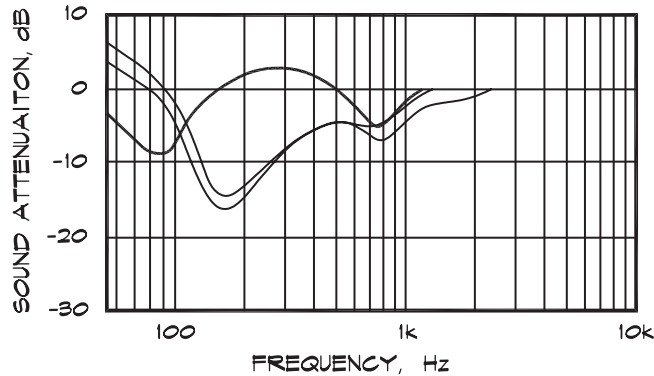
Absorption by Seats

It has been recognized for some time that theater seating, both occupied and unoccupied, produces excess attenuation of the direct sound coming from a stage, primarily at about 150 Hz, in much the same way as soft earth or vegetation contributes to excess ground attenuation. Padded opera chairs in a theater subdivide the floor into a regular lattice having a particular depth and spacing. As such they are like an array of quarter-wave resonators over which a sound wave, coming from the stage, grazes. In addition, the porous padding that covers them adds a resistive component to the impedance they present to a wave. A measurement of the excess attenuation due to theater seating, is shown in Fig. 7.44. Note that the dip is broader than the behavior predicted in Fig. 7.43 due to the resistive padding and the fact that the higher modes are not as prevalent. This may be due in part to the fact that the seat spacing is no longer small compared with a wavelength.

Ando (1985) published a detailed theoretical study of the absorptive properties of different chair-shaped periodic structures. Although the absorption varies somewhat with the precise shape selected, the basic pattern of the excess attenuation exhibits a steep dip at the frequency whose quarter wavelength is equal to the chair-back height above the floor. This agrees well with measurements made in concert halls. The excess grazing attenuation contributes to decreased bass response particularly in the orchestra seating section on the first floor of a hall. To help offset the extra attenuation, overhead reflectors can be used, which increase the angle of grazing incidence.

Quadratic-Residue Diffusers

One particular type of resonant tube absorber originally suggested by Schroeder (1979) uses a series of wells of different depths in a particular sequential order. Since each well is a small narrow-band omnidirectional radiator, a series of wells of different depths can cover a range of frequencies and provide diffusion over a reasonable bandwidth. The depth d_n of the nth well is chosen such that

$$d_n = \left(\frac{\lambda}{2N}\right) s_n \qquad (7.128)$$

where the sequence $s_n = (n^2 \bmod N)$ for $n = 0, 1, 2, \ldots$ and N is an odd prime number. For example, for $N = 11$ starting with $n = 0$, the sequence is [0, 1, 4, 9, 5, 3, 3, 5, 9, 4, 1] and then it repeats so that the period is N numbers long. This sequence of wells produces an essentially hemispheric polar reflection pattern within certain frequency limits. For a more detailed treatment, refer to Ando (1985).

The design process for a quadratic-residue diffuser is as follows:

1. Determine the frequency range f_{high} to f_{low} for the diffuser. The period N is given by the ratio f_{high} / f_{low}.

2. The width w of each well must be small compared with the wavelength of the highest frequency.

$$w \leq \frac{c_0}{2 \, f_{high}} \tag{7.129}$$

3. Calculate the depth of each well using Eq. 7.128, where $\lambda = \frac{c_0}{f_{low}}$ is called the design wavelength.

Figure 7.45 shows a side view of a quadratic-residue diffuser. One feature of quadratic-residue diffusers is that they absorb sound at low frequencies as might be expected from our previous analysis.

FIGURE 7.45   Quadratic Residue Diffusers

A typical quadratic residue diffuser based upon the prime number 17.

This page intentionally left blank

8
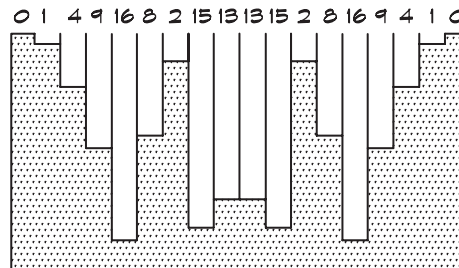
8.1   STANDING WAVES IN PIPES AND TUBES

Resonances in Closed Tubes

When a sound is generated within a solid enclosure such as a pipe, tube, or room, it expands naturally to fill the space. If the lateral dimensions of the space are small compared with a wavelength, as is the case with a tube, duct, or organ pipe, the sound propagates along the tube as a plane wave until it encounters an impedance boundary. If the tube is closed, the impedance at the end is very high, assumed to be infinite in a simple model, and the wave reflects back along the tube in the direction from which it came. If both ends are closed, the wave can reflect back and forth many times with little attenuation. The length of the tube in the direction of wave propagation determines the frequencies of the sound waves that persist under these conditions. These resonant frequencies are self-reinforcing since they combine in phase and continue for a long time after an exciting source is turned off. Other frequencies may be present initially; however, because of the geometry of the tube, they tend to cancel each other and average out to zero.

The behavior of the pressure in a one-dimensional plane wave propagating along a tube can be described using the formula

$$\mathbf{p} = \mathbf{A} \, \cos \, (k \, x + \phi) \tag{8.1}$$

where x is the distance from the end of the tube. If both ends of the tube are rigid this fact establishes the mathematical boundary conditions at the end points. At x = 0, the rigid boundary condition requires that the change in pressure with distance be zero at the boundary,

$$\left(\frac{\partial \mathbf{p}}{\partial x} \right)_{x=0} = 0 \quad \text{consequently } \phi = 0 \tag{8.2}$$

If the same condition is applied at the other termination

$$\left(\frac{\partial \mathbf{p}}{\partial x} \right)_{x=l} = \sin k \, l = 0 \tag{8.3}$$

which is satisfied for $k\,l = n\,\pi$. The resonant frequencies of the sound wave in a closed tube are given by

$$f_n = \frac{n\,c}{2\,l} \tag{8.4}$$

where n is an integer. The lowest frequency is called the fundamental mode, where $n = 1$, and the length of the tube is half of the fundamental wavelength.

Standing Waves in Closed Tubes

There are two possible solutions for plane wave propagation in a closed tube, one for sound moving in each direction. They take the form of two traveling waves

$$\mathbf{p} = \mathbf{A}\,\cos\,(-k\,x + \omega\,t) + \mathbf{A}\,\cos\,(k\,x + \omega\,t) \tag{8.5}$$

Using a trigonometric identity for the sum of two cosine waves, the equation can be written as

$$\mathbf{p} = 2\,\mathbf{A}\,\cos\,(k\,x)\,\cos\,(\omega\,t) \tag{8.6}$$

which is a standing wave. At any particular point a particle vibrates back and forth in simple harmonic motion at a particular frequency; however, its amplitude is larger or smaller depending on its location along the x axis.

The locations of the values of maximum pressure, called *antinodes*, occur at positions where

$$k\,x = 0, \pi,\ 2\pi,\ 3\pi, \ldots \tag{8.7}$$

which means

$$x = 0,\ \frac{\lambda}{2},\ \frac{2\,\lambda}{2},\ \frac{3\,\lambda}{2}, \ldots = \frac{n\,\lambda}{2} \tag{8.8}$$

These pressure antinodes occur at the rigid boundaries and have an amplitude that is twice the amplitude of a free traveling wave.

If we compare the behavior of a sound wave near a solid boundary to that of a water wave there is considerable similarity. When an ocean wave washes up against a sea wall the water rises to a height twice that of a freely propagating surface wave and falls by a similar amount. A water particle close to the wall experiences the maximum displacement up and down in response to the impact of the wave. With a sound wave there is a pressure doubling at a solid boundary resulting in a 6 dB increase in sound pressure level.

Minimum values of the sound pressure are called *nodes* and occur at positions where

$$k\,x = \frac{\pi}{2},\ \frac{3\,\pi}{2},\ \frac{5\,\pi}{2}, \ldots \tag{8.9}$$

and

$$x = \frac{\lambda}{4},\ \frac{2\,\lambda}{4},\ \frac{3\,\lambda}{4}, \ldots = \frac{n\,\lambda}{4} \tag{8.10}$$

The pressure node in the fundamental occurs at the quarter-wavelength point, which is at the midpoint of the enclosure. This leads to a phenomenon in studios, graphically described as

FIGURE 8.1   Standing Waves in a Closed-Closed Tube

Relative pressure is plotted along the length of the tube.
Areas of maximum velocity are indicated with arrows.

FIRST MODE $f_1 = \dfrac{c}{2l}$

SECOND MODE $f_2 = 2f_1 = \dfrac{c}{l}$
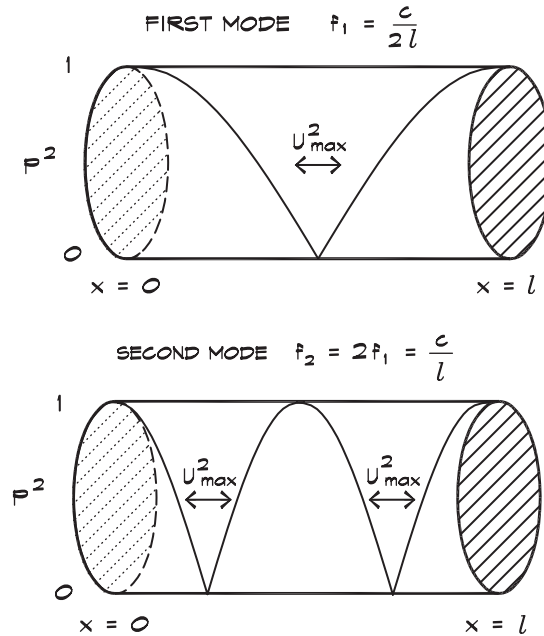
bass suckout—a lack of low-frequency energy at the mixer position near the center of the room, which is accentuated by the placement of bass loudspeakers at the ends of the room where the fundamental mode is easily excited.

An example of standing waves is shown in Fig. 8.1. These are constructed from continuously propagating rightward and leftward traveling waves. As they move past one another and combine, their sum produces the nodes and antinodes shown in the figure.

Standing Waves in Open Tubes

When a plane wave propagates along a tube that is open at the end, some of the sound energy is reflected from the open boundary. The reflection at this pressure release surface comes about due to the mass and springiness of the air column. An analogy may be drawn using the example of a toy paddle ball, where a rubber ball is attached to the paddle by means of an elastic band. When the ball strikes the paddle it is like a sound wave reflecting off the closed end of the tube. There is a pressure maximum, corresponding to squeezing the ball together, which forces a rebound. When the ball reaches the end of the elastic tether, it acts like the open end of the tube. A mass of air moves beyond the end of the tube and is pulled back by the elastic-spring force caused by the low-pressure region behind it. Air that is confined by the boundaries of the tube acts like a spring since the pressure cannot equalize in directions normal to the direction of wave propagation.

When both ends of the tube are open, the boundary condition requires that the acoustic pressure goes to zero at each end. The allowed solutions for the pressure take the form of a

FIGURE 8.2   Standing Waves in an Open-Open Tube

Relative pressure is plotted along the length of the tube.
Areas of maximum velocity are indicated with arrows.
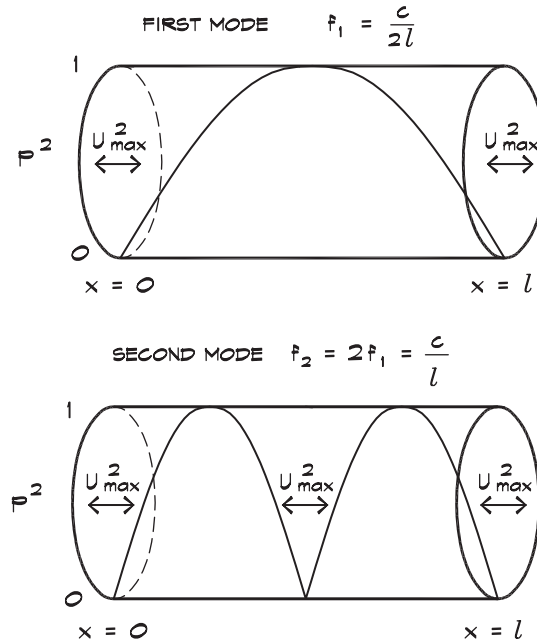
sine wave

$$\mathbf{p} = \mathbf{A} \; \sin k \; x = \mathbf{A} \sin \frac{n \, \pi \, x}{l} \qquad (8.11)$$

having the same resonant frequencies as those given in Eq. 8.4. The difference between a totally open pipe and a totally closed pipe is that, with an open pipe, the pressure maximum (antinode) in the fundamental frequency is at the center of the pipe, rather than at the ends, as shown in Fig. 8.2. This is to be expected since a sine wave is simply a cosine wave shifted by 90°.

In a real pipe the boundary condition is not as simple as a perfect pressure null. Instead there is a finite impedance at the end, which introduces a length correction much like that discussed in Chapt. 7 for perforated plates. For long pipes, this correction is generally small. Refer to Kinsler et al., (1982) for a more detailed treatment.

Combined Open and Closed Tubes

When a tube has one open end and one closed end, the boundary conditions can be applied to a sine wave to obtain

$$\mathbf{p} = \mathbf{A} \; \sin \; k \; x = \mathbf{A} \sin \frac{(2 \, n - 1) \, \pi \, x}{2} \qquad (8.12)$$

where n = 1, 2, and so on, and the resonant frequencies are

$$f_n = \frac{(2 \, n - 1) \, c_0}{4 \, l} \qquad (8.13)$$

FIGURE 8.3 **Standing Waves in a Closed-Open Tube**

Relative pressure is plotted along the length of the tube.
Areas of maximum velocity are indicated with arrows.

FIRST MODE $f_1 = \dfrac{c}{4l}$

SECOND MODE $f_2 = 3f_1 = \dfrac{3c}{4l}$
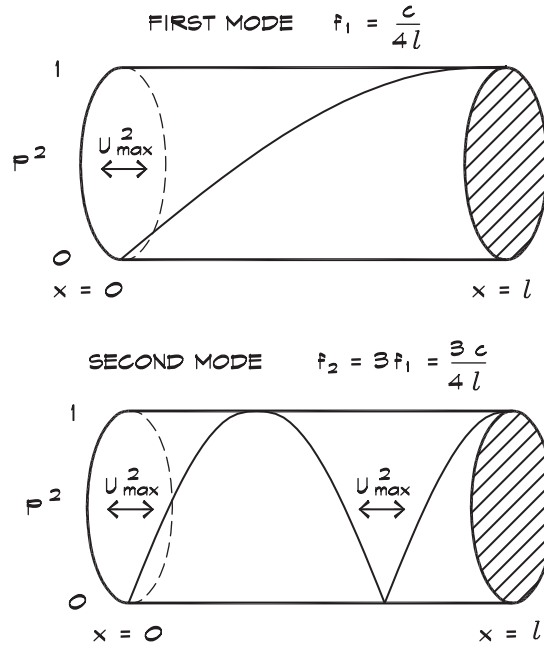
An organ pipe is open at the source end and can be either open or closed at the opposite end. For a given length the fundamental is one octave lower in a pipe, closed at one end, compared to one that is open. The even harmonics are missing; however, the density of modes remains the same as in the previous two examples. Fig. 8.3 shows the fundamental mode shapes.

8.2 SOUND PROPAGATION IN DUCTS

Rectangular Ducts

Sound waves that can propagate down a duct take on a form that is controlled by the duct dimensions relative to a wavelength. If a long duct is rectangular in cross section, standing waves can form in the lateral directions and a traveling wave in the third direction. The equation for the pressure takes the form

$$\mathbf{p} = \mathbf{A} \cos(k_x\, x) \cos(k_y\, y)\, e^{-j k_z z}\, e^{j \omega t} \tag{8.14}$$

where, in the lateral directions, there are allowed values of the wave number

$$k_x = m\pi/a \quad m = 0, 1, 2, \ldots \tag{8.15}$$

and

$$k_y = n\pi/b \quad n = 0, 1, 2, \ldots \tag{8.16}$$

where a and b are the lateral dimensions of the duct. The wave number k is related to its components

$$k^2 = k_x^2 + k_y^2 + k_z^2 \qquad (8.17)$$

and to the frequency

$$k = \frac{2\,\pi\,f}{c} = \frac{2\,\pi}{\lambda} \qquad (8.18)$$

The z-component of the wave number can be written as

$$k_z = \sqrt{k^2 - (k_x^2 + k_y^2)} \qquad (8.19)$$

and inserting Eq. 8.15 and Eq. 8.16 into Eq. 8.19 we obtain

$$k_z = k\sqrt{1 - (f_{mn}/f)^2} \qquad f \geq f_{mn} \qquad (8.20)$$

where

$$f_{m,n} = \frac{c}{2\,\pi}\sqrt{k_x^2 + k_y^2} = \frac{c}{2}\sqrt{\left(\frac{m}{a}\right)^2 + \left(\frac{n}{b}\right)^2} \qquad (8.21)$$

is known as the *cutoff frequency* for a given mode (m,n). The indices take on integer values m, n $= 0, 1, 2,$ and so on. By examining Eq. 8.20 it is clear that when $f = f_{m,n}$, k_z (m, n) $= 0$, and there is no wave propagation in the z direction for that particular mode. If the frequency is above cutoff, then k_z (m, n) is real and positive and the mode m,n is called a propagating mode. Consequently plane waves will not be formed when the lateral dimensions of the duct are wider than half a wavelength.

When the frequency is below cutoff for a particular mode, the wave number is imaginary and the mode, which dies out exponentially, is called *evanescent*.

$$\mathbf{k}_z = -j\,\mathbf{k}\sqrt{(f_{mn}/f)^2 - 1} \qquad f < f_{mn} \qquad (8.22)$$

Note that when m and n are zero, the wave is planar, and the lower cutoff frequency is zero. Thus there is no lower cutoff frequency for plane waves. The phenomenon of cutoff does not mean that the propagation of sound is cut off. It only means that below the cutoff frequency only plane waves propagate, and above the cutoff frequency only nonplane waves can be formed.

The propagation angle is the angle that a particular mode makes with the z axis. It is determined by using the relationship

$$k_z = k\,\cos\theta_{m,n} \qquad (8.23)$$

where the propagation angle is defined as

$$\theta_{m,n} = \cos^{-1}\left(\sqrt{1 - \left(f_{mn}/f\right)^2}\right) \qquad f \geq f_{mn} \qquad (8.24)$$

For plane waves the propagation direction is along the z axis since the cutoff frequency is zero. For a nonzero cutoff frequency, the propagation direction at cutoff for a particular mode is perpendicular to the z axis, so the wave does not propagate down the duct.

At high frequencies the propagation angle is small and the propagation direction approaches the z axis, which means that these modes tend to beam and have very little interaction with the duct walls. We will see the effects of this behavior in a later chapter. Lined ducts provide little attenuation both at very low frequencies, where the thickness of the lining is small compared with a wavelength, and at very high frequencies, where the wave does not interact with the lining due to beaming.

For a circular duct the cutoff frequency for the lowest mode is given by

$$f_{co} = 0.586 \, \frac{c_0}{d} \tag{8.25}$$

where d is the duct diameter. Above that frequency, modes can be formed across the duct, which combine with waves moving down the duct to generate cross or spinning modes depending on their shape.

Changes in Duct Area

If a plane wave, below the cutoff frequency, propagates down a duct that contains an abrupt change in area, energy will be reflected from the discontinuity. In Fig. 8.4 the area of the rectangular or conical duct changes abruptly from S_1 to S_2 at a point in the duct that marks the transition from region 1 to 2. At this point the pressure and volume velocity amplitudes must be continuous.

$$\mathbf{p}_i + \mathbf{p}_r = \mathbf{p}_t \quad \text{and} \quad S_1 \left(\mathbf{u}_i - \mathbf{u}_r \right) = S_2 \, \mathbf{u}_t \tag{8.26}$$

FIGURE 8.4   Area Changes in Various Types of Ducts

A. Transition, Round, Conical
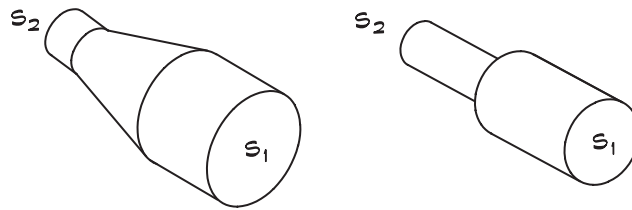
B. Transition, Rectangular, Pyramidal
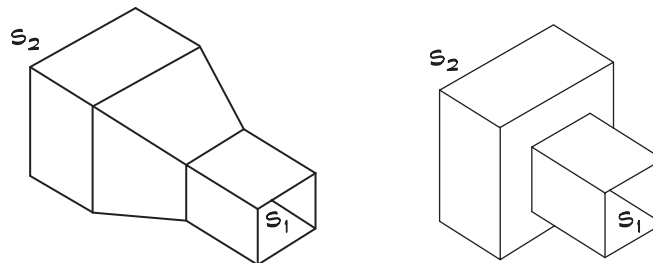
where the subscript i refers to the incident wave, r to the reflected wave, and t to the transmitted wave. The boundary conditions yield

$$\frac{\mathbf{p}_i + \mathbf{p}_r}{\mathbf{u}_i - \mathbf{u}_r} = \frac{S_1}{S_2}\left(\frac{\mathbf{p}_t}{\mathbf{u}_t}\right) \tag{8.27}$$

and using the plane wave relationships $\mathbf{u} = \mathbf{p}/\rho_0\,c_0$

$$\frac{\rho_0\,c_0\,(\mathbf{p}_i + \mathbf{p}_r)}{\mathbf{p}_i - \mathbf{p}_r} = \frac{S_1}{S_2}\left(\frac{\mathbf{p}_t}{\mathbf{p}_t/\rho_0\,c_0}\right) = \frac{\rho_0\,c_0\,S_1}{S_2} \tag{8.28}$$

The reflected amplitude coefficient is

$$\mathbf{r} = \frac{\mathbf{p}_r}{\mathbf{p}_i} = \frac{S_1 - S_2}{S_1 + S_2} \tag{8.29}$$

and the sound energy reflection coefficient is

$$\alpha_r = \left[\frac{S_1 - S_2}{S_1 + S_2}\right]^2 \tag{8.30}$$

and the transmission coefficient is

$$\tau = 1 - \left[\frac{S_1 - S_2}{S_1 + S_2}\right]^2 \tag{8.31}$$

The change in level in decibels, experienced by a plane wave passing through the area change boundary, is

$$\Delta\,L_a = 10\,\log\tau = 10\,\log\left[1 - \left(\frac{S_1 - S_2}{S_1 + S_2}\right)^2\right] \tag{8.32}$$

Clearly when the areas are equal there is no loss. For a 50% area reduction the loss is about 1.8 dB. Note that the formula can be used for an area increase or decrease with the same result. The loss due to changes in area contributes to the low-frequency attenuation in duct silencers as well as to the loss in plenums and expansion chambers.

Expansion Chambers and Mufflers

If a plane wave propagates down a duct and enters an area expansion for a certain distance followed by a contraction, there is an acoustical loss. This fundamental shape change is the basis of a reactive (nonlined) muffler used to quiet internal combustion engines and other noise sources, where a dissipative interior liner is not practical. It also furnishes most of the low-frequency loss in small plenums. Figure 8.5 illustrates the configuration.

When a plane wave encounters the changes in area, the pressure and volume velocities must be matched at the two boundaries. This leads to four boundary conditions similar to

FIGURE 8.5   Expansion Chamber Muffler
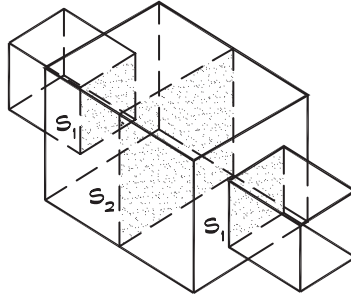
those in Eq. 8.26, which must be solved for the coefficients (Davis, 1957). At the first boundary

$$\mathbf{p}_{i\,1} + \mathbf{p}_{r\,1} = \mathbf{p}_{t\,2} + \mathbf{p}_{r\,2} \tag{8.33}$$

$$\left(\mathbf{u}_{i\,1} - \mathbf{u}_{r\,1}\right) = m\left(\mathbf{u}_{t\,2} - \mathbf{u}_{r\,2}\right) \tag{8.34}$$

where $m = S_2/S_1$. At the second boundary

$$\mathbf{p}_{t\,2}\,e^{-j\,k\,l} + \mathbf{p}_{r\,2}\,e^{j\,k\,l} = \mathbf{p}_{t\,3} \tag{8.35}$$

$$m\left[\mathbf{p}_{t\,2}\,e^{-j\,k\,l} - \mathbf{p}_{r\,2}\,e^{j\,k\,l}\right] = \mathbf{p}_{t\,3} \tag{8.36}$$

When these four equations are solved simultaneously, the transmission coefficient can be obtained from $\tau = \dfrac{\mathbf{p}_{t\,3}}{\mathbf{p}_{i\,1}}$

$$\tau = \left[\cos k\,l + j\,\frac{1}{2}\left(m + \frac{1}{m}\right)\sin k\,l\right]^{-1} \tag{8.37}$$

and the transmission loss through the expansion is

$$\Delta\,L_m = 10\,\log\left[1 + \frac{1}{4}\left(m - \frac{1}{m}\right)^2 \sin^2 k\,l\right] \tag{8.38}$$

Recall that these equations were obtained by assuming plane waves in all three sections of the duct. For this equation to hold, the lateral dimensions of the chamber must be smaller than $0.8\,\lambda$ (Beranek, 1992). A graph of the attenuation versus normalized length is shown in Fig. 8.6. Notice that the result repeats each time $k\,l = \pi$.

8.3   SOUND IN ROOMS

The analysis of sound in rooms falls into regions according to the frequency (wavelength) of the sound under consideration. At low frequencies, where the wavelength is greater than twice the length of the longest dimension of the room, only plane waves can be formed and the room behaves like a duct. This condition can occur in very small rooms. Above the cutoff

FIGURE 8.6   Transmission Loss of a Single Expansion Chamber (Beranek, 1971)
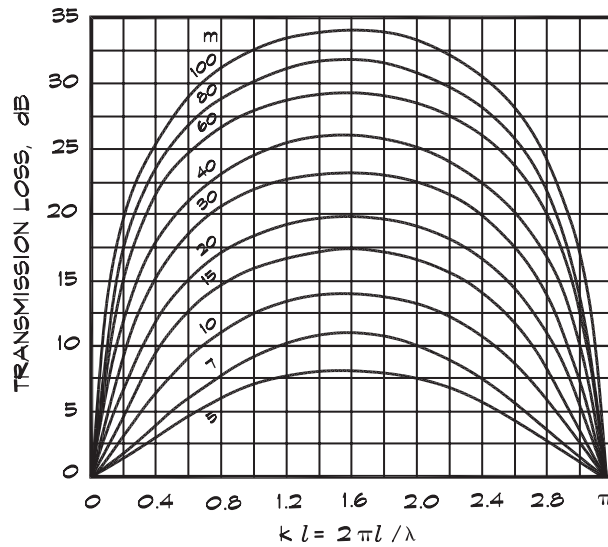
Transmission loss of a single expansion chamber of length l and $S_2 / S_1 = m$. For values of $k\,l$ above π use $k\,l$ mod π.

frequency of a room, normal modes are formed, which are manifest as standing waves having localized regions of high and low pressure. At still higher frequencies the density of modes is so great that there is a virtual continuum in each frequency range and it becomes more useful to model room behavior based on the energy density or other statistical considerations.

Normal Modes in Rectangular Rooms

Let us consider a rectangular room having dimensions l_x, l_y, and l_z. When the room is ensonified and then the sound source removed, certain frequencies persist, much like those that remained in the case of a closed tube. In this case, however, the modes may develop in several directions, since no room dimension is small compared with a wavelength. If we apply the three-dimensional wave equation in rectangular coordinates given as Eq. 6.32 and write a general solution, it takes the form of

$$\mathbf{p} = \mathbf{A}\, e^{j\,(\omega t - k_x\, x - k_y\, y - k_z\, z)} \tag{8.39}$$

If this expression is substituted into Eq. 6.32, the values for the wave numbers k_x, k_y, and k_z must satisfy the relationship

$$k = \frac{\omega}{c} = \sqrt{k_x^2 + k_y^2 + k_z^2} \tag{8.40}$$

We can replace the negative signs in Eq. 8.39 with one or more positive signs to obtain seven additional equations, which represent the group of waves moving about the room and reflecting off the boundaries. When we apply the boundary conditions as we did for a closed tube, we find that the allowed values of the wave number are

$$k_i = \frac{n_i\, \pi}{l_i} \tag{8.41}$$

where i refers to the x, y, and z directions. The equation for the sound-pressure standing wave in the room, which has the same form as Eq. 8.6, is separable into three components

$$\mathbf{p} = 8\,\mathbf{A}\,\cos\left(\frac{n_x\,\pi x}{l_x}\right)\,\cos\left(\frac{n_y\,\pi y}{l_y}\right)\,\cos\left(\frac{n_z\,\pi z}{l_z}\right)\,e^{j\omega t} \tag{8.42}$$

The natural frequencies are

$$f_{\ell\,m\,n} = \frac{c_0}{2}\left[\left(\frac{\ell}{l_x}\right)^2 + \left(\frac{m}{l_y}\right)^2 + \left(\frac{n}{l_z}\right)^2\right]^{\frac{1}{2}} \tag{8.43}$$

where the ℓ, m, and n are integers that indicate the number of nodal planes perpendicular to the x, y, and z axes.

The normal modes of a rectangular room are referenced by whole number indices represented by the three letters ℓ, m, and n. The 1,0,0 mode, for example, would be the fundamental frequency in the x direction. The 2,1,0 mode is a tangential mode in the x and y directions as in Fig. 8.7. If we take a room having dimensions $7 \times 5 \times 3$ m high ($23 \times 16.4 \times 9.8$ ft) and calculate the first few modes, the results would be those in Table 8.1.

Several things are important to notice. If the room dimensions are a low integer multiple of one another, then modal frequencies will coincide. Under these conditions the energy in

FIGURE 8.7   Standing Waves in a Rectangular Room (Bruel and Kjaer, 1978)
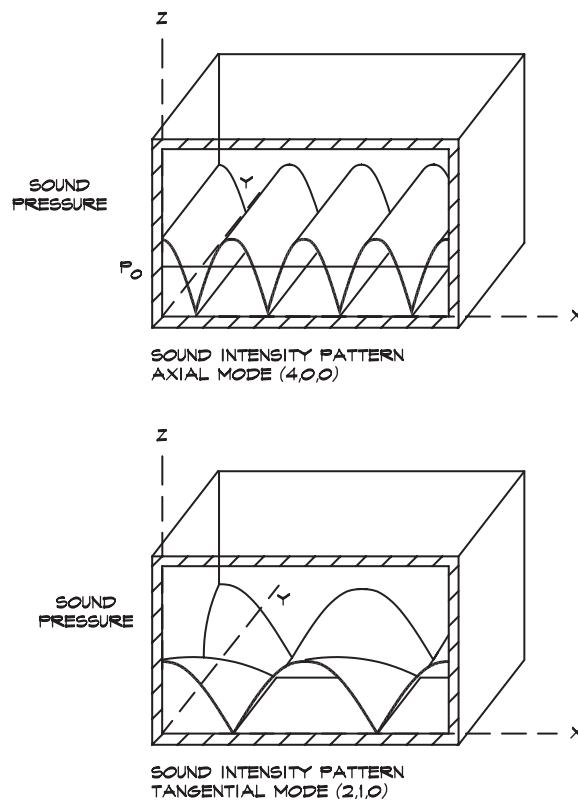
TABLE **8.1** **Normal Modes of a Rectangular Room**

Number	n_x	n_y	n_z	f_n (Hz)
1	1	0	0	24.6
2	0	1	0	34.5
3	1	1	0	42.4
4	2	0	0	49.2
5	0	0	1	57.4
6	2	1	0	60.1

the room will tend to coalesce into a few modes, which will strongly color the sound. Note also that as the frequency increases, the resonances move closer and closer together. They segue from a discrete set of identifiable frequencies into a continuum of modes.

The number of normal modes in a given frequency range can be calculated by plotting the allowed wave numbers in a three-dimensional graph, known as k-space (Fig. 8.8), having dimensions of wave number in the x, y, and z directions. A given value of k in Eq. 8.40 is represented as a point at the intersection of three lattice lines. The total number of frequencies is contained in a sphere having radius k in the positive octant of the sphere divided by the unit volume per k point. The distance between each k_i value is $\dfrac{\pi}{l_x}$, $\dfrac{\pi}{l_y}$, or $\dfrac{\pi}{l_z}$ and the unit volume per k point is $\dfrac{\pi^3}{V}$, where $V = l_x\, l_y\, l_z$ is the volume of the room. The number of allowed k values between 0 and a given value of k is

$$N_f = \frac{\pi k^3/6}{\pi^3/V} = \frac{4\pi}{3}\left(\frac{f}{c_0}\right)^3 \tag{8.44}$$

In calculating this number we have left out all k values outside of the positive octant, so we need to add back a correction for frequencies located on the axis planes, which are counted

FIGURE **8.8** **Normal Modes Falling between Two Frequencies**
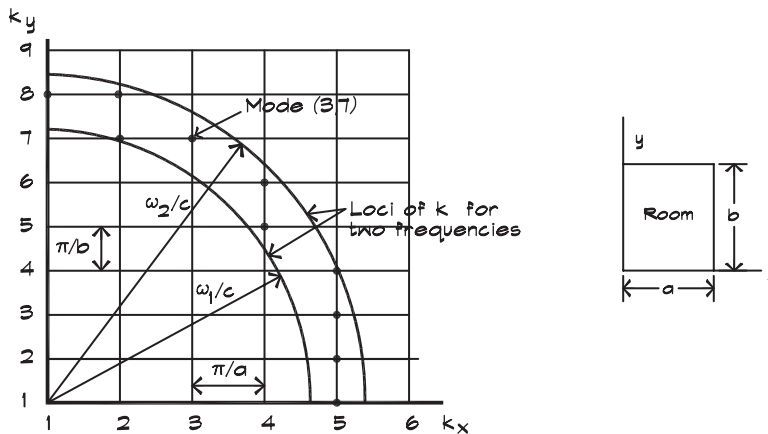
as one half, and on the axes themselves, which are counted as one quarter of their actual value. This yields

$$N_f = \frac{4\pi}{3} V \left(\frac{f}{c_0}\right)^3 + \frac{\pi}{4} S \left(\frac{f}{c_0}\right)^2 + \frac{L}{8} \left(\frac{f}{c_0}\right) \tag{8.45}$$

where S is the area of all the walls and L is the sum of all the edge lengths.

The number of modes in a given frequency range can be determined by taking the derivative of Eq. 8.45 with respect to frequency,

$$\frac{d\,N_f}{d\,f} = 4\pi V \frac{f^2}{c_0^3} + \frac{\pi}{2} S \frac{f}{c_0^2} + \frac{L}{8\,c_0} \tag{8.46}$$

At high frequencies the density of modes is extremely large—for all practical purposes, a continuum. For the room dimensions given in Fig. 8.8, at 1000 Hz, the modal density is 34 modes per Hertz.

Preferred Room Dimensions

A number of authors, including Bolt, Rettinger, and others have offered suggestions on preferred room dimensions for listening rooms and studios. These are given in terms of the ratios of the lengths of the sides of a rectangular room. The one published by Bolt is shown in Fig. 8.9.

FIGURE 8.9 Preferred Dimensions of a Rectangular Room (Bolt, 1946)

The curve encloses dimension ratios of width to length of a rectangular room having a unity ceiling height to give a smooth response at low frequencies.
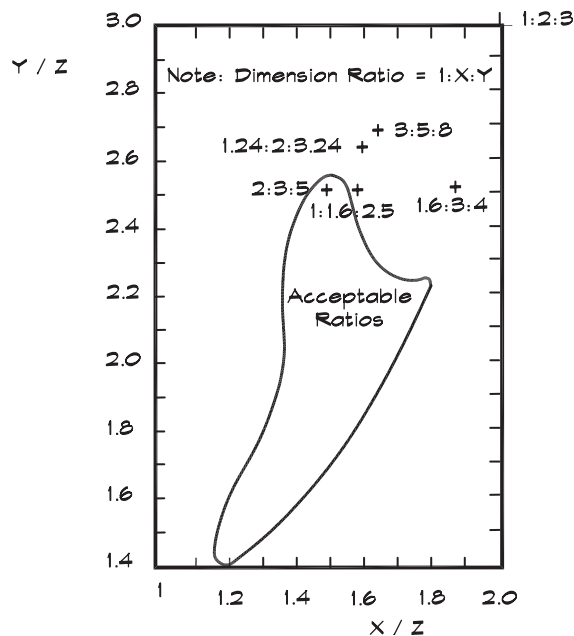
Recommendations such as those shown in Fig. 8.9 are most useful in designing reverberation chambers for acoustical-testing purposes, when a rectangular room is desired. They could be useful in the design of small studios; however, sound studios are rarely built in a rectangular shape. Normal-mode calculations for nonrectangular rooms are more difficult and can be done using finite element methods.

8.4   DIFFUSE-FIELD MODEL OF ROOMS

In a room whose dimensions are large enough that there is a sufficient density of modes, it is customary to describe the space in terms of a statistical model known as a diffuse field. A diffuse field is one in which there is an equal energy density at all points in the room. This implies that there is an equal probability that sound will arrive from any direction.

Schroeder Frequency

The transition between the normal-mode model and the statistical model is not a bright line, but is generally taken to occur at a modal spacing that has at least three modes within a given mode's half-power bandwidth. This point is marked by the so-called *Schroeder frequency* (Schroeder, 1954 and 1996), which is defined in metric units as

$$f_s = 2000 \sqrt{\frac{T}{V}} \qquad (8.47)$$

where V is the volume of the room and T is the reverberation time. In FP units, where V is in cubic feet, the multiplication constant is 12,000. Above the Schroeder frequency it is appropriate to analyze the room without having to take into account the behavior of its normal modes.

   The Schroeder frequency allows us to subdivide the room behavior into regions. Figure 8.10 (Davis and Davis, 1987) shows a plot of the type of behavior we can expect from the sound pressure level in a room plotted against frequency. It also indicates the techniques that can be used to control the steady state room response. In small rooms, where the normal mode region can extend to several hundred Hertz, a statistical model can only be used at relatively high frequencies.

FIGURE 8.10   Controllers in Steady State Room Response (Davis and Davis, 1987)
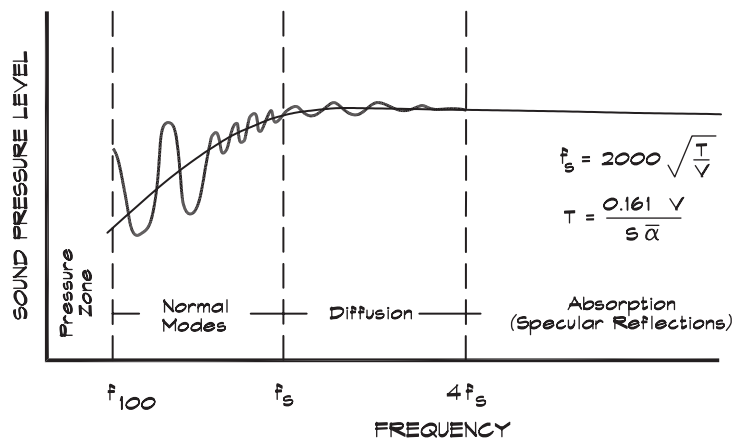
Mean Free Path

Above the Schroeder frequency, sound waves in a room can be treated as rays or particles in terms of their reflections off the room's surfaces. This can be done by following the ray path around a room and studying its interaction with the walls, or by constructing an image source for each reflecting surface and summing their contributions at the receiver. If we follow a sound ray around a room it will travel until it encounters a surface. The sound particle travels a distance (c_0 t) in time t and if it undergoes N collisions during that time, the average distance between collisions is

$$\Lambda = \frac{c_0\, t}{N} = \frac{c_0}{n} \tag{8.48}$$

where *n* is the average number of collisions per unit time and Λ is the *mean free path* between collisions. Knudsen (1932) determined the mean free path experimentally for a number of differently shaped rectangular rooms, and others (Kuttruff, 1973) have derived the equation from first principles. The result is

$$\Lambda = \frac{4\,V}{S_T} \tag{8.49}$$

where V is the volume and S_T is the total surface area of the room. Here both Λ and *n* are averages and Eq. 8.49 holds only for diffuse-field conditions. Using Eq. 8.48 the average collision frequency can be obtained

$$n = \frac{c_0\, S_T}{4\,V} \tag{8.50}$$

Decay Rate of Sound in a Room

The reciprocal of the average collision frequency is the mean time between collisions, which for a diffuse field is

$$t = \frac{4\,V}{c_0\, S_T} \tag{8.51}$$

If we ride along with the sound ray, the energy density in the vicinity of the ray after each reflection, shown in Fig. 8.11, is

$$D\,(t) = D_0\,(1 - \overline{\alpha})$$
$$D\,(2\,t) = D_0\,(1 - \overline{\alpha})^2 \tag{8.52}$$
$$D\,(n\,t) = D_0\,(1 - \overline{\alpha})^n$$

The total number of reflections n is the total time divided by the mean time between reflections, so we can write

$$D\,(t) = D_0\,(1 - \overline{\alpha})^{(c_0\, S_T/4\,V)\,t} \tag{8.53}$$

Now using the identity

$$(1 - \overline{\alpha}) = e^{\ln(1-\overline{\alpha})} \tag{8.54}$$

FIGURE 8.11   **Path of a Sound Ray Having Energy Density D**

Path of a sound wave modelled as a ray as it reflects off of surfaces having an average absorption coefficient $\overline{\alpha}$. The surfaces are spaced a distance equal to the mean free path $l = 4 V/S_T$ apart.
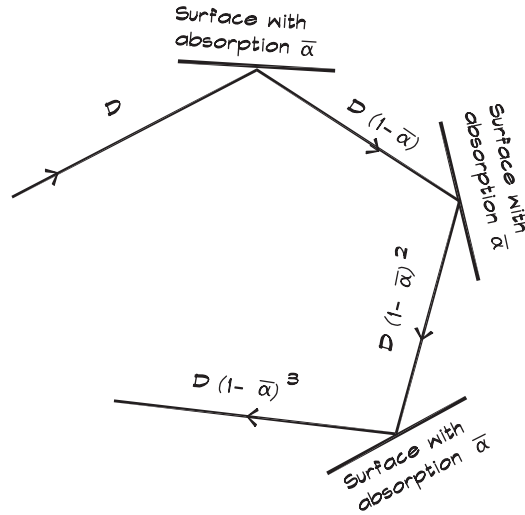
we obtain

$$D(t) = D_0 \, e^{-(c_0 \, S_T / 4 \, V)[-\ln(1-\overline{\alpha})] \, t} \tag{8.55}$$

Multiplying each side by the speed of sound, we can convert this equation into a sound pressure level as a function of time

$$L_p(t) = L_p(t = 0) - 4.34 \, \frac{c_0 \, S_T}{4V} \, [-\ln(1 - \overline{\alpha})] \, t \tag{8.56}$$

which is the rate of decay of sound in a room under diffuse-field conditions. Note that the average absorption coefficient can be expressed as a weighted average of the individual coefficients for each of the surfaces of the room.

$$\overline{\alpha} = \frac{S_1 \, \alpha_1 + S_2 \, \alpha_2 + S_3 \, \alpha_3 + \cdots + S_n \alpha_n}{S_T} \tag{8.57}$$

Sabine Reverberation Time

The idea that there exists a characteristic time for sound to die out in a room originated with Wallace Clement Sabine. When he undertook the task of correcting a problem of unintelligible speech in the Fogg Art Museum lecture hall at Harvard College; the sound in the room would persist for over 5 seconds. Because an English-speaking person can complete about 15 syllables in that time, most of the words were impossible to understand (Egan, 1988). Sabine measured the *reverberation time*, the time it took for the sound level to drop 60 dB, for varying amounts of absorptive materials. He borrowed 3-inch thick seat cushions from the nearby Sanders Theater and found that the more cushions he placed around the room, the more quickly the sound would die out. When 550 cushions were arranged in the

space on the platform, seats, aisles and the rear wall, the reverberation time had decreased to about 1 second. The empirical formula he discovered, now called the Sabine reverberation time, is

$$T_{60} = .049 \frac{V}{A} \tag{8.58}$$

where T_{60} = reverberation time, or the time it takes for sound to decrease by
          60 dB in a room (s)
     V = volume of the room (cu ft)
     A = total area of absorption in the room (sabins)
       = $S_1 \, \alpha_1 + S_2 \, \alpha_2 + S_3 \, \alpha_3 + \cdots + S_n \, \alpha_n$

The standard unit of absorption, now called the sabin in his honor, has units of sq ft. The metric sabin has units of sq m. In metric units the Sabine formula is

$$T_{60} = 0.161 \frac{V}{A} \tag{8.59}$$

Norris Eyring Reverberation Time

Carl Eyring published (1930) a theory of reverberation time in rooms based on an idea that was attributed to R. F. Norris (Andree, 1932). Using the arguments that lead to Eq. 8.56, he set the difference in level to 60 dB and calculated the resulting decay time

$$T_{60} = \frac{4 \, V \, (60)}{-4.34 \, c_0 \, S_T \, \ln \, (1 - \overline{\alpha})} = \frac{0.161 \, V}{-S_T \, \ln \, (1 - \overline{\alpha})} \tag{8.60}$$

where the volume is in metric units. In FP units the equation is

$$T_{60} = \frac{.049 \, V}{-S_T \, \ln \, (1 - \overline{\alpha})} \tag{8.61}$$

This equation is more accurate in dead (very absorptive) rooms than the Sabine equation. For example, in a perfectly absorbing room with a given area of absorption, the Sabine equation will give a nonzero result whereas the Eyring equation will correctly give zero. Care must be exercised in using the Norris Eyring equation with absorption coefficients measured with the Sabine equation, since occasionally an absorption coefficient greater than one is obtained. All Norris Eyring coefficients must be less than one.

Derivation of the Sabine Equation

When value of the average absorption coefficient is small, that is when we have an acoustically live space, we can use a series expansion for the natural logarithm,

$$\ln \, (x) = (x - 1) - \frac{1}{2} \, (x - 1)^2 + \frac{1}{3} \, (x - 1)^3 - \ldots$$

to obtain an approximation for small ($\overline{\alpha} < 0.2$) values of the average absorption coefficient,

$$-\ln \, (1 - \overline{\alpha}) \cong \overline{\alpha} \tag{8.62}$$

This leads us back to the Sabine equation, which is accurate under these conditions. The Sabine equation is the preferred formula for use in normal rooms and auditoria.

Millington Sette Equation

The average absorption coefficient for a given room is usually not readily available, but may be calculated from the absorption coefficients of the individual surfaces (Millington, 1932 and Sette, 1933)

$$S_T \, \overline{\alpha} = \sum_{i=1}^{n} S_i \, \alpha_i \tag{8.63}$$

which was adopted by Eyring.

$$T_{60} = \frac{0.161 \, V}{-S_T \, \ln \left[1 - \sum (S_i \, \alpha_i / S_T) \right]} \tag{8.64}$$

Highly Absorptive Rooms

When the average absorption coefficient for a room is large ($\overline{\alpha} > 0.5$), another series expansion for the natural logarithm can be applied to the Norris Eyring equation, namely

$$\ln(x) = \frac{x-1}{x} + \frac{1}{2} \left(\frac{x-1}{x} \right)^2 + \frac{1}{3} \left(\frac{x-1}{x} \right)^3 + \dots$$

to obtain

$$-\ln(1 - \overline{\alpha}) \cong \frac{\overline{\alpha}}{1 - \overline{\alpha}} \tag{8.65}$$

which yields the absorbent room approximation for the reverberation time

$$T_{60} \cong \frac{0.161V}{S_T \left(\dfrac{\overline{\alpha}}{1 - \overline{\alpha}} \right)} \tag{8.66}$$

This equation is limited to relatively high values of the average absorption coefficient. Neither Eq. 8.66 or the Norris Eyring equation can be used when average absorption coefficients exceed a value of one—a relatively common occurrence since we use the Sabine formula to measure absorption.

Air Attenuation in Rooms

In Chapt. 4 we discussed how sound is attenuated as it moves through the atmosphere due to its interaction with the air molecules. If we assume there is an attenuation constant that characterizes the atmospheric loss in terms of so much per distance, we can write an equation in terms of the loss, m, in energy density per meter. After a given time, say the mean time between collisions, the ray has traveled a certain distance, in this case the mean free path, and the resulting energy density has the form

$$D(t) = D_0 \, e^{-m \Lambda} \tag{8.67}$$

By inserting this relationship into Eq. 8.53 and recalculating Eq. 8.55 we get

$$D(t) = D_0 e^{-(c_0 S_T / 4V)\left[-\ln(1-\overline{\alpha}) - 4mV/S_T\right]t}$$ (8.68)

and the Norris Eyring reverberation time with air attenuation becomes

$$T_{60} = \frac{0.161\ V}{-S_T \ln(1-\overline{\alpha}) + 4\ m\ V}$$ (8.69)

in metric units and

$$T_{60} = \frac{.049\ V}{-S_T \ln(1-\overline{\alpha}) + 4\ m\ V}$$ (8.70)

in FP units. In terms of loss in dB/m or dB/ft the relationship is

$$m = \frac{\Delta L_{air}}{4.34}$$ (8.71)

where m has units of inverse meters or feet.

Air losses can be included in the Sabine reverberation time formulas, which devolve from the Eqs. 8.68 and 8.69, in the limit of small values of the average absorption coefficient. In metric

$$T_{60} = \frac{0.161\ V}{A + 4\ m\ V}$$ (8.72)

and in FP units,

$$T_{60} = \frac{.049\ V}{A + 4\ m\ V}$$ (8.73)

The total absorption in a room, including the air absorption, is called the room constant and is given the designation R

$$R = A + 4\ m\ V$$ (8.74)

The units are in sabins or metric sabins.

Laboratory Measurement of the Absorption Coefficient

It is standard practice (ASTM C423) to measure the absorption of an architectural material in a reverberant test chamber using the reverberation time method. A reverberation chamber is a hard room with concrete surfaces and a long reverberation time, with sufficient volume to have an adequate density of modes at the frequency of interest. Since the average absorption coefficient in the room is quite small under these conditions, the Sabine equation can be used. The reverberation time of the empty chamber is

$$T_{60}(1) = \frac{0.161\ V}{S_T\ \overline{\alpha}}$$ (8.75)

If a sample of absorptive material having an area S_1 is placed on the floor and the test repeated, the new reverberation time is

$$T_{60}(2) = \frac{0.161 \, V}{S_T \, \bar{\alpha} - S_1 \alpha_0 + S_1 \alpha_1} \tag{8.76}$$

where α_0 is the absorption coefficient of the covered portion of the floor and α_1 is the absorption coefficient of the sample material under test. Combining Eqs. 8.75 and 8.76 we obtain the desired coefficient

$$\alpha_1 = \alpha_0 + \frac{0.161 \, V}{S_1} \left(\frac{1}{T_{60}(2)} - \frac{1}{T_{60}(1)} \right) \tag{8.77}$$

In these tests there is some dependence on the position of the sample in the room. Materials placed in the center of a surface are more effective absorbers, and yield higher absorption coefficients, than materials located in the corners. This is because the average particle velocity is higher there. There are also diffraction effects and edge absorption attributable to the sides of the sample. For these reasons Sabine absorption coefficients that are greater than one sometimes are obtained and must be used with caution in the Norris Eyring equation.

8.5   REVERBERANT FIELD EFFECTS

Energy Density and Intensity

We have seen that, as the modal spacing gets closer and closer together, it becomes less useful to consider individual modes and we must seek other ways of describing the behavior of sound in a room. One concept is the energy density . A plane wave moves a distance c_0 in one second and carries an energy per unit area equal to its intensity, I. The direct-field energy density D_d per unit volume is

$$D_d = \frac{I_d}{c_0} = \frac{p^2}{\rho_0 \, c_0^2} \tag{8.78}$$

where p^2 is the rms acoustic pressure.

The energy density in a diffuse field has the same relationship to the pressure squared, which is not a vector quantity, but a different relationship to the intensity. In a diffuse field the sound energy can be coming from any direction. The intensity is defined as the power passing through an area in a given direction. In a diffuse field, half the energy is passing through the area plane in the opposite direction to the one of interest. When we integrate the energy incident on the area in the remaining half sphere, the cosine term reduces the intensity by another factor of two. Thus in a reverberant field the intensity is only a quarter of the total power passing through the area. This is shown in Fig. 8.12.

$$I_r = \frac{1}{4} \left(\frac{p^2}{\rho_0 \, c_0} \right) \tag{8.79}$$

FIGURE 8.12   Intensity in a Reverberant Field
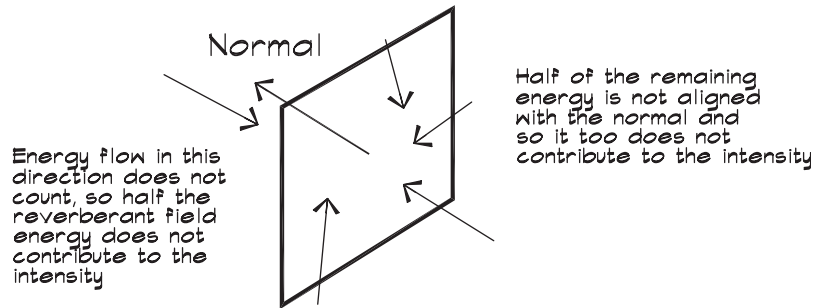
Semireverberant Fields

Occasionally we encounter a semireverberant field, where energy falls onto one side of a plane with equal probability from any direction. Most often this occurs when sound is propagating from a reverberant field through an opening in a surface of the room. Under these conditions the power passing through the plane of an opening having area S_w is given by

$$W_{sr} = \frac{S_w}{2} \left(\frac{p^2}{\rho_0 \, c_0} \right)$$

(8.80)

Room Effect

When a sound source that emits a sound power W_S is placed in a room, the energy density will rise until the energy flow is balanced between the energy being created by the source and the energy removed from the room due to absorption. After a long time the total energy in a room having a volume V due to a source having a sound power W_S is

$$V \, D_r = \frac{W_S \, \Lambda}{c_0} \left[1 + (1 - \overline{\alpha}) + (1 - \overline{\alpha})^2 + \cdots \right] = \frac{W_S \, \Lambda}{c_0 \, \overline{\alpha}}$$

(8.81)

which has been simplified using the limit of a power series for $\overline{\alpha}^2 < 1$

$$V \, D_r = \frac{4 \, W_S \, V}{c_0 \, S_T \, \overline{\alpha}}$$

(8.82)

and the sound pressure in the room will be

$$\frac{p^2}{\rho_0 \, c_0} = \frac{4 \, W_S}{S_T \overline{\alpha}} = \frac{4 \, W_S}{R}$$

(8.83)

Equation 8.83 is the reverberant-field contribution to the sound pressure measured in a room and can be combined with the direct-field contribution to obtain

$$\frac{p^2}{\rho_0 \, c_0} = \frac{Q \, W_S}{4 \, \pi r^2} + \frac{4 \, W_S}{R}$$

(8.84)

Taking the logarithm of each side we can express this equation as a level

$$L_p = L_W + 10 \log \left[\frac{Q}{4 \pi r^2} + \frac{4}{R} \right] + K \tag{8.85}$$

where K is 0.1 for metric units and 10.5 for FP units. The numerical constants follow from the reasoning given in Eq. 2.67.

Equation 8.85 is based on Sabine's theory and was published in 1948 by Hopkins and Stryker. It is a useful workhorse for the calculation of the sound level in a room given the sound power level of one or more sources. It holds reasonably well where the diffuse field condition exists; that is, in relatively large rooms with adequate diffusion if we are not too close (usually within $\frac{\lambda}{2}$) to reflecting surfaces. The increase in sound pressure level due to the reverberant field over that which we would expect from free field falloff is called the room effect.

Figure 8.13 gives the result from Eq. 8.85 for various values of the room constant. Near the source the direct-field contribution is larger than the reverberant-field contribution and the falloff behavior is that of a point source in a free field. In the far field the direct-field contribution has dropped below the reverberant-field energy, and the sound pressure level is constant throughout the space. The level in the reverberant field can be reduced only by adding more absorption to the room. According to this theory, only the total amount of absorption is important, not where it is placed in the room. In practice absorption placed where the particle velocity is the highest has the greatest effect. Thus absorption mounted in a corner, where the pressure has a maximum and the velocity a minimum, would be less effective than absorption placed in the middle of a wall or other surface. Absorption, which is hung in the center of a space, has the greatest effect but this is not a practical location.

FIGURE 8.13   Difference between Sound Power and Pressure Level in a Diffuse Room Due to an Omnidirectional Source
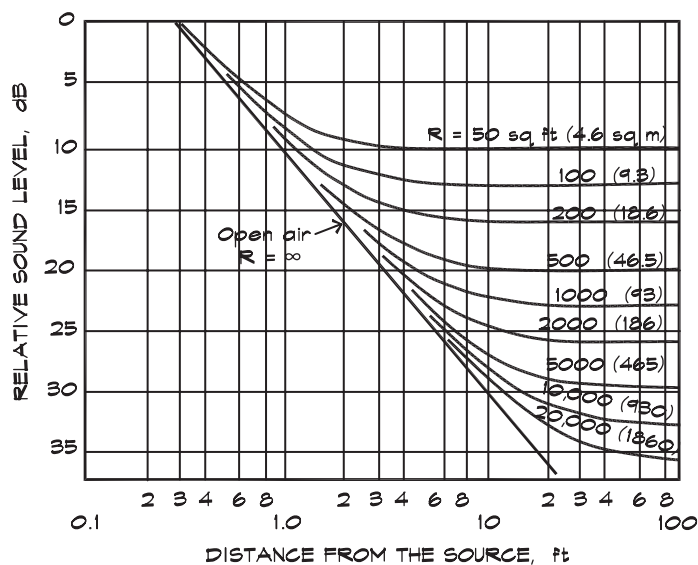
At a given distance, known as the *critical distance*, the direct-field level equals the reverberant-field level. We can solve for the distance by setting the direct and reverberant contributions equal.

$$r_c = \sqrt{\frac{Q\,R}{16\,\pi}} \tag{8.86}$$

Beyond the critical distance the reverberant field predominates.

Radiation from Large Sources

When the source of sound is physically large, such as the wall of a room, it can radiate energy over its entire surface area. The idea of a displaced center was introduced in Eq. 2.91 to relate the sound power to the sound pressure level in free space for a receiver located close to a large radiating surface. Similarly in a reverberant space the direct and reverberant contributions are combined

$$L_p = L_W + 10\,\log\left[\frac{Q}{4\,\pi\left[z + \sqrt{\dfrac{S\,Q}{4\,\pi}}\right]^2} + \frac{4}{R}\right] + K \tag{8.87}$$

where K is 0.5 for metric and 10.5 for FP units.

As the distance z, between the surface of the source and the receiver, is reduced to zero, Eq. 8.87 can be simplified to

$$L_p \cong L_W + 10\,\log\left[\frac{1}{S} + \frac{4}{R}\right] + K \tag{8.88}$$

where S is the surface area of the source. When the receiver is far from the source the area contribution is small and the distance to the surface of the source and to its acoustic center are nearly equal ($z \cong r$). The equation then reverts to its previous form

$$L_p = L_W + 10\,\log\left[\frac{Q}{4\,\pi\,r^2} + \frac{4}{R}\right] + K \tag{8.89}$$

Departure from Diffuse Field Behavior

In the power-pressure conversion, when we do not measure the sound pressure level close to the reflecting surfaces, we neglect some energy near the boundary given in Eq. 8.74. Waterhouse (1955) has investigated this energy and has suggested the addition of a correction term to the room constant, which is only significant at low frequencies.

$$R = A\left(1 + \frac{S_T\,\lambda}{8\,V}\right) + 4\,m\,V \tag{8.90}$$

where S_T is the total surface area and V the volume of the room. The correction is used in certain test procedures (e.g., ISO 3741 and ASTM E336).

FIGURE 8.14   **Measured (Power – Pressure) Level Differences (Davis and Davis, 1978)**
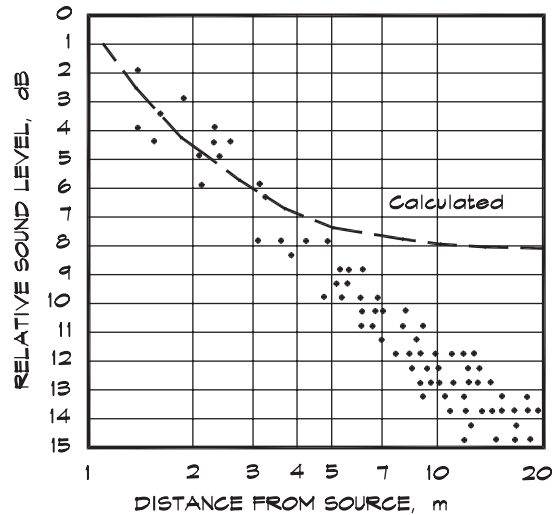
FIGURE 8.15   **Rectangular Room with Source Wall ($x = -\ell_x$), Absorbing End-Wall ($x = 0$), and Absorbing Side Surfaces ($y = \ell_y$ and $z = \ell_z$) (Franzoni, 2001)**
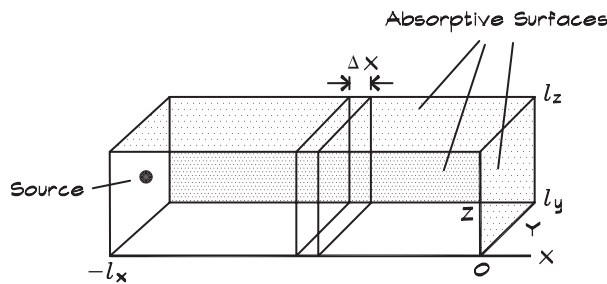
When rooms have a significant dimensional variation in different directions, particularly where there are low ceilings with a large amount of absorption, there is a departure from the behavior predicted by the Hopkins Stryker equation. Figure 8.14 shows measurements taken by Ogawa (1965) in Japan. A number of authors have attempted to account for this behavior by adding additional empirical terms or multipliers to the equation. Hodgson (1998) has published a review of several of these methods.

Franzoni and Labrozzi (1999) developed an empirical formula that applies to long, narrow, rectangular rooms, when the absorption is not uniformly distributed on all surfaces. For a source positioned near one wall and the geometry shown in Fig. 8.15,

$$\overline{p}_{rev}^2 = \frac{4\,\rho_0\,c_0\,W}{A}\left[\frac{(1-\overline{\alpha}_{total})(1-\overline{\alpha}_{total}/2)}{(1-\overline{\alpha}_w\,\overline{S}/2)}\right] e^{-(1/2)\,\overline{\alpha}_w\,\overline{S}\overline{x}} \qquad (8.91)$$

where $\overline{p}^2_{rev}$ = cross-sectionally averaged mean square acoustic pressure (Pa^2) at a
distance x from the origin (not the source)

A = total area of absorption in the room (sabins)

$= S_1 \alpha_1 + S_2 \alpha_2 + S_3 \alpha_3 + \cdots + S_n \alpha_n$

$\overline{\alpha}_{total} = A / S_{total}$

$\overline{\alpha}_w$ = total absorption of the side surfaces divided by the area of the side surfaces

$\overline{x} = x / l_x$

$\overline{S}$ = ratio of the side wall surface area to the cross sectional surface area

Reverberant Falloff in Long Narrow Rooms

Franzoni (2001) also published a theoretical treatment of the long-narrow room problem by considering an energy balance for diffuse-field components traveling to the right and to the left using the geometry in Fig. 8.15. She assumes that there is a locally diffuse condition, where energy incidence is equally probable in all directions from a hemisphere at a planar slice across the room, but the rightward energy does not necessarily equal the leftward energy. The total energy at a point is taken to be uncorrelated and can be expressed as the sum of the two directional components

$$\overline{p}^2 = \overline{p}^2_{+x} + \overline{p}^2_{-x} \tag{8.92}$$

At a given slice the reverberant intensity, due to rightward moving waves, is

$$I_{+x} = \frac{\overline{p}^2_{+x}}{\rho_0 c_0} \tag{8.93}$$

and similarly for the leftward moving waves.

To evaluate the effect of reflections from the side surfaces we write the mean square pressure near the wall as the sum of the incident and reflected components interacting with the sides

$$\overline{p}^2_{+x} = \overline{p}^2_{+x_{incident}} + \overline{p}^2_{+x_{incident}} (1 - \alpha_w) = (2 - \alpha_w)\overline{p}^2_{+x_{incident}} \tag{8.94}$$

The incident intensity into the side wall boundary (y or z) is

$$I_{sidewall} = I_s = I_y = I_z = \frac{\overline{p}^2_{+x_{incident}}}{2 \rho_0 c_0} = \frac{\overline{p}^2_{+x}}{2 \rho_0 c_0} \left[\frac{1}{2 - \alpha_w} \right] \tag{8.95}$$

where $\overline{p}^2_{+x}$ = mean square pressure associated with rightward traveling waves, incident plus reflected.

If we define β as the fraction of the surface area at a cross section, covered with an absorbing material having a random incidence absorption coefficient α_w, and l_p and S as the perimeter and area of the cross section, we can write a power balance relation equating the power in to the power out of the cross section.

$$I_x S = \left(I_x + \frac{d I_x}{d x} \Delta x \right) S + \alpha_w \beta l_p \Delta x I_s \tag{8.96}$$

This can be written as a differential equation

$$\frac{d\left(\overline{p}_{+x}^2\right)}{dx} + \frac{\alpha_w\,\beta\,l_p}{(2-\alpha_w)\,S}\,\overline{p}_{+x}^2 = 0 \tag{8.97}$$

which has a solution for right-running waves

$$\overline{p}_{+x}^2 = P_{+x}\,e^{-(\alpha_w\,\beta\,l_p)/((2-\alpha_w)\,S)\,x} \tag{8.98}$$

and another for left-running waves

$$\overline{p}_{-x}^2 = P_{-x}\,e^{+(\alpha_w\,\beta\,l_p)/((2-\alpha_w)\,S)\,x} \tag{8.99}$$

where P_{-x} and P_{+x} are coefficients to be determined by the boundary conditions at each end. At the absorbing end ($x = 0$) the right and left intensities are related

$$I_{-x}(0) = (1 - \alpha_b)\,I_{+x}(0) \tag{8.100}$$

with α_b being the end wall random incidence absorption coefficient. The coefficients in Eqs. 8.98 and 8.99 are related

$$P_{-x} = (1 - \alpha_b)\,P_{+x} \tag{8.101}$$

At the source-end wall, the power of the sources is equal to the power difference in right and left traveling waves

$$W = S\left[I_{+x}(-l_x) - I_{-x}(-l_x)\right] \tag{8.102}$$

Plugging in the mean square pressure terms and using Eq. 8.101 (Franzoni, 2001),

$$\overline{p}^2(x) = \frac{2\,\rho_0\,c_0\,W}{S}\left[\frac{\cosh(\gamma x) - \frac{1}{2}\alpha_b\,e^{+\gamma x}}{\sinh(\gamma l_x) + \frac{1}{2}\alpha_b\,e^{-\gamma l_x}}\right] \tag{8.103}$$

where $\gamma = \alpha_w\,\beta\,l_p/\left[(2-\alpha_w)\,S\right]$. Although this formula is somewhat more complicated than Eq. 8.91 it is still straightforward to use.

    The result given by Eqs. 8.91 and 8.103 can be compared to more detailed calculations in Fig. 8.16. The agreement is good for both equations. Franzoni (2001) gives several other examples for different absorption coefficients, which also yield good agreement.

Reverberant Energy Balance in Long Narrow Rooms

An energy balance must still be maintained, where the energy produced by the source is absorbed by the materials in the room. In the Sabine theory, the balance is expressed as Eq. 8.83 and the reverberant field energy is assumed to be equally distributed throughout the room. In Franzoni's modified Sabine approach, the average reverberant field energy is the same as Sabine's, but the distribution is uneven. The average energy can be obtained either by integrating Eq. 8.103 over the length of the room or from the following arguments.

FIGURE 8.16   Comparison of Falloff Data—Empirical Fit and Theoretical (Franzoni, 2001)
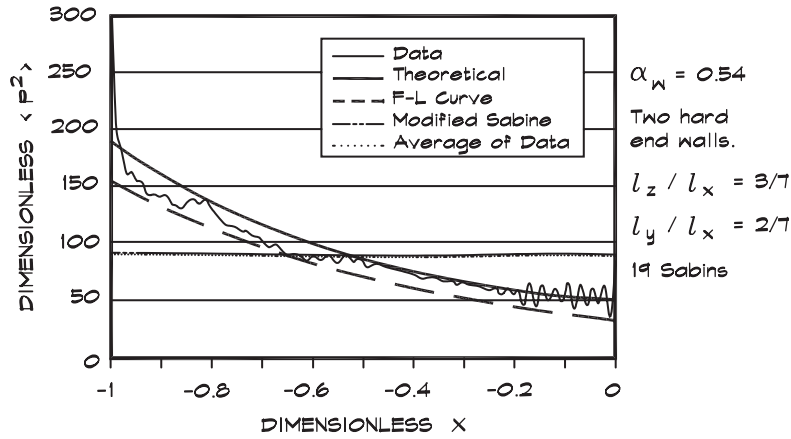
The power removed from the room is

$$
W_{out} = \sum_{\substack{absorbing \\ surfaces, i}} I_{\substack{into \\ surface}} \; \alpha_i \, S_i
\tag{8.104}
$$

The intensity incident on a surface is due to both the direct and reverberant-field components. From Eq. 8.94 the reverberant energy into a boundary surface is

$$
I_r = \frac{\overline{p}_{incident}^2}{2\,\rho_0 c_0} = \frac{\overline{p}^2}{2\,\rho_0\,c_0} \frac{1}{(2 - \alpha_i)}
\tag{8.105}
$$

and the average direct-field energy is

$$
I_d = \frac{W_{in}}{S_{total}}
\tag{8.106}
$$

The power removed by the absorbing surfaces is

$$
W_{out} = \sum_i \frac{\overline{p}^2}{2\,\rho_0\,c_0\,(2 - \alpha_i)} \alpha_i\,S_i + \sum_i \frac{W_{in}}{S_{total}} \alpha_i\,S_i
\tag{8.107}
$$

which in terms of the average mean square pressure is the modified Sabine equation (Franzoni, 2001)

$$
\overline{p}^2_{\substack{spatial \\ average}} = \sum_i \frac{4\,W_{in}\,\rho_0\,c_0}{\sum_i \alpha_i\,S_i/(1 - \alpha_i/2)} \left(1 - \sum_i \alpha_i\,S_i/S_{total}\right)
\tag{8.108}
$$

When the same absorption coefficient applies to all surfaces this simplifies to

$$\bar{p}^2_{\substack{\text{spatial} \\ \text{average}}} = \frac{4\,W_{in}\,\rho_0\,c_0}{A}\,(1 - \alpha/2)\,(1 - A/S_{total}) \tag{8.109}$$

The first term in the parentheses is a correction to the Sabine formula for the difference between the incoming and outgoing waves, and the second term is the power removed by the first reflection. Figure 8.16 also shows the results to be quite close to exact numerical simulations of the sound field.

Fine Structure of the Sound Decay

When an impulsive source such as a gunshot, bursting balloon, or electronically induced pulse excites a room with a brief impulsive sound, the room response contains a great deal of information about the acoustic properties of the space. First there is the initial sound decay in the first 10 to 20 msec of drop after the initial burst. The reverberation time based on this region is called the early decay time (EDT) and it is the time we react to. After the first impulse there is a string of pulses, which are the reflections from surfaces nearest the source and receiver. Thereafter follows a complicated train of pulses, which are the first few orders of reflections from the room surfaces. In this region the acoustical defects present in the room begin to appear. Long-delayed reflections show up as isolated pulses. Flutter echoes appear as repeated reflections that do not die out as quickly as the normal reverberant tail. Focusing can cause sound concentrations, which increase the reflected sound above the initial impulse. If the energy-time behavior of the room is filtered, it can be used to explore regions where modal patterns have formed and can contribute to coloration. A typical graph is shown in Fig. 8.17.

When two rooms are acoustically coupled the reverberation pattern in one room affects the sound in the other. When one has a longer reverberation time it may lead to a dual-slope reverberation pattern in the other. Consequently it is good practice to match the decay patterns of adjacent rooms unless it is the purpose to use one to augment the reverberant tail of the other.

FIGURE 8.17   Energy vs Time for an Impulsive Source

Sound pressure level at a point in a room for an impulsive sound. The direct sound arrives first followed by discrete reflections separated in time. Multiple reflections merge to become the reverberant field.
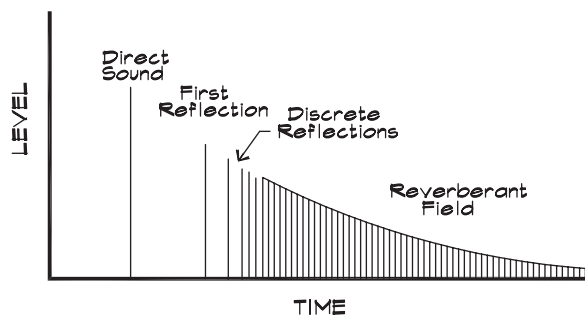
The room resonances that we examined in earlier sections contribute to the long-term behavior of the sound field. If an initial source of sound is turned on, the direct-field energy reaches a listener first, followed closely by the early reflections and lastly by the reverberant field. In the low frequencies the reverberant field is colored by the room modes where energy is preferentially stored. These modes build up and persist longer than nonresonant sound fields. The early reflections are determined by the position and orientation of reflecting surfaces near the source, whereas the reverberant field is defined by the total absorption and position of materials in the room, by the presence of diffusion in the space, and the room modes by the room size and surface orientation. By controlling these variables we can shape the room response according to its use.

This page intentionally left blank

9 SOUND TRANSMISSION LOSS

9.1 TRANSMISSION LOSS

Sound Transmission Between Reverberant Spaces

The transmission of sound from one space to another through a partition is a subject of some complexity. In the simplest case, there are two rooms separated by a common wall having area S_w, as in Fig. 9.1. If we have a diffuse sound field in the source room that produces a sound pressure p_s and a corresponding intensity

$$I_s = \frac{p_s^2}{4 \, \rho_0 \, c_0} \qquad (9.1)$$

which is incident on the transmitting surface, a fraction τ of the incident power is transmitted into the receiving room through the wall

$$W_r = I_s \, S_w \, \tau = \frac{p_s^2 \, S_w \, \tau}{4 \, \rho_0 \, c_0} \qquad (9.2)$$

where it generates a sound pressure level. If the receiving room is highly reverberant, the sound field there also will be dominated by the diffuse field component. We use Eq. 8.83 for the reverberant-field contribution to the energy and obtain the mean square pressure in the receiving room

$$\frac{p_r^2}{\rho_0 \, c_0} = \frac{p_s^2 \, S_w \, \tau}{R_r \, \rho_0 \, c_0} \qquad (9.3)$$

We can express this as a level by taking 10 log of each side and using the definition of the *transmission loss*

$$\Delta L_{TL} = -10 \, \log \, \tau \qquad (9.4)$$

FIGURE 9.1   Laboratory Measurements of the Transmission Loss
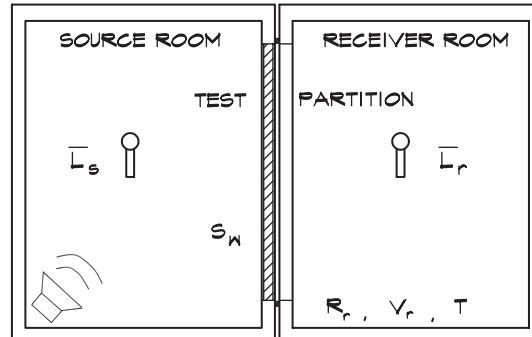
$S_w = 64$ sq ft (6 sq m)

$V_r \geq 80$ cu m (2900 cu ft) for 125 Hz

$\quad \geq 125$ cu m (4400 cu ft) for 100 Hz

we obtain the equation for the transmission of sound between two reverberant spaces

$$\overline{L}_r = \overline{L}_s - \Delta L_{TL} + 10 \log \left(\frac{S_w}{R_r} \right) \tag{9.5}$$

where $\overline{L}_r$ = spatial average sound pressure level in the receiver room (dB)

$\quad\quad \overline{L}_s$ = spatial average sound pressure level in the source room (dB)

$\quad \Delta L_{TL}$ = reverberant field transmission loss (dB)

$\quad\quad S_w$ = area of the transmitting surface (m^2 or ft^2)

$\quad\quad R_r$ = room constant in the receiving room (m^2 or ft^2 sabins)

Measurement of the Transmission Loss

Under laboratory conditions, both the source and receiving rooms are highly reverberant and the transmission loss of the common partition is given by

$$\Delta L_{TL} = \overline{L}_s - \overline{L}_r + 10 \log S_w - 10 \log R_r \tag{9.6}$$

where the bars over the source and receiver room levels indicate a spatial average in the reverberant-field portion of the rooms. Formal procedures have been established for laboratory (ASTM E90 and ISO 140/III) and field (ASTM E336 and ISO 140/IV) measurements of the transmission loss of partitions, which establish the partition size, the minimum room volume, the method of determining of the room constant, and the appropriate measurement techniques. Loudspeakers are used to generate a sound field in the source room and are positioned in the corners of the room far enough from the transmitting partition that a diffuse field is produced. Sound levels are measured at least a distance $r \geq 0.63 \sqrt{R}$ from the source and 1 m (3 ft) from large reflecting surfaces.

Two methods are used for the determination of the room constant. The reverberation time method measures the value of R_r using the Sabine equation (Eq. 8.72). A second method, called the source substitution method, uses a calibrated noise source having a known sound power level to determine R_r by means of Eq. 8.83. The standard source is usually an unhoused centrifugal fan, which produces a relatively flat noise spectrum.

Transmission loss measurements are done in third-octave bands over a standard range of frequencies, from 125 Hz to 4000 Hz. Below 125 Hz, the size of the test room necessary to achieve the diffuse-field condition becomes large and many labs do not meet this requirement. Data are sometimes taken below the 125 Hz third-octave band for research or other specialized purposes. When measured low-frequency data are unavailable, they can be calculated based on theoretical models. When the room size does not meet the minimum volume requirements for a diffuse field, the noise reduction is used instead of the transmission loss in standard tests and a notation to that effect is included in the test report.

Sound Transmission Class (STC)

Although transmission loss data in third-octave or full-octave bands are used for the calculation of sound transmission between adjacent spaces, it is convenient to have a single-number rating system to characterize the properties of a construction element. The *Sound Transmission Class* is such a system and is calculated in accordance with ASTM E413 and ISO/R 717. It begins with a plot of the third-octave transmission loss data versus frequency. The three-segment STC curve, shown in Fig. 9.2, is compared to the measured data by sliding it vertically until certain criteria are met: 1) no single transmission loss may fall below the curve by more than 8 dB and 2) the sum of all deficiencies (the difference between the curve value and the transmission loss falling below it) may not exceed 32 dB. When the curve is positioned at its highest point consistent with these criteria, as in Fig. 9.3, the STC rating is the transmission loss value at the point where the curve crosses the 500 Hz frequency line. The shape of the STC curve is based on a speech spectrum on the source-room side so this rating system is most useful for evaluating the audibility of conversations, television, and radio receivers. It is less accurate for low-frequency sounds such as music or industrial noise, where energy in the bass frequencies may predominate.

FIGURE 9.2   Reference Contour for Calculating Sound Transmission Class and Other Ratings
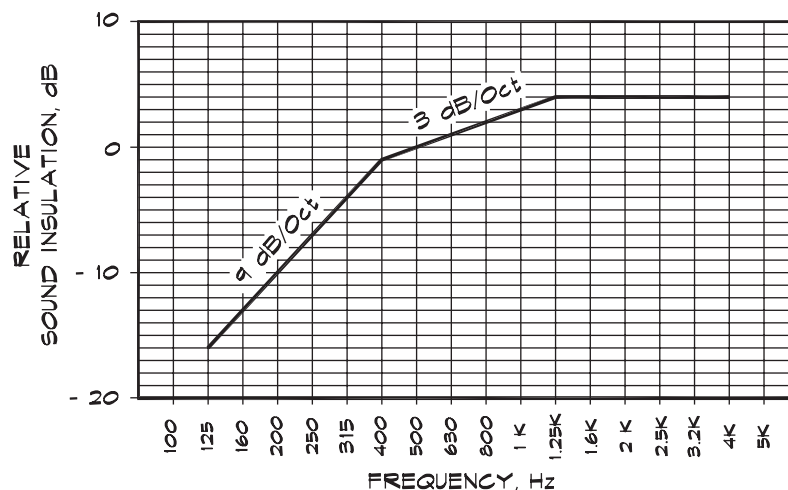
FIGURE 9.3   **Example of the Reference Contour Fitted to Transmission Loss Data (STC 25)**
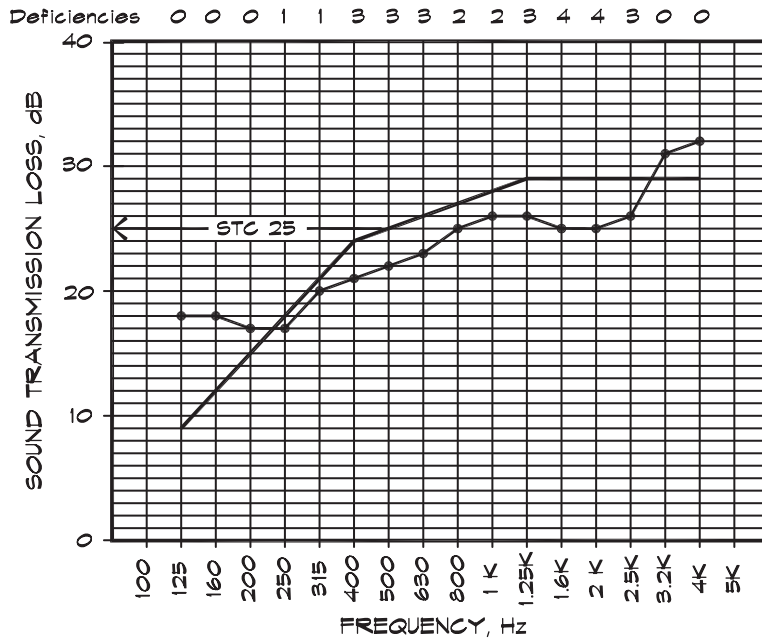
Field Sound Transmission Class (FSTC)

Field measurements of the STC can be made in existing buildings and are designated FSTC. Care must be exercised to minimize flanking, where sound is transmitted by paths other than directly through the test partition. The FSTC rating is about five points lower than the STC rating for a given partition, due to flanking and direct-field contributions. It applies only to the partition on which it is measured, but it can serve as an example of the rating of other partitions in a group of similarly constructed structures. It is not generally applicable to a construction type as a laboratory test would be. In building codes, if a given STC rating is required, an FSTC test that is five points lower is sufficient to demonstrate compliance.

Noise Reduction and Noise Isolation Class (NIC)

The arithmetic difference between the sound pressure levels in adjacent spaces is called the *noise reduction*.

$$\Delta L_{NR} = \overline{L}_s - \overline{L}_r \qquad (9.7)$$

At frequencies where rooms do not meet the minimum volume requirements necessary to establish the required modal density for a diffuse field, the noise reduction is used instead of the transmission loss to calculate the Sound Transmission Class.

A *Noise Isolation Class* (NIC) can be calculated from noise reduction values by comparing the measured data to the standard reference contour, using the STC calculation criteria (ASTM E413). The NIC is measured in the field, since a laboratory measurement would require knowledge of the transmitting area and the absorption in the receiving room to be useful. A field NIC rating is not applicable to a type of partition since it relates only to the unique combination of partition type, partition area, and the amount of absorption present in

the receiving room at the time of the measurement. Thus, it is not appropriate to assign an NIC rating to a specific construction element or to use it in place of an FSTC value.

9.2   SINGLE PANEL TRANSMISSION LOSS THEORY

Free Single Panels

When a sound wave strikes a freely suspended solid panel, there is a movement imparted, which in turn transmits its motion to the air on the opposite side. Figure 9.4 shows the geometry. The total pressure acting on the panel along its normal is

$$\Delta \mathbf{p} = \mathbf{p}_i + \mathbf{p}_r - \mathbf{p}_t \tag{9.8}$$

The velocity of a normally reacting panel can be calculated using Newton's law

$$\Delta \mathbf{p} = m_s \frac{d \mathbf{u}_p}{d t} = m_s \left(j \omega \mathbf{u}_p \right) \tag{9.9}$$

Note that the normal panel impedance in this model, $j \omega m_s$, is only due to the panel mass.

If a plane wave approaches at an angle θ to the surface normal and is specularly reflected,

$$\mathbf{u}_i = \frac{j k \cos \theta}{j \omega \rho_0} \mathbf{p}_i = \frac{\cos \theta}{\rho_0 c_0} \mathbf{p}_i \tag{9.10}$$

and

$$\mathbf{u}_r = -\frac{\cos \theta}{\rho_0 c_0} \mathbf{p}_r \quad \text{and} \quad \mathbf{u}_t = \frac{\cos \theta}{\rho_0 c_0} \mathbf{p}_t \tag{9.11}$$

Substituting Eq. 9.10 and 9.11 into 9.9, we obtain the force balance equation along the normal

$$\frac{\rho_0 c_0 \mathbf{u}_i}{\cos \theta} - \frac{\rho_0 c_0 \mathbf{u}_r}{\cos \theta} = \frac{\rho_0 c_0 \mathbf{u}_t}{\cos \theta} + m_s \left(j \omega \mathbf{u}_t \right) \tag{9.12}$$

At the surface, the particle velocities on both sides of the plate are the same as the plate velocity, so

$$\mathbf{u}_i + \mathbf{u}_r = \mathbf{u}_t = \mathbf{u}_p \tag{9.13}$$

FIGURE 9.4   Pressure on a Plate Having a Mass, m, Per Unit Area
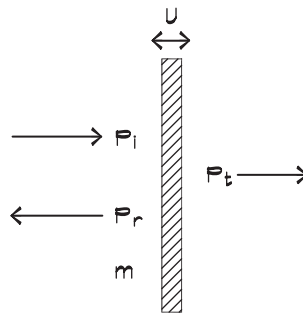
Substituting these into Eq. 9.9 to eliminate the $\mathbf{u}_r$ term we get the ratio of the transmitted to incident pressures, which is

$$\frac{\mathbf{p_t}}{\mathbf{p_i}} = \frac{1}{1 + \dfrac{j\,\omega\,m_s\,\cos\theta}{2\,\rho_0\,c_0}} = \frac{1}{1 + \dfrac{\mathbf{z_n}\cos\theta}{2\rho_0\,c_0}} \tag{9.14}$$

If we use $\zeta_n = \dfrac{\mathbf{z_n}}{\rho_0\,c_0}$ for the normalized impedance, and define the transmissivity as the ratio of the transmitted to the incident power, the square of Eq. 9.14

$$\tau_\theta = \left[\frac{\mathbf{p_t}}{\mathbf{p_i}}\right]^2 = \frac{1}{\left|1 + \dfrac{\zeta_n\cos\theta}{2}\right|^2} \tag{9.15}$$

The generalized transmission loss is

$$\Delta L_{TL}(\theta) = 10\,\log\left|1 + \frac{\zeta_n\cos\theta}{2}\right|^2 \tag{9.16}$$

Mass Law

The limp mass approximation for the normalized panel impedance $\zeta_n = \dfrac{\mathbf{z_n}}{\rho_0 c_0} \cong \dfrac{j\,\omega\,m_s}{\rho_0\,c_0}$ holds for thin walls or heavy membranes in the low-frequency limit, where the panel acts as one mass, moving along its normal, and bending stiffness is not a significant contributor. Using this impedance and recalling that the square of an imaginary number is the sum of the squares of its real and imaginary parts, we can write the *transmissivity* as

$$\tau_\theta = \left[1 + \left(\frac{\omega\,m_s\,\cos\theta}{2\,\rho_0\,c_0}\right)^2\right]^{-1} \tag{9.17}$$

where τ_θ = transmissivity or the fraction of the incident energy transmitted through the panel as a function of incident angle θ
       ω = radial frequency (rad / s)
       m_s = surface mass density (kg / m^2 or lbs / ft^2)
       ρ_0 = density of air (1.18 kg / m^3 or 0.0745 lbs / ft^3)
       c_0 = speed of sound in air (344 m / s or 1128 ft / s)

By taking 10 log of Eq. 9.17, we obtain the transmission loss of a panel for a plane wave incident at an angle θ to the normal. A graph of the behavior of the mass law transmission loss as a function of the angle of incidence of the sound wave is given in Fig. 9.5.

$$\Delta L_{TL}(\theta) = 10\,\log\left[1 + \left(\frac{\omega\,m_s\,\cos\theta}{2\,\rho_0 c_0}\right)^2\right] \tag{9.18}$$

For most architectural materials, the normalized mass impedance is much greater than one so that the term on the right-hand side of the bracket dominates.

FIGURE 9.5   Theoretical Sound Transmission Loss of Panels (Beranek, 1971)
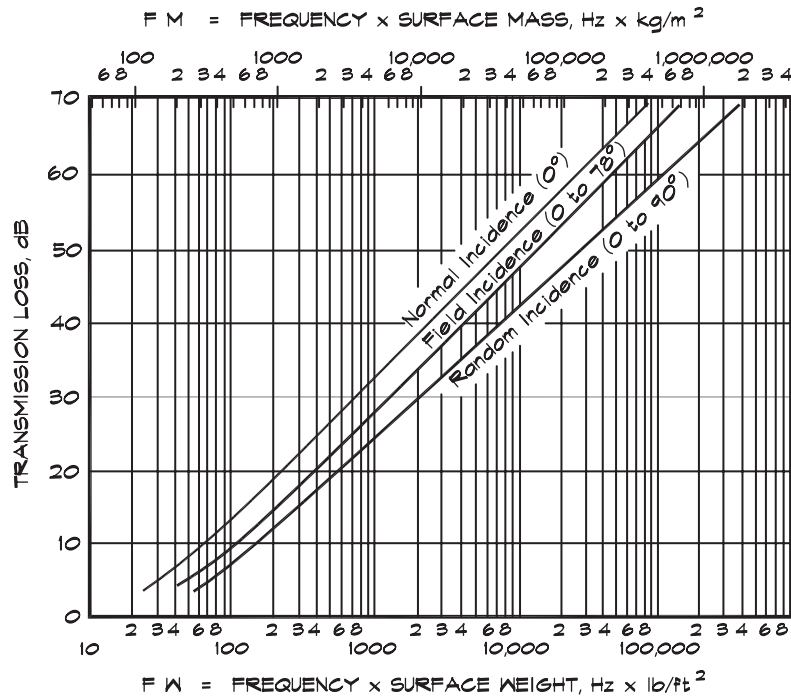
When the incident sound field is diffuse, there is an equal probability that sound will come from any direction. The diffuse incidence transmissivity is obtained by integrating Eq. 9.17 over all angles of incidence up to a limiting value of θ_{Max}.

$$\tau = \frac{\int_{0}^{\theta_{Max}} \tau_{\theta} \cos \theta \sin \theta \, d\theta}{\int_{0}^{\theta_{Max}} \cos \theta \sin \theta \, d\theta} \qquad (9.19)$$

The reason for this approach is that the elementary theory of Eq. 9.18 predicts a transmission loss of zero for grazing incidence, so if the limiting angle is 90°, we obtain a result that does not occur in practice. It has become standard procedure to select a maximum angle that yields the best fit to the measured data. This turns out to be about 78°, and gives what is known as the field-incidence transmission loss

$$\Delta L_{TL} = 10 \log \left[1 + \left(\frac{\omega \, m_s}{3.6 \, \rho_0 c_0} \right)^2 \right] \qquad (9.20)$$

or

$$\Delta L_{TL} = 20 \log \left(f \, m_s \right) - K_{TL} \qquad (9.21)$$

where ΔL_{TL} = diffuse field transmission loss (dB)
         f = frequency (Hz)

   m_s = surface mass density of the panel material (kg / m^2 or lbs / ft^2)

   K_{TL} = numerical constant
      = 47.3 dB in metric units and 33.5 dB in FP units

Equation 9.21 is known as the mass law since the transmission loss at a given frequency is only dependent on the surface mass of the panel. The transmission loss increases six dB for each doubling of surface mass or frequency. Under field-incidence conditions, the integration over the angle of incidence results in an effective mass that is lower by a factor 1.8 than the actual mass. Comparing Eq. 9.18 with Eq. 9.20, we see that this is the same as a difference between the field and normal incidence transmission losses of 5 dB.

$$\Delta L_{TL} \cong \Delta L_{TL} \ (\theta = 0) - 5 \tag{9.22}$$

Figure 9.6 shows a graph of the diffuse field transmission loss measured for a 3-mm (1/8") hardboard panel compared with the calculated value. In this frequency range, the agreement with measured data for thin panels is quite good.

Large Panels—Bending and Shear

Panels that are large compared to a wavelength, react to an applied pressure not only as a limp mass but also as a plate, which can bend or shear. As such, they have an impedance that is more complicated than that previously assumed. When the possibility of bending or shear is present, the two transmission mechanisms act much like resistors in an electric circuit. The composite panel impedance is treated mathematically like two resistors in parallel, which are in series with the mass impedance

$$\mathbf{z} \cong j \omega m_s + \frac{\mathbf{z_B} \mathbf{z_s}}{\mathbf{z_B} + \mathbf{z_s}} \tag{9.23}$$

FIGURE 9.6   Transmission Loss of 3 mm (1/8") Hardboard (Sharp, 1973)
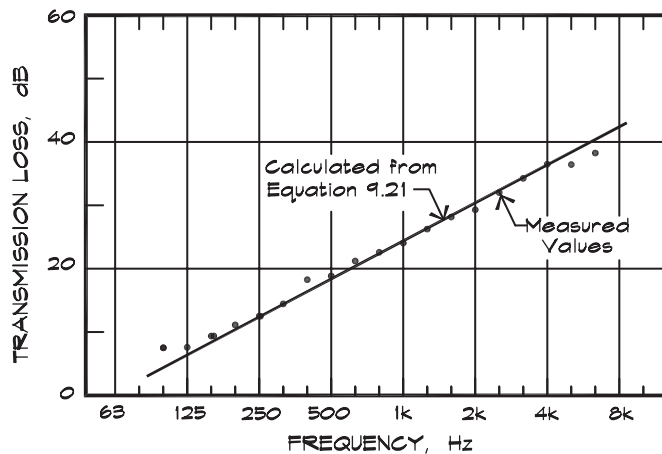
For an isotropic plate, the bending impedance (Sharp, 1973; Cremer, Heckel, and Ungar, 1973; or Fahy, 1985) is given by

$$\mathbf{z}_B \cong -\frac{j\,\omega^3\,B}{c_0^4}\,\sin^4\theta \tag{9.24}$$

and the shear impedance (Mindlin, 1951; Cremer, Heckel, and Ungar, 1973; or Beranek and Ver, 1992) is

$$\mathbf{z}_s = -j\,\frac{G\,h\,\omega\,\sin^2\theta}{c_0^2} \tag{9.25}$$

where ω = radial frequency = $2\,\pi\,f$ (rad/s)
   m_s = surface mass density of the panel (kg / m^2 or lbs / ft^2)
   $j = \sqrt{-1}$
   E = Young's modulus of elasticity (N / m^2 or lb / ft^2)
   $B = \dfrac{E\,h^3}{12\,(1-\sigma^2)}$ = bending stiffness (N m or ft lbs)
   $G = \dfrac{E}{2\,(1+\sigma)}$ = shear modulus (N / m ^{2} or lbs / ft^2)
   c_0 = speed of sound in air (m / s or ft / s)
   σ = Poisson's ratio
   h = panel thickness (m or ft)

Thin Panels—Bending Waves and the Coincidence Effect

In Eq. 9.23, the impedance is composed of three imaginary terms: the inertial mass, the bending stiffness, and the shear impedance. At low frequencies, the mass term predominates; at high frequencies it is the combination of bending and shear that determines the composite impedance. Thin panels are easier to bend than to shear, so more of the energy will flow into this mode. The resulting plate impedance becomes

$$\mathbf{z} \cong j\,\omega\,m_s - \frac{j\,\omega^3\,B}{c_0^4}\,\sin^4\theta \tag{9.26}$$

At one frequency, called the *coincidence frequency*, the mass and bending impedance terms are equal and, since they have opposite signs, the composite impedance is zero. Figure 9.7 illustrates the crossover point for this condition.

   Coincidence can be understood by realizing that the velocity of bending waves in a panel is a function of frequency. At the coincidence frequency, the bending wave velocity is the same as the trace velocity of the airborne sound moving along the panel. Since the pressure maxima and minima are spatially matched, as in Fig. 9.8, energy is easily transmitted from the air into the panel and vice versa. The frequency at which coincidence occurs varies with the angle of incidence and is obtained by setting Eq. 9.26 to zero

$$f_{co}\,(\theta) = \frac{c_0^2}{2\,\pi\,\sin^2\theta}\,\sqrt{\frac{m_s}{B}} \tag{9.27}$$

FIGURE 9.7   Imaginary Part of the Thin Panel Impedance (Sharp, 1973)

The imaginary part of the transmission impedance of a thin panel for grazing incidence ($\theta = \pi / 2$) showing the effect of coincidence.
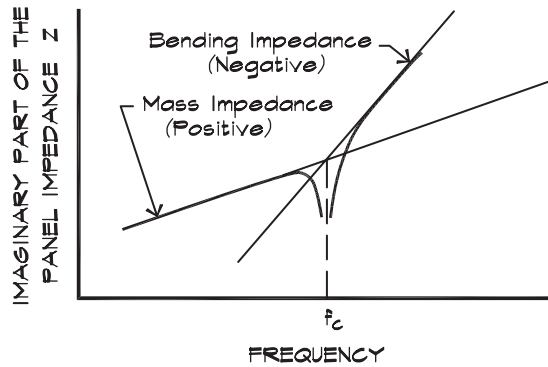
FIGURE 9.8   Coincidence Effect

The coincidence effect matches the trace of the airborne wavelength and the bending wavelength in the panel.
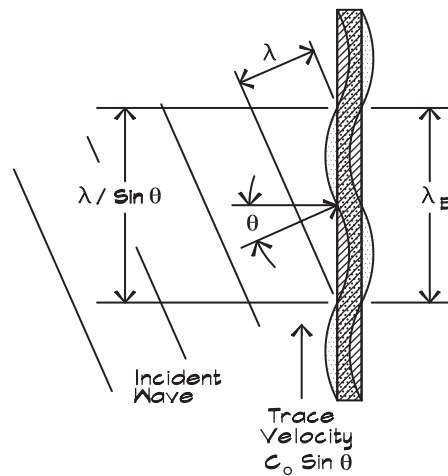
For normal incidence, the coincidence frequency is infinite, so there is no effect. The minimum value of the matching frequency occurs at grazing incidence and is called the *critical frequency*.

$$f_c = \frac{c_0^2}{2\pi} \sqrt{\frac{m_s}{B}} = \frac{c_0^2}{2\pi h} \sqrt{\frac{12\,(1 - \sigma^2)\,\rho_m}{E}} \tag{9.28}$$

where ρ_m = bulk density of the panel material (kg/m^3 or lbs/ft^3).

The two frequencies are related by means of

$$f_{co}\,(\theta) = \frac{f_c}{\sin^2 \theta} \tag{9.29}$$

FIGURE 9.9   Single Panel Direct Field Transmission Loss (Fahy, 1985)
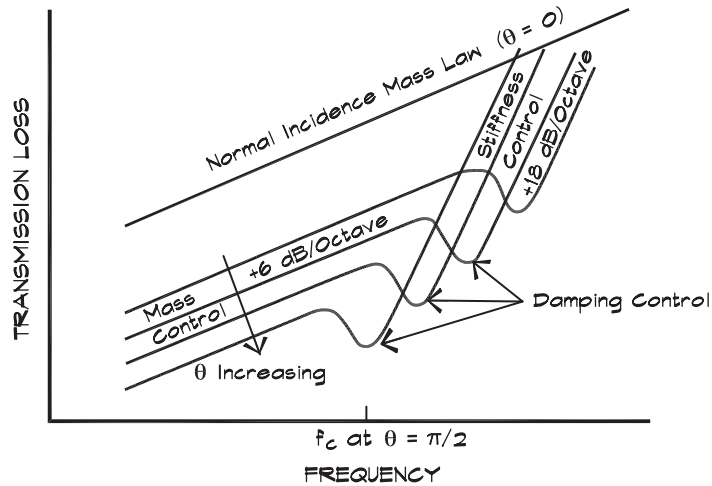
which implies that the *coincidence effect* always occurs at or above the critical frequency. Figure 9.9 gives examples in which the position of the coincidence dip varies with the angle of incidence.

Above coincidence the bending impedance term increasingly dominates and the transmission loss becomes (Fahy, 1985)

$$\Delta L_{TL}(\theta) \cong 10 \log \left[1 + \left(\frac{B k^4 \sin^4 \theta \cos \theta}{2 \rho_0 c_0 \omega} \right)^2 \right] \qquad (9.30)$$

The bending transmission loss is stiffness controlled in this region and has an 18 dB per octave slope as well as a strong angular dependence.

At the critical frequency, the transmission loss does not fall to zero because internal damping prevents it. To treat this theoretically, a complex bending stiffness $\mathbf{B} = B(1 + j\eta)$ is introduced with a damping term η having a value less than one. Since the mass term and the bending term cancel out at coincidence, damping is left. Using Eq. 9.27, Eq. 9.30 can be written as an inertial term with a damping coefficient (Fahy, 1985)

$$\Delta L_{TL}(\theta) \cong 10 \log \left(1 + \frac{\eta \omega_{co} m_s \cos \theta}{2 \rho_0 c_0} \right)^2 \qquad (9.31)$$

At coincidence, the transmission loss is expressed as the direct-field mass law plus a damping term $20 \log \eta$. Figure 9.9 also shows where internal damping becomes important.

The diffuse-field transmission loss is normally calculated by integrating the direct-field transmission loss expression over all relevant angles of incidence. The integration in the coincidence region is difficult because different equations apply, depending on the angle and the frequency. Although the coincidence frequency varies with angle of incidence,

the diffuse-field transmission loss still has a minimum at the critical frequency, since the dominant path is that having the lowest loss.

Several authors have developed approximate relations to use in this region. Fahy (1985) gives an equation for the transmission loss at the diffuse-field coincidence point, which is written in terms of a combination of the normal-incidence mass law and a damping term, dependent on the bandwidth

$$\Delta L_{TL} \, (f = f_c) \cong 20 \, \log \left(\frac{\omega_c \, m_s}{2 \, \rho_0 \, c_0} \right) + 10 \, \log \left\{ \frac{2 \, \eta}{\pi} \left(\frac{\Delta f}{f_c} \right) \right\} \tag{9.32}$$

where Δf = bandwidth (Hz) - - typically one - third octave or one octave wide
f_c = critical frequency (Hz)
η = damping coefficient ($\eta < 1$)

When the transmission loss is calculated just below coincidence, a line is drawn between the field-incidence mass law value at $f_c/2$ and the critical-frequency transmission loss from Eq. 9.32. Above the coincidence frequency, Eq. 9.30 predicts an 18 dB per octave increase in transmission loss for a given angle of incidence. Measured diffuse-field data yield a slope that is about half that (Sharp, 1973), due to the shifting location of the coincidence dip with angle. Cremer (1942) has derived an approximate diffuse-field equation for use above the coincidence frequency that combines the normal-incidence mass law and a frequency-dependent damping term.

$$\Delta L_{TL} \, (f > f_c) \cong 20 \, \log \left(\frac{\omega \, m_s}{2 \, \rho_0 \, c_0} \right) + 10 \, \log \left\{ \frac{2 \eta}{\pi} \left(\frac{f}{f_c} - 1 \right) \right\} \tag{9.33}$$

Above coincidence, Eq. 9.33 yields a transmission loss that increases 9 dB per octave for a single panel, which agrees with measured values.

Table 9.1 and Fig. 9.10 give a compilation of material properties: the product of the critical frequency and the panel thickness along with the damping coefficients for use in these equations. Figure 9.11 plots the measured transmission loss for a sheet of 5/8" drywall, which exhibits a coincidence dip around 2500 Hz. Data calculated from Eqs. 9.32 and 9.33 are also shown.

Thick Panels

As panel thickness increases, the composite panel impedance utilized in thin panel theory is no longer accurate. At high frequencies a shear wave can develop and propagate in a thick panel. When shear presents a lower impedance than bending, it will become the predominant transmission mode. The composite impedance is given by Eq. 9.25.

The crossover point between bending and shear occurs where the thickness of the plate is equal to a bending wavelength in the plate material. When the panel is thicker than a wavelength, shear predominates, as illustrated in Fig. 9.12. The shear limiting frequency is (Sharp, 1973)

$$f_s = \frac{c_0^2 \, (1 - \sigma)}{59 \, h^2 \, f_c} \tag{9.34}$$

TABLE 9.1 Product of Plate Thickness and Critical Frequency in Air (20° C) (Beranek, 1971; Cremer et al., 1973; Fahy, 1985)

Material	f_c (m sec^{-1})	h f_c (ft sec^{-1})
Steel	12.4	41
Aluminum	12.0	39
Brass	17.8	58
Copper	16.3	54
Glass or Sand Plaster	12.7	42
Gypsum Board	38	125
Chipboard	23	75
Plywood or Brick	20	66
Asbestos Cement	17	56
Concrete		
Dense	19	62
Porous	33	108
Light	34	112
Lead	55	180

Note that variations of 10% are not uncommon.

FIGURE 9.10   Values of Material Loss Factors (Beranek and Ver 1992)

Typical ranges of loss factors of materials at small strain, near room temperatures at audio frequencies.
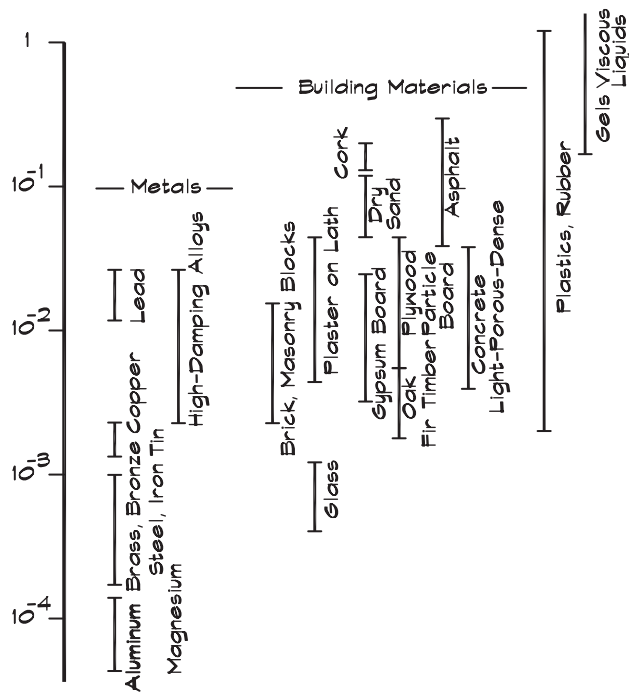
FIGURE 9.11   **Transmission Loss of 16 mm (5/8") Gypboard (Sharp, 1973)**
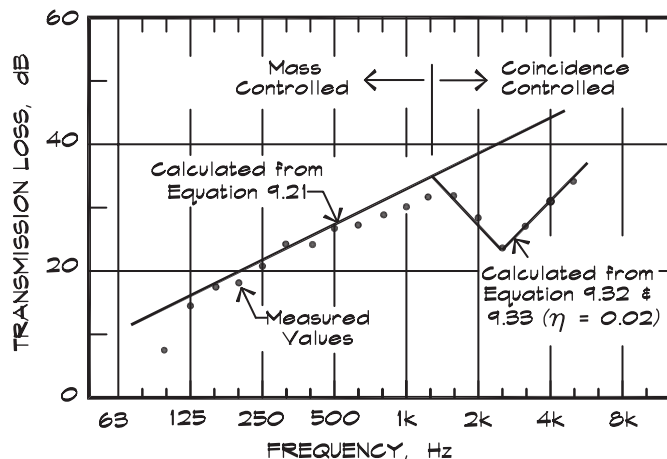
FIGURE 9.12   **Transmission Impedance of Thick Panels (Sharp, 1973)**
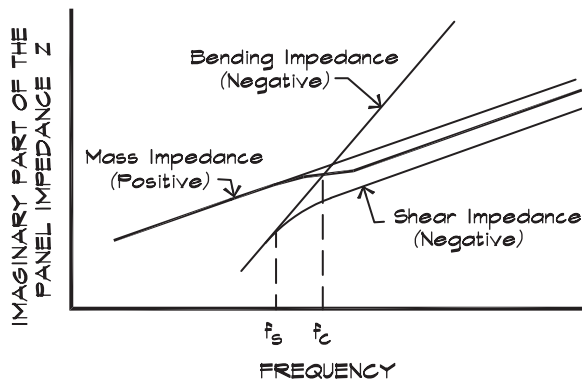
When the shear frequency falls below the critical frequency, as it can with thick panels such as concrete slabs and brick or masonry walls, there is no coincidence dip and the shear mechanism lowers the transmission loss even below that which might be expected from purely mass law considerations. This can be very important since in Fig. 9.13, it occurs in the frequency range around 200 Hz for a 15 cm (6") concrete slab. A good estimate of the transmission loss can be made above this point by using 6 dB less than the diffuse field mass law. For concrete or solid brick structures this is equivalent to assuming that there is half the actual mass.

If the shear frequency is greater than the coincidence frequency, the shear wave impedance eventually becomes lower than the bending impedance. All materials appear thick at a high enough frequency. The shear-wave impedance limits the slope of the transmission loss line above the shear-bending frequency to 6 dB per octave. Figure 9.14 gives

Figure 9.13   Transmission Loss of a 6" Concrete Panel (Sharp, 1973)

The measured values of transmission loss for a 6-inch (150 mm) concrete panel compared to values predicted by means of the thin and thick panel theories.
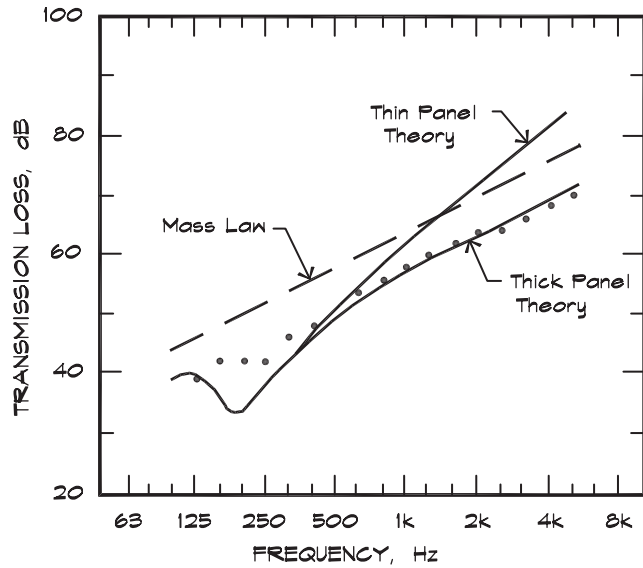
Figure 9.14   Imaginary Part of the Transmission Impedance (Sharp, 1973)

The imaginary part of the transmission impedance of a thin panel for grazing incidence $(\theta = \pi/2)$ showing the effect of coincidence. The shear frequency is greater than the critical frequency.
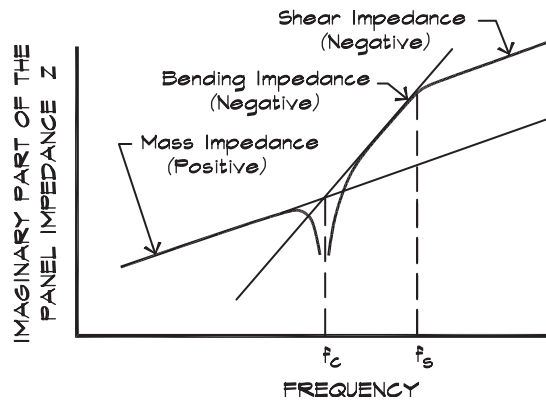
an example. Since coincidence in lightweight construction materials such as sheet metal, gypsum board, or thin wood panels occurs at a relatively high frequency (e.g., above 2000 Hz), there is little practical impact from shearing effects since there is little sound transmission in this region.

Finite Panels—Resonance and Stiffness Considerations

For a finite-sized panel, an additional term must be added to the impedance at very low frequencies, to account for panel bending resonances. This term is given by (Leissa, 1969; Sharp, 1973)

$$\mathbf{z}_P = -j \frac{K_P}{\omega} \tag{9.35}$$

where

$$K_P = \pi^4 \, B \left[\frac{1}{a^2} + \frac{1}{b^2} \right]^2 \tag{9.36}$$

and a and b are the dimensions of the panel. In this frequency range, the overall impedance is the sum of the panel impedance and the mass impedance. When the two terms are equal, a panel resonant frequency is produced

$$f_P = \frac{\pi}{2} \sqrt{\frac{B}{m_s}} \left[\frac{1}{a^2} + \frac{1}{b^2} \right] \tag{9.37}$$

Typically, the dimensions of a panel such as a wall are large enough that the panel resonance is quite low, on the order of 10 Hz or less. A 2 m × 3 m sheet of gypboard, for example, has a panel resonance of about 5 Hz. Note that Eq. 9.37 is based on the fundamental resonant frequency of the panel. There are also higher panel modes; however, due to damping these rarely contribute to the transmission loss. The frequency appears in the denominator in Eq. 9.35, so below the panel resonance the transmission loss increases with decreasing frequency at 6 dB per octave. Sharp (1973) has given an approximate relationship for this region.

$$\Delta L_{TL} \cong 20 \log \left(f \, m_s \right) - K_{TL} + 40 \log \left(\frac{f_P}{f} \right) \tag{9.38}$$

for $f < f_P$ the lowest panel resonance frequency.

Design of Single Panels

For single panels the transmission loss is influenced by four factors: 1) size, 2) stiffness, 3) mass, and 4) damping. Josse and Lamure (1964) have developed a comprehensive, albeit somewhat more complex, formulation for the region below the critical frequency

that includes all four components

$$\Delta L_{TL} = 20 \, \log\left(\frac{\omega \, m_s}{2 \, \rho_0 \, c_0}\right) - 10 \, \log\left\{\left[\frac{3}{2} + \ln\left(\frac{2 \, \omega}{\Delta \omega}\right)\right]\right.$$

$$\left. + \frac{16 \, c_0^2}{\eta \, \omega_c} \frac{1}{(\omega \, \omega_c)^{1/2}} \left(\frac{a^2 + b^2}{a^2 \, b^2}\right)\left[1 + \frac{2 \, \omega}{\omega_c} + 3\left(\frac{\omega}{\omega_c}\right)^2\right]\right\} \qquad (9.39)$$

For typical panel sizes, in the mass-law region Eq. 9.39 gives about the same result as Eq. 9.21. Above the critical frequency, Eq. 9.32 or Eq. 9.33 can be used to predict the transmission loss. For thick panels, the mass law holds up to the point where shear predominates. Above this point, mass law less 6 dB gives a good estimate.

The transmission loss of a thin panel falls into five frequency regions illustrated in Fig. 9.15. At very low frequencies the transmission loss is stiffness controlled. The greater the bending stiffness and the shorter the span, the higher the transmission loss. These considerations become important in low-frequency sound transmission problems in long-span floor structures, particularly in lightweight wood construction, where the bending stiffness of the structure is not great. Although floors are a composite structure, they can be thought of as a single bending element at these low frequencies.

Above the fundamental panel mode, the transmission loss of a thin single panel is primarily a function of its mass. Techniques such as mass loading can be used to increase the intrinsic panel mass, by adding asphalt roofing paper, built-up roofing, sand, gravel, lightweight concrete, gypboard, or discrete masses. Lead-loaded gypsum board panels are available for critical applications. Mass loading increases the weight of the panel without increasing the panel stiffness. Loading materials need not cover the entire panel but can be located at regular intervals over the surface. In existing wooden floor structures mass can be added by screwing sheets of gypboard to the underside of wood subfloors between the

FIGURE 9.15   General Form of the Diffuse Field Transmission Loss vs Frequency Curve for a Thin Panel
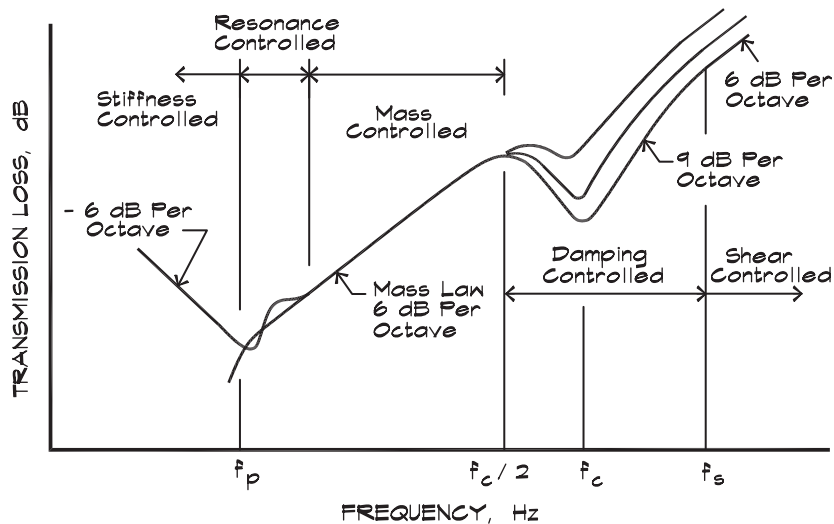
joists, a technique that also helps close off any cracks in the subflooring. Although a high mass is desirable, a high thickness is not, due to its effect on the coincidence frequency. For example, 9 mm (3/8") glass has a higher STC rating (STC 34) than a normal 44 mm (1 3/4") solid core door (STC 30) even though it weighs less per unit area, due to the fact that its coincidence frequency is much higher.

In the region around coincidence, damping controls the depth of the notch. Several techniques can be used to increase the transmission loss. In windows and glazed doors, a resin interlayer of 0.7 to 1.4 mm (30 to 60 mils) thickness can be introduced between two layers of glass to increase damping. Products of this type are called laminated glass or sometimes acoustical glass. Sheets of 6 mm (1/4 in) laminated glass make good acoustical windows and can achieve an STC rating of 34 in fixed stops or high-quality frames.

Damping compounds are also commercially available. Products come in sheet or paste form and add both mass and damping. They are primarily used to treat thin materials such as sheet-metal panels on vibrating equipment. Asphalt materials such as undercoat on car bodies serve the same function and reduce the vibration amplitudes of these surfaces.

Spot Laminating

Spot laminating is a technique used to increase transmission loss near coincidence. In this region, it is important not to thicken the panel, which decreases the critical frequency. If the mass is increased through the addition of an extra layer, it may decrease the transmission loss in the frequency range of interest. One way to achieve a combination of high mass and low stiffness is to laminate panels together using dabs (spots) of panel adhesive at regular intervals. At low frequencies, the panels act as one and their composite bending stiffness is greatly increased. At high frequencies the shearing effect of the adhesive acts to reduce the bending stiffness to that of an individual panel. The panels act individually and the critical frequency remains high, since it is that of a single panel in bending.

When using the spot laminating technique the spacing of the adhesive dots determines the frequency at which the two panels begin to decouple. Decoupling begins when the dot spacing is equal to the wavelength of bending waves. The bending wavelength of a single panel at a frequency f is given by (Sharp, 1973) as

$$\lambda_B = \frac{c_0}{\sqrt{f\,f_c}} \tag{9.40}$$

At low frequencies, the critical frequency is that of the composite panel since the bending wavelength is much greater than the spacing of the adhesive. If two panels of identical materials are joined together, the coincidence frequency of each sheet is about twice that of the composite. The decoupling frequency can be written as

$$f_d = \frac{2\,c_0^2}{a^2\,f_c} \tag{9.41}$$

where a is the adhesive spacing and f_c is the critical frequency of a single sheet of material. If the two panels are 1/2" gypboard, which has a coincidence frequency of about 3000 Hz, and the adhesive dot spacing is 24", then the decoupling frequency is 210 Hz. This is well below the composite panel's coincidence frequency, which would be about 1500 Hz.

9.3   DOUBLE-PANEL TRANSMISSION LOSS THEORY

Free Double Panels

The transmission loss of a double panel system is based on a theory that first considers panels of infinite extent, not structurally connected, and subsequently addresses the effects of various types of attachments. The treatment here follows that first developed by London (1950) and later by Sharp (1973). It is assumed that the air cavity is filled with batt insulation, which damps the wave motion parallel to the wall, so we are mainly concerned with internal wave motion normal to the surface. The airspace separating the panels acts as a spring and at a given frequency, a mass-air-mass resonance occurs. The resonance is the same as that given in Eq. 7.103, which was developed in the discussion of air-backed panel absorbers, but the mass has been modified to account for the diffuse field and for the fact that both panels can move

$$f_0 = \frac{1}{2\pi} \sqrt{\frac{3.6 \, \rho_0 \, c_0^2}{m' \, d}} \tag{9.42}$$

where $m' = \dfrac{2 \, m_1 \, m_2}{m_1 + m_2}$ = effective mass per unit area of the
construction $(\mathrm{kg/m^2}$ or $\mathrm{lbs/ft^2})$

$\quad$ d = panel spacing (m or ft)

For a double panel wall, consisting of 16 mm (5/8") gypboard separated by a stud space of 9 cm (3.5"), the mass-air-mass resonance occurs at about 66 Hz. At low frequencies, below the resonant frequency, the two panels act as one mass. If the individual panels are mass controlled then the transmission loss follows the mass law of the composite structure.

At frequencies above the mass-air-mass resonance, the effect of the air cavity is to increase the transmission loss significantly. In fact for N separate panels, the ideal theoretical transmission loss increases 6(2N-1) dB per octave. At high frequencies, constructions having multiple panels with intervening air spaces can provide significant increases in transmission loss over that achieved by a single panel. Since it is rarely practical to construct walls or floors with more than about three panels, consideration of large numbers of panels is generally not useful.

A plane wave encountering a double-panel system sees the impedance of the nearest panel, the impedance of the airspace, the impedance of the second panel, and finally the impedance of the air beyond. The transmissivity has been given by London (1950) as

$$\tau_\theta = \left[1 + (X_1 + X_2) + X_1 X_2 \left(1 - e^{-j\sigma}\right)\right]^{-2} \tag{9.43}$$

where $X = \dfrac{z_n \, \cos \theta}{2 \, \rho_0 \, c_0}$

$\quad z_n$ = normal impedance of a panel (rayls)

$\quad \sigma = 2 \, k \, d \, \cos \theta$

$\quad k = \dfrac{2 \, \pi \, f}{c_0}$ = wave number (m^{-1})

Below the critical frequency the panel impedance is equal to its mass reactance and, for a diffuse field, the transmission loss of an ideal double panel system of infinite extent, attached

only through the air spring coupling, is

$$\Delta L_{TL} \cong 10 \log \left\{ 1 + \left[\frac{\omega\, M}{3.6\, \rho_0\, c_0} - \frac{\omega^2\, m_1\, m_2}{\left(3.6\, \rho_0\, c_0\right)^2} \left(1 - e^{-2jkd} \right) \right]^2 \right\} \tag{9.44}$$

where   m = mass per unit area of an individual panel (kg/m^2)

M = total mass per unit area of the construction (kg/m^2)

At low frequencies, below the mass-air-mass resonance, the panel spacing is small compared with a wavelength so the rightmost term in Eq. 9.44 approaches zero and the transmission loss can be approximated by

$$\Delta L_{TL} \cong 10 \log \left\{ 1 + \left[\frac{\omega\, M}{3.6\, \rho_0\, c_0} \right]^2 \right\} \tag{9.45}$$

which is just the mass law for the composite panel.

$$\Delta L_{TL} \cong 20 \log (f\, M) - K_{TL} \qquad f < f_0 \tag{9.46}$$

At frequencies above f_0, but still below the point where the wavelength is comparable to the panel separation, the rightmost term in Eq. 9.44 begins to dominate. In this region the wavelength is still larger than the panel spacing, so (2 k d) is small and $e^{-2jkd} \cong 1 - 2jkd$. The transmission loss can be approximated by

$$\Delta L_{TL} \cong 20 \log \left[\frac{\omega^2\, m_1\, m_2}{\left(3.6\, \rho_0\, c_0\right)^2}\, 2\, k\, d \right] \tag{9.47}$$

which can be written as

$$\Delta L_{TL} \cong \Delta L_{TL1} + \Delta L_{TL2} + 20 \log (2\, k\, d) \qquad f_0 > f > f_\ell \tag{9.48}$$

where ΔL_{TL1} and ΔL_{TL2} are the mass law transmission losses for each panel. Each term in Eq. 9.48 increases 6 dB per octave so the overall transmission loss rises 18 dB per octave in this frequency range. It also increases 6 dB for each doubling of the separation distance between the panels. At still higher frequencies resonant modes can be sustained in the airspace between the panels and there arises a series of closed tube resonances, normal to the surfaces, having frequencies

$$f_n = \frac{n\, c_0}{2\, d} \quad \text{for } n = 1, 2, 3 \ldots \tag{9.49}$$

These aid in the transfer of sound energy between the panels and result in a series of dips in the double-panel transmission loss, shown in Fig. 9.16. Due to the damping provided by batt insulation, we usually do not see this pattern in actual transmission loss measurements, which are carried out in third-octave bands. Batt flattens out the slope of the transmission

FIGURE 9.16   Theoretical Transmission Loss of an Ideal Double Panel (Sharp, 1973)
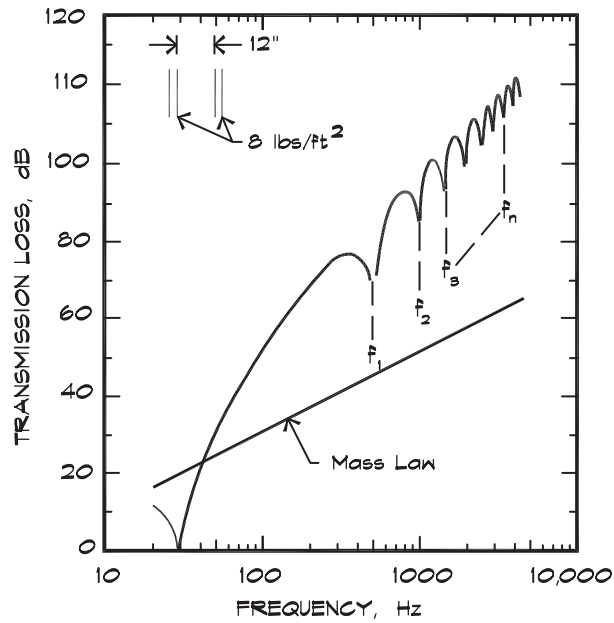
loss curve from 18 dB/octave down to 12 dB/octave in this region. The transmission loss behavior above a limiting frequency is given by

$$\Delta L_{TL} \cong \Delta L_{TL1} + \Delta L_{TL2} + 6 \qquad f_{\ell} < f \qquad (9.50)$$

The crossover frequency, which can be obtained by setting Eq. 9.48 equal to Eq. 9.50, is equal to the first cavity resonance frequency divided by π.

$$f_l = \frac{c_0}{2\pi d} = \frac{f_1}{\pi} \qquad (9.51)$$

Equations 9.46, 9.48, and 9.50 give the transmission loss of an ideal double panel system in three frequency ranges separated by the frequencies in Eqs. 9.42 and 9.51. Measurements by Sharp (1973) have shown that there is good agreement between theoretical and measured data for both the mass-reactance region (Fig. 9.17) and the critical region (Fig. 9.18). The panel transmission loss values in the critical region were used instead of simple mass law predictions.

Cavity Insulation

The theory that has been developed here has assumed that the air cavity is well damped. When there is no absorptive material between the panels, cavity resonances contribute to the transmission of sound from one side to the other in much the same way as a mechanical coupling would. The addition of damping material such as fiberglass batt insulation attenuates these modes. Figure 9.19 (Sharp, 1973) shows the effects of a fully isolated double-panel system, with and without batt insulation. The panels used were 1/4" and 1/8" hardboard so that the coincidence frequencies were above the frequency range of interest. Below the first

FIGURE **9.17** **Measured and Calculated Transmission Loss Values for a Separated Double Panel (Sharp, 1973)**
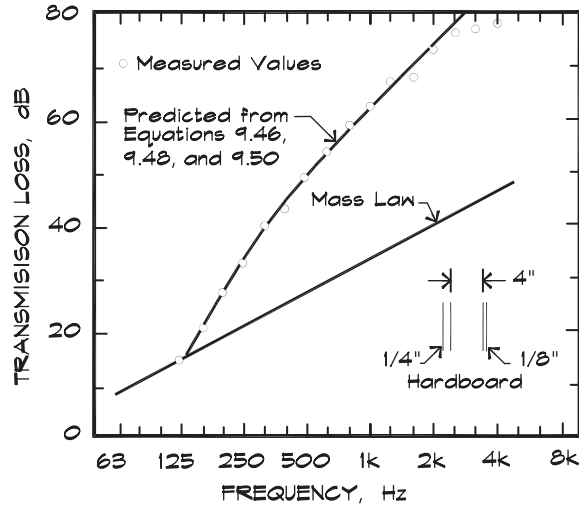
FIGURE **9.18** **Transmission Loss Values for a Separated Double Panel Including Coincidence (Sharp, 1973)**
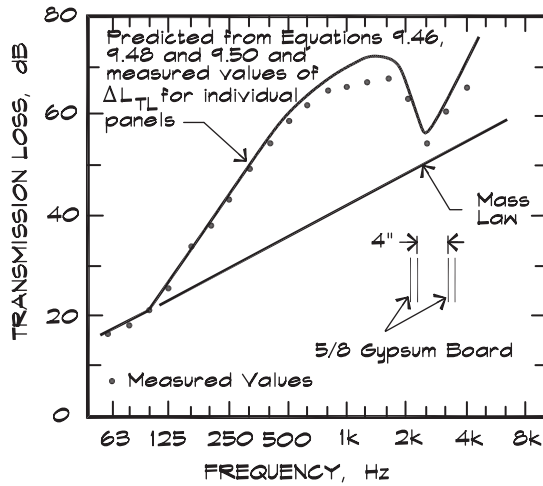
FIGURE 9.19   Transmission Loss of an Isolated Double Panel Construction with and without Insulation (Sharp, 1973)

The construction consists of 1/4" and 1/8" hardboard with a spacing of 6-1/4 inches.
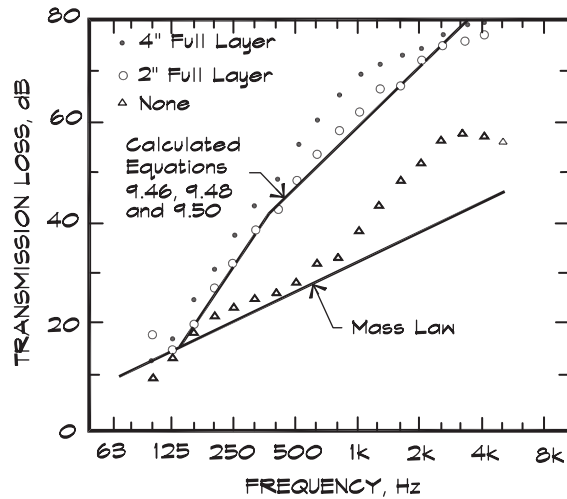
cavity resonance (1100 Hz), the panels are so coupled by the cavity resonances that the transmission loss follows the mass law. Above the first resonance, the phase varies over the depth of the cavity and the coupling is weaker. When 2" insulation is introduced into the cavity the wall begins to act like a double-panel system. With 4" of insulation, the mass of the insulation is comparable to that of the panel and transmission losses are greater than those predicted using simple theory.

Table 9.2 shows measured increases in STC values for various thicknesses of insulation between separately supported 16-mm (5/8") gypboard wall panels. The effectiveness of batt insulation in a wall cavity is almost entirely dependent on its thickness. The density of the fill for a given thickness makes only a small difference at relatively high frequencies, above 1000 Hz. The presence of paper backing on the fiberglass makes no difference for gypboard partitions, nor does the position of the partial thickness within the cavity, including contact with either side. Weaving a blanket of insulation around staggered studs is no more effective than the simpler method of placing the batt vertically between the studs. The

TABLE 9.2   Measured Effects of Fiberglass Batt in Completely Separated Double Panel Walls (Owens Corning Fiberglass, 1970)

Thickness of Cavity Fill	Average Increase in STC (dB)
1 1/2"	10
2"	11
3"	12
4"	13
6"	15
8"	16

FIGURE 9.20   **Transmission Loss of an Isolated Double Panel Construction with Perimeter Insulation (Sharp, 1973)**

The construction is 1/4" and 1/8" hardboard panels with a 6 1/4" airspace.
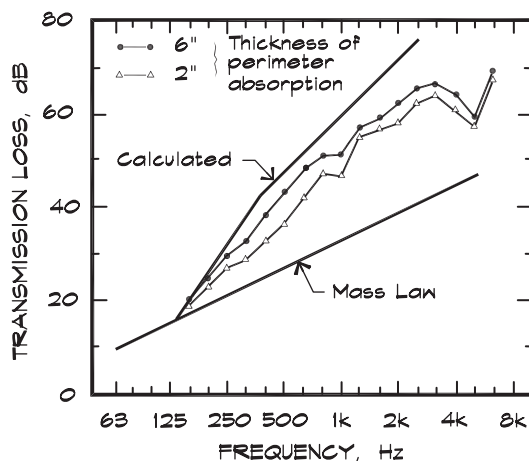
effectiveness of insulation in staggered stud and single stud walls is much less than in ideal walls due to the high degree of mechanical coupling between the two sides. Improvements in real (with studs, etc.) walls of from 3 to 7 dB were obtained, with insulation thicknesses of 2 to 6 inches. For most walls and floor-ceilings, where the two sides are mechanically coupled together in some way, the addition of batt insulation increases the STC from 3 to 5 dB for the first three inches of material and about a dB per inch above that point. Thicknesses of batt insulation beyond the stud spacing are not helpful since the compressed batt can form a structural bridge between the panels.

Higher order cavity modes, which are not necessarily perpendicular to the panels, can contribute to the sound transmission in the mid and high frequencies. Therefore, absorptive material is quite effective even if it is placed only around the perimeter of the cavity. This is a common technique used in the construction of double-glazed sound-rated windows for studios. Figure 9.20 illustrates the effect of insulation placed only around the perimeter of the cavity. At low frequencies, the transmission loss increases with the thickness of the insulation. In studio window construction it is helpful to leave an opening into the wall cavity, which acts as a Helmholtz resonator absorber, tuned to the mass-air-mass resonance frequency.

Double-Panel Design Techniques

At frequencies below the mass-air-mass (m-a-m) resonance, a double-panel wall acts as a single unit and the stiffness and mass are the most important contributors to transmission loss. Above the m-a-m resonance, both mass and panel spacing are important as shown in Fig. 9.21. Equation 9.47 holds that, for a given total mass, the transmission loss is greatest if the mass is distributed equally on both sides of the wall. This is generally true although it is a commonly held belief that unbalanced construction is preferred because of the desirability of mismatching the critical frequencies of the panels. Recent studies (Uris et al., 2000) have

**FIGURE 9.21   Effect of Mass and Spacing on Transmission Loss Ideal Double Panel
Construction (Sharp, 1973)**
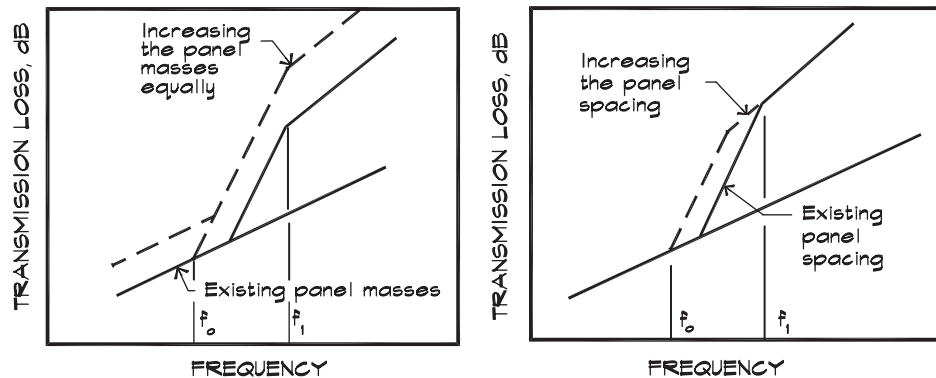
shown that, for a given mass, there is little difference between balanced and unbalanced gypsum board wall constructions, even at coincidence. The coincidence effect can be controlled by adding damping or by using different thicknesses of gypboard, while maintaining an overall equality of mass on each side (Green and Sherry, 1982).

Because of the m-a-m resonance, a certain minimum air space is necessary before double-panel construction becomes significantly better than a single panel. Figure 9.22 shows a series of transmission loss tests (Vinokur, 1996) for single-glazed and various configurations of dual-glazed windows. The large dip at about 700 Hz for curve 6 corresponds to the m-a-m resonant frequency. Curves 2 and 4 illustrate the effects of mechanical coupling through direct connection between the window frames. Bridging provides a short circuit across the main air gap and magnifies the importance of the coincidence effects.

Additional tests by Vinokur using 3 mm (1/8") laminated and plate glass are summarized in Fig. 9.23. An STC of 34 was achieved with the two sheets of glass laminated together, and this result was not bettered for double-glazed windows until the airspace exceeded 25 mm (1"). The lesson here is that not all double-glazed windows are better than single-glazed even when the total overall thickness of glass is the same. When the spacing between panels is small, it is not uncommon to find that a double-panel construction has a lower transmission loss than that of the two individual single panels sandwiched together. This accounts for the failure of thin double-panel windows, sometimes referred to as thermopane windows, to provide appreciable noise reduction.

In the region around coincidence, panels may be deadened using a sandwiched damping compound. In the Vinokur tests, glass panels were laminated together using 0.7 or 1.4 mm thick polyvinylbutyral. The coincidence dip for a laminated panel (curve 6) is significantly smaller than for single (curve 5) or double (curve 2) plate glass, where there is structural bridging. Harris (1992) reports that a sandwiched viscoelastic layer contained between two layers of 5/8" plywood can improve the transmission loss of lightweight wood floor systems. Gluing plywood floor sheathing can also be helpful.

Increasing the spacing between the partitions drives down the m-a-m resonance frequency and increases the transmission loss above that point. Measured window data show that above a spacing of about 20 mm the improvement is about 3.5 STC points per doubling

FIGURE 9.22   **Transmission Loss of Various Glazing Configurations (Vinokur, 1996)**

Curves 1 and 3 describe separate panels. Curves 2 and 4 were obtained from units with rigidly interconnected frames.
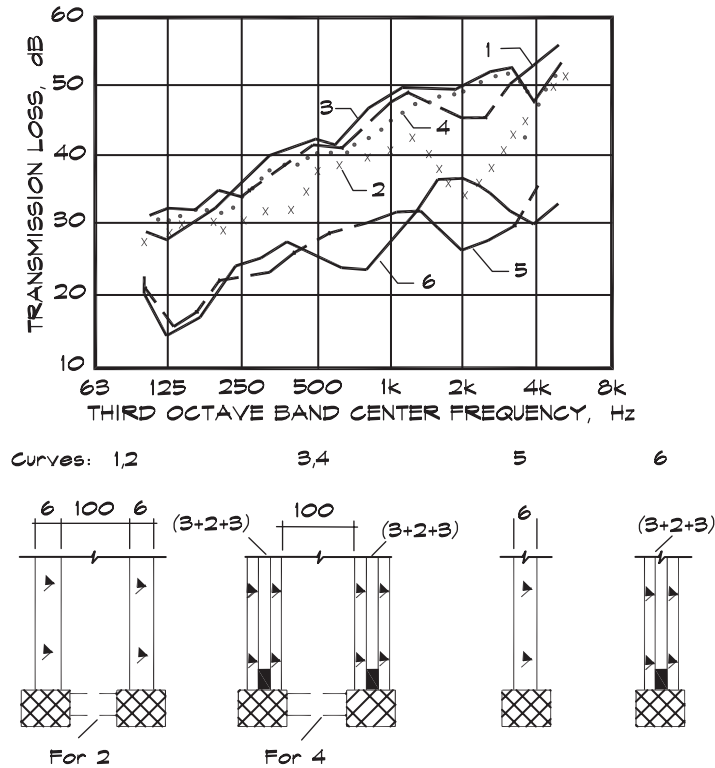
of distance between the panes and about the same increase per doubling of mass. Figure 9.24 gives laboratory data taken by Quirt (1982) for various thicknesses and spacings of window glazing. The upward trend for both mass and spacing is clear.

In the case of gypboard panels, the coincidence frequency can be kept high by using multiple sheets of differing thicknesses that are spot laminated together. In other cases, panels can be designed so that the coincidence frequency is greater than the frequency range of interest. Where thick panels such as concrete slabs or grouted concrete masonry units are used, an additional separately supported panel of gypsum board can be used to offset the low shear frequency of the concrete with a high coincidence frequency in the gypboard. In the coincidence region, the ideal mismatch is on the order of a factor of two; however, more modest ratios can provide several dB of benefit.

The coincidence effect is emphasized, perhaps overemphasized, by the STC test procedure since the knee in the standard STC curve falls at about half the critical frequency of 16-mm (5/8") drywall. Due to this fact double walls with single 13 mm (1/2") gypboard often test higher than 16 mm (5/8") gypboard and 10 mm (3/8") higher than 13 mm (1/2") (California Office of Noise Control, 1981). For a given mass of panel the thinner material is more effective due to the higher critical frequency. A higher STC value in these cases does not necessarily mean that a given construction is more effective at reducing noise, since

FIGURE 9.23   Transmission Loss Tests on Laminated and Double Glazed Windows (Vinokur, 1996)

Curves 1 and 3 describe separate panels. Curves 2 and 4
were obtained from units with rigidly interconnected frames.
4 x 4 is the descriptive code for a laminated pane.

THIRD OCTAVE BAND CENTER FREQUENCY, Hz
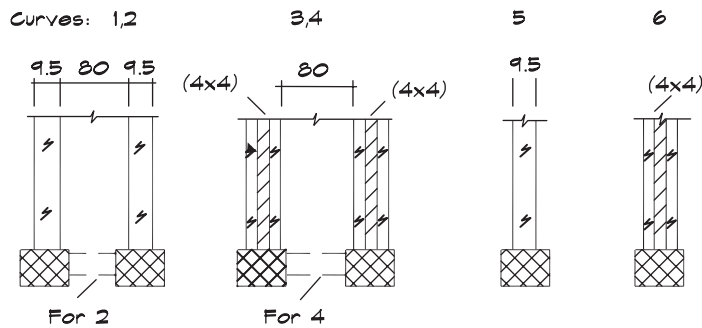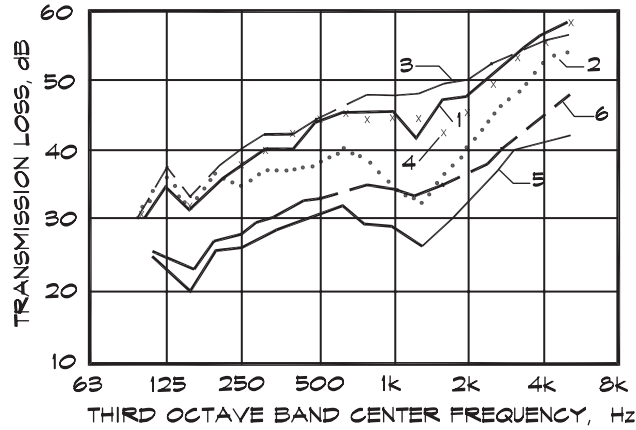
noise reduction depends on the source spectrum. At low frequencies, the heavier panels are more effective regardless of their STC rating.

There is a common misunderstanding, particularly in the design of windows in sound studios, that the slanting of one of the panes of glass with respect to the other provides some acoustical benefit. The mass-air-mass resonance is a bulk effect and is shifted only slightly by the use of a slanted panel. A careful study of window design effects, undertaken by Quirt (1982), showed that slanting had no appreciable effect on the transmission loss of double pane windows. However the technique of slanting one sheet of glass in studio control room windows is useful in reducing the ghost images from light reflections between the panes.

The introduction into the airspace of a gas such as argon, carbon dioxide, or SF_6, which have a sound velocity lower than that of air, has much the same effect as batt insulation in the cavity. Gasses that have a higher velocity than air, such as helium, can also be effective. These gasses are used in hermetically sealed dual-paned windows. The mismatch in velocity reduces the coincidence effect since, when the interior wave matches the bending velocity, the exterior wave does not.

FIGURE 9.24   STC vs Interpane Spacing for Separately Supported Double Glazing (Quirt, 1982)
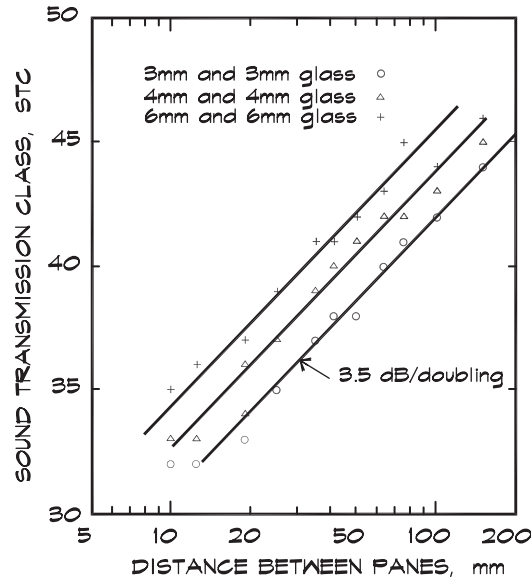
9.4   TRIPLE-PANEL TRANSMISSION LOSS THEORY

Free Triple Panels

The impedance of ideal triple panels, with no mechanical connections, can be calculated in a similar fashion to that used to obtain the double panel result. The system is pictured in Fig. 9.25. It consists of three masses and two air springs and is a two-degree of freedom system. As such it has two resonant frequencies given by the equation (Vinokur, 1996)

$$f_{\alpha,\beta} = \frac{1}{2\,\pi}\,\sqrt{3.6\,\rho_0\,c_0^2}\,\sqrt{a \pm \sqrt{a^2 - b}} \qquad \left(f_\beta > f_\alpha\right) \qquad (9.52)$$

where $a = \dfrac{1}{2\,m_2}\left(\dfrac{m_1 + m_2}{m_1\,d_1} + \dfrac{m_2 + m_3}{m_3\,d_2}\right)$

$\qquad b = \dfrac{M}{m_1\,m_2\,m_3\,d_1\,d_2}$

FIGURE 9.25   General Model of a Triple Panel System

Triple Panel

Mass-Spring-Mass-Spring-Mass
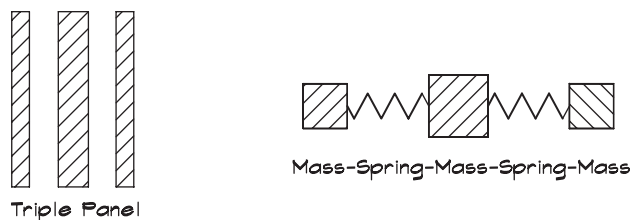
m_i = mass of the i th panel (kg/m^2 or lbs/ft^2)
d_j = spacing of the j th air gap between the layers (m or ft)
$M = m_1 + m_2 + m_3$

The resulting transmission loss can be simplified (Sharp,1973) to provide approximations, which fall into three frequency ranges

$$\Delta L_{TL} \cong \begin{cases} 20 \log (M f) - K_{TL} & f < f_\alpha \\ \Delta L_{TL1} + \Delta L_{TL2} + \Delta L_{TL3} + 20 \log (2 k d_1) + 20 \log (2 k d_2) & \\ & f_\beta < f < f_l \\ \Delta L_{TL1} + \Delta L_{TL2} + \Delta L_{TL3} + 12 & f_l > f \end{cases} \quad (9.53)$$

Below the lower mass-air-mass resonance, the triple-panel construction reverts to mass-law behavior. Above the higher mass-air-mass resonance, but lower than the lowest cavity resonance divided by π (as defined by Eq. 9.51), the transmission loss increases at a rate of 30 dB per octave compared with 18 dB per octave for the double panel. In this frequency range the transmission loss is increased 18 dB per doubling of mass.

Comparison of Double and Triple-Panel Partitions

It is useful to compare the behavior of double- and triple-panel walls, which are available for the construction of critical separations such as those found in sound studios and high-quality residential construction. At low frequencies, below f_0, the mass law applies to both types of construction, so for a given mass and thickness the performance is the same. Figure 9.26 shows a graph of the transmission loss achieved by the two types. Here the triple panel has a symmetric construction with the center panel having twice the mass of the outer panels and equal air spaces on either side. For this configuration, the lowest mass-air-mass resonant frequency, f_α, is twice that of the double construction frequency f_0. The two transmission

FIGURE 9.26   Double and Triple Panel ΔL_{TL} Comparison (Sharp, 1973)

A comparison of the transmission loss provided by double and triple panel constructions of equal total mass and overall thickness.
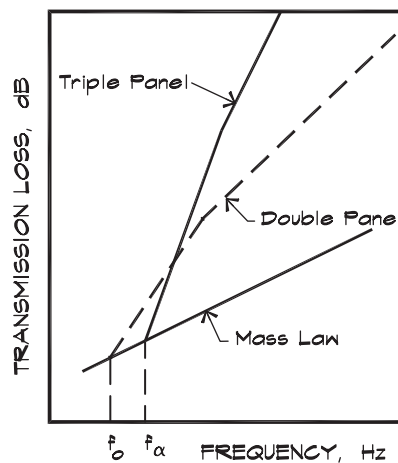
loss curves cross at a frequency that is four times f_0. Thus, assuming no connections between the panels, the double panel system is better below $4f_0$ and the triple panel is better above $4f_0$. For a wall consisting of one layer of 16 mm (5/8") gypboard on the outer panels and two layers on the inside, separated by two 90 mm (3.5") airspaces, the crossover point $4f_0$ is about 260 Hz.

In general, walls with double panels are more efficient for the isolation of music, where bass is the main concern, and triple panels for the isolation of speech. Triple panels, however, are more forgiving of poor construction practice, such as improperly isolated electrical boxes and noisy plumbing, since they provide an additional layer in the middle of the wall or floor. These practical effects in many cases may be more important than a theoretically higher transmission loss.

For a given total mass and thickness, triple-glazed windows are not as effective as double glazing, since the separation between panes in triple-glazed windows is not large. They are most effective when the heaviest sheet of glass is an outer layer and not in the center, and when the airspace dimensions are not the same. Figure 9.27 illustrates this point through a series of tests carried out by Vinokur (1996). Example 2 shows the effect of the transposition of position of the heavy and light sheets of glass. Example 3 shows that it is effective to closely space the two light panes of glass even when the larger airspace does not increase. This configuration acts more like a double-glazed unit. At the higher frequencies, the primary transmission path in windows is from pane to pane through the edge connections at the frame.

FIGURE 9.27   Measurements of Triple Panel Glass Units (Vinokur, 1996)

Glazed units have the following glazing descriptive codes:
(1) 3+20+10+20+3; (2) 10+20+3+20+3; (3) 10+20+3+2+3
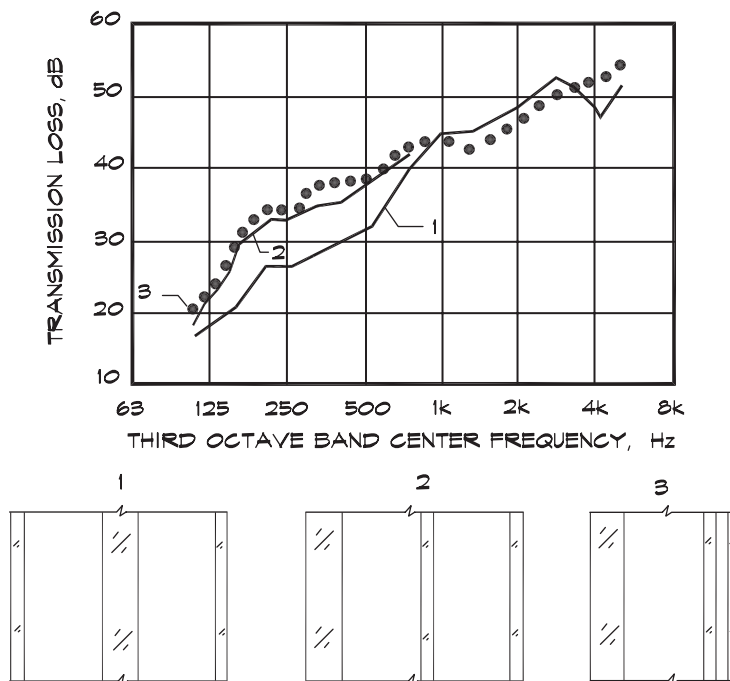
9.5   STRUCTURAL CONNECTIONS

Point and Line Connections

In the previous theoretical analysis, it has been assumed that there were no structural connections linking the panels, in either the double or the triple constructions. The only means of connection between the panels was through the coupling provided by the air space. In actual building construction, there are studs, joists, and other elements that provide the structural support system and physically connect panels together. These produce a parallel means of sound transmission, by way of mechanical connections from one panel to another. In general there are two types of connections: a line connection, such as that provided by wood or metal studs, which touch the panels continuously along their length; and a point connection, in which the contact is made over a relatively small area that approximates a point.

The theory published by Sharp (1973) for the transmission of sound through mechanical connections assumes that the power transmitted by the panel on the receiving side is proportional to the square of the velocity of the panel and to its radiating area. It further assumes that, in the local area around the connection, the panel velocity on the receiving side is the same as on the sending side, and that the sending side panel is unaffected by the presence of the receiving side panel. He develops the equivalent radiating area for point and line connections, since these areas act as localized sources, which transmit energy in addition to that transmitted by the air-gap transmission path. The bridging energy transmitted is proportional to the transmitting area, which decreases with frequency since its effective radius is about one-quarter of the bending wavelength. The power radiated by this area, however, increases with frequency so that the total bridging energy transmitted stays constant.

The effect of sound bridges in double-panel construction is shown in Fig. 9.28. The normal double-panel transmission loss is truncated by the extra energy transmitted through the solid connections above the bridging frequency. The limiting value of the transmission

FIGURE 9.28   Transmission Loss of a Double Panel with Structural Bridges (Sharp, 1973)
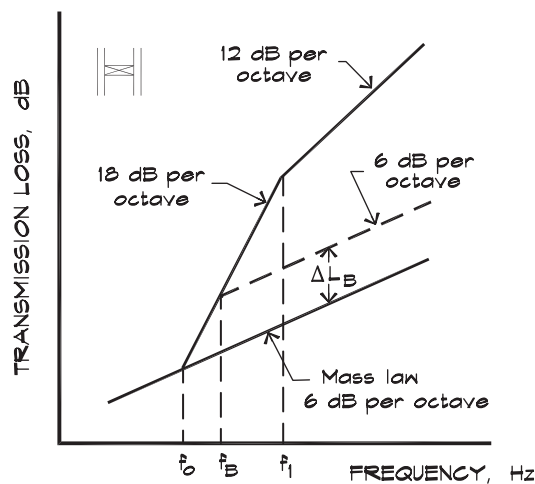
loss above the composite mass law is given for point connections (Sharp, 1973)

$$\Delta L_{BP} = 20 \log \left(e\, f_c \right) + 20 \log \left(\frac{m_1}{m_1 + m_2} \right) - K_{BP} \tag{9.54}$$

and for line connections

$$\Delta L_{BL} = 20 \log \left(b\, f_c \right) + 20 \log \left(\frac{m_1}{m_1 + m_2} \right) - K_{BL} \tag{9.55}$$

where e = point lattice spacing (m or ft)
b = line stud separation (m or ft)
m_1 = mass per unit area of the panel (kg / m^2 or lb / ft^2)
m_2 = mass per unit area on the side supported by point or line connections (kg / m^2 or lb / ft^2)
f_c = critical frequency of the panel supported by point connections or, in the case of line connections, the higher critical frequency of the two panels (Hz)
K_{BP} = constant for point connections
= − 44.7 for metric units
= − 55 for FP units
K_{BL} = constant for line connections
= − 22.8 for metric units
= − 28 for FP units

The bridging frequency for point connections is

$$f_{BP} = f_0 \left(\frac{e}{\lambda_c} \right)^{1/2} \tag{9.56}$$

and for line connections

$$f_{BL} = f_0 \left(\frac{\pi\, b}{8\, \lambda_c} \right)^{1/4} \tag{9.57}$$

Note that e^2 = the area associated with each point connection (m^2 or ft^2)
f_0 = fundamental resonance of the double panel (Hz)

The overall transmission loss for a bridged double panel is given by

$$\Delta L_{TL} \cong \begin{cases} 20 \log \left(M\, f \right) - K_{TL} & f < f_0 \\ \Delta L_{TL1} + \Delta L_{TL2} + 20 \log \left(2\, k\, d \right) & f_0 < f < f_B \\ 20 \log \left(M\, f \right) - K_{TL} + \Delta L_B & f_B < f < 0.5 f_c \end{cases} \tag{9.58}$$

FIGURE 9.29 ΔL_{TL} for a Point Mounted Double Panel Sharp (1973)

Measured values of transmission loss for a double panel with one and both panels mounted with point connections.
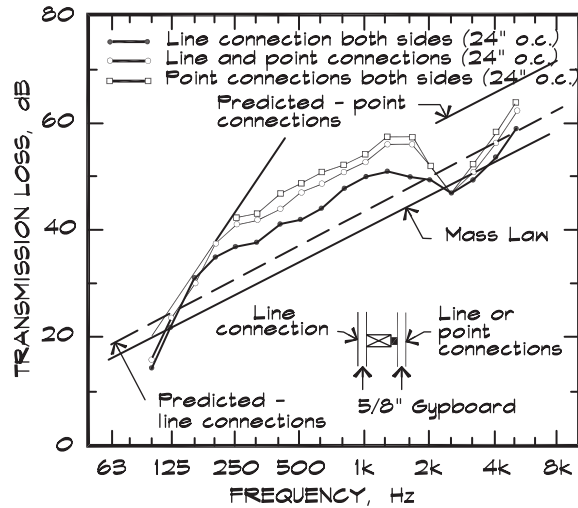
Figure 9.29 shows the results of measurements of bridged double panels done by Sharp (1973). The figure illustrates that there is little advantage to mounting both sides on point connections. Note that Eq. 9.58 does not account for the behavior at the critical frequency where the energy is transmitted by an airborne path. At the critical frequency, the various connection methods yield the same results.

When making a comparison between theoretical and laboratory transmission loss data, calculated data yield a higher result. Better agreement is obtained by assuming line bridging at a spacing based on edge connections for the panel area specified in the test standard.

Transmission Loss of Apertures

The sound transmission through apertures has been treated in some detail. Wilson and Soroka (1965) utilize an approach that analyzes a normally incident plane wave falling on a circular opening of radius a and depth h. They assume massless rigid pistons of negligible thickness at the entrance and exit of the aperture, which simulate the air motion. The radiation impedance is assumed to be that of a rigid piston in a baffle discussed in Chapt. 6. The transmission coefficient is

$$\tau = 4\,w_r \left\{ \begin{array}{l} 4\,w_r^2(\cos k\,h - x_r\ \sin k\,h)^2 + \\ \left[(w_r^2 - x_r^2 + 1)\ \sin k\,h + 2\,x_r\ \cos k\,h\right]^2 \end{array} \right\}^{-1} \tag{9.59}$$

where w_r and x_r are the resistive and reactive components of the mechanical radiation impedance of the piston radiator from Eq. 6.65. The real and imaginary parts are given in Eqs. 6.66 and 6.68.

Figure 9.30   Transmission Loss through a 1" (25 mm) Diameter 4"(100 mm) Long Hole (Gibbs and Balilah, 1989)
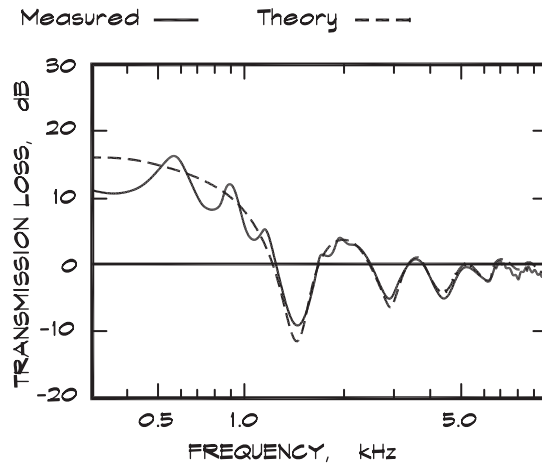
Figure 9.31   Transmission Loss through a Circular Aperture vs Frequency for Various h/a Ratios (Wilson and Soroka, 1965)
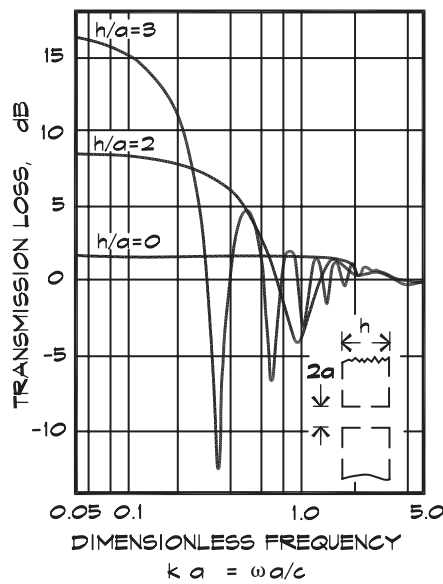
Apertures in enclosures can create Helmholtz resonator cavities, which increase the noise emitted from a source housed within them in much the same way that bass-reflex enclosures are used with cone loudspeakers to augment the low-frequency response. Figure 9.30 (Gibbs and Balilah, 1989) plots the theoretical and measured transmission loss of a 1" (25 mm) diameter hole having a 4" (100 mm) length. At low frequencies there is

about a 16 dB (theoretical) loss in this example, which drops sharply at the first open-open tube resonance. The transmission loss is negative in the vicinity of the tube resonant frequencies and gradually goes to zero as the wavelength approaches the hole diameter. Similar results were obtained by Sauter and Soroka (1970) for rectangular apertures. The loss at low frequencies depends on the ratio of the depth, h, to the hole radius, a. Figure 9.31 illustrates this effect.

This page intentionally left blank

10.1   DIFFUSE FIELD SOUND TRANSMISSION

Reverberant Source Room

The problem of sound transmission between rooms is one of considerable interest in architectural acoustics. When two rooms are separated by a common wall having an area S_w, as shown in Fig. 10.1, we model (Long, 1987) the behavior by first assuming that there is a diffuse field in the source room that produces a sound pressure p_s and a corresponding intensity

$$I_s = \frac{p_s^2}{4 \rho_0 \, c_0} \tag{10.1}$$

that is incident on the intervening partition. A fraction τ of the incident energy is transmitted into the receiving room

$$W_r = I_s \, S_w \, \tau = \frac{p_s^2 \, S_w \, \tau}{4 \, \rho_0 \, c_0} \tag{10.2}$$

where it generates a sound pressure due to both the direct and the reverberant field contributions. Since the partition is a planar surface, we use Eq. 2.91 for the direct field and Eq. 8.83 for the reverberant field portion of the energy. The receiving room sound energy is

$$\frac{p_r^2}{\rho_0 c_0} = \frac{p_s^2 \, S_w \, \tau \, Q}{16 \, \pi \, \rho_0 \, c_0 \left[z + \sqrt{\dfrac{S_w \, Q}{4 \, \pi}} \right]^2} + \frac{p_s^2 \, S_w \, \tau}{R_r \, \rho_0 \, c_0} \tag{10.3}$$

which we can convert to a level relationship by taking 10 log of each side and using the definition of the transmission loss

$$\Delta L_{TL} = -10 \log \tau \tag{10.4}$$

FIGURE 10.1 Sound Transmission between Rooms
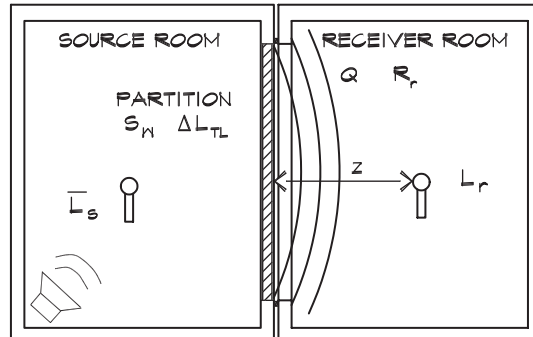
to obtain the expression for the transmission between two rooms for a diffuse source field and a combination of a direct and diffuse receiving room sound field

$$L_r = \overline{L}_s - \Delta L_{TL} + 10 \log \left[\frac{S_w\, Q}{16\,\pi \left[z + \sqrt{\dfrac{S_w\, Q}{4\,\pi}} \right]^2} + \frac{S_w}{R_r} \right] \qquad (10.5)$$

where L_r = sound pressure level at a point in the receiver room (dB)

$\overline{L}_s$ = diffuse sound pressure level in the source room (dB)

the line over the L denotes a spatial average throughout the room

ΔL_{TL} = transmission loss (dB)

S_w = area of the transmitting surface (m^2 or ft^2)

R_r = room constant in the receiving room (m^2 or ft^2 sabins)

z = distance from the surface of the source to the receiver (m or ft)

Q = directivity of the wall (usually 2)

If the receiving room is very reverberant, the S_w / R_r term is larger than the direct field term and Eq. 10.5 can be simplified to the equation we obtained in Chapt. 9 for the transmission loss between two reverberant rooms

$$\overline{L}_r \cong \overline{L}_s - \Delta L_{TL} + 10 \log \left[\frac{S_w}{R_r} \right] \qquad (10.6)$$

It is important to realize that although Eq. 10.6 is accurate for reverberant spaces with good diffusion, it is not accurate when the receiver is close to a transmitting surface or when the absorption in the receiving space is large. For example, if the receiving space is outdoors where the room constant is infinite this equation predicts that no sound will be transmitted.

Sound Propagation through Multiple Partitions

When two reverberant rooms are separated by a partition consisting of two separate components, such as a wall with a window in it, each having a different transmission loss, a *composite transmission loss* may be calculated based on Eqs. 10.4 and 10.6

$$\Delta L_{TL} = 10 \log \left(\frac{S_w}{S_1 \tau_1 + S_2 \tau_2 + \cdots + S_n \tau_n} \right) \tag{10.7}$$

Using this expression, it soon becomes clear that the component having the lowest transmission loss will control the process. It is much like having a bucket full of water with several holes in it. The largest hole (lowest transmission loss) controls the rate at which water flows out. Let us take, for example, the case where a $3^0 \times 4^0$ (915 mm × 1220 mm) window having a 25 dB transmission loss occupies part of a $20^0 \times 8^0$ (6.1 m × 2.4 m) gypboard and stud wall having a transmission loss of 45 dB. The composite transmission loss may be calculated

$$\Delta L_{TL} = 10 \log \left(\frac{160}{12(.0034) + 148(.00003)} \right) = 35.5 \text{ dB}$$

Thus, although the window has a much smaller area than the wall, it significantly reduces the overall transmission loss of the composite structure.

Composite Transmission Loss with Leaks

An even more dramatic example of a reduction in composite transmission loss is that produced by a zero transmission loss path such as an opening under a door. Using a $3^0 \times 6^8$ (0.9 m × 2 m) solid core door having a transmission loss of 30 dB and a 1/2" (13 mm) high opening under the door with a transmission loss of zero dB (at high frequencies), we obtain an overall loss of

$$\Delta L_{TL} = 10 \log \left(\frac{20.125}{20(.001) + .125(1)} \right) = 21.4 \text{ dB}$$

In this case, 8 dB, more sound energy comes through the slot under the door than through the remainder of the door. Figure 10.2 shows the effects leaks on the overall transmission loss of a structure. The relative area of the leak when compared with the overall area of the partition determines the composite transmission loss of the structure in the diffuse field model.

Transmission into Absorptive Spaces

Where sound is transmitted from a reverberant space, through a partition, and into an absorbent space, we can no longer use the approximations given in Eqs. 10.6 and 10.7. Instead, we must use Eq. 10.5, which includes consideration of the direct field contribution in the receiving space. Under these conditions, the composite transmission loss equation becomes inaccurate and we must calculate the energy contribution from each transmitting surface separately, and combine the levels in the receiving space. The results are then dependent on the physical proximity of the receiver to each transmitting surface.

If we repeat the calculation we just did using the half-inch crack under a solid core door, we will get a different answer for different distances between the observer and the

FIGURE 10.2 **Composite Transmission Loss with Leaks (Reynolds, 1981)**

Composite transmission loss of a leaky panel as a function of the total precentage of leaks.
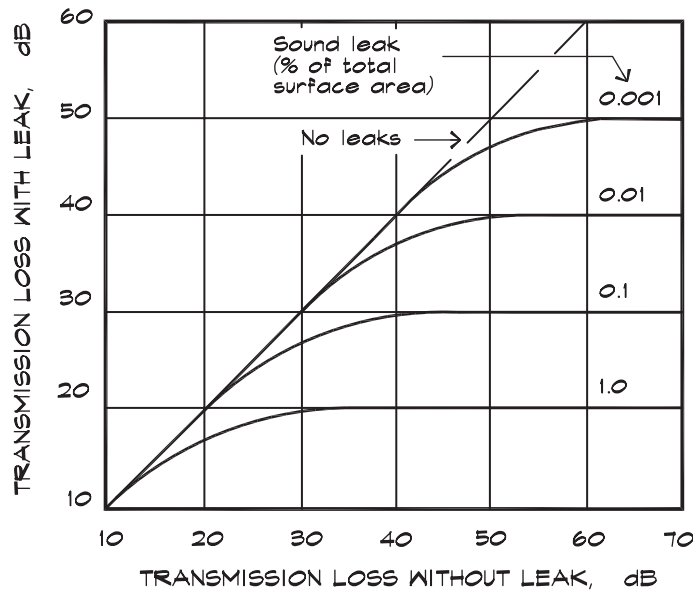
transmitting surfaces. Let us assume that the receiver is located 2 feet (0.6 m) away from the door in a space having a room constant of 1000 sq. ft. (93 sq. m) sabins, and that there is an 80 dB sound pressure level in the source room. A computation of the level through the door yields a 39 dB level in the receiving room through this path. We then perform a separate calculation for the hole. If the observer is kneeling 2 feet from the hole, the resulting level is 51 dB and the combined (door + hole) level is also 51 dB. If instead, he is standing 2 feet from the door and 6 feet from the hole, the resultant level is 44 dB and the combined level is 45 dB, which is significantly less. Note that for the same conditions Eq. 10.6 and 10.7 would predict 42 dB—less than either of the other two answers since there is no direct-field contribution.

For sound that is radiated from an enclosed reverberant space into the outdoors there is no longer a reverberant field in the receiving space so the room constant goes to infinity. Equation 10.5 then reduces to

$$L_r = \overline{L}_S - \Delta L_{TL} + 10 \log \left[\frac{S_w\, Q}{16\,\pi \left[z + \sqrt{\dfrac{S_w\, Q}{4\,\pi}} \right]^2} \right] \qquad (10.8)$$

If we use Eq. 10.8 to calculate the expected level for a receiver in the free field, close to a radiating surface, where z is nearly zero, we obtain

$$L_r \cong \overline{L}_S - \Delta L_{TL} - 6 \qquad (10.9)$$

When the distance between the surface and the receiver is large, Eq. 10.8 becomes

$$L_r \cong \overline{L}_S - \Delta L_{TL} + 10 \log \left(S_w \, Q/16 \, \pi \, z^2 \right) \tag{10.10}$$

A similar approximation can be made in an enclosed receiving space when the receiver is sufficiently far from the transmitting surface that the receiving area is large compared with the area of the surface

$$L_r \cong \overline{L}_S - \Delta L_{TL} + 10 \log \left[\frac{S_w \, Q}{16 \, \pi \, z^2} + \frac{S_w}{R_r} \right] \tag{10.11}$$

When there are multiple transmitting surfaces, the energy contribution through each surface must be calculated and the energies added to obtain the overall receiver level.

Transmission through Large Openings

When sound is transmitted through an opening in a wall that is large compared with a wavelength, an adjustment must be made to Eq. 10.8. When the formula for transmission loss is derived, it is based on the intensity passing through an area, a fraction of which is transmitted into a partition. The reason the intensity, a vector quantity, is used is that for the mass law model a panel moves as a monolithic object along one axis, normal to its surface. The only forces that move it are those with components along the normal. When reverberant sound energy passes through a large opening, all the energy falling on the opening passes through, not just the components normal to the surface. Consequently the energy transmitted is twice the reverberant-field intensity times the area as in Eq. 8.80. The difference lies in the fact that there is no longer a cosine term to integrate in the conversion from energy into intensity. If we use Eq. 10.8, whose derivation was based on intensity, the calculated value underpredicts the actual result. For transmission through a large opening in a wall, such as a door or window having a zero transmission loss,

$$L_r = \overline{L}_S + 10 \log \left[\frac{S_w \, Q}{8 \, \pi \left[z + \sqrt{\dfrac{S_w \, Q}{4 \, \pi}} \right]^2} \right] \tag{10.12}$$

Hessler and Sharp (1992) have tested this relationship by measuring the sound pressure level, generated by a reciprocating compressor in a reverberant concrete-and-steel mechanical equipment room, passing through a doorway into an open yard. The results are shown in Fig. 10.3 along with calculated levels for a Q of 4. The measured values closely match the predicted levels, indicating baffling by both the wall and the ground. It is interesting to note in the figure that the measured level at $z = 0$ is 3 dB below the interior level. This transitional behavior can be expected to occur not only for an opening, but also with any porous material, whose impedance was primarily due to flow resistance rather than mass. If the transmission loss of such a material were measured in the laboratory, the effect would be included in the measured data so the normal equation could be used, although negative transmission loss values might be found for light materials.

FIGURE 10.3 Sound Level Falloff from an Open Doorway (Hessler and Sharp, 1992)

Measured (Δ) and calculated sound levels emanating from an open
3' x 8' doorway.
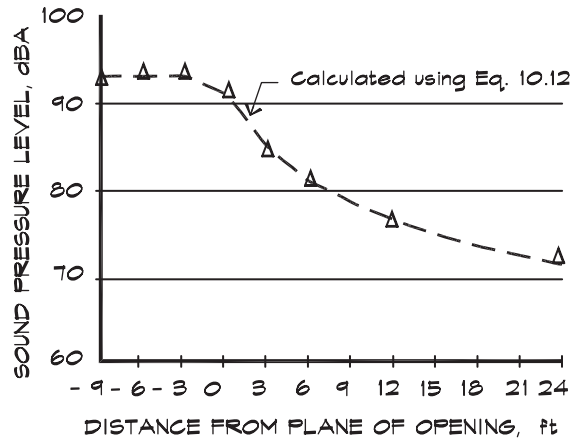
Noise Transmission Calculations

Calculations of sound propagation between spaces are done with diffuse-field transmission loss data, in individual octave or third-octave bands, and the receiving levels are combined to obtain an overall result. Most transmission loss data on walls and other components are measured in third octaves and source data (either sound power levels or sound pressure levels) are available in octave bands. Absorption coefficient data also are published primarily in octave bands. If third octave transmission loss data are used in an octave-band calculation, a composite value should be calculated.

$$\Delta L_{TL} = -10 \log \frac{1}{3} \sum_{i=1}^{3} 10^{-0.1 \Delta L_{TL_i}} \tag{10.13}$$

The exact value of course depends on the actual source spectrum and cannot be determined a priori. The same equation can be applied to the composite dynamic insertion loss of silencers.

When laboratory transmission loss data are used to predict sound levels under field conditions, the standard expectation is about a 5 dB underestimation of the receiver levels when Eq. 10.6 is used. This is acknowledged in many standards. For example, the California Noise Insulation Standards (1974) require the use of minimum STC 50 rated walls and floor-ceiling systems between dwelling units, but allow an FSTC rating of 45 under a field test. The normal reason given for this difference is the care taken in the construction of laboratory test partitions as compared to typical construction practice. A portion of the difference between laboratory and field test results may be due to the lack of consideration of the direct field contribution as well as the lack of the purely diffuse field in the receiving space assumed in the standard formula.

10.2   STC RATINGS OF VARIOUS WALL TYPES

Laboratory vs Field Measurements

The sound transmission class (STC) ratings of various construction elements are of considerable interest to architects and acoustical engineers. Although these ratings are in general use, it is also important to examine the third octave band transmission loss data that form the basis for the rating and to compare it to the theoretical predictions discussed previously. Several sets of measured data are included, which are based in part on the State of California compendium of STC and IIC ratings. It is important to note that an STC rating should not be the sole basis on which a decision to use a particular construction is made. This is particularly true in the case of floor-ceilings, where the length of the structural span and floor coverings play a major role.

Measurements of the sound transmission class in the field, as contrasted to the laboratory, are designated FSTC ratings. It is generally agreed that these ratings are five or more points lower than the laboratory ratings. The reason for this difference is attributed to the extra care in blocking the various flanking paths associated with laboratory tests and the lack of electrical outlets and other paths. It may also be in part attributable to more absorption in a typical receiving space and to the fact that the direct field transmission is not considered in the standard equation. In either case, it is prudent to design critical partitions with a margin of safety, which takes into account the expected in-field performance.

Single Wood Stud Partitions

Several single wood stud walls are shown in Fig. 10.4. Note that the effectiveness of batt insulation is much less than the ideal improvement from Fig. 9.19. This is because much of the sound is transmitted through structural coupling by the studs. Nevertheless, it is important to include batt insulation for sound control even in single stud walls.

Single Metal Stud Partitions

Examples of metal stud partitions are shown in Fig. 10.5. Single lightweight (26 Ga) metal studs are more effective than wood studs since they are inherently flexible. The studs themselves act as vibration isolators and decouple one side from another, thereby reducing structureborne noise transmission. Consequently, it is of little value to add resilient channel or other flexible mounts to nonstructural metal studs. The method of attachment also affects the transmission loss. Panels that are glued continuously to studs yield lower transmission loss values than panels that are screw attached. The gluing apparently increases the stiffness of the stud flange, which then increases transmission via the studs (Green and Sherry, 1982).

Gypsum board panels are lifted into place during construction using a spacer under their bottom edge, so there is a 3 mm to 6 mm (1/8" to 1/4") gap at the bottom of the sheet. Holes such as these must be sealed if the transmission loss of the construction is to be maintained. Closing off openings in partitions is critical to acoustical performance, particularly for the case of high transmission loss partitions. Gaps are closed off with a nonhardening caulk so the acoustical rating of the wall can be maintained. Figure 10.6 shows the effect of gaps on the STC ratings. Similar openings can be left by electrical box penetrations, pipe penetrations, cutouts for medicine cabinets, light fixtures, and duct openings. Caulk should not be used

FIGURE 10.4 Transmission Loss of Single Wood Stud Walls (California Office of Noise Control, 1981)

Single Wood Stud Wall – 2 × 4 Stud
1 Layer 5/8" Drywall Each Side
A – Without Insulation   B – R-11 Batt Insulation

	125	160	200	250	315	400	500	630	800	1K	1.3K	1.6K	2K	2.5K	3.2K	4K	STC
A	15	15	20	24	27	29	32	36	39	41	41	40	37	36	39	43	34
B	17	15	25	35	34	32	37	40	40	43	44	45	37	34	41	47	36

Single Wood Stud Wall – 2 × 4 Stud
1 Layer 5/8" Drywall One Side
Two Layers Opposite Side
A – Without Insulation   B – R-11 Batt Insulation

	125	160	200	250	315	400	500	630	800	1K	1.3K	1.6K	2K	2.5K	3.2K	4K	STC
A	19	19	23	26	28	28	34	36	39	38	38	41	43	44	49	52	36
B	19	21	27	30	32	32	36	40	42	40	40	43	44	46	50	52	39

Single Wood Stud Wall – 2 × 4 Stud
2 Layers 1/2" Drywall Each Side
A – Without Insulation   B – R-11 Batt Insulation

	125	160	200	250	315	400	500	630	800	1K	1.3K	1.6K	2K	2.5K	3.2K	4K	STC
A	15	19	35	35	34	42	43	43	47	48	50	52	53	48	46	50	39
B	21	24	40	37	36	42	45	46	48	50	51	54	55	50	47	51	45

to span more than a 6 mm (1/4") gap. Larger openings should be filled with drywall mud or gypboard.

Resilient Channel

Resilient channel is a flexible strip of metal designed to support layers of gypboard, while providing a measure of mechanical isolation against structure borne vibrations. A group of wall constructions is shown in Fig. 10.7. Note that the channel is attached to the studs only on one side. Resilient channel should be installed with the open side up so that the weight of the gypboard tends to open the gap between the stud and the board. A filler strip is used at the base plate as a solid protection against impact. The gypboard is attached with drywall screws to the channel and care must be exercised to avoid screwing through the channel and into the studs, which short-circuits the isolation. When there are bookcases or other heavy objects that must be wall mounted, resilient channel is not a good choice since these items must be bolted through into the structure.

There are a number of products called resilient channel on the market. Some are more effective than others. A type that is spoon-shaped and can be attached only on one side is preferable to the furring channel type, which is hat-shaped and may be attached on both sides. The latter is often improperly installed, rendering it ineffective.

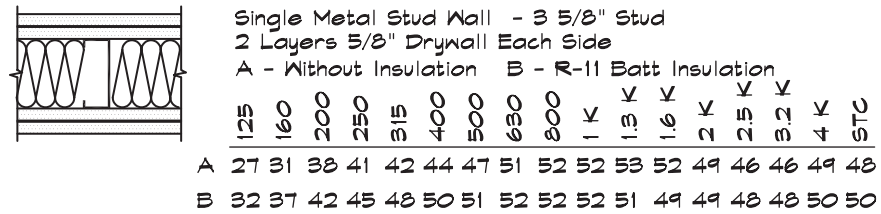**FIGURE 10.5 Transmission Loss of Single Metal Stud Walls (California Office of Noise Control, 1981)**

Single Metal Stud Wall – 3 5/8" Stud
1 Layer 5/8" Drywall Each Side
A – Without Insulation   B – R-11 Batt Insulation

	125	160	200	250	315	400	500	630	800	1	1.3	1.6	2	2.5	3.2	4	STC
A	20	23	30	31	30	34	40	41	45	48	49	47	39	38	40	46	39
B	29	35	40	42	43	48	52	55	57	57	57	54	45	40	44	50	44

Single Metal Stud Wall – 3 5/8" Stud
1 Layer 5/8" Drywall One Side
Two Layers Opposite Side
A – Without Insulation   B – R-11 Batt Insulation

	125	160	200	250	315	400	500	630	800	1	1.3	1.6	2	2.5	3.2	4	STC
A	29	31	35	38	41	44	48	47	49	51	53	56	53	44	41	46	45
B	35	37	40	39	40	42	44	47	50	54	56	55	50	44	46	50	47

Single Metal Stud Wall – 3 5/8" Stud
2 Layers 5/8" Drywall Each Side
A – Without Insulation   B – R-11 Batt Insulation

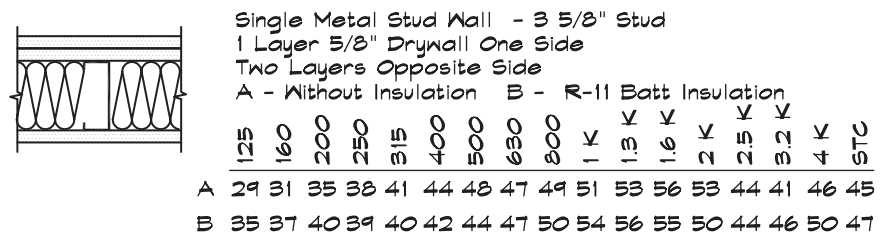|	125	160	200	250	315	400	500	630	800	1	1.3	1.6	2	2.5	3.2	4	STC
A	27	31	38	41	42	44	47	51	52	52	53	52	49	46	46	49	48
B	32	37	42	45	48	50	51	52	52	52	51	49	49	48	48	50	50

FIGURE 10.6 Dependence of the STC Rating on Caulking (Ihrig, Wilson. 1976)

MEASURED LABORATORY
STC RATING

NO CAULKING   STC 19

ONE BEAD OF
CAULKING UNDER   STC 30
RUNNER

TWO BEADS OF   STC 50
CAULKING AT EDGES
OF GYPSUM BOARD
AND SIDES OF RUNNER

FIGURE 10.7 Transmission Loss of Single Stud Resilient Walls (California Office of Noise Control, 1981)

Single Wood Stud Wall – 2 × 4 Stud
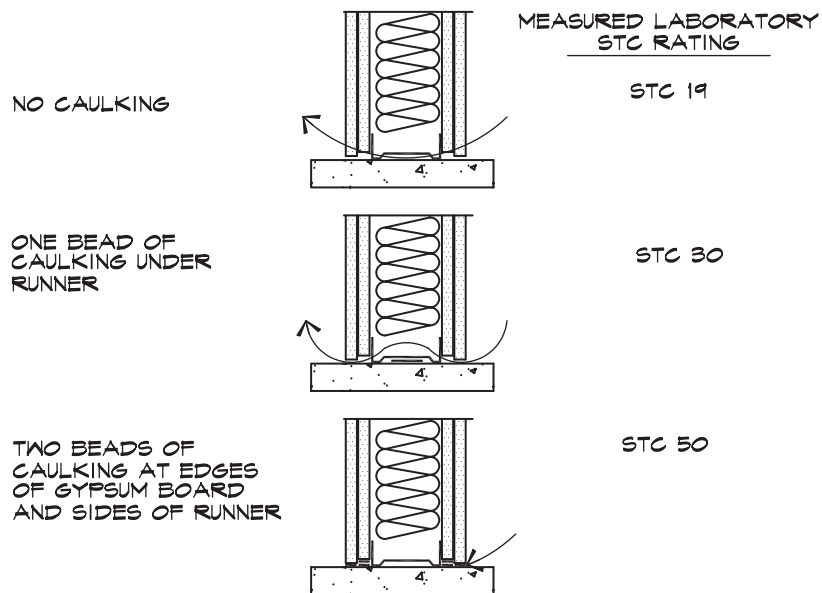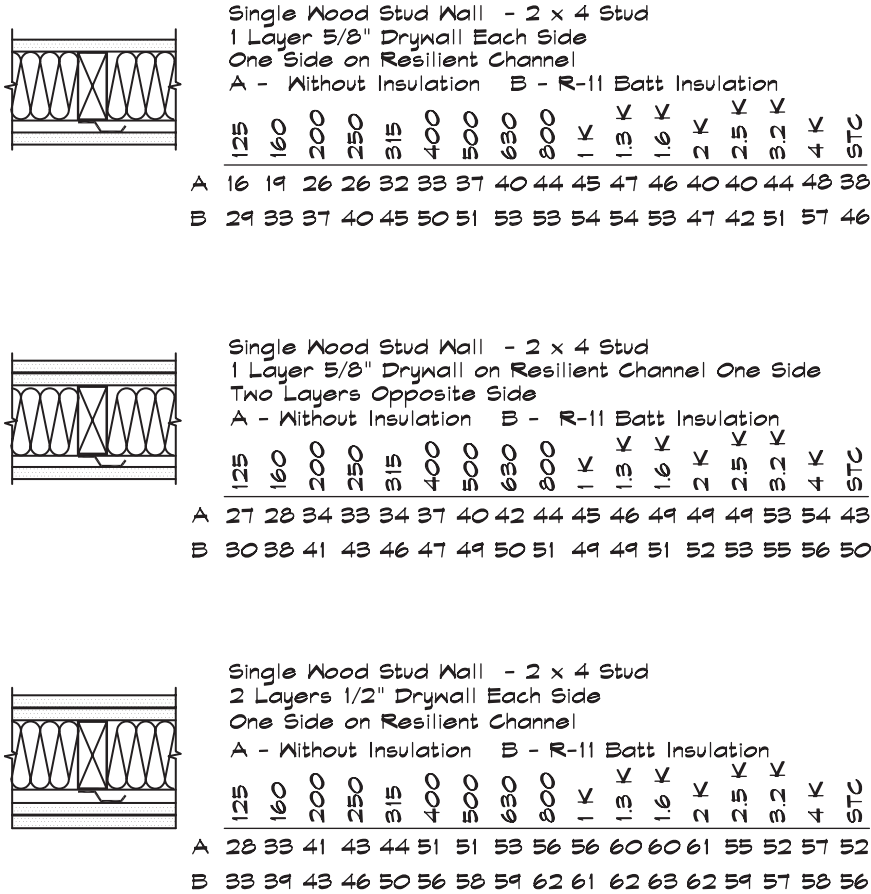1 Layer 5/8" Drywall Each Side
One Side on Resilient Channel
A – Without Insulation   B – R-11 Batt Insulation

	125	160	200	250	315	400	500	630	800	1K	1.3K	1.6K	2K	2.5K	3.2K	4K	STC
A	16	19	26	26	32	33	37	40	44	45	47	46	40	40	44	48	38
B	29	33	37	40	45	50	51	53	53	54	54	53	47	42	51	57	46

Single Wood Stud Wall – 2 × 4 Stud
1 Layer 5/8" Drywall on Resilient Channel One Side
Two Layers Opposite Side
A – Without Insulation   B – R-11 Batt Insulation

	125	160	200	250	315	400	500	630	800	1K	1.3K	1.6K	2K	2.5K	3.2K	4K	STC
A	27	28	34	33	34	37	40	42	44	45	46	49	49	49	53	54	43
B	30	38	41	43	46	47	49	50	51	49	49	51	52	53	55	56	50

Single Wood Stud Wall – 2 × 4 Stud
2 Layers 1/2" Drywall Each Side
One Side on Resilient Channel
A – Without Insulation   B – R-11 Batt Insulation

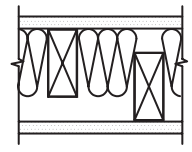|	125	160	200	250	315	400	500	630	800	1K	1.3K	1.6K	2K	2.5K	3.2K	4K	STC
A	28	33	41	43	44	51	51	53	56	56	60	60	61	55	52	57	52
B	33	39	43	46	50	56	58	59	62	61	62	63	62	59	57	58	56

The purpose of resilient channel is to provide a flexible connection to mechanically decouple the partitions on either side of the framing. When the panels are already separately or flexibly supported, the addition of resilient channel does little to improve the transmission loss. Thus there is little or no advantage in adding channel to double stud, staggered stud, or single lightweight metal stud construction.

Resilient channel is not effective when it is installed between two layers of gypboard, since the air gap is small (typically 13 mm or 1/2") and the trapped air creates an air spring, which makes an additional mass air mass resonance. If a single metal stud wall with batt insulation has drywall on each side and another layer is added on resilient channel, the result is worse than without the additional layer (Green and Sherry, 1982).
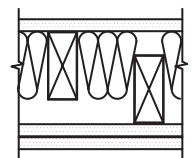
Resilient channel is utilized in floor-ceilings more often than in walls since it is compromised by mounting bookcases or cabinets to the supporting studs. It is only effective in isolating small-amplitude vibrations that are much less than the structural deflection under load. It is generally not effective in preventing the transmission of low-frequency sound created by the large-scale deflection of long-span joists under a dynamic load. However, it can provide an improvement at high frequencies to both the STC and IIC ratings in floor-ceiling systems. In floor-ceilings, it should be installed so that the ceiling gypboard is butted

FIGURE 10.8 Transmission Loss of Staggered Stud Walls (California Office of Noise Control, 1981)
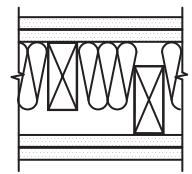
Staggered Wood Stud Wall
2 x 4 Studs on a 2 x 6 Plate
1 Layer 5/8" Drywall Each Side
A – Without Insulation   B – R-11 Batt Insulation

	125	160	200	250	315	400	500	630	800	1K	1.3	1.6	2K	2.5	3.2	4K	STC
A	29	30	33	36	39	43	44	44	46	46	50	50	43	39	46	51	43
B	34	36	40	43	45	45	45	46	47	49	50	49	45	42	46	53	46

Staggered Wood Stud Wall
2 x 4 Studs on a 2 x 6 Plate
1 Layer 1/2" Drywall One Side
Two Layers Opposite Side
A – Without Insulation   B – R-11 Batt Insulation

	125	160	200	250	315	400	500	630	800	1K	1.3	1.6	2K	2.5	3.2	4K	STC
A	32	32	35	36	39	46	46	49	50	53	54	55	47	44	50	55	47
B	38	41	41	44	47	51	51	53	54	55	56	57	58	54	50	55	53

Staggered Wood Stud Wall
2 x 4 Studs on a 2 x 6 Plate
2 Layers 5/8" Drywall Each Side
A – Without Insulation   B – R-11 Batt Insulation

	125	160	200	250	315	400	500	630	800	1K	1.3	1.6	2K	2.5	3.2	4K	STC
A	31	35	36	42	45	47	49	51	54	54	56	56	53	51	55	59	51
B	35	39	45	45	49	49	52	53	54	55	56	57	54	50	53	57	53

against the wall gypboard, leaving the resiliently supported surface free to move. If the ceiling surface rests on the wall gypboard, the mechanical isolation is compromised at the edges.
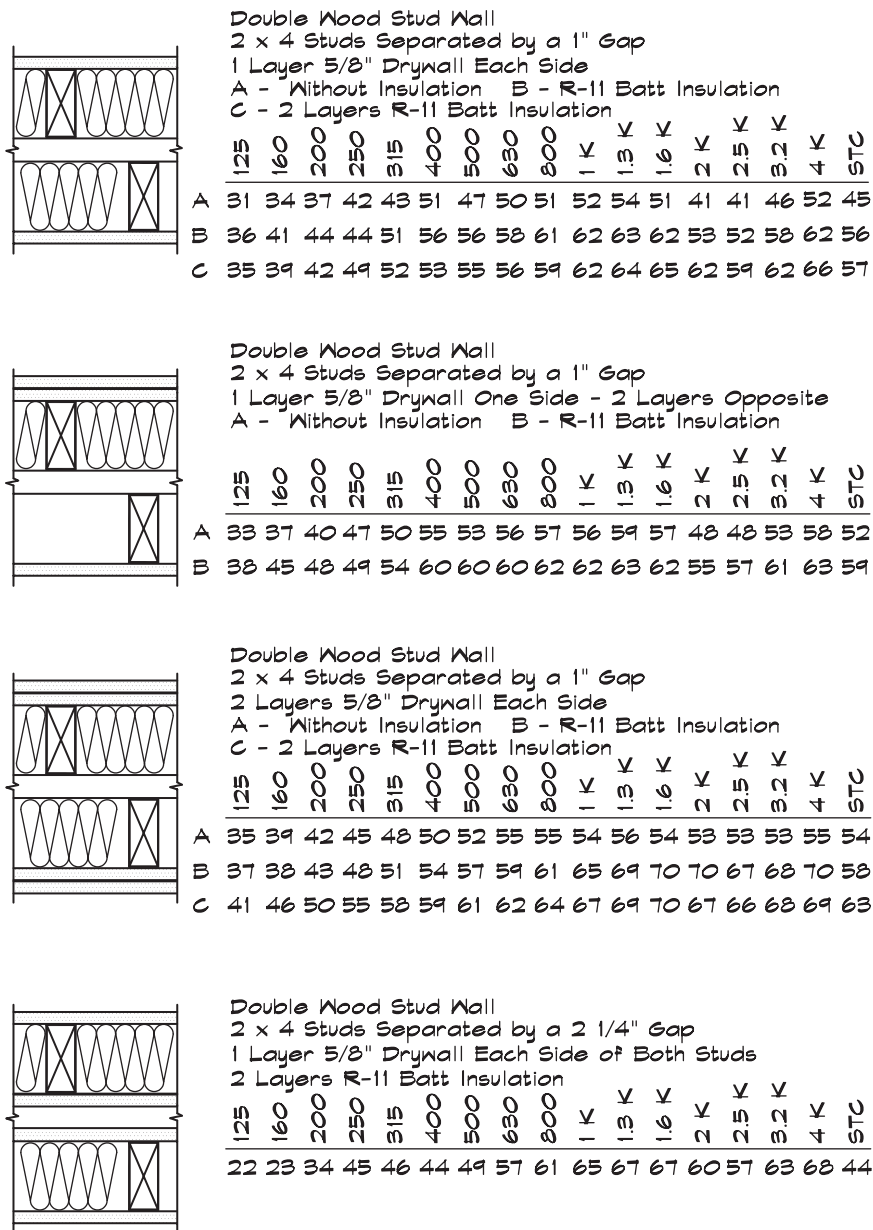
Staggered-Stud Construction

Staggered stud wall construction represents a compromise between single-stud and double-stud construction. The use of staggered wood studs on a common 2 × 6 (38 mm × 140 mm) base plate, which is shown in Fig. 10.8, can provide some mechanical decoupling between the panels on either side of a wall, but is limited by the flanking transmission through the plates. It produces transmission loss values that are comparable to resilient channel and, since a solid stud is used, this wall construction will support bookcases and the like and is thus preferred. It is difficult to use a staggered stud configuration with metal studs because at the top and bottom plates, a continuous runner cannot be used. A 3 5/8" (92 mm) 26 Ga metal stud has significant decoupling, due to its inherent softness, so there is little advantage to staggering metal studs. If a higher transmission loss is required and the width is limited, a double 2 1/2" (64 mm) metal stud with a 1/2" (13 mm) air gap will yield the same wall thickness as a staggered wood stud system and better isolation.

Double-Stud Construction

Where high transmission loss values are desired, double-stud construction, with multiple layers of gypboard or heavy plaster, is preferred. The losses are limited by the flanking transmission through the structure, which can be improved by setting one or both sides of the wall on a floating floor or isolated stud supports in specialized applications such as studios. Typical double-stud constructions are given in Fig. 10.9. There is no appreciable difference

FIGURE 10.9 Transmission Loss of Double-Stud Walls (California Office of Noise Control, 1981)

Double Wood Stud Wall
2 x 4 Studs Separated by a 1" Gap
1 Layer 5/8" Drywall Each Side
A – Without Insulation   B – R-11 Batt Insulation
C – 2 Layers R-11 Batt Insulation

	125	160	200	250	315	400	500	630	800	1K	1.3K	1.6K	2K	2.5K	3.2K	4K	STC
A	31	34	37	42	43	51	47	50	51	52	54	51	41	41	46	52	45
B	36	41	44	44	51	56	56	58	61	62	63	62	53	52	58	62	56
C	35	39	42	49	52	53	55	56	59	62	64	65	62	59	62	66	57

Double Wood Stud Wall
2 x 4 Studs Separated by a 1" Gap
1 Layer 5/8" Drywall One Side – 2 Layers Opposite
A – Without Insulation   B – R-11 Batt Insulation

	125	160	200	250	315	400	500	630	800	1K	1.3K	1.6K	2K	2.5K	3.2K	4K	STC
A	33	37	40	47	50	55	53	56	57	56	59	57	48	48	53	58	52
B	38	45	48	49	54	60	60	60	62	62	63	62	55	57	61	63	59

Double Wood Stud Wall
2 x 4 Studs Separated by a 1" Gap
2 Layers 5/8" Drywall Each Side
A – Without Insulation   B – R-11 Batt Insulation
C – 2 Layers R-11 Batt Insulation

	125	160	200	250	315	400	500	630	800	1K	1.3K	1.6K	2K	2.5K	3.2K	4K	STC
A	35	39	42	45	48	50	52	55	55	54	56	54	53	53	53	55	54
B	37	38	43	48	51	54	57	59	61	65	69	70	70	67	68	70	58
C	41	46	50	55	58	59	61	62	64	67	69	70	67	66	68	69	63

Double Wood Stud Wall
2 x 4 Studs Separated by a 2 1/4" Gap
1 Layer 5/8" Drywall Each Side of Both Studs
2 Layers R-11 Batt Insulation

125	160	200	250	315	400	500	630	800	1K	1.3K	1.6K	2K	2.5K	3.2K	4K	STC
22	23	34	45	46	44	49	57	61	65	67	67	60	57	63	68	44

in the performance of wood and metal double studs, since there is no additional decoupling due to the intrinsic stiffness of the stud.

Gypboard layers placed in the air gap between the studs reduce the transmission loss because a bridging air pocket is formed. For a given number of layers it is most effective to place them on the outside faces of the double studs. For example, the last wall shown in Fig. 10.9 rates an STC 44 with inner drywall layers as compared to a 63 rating for the same number of layers on the outside. As the air gap increases this disadvantage is offset by the effectiveness of the separation. If the distance between the studs is several feet, such as two stud walls separated by a corridor, the mass-air-mass resonance is so low that it would have no appreciable effect.

High-Mass Constructions

Heavy materials such as concrete, grouted cmu blocks, concrete-filled metal decking, and similar products can provide substantial transmission loss due to their intrinsic mass. Although a single panel structure is less efficient in the loss per mass than a multiple layer construction, in many cases there is no viable substitute. Figure 10.10 shows the measured

FIGURE 10.10   High Mass Wall Construction (California Office of Noise Control, 1981)

4" Solid Concrete Panel – 54 lbs/sq ft

125	160	200	250	315	400	500	630	800	1K	1.3K	1.6K	2K	2.5K	3.2K	4K	STC
48	44	43	42	39	41	45	46	48	56	53	51	57	62	65	66	44

6" Solid Concrete Panel – 75 lbs/sq ft

125	160	200	250	315	400	500	630	800	1K	1.3K	1.6K	2K	2.5K	3.2K	4K	STC
38	41	41	43	45	48	52	54	57	59	62	65	67	69	71	73	55

8" Solid Concrete Panel – 95 lbs/sq ft

125	160	200	250	315	400	500	630	800	1K	1.3K	1.6K	2K	2.5K	3.2K	4K	STC
44	44	45	48	51	53	55	56	56	58	60	62	63	65	66	67	58

8 x 8 x 16 3-cell Lightweight Concrete Masonry Unit
A No Center Grout – 28 lbs/block
B Center Grouted + #5 Rebar
C Center Grouted + #5 Rebar + 2 Coats Flat Oil Base
   Paint Each Side

	125	160	200	250	315	400	500	630	800	1K	1.3K	1.6K	2K	2.5K	3.2K	4K	STC
A	34	31	37	36	37	38	41	45	43	44	48	49	52	52	54	55	45
B	35	33	37	37	41	40	44	45	49	54	57	60	64	66	70	73	48
C	36	37	39	44	46	49	54	54	57	59	62	66	69	71	75	75	55

transmission loss values of concrete panels used in wall or floor construction. Note the difference in the grouted block data between painted and nonpainted conditions. Blocks are intrinsically porous and must be sealed with a bridging (oil-based) paint to achieve their full potential.

High Transmission Loss Constructions

An important study was undertaken by Sharp (1973) to try to develop construction methods that would achieve transmission loss ratings 20 dB or more above the mass law. In this work several techniques were utilized, not normally seen in standard construction practice but which could easily be implemented. These included spot lamination, which has been previously discussed, and point mounting. The point mounting technique he devised was to use 1/4" (6 mm) thick foam tape squares between the gypboard and the stud and then to attach the sheet with drywall screws through the tape into the stud. This technique resulted in panel isolation that approaches the theoretical point mounting discussed in Eq. 9.54. A triple panel wall having an STC of 76 utilizing these techniques is shown in Fig. 10.11. This wall has a relatively low transmission loss value of 33 dB in the 80 Hz band.

FIGURE 10.11   High Transmission Loss Wall Construction (Sharp, 1973)

Double Wood Stud Wall
2 x 4 Studs Separated by a 3" Gap
Outside Layers 3/8" + 1/2" Drywall on 1/4" Foam Tape
Inside 5/8" + 1/2" + 5/8" Drywall on 1/4" Wood Squares
All Layers Spot Laminated at 24" OC and Screwed
Through Mounts - 2" Batt Insulation in all Cavities

125	160	200	250	315	400	500	630	800	1 k	1.3 k	1.6 k	2 k	2.5 k	3.2 k	4 k	STC
53	56	60	66	70	75	78	80	78	79	83	83	84	87	88	89	76

Single Wood Stud Wall - 2 x 8 Studs
1/2" + 3/8" + 1/2" + 3/8" Drywall on 1/4" Foam Tape
5/8" + 1/2" + 5/8" Drywall on 1/4" Wood Squares
All Layers Spot Laminated at 24" OC and Screwed
Through Mounts - 2" Batt Insulation in all Cavities

125	160	200	250	315	400	500	630	800	1 k	1.3 k	1.6 k	2 k	2.5 k	3.2 k	4 k	STC
49	53	54	57	60	62	64	66	68	74	79	80	82	83	84	85	69

Concrete and Metal Double Stud Wall
2" Reinforced Concrete Panel
2 Layers 1/4" Drywall On 1/4" Foam Tape Each Side
2 1/2" Metal Studs - All Panels Spot Laminated at 24"
OC and Screwed Throught the Mounts
2" Batt Insulation in the Airspace

125	160	200	250	315	400	500	630	800	1 k	1.3 k	1.6 k	2 k	2.5 k	3.2 k	4 k	STC
49	53	60	63	66	68	71	73	76	78	77	78	81	83	87	88	72

Figure 10.11 also shows a double panel wall having the same mass as the previous construction. This has a lower rating (STC 69) due to reduced performance in the mid-frequencies but much better performance at low frequencies (41 dB at 80 Hz). The multiple layers of spot laminated drywall significantly reduce the coincidence effects. Similar performance should be obtained using separate double stud construction assuming that flanking paths have been controlled.

10.3   DIRECT FIELD SOUND TRANSMISSION

Direct Field Sources

We previously examined the transmission of sound through partitions for a diffuse or reverberant source field. For a direct source field the behavior of the transmission loss is somewhat different. A direct field consists of a plane or nearly plane wave that proceeds unimpeded from the source to the transmitting surface. The energy density and thus the relationship between the sound pressure levels and the sound intensity levels for a plane wave differs by 6 dB from the relationship for a diffuse field. The transmission loss of a surface is also dependent on the angle of incidence, and this must be taken into account in any comprehensive theory.

In a plane wave the power transmitted through a surface is simply related to the intensity incident on the surface

$$W = I \, S \cos \theta \, \tau(\theta) \tag{10.14}$$

where W = power transmitted through a surface (W)
$\quad\quad I$ = direct field intensity incident on the surface (W/m^2)
$\quad\quad S$ = area of the surface (m^2)
$\quad\quad \theta$ = angle of incidence with the normal to the surface (rad)
$\quad\quad \tau(\theta)$ = transmissivity of the surface for angle θ

For an exposed surface and an interior observer Eq. 10.14 can be inserted into Eq. 8.87 to obtain

$$L_r = L_s - \Delta L_{TL}(\theta) + 10 \log (4 \cos \theta)$$

$$+ 10 \log \left[\frac{S_w \, Q}{16 \, \pi \left[z + \sqrt{\dfrac{S_w \, Q}{4 \, \pi}} \right]^2} + \frac{S_w}{R_r} \right] \tag{10.15}$$

where L_s = direct field sound pressure level near, but in the absence of, reflections from the transmitting surface (dB)
$\quad\quad L_r$ = direct plus reverberant field sound pressure level in the receiving space (dB)
$\quad\quad \Delta L_{TL}(\theta)$ = direct field transmission loss of a partition for a given angle θ, (dB)

Let us define a receiver correction C, such that

$$C = 10 \log \left[\frac{S_w\, Q}{16\,\pi \left[z + \sqrt{\dfrac{S_w\, Q}{4\,\pi}} \right]^2} + \frac{S_w}{R_r} \right] \tag{10.16}$$

Then for normal incidence

$$L_r = L_s - \Delta L_{TL}(\theta = 0) + C + 6 \tag{10.17}$$

This is the same form as Eq. A3 in ASTM Standard E336 for normal incidence sound transmission loss. Note that if $z = 0$ and $\Delta L_{TL}(\theta = 0)$ at the center of an open window, then $L_r = L_s$. This is the correct result since the transmission loss of large openings for plane waves is zero.

Direct Field Transmission Loss

Transmission loss measurements are conducted in two highly reverberant laboratory test rooms. On the source side, by control of the absorption in the room and the number and orientation of the loudspeakers, a diffuse (reverberant) field is achieved at the test partition. Under these conditions, Eq. 10.6 holds and defines the diffuse field transmission loss. The bulk of the transmission loss data are measured in this manner. There is some difficulty in applying these data to direct-field calculations, since there is no specific angular dependence in the laboratory data. We can return to the fundamental mass law relationship given in Eq. 9.18

$$\Delta L_{TL}(\theta) = 10 \log \left[1 + \left(\frac{\omega\, m_s \cos \theta}{2\,\rho_0\, c_0} \right)^2 \right] \tag{10.18}$$

where $\Delta L_{TL}(\theta) =$ direct field transmission loss of a partition for a
given angle θ, (dB)
$\omega =$ radial frequency (rad / s)
$\rho_s =$ surface mass density (kg / m^2)
$\rho_0 =$ density of air (kg / m^3)
$c_0 =$ velocity of sound in air (m / s^2)

In Chapt. 9 this equation was integrated over values of θ between 0° and about 78° to obtain agreement with the measured results. The laboratory transmission loss data are found to be some 5 dB below the $\Delta L_{TL}(\theta = 0)$ data (Ver and Holmer, 1971). For this treatment we assume that the angular dependence of the transmission loss is given by Eq. 10.18. This does not preclude the use of actual measured transmission loss data, but only means that this angular dependence is assumed. We also assume that the density of most walls is large so that $\left(\omega\, m_s \cos \theta / 2\,\rho_0 c_0 \right)^2 \gg 1$ for angles less than 78°. Under these conditions the angular dependence can be written as

$$\Delta L_{TL}(\theta) \cong \Delta L_{TL}(\theta = 0) + 20 \log (\cos \theta) \tag{10.19}$$

and substituting in Eq. 9.22

$$\Delta L_{TL}(\theta) \cong \Delta L_{TL} + 5 + 20 \log (\cos \theta) \qquad (10.20)$$

Note that while this equation is used in subsequent calculations, if the transmission loss is zero, then we must revert to Eq. 10.15 to obtain accurate results.

Using these components we can assess the sound transmission due to an exterior plane wave passing through the structure of a building.

$$L_r = L_s - \Delta L_{TL} - \Delta L_{SH} + C + G \qquad (10.21)$$

where ΔL_{SH} = correction for self shielding, (dB)
G = geometrical factor, which includes the orientation of
the source relative to the transmitting surface, (dB)
G = 10 log (4 cos θ) + [−5 − 20 log (cos θ)]
= 10 log(1.26/cos θ) = 1 − 10 log (cos θ)

Equation 10.21 includes the diffuse field transmission loss measured in a laboratory with the angular behavior included in the G term. The other terms are defined in Eq. 10. 15.

Free Field—Normal Incidence

When a plane wave is normally incident on a transmitting surface,

$$L_r = L_s - \Delta L_{TL} + C + 1 \qquad (10.22)$$

Free Field—Non-normal Incidence

For angles of incidence other than zero the value of G is shown in Table 10.1.

Line Source—Exposed Surface Parallel to It

The line source G factor for an exposed surface, whose normal is perpendicular to the line source, can be determined by energy averaging the G term over all values of θ. The G factors at 0° and 80° are single counted, and all others are double counted. The result is

$$G = 3.6 - 10 \log (\cos \phi) \qquad (10.23)$$

where ϕ is the angle between the normal to the transmitting surface and the normal to the line source that intersects the center of the surface. The geometry is shown in Fig. 10.12.

Since the transmission loss is highest when the sound is normally incident, there is often an increase in noise level in high rise buildings with height of the floor above the

TABLE 10.1   Geometrical (G) Factor

	Angle θ, Degrees								
	0	**10**	**20**	**30**	**40**	**50**	**60**	**70**	**80**
G (dB)	1.0	1.1	1.3	1.6	2.2	2.9	4.0	5.7	8.6

It is common practice not to include angles above 78°.

FIGURE 10.12   **Angle between a Plane and a Line Source**
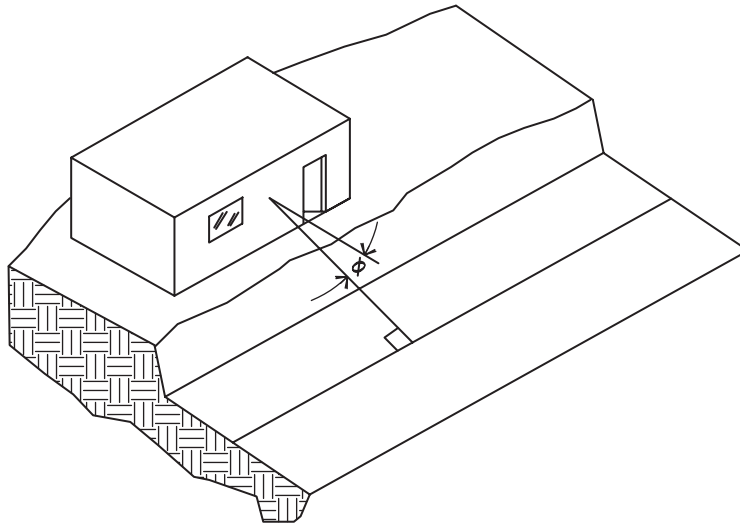
street. As one goes from floor to floor the distance from the street increases so the noise level decreases. The G factor, however, increases as well since the angle ϕ is increasing. This effect offsets the distance loss. The result is that frequently, the loudest interior sound levels occur, not on the first floor, but on about the third floor above street level.

Self Shielding and G Factor Corrections

When a building element is exposed to sound emanating from a point source, the interior level may be calculated using the G factors given in Table 10.1. If the source is shielded by the side of a building it will be attenuated by an amount that can be calculated from the barrier loss relationships previously discussed.

In the case of a line source, where the transmitting surface is a side wall, parallel to the normal, the G factor is theoretically the same as for a wall perpendicular to the normal since for a line source equal energy is radiated from equal angular segments. There is a difference in the self shielding factor, which arises from the fact that the building cuts off half of the line source as seen by the side wall. Figure 10.13 shows ground level self shielding factors for various surface orientations. Both the self shielding and the changes in the G factor are most conveniently subsumed into the self shielding correction.

The difficulty in accurately assessing the geometrical and self shielding corrections for all site configurations is apparent. For odd orientations relative to a line source there is always a tradeoff between the two. For practical calculations shielding is more important than orientation, but it can be influenced by reflections from other structures. If the primary transmitting surface is not facing the roadway, but is within 30° or so, it makes little difference in the G factor while making about a dB difference in the shielding. In general, changes in the two factors due to surface orientation offset one another. For aircraft and other elevated sources, roofs are given a zero shielding factor. Side walls facing the direction of takeoff are considered unshielded, but walls on the approach side are given a 3 dB shielding factor. Surfaces on the side opposite the line of travel are given a 10 dB shielding factor so long as there is no significant sound reflection from nearby structures.

FIGURE 10.13   Line Source Self Shielding Factors
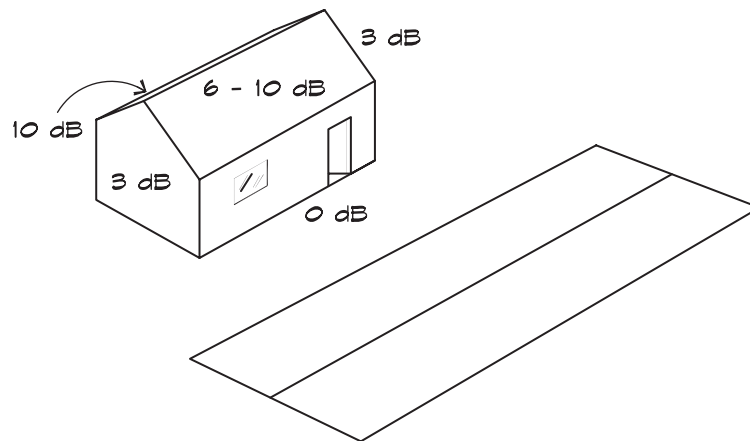
10.4   EXTERIOR TO INTERIOR NOISE TRANSMISSION

As was the case for room to room transmission loss, exterior to interior noise transmission depends on the weakest link in the chain, which in most cases is either the windows or the doors. Where a site is located in a noisy area and a quiet interior noise environment is desired, windows and doors that have a high transmission loss values are critical. Unless exterior levels are quite high, standard California building practices, including stucco exterior walls on wood studs with R-11 (3 1/2" or 90 mm) batt insulation, and 5/8" interior drywall, are adequate to obtain STC ratings that exceed those available in heavy double paned glass windows by a large margin. Thus the doors, both wood and glass, and windows are the main transmission path.

Exterior Walls

The sound transmission characteristics of several types of exterior walls have been measured by the National Bureau of Standards (Sabine et al., 1975) and are summarized in Fig. 10.14. Where the exterior surface is a lightweight material such as wood or aluminum siding, thin sheet metal or skim coat plaster over Styrofoam, a layer of 5/8" plywood against the stud is usually necessary to bring the mass up to satisfactory levels. It can be seen from Fig. 10.14 that most windows and doors have STC ratings that fall well below the ratings of the commonly used exterior walls. Thus it is necessary to use resilient mounts or separate stud construction on exterior walls only when there are no windows or doors on the wall or where the ratings of these penetrating elements are higher than standard construction will produce.

Windows

Sound transmission through windows depends on the intrinsic rating of the glazing itself and on the treatment of cracks or openings in the window frame. For single paned sealed glazing, the STC ratings are primarily dependent on the thickness of the glass and somewhat dependent on damping provided by a sandwiched interlayer. Figure 10.15 gives transmission loss ratings of various thicknesses of fixed glazing.

   Laminated glazing can provide improved transmission loss performance, especially around the critical frequency. Recognize that although a thinner sheet of laminated glass

370 ARCHITECTURAL ACOUSTICS

FIGURE 10.14 Transmission Loss of Exterior Walls (National Bureau of Standards, 1975)
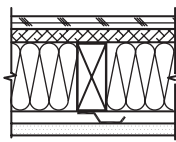
Single Wood Stud Wall - 2 x 4 Stud
1 Layer 5/8" Redwood Siding
3/4" Insulation Board Sheathing
1 Layer 5/8" Drywall
A - Without Insulation   B - R-11 Batt Insulation
C - No Insulation - With Resilient Channel
D - R-11 Batt Insulation - With Resilient Channel

	125	160	200	250	315	400	500	630	800	1K	1.3K	1.6K	2K	2.5K	3.2K	4K	STC
A	16	16	22	26	33	35	36	39	43	46	50	51	52	51	48	49	37
B	18	18	28	30	33	34	40	42	45	47	50	50	51	50	50	53	39
C	24	22	26	32	35	38	43	45	50	51	56	57	58	56	54	57	43
D	26	27	30	35	41	43	49	52	56	58	59	60	61	60	58	60	47
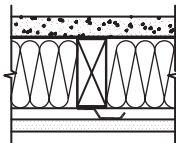
Single Wood Stud Wall - 2 x 4 Stud
1 Layer 7/8" Stucco
1 Layer 5/8" Drywall
A - R-11 Batt Insulation
B - No Insulation - With Resilient Channel
C - R-11 Batt Insulation - With Resilient Channel

	125	160	200	250	315	400	500	630	800	1K	1.3K	1.6K	2K	2.5K	3.2K	4K	STC
A	25	30	42	41	44	43	45	45	46	45	46	48	50	50	50	55	46
B	28	32	34	37	41	46	50	50	50	51	54	55	57	55	55	58	49
C	35	41	50	49	53	55	58	58	58	59	59	60	58	57	60	64	57
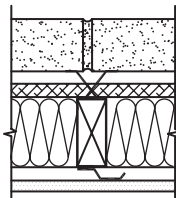
Red Brick Wire Tied to 2 X 4 Studs
1/2" Airspace
3/4" Insulation Board Sheathing
1/2" Drywall
A - R-11 Batt Insulation - No Resilient Channel
B - No Insulation - With Resilient Channel
C - R-11 Batt Insulation - With Resilient Channel

	125	160	200	250	315	400	500	630	800	1K	1.3K	1.6K	2K	2.5K	3.2K	4K	STC
A	39	36	42	46	49	51	54	56	58	61	67	67	69	69	70	73	56
B	33	34	41	41	47	50	52	55	59	61	65	66	68	68	69	72	54
C	38	39	46	47	52	54	57	58	60	61	69	68	71	71	72	74	58

may have a higher STC rating, it may be less effective than a heavier sheet of plate glass at low frequencies. The selected product should be based on the actual noise spectrum and the transmission losses in all bands. Transmission loss values for several thicknesses of laminated glass are shown in Fig. 10.16.

When sealed insulating glass is used, the STC rating depends both on the thickness of the glass and the interior air space thickness. Double wall transmission loss theory predicts that a double panel system has a higher transmission loss than a single panel of the same surface weight. This only occurs above the mass-air-mass resonant frequency, which is determined by the weight of each layer and the separation. At or near the resonant frequency the transmission loss of a double panel system is lower than that of a single panel. Even above

FIGURE 10.15   Transmission Loss of Window Glass (National Bureau of Standards, 1975)

Single Strength (3/32" – 2 mm) Glass

125	160	200	250	315	400	500	630	800	1k	1.3k	1.6k	2k	2.5k	3.2k	4k	STC
20	19	18	21	23	22	25	26	26	26	29	30	31	30	33	30	28

Double Strength (1/8" – 3 mm) Glass

125	160	200	250	315	400	500	630	800	1k	1.3k	1.6k	2k	2.5k	3.2k	4k	STC
23	23	21	23	24	24	27	27	28	28	31	32	34	34	30	25	29

7/16" (11 mm) Insulating Glass

125	160	200	250	315	400	500	630	800	1k	1.3k	1.6k	2k	2.5k	3.2k	4k	STC
25	24	23	23	23	21	24	26	30	30	34	35	37	38	40	42	30

3/16" (5 mm) Glass

125	160	200	250	315	400	500	630	800	1k	1.3k	1.6k	2k	2.5k	3.2k	4k	STC
21	23	23	24	25	27	27	28	28	28	28	30	30	27	28	31	28

1/4" (6 mm) Glass

125	160	200	250	315	400	500	630	800	1k	1.3k	1.6k	2k	2.5k	3.2k	4k	STC
21	18	19	24	25	26	27	28	30	31	31	28	25	27	29	32	29

3/8" (9 mm) Glass

125	160	200	250	315	400	500	630	800	1k	1.3k	1.6k	2k	2.5k	3.2k	4k	STC
20	21	24	27	28	29	31	32	33	30	28	26	32	36	38	40	30

1" (25 mm) Insulating Glass (1/8 + 3/4 + 1/8)

125	160	200	250	315	400	500	630	800	1k	1.3k	1.6k	2k	2.5k	3.2k	4k	STC
27	23	20	24	26	28	33	34	37	36	37	38	39	32	35	41	34

this frequency the improvement is limited by mechanical coupling between the two sides. In general it is not effective to use thin double paned windows with air spaces of less than about 3/4" (19 mm) for noise control. Typical transmission loss data are given in Fig. 10.17 for these types of windows.

   If window glass is installed in an operable frame there can be a significant degradation in the transmission loss performance due to leakage of air through the seals as well as direct transmission through the frame itself. If we examine the performance of single strength (3/32" or 2.4 mm) glass in various types of frames we find (NBS, 1975) the results shown in Table 10.2. In the case of an aluminum sliding frame, there is a drop of 4 to 5 STC points from the sealed condition.

FIGURE 10.16 Transmission Loss of Laminated Glass

3/16" (5 mm) Safety Glass

125	160	200	250	315	400	500	630	800	1k	1.3k	1.6k	2k	2.5k	3.2k	4k	STC
23	24	25	26	27	28	30	30	31	32	34	34	31	27	30	34	31

1/4" (6 mm) Laminated Glass

125	160	200	250	315	400	500	630	800	1k	1.3k	1.6k	2k	2.5k	3.2k	4k	STC
27	25	26	28	30	30	33	33	33	33	34	35	36	36	38	41	34

3/8" (9 mm) Laminated Glass

125	160	200	250	315	400	500	630	800	1k	1.3k	1.6k	2k	2.5k	3.2k	4k	STC
29	30	31	34	32	33	35	35	35	35	34	35	34	38	42	45	36

1/2" (13mm) Laminated Glass

125	160	200	250	315	400	500	630	800	1k	1.3k	1.6k	2k	2.5k	3.2k	4k	STC
29	30	31	34	33	34	35	35	35	35	33	35	39	42	45	46	37

5/8" (16 mm) Laminated Glass

125	160	200	250	315	400	500	630	800	1k	1.3k	1.6k	2k	2.5k	3.2k	4k	STC
29	30	31	36	35	36	35	35	35	35	37	40	43	45	47	49	38

3/4" (9 mm) Laminated Glass

125	160	200	250	315	400	500	630	800	1k	1.3k	1.6k	2k	2.5k	3.2k	4k	STC
35	33	33	34	36	36	37	36	35	34	39	41	46	48	50	52	39

3/4" (9 mm) Laminated Glass (3 Layer)

125	160	200	250	315	400	500	630	800	1k	1.3k	1.6k	2k	2.5k	3.2k	4k	STC
33	30	33	36	38	37	39	38	37	37	39	42	44	47	49	53	41

Similar behavior is given in Table 10.3 for insulating glass in various types of frames (NBS, 1975).

When operable frames are part of the window assembly the losses are typically lower than those of the glass alone and can be manufacturer dependent. In critical locations laboratory test data should be obtained from a prospective window supplier and calculations performed using these data.

Doors

Like windows, exterior and interior doors are a major source of sound leakage in critical applications. Unlike windows, doors are frequently opened and closed and it is the gaps at the joints and at the threshold that present the greatest problem in controlling noise. The standard exterior door thickness in the United States is 1 3/4" (44 mm), and a solid core

FIGURE 10.17   Transmission Loss of Double Glazed Windows
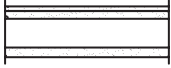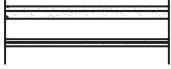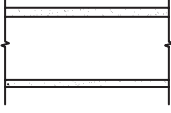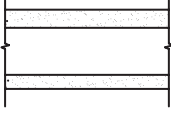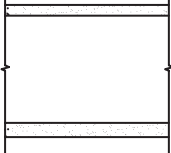
1/4" (6 mm) + 3/4" (19 mm) AS + 1/4" (6 mm) Laminated

125	160	200	250	315	400	500	630	800	1K	1.3	1.6	2K	2.5	3.2	4K	STC
18	24	23	28	32	33	36	39	39	43	43	42	38	37	42	48	38

1/4" (6 mm) + 5/8" (16 mm) AS + 3/8" (9 mm) Laminated

125	160	200	250	315	400	500	630	800	1K	1.3	1.6	2K	2.5	3.2	4K	STC
20	26	26	30	34	34	37	39	40	41	41	40	39	39	46	49	39

3/16" (5 mm) Lam + 1/2" (13 mm) AS + 3/8" (9 mm) Lam

125	160	200	250	315	400	500	630	800	1K	1.3	1.6	2K	2.5	3.2	4K	STC
24	26	27	32	32	35	37	38	41	42	39	38	44	50	56	61	40

3/16" (5 mm) + 2 1/2" (64 mm) AS + 1/4" (6 mm)

125	160	200	250	315	400	500	630	800	1K	1.3	1.6	2K	2.5	3.2	4K	STC
23	23	32	31	37	38	41	43	47	50	52	52	48	43	50	46	43

3/8" (9 mm) + 2 1/2" (64 mm) AS + 1/2" (13 mm)

125	160	200	250	315	400	500	630	800	1K	1.3	1.6	2K	2.5	3.2	4K	STC
28	31	29	35	40	40	44	45	47	46	49	52	53	52	49	51	46

3/8" (9 mm) + 4" (100 mm) AS + 1/4" (6 mm)

125	160	200	250	315	400	500	630	800	1K	1.3	1.6	2K	2.5	3.2	4K	STC
30	33	39	39	41	46	50	51	54	54	52	55	56	59	65	69	51

TABLE 10.2   STC Ratings of Single Strength Glass in Various Frames

Frame Configuration	STC Rating
Sealed (Average of 5 Tests)	28–29
Wood Double-hung, Locked	26
Wood Double-hung, Unlocked	26
Aluminum Sliding, Latched	24

wood door typically weighs about 4–5 lbs/sq ft (20–25 kg/sq m). Based on the mass law one would expect a transmission loss at 500 Hz of about 32 dB for a sealed door. Figure 10.18 shows that this is about what we measure.

In field installations there can be considerable leakage through a door seal at the jamb, head, and threshold. These seals tend to degrade in time due to wear and mechanical failure.

TABLE 10.3   STC Ratings of 7/16" Insulating Glass in Frames

Frame Configuration	STC Rating
Sealed (Average of 2 Tests)	28–30
Wood Double-hung, Locked	26
Wood Double-hung, Unlocked	22
Aluminum Single-hung, Locked	27
Aluminum Single-hung, Unlocked	25

FIGURE 10.18   Transmission Loss of Openable Doors (National Bureau of Standards, 1975)

1 3/4" (45 mm) Hollow Core Door
A – Sealed into Frame
B – Mounted in Frame with Brass Weatherstrip

	125	160	200	250	315	400	500	630	800	1K	1.3K	1.6K	2K	2.5K	3.2K	4K	STC
A	14	14	14	15	15	17	17	17	15	18	22	22	22	24	27	29	21
B	16	15	15	15	16	17	18	17	15	18	24	24	27	28	30	32	20

1 3/4" (45 mm) French Door – Single Strength Glass
A – Sealed into Frame
B – Mounted in Frame with Brass Weatherstrip

	125	160	200	250	315	400	500	630	800	1K	1.3K	1.6K	2K	2.5K	3.2K	4K	STC
A	23	20	24	23	24	24	26	29	30	30	32	32	34	35	36	35	31
B	20	20	24	25	23	24	28	29	28	28	25	25	23	25	27	28	26

1 3/4" (45 mm) Hollow Metal Door
A – Sealed into Frame
B – Mounted in Frame with Magnetic Weatherstrip

	125	160	200	250	315	400	500	630	800	1K	1.3K	1.6K	2K	2.5K	3.2K	4K	STC
A	22	21	27	28	28	29	30	31	32	33	33	27	24	34	35	37	28
B	23	21	25	26	26	27	28	29	31	31	32	27	24	32	36	39	28

1 3/4" (45 mm) Solid Core Door
A – Sealed into Frame
B – Mounted in Frame with Brass Weatherstrip

	125	160	200	250	315	400	500	630	800	1K	1.3K	1.6K	2K	2.5K	3.2K	4K	STC
A	14	14	14	15	15	17	17	17	15	18	22	22	22	24	27	29	30
B	21	24	27	27	27	27	30	30	28	26	25	25	25	27	28	29	27

The most common types of threshold in residential doors are a bulb seal, brass v-shaped strips, and a brush seal. Of these the bulb seal is probably the most effective. All weather stripping in order to be effective must seal against a solid threshold of wood, metal, or smooth concrete or vinyl tile. Carpet is ineffective since the sound passes through it under the door.

For the head and jamb, weather stripping is commercially available as foam tape, bulb, or neoprene seals. Steel door frames are also available with a bulb seal built into the frame. This type of device is very effective since it gives the bulb an area to move into when the door is closed. Seals that are located between the door and the jamb can become crushed over time and lose their effectiveness. Note that all seals must be used in compression, rather than in shear if they are to perform effectively.

In moderately critical applications such as a private office, drop closures can be used. These are mechanical devices that are spring loaded and drop down when a latch pin is activated by the closure of the door. They may be mortised into the bottom of the door or surface applied. When they are mortised the appearance of the door is more pleasing but they are more difficult to adjust and maintain. Over time drop closures can malfunction and leave a gap under the door so that periodic maintenance and adjustment is required.

Commercially available sound rated doors are the most effective choice in highly critical applications. STC ratings from 45 to 53 are available in steel doors and from about 40 to 49 in wood doors. The most effective seals are made using a cam lift hinge that lifts the door as it is opened. The bottom of the door incorporates a piece of hard rubber with no moving parts to go out of adjustment. These doors are provided with custom steel frames and adjustable head and jamb seals to close off these paths.

Some sound rated doors are available with flexible magnetic strips that are attracted to the metal surface. These require less maintenance than compression seals and do not cause the door to warp in time. A compression seal requires constant pressure to maintain closure. Most of the force is provided by the latch at the door knob near the center of the panel. In time the top and bottom corners can be pushed out by the force of the seals, which can cause leakage. Since the magnetic seals do not depend on a constant compressive force there is no pressure on the corners.

Where there is a pair of doors in an opening, one of the leaves should be fixed and held into place with a sliding bolt at the top and bottom. At the center the doors should overlap with a dadoed joint or a separate astrigal so that the two leaves do not have a butt joint, which is difficult to seal.

Other transmission paths in doors include louvered openings, undercut thresholds, and lightweight vision panels. Return air paths under or through doors generally preclude effective sound isolation. When these paths are closed off an alternate route for the return air flow must be provided. When vision panels are included in sound rated doors, they require a transmission loss equivalent to that of the door itself.

Electrical Boxes

In many buildings flanking paths between rooms occur through electrical boxes. Nightingale and Quirt (1998) have investigated the phenomenon in gypsum board walls in some detail. They tested boxes in various locations built into a double stud double drywall wall, as illustrated in Fig. 10.19.

FIGURE 10.19   Electrical Box Test Configuration (Nightingale and Quirt, 1998)
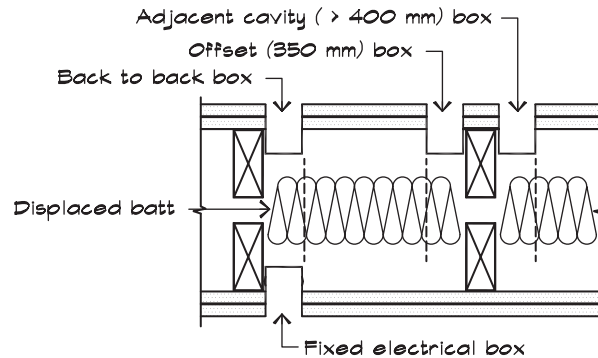
TABLE 10.4   STC Ratings of Walls with Electrical Boxes in Various Locations (Nightingale and Quirt, 1998)

Untreated Metal Boxes			Electrical Box Location		
Wood stud framing	Cavity absorption	Reference case	Back to back no offset	Same cavity offset 350 mm	Adjacent cavity
Double	None	55	51	49	53
	90 mm displaced	61	55	60	61
	90 mm	62	61	61	61
Single	90 mm displaced	55	50	54	54

The technique they used was to construct the boxes, as shown in Fig. 10.19, and to cover the unused ones with two sheets of drywall. The wall was tested with selected boxes exposed. Three insulation configurations were used: 1) no insulation, 2) insulation displaced around the box, and 3) insulation filling the cavities. The test results are summarized in Table 10.4. When the boxes are offset by a stud space (> 400 mm) the ratings are virtually unchanged, particularly with insulation in the cavity.

Figure 10.20 shows the transmission loss data for double stud walls with back-to-back boxes. At low frequencies the transmission loss through the box is high enough, due to the impedance mismatch, that there is little effect. At mid and high frequencies the flanking transmission becomes apparent through the boxes both with and without insulation.

Transmission through the boxes can be blocked by adding a drywall baffle to the inside face of the studs on the box side. Baffles in this research covered one stud cavity, extending from the sole plate to 300 mm (1 ft) above the top of the electrical box. The results are summarized in Table 10.5 and Fig. 10.21. The baffle solution is quite effective and simpler to construct than wrapping the box with drywall. Blocking the back of the box with mastic was shown in this study to be less effective than a baffle. The sides of the box still need to be caulked at the penetration through the drywall surface.

FIGURE 10.20   **Measured Transmission Loss of a Double Wood Stud Wall with Cavity Absorption Displaced around the Back-to-Back Metal Boxes (Nightingale and Quirt, 1998)**
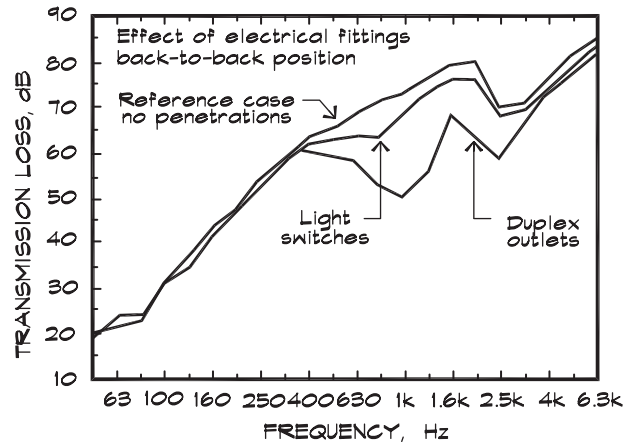
TABLE 10.5   **STC Ratings of Walls with Electrical Boxes with Baffles (Nightingale and Quirt, 1998)**

	Untreated Metal Boxes		Electrical Box Location		
			Same cavity offset 350 mm		
Cavity Absorption	**Reference Case**	**Back to back No treatment**	**Baffle**	**No treatment**	**Baffle**
None	55	51	52	49	52
90 mm displaced	61	55	62	60	61

FIGURE 10.21   **Effect of a Baffle Separating Back-to-Back Electrical Boxes in a Double Wood Stud Wall that Has 90 mm Glass Fiber Cavity Absorption (Nightingale and Quirt, 1998)**
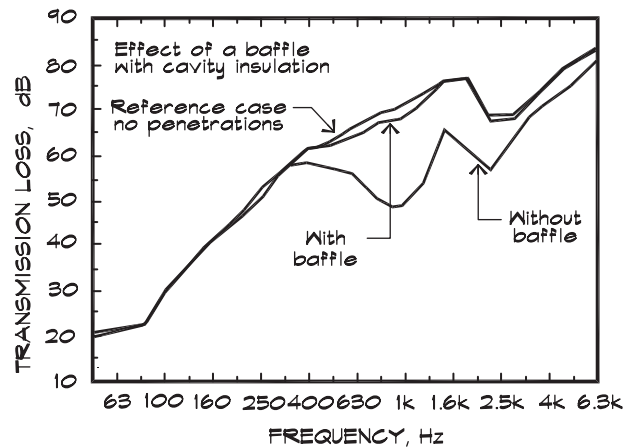
Aircraft Noise Isolation

With structures located in high noise level areas adjacent to major commercial or military airports, particular care must be exercised to insure a comfortable interior noise environment. In a study at LAX (Long, 1980) Ldn levels were near 80 dBA and the maximum allowable level was an Ldn 45 in the bedrooms. This required an A-weighted noise reduction of 35 dB. A 2 dB safety factor was included, which meant that the design was carried out based on a noise reduction of 37 dB. In homes in this area STC 38 double glazed windows were used along with heavy solid core doors, which were shielded by the structure and a roof overhang and alcove.

For control of aircraft noise the roof is the most critical parameter. Ceiling roofs are generally the largest exposed area, the most complicated structure, and acoustically the least well known. If the roof is a concrete slab or steel deck with a lightweight concrete fill, the problem of sufficient mass usually is ameliorated.

In wood structures, roofs must be solid sheeted with plywood and coverings added to increase the mass to the design level. An inexpensive way of increasing the roof mass is by using layers of 90 lb (0.9 lb/sq ft or 4.4 kg/sq m) felt roofing paper with a cap sheet and shingles or built-up roofing over it. With gravel, concrete tile, or mission tile roofs, the weight is significantly increased and additional layers of roofing paper are not required.

Estimation of the transmission loss of roofs is particularly difficult since there is no directly measured data for peaked roofs and no single separation distance. Flat roof data can be measured in a laboratory or approximated using floor-ceiling data. In the LAX study (Long, 1980), roof transmission losses were estimated using the mass law value of the heavier of the roof or ceiling panel plus two-thirds of the mass law value of the lighter panel. All roofs had solid plywood sheathing with wood shingles over. Eave vents were baffled with lined sheet-metal elbows.

Blocking, where the roofs meet the outside wall, is particularly difficult to control. In plaster homes the most practical solution is to stucco under the eaves to avoid having to caulk the blocking. Since attics must be ventilated, openings are required that must be acoustically treated—usually with a lined sheet metal duct having at least one 90° bend, located in the gable end.

Ceilings are one to two layers of gypsum board. In flat roofs resilient channel can be helpful. Where an open beam look is desired the ceiling can span between the beams but this reduces the airspace dimension and increases the length of joint.

Windows are generally heavy double glazed in noisy sites, although 1/4" laminated glass can be used up to about a 30 dB noise reduction. Highly rated French or sliding glass doors are difficult to find, although some manufacturers can provide a separate storm window or door that can be helpful.

HVAC outside air requirements can be met by providing a sheet metal duct with a commercial silencer. Where bathrooms require an exhaust fan, it too must have a treated duct with either a silencer or an appropriate length of lined duct. For noise reductions on the order of 30 dB, an 8' length of nonmetallic flex duct nested in a fiberglass-filled cavity between two joists will usually provide sufficient loss.

Traffic Noise Isolation

Control of interior noise levels from traffic is much the same as with aircraft noise. The major difference is that, when residences are located above the roadways, ceiling-roofs play a less significant part and windows a more significant part in the overall transmission path. Roofs or

patios that overhang a window or sliding glass door can reflect the sound down toward these surfaces and offset shielding that might otherwise have reduced the exterior sound pressure level. In areas of significant truck traffic, exterior windows should be heavy single glazed or double glazed with a wide airspace between panes. Trucks generate significant energy in the 125 and 250 Hz octave bands so the mass-air-mass resonance should be positioned below these bands. Where barrier shielding is present it is important to remember to use the shielded noise spectrum, which will contain a greater contribution from the lower bands than the unshielded spectrum.

This page intentionally left blank

VIBRATION
AND
VIBRATION ISOLATION

11.1   SIMPLE HARMONIC MOTION

Units of Vibration

In most vibration problems we are dealing with harmonic motion, where the quantities can be expressed as sine or cosine functions. The general formula for the harmonic displacement of a body is given by

$$x = X \sin \omega t \tag{11.1}$$

The velocity can be calculated by differentiating the displacement with respect to time

$$\dot{x} = \frac{dx}{dt} = X \omega \cos \omega t = V \sin (\omega t + \frac{\pi}{2}) \tag{11.2}$$

and the acceleration by differentiating the velocity

$$\ddot{x} = \frac{dv}{dt} = \frac{d^2 x}{dt^2} = -X \omega^2 \sin \omega t = -A \sin (\omega t) \tag{11.3}$$

These lead to simple relationships between the amplitudes

$$A = \omega V = \omega^2 X \tag{11.4}$$

Displacement, velocity, and acceleration are vector quantities that have a fixed angular relationship with each other, as the vector plot in Fig. 11.1 illustrates. Each vector rotates counterclockwise in time about the origin at the radial frequency, ω. Velocity leads displacement by 90° and acceleration leads displacement by 180°.

The units used in vibration measurements are more varied than those for sound level measurements. Amplitudes can be expressed in terms of displacement, velocity, acceleration, and jerk (the rate of change of acceleration). Accelerations are given not only in terms of length per time squared but also in terms of the standard gravitational acceleration, g. The peak amplitudes are simply coefficients such as those shown in Eq. 11.4. The root mean

FIGURE 11.1   **Vector Representation of Harmonic Displacement, Velocity, and Acceleration**
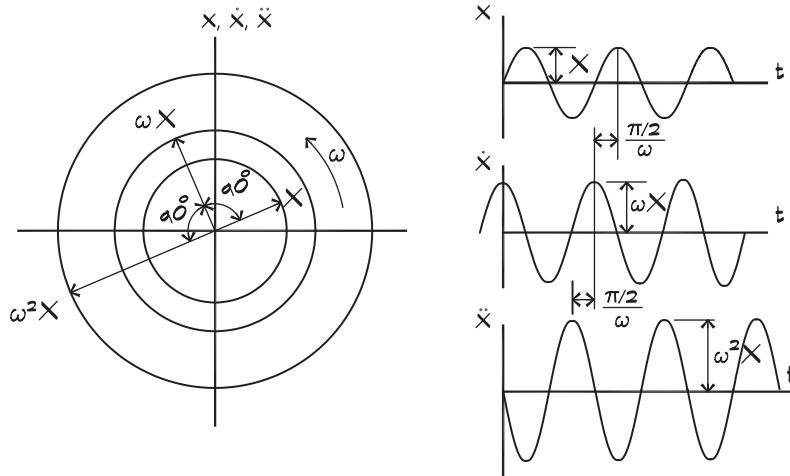
TABLE 11.1   **Reference Quantities for Vibration Levels (Beranek and Ver, 1992)**

Level (dB)	Formula	Reference (SI)
Acceleration	$L_a = 20 \log (a / a_0)$	$a_0 = 10 \ \mu m / s^2$
		$a_0 = 10^{-5} \ m / s^2$
		$a_0 = 1 \ g$
		$a_0 = 9.8 \ m / s^2$
Velocity	$L_v = 20 \log (v / v_0)$	$v_0 = 10 \ n \ m / s$
		$v_0 = 10^{-8} \ m / s$
Displacement	$L_d = 20 \log (d / d_0)$	$d_0 = 10 \ p \ m$
		$d_0 = 10^{-11} \ m$

Note: Decimal multiples are 10^{-1} = deci (d), 10^{-2} = centi (c), 10^{-3} = milli (m), 10^{-6} = micro (μ), 10^{-9} = nano (n), and 10^{-12} = pico (p).

square (rms) value is the square root of the average of the square of a sine wave over a complete cycle, which is $\left(\sqrt{2} \right)^{-1}$ or .707 times the peak amplitude. Vibration amplitudes also can be expressed in decibels and Table 11.1 shows the preferred reference quantities.

11.2   SINGLE DEGREE OF FREEDOM SYSTEMS

Free Oscillators

In its simplest form a vibrating system can be represented as a spring mass, shown in Fig. 11.2. Such a system is said to have a single degree of freedom, since its motion can be described with a knowledge of only one variable, in this case its displacement.

FIGURE 11.2 Free Body Diagram of a Spring Mass System
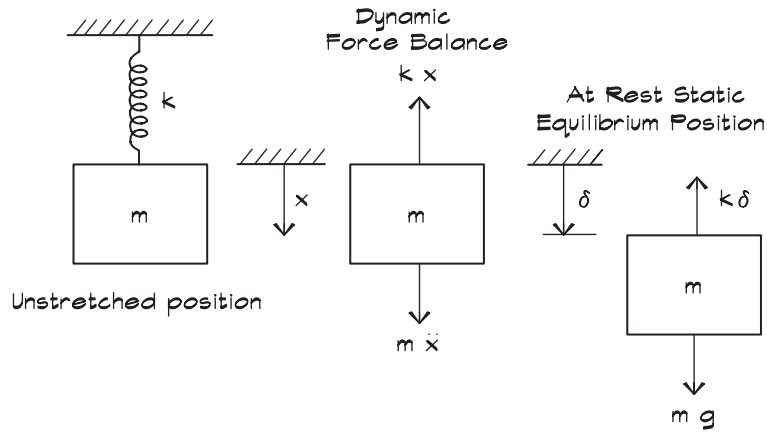
In general if a system requires n numbers to describe its motion it is said to have n degrees of freedom. A completely free mass has six degrees of freedom: three orthogonal displacement directions and three rotations, one about each axis. A stretched string or a flexible beam has an infinite number of degrees of freedom, since there are an infinite number of possible vibration shapes. These can be analyzed in a regular manner using a superposition of all possible vibrational modes added together; however, to do so exactly requires an infinite number of constants, one for each mode. This mathematical construct, called a Fourier series, is a useful tool even if it is not carried out to infinity.

The forces on a simple spring mass system are the spring force, which depends on the displacement away from the equilibrium position, and the inertial force of the accelerating mass. The equation of motion was discussed in Chapt. 6 and is simply a summation of the forces on the body

$$m \ddot{x} + k x = 0 \tag{11.5}$$

which has a general solution

$$x = X \sin (\omega_n t + \phi) \tag{11.6}$$

where $\omega_n = \sqrt{k/m}$ = undamped natural frequency (rad / s)
k = spring constant (N / m)
m = mass (kg)
ϕ = phase angle at time t = 0 (rad)
X = maximum displacement amplitude (m)

Although the spring mass model is simple, it is applicable as an approximation to many complicated structures. Building elements such as beams, wood or concrete floors, high-rise buildings, and towers can be modeled as spring mass systems and in more complex structures as series of connected elements, each having mass and stiffness.

Damped Oscillators

In vibrating systems, when bodies are set into motion, dissipative forces arise that damp or resist the movement. These are viscous forces that are proportional to the velocity of the

body; however, not all types of damping are velocity dependent. Coulomb damping due to sliding friction, for example, is a constant force. To model viscous damping, such as that provided by a shock absorber, we refer to the spring mass system shown in Fig 11.3. Here the damping force is proportional to the velocity and is negative because the force opposes the direction of motion.

$$F_r = -c\,\dot{x} \tag{11.7}$$

where F_r = viscous damping force, (N)

c = resistance damping coefficient (N s/m)

$\dot{x} = \dfrac{dx}{dt}$ = first time derivative of the displacement

= velocity (m/s)

If we gather together all forces operating on the mass on the left-hand side, and equate it to the mass times the acceleration on the right-hand side in accordance with Newton's law, and rearrange the terms, we get

$$m\,\ddot{x} + c\,\dot{x} + k\,x = 0 \tag{11.8}$$

The general solution has the form $x = e^{a\,t}$, where a is a constant to be determined. Substituting into Eq. 11.8 we obtain

$$\left(a^2 + \frac{c}{m}\,a + \frac{k}{m}\right) e^{a\,t} = 0 \tag{11.9}$$

which holds for all t when

$$\left(a^2 + \frac{c}{m}\,a + \frac{k}{m}\right) = 0 \tag{11.10}$$

This equation, known as the characteristic equation, has two roots

$$a_{1,2} = -\frac{c}{2\,m} \pm \sqrt{\left(\frac{c}{2\,m}\right)^2 - \frac{k}{m}} \tag{11.11}$$

from which we can construct a general steady-state solution in the underdamped condition, where the term under the radical is negative.

$$x = X\,e^{\frac{-c\,t}{2\,m}} \sin\,(\omega_n\,t + \phi) \tag{11.12}$$

The damped natural frequency of vibration is given by

$$\omega_d = 2\,\pi\,f_d = \sqrt{\omega_n^2 - \left(\frac{c}{2\,m}\right)^2} \tag{11.13}$$

The damping coefficient, c, influences both the amplitude and the damped natural frequency of oscillation, ω_d, by slowing it down slightly.

An example of a damped oscillation is shown in Fig. 11.4. The envelope of the decay is controlled by the damping coefficient. One measure of the degree of damping is the decay

FIGURE 11.3 A Spring Mass System with Viscous Damping (Thomson, 1965)
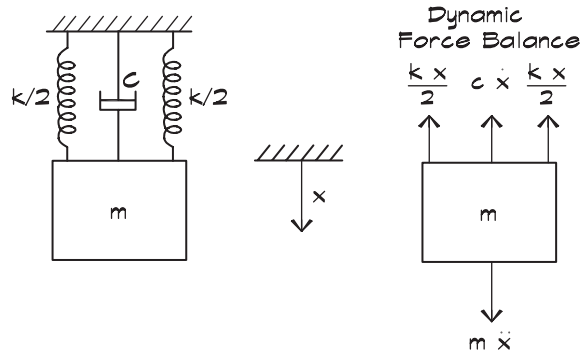
FIGURE 11.4 Response of a Damped Oscillator to an Impulse (Rossing and Fletcher,1995)
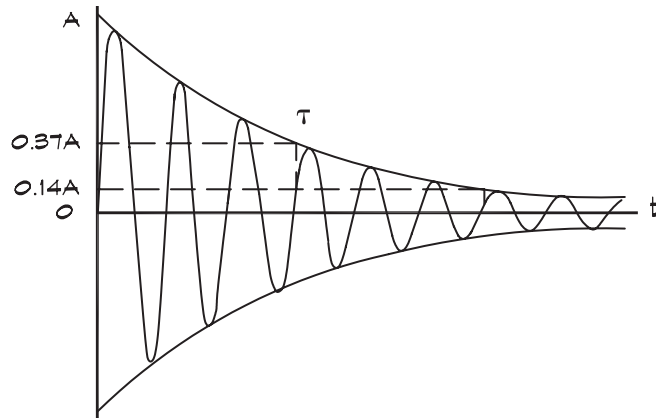
time, $\tau = \dfrac{2\,m}{c}$, which is the time it takes for the amplitude of the envelope to fall to $1/e$ (37%) of its initial value. It can be seen from Eq. 11.13 that, when one over the decay time is equal to the undamped natural frequency, the term under the radical is zero and the system does not oscillate. Such a system is said to be critically damped. The value of the damping coefficient at this point is given the symbol $c_c = 2\,m\,\omega_n$, and the degree of damping is expressed in terms of the ratio of the damping coefficient to the critical damping coefficient $\eta = \dfrac{c}{c_c}$, which is called the damping ratio, and is expressed as a percentage of critical damping.

Damping Properties of Materials

All materials have a certain amount of intrinsic internal damping, which depends on the internal structure of the substance. Figure 9.10 showed the damping coefficients for a number of common construction materials, which range from extremely low values in steel and other

metals to very high values in resins and viscous liquids. These latter materials are used in laminated glass specifically for their damping characteristics. In laminated glass a resin is sandwiched between the two layers. This is called a constrained layer damper. Damping compounds are commercially available in bulk and can be trowelled directly onto lightweight metal panels. In order to be effective they should be applied thickly–to at least the thickness of the vibrating panel.

In wood floor systems panel adhesive can help provide damping when applied between sheets of flooring, between wood joists and plywood subfloors, and to stepped blocking installed within the floor joists. In concrete floor systems the thickness and density of the concrete determines the amount of damping. Additional damping can be provided by plates welded to the joist webs and by lightweight interior partitions attached either above or below the floor. Even if partitions are not load bearing, they can contribute significantly to damping.

Driven Oscillators and Resonance

When a spring mass system is driven by a periodic force, it will respond in a predictable manner, which depends on the frequency of the driving force. A familiar example is a child's swing. If a child pumps the swing by kicking his legs out at the proper moment, he can increase the amplitude of the swing oscillation. The swing responds at the frequency of the driving force but its amplitude increases substantially only when the period of the driving force matches the natural period of vibration. Thus the child soon learns that he must kick out his legs at the proper time if he is to increase his swing's height.

There are many examples of resonant systems in architecture, including sound waves in rectangular rooms, organ pipes, and other open or closed tubes; and structural systems including floors, walls and wall panels, piping, and mechanical equipment. Each of these can act as an oscillator and be driven into resonance by a periodic force. The equation describing the motion of a forced oscillator with damping is

$$m \ddot{x} + c \dot{x} + k x = F_0 \sin (\omega t) \tag{11.14}$$

The general solution has the form

$$x = X \sin (\omega t - \phi) \tag{11.15}$$

By substituting into Eq. 11.14 we obtain

$$m \omega^2 X \sin (\omega t - \phi) - c \omega X \sin (\omega t - \phi + \frac{\pi}{2})$$
$$- k X \sin (\omega t - \phi) + F_0 \sin (\omega t) = 0 \tag{11.16}$$

The relationship among all the forces acting on the mass is shown in Fig. 11.5, and from the geometry of the force triangle we can solve for the amplitude X

$$X = \frac{F_0}{\sqrt{\left(k - m \omega^2\right)^2 + (c \omega)^2}} \tag{11.17}$$

and

$$\tan \phi = \frac{c \omega}{k - m \omega^2} \tag{11.18}$$

FIGURE 11.5 Forced Response of a Spring Mass System with Viscous Damping (Thomson, 1965)
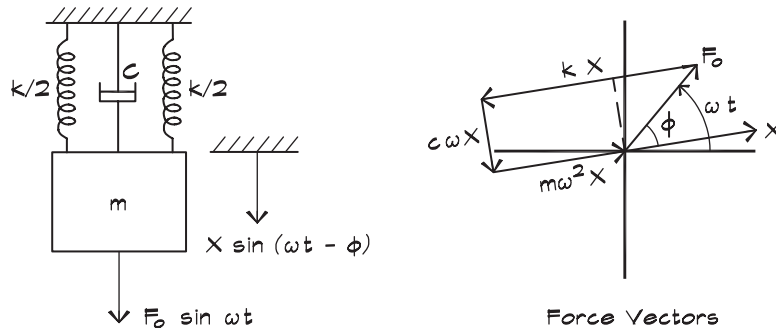
We can use more general notation as follows

$\omega_n = \sqrt{k/m}$ = undamped natural frequency (rad / s)

$c_c = 2\,m\,\omega_n$ = critical damping coefficient (N s / m)

$\eta = c/c_c$ = damping factor

$X_0 = F_0 / k$ = static deflection of the spring mass under the steady force F_0 (m)

and write Eq. 11.17 as

$$\frac{X}{X_0} = \frac{1}{\sqrt{\left[1 - (\omega/\omega_n)^2\right]^2 + \left[2\eta\,(\omega/\omega_n)\right]^2}} \qquad (11.19)$$

and Eq. 11.18 as

$$\tan \phi = \frac{2\,\eta\,(\omega/\omega_n)}{1 - (\omega/\omega_n)^2} \qquad (11.20)$$

Looking at Eqs. 11.15, 11.17, and 11.19 we see that the mass vibrates at the driving frequency ω, but the amplitude of vibration depends on the ratio of the squares of the resonant and driving frequencies. When the driving frequency matches the resonant frequency a maximum in the displacement occurs. Note that the damping term $2\,\eta\,(\omega/\omega_n)$ keeps the denominator from vanishing and limits the excursion at resonance.

Figure 11.6 shows a plot of the response of the system. As the driving frequency moves toward the resonant frequency the output increases—theoretically reaching infinity at resonance for zero damping. The damping not only limits the maximum excursion at resonance but also shifts the resonant peak downward in frequency.

Vibration Isolation

When a simple harmonic force is applied to a spring mass system, it induces a response that reaches a maximum at the resonant frequency of the system. If we ask what force is transmitted to the foundation through the spring mass support we can refer again to Fig. 11.5.

The forces are transmitted to the support structure through the spring and shock absorber system. The formulas remain the same whether the mass is resting on springs or hung

Figure 11.6 Normalized Excursion vs Frequency for a Forced Simple Harmonic System with Damping (Thomson, 1965)
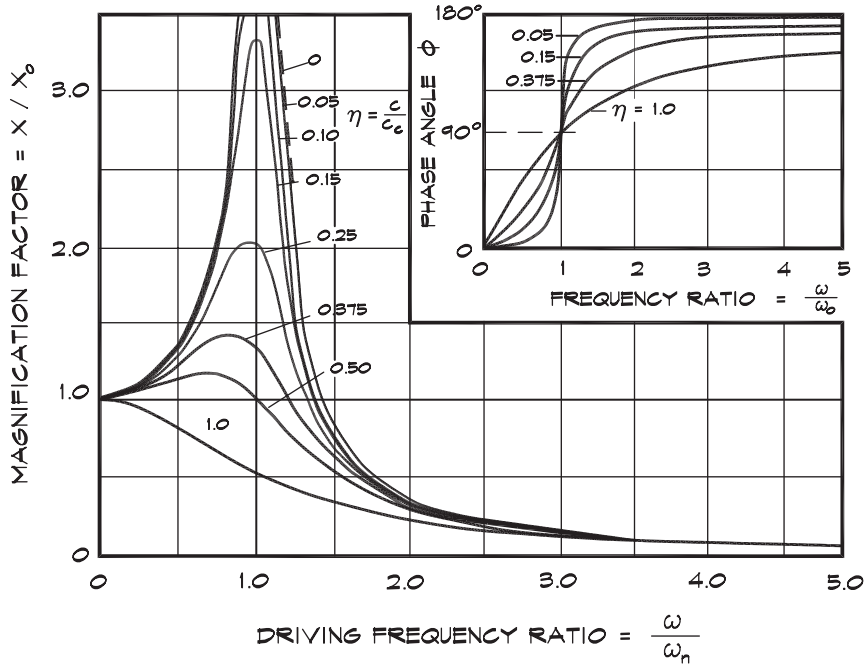
from springs. The balance of dynamic forces is shown, and using this geometry we can resolve the force on the support system as

$$F_t = \sqrt{(k\,X)^2 + (c\,\omega\,X)^2} = X\sqrt{k^2 + c^2\,\omega^2} \tag{11.21}$$

Using the expression given in Eq. 11.19 for the relationship between the applied force and the displacement amplitude, we can solve for the ratio of the impressed and transmitted forces

$$F_t = \frac{F_0\sqrt{1 + \left(\dfrac{c\,\omega}{k}\right)^2}}{\sqrt{\left[1 - \dfrac{m\,\omega^2}{k}\right]^2 + \left(\dfrac{c\,\omega}{k}\right)^2}} \tag{11.22}$$

which can be written as

$$\tau = \frac{F_t}{F_0} = \frac{\sqrt{1 + \left(2\,\eta\,\dfrac{\omega}{\omega_n}\right)^2}}{\sqrt{\left[1 - \left(\dfrac{\omega}{\omega_n}\right)^2\right]^2 + \left(2\,\eta\,\dfrac{\omega}{\omega_n}\right)^2}} \tag{11.23}$$

FIGURE 11.7 Transmissibility of a Viscous Damped System
The Force Transmissibility and Motion Transmissibility of a Viscous
Damped Single Degree of Freedom are Numerically Identical
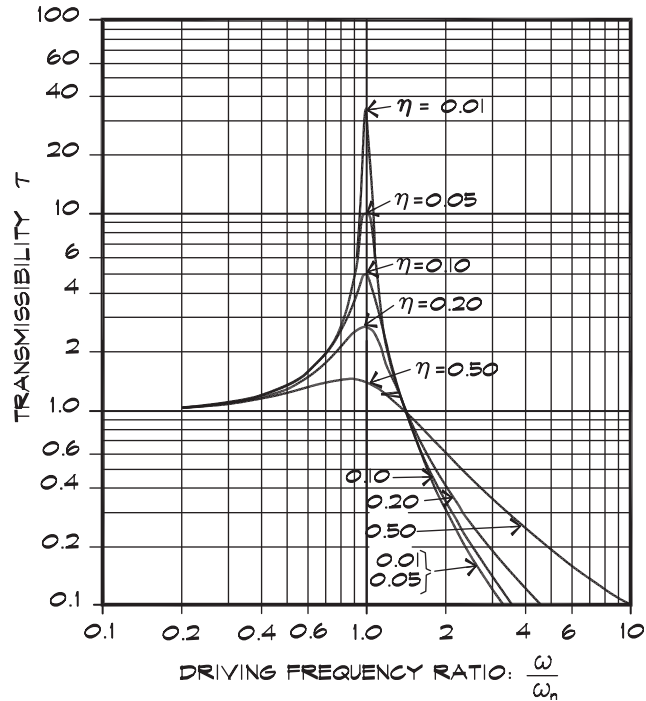
Figure 11.7 shows a plot of this expression in terms of the transmissibility, which is the ratio of the transmitted to the imposed force. We can see that above a given frequency $\left(\sqrt{2}\, f_n\right)$, as the frequency of the driving force increases, the transmissibility decreases and we achieve a decrease in the transmitted force. This is the fundamental principle behind vibration isolation.

Since the isolation is dependent on frequency ratio, the lower the resonant frequency, the greater the isolation for a given excitation frequency. The natural frequency of the spring mass system is

$$f_n = \frac{\omega_n}{2\,\pi} = \frac{1}{2\,\pi}\,\sqrt{k/m} = \frac{1}{2\,\pi}\,\sqrt{k\ g/m\ g} \qquad (11.24)$$

which can be written in terms of the static deflection of the vibration isolator under the weight of the supported object,

$$f_n = \frac{1}{2\,\pi}\,\sqrt{g/\delta} = \frac{3.13}{\sqrt{\delta_i}}\ (\text{Hz},\ \delta_i\ \text{in inches}) \qquad (11.25)$$

or

$$f_n = \frac{1}{2\,\pi}\,\sqrt{g/\delta} = \frac{5}{\sqrt{\delta_{cm}}}\ (\text{Hz},\ \delta_{cm}\ \text{in centimeters}) \qquad (11.26)$$

A fundamental principle for effective isolation is that the greater the deflection of the isolator, the lower the resonant frequency of the spring mass system, and the greater the vibration isolation. We must counterbalance this against the mechanical stability of the isolated object since very soft mounts are generally less stable than stiff ones. To increase the deflection, we must increase the load on each isolator, so a few point-mount isolators are preferable to a continuous mat or sheet. Thick isolators are generally more effective than thin isolators since thick isolators can deflect more than thin ones. Finally, trapped air spaces under isolated objects should be avoided and, if unavoidable, then wide spaces are better than narrow spaces, because the trapped air acts like another spring. Note that the greater the damping, the less the vibration isolation, but the lower the vibration amplitude near resonance. This leads to a second important point, which is that damping is incorporated into vibration isolators, not to increase the isolation, but to limit the amplitude at resonance. An example might be a machine that starts from a standstill (zero frequency), goes through the isolator resonance, and onto its operating point frequency. If this happens slowly we may be willing to trade off isolation efficiency at the eventual operating point for amplitude limitation at resonance.

If there is zero damping Eq. 11.23 can be simplified further. Assuming that the frequency ratio is greater than $\sqrt{2}$, the transmissibility is given by

$$\tau \cong \left[\left(\frac{\omega}{\omega_n} \right)^2 - 1 \right]^{-1} \tag{11.27}$$

We substitute $\omega_n^2 = g/\delta$, where g is the acceleration due to gravity and δ is the static deflection of the spring under the load of the supported mass, and the transmissibility becomes

$$\tau \cong \left[\frac{(2 \pi f)^2 \delta}{g} - 1 \right]^{-1} \tag{11.28}$$

which is sometimes expressed as an isolation efficiency or percent reduction in vibration in Fig. 11.8. This simplification is occasionally encountered in vibration isolation specifications that call for a given percentage of isolation at the operating point. It is better to specify the degree of isolation indirectly by calling out the deflection of the isolator, which is directly measurable by the installing contractor, rather than an efficiency that is abstract and difficult to measure in the field.

It is important to recall that these simple relationships only hold for single degree of freedom systems. If we are talking about a piece of mechanical equipment located on a slab the deflection of the slab under the weight of the isolated equipment must be very low—typically 8 to 10 times less than the deflection of the isolator for this approximation to hold. As the stiffness of the slab decreases, softer vibration isolators must be used to compensate.

When the excitation force is applied directly to the supported object or when it is self excited through eccentric motion, vibration isolators do not decrease the amplitude of the driven object but only the forces transmitted to the support system. When the supported object is excited by the motion of the support base, there is a similar reduction in the forces transmitted to the object. For a given directly applied excitation force, an inertial base consisting of a large mass, such as a concrete slab placed between the vibrating equipment and the support system, can decrease the amplitude of the supported equipment, but interestingly

FIGURE 11.8 Isolation Efficiency for a Flexible Mount
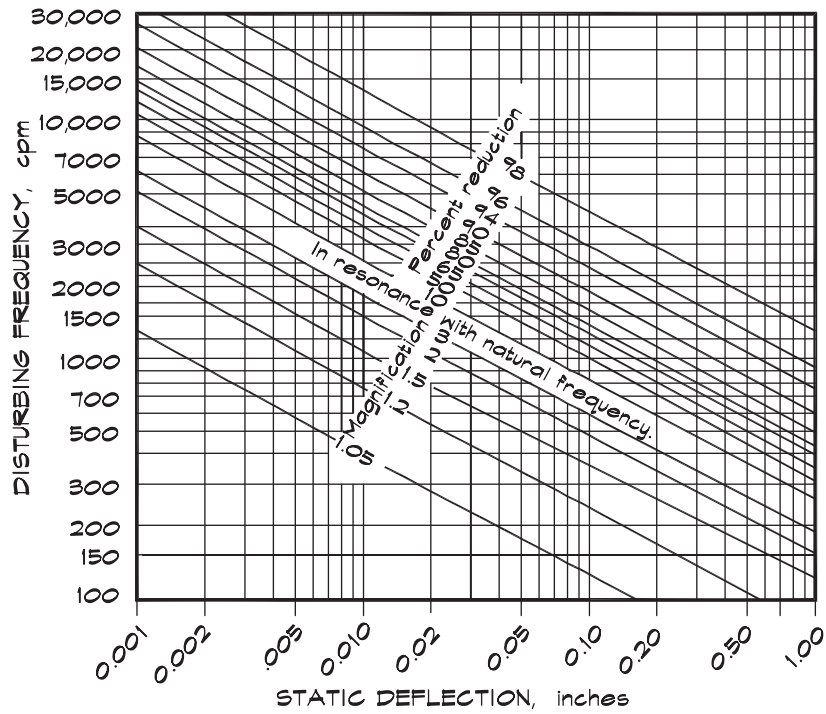
not the amplitude of the transmitted force. Inertial bases are very helpful in attenuating the motion of mechanical equipment such as pumps, large compressors, and fans, which can have eccentric loads that are large compared to their intrinsic mass.

Isolation of Sensitive Equipment

Frequently there are requirements to isolate a piece of sensitive equipment from floor-induced vibrations. The geometry is that shown in Fig. 11.9. Since the spring supports are in their linear region the relations are the same for equipment hung from above or supported

FIGURE 11.9 Force Vectors of a Spring Mass System with Viscous Damping for a Moving Support

Moving Support   Force Vectors
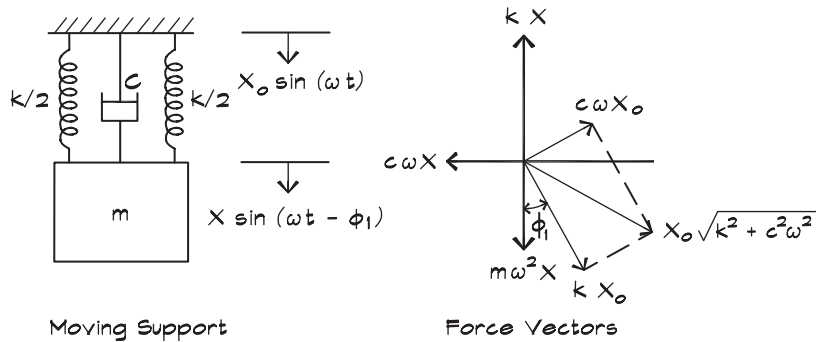
FIGURE 11.10   Transmissibility Curves for Vibration Isolation (Ruzicka, 1971)
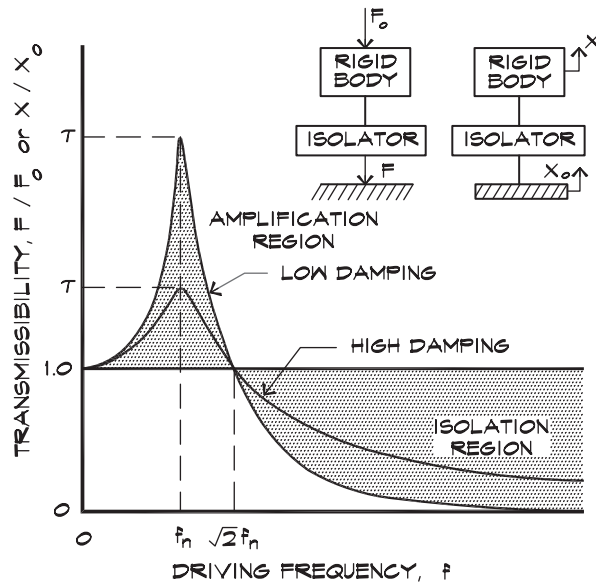
from below. The transmissibility is the same as that given in Eq. 11.23. In the case of isolated equipment, instead of the force being generated by a vibrating machine, a displacement is created by the motion of the supporting foundation. In Eq. 11.23 the terms for force amplitudes are replaced by displacement amplitudes.

Summary of the Principles of Isolation

Figure 11.10 shows the result of this analysis for both self-excited sources and sensitive receivers. The transmission equation is the same in both cases, differing only in the definition of transmissibility, which for an imposed driving force is the force ratio and for base motion is the displacement ratio. Above the resonant frequency of the spring mass system the response to the driving function decreases until, at a frequency just over 40% above resonance, the response amplitude is less than the imposed amplitude. At higher driving frequencies the response is further decreased. The lower the natural frequency of the isolator—that is, the greater its deflection under the load of the equipment—the greater the isolation.

11.3   VIBRATION ISOLATORS

Commercially available vibration isolators fall into several general categories: resilient pads, neoprene mounts, and a combination of a steel spring and neoprene pad (Fig. 11.11). An isolator is listed by the manufacturer with a range of rated loads and a static deflection, which is the deflection under the maximum rated load. Most isolators will tolerate some loading beyond their rated capacity, often as much as 50%; however, it is good practice to check the published load versus deflection curve to be sure. An isolator must be sufficiently loaded to achieve its rated deflection, but it must also remain in the linear range of the load versus deflection curve and not bottom out.

FIGURE 11.11   Types of Vibration Isolators
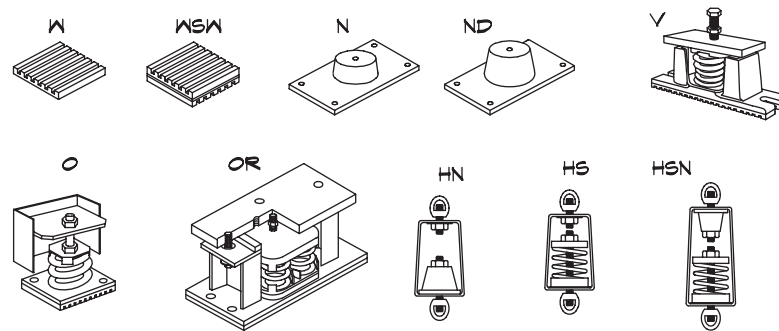
Isolation Pads (Type W, WSW)

Isolation pads of felt, cork, neoprene impregnated fiberglass, or ribbed neoprene sometimes sandwiched by steel plates usually have about a .05 inch (1 mm) deflection ($f_n = 14$ Hz) and are used in noncritical or high-frequency applications. Typically these products are supplied in small squares, which are placed under vibrating equipment or piping. Depending on the stiffness of the product, they are designed to be loaded to a particular weight per unit area of pad. For 40 durometer neoprene pads, for example, the usual load recommendation is about 50 lbs/sq in. Where higher deflections are desired or where there is a need to spread the load, pads are sandwiched with thin steel plates. Such pads are designated WSW or WSWSW depending on the number of pads and plates.

Neoprene Mounts (Type N, ND)

Neoprene isolators are available in the form of individual mounts, which have about a 0.25 inch (6 mm) rated deflection, or as double deflection mounts having a 0.4 inch (10 mm) deflection. These products frequently have integral steel plates, sometimes with tapped holes, that allow them to be bolted to walls or floors. They are available in neoprene of various durometers from 30 to 60, and are color-coded for ease of identification in the field. The double deflection isolators can be used to support floating floors in critical applications such as recording studios.

Steel Springs (Type V, O, OR)

A steel spring is the most commonly used vibration isolator for large equipment. Steel springs alone can be effective for low-frequency isolation; however, for broadband isolation they must be used in combination with neoprene pads to stop high frequencies. Otherwise these vibrations will be transmitted down the spring. Springs having up to 5 inches (13 cm) static deflection are available, but it is unusual to see deflections greater than 3 inches (8 cm) due to their lateral instability. Unhoused open-spring mounts (Type O) must have a large enough diameter (at least 0.8 times the compressed height) to provide a lateral stiffness equal to the vertical stiffness. Housed springs have the advantage of providing a stop for lateral (Type V) or vertical motion and an integral support (Type OR) for installing the equipment at or near its eventual height, but are more prone to ground out when improperly positioned. These stops are useful during the installation process since the load of the equipment or piping may vary; particularly if it can be filled with water or oil. Built in limit stops are not

the same as earthquake restraints, which must resist motion in any direction. Threaded rods, allowing the height of the equipment to be adjusted and locked into place with double nuts, are also part of the isolator assembly.

Spring isolators must be loaded sufficiently to produce the design deflection, but not so much that the springs bottom out coil to coil. A properly isolated piece of equipment will move freely if one stands on the base, and should not be shorted out by solid electrical or plumbing connections.

Hanger Isolators (Type HN, HS, HSN)

Hanger isolators contain a flexible element, either neoprene (Type HN) or a steel spring (Type HS), or a combination of the two (Type HSN), which supports equipment from above. Spring hangers, like free standing springs, must have a neoprene pad as part of the assembly. Hangers should allow for some misalignment between the housing and the support rod (30°) without shorting out and be free to rotate 360° without making contact with another object. Threaded height-adjusting rods are usually part of these devices.

Air Mounts (AS)

Air springs consisting of a neoprene bladder filled with compressed air are also available. These have the disadvantage of requiring an air source to maintain adequate pressure along with periodic maintenance to assure that there is no leakage. The advantage is that they allow easy level adjustment and can provide larger static deflections than spring isolators for critical applications.

Support Frames (Type IS, CI, R)

Since the lower the natural frequency of vibration the greater the vibration isolation, it is advantageous to maximize the deflection of the isolation system consistent with constraints imposed by stability requirements. If the support system is a neoprene mount—for example, under a vibrating object of a given mass—it is generally best to use the fewest number of isolators possible consistent with other constraints. It is less effective to use a continuous sheet of neoprene, cork, flexible mesh, or other similar material to isolate a piece of equipment or floating floor since the load per unit area and thus the isolator deflection is relatively low. Rather, it is better to space the mounts under the isolated equipment so that the load on each mount is maximized and the lowest possible natural frequency is obtained. A structural frame may have to be used to support the load of the equipment if its internal frame is not sufficient to take a point load. Integral steel (IS) or concrete inertial (CI) or rail frame (R) bases (Fig. 11.12) are used in these cases. A height-saving bracket that lowers the bottom of the frame to 25 to 50 mm (1" to 2") above the floor is typically part of an IS or CI frame. Brackets allow the frame to be placed on the floor and the equipment mounted to it before the springs are slid into place and adjusted.

When equipment is mounted on isolators the load is more concentrated than with equipment set directly on a floor. The structure beneath the isolators must be capable of supporting the point load and may require a 100 to 150 mm (4" to 6") housekeeping pad to help spread the load. Equipment such as small packaged air handlers mounted on a lightweight roof can be supported on built up platforms that incorporate a thin (3") concrete pad. Lighter platforms may be used if they are located directly above heavy structural elements such as steel beams or columns. In all cases the ratio of structural deflection to spring deflection must be less than 1:8 under the equipment load.

FIGURE 11.12   Vibration Isolation Bases
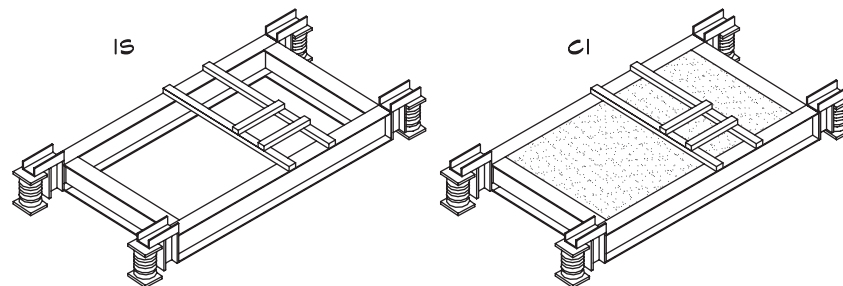
Isolator Selection

A number of manufacturers, as well as ASHRAE, publish recommendations on the selection of vibration isolators. By and large these recommendations assume that the building structure consists of concrete slabs having a given span between columns. One of the most useful is that published by Vibron Ltd. (Allen, 1989). This particular guide is reproduced as Tables 11.2 through 11.4. To use it, first determine the sensitivity of the receiving space, the floor thickness, and span. The longer the span, the more the deflection of the floor, the lower its resonant frequency, and the harder it is to isolate mechanical equipment that it supports. From step one we obtain an isolation category, a number from 1 to 6, which is a measure of the difficulty of successfully isolating the equipment. We then enter the charts in Tables 11.3 or 11.4 and pick out the base type and isolator deflection appropriate to the type of equipment and the isolation category.

When a concrete inertial (type CI) base is required, we can calculate its thickness from the nomographs given in Fig. 11.13. Using such a table is a practical way of selecting an appropriate isolator for a given situation. Although these tabular design methods are simple in practice, there is a great deal of calculating and experience that goes into their creation.

11.4   SUPPORT OF VIBRATING EQUIPMENT

Structural Support

A spring mass system, used to isolate vibrating equipment from its support structure, is based on a theory that assumes that the support system is very stiff. In practice it is important to construct support systems that are stiff, compared to the deflection of the isolators, and to minimize radiation from lightweight diaphragms. Where the support structure is very light— which can be the case for roof-mounted units—mechanical equipment is best supported on a separate system of steel beams that in turn are supported on columns down to a footing. A lightweight roof or similar structure can radiate sound like a driven loudspeaker, so mechanical equipment should not be located directly on lightweight roof panels. Where there is no other choice, and the roof slab is less than 4.5" (11 cm) of concrete, a localized concrete housekeeping pad should be used, having a thickness of 4" (10 cm) to 6" (15 cm) and a length 12" (30 cm) longer and wider than the supported equipment. These pads help spread the load and provide some inertial mass to increase the impedance of the support. Where it is not possible to locate equipment above a column, it should be located over one or more heavy structural members. Where supporting structures are less than 3.5" of solid concrete, use one isolation category above that determined from Table 11.2 along with the concrete subbase.

TABLE 11.2   Vibration Isolation Selection Guide (Vibron, 1989)

LOCATION OF VIBRATION ISOLATION		ISOLATION CATEGORY		
			UPPER CONCRETE FLOORS - OVER AND ADJACENT TO OCCUPIED AREAS	
TYPE OF BUILDING	FLOOR SPAN (ft)	BASEMENT BELOW GRADE	6" THICK & UP	TO 6" THICK
AUDITORIUMS CHURCHES - CRITICAL AREAS HOSPITALS - CRITICAL AREAS MUSIC HALLS OFFICE BUILDINGS - CRITICAL CONDOMINUIMS RADIO AND TV STATIONS	ON GRADE - ALL SPANS THROUGH 20 21 - 30 31 - 40 41 - 50 51 & UP	— 1 1 1 1 1	2 2 3 4 5 6	2 3 4 5 6 6
APARTMENT BUILDINGS CHURCHES HOSPITALS HOTELS OFFICE BUILDINGS PUBLIC BUILDINGS SCHOOLS	ON GRADE - ALL SPANS THROUGH 20 21 - 30 31 - 40 41 - 50 51 & UP	— 1 1 1 1 1	2 2 3 3 4 5	2 3 3 4 5 6

INDUSTRIAL BUILDINGS -
   NEAR OFFICE AREAS
SPORTS ACTIVITY AREAS -
   INDOORS
RESTAURANTS
TRANSPORTATION - AIRPORTS
   AND BUS TERMINALS
	ON GRADE - ALL SPANS
	THROUGH 20
	21 - 30
	31 - 40
	41 - 50
	51 & UP
		—
		1
		1
		1
		1
		1
			2
			2
			2
			3
			3
			4
				2
				2
				3
				3
				5
				5

TYPES OF ISOLATORS AND BASES USED IN THE TABLES

W   3/8" THICK, 40 DUROMETER RIBBED NEOPRENE PADS

WSW   3/8" THICK, 40 DUROMETER RIBBED NEOPRENE PADS SEPARATED BY A
10 GAUGE STEEL SHEET - LOADED TO 50 PSI

N   NEOPRENE IN SHEAR MOUNTS HAVING A 0.25" RATED DEFLECTION WITH
INTEGRAL STEEL PLATES AND TAPPED HOLES FOR BOLTING EQUIPMENT

ND   DOUBLE DEFLECTION NEOPRENE MOUNTS HAVING A 0.4" RATED DEFLECTION
WITH STEEL PLATES AND TAPPED HOLES FOR BOLTING EQUIPMENT

V   HOUSED STEEL SPRING AND 3/8" NEOPRENE ISOLATORS
WITH RUBBER SNUBBERS SEPARATING THE TOP AND BOTTOM HOUSINGS

O   OPEN FREE STANDING STEEL SPRING AND 3/8" NEOPRENE ISOLATORS
WITH EQUAL STIFFNESS IN THE HORIZONTAL AND VERTICAL DIRECTIONS

OR   OPEN RESTRICTED STEEL SPRING AND 3/8" NEOPRENE ISOLATORS
WITH EQUAL STIFFNESS IN THE HORIZONTAL AND VERTICAL DIRECTIONS
AND LIMIT STOPS TO PREVENT LIFTING AND STRESSING OF EQUIPMENT

HN   NEOPRENE MOUNT HANGERS FOR SUSPENDED EQUIPMENT - HANGERS
SHALL ACCOMMODATE A 30 DEG. MISALIGNMENT WITHOUT SHORTING OUT

HS   SPRING AND NEOPRENE PAD HANGERS FOR SUSPENDED EQUIPMENT HANGERS
SHALL ACCOMMODATE A 30 DEG. MISALIGNMENT WITHOUT SHORTING OUT

HSN   SPRING AND NEOPRENE MOUNT HANGERS FOR SUSPENDED EQUIPMENT HANGERS
SHALL ACCOMMODATE A 30 DEG. MISALIGNMENT WITHOUT SHORTING OUT

R   SPRING MOUNT SYSTEM WHICH INCORPORATES AN INTEGRAL RAIL FRAME

IS   INTEGRAL STEEL FRAME DESIGNED TO SUPPORT THE EQUIPMENT AND MOTOR

CI   CONCRETE INERTIAL BASE WITH FULL DEPTH PERIMETER STEEL FRAMES

TABLE 11.3 Vibration Isolation Selection Guide (Vibron, 1989)

TYPE OF EQUIPMENT			VIBRATION ISOLATION CATEGORY																	
			1			2			3			4			5			6		
DESIGNATION	DESCRIPTION		BASE	ISL/TR	DEFL	BASE	ISL/TR	DEFL	BASE	ISL/TR	DEFL	BASE	ISL/TR	DEFL	BASE	ISL/TR	DEFL	BASE	ISL/TR	DEFL
CENTRIFUGAL FANS	THROUGH 40 HP	TO 275 RPM	IS	O	3.0	IS	O	3.0	IS	O	3.0	IS	O	3.0	IS	O	3.0	IS	O	3.0
		276-600 RPM	IS	O	1.5	IS	O	1.75	IS	O	2.0	IS	O	2.0	IS	O	2.0	IS	O	2.5
		601 RPM & UP	IS	O	1.0	IS	O	1.0	IS	O	1.0	IS	O	1.75	IS	O	1.75	IS	O	2.0
	50 HP & UP	TO 275 RPM	CI	O	3.0	CI	O	3.0	CI	O	3.5	CI	O	4.0	CI	O	4.0	CI	O	4.0
		276-600 RPM	CI	O	1.5	CI	O	1.75	CI	O	2.0	CI	O	2.5	CI	O	3.0	CI	O	3.0
		601 RPM & UP	CI	O	1.0	CI	O	1.0	CI	O	1.0	CI	O	1.75	CI	O	2.0	CI	O	3.0
TUBULAR CENTRIFUGAL AND AXIAL FANS	ALL SIZES SUSPENDED	TO 750 RPM	-	HS	1.0	-	HS	1.1	-	O	1.5	-	O	2.0	-	O	2.75	-	O	3.0
		751 RPM & UP	-	HS	0.7	-	HS	1.0	-	O	1.1	-	O	1.5	-	O	2.0	-	O	2.75
	ALL SIZES FLOOR MOUNTED	TO 750 RPM	IS	O	0.7	IS	O	1.1	IS	O	1.5	CI	O	2.0	CI	O	2.75	CI	O	3.0
		751 RPM & UP	IS	O	0.7	IS	O	1.0	IS	O	1.1	CI	O	1.5	CI	O	2.0	CI	O	2.75
PACKAGED AH, AC AND H & V UNITS (SUSPENDED)	THRU 7.5 HP	ALL RPM	-	HS	0.7	-	HS	0.7	-	HS	0.7	-	HS	1.0	-	HSN	1.0	-	HSN	1.0
	10 HP & UP AND TO 5" S.P.	TO 600 RPM	-	HS	0.7	-	HS	0.7	-	HS	1.0	-	HS	1.0	-	HSN	1.5	-	HSN	1.75
		601-1000 RPM	-	HS	0.7	-	HS	0.7	-	HS	1.0	-	HS	1.0	-	HSN	1.0	-	HSN	1.5
		1001 RPM & UP	-	HS	0.7	-	HS	0.7	-	HS	0.7	-	HS	0.7	-	HSN	1.0	-	HSN	1.0
PACKAGED AH, AC AND H & V UNITS (FLOOR MOUNTED)	THRU 7.5 HP	ALL RPM	-	ND	0.25	-	V	0.75	-	V	0.75	-	V	1.0	-	V	1.0	-	V	1.0
	10 HP & UP AND TO 5" S.P.	TO 600 RPM	-	V	0.7	-	V	0.7	-	V	1.0	-	O	1.0	-	O	1.5	-	O	1.75
		601-1000 RPM	-	V	0.7	-	V	0.7	-	V	1.0	-	O	1.0	-	O	1.0	-	O	1.5
		1001 RPM & UP	-	V	0.7	-	V	0.7	-	V	0.7	-	O	1.0	-	O	1.0	-	O	1.0
UTILITY SETS	SUSPENDED	TO 500 RPM	-	HS	0.35	-	HS	1.0	-	HS	1.0	-	HS	1.5	-	HS	2.0	-	HS	2.5
		501 RPM & UP	-	HS	0.35	-	HS	1.0	-	HS	1.0	-	HS	1.0	-	HS	1.5	-	HS	2.0
	FLOOR MOUNTED	TO 500 RPM	R	ND	0.35	IS	O	1.0	IS	O	1.5	IS	O	2.0	IS	O	2.5	IS	O	2.75
		501 RPM & UP	R	ND	0.35	IS	O	1.0	IS	O	1.0	IS	O	1.5	IS	O	2.0	IS	O	2.5
AIR COOLED CONDENSERS AND CLOSED CIRCUIT COOLING TOWERS COOLERS	CENTRIFUGAL UNITS	TO 400 RPM	-	OR	2.0	-	OR	2.0	-	OR	2.0	-	OR	2.5	-	OR	3.0	-	OR	3.0
		401 RPM & UP	-	OR	1.0	-	OR	1.0	-	OR	1.5	-	OR	1.5	-	OR	2.0	-	OR	2.0
	AXIAL FLOW UNITS	TO 300 RPM	-	OR	2.0	-	OR	2.0	-	OR	2.0	-	OR	3.0	-	OR	3.0	-	OR	3.5
		301-700 RPM	-	OR	1.5	-	OR	1.5	-	OR	1.5	-	OR	2.0	-	OR	2.0	-	OR	3.0
		701 RPM & UP	-	OR	1.0	-	OR	1.0	-	OR	1.5	-	OR	1.5	-	OR	2.0	-	OR	3.0
PACKAGED STEAM GENERATORS	ALL SIZES		-	OR	1.0	-	OR	1.5	-	OR	1.75	-	OR	2.0	-	OR	2.5	-	OR	2.5

TABLE 11.4   Vibration Isolation Selection Guide (Vibron, 1989)

TYPE OF EQUIPMENT			VIBRATION ISOLATION CATEGORY															
			1			2			3			4			5			6		
DESIGNATION	DESCRIPTION		BASE	ISL.TR	DEFL	BASE	ISL.TR	DEFL	BASE	ISL.TR	DEFL	BASE	ISL.TR	DEFL	BASE	ISL.TR	DEFL	BASE	ISL.TR	DEFL
CENTRIFUGAL PUMPS	CLOSE COUPLED ALL RPM	THRU 5 HP	CI	O	1.0	CI	O	1.0	CI	O	1.0	CI	O	1.0	CI	O	1.5	CI	O	1.5
		7.5 HP & UP	CI	O	1.0	CI	O	1.0	CI	O	1.0	CI	O	1.5	CI	O	2.0	CI	O	2.0
	BASE MOUNTED ALL RPM	THRU 5 HP	CI	O	1.0	CI	O	1.0	CI	O	1.0	CI	O	1.5	CI	O	2.0	CI	O	2.0
		7.5 HP - 75 HP	CI	O	1.0	CI	O	1.0	CI	O	1.0	CI	O	1.5	CI	O	2.0	CI	O	3.5
		75 HP & UP	CI	O	1.0	CI	O	1.0	CI	O	1.5	CI	O	2.0	CI	O	2.5	CI	O	3.0
INLINE PUMPS	THRU 40 HP		-	WSW	0.15	-	V	0.7	CI	O	1.0	-	O	1.0	CI	O	1.5	CI	O	2.0
	40 HP & UP		-	WSW	0.15	-	V	1.0	CI	O	1.0	CI	O	1.5	CI	O	2.0	CI	O	2.5
RECIPROCATING AIR OR REFRIGERATION COMPRESSORS	THRU 15 HP	TO 500 RPM	CI	O	1.0	CI	O	1.0	CI	O	1.5	CI	O	1.75	CI	O	2.0	CI	O	2.5
		501-750 RPM	CI	O	0.75	CI	O	1.0	CI	O	1.5	CI	O	1.5	CI	O	2.0	CI	O	2.0
		751 RPM & UP	CI	O	0.75	CI	O	1.0	CI	O	1.5	CI	O	1.5	CI	O	2.0	CI	O	2.0
	20 HP AND UP	TO 500 RPM	CI	O	1.0	CI	O	1.5	CI	O	1.75	CI	O	2.0	CI	O	2.0	CI	O	1.75
		501-750 RPM	CI	O	1.0	CI	O	1.25	CI	O	1.5	CI	O	1.75	CI	O	1.75	CI	O	1.5
		751 RPM & UP	CI	O	0.75	CI	O	1.0	CI	O	1.25	CI	O	1.5	CI	O	1.5	CI	O	1.0
CENTRIFUGAL & REFRIGERATION MACHINES	ALL SIZES		IS	OR	1.0	IS	OR	1.5	IS	OR	2.0	IS	OR	2.0	IS	OR	2.5	IS	OR	2.5
ABSORPTION REFRIGERATION MACHINES	ALL SIZES		IS	OR	1.0	IS	OR	1.0	IS	OR	1.5	IS	OR	1.5	IS	OR	2.0	IS	OR	2.0
ELECTRICAL DISTRIBUTION TRANSFORMERS	0 - 50 KVA		-	W	0.06	-	WSW	0.12	-	WSW	0.12	-	WSW	0.12	-	V	0.7	-	V	0.7
	51 - 250 KVA		-	N	0.25	-	N	0.25	-	ND	0.35	-	ND	0.4	-	ND	0.4	-	ND	0.4
	251 KVA & LARGER		-	ND	0.35	-	V	0.7	-	V	0.7	-	V	0.7	-	V	1.0	-	V	1.0

FIGURE 11.13   The Thickness of Concrete Inertial Bases (Vibron, 1989)
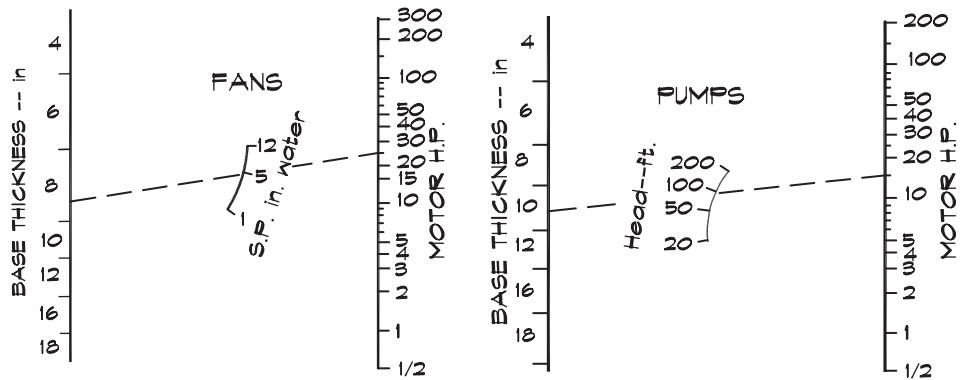
For T-shaped Pump Bases
Reduce To Next Lower
Thickness

AIR AND REFRIGERATION COMPRESSORS	
Motor H.P.	Base Thickness -- in.
through 2	8
3 & 5	10
7 1/2 to 20	12
25 to 40	14
50 to 75	16
100 & 125	20
125 up	24

Examples of various recommendations on the support of rooftop equipment are shown in Fig. 11.14 (Schaffer, 1991).

Inertial Bases

When the source of vibration is a piece of mechanical equipment with a large rotating mass or a high initial torque, it is good practice to mount it on a concrete base that is itself supported on spring isolators. The additional mass does not increase the isolation efficiency since the springs must be selected to support both the equipment and the base, and the overall spring deflection will probably not change appreciably. The advantage of having the base is that for a given driving force, such as the eccentricity of a rotating part, there is a lower overall displacement due to the extra mass of the combined base plus equipment. Inertial bases also aid in the stabilization of tall pieces of equipment, equipment with a large rocking component, and equipment requiring thrust restraint.

Concrete inertial bases are used in the isolation of pumps and provide additional frame stiffness, which a pump frequently requires. Pump bases are sized so that their weight is about two to three times that of the supported equipment. Any piping, attached to a pump mounted on an isolated base, must be supported from the inertial base or by overhead spring hangers. It must not be rigidly supported from a wall, floor, or roof slab unless it is in a noncritical location.

Where unbalanced equipment, such as single- or double-cylinder low-speed air compressors are to be isolated, the weight of the inertial base is calculated from the unbalanced

FIGURE 11.14 Structural Support of Rooftop Equipment (Schaffer, 1991)

Poor
Concentration of equipment weight between beams causes excessive roof deflection and vibration transmission, even for isolated equipment.

Fair
Additional beam under equipment stiffens roof.

Good
Further addition of housekeeping pad adds mass and stiffness to roof.

Very Good
A column directly under the equipment gives the roof a very high local stiffness, but some equipment vibration still enters the roof slab.

Best
Mounting equipment on a steel frame supported by column extensions keeps virtually all vibration out of the roof slab.

force, which can be obtained from the manufacturer. These bases frequently must be five to seven times the weight of the compressor to control the motion.

Concrete bases also offer resistance to induced forces such as fan thrust. Isolation manufacturers (Mason, 1968) recommend that a base weighing from one to three times the fan weight be used to control thrust for fans above 6" of static pressure.

Earthquake Restraints

In areas of high seismic activity, vibration isolated equipment must be constrained from moving during an earthquake. The seismic restraint system must not degrade the performance

FIGURE 11.15   Earthquake Restraint (Mason Industries, 1998)
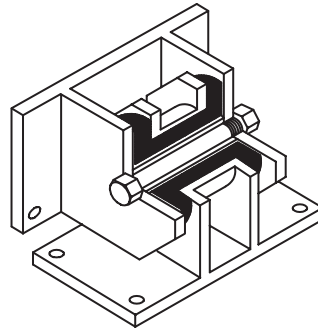
of the vibration isolation. Some specialized isolators incorporate seismic restraints, but most vibration isolators do not since a restraint device must control motion in any direction. A standard method of providing three-dimensional restraint is shown in Fig. 11.15 using a commercial three-axis restraint system. Lightweight hanger-supported equipment can be restrained by means of several slack braided-steel cables. Any earthquake restraint system must comply with local codes and should be reviewed by a structural engineer.

Pipe Isolation

Piping can conduct noise and vibration generated through fluid motion and by being connected to vibrating equipment. Fluid flow in piping generates sound power levels that are dependent on the flow velocity. Pipes and electrical conduits that are attached directly to vibrating equipment and to a supporting structure serve as a transmission path, which short circuits otherwise adequate vibration isolation. Any rigid piping attached to isolated equipment such as pumps, refrigeration machines, and condensers must be separately vibration isolated, typically at the first three points of support, which for large pipe is about 15 m (50 ft). It should be suspended by means of an isolator having a deflection that is at least that of the supported equipment or 3/4", whichever is greater.

There is a significant difference in the weight of a large water pipe, depending on whether it is empty or filled. Isolated equipment will move up when the pipe system is drained, and in doing so, will stress elbows and joints. The suspension system should allow for normal motion of the pipe under these conditions. Risers and other long pipe runs will expand and contract as they are heated and cooled and should be resiliently mounted. Even when fluid is not flowing, a popping noise can be generated as the pipe slides past a stud or other support point during heating or cooling.

In critical applications such as condominiums, water, waste, and refrigeration pipes should be isolated from making contact with structural elements for their entire length. Table 11.5 gives typical recommendations on the types of materials used for the isolation of plumbing and piping. These recommendations also apply to the support of piping at points where it penetrates a floor.

Several examples of proper isolation of piping connected to pumps are shown in Fig. 11.16. On all piping greater than 5" (13 cm) diameter, flexible pipe couplings are necessary between the pump outlet and the pipe run. Even with smaller diameter pipes they can be very helpful in decreasing downstream vibrations and associated noise. They act as vibration isolators by breaking the mechanical coupling between the pump and the pipe, and they

TABLE 11.5   **Typical Plumbing Isolation Materials**

NOMINAL PIPE SIZE (Dia, in)	REQUIRED ISOLATION HORIZONTAL	REQUIRED ISOLATION VERTICAL
1/2	1/4" FELT	1/4" FELT
3/4	3/8" FELT	3/8" FELT
1	3/8" FELT	3/8" FELT
1 1/2	3/8" FELT	3/8" FELT
2	1/2" FELT	WSW PADS
3	HN ISOLATORS	ND MOUNTS
4	HN ISOLATORS	ND MOUNTS
> 5	HS ISOLATORS 3/4" DEFL	V ISOLATORS 3/4" DEFL
* NOT REQUIRED FOR VENT STACKS, FIRE SPRINKLERS, OR GAS PIPING.		

help compensate for pipe misalignment and thermal expansion. Flexible pipe connections alone are usually not sufficient to isolate pipe transmitted vibrations but are part of an overall control strategy, which includes vibration isolation of the mechanical equipment and piping.

In high pressure hydraulic systems much of the vibration can be transmitted through the fluid so that pulse dampeners inserted in the pipe run can be helpful. These consist of a gas filled bladder, surrounding the fluid, into which the pressure pulse can expand and dissipate.

Where pipes are located in rated construction elements, closing off leaks at structural penetrations is critical to maintain the acoustical rating. Here the normal order of construction dictates the method of isolation. In concrete and steel structures, slabs are poured and then cored to accommodate pipe runs. In wood construction, piping is installed along with the framing, often preceding the pouring of any concrete fill. In both building types holes should be oversized by 1" (25 mm) more than the pipe diameter to insure that the pipe does not make direct structural contact. They are then stuffed with insulation, safing, or fire stop, and sealed. In slab construction the sealant can be a heavy mastic. With walls, the holes are covered with drywall leaving a 1/8" (3 mm) gap that is caulked. Pipe sleeves, which wrap the pipe at the penetration, are also commercially available. Details are shown in Fig. 11.17.

Electrical Connections

Where electrical connections are made to isolated equipment, the conduit must not short out the vibration isolation. If rigid conduit is used it should include a flexible section to isolate this path. The section should be long enough and slack enough that a 360° loop can be made in it.

Duct Isolation

High-pressure ductwork having a static pressure of 4" (10 cm) or greater should be isolated for a distance of 30 ft (10 m) from the fan. Ducts are suspended on spring hangers with a minimum static deflection of 0.75" (19 mm), which should be spaced 10 ft (3 m) or less apart.

Roof-mounted sheet metal ductwork, located above sensitive occupancies such as studios, should be supported on vibration isolators having a deflection equal to that of the

FIGURE 11.16   Vibration Isolation of Piping and Ductwork (Vibron, 1989)

Vibration Isolation of Piping Connected to Isolated Equipment
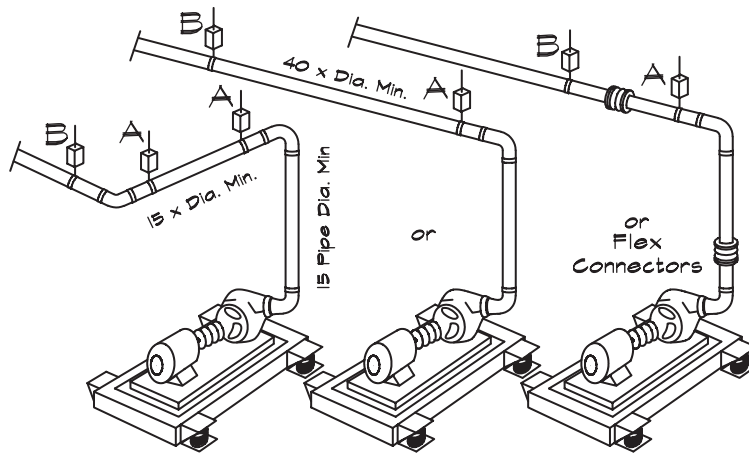
Each of the above alternatives will result in equivalent piping isolation from a flexibly supported pump if the following suggestions are implemented.

(1) The pump inertia bases should be at least 2.5 times the unit weight.

(2) Piping isolators should have the following static deflections:
Points A and B - Equal to the pump base static deflection
Beyond Point B - At least 0.7" for 20 ft. from point B with isolators spaced at 10 ft. intervals. For critical locations the complete pipe run should be isolated, with isolator static deflection of at least 0.7" and spaced at 10 ft. intervals.

(3) For pipe diameters above 5", flexible connections are necessary.

Vibration Isolation of High Pressure Ductwork

High pressure (above 4" static pressure) duct runs should be isolated for a distance of 30 ft. from the fan. Ducts supported by hanger isolators should have a static deflection of at least 3/4" and be spaced 10 ft. apart.

FIGURE 11.17   Pipe or Duct Penetration

The opening is oversized to allow for the penetration and covered with the same number of layers as are on the wall.
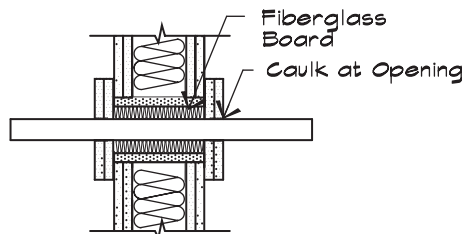
FIGURE 11.18 **Forced Excitation of an Undamped Two Degree of Freedom System (Ruzicka, 1971)**
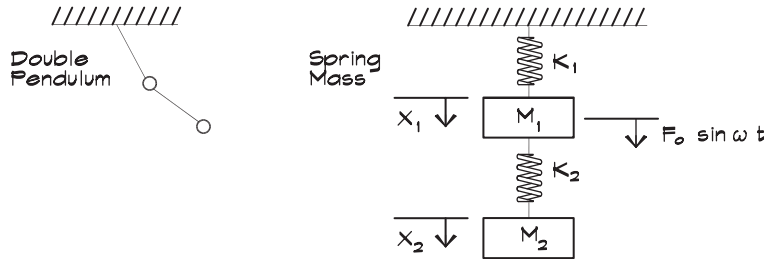
isolated equipment to which they are attached, for the first three points of support. Beyond that point the ducts can be supported on mounts having half that deflection.

11.5 TWO DEGREE OF FREEDOM SYSTEMS

Two Undamped Oscillators

Although the one degree of freedom model is the most commonly utilized system for most vibration analysis problems, often situations arise that exhibit more complex motion. A model of a two degree of freedom system is shown in Fig. 11.18. This system consists of two masses and two springs with a sinusoidal force applied to one of the masses. The equations of motion can be written as

$$m_1 \ddot{x}_1 = k_2 (x_2 - x_1) - k_1 x_1 + F_0 \sin \omega t \tag{11.29}$$

$$m_2 \ddot{x}_2 = - k_2 (x_2 - x_1) \tag{11.30}$$

If we make the following substitutions

$$\omega_1 = \sqrt{k_1 / m_1} \qquad X_0 = F_0 / k_1$$

$$\omega_2 = \sqrt{k_2 / m_2}$$

and write the solution in terms of sinusoidal functions of displacement

$$x_1 = X_1 \sin \omega t$$

and

$$x_2 = X_2 \sin \omega t$$

Substituting these expressions into Eqs. 11.29 and 11.30, we obtain an expression for the relationship between the amplitude displacements

$$\left[1 + \frac{k_2}{k_1} - \left(\frac{\omega}{\omega_1} \right)^2 \right] X_1 - \left(\frac{k_2}{k_1} \right) X_2 = X_0 \tag{11.31}$$

and

$$-X_1 + \left[1 - \left(\frac{\omega}{\omega_2}\right)^2\right] X_2 = 0 \qquad (11.32)$$

We can then study the system behavior by looking at the expressions for the ratio of the two amplitudes

$$\frac{X_1}{X_0} = \frac{\left[1 - (\omega/\omega_2)^2\right]}{\left[1 + \frac{k_2}{k_1} - \left(\frac{\omega}{\omega_1}\right)^2\right]\left[1 - \left(\frac{\omega}{\omega_2}\right)^2\right] - \frac{k_2}{k_1}} \qquad (11.33)$$

$$\frac{X_2}{X_0} = \frac{1}{\left[1 + \frac{k_2}{k_1} - \left(\frac{\omega}{\omega_1}\right)^2\right]\left[1 - \left(\frac{\omega}{\omega_2}\right)^2\right] - \frac{k_2}{k_1}} \qquad (11.34)$$

Now there are two resonant frequencies of the spring mass system, ω_1 and ω_2. From Eq. 11.33 we see that when the natural frequency of the second spring mass system matches the driving frequency of the impressed force, the numerator, and thus the amplitude X_1, goes to zero. At this frequency the amplitude of the second mass is

$$X_2 = -\frac{k_1}{k_2} X_0 = -\frac{F_0}{k_2} \qquad (11.35)$$

where the minus sign indicates that the motion is out of phase with, and just counterbalances, the driving force. This is the principal behind a second form of vibration isolation known as mass absorption or mass damping. The absorber mass must be selected so as to match the applied force, taking into consideration the allowable spring deflection.

Two Damped Oscillators

Figure 11.19 gives the results of an imposed force on a damped two-degree of freedom spring mass system. The two resonant peaks are at different frequencies, with $\omega_2 > \omega_1$. In this example there is a relatively narrow frequency range where the second mass provides appreciable mass damping. Indeed it may generate an unwelcome resonant peak, slightly above the fundamental frequency of the second mass.

A mass absorber is most effective when it is used to damp the natural resonant frequency of the first spring mass system. If the ω_2 is selected to match ω_1, then the two resonant peaks coincide. When a broadband vibration or an impulsive load is applied to the system, the zero in the numerator in Eq. 11.33 smothers the resonant peaks and mass damping occurs. Figure 11.20 illustrates this case.

In long-span floor systems the floor itself acts like a spring mass system. A weight, suspended by isolator springs below a floor at a point of maximum amplitude, can be used as a dynamic absorber. These weights, which are usually 1% to 2% of the weight of the

FIGURE 11.19   Forced Response of a Two Degree of Freedom System (Ruzicka, 1971)

Transmissibility curves for a vibration isolation system to which is
attached a passive vibration absorber tuned to a high frequency
component of vibration excitation.
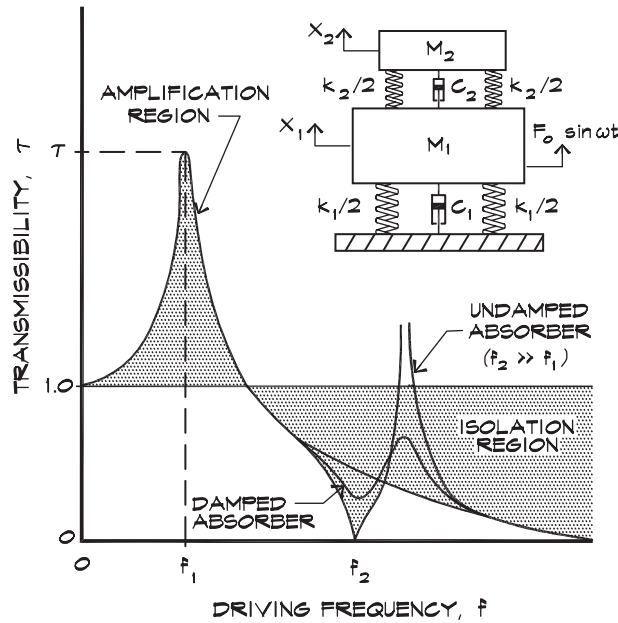
**FIGURE 11.20   Forced Response of a Two Degree of Freedom System Near Resonance
(Ruzicka, 1971)**

Transmissibility curve for a spring mass system to which is attached
a passive vibration absorber tuned so as to suppress the main
system resonant response.
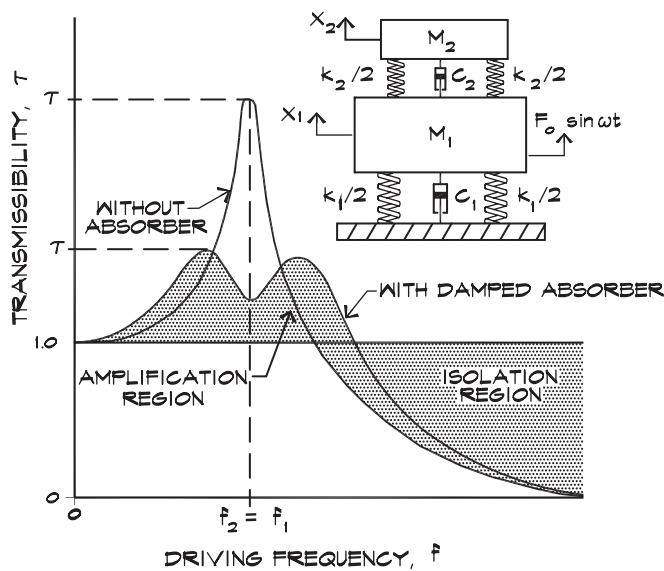
relevant floor area, are hung between the ceiling and the slab. It is not advisable to use the ceiling itself as the dynamic absorber, since mass damping works to minimize floor motion by maximizing the motion of the suspended mass. If the ceiling motion is maximized, it will radiate a high level of noise at the floor resonance.

Mass absorbers have also been used to damp the natural swaying motion of large towers such as the CN Tower in Toronto, Canada, using a dynamic pendulum. The double pendulum is another two degree of freedom system whose behavior is similar to that of a double spring mass. In this example the tower is encircled with a donut-shaped mass that is suspended as a pendulum. The mass is located at the point of maximum displacement of the normal modes of the structure. In the case of tall towers, the second and third modes are usually damped. The maximum displacement of the first mode occurs at the top of the tower and practical considerations prevent the suspension of a pendulum from this point. Two donut-shaped pendulums were used at the 1/3 and 1/2 points of the structure where they counter the second and third modes of vibration.

11.6   FLOOR VIBRATIONS

The vibration of floors due to motions induced by walking or mechanical equipment can be a source of complaints in modern building structures, particularly where lightweight construction such as concrete on steel deck, steel joists, or concrete on wood joist construction is used. Usually the vibration is a transient flexural motion of the floor system in response to impact loading from human activity (Allen and Swallow, 1975), which can be walking, jumping, or continuous mechanical excitation. The induced amplitudes are seldom enough to be of structural consequence; however, in extreme cases they may cause movement in light fixtures or other suspended items. The effects of floor vibrations are not limited to receivers located immediately below. With the advent of fitness centers, which feature aerobics, induced vibrations can be felt laterally 100 feet away on the same slab as well as up to 10 stories below (Allen, 1997).

Sensitivity to Steady Floor Vibrations

People, equipment, and sophisticated manufacturing processes, such as computer chip production, are sensitive to floor vibrations. The degree of sensitivity varies with the process and various authors have published recommendations. One of the earliest was documented by Reiher and Meister (1931) and is shown in Fig. 11.21. These were human responses determined by standing subjects on a shaker table and subjecting them to continuous vertical motion. Subjects react more vigorously to higher velocities, and for high amplitudes, awareness increases with frequency. Also shown are the Rausch (1943) limits for machines and machine foundations and the US Bureau of Mines criteria for structural safety against damage from blasting.

Sensitivity to Transient Floor Vibrations

Vibrational excitation of floor systems may be steady or transient; however, it is usually the case that steady sources of vibration can be isolated. Transient vibrations due to footfall or other impulsive loads are absorbed principally by the damping of the floor. Damping provides a function somewhat akin to absorption in the control of reverberant sound in a room. People react, not only to the initial amplitude of the vibration, but also to its duration.

FIGURE 11.21 Response Spectra for Continuous Vibration (Richart et al., 1970; Reiher and Meister, 1931)
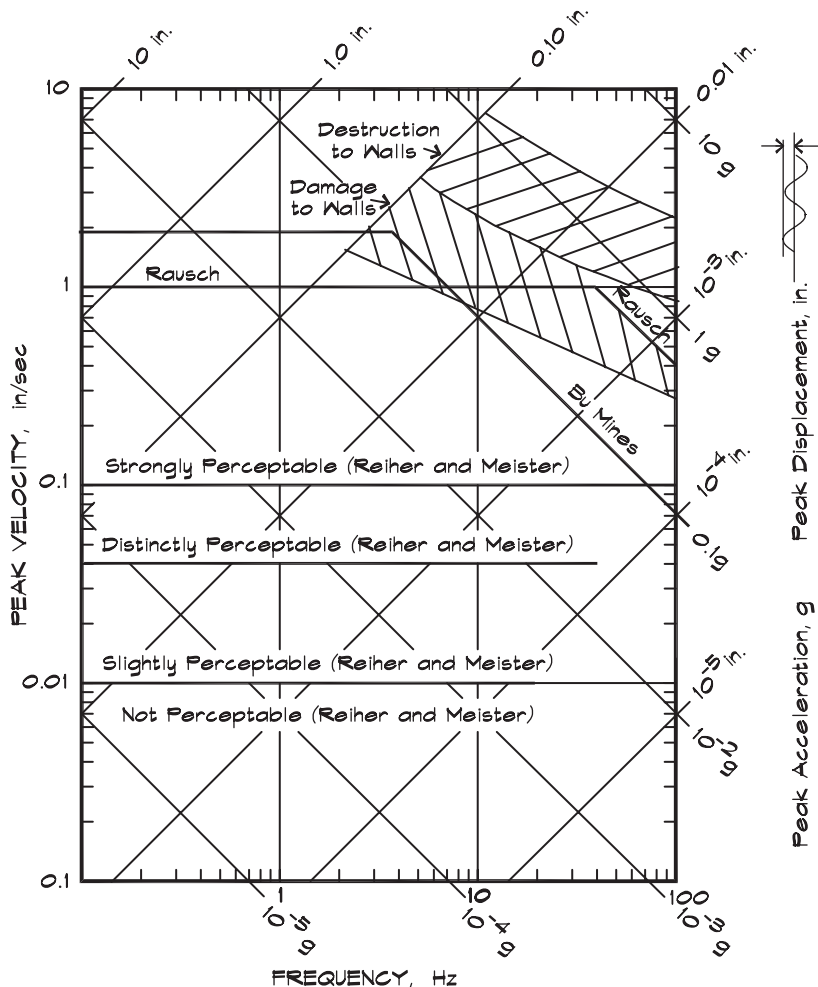
Investigators use tapping machines, walking at a normal pace (about 2 steps per second), and a heel drop test, where a subject raises up on his toes and drops his full weight back on his heels, as impulsive sources. This latter test represents a nearly worst-case scenario for human induced vibration, with aerobic studios and judo dojos being the exception.

After studying a number of steel-joist concrete-slab structures, Lenzen (1966) suggested that the original Reiher-Meister scale could be applied to floor systems having less than 5% of critical damping, if the amplitude scale were increased by a factor of 10. This means that we are less sensitive to floor vibration when it is sufficiently damped, in this case when only 20% of the initial amplitude remains after five cycles. He further suggested that if a vibration persists 12 cycles in reaching 20% of the initial amplitude, human response is the same as to steady vibration. Allen (1974), using his own experimental data along with observations of Goldman, suggested a series of annoyance thresholds for different levels of damping. This work, along with that of Allen and Rainer (1976), was adopted as a Canadian National Standard, which is shown in Fig. 11.22.

FIGURE 11.22   Annoyance Thresholds for Vibrations (Allen, 1974)
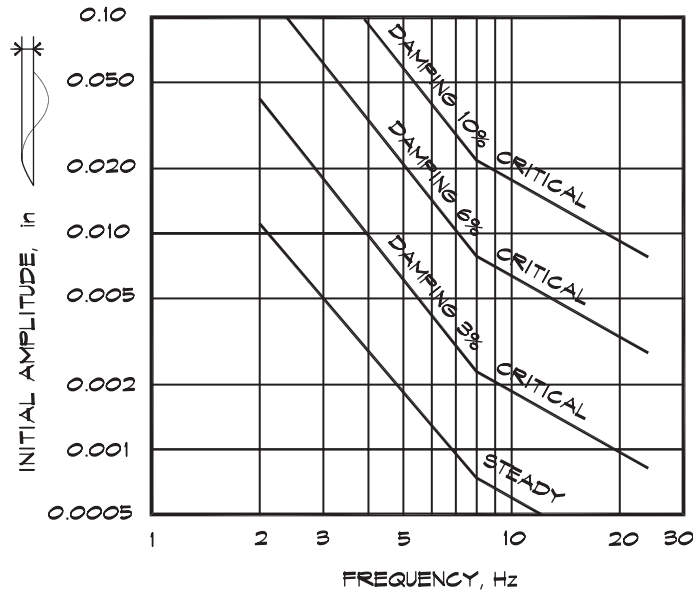
FIGURE 11.23   Impulsive Force
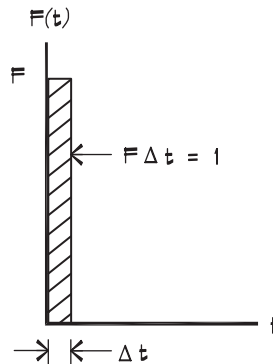
Vibrational Response to an Impulsive Force

When a linear system, such as a spring mass damper, is driven by an impulsive force we can calculate the overall response. For the study of vibrations in buildings the system of interest here is a floor and the impulsive force is a footfall generated by someone walking. An impulse force is one in which the force acts over a very short period of time. An impulse can be defined as

$$\hat{F} = \int_{t}^{t+\Delta t} F \, dt \cong F \, \Delta t \tag{11.36}$$

Figure 11.23 shows an example of an impulsive force, having a magnitude F and a duration Δt. An impulsive force, such as a hammer blow, can be very large; however, since it occurs over a rather short period of time, the impulse is finite. When the impulse is normalized to 1 it is called a unit impulse.

**FIGURE 11.24 Response of a Damped System to a Delta Function Impulse $\widehat{F}$
(Thomson, 1965)**
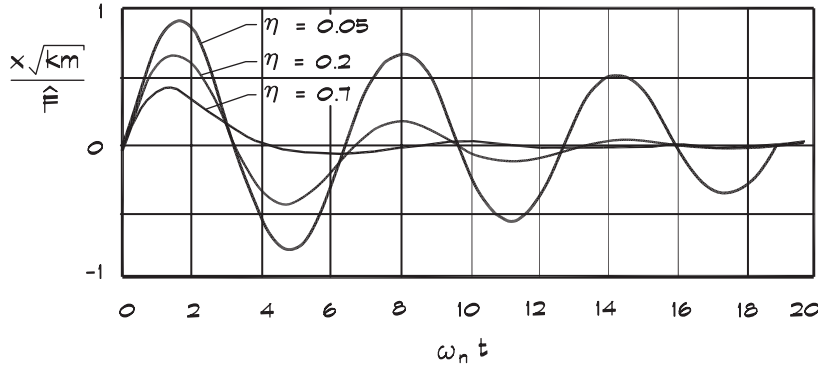
Figure 11.24 illustrates the response of a damped spring mass system under an impulse force for various values of the damping coefficient. From Newton's law, $F \Delta t = m \dot{x}_2 - m \dot{x}_1$. When an impulsive force is applied to a mass for a short time the response is a change in velocity without an appreciable change in displacement. The velocity changes rapidly from zero to an initial value of $\widehat{F} / m$. We can use this as the initial boundary condition, assuming an initial displacement of zero, by plugging into the general undamped solution (Eq. 11.6). We get the response to the impulse force

$$x = \frac{\widehat{F}}{m \, \omega_n} \sin \omega_n \, t \tag{11.37}$$

where ω_n is the undamped natural frequency of the spring mass system. If the system is damped, we can use the same procedure to calculate the response by plugging into Eq. 11.12.

$$x = \frac{\widehat{F}}{m \, \omega_n \, \sqrt{1 - \eta^2}} e^{- \eta \, \omega_n \, t} \quad \sin \left(\sqrt{1 - \eta^2} \, \omega_n \, t \right) \tag{11.38}$$

Response to an Arbitrary Force

The impulse response in Eq. 11.38 is a fundamental property of the system. It is given a special designation, g (t), where $x = \widehat{F} \, g$ (t). Once the system response to a unit impulse (sometimes called a delta function) has been determined, it is possible to calculate the response to an arbitrary force f (t) by integrating (summing) the effects of a series of impulses as illustrated in Fig. 11.25.

At a particular time τ, the force function has a value, which can be described by an impulse $\widehat{F} = f(\tau) \, \Delta \, \tau$. The contribution of this slice of the force function on the system response at some elapsed time $t - \tau$ after the beginning of that particular pulse is given by

$$x = f(\tau) \, \Delta \tau \; g \, (t - \tau) \tag{11.39}$$

and the response to all the small force pulses is given by integrating over the total time, t_p, the force is applied. If the time of interest is less than t_p, the limit of integration becomes the

FIGURE 11.25   An Arbitrary Pulse as a Series of Impulses (Thomson, 1965)
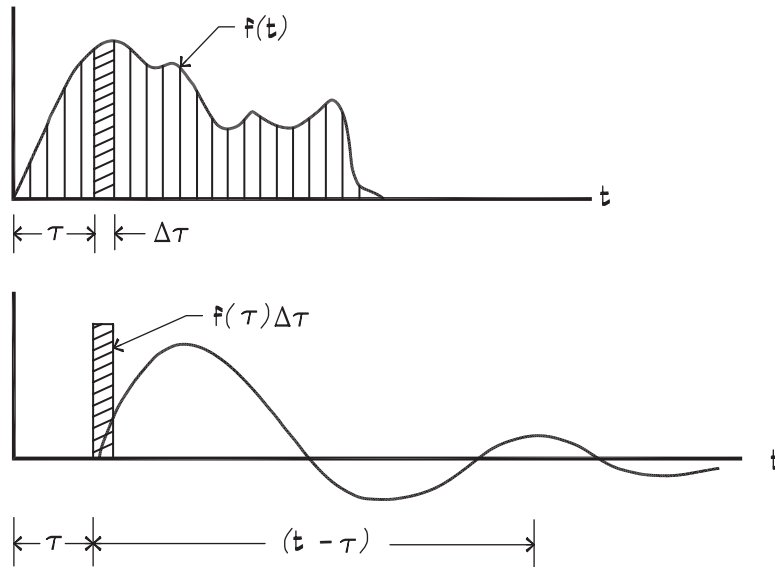
time of interest.

$$x(t) = \int_0^{t_p} f(\tau) \, g(t - \tau) \, d\tau \qquad (11.40)$$

This integral is known by various names including the Duhamel integral, the summation integral, and the convolution integral. It says that if we know the system impulse response, we can obtain the system response for any other type of input by performing the integration. This has profound implications for the modeling of concert halls and other spaces since the impulse response of a room can be modeled and the driving force can be music. Thus we can listen to the sound of a concert hall before it is built.

Response to a Step Function

If the shape of a force applied to a spring mass system consists of a constant force that is instantaneously applied, we can substitute the force time behavior, $f(t) = F_0$, into Eq. 11.40 along with the system response to obtain the response behavior. For an undamped spring mass system the result is

$$x(t) = \int_0^t \frac{F_0}{m \, \omega_n} \sin \omega_n (t - \tau) \, d\tau \qquad (11.41)$$

which is

$$x(t) = \frac{F_0}{k} (1 - \cos \omega_n t) \qquad (11.42)$$

FIGURE 11.26   **Response of a Damped System to a Unit Step Function (Thomson, 1965)**
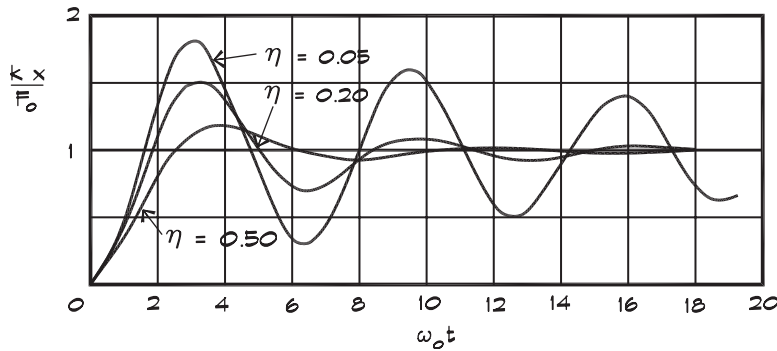
and for the damped system the result is (see Harris and Crede, 1961; or Thomson, 1965)

$$x = \frac{F_0}{k} \left[1 - \frac{e^{-\eta \omega_n t}}{\sqrt{1 - \eta^2}} \cos \left(\sqrt{1 - \eta^2} \, \omega_n t - \psi \right) \right] \quad (11.43)$$

where $\tan \psi = \dfrac{\eta}{\sqrt{1 - \eta^2}}$

Figure 11.26 shows the system response for a damped spring mass as a function of damping. When the damping is zero the maximum amplitude is twice the displacement that the system would experience if the load were applied slowly.

Vibrational Response of a Floor to Footfall

A footstep consists of two step functions, one when the load is applied and one when it is released. Ungar and White (1979) have modeled this behavior using a versed sine pulse in Fig. 11.27, and have calculated the envelope for the dynamic amplification, defined as the ratio of the maximum dynamic amplitude divided by the static deflection obtained under the load, F_m.

$$A_m = \frac{X_{max}}{X_{static}} = \frac{\sqrt{2 \left(1 + \cos 2 \pi f_n t_0 \right)}}{\left[1 - \left(2 f_n t_0 \right)^2 \right]} \quad (11.44)$$

FIGURE 11.27   **Idealized Footstep Force Pulse (Ungar and White, 1979)**
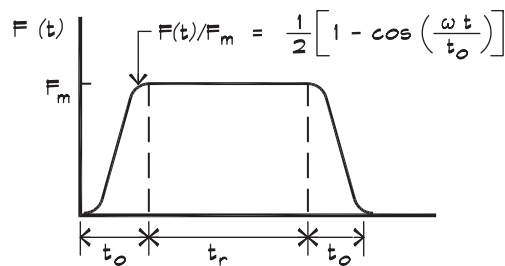
FIGURE 11.28   Maximum Dynamic Deflection Due to a Footstep Pulse (Ungar and White, 1979)
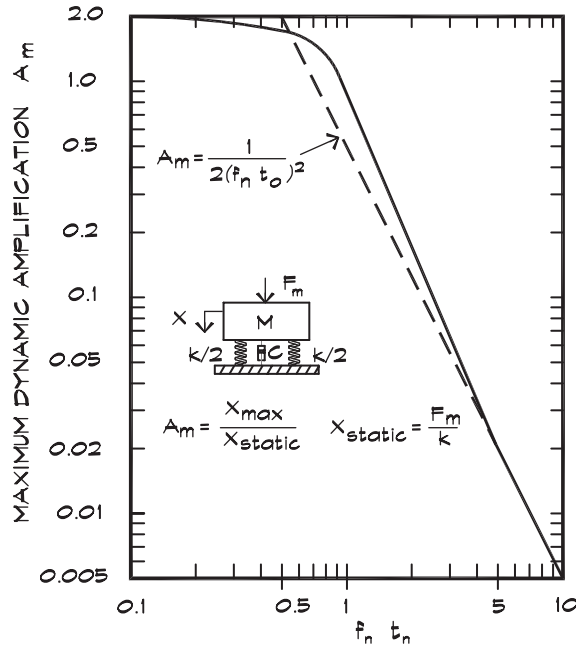
where $f_n = \dfrac{1}{2\pi}\sqrt{\dfrac{k}{m}}$ and t_0 is the rise time of the pulse. Note that k is the stiffness at the point where the footstep is taken. This equation does not give us the detailed behavior of the motion but gives us the envelope of the maximum deflection with resonant frequency, which is often sufficient for design purposes. For values of $f_n t_0$ that are small when compared to 1, the maximum dynamic amplification $A_m \cong 2$. For large values of $f_n t_0$, the amplification becomes $A_m \cong a / (2 f_n t_0)^2$, where a varies between 0 and 2, so that under these conditions $A_m \leq 1/\left[2 (f_n t_0)^2\right]$. Figure 11.28 gives a plot of the upper bound envelope for A_m. In Eq. 11.44 we note that the product $f_n t_0$ is equal to t_0 / t_n, the ratio of the pulse rise time to the natural period of floor vibration.

Figure 11.29 shows published data on footstep forces generated by a 150 lb (68 kg) male walker, and Fig. 11.30 shows the dependence of the rise time and force on walking speed. The figures allow us to estimate the maximum deflection of a floor system for various values of the resonant floor frequency.

While floors have a multitude of vibrational modes, the fundamental is usually the most important. It exhibits the lowest resonant frequency, is the most directly excitable structural motion, and has the softest (lowest impedance) point at its antinode. Some measured results are shown in Fig. 11.31 for a concrete I-beam structure. Although only two floor modes have been predicted, and floors are not pure undamped spring mass systems, the curve neatly bounds the remainder of the modes.

Control of Floor Vibrations

When it is desirable to control floor vibration for human comfort, it is important to limit the maximum amplitude as well as increase the damping. If the driving force is footfall, we

FIGURE 11.29   The Footstep Force Pulse Produced by a 150 lb (68 kg) Male Walker (Ungar and White, 1979)
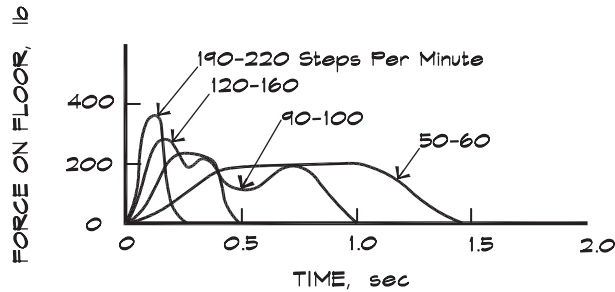
FIGURE 11.30   Dependence of the Maximum Force F and the Rise Time t of a Footstep Pulse on the Walking Speed (Ungar and White, 1979)
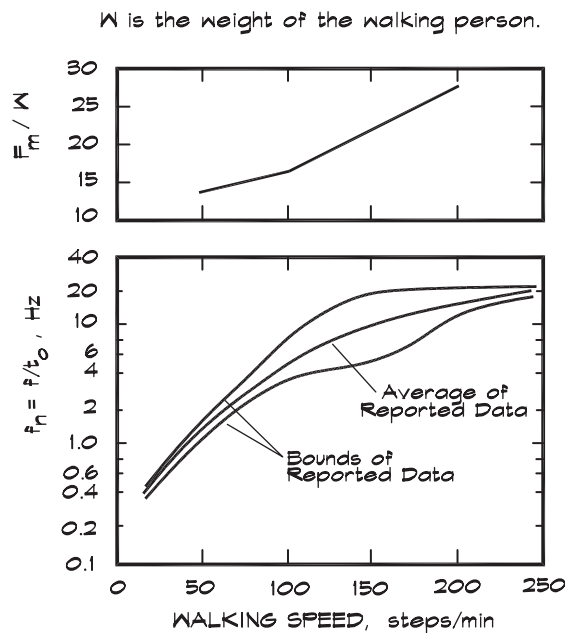
can use the amplification factor rise time t_0 to the natural period t_n of the structural mode. When the pulse rise time is a small fraction of the natural period we might expect a different behavior than for cases where the rise time is a large multiple of the period. This is illustrated in Fig. 11.28. From the graph it is reasonable to take the value of $f_n t_0 = 0.5$ as the dividing point between these two regions. From Fig. 11.29, the rise time for a typical rapid walker is about a tenth of a second, which means that the dividing point corresponds to a floor resonance of about 5 Hz. The fundamental resonances of most concrete floor systems fall into the region between 5 and 8 Hz, so that rapid walking on these structures corresponds to the region where $f_n t_0 \geq 0.5$. For this region,

$$x_{max} = F_m / 2 \, k \, (f_n \, t_0)^2 \cong 2 \, \pi^2 \, F_m \, M / t_0^{\;2} \, k^2 \qquad (11.45)$$

FIGURE 11.31   Footfall Response of a Concrete I-Beam Floor Structure (Ungar and White, 1979)

and
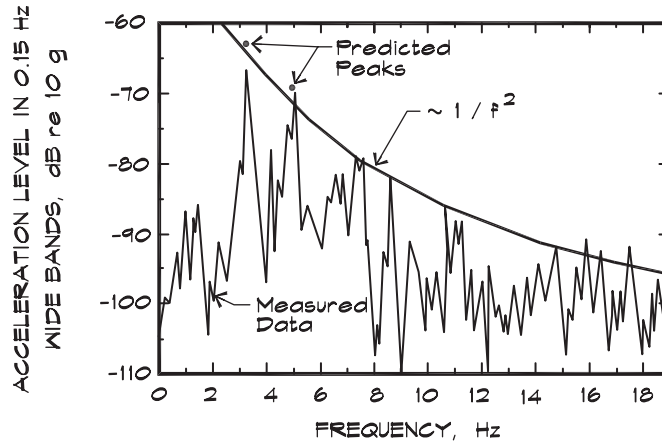
$$a_{max} \cong \left(2 \pi f_n\right)^2 x_{max} = 2 \pi^2 F_m / = t_0^2 k \qquad (11.46)$$

where a_{max} represents the maximum floor acceleration, k the local modal stiffness, and M the corresponding mass. It is clear that the structural stiffness is the most important component in decreasing both the maximum amplitude and the maximum acceleration. The floor mass does not appear in the equation for acceleration. The maximum displacement increases with mass, unless the mass increases the stiffness.

In the region where $f_n t_0 \leq 0.5$, which would correspond to a very long span floor, we find that

$$x_{max} \cong F_m / k \qquad (11.47)$$

and

$$a_{max} \cong \left(2 \pi f_n\right)^2 x_{max} = 2 F_m / M \qquad (11.48)$$

Here only the stiffness affects the maximum displacement and only the mass affects the maximum acceleration.

Allen and Swallow (1974) have addressed the design of concrete floors for vibration control. It is difficult to change the fundamental resonant frequency. A concrete floor might weigh 200,000 lbs (91,000 kg) and changing the gross physical properties requires major structural changes. Damping, however, is a factor that produces significant results and may be easier to control. These authors make the following preconstruction design considerations:

1. Cross bracing in steel structures has little effect (Moderow, 1970).
2. Noncomposite construction tends to increase damping by 1 to 2% over composite construction (Moderow, 1970).
3. Concrete added to the lower cord of the structural steel can increase damping of a completed floor by 2%.

4. Increasing the thickness of the concrete slab decreases the maximum amplitude and the natural frequency and increases the damping.

5. Cover plates on the joists increase the natural frequency and decrease amplitudes, due to the increased stiffness of the floor. When the data are plotted to determine human response it is found that the change moves downward with frequency, essentially paralleling the human response curve, so little is gained.

After construction, there are still some therapeutic measures available, principally to increase damping. Partitions are very effective in adding damping to an existing structure and can increase the overall damping to 14% of critical. Even lightweight low partitions, planter boxes, and the like can increase damping to 10% of critical. Partitions may be attached to a slab either above or below. Damping posts at critical locations can improve damping somewhat, but they may interfere with the decor. A dynamic absorber can be hung from a floor and can include a damper as part of the design. Allen and Swallow (1975) report that a mass damper tuned to 0.9 of the fundamental frequency and with 10% of critical damping reduced the floor amplitude by 50% and increased floor damping from 3 to 15% of critical. The added mass was 1 percent of the total floor mass.

NOISE TRANSMISSION
IN
FLOOR SYSTEMS

12.1   TYPES OF NOISE TRANSMISSION

The noise and vibration problems encountered in real floor-ceilings generally fall into four categories: airborne, footfall, structural deflection, and floor squeak. Each is a distinct class of problem with unique solutions.

Airborne Noise Isolation

Airborne noise isolation in floors follows the same principles and is tested in the same manner as airborne noise isolation in walls. STC tests are done by placing the noise source in the downstairs room to insure vibrational decoupling between the loudspeakers and the floor-ceiling system being tested.

   As was the case with wall transmission, the isolation of airborne noise such as speech is well characterized by the STC rating. The best floor systems combine a high-mass floor slab with a large separation between the floor and ceiling. The two panels should be vibrationally decoupled either by means of a separate structure or by a resilient support. At low frequencies a high structural stiffness is desirable, to minimize the floor deflection. In all cases at least 3" (75mm) of batt insulation should be placed in the air cavity and openings and joints must be sealed air tight.

Footfall

The act of walking across a floor generates noise due to two mechanisms: footfall and structural deflection. Footfall noise is created by the impact of a hard object, such as a heel, striking the surface of a floor. The heel is relatively lightweight and the noise associated with its fall is considered separately from the transfer of weight due to walking. Impact noise can be measured using a standard tapping machine as a source, which leads to an Impact Insulation Class (IIC) rating. The IIC test measures the reaction of a floor system to a series of small hammers dropped from a standard height. Although this may accurately characterize the noise of a heel tap against the floor surface, it does not measure the effect of loading and unloading under the full weight of a walker. Thus the achievement of a particular IIC rating in a given floor-ceiling system does not guarantee that footfall noise will not be a problem, or that the sound of walking will not be audible in the spaces below. The level of impact

noise in the receiving space is primarily dependent on the softness of the floor covering, and is best attenuated using a thick carpet and pad.

Structural Deflection

When a person walks or bounces up and down, a floor will deflect under the static and dynamic load of his weight. Under these conditions the floor acts like a large spring mass system, which responds to a periodic or impulsive force. If the underside of the moving structure is exposed to the room below, the low-frequency sound generated by the movement will radiate directly into the receiving space. Noise created by structural deflection sounds like low-frequency thumps similar to the sound of a very large bass drum, whereas footfall sounds like a high-frequency click. Noise associated with floor deflection is more difficult to correct than footfall noise since the joist system must be stiffened and damped and the ceiling must be physically decoupled from it. Where resilient ceiling supports are used to provide effective vibration isolation, their static deflection must be much greater than the potential structural deflection under the excitation force.

Squeak

Floor squeak is a phenomenon found in wood structures, which is most often caused by the rubbing of nails against wood framing members or metal hangers. It is high pitched and localized to the area around the point of contact. It can occur when there are gaps between the floor diaphragm and the supporting joists and when no glue has been used, or when joists are supported by metal hangers. It can also be exacerbated by the use of wood products having a high glue content, which do not allow the nail to grip the wood.

To control squeak all nonbedded nails (sometimes called shiners) that can rub against a joist or other wood or metal members should be removed and wood diaphragms should be glued to their supporting joists. Shiners must be removed before any concrete topping is poured. When the squeak originates at a joist hanger, it can be caused by inconsistencies in the joist size, and can be treated with small wood shims inserted between the joist and the hanger.

12.2   AIRBORNE NOISE TRANSMISSION

Concrete Floor Slabs

The transmission loss in thick, monolithic concrete floor slabs can be modeled by subtracting 6 dB from the mass law relationship previously developed. In thick panels the shear wave impedance is below the bending impedance so there is no coincidence effect. Typical examples of measured transmission loss data are given in Fig. 10.10. Because of the mass law, we quickly reach a point of diminishing returns if we wish to increase the transmission loss by thickening the slab. A thickness of 8 to 10 inches, which rates around an STC 58, is usually the practical limit for multistory buildings.

In order to achieve significantly higher STC ratings we must use double panel or other compound construction techniques. In many situations, a concrete floor slab is an excellent choice. Although it may not by itself provide an extremely high STC rating, it has many other advantages. Its low-frequency performance is excellent. If the spans are controlled it can be relatively stiff, and there are no squeak problems.

FIGURE 12.1 Transmission Loss of Metal Deck Floor-Ceilings (National Research Council Canada, 1966)

5" Thick Concrete Slab on Metal Decking (42 lbs/sq ft)
3/4" Fireproofing

125	160	200	250	315	400	500	630	800	1k	1.3k	1.6k	2k	2.5k	3.2k	4k	STC
34	37	38	38	39	41	42	50	54	55	54	54	54	56	60	65	50

5" Thick Concrete Slab on Metal Decking (42 lbs/sq ft)
3/4" Fireproofing
16" Airspace
5/8" Mineral Tile in T-Bar

125	160	200	250	315	400	500	630	800	1k	1.3k	1.6k	2k	2.5k	3.2k	4k	STC
41	47	50	52	53	53	52	62	67	71	72	75	75	76	77	78	60

5" Thick Concrete Slab on Metal Decking (42 lbs/sq ft)
16" Airspace
5/8" Gypsum Board on Resilient Channel
NIOSH, 1980

125	160	200	250	315	400	500	630	800	1k	1.3k	1.6k	2k	2.5k	3.2k	4k	STC
35	37	39	44	48	50	53	55	58	60	63	62	59	61	65	67	55

(PAC International, 2001)

3.5" Thick Concrete Slab on Metal Decking (39 lbs/sq ft)
9.6" Steel Joists at 24" O.C.
RSIC-1 Neoprene Clips Screwed to Joists at 24" O.C.
2 X 5/8" Gypsum Board on 7/8" Hat Channel
Riverbank, TL01-220

125	160	200	250	315	400	500	630	800	1k	1.3k	1.6k	2k	2.5k	3.2k	4k	STC
42	42	44	48	52	57	59	61	66	70	73	76	76	78	82	84	60

Concrete on Metal Pans

Concrete poured into a sheet metal pan supported on metal joists can deliver reasonable sound isolation if it is combined with a suspended drywall ceiling. Figure 12.1 gives several examples. The ceiling is supported from hanger wires at 4'-0" (1.2 m) on center that are tied to a 1.5" (38 mm) carrying channel (called black iron). A 7/8" (22 mm) thick hat channel is wire tied or clipped to the black iron and the gypsum board is screwed to it. STC ratings for this construction vary with the airspace depth and the softness of the ceiling support system. Since the slab is relatively stiff, good transmission loss values can be achieved using a neoprene mount, or a neoprene or spring hanger in the ceiling support wires.

Wood Floor Construction

Wood floor construction consists of separate floor and ceiling panels, which may be supported from the same joists or supported separately. Wood construction is lightweight and, if limited to short spans, relatively stiff, compared to long span concrete and steel floors. There is considerable damping in wood structures, so that vibrations do not propagate laterally as easily as in steel framing. Being lightweight, high transmission loss values are achieved only in compound, vibrationally isolated structures. The advantage of isolated construction is that it can approach ideal double panel performance if the floor and ceiling are sufficiently decoupled. Examples of lightweight wood and gypsum board floor-ceiling systems are shown in Fig. 12.2. In several of these the ceiling is attached directly to the underside of the wood joists, so the sound isolation ratings are relatively poor. In others the ceiling is mounted on resilient channels, which results in a modest improvement in STC rating. Resilient channel helps to provide a degree of vibration isolation between the joist system and the ceiling. The preferred type of channel is z-shaped rather than hat-shaped and can be attached only on one side. In order for a hat-shaped channel to be effective, one side of the flange and then the other must be alternately screwed to each joist. Both sides must never be screwed to the same joist. This is an important installation detail, which is rarely implemented correctly in the field, and renders the channel ineffective if not properly done. With all resilient channel, the length of the drywall screws must be controlled so that when the gypsum board is attached to the channel, the screws do not penetrate the joist and short out the isolation.

The third floor in Fig. 12.2 shows an example of adding mass to the underside of the diaphragm. This technique can be used to make improvements to existing construction. It has the advantage of adding mass without adding thickness to the diaphragm and consequently the coincidence frequency of the floor panel is not lowered. The addition of an extra layer of gypsum board on resilient channel over an existing layer is not effective due to the coupling through the air spring between the layers. Improvements of 1 dB or less are the usual result. In cases where there is an existing ceiling and substantial improvement is desired it is most effective to remove the ceiling drywall and add mass, batt insulation, and stepped blocking between the joists before resiliently supporting a double layer gypsum board ceiling.

Resiliently Supported Ceilings

Supporting ceilings on resilient mounts can increase the sound transmission class. Resilient channels are one such support system. Working as a spring isolator they rarely achieve a deflection of more than about 1/8" (3 mm). Thus they do not have the softness required to isolate noise due to structural deflection. They are, however, helpful in providing a degree of decoupling of airborne or footfall vibrations transmitted through the structure. In Fig. 12.2 we can see an example in the difference between constructions B and D in the second example.

Where a moderate degree of decoupling is desired, the ceiling can be suspended from neoprene mounts. These can be cut into the hanger wire or screwed directly to the support framing. Test ratings are included in Fig. 12.1 in the last example. This system has the advantage of being able to support multiple layers of drywall in critical applications.

If high STC ratings are desired the ceiling must be independently supported on a separate joist system or suspended from springs, having a deflection of one-inch (25 mm)

Figure 12.2 Transmission Loss of Floor-Ceilings (California Office of Noise Control, 1981)
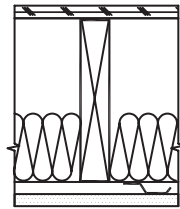
Double Layer Plywood – 1" Thick
2 x 10 Wood Joists
1 Layer 1/2" Gypsum Board
A – No Batt Insulation – No Resilient Channel
B – R-11 Batt Insulation – No Resilient Channel
C – No Insulation – With Resilient Channel
D – R-11 Batt Insulation – With Resilient Channel

	125	160	200	250	315	400	500	630	800	1K	1.3K	1.6K	2K	2.5K	3.2K	4K	STC
A	23	23	21	27	31	31	31	35	37	41	42	45	44	41	42	45	37
B	20	23	29	32	38	41	44	41	43	45	47	50	51	50	51	54	43
C	27	29	31	33	38	41	43	45	47	48	49	52	54	52	51	54	45
D	27	33	36	35	38	41	44	47	51	51	54	57	59	61	57	60	47
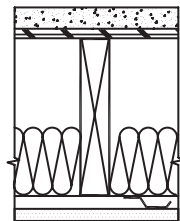
1 1/2" Lightweight Concrete (110 lbs/cu ft)
1 Layer 5/8" Plywood
2 x 10 Wood Joists
1 Layer 1/2" Gypsum Board
A – No R-11 Batt Insulation – No Resilient Channel
B – R-11 Batt Insulation – No Resilient Channel
C – No Insulation – With Resilient Channel
D – R-11 Batt Insulation – With Resilient Channel

	125	160	200	250	315	400	500	630	800	1K	1.3K	1.6K	2K	2.5K	3.2K	4K	STC
A	26	30	35	36	41	43	46	43	43	47	52	55	57	57	57	60	46
B	28	32	34	37	41	46	50	50	50	51	54	55	57	55	55	58	49
C	36	38	34	38	41	44	51	53	54	57	61	63	64	63	60	62	52
D	40	40	37	41	45	49	51	51	52	54	59	61	63	62	60	63	53
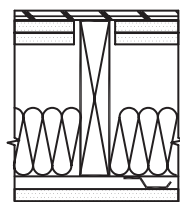
1 Layer 5/8" Plywood
2 x 5/8" Gypsum Board Screwed to the Subfloor
2 x 10 Wood Joists
1 Layer 5/8" Gypsum Board

A – R-11 Batt Insulation – With Resilient Channel

	125	160	200	250	315	400	500	630	800	1K	1.3K	1.6K	2K	2.5K	3.2K	4K	STC
A	37	40	44	46	51	51	54	56	57	58	63	63	62	58	59	61	56

or greater. In these cases the floor and ceiling panels begin to act separately and we gain the advantages of double panel construction, which were discussed in Chapt. 9. With a spring-supported ceiling the transmission loss behavior approaches, but does not reach, the ideal double panel values. In practice, with one-inch deflection isolators, transmission losses are approximately the simple sum of the mass law values above the mass-air-mass resonance or about 6 dB below the ideal behavior. Several examples are given in Fig. 12.3 for suspended gypsum ceilings.

FIGURE 12.3 Transmission Loss of Floors and Spring Supported Ceilings (Kinetics Corporation Test Data)

3/4" Thick Hardwood Flooring
3/4" Plywood
2 x 10 Wood Joists
R-11 Batt Insulation
1" Deflection Spring Isolators
2 Layers 5/8" Gypsum Board

125	160	200	250	315	400	500	630	800	1K	1.3K	1.6K	2K	2.5K	3.2K	4K	FSTC
42	39	38	40	44	42	47	48	51	53	55	54	56	59	67	66	51

1 1/2" Lightweight Concrete (110 lbs/cu ft)
1 Layer 5/8" Plywood
2 x 10 Wood Joists
R-11 Batt Insulation
1" Deflection Spring Isolators
2 Layers 5/8" Gypsum Board

125	160	200	250	315	400	500	630	800	1K	1.3K	1.6K	2K	2.5K	3.2K	4K	STC
50	56	58	59	62	70	74	79	84	86	90	94	97	100	100	95	73

6" Concrete Slab
R-11 Batt Insulation
1" Deflection Spring Isolators
2 Layers 5/8" Gypsum Board

125	160	200	250	315	400	500	630	800	1K	1.3K	1.6K	2K	2.5K	3.2K	4K	STC
63	64	66	72	73	83	84	86	91	92	96	104	104	105	105	105	84

A number of details are important to the successful installation of hanger-supported ceilings. When sheets of drywall are applied to a ceiling, supported from a series of springs, the weight due to each additional layer will cause the ceiling to drop. As it drops it is important that neither the drywall nor the hat or carrying channel above it rests on the side wall structure or gypsum board. If it does an uneven load distribution will result and the ceiling will bow. The ceiling should be free to move so that the isolators can work effectively. This is accomplished most easily by building the ceiling within the confines of the side wall finish material as in Fig. 12.4. Joints between the two may then be caulked and molding can be applied slightly below the finish ceiling.

The second detail has to do with the load carried by each spring hanger. Typically hangers are located at 4'-0" (1.2 m) on center so that each spring supports 16 sq. ft. (1.5 sq m) of ceiling material. For a ceiling constructed of double 5/8" (16 mm) drywall the total weight along with the support framing works out to be about 100 lbs (45 kg) per isolator. When a spring is located near a wall it may support as little as half the load of a center

FIGURE 12.4 Resiliently Suspended Ceiling Detail

Ceiling drywall and support
structure must be free of wall.
Caulk all gaps.
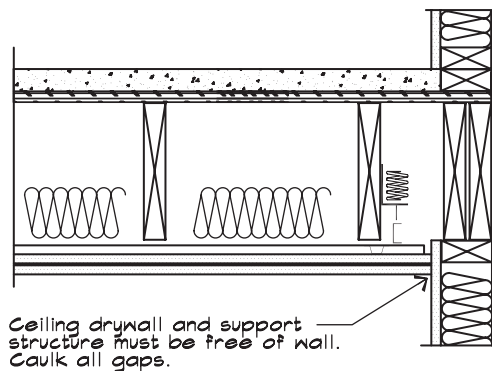
spring and when it is in a corner, as little as one-quarter. If a hanger supports a vertical portion of a soffit and therefore more than its normal load, the stiffness of each spring must be matched to the load it carries so that the deflection across the ceiling is uniform. This is done by calculating the load on each hanger and by having springs of varying stiffness (usually color-coded) available at the construction site to insert into a hanger. The deflection can also be adjusted by means of a threaded cap screw on top of each spring. This is often required in corner springs supporting more than a quarter load.

Floating Floors

Floating floors, which are resiliently supported panels located above the structural system, can be used to attenuate vertical as well as lateral noise and vibration transmission. They are usually heavier than resiliently hung ceilings and thus have the attendant advantages of mass. This is offset somewhat by the narrow air gap and low deflections inherent in the neoprene or pressed fiberglass isolators that normally are employed. Where low-deflection (< 0.1" or 3 mm) continuous support systems such as sheets of neoprene, pressed fiberglass board, pressed paper, or wire mesh materials are used, the degree of decoupling is much less, due to the low deflection as well as the additional stiffness attributable to the trapped air. Some of these materials can become overloaded and crush over time, further reducing their effectiveness. Any concrete, which flows into the space beneath the floating floor and shorts out the resilient support, also severely reduces its effectiveness.

Since the floating floor supports are acting as vibration isolators it is desirable to reduce their natural frequency by maximizing the static deflection under load. Consequently a grid of regularly spaced individual mounts is much more effective than a continuous material since the loading on each isolator is much greater.

Where very high transmission loss values are required, such as in the construction of sound studios, floating floors in combination with resiliently supported ceilings can yield very good results. Figure 12.5 shows an example of a continuous floor support system and two point-mounted floor systems. Note that the floating floor is most effective if it is heavy and point mounted. The weight is important for several reasons. First, it provides the additional mass for sound attenuation. Second, it yields good isolator deflection without softening the floating floor. A high stiffness in the floating floor is important since it should not deflect appreciably between the mounts. Lightweight floating floors, such as those used

FIGURE 12.5 Transmission Loss of Floating Floors (Kinetics Corporation Test Data)

1 1/2" Lightweight Concrete (110 lbs/cu ft)
5/8" Continuous Resilient Underlayerment
1 Layer 3/4" Wood Subfloor
2 x 10 Wood Joists
R-11 Batt Insulation
Resilient Channel
1 Layer 5/8" Gypsum Board

125	160	200	250	315	400	500	630	800	1K	1.3K	1.6K	2K	2.5K	3.2K	4K	FSTC
37	35	42	45	47	49	52	52	54	55	59	60	61	60	64	68	54

4" Concrete Slab (144 lbs/cu ft)
2" Thick Pressed Fiberglass Isolators at 16" on Center
R-11 Batt Insulation
6" Concrete Structural Slab (144 lbs/cu ft)

125	160	200	250	315	400	500	630	800	1K	1.3K	1.6K	2K	2.5K	3.2K	4K	STC
53	54	55	57	63	70	72	78	83	86	91	93	98	101	101	100	72

4" Concrete Slab (144 lbs/cu ft)
2" Thick Pressed Fiberglass Isolators at 16" on Center
R-11 Batt Insulation
6" Concrete Structural Slab (144 lbs/cu ft)
R-11 Batt Insulation
1" Deflection Spring Isolators
2 Layers 5/8" Gypsum Board

125	160	200	250	315	400	500	630	800	1K	1.3K	1.6K	2K	2.5K	3.2K	4K	STC
71	74	81	84	86	96	99	101	101	106	105	106	106	106	107	107	94

as gymnasium floors, tend to be springy and walkers can perceive a noticeable movement. Thus concrete floating floors are preferred for residential and studio applications.

12.3   FOOTFALL NOISE

Impact Insulation Class—IIC

The Impact Insulation Class (IIC) is a laboratory rating much like the Sound Transmission Class; however, it represents the isolation provided by a floor system subjected to a controlled impulsive load. Since there is no standard footstep, the impulsive loads are generated by a tapping machine pictured in Fig. 12.6. The machine consists of a frame supporting a row of five cylindrical hammers, each weighing a half-kilogram (1.1 lbs), which are raised by a cam mechanism and dropped sequentially from a height of 4 cm (1.6 in) onto the surface of the floor. The cam is driven by an electric motor that is set to deliver 10 impacts per second at equal intervals.

There are test standards in the United States and Europe that regulate the laboratory (ASTM E 492 and ISO 140/6) as well as field (ASTM E 1007 and ISO 140/7) test methodologies. The test is performed by placing the tapping machine near the center of the

FIGURE 12.6 Tapping Machine Showing Inner Workings

HAMMERS
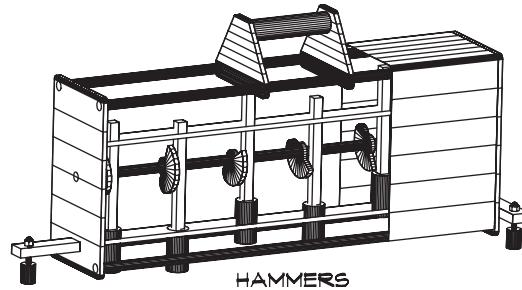
FIGURE 12.7 IIC Tapping Machine Positions
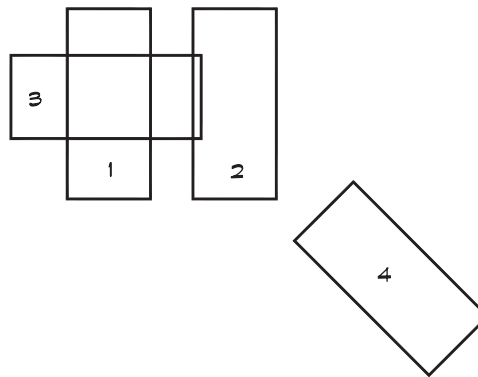
floor under test. Spatially averaged sound pressure levels are then measured in the room below in third-octave bands ranging from 100 through 3150 Hz. The readings are done for four specified tapping machine positions illustrated in Fig. 12.7. A normalized impact sound pressure level in the receiving room is then obtained from the spatial average sound pressure levels

$$L_n = \overline{L}_p - 10 \log (A_0 / R) \tag{12.1}$$

The absorption in the receiving room is measured either by using the reverberant field approximation (Eq. 12.2) and a source of known sound power, or by measuring the reverberation time, from which the total absorption is obtained using the Sabine equation.

$$\overline{L}_p \cong L_w + 10 \log (4 / R) + K \tag{12.2}$$

where $\overline{L}_p$ = average one - third octave sound pressure level measured in the receiving room (dB)

L_w = one - third octave sound power level of the reference source (dB)

R = sound absorption in the receiving room (m^2 or ft^2)

A_0 = reference absorption in the same units as R (either 10 metric sabins or 108 sabins)

K = 0.1 for SI units or 10.5 for FP units

FIGURE 12.8 Reference Contour for Calculating Impact Insulation Class and Other Ratings (ASTM E989, 1989)
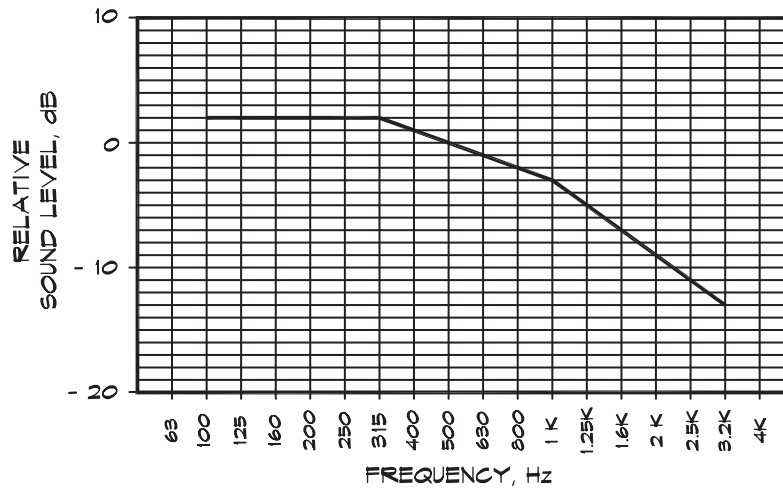
Note that $\overline{L}_p$ in Eq. 12.1 is measured using the tapping machine as the noise source, whereas in Eq. 12.2 a standard reference noise source such as a calibrated fan or loudspeaker is used.

Once the normalized levels have been obtained, they are compared to the standard IIC curve (ASTM E 989) in Fig. 12.8 by taking the deficiencies (differences) at each third-octave frequency band. The standard curve is shifted vertically relative to the test data until two conditions are fulfilled: 1) the sum of the deficiencies above the contour does not exceed 32 dB, and 2) the maximum deficiency at a single frequency band does not exceed 8 dB. Once these criteria are satisfied, the normalized sound pressure level at the intersection of the standard curve and the 500 Hz ordinate is subtracted from 110 to obtain the Impact Insulation Class. A typical example is given in Fig. 12.9.

Field tests of the IIC rating also may be carried out after a building has been constructed. These are designated FIIC, and like the FSTC tests fall about five points below the laboratory test for the same construction. They apply only to the room in which they are measured and are not generally applicable to a type of construction. Test standards set minimum limits on the volume of the receiving space at each third-octave frequency. Receiving rooms are required to meet minimum volume requirements such that there are at least 10 room modes at 125 Hz and the same modal spacing at 100 and 160 Hz. Minimum room volumes are 2100 cu ft (60 cu m) at 100 Hz, 1400 cu ft (40 cu m) at 125 Hz, and 800 cu ft (25 cu m) at 160 Hz. If room volumes fall below these limits the field report must include a notation to that effect.

The State of California has modified the standard FSTC and FIIC procedures to make them less strict by dropping the room constant term. In the revised code only the raw receiving levels are used to compute $L_n \cong \overline{L}_p$. Nonnormalized field tests generally produce ratings that are 3 to 5 dB higher than tests properly done, in accordance with the accepted ASTM standards. They yield an FIIC rating that is not normalized to the absorption in the receiving room and thus may vary from room to room or for the same room if the receiving space contains different amounts of furniture or other absorptive materials. Field tests made under these requirements are representative only of the rooms and conditions under which they

FIGURE 12.9 Calculation of an IIC Rating
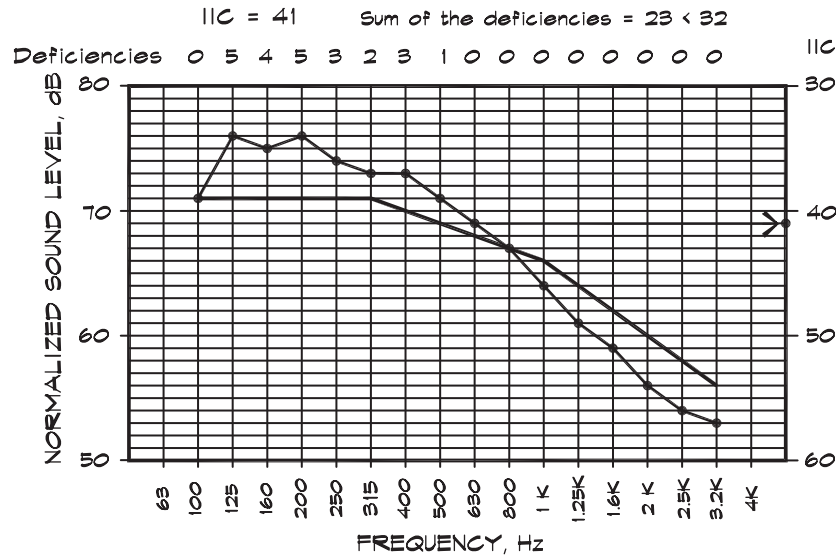
were measured and are not generally applicable to other rooms, even those having the same nominal construction.

Impact Insulation Class Ratings

The IIC rating reflects the softness of the floor covering including any resilient support system. IIC ratings are shown for various floor coverings in Fig. 12.10 for a concrete slab and in Figs. 12.11 and 12.12 for wood floor-ceiling systems. The Uniform Building Code (UBC) and the State of California set minimum standards of 50 IIC (laboratory) and 45 FIIC (field) ratings in multifamily dwellings. At this rating footfall noise from a person walking on a floor above is clearly audible, and it is possible to follow the progress of the walker around the room. Thus these building code standards do not represent good building practice. Rather they represent minimums below which it is illegal to build. It is only when the ratings are above an IIC 65 that heel clicks begin to become inaudible (Kopec, 1990).

Vibrationally Induced Noise

To construct a theoretical model of vibration transmitted through floor systems we can assume that a mechanical force is applied to one or more points on the floor, which induces a motion in the ceiling below. Clearly if the ceiling vibrates, an airborne sound will be radiated. Assuming that the ceiling is a flat plate moving vertically, the intensity near its surface is the same as that radiated by a plane wave.

$$W_{rad} = I \, S = \frac{p^2}{\rho_0 \, c_0} S \tag{12.3}$$

The radiated acoustic power can be written in terms of the surface velocity and a radiation efficiency, which is an empirical constant expressing the ratio of the actual power emitted

FIGURE 12.10 Impact Insulation Class of Concrete Floors (Kinetics Corporation Test Data)
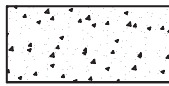
6" Concrete Slab (144 lbs/cu ft)
A 1/2" Wood Fiber Board glued to Concrete
   44 oz Carpet on 40 oz Pad
B No Floor Covering

	100	125	160	200	250	315	400	500	630	800	1K	1.3K	1.6K	2K	2.5K	3.2K	IIC
A	39	36	34	28	29	29	25	18	14	11	0	0	0	0	0	0	81
B	62	63	67	73	71	74	73	74	74	75	74	74	73	73	73	72	28
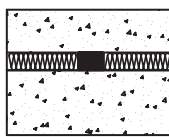
4" Concrete Slab (144 lbs/cu ft)
2" Thick Pressed Fiberglass Isolators at 16" on Center
R-11 Batt Insulation
6" Concrete Structural Slab (144 lbs/cu ft)
R-11 Batt Insulation
No Floor Covering

100	125	160	200	250	315	400	500	630	800	1K	1.3K	1.6K	2K	2.5K	3.2K	IIC
50	52	53	60	58	52	48	47	46	45	45	41	40	41	34	36	60
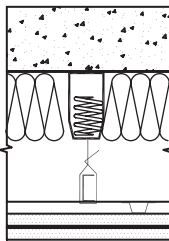
6" Concrete Structural Slab (144 lbs/cu ft)
R-11 Batt Insulation
1" Deflection Spring Isolators
2 Layers 5/8" Gypsum Board
No Floor Covering

100	125	160	200	250	315	400	500	630	800	1K	1.3K	1.6K	2K	2.5K	3.2K	IIC
42	42	43	44	41	45	37	39	38	39	41	36	29	29	32	30	70
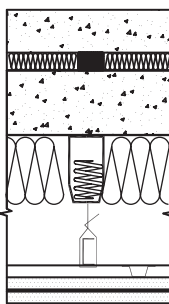
4" Concrete Slab (144 lbs/cu ft)
2" Thick Pressed Fiberglass Isolators at 16" on Center
R-11 Batt Insulation
6" Concrete Structural Slab (144 lbs/cu ft)
R-11 Batt Insulation
1" Deflection Spring Isolators
2 Layers 5/8" Gypsum Board
No Floor Covering

100	125	160	200	250	315	400	500	630	800	1K	1.3K	1.6K	2K	2.5K	3.2K	IIC
38	37	27	27	27	26	24	16	15	13	12	13	7	4	4	4	82

by a source compared with that emitted by an ideal radiating surface.

$$W_{rad} = \sigma \, u^2 \, \rho_0 \, c_0 \, S \tag{12.4}$$

where W_{rad} = radiated sound power, (W)
   σ = radiation efficiency (usually ≤ 1)
   u = rms velocity of the radiating surface, (m / s)

FIGURE 12.11 Impact Insulation Class of Wood Framed Floors (California Office of Noise Control, 1981)
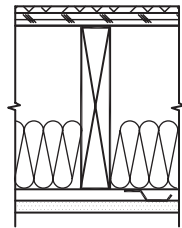
1/4" Particle Board Glued
5/8" Plywood Glued and Nailed
2 x 10 Wood Joists
R-11 Batt Insulation
1 Layer 1/2" Gypsum Board on Resilient Channel
A - 76 oz Carpet on 50 oz Hair Pad
B - 65 oz Carpet on 30 oz Foam Rubber Pad
C - 50 oz Carpet on 24 oz Hair Pad
D - Cushioned Vinyl Tile
E - 1/16" Vinyl Asbestos Tile
F - 1/2" Wood Parquet Flooring
G - No Floor Covering

	100	125	160	200	250	315	400	500	630	800	1K	1.3K	1.6K	2K	2.5K	3.2K	IIC
A	50	43	42	37	34	34	33	30	31	31	32	29	0	0	0	0	70
B	49	42	39	35	34	32	32	28	28	29	29	0	0	0	0	0	71
C	62	57	56	52	47	42	38	33	34	34	34	32	0	0	0	0	58
D	68	66	68	67	65	61	53	47	45	44	41	37	33	34	0	0	51
E	69	65	69	69	69	69	67	65	64	64	60	56	50	48	48	48	47
F	65	64	64	65	64	63	63	60	60	59	57	55	49	45	45	49	50
G	66	64	68	67	66	67	65	62	62	61	58	54	49	47	46	47	49
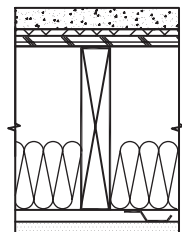
1 5/8" Lightweight Concrete (110 lbs/cu ft)
1/4" Particle Board Glued to Plywood
5/8" Plywood Glued and Nailed to Joists
2 x 10 Wood Joists
R-11 Batt Insulation
1 Layer 1/2" Gypsum Board on Resilient Channel
A - 76 oz Carpet on 50 oz Hair Pad
B - 65 oz Carpet on 30 oz Foam Rubber Pad
C - 50 oz Carpet on 24 oz Hair Pad
D - Cushioned Vinyl Tile
E - 1/16" Vinyl Asbestos Tile
F - 1/2" Wood Parquet Flooring
G - No Floor Covering

	100	125	160	200	250	315	400	500	630	800	1K	1.3K	1.6K	2K	2.5K	3.2K	IIC
A	47	42	39	34	34	29	30	26	25	27	28	23	22	21	0	0	73
B	44	38	35	31	32	27	28	24	24	25	27	22	19	19	0	0	76
C	56	54	50	46	43	37	35	31	30	31	32	29	0	0	0	0	64
D	64	61	62	60	58	52	48	40	36	37	39	34	33	34	0	0	56
E	62	59	60	60	61	60	62	62	62	65	66	64	62	60	60	55	43
F	64	61	63	63	63	60	61	60	59	58	55	50	46	42	40	40	52
G	62	61	60	60	61	59	62	63	63	65	66	65	62	61	61	62	38

ρ_0 = density of air, (kg/m^3)
c_0 = speed of sound in air, (m/s)
S = area of the radiating surface, (m^2)

Radiation efficiencies are helpful in describing the process since real sources do not move in a perfectly planar manner and are not infinite. Sound radiation by heavy thick materials such as brick or concrete, where shear waves predominate at high frequencies, usually can be

FIGURE 12.12   Impact Insulation Class of Floors with Resiliently Supported Ceilings

(Kinetics Corporation Test Data)

1 1/2" (40 mm) Lightweight Concrete
(12.8 lbs/sq ft or 63.4 kg/sq m)
1 Layer 5/8" (16 mm) Plywood
2 × 10 (240 mm) Wood Joists
R-11 Batt Insulation
1" (25 mm) Deflection Spring Isolators
2 Layers 5/8" (16 mm) Gypsum Board
A - Carpet on 3/8" (10 mm) Hair Pad
B - 5/16" (8 mm) Parquet Flooring

	100	125	160	200	250	315	400	500	630	800	1K	1.3K	1.6K	2K	2.5K	3.2K	IIC
A	31	29	27	22	19	16	14	10	10	6	6	5	6	7	7	9	89
B	56	56	53	53	55	54	50	48	46	44	43	40	36	34	31	24	62

(PAC International Test Data)

1/4" (13 mm) Ceramic Tile
1" (25 mm) Lightweight Concrete
(130 lb/cu ft or 2,083 kg/cu m)
1 Layer 3/4" (18 mm) Plywood
18" (457 mm) Truss Wood Joist
R-11 Batt Insulation
RSIC-1 Isolation Clips with 7/8" (22 mm) Hat Channel
2 Layers 5/8" (16 mm) Gypsum Board
A - As Shown
B - 3/8" (10 mm) Carpet on 3/8" (10 mm) Pad on Tile
     with 1 × 5/8" (16 mm) Gypsum Board Ceiling

	100	125	160	200	250	315	400	500	630	800	1K	1.3K	1.6K	2K	2.5K	3.2K	IIC
A	64	55	57	57	54	52	53	54	57	55	53	51	50	52	50	45	53
B	46	32	32	28	28	29	22	13	9	8	8	5	5	5	4	4	74

assumed to have a radiation efficiency of one. If bending waves are part of the transmission mechanism they result in a pronounced increase in the radiation efficiency around the critical frequency and a decrease below it, as shown in Fig. 12.13. For finite-sized panels there are also contributions due to edge effects, so that there are additional terms contributing to Eq. 12.4.

Mechanical Impedance of a Spring Mass System

A vibrationally driven system such as a floor can be analyzed in terms of its mechanical impedance, which is the ratio of an applied force to the induced velocity. This is somewhat different from the specific acoustic impedance in which the force was expressed as a pressure. The mechanical or driving point impedance is given by

$$\mathbf{z}_m = \frac{\mathbf{F}}{\mathbf{u}} \tag{12.5}$$

The model of vibrational point excitation of structures is analogous to the use of point sources in the study of sound propagation. They allow us to deal with complex force distributions by integrating (summing) over a distribution of point forces. Point impedances can be measured

FIGURE 12.13 Design Curve for Approximating the Radiation Efficiency (Beranek, 1971)

Design curve for a finite panel having perimeter P and area S with simply supported or clamped edges. (Note that $\lambda_c = c/f_c$ = wavelength in the panel or in air at the critical frequency.)
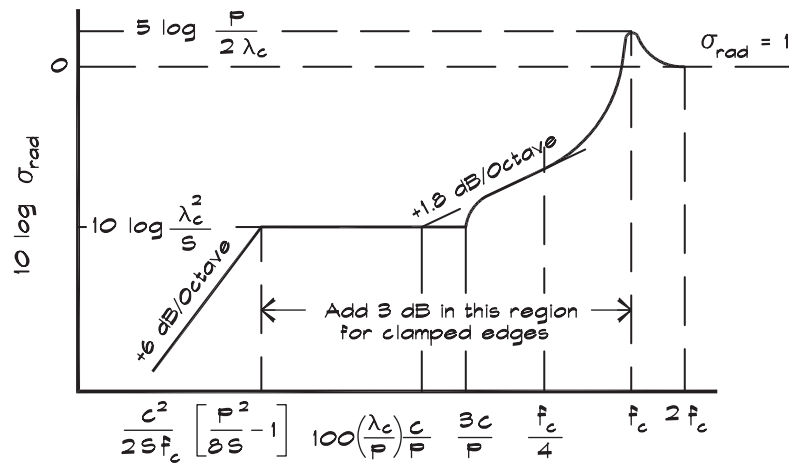
in the laboratory under controlled conditions and are a useful tool in characterizing complex systems.

If a force is applied to a simple spring mass system the mechanical impedance is the sum of the impedances of the individual components, namely the mass, spring, and damping.

$$\mathbf{z}_\mathrm{m} = c + j\,\omega\,m + \frac{k}{j\,\omega} \qquad (12.6)$$

Note that at resonance the mechanical impedance is zero, since a large velocity is produced by a very small force. If we set the impedance to zero and solve Eq. 12.6 for the resonant frequency, we get Eq. 6.4 for zero damping.

For a sinusoidal force $\mathbf{F} = F_0\,e^{j\,\omega t}$ applied to a spring-mass system, the induced velocity is

$$\mathbf{u} = \frac{F_0\,e^{j\,\omega t}}{\mathbf{z}_\mathrm{m}} = \frac{F_0\,e^{j\,\omega t}}{c + j\,\omega\,m + \dfrac{k}{j\,\omega}} \qquad (12.7)$$

It is clear that for low induced velocities we want high mass, high stiffness, and high damping. Although floors are not pure spring-mass systems, the model is a helpful analogy. An examination of Eq. 12.7 reveals that at high frequencies the mass and damping terms predominate, while at very low frequencies the stiffness and damping terms are more important.

In a generalized system having a complex impedance the power is

$$W = \frac{\omega}{2\pi} \int_0^{2\pi/\omega} \mathbf{F}(t)\, \mathbf{u}(t)\, dt = \frac{1}{2} \left| F_0 \right| \left| u_0 \right| \cos\phi \qquad (12.8)$$

so

$$W = \frac{1}{2} \left| F_0 \right|^2 \mathrm{Re} \left\{ \frac{1}{\mathbf{z}_m} \right\} = \frac{1}{2} \left| u_0 \right|^2 \mathrm{Re} \left\{ \mathbf{z}_m \right\} \qquad (12.9)$$

where F_0 is the peak force amplitude, u_0 is the peak velocity amplitude, and ϕ is the relative phase between the force and the velocity. The bracketed terms are the real parts of the complex impedance or its reciprocal. If a sinusoidal force is applied to a spring mass system the steady state energy is dissipated in the dashpot. The dashpot impedance c is real and the velocity of the mass is in phase with the resistance force. The power expended is

$$W = \frac{\left| F_0^2 \right|}{2\,c} \qquad (12.10)$$

Spring mass models are useful abstractions when the structural wavelengths are large compared to the dimensions of the system (Ver, 1992). When the wavelengths are small compared to the dimensions of the floor, we use another approximation, the driving point impedance. In this model we assume that the panel is infinite so we can ignore the reflection of structural waves from the plate boundaries. We then use the infinite plate model to approximate the result for a finite structure.

Driving Point Impedance

The driving point impedance of a structural system can be measured directly or calculated from its mass and bending stiffness. This exercise has been carried out by a number of authors. Results have been published by Cremer (1973), Pinnington (1988), and Beranek and Ver (1992). The structural configuration that is generally of the greatest interest in architectural acoustics is a flat plate. The point impedance of an infinite thin plate in bending is

$$z_m = 8 \sqrt{D\, \rho_m\, h} \cong 2.3\, c_L\, \rho_m\, h^2 \qquad (12.11)$$

where D = flexural rigidity per unit length = $\dfrac{E\, h^3}{12\,(1 - \mu^2)}$ (N m)

$\quad \rho_m$ = density of the plate (kg / m^3)

$\quad c_L$ = longitudinal sound velocity in the plate = $\sqrt{\dfrac{E}{\rho_m}}$ (m / s)

$\quad h$ = plate thickness (m)

$\quad \mu$ = Poisson's ratio $\cong 0.3$

$\quad E$ = Young's modulus (N / m^2)

Cremer (1973, pp. 260–264) gives the derivation of this relationship.

Power Transmitted through a Plate

For vibrational energy transmitted into and out of a plate, there is an energy balance whereby the energy entering the plate is either dissipated within the plate or radiated away as sound.

$$W_{in} = W_{dis} + W_{rad} \tag{12.12}$$

There are several possible energy dissipation mechanisms. The energy may be transmitted away as a bending wave in an infinite plate, or in a finite plate it may end up exciting the normal modes of vibration, which decay out due to internal losses. In both cases we can assume there is internal damping, which attenuates energy by some amount over time.

$$E_{dis}(t) = E_0 \left(1 - e^{-\eta \omega t}\right) \tag{12.13}$$

where $E_{dis}(t)$ = energy dissipated as a function of time (W)

E_0 = initial vibrational energy (W)

η = damping constant
ω = radial frequency (s^{-1})
t = time (s)

We can calculate the energy lost in one period ($T = 2\pi / \omega$) assuming a damping constant much less than one

$$E_{dis} \cong 2\pi\,\eta\,E_0 \tag{12.14}$$

Now we examine a small element of plate, which is vibrating. The initial energy in that element is

$$E_0 = \frac{1}{2}\rho_s\,u_0^2\,dx\,dz \tag{12.15}$$

where $\rho_s = \rho_m h$ is the surface density of the plate. Dividing the energy by the period $T = 1 / f$, we obtain the energy dissipated per unit time

$$E_{dis} = \frac{1}{2}\,\omega\,\eta\,\rho_s\,u_0^2\,dx\,dz \tag{12.16}$$

so the power converted to heat for a total plate area S is

$$W_{dis} = \frac{1}{2}\,\omega\,\eta \int_S \rho_s\,u_0^2\,dx\,dz = \frac{1}{2}\,\omega\,\eta\,\rho_s\,S\,u_0^2 \tag{12.17}$$

Therefore the power balance equation can be written as

$$\frac{1}{2}\,F_0^2\,Re\left\{\frac{1}{\mathbf{z}_m}\right\} = u^2\,S\left[\omega\,\eta\,\rho_s + 2\,\rho_0\,c_0\,\sigma\right] \tag{12.18}$$

and using the mechanical impedance given in Eq. 12.11, the mean square velocity in a thin infinite plate that results from an imposed force having an amplitude F_0 is

$$u^2 = \frac{F_0^2}{4.6\,\rho_S^2\,c_L\,h\,\omega\,\eta\,S\,(1 + 2\,\rho_0\,c_0\,\sigma/\omega\,\eta\,\rho_s)} \tag{12.19}$$

When $\omega \eta \rho_s \gg 2 \rho_0 c_0 \sigma$, Eq. 12.19 simplifies to

$$u^2 \cong \frac{F_0^2}{4.6 \, \rho_S^2 \, c_L \, h \, \omega \, \eta \, S} \tag{12.20}$$

Thus the transmission mechanism for impact noise in a thin plate is primarily due to bending waves.

Impact Generated Noise

When a standard tapping machine is used to test the Impact Insulation Class of a floor, a series of blows is created by releasing hammers timed to fall on the floor 10 times per second. This generates a train of force pulses that can be analyzed in terms of a Fourier series (Ver, 1971). The reason we use this methodology is that we wish to be able to calculate noise generated in each frequency band and thus we must determine the vibrational frequency spectrum of the exciting force. The Fourier series describes any repeated wave form using an infinite sum having the form

$$F(t) = \sum_{n=1}^{\infty} F_n \cos(n \, \omega \, t) \tag{12.21}$$

where the amplitudes are given by

$$F_n = \frac{2}{T_r} \int_0^{T_r} f(t) \cos\left(\frac{2 \pi n}{T_r} t\right) dt \tag{12.22}$$

and $f(t)$ is the shape of a typical force pulse, T_r is the time period between hammer blows, and $n = 1, 2, 3 \ldots$ The duration of the force impulse for a hard concrete slab is small compared to the period of the highest frequency of interest. Thus the term

$$\cos\left(\frac{2 \pi n}{T_r} t\right) \cong 1 \tag{12.23}$$

and the Fourier amplitude of the pulse train can be simplified to

$$F_n \cong \frac{2}{T_r} \int_0^{T_r} f(t) \, dt = 2 \, f_r \, m \, v_0 = 2 \, f_r \, m \, \sqrt{2 \, g \, d} \tag{12.24}$$

where f_r = repetition frequency, (Hz)
   m = mass of the hammer, (kg)
   v_0 = velocity of the hammer at impact, (m / s)
   d = drop distance, (m)
   g = gravitational acceleration (9.8 m / s^2)

Figure 12.14 shows a pulse train and its spectrum. The frequency spectrum is a series of lines of the same length that are separated by the frequency interval f_r.

FIGURE 12.14 Time Dependence and Frequency Spectrum of Tapping Machine Noise (Cremer and Heckl, 1973)
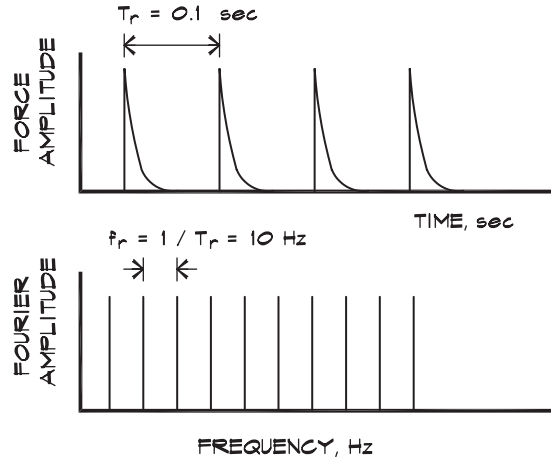
This relationship holds for ideal impacts. For real impacts, which have a finite duration, the length of the lines decreases slowly at high frequencies (Lange, 1953).

To determine the force spectrum at a given frequency, we define a mean square force spectrum density, S_f, which when multiplied by the bandwidth yields the mean square force in the same bandwidth (Ver, 1971 and Cremer, 1973)

$$S_f = \frac{1}{2} T_r F_n^2 = 4 f_r m^2 g d \quad (N^2 / Hz) \tag{12.25}$$

For a standard tapping machine the value of S_f can be calculated from the fixed mass, the drop frequency, and the drop distance to be 4 N^2 / Hz. The mean square force in a standard octave band is the spectrum density times the octave bandwidth or

$$F_{rms}^2 \, (oct) = 4 \frac{f}{\sqrt{2}} \quad (N^2) \tag{12.26}$$

Using Eqs. 12.3 and 12.18 we can calculate the sound power level generated by a tapping machine in a given frequency range

$$L_w \, (oct) = 10 \log \left(\frac{\rho_0 \, c_0 \, \sigma_{rad}}{5.1 \, \rho_m^2 \, c_L \, \eta \, h^3} \right) + 120 \tag{12.27}$$

and using Eqs. 12.1 and 8.83, the normalized impact sound level in each octave band is

$$L_n \, (oct) = 10 \log \left(\frac{4}{5.1} \frac{(\rho_0 \, c_0)^2 \, \sigma_{rad}}{p_{ref}^2 \, A_0 \, \rho_m^2 \, c_L \, \eta \, h^3} \right) \tag{12.28}$$

where $p_{ref} = 2 \times 10^{-5} \, (N / m^2) = 0.0002 \, \mu$ bar. Note that in Eq. 12.28, the transmitted sound level follows the normal mass law, increasing 6 dB per doubling of density; however, it decreases 9 dB per doubling of slab thickness. The normalized level, L_n, decreases with

increasing damping and is independent of the frequency, as long as the radiation efficiency and damping are frequency independent. To calculate the spatial average diffuse field sound level in the room below the tapping machine we use

$$\overline{L}_p = L_n \text{ (oct)} + 10 \log \frac{A_o}{S\overline{\alpha}} \tag{12.29}$$

To estimate the sound levels radiated by structural concrete or lightweight concrete floors we can use the material constants for the propagation speed of longitudinal waves and the characteristic density, which are: 1) for dense concrete $\rho_m = 2.3 \times 10^3$ (kg / m^3) and $c_L = 3.4 \times 10^3$ (m/s), and 2) for lightweight concrete $\rho_m = 6 \times 10^2$ (kg/m^3) and $c_L = 1.7 \times 10^3$ (m/s). Using these constants the expected levels for dense concrete are

$$L_n \text{ (oct)} = 32.5 - 30 \log h_m + 10 \log (\sigma_{rad} / \eta) \tag{12.30}$$

or

$$L_n \text{ (oct)} = 80.5 - 30 \log h_{in} + 10 \log (\sigma_{rad} / \eta) \tag{12.31}$$

and for lightweight concrete

$$L_n \text{ (oct)} = 47 - 30 \log h_m + 10 \log (\sigma_{rad} / \eta) \tag{12.32}$$

or

$$L_n \text{ (oct)} = 95 - 30 \log h_{in} + 10 \log (\sigma_{rad} / \eta) \tag{12.33}$$

where h_m is the thickness of the floor slab in meters and h_{in} is the thickness in inches.

Ver (1971) published a plot of the calculated levels, which is reproduced as Fig. 12.15. The quantity $L_n \text{ (oct)} + 10 \log (\eta/\sigma_{rad})$ is shown on the left-hand scale as a function of slab thickness. On the right-hand scale $L_n \text{ (oct)}$ is given for the typical values, $\eta = 0.01$

FIGURE 12.15   Normalized Impact Sound Level as a Function of Slab Thickness for Lightweight and Dense Concrete Floor Slabs (Ver, 1971)
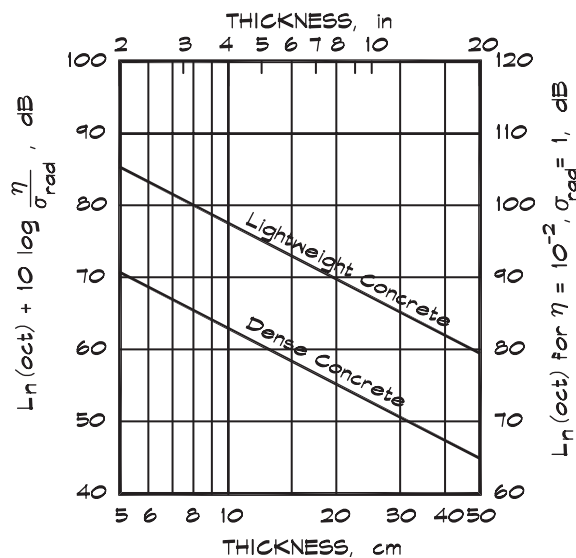
FIGURE 12.16   Forces and Velocities for Soft Floor Covering (Ver, 1971)
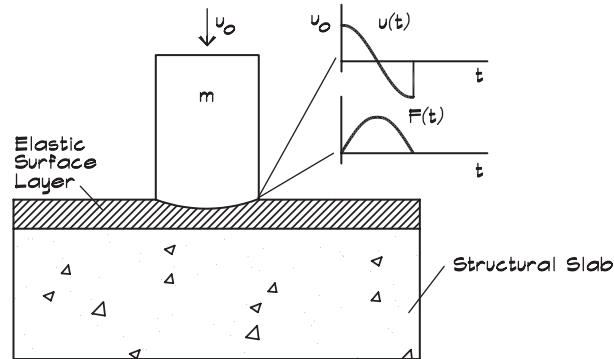
and $\sigma_{rad} = 1$. If we assume a 15 cm (6 in) dense concrete slab and use the figure, we get about 78 dB, and for a lightweight concrete structure of the same thickness we get about 92 dB with no surface covering. Human heel drops are not this loud, but the numbers are close to the measured levels for a tapping machine test (Fig. 12.18). Since it is usually impractical to increase the slab thickness and density enough to make a significant change, we turn to the floor surface covering for improvement.

Improvement Due to Soft Surfaces

Ver (1971) and Cremer (1973) have analyzed the impact of a carpet or other similar elastic surfaces on tapping machine noise transmitted through a floor. An illustration of Ver's model is given in Fig. 12.16.

The falling weight strikes a surface, whose stiffness is the elasticity of the carpet. In this model damping is ignored and the weight is assumed to strike the surface and recoil elastically once without multiple bounces. The equation of motion of the spring mass system is

$$m\,\frac{d^2 x}{d\,t^2} - k\,x = 0 \tag{12.34}$$

and

$$m\,\frac{d\,u}{d\,t} + \frac{k}{j\,\omega_0}u = 0 \tag{12.35}$$

where the natural frequency of the spring mass system is

$$\omega_n = \sqrt{\frac{k}{m}} \tag{12.36}$$

The spring constant is given by

$$k = \frac{E_d\,S_h}{h} \tag{12.37}$$

where E_d = dynamic Young's modulus of elasticity (N/m^2)
   which is about twice the static modulus
S_h = area of the striking surface of the hammer = 0.0007 m^2
h = thickness of the elastic layer (m)
m = mass of the hammer = 0.5 kg

When the hammer is dropped it strikes the elastic layer with a velocity u_0 at time $t = 0$ and its subsequent motion can be calculated from Eq. 12.34 to be

$$u(t) = u_0 \cos(\omega_n t) \qquad \text{for } 0 < t < \pi/\omega_n \tag{12.38}$$

and

$$u(t) = 0 \qquad \text{for } t < 0 \text{ and } t > \pi/\omega_n \tag{12.39}$$

Figure 12.16 also shows this velocity function. The force is given by

$$F(t) = m\frac{du}{dt} = u_0 \omega_n m \sin(\omega_n t) \quad \text{for } 0 < t < \pi/\omega_n \tag{12.40}$$

$$F(t) = 0 \qquad \text{for } t < 0 \text{ and } t > \pi/\omega_n \tag{12.41}$$

Now the Fourier amplitude of the tapping machine pulse train as given in Eq. 12.22

$$F_n' = 2 f_r \int_0^{1/(2 f_0)} u_0 \, 2\pi f_0 \, m \sin(2\pi f_0 t) \cos(2\pi n f_r t) \, dt \tag{12.42}$$

where $n = 1, 2, 3, \ldots$ This yields the force coefficients of the Fourier series

$$F_n' = F_n \frac{\pi}{4}\left(\frac{\sin\alpha}{\alpha} + \frac{\sin\beta}{\beta}\right) \tag{12.43}$$

in terms of the coefficients given in Eq. 12.43 and

$$\alpha = \frac{\pi}{2}\left(1 - n\frac{f_r}{f_0}\right) \quad \text{and} \quad \beta = \frac{\pi}{2}\left(1 + n\frac{f_r}{f_0}\right) \tag{12.44}$$

The improvement due to the elastic surface in the impact noise isolation is given in terms of a level

$$\Delta L_n = 20 \log \frac{F_n}{F_n'} = 20 \log\left(\frac{4/\pi}{\sin\alpha/\alpha + \sin\beta/\beta}\right) \tag{12.45}$$

which is shown graphically in Fig. 12.17.

Note that in this model we have ignored the contribution of the floor impedance and have assumed that it is very stiff compared with the elastic covering. At very low frequencies—that is, below the spring mass resonance—the improvement due the covering is zero. Above this frequency the surface covering becomes quite effective, giving a 12 dB per

FIGURE 12.17 Improvement in Impact Noise Isolation by an Elastic Surface (Ver, 1971)
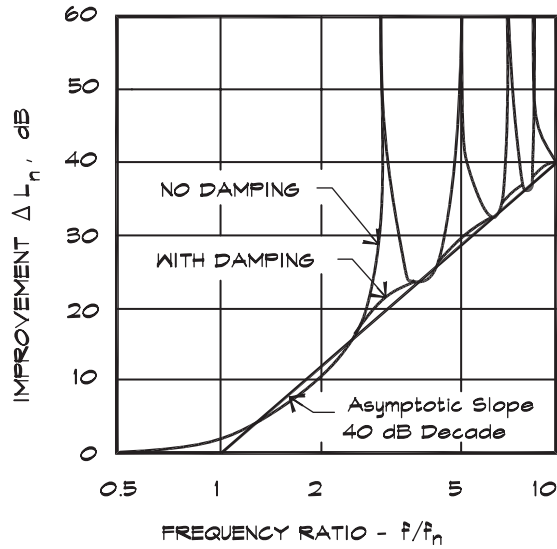
octave attenuation. The resonant peaks, which occur at odd multiples of the fundamental resonance, are diminished in actual field conditions by the damping in the surface treatment.

The normalized impact sound level for composite floor systems is given by

$$L_{n\ comp} = L_{n\ bare} - \Delta L_n \tag{12.46}$$

which is shown in Fig. 12.18 and compared with measured data. Note that while carpet and other elastic surface treatments improve the high-frequency loss for tapping noise, they

FIGURE 12.18 Calculated and Measured Impact Noise Levels

Footfall noise level under a 12 cm thick concrete floor with various floor coverings   (Measured data by Cremer and Heckl, 1973)
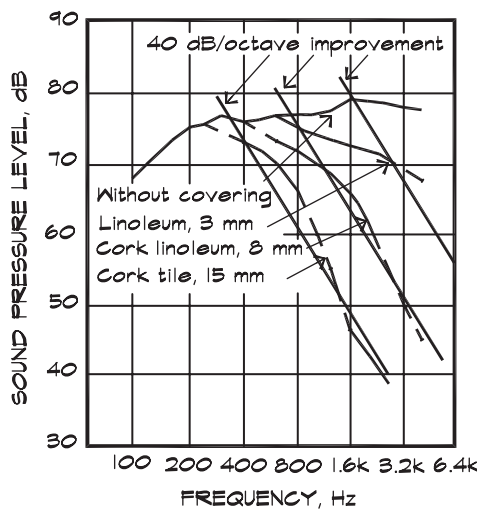
do not change the low-frequency transmission due to the weight of the walker, which is controlled by the stiffness and damping of the structural system. Likewise, they have little effect on the sound transmission loss of the structure since they do not alter the mass or stiffness of the floor system.

Improvement Due to Locally Reacting Floating Floors

A number of systems have been developed to provide noise and vibration isolation through the use of resilient floor or ceiling supports. These include continuous and point-supported floating floors, which are built on top of the structural floor system, as well as resiliently hung or separately supported ceilings. Each of these systems can provide improved isolation for footfall noise and some for walking noise, which as we will see, will depend on the softness of the mounts.

A locally reacting floating floor is one in which the influence of the initial force impulse is confined to the region around the point of impact. There is no vibrational wave in the upper slab, which is considered highly damped. An example might be a single layer of plywood without structural support other than the resilient mounts. Since the upper surface is hard the Fourier amplitude coefficients of the force pulse given in Eq. 12.24 can still be used. Ver (1971), citing Cremer (1952), has published the expected improvement

$$\Delta L_n = 20 \log \left[1 + \left(\frac{f}{f_1} \right)^2 \right] \cong 20 \log \left(\frac{f}{f_1} \right)^2 \tag{12.47}$$

where f_1 is the resonant frequency of the floating floor system is

$$f_1 = \frac{1}{2\pi} \sqrt{\frac{k'}{\rho_{S1}}} \tag{12.48}$$

and k' is the dynamic stiffness per unit area of the resilient layer between the floors, including the stiffness of the trapped air, and ρ_{S1} is the mass per unit area of the upper floor. As with a resilient surface, the result is a 12 dB per octave decrease in level above the resonant frequency. Below resonance there is no improvement.

Improvement Due to Resonantly Reacting Floating Floors

A resonantly reacting floor is a rigid, lightly damped floating slab in which bending waves are generated in response to the impulsive load. The input power into the upper slab is given by Eq. 12.9. The power balance equation for the upper slab is

$$W_{in} = W_{dis(1)} + W_{12} - W_{21} \tag{12.49}$$

and for the lower slab is

$$W_{12} = W_{dis(2)} + W_{21} \tag{12.50}$$

where powers with the subscript "dis" are the dissipated powers in slabs 1 and 2. The numerical subscripts indicate the direction of travel of the particular transmitted power

through the mounts. Three equations permit the calculation of the transmitted power through the mount

$$F = (u_1 - u_2) z_m$$
$$u_1 = u_0 - \frac{F}{z_1}$$
$$u_2 = \frac{F}{z_2}$$
(12.51)

where u_n = peak velocity amplitude in slab n (m/s)
z_n = point impedance of slab n (Ns/m)
z_m = point impedance of the support system (Ns/m)

When these equations are solved (Beranek and Ver, 1992) for the transmitted forces in terms of the point impedances, the improvement in the high-frequency limit, given in terms of the ratio of the initial to the transmitted forces is

$$\Delta L_n(\omega) \cong 10 \log \left[2.3 \, c_{L1} \, h_1 \, \eta_1 \, n' \left(\frac{\omega^3}{\omega_1^4} \right) \right]$$
(12.52)

where c_{L1} = speed of longitudinal waves in the floating slab (m/s)
h_1 = thickness of the floating slab (m)
η_1 = damping factor in the floating slab
n' = number of resilient mounts per unit area (m^{-2})
$\omega_1 = \sqrt{\dfrac{k_m \, n'}{\rho_{s1}}}$ = resonant frequency of the floating slab (s^{-1})
k_m = dynamic stiffness of an individual mount (N/m)
ρ_{m1} = surface mass density per unit area of the floating slab (kg/m^2)

In obtaining this relationship we have assumed that the power is transmitted only through the mounts, which can be represented by a spring constant, and that the point impedance of the slab is that of an infinite thin plate. Typical material constants are given in Table 12.1 and calculated data are shown in Fig. 12.19, along with measured results published by Josse and Drouin (1969). The improvement follows a 9 dB/octave slope above the resonant frequency.

12.4   STRUCTURAL DEFLECTION

Sound can be produced by the deflection of the structure in a gross way under the weight of a walker or other moving object. When a load is applied to a floor, the structure will deflect and transmit the movement to the space below. The weight may be statically or dynamically applied. We have discussed the vibrations induced in a floor system due to a walker in Chapt. 11. Where the floor system is a slab or a nonisolated structure the motion imparted to the floor will be faithfully reproduced on the ceiling side. Where the ceiling is decoupled from the floor support system considerable improvement can be expected.

Floor Deflection

If a person stands in the center of an upper-story floor, the structure will deflect under the concentrated load of his weight. This is a static, as contrasted to a dynamic, effect since it

TABLE 12.1   Speed of Longitudinal Waves, Density, and Internal Damping Factors
for Common Building Materials (Beranek and Ver, 1992)

Material	c m/sec	ρ lb/ft^3	ρ kg/m^3	Damping Factor η*
Aluminum	5,150	170	2,700	10^{-4}- 10^{-2}
Brick	......	120-140	1,900-2,300	0.01
Concrete, poured	3,400	150	2,300	0.005-0.02
Masonry block				
Hollow cinder (nominal 6 in. thick)	......	50	750	0.005-0.02
Hollow cinder 5/8 in. sand plaster each side (nominal 6 in. thick)	......	60	900	0.005-0.02
Hollow dense concrete (nominal 6 in. thick)	......	70	1,100	0.007-0.02
Hollow dense concrete, sand-filled (6 in. thick)	......	108	1,700	Varies with frequency
Solid dense concrete block (4 in. thick)	.....	110	1,700	0.012
Fir timber	3,800	40	550	0.04
Glass	5,200	156	2,500	0.001-0.01†
Lead:				
Chemical or tellurium	1,200	700	11,000	0.015
Antimonial (hard)	1,200	700	11,000	0.002
Plaster solid, on metal or gypsum lath	......	108	1,700	0.005 - 0.01
Plexiglas or Lucite	1,800	70	1,150	0.002
Steel	5,050	480	7,700	10^{-4}- 10^{-2}
Gypboard (0.5 to 2 in)	6,800	43	650	0.01 - 0.03
Plywood (0.25 to 1.25 in)	......	40	600	0.01 - 0.04
Wood chip board, 5 lb/ft^2	......	48	750	0.005 - 0.01

*The range in values of η are based on limited data at 1000 Hz. The lower values are typical for
the material alone.
† The loss factor for structures of these materials is very sensitive to construction techniques
and edge conditions.

FIGURE 12.19 Improvement in Impact Noise Isolation for a Resonantly Reacting Floating Floor (after Beranek and Ver, 1992)

a) Standard tapping machine b) High heeled shoes
Note the negative ΔL_n in the vicinity of the resonant frequency.
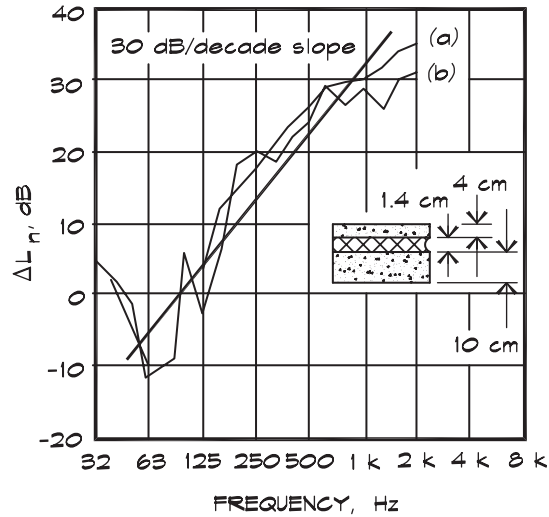
takes place without any repetitive motion—at zero frequency. The deflection of the floor can be modeled in a number of ways, but let us take a simple example using standard structural equations (Roark and Young, 1975). If we assume that the load is supported entirely by a simply supported beam, the midpoint deflection, ignoring the weight of the beam, is

$$\delta = -\frac{W L^3}{48\,E\,I} \tag{12.53}$$

where δ = deflection at midspan (in)
  W = weight of the impressed load (lbf)
  L = length of the beam (in)
  E = modulus of elasticity (lb / in^2)
   = 1.92×10^6 lb / in^2 for douglas fir
  I = moment of inertia (in^4) = b d^3 / 12
  b = beam width and d = beam depth (in)

If the beam is a wood 2 × 12 that is 20 feet long and a 200 lb man is standing at the midpoint, the deflection is about 0.16 inch and the natural frequency, using a simple spring mass relationship is about 8 Hz.

If the floor is 5/8" plywood with a 1.5" lightweight concrete topping, each beam (assuming 16" centers) bears a distributed load of about 20 lbs/ft (w = 1.7 lbs/in). The midspan deflection is

$$\delta = -\frac{5\,w\,L^4}{384\,E\,I} \tag{12.54}$$

For the same beam the deflection is about 0.2" with no concentrated load, and adding the deflection due to the weight of a person it is about 0.36". The natural frequency of this system, modelled as a spring mass, is 5 Hz.

Now this is a very simple model. The plywood flooring can increase the moment of inertia of the beam somewhat. The point load may be distributed over more than one beam. The beams may not be simply supported. So we may get a bit higher resonant frequency. The result, however, will be a relatively low frequency, less than 10 to 15 Hz at these spans, and somewhat higher frequencies at shorter spans. When the floor resonance is excited by a walker we can get a high ceiling deflection unless the floor is stiffened, damped, and decoupled from the ceiling support structure.

Low-Frequency Tests

There are a few tests available to measure the results of noise generated by floor deflection. A few years ago ASTM committee E33 proposed a single microphone located 1 m below the midpoint of the ceiling. The receiving room is deadened by placing absorbing material in it. Three types of sources are used: a male walker, a heavy ball, and an automobile tire. The Japanese measurement standard JIS 1418 specifies an automobile tire mounted on an arm attached to a motor. The motor arm lifts the tire and drops it on the floor. A cam system catches the tire on the rebound before it can strike the floor again and lifts it again to the proper height. The standard specifies many drop positions and several microphone positions; however, since the fundamental resonance is excited, only a few drop positions and a single mic position are adequate for comparative measurements. Test results are shown in Fig. 12.20

FIGURE 12.20 Peak Impact Sound Level Measurements Using Various Excitation Sources (Kinetics, 1990)

Floor Construction: 6" Concrete Slab
12 " Airspace with 3 1/2" Batt Insulation
2 x 5/8" Drywall Suspended on 1" Deflection Isolators
See Fig. 12.10 third example for section
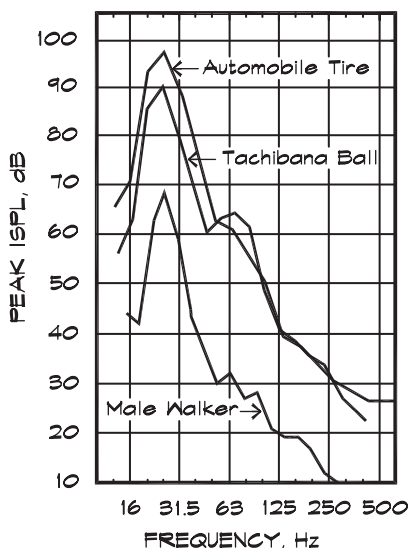
for a 6" thick concrete slab floor with a resiliently suspended drywall ceiling below. Note the peak impulse response is around 25 Hz, which is characteristic of the short span concrete floor used in these tests. The Tachibana ball, used in a Japanese test, is 180 mm in diameter and weighs 2.5 kg and is dropped from a height of 900 mm, and produces a very similar curve. A male walker yields similar results although the absolute levels vary.

Blazier and DuPree (1994) published measurements of the impact sound pressure level, taken on the wood floor system shown in Fig. 12.21, using a standard tapping machine as a source. Part of their study sought to quantify the importance of structural flanking in floating floors; however, these authors also extended their measurements to very low frequencies. In Fig 12.22 we see a comparison of a tapping test done on carpeted floor, a floating tile floor, and a partially floating tile floor. Below the 63 Hz band, there is little difference between surface treatments and we see two resonant peaks associated with the structural modes of the floor. Note that the difference between the unflanked and the partially flanked floating floor does not exceed 5 to 6 dB until the frequency is around 500 Hz, indicating a very

FIGURE 12.21 Wood Framed Floating Floor

10 mm (3/8") Ceramic Tile (or Carpet and Pad)
32 mm (1 1/4") Mortar Bed
10 mm (3/8") Mesh Mat
19 mm (3/4") Plywood
Double 38 x 292 mm (2 x 12) Wood Joists
165 mm (6 1/2" in) Batt Insulation
25 Ga Resilient Channels @ 16" O.C.
2 x 13 mm (1/2") Gypsum Board
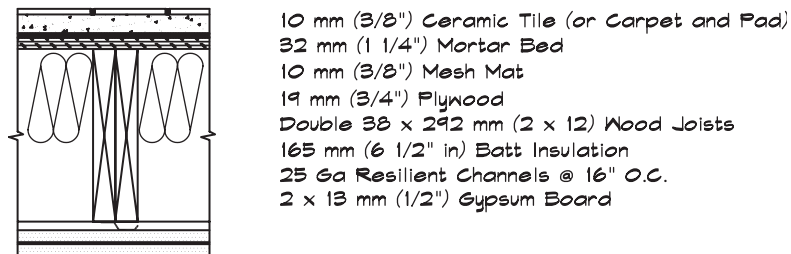
FIGURE 12.22 Impact Noise Spectrum of ISO Tapping Machine on a Floated Floor vs Percent of Floor Area Flanked and Type of Surface Covering (Blazier and DuPree, 1994)
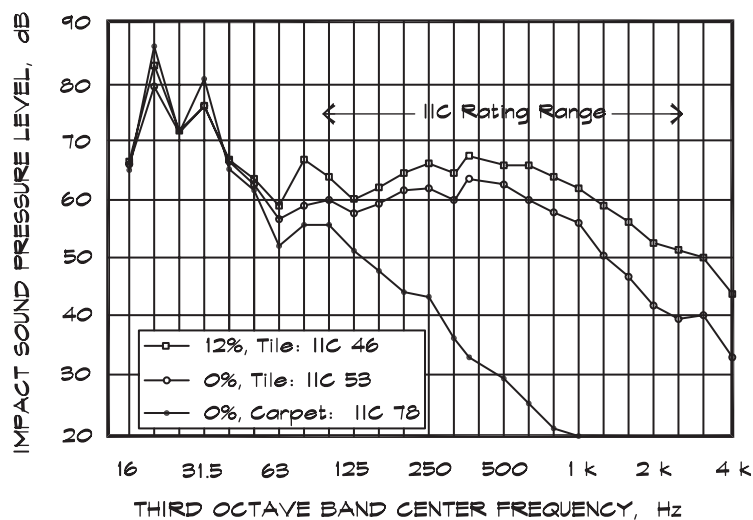
FIGURE 12.23   Impact Noise Spectrum of a Male Walker on a Floated Floor vs Percent of Surface Area Flanked and Type of Surface Covering (Blazier and DuPree, 1994)
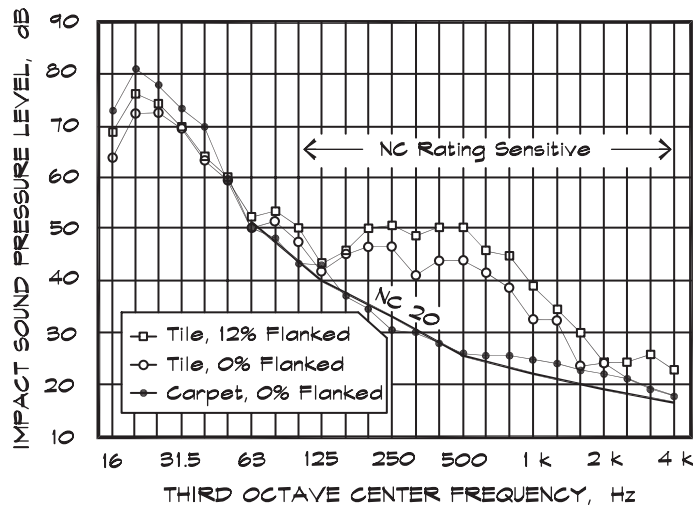
low deflection support system. The structural flanking referred to in Fig. 12.22 was due to concrete in the mortar bed flowing around the pour dam and under the matting.

Figure 12.23 shows additional measurements from the same study on the noise produced by normal walking compared with a standard NC curve. Even with carpet the levels are audible at low frequencies and very audible for tile floors. At these very low frequencies, it is the structural resonance that is being excited by the walker. Since the effect is a gross property of the structure, it is unaffected by the surface covering. For this construction there is little decoupling between the floor and the ceiling, so relatively poor isolation results.

It is interesting to compare the data from the walking test in Fig. 12.20 for a concrete slab with similar tests done on the Fig. 12.23 construction, which is poorly isolated. The difference above 20 Hz is at least 10 dB and as much as 30 dB quieter in the concrete structure.

Structural Isolation of Floors

Three mechanisms are available to improve low-frequency sound transmission: 1) increase the stiffness of the floor support system, 2) increase the structural damping, and 3) increase the vibrational decoupling between the floor and the ceiling. In concrete structures both the stiffness and the damping increase with slab thickness. In Chapt. 11 we discussed the treatment of vibrations in concrete slab floors.

In wood floor structures both stiffness and damping can be increased by using stepped blocking, shown in Fig. 12.24. Blocking, using 2 × lumber one size smaller than the joist material, is installed in a series of inverted U shapes, glued and end-nailed into place. The next set of blocks is stepped (i.e., installed in a position that is offset relative to the first set) so that it can also be end-nailed. Both careful trimming and liberal application of glue are important to the installation. Blocks must be trimmed so that no more than a 1/8" gap is left between the block and the joist. The object of the blocking is to build an additional beam at right angles to the joists near the midpoint of the span and to provide additional damping.

FIGURE 12.24 Stepped Blocking in 2 × Wood Framing

Staggered wood blocking one size smaller than the framing, glued and end nailed. Locate blocks at the mid point for spans greater than 12', at the one third points for spans greater than 18', and at the one quarter points for spans greater than 25'. Cut blocks to within 1/8" of the space and glue.

Nailing pattern
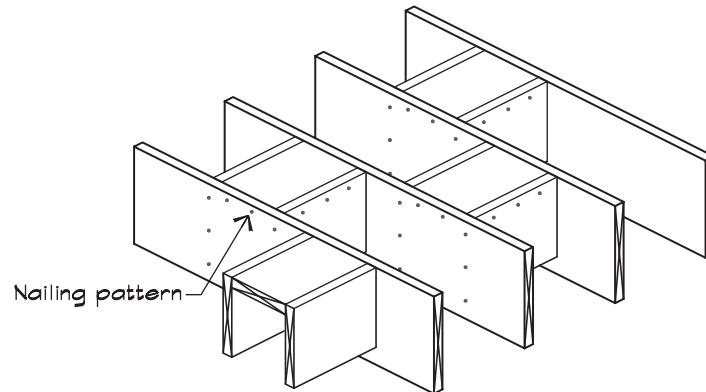
Stepped blocking is used at the midspan in wood floors having a joist span of more than 12 feet (3.7 m) and less than 18 feet (5.5 m), and at the one-third points in spans 18 feet or greater. This type of blocking is most effective when it is installed before the floor is covered with a diaphragm and concrete, since the additional loads cause the structure to deflect and distributes some of the static load to the blocking. It can also be used as a retrofit; however, the joists have already deflected and the static load is not distributed as efficiently.

Figure 12.25 shows the results of tapping machine tests done on the floor system, drawn in Fig. 12.26, that incorporates stepped blocking, compared with the mesh mat construction. Note that the low-frequency transmission loss is much better than the Blazier and DuPree results.

12.5   FLOOR SQUEAK

Shiners

Floor squeak is generated most often in wood construction by the rubbing of a joist or panel on a nail that is not completely embedded. Called *shiners*, these nails occur when framers use nail guns to secure the plywood diaphragms to the joists and miss their target. If the nail is not centered it will pass through the plywood and lay alongside the joist as in Fig. 12.27. When the floor deflects due to the passage of a walker, the joist moves and the nail rubs against the wood, creating a high-pitched squeak much like a bird call.

If shiners are found in the field they should be removed by pounding them up from the bottom and pulling them out from the top. It is critical to listen below to the floor response, while someone walks over each portion of the floor, to locate nonbedded nails before any lightweight concrete or other flooring is applied. Since squeak is not dependent on mass or damping in the floor structure, it is not affected by the addition of lightweight concrete, and the presence of these materials make the nails much more difficult to remove.

FIGURE 12.25 **Impact Noise Spectrum of ISO Tapping Machine on Two Types of Floors, Both Carpeted**
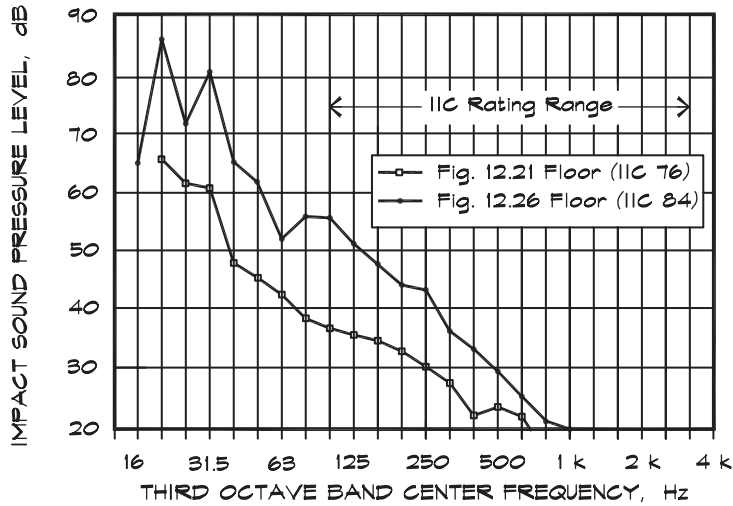
FIGURE 12.26 **Separately Supported Wood Floor**
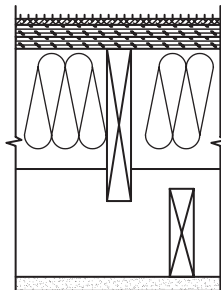
44 oz Carpet on 40 oz Pad
2 x 19 mm (3/4") Plywood Glued and Screwed
38 x 204 mm (2 x 10) Wood Studs @ 16" O.C.
38 x 190 mm (2 x 8) Stepped Mid Span Blocking
150 mm (6" in) Batt Insulation
38 x 140 mm (2 x 6) Wood Joists
22 mm (7/8") Plaster

FIGURE 12.27 **Sources of Floor Squeak**
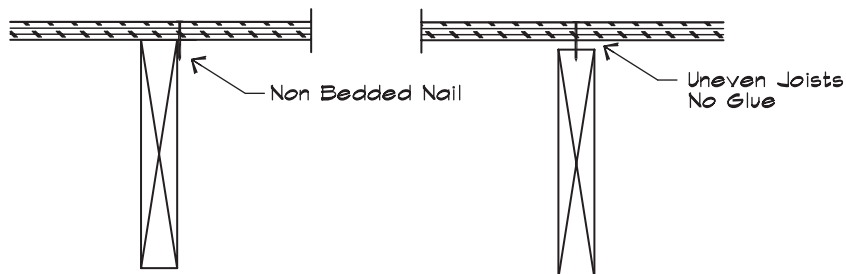
Figure 12.28   Truss Joists with Stepped Blocking

Note the spacer piece to fill the web.
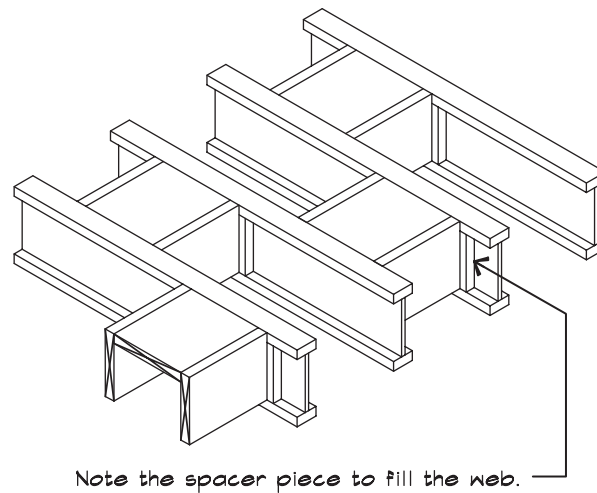
Uneven Joists

Nail squeak also can occur in a wood floor when the joists are of an uneven height. In these cases, the diaphragm does not make contact with the top of the joist and, in time, can move up and down on a nail, even one embedded in the joist. These conditions are particularly difficult to locate and remedy after the fact. Liberal application of panel adhesive to the top side of the joist before the plywood is installed will bond the subfloor to the joist and help fill in gaps that may be present. Factory manufactured truss joists can provide a better size consistency, which helps problems due to the variability in lumber. With truss joists, however, it is more difficult to construct stepped blocking since a spacer piece is required to fill the webbing, as illustrated in Fig. 12.28.

Hangers

Squeak can also occur when metal hangers are used to support the joists. In these cases the nails securing the hanger to the joist may rub on the hanger as the joist deflects. If the lumber varies in size, the diaphragm may not make contact with the joist and a gap will result. The best solution in these cases is to shim the joist so the top is even, and to glue the plywood down before nailing. It is preferable to frame the joists on the top plate of the bearing wall rather than being carried on wall-mounted metal hangers.

Nailing

A smooth nail, which does not grip the wood, is more prone to squeak than a ribbed nail. Ribbed or ring shank nails are helpful in preventing squeak since the wood is less likely to move vertically. Floor panel materials fabricated from strands of wood glued together are more prone to squeak than plywood since the high glue content material abrades and leaves a small hole where the nail can rub. Panel screws along with glue can give additional protection against squeak since they grip the wood more firmly. Drywall screws can be used; however, they are thinner than panel screws and more prone to break off.

This page intentionally left blank

13 NOISE IN MECHANICAL SYSTEMS

13.1 MECHANICAL SYSTEMS

Occupied spaces need the continuous delivery of the requirements for the human habitat—air, water, power, a controlled thermal environment—and the return of the waste products back to the surroundings in the form of carbon dioxide, waste water, sewage, refuse, and heat. To carry out these functions specialized machines are included in every building. The delivery of air and environmental control is provided by a heating, ventilating, and air conditioning (HVAC) system, water is circulated by pumps, and waste is removed through piping.

Fresh air is delivered by electric fans, most often centrifugal, but occasionally a plug, vane axial, or propeller type. Since thermal requirements necessitate the movement of more air than the oxygen requirements, most of the air in a room is recirculated to add or remove heat, and a portion of it is replaced with fresh air from the outside. Since the building is slightly pressurized by this process, some air leaks out through openings and the rest is removed by the mechanical system.

Temperature is controlled by blowing room air over a heat exchanger, a series of tubes, like the radiator in a car, through which a heated or cooled liquid is circulated. Heat, which is produced by electric resistive elements or a gas-fired boiler, is much easier to generate than cooling. Cooling is created by forcing a pressurized liquid or gas through an orifice, where it expands and some of the liquid changes to a gas, thereby absorbing heat from the surroundings. In the heat exchanger the cooled refrigerant is evaporated by taking heat from the circulating air. Once this process is complete the gas is recycled back to the condenser, where it is pressurized and converted back to a liquid, thereby releasing heat to the atmosphere. Figure 13.1 illustrates the process in a packaged air handler, which contains a compressor, a fan to exhaust the heat given off by the compressor, a pump to circulate the cooling fluid, a heat exchanger coil, and another fan to circulate the air in the room. When the compressor is physically separated from the fan coil unit as in Fig. 13.2, it is called a split system and the refrigerant is circulated through pipes connecting the two components.

Noise and vibration are often the byproducts of these mechanical processes. Figure 13.3 shows an example of an HVAC unit and several of the most common structural and airborne noise transmission paths. Each of the paths must be treated to assure overall noise control.

FIGURE 13.1 Heat Flow in a Package Air Handler
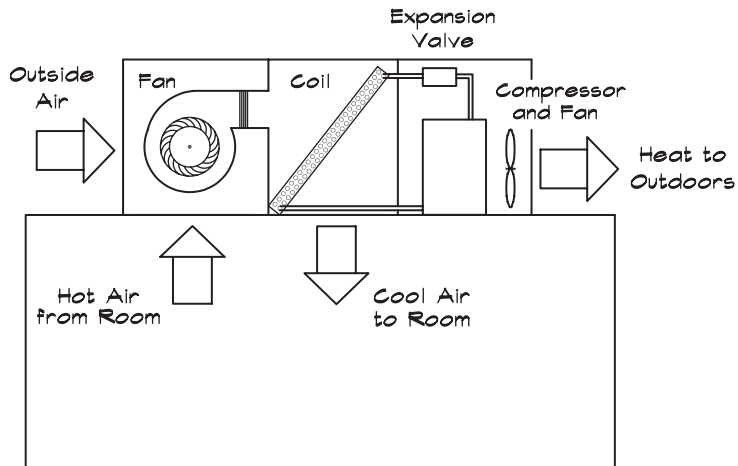
FIGURE 13.2 Air and Heat Flow in a Split System Air Conditioner
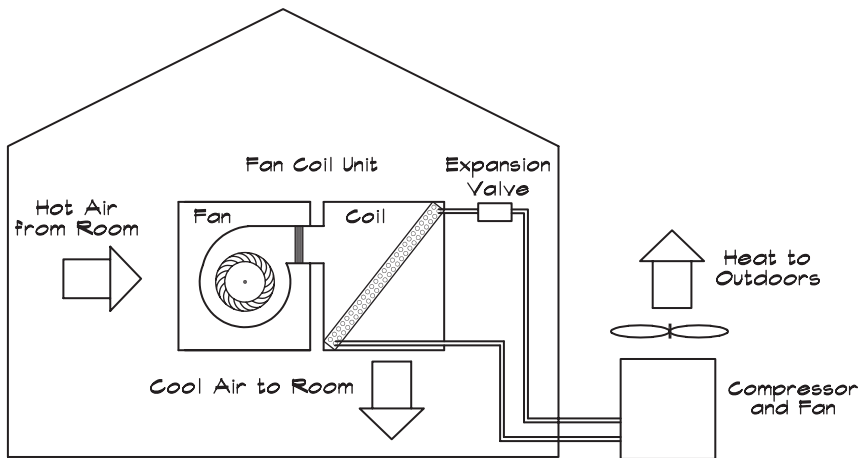
FIGURE 13.3 Rooftop Air Handling Unit Showing Noise Transmission Paths
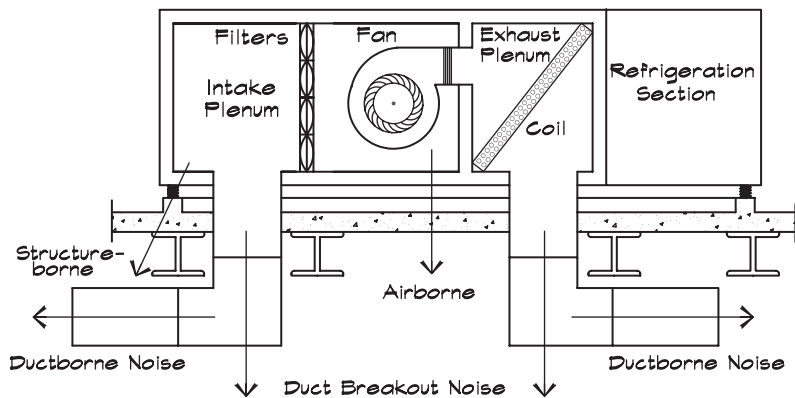
If a generalization can be made, first it is important to insure that the structure-borne path is isolated. This may be accomplished by locating equipment away from sensitive receivers, and by vibration isolating it, along with all solid connections to it. Once the vibrational path is controlled, then the airborne path can be treated.

Manufacturer Supplied Data

An airborne sound transmission calculation begins with the sound power level generated by a piece of equipment. Often the manufacturer can provide measured sound power level data in octave bands or sound pressure levels at a known distance. The fact that data are available, however, should not lead to the suspension of disbelief about their accuracy. It is important to ferret out the origin of the measurements, and then to compare manufacturer-supplied data with data calculated from standard equations to see if the two are in general agreement. If they are not, further inquiries may be necessary to clarify the reason for the difference.

It seems logical that manufacturers would simply measure the noise their equipment makes and publish the data. Logic does not always prevail and companies may rely instead on calculations or other methods to determine noise level data. Although calculated data are better than nothing, the user does not necessarily know if the data are measured or calculated, and if calculated, which equations were used. In some instances, manufacturers will measure sound data on one unit and will publish data for other models, sizes, or speeds based on scaling relationships. This is standard practice among silencer manufacturers. The precise methodology and measurement techniques are important to learn, to confirm the appropriateness and applicability of the data. Occasionally manufacturers publish data with substantial errors. Here again a comparison to generic formulas can help uncover inconsistencies. Even when data have been measured directly on one unit, there can be some variation in levels due to the production process and details of the installation. The actual sound power level, based on carefully measured data, can still vary by a few dB in a given band from unit to unit, even under ideal conditions.

Airborne Calculations

If we have the sound power level of a source we can calculate the sound pressure level at the location of interest. When we are inside a room and sufficiently far from the source the reverberant field will predominate and we can proceed using Eq. 8.83 to predict the airborne sound pressure level in a space. If there is a significant contribution from a direct field component, such as when equipment is located outdoors, a separate calculation should be carried out using Eq. 2.74. If both types of field contribute, the levels from each should be combined.

When the sound wave cannot expand, such as when it is contained within a duct, there is no attenuation due to geometrical spreading. Instead the attenuation due to the duct lining or other elements in the ductwork is subtracted from the overall power, in each band, before the sound is introduced into a room. There it is analyzed as any other source would be.

13.2   NOISE GENERATED BY HVAC EQUIPMENT

Compilations of sound power level data radiated by mechanical equipment have been published and are sometimes available from equipment manufacturers. One of the best was developed in the 1960s by Laymon Miller (1968) for the U.S. Army. He continued this work through the 1980s and his studies are excellent references. The American Society of

TABLE 13.1   Sound Pressure Levels at 3 ft from Packaged Chillers, dB (Miller, 1980)

Freq	Rotary Screw Compressor	Reciprocating 10-50 Tons	Reciprocating 51-200 Tons	Centrifugal < 500 Tons	Centrifugal > 500 Tons
31 Hz	70	79	81	92	92
63 Hz	76	83	86	93	93
125 Hz	80	84	87	94	94
250 Hz	92	85	90	95	95
500 Hz	89	86	91	91	93
1 k Hz	85	84	90	91	98
2 k Hz	80	82	87	91	98
4 k Hz	75	78	83	87	93
8 k Hz	73	72	78	80	87
A-Weighted	90	89	94	97	103

Heating Refrigeration and Air Conditioning Engineers, ASHRAE, also publishes data on fans, pumps, and air handlers, and is another good source. Other manufacturers and trade associations make available data on specific pieces of equipment.

Refrigeration Equipment

Miller (1980) has collected and studied noise data on nearly 40 packaged chillers and recipro-cating compressors. These units ranged in size from 15 tons to more than 500 tons of cooling capacity. A ton of refrigeration capacity is defined as the amount of heat removal required to produce one ton of ice from water at 32° F (0° C), 288,000 Btu (84.5 kW), in 24 hours or 12,000 Btuh (3.52 kWh). In air handling systems, fans generally are sized to provide about 400 cfm/ton of refrigeration. Sound data are given in terms of the sound pressure level at 3 ft. (1 m) from the equipment. No information on the physical size of the equipment is available. Several types of packaged chillers were investigated, differing primarily in the type of compressor. Table 13.1 shows the sound pressure levels at 3 ft. (1 m) for each type.

Cooling Towers and Evaporative Condensers

Cooling towers serve to cool water by using the latent heat absorbed during the process of evaporation. Water is introduced at the top of a cooling tower and falls to the bottom. Simultaneously air is blown or drawn upward through the falling water to aid in the mixing and increase evaporation. Noise is generated primarily by the fans; however, in certain cases the water itself can also contribute. Figure 13.4 shows examples of various types of cooling towers.

Overall sound power levels for each type are listed in Table 13.2 along with corrections to be subtracted from the overall level to obtain the level for each octave band. Cooling towers have a definite directivity, which depends on the type of fan, its location, and the side in question. Table 13.3 gives the approximate directional corrections to be added to the sound pressure levels calculated from the sound power levels in Table 13.2.

Note that these sound power level data have been calculated from sound pressure level measurements that are taken sufficiently far away from the unit that consideration of the size

FIGURE 13.4 Principal Types of Cooling Towers (Miller, 1980)
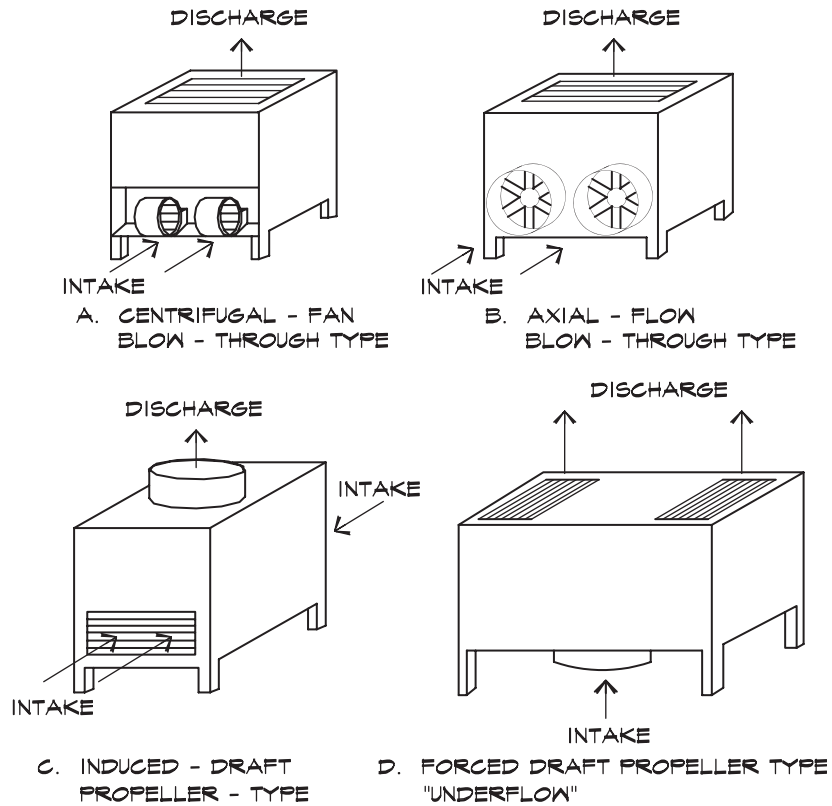
TABLE 13.2   Sound Power Levels of Cooling Towers, dB (Miller,1980)

	Propeller Type	Centrifugal Type
	$L_W = 95 + 10 \log \text{(fan hp)} - \text{Corr}$	$L_W = 85 + 10 \log \text{(fan hp)} - \text{Corr}$
31 Hz	8	6
63 Hz	5	6
125 Hz	5	8
250 Hz	8	10
500 Hz	11	11
1 k Hz	15	13
2 k Hz	18	12
4 k Hz	21	18
8 k Hz	29	25

TABLE 13.3   **Corrections to Average Sound Pressure Levels for the Directivity of Cooling Towers, dB (Miller, 1980)**

Octave Band (Hz)	31	63	125	250	500	1k	2k	4k	8k
Centrifugal Fan Blow-through Type									
Front (Fan Inlet)	3	3	2	3	4	3	2	2	2
Side (Enclosed)	0	0	0	−2	−3	−4	−5	−5	−5
Rear (Enclosed)	0	0	−1	−2	−3	−4	−5	−6	−6
Top (Discharge)	−3	−3	−2	0	1	2	3	4	5
Axial Flow Blow-through Type									
Front (Fan Inlet)	2	2	4	6	6	5	5	5	5
Side (Enclosed)	1	1	1	−2	−5	−5	−5	−5	−4
Rear (Enclosed)	−3	−3	−4	−7	−7	−7	−8	−11	−8
Top (Discharge)	−5	−5	−5	−5	−2	0	0	2	1
Induced Draft Propeller Type									
Front (Air Inlet)	0	0	0	1	2	2	2	3	3
Side (Enclosed)	−3	−3	−3	−3	−3	−3	−4	−5	−6
Top (Discharge)	3	3	3	3	3	4	4	3	3
Underflow Forced Draft Propeller Type									
Any Side	−1	−1	−1	−2	−2	−3	−3	−4	−4
Top	2	2	2	3	3	4	4	5	5

was unnecessary for the pressure to power conversion. If near field sound pressure levels are needed, then the physical size of the source must be taken into account by using Eq. 2.91.

Air Cooled Condensers

In single or multifamily residences, air cooled condensers are used in place of the larger cooling towers or evaporative condensers. The noise from these units is due to the fan, usually a propeller type, with a small contribution from the air flow through the condenser coil decks. Figure 13.5 shows a sketch and measured data. These data are for a 3–5 ton residential unit based on sound pressure levels measured at 6 ft from the center of the fan and at 90° to the direction of airflow, which is out the top of the unit.

Pumps

Pumps are found in virtually every building. When they are located above grade they are best mounted on an inertial base and housekeeping pad, such as that in Fig. 13.6. Pipe elbows that are connected to the pump should be supported from the isolation base. Flexible couplings are used to compensate for pipe misalignment and to provide structural decoupling. Piping should be resiliently supported in accordance with the recommendations given in Chapt. 11.

FIGURE 13.5 Sound Power Levels from a 3–5 Ton Air Cooled Compressor
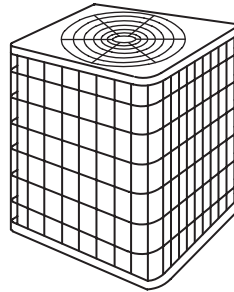
Octave Band (Hz)	63	125	250	500	1k	2k	4k	8k
Level	87	84	75	75	74	71	64	56

FIGURE 13.6 Water Pump Installation with Inertial Base

Note that the piping is supported off the inertial base.

Flex Connection

Flex Connection
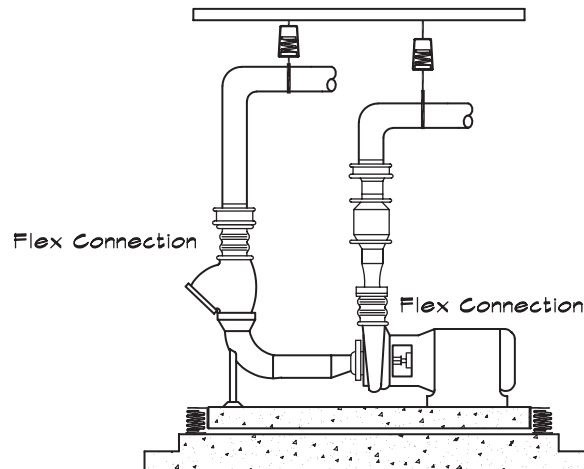
Sound pressure level data at a distance of 3 ft have been published by Miller (1980) and are reproduced in Table 13.4. Also shown in the table are the corrections to be subtracted from the overall level to obtain the octave band values. A-weighted levels are 2 dB lower than the overall levels.

13.3   NOISE GENERATION IN FANS

Noise in HVAC systems is created both actively by mechanical equipment, primarily fans, and passively by static components in the air stream, which can create flow-generated noise. Nearly every component in an HVAC system, no matter how benign, can contribute to noise creation. It is critical to be aware of the noise generating mechanisms and their relative impact on the overall system.

TABLE 13.4   **Overall Sound Pressure Levels at 3 ft for Pumps (Miller, 1980)**

Speed Range (rpm)	Drive Motor Nameplate Power	
	Under 100 hp	Above 100 hp
	Overall Sound Pressure Level, dB	
3000–3600	71 + 10 log (hp)	85 + 3 log (hp)
1600–1800	74 + 10 log (hp)	88 + 3 log (hp)
1000–1500	69 + 10 log (hp)	83 + 3 log (hp)
450–900	67 + 10 log (hp)	81 + 3 log (hp)

Corrections to Overall SPL for Pumps, dB

Octave Band (Hz)	31	63	125	250	500	1k	2k	4k	8k
Level Subtracted	13	12	11	9	9	6	9	13	19

Fans

All buildings have fans of one sort or another for air circulation. Fans are typed according to the mechanism used to propel the air in Fig. 13.7, and further subdivided according to the type of blade in Fig. 13.8. The basic types are axial and centrifugal. Axial fans are the simplest to understand; they have a fixed-pitch multiple-bladed rotor. Propeller fans are unhoused, whereas vane axial and tube axial fans include a shroud or housing around the impeller.

FIGURE 13.7 **Types of Fans**

CENTRIFUGAL

VANEAXIAL

PROPELLER

PLUG
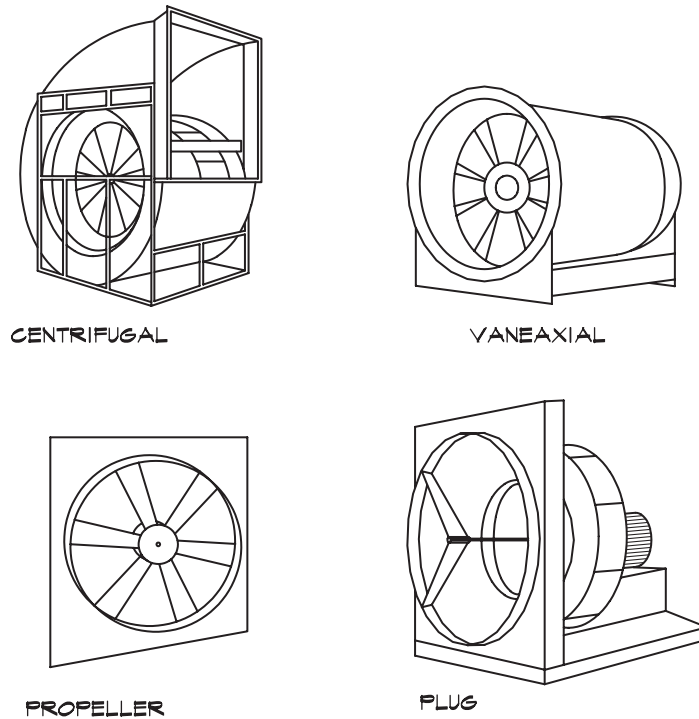
FIGURE 13.8 Types of Centrifugal Fans
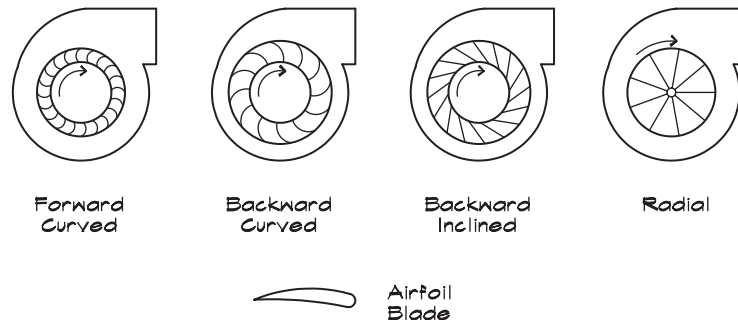
Vane axial fans have fixed stator blades to straighten the flow after it passes through the rotor blades; tube axial fans do not.

Centrifugal fans consist of a series of blades, arranged at even intervals around a circle like a waterwheel, that throw the air from the inside to the outside of the circle as they rotate. Forward curved blades push the air out much like a jai alai racket. The air leaves the fan blade at a velocity higher than that of the blade tip. In backward-curved or backward-inclined blades the air velocity is lower than the tip velocity, so a lower noise level is generated. The forward-curved blades can generate the same air volume at a lower rotational speed, which means that the peak in their spectrum occurs at a lower frequency.

Fan noise is generated by several mechanisms, including the surge of the air pressure and velocity each time a blade passes, turbulent airflow in the air stream, and physical movement of the fan casing or enclosure. The noise emitted by each fan type follows a series of generalized laws called scaling laws, originally developed by Beranek, which have the general form (Graham, 1975 as given in ASHRAE, 1987)

$$L_W = K_F + 10 \log Q_F / Q_{REF} + 10 \log P_F / P_{REF} + C_{EFF} + C_{BFI} \qquad (13.1)$$

where L_W = sound power level (dB re 10^{-12} Watts)
   K_F = spectral constant which depends on the type of fan (dB) shown in Fig. 13.8
   Q_F = volume of air per time passing through the fan (cfm or L/s)
   Q_{REF} = reference volume (1 for cfm or 0.472 for L/s)

   P_F = static pressure produced by the fan (in of water or Pa, gage)
   P_{REF} = reference pressure (1 for in of water or 249 for Pa)

   C_{EFF} = efficiency correction factor (dB)
   C_{BFI} = blade frequency increment correction (dB)

Table 13.6 gives the off-peak the efficiency correction factor for fans running at less than peak efficiency. Equation 13.2 gives the method for calculating the fan's efficiency in FP units

$$\eta = \frac{100 \, Q_F \, P_F}{6356 \, W_{hp}} \qquad (13.2)$$

TABLE 13.5   Level Correction K_F for Total Sound Power of Fans, dB (ASHRAE, 1987)

Fan Type	Octave Band Center Frequency (Hz)							
Centrifugal	63	125	250	500	1k	2k	4k	8k
Airfoil, Backwards Curved, Backward Inclined Wheel Diameter (inches)								
> 36 in	40	40	39	34	30	23	19	17
< 36 in	45	45	43	39	34	28	24	19
Forward Curved								
All	53	53	43	36	36	31	26	21
Radial Total Pressure (in. w.g.)								
Low 4–10	56	47	43	39	37	32	29	26
Med 6–15	58	54	45	42	38	33	29	26
High 15–60	61	58	53	48	46	44	41	38
Vaneaxial Hub Ratio								
0.3–0.4	49	43	43	48	47	45	38	34
0.4–0.6	49	43	46	43	41	36	30	28
0.6–0.8	53	52	51	51	49	47	43	40
Tubeaxial								
Wheel Diameter (inches)								
> 40 in	51	46	47	49	47	46	39	37
< 40 in	48	47	49	53	52	51	43	40
Propeller								
General ventilation and Cooling towers								
All	48	51	58	56	55	52	46	42

TABLE 13.6   Efficiency Corrections, C_{EFF} (ASHRAE, 1987)

Static Efficiency	Correction Factor
(% of Peak)	(dB)
90–100	0
85–89	3
75–85	6
65–74	9
55–64	12
50–54	15
below 50	16

TABLE 13.7   Blade Frequency Increment Correction, C_{BFI} (ASHRAE, 1987)

Fan Type	Blade Passing Octave, f_{bp}	C_{BFI}
Centrifugal		
Airfoil, backward curved, backward inclined	250 Hz	3
Forward curved	500 Hz	2
Radial blade pressure blower	125 Hz	8
Vaneaxial	125 Hz	6
Tubeaxial	63 Hz	7
Propeller		
Cooling Tower	63 Hz	5

where W_{hp} = power rating of the fan in horse power. The relative fan efficiency expressed as a percentage is

$$\eta_{rel} = 100 \left[\frac{\eta}{\eta_{peak}} \right] \tag{13.3}$$

If the peak efficiency is not known, it is normal to assume a relative efficiency of about 80% , a value that adds about 6 dB to the data. If the peak efficiency is available from the manufacturer usually the actual sound power levels are as well.

The additional factor known as the blade frequency increment correction C_{BFI}, shown in Table 13.7, is a number to be added to the overall level in the octave band containing the blade passing frequency, f_{bp}

$$f_{bp} = \frac{\text{fan rpm} \times \text{number of blades}}{60} \tag{13.4}$$

The sound is radiated from both the fan intake and discharge. The formula assumes ideal inlet and outlet flow conditions and operation of the fan at a given efficiency.

Fans can also radiate noise through their enclosures and into the surrounding space. This is referred to as casing radiation and may be calculated by subtracting a factor for the insertion loss of the casing. Insertion losses are very dependent on the gauge and construction of the fan housing and those cited in Table 13.8 are only approximate.

Housing attenuation values are subtracted from the fan sound power level data to obtain a rough estimate of the power levels radiated by the fan through the housing when the fan is attached to ductwork. At low frequencies the power is unaffected by the casing since the enclosure vibration radiates as much noise as the unhoused fan would. The attenuations reflect the assumption that there is no separate enclosure around the fan housing and no absorption inside the housing, but that there is a silencer or lining in the ductwork close to the fan.

TABLE **13.8** **Adjustments for the Attenuation of the Fan Housing, dB (Miller, 1980)**

	Octave Band Center Frequency (Hz)								
	31	**63**	**125**	**250**	**500**	**1k**	**2k**	**4k**	**8k**
Attenuation	**0**	**0**	**0**	**5**	**10**	**15**	**20**	**22**	**25**

Fan Coil Units and Heat Pumps

In small offices and residential installations split HVAC systems are often used. These consist of an air-cooled condenser outdoors and a fan coil indoors as illustrated in Fig. 13.2. A refrigerant is circulated between the two devices moving under pressure in mostly liquid form between the condenser and the fan coil, and returning as a gas. The high-pressure liquid is forced through an expansion valve and thence into a cooling coil, where heat is removed from the room air.

The main source of noise in a fan coil is the small fan that circulates air through the coil and into the conditioned space. Figure 13.9 gives measured sound power levels at several rates of flow. When a fan coil unit is located above a T-bar ceiling the noise it generates is difficult to control even with lined ductwork or silencers. Wherever possible fan coils should be installed in closets or above drywall ceilings, which provide the necessary transmission loss. Lined ducts or silencers are usually required.

The compression expansion cycle can be used to heat as well as cool a space. The process is reversible in a device known as a heat pump, which literally can carry heat into or out of a building. Figure 13.10 illustrates this process. In the winter or heating mode, at the top of the figure, refrigerant is circulated through a refrigerant-to-water heat exchanger, where it absorbs heat from water that is colder than the exterior environment but warmer than the refrigerant. The heat absorbed warms the refrigerant and converts it to a gas. It then

FIGURE **13.9** **Discharge Noise Levels of Fan Coil Units (Fry, 1988)**
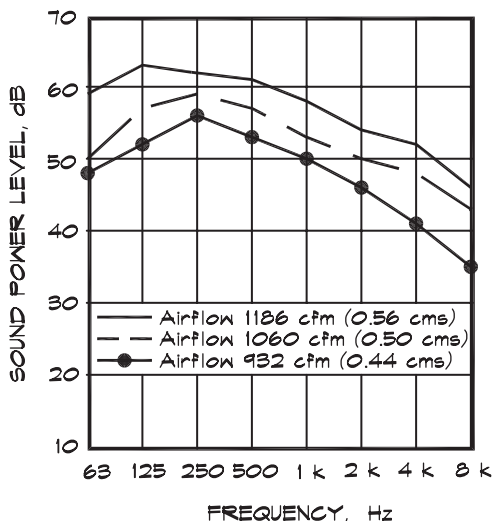
FIGURE 13.10   Air and Heat Flow in a Heat Pump System (California Heat Pump)

The shaded pipes indicate areas of high pressure.

HEATING

Cold Air In

Warm Air Out

Filter

Refrigerant
to air heat
exchanger

Hot Gas

Liquid

Compressor

Capillary tube

C.   H.

Reversing valve
Heating mode

Refrigerant to
water heat
exchanger

Low temp. gas

Supply
water

Return
water

To outdoor heat exchanger

COOLING

Hot Air In

Cool Air Out

Filter

Refrigerant
to air heat
exchanger

Low temp. gas

Liquid

Compressor

Capillary tube

C.   H.

Reversing valve
Cooling mode

Refrigerant to
water heat
exchanger

Hot gas

Supply
water

Return
water

To outdoor heat exchanger

flows to the compressor, which further warms and pressurizes it by performing mechanical work on it. The hot gas then flows through a coil where a fan blows air over it and into the occupied space. The gas gives off heat in the exchange and condenses into a liquid. The liquid is then forced under pressure through the capillary tube where it expands and is returned to the heat exchanger. The cooling cycle is just the reverse of this process and is enabled by changing the direction of flow of the reversing valve. Noise generated by heat pump units can be greater than fan coils since the compressor is located in the same unit as the coil.

VAV Units and Mixing Boxes

In recent years, due to the emphasis being placed on energy conservation, the variable air volume or VAV system has become a commonly used design. A VAV system consists of a fan operating at a constant velocity that pressurizes a series of valves, which in turn feed a network of diffusers, distributed throughout the occupied space. The valves consist of remotely controlled dampers, which regulate the airflow to each space. A bypass duct is used to route the unused air back to the inlet side of the air handler in order to maintain a constant volume through the fan. A VAV unit, pictured in Fig. 13.11, must be capable of regulating the airflow from the full design capacity down to a very small flow, usually by means of butterfly dampers.

Blazier (1981) has published discharge (in Fig. 13.12) and radiated (in Fig. 13.13) sound power levels generated by VAV units for two rates of flow. The noise is generated by disturbed flow around the dampers.

Many manufacturers publish data on both discharge and casing radiated sound from VAV units. The most useful data are given in terms of sound power levels; however, some manufacturers list data in terms of NC levels, which are obtained by assuming a certain

FIGURE 13.11   A Variable Air Volume Unit
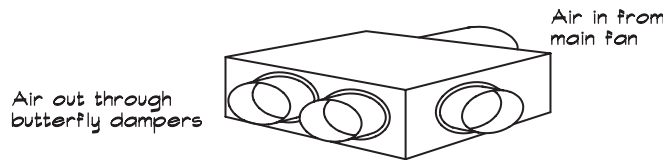
FIGURE 13.12   Range of Discharge VAV Noise Levels at Two Operating Points (Blazier, 1981)

FIGURE 13.13   Range of Radiated VAV Noise Levels at Two Operating Points (Blazier, 1981)

Tests on 5 manufacturers' boxes (average ± 1 standard deviation)
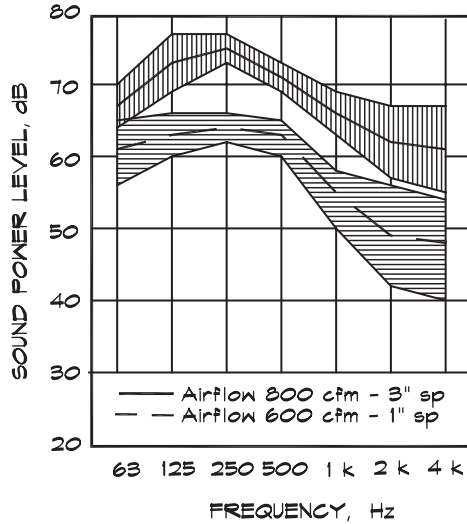
FIGURE 13.14   Comparison between Published and Measured Sound Power Levels (Blazier, 1981)

Based on a survey of 7 manufacturers at 6 operating points
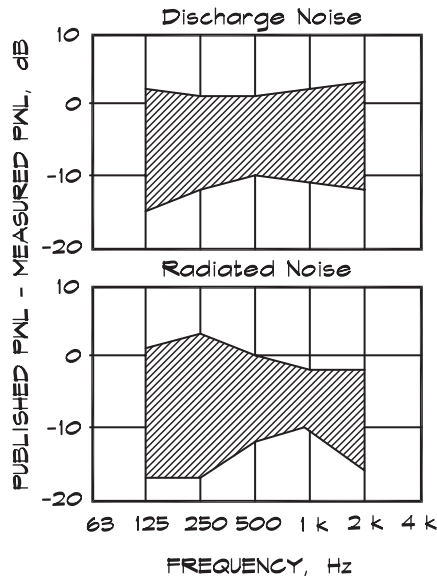
power-to-pressure conversion in the receiving room (usually −10 dB) and sometimes an additional noise reduction (also −10 dB) due to the ceiling tile. Blazier (1981) has measured the noise generated by VAV units as they compare to data published by the manufacturers. He lists in Fig. 13.14 the difference between published and measured sound power levels citing a 6 to 10 dB understatement of the noise furnished by manufacturers. Some of the

FIGURE 13.15 Measured Insertion Loss of Typical Lay-in Acoustical Ceiling Systems (Blazier, 1981)
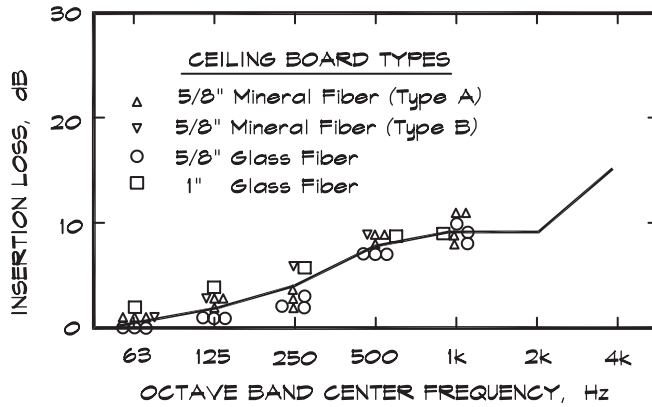
discrepancy may be due to the difficulty in duplicating in the field the smooth entry and exit flow conditions under which the laboratory data are taken. Blazier (1981) has also measured the insertion loss due to acoustical tile ceilings given in Fig 13.15. Note that the loss approaches 10 dB only at high frequencies.

13.4 NOISE GENERATION IN DUCTS

Flow Noise in Straight Ducts

Once air has been set in motion it can generate noise by creating pressure fluctuations through turbulence, vortex shedding, mixing, and other mechanisms. Steady flow in a straight duct does not generate appreciable noise, when compared with other sources such as abrupt transitions in the air path, takeoffs, and elbows. Figure 13.16 (Fry, 1988) shows sound power

FIGURE 13.16 Sound Power Spectra of 600 mm (24 in) × 600 mm Straight Steel Duct for Various Air Velocities (Fry, 1988)
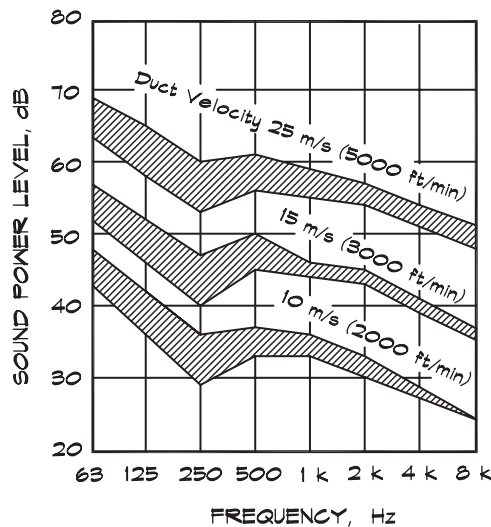
FIGURE 13.17   Buffeting in Rectangular Ducts (Fry, 1988)
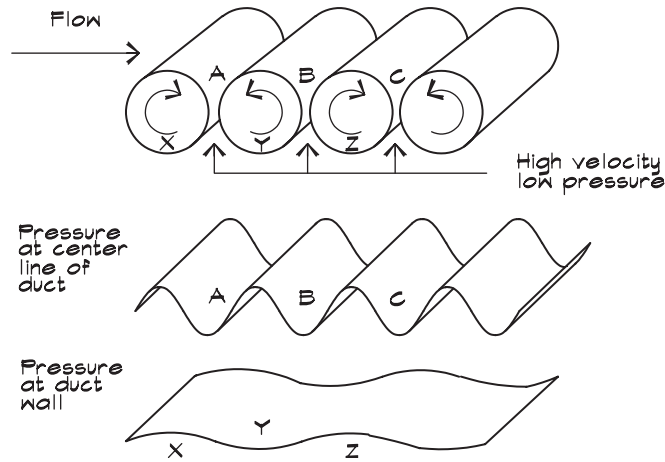
level data on noise generated in straight duct runs for straightened flow. Levels generally follow an 18 dB per doubling of velocity scaling law.

The cited data show a significant rise in level when the cross sectional duct dimension is equal to a wavelength, which for this example is about 500 Hz. This bump coincides with the establishment of full cross duct turbulent eddies illustrated in Fig. 13.17. Eddies form downstream of disturbing elements such as rods or dampers. By themselves eddies are not particularly efficient sound radiators; however, they can generate noise when they impinge on a flat plate or other low-frequency radiator. In an open duct, eddies cause the flow to alternately speed up and slow down, producing pressure maxima at points X and Z and a pressure minimum at point Y.

In air distribution design it is prudent to control the duct velocity by increasing the cross sectional area of the duct, thus slowing the flow as it approaches the space served. A duct layout is pictured in Fig. 13.18.

FIGURE 13.18   Typical Duct Run in an HVAC System
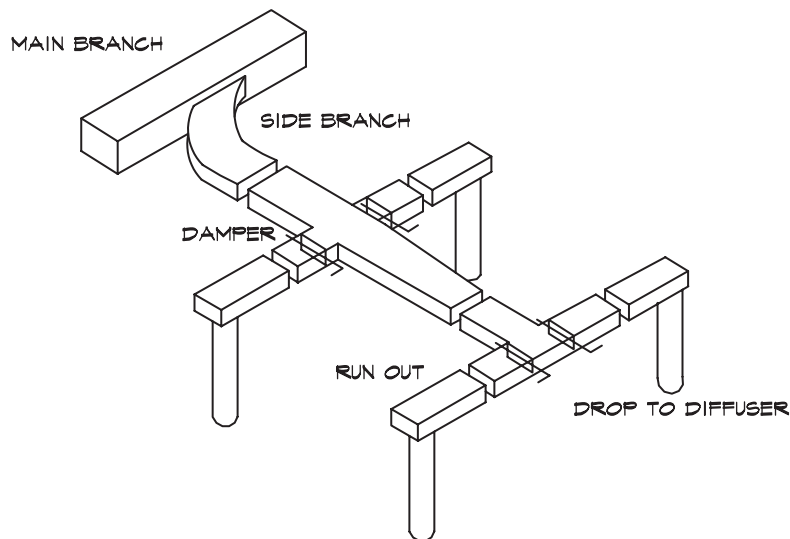
TABLE 13.9   Velocity Criteria for Air Distribution Systems

		Maximum Air Velocities (ft/min)					
Description		**Distance from Termination**					
	Slot Speed at Termination	**< 10 ft (3 m) No Lining**	**> 5 ft (1.5 m)**	**> 10 ft (3 m)**		**> 20 ft (6 m)**	
NC Criteria		**< 5 ft (1.5 m) Lining***	**Lining***	**No Lining**	**Lining***	**No Lining**	**Lining***
NC 15 supply	250	300	500	350	800	425	1000
NC 15 return	300	350	600	350	950	500	1200
NC 20 supply	300	350	600	425	950	550	1200
NC 20 return	350	425	725	500	1150	650	1450
NC 25 supply	350	425	725	500	1150	700	1450
NC 25 return	425	500	875	650	1375	800	1725
NC 30 supply	425	500	875	700	1375	850	1725
NC 30 return	500	600	1050	800	1650	950	2075
NC 35 supply	500	600	1050	800	1650	1000	2075
NC 35 return	600	700	1250	900	2000	1150	2500
NC 40 supply	600	700	1250	900	2000	1150	2500
NC 40 return	725	850	1500	1075	2400	1380	3000
NC 45 supply	725	850	1500	1075	2400	1375	3000
NC 45 return	875	1000	1800	1300	2875	1675	3575

*   Duct must be lined with 1" fiberglass duct   1 m/sec = 196.8 ft/min
      liner or flexible duct from this point to termination.

FIGURE 13.19   Sound Power Levels of Abrupt and Gradual Area Transitions from 600 mm × 600 mm to 200 mm × 200 mm Duct Cross Sections (Fry, 1988)
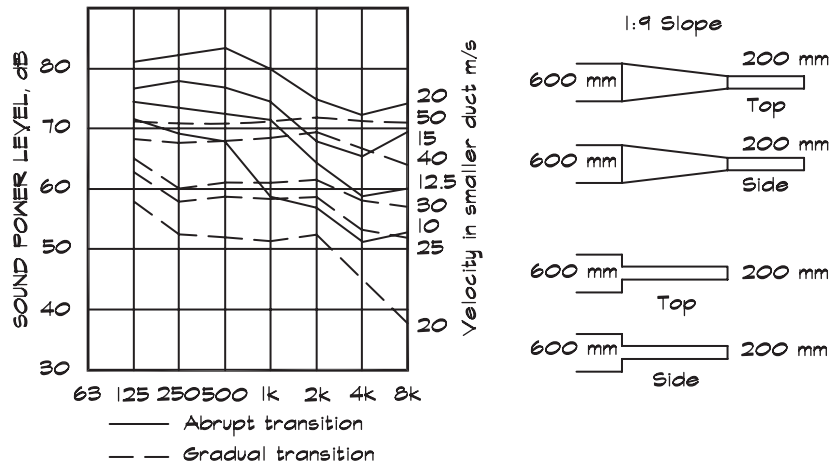
Table 13.9 gives velocity recommendations appropriate for various NC levels in the receiving space. These include consideration of the attenuation of downstream sections of lined duct. For the lined duct velocities, it is assumed that the remaining ductwork is covered on the inside with a 1" (25 mm) thick fiberglass duct liner or is flex duct.

Noise Generated by Transitions

Aerodynamic noise is generated at both gradual and abrupt changes in duct area. Gradual transitions and low velocities generate less turbulence than abrupt transitions and high velocities. Beyond these generalizations there are few models to use for sound power level prediction. Fry (1988) has published measured data for several expansion ratios in rectangular ducts, which are reproduced in Figs. 13.19 and 13.20.

Air Generated Noise in Junctions and Turns

Noise generated in transition elements such as turns, elbows, junctions, and takeoffs can run 10 to 20 dB higher than the sound power levels generated in straight duct runs. Ducts having radiused bends, with an aspect ratio of 1:3 generated, no more noise than a straight duct (Fry, 1988). Elbows having a 90° bend are about 10 dB noisier than straight duct. One or more turning vanes can reduce the noise 8 to 10 dB at high and low frequencies while increasing it 3 to 4 dB in the mid frequencies.

Ver (1984) published an empirical equation for the sound power levels given off by various fittings, which was reproduced in the 1987 ASHRAE guide. For branches, turns (including elbows without turning vanes), and junctions such as those pictured in Fig. 13.21, it is

$$L_{W \, OCT}(f_0) = K_J + 10 \log (f_0/63) + 50 \log (U_B) + 10 \log (S_B)$$
$$+ 10 \log (D_B) + C_B + \Delta r + \Delta T \tag{13.5}$$

FIGURE 13.20   **Sound Power Levels of Abrupt and Gradual Area Transitions from 600 mm x 600 mm to 600 mm x 200 mm Duct Cross Sections (Fry, 1988)**
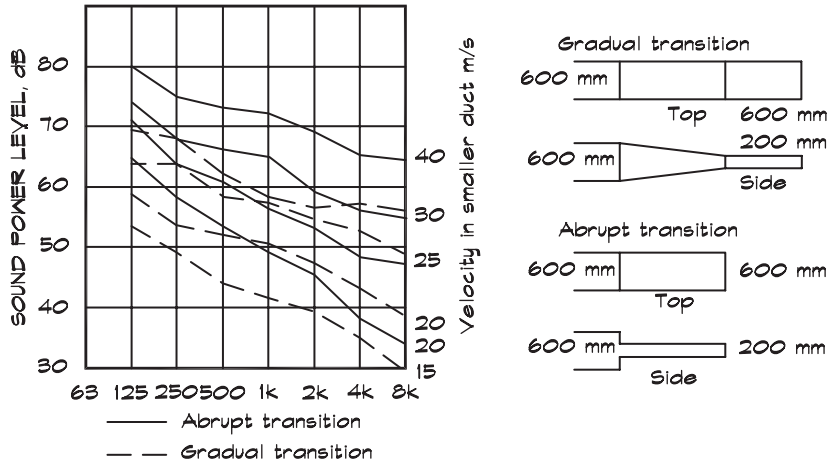
FIGURE 13.21   **Elbows, Junctions, and Branch Takeoffs**
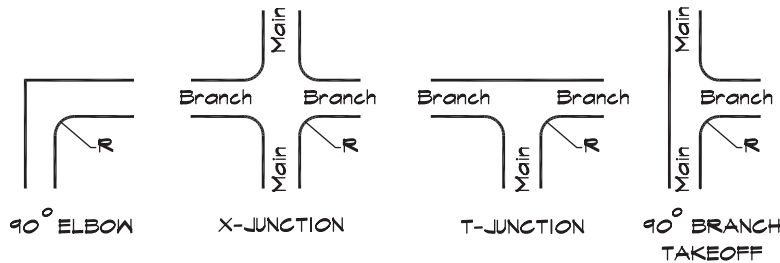
where $L_{W\ OCT}$ = octave band sound power level (dB re 10^{-12} Watts)
f_0 = center frequency of the octave band (Hz)
K_J = characteristic spectrum of the junction or turn, based on the Strouhal number
U_B = velocity in the branch duct (ft/s)
S_B = cross sectional area of the branch duct (ft^2)
D_B = equivalent diameter of the branch duct or in the case of junctions, $D_B = \sqrt{4\ S_B/\pi}$ (ft)
C_B = a constant which depends on the type of branch or junction

The flow velocity in the branch is calculated using

$$U_B = Q_B/(60\ S_B)\ \text{(ft/s)} \tag{13.6}$$

where Q_B = flow volume in the branch, (cfm)

The term Δr is a correction for the roundness of the bend or elbow associated with the turn or junction (Reynolds, 1990)

$$\Delta r = \left\{ 1.0 - \frac{R_D}{0.15} \right\} \left[6.793 - 1.86 \log (S_t) \right] \tag{13.7}$$

where R_D is the rounding parameter $R_D = \dfrac{R}{12\,D_B}$ for the radius, R (inches), of the inside edge of the bend, and $S_t = f_0\,D_B/U_B$ is the Strouhal number.

The term ΔT is a correction for upstream turbulence, which is applied only when there are dampers, elbows, or branch takeoffs upstream, and within five main duct diameters, of the turn or junction under consideration.

$$\Delta T = -1.667 + 1.8\,m - 0.133\,m^2 \tag{13.8}$$

$$m = U_M/U_B \tag{13.9}$$

where U_M = velocity in the main duct (ft/min)
       U_B = velocity in the branch duct (ft/min)

The characteristic spectrum K_J in Eq. 13.5 may be calculated (Reynolds, 1990) using

$$\begin{aligned} K_J = {} & -21.61 + 12.388\,m^{0.673} \\ & - 16.482\,m^{-0.303} \log (S_t) \\ & - 5.047\,m^{-0.254} \log (S_t)^2 \end{aligned} \tag{13.10}$$

Finally the correction term C_B depends on the type of junction in Fig. 13.21.

For X - junctions

$$C_B = 20 \log \left[\frac{D_M}{D_B} \right] + 3 \tag{13.11}$$

and for T junctions

$$C_B = 3 \tag{13.12}$$

For 90° elbows without turning vanes,

$$C_B = 0 \tag{13.13}$$

For a 90° branch takeoff,

$$C_B = 20 \log \left[\frac{D_M}{D_B} \right] \tag{13.14}$$

Air Generated Noise in Dampers

Damper noise follows the same general spectrum equation (Eq. 13.5) as was used for branches and turns, although the terms are defined somewhat differently

$$L_{W \text{ OCT}}(f_0) = K_D + 10 \log (f_0/63) + 50 \log (U_C)$$
$$+ 10 \log (S) + 10 \log (D_H) + C_D \tag{13.15}$$

where $L_{W \text{ OCT}}$ = octave band sound power level (dB re 10^{-12} Watts)
   f_0 = center frequency of the octave band (Hz)
   K_D = characteristic spectrum of the damper, based on the pressure loss factor and the Strouhal number
   U_C = flow velocity in the constricted part of the duct (ft/s)
   S = cross sectional area of the branch duct (ft^2)
   D_H = duct height normal to the damper axis (ft)

Before solving Eq. 13.15, several preliminary calculations must be undertaken. The characteristic spectrum is determined from the Strouhal number, which depends on the velocity, the blockage factor, and the pressure loss coefficient, C.

The pressure loss coefficient in FP units is

$$C = 15.9 \cdot 10^6 \frac{\Delta P}{(Q/S)^2} \tag{13.16}$$

where ΔP = pressure drop across the fitting (in. w.g.)
   Q = flow volume, (cfm)

The blockage factor, B, for multiblade dampers and elbows with turning vanes is

$$B = \frac{\sqrt{C} - 1}{C - 1} \quad \text{for } C \neq 1 \tag{13.17}$$

or

$$B = 0.5 \quad \text{if } C = 1 \tag{13.18}$$

For single blade dampers, it is

$$B = \frac{\sqrt{C} - 1}{C - 1} \quad \text{if } C < 4 \tag{13.19}$$

or

$$B = 0.68 \, C^{-0.15} - 0.22 \quad \text{if } C > 4 \tag{13.20}$$

Next the constricted velocity is calculated using

$$U_c = Q/(60 \text{ SB}) \quad \text{(ft/sec)} \tag{13.21}$$

which gives the Strouhal number

$$S_t = f_0 \, D / U_c \tag{13.22}$$

Having calculated these numbers for the particular fitting we can find the characteristic spectrum for dampers (Reynolds, 1990)

$$K_D = -36.6 - 10.7 \log (S_t) \quad \text{for } S_t \le 25$$
$$K_D = -1.1 - 35.9 \log (S_t) \quad \text{for } S_t > 25 \tag{13.23}$$

Air Noise Generated by Elbows with Turning Vanes

For elbows with turning vanes we use Ver's equation with a slightly different definition of the terms

$$L_{W \, OCT}(f_0) = K_T + 10 \log (f_0/63) + 50 \log (U_C)$$
$$+ 10 \log (S) + 10 \log (D_C) + 10 \log n \tag{13.24}$$

where $L_{W \, OCT}$ = octave band sound power level (dB re 10^{-12} Watts)
f_0 = center frequency of the octave band (Hz)
K_T = characteristic spectrum of an elbow with turning vanes
U_C = flow velocity in the constricted part of the flow field (ft/s)
S = cross sectional area of the elbow (ft^2)
D_C = chord length of a typical vane (in)
n = number of turning vanes

Figure 13.22 shows the definition of the chord length.
   The characteristic spectrum (Reynolds, 1990) is

$$K_T = -47.5 - 7.69 \, [\log (S_t)]^{2.5} \tag{13.25}$$

where the Strouhal number in Eq. 13.22 is calculated from the pressure loss coefficient in Eq. 13.16, the blockage factor,

$$B = \frac{\sqrt{C} - 1}{C - 1} \tag{13.26}$$

and the constricted velocity in Eq. 13.21.

FIGURE 13.22   Ninety Degree Elbow with Turning Vanes
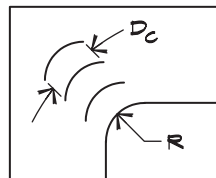
Grilles, Diffusers, and Integral Dampers

Diffuser generated noise is of paramount importance in HVAC noise control since it cannot be attenuated by the addition of downstream devices. Since diffuser noise is primarily dependent on the air velocity through the device, the only method for attenuating it is to reduce it, either by adding additional diffusers, or by increasing the size of the existing diffusers. Often diffuser noise is influenced by the upstream flow conditions that can be modified. Pressure equalizing grilles at the entry to the diffuser can help reduce the contribution due to turbulence.

Sound data on diffuser noise is published by manufacturers in terms of NC levels; however, these are only valid for ideal flow conditions. To achieve ideal conditions, flexible ducts must be straight for at least one duct diameter before the connection to the diffuser and must not be pinched or constricted. Figure 13.23 shows examples of correct and incorrect flexible duct connections.

It should be noted that manufacturer published data are given for one diffuser or, in the case of linear diffusers, for one four-foot long segment, with a power-to-pressure conversion of 10 dB, which corresponds to a room absorption of about 400 sabins and a distance of about 12 ft. The actual power-to-pressure conversion factor should be calculated for the specific room in question. Where there are multiple diffusers in a space, a factor of 10 log n, where n is the number of diffusers or the total number of four-foot segments of linear diffuser, must be added to the published noise levels.

When sound levels from diffusers are not available, they can be approximated using a general equation (Reynolds, 1990). It relates the diffuser noise to the sixth power of the flow

FIGURE 13.23   Correct and Incorrect Diffuser Installation (Fry, 1988)

Basis of manufacturer's rating

Sound levels, same as manufacturer's rating with equalizing grid

Sound levels up to 12 dB higher with no equalizing grid

EFFECT OF CORRECT AND INCORRECT ALIGNMENT OF FLEXIBLE DUCT CONNECTOR

Sound levels same as manufacturer's ratings

Sound levels 12 to 15 dB higher than manufacturer's ratings
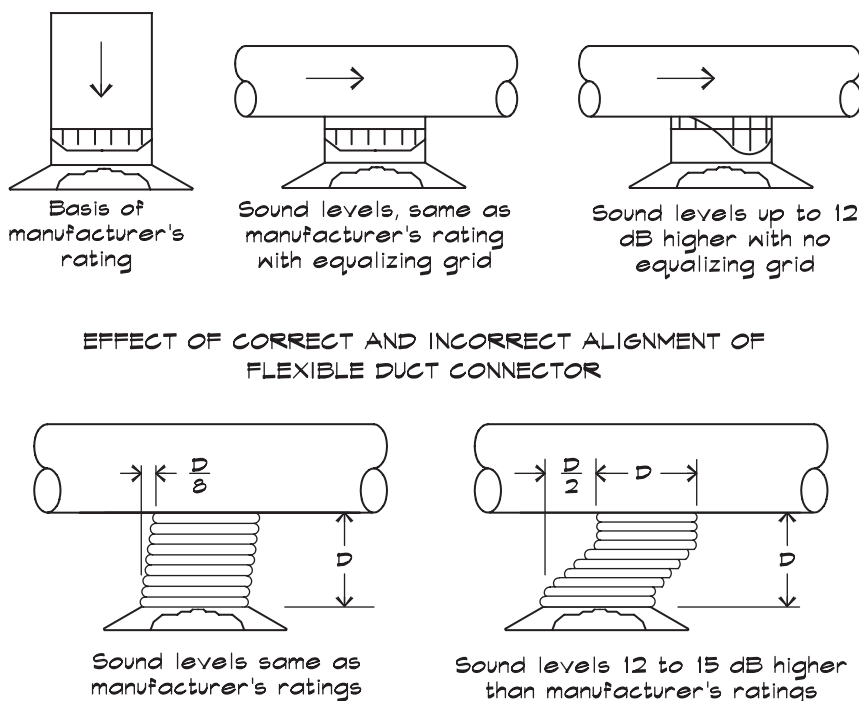
velocity and the third power of the pressure drop.

$$L_w = 10 \log S_G + 30 \log \xi + 60 \log U_G - 31.3 \qquad (13.27)$$

where L_W = overall sound power level (dB re 10^{-12} Watts)
S_G = cross sectional face area of the grille or diffuser (ft^2)
U_G = flow velocity prior to the diffuser (ft/s)
ξ = normalized pressure drop coefficient

It is clear that the noise emitted by diffusers is very dependent on the flow velocity and the formula yields an 18 dB per doubling of velocity relationship. For a given flow volume a doubling of grill area will reduce noise by 15 dB.

The normalized pressure drop is

$$\xi = 334.9 \ \frac{\Delta P}{\rho_0 \ U_G^2} \qquad (13.28)$$

where ΔP = pressure drop across the diffuser (in w.g.)
ρ_0 = density of air (0.075 lb/ft^3)
U_G = flow velocity prior to the diffuser (ft/min)
$= \dfrac{Q}{60 \ S_G}$ (for Q in cfm)

The octave band sound power levels can be calculated from the overall level by adding a correction factor to Eq. 13.27

$$L_{W \ OCT} = L_W + C_D \qquad (13.29)$$

The correction term for round diffusers is

$$C_D = -5.82 - 0.15A - 1.13 \ A^2 \qquad (13.30)$$

and for rectangular (including slot) diffusers,

$$C_D = -11.82 - 0.15A - 1.13 \ A^2 \qquad (13.31)$$

and is normalized to a peak frequency

$$f_P = 48.8 \ U_G \qquad (13.32)$$

The term A is

$$A = N_B \ (f_P) - N_B \ (f) \qquad (13.33)$$

where $N_B(f)$ is the band number of the octave of interest and $N_B(f_P)$ is the band number of the octave where the peak frequency occurs. Octave band numbers are 0 for 32 Hz, 1 for 63 Hz, 2 for 125 Hz, and so forth. So, for example, if the peak frequency falls within the 125 Hz octave band, the band number is 2. The value of A for the 63 Hz octave band would be $A = 2 - 1 = 1$ and would decrease by 1 for each octave above that. The shape of the diffuser spectrum curve is given in Fig. 13.24.

FIGURE 13.24 Generalized Shape of the Diffuser Spectrum (ASHRAE, 1995)
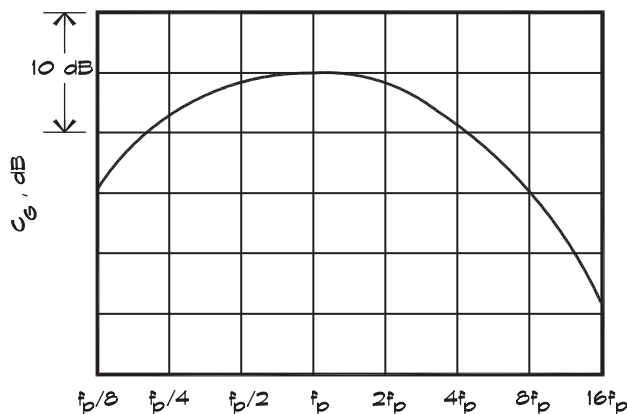
Dampers located close to an outlet diffuser can add appreciably to the noise generated by the termination. First the damper generates vortex shedding in its wake, which is a source of noise. Second, downstream turbulence increases the noise generated by the grille. Manufacturers of these devices can provide sound power levels for a given flow volume. If these are not available it can be assumed that levels will increase 5 dB in all bands with the dampers in the fully open position. As the dampers are closed, there is an increase in the pressure drop across the damper, which restricts the flow. The overall sound power level increases approximately as (Fry, 1988)

$$\Delta L_w = 33 \log (\Delta P/\Delta P_0) \qquad (13.34)$$

where ΔL_W = increase in sound power level radiated by the diffuser (dB)
ΔP = new static pressure drop across the unit (in. w.g.)
ΔP_0 = initial static pressure drop with the damper in place but with the vanes fully open with the same flow volume (in. w.g.)

Figure 13.25 shows the effect of integral dampers on noise radiated by ceiling diffusers for various settings. For dampers and grills to act as separate sources they should be located at least 4 duct diameters apart.

13.5   NOISE FROM OTHER MECHANICAL EQUIPMENT

Air Compressors

Air compressors in buildings generally fall into two categories: small units, under 5 hp, used to provide high pressure air for pneumatically controlled HVAC systems; and large units of up to 100 hp, which provide shop air to machine shops, laboratories, and maintenance areas. Miller (1980) has published sound pressure levels at 3 ft based on measurements of nine machines. Seven of these were reciprocating with motors ranging from 1 to 75 hp, and two were centrifugal, one of 10 hp and another 20 hp. Figure 13.26 reproduces his results. The principal source of air compressor noise is the air intake, which can be treated using a muffler between the filter and the intake manifold.

FIGURE 13.25   Ceiling Diffuser Damper—Sound Power Spectra (Fry, 1988)
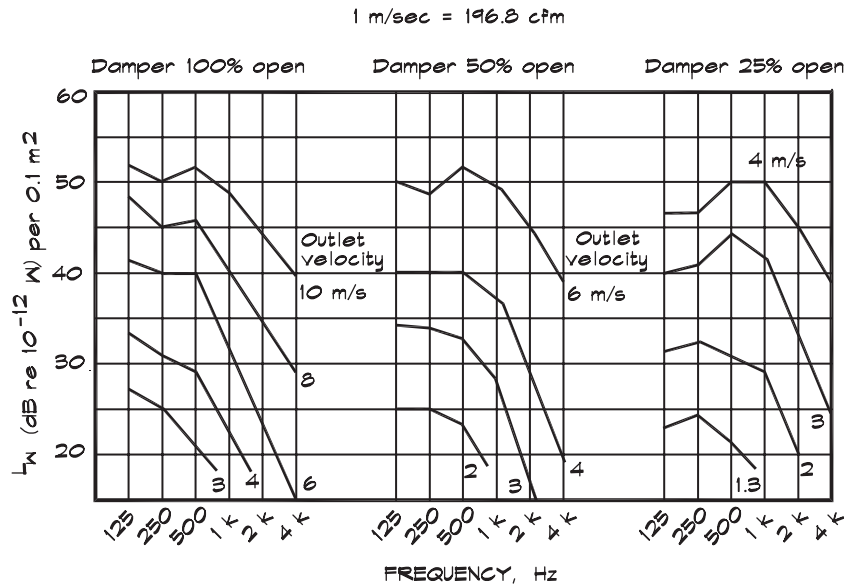
FIGURE 13.26   Sound Pressure Levels of Air Compressors at a Distance of 3 Feet (Miller, 1980)
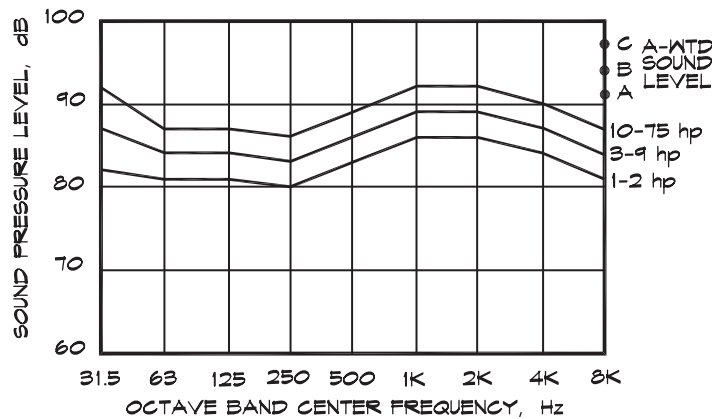
Transformers

Transformers are usually located in an electrical equipment room, where they are sequestered from sensitive receivers. Ideally these rooms do not have common walls or floor-ceiling separations. Transformer noise is created through a process of magnetostriction, an expansion and contraction due to a magnetic field, caused by current within the coils. For a sinusoidal input voltage this phenomenon occurs twice every cycle, at 120 Hz, in single phase units and at harmonics of this frequency. Miller (1980) has published a conversion equation to obtain the sound power spectrum from the manufacturer's NEMA rating (the average of A-weighted sound pressure levels taken at a distance of 1 ft from an imaginary vertical surface passing

TABLE 13.10 **Level Adjustments for the NEMA Rating of a Transformer, dB (Miller, 1980)**

Octave Band Center Frequency, Hz

	31	63	125	250	500	1k	2k	4k	8k
C_T	-1	5	7	2	2	-4	-9	-14	-21

through a string tied around the unit), and the correction term, which includes the 10.5 dB adjustment for the power to pressure conversion. Table 13.10 gives the correction term for an unenclosed transformer.

$$L_w = \text{NEMA rating} + 10 \log S_T + C_T \qquad (13.35)$$

where $L_{w\,OCT}$ = octave band sound pressure level (dB)
        S_T = surface area of the transformer (ft^2)
        C_T = octave band correction (dB)

Over time, transformers can grow noisier as their laminations and tie bolts become loose. Miller cites increases as large as 5 dB at the fundamental and 10 dB in the second and third harmonic frequencies. When transformers are enclosed in small vaults they can induce standing wave patterns in the room, which have the effect of increasing the transmitted power by 6 dB in the same bands.

Transformers that are directly tied to a wall can induce structure-borne noise. Jones (1984) recommends isolation techniques shown in Fig. 13.27 to prevent this. In areas of seismic activity, one or more sway braces may be necessary to provide stability at the top of the unit.

Reciprocating Engines and Emergency Generators

Most large buildings have emergency generators to provide power when the normal sources fail. It is often argued that noise control of emergency generators is unnecessary since they would be used only in an emergency, when noise is a secondary concern. Although this is probably true, generators must be tested periodically, an hour a month, and during these test periods the building functions normally and noise is still a concern. During power outages generators can be needed over longer periods of time.

Generator sets are powered by a diesel, methane, or propane fuel reciprocating engine and radiate sound from their casing, intake, and exhaust. Miller (1980) measured the casing radiated power levels, which followed the relationship

$$L_w = 93 + 10 \log (\text{rated hp}) + A + B + C + D \qquad (13.36)$$

where L_w = overall sound power level (dB)
   rated hp = engine manufacturer's continuous full load rating
             for the engine, (horse power)
 A, B, C, D = correction terms given in Table 13.11 (dB)

Octave-band casing-radiated noise can be obtained from the overall sound power level spectrum by subtracting the levels given in Table 13.12.

FIGURE 13.27   Vibration Isolation of Floor-Mounted Transformers (Jones, 1984)
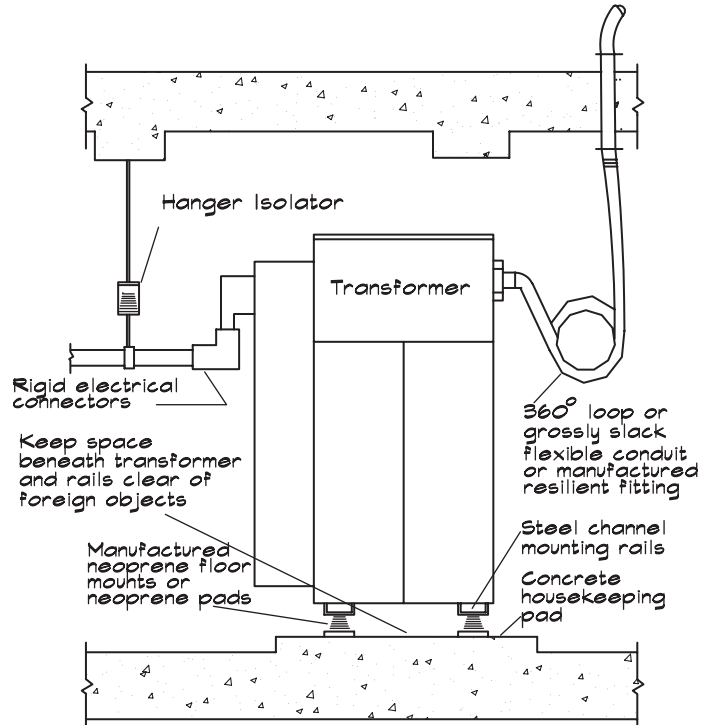
TABLE 13.11   Level Adjustments for Engine Casing Radiated Noise, dB (Miller, 1980)

Speed Correction Term, A	
Under 600 rpm	−5
600 - 1500 rpm	−2
Above 1500 rpm	0
Fuel Correction Term, B	
Diesel fuel only	0
Diesel and/or natural gas	0
Natural gas only (may have small amounts of "pilot oil")	−3
Cylinder Arrangement Term, C	
In-line	0
V-type	−1
Radial	−1
Air Intake Correction Term, D	
Unducted air inlet to unmuffled Roots Blower	+3
Ducted air from outside the room or into muffled Roots Blower	0
All other inlets to engine (with or without turbochargers)	0

Noise radiated from the inlet is usually the same as the casing radiation unless there is a separate ducted inlet to a turbocharger. In these cases the inlet noise is given by

$$L_w = 94 + 5 \log (\text{rated hp}) \tag{13.37}$$

TABLE 13.12 **Frequency Adjustments for Casing Radiated Noise of Reciprocating Engines (Miller, 1980)**

Octave Frequency Band (Hz)	Value to be Subtracted from Sound Power Level, dB			
	Engine Speed Under 600 rpm	Engine Speed 600-1500 rpm		Engine Speed Over 1500 rpm
		Without Roots Blower	With Roots Blower	
31	12	14	22	22
63	12	9	16	14
125	6	7	18	7
250	5	8	14	7
500	7	7	3	8
1000	9	7	4	6
2000	12	9	10	7
4000	18	13	15	13
8000	28	19	26	20
A	4	3	1	2

TABLE 13.13 **Level Adjustments for Turbocharger Air Inlet, dB (Miller, 1980)**

	Octave Band Center Frequency (Hz)									
	31	**63**	**125**	**250**	**500**	**1k**	**2k**	**4k**	**8k**	**A**
Correction	4	11	13	13	12	9	8	9	17	3

Any losses due to inlet ductwork or silencers must be subtracted from the octave band sound power levels. The corrections for each octave band are given in Table 13.13 and are subtracted from the overall sound power level.

The exhaust is the loudest source. The overall sound power level for noise radiated from an unmuffled engine exhaust is

$$L_w = 119 + 10 \log (\text{rated hp}) - T \tag{13.38}$$

where the factor T is the turbocharger correction term (T = 0 dB for no turbocharger and T = 6 dB for an engine with a turbocharger). The effects of any downstream exhaust piping or mufflers must be subtracted from the sound power level in each band. Octave-band adjustments to be subtracted form the overall sound power level are shown in Table 13.14.

TABLE 13.14 **Level Adjustments for Engine Exhaust, dB (Miller, 1980)**

	Octave Band Center Frequency (Hz)									
	31	**63**	**125**	**250**	**500**	**1k**	**2k**	**4k**	**8k**	**A**
Correction	5	9	3	7	15	19	25	35	43	12

14.1 SOUND PROPAGATION THROUGH DUCTS

When sound propagates through a duct system it encounters various elements that provide sound attenuation. These are lumped into general categories, including ducts, elbows, plenums, branches, silencers, end effects, and so forth. Other elements such as tuned stubs and Helmholtz resonators can also produce losses; however, they rarely are encountered in practice. Each of these elements attenuates sound by a quantifiable amount, through mechanisms that are relatively well understood and lead to a predictable result.

Theory of Propagation in Ducts with Losses

Noise generated by fans and other devices is transmitted, often without appreciable loss, from the source down an unlined duct and into an occupied space. Since ducts confine the naturally expanding acoustical wave, little attenuation occurs due to geometric spreading. So efficient are pipes and ducts in delivering a sound signal in its original form, that they are still used on board ships as a conduit for communications. To obtain appreciable attenuation, we must apply materials such as a fiberglass liner to the duct's inner surfaces to create a loss mechanism by absorbing sound incident upon it.

In Chapt. 8, we examined the propagation of sound waves in ducts without resistance and the phenomenon of cutoff. Recall that cutoff does not imply that all sound energy is prevented from being transmitted along a duct. Rather, it means that only particular waveforms propagate at certain frequencies. Below the cutoff frequency only plane waves are allowed, and above that frequency, only multimodal waves propagate.

In analyzing sound propagation in ducts it is customary to simplify the problem into one having only two dimensions. A duct, shown in Fig. 14.1, is assumed to be infinitely wide (in the x dimension) and to have a height in the y dimension equal to h. The sound wave travels along the z direction (out of the page) and its sound pressure can be written as (Ingard, 1994)

$$\mathbf{p}\,(y, z, \omega) = A \, \cos\,(\mathbf{q}_y \, y) \, e^{j\,\mathbf{q}_z\,z} \qquad (14.1)$$

FIGURE 14.1 Coordinate System for Duct Analysis
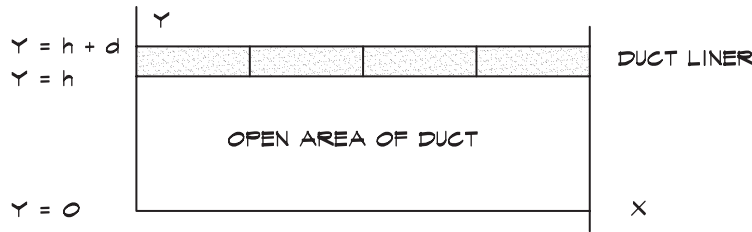
where p = complex sound pressure (Pa)
   A = pressure amplitude (Pa)
   q_z and q_y = complex propagation constant in the z and y
      directions (m^{-1})

   $j = \sqrt{-1}$
   $\omega = 2\pi f$ (rad/s)

The propagation constants have real and imaginary parts as we saw in Eq. 7.79, which can be written as

$$\mathbf{q} = \delta + j\beta \tag{14.2}$$

where the z-axis subscript has been dropped. The value of the imaginary part of the propagation constant, β, in the z direction is dependent on the propagation constant in the y direction, and the normal acoustic impedance of the side wall of the duct or any liner material attached to it. The propagation constants are complex wave numbers and are related vectorially in the same way wave numbers are. As we found in Eq. 8.19,

$$\mathbf{q}_z = \sqrt{(\omega/c)^2 - \mathbf{q}_y^2} \tag{14.3}$$

At the side wall boundary the amplitude of the velocity in the y direction can be obtained from Eq. 14.1

$$\mathbf{u}_y = \frac{1}{-j\omega\rho_0} \frac{\partial \mathbf{p}}{\partial y} = \frac{A}{-j\omega\rho_0} \mathbf{q}_y \sin(\mathbf{q}_y \, y) \, e^{j\mathbf{q}_z z} \tag{14.4}$$

The boundary condition at the surface of the absorptive material at $y = h$ is

$$\frac{\mathbf{u}_y}{\mathbf{p}} = \frac{1}{\mathbf{z}_n} \tag{14.5}$$

where $\mathbf{z}_n$ is the normal specific acoustic impedance of the side wall panel material. Substituting Eqs. 14.1 and 14.4 into 14.5 we obtain

$$\mathbf{q}_y \, h \, \tan(\mathbf{q}_y \, h) = \frac{-j \, k \, h \, \rho_0 \, c_0}{\mathbf{z}_n} \tag{14.6}$$

where $k = \omega/c$. Values of the normal impedance for fiberglass materials were given in Chapt. 7 by the Delany and Blazey (1969) equations. Once the material impedance $\mathbf{z}_n$ has

been obtained, the propagation constant $\mathbf{q}_y$ can be extracted numerically from Eq. 14.6. Equation 14.3 then gives us a value for $\mathbf{q}_z$, from which we can solve for its imaginary part, β, in nepers/ft.

The ratio of the pressure amplitudes at two values of z is obtained from Eq. 14.1

$$\left| \frac{\mathbf{p}(0)}{\mathbf{p}(z)} \right| = e^{\beta z} \tag{14.7}$$

from which we obtain the loss in decibels over a given distance *l*

$$\Delta L_{duct} = 20 \log \left| \frac{\mathbf{p}(0)}{\mathbf{p}(z)} \right| = 20 (\beta l) \log (e) \cong 8.68 \, \beta \, l \tag{14.8}$$

In this way we can calculate the attenuation from the physical properties of the duct liner. The lined duct configurations shown in Fig. 14.2 yield equal losses in the lowest mode. The splitters shown on the right of the figure are representative of the configuration found in a duct silencer.

In practice, lined ducts and silencers are tested in a laboratory by substituting the test specimen for an unlined sheet metal duct having the same face dimension. Figure 14.3 shows measured losses for a lined rectangular duct. The data take on a haystack shape that shifts slightly with flow velocity. At low frequencies the lining is too thin, compared with a wavelength, to have much effect. At high frequencies the sound waves beam and the interaction with the lining at the sides of the duct is minimal. The largest losses are at the mid frequencies, as evidenced by the peak in the data.

Air flow affects the attenuation somewhat. When the sound propagates in the direction of flow, it spends slightly less time in the duct so the low-frequency losses are slightly less. The high frequencies are influenced by the velocity profile, which is higher in the center

FIGURE 14.2 Equivalent Duct Configurations (Ingard, 1994)
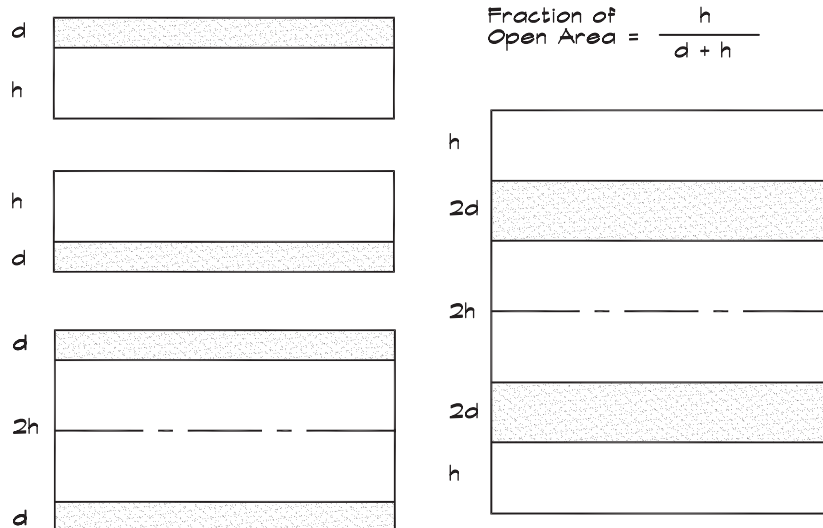
FIGURE 14.3 **Attenuation in a Lined Duct (Beranek and Ver, 1992)**

The effect of flow on the sound attenuation for Mach numbers
M = 0, 0.15, 0.3 for a) sound propagation in the direction of flow
and b) sound propagation against the direction of flow
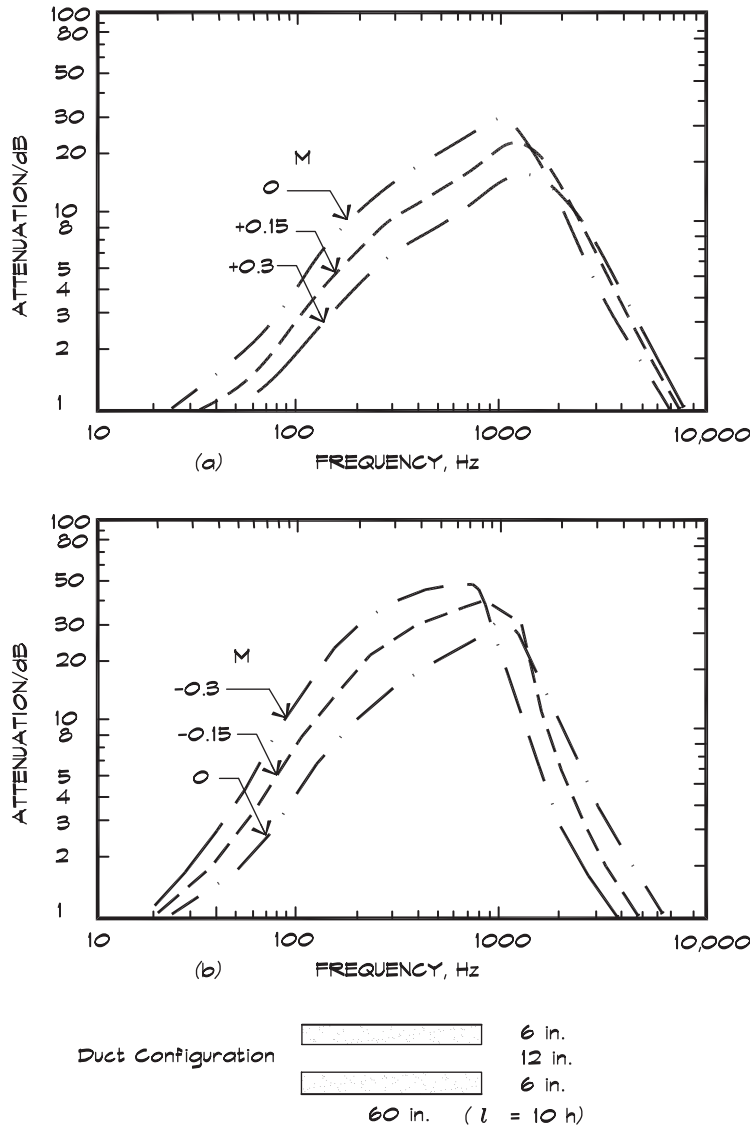
of the duct. The gradient refracts the high frequency energy toward the duct walls yielding somewhat greater losses for propagation in the downstream direction. Figure 14.4 shows this effect.

Ingard (1994) published a generalized design chart in Fig. 14.5 for lined rectangular ducts giving the maximum attainable attenuation in terms of the percentage of the open area of the duct mouth and the resistivity of the liner. The chart is useful for visualizing the effectiveness of lined duct, as well as for doing a calculation of attenuation. The peak in the

FIGURE 14.4 Influence of Air Velocity on Attenuation (IAC Corp., 1989)
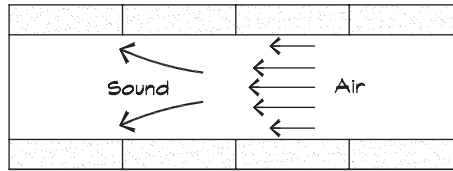
Under FORWARD FLOW conditions, high-frequency sound is refracted toward the duct walls.
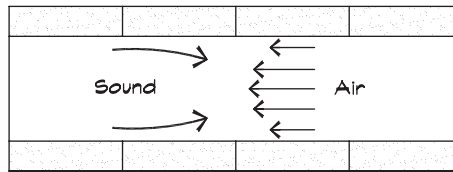
Under REVERSE FLOW conditions, high-frequency sound is refracted away from the walls and toward the center of the duct.

FIGURE 14.5 Approximate Relationship between Optimized Liner Resistance and the Corresponding Maximum Attenuation (Ingard, 1994)
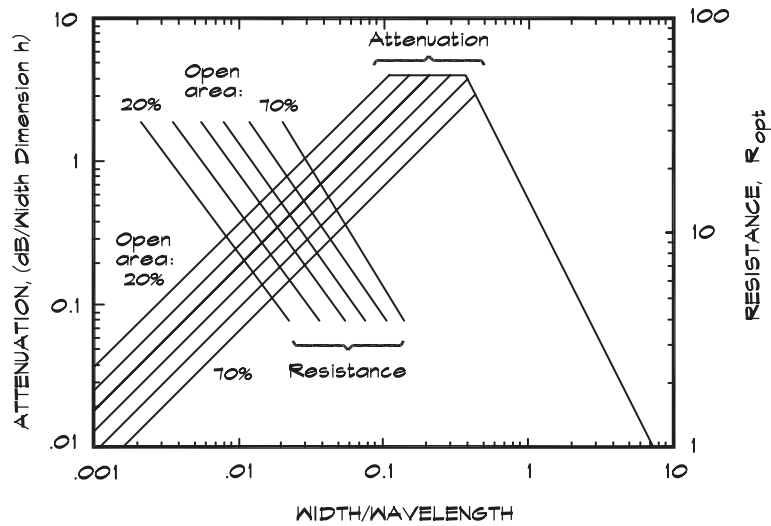
Relationship between the optimized liner resistance and the maximum attenuation that can be achieved for the fundamental mode in a rectangular duct with one side lined with a locally reacting porous liner. The left axis is the attenuation in a length of duct equal to the air channel width h and the right axis is the optimum value of the normalized flow resistance.

curve is extended downward in frequency with lower open area percentages. Thus there is a tradeoff between low-frequency attenuation and back pressure.

Attenuation in Unlined Rectangular Ducts

As a sound wave propagates down an unlined duct, its energy is reduced through induced motion of the duct walls. The surface impedance is due principally to the wall mass, and the duct loss calculation goes much like the derivation of the transmission loss. Circular sheet-metal ducts are much stiffer than rectangular ducts at low frequencies, particularly in their first mode of vibration, called the breathing mode, and therefore are much more difficult to excite. As a consequence, sound is attenuated in unlined rectangular ducts to a much greater degree than in circular ducts.

Since a calculation of the attenuation from the impedance of the liner is complicated, measured values or values calculated from simple empirical relationships are used. Empirical equations for the attenuation can be written in terms of a duct perimeter to area ratio. A large P/S ratio means that the duct is wide in one dimension and narrow in the other, which implies relatively flexible side walls. The attenuation of rectangular ducts in the 63 Hz to 250 Hz octave frequency bands can be approximated by using an equation by Reynolds (1990)

$$\Delta L_{duct} = 17.0 \left(\frac{P}{S} \right)^{-0.25} f^{-0.85} l \tag{14.9}$$

for $\dfrac{P}{S} \geq 3$ and

$$\Delta L_{duct} = 1.64 \left(\frac{P}{S} \right)^{0.73} f^{-0.58} l \tag{14.10}$$

for $\dfrac{P}{S} < 3$.

Note that these formulas are unit sensitive. The perimeter must be in feet, the area in square feet, and the length, l, in feet. Above 250 Hz the loss is approximately

$$\Delta L_{duct} = 0.02 \left(\frac{P}{S} \right)^{0.8} l \tag{14.11}$$

When the duct is externally wrapped with a fiberglass blanket the surface mass is increased, and so is the low-frequency attenuation. Under this condition, the losses given in Eqs. 14.9 and 14.10 are multiplied by a factor of two.

Attenuation in Unlined Circular Ducts

Unlined circular ducts have about a tenth the loss of rectangular ducts. Typical losses are given in Table 14.1

TABLE 14.1   Losses in Unlined Circular Ducts

Frequency (Hz)	63	125	250	500	1000	2000	4000
Loss (dB/ft)	0.03	0.03	0.03	0.05	0.07	0.07	0.07

TABLE 14.2   Constants Used in Eq. 14.12 (Reynolds, 1990)

Octave Band Center Frequency (Hz)

	63	125	250	500	1000	2000	4000	8000
B	0.0133	0.0574	0.2710	1.0147	1.7700	1.3920	1.5180	1.5810
C	1.959	1.410	0.824	0.500	0.695	0.802	0.451	0.219
D	0.917	0.941	1.079	1.087	0.000	0.000	0.000	0.000

Attenuation in Lined Rectangular Ducts

When a duct is lined with an absorbent material such as a treated fiberglass board, sound propagating in the duct is attenuated through its interaction with the material as discussed earlier. A regression equation for the insertion loss of rectangular ducts has been published by Reynolds (1990).

$$\Delta L_{duct} = B \left(\frac{P}{S}\right)^C t^D l \tag{14.12}$$

where P = perimeter of the duct (ft)
        S = area of the duct (sq ft)
        l = length of the duct (ft)
        t = thickness of the lining (inches)

Table 14.2 lists the constants B, C, and D.

Reynolds' equation was based on data using a 1 to 2 inch (25 mm to 51 mm) thick liner having a density of 1.5 to 3 lbs / ft^3 (24 to 48 kg / m^3). Linings less than 1 inch (25 mm) thick are generally ineffective. The P/S ratios ranged from 1.1667 to 6, in units of feet. The equation is valid within these ranges.

The insertion loss of ducts is measured by substituting a lined section for an unlined section and reporting the difference. Since there may be a significant contribution to the overall attenuation furnished by the induced motion of the side walls, the unlined attenuation should be added to the lined attenuation to obtain an overall value.

Attenuation of Lined Circular Ducts

An empirical equation for the losses in lined circular ducts has been developed in the form of a third order polynomial regression by Reynolds (1990).

$$\Delta L_d = \left[A + Bt + Ct^2 + Dd + Ed^2 + Fd^3\right] l \tag{14.13}$$

where t = thickness of the lining (inches)
        d = interior diameter of the duct (inches)
        l = length of the duct (ft)

The constants are given in Table 14.3

Reynolds developed this relationship for spiral ducts having 0.75 lb/cu ft (12 kg/cu m) density fiberglass lining in thicknesses ranging from 1 to 3 inches (25 to 76 mm) thick with a 25% open perforated metal facing. The inside diameters of the tested ducts ranged from 6 to 60 inches (0.15 to 1.5 m).

TABLE 14.3   Constants Used in Eq. 14.13 (Reynolds, 1990)

Freq., Hz	A	B	C	D	E	F
63	0.2825	0.3447	−5.251E-2	−3.837E-2	9.132E-4	−8.294E-6
125	0.5237	0.2234	−4.936E-3	−2.724E-2	3.377E-4	−2.490E-6
250	0.3652	0.7900	−0.1157	−1.834E-2	−1.211E-4	2.681E-6
500	0.1333	1.8450	−0.3735	−1.293E-2	8.624E-5	−4.986E-6
1000	1.9330	0.0000	0.0000	6.135E-2	−3.891E-3	3.934E-5
2000	2.7300	0.0000	0.0000	−7.341E-2	4.428E-4	1.006E-6
4000	2.8000	0.0000	0.0000	−0.1467	3.404E-3	−2.851E-5
8000	1.5450	0.0000	0.0000	−5.452E-2	1.290E-3	−1.318E-5

Because of flanking paths, the duct attenuation in both round and rectangular ducts is limited to 40 dB. As with rectangular ducts, the unlined attenuation may be added to the lined attenuation. For circular ducts it is such a small contribution that it is usually ignored.

Flexible and Fiberglass Ductwork

It is frequently the case that the last duct run in a supply branch is made with a round flexible duct with a lightweight fiberglass fill, surrounded on the outside with a light plastic membrane, and lined on the inside with a fabric liner. The published insertion losses of these flexible ducts are quite high, sometimes as much as 2 to 3 dB per foot or more. Table 14.4 is based on data published in ASHRAE (1995).

Since the insertion loss testing is done by replacing a section of unlined sheet-metal duct with the test specimen, some of the low-frequency loss obtained from flexible duct occurs due to breakout. This property can be used to advantage, since in tight spaces where there is little room for a sound trap, flexible duct surrounded with fiberglass batt can be used to construct a breakout silencer. Such a silencer can be built between joists in a floor-ceiling to isolate exterior noise that might otherwise enter a dwelling through an exhaust duct attached to a bathroom fan. A serpentine arrangement of flexible duct 6 to 8 feet in length in an attic can often control the noise from a fan coil unit located in this space, so long as there is a drywall or plaster ceiling beneath it.

The transmission loss properties of flexible duct are not well documented; however, a conservative approach is to assume that the flex duct is not present and to calculate the insertion loss of the ceiling material. When the attenuation of the flexible duct is greater than the insertion loss of the ceiling the latter is used.

End Effect in Ducts

When a sound wave propagates down a duct and encounters a large area expansion, such as that provided by a room, there is a loss due to the area change known as the end effect. The end effect does not always follow the simple relationship shown in Chapt. 8, which was derived assuming that the lateral dimensions of both ducts were small compared with a wavelength. At low frequencies sound waves expand to the boundaries of the duct. At very high frequencies the sound entering a room from a duct tends to radiate like a piston

TABLE 14.4   Lined Flexible Duct Insertion Loss, dB (ASHRAE, 1995)

Diameter (in/mm)	Length (ft/m)	Octave Band Center Frequency—Hz						
		63	125	250	500	1000	2000	4000
4/100	12/3.7	6	11	12	31	37	42	27
	9/2.7	5	8	9	23	28	32	20
	6/1.8	3	6	6	16	19	21	14
	3/0.9	2	3	3	8	9	11	7
5/127	12/3.7	7	12	14	32	38	41	26
	9/2.7	5	9	11	24	29	31	20
	6/1.8	4	6	7	16	19	21	13
	3/0.9	2	3	4	8	10	10	7
6/152	12/3.7	8	12	17	33	38	40	26
	9/2.7	6	9	13	25	29	30	20
	6/1.8	4	6	9	17	19	20	13
	3/0.9	2	3	4	8	10	10	7
7/178	12/3.7	8	12	19	33	37	38	25
	9/2.7	6	9	14	25	28	29	19
	6/1.8	4	6	10	17	19	19	13
	3/0.9	2	3	5	8	9	10	6
8/203	12/3.7	8	11	21	33	37	36	22
	9/2.7	6	8	16	25	28	28	18
	6/1.8	4	6	11	17	19	19	12
	3/0.9	2	3	5	8	9	9	6
9/229	12/3.7	8	11	22	33	37	36	22
	9/2.7	6	8	17	25	28	27	17
	6/1.8	4	6	11	17	19	18	11
	3/0.9	2	3	6	8	9	9	6
10/254	12/3.7	8	10	22	32	36	34	21
	9/2.7	6	8	17	24	27	26	16
	6/1.8	4	5	11	16	18	17	11
	3/0.9	2	3	6	8	9	9	5
12/305	12/3.7	7	9	20	30	34	31	18
	9/2.7	5	7	15	23	26	23	14
	6/1.8	3	5	10	15	17	16	9
	3/0.9	2	2	5	8	9	8	5
14/356	12/3.7	5	7	16	27	31	27	14
	9/2.7	4	5	12	20	23	20	11
	6/1.8	3	4	8	14	16	14	7
	3/0.9	1	2	4	7	8	7	4
16/406	12/3.7	2	4	9	23	28	23	9
	9/2.7	2	3	7	17	21	17	7
	6/1.8	1	2	5	12	14	12	5
	3/0.9	1	1	2	6	7	6	2

in a baffle and forms a beam. Therefore it does not interact with the sides of the duct and is relatively unaffected by the end effect. An empirical formula for calculating end effect has been published by Reynolds (1990). Its magnitude depends on the size of the duct, measured in wavelengths. This is expressed in the formula as a frequency-width product. The attenuation associated with a duct terminated in free space is

$$\Delta L_{end} = 10 \log \left[1 + \left(\frac{c_0}{\pi f d} \right)^{1.88} \right] \tag{14.14}$$

and for a duct terminated flush with a wall

$$\Delta L_{end} = 10 \log \left[1 + \left(\frac{0.8 \, c_0}{\pi f d} \right)^{1.88} \right] \tag{14.15}$$

where d is the diameter of the duct in units consistent with those of the sound velocity. If the duct is rectangular the effective diameter is

$$d = \sqrt{\frac{4 S}{\pi}} \tag{14.16}$$

where S is the area of the duct. End effect attenuation does not occur when the duct is terminated in a diffuser, since these devices smooth the impedance transition between the duct and the room.

Split Losses

When there is a division of the duct into several smaller ducts there is a distribution of the sound energy among the various available paths. The loss is derived in much the same way as was Eq. 8.32; however, multiple areas are taken into account. The split loss in propagating from a main duct into the ith branch is

$$\Delta L_{split} = 10 \log \left[1 - \left(\frac{\sum S_i - S_m}{\sum S_i + S_m} \right)^2 \right] + 10 \log \left[\left(\frac{S_i}{\sum S_i} \right) \right] \tag{14.17}$$

where S_m = area of the main feeder duct (ft^2 or m^2)

S_i = area of the i th branch (ft^2 or m^2)

$\sum S_i$ = total area of the individual branches that
continue on from the main duct (ft^2 or m^2)

The first term in Eq. 14.17 comes from reflection, which occurs from the change in area, when the total area of the branches is not the same as the area of the main duct and the frequency is below cutoff. The second term comes from the division of acoustic power among the individual branches, which is based on the ratio of their areas.

Elbows

A sharp bend or elbow can provide significant high-frequency attenuation, particularly if it is lined. In order for a bend to be treated as an elbow its turn angle must be greater than 60°.

TABLE 14.5   **Insertion Loss of Unlined and Lined Square Elbows without Turning Vanes**

f w	Insertion Loss, dB	
	Unlined	**Lined**
f w < 1.9	0	0
1.9 < f w < 3.8	1	1
3.8 < f w < 7.5	5	6
7.5 < f w < 15	8	11
15 < f w < 30	4	10
f w > 30	3	10

The term f w = f times w, where f is the octave-band center frequency (kHz) and w is the width of the elbow (in).

TABLE 14.6   **Insertion Loss of Unlined and Lined Square Elbows with Turning Vanes**

f w	Insertion Loss, dB	
	Unlined	**Lined**
f w < 1.9	0	0
1.9 < f w < 3.8	1	1
3.8 < f w < 7.5	4	4
7.5 < f w < 15	6	7
f w > 15	4	7

The losses in unlined elbows are minimal, particularly if the duct is circular.

TABLE 14.7   **Insertion Loss of Round Elbows**

f w	Insertion Loss, dB
f w < 1.9	0
1.9 < f w < 3.8	1
3.8 < f w < 7.5	2
f w > 15	3

To be considered a lined elbow, the lining must extend two duct widths (in the plane of the turn) beyond the outside of the turn, and the total thickness of both sides must be at least 10% of the duct width. Reynolds (1990) has published data on unlined rectangular elbows, given in Tables 14.5 and 14.6 and for round elbows, shown in Table 14.7.

Lined round elbow losses can be calculated using an empirical regression formula published by Reynolds (1990). The testing was done on double-wall circular ducts having a perforated inner wall, with an open area of 25%, and the space between filled with 0.75 lb/cu ft (12 kg/cu m) fiberglass batt, between 1 to 3 inches (25–75 mm) thick. The ducts ranged

FIGURE 14.6 **Schematic of a Plenum Chamber**
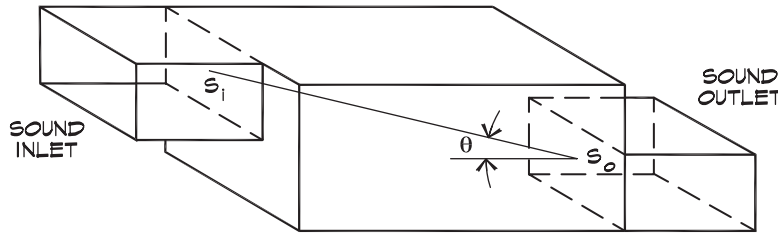
from 6 inches to 60 inches (150–1500 mm) in diameter. For elbows where $6 \leq d \leq 18$ inches (150–750 mm),

$$
\Delta L_e \left(\frac{d}{r}\right)^2 = 0.485 + 2.094 \log (fd) + 3.172 [\log (fd)]^2
$$
$$
- 1.578 [\log (fd)]^4 + 0.085 [\log (fd)]^7
$$

(14.18)

and for elbows where $18 < d \leq 60$ inches (750–1500 mm),

$$
\Delta L_e \left(\frac{d}{r}\right)^2 = -1.493 + 0.538 \, t + 1.406 \log (fd) + 2.779 [\log (fd)]^2
$$
$$
- 0.662 [\log (fd)]^4 + 0.016 [\log (fd)]^7
$$

(14.19)

where ΔL_e = attenuation due to the elbow (dB)
   d = diameter of the duct (in)
   r = radius of the elbow at its centerline (in)
   t = thickness of the liner (in)
   f = center frequency of the octave band (kHz)

Note that if calculated values are negative, the loss is set to zero. In the ducts tested, the elbow radius geometry followed the relationship $r = 1.5 \, d + 3 \, t$.

14.2   SOUND PROPAGATION THROUGH PLENUMS

A plenum is an enclosed space that has a well-defined entrance and exit, which is part of the air path, and that includes an increase and then a decrease in cross-sectional area. The geometry is shown in Fig. 14.6. A return-air plenum located above a ceiling may or may not be an acoustical plenum. If it is bounded by a drywall or plaster ceiling, it can be modeled as an acoustic plenum; however, if the ceiling is constructed of acoustical tile, it is usually not. Rooms that form part of the air passageway are modeled as plenums. For example a mechanical equipment room can be a plenum when the return air circulates through it. In this case the intake air opening on the fan is the plenum entrance.

Plenum Attenuation—Low-Frequency Case

Plenum attenuation depends on the relationship between the size of the cavity and the wavelength of the sound passing through it. When the wavelength is large compared with the cross-sectional dimension—that is, below the duct cutoff frequency—a plenum is modeled as a muffler, using plane wave analysis. This approach follows the same methodology

used in Chapt. 8 for plane waves incident on an expansion and contraction, which was treated in Eqs. 8.35 and 8.36. The transmissivity can be written in terms of the area ratio $m = S_2/S_1$

$$\alpha_t = \frac{4}{4 \cos^2 k\,l + \left(m + \dfrac{1}{m}\right)^2 \sin^2 k\,l} \tag{14.20}$$

When the plenum is a lined chamber having a certain duct loss per unit length, the wave number k within that space becomes a complex propagation constant **q**, having an imaginary term $j\,\beta$. The plenum attenuation is then given by (Davis et al., 1954)

$$\Delta L_p = 10 \log \left[\begin{array}{l} \left(\cosh[\beta\,l] + \dfrac{1}{2}\left[m + \dfrac{1}{m}\right] \sinh[\beta\,l] \right)^2 \\[4pt] \times \cos^2\left(\dfrac{2\,\pi\,f\,l}{c_0}\right) \\[8pt] + \left(\sinh[\beta\,l] + \dfrac{1}{2}\left[m + \dfrac{1}{m}\right] \cosh[\beta\,l] \right)^2 \\[4pt] \times \sin^2\left(\dfrac{2\,\pi\,f\,l}{c_0}\right) \end{array} \right] \tag{14.21}$$

The loss term, $\beta\,l$, due to the plenum liner, can be calculated using empirical equations for a lined rectangular duct (Reynolds, 1990)

$$\begin{array}{ll} 63\,\text{Hz} & \beta\,l = \left[0.00153\,(P/S)^{1.959}\,t^{0.917}\right] l \\[4pt] 125\,\text{Hz} & \beta\,l = \left[0.00662\,(P/S)^{1.410}\,t^{0.941}\right] l \\[4pt] 250\,\text{Hz} & \beta\,l = \left[0.03122\,(P/S)^{0.824}\,t^{1.079}\right] l \\[4pt] 500\,\text{Hz} & \beta\,l = \left[0.11690\,(P/S)^{0.500}\,t^{1.087}\right] l \end{array} \tag{14.22}$$

where β = attenuation in the open area of the plenum (nepers/ft
      or dB/8.68 ft)
   P/S = perimeter of the cross - section of the plenum divided
      by the area (ft^{-1})
   t = thickness of the fiberglass liner (in)
   l = length of the plenum (ft)

Plenum Attenuation—High Frequency Case

When the wavelength is not large compared with the dimensions of the central cross section, the plane wave model is no longer appropriate, since the plenum behaves more like a room than a duct. Under these conditions we return to the methodology previously developed for the behavior of sound in rooms. First, we assume that the sound propagating down a duct and into a plenum is nearly plane, so the energy entering the plenum is

$$W_i = S_i\,I_i \tag{14.23}$$

and using Eq. 2.74, the direct field intensity at the outlet is

$$I_o = \frac{S_i \, I_i \, Q_i}{4 \pi \left[r + \sqrt{\dfrac{S_i \, Q_i}{4 \pi}} \right]^2}$$ (14.24)

The direct field energy leaving the plenum is

$$W_o = S_o \cos \theta \, I_o$$ (14.25)

and the ratio of the direct field outlet energy to the inlet energy is

$$\frac{W_o}{W_i} = \frac{Q_i \, S_o \, \cos \theta}{4 \pi \left[r + \sqrt{\dfrac{S_i \, Q_i}{4 \pi}} \right]^2}$$ (14.26)

A similar treatment can be done for the reverberant energy, with the intensity in a reverberant field, from Eqs. 8.79 and 8.83

$$I_o = \frac{W_i}{R}$$ (14.27)

so that the reverberant field power out is

$$W_o = S_o \, I_o = \frac{W_i \, S_o}{R}$$ (14.28)

Combining the direct and reverberant field contributions the overall transmission loss is

$$\Delta L_p = 10 \log \frac{W_o}{W_i} = 10 \log \left\{ \frac{Q_i \, S_o \, \cos \theta}{4 \pi \left[r + \sqrt{\dfrac{S_i \, Q_i}{4 \pi}} \right]^2} + \frac{S_o}{R} \right\}$$ (14.29)

where ΔL_p = attenuation due to the plenum (dB)
   S_i = sound inlet area of the plenum (m^2 or ft^2)

   Q_i = directivity of the inlet
   S_o = sound outlet area of the plenum (m^2 or ft^2)

   R = room constant of the plenum
      = $S_p \, \bar{\alpha} / (1 - \bar{\alpha})$ (m^2 or ft^2)

   S_p = interior surface area of the plenum (m^2 or ft^2)
   θ = angle between the inlet and the outlet
   r = distance between the inlet and the outlet (m or ft)

When the characteristic entrance dimension is small compared with the inlet to outlet distance, $\sqrt{\dfrac{S_i\,Q_i}{4\,\pi}} \ll r$, Eq. 14.28 can be simplified to (Wells, 1958)

$$\Delta\,L_p = 10\log\left\{\frac{S_o\cos\theta}{4\,\pi r^2} + \frac{S_o}{R}\right\} \qquad (14.30)$$

which assumes that the inlet directivity is one.

These plenum equations begin with the assumption that the inlet and outlet waveforms are planar. At high frequencies the field at the exit can be semidiffuse rather than planar, particularly above the cutoff frequency. This is similar to the situation encountered in the transmission from a reverberant space through an open door, which was discussed in Chapt. 10. When the inlet condition is semidiffuse and the outlet condition is planar, the plenum is 3 dB more effective than Eq. 14.28 predicts, since there is added attenuation through the conversion of the waveform. If the outlet condition is semidiffuse and the inlet planar, the plenum is 3 dB less effective since there is more energy leaving than predicted by the plane wave relationship. Usually semidiffuse conditions occur when the inlet and outlet openings are large, so that the frequencies are above cutoff, and the upstream and downstream duct lengths are short. If both inlet and outlet conditions are semidiffuse, these relations still hold since the extra energy is passed along from the inlet to the outlet.

Sometimes, the Sabine absorption coefficients of plenum materials are greater than one at certain frequencies, and in many instances a large fraction of the plenum surface is treated with such a material. In these cases the average absorption coefficient may calculate out greater than one, and the room constant is not defined. As a practical guide, when the Norris Eyring room constant is employed a limiting value of the average absorption coefficient should be established, on the order of 0.98.

As was discussed previously, a mechanical plenum is not always an acoustic plenum. For example, if air is returned through the space above an acoustical tile ceiling, the return-air plenum is not an acoustic plenum since the noise breaks out of the space through the acoustical tile ceiling, which has a transmission loss lower than the theoretical plenum loss. The problem is treated as if the return-air duct entering the plenum were the source, and the insertion loss of the acoustical tile is subtracted from the sound power level along with the room correction factor to obtain the sound pressure level in the space. Figure 13.15 gives the insertion loss of acoustical tile materials (Blazier, 1981).

In other cases a duct may act as a plenum. If a flexible duct is enclosed in an attic filled with batt insulation, the sound breaks out of the duct and enters the attic plenum space. At the opposite end of the duct it breaks in again, completing the plenum path. This effect can provide significant low-frequency loss in a relatively short distance, particularly when the length of the duct is maximized by snaking. In this manner flexible ducts can be made into quasi-silencers by locating them in joist or attic spaces that are filled with batt.

14.3   SILENCERS

Silencers are commercially available attenuators specifically manufactured to replace a section of duct. They are available in standard lengths in one-foot increments between 3 and 10 feet, and sometimes in an elbow configuration. They consist of baffles of perforated

FIGURE 14.7 Duct Silencer Construction
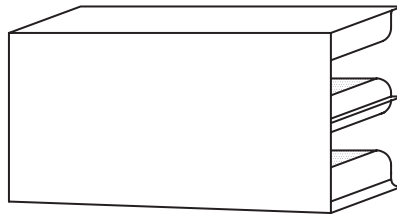
metal filled with fiberglass, which alternate with open-air passage ways. An example is shown in Fig. 14.7.

Dynamic Insertion Loss

Silencer manufacturers publish dynamic insertion loss (DIL) data on their products. This is the attenuation achieved when a given length of unlined duct is replaced with a silencer. Insertion loss data are measured in both the upstream and downstream directions at various air velocities. As with lined ducts, silencer losses in the upstream direction are greater at low frequencies and less at high frequencies.

Insertion loss values are measured in third-octave bands and published as octave-band data. At very low frequencies, below 63 Hz, there are significant comb filtering effects, probably due to the silencer acting as a tuned pipe. In these regions it is more accurate to perform calculations in third-octave bands rather than in octaves. Figure 14.8 gives an example of measured data.

Self Noise

The flow of air through a silencer can generate *self noise*, and sound power level data are published by silencer manufcturers. Self-noise levels are measured on a 24" × 24" (600 × 600 mm) inlet area silencer, and a factor of 10 log (S/S_o) must be added to account

FIGURE 14.8 Silencer Dynamic Insertion Loss Data (PCI Industries, 1999)
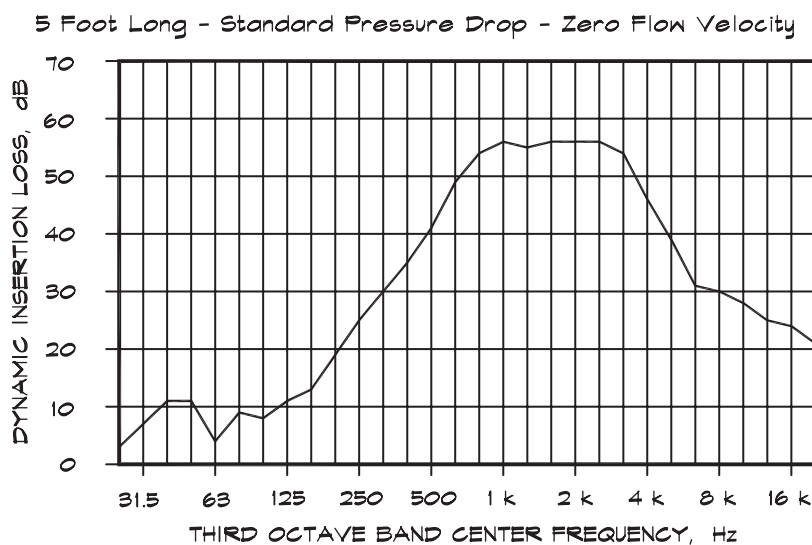
TABLE 14.8   **Silencer Self Noise Octave Band Corrections (dB)**

Freq. (Hz)	63	125	250	500	1k	2k	4k	8k
Correction	4	4	6	8	13	18	23	28

for the actual area of the silencer being used. In most cases $S_o = 4 \, \text{ft}^2$ (0.37 sq m), but when the measurements were made on a different unit, the actual face area must be utilized. Self noise is the power radiated from the receiver end of the silencer and is combined with the sound power levels from other sources exiting the silencer. Most of the high-frequency self noise is generated at the air inlet, so it is attenuated in its passage through the silencer in the downstream direction but not in the upstream direction. Hence high-frequency ($> 1\text{k Hz}$) self noise levels are greater on the return-air side of an HVAC system. Low-frequency self-noise levels do not vary significantly with flow direction.

When self-noise data are not available, they can be estimated using (Fry, 1988)

$$L_w \cong 55 \log \frac{V}{V_0} + 10 \log N + 10 \log \frac{H}{H_0} - 45 \qquad (14.31)$$

where L_w = sound power level generated by the silencer (dB)
V = velocity in the splitter airway (m / s or ft / min)
V_0 = reference velocity (1 for m / s and 196.8 for ft / min)
N = number of air passages
H = height or circumfrence (round) of the silencer (mm or in)
H_0 = reference height (1 for mm or 0.0394 for in)

The spectrum of noise generated by the silencer is calculated by subtracting octave band corrections given in Table 14.8 from the overall sound power level.

Back Pressure

Silencers create some additional back pressure or flow resistance due to the constriction they present. Silencers that minimize this pressure loss are available but there is generally a trade off between back pressure and low-frequency attenuation. Sometimes it is necessary to expand the duct to increase the silencer face area and reduce the pressure loss. It is desirable to minimize the silencer back pressure, usually limiting it to less than 10% of the total rated fan pressure. The position of the silencer in the duct, relative to other components, also affects the back pressure. Figure 14.9 shows published data (IAC Corp.) that give the multiplier of the standard back pressure for various silencer positions.

14.4   BREAKOUT

The phenomenon known as breakout describes the transmission of sound energy from the interior of the duct out through its walls and into an occupied space. The analysis of the process combines elements of duct attenuation as well as the transmission loss through the duct walls.

Silencers Before and After Elbows

Downstream $\quad\longmapsto\quad L \quad\longrightarrow\quad$ Upstream

Pressure Drop = Rated Pressure Drop x Multiplier

Elbows (without turning vanes)   Multiplier
      L = D x 3   1.0
      L = D x 2   1.5
      L = D x 1   2.0

Elbows (with turning vanes)
      L = D x 3   1.0
      L = D x 2   1.2
      L = D x 1   1.75
      L = D x 0.5   3.0
      L = 0   4.0 (Not advised downstream)

Note: Silencer baffles should be parallel to the plane of the turn.
Check manufacturer recommendations for multipliers associated with
individual products.
D = Duct Diameter or Equivalent from Eq. 14.16
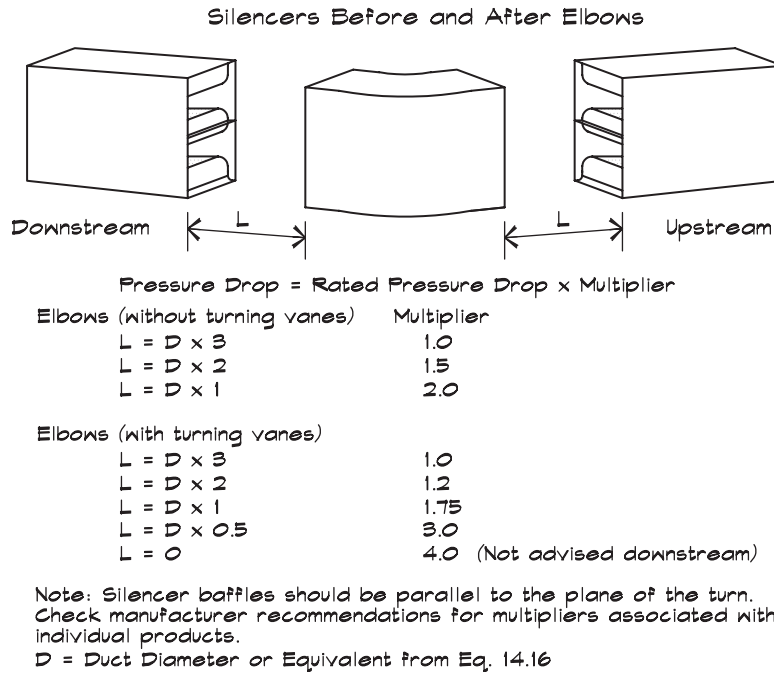
Transmission Theory

The breakout transmission loss defines the relationship between the sound power level entering an incremental slice of the duct at position z and that radiating out through the walls of that slice. Figure 14.10 illustrates the geometry (following Ver, 1983).

The breakout transmission loss at a given point is

$$\Delta L_{TLio} = 10 \log \left[\frac{d W_i (z)}{d W_{io} (z)} \right] \qquad (14.32)$$

FIGURE 14.10   Duct Breakout Geometry

Duct Breakout
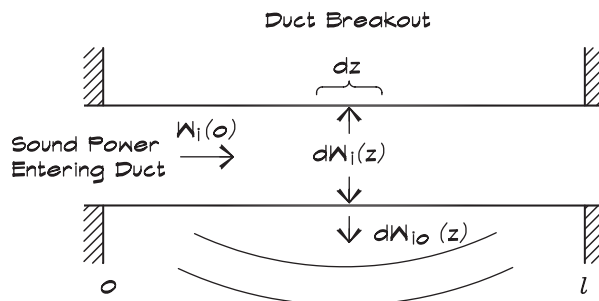
where the sound power incident on the increment of duct length, dz is

$$d W_i (z) = \left| I_i (z) \right| P \, d z = W_i (z) \frac{P}{S} \, d z \tag{14.33}$$

and the radiated power emanating from this slice on the outside of the duct is

$$d W_{io} (z) = d W_i (z) \, 10^{-0.1 \, \Delta L_{TLio}} = \frac{W_i (z)}{S} \, 10^{-0.1 \, \Delta L_{TLio}} \, P \, d z \tag{14.34}$$

If the internal sound power decreases with distance along the duct due to radiation through the duct walls and interaction with the interior surface, according to the relationship

$$W_i (z) = W_i (0) \, e^{-(\tau + 2\beta) \, z} \tag{14.35}$$

the sound power radiated by a length l of duct is given by

$$W_{io} (z) = \int_0^l d W_i (z) \, d z$$

$$= W_i (0) \frac{P}{S} \, 10^{-0.1 \, \Delta L_{TLio}} \int_0^l e^{-(\tau + 2\beta) \, z} \, d z \tag{14.36}$$

which yields

$$W_{io} (z) = W_i (0) \frac{P \ell}{S} \, 10^{-0.1 \, \Delta L_{TLio}} \left[\frac{1 - e^{-(\tau + 2\beta) l}}{(\tau + 2\beta) l} \right] \tag{14.37}$$

and converting to levels

$$L_{wio} = L_{wi} - \Delta L_{TLio} + 10 \log \frac{P l}{S} + D \tag{14.38}$$

where L_{wio} = sound power radiated out of the duct (dB)
L_{wi} = sound power level entering the duct (dB)
ΔL_{TLio} = sound transmission loss from the inside to the outside of the duct (dB)
P = perimeter of the duct (m or ft)
l = length of the duct (m or ft)
S = cross sectional area of the duct (m^2 or ft^2)

D, the duct loss term, is defined as

$$D = 10 \log \left\{ \frac{1 - e^{-(\tau + 2\beta) l}}{(\tau + 2\beta) l} \right\} \tag{14.39}$$

where $\beta = \dfrac{\Delta L_{duct}}{8.68}$ (Nepers / ft or Nepers / m)
ΔL_{duct} = attenuation per unit length inside the duct (dB)
$\tau = \dfrac{P}{S} \, 10^{-0.1 \, \Delta L_{TLio}}$

The D term in Eq. 14.39 can be ignored in short sections of duct, particularly when the duct is unlined and unwrapped. However, for lined duct it should be included. In internally lined ducts the attenuation term is usually larger than the breakout term. In flex or fiberglass ducts the breakout term may dominate, though transmission loss data for these products is difficult to obtain. The breakout sound power can never exceed the internal sound power.

Once the sound has penetrated the duct walls it radiates into the room at high frequencies as a normal line source. Equation 8.85 can be used to predict the expected sound pressure level in the room. Alternatively if the duct is long and unlined it radiates like a line source at high frequencies and the sound pressure level is given by

$$L_p = L_{wio} + 10 \log \left[\frac{Q}{2 \pi r l} + \frac{4}{R} \right] + K \qquad (14.40)$$

where K is 0.1 for SI units and 10.5 for FP units.

At low frequencies if the duct is oriented perpendicular to two parallel walls it may excite resonant modes in the room, in which case the simple diffuse field condition does not exist (Ver, 1984).

Transmission Loss of Rectangular Ducts

The duct transmission loss for breakout of rectangular ducts is divided into regions by frequency that are similar to those discussed in Chapt. 9 for flat panels (ASHRAE, 1987). The transmission loss behavior with frequency is first stiffness controlled, then mass controlled, and finally coincidence controlled. Figure 14.11 shows the general structure of the loss for rectangular ducts.

For all but very small ducts the fundamental wall resonance falls below the frequency range of interest. In this region there is a minimum transmission loss that is dependent on the duct dimensions (a, b in inches and l in feet)

$$\Delta L_{TLio}(min) = 10 \log \left[24 l \left(\frac{1}{a} + \frac{1}{b} \right) \right] \qquad (14.41)$$

At higher frequencies, in the mass controlled region, there is a crossover frequency, below which the transmission loss is affected by the duct dimensions, and above which it follows

Figure 14.11 Interior to Exterior Transmission Loss for Rectangular Ducts (ASHRAE, 1987)
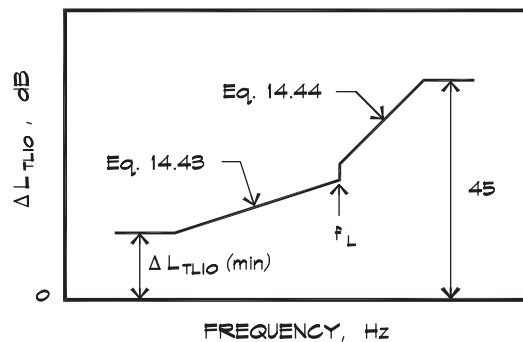
normal mass law. The crossover frequency is given by

$$f_L = \frac{24120}{\sqrt{a\,b}} \qquad (14.42)$$

where a is the larger and b the smaller duct dimension in inches. Below this frequency the transmission loss is given by

$$\Delta L_{TLio} = 10 \log \left[\frac{f\,m_s^2}{a+b} \right] + 17 \qquad (14.43)$$

where f is the frequency, and m_s is the duct wall surface mass in lbs/sq ft.

Above the crossover frequency where the normal mass law holds, the transmission loss for steel ducts is given (as in Eq. 9.21) by

$$\Delta L_{TLio} = 20 \log \left[f\,m_s \right] - K_{TL} \qquad (14.44)$$

where $K_{TL} = 47.3$ in SI units and $= 33.5$ in FP units. At very high frequencies side walls exhibit the normal behavior at the coincidence frequency, but for thin sheet metal this lies above 10 kHz and is of little practical interest.

Transmission Loss of Round Ducts

When sound breaks out of round ducts the definitions in Eq. 14.38 are the same as those used in rectangular ducts. The inside area is $S = \dfrac{\pi\,d^2}{4}$ and the outside transmitting area is $P\,l = 12\,\pi\,d\,l$, where d is in inches and l is in feet. The behavior of round ducts is less well understood and more complicated than with rectangular ducts; however, if the analysis is confined to octave bands, the transmission loss can be approximated by a curve, shown in Fig. 14.12. The low-frequency transmission loss is theoretically quite high because the hoop strength of the ducts in their fundamental breathing mode is very large. In practice we do not achieve the predicted theoretical maximum, which may be as high as 80 dB, and a practical limit of 50 dB is used. As the frequency increases the transmission loss is dependent on the localized bending of the duct walls.

FIGURE 14.12 **Interior to Exterior Transmission Loss for Round Ducts (Reynolds, 1990)**
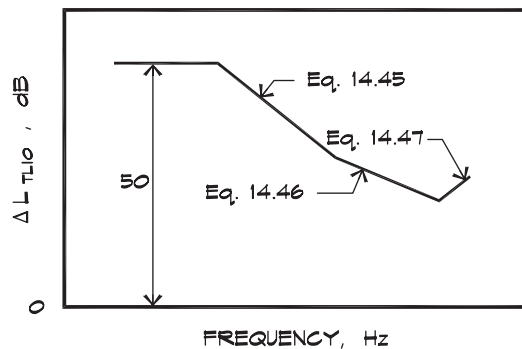
Reynolds (1990) has given three formulas to approximate the curve segments shown in Fig. 14.12. The transmission loss is given by the larger of the following two formulas:

$$\Delta L_{TLio} = 17.6 \log (m_s) - 49.8 \log (f) - 55.3 \log (d) + C_o \qquad (14.45)$$

$$\Delta L_{TLio} = 17.6 \log (m_s) - 6.6 \log (f) - 36.9 \log (d) + 97.4 \qquad (14.46)$$

where ΔL_{TLio} = sound transmission loss from the inside to the outside of the duct (dB)
  m_s = mass/unit area (lb / sq ft)
  d = inside diameter of the duct (in)
  C_o = 230.4 for long - seam ducts or 232.9 for spiral - wound ducts

In the special case where the frequency is 4000 Hz and the duct is greater than or equal to 26 inches in diameter there is a coincidence effect and

$$\Delta L_{TLio} = 17.6 \log (m_s) - 36.9 \log (f) + 90.6 \qquad (14.47)$$

Since the maximum allowable level is 50 dB, if the calculated level exceeds this limit the transmission loss is set to 50.

Transmission Loss of Flat Oval Ducts

The transmission loss of flat oval or obround ducts falls in between the behavior of square and rectangular ducts. The lower limit of the transmission loss is given by

$$\Delta L_{TLio} = 10 \log \left[\frac{P\,l}{S} \right] \qquad (14.48)$$

since if it were any less, according to the definition of transmission loss in Eq. 14.38, it would imply amplification. For obround ducts the areas are given by

$$S = b (a - b) + \frac{\pi b^2}{4} \qquad (14.49)$$

and

$$P\,l = 12\,l\,[2 (a - b) + \pi b] \qquad (14.50)$$

At low to mid frequencies the wall strength is close to a rectangular duct because of bending of the flat sides. Assuming the radiation is entirely through the flat sides the transmission loss is given by (Reynolds, 1990)

$$\Delta L_{TLio} = 10 \log \left[\frac{f\,m_s^2}{\delta^2\,P} \right] + 20 \qquad (14.51)$$

where ΔL_{TLio} = sound transmission loss from the inside to the outside of the duct (dB)
  m_s = mass/unit area (lbs / sq ft)
  f = octave band center frequency (Hz)
  P = perimeter (in) = $2 (a - b) + \pi b$
  δ = fraction of the perimeter taken up by the flat sides
  $\delta = \dfrac{1}{\left[1 + \dfrac{\pi b}{2 (a - b)} \right]}$

Eq. 14.51 holds up to a limiting frequency $f_L = \dfrac{8115}{b}$.

FIGURE 14.13   Duct Break-in Geometry
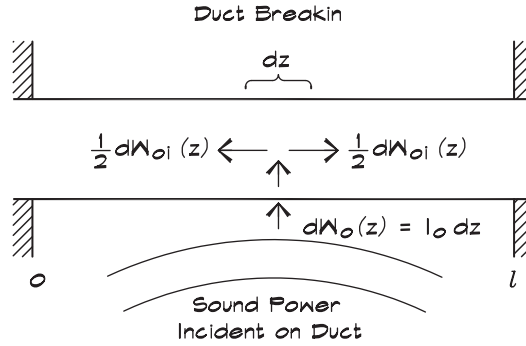
14.5   BREAK-IN

The phenomenon known as break-in encompasses the transmission of sound energy from the outside of a duct to the inside. The approach is quite similar to that applied to breakout.

Theoretical Approach

The geometry is shown in Fig. 14.13 and the definition of the transmission loss is similar to that given for breakout.

$$\Delta L_{TLoi} = 10 \, \log \left[\frac{d \, W_o \, (z)}{d \, W_{oi} \, (z)} \right] \tag{14.52}$$

where $d \, W_o \, (z) = I_o P \, d \, z$ and I_o is the intensity of the diffuse sound field incident on the exterior of the duct. The quantity $d \, W_{oi} \, (z)$ is the sound power transmitted from the outside to the inside of the duct by the segment of duct dz, located a distance z from the reference end. The power is given by

$$d \, W_{oi} \, (z) = d \, W_o \, (z) \, 10^{-0.1 \, \Delta L_{TLoi}} = I_o P \, dz \, 10^{-0.1 \, \Delta L_{TLoi}} \tag{14.53}$$

The sound then travels down the duct toward the reference end and is attenuated as it is carried along. A factor of two is included since the energy is split with half traveling in each direction. Adding the contributions from all the incremental lengths dz from $z = 0$ to $z = l$

$$W_{oi} \, (z) = \int_0^l \frac{1}{2} \, d \, W_{oi} \, (z) \, e^{-(\tau + 2\beta) z} \, d \, z \tag{14.54}$$

which is

$$W_{oi} \, (z) = \frac{I_o \, P \, l}{2} \, 10^{-0.1 \, \Delta L_{TLio}} \left[\frac{1 - e^{-(\tau + 2\beta) l}}{(\tau + 2\beta) l} \right] \tag{14.55}$$

and simplifying, we obtain the sound power level at the reference end in terms of the break-in transmission loss

$$L_{woi} = L_{wo} - \Delta L_{TLoi} - 3 + D \tag{14.56}$$

where L_{woi} = sound power breaking into the duct at a given point (dB)
   L_{wo} = sound power level incident on the outside of the duct (dB)
   ΔL_{TLoi} = sound transmission loss from the outside to the inside of the duct (dB)
   D = duct loss correction term (dB)

Ver (1983) has developed simple relationships between the breakout and break-in transmission loss values based on reciprocity. Above cutoff where higher order modes can propagate,

$$\Delta L_{TLoi} = \Delta L_{TLio} - 3 \quad \text{for } f > f_{co} \tag{14.57}$$

and below cutoff,

$$\Delta L_{TLoi} = \text{the larger of} \begin{cases} \Delta L_{TLio} - 4 + 10 \log \dfrac{a}{b} + 20 \log \dfrac{f}{f_{co}} \\ 10 \log \dfrac{P\,l}{2\,S} \end{cases} \tag{14.58}$$

Note that for round and square ducts, the duct dimensions a and b are equal. The lowest cutoff frequency is given in Eq. 8.21, in terms of the larger duct dimension, a

$$f_{co} = \frac{c_o}{2\,a} \tag{14.59}$$

The sound power impacting the exterior of the duct will depend on the type of sound field present in the space. Where the reverberant field predominates, the sound power level incident on the exterior is

$$L_{wo} = L_p + 10 \log P\,l - 14.5 \tag{14.60}$$

where L_p is the sound pressure level measured in the reverberant field and the dimensions are in feet.

14.6   CONTROL OF DUCT BORNE NOISE

Duct Borne Calculations

A typical duct borne noise transmission problem is illustrated in Fig. 14.14. A fan is located in a mechanical enclosure and transmits noise down a supply duct and into an occupied space. On the return side the ceiling space acts as a plenum for return air, which enters through a lined elbow. There could well be more paths to analyze, such as breakout from the side of a supply or return elbow before the silencer; however, for purposes of this example, we limit it to these two.

The starting point is the sound power level emitted by the fan, which we calculate from the operating point conditions. In this example the fan has a forward curved blade, producing 5000 cfm at 2" of static pressure.

FIGURE 14.14 **Roof-mounted Built-up Air Handler**
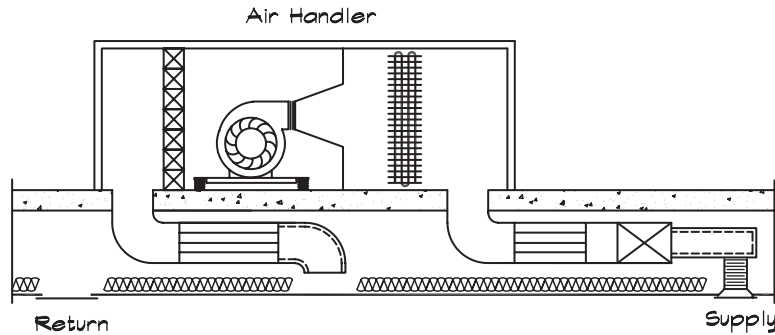
Using the fan equations, we can calculate the sound power in octave bands as shown in Table 14.9. We then follow along each path, subtracting the attenuation due to each element and then adding back the sound power that each generates. The computer program used to generate these numbers uses a 0 dB self-noise sound power level as the default value or when calculated levels are negative. This has a slight effect on the very low levels but is of no practical consequence.

TABLE 14.9 **HVAC System Loss Calculations, dB**

No.	Description	Octave Band Center Frequency, Hz							
		63	125	250	500	1000	2000	4000	8000
Supply									
1	**Fan, Centrifugal, FC—5000 cfm, 2" s.p.**								
		90	86	82	79	77	75	71	61
2	**Elbow—36" × 24", Unlined**								
		0	−1	−2	−3	−3	−3	−3	−3
	Sum	90	85	80	76	74	72	68	58
	Self Noise—0.05" pd								
		41	39	36	29	20	6	0	0
	Combined	90	85	80	76	74	72	68	58
3	**Silencer, Standard Pressure Drop Type—3' long, 36" × 24"**								
		−7	−12	−16	−28	−35	−35	−28	−17
	Sum	83	73	64	49	39	37	40	41
	Self Noise—0.25" pd								
		49	43	44	42	42	45	35	24
	Combined	83	73	64	49	44	45	41	41

TABLE 14.9　HVAC System Loss Calculations, dB　(Continued)

No.	Description	Octave Band Center Frequency, Hz							
		63	125	250	500	1000	2000	4000	8000
4	Duct, Rectangular Sheet Metal—36" × 24", 5' long, 1" lining								
		−2	−2	−3	−7	−15	−12	−11	−9
	Sum	81	71	61	42	29	33	30	32
	Self Noise								
		0	0	0	0	0	0	0	0
	Combined	81	71	61	42	29	33	30	32
5	Split, 25%								
		−6	−6	−6	−6	−6	−6	−6	−6
	Sum	75	65	55	36	23	27	24	26
	Self Noise								
		0	0	0	0	0	0	0	0
	Combined	75	65	55	36	23	27	24	26
6	Duct, Rectangular Sheet Metal—18" × 12", 6' long, 1" lining								
		−3	−3	−5	−11	−25	−22	−16	−13
	Sum	72	62	50	25	−2	5	8	13
	Self Noise								
		0	0	0	0	0	0	0	0
	Combined	72	62	50	25	2	6	9	13
7	Duct, Round Flex Duct—12" diameter, 6' long								
		−14	−14	−16	−15	−17	−22	−16	−13
	Sum	58	48	34	10	−15	−16	−7	0
	Self Noise								
		0	0	0	0	0	0	0	0
	Combined	58	48	34	10	0	0	1	3
8	Rectangular Diffuser, 312 cfm—0.05" pd, 6' to receiver								
		0	0	0	0	0	0	0	0
	Sum	58	48	34	10	0	0	1	3
	Self Noise								
		33	32	29	23	15	4	0	0
	Combined	58	48	35	23	15	5	4	5

TABLE 14.9   HVAC System Loss Calculations, dB   (Continued)

No.	Description	Octave Band Center Frequency, Hz
		63	125	250	500	1000	2000	4000	8000
9	Room Effect—20' × 20' × 8' Room, Drywall Walls, Carpeted Floor								
		−6	−6	−5	−5	−6	−7	−6	−6
	Sum	52	42	30	18	9	−2	−2	−1
Return									
1	Fan, Centrifugal, FC—5000 cfm, 2" s.p.								
		90	86	82	79	77	75	71	61
2	Elbow—36" × 24", Unlined								
		0	−1	−2	−3	−3	−3	−3	−3
	Sum	90	85	80	76	74	72	68	58
	Self Noise 0.05" pd - 4500 cfm								
		43	42	39	33	24	12	0	0
	Combined	90	85	80	76	74	72	68	58
3	Silencer, Low-frequency Standard Pressure Drop Type—5' long, 36" × 24"								
		−16	−21	−35	−41	−41	−28	−21	−15
	Sum	74	64	45	35	33	44	47	43
	Self Noise 0.3" pd - 4500 cfm								
		51	49	53	56	56	59	60	53
	Combined	74	64	54	56	56	59	60	53
4	Elbow—36" × 24", Lined, 1"								
		−1	−2	−3	−4	−5	−6	−8	−10
	Sum	73	62	51	52	51	53	52	43
	Self Noise 0.05" pd - 4500 cfm								
		39	38	34	28	18	4	0	0
	Combined	73	62	51	52	51	53	52	43
5	Plenum, 2" Duct Liner on Gypboard—800 sq ft, 50% Lined, 8 ft @ 85°								
		−12	−13	−19	−20	−20	−20	−21	−21
	Sum	61	49	32	32	31	33	31	22
	Self Noise								
		0	0	0	0	0	0	0	0
	Combined	61	49	32	32	31	33	31	22

TABLE 14.9   HVAC System Loss Calculations, dB   (Continued)

No.	Description	Octave Band Center Frequency, Hz							
		63	125	250	500	1000	2000	4000	8000
6	Rectangular Grille—24" × 24", 563 cfm, 0.05" pd, 6' to receiver								
		0	0	0	0	0	0	0	0
	Sum	61	49	32	32	31	33	31	22
	Self Noise								
		30	29	26	20	12	1	0	0
	Combined	61	49	33	33	31	33	31	22
7	Room Effect—20' × 20' × 8' Room, Drywall Walls, Carpeted Floor								
		−9	−8	−6	−8	−8	−8	−9	−10
	Sum	52	41	27	25	23	25	22	12
Combined Supply and Return									
	Supply	52	42	30	18	9	−2	−2	−1
	Return	52	41	27	25	23	25	22	12
	Combined	55	45	32	26	23	25	22	12
	NC 30	57	48	41	35	31	29	28	27

By making the comparison to the room criterion we surmise that the design is satisfactory. We have not checked the breakout level in the plenum through the walls of the first elbow, which should be done. Breakout levels through the walls of a silencer are on the same order as the low-frequency levels passing through the silencer and are not a concern at high frequencies.

Calculations such as these are routine in new construction. They are also useful in trouble shooting existing installations. Low-frequency noise can be generated by duct rumble or by the fans themselves. Mid frequency noise is often due to excessive duct velocities and high frequency noise to diffusers. When the measured levels do not agree with the calculated values, other causes such as flanking paths and duct velocity problems should be examined.

15 DESIGN AND CONSTRUCTION OF MULTIFAMILY DWELLINGS

As the growing population is extruded into urbanized areas, multifamily dwellings must be constructed to accommodate the higher densities. Pressures of population and cost force people together, and noise and noise transmission between occupied spaces become significant concerns. People want their homes to be quiet and free from intrusions, like a single-family residence. The most common complaints are about noise transmission through floor-ceilings, footfall noise, and noise due to the movement of people on floors and stairways. The next most common problem is audibility of plumbing and piping. Airborne noise transmission can also be problematic, but is encountered less frequently.

The design and construction of multifamily dwellings must include consideration of privacy, which in many cases is legally mandated; even if it is not controlled by a building code or property line ordinance, it nevertheless forms part of the basis of the home buyer's or occupant's reasonable expectation of quality. If the dwelling, by dint of its construction, does not meet this expectation there may be sufficient cause for the finding of a construction defect in the building for which the developer and his design team may be held liable. As the perceived quality of a residence increases, so too do the expectations for a quiet environment. This perception of quality may be based on cost, location, sales information provided to the buyer, or due to the fact that a person is purchasing a permanent home rather than renting an apartment.

Since buildings increasingly are constructed from lightweight materials, the sound transmission between spaces increases. In the older masonry and concrete structures, the mass law insured that isolation would be quite high. The exigencies of cost and time have pushed building construction toward lighter and lighter materials, and hence to greater sound transmission. Given these very real constraints it is incumbent upon architects and engineers to find ways of providing adequate sound isolation in residential structures using the commonly available materials. Where dwelling units are separated by design, good results can be achieved without heroic measures. For example, in multifamily dwellings a townhouse plan is preferred over stacked units to avoid common floor-ceilings. When multistory units are necessary, a plan that stacks similar rooms, one above another, avoids incompatible uses such as a bathroom located above a bedroom. Closets and other nonsensitive spaces can be located on party walls to provide additional shielding.

15.1   CODES AND STANDARDS

Sound Transmission Class—STC

In Chapt. 9 we discussed the formal procedures for the measurement of the airborne sound transmission loss and the determination of the sound transmission class (STC) of a partition. The STC is a weighted average of the transmission loss values at 16 third-octave band frequencies, which is normalized using the area of the common partition and the absorption in the receiving room. Many cities and states have adopted minimum code standards for the STC ratings in multifamily dwellings and these can be used to develop prudent design objectives for various levels of construction quality.

The legally mandated minimum STC ratings are usually set to 50 (State of California, 1974; the Uniform Building Code or UBC, Appendix Chapter 35, 1982); however, in some cases stricter standards have been adopted. For example, the City of Redondo Beach, CA requires a minimum STC of 55 in condominium homes. Under field conditions the measured FSTC rating is about five points lower than the laboratory rating, and this difference is acknowledged in the building code. Thus if a field test is performed to check the rating of a separation after the building has been completed, an FSTC 45 is the minimum allowed under UBC requirements.

In California (Title 24 CAC, 1990), the NIC, which is an FSTC measurement based on the noise reduction without normalization, is allowed to be measured in lieu of the FSTC. The NIC, defined in Chapt. 9, is generally three to five points higher than the FSTC, and varies from room to room depending on the absorption in the receiving space. Thus this provision not only introduces a substantial weakening of the FSTC 45 minimum code standard, but also presents a standard, which may not be representative of the type of partition being tested.

An STC 50 may be the lowest allowable laboratory rating for a given partition. This does not necessarily represent a level of quality that guarantees owner satisfaction with the dwelling or acoustical privacy between units. Rather, it is the minimum level of quality legally acceptable; it is illegal to build a building any worse. The degree of isolation for airborne noise transmission depends not only on the building construction but also on the type of source, the level of the noise, and on the background noise in the receiving space. Table 15.1 and Fig. 15.1 give the assumptions used in a hypothetical sound transmission calculation. The music spectrum is taken to be flat between 125 Hz and 1000 Hz and rolls off 3 dB per octave above and below these limits. Calculations lead us to the levels shown in Table 15.2. The background level is typical of that found in a quiet bedroom at night.

TABLE 15.1   Source and Background Level Assumptions

Source Level	Receiver Level
Normal Voice = 58 dBA at 3'	Understandable => 30 dBA
Raised Voice = 65 dBA at 3'	Plainly Audible => 25 dBA
Loud Voice = 75 dBA at 3'	Background = 25 dBA
Shouting Voice = 88 dBA at 3'	Audible => 20 dBA
Loud Stereo = 95 dBA at 3'	Not Audible < 20 dBA

FIGURE 15.1 Male and Female Speech Spectra (Pearsons et al., 1977)
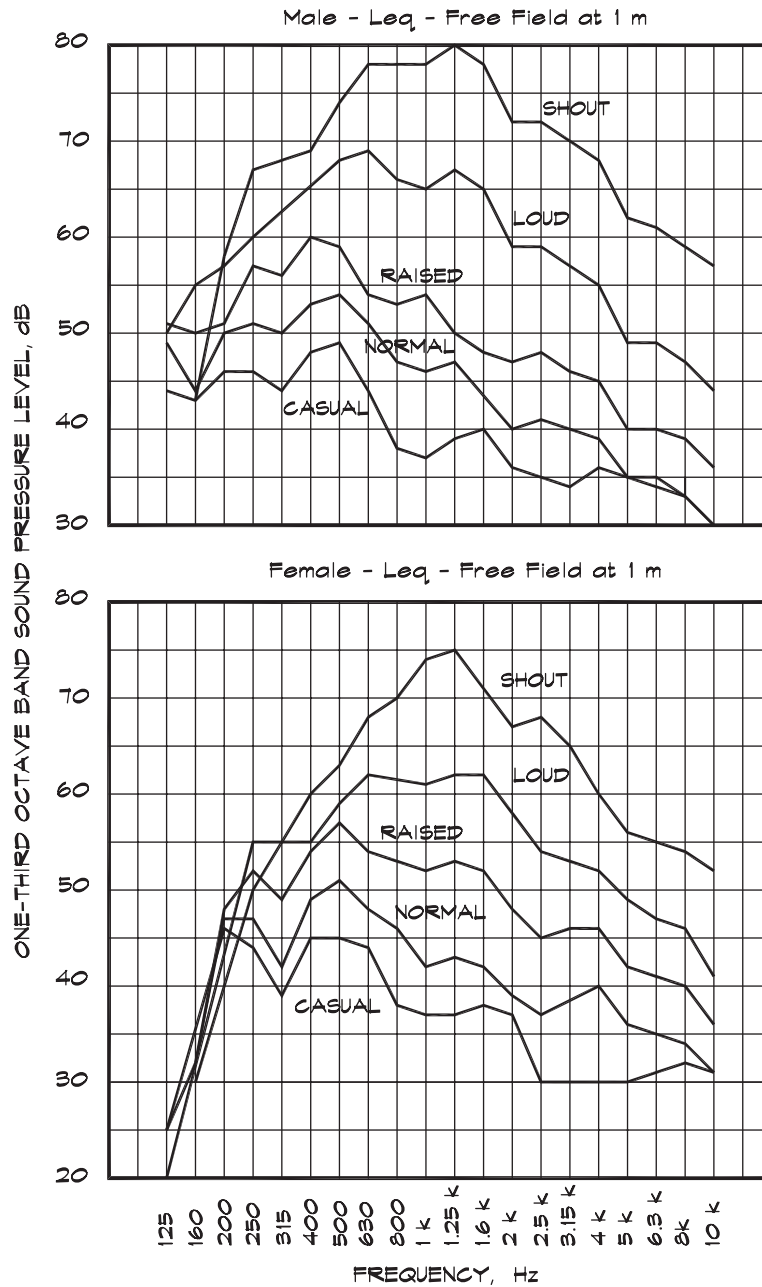
The calculations in Tables 15.1 and 15.2 are meant to be illustrative rather than being a result that holds for all sources and wall types. They give a portrait of the transmission of various source levels between spaces and demonstrate that not all sources, even if they are voice, generate the same level, and that minimum code compliance is not necessarily sufficient for adequate acoustical isolation. At the upper end of the level range the numbers show the problems encountered in the design of recording studios where high acoustic levels occur near very quiet recording spaces.

TABLE 15.2 **Sound Transmission Class vs Expected Field Result**

STC	FSTC	Expected Field Result
80	75	Very loud music audible
75	70	Very loud music plainly audible
70	65	Very loud music understandable
		No unamplified voice audible
65	60	Shouting audible
		Loud voice not audible
60	55	Shouting plainly audible
		Loud voice audible
55	50	Shouting voice understandable
		Loud voice plainly audible
50	45	Loud voice understandable
		Raised voice not audible
45	40	Raised voice plainly audible
		Normal voice not audible

Reasonable Expectation of the Buyer

In selecting the appropriate design criterion for a given level of quality the designer should consider the type of building and the reasonable expectation of quality of the buyer. Unfortunately, too often builders put money into the appearance of a residential building but little into noise isolation. The words *luxury* or *high quality* or *soundproof* are sometimes used to describe projects that barely meet minimum code requirements. If a builder or sales broker is going to characterize the product in this manner, he is well advised to provide a level of noise control commensurate with the description.

Multifamily dwellings can be grouped into three quality categories as shown in Table 15.3. Table 15.4 shows general guidelines according to the level of quality, which assumes a minimum code standard of STC 50.

TABLE 15.3 **Level of Quality vs Type of Use**

Classification	Residential Use
Minimum Quality	Normal Apartments
	Hotels and Motels
	Nursing Homes
	Hospitals
Medium Quality	Good Apartments
	Normal Condominiums
High Quality	High Quality Condominiums

TABLE 15.4   Sound Transmission Class vs Level of Quality for Party Wall and Floor-Ceiling Construction

Classification	STC	FSTC
Minimum Code	50	45
Minimum Quality	55	50
Medium Quality	60	55
High Quality	65	60

To achieve a minimum code standard of STC 50, one should design to the code plus a reasonable safety factor. Generally low-cost rental property, subsistence housing, and temporary housing such as hotels and motels would be designed to the minimum-quality level. Note that the minimum-quality design level is not the same as minimum-code level, since there must be a certain safety factor included to assure code compliance. If one were to design exactly to the code minimum it would mean that the selected construction would have a 50% probability of passing a field test. This is not considered good design practice, and a 3–5 dB minimum margin of safety is recommended. In practice, published test results for a given wall or floor will vary by a few points. It is prudent to examine the range of test results for a given configuration and to expect the lowest values in the test range rather than the highest.

The medium-quality level is appropriate for use for high-quality apartments and normal condominiums. In general, any condominium should be designed to at least the medium quality standard. If noise problems arise, the owner of a condominium does not have the freedom of movement of an apartment dweller. Under California law the seller must reveal any known defects to a potential buyer, including any problems associated with noise transmission. A first-time condominium purchaser may be moving from a single family home and have an expectation of quality based on his previous housing experience.

Into the high-quality category fall those condominiums where there is a level of isolation similar to that found in a single family home. In these cases owners may complain if they can hear any activities in adjacent dwelling units. They are particularly sensitive to footfall and plumbing noise since these may occur relatively frequently. Even for this type of structure the ratings given in Table 15.4 will not guarantee isolation of every noise, as illustrated in Table 15.2.

Impact Insulation Class—IIC

Minimum IIC ratings are set to 50 in the UBC with a minimum field tested FIIC of 45 allowed. At this rating, footfall noise is quite pronounced and very audible in the unit below. In response some cities and condominium associations have adopted more stringent laws. The City of Redondo Beach, for example, sets a minimum IIC rating of 65 in condominiums. Other cities such as Beverly Hills control noise through a property line ordinance as discussed next. The point at which footfall-generated impact noise becomes inaudible is closer to an IIC of 75, as shown in Fig. 12.23. The level of quality due a buyer in the control of impact-generated noise is numerically higher than that for airborne noise.

TABLE 15.5   **Impact Insulation Class vs Level of Construction for Party Floor-Ceiling Construction**

Classification	IIC	FIIC
Minimum Code	50	45
Minimum Quality	55	50
Medium Quality	65	60
High Quality	75	70

Property Line Ordinances

Cities and counties have ordinances restricting the levels of noise that are allowed within a real property boundary. These are known as property line ordinances and are tied to the zoning of the receiving property. Allowable levels are based on a measured or assumed ambient level within the receiving property, since a noise maker cannot be expected to be responsible for noise generated by other sources. A law usually establishes an absolute maximum at a level 5 dBA above the higher of the measured or assumed ambient. Normally the assumed ambient is reduced at night (before 7 AM and after 10 PM) by 10 dB to account for our increased sensitivity. Assumed ambient background levels provide the basis for the lowest level to which a standard may fall. For example in the City of Los Angeles, the nighttime assumed ambient is 40 dBA, so a noise maker would be allowed to create 45 dBA, even if the actual ambient background were below 40 dBA. This approach gives the noise maker a clear numeric design target even if the actual ambient falls below the assumed ambient.

The wording of these ordinances varies. Some are stated in terms of an absolute level such as the US EPA Model Noise Ordinance (1973), which reads:

> "No person shall operate or cause to be operated on private property any source of sound in such a manner as to create a sound level, which exceeds the limits set forth for the receiving land use category in Table ___ when measured at or within the property boundary of the receiving land use."

In this case the ambient must still be taken into consideration since the ordinance applies only to the intrusive source.

The specific wording of an ordinance, particularly the definition section, is important. In many cases they set maximum limits on interior noise levels, which apply within the property boundaries of a dwelling unit. Thus if a person in one unit walks across a floor or turns on a tub faucet and the occupant of another unit is subjected to a noise in excess of the property line ordinance, there may be a cause of action against the builder who caused the condition to exist. It is not an action that is taken against the occupant unless the noise-making activity is unusual or excessive, such as playing a stereo too loudly, or unless the owner has changed the construction so as to worsen its sound reduction capability, for example by replacing a carpeted floor with a wood or tile floor. If an occupant runs the bath or shower, this would not be considered an unusual activity. If, however, he is doing midnight body slams, the resulting noise could not necessarily be blamed entirely on the developer.

TABLE 15.6   Recommended Maximum Interior Day Night Noise Levels from Exterior Sources

Classification	L_{dn} (dBA)
Minimum Code	45
Minimum Quality	40
Medium Quality	35
High Quality	30

Under California law developers are liable for the cost of testing and repair if party wall or floor-ceiling separations do not meet the minimum codes. Architects and engineers who design multifamily dwellings are well advised to consult local property line ordinances to make sure they are in compliance. The City of Beverly Hills, for example, limits interior noise levels to no more than 5 dB over the actual interior ambient. This is not an unusual provision; however, Beverly Hills defines the ambient as the quietest level present at any time of day at a given location with no minimum. An ordinance of this type can put a greater restriction on intrusive noise levels than a minimum STC or IIC rating does.

Exterior to Interior Noise Standards

The State of California (CAC Title 25, 1974) and other regulating bodies set maximum allowable interior levels generated by exterior noise sources such as street traffic. Housing and Urban Development (HUD) financed housing projects are subject to the same interior requirements (24 CFR 51B, 1979) as well as additional exterior requirements. Under both California law and the HUD regulations the limit is an interior L_{dn} of 45 dBA. In much the same way as the limits on STC and IIC were minimum code levels, so too are the allowable interior noise levels. Occupants are seldom happy with the minimum code noise level. Table 15.6 lists recommended interior levels for different types of construction quality. The interior standards assume that all windows and doors are closed so that adequate mechanical ventilation must be provided.

15.2   PARTY WALL CONSTRUCTION

General Principles

In actual building practice there are relatively few construction materials that are utilized, and a knowledge of transmission loss theory is most helpful in properly applying them. The most common materials are concrete, concrete masonry units (cmu), stucco, gypsum plaster, gypboard, and wood or metal sheets in various combinations. The structural supports are wood or metal studs for walls, and concrete, steel, or wood-joist systems for floors.

At low frequencies providing adequate stiffness and mass are the most important factors in achieving high transmission loss values. Stiffness can be increased by decreasing the support span and by increasing the bending stiffness. Short-span concrete slabs have both high mass and a large intrinsic stiffness and thus give excellent low-frequency transmission loss. Fully grouted cmu blocks or brick can provide nearly as much mass and stiffness; however, concrete blocks have significant porosity and must be sealed with an oil-based paint or plaster to realize the full effectiveness of their mass. Double concrete or cmu walls

can be used, but the spacing between panels must be sufficiently large that the two are not coupled through the air gap. Usually at least 10 to 15 cm (4"–6") of spacing is required. Details of the STC ratings were discussed in Chapt. 10.

At higher frequencies, separately supported gypboard partitions, which have a high critical frequency and a large air space, are a good choice. If the separation distance is large enough, these can be more effective than a single concrete panel. In separately supported structures, either wood or metal studs yield the same results. Offsetting or staggering studs, which are already on separate base plates, is not necessary.

In single-stud construction there is a more limited range of options available. With wood studs the two panels are rigidly attached by means of the line connections. The addition of multiple layers of drywall is only somewhat effective. A resilient attachment provides some decoupling, though not as much as a separated stud. Metal studs, because they are inherently flexible, can also provide significant decoupling. Resilient supports can be helpful in decoupling gypboard layers on either side of a wood stud or floor joist. Resilient channel must be properly installed so that the screws do not short circuit. Channels applied directly over layers of gypboard or other panel materials are ineffective due to bridging by the trapped air pocket. Products that can be attached only on one side are preferred over hat-shaped channels, which can be attached on both sides. Resilient channels are not recommended for party walls since they are not suitable for the mounting of bookshelves or heavy pictures. When applied to double stud and lightweight metal stud walls, resilient supports do not significantly increase the sound transmission loss since the structures are already isolated.

Party Walls

The selection of a party-wall construction should be based on the level of quality and the ultimate use of a given development. An example of party wall construction for minimum-quality construction is shown in Fig. 15.2. The minimum-quality construction consists of two layers of 5/8" (16 mm) drywall on each side of staggered 2 × 4 (38 × 89 mm) studs set

FIGURE 15.2 Minimum-Quality Party Walls

Staggered Wood Stud Wall
2 x 4 (50 mm x 100 mm) Studs on a 2 x 6
(50 mm x 150 mm) Plate
2 Layers 5/8" (19 mm) Drywall Each Side
R-11 Batt Insulation

125	160	200	250	315	400	500	630	800	1 K	1.3 K	1.6 K	2 K	2.5 K	3.2 K	4 K	STC
35	39	45	45	49	49	52	53	54	55	56	57	54	50	53	57	53

Metal Stud Wall
3 5/8" (90 mm) Metal Stud
2 Layers 1/2" (13 mm) Drywall Each Side
R-11 Batt Insulation

125	160	200	250	315	400	500	630	800	1 K	1.3 K	1.6 K	2 K	2.5 K	3.2 K	4 K	STC
40	44	46	48	52	56	59	58	59	59	62	63	62	58	52	57	56

on a 2 × 6 (38 × 140 mm) wood plate. An alternative to staggered studs would be the use of a light-gauge 3 5/8" (92 mm) metal stud. The wall should have 3 1/2" (90 mm) fiberglass batt insulation having a thermal rating of R-11 in the air space. The staggered-stud wall rates an STC 53 while the metal-stud wall rates an STC 56 (CONC, 1981) with double 1/2" (13 mm) drywall. Generally a wall with two layers of drywall each side is preferable to one with only one layer even when the stud configuration yields comparable STC ratings. The small advantage in using mismatched drywall thicknesses in low-rated party walls (< 55 STC) is probably not worth the confusion it produces in having two thicknesses of drywall on the job site.

For medium-quality construction the first wall shown in Fig. 15.3 is a good choice. It consists of two layers of 5/8" (16 mm) drywall on each side of separate 2 × 4 (38 mm × 89 mm) wood or 3 5/8" (92 mm) metal studs separated by at least 1" (25 mm). There are two layers of R-11 fiberglass batt in the airspace. This wall has achieved an STC 63 in a laboratory test (CONC, 1981).

In high-quality construction projects the triple-panel wall shown in Fig. 15.3 has been used successfully. It consists of two layers of drywall, one 1/2" (13 mm) and the other 5/8" (16 mm) thick in the outside of separate 2 × 4 (38 mm × 89 mm) studs. On the inside of one set of studs are three layers of drywall: two 5/8" (16 mm) and one 1/2" (13 mm) thick. The layers are spot laminated and screwed together as described in Chapt. 9. There is R-11 fiberglass insulation in the air cavities. The STC test data shown are for a similar wall cited in Fig. 10.11, which was tested by Sharp (1973). The wall shown here will test a few points lower since the panels are not point mounted.

FIGURE 15.3 Medium- and High-Quality Party Walls

Medium Quality Party Wall

Double Wood Stud Wall
2 × 4 Studs Separated by a 1" Gap
2 Layers 5/8" Drywall Each Side
2 Layers R-11 Batt Insulation

125	160	200	250	315	400	500	630	800	1K	1.3K	1.6K	2K	2.5K	3.2K	4K	STC
41	46	50	55	58	59	61	62	64	67	69	70	67	66	68	69	63

High Quality Party Wall

Double Wood Stud Wall
2 × 4 Studs Separated by a 1" Gap
Outside Layers 5/8" + 1/2" Drywall
Inside 5/8" + 1/2" + 5/8" Drywall
All Layers Spot Laminated at 24" OC and Screwed
to Studs – 3" Batt Insulation in all Cavities

125	160	200	250	315	400	500	630	800	1K	1.3K	1.6K	2K	2.5K	3.2K	4K	STC
53	56	60	66	70	75	78	80	78	79	83	83	84	87	88	89	76

Structural Floor Connections

In certain cases there can be significant flanking of a wall through structural connections such as a floor diaphragm. In wood-frame buildings there are requirements that there be a fire stop between wall studs or joists supporting a floor. In earthquake country there are also requirements that the building have adequate stability to withstand vibration-induced lateral motion. In many cases this stability is provided through a plywood diaphragm, which runs continuously from floor to floor beneath a sound rated partition such as a party wall in a multifamily residence. Craik, Nightingale, and Steel (1997) published a study of the flanking due to the presence of several types of fire stops: wood, metal, drywall, and safing (no connection). Their calculations (Craik, 1996), which used statistical energy analysis, assumed that the floor and wall could be modeled using four plates, one for each side of the wall and one for the floor on each side, with only a moment connection between them. Both calculated and measured results were reported. The measured results are summarized in Fig. 15.4. Note that the wall has a double stud with double 1/2" (13 mm) gypsum board, a 1" (25 mm) air gap, and two layers of batt insulation. The floor was constructed of a single layer of 5/8" (16 mm) plywood.

Figure 15.4 Effects of Structural Decoupling (Craik, Nightingale, and Steel, 1997)
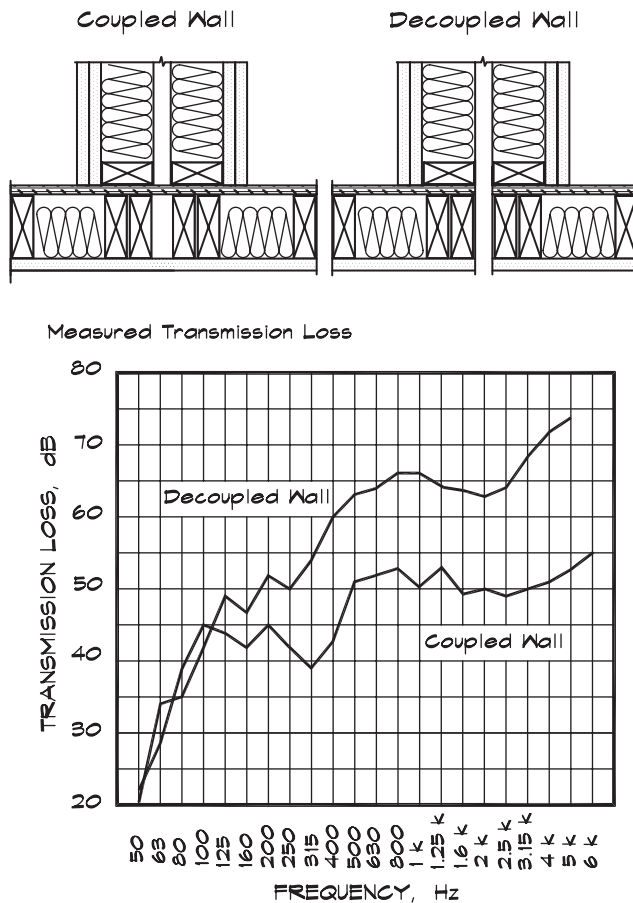
The results show that there can be significant flanking due to the structural path through the floor when there is continuous plywood. In fact, the calculations indicated that for coupled structures the most important noise path is from the source room into the floor, through the diaphragm, into the adjacent floor, and into the receiving room. Improvements can be obtained by separating the two sides and by using a thin sheet metal or safing fire stop and by increasing the mass of the floor structure through the use of a concrete topping layer or by the installation of a floating floor system. Horizontal fire stops in double stud party walls can be achieved with drywall, which is attached only to one side. On the opposite side the gap between the drywall and the stud is minimized and stuffed with safing.

In concrete-slab construction the high mass of the floor helps block the room-floor-floor-room path. In wood construction a continuous diaphragm may be required for structural reasons, but here concrete topping slabs increase the floor mass and help decrease the floor transmission path. Metal straps may provide the coupling required by structural or earthquake requirements, while still providing a significant impedance mismatch.

Flanking Paths

In party-wall construction there can also be nonstructural flanking paths. When double drywall is used as a surface material, the joints on the second layer should be staggered with respect to the first layer. At the corners, layers should be overlapped and all joints must be premudded before taping. When this is not done a gap can remain between the two layers of drywall, which is covered over only with drywall tape.

At the base plate, the gap between the drywall and the floor should be caulked with a nonhardening caulk. Base plates should not be completely sawed through to accommodate piping. This is important because the drywall needs a continuous backing to seal against. It is more important to caulk under the drywall than it is to caulk under the bottom plate. The principal reason for caulk under the bottom plate is to provide blockage when the lumber is warped; however, this path should also be blocked by caulking the drywall. The addition of a caulked wood base strip along the bottom of the drywall helps to close off the gaps under the drywall.

Blocking headers, located above the top plates of the wall framing, should be doubled and joints between the headers and the joists should be kept tight. This prevents sound, which makes its way into the ceiling cavity, from migrating into an adjacent unit by way of the joist space.

Where bathtubs and showers are located on a party wall they must be installed so that the integrity of the wall is not compromised. This means that the drywall (or green board) must be continuous behind tubs, showers, and other wall-mounted fixtures such as lavatories. Party walls should not be cut out to accommodate medicine cabinets or other surface-mounted millwork.

Drywall must also be continuous behind stairwells. Party wall framing should not provide structural support for stair risers. Even with double stud walls and carpeted stair treads, footfall noise on stairways can be audible when the stair framing is structurally attached.

Electrical Boxes

Once a decision has been made on the construction of the separating partition, care must be exercised to insure that the rating of the partition is maintained. One example, which we have already discussed, is through a hole or other area of reduced transmission loss in a wall.

FIGURE 15.5 Treatment of Electrical Boxes in Rated Walls

Offset electrical boxes 24" or two stud spaces and box with drywall on the exposed sides. Use one layer less than the surface treatment but at least one. Caulk or mud gap between box and surface drywall.
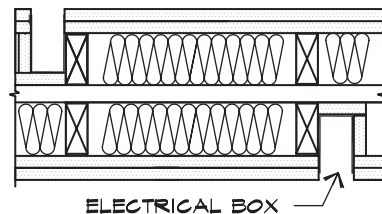
ELECTRICAL BOX

These can be gaps in and around electrical boxes or simple cutouts in walls for telephone, computer or television cabling. Too often wiring is run freely in walls and not contained in conduit and metal boxes. When this occurs the plastic electrical wall plate becomes the weak part of the structure and can lead to a degradation of the performance of the partition. Even a small opening such as a 1/2" (13 mm) emt conduit between two 2 × 4 electrical boxes can significantly degrade the transmission loss.

It is good practice to enclose all wiring, including low voltage computer, telephone, and cable TV wiring, that is located in sound-rated partitions, in metal boxes and conduit. Where these boxes penetrate the wall surface the openings between the drywall and the box should be sealed with caulk or plaster. Electrical boxes should be offset 24" (0.6 m) or two studs when they are located on opposite sides of a wall. Figure 15.5 illustrates this principle. The backs and sides of the boxes should be buttered with plaster, wrapped with drywall, or sealed with clay pads to attenuate sound penetration out of the back of the box. Wrapping with drywall is preferred since clay pads can peel away from the box over time. A 1/2" (13 mm) sheet of drywall, which spans the stud bay containing the electrical box from the base plate to a height 12" (300 mm) above the electrical box, can be used in place of wrapping. Batt insulation must be placed within and behind the drywall cavity. At the point where the electrical boxes penetrate the drywall, all gaps between the outside of the box and the drywall must be sealed with drywall mud or caulk.

Wall Penetrations

Where plumbing pipes are located in party walls (this is not recommended), penetrations should be avoided. If a pipe must penetrate a party wall a resilient escutcheon or caulked opening should be used; however, these openings can compromise the sound isolation over time. When water flows through a pipe it can move the pipe around, due to the forces produced by the fluid as well as thermal expansion and contraction. Pipe movement tends to open up the hole at the penetration even when it is caulked. Piping penetrations on opposite sides of a party wall should be offset by 24" (610 mm). Piping to adjacent units should be separate and the piping should only be supported on the studs on the side of the wall whose unit it serves. Plumbing piping or rigid conduit connected to the structure on both sides will short circuit the stud separation. Sufficient space must be allowed for the passage of waste piping so that it does not make contact with the panels or support structure on either side. When there are back to back pipe penetrations in a double stud party wall, a layer of drywall should

FIGURE 15.6 Treatment of Rated Wall Penetrations

When a large duct or pipe penetrates a rated wall, the opening is
oversized by about 1" (25mm) and filled with fiberglass board. The
ends are capped with drywall closely fitted to the penetrating body
and caulked. Use the same number of layers as are on the wall.

DUCT SILENCER
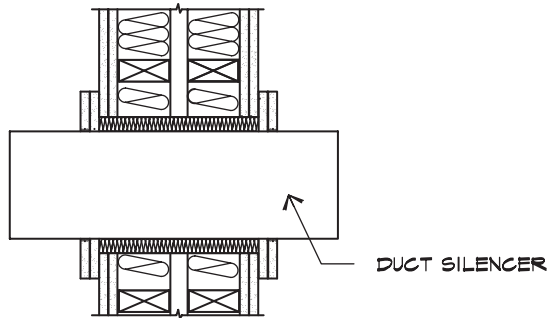
be installed on the inside face of a stud behind one penetration, a stud space wide extending 18" (457 mm) above and below the penetration.

When a duct or pipe penetrates a rated separation the penetration must be treated so as to retain the rating of the partition. If the penetrating element is a large pipe or duct, as shown in Fig. 15.6, a hole in the wall is cut, leaving about a 1" (25 mm) gap that is filled with fiberglass board. The opening is then sealed off with the same number of layers of drywall as the original wall surface and the remaining gap is caulked. In the case of a pipe penetrating a concrete floor, the opening above and below the fiberglass can be filled with a sealant.

Holes

At the top of a wall the attachment of a stud wall to a metal deck can be tricky. Sheet metal plates or rubber filler strips can be used to close off the openings above the top track as shown in Fig. 15.7. Where nested tracks are employed to allow for floor movement, the outer layers of drywall should overlap the inner track and be caulked against the floor plate. When a wall

FIGURE 15.7 Wall Connection at a Metal Deck

A wall butting up against a metal deck should be attached to a sheet
metal plate, typically 16 ga. The webs are stuffed with safing or
prefabricated neoprene strips.
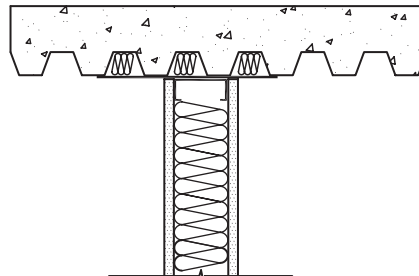
parallels the deck webs, a plate of 16 Ga sheet metal with safing in the cavities will close off the path above the wall. A wall that runs perpendicular to the webbing can be topped with a wide sheet metal plate, neoprene inserts, or cut drywall. Walls that lie at an oblique angle to the webbing can also be sealed with a wide plate with the cavities stuffed with safing.

15.3   PARTY FLOOR-CEILING SEPARATIONS

Noise and vibration problems encountered in floor-ceiling systems fall into the four categories discussed in Chapt. 12: airborne noise, structural deflection, footfall, and floor squeak. Floor vibration and vibration isolation of mechanical equipment are separate topics, which were discussed in Chapt. 11.

Airborne Noise Isolation

Airborne noise isolation in floors follows the same principles and is tested in the same manner as airborne isolation in walls. As was the case with wall transmission, the isolation of airborne noise such as speech is well characterized by the STC rating. STC tests are done by placing the noise source in the downstairs room to insure vibrational decoupling between the loudspeakers and the floor-ceiling being tested. The ratings shown in Table 15.4 apply to floor-ceiling separations just as they applied to walls, but the choice of floor systems is greater.

Highly rated floor-ceilings combine a high-mass floor with a large separation between panels as in a double panel wall system. Ideally the two panels should be structurally decoupled either by separate structural supports or by means of a resiliently hung ceiling or floating floor. At low frequencies a high structural stiffness is desirable to minimize the plate deflection.

A simple concrete slab of sufficient thickness can provide a good floor-ceiling. A 6" (152 mm) thick slab has an STC rating of 55 and is sufficient by itself for a minimum quality floor. Six-inch concrete slabs with a wire-hung drywall ceiling can provide sufficient isolation for airborne noise to be used in medium-quality construction. For high-quality construction even with concrete slabs a drywall ceiling suspended from neoprene isolators is preferred. Figure 15.8 shows some examples of concrete floor-ceiling systems.

In wood construction the structures are light and stiff. The problem with wood floors for airborne noise isolation is in achieving sufficient mass. Lightweight-concrete fill weighs 110 to 115 lbs/cu ft (540–560 kg/sq m) and should be poured to a thickness of at least 1.5" (38 mm). A hard concrete fill (140–150 lbs/cu ft or 685–735 kg/sq m) is preferred; however, the structural system must be designed to accommodate the additional weight. Figure 15.9 gives examples of wood floor-ceiling systems suitable for various levels of quality in multifamily dwellings. Note the increasing thickness of plywood subflooring.

Composite floor-ceiling systems fall somewhere between wood and concrete. A composite floor can be constructed using a 5" (127 mm) lightweight concrete fill poured into a webbed sheet metal deck with a suspended ceiling below. With this configuration a drywall ceiling is required even for the minimum design standard. Several designs are shown in Fig. 15.10. Note that there is no structural support provided by the lightweight concrete or the sheet metal pan. The structural floor stiffness is due to the supporting beams. When these beams have a long span, floor deflection can be a greater problem than noise transmission.

FIGURE 15.8 Concrete Floor-Ceiling Assemblies
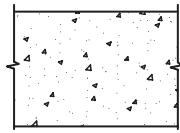
Minimum Quality

6" (150 mm) Solid Concrete Panel
75 lbs/sq ft (365 kg/sq m)
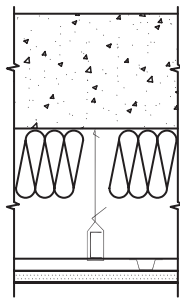
Medium Quality

6" (150 mm) Solid Concrete Panel
75 lbs/sq ft (365 kg/sq m)
R-11 (3.5" or 90 mm) Batt Insulation
1 Layer 5/8" (16 mm) Gypsum Board
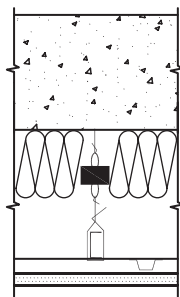
High Quality

6" (150 mm) Solid Concrete Panel
75 lbs/sq ft (365 kg/sq m)
R-11 (3.5" or 90 mm) Batt Insulation
0.15" (4 mm) Deflection Neoprene Isolators
1 Layer 5/8" (16 mm) Gypsum Board

Structural Stiffness

The achievement of a high IIC rating in a given floor-ceiling system does not guarantee that noise will not be a problem or that the sound of walking will not be audible in the units below. The IIC test measures the reaction of a floor system to the impact of a series of 1.1 lb (0.5 kg) weights dropped on the surface. Although this may model the noise of a heel tap, it does not represent the full effect of the loading and unloading under the weight of a walker. When a person steps or even stands on a floor, it will deflect under the static and dynamic load of his weight, as we discussed in Chapt. 12. If the underside of the floor is exposed to the room below, a sound generated by this motion will radiate directly into the receiving space. Noise generated by floor deflection sounds like low-frequency thumps, whereas heel clicks have a spectral character largely dominated by the high frequencies.

Three mechanisms are available to improve this condition: 1) increase the stiffness of the floor system, 2) increase the structural damping, and 3) increase the vibrational decoupling between the floor and the ceiling. In concrete structures both the stiffness and damping increase with slab thickness. For the 6" (152 mm) concrete slab required to achieve an STC of 53-55 structural deflection is rarely a problem for moderate spans. In wood structures the most common type of minimum quality construction consists of 1.5" (38 mm) lightweight concrete on plywood on joists with ceilings of drywall on resilient channel. This construction

FIGURE 15.9 Wood Floor-Ceiling Constructions

Minimum Quality
1 1/2" (38 mm) Lightweight Concrete
(110 lbs/cu ft or 1760 kg/cu m)
1 Layer 5/8" (16 mm) Plywood Glued and Screw Nailed
2 (50 mm) x Wood Joists
R-11 (3.5" or 90 mm) Batt Insulation
Resilient Channel
1 Layer 1/2" (13 mm) Gypsum Board

Medium Quality
1 1/2" (38 mm) Lightweight Concrete
(110 lbs/cu ft or 1760 kg/cu m)
1 Layer 3/4" (19 mm) Plywood Glued and Screw Nailed
2 (50 mm) x Wood Joists
R-11 (3.5" or 90 mm) Batt Insulation
RSIC-1 Isolators with 7/8" Hat Channel
2 Layers 5/8" (16 mm) Gypsum Board

High Quality
1 1/2" (38 mm) Lightweight Concrete
(110 lbs/cu ft or 1760 kg/cu m)
1 Layer 3/4" (19 mm) Plywood Glued and Screw Nailed
2 (50 mm) x Wood Joists
R-11 (3.5" or 90 mm) Batt Insulation
1" (25 mm) Deflection Spring Isolators
2 Layers 5/8" (16 mm) Gypsum Board

can transmit considerable low-frequency noise, since for normal joist lengths the deflection of the resilient channel is not sufficient to overcome the deflection of the joists.

In wood construction both stiffness and damping can be increased by using the stepped blocking shown in Fig. 12.24. The blocking works for several reasons. The first is the damping added by the moment connection provided by the glued faces and end nailing. Second the stiffness is increased by building the equivalent of another beam in the middle of the joist system. The third effect is additional load spreading, which distributes a point load over several joists and helps increase the composite floor stiffness. Stepped blocking is more effective than doubling joists or reducing joist spacing, although the two can be combined to good effect. When prefabricated truss joists are used, a spacer plate must be installed as in Fig. 12.28. Stepped blocking should be located at the mid-span in joists having a length of between 12 to 18 feet (3.7—5.5 m) and at the one-third points in joists greater than 18 feet.

Structural Decoupling

If a floor-ceiling system is not a monolithic slab, it generally includes an independently supported ceiling, which may be isolated vibrationally from the structure. In concrete

FIGURE 15.10   Steel Deck and Concrete Floor-Ceiling Constructions

Minimum Quality

5" (125 mm) Thick Lightweight Concrete on Metal Decking
(42 lbs/sq ft or 200 kg/sq m)
16" (400 mm) Airspace
R-11 Batt (3.5" or 90 mm) Insulation
5/8" (16 mm) Gypsum Board on Hat Channel
and Carrying Channel

Medium Quality

5" (125 mm) Thick Lightweight Concrete on Metal Decking
(42 lbs/sq ft or 200 kg/sq m)
16" (400 mm) Airspace
R-11 Batt (3.5" or 90 mm) Insulation
0.15" Deflection Neoprene Isolators
5/8" (16 mm) Gypsum Board on Hat Channel
and Carrying Channel

High Quality

5" (125 mm) Thick Lightweight Concrete on Metal Decking
(42 lbs/sq ft or 200 kg/sq m)
16" (400 mm) Airspace
R-11 Batt (3.5" or 90 mm) Insulation
1" (25 mm) Deflection Spring Isolators
5/8" (16 mm) Gypsum Board on Hat Channel
and Carrying Channel

construction the most common support system is hanger wires at 4' (1.2 m) on center wrapped around 1 1/2" (38 mm) carrying channel (black iron) to which 7/8" (22 mm) metal furring channels (hat channels) are wire-tied. This system provides some isolation because it uses a point connection (Chapt. 9) rather than a line connection. It can be improved further by utilizing vibration isolators either in the form of neoprene hangers or steel spring isolators cut into the hanger wires.

In wood structures a common type of structural decoupling is resilient channel. At high frequencies resilient channel can provide some improvement to the structural isolation; at very low frequencies, however, it is not particularly effective. Several different kinds of resilient channel are available on the market, some of which are shown in Fig. 15.11.

When resilient channel is installed improperly, it is ineffective, so the manufacturer's installation instructions must be followed closely. A z-shaped channel is one of the easiest to install, but screws that are too long can still short out the decoupling as shown in Fig. 15.12. Z-shaped resilient channels should be installed with the open side up when they are attached to studs so that the weight of the applied drywall pulls the channel open and away from the stud.

Hat-shaped resilient channels must be installed so that there is an attachment screw on only one side of the flange. Each screw attachment alternates from one side to the next.

FIGURE 15.11   **Types of Resilient Channel**

Z Shaped Resilient Channel

Hat Shaped Resilient Channel
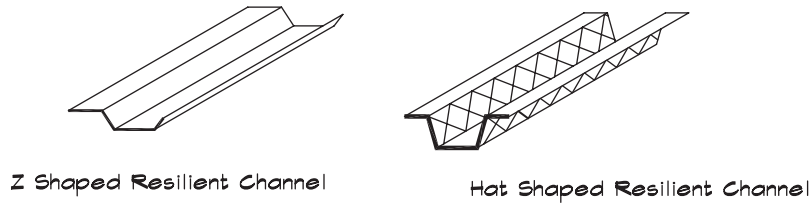
FIGURE 15.12   **Improperly Attached Resilient Channel**

Z Shaped Resilient Channel
Screw is so long that it enters the joist,
shorting out the channel.

Hat Shaped Resilient Channel
Screws are attached on both sides,
which destroys the flexibility of the channel.
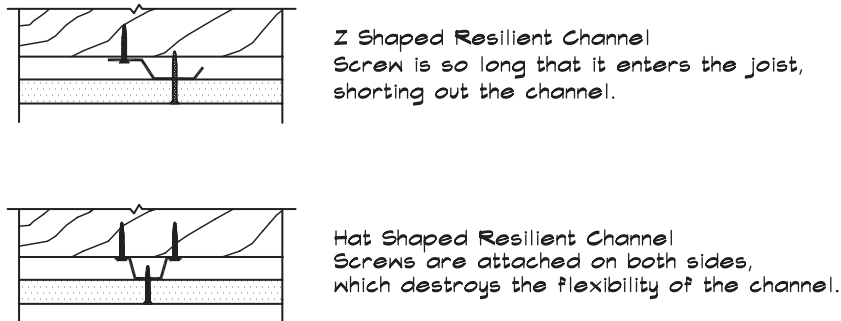
If it is screwed to a joist on both sides the hat channel is not free to deflect and is ineffective. The side webbing of hat-shaped resilient channels have openings to reduce their stiffness; however, they are still too stiff to provide appreciable isolation if they are screwed to the joists on both sides.

Neoprene mounts, which include a clip to support hat channels, recently have become available. These give somewhat better floor isolation than resilient channels (STC 61) and can support a double layer of drywall. They are installed on 24" (0.6 m) centers in one direction and at twice the joist spacing (typically 32" or 0.8 m) in the other. They provide the advantages of a resilient point-mount support along with ease of installation. A sketch is included in Fig. 15.13.

The most effective structural decoupling in wood floor-ceiling systems is a resiliently supported ceiling hung from spring hangers shown in Fig. 12.3 (STC 73). Note that the hangers are located high on the joist to preserve as much ceiling height as possible. Spring hangers are more effective than a ceiling supported on separate joists since with the latter system there is still the possibility of structural transmission through the joist supports. When a spring-hung ceiling is installed, unless the springs are precompressed, it will drop by the amount of the hanger isolator deflection. Hence the ceiling drywall must not extend beyond the top of the wall drywall, or else its weight will be supported by the walls and the ceiling will bow. An example of a proper installation is given in Fig. 12.4. Once the ceiling has come to its final elevation the gap between the ceiling and wall material may be caulked. Molding or other trim pieces then can be added since they are nonbearing.

FIGURE 15.13   RSIC Resilient Point Mount Supports (Pac International)
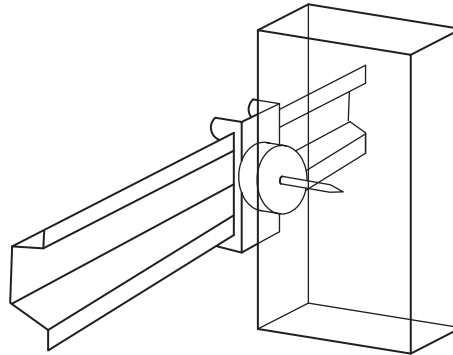
Spring precompression can minimize the actual deflection; in practice, however, this is somewhat tricky since the final load must be determined carefully. Springs are located at 4' (1.2 m) on center, and if they support 16 sq. ft. (1.5 sq m) of ceiling, at 5.5 lbs/sq ft (27 kg/sq m), they will each carry about 90 lbs (41 kg). A spring located along an edge will carry a little more than half that load, and one in a corner somewhat more than one quarter. In irregularly shaped ceilings or one with coffers and light fixtures the loading is more complex. It is prudent to have springs of several different sizes at a job site in case the odd hanger is needed. When stepped blocking and a resiliently hung ceiling are used in combination, the black iron can run parallel to the joists just below the blocking. The hat channels run perpendicular to the joists just below them. When the drywall is installed its weight will pull the hat channel away from the joists so it does not touch.

Floors should be structurally decoupled laterally as well as vertically. Joists should not be run continuously across a party wall separation but should be supported on the nearest side of the party wall framing.

Floor Squeak

Creaking floors are caused by the relative motion of wood on wood or nails rubbing against diaphragms, joists, or metal joist hangers. One common cause are shiners, as they are called— nonbedded nails that lay alongside a joist and rub as the floor structure deflects. These must be removed before any lightweight or other concrete fill is poured.

Another cause is unevenness in the top surface of the joists, either due to imperfections in the wood or in the case of joist hangers, to differences in the joist level, which allows motion of the floor diaphragm against the nails. Gluing diaphragms to the joists, prevents much of the panel motion and increases damping. Joists can also be shimmed at the hanger to assure even floor support. In tongue and groove flooring the individual planks can move relative to one another. Gluing or applying paraffin to the plank edges helps prevent this cause of squeak.

In some cases subflooring, made of wood strands bonded together with a resin material, has been found to contribute to floor squeak. When these materials deflect they rub against the nails, which powders the binder and opens up a small hole around the nail, which in

turn loosens the grip of the nail on the board. This effect can be offset somewhat by gluing under the flooring and using a gripping ring shank nail. Ring shank nails are recommended for nailing all wood diaphragms since they provide some additional grip on the plywood. To repair existing wood floors, screws can be added to cinch down the flooring to the joists and reduce panel movement. Glue should be applied from below along the top edges on both sides of the joists.

Floor Coverings

It is relatively easy to achieve high impact insulation class ratings by using carpet and pad. Medium quality ratings are achievable with a cushioned or padded vinyl floor surface. It is where hard materials such as quarry tile, marble, sheet vinyl, or hardwood floors are used that low impact ratings are encountered. As an example Fig. 12.11 shows the results of several IIC tests carried out on a minimum quality lightweight concrete and wood floor-ceiling construction. The ratings range from an IIC 76 for a heavy carpet and pad to an IIC 38 for exposed concrete.

Where hard surface floors are desired a spring isolated ceiling or concrete floating floor are usually required to achieve medium quality. Figure 12.12 gives an example. Thin layers of resilient material such as fiberglass board, cardboard-like materials, and wire mesh mats can raise the IIC ratings modestly, three to five points, but seldom provide sufficient deflection to achieve the impact isolation necessary for condominium construction. A number of products are commercially available, which are intended as a resilient underlayerment for hard-surfaced flooring. A typical construction consists of a plywood diaphragm on joists with the underlayerment above followed by a spanning cementatious board with tile set into a mortar bed on top of that. When combined with a drywall ceiling supported on resilient channel these constructions can provide IIC ratings a few points above minimum code. At this rating footfall noise is still clearly audible, and although the system may pass the minimum code requirements, it is unlikely to meet a condominium buyer's reasonable expectation of quality. The general failing of these materials is that they are so thin (1/4–3/8" thick) that they provide very little deflection. Hence their natural frequency of vibration is relatively high. When combined with the reduced impedance of the support system below due to the lack of lightweight concrete, their overall effectiveness is modest. Figure 12.22 shows the test results using a mesh mat underlayerment below a tile floor, which has an IIC 53 rating, barely above the minimum code.

The preferred floor covering in multifamily dwellings is carpet and pad. Hard surface floor coverings such as marble tile, quarry tile, and hardwood flooring are not recommended unless a spring-supported ceiling and a resilient floating floor are used. Even in these cases high quality IIC ratings are difficult to achieve. Figure 15.14 gives an example of a hardwood floor, which has achieved a field IIC rating of 69. The floating floor rests on 1" (25 mm) thick, 20 durometer dimpled rubber mats. The ceiling is supported on 1" deflection spring isolators. A similar installation with tile would likely have a lower rating. Note that the overall thickness of this construction is 18" (460 mm).

Where the appearance of wood or tile is desired, a hard surface can be used in non-walking areas such as within 1 to 2 feet (0.3–0.6 m) of a wall with carpet installed where walking traffic occurs. In kitchen and bathroom areas vinyl tile over a soft backing material such as a 20 durometer, 11/16" (17 mm) thick, dimpled rubber mat can provide reasonable IIC ratings, particularly when combined with a point-mounted resiliently suspended ceiling.

FIGURE 15.14   Double Isolated Wood Floor –Ceiling (Adams, 2002)

3/4" (19 mm) Wood Flooring on 1" (25 mm) Wood Sleepers
1" (25 mm) Lightweight Concrete Between the Sleepers
(110 lbs/cu ft or 1760 kg/cu m)
1" (25 mm) Thick Regupol QT2025.8 Underlayerment
3/4" (19 mm) Plywood Subfloor Glued and Screw Nailed
12" (300 mm) TJI Wood Joists
R-19 (6" or 150 mm) Batt Insulation
1" (25 mm) Deflection Spring Isolators
1 1/2" (38 mm) Carrying Channel
2 Layers 5/8" (16 mm) Gypsum Board on Hat Channel

100	125	160	200	250	315	400	500	630	800	1 K	1.3 K	1.6 K	2 K	2.5 K	3.2 K	FIIC
47	49	48	48	49	47	41	38	36	33	30	29	28	27	25	20	69

15.4   PLUMBING AND PIPING NOISE

Noise from plumbing and piping is one of the most important causes of dissatisfaction in residential structures. It has become much more noticeable with the unfortunate use of plastic pipe in waste stacks, but it can also be caused by excessive flow velocities in supply pipes and be exacerbated by poor isolation. Plumbing and piping noise frequently originates with turbulent flow in pipes and fixtures and is transmitted primarily through vibrational coupling to the building structure and into the occupied spaces. Several other noise generation mechanisms are present in plumbing including cavitation, water hammer, vibrational transmission of pump or other mechanical noise, and water impact or splash noise; however, noise produced by turbulent flow is the primary source.

Supply Pipe

For normal velocities, the flow of water in straight residential supply pipes can be considered to be turbulent. In turbulent flow, regions of highly varying pressure are created, which transfer to the walls of the pipe and from there to the structure. Although turbulence is present in straight pipe, it is mainly caused by valves, fixtures, elbows, and constrictions. Several factors influence the noise generated by a supply pipe. The first is the velocity of flow within the pipe itself, which affects the amount of noise created by any valves or fixtures. The second is the way in which the pipe is attached to the structural framing, both to the structure and to the surface material.

Measurements have been made by Van Houten (1979), who investigated both these factors. Figure 15.15 shows his experimental setup. The test apparatus consisted of a double stud wall with one layer of drywall on each side and supply piping through the studs on the far side of the wall. Pressure was regulated with a valve and the pipe was terminated in a flexible hose. This is perhaps not the most realistic test condition since in a real situation the flow regulating fixture would probably be remotely located.

The attachment methods are sketched in Fig. 15.16. When pipes are routed through holes drilled in a series of studs it is rare that each hole is perfectly aligned with its neighbor. Consequently the pipe, which courses through these holes, will lie closer to the stud on one side or the other at each penetration. Isolators that are wedged into the holes will be pinched on the close side or will be loose if the holes are oversized. The preferred mounting method is to wrap felt around the pipe, outside the hole, and to band it with plumbers tape. This

FIGURE 15.15 Piping Noise Test Configuration (Van Houten, 1979)
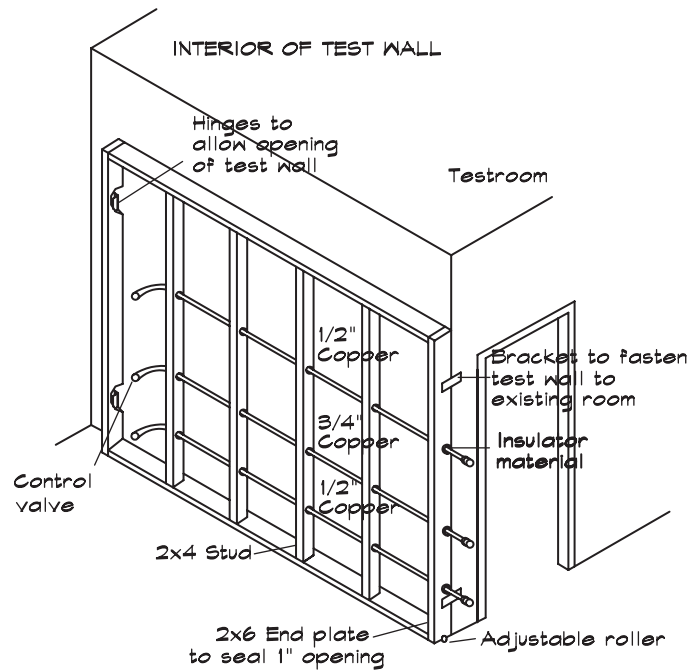
FIGURE 15.16 Pipe Mounting Methods and Descriptions (Van Houten, 1979)

MOUNTING	METHOD OF PIPE MOUNTING	ILLUSTRATION
A	Wood wedges, two wood wedges forced between the pipe and stud	Wood
B	"J" Hook nail ons, Type 3/4" E.M.T. nail on at each pipe penetratio of stud	Nail-on
C	Felt packing, 1/2" thick carpet felt packed between the pipe and stud	Felt
D	Pipe insulator, insulator without foam insert	Insulator
E	Pipe insulator, with polyethylene foam insert	Polyethylene Foam
F	Rubber bands	Rubber bands

TABLE 15.7   Sound Levels Transmitted by Supply Piping, dBA (Van Houten, 1979)

Mounting Description		Supply Pressure			
1/2" Copper Water Pipe		**30 psi**	**45 psi**	**60 psi**	**70 psi**
A	Wood Wedges	50	54.5	56	57
B	J Hooks	50	54.5	56	
C	Felt Packing	44.5	48.5	49.5	
D	Plastic Pipe Insulator	51.5	55.5	57.5	
E	Foam Pipe Insulator	40.5	43.5	44	
F	Rubber Bands	35.5	35.5	31	
3/4" Copper Water Pipe					
A	Wood Wedges	47.5	51.5	52.5	
C	Felt Packing	42.5	45.5	46	
E	Foam Pipe Insulator	39.5	42.5	43.5	

allows the pipe to move without making contact with the stud. In general piping should be free to move slightly but must not touch the structure or the drywall. When a pipe cannot move, it indicates that it is being rigidly constrained, either by the structure or by an isolator that is overly compressed.

For a specific diameter pipe, the noise generated at a given back pressure is illustrated in Table 15.7. The data show the dependence of the noise level on pressure and mounting for 1/2" (13 mm) and 3/4" (19 mm) diameter pipe. Clearly there is substantial benefit to lower pressures; however in practice, pressures of 45 psi are usually required to maintain adequate flow. High pressures, on the order of 60 to 70 psi, are not necessary and should be avoided.

The data shown in Table 15.7 illustrate that there is little difference in noise level among the different types of rigid connections. Wood wedges, J hooks, and hard plastic pipe supports all lead to high levels even when contained in a double stud wall with batt insulation. There is substantial improvement afforded by resilient supports and the softer the mount the greater the isolation, although considerable effort is required to achieve satisfactory levels. This may be due in part to the setup of this experiment with the control valve upstream of the test section located close to the wall. It emphasizes the importance of keeping plumbing fixtures off party walls.

Table 15.7 lists the pipe diameter, mounting method, and back pressure as independent variables. In most real situations the flow volume is fixed by the downstream conditions. For example, if a pipe serves a shower nozzle the conditions at the outlet determine the flow rate. Upstream the piping can be sized to control the fluid velocity and thus the local turbulent noise. Careful selection of valves and nozzles can help reduce noise generation at the termination.

Intrusive noise due to plumbing and piping should be limited to the levels set forth in Table 15.8. These apply to any occupied space within a dwelling unit, including bathrooms. As we have previously discussed, as the level of quality increases the tolerance for neighbor-generated intrusive noise decreases.

In order to control turbulence-generated noise in supply piping a combination of several steps is required. First, the line pressure in the supply pipes should be below 60 psi. Second,

TABLE 15.8   Maximum Intrusive Noise Levels Due to Plumbing

Classification	SPL (dBA)
Minimum Quality	35
Medium Quality	30
High Quality	25

the pipes must be sized large enough that flow generated noise is kept to a minimum. Table 15.9 shows recommended pipe sizes and the maximum flow velocities and flow rates (Wilson, Ihrig & Associates, 1976).

A tub fills at a rate of about 8 gal/min so that a 1" (25 mm) pipe would be appropriate. A low-flow shower supplies water at about 3 gal/min so a minimum 3/4" (19 mm) pipe could be used. Where multiple fixtures are served the supply pipes should be scaled up accordingly. The larger pipe diameters allow local flow velocities to remain low even when it is necessary to neck down a pipe size to accommodate a valve or fixture. The third factor is wall construction. In walls containing piping that serves another unit, the wall surface should be a minimum of two layers of 5/8" (16 mm) drywall. There should be a full layer of batt insulation in all walls where supply, waste, or other fluid-carrying pipes are located.

The fourth factor, mechanical decoupling, is perhaps the most important. Piping must be physically decoupled from both support structure and from the wall surface. In party walls the piping should be supported only on the side of the wall that is served by the pipe. The type of resilient support is summarized in Table 15.10. Note that the isolation shown above is for water supply pipes. It is not required for vent stacks, fire sprinkler pipes, or gas pipes, although when vent stacks are rigidly attached to waste stacks they too should be isolated.

TABLE 15.9   Maximum Flow Velocities in Supply Pipe (Wilson, Ihrig & Associates, 1976)

Nominal Pipe Size (inches)	Max. Velocity (ft/sec)	Max. Flow Rate (gal/min)
1/2	1	1
3/4	2	3
1	3	8
1 1/4	3.2	15
1 1/2	3.5	22
2	4	42
2 1/2	5	74
3	6	138
3 1/2	6.5	200
4	7	277
5	7.5	467
6	8	720

TABLE 15.10   Vibration Isolation of Supply Piping

Nominal Pipe Size	Required Isolation Type	
(inches)	Horizontal	Vertical
1/2	1/4" Felt	1/4"Felt
3/4	3/8" Felt	3/8"Felt
1	3/8" Felt	3/8" Felt
1 1/4	3/8" Felt	3/8" Felt
1 1/2	3/8" Felt	3/8" Felt
2	1/2" Felt	WSW Pads
2 1/2	HN Hangers	WSW Pads
3	HN Hangers	ND Mounts
3 1/2	HN Hangers	ND Mounts
4	HS Hangers*	V Mounts*
5	HS Hangers*	V Mounts*
6	HS Hangers*	V Mounts*

*Nominal 1" deflection isolators

The details of the pipe isolation vary somewhat. For small diameters (< 2") the pipe can be secured with a full wrap of plumbers tape around a 1/4" (6 mm) felt pad. Foam and plastic isolators are commercially available, but they must contain a sufficient thickness (1/4–3/8") of foam or other isolating material to be effective. Hard-plastic mounts without soft inserts are ineffective. Neoprene in shear isolators can be effective in securing shower supply pipe as shown in Fig. 15.17.

With larger pipe sizes it may be more convenient to mount a number of pipes to a common structural frame, which is itself supported on neoprene mounts as Fig. 15.18 shows. Vertical riser pipes are held in place with a pipe clamp, which then rests on neoprene mounts or pads, as in Fig. 15.19.

In critical applications such as high-quality construction, it is sometimes necessary to wrap supply pipes with foam lead sheets where the pipes are located within walls or floor-ceilings of other occupied spaces, or where they are contained in the wall of a bedroom. Foam lead sheets consist of 1/4" (6 mm) foam adhesively attached to both sides of a 2 lb/sq ft (9.8 kg/sq m) lead sheet approximately 1/16" (1.6 mm) thick, which provides both vibration isolation and noise reduction. They can be cut to the appropriate size with shears and tied

FIGURE 15.17   Felt Isolated Shower Attachment
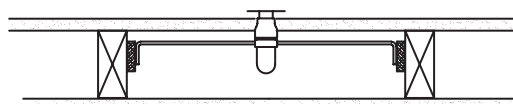
Screws are inserted through the felt pads.

FIGURE 15.18 Resilient Multiple Pipe Support
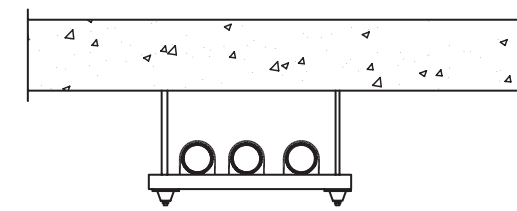
Type N neoprene isolator with threaded rod.
Rods shall not touch pipe or framing.

FIGURE 15.19 Floor Penetration Detail for Pipe Risers

Conventional
pipe clamp

Type WSW Pad

Floor
construction

Pipe

Pack with
safing
material
all around
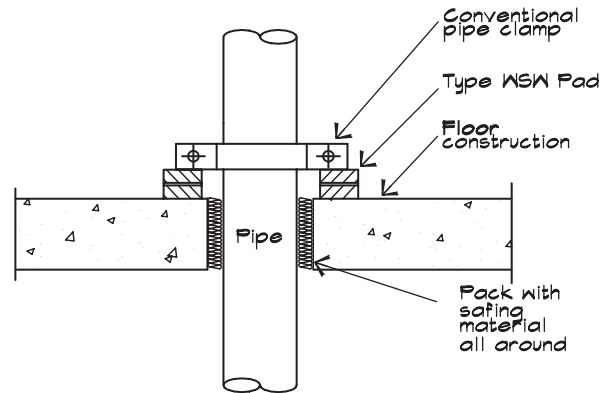
Neoprene waffle pads should be 40 durometer, and sized
to accommodate the calculated load. For heavy pipes
a 10 Ga top plate may be used to spread the load.

with wires so that they completely encircle the pipe and overlap at least an inch (2.5 cm). Additional felt at points of support is not required for foam lead wrapped pipe.

Water Hammer

Water hammer is a shock wave, usually generated by the rapid closure of a valve, but occasionally caused by a pressure wave resonance within a pipe. In the case of an isolated occurrence, it produces a violent slamming, which physically moves the pipe and causes a loud banging noise. In the case of a resonance the passage of a shock wave back and forth results in a very loud low-frequency buzzing sound.

Water hammer creates a dramatic effect, which if allowed to continue, can result in damage to the pipe. Control is effected by exposing the fluid stream to a confined air pocket, which allows the high pressure shock to expand into a pressure release surface. These devices, called water hammer arrestors, contain a gas trapped in a flexible bladder that encircles the fluid or is contained in a separate branch on a threaded T-fixture. In residential structures

such devices are very effective when mounted to the outlet pipe of the water heater and near any quick-closing valves, such as automatic sprinkler systems. Occasionally they may also be necessary to control resonances in long runs of pipe or near a particularly troublesome valve.

Waste Stacks

Waste stacks, which carry water and effluent from toilets and other fixtures, are a frequent cause of noise complaints, particularly when plastic (PVC or ABS) pipe is used. This lightweight pipe transmits annoying levels of noise when water flows through it. When a toilet is flushed upstairs and the water rushes through a plastic pipe, levels as high as 60 to 65 dBA have been measured in downstairs units. This is loud enough that it makes normal conversations difficult and is certainly a show-stopper for the party guests. The cause is the lightweight plastic material, which vibrates due to the turbulent flow created by the passage of the waste water, and any direct coupling of the pipe to the structure. Consequently plastic waste stacks should never be used in residential buildings or sensitive commercial structures such as offices, classrooms, hospitals, studios, or theaters even for short runs such as P-traps.

Instead of plastic, cast iron is the preferred material for waste stacks due to its mass. Even with cast iron problems may arise if the pipe is not properly isolated. Waste stacks must be vibrationally isolated just as supply pipes were isolated. The inherent mass of cast iron and the relatively slow fluid velocity makes the isolation requirements less stringent than similarly sized supply pipes. Vertical risers should be supported on type WSW neoprene waffle pads as shown in Fig. 15.19. Horizontal runs may be isolated with 1/2" (13 mm) felt or neoprene pads. Frequently waste stacks exceed 2.5" (64 mm) in diameter, and when they are wrapped with a felt isolation material the combination may not fit within a single stud space without binding. Thus it is prudent to allow at least a 2 × 6 stud for all walls housing waste stacks. This permits a neatly drilled round hole of sufficient size to allow the pipe to pass through the base plate or stud without touching the structure.

When treating an existing condition where plastic pipe has been used as a waste stack, noise levels have been reduced to inaudibility by decoupling the pipe from the structure, wrapping it with 2 lb/sq ft (9.8 kg/sq m) foam lead sheets, installing R-11 batt insulation in the airspace, and applying two layers of 5/8" (16 mm) drywall on resilient channel to the stud. In some cases the replacement of plastic pipe with cast iron pipe may be less expensive. Note that if the plastic pipe is replaced it should be removed completely for its entire length.

Tubs, Toilets, and Showers

Tubs, toilets, and showers should be installed over a floor-ceiling, which is equivalent to that constructed in the rest of the residence. In wood construction if the floor has lightweight concrete it should extend under the tub or shower. Where fiberglass tubs are installed, it is good practice to pour additional lightweight concrete around the bottom of the tub to add mass and damping.

Below the tub, where the piping penetrates the floor, builders sometimes leave a sizable opening in the floor for ease of installation. This must be closed for both acoustical and fire

FIGURE 15.20   Bathtub Installation Detail
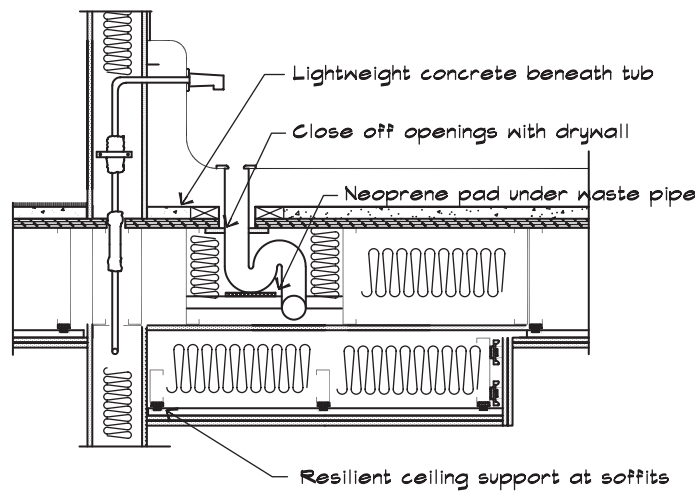
code reasons using at least two layers of 5/8" (16 mm) drywall as in Fig. 15.20. Where the P-trap is supported on a crosspiece the pipe should rest on a neoprene waffle pad isolator consistent with its size.

Since the noise generated by supply piping is velocity dependent, low-flow devices like an aerated showerhead can reduce supply-pipe noise. Upstream noise from the pipe serving a toilet can be reduced by restricting the flow locally at the wall valve. Careful selection of quiet fixtures such as ball valves can prevent noise creation at a critical location.

Pump and Piping Vibrations

When a pump is located in a residential or other noise-sensitive structure the pulsations imparted to both the pipe and the driven fluid can create noise both by vibrational and airborne transmission paths. Control of pump vibrations begins with the location of the pump in a nonsensitive area such as a basement; however, it is not uncommon to find rooftop installations in large condominium complexes. Both the pump and the pipe must be properly isolated, beginning with a concrete housekeeping pad and inertial base such as that shown in Fig. 13.6. Any piping attached to isolated equipment, which includes not only pumps but cooling towers, compressors, boilers, refrigeration equipment, and fan coil units, must itself be isolated with an isolator having the same deflection as the isolated equipment for a distance of 50 feet or 50 pipe diameters, whichever is greater. At the first point of support an isolator having twice the pump deflection can be used, since when the pipe is drained it weighs considerably less than when it is full. The pump isolators are installed when the pipe is empty, and when it is filled the pump and pipe assembly drops down under the increased load. This motion may crack the pipe unless it is given the freedom to move. All piping must be resiliently supported either from the pump's inertial base or with separate vibration isolators. In addition to isolating the pipe, flexible couplings can be installed near the pump. These serve to compensate for minor pipe misalignments and provide some vibrational decoupling for impulses transmitted along the pipe.

Fluid Pulsations

Occasionally the pulsations induced by a pump impeller will travel from the pump along the pipe and into a structure, through mechanical coupling between the pipe and a wall or floor. In existing buildings some reduction can be obtained by inserting a flexible coupling in the pipe between the pump and the receiver.

In high-pressure lines the impeller impulses may also be transmitted within the fluid so that a pulse dampener is recommended on the supply side of the pump after the flexible coupling. Pulse dampeners work in much the same way as a water hammer arrestor with an encapsulated gas-filled bladder. The pressure surge is allowed to expand into the bladder, which removes it from the liquid in the pipe. These devices are commercially available and are quite effective for attenuating vibrations in high-pressure lines including hydraulic lines.

15.5   MECHANICAL EQUIPMENT

Split Systems

Mechanical systems in residential structures provide heating, ventilating, and air conditioning (HVAC) services to the building. The thermodynamic principles were discussed in Chapt. 13. A typical system consists of an external air-cooled condenser, which gives up heat to the outdoors in the process of compressing a circulating refrigerant. The refrigerant is pumped through copper pipes to a fan coil unit where it is forced through an expansion valve and a coil, where it changes state from a liquid to a gas and absorbs heat from its surroundings. Air is blown over the cooling coil through which the refrigerant passes and heat is transferred to the coils and then to the refrigerant. Heat can be generated by an electric coil or separate gas-fired boiler.

Roof-mounted compressors, unless properly configured, can be a source of annoying vibration. Units should be installed as in Fig. 15.21. In wood buildings compressors are set on small platforms built of 3" (75 mm) lightweight concrete pads extending at least 12" (150 mm) beyond the outside of the unit. The unit itself is supported on 1" (25 mm) deflection spring isolators. Any electrical connections to the compressor are made using a minimum of 3' (1 m) flexible wiring, which allows the unit to move freely back and forth and up and

FIGURE 15.21   Rooftop Condenser Installation
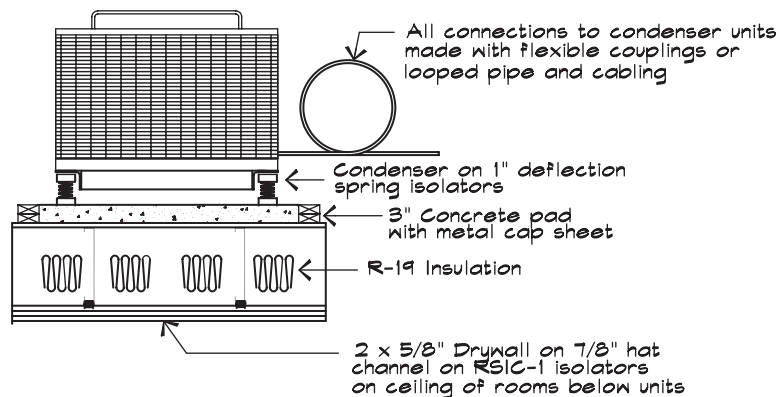
FIGURE 15.22 Vertical Fan Coil Unit
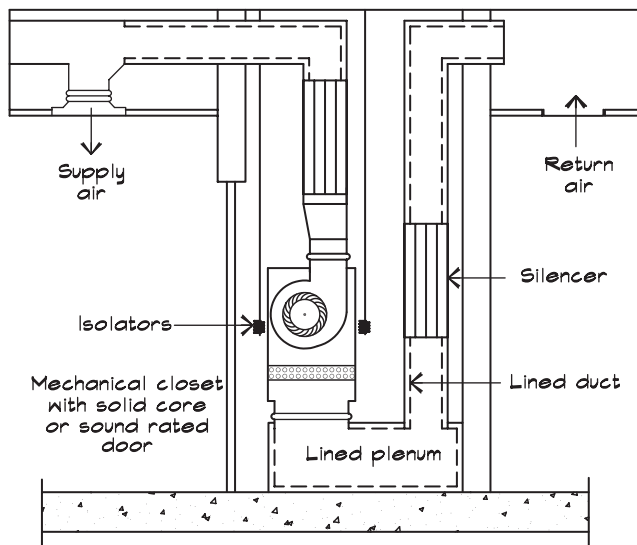
down on its isolators. Since the refrigerant lines are connected rigidly to the compressor it is good practice to wrap them one full turn around the unit before they penetrate the roof. This reduces the transmitted vibration that travels along the tubing. Refrigerant lines can create noise in the 35 to 40 dBA range if improperly isolated. They should be wrapped with foam insulation and be routed through a chase or within stacked fan coil closets. Where refrigerant lines are located in walls adjacent to critical areas such as bedrooms they should be wrapped with foam lead sheets. In any case they must not make direct contact with the structure or drywall.

Fan coil units are also a source of noise in residential buildings. They can be located in an attic in single-family residences or in a closet in multifamily dwellings and usually require a 3' (1 m) medium pressure drop silencer or equivalent loss in lined duct and elbows on the supply and return ducts to control duct borne noise. One effective mounting method is to arrange the fan coil vertically in a closet with a ducted supply and return as in Fig. 15.22.

Where the air is returned to the closet through a louvered panel located under the fan coil, noise levels are generally unacceptable, ranging from 45 to 55 dBA in the room containing the intake. Lining the area beneath the fan coil is of marginal value. Generally this space is too small to act as a plenum and at best becomes a lined elbow, which provides only a few dB of loss. Figure 15.23 shows a way of installing a fan coil or heat pump without a ducted return so that the return-air noise transmission path is attenuated by using a transfer-duct silencer. A heavy solid-core or sound-rated door with air-tight weather stripping, along with 2" (50 mm) fiberglass duct-liner board and 0.4" (10 mm) deflection neoprene isolators are necessary to properly isolate a vertical fan coil unit. Detailed calculations based on the casing radiated sound power levels of the unit can clarify the level of isolation required.

Packaged Units

Small packaged air handling units can be rooftop-mounted and contain a compressor, fan coil, and cooling fan in a single unit. These units are available in a side-discharge or

FIGURE 15.23   Fan Coil Unit with a Transfer Duct
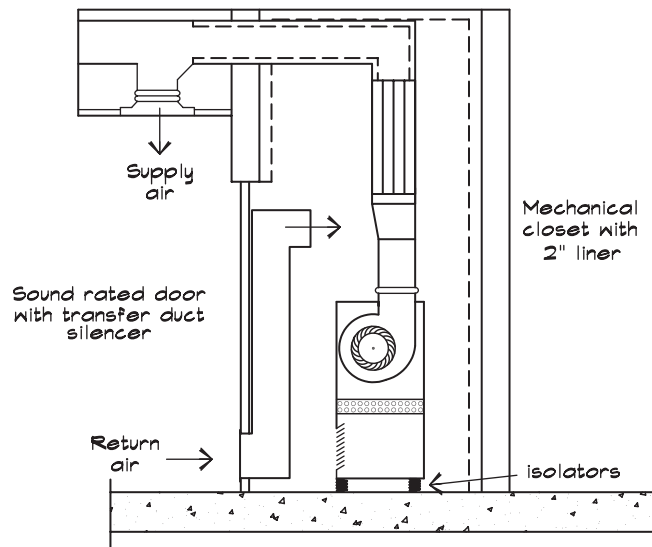
FIGURE 15.24   Roof-Mounted Packaged Air Handlers
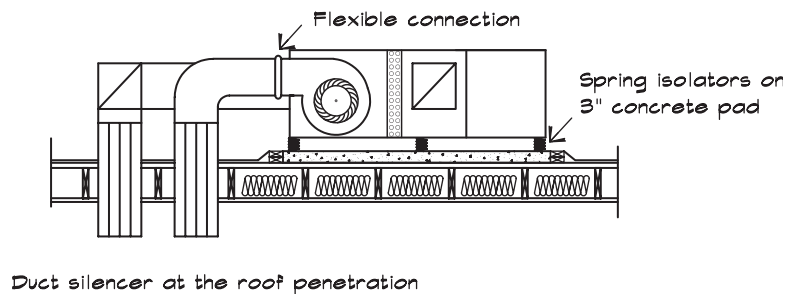
down-discharge configuration. For purposes of noise control, the side-discharge units are much preferred since this allows space for the installation of silencers in a horizontal run of duct. In down-blast units, the air and noise issue straight down out of the unit, allowing very little room for a silencer or other attenuating mechanism. Figure 15.24 shows the preferred configuration for side-discharge units with silencers installed in the vertical drop. This location is optimal for the attenuation of both duct borne noise and exterior noise breaking into the duct.

Sound power levels associated with small packaged units vary according to the fan scaling laws discussed in Chapt. 13. They usually require some lined duct and either a 3' (1 m) or a 5' (1.5 m) medium pressure drop silencer to reduce levels to below an NC 30. An analysis along the lines of the calculation set forth in Chapt. 14 can yield the required attenuation.

Vibration isolation for these packaged units is similar to that for compressors. Rooftop units should be set on 3" (150 mm) lightweight concrete housekeeping pads and supported on 1" (25 mm) deflection spring isolators. In areas requiring seismic restraint separate limit

stops are installed. Electrical connections are by means of 3' (1 m) long flexible cables. A flexible connection is used to couple the duct to the package unit. When they are located above critical areas, roof-mounted ductwork should be supported on neoprene isolators having a 0.25" (6 mm) deflection. Any condensate lines should be supported from the isolated equipment and not from the roof deck.

Roof-mounted boilers and associated piping must also be vibration isolated. Boilers with integral pumps need 1" (25 mm) deflection isolators and those with separate pumps should have 0.25" (6 mm) deflection neoprene mounts. Gas lines, which cannot include flexible connections, attached to isolated equipment should have four or more 90° bends separated by 3' (1 m) of straight pipe and be supported on 0.25" (6 mm) deflection neoprene isolators.

15.6 APPLIANCES AND OTHER SOURCES OF NOISE

Stairways

Footfall impacts on stairways can be conducted structurally through the studs, which support the stair risers. This, in turn, is radiated by the panels attached to the wall studs. In townhouse (two-story) condominiums and apartments it is good practice to locate the stairways on the interior of the unit away from the party walls. When this is not possible the stairways should be supported separately and the risers must not be physically attached to the wall framing or drywall. The party wall surface must be continuous behind the stairs and the treads, and risers and framing must not touch the drywall. Separate pipe columns may be used to support the stair landing and the diagonal supports should be attached only at the landing and the floor.

Appliances

In critical residential structures such as condominium units, free-standing appliances such as washers, dryers, and dishwashers should be isolated from the floor by using neoprene mounts. When this arrangement affects the lateral stability of the unit such as during a spin cycle in a washing machine, a lateral stabilizer may be necessary. This, too, should be in the form of a neoprene isolator having the same stiffness as the vertical one. The lateral stabilizer can be bolted to a crosspiece of plywood, which in turn is bolted to the washer. Quick acting valves in washing machines can cause water hammer in certain cases. Generally the hoses used to connect to the supply pipes have sufficient flexibility to dissipate the pressure pulse. Where this is not the case a water hammer arrestor located near the valve on the supply pipe will solve the problem and extend the life of the hose.

Garbage disposals present a unique set of problems for vibration isolation. Internally isolated units have become available, which have a shell within a shell construction and internal neoprene mounts. These are much preferred over the standard models, but they must be installed with a piece of flexible hose approximately 18" (450 mm) long to decouple the waste pipe from the disposal.

Jacuzzis

Jacuzzi tubs have an aerator, which mixes air with the tub water, and a circulation pump forces the mixture back into the tub in a closed-loop cycle. The combination can produce relatively high noise levels in multifamily dwellings both directly under the tub as well as in rooms adjacent to the epicenter. Noise levels as high as 50 to 60 dBA have been measured

directly beneath a Jacuzzi tub in wood structures with lightweight concrete floors, and in the 40 to 50 dBA range in nearby rooms one floor below. Resiliently mounting the motor and pump provide some relief, on the order of 5 dB, but not enough to meet the levels set forth in Table 15.8.

In concrete structures Jacuzzi tubs have been installed on 4" (100 mm) concrete floating floors with 1" (25 mm) deflection spring isolators on a 6" (150 mm) slab. This approach addresses the sound and vibration problem but introduces a significant floor height change up to the base of the tub. The variation in floor height with the addition of water and bathers must also be accommodated. In general Jacuzzi tubs should not be installed in multifamily dwellings above the first floor.

Trash Chutes

Trash chutes are constructed of sheet metal tubes mounted in shafts, which carry trash from upper floors to a receptacle in the basement. They are best located in a masonry shaft, which is not on a wall of a dwelling unit. Shafts can be constructed of grouted concrete block units. Where they are located on common walls an additional batted stud wall with two layers of drywall, which does not make physical contact with the shaft wall, should be used to reduce their impact. Some authors (Harris, 1994) recommend that the steel trash chutes themselves be isolated and that the trash receptacles be covered with damping material.

Elevator Shafts and Equipment Rooms

Elevator shafts in multifamily dwellings and in office complexes are best located in a separate utility core, which is not contiguous to occupied spaces. Even if an elevator equipment room is remotely located, the elevator passage itself can cause noise levels in the 50 dBA range due to the vibration transmitted through the vertical guide rails. Where elevator shafts are located adjacent to occupied spaces a double stud double drywall wall has been used. Even in these cases vibration may still be transmitted into the adjacent space via the direct coupling of the rails to the slab or floor system.

Elevator equipment is either hydraulic or electric. Hydraulic equipment is located near the bottom of the shaft and consists of a pump, associated piping, and a thrust cylinder. The pump and piping is of greatest concern whereas the cylinder is rarely a factor. When the pump is located on a structural slab on grade below occupied areas it rarely presents a problem. Hydraulic pumps above grade should be vibration isolated using neoprene mounts. Code requirements prohibit flexible hose from being used as hydraulic lines so solid piping should be separated from the structure using isolators.

Electric winches control the elevator height by a cable wound on a drum located at the top of the shaft. In critical applications the drum and winch can be isolated by mounting the entire assembly on a concrete slab, which is set on isolators. Due to safety considerations, the mechanism must be designed so as to tolerate a failure or bottoming out of the isolation system.

Garage Doors

Where parking is provided below a multifamily dwelling or office building steel gates sometimes are installed for security. In an overhead installation the gate is supported at the sides on two vertical pipe columns attached top and bottom to the slabs. An electric motor hung from the slab above drives a chain or gear mechanism, which raises and lowers the gate.

When these gates are attached in this manner the vibration from the opening and closing of the gate can produce considerable annoyance to occupants of the floor above.

A preferable alternative to the overhead attachment is a side-opening gate, which is supported from below. Here the gate rides on a V rail and rolls to the side, driven by a chain drive motor bolted to the floor. In these installations a simple neoprene isolator supporting the track attached to the upper slab is usually sufficient to control the transmitted vibration. The important feature is that the upper rail system must not be directly coupled to the slab above. Where there is insufficient space for a side-opening gate an overhead gate can be supported using an independent structure on steel columns that do not make contact with the floor above.

16

DESIGN AND
CONSTRUCTION OF
OFFICE BUILDINGS

Commercial buildings present a set of design issues that differ somewhat from those encountered in residential structures. In critical spaces such as classrooms, theaters, and studios, much of the information presented in Chapt. 15 is still applicable. In commercial office buildings the uses can vary, and may include less sensitive spaces. Structures are likely to be multistory, with an air handling unit on each floor located in a central core, along with other services such as elevator shafts, stairwells, and bathrooms. Mechanical equipment is also located on the roof, sometimes directly above the most prestigious and expensive floor space. The main air ducts are sized, based on the clearance afforded by the ceiling heights, and velocities may be relatively high. Air is likely to be returned through a common plenum, which complicates the room-to-room noise transmission problem.

In high-rise office towers exterior walls can be continuously glazed curtain walls, framed outside the flooring system, with narrow mullions, leaving little opportunity for closure of gaps at the interior walls and floors. Floor coverings may not be selected based on considerations of footfall noise. Conflicting uses may abut one another. These and many more details, which are critical to a satisfactory work environment, may not be totally under the control of the acoustical engineer, but nevertheless should be addressed.

16.1 SPEECH PRIVACY IN OPEN OFFICES

Privacy

When the intelligibility of speech is low, not surprisingly it follows that the privacy is high. Table 16.1 (ANSI S3.5) shows the relationship between Articulation Index, signal-to-noise ratio, and privacy. Written characterizations of these degrees of privacy were given in Table. 3.6.

In an office environment, where speech privacy is the goal, we can strive to achieve the required signal-to-noise ratio in several ways. The general form of the intelligibility equation is

$$
\begin{bmatrix} \text{Source} \\ \text{Sound} \\ \text{Level} \end{bmatrix} - \begin{bmatrix} \text{Sound} \\ \text{Attenuation} \\ \text{(Reduction)} \end{bmatrix} - \begin{bmatrix} \text{Masking} \\ \text{Sound} \\ \text{Level} \end{bmatrix} = \begin{bmatrix} \text{Signal to} \\ \text{Noise Ratio} \\ \text{(Privacy)} \end{bmatrix} \qquad (16.1)
$$

TABLE 16.1   **The Relationship between Intelligibility and Privacy**

Articulation Index	Signal to Noise	% Sentences Understood	Intelligibility	Privacy
> 0.4	> 0 dB	> 90	Very Good	None
0.3	−3 dB	80	Good	Poor
0.2	−6 dB	50	Fair	Transitional
0.1	−9 dB	20	Poor	Normal
< 0.05	−12 dB	0	Very Poor	Confidential

Clearly we have three possible ways of influencing the signal-to-noise ratio: 1) control the sound source, 2) increase the path attenuation, and 3) raise the masking sound level. The source can be oriented to take advantage of the natural directivity of the human voice. The direct sound path can be controlled by using full or partial height barriers. Reflections can be attenuated with absorptive materials, and we can electronically generate background noise to mask intrusive speech. The details of each of these features depend on the office configuration and other design considerations.

Privacy Calculations

Calculations based on Eq. 16.1 can be carried out in individual third-octave or full-octave bands. The most accurate method is to use third octaves and the Articulation Index to determine intelligibility; however, there are also useful composite methods. Articulation calculations begin with the layout of the working environment.

Offices are configured either as separate rooms with full or partial height walls or as an open plan layout. Open-office plan refers to a system of workstations, distributed about an open floor, separated by partial height barriers. This design approach yields a flexible and relatively inexpensive work space, which if properly designed can furnish a degree of privacy for telephone and other conversations. Originally developed in the 1960s, its effectiveness unfortunately was oversold at first and its reputation subsequently suffered from unfulfilled expectations. Problems also arose when the system was only partially implemented.

Privacy in an open-office work environment can be achieved only when all the critical components are present and properly implemented. These include: 1) careful arrangement of the furniture and occupants, including the orientation of both talkers and listeners; 2) partial height barriers of the correct type, height, and location; 3) highly absorbent ceiling and wall panels; and 4) masking sound having the proper spectral content and level.

Chanaud (1983) and others have developed detailed methodologies for evaluating speech privacy in open offices by calculating the speech intelligibility between workstations. All calculations are based on Eq. 16.1; in the office environment, however, there is a large number of potential sound paths to be considered. Figure 16.1 shows several, each of which must be evaluated to arrive at the final signal-to-noise ratio at a receiver. Figure 16.2 presents a diagram of the separate calculations broken down into individual steps. The final result is a composite signal-to-noise ratio, which leads to the Articulation Index at the receiver. Note that each of these calculations is based on direct-field transmission, where the sound wave has undergone at most one or two reflections. In open-office environments a classic

FIGURE 16.1 Panels and Screens as Speech Barriers
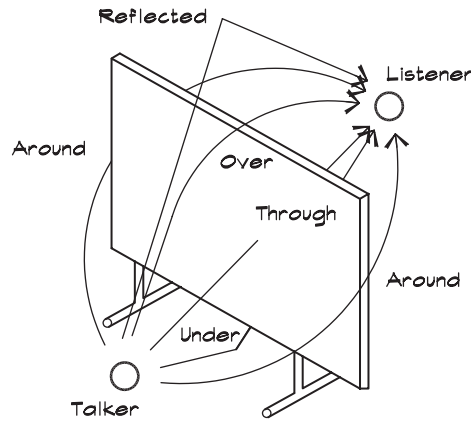
reverberant field does not exist, particularly with intervening barriers and highly absorptive ceilings.

The Articulation Index (AI) is calculated from partial articulation indices (PAI), which are signal-to-noise ratios in each third-octave band, weighted according to the importance of the band for the understanding of speech. The Articulation Index is the sum of these individual weighted signal-to-noise ratios

$$AI = \sum_{i=200}^{5000} PAI_i \qquad (16.2)$$

The signal-to-noise ratio in a particular third-octave band, between 200 Hz and 5000 Hz, is calculated from the source strength, the particular path attenuation (which is called the speech reduction), and the masking spectrum present at the receiver location. Each partial Articulation Index is determined from the signal-to-noise ratio multiplied by the weighting factor particular to a given band

$$PAI_i = (VS_i - SR_i - MS_i)WF_i \qquad (16.3)$$

where   PAI = partial Articulation Index in a given third-octave band

   VS = average peak voice spectrum, in a given third-octave band, of the male voice at one meter, on axis (dB)

   SR = speech reduction—difference between the VS level and the level at the receiver in a given third-octave band (dB)

   MS = third-octave masking sound spectrum (dB)

   WF = third-octave Articulation Index weighting factor

All calculations are limited by conditions on the partial AI components such that

$$If\ PAI_i < 0 \quad then\ set \quad PAI_i = 0 \qquad (16.4)$$

$$PAI_i > 30\ WF_i \quad then \quad PAI_i = 30\ WF_i$$

FIGURE 16.2 Open Plan Speech Rating Diagram (Chanaud, 1983)

PRIMARY FACTORS
VSR – Voice Spectrum Rating
AC – Articulation Class
MSR – Masking Sound Rating
AI – Articulation Index

SECONDARY FACTORS
VDC – Voice Directivity Correction
DR – Distance Rating
SDR – Speech Diffraction Rating
SAR – Speech Absorption Rating
STR – Speech Transmission Rating

GENERALIZED CALCULATION CATEGORIES

```
┌─────┐        ┌─────┐        ┌─────┐     ┌─────┐
│ VSR │───────▶│ AC  │───────▶│ MSR │────▶│ AI  │
└─────┘        └─────┘        └─────┘     └─────┘
```

Direct Path
VDC → DR

Over Barrier
VDC → DR → SDR

Under Barrier
VDC → DR → SDR

Around Barrier
VDC → DR → SDR

Through Barrier
VDC → DR → STR → AC

Ceiling Reflection
VDC → DR → SAR → SDR

Floor Reflection
VDC → DR → SAR → SDR

Wall Reflection
VDC → DR → SAR → SDR

Multiple Reflections
VDC → DR → SAR → SDR
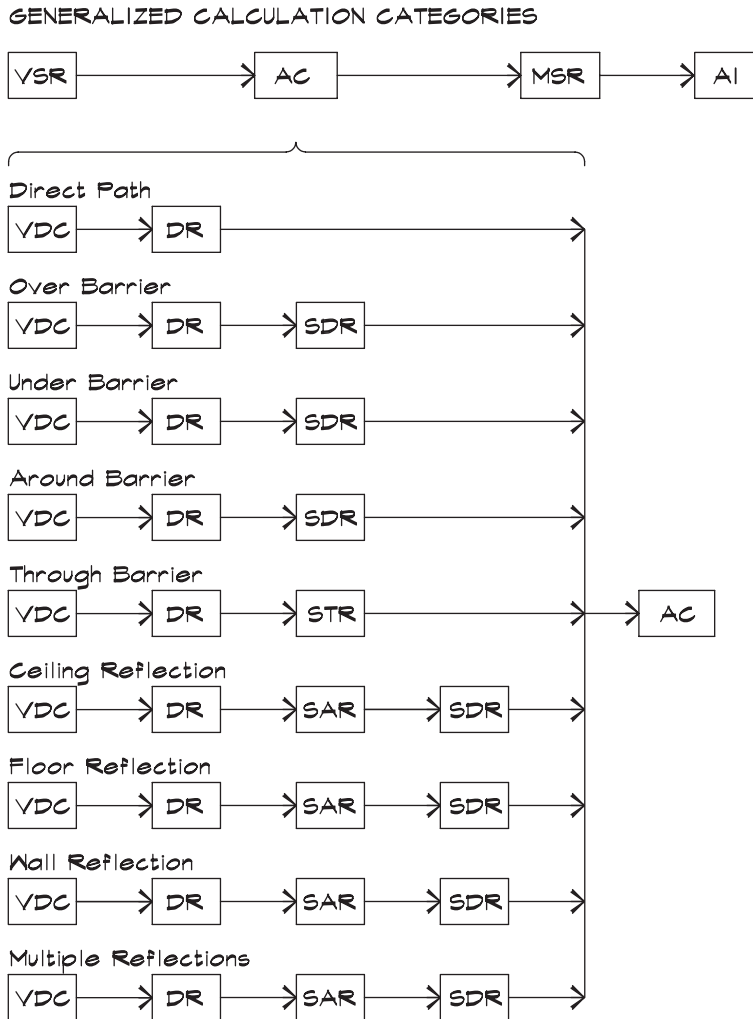
We begin with the sound pressure level and spectrum generated by a male voice adjusted for voice effort and weight it according to the way the ear hears. The voice spectrum (VS) in Fig. 16.3 is the third-octave sound pressure level of the male voice peaks, which differs somewhat from the energy average levels cited previously. The levels in each band are weighted with the AI speech weighting factors, WF, given in Table 16.2. For simplicity we can use the Speech Rating Factor (SRF), which is 30 times the AI weighting factor (WF) and sums to one.

FIGURE 16.3 Average Peak Male Speech Spectra (ANSI S3.5, 1997)

Male - Free Field at 1 m
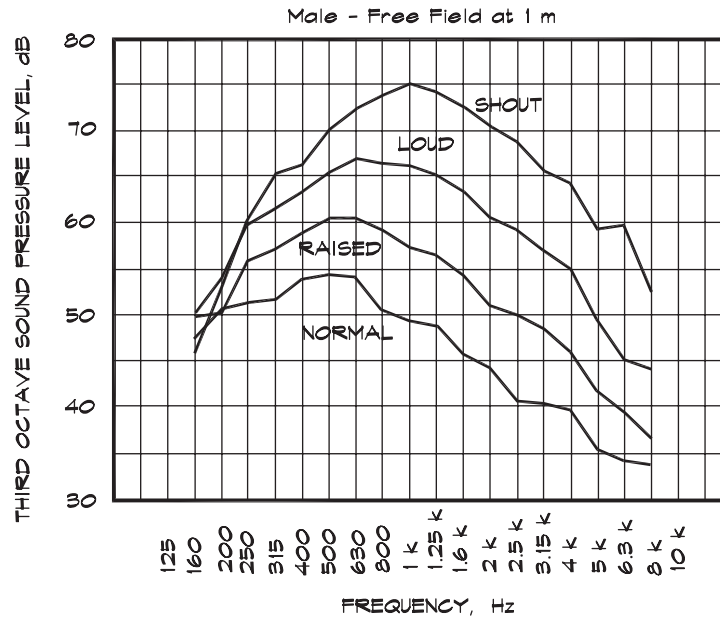
TABLE 16.2   Speech Weighting Factors (ASTM E1110-86)

Freq.	One Third Octave SRF	One Third Octave WF	One Octave SRF	One Octave WF	A-Weighting
200	.012	.0004			−11
250	.030	.0010	.072	.0024	−9
315	.030	.0010			−7
400	.042	.0014			−5
500	.042	.0014	.144	.0048	−3
630	.060	.0020			−2
800	.060	.0020			−1
1000	.072	.0024	.222	.0074	0
1250	.090	.0030			1
1600	.111	.0037			1
2000	.114	.0038	.328	.0109	1
2500	.103	.0034			1
3150	.102	.0034			1
4000	.072	.0024	.234	.0078	1
5000	.060	.0020			1

The speech reduction (SR) is calculated from the directivity relative to the on-axis level associated with the listener direction, the loss due to distance, and the attenuation due to the interaction with objects associated with the particular sound path, including diffraction over barriers, transmission through barriers, or absorption due to reflections. When each path level is computed the overall level in each third-octave band is determined and we compare the composite sound pressure level with the masking sound spectrum $(MS)_i$ to calculate the Articulation Index and the degree of privacy.

To make the AI easier to understand, a metric called the Privacy Index (Chanaud, 1983) was introduced, which increases as the isolation increases. The Privacy Index (PI) is defined as the percentage of privacy in terms of the Articulation Index as

$$PI = 100 \, (1 - AI) \qquad (16.5)$$

The Privacy Index is easier to understand for many users. For example, a 95% Privacy Index is excellent privacy, and 60% is poor.

Articulation Weighted Ratings

The Articulation Index can be estimated (Chanaud, 1983) from three ratings instead of being calculated individually in each third-octave band.

$$AI \cong \frac{1}{30} \, [VSR - AC - MSR] \qquad (16.6)$$

where the AI weightings have been included in the individual rating terms. The ratings are the voice spectrum rating (VSR), which is based on voice level; the speech reduction rating (SRR), originally developed by Chanaud (1983), which has been standardized (ASTM E1110-86) and renamed the Articulation Class (AC); and the masking spectrum rating (MSR) defined in Eq. 16.9.

$$VSR = \sum_{i=200}^{5000} (VS_i)\,(SRF_i) \qquad (16.7)$$

$$AC = \sum_{i=200}^{5000} (SR_i)\,(SRF_i) \qquad (16.8)$$

$$MSR = \sum_{i=200}^{5000} (MS_i)\,(SRF_i) \qquad (16.9)$$

The speech reduction calculation varies depending on the attenuation mechanism associated with a particular path. Each path attenuation can also be discussed in terms of a composite rating. The Articulation Class (AC), as contrasted to the STC rating, is a weighted measure of the noise reduction between two given positions. It can be determined by calculating the losses associated with each sound path.

For example, if the sound is diffracted over a barrier, we can calculate the barrier loss and the associated speech diffraction rating (SDR).

$$SDR = \sum_{i=200}^{5000} (\Delta L_B)_i \, SRF_i \qquad (16.10)$$

For transmission through a barrier, the sound attenuation is the point-to-point direct-field noise reduction, based on the direct-field transmission loss at a given angle and frequency. The speech transmission rating (STR) is written as

$$STR = \sum_{i=200}^{5000} \left\{ \left[\Delta L_{TL}(\theta) \right]_i SRF_i \right\} \qquad (16.11)$$

For surface reflections the speech absorption rating (SAR) is

$$SAR = \sum_{i=200}^{5000} \left\{ \left[\Delta L_s \right]_i SRF_i \right\} \qquad (16.12)$$

where ΔL_s is the attenuation due to a reflection, based on the specular absorption coefficient given in Eq. 16.13.

These rating simplifications have the advantage of allowing a general discussion of the components, while retaining most of the original accuracy. The differences between the results using the separate calculation method and the one-number ratings are shown in Fig. 16.4, where Eq. 16.5 has been inserted into Eq. 16.6 for the estimation of the Privacy Index. The only thing that is dropped in this generalization is the limitation imposed under Eq. 16.4, which leads to a slight over-design at high isolation values.

Experience has shown that there is no single masking spectrum, which provides the most privacy at the lowest overall sound level, and is best for every situation. The shape of the spectrum depends critically on the details of the sound attenuation. Chanaud (2002)

FIGURE 16.4 Privacy Index vs Articulation Class Rating (Chanaud, 2000)
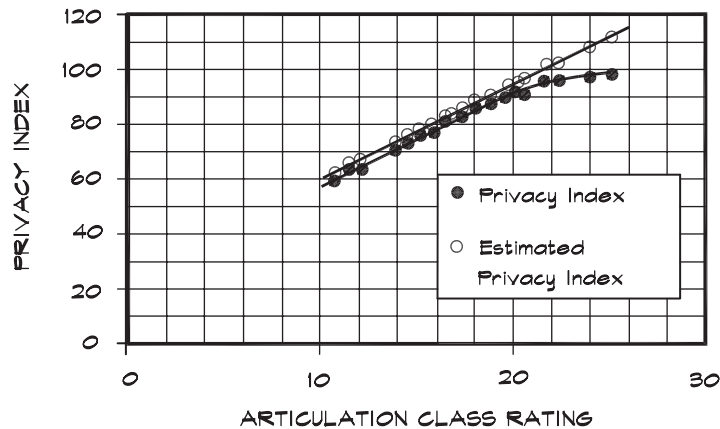
TABLE 16.3   **Masking Sound Spectra (Chanaud, 2002)**

Freq.	One-Third Octave		One Octave	
	Open Office	**Closed Office**	**Open Office**	**Closed Office**
200	43	43		
250	43	41	47	46
315	42	40		
400	41	39		
500	41	37	45	42
630	40	35		
800	39	34		
1000	38	32	43	37
1250	36	30		
1600	34	29		
2000	32	27	37	32
2500	30	25		
3150	28	23		
4000	26	21	31	26
5000	24	19		
dBA	47	43		
MSR	41	37		

suggests two good compromise spectra, one for open offices and another in closed offices, in Table 16.3.

Speech Reduction Rating and Privacy

In a calculation of the Articulation Index, based on the geometry sketched in Fig. 16.5, we begin with the source level and associated spectrum, and calculate the attenuation due to the directivity of the talker, the intervening distance, and barriers or absorbers, finally comparing the level in third octaves to the background level. The masking spectrum (MS) is the actual background noise in the receiving space.

For purposes of this analysis it has been assumed to be the open-office spectrum from Table 16.3. The worst case (least private) condition, at a given distance, would be represented by a face-to-face orientation with no intervening barriers. Table 16.4 shows the results of such a calculation, giving a compilation of the privacy expected from various speech reduction ratings, for a person talking at a normal voice level based on face-to-face orientation and an open-office masking sound level.

What we learn from this figure is that the entire span of privacy ratings falls within a 10 dB range of levels, and that a change of 1 dB in a rating results in a change of .03 in the Articulation Index. Thus even a one-point difference can have a noticeable effect on the degree of privacy. Given these relationships, we can refer to this chart when discussing speech privacy in terms of calculated AC values in more complicated configurations.

FIGURE 16.5 Noise Reduction Ratings by Path
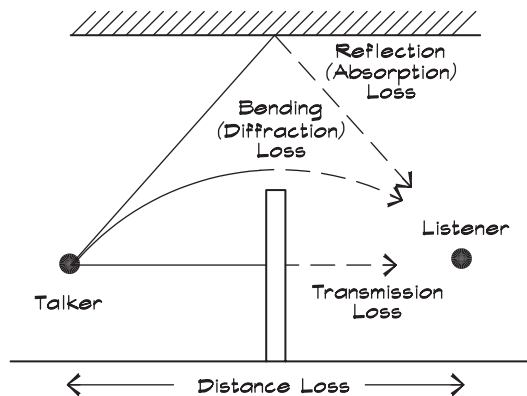
TABLE 16.4   Influence of Sound Attenuation on Speech Privacy (Chanaud, 1983)

Articulation Class	Articulation Index	Privacy Index	Degree of Privacy
16	.37	63	None
17	.33	67	None
18	.30	70	Poor
19	.27	73	Poor
20	.23	77	Poor
21	.20	80	Transitional
22	.17	83	Transitional
23	.13	87	Normal
24	.10	90	Normal
25	.07	93	Normal
26	.05	95	Confidential

Source Control

In open plan analyses the source model is the male voice, which has a characteristic spectrum, level, and directivity. In the analysis of speech, average voice peaks from Fig. 16.3 are used. The overall changes can be approximated by the vocal effort table in Table 16.5.

There are characteristic directivities associated with the human voice, which are shown in Fig. 16.6, relative to on-axis. It is assumed that the receiver has no directivity. From this table we see that a degree of natural attenuation may be achieved by taking advantage of the directivity of the human voice and the orientation of the talker and listener. If workstations are arranged so that the line between two conversing individuals in one workstation is at right angles to the direction of the listener in the next workstation, the directivity correction is maximized.

TABLE 16.5   Voice Level Corrections

Vocal Effort	Correction to Voice Spectrum
Normal	0 dB
Raised	+ 6
Loud	+ 10
Shouting	+ 20

FIGURE 16.6 Comparison of the Relative A-Weighted Levels in the Frontal Vertical and Horizontal Planes for Male and Female Talkers (Chu and Warnock, 2002)
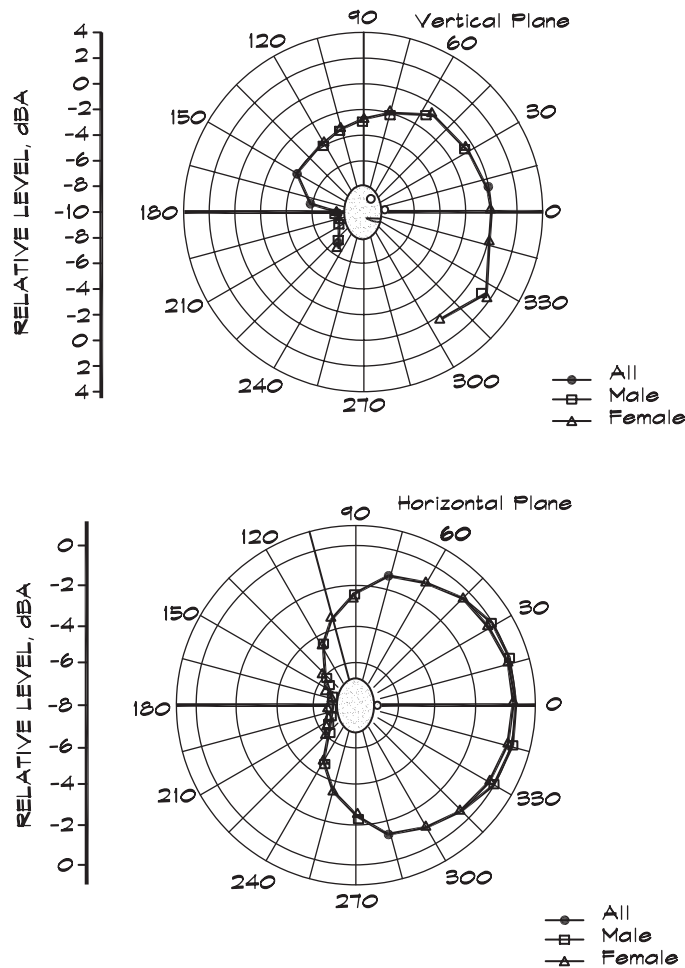
Outside noise sources should also be controlled in open-plan offices. HVAC noise should be limited to NC 35 in open-office areas and to NC 30 in private offices. HVAC noise is not helpful as a masking source, since its spectrum is rarely the proper shape and, in any case, it is not adjustable or uniformly distributed throughout the space. Noisy office equipment should be located in separate rooms. Offices should be carpeted to reduce walking

and furniture noise. The use of intercoms, personal radios, pagers, speaker phones, and other extraneous noise sources should be discouraged. Telephone rings should be set to their minimum volume.

Partial Height Panels

Although source orientation and control are helpful, barriers are always necessary. Partial height barriers include walls, which extend up to or even beyond the acoustical tile ceiling, but not to the slab or roof above. Prefabricated furniture panels can be used as speech barriers, but their inherent transmission loss limits their ability to perform this function. All the potential transmission paths must be considered, namely over, under, around, and through the barrier.

The total direct-field attenuation of a panel is the composite of the paths in Fig. 16.2. First, the barrier must block the direct path between talker and listener. If the listener is within 12 m (40 ft) of the talker, as in Fig. 16.7, the barrier must overlap the line of sight by at least 0.3 m (1 ft) to be effective. At distances of less than 4.5 m (15 ft) the sound path should have to bend at least 90° or more, as in Fig. 16.8, to be sufficiently attenuated.

Panel height is also an important factor. Barrier attenuation for both over and around paths may be calculated using Maekawa's relationship from Eqs. 5.10 and 5.11. The attenuation depends on the relative heights of the talker, barrier, and listener, as well as the frequency, and approximate results are given in Fig. 16.9.

FIGURE 16.7 Determining the Line of Sight for Distant People (Chanaud, 1983)
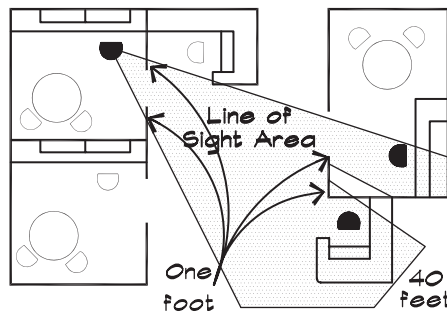
FIGURE 16.8 Determining the Line of Sight for Near People (Chanaud, 1983)
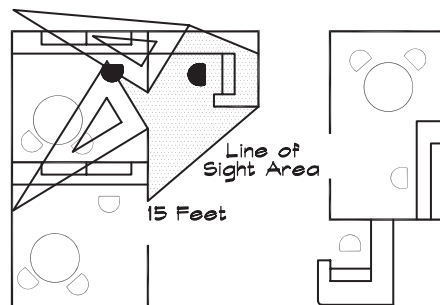
FIGURE 16.9 Influence of Panel Height on Speech Diffraction (Chanaud, 1983)
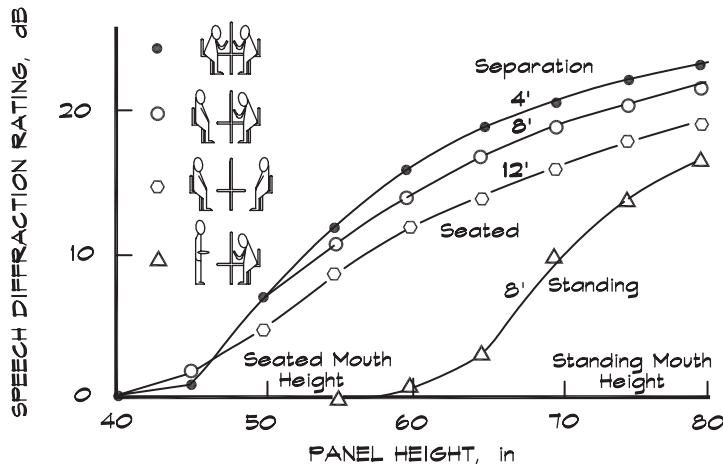
FIGURE 16.10 Influence of Panel Height and Distance on Speech Reduction (Chanaud, 1983)
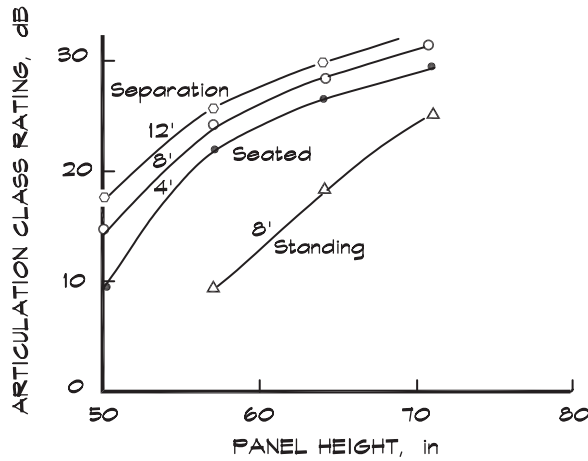
When the distance and directivity attenuations are taken into account, the results are the speech reductions shown in Fig. 16.10. For seated occupants, at least a 1.8 m (70 in) panel height should be used, and if there are a significant number of standing conversations, a 2 m (80 in) panel height is recommended. In some situations it is desirable to be able to look around the room or over individual panels. In these cases panels may incorporate sections of glass without significant degradation.

In all cases it is also important that partial height barriers extend down to the floor to seal off the transmission path under the panel. A well-designed system includes blockage of this reflection. Panels should leave no more than a 25 mm (1 in) gap at the floor since carpet yields relatively low absorption values in the speech frequencies.

FIGURE 16.11   Influence of Panel Width on Speech Reduction (Chanaud, 1983)
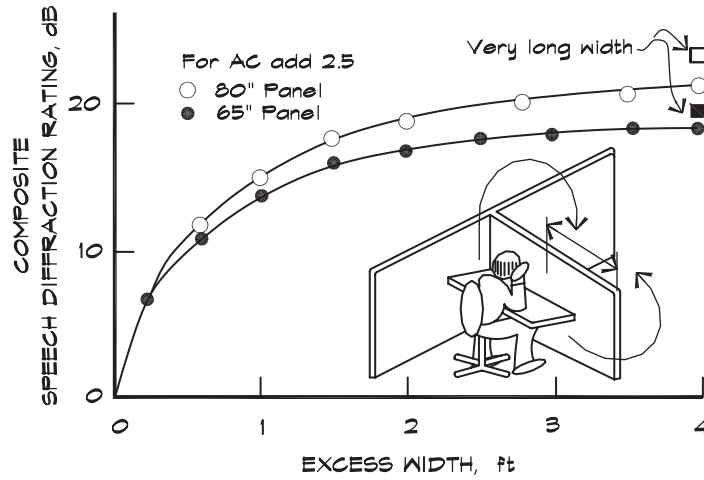
FIGURE 16.12   Influence of Transmission Loss on Speech Reduction (Chanaud, 1983)
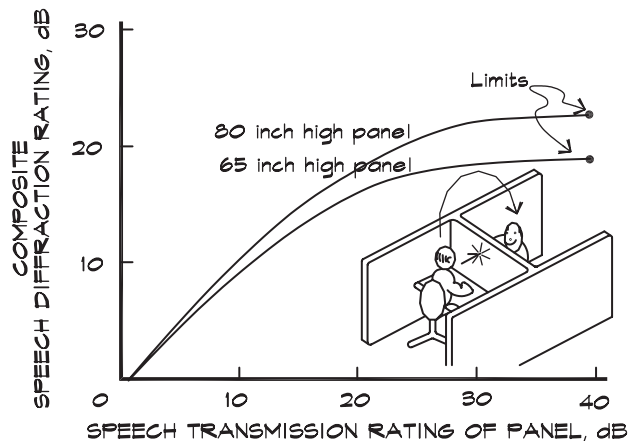
Diffraction around the end of a panel must also be controlled. Figure 16.11 shows the effect of excess width on the speech diffraction rating of a side panel. Free-ended panel runs should be avoided and the ends capped with a right-angle piece. For 1.8 m (70 in) high panels the free end should extend at least 1.2 m (4 ft) beyond a seated worker. For 2 m (80 in) high barriers, no free-end conditions should be allowed. Free-ended panels are a problem, not only because of the diffraction, but also because they allow easy transmission of reflected sound.

Transmission of sound directly through a panel is also a concern. Since there is a natural limit to the effectiveness of a panel for diffraction losses, this sets a maximum on the necessary transmission loss. Figure 16.12 gives the diffraction limits for two heights of panel. The corresponding STC limits are 20 for 1.65 m (65") panels and 24 for 2 m (80") panels.

To achieve an STC rating of 20 to 24 a surface mass density of about 5 kg/sq m (1 lb/sq ft) is required. This can be accomplished using 3/8" plywood, 1/4" gypboard, or a 22 Ga steel sheet sandwiched between two absorbent fiberglass boards. Manufacturers of office furniture sometimes refer to this type of panel as "acoustical" or "high performance" in their literature, although the presence of these descriptors does not guarantee this rating. Manufacturers must be contacted for the actual STC ratings of a prospective material.

Absorptive and Reflective Surfaces

Absorptive surfaces should be used in locations where they will prevent reflected sound from flanking the main barrier, including ceilings, rear, and sometimes side walls. The sound reflecting from a surface is attenuated by an amount given by

$$\Delta L_s = 10 \log (1 - \alpha_s) \tag{16.13}$$

where α_s is the specular absorption coefficient.

Although the NRC ratings are useful for a general discussion of the properties of a given panel, if calculations are to be undertaken more detailed data are necessary. Random-incidence absorption coefficients are measured in third-octave bands, although they are published in octaves. Due to the details of the testing process, values of these coefficients sometimes exceed 1. In the case of ceilings and other reflecting surfaces the specular absorption coefficients are of more interest but are rarely available. Chanaud (2000) has developed an empirical relationship relating the diffuse (α) and specular (α_s) absorption coefficients for open-office calculations. He suggests

$$\alpha_s \cong \alpha \quad \text{for} \ \alpha < 0.5$$

$$\alpha_s \cong .092 + .82\,\alpha \quad \text{for} \ 0.5 < \alpha \leq 1.1 \tag{16.14}$$

$$\alpha_s \cong 0.999 \quad \text{for} \ \alpha > 1.1$$

Since most reflections between workstations are within 20° to 30° of the normal, there is little change in absorption with angle, as we saw in Fig. 7.19. When losses from reflections are combined with the directivity and the distance attenuation, we obtain the speech reduction for a reflected path

$$\text{SR} = \Delta L_\theta + \Delta L_s + 20 \log (D_s) \tag{16.15}$$

where D_s is the total reflected path length in meters.

Figure 16.13 shows several examples of absorptive panel placement. If the separating panel, located directly along the line of sight between the source and receiver, is absorptive, its first reflection does not go toward the receiver, so the absorption is not in the most beneficial position. A side-panel reflection may not go directly to the receiver and so here, too, absorption may not be effective. An absorbing ceiling and rear panels decrease the sound transmission reflecting to the receiver and are effective. We therefore arrive at the conclusion that we place absorptive panels overhead and in the direction opposite the person to be given the privacy. Where there are people in all directions the application of this rule will result in several panels being covered with soft material.

Absorption should also be placed where a reflection would create a flanking path around the barrier panel. Reflections can occur from other panels, or from the walls and windows of

FIGURE 16.13 Absorbing Panels in Workstations (Chanaud, 1983)
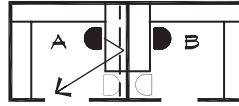
Case 1 Separating panel is absorptive. B gets no benefit.

Case 2 Side panel is absorptive. Again B gets no benefit.
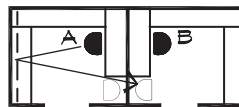
Case 3 Rear panel is absorptive. B gets some benefit.

Panel Type	Typical NRC	Reflection Attenuation
Hard Surface	0.05	0 dB
Acoustical	0.80	13 dB
Sound Screens	0.90	15 dB

FIGURE 16.14 Open Plan Panel to Window Connections

Best if it touches the wall

Extend wing walls 2' on either side

Slide the panels to meet at the wall

Flat extensions are best
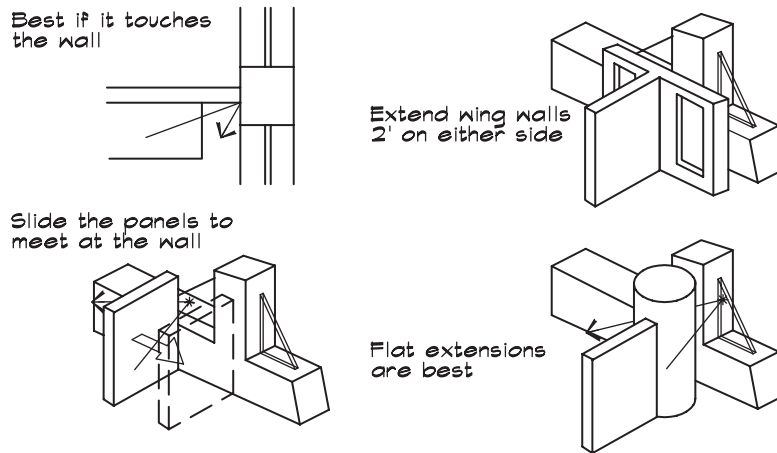
the building. If the reflecting surface is within 2 m (6.6 ft) of the talker the noise reduction coefficient (NRC) of the panel must be at least 0.9. For each additional 0.3 m (1 foot) of separation the NRC of the panel may be reduced by 0.05. Absorbent panels placed on potential reflecting surfaces must be long enough to cover all possible talker and listener mirror locations within their respective workstations. This is illustrated in Fig. 16.14.

Carpeted floors do little to improve speech privacy when panels extend all the way down to the floor. They do help control extraneous noise from sliding furniture, walking, and general reverberant noise at high frequencies. Their use is recommended in open-office areas for these reasons; however, they do not have to be chosen based on their NRC ratings.

Open-Plan Ceilings

The ceiling is a potential reflecting surface, which must be treated in open offices. The choice of ceiling materials was once limited to plaster, gypsum board, and mineral or fiberglass tile. Recently these traditional materials have been supplemented with many additional products including perforated and linear metal shapes, wire mesh, and sintered metal products. The traditional acoustical tile products have become more interesting visually and may be wrapped with cloth, perforated vinyl, or other porous materials.

An absorptive ceiling tile consists of three parts: backing, core, and facing. The most commonly available combinations are listed in Table 16.6. For open-plan offices, ceilings must be highly absorptive. Fiberglass tiles with a cloth facing have the highest ratings. A fiberglass tile having a 19 mm (3/4") thickness will have an NRC rating of about 0.90 and at a 38 mm (1.5") thickness its rating can sometimes exceed 1.0. Mineral-tile ceilings have NRC ratings, which range from 0.55 to 0.65 depending on thickness and surface treatment, whereas a gypboard ceiling has an NRC of about 0.05. Metal-foil backings should be used where the ceiling plenum is also a return air conduit. Table 16.7 (Chanaud, 1983) gives the speech reduction rating or Articulation Class for various ceiling absorption coefficients at an 8-foot talker-to-listener separation distance.

A comparison with the privacy ratings in Table 16.4 reveals that Normal Privacy will not be achieved if an acoustically hard ceiling is present. Transitional Privacy can be achieved with a mineral tile ceiling, but Normal Privacy can only be achieved by using a fiberglass ceiling tile in conjunction with 2 m (80 inch) high panels with masking. Figure 16.15 shows the variation of Articulation Index with ceiling material in the presence of masking sound.

The ceiling height can also have an effect on the degree of privacy. As the ceiling height increases the distance loss for reflected sounds becomes greater. Since speech reduction is a combination of distance attenuation and the absorption of the ceiling panels, a higher ceiling may allow the selection of a less expensive ceiling material. Table 16.8 (Chanaud, 1983) shows a comparison of the speech reduction rating for various ceiling heights.

A mineral tile ceiling must be 4.6 m (15 ft) high if it is to result in the same attenuation as a fiberglass tile ceiling at 2.6 m (8.5 ft). There is little advantage to be gained from raising

TABLE 16.6   Ceiling Tile Combinations

Backing	Core	Facing
None	Mineral Tile	Glass Cloth
Metal Foil	Fiberglass	Vinyl
		Perforated Vinyl
		Painted Cloth
		Metal Pan

TABLE 16.7   Speech Reduction Caused by Ceiling Absorption (Chanaud, 1983) 2.5 m (8 Foot) Separation

Ceiling Type	NRC	AC (dB)
1.65 m (65 Inch) Panels		
None		27
Ideal Material	1.15	26.5
Good Fiberglass Tile	1.00	25
Standard Mineral Tile	0.65	21.5
Gypsum Board	0.05	17
2 m (80 Inch) Panels		
None		33
Ideal Material	1.15	31.5
Good Fiberglass Tile	1.00	28
Standard Mineral Tile	0.65	22.5
Gypsum Board	0.05	17

FIGURE 16.15   Factors Influencing Speech Privacy with Masking Sound (Chanaud, 1983)
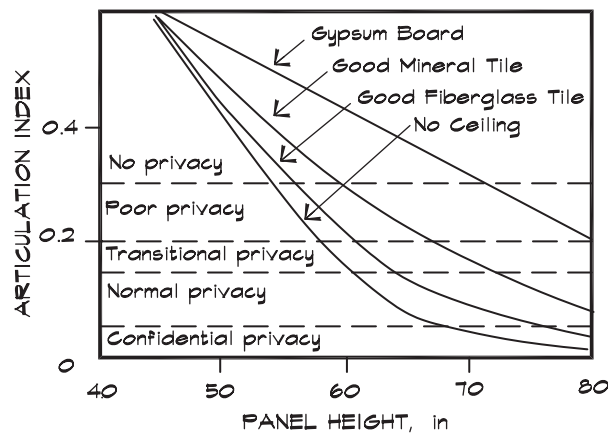
a ceiling, if it is already highly absorbent. Conversely, if a ceiling is quite high, there is little privacy improvement to be gained by changing to a more absorbent material.

Reflective light fixtures and metallic diffusers should not be located where a reflection will cause a degradation of the ceiling absorption. A flat reflective light fixture, such as those in Fig. 16.16, located above a separating partition, can produce a reflected level equal to the effect of changing the entire ceiling from fiberglass to mineral tile.

TABLE 16.8   Influence of Ceiling Height on Speech Reduction (Chanaud, 1983)
1.3 m (4 foot) Separation—1.35 m (65 Inch) Panels

Ceiling Height (m/ft)	AC (dB) Fiberglass	AC (dB) Mineral Tile
2.4 (8)	23	19
2.6 (8.5)	23	19.5
2.7 (9)	23.5	20
3.0 (10)	23.5	21
3.7 (12)	24	22
4.6 (15)	24	23
6.1 (20)	24.5	23.5
30 (100)	24.5	24.5

FIGURE 16.16   Influence of Light Fixtures on Ceiling Reflections (Chanaud, 1983)
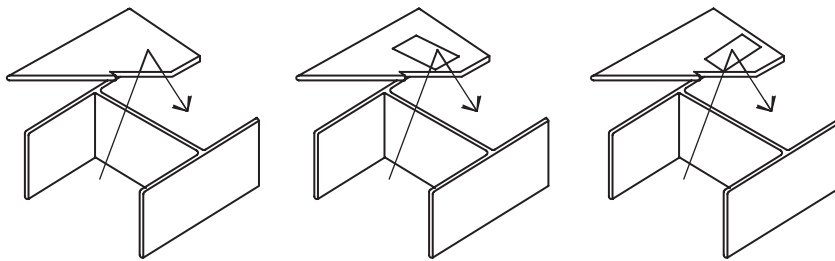
Privacy for 65 inch panels on three sides,
fiberglass ceiling, and masking sound

Condition	Privacy Index	Degree of Privacy
No light fixture	84	Normal
Fixture in short direction	69	Poor
Fixture in long direction	67	Poor

Masking Sound

The addition of background or masking sound to an open-office environment is a critical component to obtaining overall privacy in the workplace. When properly done, masking sound raises the noise level in an unobtrusive way that increases privacy without being noticed by the occupants. It can be used in open-office plans with partial-height barriers and in private offices with walls that are either full or partial height. Even when a private office with a full-height wall is adjacent to an open-office area, it is still a good idea to introduce masking sound into the private office. This smoothes the transition between the spaces and makes the noise in the open area much less noticeable. Masking sound is produced by using an electronic pink noise generator and a filter that results in a spectrum that falls off at about

FIGURE 16.17   Influence of Masking Sound on Speech Privacy (Chanaud, 1983)
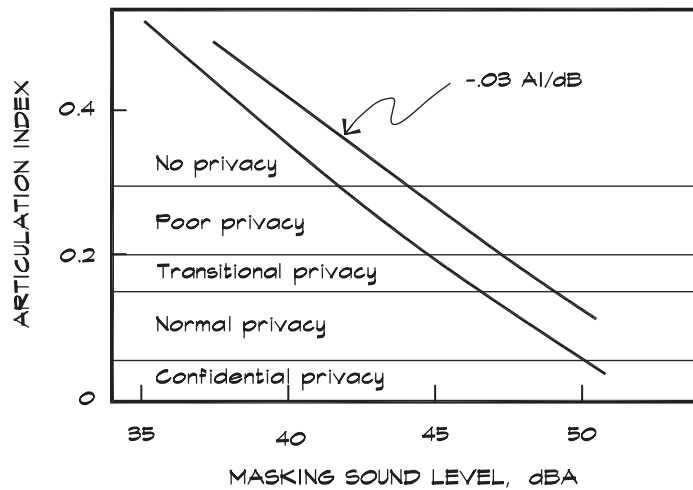
FIGURE 16.18   Masking Sound Loudspeaker Locations
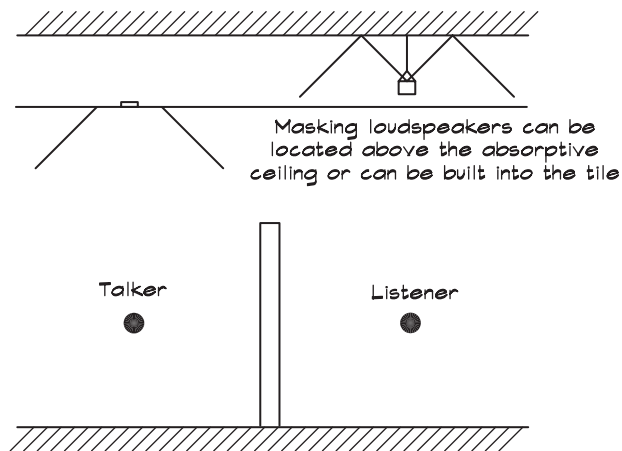
5 to 6 dB per octave at the receiver. A possible spectrum is shown in Table 16.3; however, there is no single ideal curve. The overall level is set between 43 and 49 dBA. Though this seems like a relatively narrow range, below 43 dBA masking sound has little effect, and above 49 dBA it is an annoyance. Most systems end up being adjusted to somewhere around 47 dBA in open offices and 44 dBA in closed offices. The effect of masking sound on privacy for a typical workstation is shown in Fig. 16.17.

Loudspeakers can be located above the ceiling tiles, out of sight, and pointed up to increase their effective distance and widen their coverage pattern. They may also be built into the tiles themselves, which decreases the installation cost. Figure 16.18 gives two examples. The introduction of masking sound above a workstation provides privacy for a listener located within the sound field of the loudspeaker. It does not provide masking of the sound made by

a talker located there. Hence, loudspeakers must be distributed through all areas where there are potential receivers. As an employee walks around the workspace, the sound level should not change drastically. He should not be aware of the presence of masking, so any changes in level or spectrum should be gradual. Work areas should be zoned so that levels may be adjusted according to the needs of a particular area. Masking systems can be controlled using a timer that varies the level in a given zone during the workday; however, the system should not be switched off during working hours.

Music and paging may be mixed into the system, but the masking sound should only be muted for emergency pages. Music is not a good source of masking sound by itself, but it can provide a pleasant background environment for certain tasks. Music is not appropriate for areas where difficult tasks are performed. When music is introduced the masking sound must remain on.

Degrees of Privacy

We now have in place the tools to provide various degrees of privacy in an open (or private) office environment. As was emphasized previously, all component parts must be in place to achieve privacy. Figure 16.19 shows the influence of panel height and masking sound on levels of speech privacy. Clearly neither high panels nor masking sound alone can yield good privacy.

A successful open-office design must include four key elements and fails if any of the four is missing. The elements are: 1) partial height barriers at least 1.65 m (65 in) high, having sufficient transmission loss, provided by a 3/8" plywood or other interior panel; 2) absorptive material typically 25 mm (1 in) fiberglass panels on the reflecting walls or additional barriers to prevent flanking; 3) a highly absorbent ceiling (NRC > .85); and 4) an electronic sound-masking system with loudspeakers located above the acoustical tile ceiling set to emit a particular spectrum in the range of 45 to 49 dBA.

FIGURE 16.19   Privacy Index with Ceiling NRC = 0.9 and a 6-Foot Separation (Chanaud, 1983)
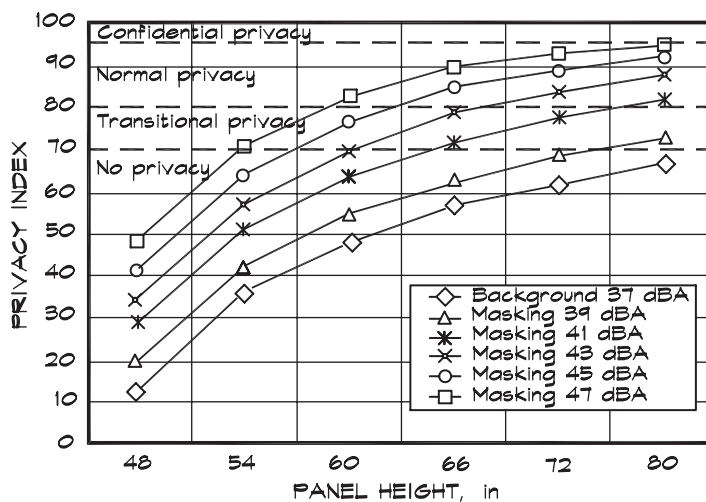
16.2   SPEECH PRIVACY IN CLOSED OFFICES

Private Offices

In a closed office the assessment of privacy is expressed in terms of STC values between adjoining spaces. Closed offices have the advantage of providing privacy throughout the enclosed space for a standing or seated occupant. The disadvantage is that the normal background level is lower, even when masking is included, and conversations may take place at raised voice levels even when confidential matters are being discussed. Specialized areas such as psychologists' offices, spaces used for conflict resolution, rooms with audio visual systems, lecture rooms, and classrooms, are all likely to have a need for extra isolation and should be identified as part of the initial planning process.

The analysis of sound transmission for private offices is similar to that for open offices. In critical locations detailed calculations using voice spectra, transmission loss, and background noise levels should be done. Figure 16.20 shows the calculated Articulation Index for various FSTC values at three voice levels, and Table 16.9 includes the corresponding sound attenuation requirements for various degrees of privacy. Chanaud (1983) recommends that the FSTC of a given structural component be 6 dB greater than the desired composite FSTC.

Full-Height Walls

The traditional approach to closed-office privacy is to use full-height walls and weather-stripped solid core doors. When the walls are full height, the total FSTC value is obtained. Sketches of several wall configurations are given in Fig. 16.21, along with estimates of their composite FSTC values. When the wall does not extend full height on both sides various plenum barrier materials can be used to make up the difference.

For Confidential Privacy with a normal voice talker, a good separation wall between rooms is a single 3 5/8" (90 mm) metal stud with 5/8" (16 mm) drywall each side and R-11 batt in the airspace. This wall rates an STC 44 (FSTC 39), and for voice provides a calculated noise reduction of approximately 42 dB. In terms of a rough calculation, a 60 dBA

FIGURE 16.20   Required FSTC for Speech Privacy for Various Voice Levels (Chanaud, 1983)
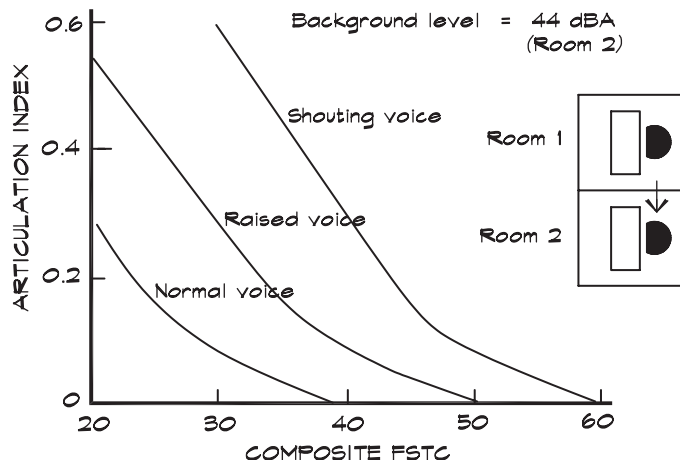
TABLE 16.9   Required Composite and Component FSTC for Various Voice Levels
(Chanaud, 1983)

Background Noise = 44 dBA

Minimum Composite FSTC for

Voice Level	Normal Privacy	Confidential Privacy
Normal	26	32
Raised	36	42
Shouting	46	52

Recommended Component FSTC for

Voice Level	Normal Privacy	Confidential Privacy
Normal	32	38
Raised	42	48
Shouting	52	58

sound pressure level due to a normal voice in one room would generate about 18 dBA sound pressure level in the adjacent room. If the masking level in the receiving space were 35 dBA, we could achieve Confidential Privacy since the signal-to-noise ratio is less than –12 dB. This describes a typical private office with a background level of about NC 30 although the NC spectrum is not identical with the masking spectrum.

Plenum Flanking

The choice of an appropriate wall type is not the end of the design exercise, since there are many other routes that the sound can take from one room to another. If the wall does not extend from slab to slab, then the sound can travel over the top of the wall, passing through the plenum above the T-bar ceiling on either side. Since the mass of acoustical tile is quite low, it does little to attenuate noise from passing through it. Blazier (1981) has published measured values of the noise reduction of an acoustical tile ceiling, which are shown in Fig. 13.15. Even if these are doubled and increased by 6 dB, following Eq. 9.50 they still represent a significant degradation in transmission loss relative to the wall performance. Grille openings for the return air plenum can further degrade these ratings.

Figure 16.22 gives several examples of FSTC values for partial-height walls flanked by plenums. In this figure there are substantial differences in FSTC values depending on the ceiling material. Manufacturers of acoustical ceilings have sought to develop so-called high transmission loss tiles, which combine both absorption and transmission loss into a single product. These tiles have a modest absorption coefficient, between 0.5 to 0.7, and a relatively low effective STC rating (as measured with a wall in the STC 30 to 35 range). Even though they are better than lighter acoustical tiles, they can be compromised by openings for return air grilles.

FIGURE 16.21   Full Height Separation Wall Configurations
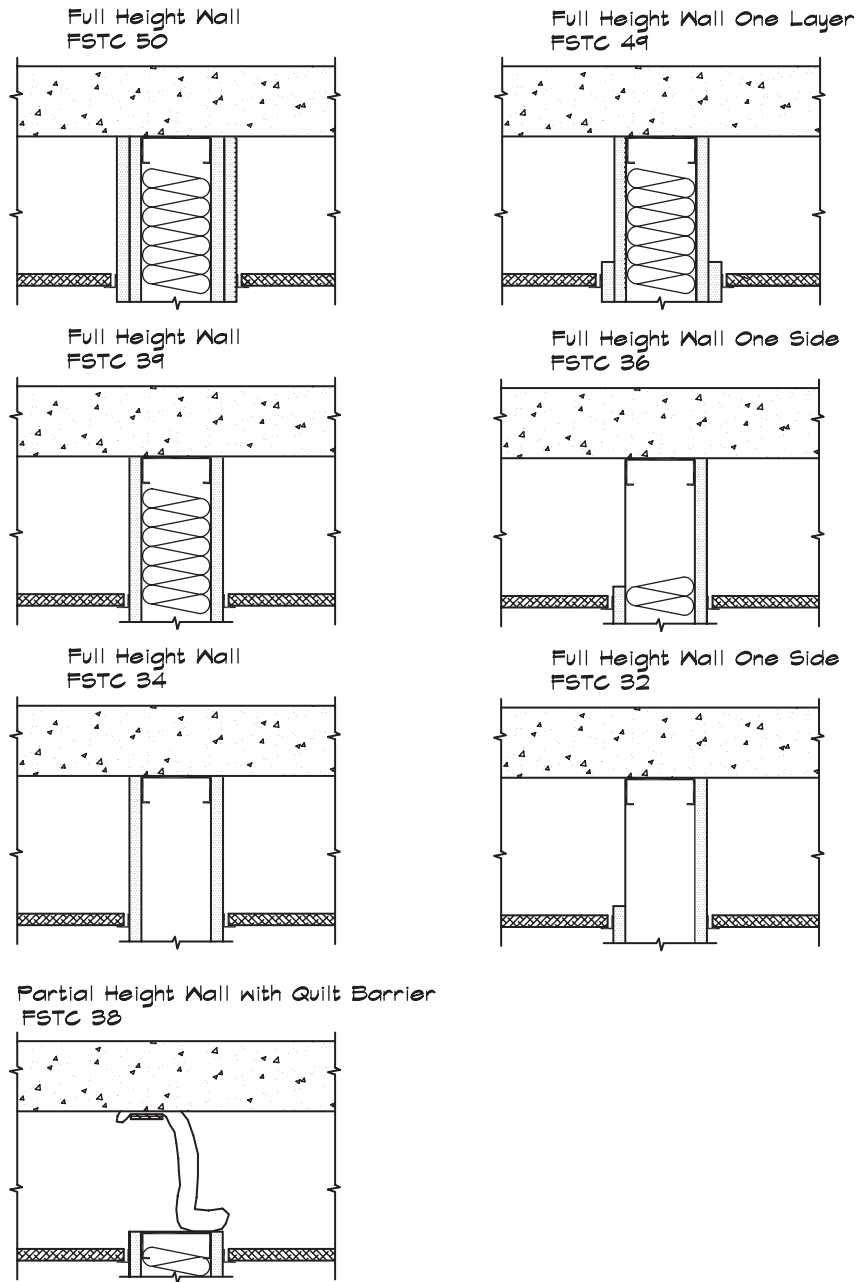
FIGURE 16.22   Wall Plenums with Estimated FSTC Values

Partial Height Wall – Drywall Ceiling
No Penetrations FSTC 47
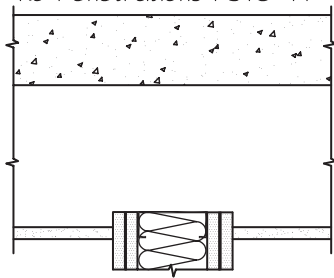
Partial Height Wall – Drywall Ceiling
Ceiling Penetrations FSTC 43
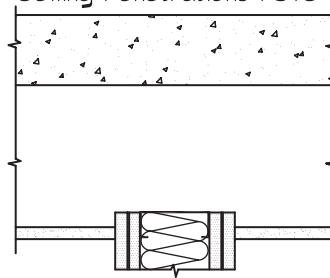
Partial Height Wall – Open Plenum
Mineral Tile   FSTC 39
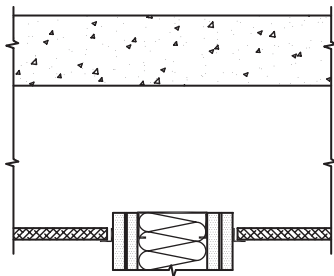
Partial Height Wall – Open Plenum
Fiberglass Tile with Overlay   FSTC 32
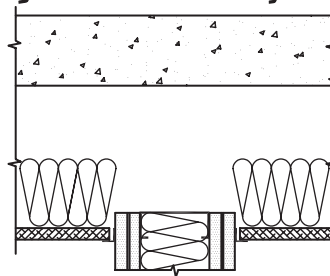
Partial Height Wall – Drywall Ceiling
No Penetrations FSTC 37
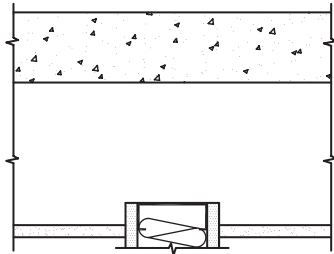
Partial Height Wall – Drywall Ceiling
Ceiling Penetrations FSTC 36
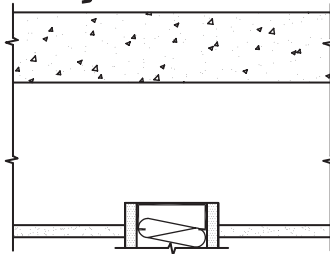
Partial Height Wall – Open Plenum
Mineral Tile   FSTC 35
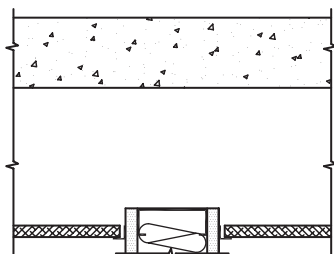
Partial Height Wall – Open Plenum
Fiberglass Tile with Overlay   FSTC 31
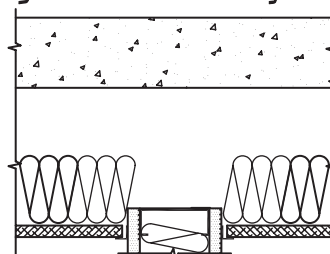
FIGURE 16.23   Flanking through Ductwork
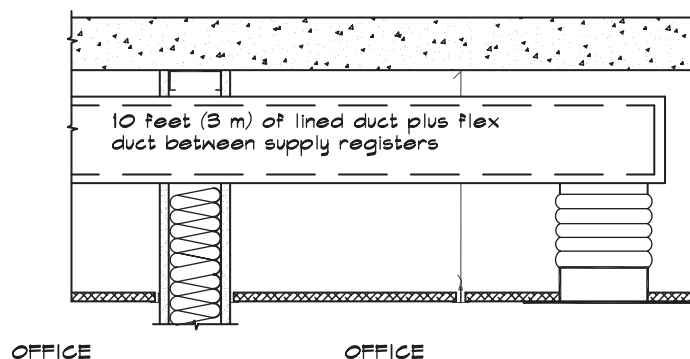
        The addition of batt insulation on top of the T-bar ceiling can provide some improvement for fiberglass tile ceilings, which have relatively low transmission loss values. Batt is not appropriate in return air plenums and instead a duct liner should be used.

Duct Flanking

HVAC ducts can also serve as a conduit for sound transmission between adjacent rooms, particularly if they are unlined. If an unlined duct directly connects diffusers in adjacent offices, sound can propagate along the duct and be heard clearly in the receiving room. To calculate this effect, the duct attenuation becomes the transmission loss and the cross sectional area of the duct becomes the transmitting area in Eq. 10.5. Where the supply or return air is ducted directly between sensitive spaces, a 3 foot (1 m) silencer or a total of 10 feet (3 m) of duct, lined with 1" (25 mm) duct liner, is required. If the ceilings are drywall, two 4-foot (1.2 m) lengths of flex duct can be substituted for the lined duct. A detail is shown in Fig. 16.23.
        Where walls are constructed full height to the floor or roof above, they cut off the free circulation of air from the plenum to the rest to the return-air system. An opening in one of the walls, with 5 ft (1.5 m) of lined duct penetrating the plenum wall, is normally sufficient to isolate the two spaces and provide a low-pressure path for the air to return. Where the return air can be transported in the space above the corridors in an office complex, it provides for additional separation by forcing the noise to traverse two segments of lined duct. Figure 16.24 shows a typical arrangement.

Exterior Curtain Walls

Interior partitions separating adjacent offices will eventually meet an exterior wall. Ideally, the interior wall should join the exterior surface at an area of solid construction, so that acoustical isolation is maintained. When the walls intersect at a window mullion or at the glazing there can be a flanking path at the junction, particularly if the window is double glazed. Exterior window mullions are constructed from thin (typically 0.090" or 2 mm), hollow, rectangular aluminum extrusions with very little mass. Where the junction with an interior wall falls on the mullion the wall can be attached as shown in Fig. 16.25. For additional isolation an extra piece of drywall or heavy sheet metal can be attached to each side.

FIGURE 16.24   Return Air Plenum at a Full Height Wall
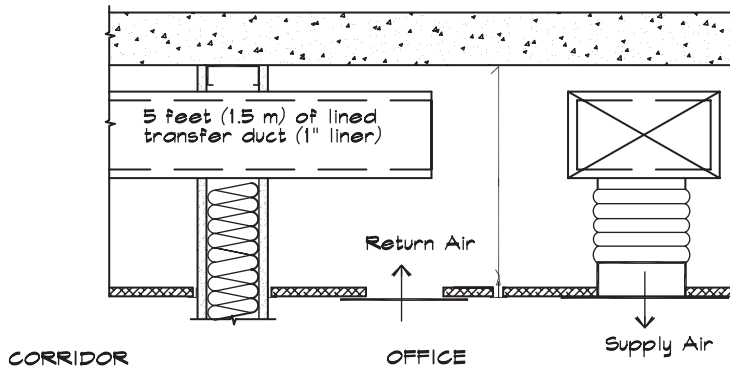
FIGURE 16.25   Flanking around Walls at Mullions

This thickens the appearance of the mullion as seen from the outside but provides much better isolation than stopping the wall short of the inner surface of the mullion.

Where the end of the wall falls between two mullions the wall should be jogged over until it falls directly on the mullion. Occasionally there is a continuous air bar around the outside of the building that penetrates the dividing wall. This can severely compromise acoustical isolation between spaces and must be closed off at the wall. Lined sections of duct can carry the air through the wall.

Not infrequently in high-rise construction the exterior curtain walls are supported from the edge of the floor slab and a gap is left between the slab and the glazing. Where there is spandrel glass and an interior wall, it is a good idea to continue the wall up past the ceiling as shown in Fig. 16.26. In other cases sheet-metal plates can be installed to bridge the gap between the slab and horizontal mullions both above and below the slab. The airspace should be filled with safing.

FIGURE 16.26   Flanking around Slabs at Curtain Walls

Section Drawing

The interior gypsum board must extend to the slab to close off the flanking path around the end to the floor above.
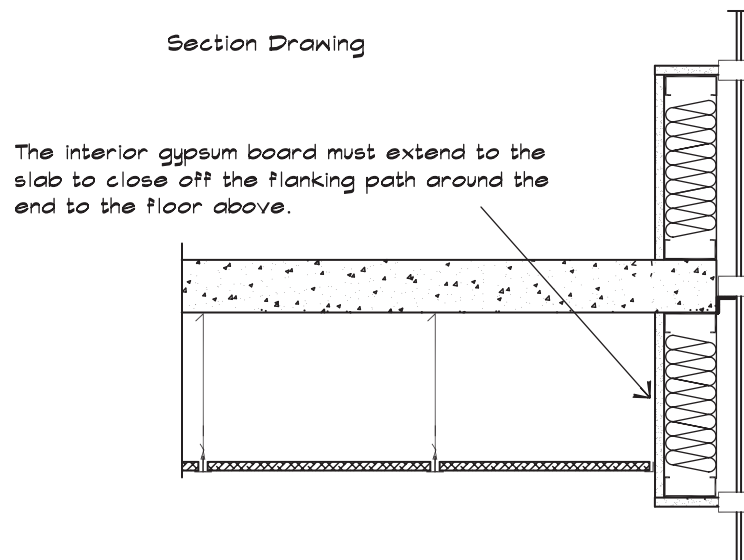
Flanking paths sometimes occur at column penetrations of slabs, particularly where the lower floor space has an open ceiling. In each of these conditions the openings around the column must be closed off with a material that has a sound transmission loss equivalent to the floor system.

Divisible Rooms

Moveable walls, used as dividers between meeting rooms, are commercially available with STC ratings as high as 50 or more. To achieve these ratings the panels weigh as much as 10 lbs/sq ft (49 kg/sq m). They are supported from a structural framework above that must be sized to carry the load without undue deflection. Unless this is taken into consideration the moveable walls can drag on the floor when they are moved into place. Some deflection is inevitable, and the panels are positioned and jacked up so that they support their own weight from the floor below. Moveable walls are the same as permanent walls in that the plenum flanking path must be blocked off. Figure 16.27 shows a design. Any stem wall must also accommodate structural deflection due to the weight of the panel.

Masking in Closed Offices

Where walls do not extend to the structural deck above the T-bar ceiling, it is not possible to achieve Confidential Privacy without the addition of masking sound. An office separation might consist of a single metal-stud wall with single layers of 1/2" gypsum board extending up to or slightly above the T-bar and a mineral-tile ceiling. Return-air grilles should be baffled with a lined sheet-metal enclosure illustrated in Fig. 16.28, with the open sides facing away from the receiver room. Table 16.10 shows the resulting degrees of privacy with this configuration for several levels of masking sound.

FIGURE 16.27 Installation of Moveable Wall Partitions

A wall of equivalent transmission loss should be built above
the moveable wall. Studs and batt not shown for clarity.
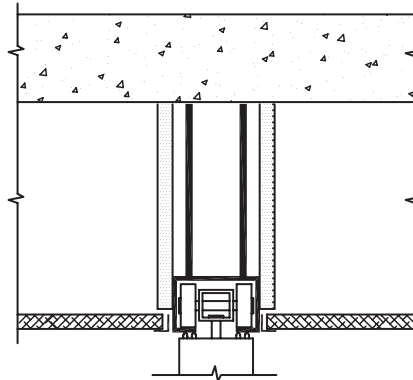
FIGURE 16.28 Return Air Boots

A sheet metal return air boot built over the return air grille.
Orient the opening away from the receiver. Nominal dimensions
24" x 24" x 8" high.
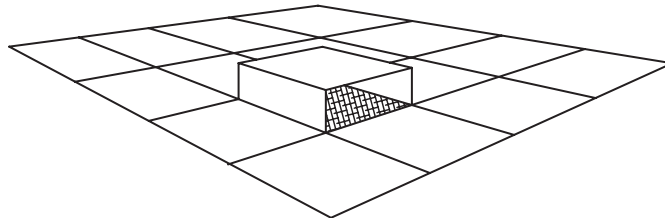
TABLE 16.10 Closed Office Speech Privacy for Mineral Tile Ceilings Normal Voice Levels (Chanaud, 1983)

	No Masking	Masking
Attenuation (NIC)	33	33
Masking Level (dBA)	35	39
Privacy Index	89	95
Degree of Privacy	Normal	Confidential

TABLE 16.11   Closed Office Speech Privacy for Fiberglass Tile Ceilings: Normal Voice Levels (Chanaud, 1983)

	Fiberglass Tile	Fiberglass with Overlay
Attenuation (NIC)	27	33
PI with 47 dBA	> 95	> 95
PI with 42 dBA	91	> 95
PI with 37 dBA	83	91

Note that in closed offices lower levels of masking sound are required to achieve Confidential Privacy than were necessary in open offices.

When fiberglass tile ceilings are present the low transmission loss values limit the attenuation between spaces. An overlay of 1/2" drywall on top of the tile can be helpful for improving the ceiling transmission loss. Table 16.11 summarizes the results of measurements for these conditions with booted return air grilles.

This solution is helpful in cases where the designer prefers the same style of ceiling tile in the open- and closed-office areas. Even with the drywall overlay the masking sound penetrates the ceiling, although the level must be increased. Loudspeakers should not be located near the return air grilles.

16.3   MECHANICAL EQUIPMENT

Mechanical systems in commercial spaces tend to be larger and more centralized than those in residential buildings. With larger units it becomes critical to address the vibration isolation aspects of the transmission problem and to enclose the mechanical spaces with heavy walls or buffer zones to protect the adjacent occupancies. Given the additional space, oft times these units are easier to treat, since there is room for silencers, lined plenums, and other conventional treatments.

System Layout

Architects and engineers can reduce the amount of treatment necessary to control mechanical noise in office spaces by shielding mechanical equipment rooms from sensitive spaces with intervening rooms such as bathrooms, storage rooms, and corridors. Bathrooms are particularly useful in this regard, since they include drywall or plaster ceilings, which can serve as return air plenums and provide additional space for the location of silencers.

Simply providing adequate space for mechanical equipment in a location that is isolated from potential receivers can be of great benefit. Many noise problems occur when this planning is not done. All too frequently air handlers or heat pumps are shoehorned into the available space in ceiling plenums above sensitive areas. Even when space is provided for the equipment, space is not left for a silencer, plenum, or other attenuating devices. This is often the case with down-shot air handlers, where the ducts emerge straight down from the underside of the unit, leaving little room for silencers and gradual turns. Where these devices are located above sensitive receptors it is very difficult to correct noise problems after installation.

Mechanical Equipment Rooms

In a typical multistory office complex there is a central core where a mechanical equipment room is located. This is an excellent design configuration since it allows the necessary space for buffers, silencers, lined duct, or the other treatments. Several possible core layouts are shown in Fig. 16.29. The designs illustrate increasingly isolated arrangements with storage and acoustically benign equipment rooms acting as buffers.

From the central mechanical equipment room the supply air is fed into a duct loop serving the tenant spaces. The return air can be ducted or drawn from the ceiling plenum or from a plenum located above the central corridor. When the space is leased by a single tenant, there is often no reason for the corridor, and the lessor builds out the whole space to his liking. The full built-out condition is more difficult to treat acoustically than the subdivided condition since there is no buffering provided by the corridor.

In a central equipment room the air handler is located (Fig. 16.30) so that the supply ducts rise vertically to an elbow and pass horizontally through the walls of the mechanical equipment room to the duct loop. The air is returned through an opening in the mechanical equipment room wall and into the side of the air handler. Makeup air is supplied to the mechanical equipment room by means of a separate fan located on the roof.

FIGURE 16.29 Comparison of Various Building Core Layouts (after Schaffer, 1991)

Poor Core Layout
Exposes 3 mechanical room walls to surrounding tenant space. Impenetrable partition between mechanical room and exit stairs results in supply and return air wall openings next to tenant space.

Fair Core Layout
Exposes 2 mechanical room walls to tenant space. Exposes mechanical room partition to elevators and exit stairs resulting in supply and return wall openings next to tenant space.

Better Core Layout
Exposes 2 mechanical room walls to tenant space. Ceiling over toilets can be used for either supply ducts or return air path.

Best Core Layout
No mechanical room walls exposed to tenant space. No supply or return air openings need be next to tenant space. Ceiling over toilets can be used for supply air ducts or return air path.

FIGURE 16.30   Central Core Air Handling Unit
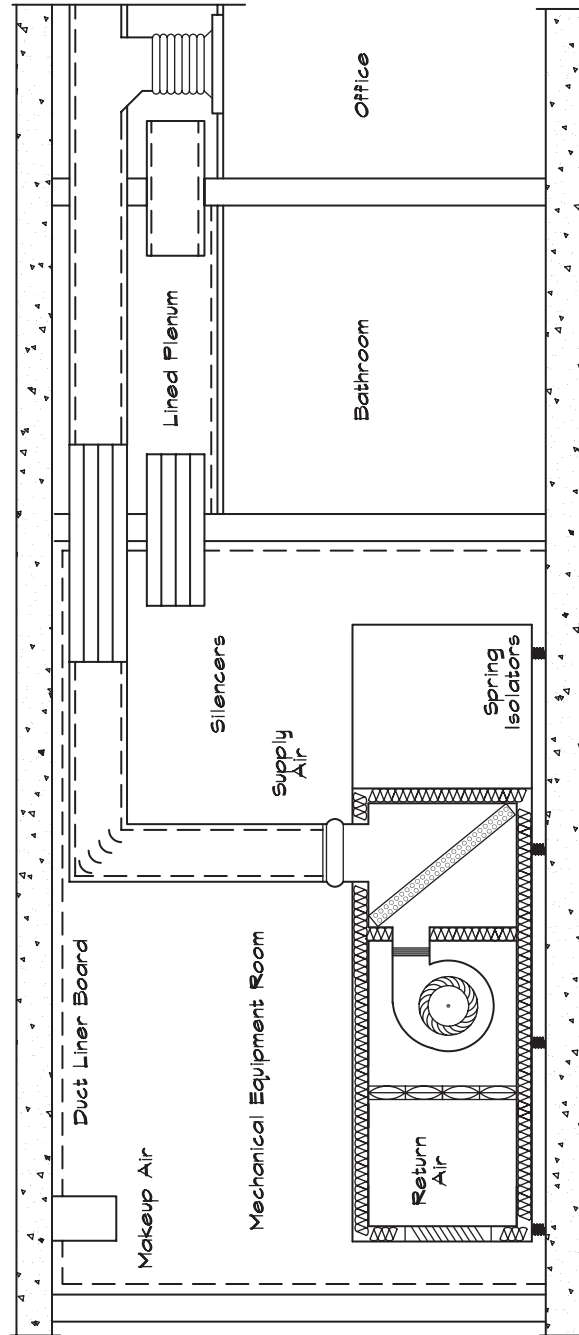
Given the sound power level data on HVAC units at the specified operating point, a calculation can be carried out on both the supply side and return sides of the equipment as outlined in Chapt. 14. The final receiver sound pressure levels are compared with the interior noise level criteria to determine if any remedial steps need to be taken. In this case a silencer is added to the supply duct to provide the necessary attenuation.

On the return side the mechanical equipment room acts as an acoustical plenum with the return air opening on the air handler being the plenum entrance. If the radiating area of the air handler is not included as the entrance area, it is common to overestimate the attenuation due to the plenum effect. When the ceiling space above the bathroom is available it is useful to create an additional plenum and to use return-air silencers as well. Assuming that the exit from the plenum opens into the area above the acoustical tile ceiling we calculate the loss through the ceiling as an insertion loss to be subtracted from the sound power level before converting it to a sound pressure level using the appropriate room constant. An additional calculation of the sound radiated through the walls of the mechanical equipment room should also be done.

Roof-Mounted Air Handlers

In single story and low multistory projects packaged air handling equipment is frequently located on the roof. A packaged unit contains its own refrigerating condensing section along with the fan coil heat exchangers, filters, and one or more circulating fans. These units should be isolated with external spring isolation, on a series of open springs or curb rails, because internal isolation provided by the manufacturers may be inadequate and does not isolate casing vibration. The unit should be located over a stiff region of the roof having a deflection under the load of the equipment of no more than 1/6 to 1/8 of the spring isolator deflection. A housekeeping pad of at least 3" (75 mm) thickness should be provided for units up to 10 tons and 6" (150 mm) thickness above that. Pads must extend at least twice their thickness beyond the isolated equipment. Pads are strongly recommended, even when units are rail mounted on grade beams.

Side inlet and discharge are much preferred over down-shot units since they afford the space to install silencers. Down-shot units are often specified by mechanical engineers and contractors since they are self flashing, less prone to leaking, and less unsightly. Schaffer (1991) has published a series of figures showing various configurations of rooftop units, which are reproduced in Figs. 16.31 through 16.34.

Figure 16.31 shows a down-shot air handling unit with a large opening in the lightweight roof beneath. The opening allows the passage of noise through this space. To correct this condition, the unit must be picked up and mounted on rails to stiffen the structure and the opening must be boxed in from below with a metal stud wall with 2 layers of 5/8" (16 mm) drywall. Silencers are then installed at the points where the ducts penetrate the box. The details of the enclosure design must be determined by doing calculations using the sound power level emanating from the underside of the unit.

Figure 16.32 illustrates a configuration where some steps have been taken to control the noise. This arrangement is not sufficient above occupied office areas; however, with the addition of return-air silencers and a drywall box around the ductwork out to the silencers, it can be made to work in nonsensitive areas. Some manufacturers can provide high transmission loss ductwork of heavy (14–16 gauge) metal, which can help reduce breakout problems.

FIGURE 16.31   A Very Noisy Rooftop Air Handling Unit (Schaffer, 1991)

No Vibration Isolation Under Unit Frame

No Roof Under Unit Frame

Lightweight Roof

Untreated Ductborne Noise

Return Air Plenum of Acoustical Tile
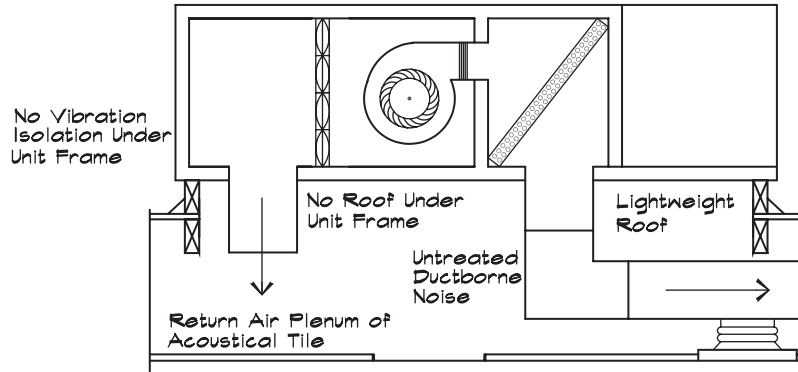
FIGURE 16.32   A Noisy Rooftop Air Handling Unit (Schaffer, 1991)

Vibration Isolation Under Unit Frame

Flex Connections

Lightweight Roof

Lined Return Air Duct Acoustical Tile Ceiling

Silencer
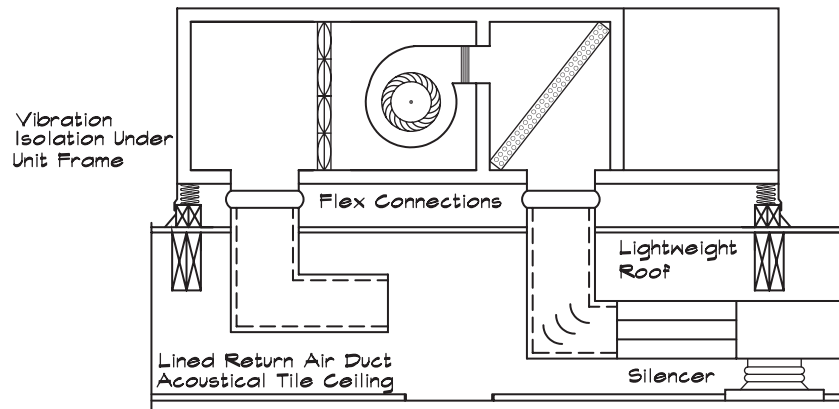
FIGURE 16.33   A Moderately Quiet Side Discharge Rooftop Air Handling Unit (Schaffer, 1991)

Slab with Housekeeping Pad Air Handler on Spring Isolators

Silencers at the Roof Penetration
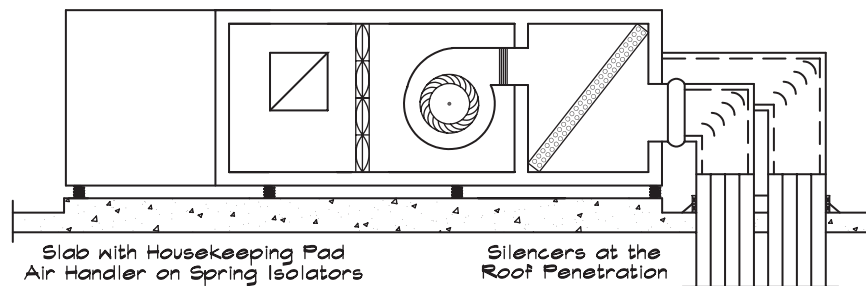
FIGURE 16.34 Quiet Rooftop Air Handling Unit (Schaffer, 1991)
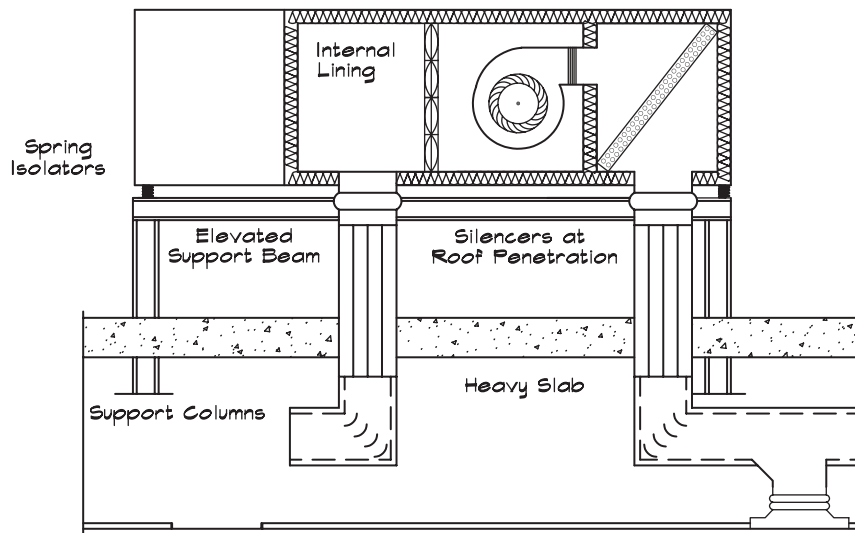
Figure 16.33 shows a side discharge configuration, which is the preferred arrangement, particularly for small installations. Where possible the ducts should penetrate the roof at a duct shaft or other nonsensitive area, since there is noise generated by the branch takeoffs. Where the building is located in a high exterior noise environment, the silencers can be located vertically at the roof penetration to reduce break-in problems.

Figure 16.34 illustrates a rooftop unit in which considerable effort has been expended to address the noise problems before the ducts penetrate the roof. The equipment support system is mounted on columns. The air handling unit is raised to allow the silencers to be installed vertically. Round ducts are used to control breakout and rumble.

Fan Coil and Heat Pump Units

In buildings such as hotels, where there is a need for temperature control in individual zones, a split system is used, which consists of an exterior condensing unit and cooling system, and an interior fan coil or heat pump unit located near the conditioned space. The fan in these units is the source of noise; as a general rule, fan coil units should not be located above or adjacent to occupied spaces when there is only an acoustical-tile or louvered-grille separation.

Fan coil units are available in two configurations, horizontal and vertical. The sound power levels vary with the fan capacity but in general a 3' (1 m) medium pressure drop silencer or equivalent is required on both the supply and return to reduce noise levels to an NC 30. Horizontal units can be located above a closet, which allows access through the closet ceiling for maintenance. Vertical units can also be placed in a closet with a silencer in the supply duct. The return can be ducted through a return air plenum in the ceiling or through a transfer duct silencer mounted to the back of a solid core or rated door (depending on the sound power level of the unit). Lined plenum returns located beneath vertical units are usually not sufficient to achieve an NC 30, but can achieve an NC 40 to 45 in the region adjacent to the return air grille. This may be sufficient for nonsensitive spaces but is not

FIGURE 16.35   Vertical Fan Coil Units

Supply air

Return air

Silencer

Isolators

Lined duct

Mechanical closet with heavy solid core or sound rated door

Lined plenum
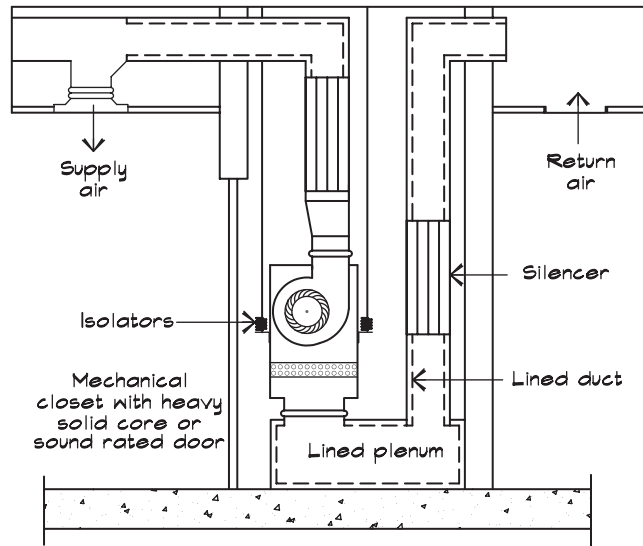
FIGURE 16.36   Horizontal Fan Coil Units

Isolators

RA plenum

Silencer

Supply air

Nonsensitive room with drywall ceiling

Return air
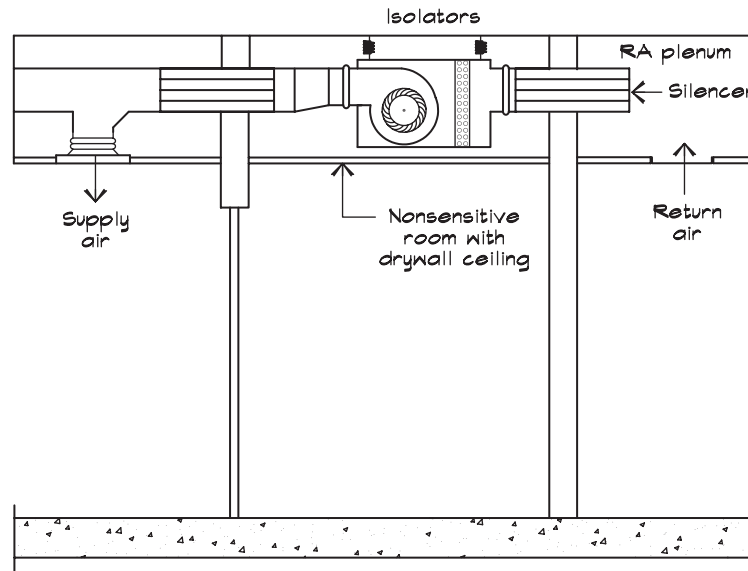
recommended for residential installations. Figures 16.35 and 16.36 illustrate these two types of fan coil installations.

Emergency Generators

Emergency generators are included in large buildings to supply power to selected equipment when the main power is lost. Although they are used infrequently, they must be tested

FIGURE 16.37 Plan of an Emergency Generator Room
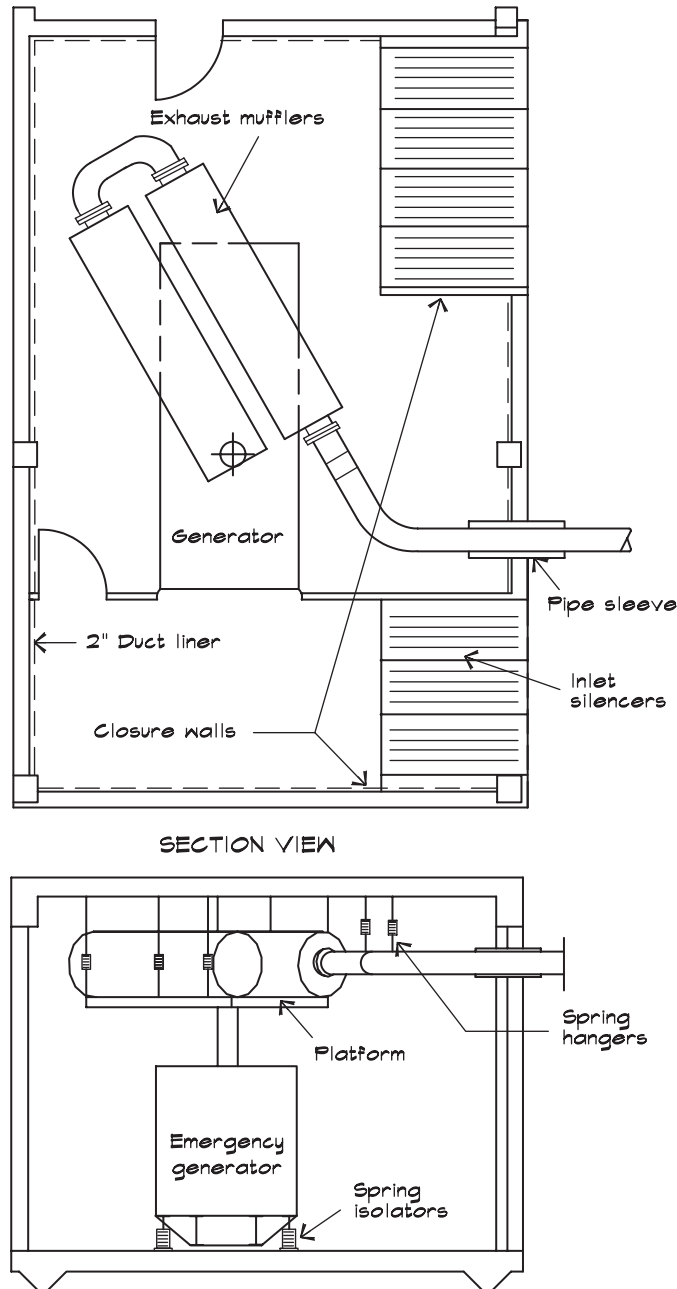
periodically, typically an hour per month, so they need to be acoustically isolated. This requires treatment of both the exhaust and the inlet/cooling air. Inlet air is drawn in through the radiator by a fan and is used to cool the engine as well as to provide the combustion air. It circulates through the generator room and exhausts out again through silencers. The air intake has a large open area since the fan can accommodate only a small back pressure. The exhaust passes through one or more large mufflers. A design is shown in Fig. 16.37.

DESIGN OF ROOMS
FOR SPEECH

17.1   GENERAL ACOUSTICAL REQUIREMENTS

General Considerations

Intelligibility depends on the masking effects of extraneous sounds on the speech we hear. Masking can be caused by noise from background sources or by reflections of the original spoken words. Speech combines the quick high-frequency sounds of consonants with the broader tones of the vowels. It is the recognition of consonants that correlates most closely with speech intelligibility, so the transmission of undistorted high-frequency information is critical. Figure 17.1 gives an illustration of a level versus time plot of the spoken word "back." Since the first part of the word is louder than the rest, its reverberant tail can mask the consonant ending.

In the design of classrooms, conference rooms, and auditoria, the ability to understand speech is very important. The architectural components of these rooms—size, shape, surface orientation, and materials, as well as the background noise level—all influence intelligibility. There are several fundamental requirements in designing rooms for speech (Doelle, 1972), each of which contributes to achieving a high signal-to-noise level at the receiver:

1. There must be adequate loudness.

2. The sound level must be relatively uniform.

3. The reverberation characteristics of the room must be appropriate.

4. There must be a high signal-to-noise ratio.

5. Background noise levels must be low enough to not interfere with the listening environment.

6. The room must be free from acoustical defects such as long delayed reflections, flutter echoes, focusing, and resonance.

Adequate Loudness

For adequate loudness in a room, there must be a high direct field level. In unamplified spaces such as classrooms, the distance between the source and the receiver should be controlled.

FIGURE 17.1 An Illustration of the Effects of Reverberation on the Intelligibility of Speech (Everest, 1994)
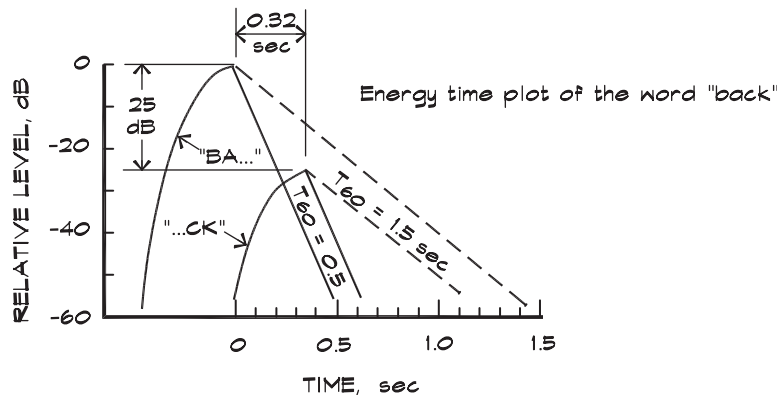
Beyond 30 to 40 feet it is difficult to understand unreinforced speech, especially in a reverberant space. The volume per seat should be low, no more than 80 to 150 cu ft (2.3 to 4.3 cu m) per seat with an optimum value of 110 (3.1 cu m) (Doelle, 1972). By reducing the volume per seat, the loudness is increased and the reverberation time decreased for a given area of absorptive material. In general the smaller the seating capacity the larger the volume per seat can be within this range. Grazing attenuation should be controlled by raising the talker height and by sloping the floor. Beneficial reflections, preferably from overhead, should be designed in to help offset the effects of geometric spreading and grazing attenuation.

Making the audience seating area more circular minimizes the source-receiver distance. As the seating circle expands, there is a region beyond which the human voice cannot extend without physical or electronic reinforcement. These limits define the shape of a simple outdoor amphitheater and with the addition of walls and ceiling, they also contribute to the shape of a classroom or small lecture hall. For an auditorium, the semicircular seating area drives the shape toward a width that is greater than the depth as in Fig. 17.2. With a hard ceiling, the depth can be increased and the length-to-width ratio can exceed one. A balcony allows more of the audience to be seated close to the talker, as it brings the center of mass of the audience forward.

Nonacoustical considerations such as sight lines also influence the choice of room shape. The included angle between the outermost seats should be less than 140°, as shown in Fig. 17.3. This seating arrangement allows a clear view of the lecturer and writing boards. For projection screens the included angle should be limited to 125°, or about 60° from the screen centerline. Multiple angled screens can improve sight lines and reduce the effects of off-axis screen gain (loss).

Floor Slope

The floor of a large auditorium should be sloped to provide adequate sight lines. Good sight lines result in good listening conditions. Sight lines are set so that the audience can see the lowest point of interest on stage, called the arrival point of sight (APS), over the head of a person sitting in front of them. Even though it is theoretically desirable to design a theater with every-row clearance, from a practical standpoint this yields floor slopes that are too steep.

FIGURE 17.2 General Shapes of Auditoria (Doelle, 1972)
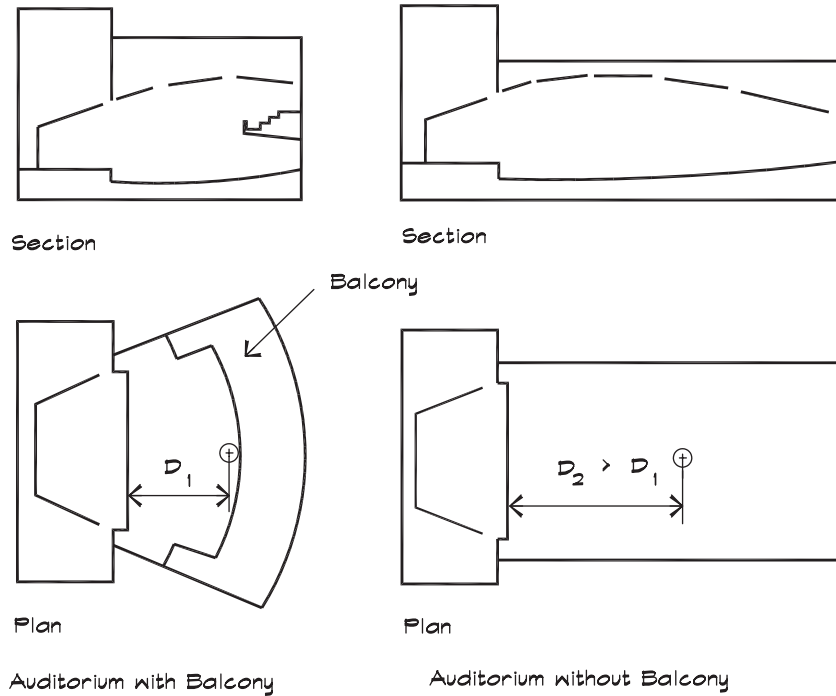
FIGURE 17.3 Seating Layout for a Lecture Hall
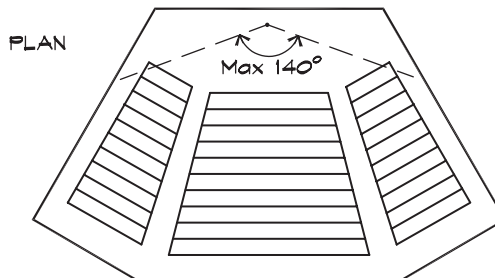
It is assumed that a person will adjust his position to look between the patrons seated in the next row so most theaters are designed for every-other-row visibility.

Figure 17.4 shows a typical sight-line design problem. The slope of the floor will depend dramatically on the APS that is selected. A high APS such as that found in a movie theater will still be visible, even with a relatively shallow floor slope. Stage floor heights are set low enough that a person sitting in the front row can see the actors' feet, but high enough that the APS does not force excessive floor rake. The eye height of a seated person ranges from 44 inches (1.12 m) for an adult female to 48 inches (1.22 m) for an adult male (Ramsey and Sleeper, 1970). Stage heights are fixed at between 40 and 42 inches (1.02–1.07 m) above the floor. The floor slope is determined by drawing a series of sight lines from the APS to a patron's ear level using standard anatomical data or by iteratively

FIGURE 17.4 Geometry of Theatrical Sight Line Calculations Every Other Row Sight Lines
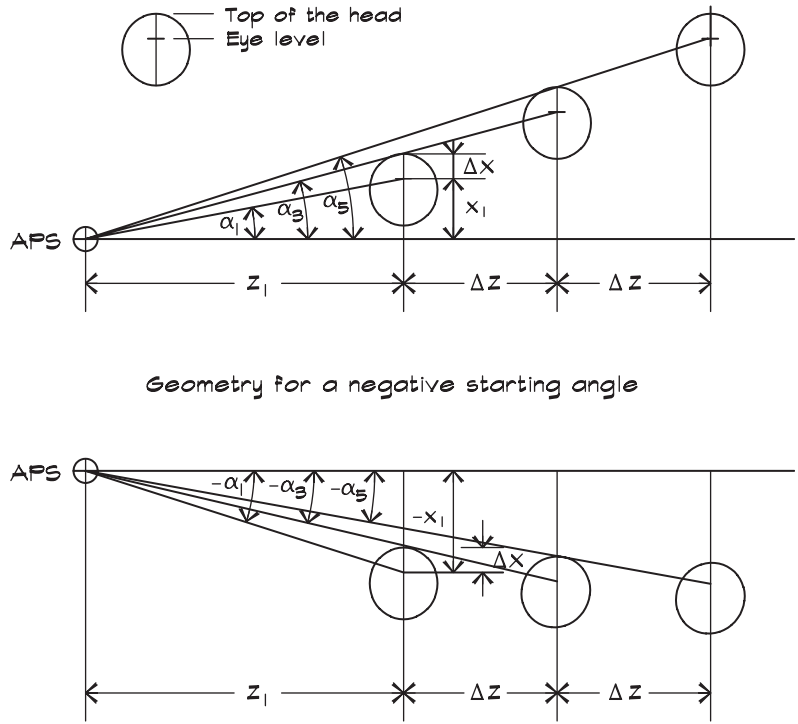
applying a mathematical relationship

$$\tan \alpha_1 = \frac{x_1}{z_1} \tag{17.1}$$

where the index 1 refers to the first row and each subsequent index to the next row. The odd numbered rows are calculated for every-other-row sight lines. For this case the third row angle is

$$\tan \alpha_3 = \frac{x_1 + \Delta x}{z_1} \tag{17.2}$$

Subsequent odd numbered rows are calculated iteratively

$$\tan \alpha_n = \frac{\left\{ z_1 + \left[\frac{(n-1)}{2} - 1 \right] \Delta z \right\} \tan \alpha_{n-2} + \Delta x}{z_1 + \left[\frac{(n-1)}{2} - 1 \right] \Delta z} \tag{17.3}$$

where n = 5, 7, 9, and so forth, Δx = 5" (12.7 cm) for two rows, and Δz = 2· (row spacing).

Where there are fixed seats, grazing effect produces an attenuation that depends on the angle of incidence. The lower the angle, the greater the effect. The angle can be increased by

FIGURE **17.5 Good Sight Lines Yield Good Direct Sound**
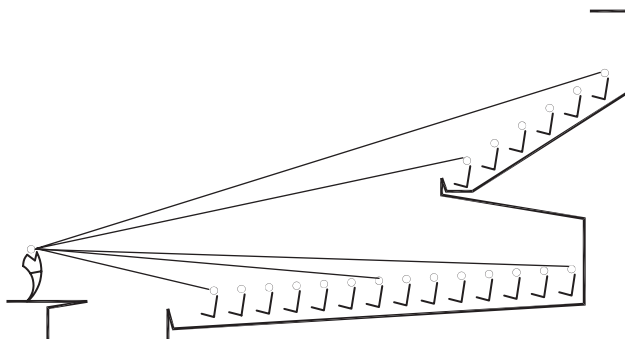
raising the talker on a platform or by raking the angle of seating as in Fig. 17.5. Seating rake is set by the sight-line requirements that are fixed by the APS and by the relative heights of each row of seats. In general the higher the APS the lower the seating rake. The rise of each row of seating can be calculated using Eq. 17.3. In the orchestra level seating a 1:9 rake for the first ten rows, and thereafter a 1:8 slope, yields a good result for a theater stage having a normal 42" (1.07 m) height. Building codes, which require no more than a 1:12 slope for handicapped access, may dictate the floor design.

In lecture halls, where the APS is selected to be at or above the waist of the lecturer or at the bottom of the writing board, the rake can be modest. In a large flat-floored classroom, a platform of 1 ft (0.3 m) height can improve the sight lines significantly. In small classrooms, seating fewer than 50 people, a platform is not necessary.

Sound Distribution

Unamplified speech can be augmented by physically placing hard surfaces in positions where they can distribute sound to the audience. Reflectors must have sufficient size that they scatter the frequencies of interest and should be close enough so that the reflection delay time is less than 30 to 50 msec. To provide this support, a hard ceiling is preferred in a lecture hall and auditorium (50–500 seats). In small classrooms (< 50 seats) the direct field, along with support from the walls, provides sufficient loudness and control of reverberant noise using an absorptive ceiling as the normal choice.

The orientation of a reflective element is determined by the required coverage area of the scattered sound. For specular reflection, the deflected angle is determined by locating the mirror image point of the sound source and by then drawing a line from the image point through the point of reflection toward the receiver. An example is given in Fig. 7.1. When the reflecting surface has a finite size, it is not an effective reflector over its entire length. Simple reflection studies illustrate the procedure. In these cases a reflection should be considered only if it occurs at a point more than one-half wavelength from the end of the reflector. Where the reflector is curved, the reflection angle is determined by mirroring the incident ray about the line connecting the center point of the curved surface with the intersection point of the ray and the surface. This is relatively straightforward in a CAD program; however, simple ray tracing does not tell the whole story since the scattered intensity falls off rapidly with increasing included angle, as was illustrated in Eq. 7.37.

The shape of the ceiling can be used to distribute sound evenly throughout an auditorium. Figure 17.7 shows a simple example of a flat ceiling. In this example the reflected rays

FIGURE 17.6 Reflection Studies from Ceiling Panels
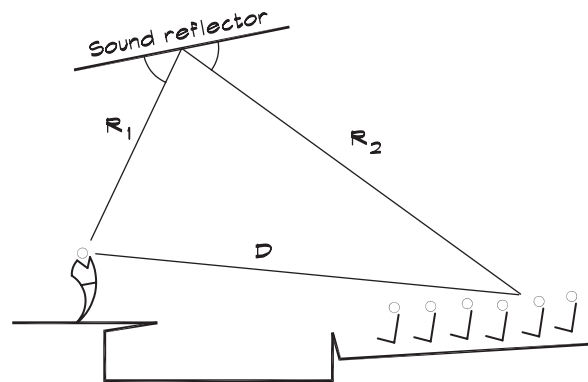
Time delay in milliseconds

$$\left[\frac{R_1 + R_2 - D}{1.13} \text{ for dimensions in feet} \right]$$

$$\left[\frac{R_1 + R_2 - D}{0.34} \text{ for dimensions in meters} \right]$$
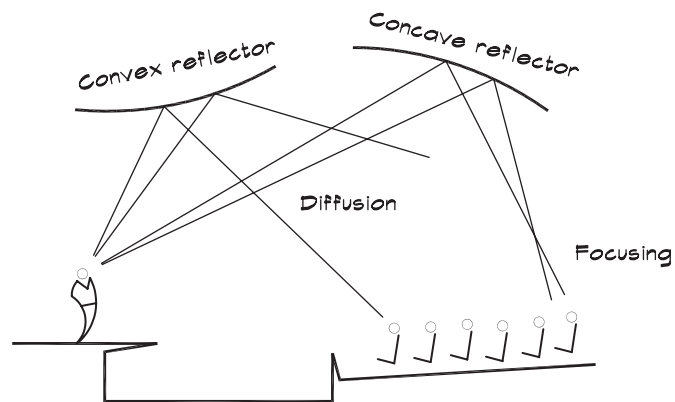
FIGURE 17.7 Reflections from a Flat Ceiling Section
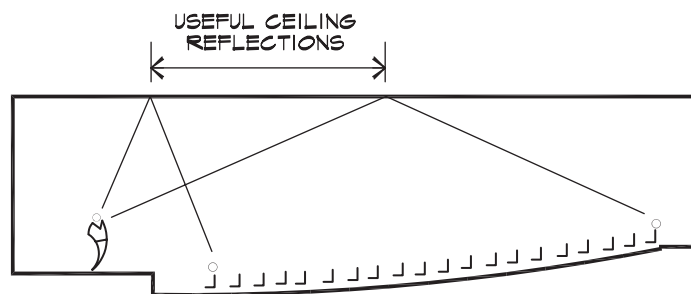
FIGURE 17.8 Reflected Sound from a Segmented Ceiling (Doelle, 1972)

SECTION
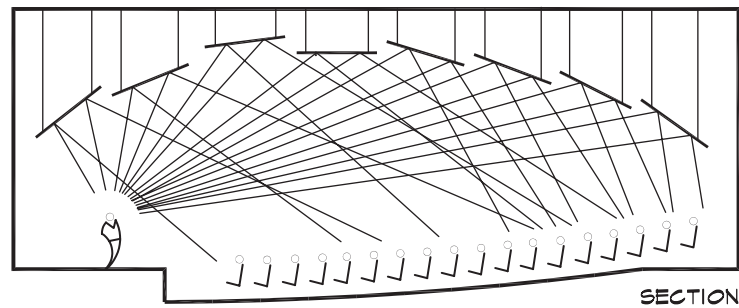
FIGURE 17.9 Reflected Sound from a Stepped Flat Ceiling

SECTION
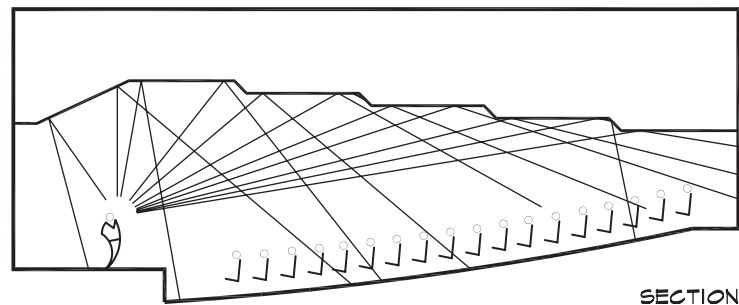
illuminate the front and middle portions of the space but much of the energy falling on the rear portion of the ceiling is grounded out on the absorptive rear wall.

To improve the design, the ceiling can be segmented as in Fig. 17.8 or the seating raised and the ceiling stepped as in Fig. 17.9. Note that only about half of the ceiling provides useful specular reflections in both Fig. 17.7 and 17.8 since the ends of the segmented reflectors are diffusive.

The energy distribution is dependent on the location of the talker, which may vary, so slightly convex panels may be used to provide additional flexibility. Panels should not be used to reflect sound directly down, or back to the listener from behind, since this shifts the perceived source location overhead.

Reverberation

Reverberation can be the boon or the bane of the acoustical performance of a room. In general, the more speech content there is to the sound, the lower the ideal reverberation time. For classrooms and small lecture halls times at or below one second are preferred. Longer reverberation times are desirable for music; the ideal length depends on both the room size and the type of music. For light opera such as Gilbert and Sullivan, where understanding the complicated play of words is critical, a time of 1.0 to 1.2 seconds would not be too low. For a Mozart opera preferred reverberation times might range from 1.2 to 1.5 seconds. A Wagnerian opera is ideal in a 1.5 to 1.6 second room, and romantic symphonies sound best in a 1.7 to 2.1 second hall. For organ concerts and chant, reverberation times between 2.5 to 3.5 seconds

FIGURE 17.10   Reverberation Times vs Room Volume
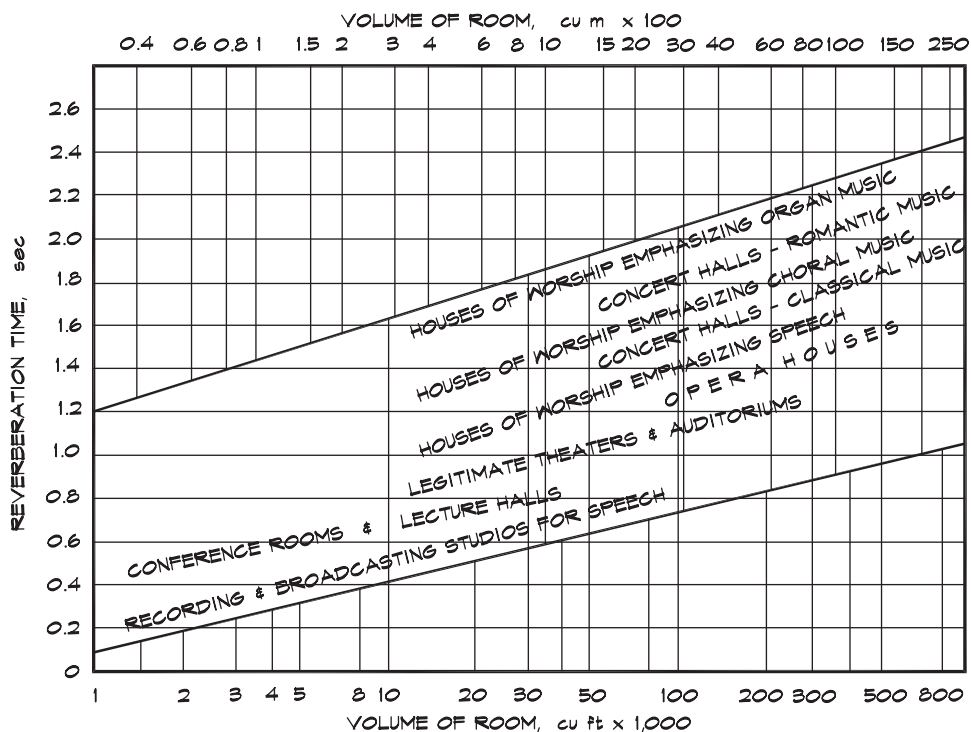
are not too long. Clearly there is no single reverberation time that is perfect for all uses of a given room. Variations of 5 to 10% from the ideal values are commonplace.

Various authors have made recommendations on ideal reverberation times for different types of spaces. Figure 17.10 shows a synthesis of a number of these graphs (e.g., Doelle, 1972; Knudsen and Harris, 1950; Long, 1999). Recent trends, particularly in the design of churches for electronically reinforced music, have driven the desirable reverberation times in large spaces downward, since reverberation can be added back electronically. Reverberation time recommendations for motion-picture theaters are given in Fig. 17.26.

Authors Knudsen and Harris (1950) and Doelle (1972) have recommended that for music the reverberation times at frequencies below 500 Hz rise to a number higher than the mid frequency value. Beranek (1996), citing measured results from various halls, recommends a factor of about 1.2 times the 500 to 1000 Hz value at 125 Hz. A recommended graph is shown in Fig. 17.11. A rising bass reverberation is good practice for performance rooms used for unreinforced music but not necessarily desirable in spaces where the low-frequency is provided by loudspeakers. As a practical matter it is difficult to achieve a rising reverberation time at very low frequencies, due to the weight and thicknesses of the materials required.

Since single-layer 16-mm (5/8") gypsum board is nearly 30% absorptive at 125 Hz, a rising bass requires the use of multiple-layer gypboard or thick plaster construction. In the best concert halls the use of 25 to 50 mm (1"–2") plaster is common. For speech the reverberation time behavior with frequency should be flat. In large rooms this is also difficult to achieve due to air attenuation, and the times fall off above 1 kHz. In large concert halls the HVAC system must include humidity control to reduce the high-frequency losses.

FIGURE 17.11   Ratio of the Bass to Mid-Frequency Reverberation Time
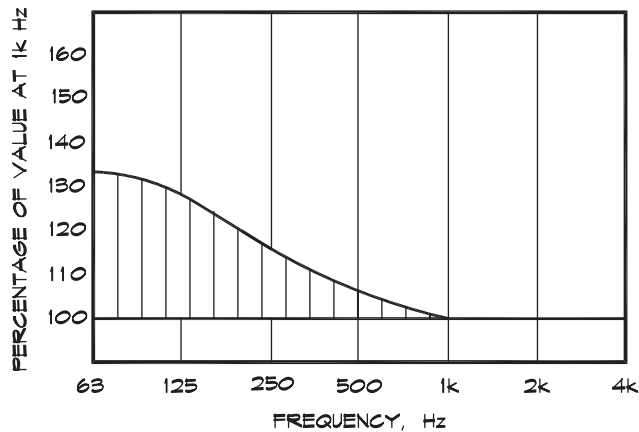
Recommended variation of T_{60} with frequency for music.
At frequencies lower than 1000 Hz the T_{60} should
increase according to the values inside the shaded area.
For speech the T_{60} should remain flat with frequency.

Signal-to-Noise Ratio

Background noise levels in small classrooms and lecture halls are designed to an NC 30 (35 dBA) and larger auditoria to an NC 25 (30 dBA). The difference is due to the greater loss of loudness in the larger space. Some authors (Peutz and Klein, 1974) recommend that the received level be at least 25 dB higher than the background noise level for adequate intelligibility. Others (Bradley, 1986) hold that a 10–15 dB margin is a more reasonable choice. The latter value is consistent with an NC 30 background level and a direct-field level of 45 dBA, based on a speaking voice sound power level of 75 dBA and a source to receiver distance of 25 feet (7.6 m).

When the reverberant field is the masking noise a higher level can be tolerated. In these cases signal-to-noise ratios are rarely positive and a signal-to-reverberant-noise of −6 dB can still yield good intelligibility. This is discussed in more detail in Chapt. 18.

Acoustical Defects

The presence of acoustical defects can contribute to poor intelligibility and general discomfort in rooms. The principal defects, in addition to those already discussed, are multiple or long delayed reflections, focusing, coloration, and low-frequency phenomena such as room resonances and locally high-amplitude sound fields. In large auditoria there are also shadowed areas under balconies, coupled spaces with mismatched reverberation characteristics, and excess attenuation due to grazing incidence. Not all these defects are important in every room and some may be present without affecting the room's primary use.

There are a number of phenomena, associated with single or multiple reflections, that can detract from good intelligibility in rooms and should be avoided. These include long-delayed reflections, echoes, and flutter. Echoes occur when a sound of sufficient loudness arrives later than the direct field by more than a given time. The cause might be a single reflection from a rear wall of an auditorium, particularly if it is concave. Figure 17.12 shows

FIGURE 17.12 Perception of Lateral Speech Reflections (Everest, 1994)
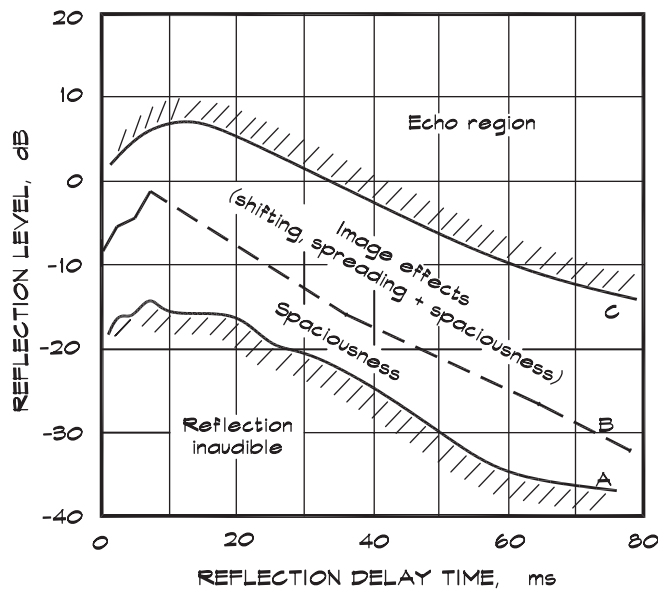
the effect of reflections for various amplitudes and delay times, as simulated in an anechoic environment. Below curve B the echo increases the perception of spaciousness, while below curve A the reflected sound is reduced to inaudibility. Above curve C the reflection is perceived as an echo.

Echo and reverberation are not the same thing. Echo is a repetition of the original sound that is distinctly perceptible, whereas reverberation is a prolongation of the sound through multiple reflections, which is frequently beneficial for music. Long-delayed reflections are like echoes, but have a somewhat shorter delay time. They are not perceived as separate sounds, but blur the understanding of the original sound. Flutter echoes are sounds that persist locally due to multiple reflections between parallel planes, concave, or chevroned surfaces. They can be caused by two, three, or more reflections. Figure 17.13 gives several examples of acoustical defects.

Coloration is the emphasis of certain frequencies or frequency bands over others. It can be caused by room-mode buildup or by absorptive materials that only absorb in certain frequency ranges. Focusing is the buildup of sound energy in localized regions of a room, due to concave surfaces. Shadowing is the blockage of sound traveling from the source, or from a significant reflecting surface, to the receiver. Each of these defects can detract from the overall acoustical environment in a room and each can be avoided with careful design.

17.2   SPEECH INTELLIGIBILITY

Speech-Intelligibility Tests

Speech-intelligibility tests for an unamplified talker are carried out using a single loudspeaker, ideally having a directivity similar to that of the human voice. Prerecorded words are presented in a neutral context carrier phrase such as, "Word number __ is ___", at one or more calibrated levels, in rooms exhibiting a variety of acoustical conditions. As we gleaned

FIGURE 17.13   Examples of Acoustical Defects (Doelle, 1972)

1) ECHO

2) LONG DELAYED REFLECTIONS

3) SHADOW ZONE

4) FOCUSING

5) FLUTTER ECHO
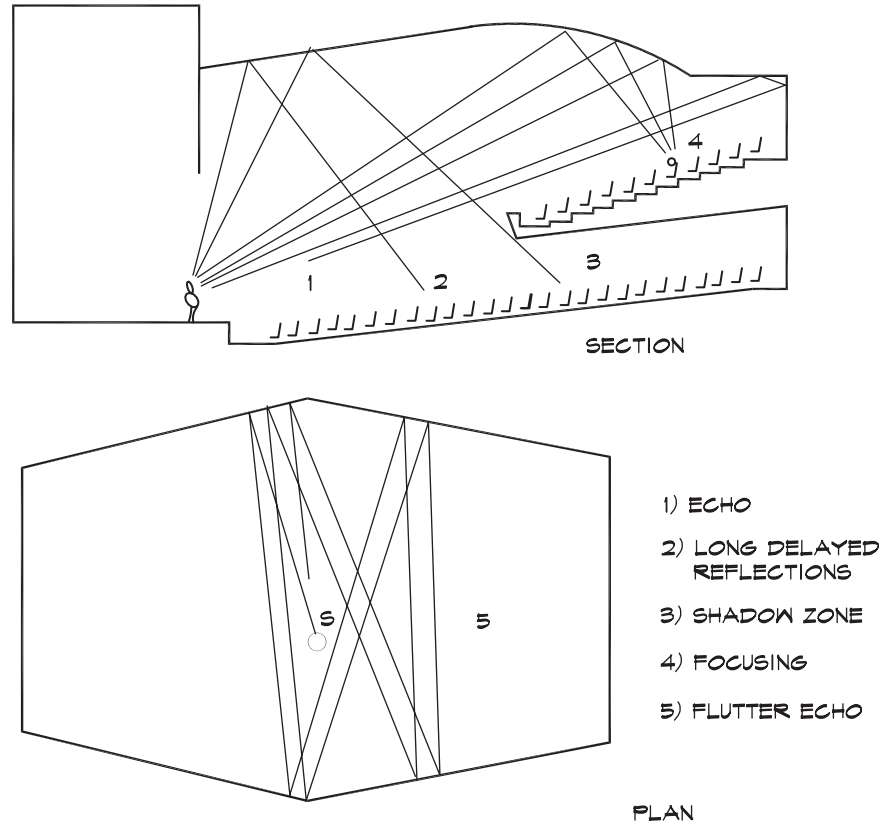
from Fig. 3.19, there is not just one test that gives the single answer for speech intelligibility. Rather there are many different results that depend on the details of the test and the type of material presented to the listener. The prediction of speech intelligibility in an enclosed space thus combines the results of listening tests with knowledge of the room's acoustical properties in such a way as to produce a predictable outcome.

Energy Buildup in a Room

When a sound is generated by a single source, the listener receives, in rapid succession, the direct-field signal followed by individual early reflections, and a rising swell of merged reflections whose sum becomes the reverberant field, which finally decays at a rate characteristic of the space. Figure 17.14 shows an example of the idealized pattern. In this figure the three temporal regions are neatly separated; in practice the divisions are not so distinct. The early reflections and the reverberation may be merged. If long-delayed reflections are present they may arrive during the reverberant decay. Sometimes individual reflections are louder than the direct sound when focusing or grazing attenuation is present. The reverberant field can be louder than the direct sound when the receiver is a relatively long way from the source.

The time between the arrival of the direct sound and the first major reflection is called the initial delay gap. If this gap is short enough, early reflections can contribute to increased

FIGURE 17.14 Idealized Acoustic Response of a Room to an Impulse Excitation
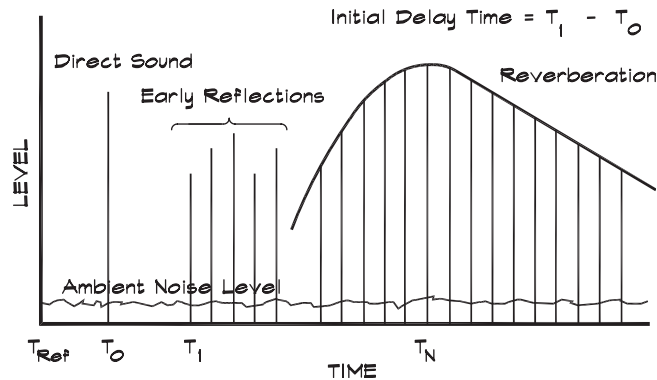
intelligibility, a broadening of the sound image, and a pleasant augmentation of the sound level. If it is too long, its effect will be to decrease intelligibility.

Background noise, along with long-delayed reflections and persistent reverberation, serve to decrease intelligibility. Background noise that interferes with the comprehension of speech can originate from many sources: people, HVAC systems, exterior noise sources such as traffic, or electronically generated masking noise, which is purposefully introduced to increase speech privacy. When words are spoken in a room, the reflections off the walls and other surfaces will eventually have a negative effect on speech intelligibility, either through long delayed individual reflections or as part of the general buildup of background noise. Thus the reverberant field of speech itself can also become the source of masking noise.

Room Impulse Response

Although it is possible to measure speech intelligibility directly in an existing room, it is also useful to have algorithms to predict it before a room is constructed. As we discussed in Chapt. 11, the impulse response completely defines the properties of a system, and we can predict the result of introducing an arbitrary forcing function (speech) by convolving (integrating) the input with the room's impulse response (Eq. 11.40). An exact formulation of a room's response is not available a priori, but it can be approximated by using the simplifying assumptions or by ray tracing.

A simple model assumes that the room is diffuse and that there exists a reverberant field characterized by a reverberation time. This model ignores common acoustical defects such as long delayed reflections, flutter echo, focusing, and the process of reverberant sound buildup. More complicated analyses utilizing ray tracing can describe these effects, but they are not expressible in a closed-form equation and are time consuming. The approximate methods yield results that are sufficiently accurate, as long as steps are taken to avoid the acoustical defects, which they do not include. The approach is to use the direct and reverberant sound energy densities previously discussed. The direct field (Eq. 2.56) energy density is given by

$$D_d = \frac{E}{S\,c_0\,t} = \frac{W_S}{S\,c_0} = \frac{p^2}{\rho_0\,c_0^2} \qquad (17.4)$$

and

$$D_{\rm d} = \frac{Q\,W_{\rm S}}{4\,\pi\,c_0\,r^2}$$

(17.5)

The steady state reverberant field (see Eq. 8.82) energy density is

$$V\,D_{\rm r} = \frac{4\,W_{\rm S}\,V}{c_0\,S_{\rm T}\,\overline{\alpha}}$$

(17.6)

or

$$D_{\rm r} = \frac{Q\,W_{\rm S}}{4\,\pi\,r_{\rm c}^2\,c_0}$$

(17.7)

where $r_{\rm c}$ is defined as the critical distance, the point at which the direct sound pressure level is equal to the reverberant field level.

$$r_{\rm c} = \sqrt{\frac{Q\,R}{16\,\pi}}$$

(17.8)

where $W_{\rm s}$ = source sound power (W)
V = room volume (m^3 or ft^3)
Q = source directivity in the receiver direction
c_0 = speed of sound in air (m / s or ft / s)
ρ_0 = density of air (kg / m^3 or lbs / ft^3)
$\overline{\alpha}$ = average room absorption coefficient
R = room constant (m^2 or ft^2)
S = area of the control surface (m^2 or ft^2)
$S_{\rm T}$ = total surface area of the room (m^2 or ft^2)
T_{60} = reverberation time (s)

We can approximate the impulse response of a room by assuming that the sound field is made up of only a direct and perfectly reverberant field that decays at a rate defined by the reverberation time. This idealized model, illustrated in Fig. 17.15, ignores all individual reflections.

The sound power density as a function of time (t $\geq$ 0) is (Houtgast et al., 1980)

$$w\,(t) = \frac{W_{\rm S}}{4\,\pi\,c_0}\left[\frac{Q}{r^2}\,\delta(t) + \frac{Q\,\kappa}{r_{\rm c}^2}\,e^{-\kappa t}\right]$$

(17.9)

where $\delta(t)$ = Dirac delta function at t = 0
κ = decay rate = 13.82 / T_{60} (1/s)
and the terms within the brackets are the impulse response of the room.

FIGURE 17.15   Simplified Room Impulse Response
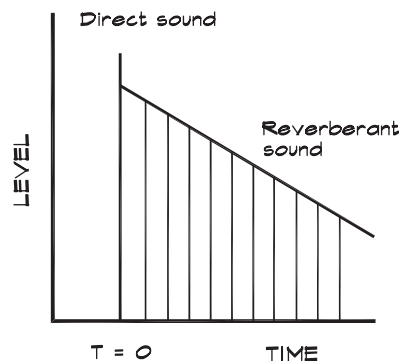
Once the impulse response is known, the sound energy density arriving at a receiver during the time period from t = 0 to t = T is found by integrating over time

$$D_{0-T} = \int_0^T w\,(t)\,dt \qquad (17.10)$$

The steady-state energy density for a continuous driving function is found by setting $T = \infty$. In this way we recover Eqs. 17.5 and 17.7.

Speech-Intelligibility Metrics—Articulation Index (AI)

There are several metrics currently enjoying use for the prediction of the intelligibility of speech in rooms: the Articulation Index (AI), the Articulation Loss of Consonants (AL_{cons}), the Speech Transmission Index (STI), and the various signal-to-noise ratios including the Useful to Detrimental Energy Ratio (U_τ) and the Useful to Late Energy Ratio (C_τ).

Much of the pioneering work in communication acoustics was done at Bell Laboratories, where engineers studied methods of improving the intelligibility of telephone conversations. Harvey Fletcher (1884–1981) was one of these early pioneers. Although Fletcher's work dates from the 1920s and 1930s, much of it was not revealed publicly until the publication of later papers and his classic book in 1953.

Fletcher (1921) proposed to quantify the speech distortion in telephone systems by relating it to articulation scores. He defined the "articulation," which ranged from 0 to 1, as an overall measure of the intelligibility of speech transmitted through a system. One of Fletcher's contributions was the discovery of the probabilistic nature of intelligibility, and indeed the definition of articulation is the probability of understanding an individual sound. If, for example, a syllable consists of a consonant-vowel-consonant (cvc) sequence, the probability of understanding the whole sequence would be the product of the probabilities of understanding each separate consonant or vowel. When this was combined with the realization that the probabilistic approach carried over into the analysis of separate frequency bands (published later in Fletcher and Galt, 1950), the basis for the Articulation Index was established. French and Steinberg (1947) formalized the method of measurement and Kryter (1970) published a method of calculating the expected speech intelligibility in rooms using the sum of weighted signal-to-noise ratios in third-octave frequency bands (Chapt. 3).

FIGURE 17.16   **Measured Intelligibility vs Articulation Index (Bradley, 1986)**
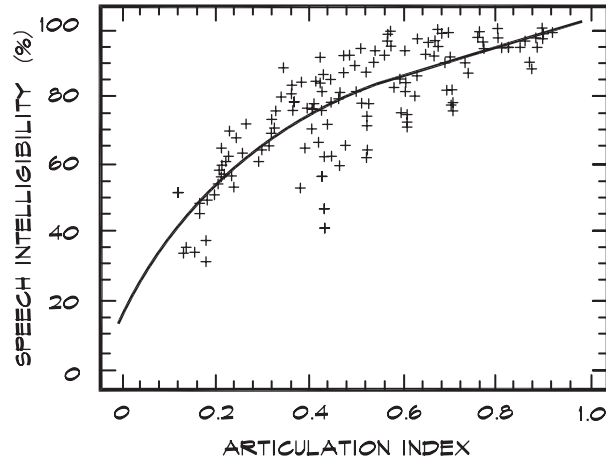
In 1986 Bradley published a study comparing the accuracy of various articulation metrics, and Figure 17.16 shows his result for Articulation Index.

Articulation Index (AI) is like virtually all other intelligibility prediction schemes in that it uses a signal-to-noise ratio as part of the calculation. The differences among the various schemes are how the terms "signal" and "noise" are defined. In AI calculations, the signal is the long-term rms average speech level (direct + reverberant) plus 12 dB, and the noise is the steady background noise level in each frequency band. AI is difficult to use as an intelligibility prediction methodology since it does not have a built-in way of accounting for reverberant noise. In the ANSI standard (ANSI S3.5-1969) there is an empirical correction table for reverberation time (Knudsen and Harris, 1950) but no way of dealing with the contribution of the reverberant field. Where an electronic masking system generates the steady background noise, AI yields good results in the assessment of privacy. Typical results of intelligibility scores versus AI values were given in Fig. 3.19.

Articulation Loss of Consonants (AL_{cons})

Early researchers (e.g., Knudsen, 1932) found that intelligibility was based on the recognition of consonants rather than vowels and developed metrics based on this concept. Maxfield and Albersheim (1947) at Bell Laboratories examined the measured articulation-loss-of-consonants data published by Steinberg (1929) and Knudsen (1932) and plotted them versus a steady-state direct-to-reverberant energy ratio. They found that the data did not lie along a straight line and subsequently developed the concept of a liveness factor, for use with microphone pickups, which they defined as

$$L = \int_0^\infty D_r(t)\, dt\, /\, D_d \qquad (17.11)$$

where $D_r(t)$ is the reflected-energy density at any time, t, and D_d is the direct-field energy density. Under the assumption of a reverberant field and unit directivity, the liveness can be

written (Bistafa and Bradley, 2000) in metric units as

$$L = \frac{T_{60} D_r}{13.82 D_d} = \frac{4\pi}{(13.82)^2} \frac{c_0 T_{60}^2 r^2}{V} = 22.6 \frac{T_{60}^2 r^2}{V} \tag{17.12}$$

which is the reverberant-to-direct energy ratio multiplied by the reverberation time. Bistafa and Bradley (2000) fitted a curve to the Maxfield and Albersheim plots, which related articulation loss (AL) to liveness based on Steinberg's data

$$AL = 4.5 L^{0.67} \tag{17.13}$$

In 1971 Peutz measured the speech intelligibility in rooms using cvc phonetically balanced words in Dutch. Like Knudsen, he also found that the articulation loss was much smaller for vowels than for consonants, so that consonant loss probabilities controlled cvc recognition. Unlike Maxfield and Albersheim, however, he found a linear relationship between the measured articulation loss of consonants and liveness. His relationship, in metric units, is shown in Eq. 17.14, and assumes a directivity of one and negligible background noise.

$$AL_{cons} = 8.9 L + a = 200 \frac{T_{60}^2 r^2}{V} + a \tag{17.14}$$

where a is a correction factor that can vary from 1.5% for a "good" listener, to 12.5% for a "bad" listener. This equation is said to hold as long as the listener is no more than a limiting distance r_ℓ away, where

$$r_\ell = 0.21 \sqrt{V/T_{60}} \quad (m) \tag{17.15}$$

This is the distance at which the direct-field level is 10 dB below the reverberant-field level for a directivity of one. Beyond that point Peutz states that the articulation loss is given by

$$AL_{cons} = 9 T_{60} + a \quad \text{for } r \geq r_\ell \tag{17.16}$$

In terms of the limiting distance, the equation is

$$AL_{cons} = 9 T_{60} \frac{r^2}{r_\ell^2} + a \quad \text{for } r < r_\ell \tag{17.17}$$

Equations 17.16 and 17.17 are known as the architectural versions of the Peutz equations. They do not account for early reflections, discrete echoes, background noise, or frequency dependence of the variables.

Bistafa and Bradley (2000) published a continuous version of the noiseless equations based on work by Peutz (1974) and Peutz and Kok (1984).

$$AL_{cons} = 9 T_{60} \left[\frac{1}{1 + (r_\ell/r)^2} \right] + a \tag{17.18}$$

FIGURE 17.17   ALcons–N vs $(r_\ell/r)^2$ with Reverberation Time as a Parameter (Bistafa and Bradley, 2000)

——— Calculated with the architectural form of the Peutz equation.

——— Calculated with the architectural form of the Peutz equation. written as a continuous function using Eq. 17.20.
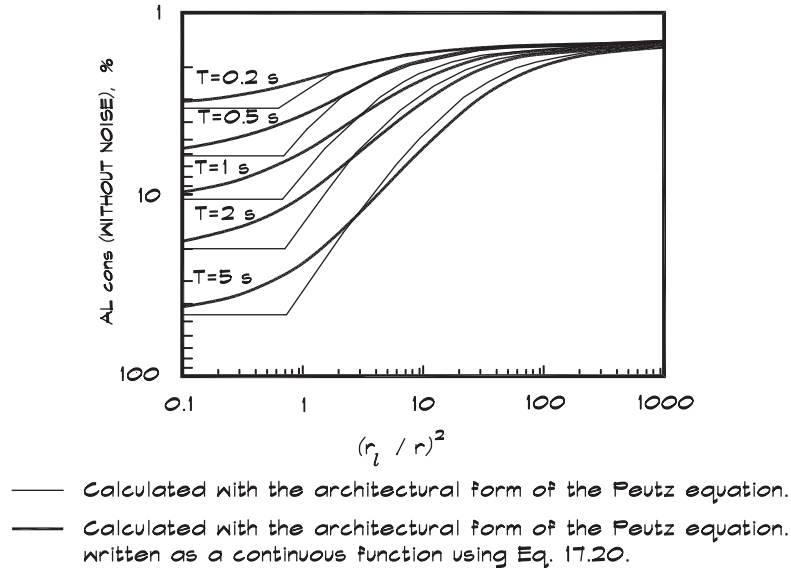
and Klein (1971) added back the directivity by defining the limiting distance in terms of the room constant.

$$r_\ell = 0.45 \sqrt{QR} \quad (m) \tag{17.19}$$

A comparison of Eqs. 17.16 and 17.17 to 17.18 is shown in Fig. 17.17.

In 1974 Peutz and Klein published a graphical method of accounting for the presence of noise. This was curve fitted by Bistafa and Bradley (2000) and in its continuous form is

$$AL_{cons} = 9\, T_{60} \left\{ \frac{1}{1 + (r_\ell/r)^2} \right\} \left[1.071\, T_{60}^{-0.0285} \right]^{(25 - L_{SN})} + a \tag{17.20}$$

where L_{SN} is the signal-to-noise ratio $L_{SN} = L_s - L_n$ in dB. According to Eq. 17.20, when the signal is less than 25 dB above the background noise there is a reduction in speech intelligibility, which becomes progressively worse as the signal level decreases. If the signal level is greater than 25 dB above the noise, there is no degradation due to background noise and the noise term is dropped. Here the signal level is the direct plus reverberant speech level, and the noise level is the steady background level having the same spectral shape as the speech level. Peutz and Klein did not include information on the spectrum of the background noise or the frequency at which the calculations are to be carried out. Standard practice is to use the 2000 Hz octave band.

Davis and Davis (1987) recommend AL_{cons} for general use in sound-system design, although in this form there is no single value of the directivity when multiple loudspeakers are used. Jacobs (1985), experimenting with single high, medium, and low-Q loudspeakers, found a poor correlation between the predicted and measured intelligibility, particularly in highly reverberant rooms. His data indicated that AL_{cons} underpredicted the speech

intelligibility for low- and medium-Q loudspeakers and overpredicted with a high-Q device. Bistafa and Bradley (2000) also found a poor correlation between AL_{cons} predictions and those based on STI and U_{50} metrics. They recommended that its use be limited to classrooms and small meeting rooms. This would seem to be a good approach. AL_{cons} includes the reverberant field as part of the signal in a signal-to-noise ratio, but switches to a different formulation when the reverberant field dominates the direct field.

Speech Transmission Index (STI)

Researchers in optics (Baker, 1970), seeking to quantify the distortion of light received from stars, developed the optical transfer function, which was based on a mathematical formulation called the modulation transfer function (MTF). Houtgast, Steeneken, and Plomp (1980) reasoned that stars are the spatial equivalent of an acoustical impulse source and this approach could be useful in evaluating distortion in rooms. As we discussed in Chapt. 4, the MTF uses a modulated sinusoidal input

$$I_{in}(t) = I_{in}(1 + \cos \omega_m t) \qquad (17.21)$$

which is introduced into a room. It is convolved with the room's impulse response g (t') to obtain an output

$$I_{out}(t) = \int_0^\infty I_{in}(t - t')\, g(t')\, dt \qquad (17.22)$$

which has the general form

$$I_{out}(t) = I_{out}\left\{1 + m\left[\cos \omega_m (t - \theta)\right]\right\} \qquad (17.23)$$

The modulation transfer function is defined as

$$m(\omega_m) = \frac{\left| \int_0^\infty g(t)\, e^{-j\,\omega_m\, t}\, dt \right|}{\int_0^\infty g(t)\, dt} \qquad (17.24)$$

and $\omega_m = 2\,\pi\,f_m$ is the modulation frequency. Schroeder (1981) pointed out that this is the normalized Fourier transform of the power density impulse response. Assuming a diffuse field, the impulse response for both the direct and reverberant field components is

$$g(t) = \frac{Q}{r^2}\, \delta(t) + \frac{Q\kappa}{r_c^2}\, e^{-\kappa t} \qquad (17.25)$$

where κ is the exponential decay constant of the reverberant energy, $\kappa = 13.82 / T_{60}$.

When background noise is added to the mix the output intensity is

$$I_{sum} = I_{out}(t) + I_n \qquad (17.26)$$

and using Eq. 17.23,

$$I_{sum} = I_{out} \left[1 + m \cos \omega_m (t - \theta) \right] + I_n \tag{17.27}$$

which can be written

$$I_{sum} = (I_{out} + I_n) \left[1 + m \frac{I_{out}}{I_{out} + I_n} \cos \omega_m (t - \theta) \right] \tag{17.28}$$

So the modulation factor due to background noise is

$$m_n = \frac{I_{out}}{I_{out} + I_n} = \left[1 + 10^{-0.1 \, L_{SN}} \right]^{-1} \tag{17.29}$$

and the signal-to-noise ratio in dB is $L_{SN} = 10 \log (I_{out} / I_n)$.

This yields the overall modulation transfer function including both

$$m (\omega_m) = \frac{\left| \int_0^\infty g(t) \, e^{-j \omega_m t} \, dt \right|}{\int_0^\infty g(t) \, dt} \left[1 + 10^{-0.1 \, L_{SN}} \right]^{-1} \tag{17.30}$$

room distortion and noise. We substitute the impulse-response function (Houtgast et al., 1980)

$$m (\omega_m) = \frac{\left(A^2 + B^2 \right)^{1/2}}{C} \tag{17.31}$$

with

$$A = \frac{Q}{r^2} + \frac{Q}{r_c^2} \left[1 + \left(\frac{\omega_m T_{60}}{13.8} \right)^2 \right]^{-1}$$

$$B = \frac{\omega_m T_{60}}{13.8} \frac{Q}{r_c^2} \left[1 + \left(\frac{\omega_m T_{60}}{13.8} \right)^2 \right]^{-1} \tag{17.32}$$

$$C = \frac{Q}{r^2} + \frac{Q}{r_c^2}$$

and the critical distance defined in Eq. 17.8. This can be simplified in the far field, $\frac{r_c^2}{r^2} \to 0$ for unit directivity to

$$m (f_m) \cong \left\{ 1 + \left(2 \pi f_m \frac{T_{60}}{13.8} \right)^2 \right\}^{-1} \left[1 + 10^{-0.1 \, L_{SN}} \right]^{-1} \tag{17.33}$$

For a given modulation frequency an apparent signal-to-noise ratio and speech transmission index (STI) is calculated from the modulation index described in Eqs. 4.23 through 4.25, and from this an intelligibility can be determined.

FIGURE 17.18 **Measured Speech Intelligibility vs Speech Transmission Index (Bradley, 1986)**
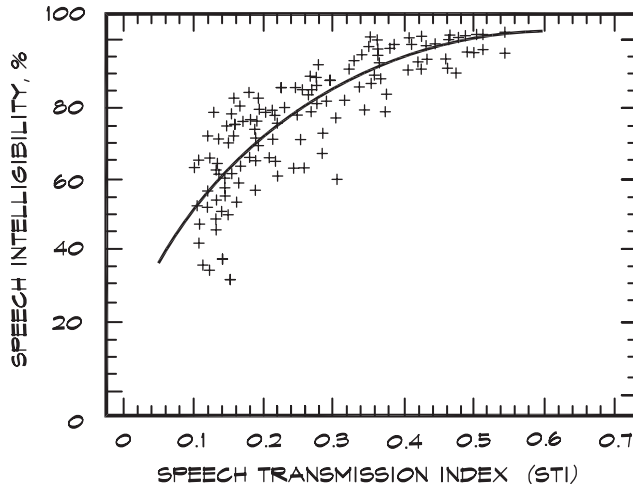
In a study of classroom intelligibility, Bradley (1986) measured speech-intelligibility scores, including the effects of noise, and compared them to calculated STI values. The results are given in Fig. 17.18. Bistafa and Bradley (2000) plotted STI values versus reverberation time for unamplified speech in classrooms, which are reproduced as Fig. 17.19. Here we see that for a given signal-to-noise ratio the intelligibility can be maximized as a function of reverberation time.

FIGURE 17.19 **Speech Transmission Index (STI) vs Reverberation Time (Bistafa and Bradley, 2000)**
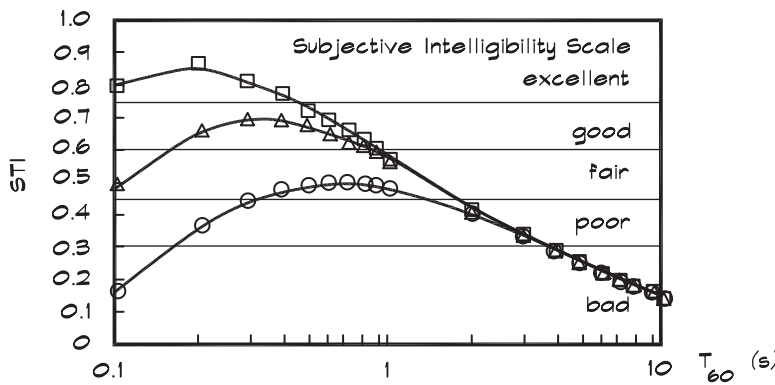
Measurements taken in a 300 sq m classroom for various differences between the background noise level, L_N and the long term average speech level at 1 m (65 dB), L_{splm} at 1000 Hz. The directivity, Q, is assumed to be 2.

□ $L_N - L_{splm} = -30$ dB

△ $L_N - L_{splm} = -20$ dB

○ $L_N - L_{splm} = -10$ dB

Signal-to-Noise Ratios (C_t and U_t)

In 1935 two researchers, F. Ainger and M. J. O. Strutt, reported on the property of the ear that combines early-reflected sounds with the direct sound so as to increase the apparent strength of the whole. They suggested an energy ratio formula to quantify the effects of background noise and room acoustics on intelligibility. They called this ratio *impression*, which they defined as

$$Q = \frac{E_d + E_e}{E_\ell + E_n} \tag{17.34}$$

where E_d = direct field energy (N m)
E_e = early part of the reflected energy (N m)
E_ℓ = late portion of the reflected energy (N m)
E_n = constant noise energy (N m)

They set the dividing line between early and late reflections at 1/16 second and set a lower limit of 1 for a satisfactory value of Q. If we write Eq. 17.34 in terms of energy densities we obtain a similar expression

$$Q = \frac{D_d + D_e}{D_\ell + D_n} \tag{17.35}$$

where D_d = direct field energy density (W s / m^3)
D_e = early part of the reflected energy density (W s / m^3)
D_ℓ = late part of the reflected energy density (W s / m^3)
D_n = constant noise energy density = $\dfrac{p^2}{\rho_0\, c_0^2}$ (W s / m^3)

Using this model and the impulse response from Eq. 17.25 we can calculate the value of the impression (Bistafa and Bradley, 2000)

$$Q = \frac{1 + (r_\ell/r)^2 - e^{-0.86/T_{60}}}{e^{-0.86/T_{60}} + 10^{\,0.1\,(L_n - L_r)}} \tag{17.36}$$

where L_n = steady background noise level (dB)
L_r = steady reverberant signal level (dB)

The metric is seldom encountered now but is interesting, not only for its historical significance, but also as an introduction to more recent versions of the same concept using different cutoff times.

In the 1950s, Thiele (1953) published one of the earliest attempts at relating early to total sound energy ratio to intelligibility, which he called the definition, D. He considered the useful energy to be the direct plus the reflected energy that arrives within 50 msec of the direct sound. The definition can be written (Bistafa and Bradley, 2000) as

$$D_{50} = \frac{1 + (r_\ell/r)^2 - e^{-0.69/T_{60}}}{1 + (r_\ell/r)^2} \tag{17.37}$$

Definition does not account for the contribution of the background noise to the detrimental energy. It represents another early attempt to quantify speech intelligibility in terms of room acoustics.

Bradley (1986) used variations of the Q metric in his study of speech intelligibility in classrooms. These included the useful-to-detrimental noise ratio

$$U_\tau = 10 \log \left[\frac{R_\tau}{(1 - R_\tau) + 10^{-0.1\,L_{SN}}} \right] \tag{17.38}$$

where R_τ is the ratio between the early and the total energy

$$R_\tau = E_e / (E_e + E_\ell) \tag{17.39}$$

and the early-to-late signal-to-noise ratio

$$C_\tau = 10 \log \left[\frac{R_\tau}{1 - R_\tau} \right] \tag{17.40}$$

which is obtained by setting the second term in the denominator of Eq. 17.38 equal to zero.

When these expressions are evaluated using the diffuse-field impulse response and a cutoff time of 50 msec we obtain

$$U_{50} = 10 \log \left[\frac{1 + (r_\ell/r)^2 - e^{-0.69/T_{60}}}{e^{-0.69/T_{60}} + 10^{0.1\,(L_n - L_r)}} \right] \tag{17.41}$$

and

$$C_{50} = 10 \log \left[\frac{1 + (r_\ell/r)^2 - e^{-0.69/T_{60}}}{e^{-0.69/T_{60}}} \right] \tag{17.42}$$

Bradley (1986) published intelligibility versus U_{80} values in his study of classrooms, which are given in Fig. 17.20. Bradley worked with several cutoff times: 35, 50, 80, and 95 msec. He found (1998) that the differences using cutoff times between 50 and 95 msec are not great, for example, $C_{80}(A) \cong C_{50}(A) + 2$. The results are plotted in Fig. 17.21.

Weighted Signal-to-Noise Ratios (C_t^α *and* U_t^α)

Early-to-late ratios were also the basis of work by Lochner and Berger (1964) in the Afrikaans language. These authors identified and separated the early sound energy, arriving at less than a certain time after the direct sound, from the later reflected sound. In their system the early arrivals are weighted and integrated over the time period and compared to the sound energy arriving after that time. They defined a useful-to-late energy ratio as

$$C_\tau^\alpha = 10 \log \left[\frac{\int_0^\tau \alpha(t)\, w(t)\, dt}{\int_\tau^\infty w(t)\, dt} \right] \tag{17.43}$$

where $\alpha(t)$ is the average fraction of the energy of an individual reflection that is integrated into the useful early energy sum. This weighting term depends on the amplitude of the

FIGURE 17.20   Speech Intelligibility vs U$_{80}$ Values (Bradley, 1986)
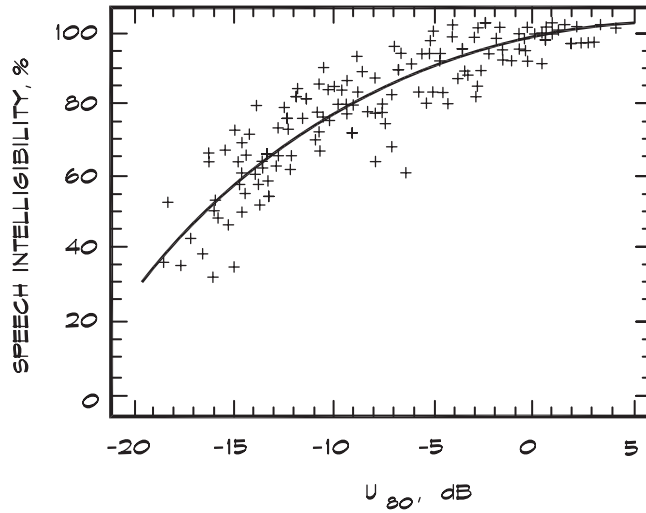
FIGURE 17.21   Measured C$_{50}$ vs C$_{95}$ values at 1 kHz (Bradley, 1986)
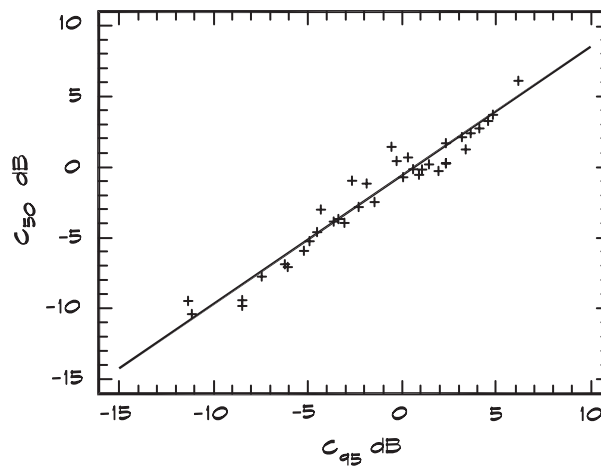
reflected energy, relative to the direct sound and the time of arrival. The $\alpha(t)$ term was included because the unweighted method proved highly sensitive to individual reflections arriving just before or just after the cutoff time. The weighting factor was set to 1 at a start time and to 0 at the finish time, and decreased linearly between them. Various algorithms have been used as a weighting function. Among them are

$$\alpha(t) = 1 \quad \text{for } 0 \leq t < t_1$$

$$\alpha(t) = \frac{t_2 - t}{t_2 - t_1} \quad \text{for } t_1 \leq t \leq t_2 \tag{17.44}$$

$$\alpha(t) = 0 \quad \text{for } t > t_2$$

FIGURE 17.22 **Measured Speech Intelligibility vs A-Weighted Signal-to Noise-Ratio (Bradley, 1986)**
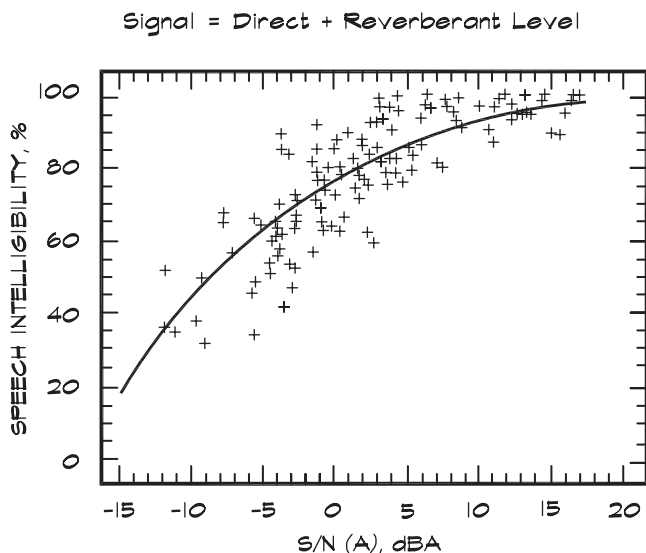
with $t_1 = 0.035$ s and $t_2 = 0.095$ s. For a diffuse field and a 95 ms cutoff time, Lochner and Burger's useful-to-detrimental ratio is

$$U^{\alpha}_{95} = 10 \, \log \left[\frac{1 + (r_{\ell}/r)^2 + 1.21 \, T_{60} \, (e^{-1.31/T_{60}} - e^{-0.48/T_{60}})}{e^{-1.31/T_{60}} + 10^{0.1 \, (L_n - L_r)}} \right] \qquad (17.45)$$

The useful-to-late ratio C^{α}_{95} can be obtained by setting the noise term in the denominator equal to zero.

A-Weighted Signal-to-Noise Ratio

Bradley (1986) also worked with a simple metric, namely the A-weighted steady-average-speech level (55 dBA at 1 m for a normal voice and 63 dBA for a raised voice in this study), based on anechoic measurements of speech. He calculated the direct plus reverberant-field level and used it to test intelligibility for various background-noise levels. The results were very similar to those found with more complicated metrics, and its ease of use makes it attractive. Figure 17.22 shows his results in terms of a signal-to-noise ratio. It is interesting to note that these data support his assertion that signal-to-noise ratios significantly less than 15 dB yield very satisfactory intelligibility.

Comparison of Speech-Intelligibility Metrics

Bradley (1986), in his comparison of several methods of predicting speech intelligibility in rooms, examined metrics in three categories: AL_{cons}, STI, and the various signal-to-noise ratios. His studies were carried out using a Fairbanks rhyme test, which gives a result similar to that obtained with nonsense syllables. He found that there was close agreement between STI and the early-to-late ratios, but poor correlation between AL_{cons} and the other metrics. Jacobs (1985), using loudspeakers of differing directivities, found a similar result with AL_{cons}, yielding errors on the order of 20% in intelligibility. In his work the use of

STI lead to a slight (5%) underprediction of intelligibility, whereas a weighted signal-to-noise ratio, similar to Eq. 17.45, yielded an overprediction of the same order of magnitude. Bistafa and Bradley (2000) found a linear relationship between STI and U_{50}

$$U_{50} \cong 31 \, STI - 16 \qquad (17.46)$$

indicating that these metrics are essentially equivalent. A similar relation was deduced for Lochner and Burger's signal-to-noise ratio

$$U_{50}^{\alpha} \cong 1.25 \, U_{50} + 3.4 \qquad (17.47)$$

The research cited in this section was done with single, as opposed to distributed, loudspeakers and is best utilized in analyzing rooms with unamplified talkers or single-source reinforcement systems. The complications introduced by multiple loudspeakers with different directivity characteristics and delay times are not addressed here.

17.3   DESIGN OF ROOMS FOR SPEECH INTELLIGIBILITY

The interior design of a given room depends on the use, interior décor, and the acoustical goals for the space. In many rooms such as restaurants or private homes, the noise may be generated by conversations other than those of interest. In these cases the addition of absorbing materials can control reverberant noise but must be balanced against the interior design goals. Acousticians must be sensitive to the appearance of their work and architects must accept the fact that design is not only visual.

The Cocktail Party Effect

The cocktail party effect* is an interesting and amusing exercise in the buildup of a sound field in a room. Let us assume that we are giving a party in a relatively reverberant room and invite a number of people to come. Let us say that the room has a carpeted floor, hard walls and ceiling, and some furniture, which contribute 93 metric (1000 sq ft) sabins of absorption. Before the guests arrive two hosts are having a conversation in the living room. They are polite so that only one speaks at a time with a sound power level of 70 dB. For purposes of this calculation let us assume that the direct sound, which is transmitted between the talker (with $Q = 2$) and the listener, is the signal, and the reverberant sound reflected from the surfaces of the room is the noise. Clearly some of the reflected sound contributes to intelligibility but we are going to ignore that for this simple analysis. Using Fig. 17.23, let us say that for barely adequate (60%) intelligibility, we need a signal-to-noise ratio of at least -6 dB to understand sentences.

The reverberant field level in our living room is

$$L_p \cong L_w + 10 \, \log \, (4 \, / \, R) \qquad (17.48)$$

so

$$L_p = 70 + 10 \, \log \, (4 \, / \, 93) = 56.3 \, dB \qquad (17.49)$$

---

*Cocktail party effect is also used to describe our ability to understand an individual talker in the presence of a noisy combination of other conversations and background noise.

FIGURE 17.23 **Percent of Words and Sentences Correctly Identified in the Presence of Background Noise (Kinsler et al., 1982)**
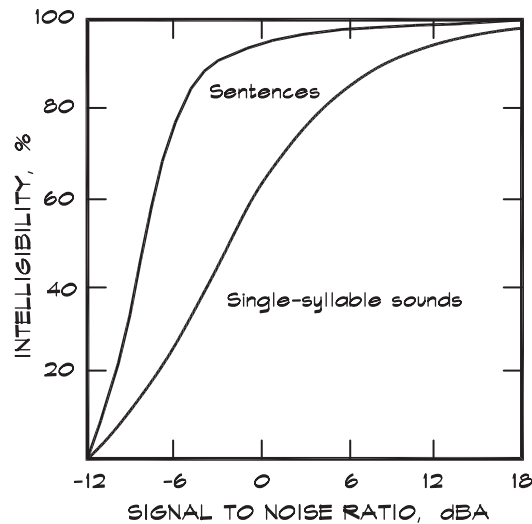
This means that speech can be understood at a direct field level of 50.3 dB. Assuming the background noise due to other sources is low, the two people can converse comfortably at a separation distance of 3.9 m (13 ft).

Our first pair of guests arrives and the two groups begin talking, only now two people, one from each group, are talking simultaneously. The reverberant level increases by 3 dB, but the direct-field remains the same, so the minimum conversation distance drops to 2.7 m (9 ft). When two more couples arrive and pair off, the comprehension distance drops to 1.9 m (6 ft). When four more arrive the distance drops to 1.3 m (4 ft), and so forth.

In practice what happens is that people may choose not just to move closer, but also to talk louder. This raises the background noise and forces everyone to elevate their voices so at the end of the evening they all go home with sore throats—a corollary of the cocktail party effect. The point of this example is that more absorption in the room allows a higher signal-to-noise ratio and more people can talk comfortably before the increasing-volume spiral begins to kick in.

Restaurant Design

Restaurant design includes a similar problem in speech intelligibility since we want patrons to be able to talk comfortably across a table, but we do not want their conversations overheard by someone at a neighboring table. Consequently we need sufficient absorption that we do not have to raise our voices to be understood at a distance of 1 to 2 m (4 to 6 ft), but we want masking at a distance of, say, 3 m (10 ft) and beyond.

Let us imagine a restaurant that has a hard ceiling and walls and some absorption in the furniture for a total of around 20 metric sabins. A normal conversational level ($L_w = 70$ dB) will produce a direct field of 60 dB at 1.2 m (4 ft). With 20 metric sabins, our self-generated reverberant-field noise is 63 dB, our signal-to-noise ratio is -3 dB, and we achieve 75% intelligibility. If there are 20 tables in the room, with one person talking at each table, the reverberant noise level rises to 76 dB, a very uncomfortable level, and we can no longer have an intelligible conversation. This simple calculation tells us something useful—in hard-surfaced restaurants it is very difficult to have a normal conversation across a table.

People who enjoy talking to their dinner companions do not come back to these establishments and the owners ultimately suffer. Yet for some unfathomable reason countless restaurants are designed in this way.

We treat the problem by adding absorption. For example, assume that we cover the ceiling with an absorbent material. If it has an absorption coefficient of 0.9, this adds 170 metric sabins to the 13.7×13.7 m (45×45 ft) room. The 20 table reverberant noise level drops to 66 dB, which is low enough to carry on a cross-table conversation. At an adjacent table 3 m (10 ft) away, the direct field level from our conversation is about 54 dB and so it is not understandable. Off-axis directivity losses also may provide some additional isolation.

What we see from these relatively simple calculations is that unless we add absorptive treatment with an area approximately equal to the restaurant ceiling area, when the room is full of patrons, conversation across a table will be difficult and the background noise level will be uncomfortable. Second, even when we add this amount of absorption, the environment is not so dead that conversations are easily overheard at a neighboring table. More formally, these two conditions can be stated as follows.

$$L_p(\text{signal}) = L_w + 10 \log\left[\frac{Q}{4\pi r^2}\right] \qquad (17.50)$$

and

$$L_p(\text{noise}) = L_w + 10 \log N + 10 \log\left[\frac{4}{N R_t}\right] \qquad (17.51)$$

where N is the number of simultaneous talkers (or tables) in the room and R_t is the absorptive area per table. The signal-to-noise ratio is the difference between these two equations

$$L_{SN} = 10 \log\left[\frac{Q}{4\pi r^2}\right] + 10 \log\left[\frac{R_t}{4}\right] \qquad (17.52)$$

To insure adequate communication for a cross-table distance equal to r_s we apply the condition that $L_{SN} > -6$ dB. This leads to the requirement that the amount of absorption per table in terms of the cross-table separation distance must be

$$R_t > 6.33\ r_s^2 \qquad (17.53)$$

To insure privacy between tables, we apply the condition that the signal-to-noise ratio $L_{SN} < -9$ dB. This leads to the requirement that the amount of absorption per table, in terms of the separation distance r_t between tables, be limited to

$$R_t < 3.16\ r_t^2 \qquad (17.54)$$

For a talker-to-listener distance of 1 m, our analysis suggests at least 6.3 or more square meters (68 sq ft) of absorption per table. If we treat the ceiling with a highly absorptive material, the minimum spacing between tables becomes about 2.5 m (8 ft), based on filling the room evenly. At that distance the maximum allowable absorption from Eq. 17.54 should be no more than 20 sq m (215 sq ft) per table. Normally we design based on Eq. 17.53 since the requirement in Eq. 17.54 is easily met.

Conference Rooms

Small conference rooms have become increasingly sophisticated primarily due to the audio-visual and computer interface requirements. Even with such systems in place face-to-face communication must still take place within a room, and the natural acoustical characteristics of the space are very important. Strong overhead reflections aid in cross-table communications so the ceiling above the table should be hard and flat. The area of reflective ceiling does not need to extend beyond the seating area. Outside this area the ceiling may be absorptive, diffuse, or recessed. In the central ceiling area acoustical diffusers are not particularly helpful. Above the conference table the ceiling should be low, preferably less than 3 m (10 ft) so the distance loss is minimized.

Most conference rooms are set up to have a table in the middle of the room with people seated around it. The shape of the conference table can help improve intelligibility. A lenticular shape allows people to see everyone seated at the table and also see plans and diagrams in the center. Horseshoe-shaped tables should be avoided, particularly if people are seated on both sides of the U, since they may face away from people on the other side.

Floors should be carpeted and absorption applied to the middle and upper portions of the walls in the form of cloth-wrapped panels, preferably with a tackable surface of 3 mm (1/8") dense fiberglass or cork between the cloth and the fiberglass. Reverberation times may be selected in accordance with the recommendations in Fig. 17.10.

Sound systems are often included in conference rooms if only to present recorded or transmitted material. Where there is a projection screen at one end of the room, loudspeakers should be located on either side. If there is also a speech-reinforcement system, loudspeakers are best located overhead with an electronic delay to maintain the correct impression of source direction. The loudspeaker system associated with the screen should not be used for speech reinforcement in order to minimize feedback.

Classrooms

The architectural design of a classroom begins with the seating layout, which is driven by the number of seats, code requirements, and the location of the audio-visual elements. Typical classrooms are relatively small, perhaps 25 feet wide by 30 feet deep, which will accommodate 30 to 40 students. Control of classroom noise, including exterior, mechanical, and reverberant, is of particular concern. For small classrooms, an NC 30 is an appropriate background level and noise from exterior sources such as traffic or aircraft should be limited to an L_{eq} of 35 dBA.

As a general rule reverberation times should be less than 0.8 seconds for good intelligibility. In his study of intelligibility in classrooms, Bradley maximized intelligibility as a function of reverberation time. The result appears in Fig. 17.19. He found that intelligibility was maximized at a reverberation time that depends on the signal-to-background-noise ratio in a range from 0.2 to 0.8 seconds. This requires a ceiling material of acoustical tile having an NRC of 0.8 or above for a ceiling height of between 9 and 12 feet. In small classrooms the ceiling is the only absorptive surface. When this is the case, the mid-frequency reverberation time can be estimated using the approximation

$$T_{60} \cong \frac{h_c}{20 \, \overline{\alpha}_{NRC}} \tag{17.55}$$

where h_c is the ceiling height in feet and $\overline{\alpha}_{NRC}$ is the NRC value of the ceiling material. For a 10-foot ceiling, an NRC of 1.0 produces a half-second reverberation time.

Similar recommendations have been memorialized in an ANSI standard (ANSI, S12.60-2002) which sets background noise levels for spaces of less than 20,000 sq ft (283 cu m) to 35 dBA. Reverberation times for classroom volumes less than 10,000 sq ft are < 0.6 sec and for rooms having between 10,000 and 20,000 sq ft (566 cu m) are < 0.7 sec.

Small Lecture Halls

In a small lecture hall the choice of room shape is between a fan and a rectilinear form with a range of floor plans between the two. Fan-shaped rooms bring the seats closer to the front whereas a rectilinear shape provides a more frontal view of the display areas. Background levels due to HVAC systems and exterior sources should be limited to no more than an NC 30 or an L_{eq} of 35 dBA. Carpeted aisles are helpful in controlling the footfall noise due to latecomers. Automatic door closures without latches help to muffle the sounds of entry doors.

As a room grows larger the direct field should be augmented with early reflections from hard surfaces. Overhead reflections are preferred since the human ear is easily fooled as to the source direction, when the image source is located above (or below) the actual source. Lateral reflections smear the perceived source direction particularly when the reflection is louder than the direct sound. This condition occurs when there is grazing attenuation due to the presence of an audience that results in a direct sound being weaker than the reflected sound. In the case of large conference rooms, small auditoria, lecture halls, and legitimate theaters, a relatively low hard ceiling is preferable to an absorbent one.

A stepped or sloped floor, along with a raised platform for the talker, aids in the useful reflections and reduces grazing attenuation. Absorptive panels should be applied to the rear and side walls of the room to control reverberation and lateral reflections. The ceiling above the podium and the side walls surrounding the podium should be slanted (a 1:12 slope is sufficient) to avoid flutter echo.

A floor plan of a typical small lecture hall of about 120 seats is shown in Fig. 17.24. This hall is typical of several designed by the author and combines the audio-visual program with the acoustical requirements of the space. Moveable writing boards can be incorporated into the front walls along with projection screens for slides or video. The side walls at the front of the room are canted to accommodate the screens and to reduce the flutter echo from the side walls on either side of the lecturer.

The ceiling is a series of flat-stepped elements, which provide beneficial early reflections. Flat ceiling elements are both more practical to build and better for intraclass discussions than more complicated ceiling shapes. The rear and side walls are treated with absorptive panels, which can be made tackable if classroom activities require the posting of student work.

The design of small lecture halls is increasingly influenced by the audio-visual requirements of the space. As room size increases the size of the projection screens must increase proportionately, and they tend to dominate the front surface of the room. A projection screen, which can be raised and lowered, is preferred to a fixed screen, since it discourages lecturers from writing on it, although surfaces are available that can be used for both functions.

Large Lecture Halls

In large lecture halls the design techniques are similar in principle to that of small halls. The distance from the source to the receiver should be short, which requires some widening of the seating area. Unsupported speech is not intelligible more than 30 to 40 ft (9 to 12 m)

FIGURE 17.24   Design of a Small Lecture Hall
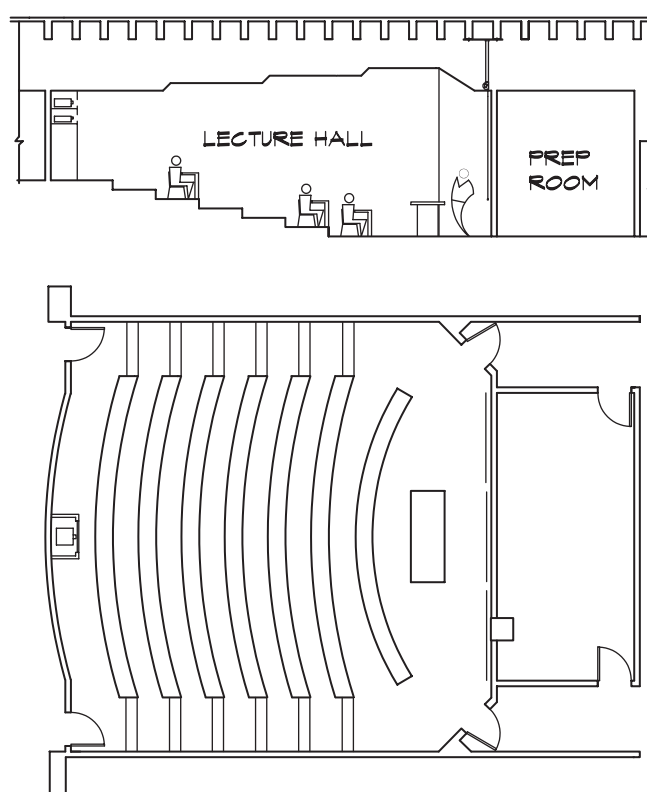
away unless considerable care is taken with the design. A fan-shaped configuration brings the audience close to the platform; however, the seating layout should be contained within a 125° maximum included angle if there is a projection screen on the front wall. The first-reflected-sound path should also be kept short. To that end the ceiling should be hard and relatively low so that the room volume (Doelle, 1972) is between 80 and 150 cu ft/seat (2.3 to 4.3 cu m/seat). Background-noise levels should be limited to no more than an NC 25 and exterior noise to an L_{eq} of 30 dBA, somewhat lower than the requirements for small halls.

A sound system should be included as part of the design and the loudspeakers should be integrated into the appearance of the room. The reverberation times can be selected from Fig. 17.10. If opera chairs are used, they should have padded seats and backs to reduce the variation in reverberation between the empty and full conditions. Reflections from the lower side walls can be helpful; however, reflections from the rear wall should be controlled with absorption.

An example of a successful lecture hall design at the Applied (Acoustics) Research Laboratory at Penn State University is shown in Fig. 17.25. This auditorium seats about 500 people and has extensive audio-visual capability. Although the room has a sound-reinforcement system, amplification is unnecessary, due to the drywall ceiling, but convenient for most lecturers. Loudspeakers are located behind a curved perforated metal screen as well as in the ceiling in the rear half of the seating area. The lower portion of the screen is backed with clear plastic to provide an overhead reflecting surface, which has the same appearance as the absorptive portion. Even though a flat ceiling yields good results when

FIGURE 17.25 Design of a Large Lecture Hall
Penn State Applied Research Laboratory (Acoustical Engineer, Marshall Long Acoustics) (Architect, The King Lindquist Partnership)

SECTION

PLAN
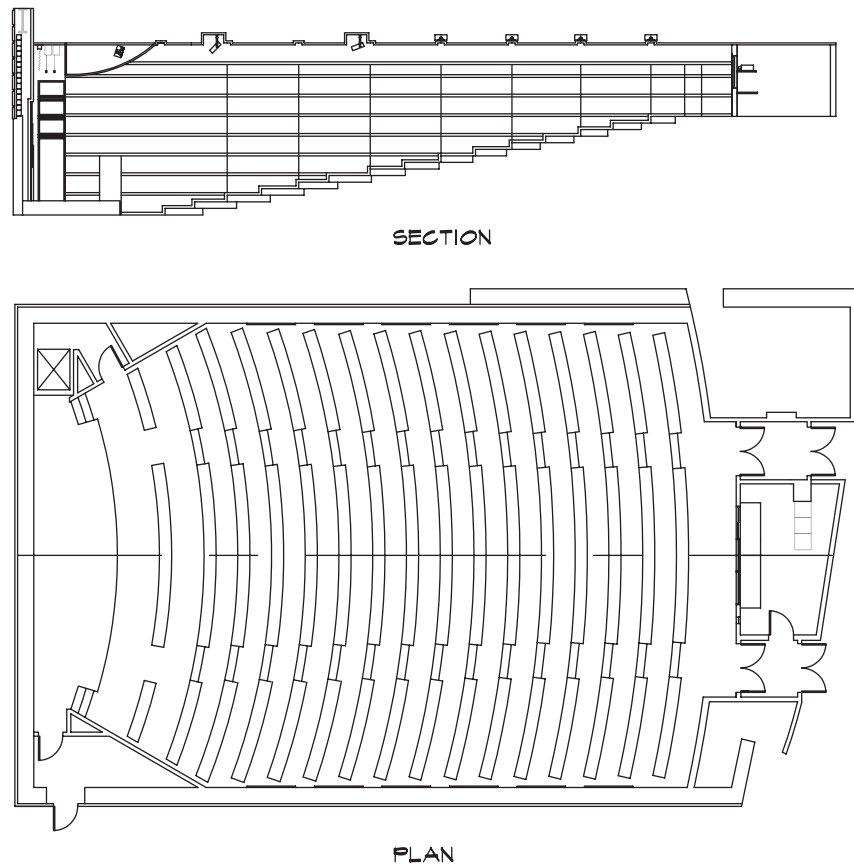
the seating is raked, a shaped ceiling is necessary in a room having a flat or shallow-angled floor. Lecture halls seating more than about 100 people should be designed with a sound reinforcement system and a hall having any type of projection or audio playback system needs to have sound reinforcement. In council chambers or courtrooms there may be a need for a recording system or for simultaneous translations. In these cases all talkers are miked and both loudspeakers and headphone feeds should be provided. The specifics of sound reinforcement design are discussed in Chapt. 18.

17.4   MOTION PICTURE THEATERS

Although motion pictures include speech and music, the design of movie theaters is driven by speech intelligibility considerations rather than by the need to provide reverberant support for unamplified music. The theater itself is an important link in the production chain since a film, as a mass-produced entertainment medium, is most effective if it is viewed in a controlled environment that yields the same auditory experience for every patron. Not all movie theaters are the same but they should be designed to achieve a consistent listening environment.

FIGURE 17.26 SMPTE Standard Reverberation Time vs Room Volume (SMPTE, 1989)
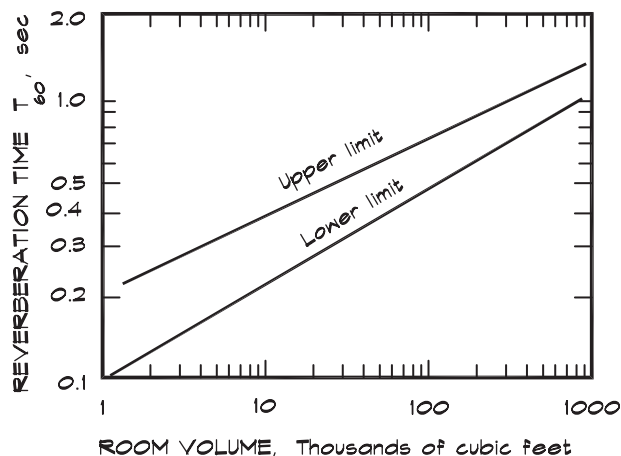
Reverberation Times

By and large, motion picture theaters are built to be acoustically dead, with absorptive material on virtually every surface except the floor, which must be washable. Ceilings are dark-colored acoustical tile and the side and rear walls are covered with minimum 1" thick cloth wrapped fiberglass panels or heavy pleated drapes. Curved rear walls should include 6" of fiberglass batt behind the panels to reduce focusing.

Recommended standards have been issued by SMPTE (Society of Motion Picture and Television Engineers) and by THX, a private company founded by George Lucas, on the preferred background noise levels, reverberation times, and sound system equalization curves. Motion picture theaters are designed to an NC 30 background-noise level and to the reverberation times shown in Fig. 17.26. THX recommends a minimum transmission loss rating (STC 65) for walls separating theaters, as well as a list of approved sound system components.

18 SOUND REINFORCEMENT SYSTEMS

Electronic sound reinforcement systems are a critical part of achieving good speech intelligibility in large rooms. When the room volume is greater than about 15,000 cu ft (425 cu m), or the seating capacity more than 100 to 150 seats, or the talker-to-listener distance greater than about 40 feet (12 m), a sound reinforcement system is necessary, even if there are no auxiliary inputs. There are many uses of electroacoustic systems beyond speech reinforcement including playback of prerecorded or transmitted material, distribution to the hearing disabled, simultaneous translation, sound effects including surround sound and bass effects in motion picture theaters, artificial reverberation, synthesized music such as electronic organs, paging, intercom, and recording. At lower seating capacities, playback requirements alone may dictate the need for a system. In this chapter, however, we will concentrate primarily on the speech reinforcement function.

The guidelines for a well-designed sound system are similar to those for general speech intelligibility:

1. There must be loudness appropriate for the program material.

2. The coverage must be uniform both spatially and over the frequency range of interest.

3. There must be adequate gain before the onset of unstable feedback.

4. The illusion that the sound is originating from the original source location should be preserved.

5. The sound system must not cause or contribute to acoustical defects such as echo, comb filtering, or long delayed reflections.

6. The sound system design should be sensitive to the architecture.

18.1 LOUDSPEAKER SYSTEMS

Loudspeaker Types

Loudspeakers in sound reinforcement systems are designed with different goals than those used in the home. Reinforcement loudspeakers emphasize efficiency, directivity control,

power handling capacity, and durability. By contrast, home listening systems stress wide-coverage angles, stereo imaging, clarity, and fidelity of reproduction. For critical listening, home systems, particularly the better quality systems, are much more accurate and much better sounding than speech reinforcement systems.

Reinforcement loudspeakers are either cones or horns or some combination of the two. Cone loudspeakers, which were discussed in Chapt. 6, are lightweight paper, metal, or composite diaphragms attached to a coil of wire immersed in a permanent magnetic field. For cone loudspeakers the greater the cone diameter and excursion, the higher the maximum sound pressure level. Large cone diameters, however, yield narrow coverage angles. Most cone loudspeakers, which span the speech frequency range and have a wide dispersion pattern, are between 5" and 8" in diameter. Large cones (having diameters greater than 10") are not used as full-range devices, but are employed in combination with a high-frequency transducer, utilizing a crossover to divide the signal at a convenient point. Coaxial loudspeakers, which include a high-frequency radiator positioned along the center axis, allow a large cone to be used for the low frequencies while maintaining the advantage of a small high-frequency transducer in a collinear position.

A horn loudspeaker, also discussed in Chapt. 6, consists of a moving coil driver coupled to a (2–4") metal or carbon-fiber diaphragm, which is coupled through a phasing plug, to the throat (usually 1", 1.5", or 2" diameter) of an expanding horn. Horns are more efficient and have a higher directivity than cones. The size of the horn's mouth opening controls the low-frequency limit of directional control. This is the most critical parameter in sound system design since it determines the visual impact as well as the degree of feedback control, and thus the gain before feedback, for a given system.

Sometimes horn and cone loudspeakers are combined into a single enclosure as in Fig. 18.1 or arranged as separate components as in Fig. 18.2. The scarcity of choices makes the commercial design problem simple when the choices are appropriate to the application but difficult when the choices are not. When the choice is between a cone and a horn for a given application, at the risk of over simplification, cone loudspeakers sound better and horn loudspeakers are louder and provide more directional control. Horns can be made to sound better by carefully matching the driver to the horn and by exercising care in the shape of the horn. Cones can be made somewhat more efficient by grouping them and can be made more directional by using line arrays over a limited bandwidth. Obviously the quality of the sound produced by an individual transducer affects the overall quality of the sound system. Cones sound better than horns since with horns there is a complex interaction between the driver and the horn, which colors the sound. This is particularly true of the small-mouth horns.

Manufacturers offer two- and three-way systems in enclosures, with the advantage of being able to match and align components so that the tonal balance is good. The disadvantage is that, due to size constraints, the directional control provided by a prepackaged box is not as good as with a large-format horn. Cabinets are available, which are trapezoidal in plan so that they can be arranged along a radius of curvature as shown in Fig. 18.3. This distributes the high-frequency components, which do not overlap, but creates a mid-frequency line array that narrows the beam width in the plane of the curve.

Loudness

Manufacturers publish data on the sensitivity of their products, along with their maximum power handling capacity and sometimes the maximum level at 1 meter from the face of

FIGURE 18.1 A Cabinet Loudspeaker
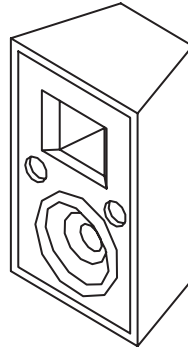
FIGURE 18.2 A Component Loudspeaker System
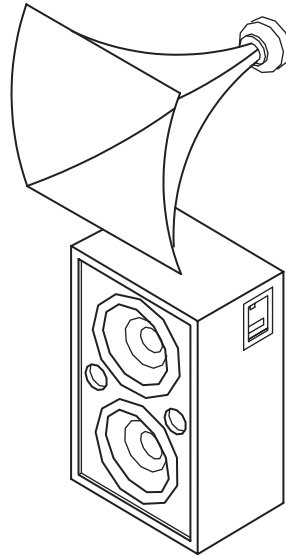
FIGURE 18.3 A Clustered Cabinet Loudspeaker System
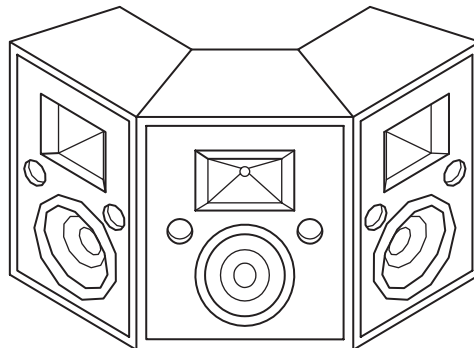
TABLE **18.1**   **Maximum Sound Pressure Levels for Various Uses**

Type of Use	Maximum Level (dBA)
Classroom	**80**
Lecture Hall	**85**
Synagogue	**85**
Home Theater	**90**
Legitimate Theater	**90**
Church, Traditional	**90**
Movie Theater	**100**
Church, Fundamentalist	**100**
Sports Arena	**105**
Rock Concert	**110–115**

the device. These data can be used to determine the highest direct-field level achievable. It is important to establish the maximum sound pressure level required in a given venue and Table 18.1 can be helpful in this regard.

The maximum sound pressure level required by use determines the power handling capacity of the sound system and the corresponding size of the amplification system. It should be remembered that overdesign is expensive but underdesign can be fatal, particularly in live entertainment venues. Thus amplifier headroom based on the peak-to-average ratio should be included.

Bandwidth

Although less critical than loudness, bandwidth is also an important concern particularly if high levels of bass are required. For speech reinforcement systems the bandwidth ranges from about 100 Hz to 4 k Hz. For paging it might require only 200 Hz to 3000 Hz. The bandwidth of the telephone system extends from 300 Hz to 3500 Hz. A refined audiophile might demand the full range of human hearing from 20 Hz to 20 k Hz from his stereo system. As a general guideline some apply the so-called "rule of 400,000," which states that the product of the upper- and lower-frequency limits of an audio system should be equal to 400,000. This is not a physical law but more of an audio urban legend.

When assembling a multiway loudspeaker system using separate components, the bandwidth of each driver needs to be matched to its adjacent unit. Table 18.2 gives the bandwidth of the most frequently encountered loudspeakers without tuned enclosures. A carefully designed enclosure can extend the low-frequency limit by about an octave.

In full range two-way systems a dual 15" midrange/bass cabinet can be matched with a 1.5" to 2" compression driver and horn combination. For speech systems a 1" driver and horn with a dual 12" cone midrange yields better high-frequency performance. A three-way system might consist of two 15" bass loudspeakers, one or more 10" midrange cone drivers, and a high-frequency 1" compression driver and horn combination. Midrange devices can also be coupled to horns to achieve both directional control and increased efficiency.

TABLE 18.2   Bandwidth of Various Loudspeakers

Type of Loudspeaker	Bandwidth (Hz)
1" Compression Driver	1200 – 16 k
1.5" Compression Driver	1000 – 12 k
2" Compression Driver	850 – 10 k
1" Dome Tweeter	2000 – 20 k
3" Cone Driver	700 – 10 k
4" Cone Driver	500 – 7 k
5" Cone Driver	350 – 6 k
8" Cone Driver	250 – 5 k
10" Cone Driver	200 – 4k
12" Cone Driver	150 – 2k
15" Cone Driver	80 – 1250
18" Cone Driver	70 – 1000

Low-Frequency Loudspeakers

When separate subwoofers are used as part of a sound system, the loudspeakers are most efficient if they are coupled to one or more reflecting surfaces no more than one-sixth of a wavelength away. Coupling can increase the efficiency and overall output. A bass loudspeaker is most efficient when placed on a solid floor near a wall or in the corner of a room. From a corner location the loudspeaker can excite all room modes since they all have pressure maxima at the corner.

If low-frequency drivers are located away from a wall and grouped together in a cluster, additional support for the bass cabinets can be obtained by constructing a baffle wall around them. To be effective the wall must be large enough to reflect all frequencies of interest and heavy enough to minimize diaphragmatic absorption.

It is particularly important in the construction of baffle walls to seal any openings between the wall and the loudspeaker cabinets. An opening around the face of the loudspeaker, along with the cavity behind, forms a Helmholtz resonator, which will selectively absorb sound at its resonant frequency. Thus if the baffle is not properly sealed, it can do more harm than good by creating notch filters in the frequency response.

Loudspeaker Systems

A range of reinforcement systems is shown in Fig. 18.4 and includes single and multiple clusters, overhead or column-mounted distributed loudspeakers, and pewback systems. In some cases a combination of clusters, point-source and distributed loudspeakers, can be used. The choice is strongly influenced by the architecture of the space. The main design considerations include adequate signal-to-noise, maintenance of the correct image, sufficient gain before feedback, and architectural sensitivity.

Distributed Loudspeaker Systems

A distributed loudspeaker system is one in which the loudspeakers are located more or less evenly throughout the space, most often in the ceiling. The direct-field coverage can be

FIGURE 18.4 Types of Sound Systems (Klepper, 1999)

Cluster

Pewback Distributed System

Split Cluster

Distributed Horn System

Distributed System

Distributed Column Loudspeakers

Cluster with a Delayed Cluster

Cluster with Distributed Fill
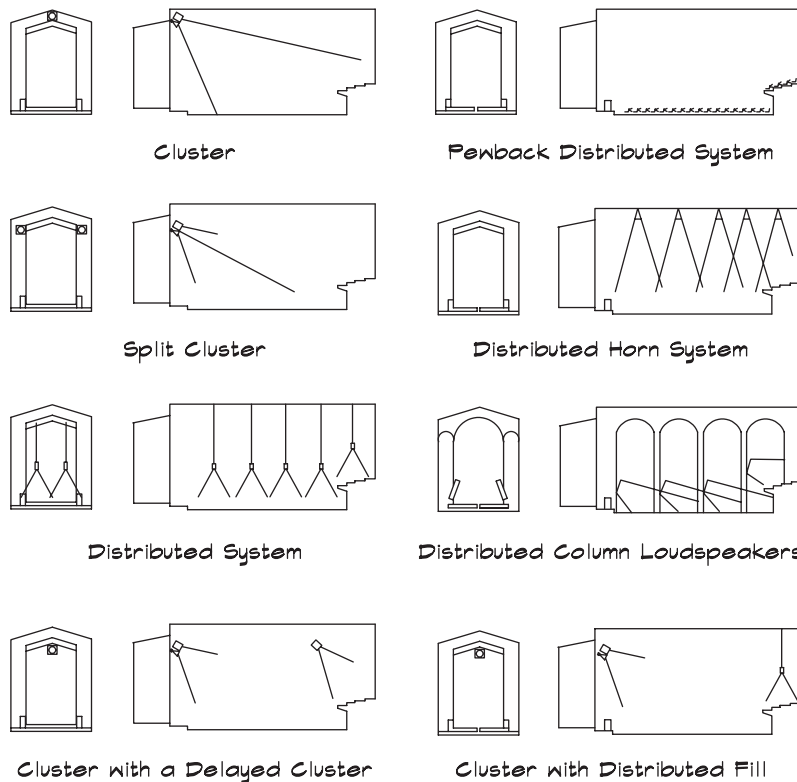
calculated; usually, for cone loudspeakers, a spacing equal to the ceiling height yields a variation of less than one dB for seated listeners. Distributed ceiling systems with cone loudspeakers can be used for ceiling heights of up to about 25 feet (7.6 m), beyond which the direct-to-reverberant ratio begins to suffer. In reverberant spaces with high ceilings, a system utilizing enclosed loudspeakers suspended in a horizontal plane can be employed, although these can be highly visible. Sometimes loudspeakers can be incorporated into light fixtures to improve their appearance, but this limits the choice to relatively small transducers. In a reverberant space such as a large airport terminal, if the system requires only a limited bandwidth, highly directional horns can be used in a distributed grid at a greater source height. In ceilings below 15 feet (4.6 m) in height, small diameter loudspeakers are preferred. A receiver standing beneath a particular loudspeaker receives the high-frequency information from the nearest source and low-frequency information from several sources. Thus even though a 5-inch (13 cm) loudspeaker may not have particularly impressive low-frequency performance, when combined with the others, it produces quite an acceptable bass output. As the ceiling height increases, the number of loudspeakers can be reduced and the aggregate contribution to the bass drops. Therefore larger transducers, having better bass response, should be used in high ceiling areas.

Distributed loudspeakers include individual transformers that increase their electrical impedance, so that several can be driven in parallel by the same amplifier. This configuration sometimes is referred to as a 70-volt or constant-voltage system, not because the impressed voltage is necessarily 70 volts, but as a shorthand. If a 70 volt (rms) signal is applied to the

input of a transformer, the rated wattage associated with each transformer tap is delivered to the loudspeaker. A constant-voltage amplifier can drive groups of loudspeakers, but they should be the same type and have the same equalization and delay. Their combined power requirements should be less than the output capacity of the amplifier.

Ceiling-mounted distributed loudspeakers can be used with or without an electronic delay system. If a delay is used, the time-base-zero source must be sufficiently loud to provide a clear directional cue to the first delay zone. Subsequent delay zones can rely in part on the zones preceding them. In small rooms the human voice is enough to provide the initial cue, but in large rooms localizing loudspeakers are required to supplement an unamplified source.

The use of electronic delays in rooms with high ceilings is a complicated problem due to the variation in delay time over the audience area. As ceiling heights increase the delay times within the area of coverage of the loudspeaker can vary enough to result in a different perceived source direction. Hence it is preferable to use delayed overhead loudspeakers in ceilings less than 20 feet (6 m) high.

Single Clusters

A loudspeaker cluster, just as the name implies, is a group of one or more loudspeakers located above the center of focus. A central cluster is one of the most effective design solutions for covering large spaces. It can deliver considerable level to the audience, while maintaining the proper relationship between the sound system and the apparent source. In a theater or auditorium this is the area above the proscenium arch. In an arena it can be the center of the room for sports events or at the end when it is used as a performance venue.

In large rooms it is difficult to design a single cluster that will provide even coverage to the whole room over the entire frequency range. In a narrow rectangular room with the focus of interest in the center of the short side, a single cluster can be successful. If the room is relatively wide, a distributed cluster is required to obtain even coverage. In a fan-shaped theater, a convex central cluster in the horizontal plane can be used. This preserves the image of sound coming from the center of the stage, even when the listener is off axis, and maintains time coincidence. The central group can be augmented with delayed clusters or distributed loudspeakers to cover hard-to-reach areas such as seats located under a balcony.

Multiple Clusters

When a single cluster is insufficient to adequately cover a space, a distributed or multiple cluster system can be used. In a wide room, loudspeakers are positioned across the front above the stage. The advantage of this type of design is that it provides excellent intelligibility and very even coverage. The disadvantage is that the apparent source is spread across the front of the room. In a long narrow room a second set of clusters located in the ceiling is sometimes necessary to cover the rear. In this type of design the second cluster must be located far enough in front of the area of coverage that it does not shift the image overhead.

If the space does not lend itself to the installation of a central cluster, other locations must be found. Loudspeakers on either side of the stage are visually benign and can yield even coverage; however, with this solution the sound image snaps to whichever side of the center aisle one is sitting on. When the talker is on the opposite side the effect is disconcerting. This may be a small price to pay for intelligibility, but it is still a design element worth consideration.

Cross-fire solutions, where one loudspeaker aims across the sound field of another, can be used as long as at the coverage overlap points, their relative levels and time delays are well matched. Cross-firing clusters can be used to preserve the source image, where there is no convenient central location, although feedback and delay times are sometimes a problem.

Other Configurations

In long narrow spaces such as cruciform-shaped churches, it is difficult to cover the entire space from the front. Supporting loudspeakers located along the sides are useful for augmenting the areas that are hard to cover. One or more small sources, built into steps or the front of the stage, should be used to assist in pulling the image back into the center.

In some churches loudspeakers are installed on the back of each pew with low-frequency augmentation under the pews. When properly designed this type of installation can provide excellent intelligibility and imaging; due to the size limitations pewback systems are limited to speech reinforcement and are not particularly successful for music.

18.2   SOUND SYSTEM DESIGN

The actual process of designing a sound system is highly iterative. It begins with an acoustical evaluation of the space, including a calculation of the reverberation times in each frequency band. The desired maximum direct-field sound pressure level should be known as well as the frequency range, type of program, location of microphones, and the preferred appearance. Based on these factors an initial choice of a system type is made. The types of reinforcement systems fall into the general categories outlined in Fig. 18.4.

The choice of loudspeaker system is based on the goal of achieving speech intelligibility through a high direct-to-reverberant ratio at the listener. This can be done in several ways: 1) by moving the sound source close to the receiver, 2) by using a loudspeaker with a high directivity, 3) by adding absorption to the space, or 4) by employing various combinations of all three.

In highly-reverberant spaces, where the signal-to-noise ratio cannot be increased by adding absorption, intelligibility can only be controlled by increasing the directivity of the loudspeakers or by decreasing the distance between the source and the receiver. This assumes that time delays and individual reflections are not a factor, which may not always be the case. The choices can be quickly narrowed to directional horns as part of one or more clusters or a distributed system. In absorptive spaces there is a greater variety of choices since the individual loudspeakers can be farther from the receiver and less directional. In rooms with low flat ceilings a distributed system is the usual selection. In long narrow rooms such as churches with high ceilings a side fill system can be used. In proscenium theaters central clusters are preferred. The system choice is largely driven by the architecture.

The second major choice is whether there will be a house mixer and where it will be located. In small conference rooms and meeting rooms an unattended automatic mixer is sufficient. As the range of program material and the number of inputs grow larger, a manual mixer becomes increasingly important. In venues such as high schools where security is a concern the mixer can be positioned in a technical booth at the rear of the auditorium with a large operable window. In legitimate theaters and concert venues where there is control over access to the facility and where the auditory experience is of the highest concern, a house mixing location in the seating area is very important. Locations may vary, however a position at the front of the balcony has many advantages including unobstructed sight lines

TABLE 18.3   Direct-to-Reverberant Levels for Speech Intelligibility in Rooms

Direct-to-Reverberant Level (dB)	Intelligibility
> –3	Excellent
–3 to –6	Very Good
–6 to –9	Good
–9 to –12	Fair
–12 to –15	Poor
< –15	Very Poor

when the audience is standing. Where there is only orchestra seating, a position in the rear of the seating area allows the mixer to stand or sit on a drafting chair to obtain a clear view of the stage.

Coverage

Once an approach has been selected, a calculation is undertaken to determine the direct sound pressure level throughout the room. Commercial computer programs are available to do these calculations or programs can be written. The design process tends to be iterative—moving loudspeakers about and determining the effect of different combinations. In a good design the predicted direct-field level should have a standard deviation of less than 2 dB in the 500 to 2k Hz octave bands throughout the seating area.

When clusters are used, the higher the elevation of the loudspeakers, the smoother the coverage but the lower the signal-to-noise ratio. For large horns, clusters should be higher than 20 feet (6 m) but lower than about 35 feet (10.6 m) above the receiver plane to achieve even coverage. For distributed ceiling systems using cone loudspeakers, the maximum practical height is around 20 to 25 feet (6 to 7.6 m). Above that height it is better to use clusters or cabinets. Cabinet systems can be very successful if there is sufficient pattern control and minimal overlap. As a general rule, the fewest number of loudspeakers possible should cover a given receiver and arrival times should be controlled so that there is no blurring or directional confusion.

Intelligibility

Once even coverage has been achieved, the next step is to insure adequate intelligibility. The algorithms discussed in Chapt. 17 were all based on single-source tests. We have excellent techniques and well-documented results under these conditions. We have much less data on speech intelligibility in rooms having multiple loudspeakers of different types and volume settings. In part this is due to the number of variables involved.

A method used by the author for many years is to calculate a signal-to-noise ratio, where the signal is the direct-field sound pressure level from all loudspeakers, combined on an energy basis, and the noise is the reverberant-field sound pressure level. The resulting signal-to-noise ratio is compared to the table shown in Table 18.3 to determine the intelligibility.

A direct-to-reverberant ratio of 0 dB is almost never achieved indoors and even a ratio greater than –3 dB is rare. Values between –3 and –6 yield very satisfactory intelligibility. Normally it is sufficient to design a room for good intelligibility and a small number of fair

FIGURE 18.5 Alcons vs Direct-to-Reverberant Ratio (JBL, 2000)
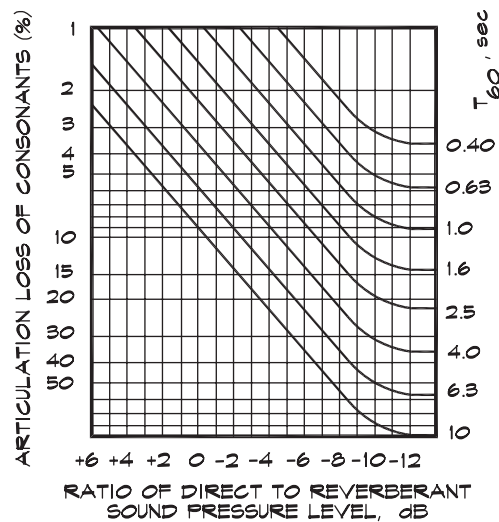
seats, particularly at the sides and rear, are tolerable. The transition from fair to poor agrees well with Davis' (1969) limiting distance of 4 D_c for adequate intelligibility.

A chart such as that given in Table 18.3 can be very useful even though it is relatively simple. This method is similar to the useful-to-late signal-to-noise ratios used by Bradley, but uses the limiting integration time of zero. It matches up well with Fig. 17.23. A more detailed analysis would take into account early reflections from nearby surfaces and possibly a factor for the reverberation time similar to the methodologies discussed previously. In most sound system designs there is a concerted effort to point the loudspeakers at the audience and to keep reflections off of the walls and ceilings. Clearly not all the reverberant field is harmful to intelligibility, but this is accounted for in the table. As a receiver moves away from the source, and closer to side walls or other reflecting surfaces, it is more likely that the direct-field levels will be augmented by beneficial reflections and the signal-to-noise ratio will increase. Therefore receiver locations in these positions can be designed with the expectation of a bit more direct-field contribution.

Table 18.3 does not account for the noise due to other sources since sound systems can be turned up enough to overwhelm most background levels. Notable exceptions to this rule include sports stadia where crowd noise can exceed 100 dBA. The overall level must therefore be calculated separately.

Intelligibility metrics, which were not originally developed for multiple sources, have been adapted to sound system calculations. JBL (2000) issued a technical note containing equations and a graph (Fig. 18.5) for the prediction of the articulation loss of consonants in terms of direct and reverberant-field energies. The note cites work by Peutz (1971).

$$\text{AL}_{\text{cons}} = 100(10^{-2(\text{A} + \text{BC} - \text{ABC})} + 0.15) \tag{18.1}$$

$$\text{A} = -0.32 \log \left(\frac{\text{E}_\text{R} + \text{E}_\text{N}}{10\,\text{E}_\text{D} + \text{E}_\text{R} + \text{E}_\text{N}} \right) \tag{18.2}$$

$$B = -0.32 \log \left(\frac{E_N}{10\, E_R + E_N} \right) \qquad (18.3)$$

$$C = -0.5 \log \left(\frac{T_{60}}{12} \right) \qquad (18.4)$$

where $E_R = 10^{0.1\, L_R} =$ reverberant - field contribution
$E_D = 10^{0.1\, L_D} =$ direct - field contribution
$E_N = 10^{0.1\, L_N} =$ noise - field contribution

Note that these terms are not simple energies but normalized intensity ratios, which are proportional to energy. This formulation is just the liveness (Eq. 17.12); that is, a constant times the reverberant-to-direct energy ratio times the reverberation time out to a direct-to-reverberant ratio of –10 dB, after which it reverts to a constant times the reverberation time. According to JBL, it is included in popular loudspeaker design programs.

When computations indicate that a loudspeaker design will not result in adequate intelligibility, the signal-to-noise ratio must be improved. There are only a few ways of doing this, namely to decrease the reverberant field or to increase the direct field. The reverberant field can be decreased by adding absorption to the room or by decreasing the sound power level of the loudspeakers. The direct field can be increased by using more directional loudspeakers or by moving the loudspeakers closer to the receiver. If highly directional loudspeakers are needed, the face area of these loudspeakers is large, and this will have architectural ramifications.

Amplifier Power Handling

The sensitivity, along with the power handling capacity, determines the maximum output level available from a loudspeaker. Horns, because they confine the energy to a narrow beam, have a higher sensitivity than cones. For example, a 1-inch driver attached to a 90° × 40° horn might have a sensitivity of 102 dB at 1000 Hz. Small cones tend to be more sensitive than large cones. An 8" cone driver has a sensitivity of about 96 dB, whereas for a 15" cone it might be 90 dB. The decreased sensitivity of large cones is offset by the fact that they will handle a higher input power.

In designing high-powered systems it is important to match the maximum output of each component so as not to waste power or overdesign in a given frequency range. If the maximum output level for a given cabinet size is the design goal, as is often the case in road systems, then component matching is very important. Amplifiers should be sized large enough to handle the maximum power that a transducer is likely to encounter. If the low-frequency input signal drives the amplifier into clipping, high-frequency components necessary to generate the clipped wave shape are produced. These components can be passed through a crossover and overdrive the high-frequency unit. Digital distortion can also generate some nasty waveforms, which are not necessarily stopped by digital limiters within the same processor system.

To obtain the amplifier power required for a given level at a receiver we use

$$10 \log J = L_p(r,\ 0,\ 0) - L_s + 20 \log r + 2\, \Delta\, L_\sigma + 10 \qquad (18.5)$$

where $L_p(r, 0, 0)$ = on - axis direct - field level produced by the loudspeaker
at the aim point (dB)

L_s = loudspeaker sensitivity (dB re 1 W at 1 m)

J = electrical power applied to the loudspeaker (W)

r = distance between the loudspeaker and the receiver (m)

ΔL_σ = standard deviation of the direct - field level (dB)

The factor of 10 at the end of Eq. 18.5 represents the peak-to-average ratio for uncompressed speech since amplifiers must have enough power to handle the peaks. The factor for the standard deviation accounts for the lower off-axis level.

Electrical Power Requirements

The electrical power required by the amplifier is based on its output power, efficiency, and duty cycle. The rated output power is available from the amplifier manufacturer in the published specifications. It will depend on the load impedance, with lower impedances drawing the greater power. The amplifier efficiency is the ratio of the electrical energy, powering the loudspeakers, to the amount of electrical power supplied to the amplifier. Most A-B amplifiers are about 65% efficient. Some, however, can be as high as 95% efficient depending on design. The duty cycle is a measure of the peak-to-average ratio of the input signal over time. Amplifiers must be sized to provide an output power high enough to handle the maximum signal level, but that power is not always required. The duty cycle for various types of source material is given in Table 18.4.

Using the duty cycle data, the electrical power requirements can be determined

$$J_e = \frac{N_c \, J \, \xi}{\eta} + \frac{N_c \, J_q}{2} \tag{18.6}$$

where J_e = electrical power from the AC main (W)

J = rated amplifier output power for one channel (W)

J_q = quiescent power for zero input voltage (W)

$\cong$ 90 W (typical value)

ξ = duty cycle

η = amplifier efficiency

N_c = number of amplifier channels (assuming 2 channels per amplifier)

TABLE 18.4   **Duty Cycles for Various Sources (Crown, 1995)**

Source Material	Duty Cycle
Pink Noise	50%
Highly Compressed Rock	40%
Rock Music	30%
Background Music	20%
Continuous Speech	10%
Infrequent Short Duration Paging	1%

To convert the power draw into current,

$$I_e = \frac{J_e}{V_e \, f} \tag{18.7}$$

where I_e = electrical current from the AC main (A)
V_e = electrical voltage from the AC main (V)
f = power factor = 0.83

The power factor accounts for the difference in phase between the voltage and current.

Heat Load

Electronic equipment is mounted in standard rack frames located in an equipment room. Cool air must be supplied to these rooms in sufficient quantities to stabilize the room temperature so the equipment does not overheat. The heat to be removed is the waste heat generated by the electronics. The heat load for processing and line-level devices can be calculated directly from their power requirements since no power leaves the room. For amplifiers it is based on the power that is not delivered to the loudspeakers (Crown, 1993).

$$\frac{dQ}{dt} = K_h \left[\frac{N_c \, J \, \xi(1 - \eta)}{\eta} + \frac{N_c \, J_q}{2} \right] \tag{18.8}$$

where Q = heat load in BTU or Joules
K_h = 0.3415 for BTU / hr
       = 360 for J / hr

Heat is removed through convective cooling, whereby hot air is exhausted from the room and is replaced by refrigerated air. The rate of heat removal must match the rate of heat generation for temperature stability. The thermodynamic model of the process assumes that the air in the equipment room is heated to a temperature ΔT above the temperature of the incoming air and is then carried off through the return air system. The heat transferred to the air is

$$Q = m \, C_p \, \Delta T \tag{18.9}$$

where m = mass of air (kg or lb_m)

  C_p = heat capacity of air at constant pressure
      = 1006 J / kg °C

      = 0.240 BTU / lb_m °F
ΔT = temperature rise (°C or °F)

The total heat removed in terms of the mass of moving air is

$$\frac{dQ}{dt} = \frac{dm}{dt} C_p \, \Delta T \tag{18.10}$$

and the required amount of cooling air for a given temperature rise and heat load is

$$\frac{dV}{dt} = \frac{1}{\rho_0 \, C_p \, \Delta T} \frac{dQ}{dt} \tag{18.11}$$

where $\dfrac{dV}{dt}$ = volume flow of air (cu m / hr or cu ft / hr)

ρ_0 = density of air

$\quad$ = 1.21 kg / cu m

$\quad$ = 0.075 lb_m / cu ft

This yields

$$\frac{dV}{dt} = \frac{K_h}{\rho_0\, C_p\, \Delta T}\left[\frac{N_c\, J\, \xi\, (1-\eta)}{\eta} + \frac{N_c\, J_q}{2}\right] \qquad (18.12)$$

For a 1000 Watt amplifier (total combined power for both channels) this works out to about 16 cfm for a 30% duty cycle and a 5° F temperature rise. For six amplifiers in a rack, the cooling requirements would be on the order of 100 cfm. It should be noted that the temperature rise is that of the air in the room, not necessarily that of the amplifiers. The amplifiers may be at a different temperature depending on the local heat transfer within the racks and the point of delivery of the refrigerated air, which depends on fans in the rack or in the amplifiers themselves.

Time Coincidence

When two sound sources are used to cover the same receiver, any physical separation between them yields a difference in arrival time and a pattern of cancellation at certain frequencies, just as it did with an image source discussed in Chapt. 7. As more sources are added, the interference pattern becomes more complex and fills in the gaps in the spectrum created by the original pair. Using this line of reasoning, Davis and Davis (1987) argue for more loudspeakers covering a given area as long as the time delays between individual loudspeakers are not excessive. Comb filtering is seldom a problem in distributed loudspeaker systems, where multiple sources cover the same area, since it is a steady-state phenomenon. Speech varies in time so rapidly that comb filtering is rarely audible.

If a cluster is used, only one or two loudspeakers will cover a given area. Arrival time differences due to loudspeaker displacements of a few inches can be perceived as a lack of speech clarity. Here it is important that the sounds from adjacent units arrive at the listener at approximately the same time, since small misalignments are more audible than large ones. For a system such as that pictured in Fig. 18.6, time coincidence can be assured on axis by aligning the drivers. If the driver diaphragms of each loudspeaker are physically aligned then the wavefronts will be coincident along the centerline. In home hi-fi systems, where the principal listener is located on the centerline, correct alignment results in a marked improvement in imaging and clarity.

An off-axis listener does not receive the same benefit from this technique since the sound paths are of different lengths. Though seldom a problem in home systems, it is an important design parameter in sound-reinforcement systems. With speech-reinforcement systems, particularly those that include horns, the physical alignment of the drivers is inconvenient and not sufficient to guarantee time alignment, because the path length difference at an off-axis receiver is not the same as that for an on-axis receiver. In these cases the faces of the individual cone loudspeakers and horns should be aligned and an electronic delay should be used to ensure arrival time coincidence, as illustrated in Fig. 18.7. Although this scheme is an excellent technique, time coincidence cannot be guaranteed for every direction, since the off-axis path lengths still vary somewhat for each component. In a two-way system where

FIGURE 18.6 Two-Way Loudspeaker with Aligned Diaphragms

High frequency driver diaphragm

On-axis travel
times are equal
at the listener
for each component

Low frequency driver diaphragm
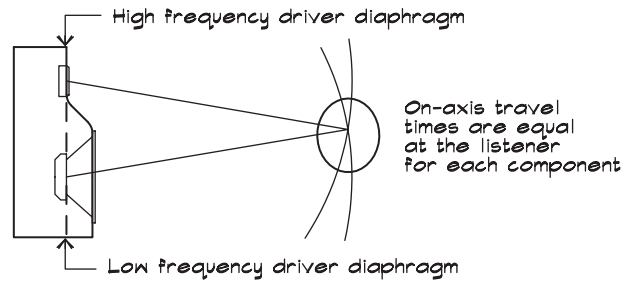
FIGURE 18.7 Two Component Loudspeaker System with Aligned Faces and an Electronic Delay

High frequency loudspeaker face

Travel times are
equal at the listener
for each component

Low frequency loudspeaker face

Delay
distance

Delay time = delay distance / speed of sound
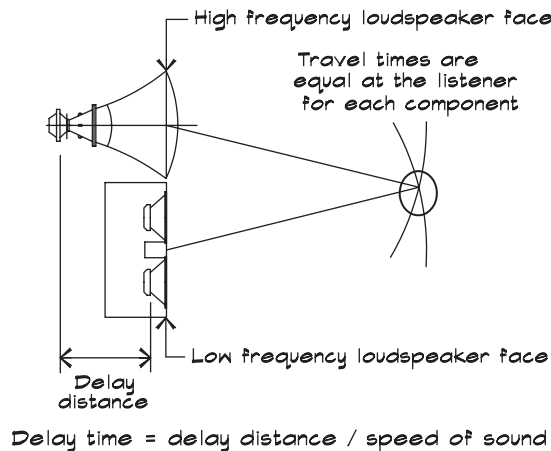
time overlap is a concern only near the crossover frequency, differences in arrival time can change the character of the sound.

Sometimes timing delay differences are introduced on purpose to achieve directivity control. In the midrange, where cone loudspeakers are used, vertical stacking of components leads to a narrowing of the coverage angle in the vertical plane. This occurs even when trapezoidal boxes with splayed sides are arrayed in a line. Just because packaged enclosures point in different directions does not mean that they do not interact in the manner of a typical line source.

Imaging

In a well-designed audio system the sound appears to be coming from the talker. This is accomplished by using the law of the first arrival, which states that the sound that reaches a listener first fixes the perceived source direction unless its level is too low. An example is pictured in Fig. 18.8. When the first-arriving sound comes from the talker or from a loudspeaker placed near him, the illusion is maintained. Since our ears are in the horizontal plane we are more sensitive to differences in azimuth than in elevation. For example, a central cluster located in front of a proscenium arch above the stage can maintain the illusion that the sound is coming from a performer on stage if the performer's voice is strong enough

FIGURE 18.8 Delay Settings for Cluster Systems
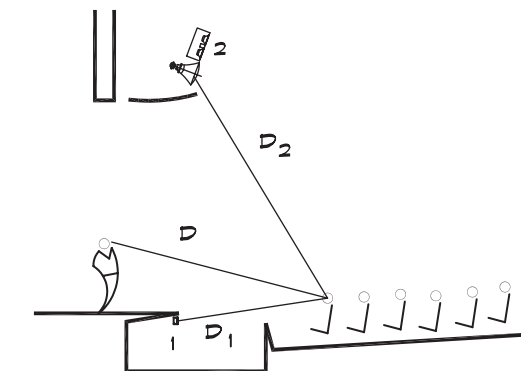
Delay for loudspeaker 1 in milliseconds

$$\left[(D - D_1) / 1.13 \right] + 5 \qquad \text{Dimensions in feet}$$

$$\left[(D - D_1) / 0.34 \right] + 5 \qquad \text{Dimensions in meters}$$

No delay for cluster 2 since $D_2 > D$

to provide the zero delay signal. Small loudspeakers located along the front of the stage can help pull the image down but they may have to be turned off when the pit orchestra is miked. The audio signal is fed into the main cluster, which may be delayed so that it arrives 5 to 10 msec later than the live sound. In the illustration, the cluster is located in front of the talker so that no additional delay is required. The actual delay setting depends on the position of the performer on stage and is a compromise since there is a range of performer locations.

In theme parks, where a live show might be combined with on-stage effects, point-source loudspeakers are positioned near an animatronic character or effect to generate the first arrival sound. This maintains the overall level and frequency balance between the live and recorded tracks and provides the physical illusion. Point-source loudspeakers do not need to have the full frequency range to preserve this imaging and can be small, as long as they produce an adequate level. If point sources are used with live microphones, the live mics must be muted during the effects to prevent feedback. In theme parks, this is done by using a show control computer to duck or gate the live mics. In live theater the ducking can be controlled either manually or automatically.

If a distributed system is used, the signal feeding the overhead loudspeakers is progressively delayed so that the illusion is maintained. Some source, either a live talker or a centrally located loudspeaker, must be used to produce the time-base-zero signal. The number of delay zones required for any given system depends on the details of the design; loudspeakers, which are no more than 10 msec apart in time delay, can be grouped into a zone. It is preferable in these systems to have only a few loudspeakers covering a given area. Thus this technique is most effective in low (< 6 m) ceiling rooms where the loudspeakers are close to the receivers. The overhead loudspeakers in the zones close to the talker help maintain the illusion for the zones farther away.

FIGURE 18.9 Delay Settings for a Lawn System
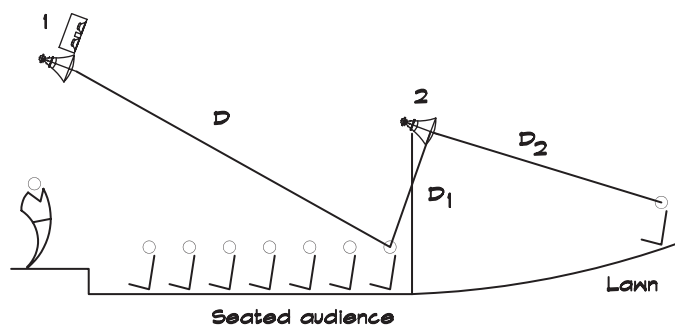
Delay for loudspeaker 2 in milliseconds

$$[D / 1.13 - 10] \quad \text{Dimensions in feet}$$

$$[D / 0.34 - 10] \quad \text{Dimensions in meters}$$

Outdoor amphitheaters often have a sound system with loudspeakers flown above a stage, with a series of loudspeakers located on poles around the rear of the fixed seating. These systems are designed to allow flexibility in servicing audiences of different sizes, with overflow patrons seated on a lawn behind the fixed seats. Setting time delays for a multiple-cluster system is difficult, particularly when the delayed cluster is elevated. In the configuration illustrated in Fig. 18.9, there are different delay times for listeners located under and behind the delayed loudspeaker. Normally the delays are set so that the time-base-zero loudspeakers lead the delayed loudspeakers by about 5–10 msec so that the illusion that the sound is coming from the stage is preserved. In this example the delayed loudspeakers are located on a tower 20 feet (6 m) in the air. If the time delay is picked to be 10 msec after the arrival of the time-base-zero signal, the sound heard at the base of the tower will lag the sound from the stage by about 30 msec and create a noticeable upward image shift. In tower systems the arrival time for the delayed loudspeakers should be set so as to lead the stage loudspeakers by about 10 msec. Then at the base of the tower the overhead sound lags the stage sound by 10 msec and the illusion is preserved. Farther back on the lawn the patrons are in line with the tower loudspeakers and even though they now lead the stage loudspeakers, the directional illusion still is preserved.

Feedback

The control of feedback and the achievement of adequate gain before the feedback becomes unstable are probably the most difficult aspects of sound system design. Figure 18.10 shows the gain structure of a sound reinforcement system. Note that gain and loss are used interchangeably. The open-loop system gain $Z_s = 20 \log z_s$ is defined as the difference between the level produced by the loudspeaker at the listener and the level produced by the talker at the microphone. The multiplier factor is 20 rather than 10 because z_s is a voltage gain. Clearly the gain must be high enough to produce an adequate level in the audience.

When there is a path for the amplified sound to travel back to the microphone, it has a transfer gain (or loss) $G_s = 20 \log g_s$, which characterizes the feedback loop. In electrical engineering terms any closed loop produces feedback, which can be stable or unstable. The transfer function for the signal moving through the entire closed loop system (with feedback)

FIGURE 18.10   Sound System Gain Block Diagrams
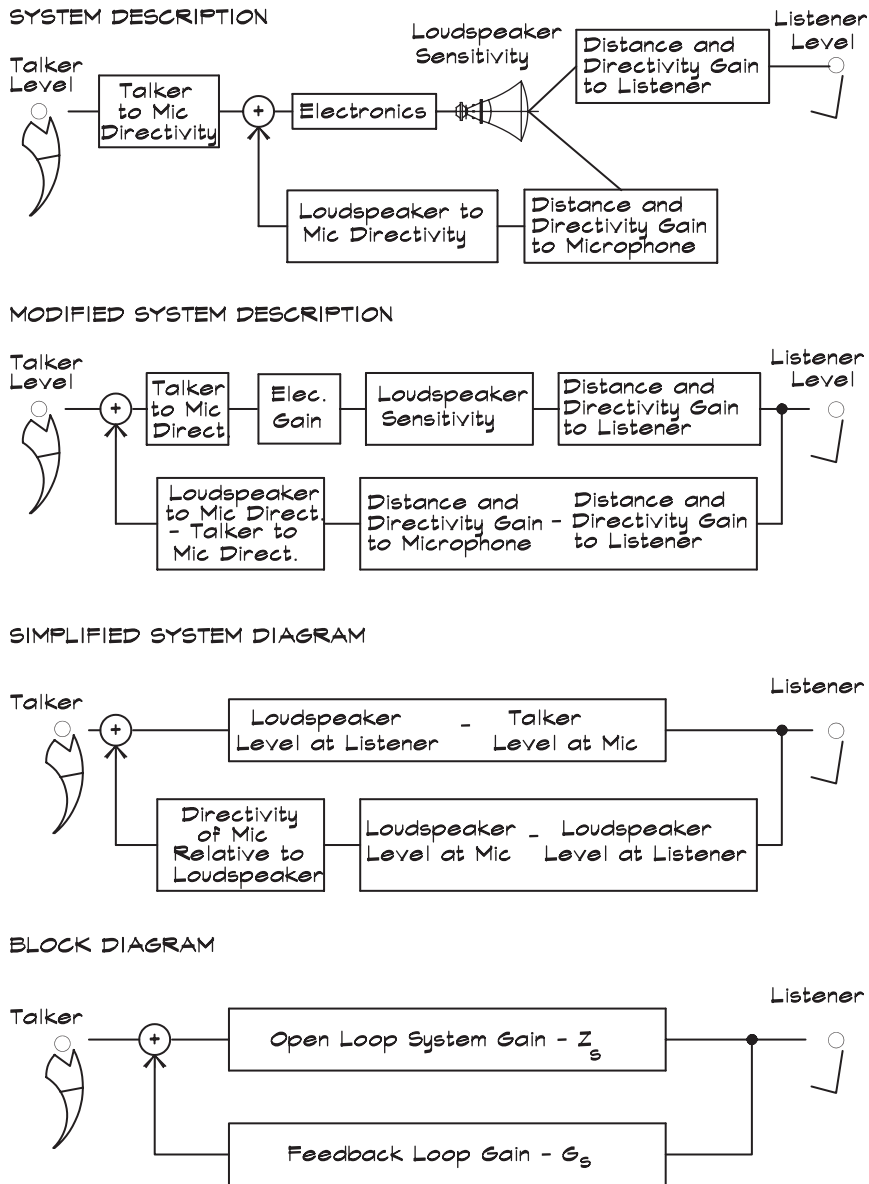
is the infinite series

$$X_S = z_s + z_s \, (z_s \, g_s) + z_s \, (z_s \, g_s)^2 + z_s \, (z_s \, g_s)^3 + \cdots \qquad (18.13)$$

which has a value in the limit of

$$X_S = \frac{z_s}{1 - z_s \, g_s} \qquad (18.14)$$

FIGURE 18.11   Parameters for Feedback Control
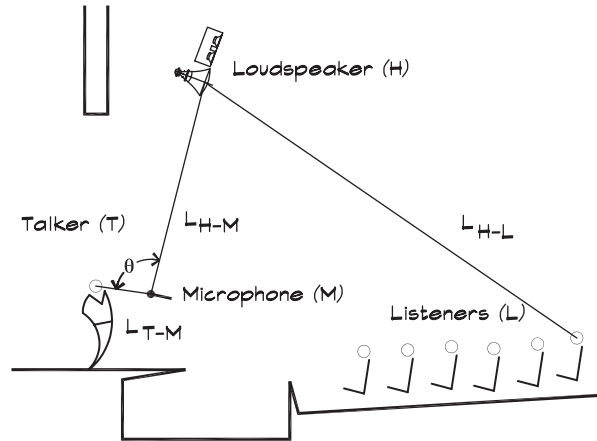
This is unstable (infinite) when the denominator goes to zero or when

$$z_s \, g_s = 1 \tag{18.15}$$

If the transfer functions are expressed in decibels (taking 20 log of Eq. 18.15) the criterion for sustained unstable feedback is

$$Z_s + G_s = 0 \tag{18.16}$$

Using Figs. 18.10 and 18.11 we can write out the gains in terms of their components. The open-loop system gain is the difference between the direct field level at an average receiver in the audience area and the direct-field level produced at the microphone by the talker

$$Z_S = L_{H\text{-}L} - L_{T\text{-}M} \tag{18.17}$$

where $L_{H\text{-}L}$ = direct field level produced by the loudspeaker
  system (H) at the listener (L), (dB)

  $L_{T\text{-}M}$ = direct field level produced by the talker (T)
  at the microphone (M), (dB)

  Z_S = system gain necessary to produce a given level at the
  listener relative to the talker level at the microphone (dB)

For a typical sound system the desired open-loop system gain might be on the order of -6 dB, which means that a comfortable communication level is achieved at a talker-to-listener distance that is twice the talker-to-microphone distance. In a rock concert, where the desired receiver sound pressure level is high, the system gain is increased as much as possible and the performer-to-microphone distance is made very short, normally less than one inch.

The feedback loop transfer function from Fig. 18.10 is

$$G_s = L_{H\text{-}M} - L_{H\text{-}L} + D_M(\theta) \tag{18.18}$$

where $L_{H\text{-}M}$ = direct - field level produced by the
loudspeaker system at the microphone, (dB)

$D_M(\theta)$ = directivity index of the microphone in the
direction of the loudspeaker relative to the talker
(usually negative), (dB)

We can substitute the levels into Eq. 18.16 to obtain the condition for sustained unstable feedback,

$$Z_S + L_{H\text{-}M} = L_{H\text{-}L} - D_M(\theta) \tag{18.19}$$

Now if we wish to have a stable system we must reduce the gain by a margin of safety called the feedback margin of stability, which is taken by some authors (Snow, 1955; Davis and Davis, 1987) to be between 12 dB for an unequalized system and 6 dB for a carefully equalized system. This text uses a middle value of 10 dB for an equalized system. In practice if a tone from the loudspeaker is sustained it may combine in phase at some frequency with the sound reflected from a hard surface yielding a 6 dB increase in the level seen by the microphone. The extra 4 dB is a safety factor. Thus we would expect the system to be stable if

$$Z_S + L_{H\text{-}M} \leq L_{H\text{-}L} - D_M(\theta) - 10 \tag{18.20}$$

For an open loop gain of −6 dB, typical of an auditorium or church, we obtain the condition for system stability with a closed feedback loop

$$L_{H\text{-}M} \leq L_{H\text{-}L} - D_M(\theta) - 4 \tag{18.21}$$

which states that for feedback prevention the direct-sound level at an omnidirectional microphone ($D_M(\theta) = 0$) should be 4 dB below the average direct level in the audience. With a cardioid microphone, having −2 or −3 dB of relative directivity, the stability criterion is

$$L_{H\text{-}M} \leq L_{H\text{-}L} - 2 \tag{18.22}$$

and the level at the microphone can rise to just under the average level in the receiving space. Although this formula is very simple, it is also quite useful since it is not explicitly dependent on the type, number, or characteristics of the loudspeaker system, only on the sound field it produces and the type and orientation of the microphone. The desired level in the audience area is determined independently and sets the maximum distance that the talker can be from the microphone. The coverage variability is also independently determined.

The sound level at the receiver can be increased either by increasing system gain or by decreasing the talker-to-microphone distance. Once the loudspeaker system has been set, the only way to increase the gain is to utilize a more directional microphone or to add electronic processing such as equalization, delay, or a frequency shifter to suppress the ring frequencies.

Note that the loop-gain equations include the directivity of the microphone. Directional microphones can be beneficial for increasing gain before feedback, but they discriminate against the talker when he is off-axis. They also emphasize sounds coming from a particular direction that may include sound scattered from nearby surfaces, including the talker's body. The precise calculation of their effectiveness is difficult since they are not always held at the same angle relative to the loudspeaker. It is prudent to incorporate a cardioid or

hypercardioid microphone into a system. Highly directional shotgun microphones are not always useful in preventing feedback since they can have complicated lobing patterns and can be sensitive to sound arriving from certain angles.

Equation 18.20 does not contain reverberant field information. That is included indirectly by using the ratios in Table 18.3 as part of the design process. The reverberant field can contribute to feedback; however, if it is uniform throughout the space as theory predicts, it should not matter where the microphone is located or in what direction it is pointed, unless it is close to a reflecting surface. Since the microphone location and orientation are found to be important in controlling feedback, the direct-field level is more useful as a design tool.

Multiple Open Microphones

When there are several microphones in use at the same time, the signal from the loudspeaker can be picked up by each of them and combined at the mixer. This increases the level of the signal being fed back and it is customary to add a factor into the gain equation to account for this effect. The standard adjustment for the number of open microphones (nom) is

$$\Delta L_{nom} = 10 \log N_m \qquad (18.23)$$

where N_m is the number of microphones simultaneously in use. Although Eq. 18.23 is a useful generalization, it is based on the assumption that all microphones contribute equally to system gain. This requires that they be the same type, that their level and equalization settings all be the same, that they all have the same physical relationship to the loudspeakers, and that none of the signals they receive be in phase with those falling on other microphones. This is almost never the case in practice. It is much more likely that one or two microphones will contribute more than the rest and be responsible for the initiation of feedback. Nevertheless it has become accepted practice to insert the nom correction into the gain equation (Eq. 18.20) since there are too many unknowns associated with the exact multiple microphone calculation.

$$Z_S + L_{H\text{-}M} + \Delta L_{nom} \leq L_{H\text{-}L} - D_M(\theta) - 10 \qquad (18.24)$$

It is good practice in speech systems, where there is no live mixer, to use an automatic microphone mixer, so that the nom correction is zero. These devices adjust the combined output level according to the number of microphones receiving signal, so that the system gain is theoretically the same as it would be if only one microphone were on at a given time. In music systems automatic mixers are not employed (with some exceptions) and the number of open microphones correction must be applied. We frequently encounter multiple open microphones in churches, where separate microphones are used to pick up the sound from the choir. Separately adjustable loudspeakers in the vicinity of the music microphones can help maintain a reasonable gain structure.

Equalization

An equalizer is an electronic device that allows the addition or subtraction of gain within a frequency range that is selectable by the user. Filters come in several flavors: constant bandwidth (rarely encountered); constant percentage bandwidth (such as octave or third octave); and parametric where the frequency, bandwidth, and level are all adjustable.For overall system equalization a third octave bandwidth filter is used. Parametric filters can be used where precise control is desired; however in the hands of an inexperienced user, parametric filters can be tricky.

FIGURE 18.12   Effect of Equalization on Feedback
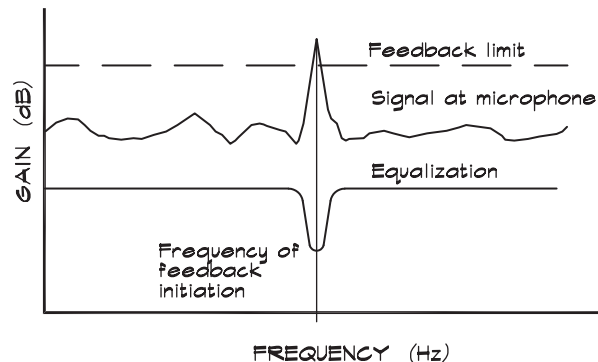
Equalizers are used to control feedback as well as even out the frequency response of a sound reinforcement system. Figure 18.12 gives an example. Since feedback begins at one particular frequency, a narrow-band filter can be used to reduce the level at the feedback frequency so that the overall gain can be increased before the instability begins. System designers debate the relative merits of adjustable-bandwidth filters versus (third-octave) constant-bandwidth filters. Either parametric or graphic equalizers can do a satisfactory job of controlling ring modes. A constant-bandwidth filter has the advantage of covering all possible frequencies within a range and providing a knowledge of where a filter is set. If digital processors are used, parametric filters require less processing real estate than the constant-bandwidth type.

Once a sound system is installed and the delay times set, it can be ensonified using a pink noise generator, which produces a random signal having equal energy per octave across the audio spectrum. In well-designed rooms, a pink noise source should yield even coverage throughout the room. Levels should vary no more than $\pm$ 2 dB, although in large rooms or in rooms having an unusual shape greater variation is sometimes encountered. A house equalization curve is introduced, which depends on the specific material to be presented. Figure 18.13 shows several examples. For speech reinforcement the equalization rolls off at about 3 dB/octave above 1 kHz.

Every designer has a favorite way of doing final equalization. Some find it helpful to listen to a well-known piece of music or a familiar voice to judge the accuracy of the system. Others prefer narrow-band analyzers, which can separate out the direct-field components by time windowing. Equalization for maximum gain is done with a live microphone in its normal location. The system gain is increased until the onset of feedback occurs. A spectrum analyzer, positioned in the space, is used to read off the frequencies of the rapidly rising levels from which the equalizer can be adjusted to notch out the worst offenders. When there are different types of microphones or even microphones in different places, it is useful to use a separate equalizer for each one. Even a relatively small change in microphone location, on the order of a few feet, can sometimes shift the feedback frequencies enough to warrant resetting the equalizer. Once a feedback mode has been identified the equalizer is used to reduce the level in that frequency band until the ringing subsides. The gain is then increased until feedback occurs again and the process is repeated until there is sufficient gain in the system.

At the end of the process there needs to be a reality check on the shape of the equalization curve to insure that the notching is not so severe that it distorts the sound. If the settings are unusually dramatic from band to band, then there may be other things happening in the room causing the problem. Typical problems to avoid include loudspeaker misalignment, background or mechanical system noise, mechanical coupling to the microphone, and room modes. None of these is best treated through equalization.

FIGURE 18.13A   Various Recommended Response Curves for Equalization (Foreman, 1987)
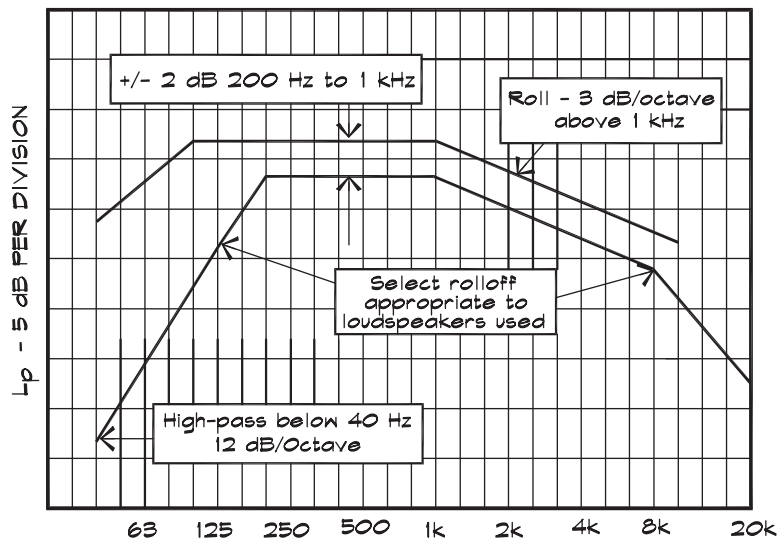
(A) Recommended response curve for speech reinforcement systems
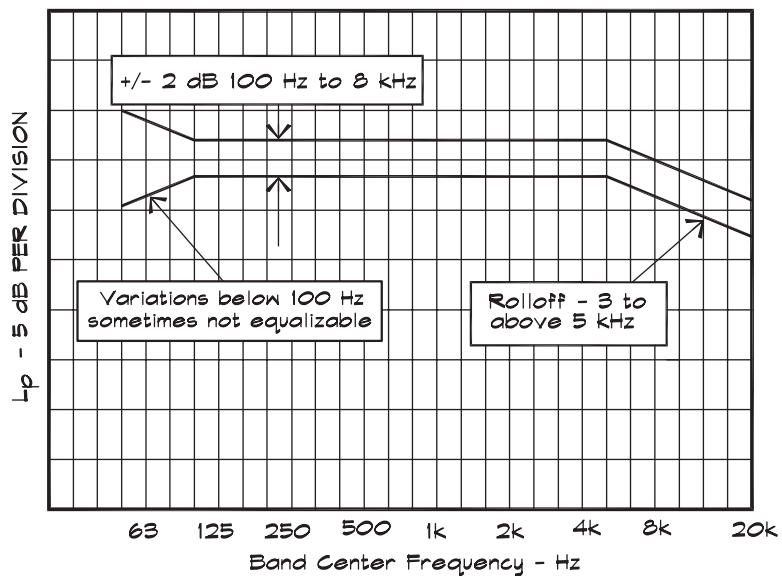
(B) Recommended response curve for studio control room monitoring systems

FIGURE 18.13B   **Various Recommended Response Curves for Equalization (Foreman, 1987)**

(C) Standard response curve for cinema playback systems.

(D) Recommended response curve for high-level rock music reinforcement systems.
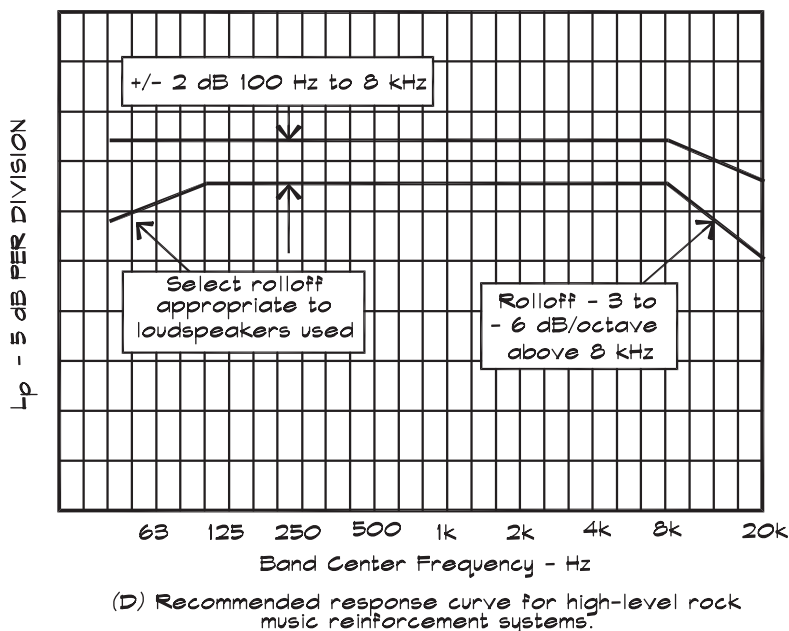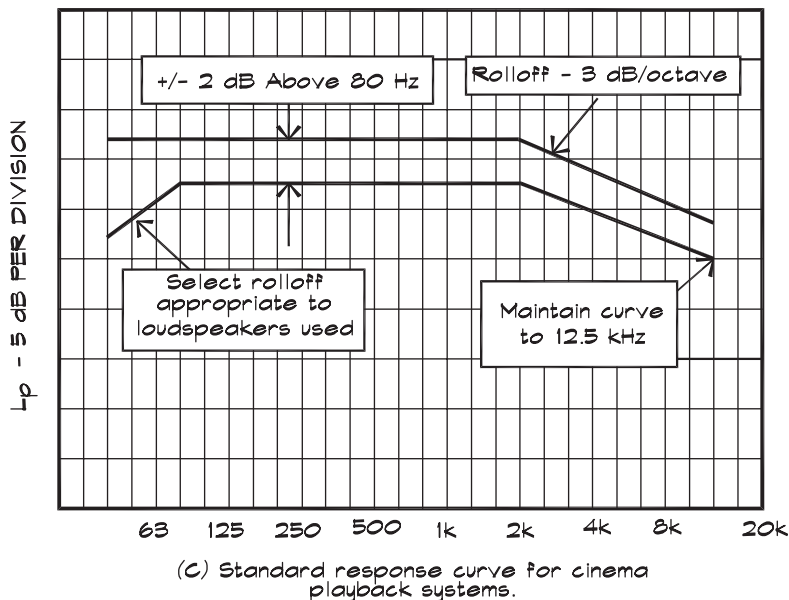
Architectural Sensitivity

Loudspeakers have the greatest architectural (visual) impact of any audio component. An early step in the sound system design process is to explore alternatives that may be used to achieve reasonable intelligibility in a space. The toolbox includes the central cluster, multiple clusters, and a combination of central cluster and delayed system, a progressively delayed system, and a distributed system. Each of these configurations has certain

advantages and disadvantages compared to the others, and each can be designed so as to provide adequate intelligibility. Not every system type, however, can be used successfully in every space.

Theaters, auditoria, churches, and concert halls all require sound systems, which can be blended into the architectural design of the space or left exposed either temporarily or permanently. Too often rooms are designed without giving consideration to the presence of the loudspeaker system that frequently must be physically large in order to provide adequate directivity control. Just as designers must accommodate mechanical and electrical systems with dedicated spaces, so too should audiovisual systems be designed into the fabric of the building, with dedicated equipment rooms and mixing locations.

Clusters can be shrouded with acoustically transparent materials such as light fabric, perforated metal screens, or wire mesh cloth. These materials should be at least 40% open to maintain acoustical transparency. Holes in solid materials must be small enough that the spacing is less than a quarter wavelength at the highest frequency of interest. This is around 0.25 inch (6 mm) apart at a maximum. They should be large enough that they are not clogged by paint, which requires a diameter greater than about 3/32 inch (2.4 mm). Hole diameters must also be larger than the thickness of the material.

Often when the loudspeaker system is not integrated, a priori, into the architecture, it is suspended as cable supported boxes or as one or more large clusters located in the center of the proscenium. This design solution may be visually acceptable; it is important to either integrate the sound system into the overall design early in the process or accept the appearance of exposed components.

18.3 CHARACTERIZATION OF TRANSDUCERS

Microphone Characterization

The ultimate goal of a sound reinforcement system is to deliver amplified speech or music in as natural sounding and intelligible form as possible. In the case of speech, which is the primary source of amplified sound, the direct-to-reverberant noise ratio determines the overall intelligibility. Thus the higher the signal-to-noise ratio of the sound gathered by the microphone, the better off we are. Even if we listen to the sound on headphones we cannot obtain a better signal-to-noise ratio than that received by the microphone, and the projection of the sound through loudspeakers can only decrease this ratio.

If we consider the reverberant sound field as the primary source of noise, the closer the microphone is to the talker and the more directional its characteristics, the higher the signal-to-noise ratio will be. From the standpoint of intelligibility, a microphone located near the source is preferable to one located farther away. Although this is true, both distance and directivity have other effects that influence the character of the sound. As we move closer to a fixed microphone, any changes in distance and head orientation can have a large influence on the level and frequency spectrum of the output signal. If the microphone is directional, the closer it is to the talker, the more severe will be the effects of head movement.

Microphones can also have an architectural impact, particularly if they are on camera. Fortunately they can be quite small with current technology. Microphones are most effective when placed close to the mouth of the user. Concert performers have come to use headset microphones, which maintain a consistent orientation and distance between the microphone and the mouth. In legitimate theater, radio microphones are located in the clothing or even the hair of the actors. In a church or synagogue the user does not have the same level of audio

sophistication or technical assistance available in a theater and choices of microphone type and location, in part, must be based on these considerations.

Omnidirectional microphones provide the most accurate reproduction of sound but are also the most prone to feedback. By using a directional microphone we can discriminate against both direct and reverberant sound coming from off-axis. A directional microphone is less likely to produce feedback, but is more sensitive to the orientation of the user's head and less natural sounding. A cardioid pattern most often represents the best compromise between feedback control and naturalness.

Unidirectional microphones are more prone to vibration and handling noise than are omnidirectional microphones. This is because the off-axis discrimination is obtained by allowing some of the signal to enter at the rear of the microphone, which decreases the net pressure on the diaphragm. At low frequencies the pressure differential, which causes the diaphragm to move, is small compared to the absolute sound pressure. Consequently the diaphragm of a unidirectional microphone must be made to move more easily in response to low-frequency sound, accomplished by reducing the damping resistance to about one-tenth that used in an omnidirectional microphone. These microphones are most sensitive to vibrations at about 150 Hz, the mechanical resonant frequency of the diaphragm and voicecoil (Ballou, 1987).

Microphones can introduce sonic artifacts due to their position and orientation. If an omnidirectional microphone is placed near a reflecting surface the signal received will include both the direct and reflected sound. The path-length difference between the direct and reflected paths will produce a series of cancellations (shown in Fig. 18.14) called comb filters which can color a steady sound.

The comb filter frequencies are given by a half wavelength path-length difference

$$f_n = \frac{(2n - 1) c}{2(d_2 - d_1)} \tag{18.25}$$

where n is a positive integer. If the path length difference is small, the first frequency is high and the reflection acts as a low pass filter shown in Fig. 6.16. Microphones can be placed near the floor to take advantage of this effect, but they are farther from the talker and more prone to

FIGURE 18.14   Comb Filters Plotted on a Linear Scale (Everest, 1994)
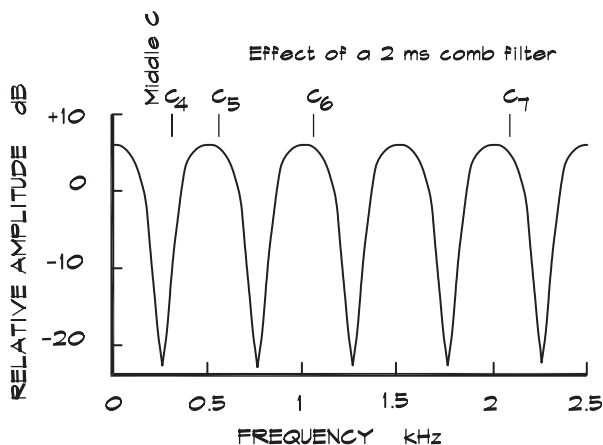
vibrational interference. Small pieces of foam located under the case can be used as vibration isolators. For large path length differences, the filter frequencies are closer together and the reflected levels are not as great as the direct level. When a microphone discriminates against off-axis sounds, the comb filtering effects are even less for the same reason. For directional microphones located on a floor-mounted stand, comb filtering is rarely a problem. Podium microphones can be positioned so that the talker's voice is not reflected directly into the capsule and these effects are minimized.

Some microphones take advantage of the reflection from a planar surface. These microphones are located close to a solid boundary where the reflected sound is in phase with the direct sound. They are generally omnidirectional, with one or two exceptions, but can be used with reflecting shields to gain some directivity. The amount of shielding is dependent on the physical size of the barrier. For small shields there is little barrier effect below a given frequency. Surface-mounted microphones placed on a table or podium are farther away from the talker than extension mounted microphones and will pick up the rustling of papers and vibrations transmitted through the mount.

In selecting a microphone several factors must be considered:

1) Directivity

2) Coloration, or changes in response with frequency

3) Ruggedness and maintainability

4) Freedom from shock and handling noise

5) Accuracy and fidelity

6) Electrical characteristics: sensitivity, phantom power requirements, impedance

7) Resistance to feedback

8) Maximum input level

Directivity patterns are available from the manufacturer and should be studied for frequency response and lobbing. The better microphones can be handled without generating excessive noise. An external vibration isolated support is sometimes helpful, but these can be cumbersome and unattractive in sound reinforcement systems. Internal vibration isolation, which is available on some microphones, is useful, as are hum-bucker coils to reduce low-frequency hum. If phantom power is required to power internal circuitry or to provide a polarizing voltage, it is supplied by the primary mixer, which applies a DC voltage (usually from $+9$ to $+52$ volts) equally to pins 2 and 3 of the preamplifier input receptacle.

Microphones typically produce a high impedance output signal at a level of a few millivolts, which is commonly referred to as mic level. These signals may be conducted in a shielded cable over a distance of a few hundred feet without appreciable loss. Where longer distances are involved a preamplifier, with a low output impedance, can be located near the microphone to drive the line.

In a critical application, a system can be designed with a certain microphone in mind, but it is difficult to predict which microphone will sound best in a space. It is helpful to try out a number of possible microphones in the finished space and to listen to each one, preferably with the person who will ultimately be using it.

In theaters and frequently in churches a small lavaliere microphone is used either on a long cord or attached to a radio transmitter carried by the user. The alternative is one or more fixed microphones located at the principal speaking locations. Each of these solutions has

FIGURE 18.15   Horizontal and Vertical Polar Data (JBL, 1997)
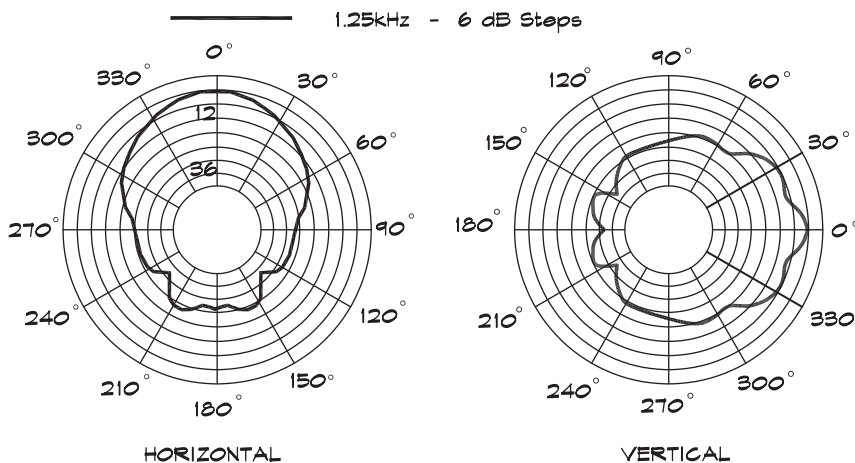
advantages and disadvantages. Wireless microphones need to have their batteries periodically replaced and some have connectors that are fragile and prone to breakage. Fixed microphones are more robust but more visible and require some microphone discipline by the user.

Loudspeaker Characterization

Loudspeakers are characterized by a few simple parameters: 1) on-axis sensitivity described in Chapt. 2, 2) on-axis directivity (Q_0) and relative directivity index as a function of angle, 3) power handling capability, and 4) frequency response.

Directivity is critical to accurate system design and most manufacturers publish directivity information in terms of the difference between the on-axis level and the level for a given direction. Until recently manufacturers listed directivity data only in the form of horizontal and vertical polars as shown in Fig. 18.15, and Q_0 versus frequency data as shown in Fig. 18.16.

$$D_{rel}(\theta,\phi) \equiv L_p(0,0) - L_p(\theta,\phi) \qquad (18.26)$$

where $D_{rel}(\theta, \phi)$ = the directivity index relative to on - axis, (dB)
  taken to be positive for $L_p(0, 0) > L_p(\theta, \phi)$

  $L_p(0, 0)$ = the on - axis sound pressure level at a given distance, (dB)

  $L_p(\theta, \phi)$ = the sound level at a given angle for the same distance, (dB)

  θ = latitude referenced to the loudspeaker centerline (deg)
  ϕ = longitude from the horizontal loudspeaker plane (deg)

Since the on-axis level is almost always higher than off-axis levels, $D_{rel}(\theta,\phi)$ is generally positive.

With the development of computer modeling programs for loudspeaker coverage calculations, the horizontal and vertical polars have given way to data published in 10° increments, and there is movement toward finer increments. The normal geometry used in standard computer modeling programs is shown in Fig. 18.17.

**FIGURE 18.16   Data for a Three-Way High Directivity Loudspeaker System
(JBL, 1997)**
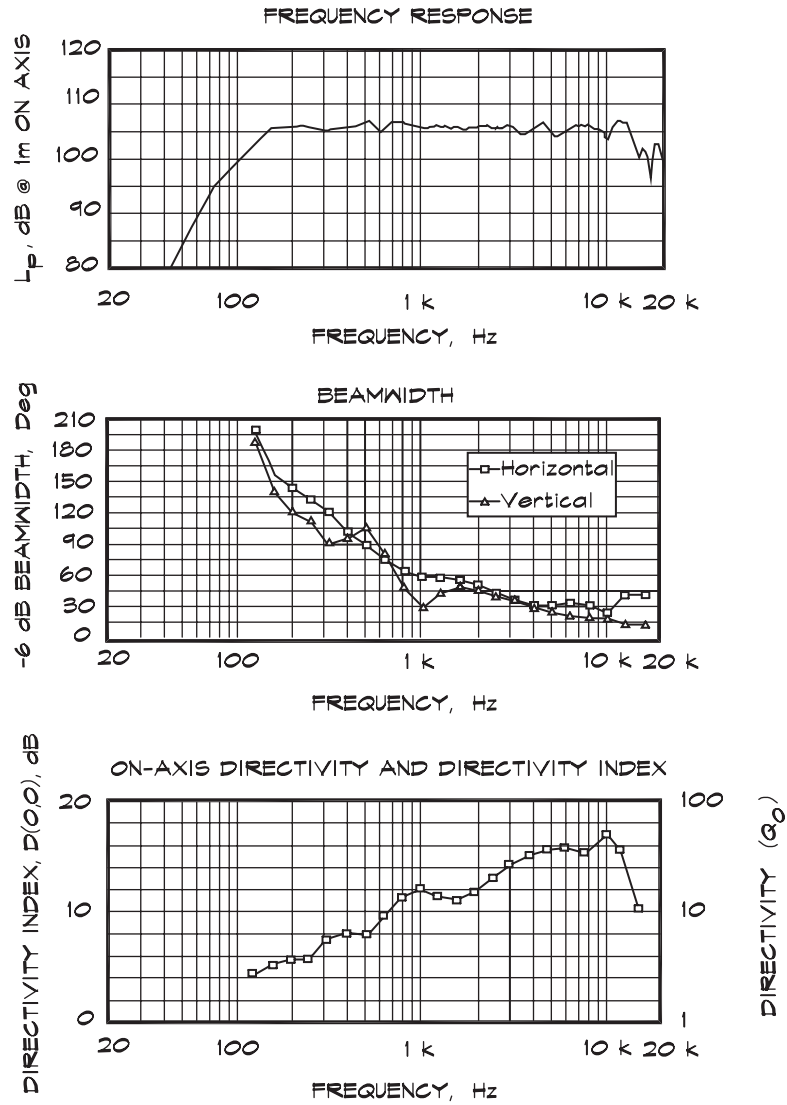
All the major modeling programs use the loudspeaker centerline as the x axis (North Pole) and measure latitude relative to it. Different programs use different axes for Greenwich, the prime meridian from which longitude is measured. These choices are subsumed in the internal coding of the program; however, in generating directivity data exchange files the starting axis must be known. The CADP program measures its longitude counterclockwise beginning from the z (vertical) axis. The EASE program and the author's program, on which this text is based, use the y axis (horizontal) as the reference line.

Given the older horizontal and vertical polar data, whose coordinates are shown in Fig. 18.18, the relative directivities based on longitude and latitude around a sphere can be calculated using an interpolation formula. There is no standard method of doing this since there is no unique relationship between the polar data and the off-axis results. An approximate

FIGURE 18.17 Loudspeaker Coordinate System
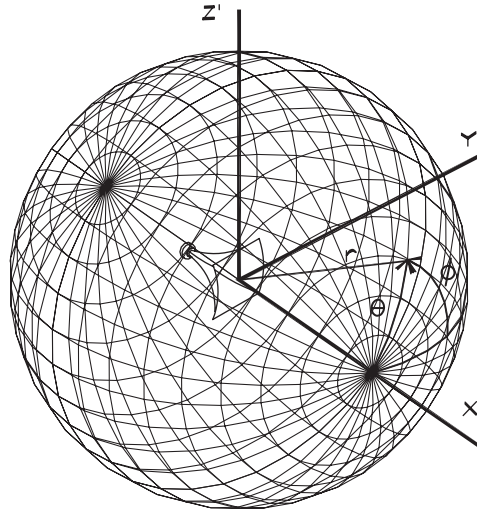
FIGURE 18.18 Horizontal and Vertical Polar Coordinates
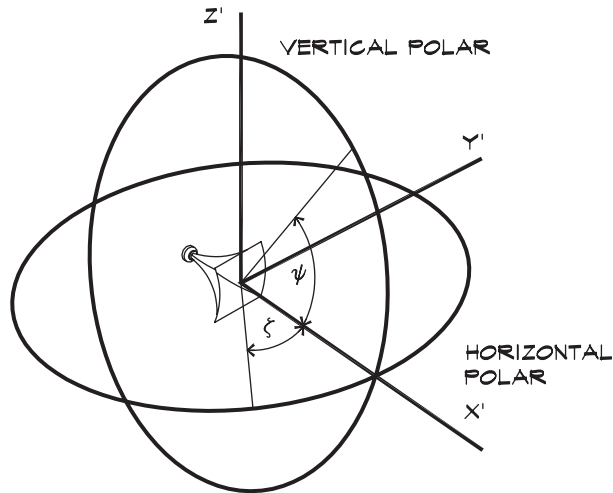
formula that can be used is

$$D_{rel}(\theta_n, \phi_n) \cong \left[\begin{array}{c} \left(D_{vert}(\psi_n = \theta_n) \sin \phi_n\right)^2 \\ + \left(D_{horiz}(\varsigma_n = \theta_n) \cos \phi_n\right)^2 \end{array} \right]^{1/2} \tag{18.27}$$

where D_{rel} = the directivity index relative to on-axis for a given direction
(taken to be positive for $L_p(0, 0) > L_p(\theta, \phi)$)
D_{vert} = the vertical directivity index relative to on-axis
D_{horiz} = the horizontal directivity index relative to on-axis

FIGURE 18.19   Interpolation of Data between Known Points
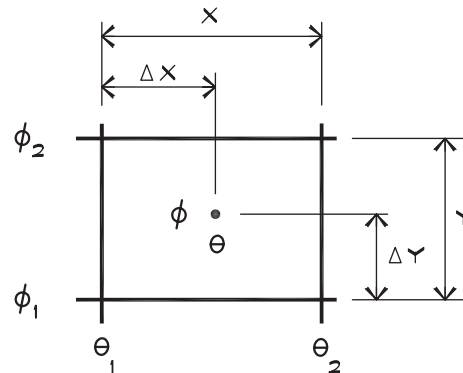
ς_n = polar angle in the horizontal plane in 10° steps
ψ_n = polar angle in the vertical plane in 10° steps
θ_n = latitude referenced to the speaker centerline in 10° steps
      (note that $\theta_n = \alpha_n = \beta_n$)
ϕ_n = longitude from the horizontal plane in 10° steps

The vertical component of D_{rel} is zero for a vertical angle of zero, that is in the horizontal plane, and the same is true for the horizontal component of D_{rel} values in the vertical plane. The difficulty with Eq. 18.27 and other similar equations is that the real off-axis directivity values are not directly dependent on the horizontal and vertical polar values. This particular equation generates a smooth elliptical coverage pattern when viewed from the front, but does not include the complex lobing that may be present in a given direction, but may not be reflected in the polar data. Thus these types of relations are only a rough approximation of the actual off-axis behavior, but can be useful when only polar data are available.

Most manufacturers now publish the directivity index relative to the on-axis level at 10° intervals measured on a sphere of receiver locations surrounding the source. When the actual angle to a receiver falls between measured points, such as those shown in Fig. 18.19, a linear interpolation must be performed.

$$\begin{aligned}
D_{rel}(\theta,\phi) = {} & D_{rel}(\theta_1,\phi_1)\left(\frac{x-\Delta x}{x}\right)\left(\frac{\Delta y}{y}\right) \\
& + D_{rel}(\theta_1,\phi_2)\left(\frac{\Delta x}{x}\right)\left(\frac{\Delta y}{y}\right) \\
& + D_{rel}(\theta_2,\phi_1)\left(\frac{x-\Delta x}{x}\right)\left(\frac{y-\Delta y}{y}\right) \\
& + D_{rel}(\theta_2,\phi_2)\left(\frac{\Delta x}{x}\right)\left(\frac{y-\Delta y}{y}\right)
\end{aligned}$$

(18.28)

where θ_n = latitude referenced to the speaker centerline in 10° steps
           ϕ_n = longitude from the horizontal plane in 10° steps

$$x = \theta_2 - \theta_1 = \text{angular increment between measurements}$$
$$\Delta x = \theta - \theta_1 = \text{angular increment between receiver direction and}$$
$$\text{the least measured angle}$$
$$y = \phi_2 - \phi_1 = \text{angular increment between measurements}$$
$$\Delta y = \phi - \phi_1 = \text{angular increment between receiver direction and the}$$
$$\text{least measured angle}$$

The Calculation of the On-axis Directivity

Loudspeaker sensitivity was defined in Eq. 2.83 and is the on-axis sound pressure level at one meter for a one Watt input power. Since the measurements are done on-axis, the relationship between the sensitivity and the sound power level is a function of Q_0, the on-axis Q. Once measured directivity data are available in 10° increments the directivity for a particular intermediate angle can be calculated. Recall from Chapt. 2 that $Q(\theta,\phi)$ was defined in terms of the on-axis directivity and a relative directivity.

$$Q(\theta,\phi) = Q_0 \, Q_{rel}(\theta,\phi) \tag{18.29}$$

where θ = latitude relative to on - axis

ϕ = longitude relative to an arbitrary plane

The directivity Q, is defined as the ratio of the intensity in a given direction to the average intensity over the whole receiver sphere. To calculate the intensity for a given direction we must know the relative level for that particular direction. The average intensity is determined from the off-axis levels and their corresponding areas in each direction.

We begin with the on-axis directivity (Q_0), which is defined as

$$Q_0 = Q(0, 0) = \frac{I(0, 0)}{I_{ave}} \tag{18.30}$$

where

$$I_{ave} = \sum_{i=1}^{N} I_i(\theta, \phi) S_i(\theta, \phi) \tag{18.31}$$

and $S_i(\theta,\phi)$ = fractional surface area of a sphere associated with a
given pair of angles θ and ϕ

Now the intensity in a given direction can also be written in terms of the directivity index relative to on-axis.

Published loudspeaker directivity indices are given relative to the on-axis directivity index, which is zero.

$$D_{rel}(\theta, \phi) = -10 \log Q_{rel}(\theta, \phi) = -10 \log \frac{I(\theta, \phi)}{I(0, 0)} \tag{18.32}$$

Thus if I_{ave} is calculated in terms of the relative directivity data,

$$I_{ave} = \sum_{i=1}^{N} I(0, 0) \, Q_{rel,i}(\theta, \phi) \, S_i(\theta, \phi) \tag{18.33}$$

$$I_{ave} = I(0, 0) \, \overline{Q}_{rel} \tag{18.34}$$

where

$$\overline{Q}_{rel} = \sum_{i=1}^{N} Q_{rel,i}(\theta, \phi) \, S_i(\theta, \phi) \tag{18.35}$$

Using Eqs. 18.30 and 18.34 it follows that

$$Q_0 = \frac{1}{\overline{Q}_{rel}} \tag{18.36}$$

In making this calculation we subdivide a sphere into area segments. The geometry of the area of a segment of a sphere is shown in Fig. 18.20. We must then find the area of a segment associated with a given pair of angles as a fraction of the total area. For the geometry shown, the fractional area is

$$S_i(\theta, \phi) = \left(\frac{\phi_2 - \phi_1}{360}\right)\left(\frac{\cos\theta_1 - \cos\theta_2}{2}\right) \tag{18.37}$$

When the increments between angles are $\Delta\theta$ and $\Delta\phi$ (usually $10°$), Eq. 18.37 can be written as

$$S_i(\theta, \phi) = \left(\frac{\Delta\phi}{360}\right)\left(\frac{\cos(\theta - \Delta\theta/2) - \cos(\theta + \Delta\theta/2)}{2}\right) \tag{18.38}$$

FIGURE 18.20   Area Associated with a Directivity Data Point
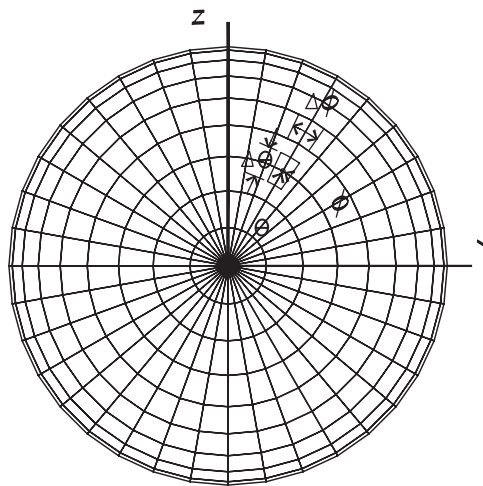
for $0 \geq \theta \geq 180$ and $(\theta - \Delta\theta/2) \geq 0$ and $(\theta + \Delta\theta/2) \leq 180$. The angle θ is incremented in $10°$ steps. Using these equations we can calculate the average intensity, the on-axis directivity, and from Eq. 2.83, the sound power level for a given loudspeaker using its sensitivity at each frequency.

18.4   COMPUTER MODELING OF SOUND SYSTEMS

Computer modeling programs are available and can be used to predict the coverage of loudspeakers individually or in combination. When they first appeared, these programs were developed, or purchased, principally by loudspeaker manufacturers as a marketing tool to encourage the use of their products. In their earliest versions programs offered by one manufacturer did not include data on another manufacturer's devices. As other programs became available, users demanded a selection of loudspeakers from more than one manufacturer, so most programs began to include a wider range of components. When the market coalesced around a few modeling programs, manufacturers found it to their advantage to provide designers with directivity and other data on all products.

Computer programs make it possible to do rather complicated calculations of coverage and intelligibility without a detailed knowledge of the mathematics involved. This shifts the decision-making process from the sound system designer to the computer programmer on whether the coverage, intelligibility, and gain before feedback will be satisfactory for a particular design. Unfortunately vendors may not provide the user with the algorithms used in generating the code, so there is no way of back-checking the conclusions offered by the program.

Coordinate Systems and Transformation Matrices

A sound-system modeling program must describe a three-dimensional space mathematically as seen from the viewpoint of the loudspeaker. To do so a coordinate system needs to be established that defines the space in which both the loudspeakers and receivers are located. To be consistent with computer-aided design programs, the x-y axes define the plane of the building floor and the z axis is vertical. The room coordinate system is shown in Fig. 18.21. The coordinates are right-handed with the x axis aligned with the centerline of the room.

FIGURE 18.21   Room Coordinate System
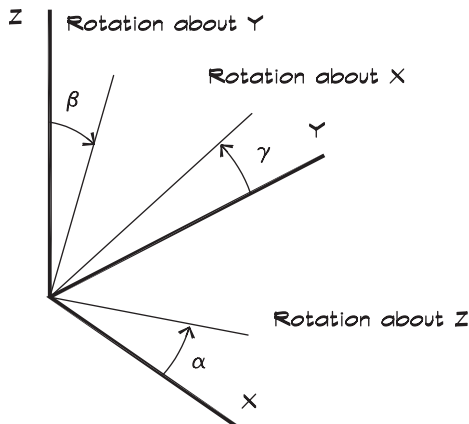
When looking from a positive point on one axis toward the origin, a 90° counterclockwise rotation will transform one axis into the following one—that is, x to y and y to −x, and so forth. Rotation angles with respect to each axis are also shown.

It is convenient to use a system of homogeneous coordinates, which contains one dimension more than the space being characterized. Thus for a three-dimensional space, a four-element vector is used, where the fourth element is a scaling parameter. In this text the scaling parameter for a point is always one. The four coordinates define a particular location in space

$$\mathbf{x} = [x, y, z, 1] \tag{18.39}$$

which is used as a column matrix when doing calculations. The effect of a translation of the coordinate system to a new location displaced by some distance $\Delta x, \Delta y, \Delta z$ from the origin can be produced by multiplication by a translation matrix

$$\mathbf{T}(\Delta x, \Delta y, \Delta z) = \begin{bmatrix} 1 & 0 & 0 & -\Delta x \\ 0 & 1 & 0 & -\Delta y \\ 0 & 0 & 1 & -\Delta z \\ 0 & 0 & 0 & 1 \end{bmatrix} \tag{18.40}$$

The new point is

$$\mathbf{x}' = \mathbf{T}\,\mathbf{x} = [x - \Delta x, \ y - \Delta y, \ z - \Delta z, 1] \tag{18.41}$$

The convenience of this notation system is apparent since all operations, including translations, can be done with matrix multiplications.

Rotations are straightforward. A counterclockwise rotation of the axes about the z axis, shown in Fig. 18.22, is accomplished using the rotation matrix

$$\mathbf{R_z}(\alpha) = \begin{bmatrix} \cos \alpha & -\sin \alpha & 0 & 0 \\ \sin \alpha & \cos \alpha & 0 & 0 \\ 0 & 0 & 1 & 0 \\ 0 & 0 & 0 & 1 \end{bmatrix} \tag{18.42}$$

The y-axis rotation matrix is

$$\mathbf{R_y}(\beta) = \begin{bmatrix} \cos \beta & 0 & \sin \beta & 0 \\ 0 & 1 & 0 & 0 \\ -\sin \beta & 0 & \cos \beta & 0 \\ 0 & 0 & 0 & 1 \end{bmatrix} \tag{18.43}$$

and the x-axis rotation matrix is

$$\mathbf{R_x}(\gamma) = \begin{bmatrix} 1 & 0 & 0 & 0 \\ 0 & \cos \gamma & -\sin \gamma & 0 \\ 0 & \sin \gamma & \cos \gamma & 0 \\ 0 & 0 & 0 & 1 \end{bmatrix} \tag{18.44}$$

Composite transformations may be carried out by applying the appropriate matrices sequentially.

FIGURE 18.22 Rotation of a Coordinate System
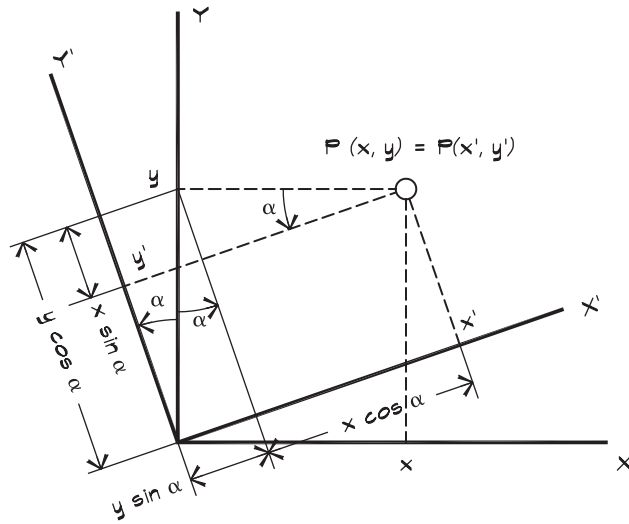
Determination of the Loudspeaker Coordinate System

If a direct-field sound pressure level is to be calculated due to a given loudspeaker, the directivity associated with the receiver must be determined. The loudspeaker is positioned in the room and aimed in a particular direction. The loudspeaker and its aim point in room coordinates are shown in Fig. 18.23.

The loudspeaker is located at

$$\mathbf{x_s} = \left[x_s, y_s, z_s, 1\right] \tag{18.45}$$

and is aimed at

$$\mathbf{x_p} = \left[x_p, y_p, z_p, 1\right] \tag{18.46}$$

FIGURE 18.23 Loudspeaker in the Room Coordinate System
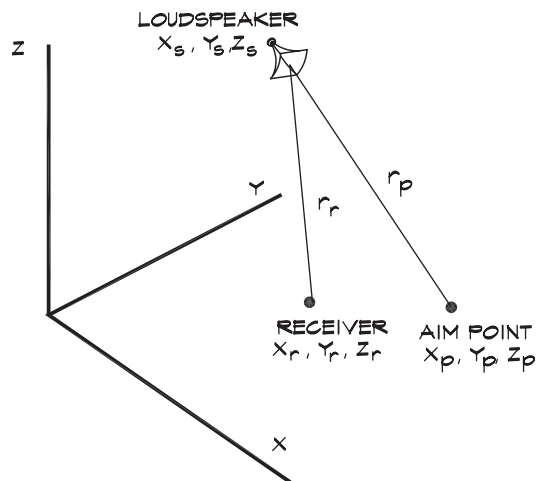
Figure 18.24 Four Steps in the Transformation to Loudspeaker Coordinates

(a) Translation to the Loudspeaker

(b) z'-axis Rotation

(c) y'-axis Rotation

(d) x'-axis Rotation
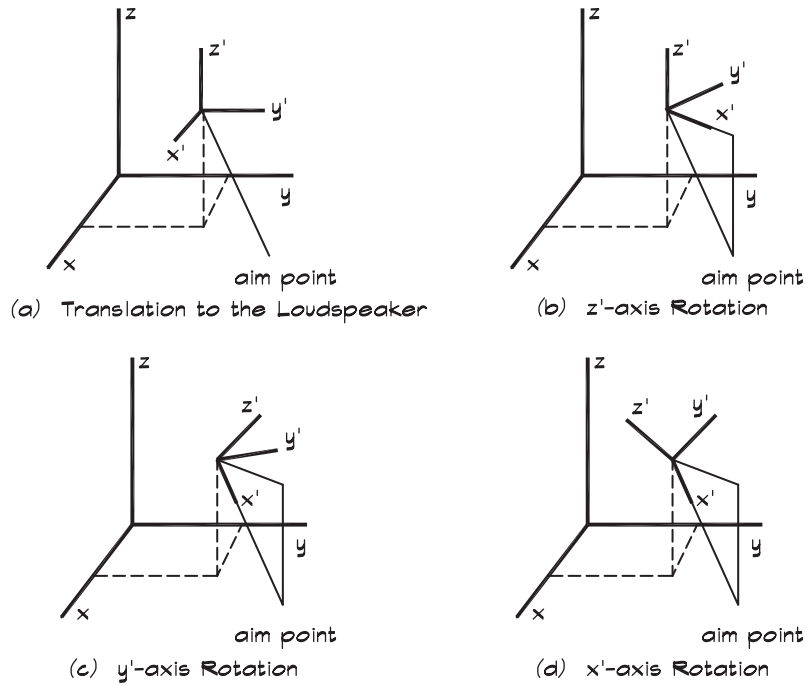
The ultimate goal is to describe the receiver location in the loudspeaker coordinate system, so that the directivity associated with the vector between the loudspeaker and the receiver can be found. We align the transformed x axis with the aim point direction and the transformed y axis with the horizontal axis of the loudspeaker in accordance with the four steps outlined in Fig. 18.24. The first step in this process is to translate the room origin to the loudspeaker location. The translation matrix is

$$\mathbf{T_s} = \begin{bmatrix} 1 & 0 & 0 & -x_s \\ 0 & 1 & 0 & -y_s \\ 0 & 0 & 1 & -z_s \\ 0 & 0 & 0 & 1 \end{bmatrix} \tag{18.47}$$

Having translated the origin, we orient the coordinate system so that its x axis is aligned with the loudspeaker centerline. Since the centerline is pointed at the aim point, we locate the loudspeaker aim point, $\mathbf{x_p}$, in room coordinates and transform it using Eq. 18.40. This yields a transformed aim point,

$$\mathbf{x'_p} = \left[x'_p, \ y'_p, \ z'_p, \ 1 \right] \tag{18.48}$$

which has a unit vector

$$\frac{\mathbf{x'_p}}{r_p} = [a, \ b, \ c, \ 1] \tag{18.49}$$

FIGURE 18.25 Two Rotations Are Used to Align the X Axis with the Aim Point Unit Vector a, b, c
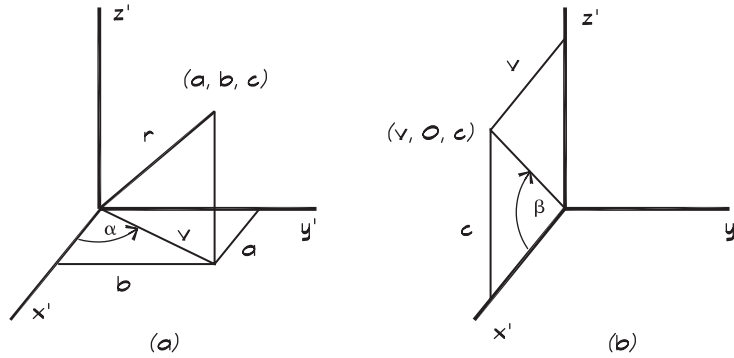
where

$$r_p = \sqrt{\left(x_{\mathbf{p}}'\right)^2 + \left(y_{\mathbf{p}}'\right)^2 + \left(z_{\mathbf{p}}'\right)^2} \qquad (18.50)$$

As outlined in Fig. 18.25, we align the x' axis with the aim point unit direction by first rotating the coordinate system around the z' axis by the angle α

$$\cos \alpha = \frac{a}{v} \qquad (18.51)$$

where

$$v = \sqrt{a^2 + b^2} \qquad (18.52)$$

This puts the loudspeaker system's x' axis in the same plane as the loudspeaker's z' axis and the aim-point vector.

Next we rotate around the new y' axis using Eq. 18.43 by an angle

$$\sin \beta = c \qquad (18.53)$$

This places the loudspeaker coordinate system collinear with the vector $\mathbf{x}_{\mathbf{p}}'$. Finally we rotate around the new loudspeaker x' axis by the loudspeaker rotation angle, γ. This last transformation establishes the loudspeaker coordinate system. The z' axis is collinear with the loudspeaker vertical, the y' axis is in the horizontal plane of the loudspeaker, and the x' axis is collinear with the aim point.

The transformation matrices may be applied sequentially so that a given receiver location, x, y, z, in room space becomes a transformed, x', y', z', in loudspeaker space according to the formula

$$\mathbf{x}' = \mathbf{R}_3 \, \mathbf{R}_2 \, \mathbf{R}_1 \, \mathbf{T}_1 \, \mathbf{x} \qquad (18.54)$$

where the transformation matrices are

$$\mathbf{T_1} = \begin{bmatrix} 1 & 0 & 0 & -x_s \\ 0 & 1 & 0 & -y_s \\ 0 & 0 & 1 & -z_s \\ 0 & 0 & 0 & 1 \end{bmatrix} \qquad \mathbf{R_1} = \begin{bmatrix} \cos\alpha & -\sin\alpha & 0 & 0 \\ \sin\alpha & \cos\alpha & 0 & 0 \\ 0 & 0 & 1 & 0 \\ 0 & 0 & 0 & 1 \end{bmatrix}$$

$$\mathbf{R_2} = \begin{bmatrix} \cos\beta & 0 & \sin\beta & 0 \\ 0 & 1 & 0 & 0 \\ -\sin\beta & 0 & \cos\beta & 0 \\ 0 & 0 & 0 & 1 \end{bmatrix} \qquad \mathbf{R_3} = \begin{bmatrix} 1 & 0 & 0 & 0 \\ 0 & \cos\gamma & -\sin\gamma & 0 \\ 0 & \sin\gamma & \cos\gamma & 0 \\ 0 & 0 & 0 & 1 \end{bmatrix} \qquad (18.55)$$

Applying these transformations yields

$$x' = (x - x_s)\cos\alpha\cos\beta - (y - y_s)\sin\alpha\cos\beta + (z - z_s)\sin\beta$$

$$y' = (x - x_s)(+\sin\alpha\cos\gamma + \cos\alpha\sin\beta\sin\gamma)$$
$$+ (y - y_s)(\cos\alpha\cos\gamma - \sin\alpha\sin\beta\sin\gamma) - (z - z_s)\cos\beta\sin\gamma \qquad (18.56)$$

$$z' = (x - x_s)(\sin\alpha\sin\gamma - \cos\alpha\sin\beta\cos\gamma)$$
$$+ (y - y_s)(+\cos\alpha\sin\gamma + \sin\alpha\sin\beta\cos\gamma) + (z - z_s)\cos\beta\cos\gamma$$

Directivity Angles in Loudspeaker Coordinates

Once the receiver is located in loudspeaker coordinates, $\mathbf{x'} = \begin{bmatrix} x', & y', & z', & 1 \end{bmatrix}$, the direction angles can be calculated directly. If ϕ and θ are the longitude and latitude of the receiver then $\mathbf{x'}$ can be written

$$x' = r_r \cos\theta$$
$$y' = r_r \sin\theta \cos\phi \qquad (18.57)$$
$$z' = r_r \sin\theta \sin\phi$$

where

$$r_r = \sqrt{(x_r')^2 + (y_r')^2 + (z_r')^2} \qquad (18.58)$$

Having transformed the coordinates, the directivity angles θ and ϕ follow

$$\theta = \cos^{-1}\left(\frac{x_r'}{r_r}\right) \qquad (18.59)$$

and

$$\phi = \tan^{-1}\left(\frac{z_r'}{y_r'}\right) \qquad (18.60)$$

From these angles along with the loudspeaker-directivity data and the loudspeaker-to-receiver distance we can determine the direct-field level associated with a given receiver location. A pictorial of the resultant coordinate system is given in Fig. 18.26.

FIGURE 18.26 **Loudspeaker Coordinate System**
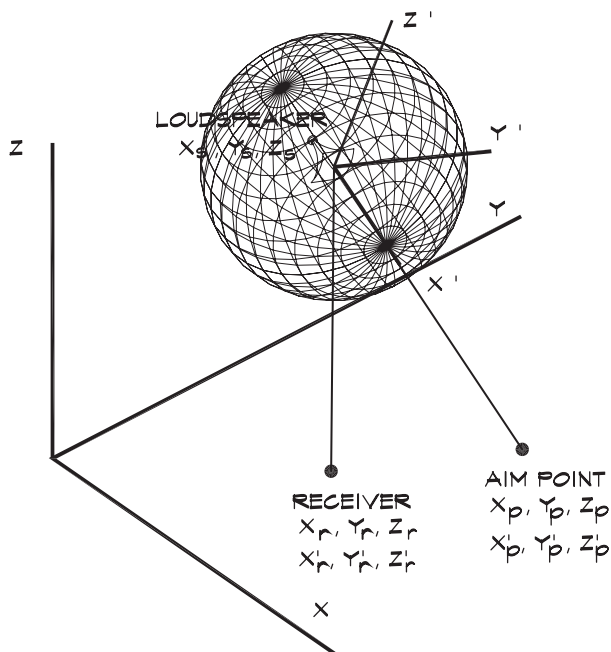
Multiple Loudspeaker Contributions

If the sound field due to several loudspeakers is present at a receiver location, the direct-field contribution from all sources may be combined to produce an overall direct field level. This can be done in several ways: 1) by adding the energy from each source in accordance with Eq. 2.62, 2) by combining signals in a coherent manner that accounts for the relative phase due to the difference in time, or 3) by coherently combining the energy and integrating over the frequency bandwidth.

An incoherent (energy) combination is the simplest methodology and is sufficiently accurate for most designs. It is inaccurate in that it does not account for the phase differences, but for most applications this is not a fatal flaw. The combined pressure squared is

$$p_{rms}^2 = \sum_{i=1}^{N} p_i^2 \tag{18.61}$$

where the index i runs over all loudspeakers covering a given receiver.

Coherent addition combines the pressures from multiple loudspeakers but also includes consideration of the phase

$$p_{rms}^2 = \left[\sum_{i=1}^{N} p_i \cos \varphi_i \right]^2 + \left[\sum_{i=1}^{N} p_i \sin \varphi_i \right]^2 \tag{18.62}$$

This calculation is carried out at one frequency, representative of the band, and requires an intimate knowledge of the phase of each loudspeaker in a given direction—data that

are not available. The time difference must include the travel time from the driver to the face of the loudspeaker, which is taken to be its location. It also requires the path-length difference between the actual sound path and the distance from the center of the mouth to the receiver. In addition it requires knowledge of the time delay for each loudspeaker due to any electronic processing in the system. Some of the delay may be due to the imposition of an electronic delay line in the signal path for time coincidence. Some may also be due to the time required to perform digital electronic manipulations associated with digital equalizers, crossovers, and other components, which use microprocessors to perform these functions. These delay times are rarely published by the equipment manufacturers but can range from 20 to 80 microseconds per device. In the final analysis, a coherent signal combination is an interesting theoretical exercise. It is only valid at one frequency, however, and relies on difficult assumptions on the directional path lengths and internal time delays of each device. The results obtained from this type of summation can overstate the degree of interference.

A third method has been proposed by JBL (2000) and is called the average complex sum. It uses coherent summation, but instead of integrating over the bandwidth it employs the center frequencies of the third-octave bands within the octave of interest.

$$p_{rms}^2 = \frac{1}{N} \sum_{j=1}^{N} \left\{ \left[\sum_{i=1}^{n} p_{ij} \cos \varphi_{ij} \right]^2 + \left[\sum_{i=1}^{n} p_{ij} \sin \varphi_{ij} \right]^2 \right\} \qquad (18.63)$$

This technique smoothes over many of the rough edges of coherent summation at single frequencies, and yields good agreement with measured results (JBL, 2000).

The phase can be defined in terms of the loudspeaker-to-receiver path length, r

$$\varphi_{ij} = 2 \pi \ \text{trunc} \left[\frac{r_i}{\lambda_j} \right] \qquad \text{(rad)} \qquad (18.64)$$

where the function "trunc" indicates a truncation of all numbers appearing to the left of the decimal point. Note that any time delays are included in the overall distance in Eq. 18.64.

This page intentionally left blank

DESIGN OF
ROOMS
FOR MUSIC

Rooms designed for unamplified music are the most visible and interesting spaces in architectural acoustics. It is here that the science of acoustics and the arts of architecture and music are blended. From the standpoint of acoustical design, the concert hall requires the most careful control, but gives the acoustician the fewest tools to accomplish the task. In contrast to sound system design, where a loudspeaker configuration can yield a very predictable result, the design of a hall for music requires the sculpting of a sound field without the ability to control the original sources, whose type, position, loudness, directivity, and number can change with every performance, or in some cases, with every note. The acoustician can only work indirectly with the room surfaces that reflect, diffuse, or absorb the primal energy. As a consequence he is left with only partial control, and general design principles to follow that have yielded good results in the past, rather than a fixed set of calculations that will produce a precise outcome.

19.1   GENERAL CONSIDERATIONS

The Language of Music

Beranek (1979, 1996), in his books on concert hall design, pointed out the importance of musicians and acousticians being able to communicate with one another. Like the British and Americans, these are two groups separated by a common language. In an attempt to provide a coherent vocabulary, Doelle (1972), Barron (1993), and Beranek (1996) have offered the definitions in Table 19.1.

Each musical term is associated with one or more acoustical properties of a performance space. Table 19.2 (Beranek, 1996; Barron, 1993) lists several of these relationships, whose properties will be explored in greater depth as we progress.

The Influence of Recording

Just as the natural acoustical properties of enclosed spaces have profoundly influenced music and the recording process, so too have electronic reinforcement and recording influenced the design of concert venues and the expectations of concertgoers. In a concert hall, the

TABLE 19.1   Definitions of Common Musical/Acoustical Terms

Term	Definition
Balance	Equal loudness among the various orchestral and vocal participants.
Blend	A harmonious mixture of orchestral sounds.
Brilliance	A bright, clear, ringing sound, rich in harmonics, with slowly decaying high-frequency components.
Clarity	The degree to which rapidly occurring individual sounds are distinguishable.
Definition	Same as clarity.
Dry or Dead	Lacking reverberation.
Dynamic Range	The range of sound levels heard in the hall (or recording). Dependent on the difference between the loudest level and the lowest background level in a space.
Echo	A long delayed reflection of sufficient loudness returned to the listener.
Ensemble	The perception that musicians are playing in unison.
Envelopment	The impression that the sound is arriving from all directions and surrounding the listener.
Glare	High-frequency harshness, due to reflections from flat surfaces.
Immediacy	The sense that a hall responds quickly to a note. This depends on the early reflections returned to the musicians.
Intimacy	The sensation that music is being played in a small room. A short initial delay gap.
Liveness	The same as reverberation, above 350 Hz.
Presence	The sense that we are close to the source, based on a high direct-to-reverberant ratio.
Reverberation	The sound that remains in a room after the source is turned off. It is characterized by the reverberation time, which has been previously defined.
Spaciousness	The perceived widening of the source beyond its visible limits. The apparent source width (ASW) is another descriptor.
Texture	The subjective impression that a listener receives from the sequence of reflections returned by the hall.
Timbre	The quality of sound that distinguishes one instrument from another.
Tonal Color	The balance between tones in different frequency ranges and the balance between sections of the orchestra.
Tonal Quality	The beauty or fullness of tone in a space. It can be marred by unwanted noises or by resonances in the hall.
Uniformity	The evenness of the sound distribution.
Warmth	Low-frequency reverberation, between 75 Hz and 350 Hz.

Table 19.2   Musical Terms and the Related Acoustical Factors

Musical Term	Acoustical Factor
Clarity	Reverberation time Early-to-late energy ratio Speed of the music
Intimacy	Initial delay gap Proximity to the musicians
Spaciousness	Apparent source width of early sound Listener envelopment by the reverberant sound
Timbre and Tone Color	Frequency balance in reflection and absorption
Color	Richness of treble Tonal distortion Texture Balance Blend Diffusion Focusing
Envelopment	Lateral reflections Reverberant sound
Ensemble	Musicians' ability to hear each other
Dynamic Range	Level of the fortissimo minus the background noise level
Warmth	Low-frequency reverberation

receiver's location determines the sound stage of his listening experience. In a rectangular room the listener is positioned facing the front of the orchestra, where the traditional arrangement of the instruments, with first violins to the left and cellos and basses on the right, is maintained. This is close to the listening experience presented by a high-quality stereo recording since the primary microphone pair is placed above the musicians near the front of the audience.

In a live performance the listener's experience is much more varied. Depending on his seat location and the shape of the hall, the orchestral sound can be quite different. Because of high-quality recordings, the audience may come with certain expectations about their musical experience. The sound of the highs in live performances is much less pronounced since close miking is employed in recordings. The concert hall designer may wish to increase the high-frequency reflections both to the audience in the center of the seating area, and to the players, to provide the extra detail that the listener has come to expect from recordings. This must be balanced against excessive brightness or glare produced by flat reflecting surfaces.

Concert Halls

Concert halls are rooms designed specifically for music in which the musicians and the audience occupy the same space. Classic concert halls are roughly rectangular and have one or more shallow balconies. In good concert halls the number of seats ranges

from 1700 to 2600, with the best halls averaging around 1850. Above 2600 seats, the chances of success are much reduced and the preferred capacity is between 1750 and 2200.

There is no division between the stage and the audience in a concert hall. The orchestra is positioned on a raised platform, sometimes with an organ and choir seating behind it. In classic rectangular halls such as Boston Symphony Hall (Fig. 19.17), there is an enclosure or shell surrounding the orchestra, which is located on one end of the room and extends nearly the full width of the room. Even in New York's Carnegie Hall (Fig. 1.23), which has the appearance of a traditional theater, the floor plan is rectangular with parallel side walls, and the orchestra shell extends out to the side wall. In surround halls, the orchestra is located toward the center of the room with the audience seating wrapped around it. There is no shell in a surround hall, although sometimes there is a wall on three sides of the orchestra and suspended reflectors overhead.

Seating in a concert hall includes a section of seats on the lowest level, about as wide as the orchestra, which runs front to back, sometimes stepping up into one or more balconies. In rectangular rooms most of the seating is located in this strip, whereas in surround halls the strip can be flanked by low side walls, which pick up the rectangular shape. In some rooms the seating rises in steps, like a vineyard cut into a hill, to minimize grazing attenuation. Rectangular rooms sometimes have one or more shallow side balconies, and surround halls can have a series of them.

Reverberation times in concert halls range from 1.5 to 2.2 seconds with preferred values between 1.8 to 2.0 seconds. Clearly the choices depend on the type of music and the volume of the space. Baroque music requires the lowest times (1.5–1.7 seconds), classical the mid-range (1.6–1.9 seconds), and romantic the longest (1.8–2.2 seconds). To attain long reverberation times, the ceilings of concert halls are high, 15 m (50 ft) or more, and diffusive, with coffered patterns having deep (15 cm or 6 in) fissures. Side walls are adorned with columns, caryatids, statuary, and convex shapes that help diffuse the reflected energy.

Opera Houses

An opera house is a mix of a legitimate theater and a concert hall, which constrains the design more than a pure concert hall. In opera, the stage performance rather than the orchestra is the main attraction. The stage house must be deep, with considerable wing space for set movement and storage. The fly tower above the stage, which accommodates the lifting of sets, is about one and a half times the height of the proscenium opening above the top of the arch.

The orchestra is seated in a pit below the stage to balance the level between the singer and the orchestra. The conductor, who must be visible to both the orchestra and the vocalists, stands with his head just at stage level. Open pits, where the orchestra is open to the audience with minimal stage overhang, give the best results in large rooms. In small auditoria some stage floor overhang is necessary to control the loudness.

Sight lines are important for theater, so opera houses tend to be shallower than concert halls. The furthest seat is no more than 30 m (98 ft) from the stage and 30° from the nearest side of the stage opening. Traditional European opera houses are horseshoe-shaped, with many tiers of box seating, stacked like a layer cake. The average seating capacity is about the same as in concert halls but smaller rooms are preferred since the vocal effort required of the singers is much less. Nevertheless a number of the most successful opera houses are relatively large, including Theatro Alla Scalla in Milan (2289 seats; Fig. 19.22), the

Metropolitan in New York (3816 seats; shown in Fig. 1.22), and the Theatro Colon in Buenos Aires (2487 seats; Fig. 19.21). Financial demands push these facilities toward larger capacities, particularly in the United States, where there is little public money available for the arts.

In opera houses most of the action takes place down stage near the center. Singers need an area where they receive adequate reflected energy returning from the room. Consequently the walls surrounding the forestage are often nearly parallel and decorated with large ornate elements such as columns and balconies. These provide diffusion and serve to create a local reverberant field where the performers stand. Reverberation times in opera houses are shorter than in concert halls, between 1.2 and 1.5 seconds. European theaters tend to fall into the low end of this range. Festspielhaus in Bayreuth, Germany (Fig. 1.16), which was built by Richard Wagner for his romantic music, is one exception with a reverberation time of 1.55 seconds occupied.

The traditional opera-house form has served us well, and opera halls have not seen the experimentation that has occurred in concert halls. The classic U-shaped Baroque theater still provides the most common model.

19.2   GENERAL DESIGN PARAMETERS

The Listening Environment

The ideal listening environment for live music depends to some degree on the type of music being played. There are, however, a number of common elements about which there is general agreement.

1. The audience should feel enveloped or surrounded by the sound. This requires strong lateral reflections with a significant fraction of the energy arriving from the side.

2. The room should support instrumental sound by providing a reverberant field, whose duration depends on the type of music being played. A reverberation time that rises with decreasing frequency below 500 Hz yields a beneficial sense of musical warmth.

3. There must be clarity and definition in the rapid musical passages so that they can be appreciated in detail. This requires reflections from supporting surfaces located close to the source or receiver so that the initial time delay gap is short.

4. Sound must have adequate loudness that is evenly distributed throughout the hall. When the number of seats becomes excessive (above 2600 seats), loudness and definition are reduced. In small auditoria the loudness must not be overbearing.

5. A wide bandwidth must be supported. Musical instruments generate sounds from 30 Hz to 12,000 Hz, which is much broader than the speech spectrum. The room must not color the natural spectrum of the music.

6. Noise from exterior sources and mechanical equipment must be controlled so that the quietest instrumental sound can be heard. Background noise levels should not exceed NC 20 in small halls and NC 15 in large concert halls.

7. The detailed reverberation characteristics of the space should be well controlled with a smooth reverberant tail and no echoes, shadowing, coloration, or other defects.

8.   The performers should have the ability to hear each other clearly and to receive from the space a reverberant return that is close to that experienced by the audience.

Hall Size

If there is a generalization about concert hall seating capacity then it is the architectural homily, "less is more." Seating capacity pays the rent so there is always pressure to increase it, particularly if there is no other source of funding. The stubborn fact still remains that the best concert halls have low seating capacities and a rectangular shape. The average seating capacity for the top nine halls in Beranek's 1996 study was about 1850, with the highest and lowest not included in the average. By contrast the average seating capacity of the eight least-liked halls (also with highest and lowest number excluded) was 2800. It is far easier to design a good sounding concert hall in the 1750 to 2200 seat range than at higher numbers.

Hall Shape

The most commonly encountered shapes in concert hall design are summarized in Fig. 19.1. The most consistent performer is the rectangular or shoebox floor plan. In Beranek's (1996) review of concert halls, the three halls rated A+, and six of the top eight have this basic form. A rectangular room provides the strong lateral reflections necessary for envelopment as a natural consequence of its shape. Narrow halls also yield low delay times for early reflected sound.

Surround halls can give the architect more freedom of expression, but less acoustical consistency than the standard forms. Any of the basic shapes can be built in a surround configuration by moving the orchestra platform toward the center of the room and arranging seating around the side and the rear. Berlin Philharmonic Hall is a typical example. It has a dazzling appearance but inconsistent acoustics (Beranek, 1994). When sitting on the side, the orchestral balance is changed and the traditional sound stage is rearranged. When the audience is behind the orchestra the spatial relationships are reversed and the balance is very uneven. French horns dominate and vocalists can be difficult to hear.

Surround halls are popular with architects and selection committees due to their dramatic appearance. Interestingly enough the overall hall shape is not infrequently chosen by the selection committee either by specifying the style directly or by selecting an acoustician based on a preference for the desired type. There are recently designed halls such as McDermott (Fig. 19.20) in Dallas, which combine traditional features such as a rectangular shape, narrow width, low seating capacity, overhead reflectors, and still provide interesting design elements.

Hall Volume

Hall volume influences both the reverberation time and room gain. At low capacities a high volume per seat is necessary to control excessive loudness. At higher capacities a low volume per seat helps preserve acoustical energy. Figure 19.2 gives the volume per seat of a number of the better-known halls. In general there is a tendency toward lower volume per seat numbers with increasing seat count; however, there is a wide range of volume per seat values that have produced good results. Each hall designer has his own preference. Those who prefer the model of Boston Symphony Hall cluster around 250 cu ft (7 cu m). Several surround halls, following the Berlin Philharmonic Hall model, are around 320 cu ft (9 cu m). Recent halls such as McDermott in Dallas, and Birmingham Symphony Hall with openable reverberation

FIGURE 19.1 Simple Plan Forms for Concert Halls in Normal and Surround Configurations

a) Shoebox

b) Fan

c) Diamond

d) Horseshoe
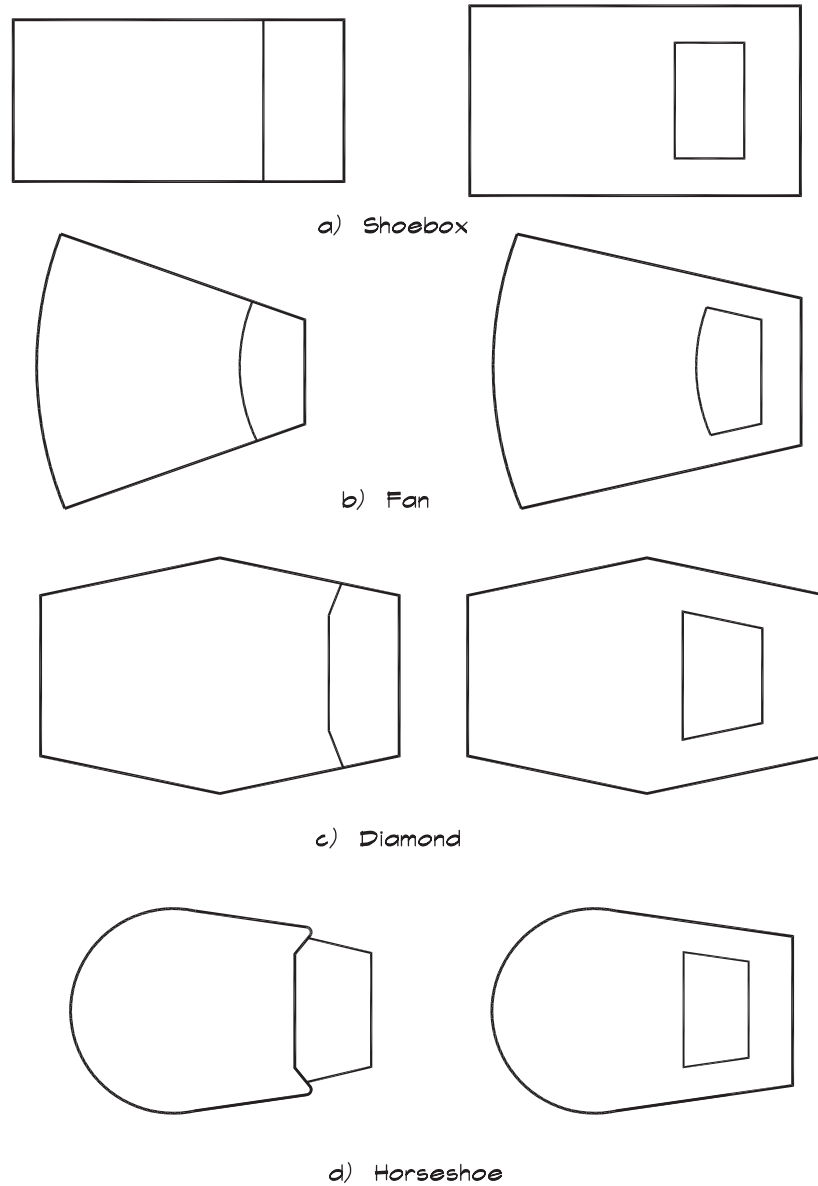
chambers, are at or above 400 cu ft (11.3 cu m); these also feature a large moveable reflector above the orchestra which offsets some of the effects of a high volume.

Surface Materials

Heavy plaster is the most commonly encountered wall and ceiling material used in concert and opera halls. In buildings more than 100 years old it was convenient since it could be worked in a semi-liquid state and would dry to a hard surface. Backings in these old buildings

FIGURE 19.2 Volume per Seat for Several Halls
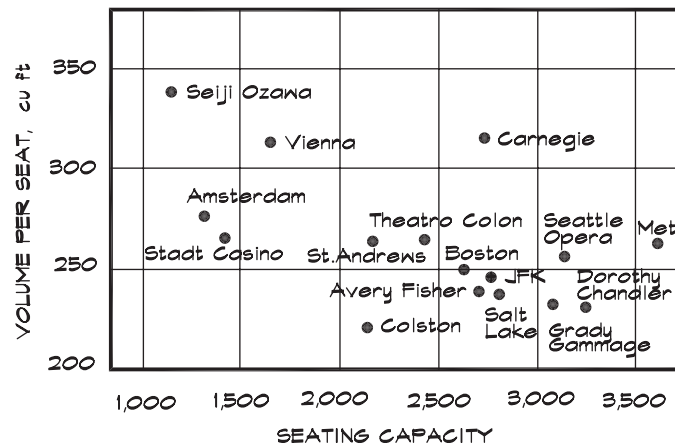
were mostly brick or wood lath. In Amsterdam it is reeds, and the plaster surface sounds dull or damped when tapped (Beranek, 1996). In newer buildings the backing is metal or gypsum lath. Plaster may also be applied directly onto grouted concrete block or concrete. In a standard application it is trowelled on in three coats—called scratch, brown, and finish—to an overall thickness of 7/8" (22 mm). Each coat is allowed to dry before the next is applied. In some cases thicker plaster, up to 2" (52 mm), has been used. The thicker the plaster and the stiffer the backing, the lower the bass absorption.

When wood is used it should be heavy, at least 1" (25 mm) thick, and be backed with a solid masonry or concrete structure. Thin wood panels over an airspace are very absorptive in the lower frequencies. Wood can be glued directly to concrete block or concrete walls or applied on furring strips. These have the advantage of allowing the surface to be faired but leave an air gap, which can be filled with pressed fiberglass board. Some designers prefer multiple wood layers of random widths, backed by randomly spaced support members. In practice the variation in spacing can be only a few inches because of structural considerations.

Floors are constructed of concrete or wood on concrete. When floors are concrete, the aisles are covered with a thin carpet walking surface. Wood floors are applied in two layers, for example a 3/4" (19 mm) finish floor on 3/4" plywood subfloor on wood sleepers over concrete. In Amsterdam the space between the sleepers is filled with 1.5" (4 cm) of sand.

Balconies and Overhangs

A balcony brings the audience closer to the musicians and improves sight lines, while dividing the room vertically into separate spaces. Under a deep balcony there is less reverberant energy and the listener has less sense of envelopment and a lower reverberation time. As a consequence under-balcony spaces should be shallow and the front openings high. Figure 19.3 gives recommendations in terms of the ratio of the height to depth ratio. Beranek (1962) suggests a D/H ratio of no more than one for concert halls and no more than two for opera. Barron (1993) recommends that there be a direct line of sight between the rearmost listener and overhead reflecting surfaces and that the angle between the listener and these surfaces not be less than 45° in concert halls and 25° in opera houses.

FIGURE 19.3 Designs for Balcony Overhangs
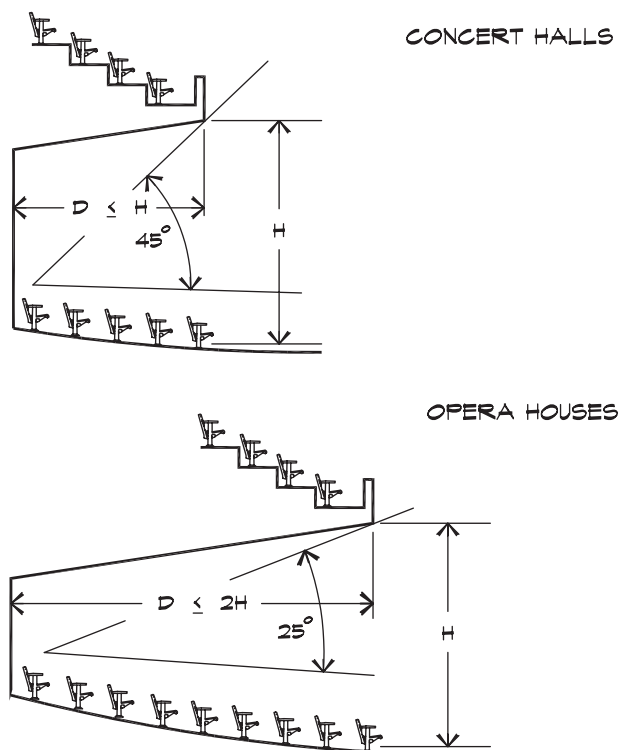
The greater the balcony overhang the more it cuts the listener off from the reverberant energy in the main portion of the hall, and the shorter the early decay time. Barron (1993) has measured early decay times under balconies and has compared them to those taken in the open part of the hall. His results are given in Fig. 19.4. Knudsen (1965), at Grady Gammage Hall in Tempe, Arizona, designed a flying balcony to allow reverberant energy to pass behind the upper balcony to reach those seated below. He wrote that in the rear seats the audience received the same sense of envelopment as in the orchestra seating area. A semi-cylindrical cavity under the balcony can help offset the lack of reverberant sound by creating some local reverberant focusing. A rising extension of the front part of the balcony can also be helpful for gathering acoustic energy and reflecting it to the rear.

Seating

In large auditoria the biggest absorbing surface is the seated audience. Since it is desirable to maintain a consistent acoustical environment, no matter the number of people, it is most important to use seats whose absorption characteristics closely resemble that of a seated occupant. Concert hall and opera house seats should be padded so that there is little acoustical variation between the rehearsal and the performance. The overall absorption of an audience area is based on the floor area occupied by the opera chairs, rather than the number of seats (Beranek, 1996). This area is increased by 0.5 m (or half the aisle width) on each side to account for the absorption of the exposed edges. Beranek emphasizes the importance of minimizing the area covered by the audience to provide adequate reverberation at minimum

FIGURE 19.4 Under Balcony Early Decay Time T_E (Barron, 1993)
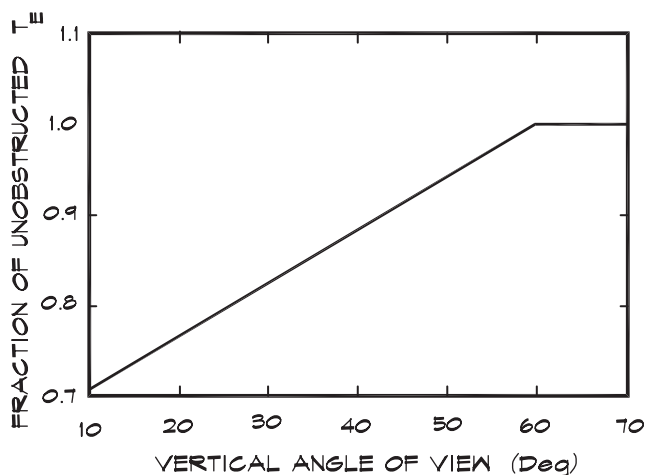
TABLE 19.3   Smoothed Average Absorption Coefficients of Seating (Beranek and Hidaka, 1998)

Type of Seat	Octave Band Center Frequency (Hz)					
	125	250	500	1k	2k	4k
Unoccupied with the weight of upholstering noted						
Heavy	0.70	0.76	0.81	0.84	0.84	0.81
Medium	0.54	0.62	0.68	0.70	0.68	0.66
Light	0.36	0.47	0.57	0.62	0.62	0.60
Occupied						
Heavy	0.72	0.80	0.86	0.89	0.90	0.90
Medium	0.62	0.72	0.80	0.83	0.84	0.85
Light	0.51	0.64	0.75	0.80	0.82	0.83

room volume. He feels that the ratio of the room volume to the seating area is a more useful figure of merit than volume per seat.

The absorption coefficients of seats show considerable variation, which depends on the thickness of the padding. Beranek and Hidaka (1998) have made a comprehensive study of the absorption coefficients of padded seats based on measurements taken in ten halls, before and after the installation of seats. Data were measured for both the occupied and unoccupied conditions. Table 19.3 gives their results grouped according to the amount of padding.

It is interesting that there are residual differences between seats having a different thickness of padding even in the occupied condition. Descriptions of the padding are given in Table 19.4.

TABLE 19.4   Upholstery Details (Beranek and Hidaka, 1998)

Type of Seat	Front Side of Seat Back	Rear Side of Seat Back	Top of Seat Bottom	Arm Rest
Heavy	7.5 cm	Sometimes	10 cm	2 cm
Medium	2.5 cm	0	5 cm	Solid
Light	1.5 cm	0	2.5 cm	Solid

As sound propagates over the seats of a theater it is found that there is an extra attenuation above that which would be expected from distance and high-frequency grazing losses. This extra attenuation is centered on 125 Hz and appears as a deep dip in the attenuation versus frequency response curve. A typical example is shown in Fig. 7.44 (Schultz and Watters, 1964). Ando (1985) has analyzed this effect and has related it to a change in the impedance due to the depth of the seats. He has proposed various solutions, including cavities in the floor and several geometrical alternatives. There is little measured field data available to determine the effectiveness of his suggestions.

One way of reducing the effect is to provide strong overhead reflections from the ceiling or from hanging reflectors. In mixed-use theaters and auditoria, low reflective ceilings are not difficult to include, however in concert halls, side wall reflections are more important and the ceiling is high and designed to diffuse sound. Overhead clouds can be helpful, however they must be of sufficient extent that they provide reflections down to 125 Hz. Another way to minimize seat dip is to group the opera chairs in clusters, which are stepped up and separated by low walls to block the reflected wave. This is called vineyard-step seating since it resembles the planting style found in hillside vineyards. A third way is to elevate the orchestra on a raised platform like those in Amsterdam or Boston to increase the grazing angle.

Platforms

Space must be provided for the musicians in a configuration where they can hear and be heard. The amount of floor space provided for the orchestra is a compromise between comfort and acoustics. This is not to say that acoustical excellence requires us to torture the musicians, but smaller stages generally yield better sound. Beranek (1962) recommends 20 sq ft (1.9 sq m) per musician, which yields a platform size of 2000 sq ft (190 sq m) for a 100 piece orchestra. Platforms in many of the best halls are considerably smaller. Vienna Musikvereinssaal has 1750 sq ft (163 sq m); Amsterdam, 1720 sq ft (160 sq m); and Boston, 1635 sq ft (152 sq m).

Barron (1993) recommends a floor area, which varies with the type of instrument:

13.5 sq ft (1.25 sq m) for upper string and wind instruments
16 sq ft (1.5 sq m) for cellos and larger wind instruments
19 sq ft (1.8 sq m) for double basses
108 sq ft (10 sq m) for timpani and up to 216 sq ft (20 sq m)
More for other percussion

He calculates that a 100-piece orchestra would require an area of 1600 sq ft (150 sq m), and suggests that Beranek's 2000 sq ft (190 sq m) also allows space for soloists, additional

percussion, losses due to risers, and a 3.3 ft (1 m) strip in front of the orchestra. Barron (1993) reckons that a choir needs 5.4 sq ft (0.5 sq m) per seated member, so a 100-voice choir would occupy 540 sq ft (50 sq m) of additional space. The choir seats can be positioned behind and on either side of the orchestra and are available to the audience when not in use. The quality of the sound in these seats is a compromise at best.

The orchestra platform should not be too deep, at most 35 to 40 ft (11–12 m), which results in a width of about 56 ft (17 m) based on Beranek's recommended area. Musicians like to spread themselves out and move forward toward the audience. Conductors frequently feel that moving an orchestra into the audience will improve the sound, but this is not always the case. It is important to keep the players close together and near the rear wall of the platform shell or enclosure, as long as it is not too deep. The double basses should be arrayed along the back wall both to enjoy the benefits of the reflection and to form a line source, which directs sound out toward the audience. Moving the orchestra against a solid reflecting surface is helpful for improving projected level, bass, and ensemble.

The platform floor material is universally wood on wood sleepers. Musicians appreciate the resonance they feel returning from the floor; however if the surface is too thin it will absorb airborne bass energy and if it is too thick it will not vibrate enough. A compromise suggested by Barron (1993) is 7/8" (22 mm) wood on wood sleepers spaced 24" (600 mm) on center. Beranek (1996), in his review of the construction of many halls, found that platform floor thickness ranged from 1/2" (13 mm) to 2" (52 mm). The depth of the airspace below the floor also varied considerably.

Risers are important to minimize shielding of the instruments in the back. Risers that are arranged in a semicircular pattern around the conductor provide an unencumbered path for the direct sound and allow good visual contact between the conductor and the players. The riser must be deep enough to accommodate both the musician and his music stand comfortably. Barron (1993) suggests a horizontal depth of 4 ft (1.25 m) for the upper strings and woodwinds, 5 ft (1.4 m) for brass and cellos, and slightly more for the brass. If the choir is placed on risers, 28" (0.7 m) is needed for a standing vocalist and 32" (0.8 m) for a seated one. The timpani and percussion need a level area about 10 ft (2.8 m) deep. Barron recommends a rise of 4" (100 mm) per step for woodwinds and slightly more further back.

The height of the stage in a theater is just below the eye level of the first row, which is about 44" (1.1 m). In a musical setting, sight lines are less critical and the platform can be higher. A higher platform helps with grazing attenuation and allows the sound to interact with the side walls in a horizontal plane. In Boston, for example, the stage is 54" (1.4 m) high and in Amsterdam it is 59" (1.5 m).

Orchestra Shells

The ability of the orchestra to hear itself is one of the most underrated factors in concert hall design. Where the orchestra is located on a platform surround by a shell such as that in Boston or New York's Avery Fisher Hall, the support provided by the ceiling and walls of the shell generates strong reflections back to the musicians, allowing them to hear themselves and each other. Therefore a goodly fraction of the overhead surface of the shell should direct the sound downward, either specularly or by means of large diffusing elements.

When the orchestra is located near the center of the room, ceiling reflections are not strong and orchestral balance is harder to achieve. In these cases panels or clouds can be

suspended below the ceiling to help generate early reflections back to the players. Individual reflectors are formed from convex sheets or discs, and are located 6 to 8 m (20 to 26 ft) above the musicians (Barron, 1993). A glass or Plexiglas surface, which produces a visible reflection of the other musicians, aids in their positioning (Nagata, 1997). When the room is narrow as in Vienna, the side walls and the overhang below the organ pipes give considerable support, which helps offset the absence of overhead reflectors. Very wide surround halls such as Berlin have low walls partially enclosing the orchestra platform on three sides, along with overhead clouds, to provide early reflections. In other surround halls like Dallas and Birmingham, the support is generated from a large overhead reflector, which can be raised or lowered according to the type of music.

In outdoor venues where the orchestra is miked, the main acoustical purpose of the shell is to provide a balanced sound onstage for the musicians. Sound that reflects out to the audience leaves the platform area and is not available to the orchestra or to the microphones. The shell at the Hollywood Bowl, a large outdoor amphitheater in Los Angeles, is a good example. It is very deep and shaped like truncated cone, which is useful for keeping the rain off, but can be an acoustical hindrance due to long delayed reflections and focusing.

A permanent shell, such as the one in Boston, is made from heavy wood or plaster, much like that of the walls and ceiling of the room. When a room has multiple uses, the shell is divided into sections, which must be light enough to be moved and stored. Permanent shells should be at least 1" (25 mm) thick wood. Portable shells can be as thin as 1/2" (13 mm) wood, but heavier materials are preferred. Where lighter materials are used it is helpful to construct shell surfaces of convex curved sheets with stiffeners in the rear to provide added structural support. Clearly the lighter materials provide less bass reflection but stiffeners help reduce panel movement and low-frequency absorption.

Pits

An orchestra pit is not normally part of a pure concert hall, but is quite important in opera halls and multiuse facilities. A pit functions to reduce the loudness of the orchestra relative to the singers and to provide a place where the musicians can be viewed by the conductor while being out of the sight of the audience. The musicians in the pit should be able to hear each other and the singers. The singers in turn must be able to hear the orchestra so that each can adjust their level to the other. Pit levels can be very high, particularly when the pit is partially enclosed. Absorbent materials lower the pit levels but also lessen the communication between players.

Pit design is difficult since the desired amount of level control depends on the size of the hall, the size of the orchestra, the ability of the singers, and the type of music. The space required is a little less than that necessary for a platform, about 16 to 18 sq ft (1.5 to 1.7 sq m) per musician. Pit orchestras tend to be smaller than concert orchestras with a few exceptions. The pit in the Metropolitan Opera House in New York, with an area of 1420 sq ft (132 sq m), accommodates up to 95 musicians and is approximately 25 ft (7.6 m) deep from the back wall to the front railing (Beranek, 1996).

Pits can be open or partially covered. A sketch of a basic pit configuration is given in Fig. 19.5. The top of the orchestra rail is at the same height as the stage. Where the pit floor is on a lift, it can be raised to form a thrust stage and act as a large freight elevator for sets and grand pianos. Open pits are located in front of the stage and have no stage overhang. Their depth, which must be sufficient to accommodate double basses, is between

FIGURE 19.5 Typical Opera Hall Pit Dimensions (Barron, 1993)
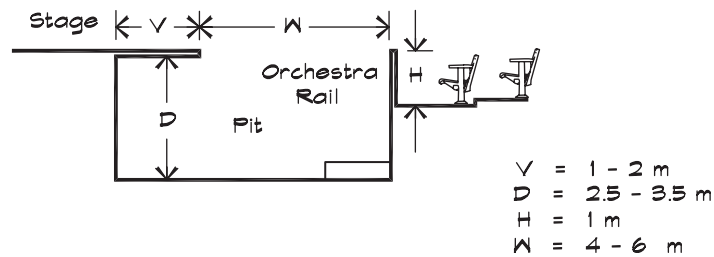
8 and 11.5 ft (2.5 to 3.5 m). The advantage of the open type is that the orchestral sound is unobstructed and the musicians have a better chance of hearing the singers and the sound in the hall. The disadvantages are that the orchestra can overwhelm the singers, there may be poor communication between players, and the lights on the music stands are visible to the audience. It also robs the theater of some very good seats.

A covered pit has its own set of design problems. Depending on the amount of overhang, which can vary from nothing in an open pit to as much as 16 ft (5 m) or more, the orchestra is increasingly isolated from the onstage activities and the audience. In small theaters this may not be a significant disadvantage since the orchestra must be muted, but in large houses it is problematic. With a large stage overhang the orchestra is in its own acoustic space with a separate reverberant field having a double slope. Barron (1993) estimates that the reverberation time in an orchestra pit ranges from 0.35 to 0.7 seconds in the early part of the decay curve. As the sound radiates out to the main room and returns, the late reverberation in the pit mirrors that of the hall.

The front wall of the pit enclosure acts as a barrier to the music for those seated in the first rows of the orchestra seating section. Barron (1993) has estimated the shielding based on floor slope (Fig. 19.6). He suggests that diffusing elements on the side walls and underside of the stage can help fill in the high frequencies in these areas. Overhead reflectors are helpful for the exposed players. If necessary, the orchestra can also be electronically reinforced. This is common practice in Broadway theaters, featuring musicals and light opera, but has not found its way into the classical opera house.

19.3 QUANTIFIABLE ACOUSTICAL ATTRIBUTES

Numerous attempts have been made to correlate subjective judgments of sound quality with objective measurements of acoustical attributes to establish a mathematically predictable assessment of concert halls. Opinion surveys by Beranek (1962), Barron and Lee (1988), and Haan and Fricke (1995), based on interviews with musicians, conductors, critics, and other knowledgeable concertgoers, were used to parse halls by perceived quality. Authors including Sabine (1900), Beranek (1962, 1992, 1996), Hawkes and Douglas (1971), Cremer and Muller (1982), Ando (1985), and Barron (1993) identified quantifiable attributes that contribute to the acoustical quality of concert halls. Beranek, in his early work (1962), identified eight objective factors and correlated them with the subjective judgments, assigning a weighting to the importance of each (Table 19.5).

FIGURE 19.6 Reduction of Sound Level Due to Diffraction over the Pit Rail for Two Floor Slopes (Barron, 1993)
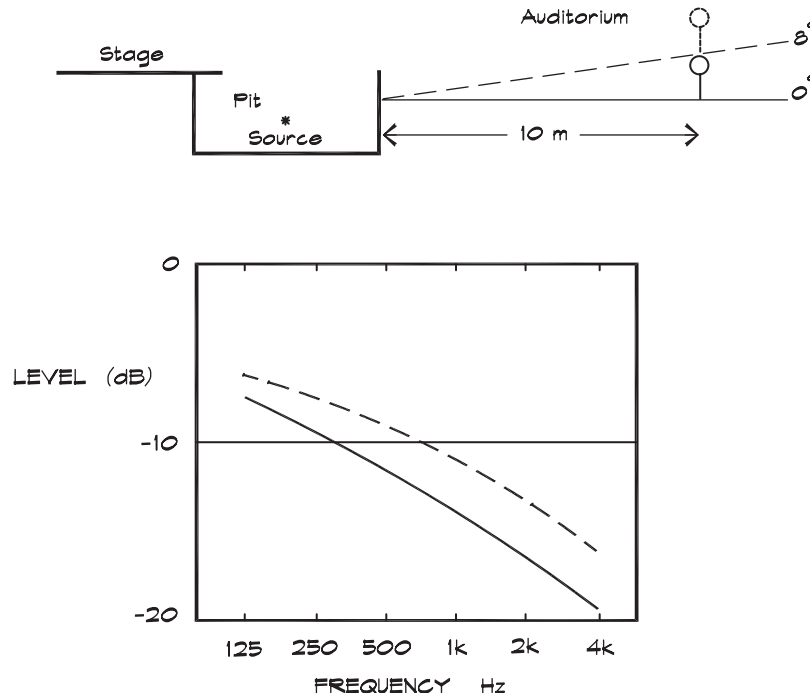
TABLE 19.5   Weightings of Acoustical Attributes (%) (Beranek, 1962)

Attribute	Concert Halls	Opera Houses
Intimacy	40	40
Liveness	15	15
Warmth	15	15
Loudness of Direct Sound	10	10
Loudness of Reverberant Sound	6	6
Balance and Blend	6	10
Diffusion	4	0
Ensemble	4	4
Total	100	100

Studies of Subjective Preference

Though studies based on recollection are useful, researchers wanted better controls and repeatability in the testing. They turned to subjective preferences, which consist of paired comparison tests carried out in a controlled listening environment. Subjects are presented

TABLE 19.6   Weightings of Acoustical Attributes (%) (Beranek, 1996)

Attribute	Concert Halls
IACC_{E3}	25
T_E	25
SDI	15
G_{mid}	15
t_I	10
BR	10
Total	**100**

where IACC_{E3} = interaural cross - correlation coefficient

T_E = early decay time (sec)

SDI = surface diffusivity index

G = difference between the level at a given point and the direct field level at 10 m for an omnidirectional source on stage (dB)

t_I = initial time delay gap (sec)

BR = bass ratio

with sounds by means of binaural headphones, or a three-dimensional array of loudspeakers. The sounds presented can be based on impulse functions recorded using a dummy head in a real hall or by a synthesized simulation using direct, reflected, and reverberant fields. The variables of interest are changed and presented to listeners in pairs so that the question is always, "Which do you prefer?"

In contrast to the comprehension of speech, where intelligibility can be measured one dimensionally, the appreciation of music in a concert hall is multidimensional. Hawkes and Douglas (1971) identified five dimensions (parameters) that have been expanded and refined since that time. These were clarity, reverberation, envelopment, intimacy, and loudness. Wilkens and Plenge (1974) cited three factors: loudness (47%), definition (28%), and appreciation (14%). In that study there was agreement on the attributes, but there was a bipolar preference in loudness with some listeners choosing a fuller sound and others a lighter one.

In his book on concert hall acoustics, Ando (1985) published a study of listener preferences done by playing music through a spherical array of loudspeakers in an anechoic room. Subjects were asked to express their preferences for several variables based on two pieces of music: motif A, Royal Pavanne by Gibbons; and motif B, Sinfonetta, Opus 48, III movement by Malcom Arnold. Based on these choices, Ando identified four orthogonal (independent) variables: loudness, reverberation, envelopment, and clarity, and developed a methodology for calculating each. Later Beranek (1996) added two more to the list: warmth, expressed in terms of the bass ratio (BR); and diffusion, in terms of a surface diffusivity index (SDI). He published the composite list with weightings given in Table 19.6.

The overall assessment of concert hall quality in Ando's scheme is calculated by means of a sum of weighted preferences

$$S = \sum_{i=1}^{N} S_i \qquad (19.1)$$

where

$$S_i = - a_i \left| x_i \right|^{3/2} \qquad (19.2)$$

and the a_i are the weightings. Each weighted preference has a maximum value of zero. The individual acoustical attributes (Beranek, 1996) are

$$x_1 = IACC_{E3} \qquad\qquad a_1 = 1.2$$

$$x_2 = 10 \log \left[t_I / (t_I)_{pref} \right] \qquad a_2 = 1.42$$

$$x_3 = G_{mid} - (G_{mid})_{pref} \qquad a_3 = 0.04 \text{ for } G_{mid} < 4.0$$

$$a_3 = 0.07 \text{ for } G_{mid} > 5.5$$

$$x_4 = \log \left[T_E / (T_E)_{pref} \right] \qquad a_4 = 9 \text{ for } T_E < 2.0 \text{ sec}$$

$$a_4 = 12 \text{ for } T_E > 2.3 \text{ sec}$$

$$x_5 = \log \left[BR / (BR)_{pref} \right] \qquad a_5 = 10 \text{ for } 2.2 \text{ sec}$$

$$x_6 = \log \left[SDI / (SDI)_{pref} \right] \qquad a_6 = 1$$

$$(19.3)$$

and the preferred values of each attribute are

$$(t_I)_{pref} = 20 \text{ msec or less}$$

$$(G_{mid})_{pref} = 4 \text{ to } 5.5 \text{ dB}$$

$$(T_E)_{pref} = 2 \text{ to } 2.3 \text{ sec}$$

$$(BR)_{pref} = 1.1 \text{ to } 1.25 \text{ for } T_{60} = 2.2 \text{ sec}$$

$$1.1 \text{ to } 1.45 \text{ for } T_{60} = 1.8 \text{ sec}$$

$$(SDI)_{pref} = 1$$

$$(19.4)$$

There is no preferred value for the IACC, but lower numbers are better than higher numbers. It should be noted that, with the addition of SDI to the attribute list, the quantities are no longer orthogonal. IACC is clearly related to diffusion (SDI).

The change from Beranek's 1962 assignment of 40% of a hall's total rating to intimacy, to his 1996 assignment of 40% to envelopment-related attributes, shows the subjective nature

of these rating schemes. Part of the difficulty is the assumption that subjective preference is additive. Under the presumption of linearity, theoretically a good score in one area can offset a bad score in another. It is equally arguable (Barron, 1993) that a long-delayed reflection or exterior noise can overwhelm the other good aspects of the design.

Modeling Subjective Preferences

Most of the acoustical attributes can be modeled relatively simply using direct and reverberant-field theory in a manner similar to that discussed in Chapt. 18. According to the simple two-field assumption, the relationship (metric) between sound power and sound pressure level is

$$L_p = L_w + 10 \log (Q / 4 \pi r^2 + 4 T_{60} / 0.161 \, V) \tag{19.5}$$

The sound pressure level at a given location may be written relative to the free-field level of an omnidirectional source at 10 m instead of the sound power level. This room gain, sometimes called the total sound level or the strength factor G, is given in metric units by

$$G = L_p - L_0 = 10 \log (100 / r^2 + 31200 \, T_{60} / V) \tag{19.6}$$

where

$$L_0 = L_w - 10 \log (400 \pi) \tag{19.7}$$

Note that these relationships are based on the Sabine reverberant field equation. In real rooms the falloff of level with distance is not always this simple. Field measurements taken in a number of halls led Barron and Lee (1988) to modify the traditional direct/reverberant field relationships since their measured data departed from predicted levels by about 2 dB on average. They found that the reverberant field levels decrease with distance from the source, although at a rate much less than in Fig. 8.14. The average falloff rate in their study was about 1 dB/10 m beyond a distance of 10 m.

Barron and Lee divide the sound fields into three categories: direct, early-reflected, and late-reflected energy, with the break point taken at 80 msec. The energy in each segment, relative to that at 10 m is

$$e_d = 100 / r^2 \tag{19.8}$$

$$e_e = (31200 \, T_{60} / V) \, e^{-0.04 \, r / T_{60}} \, (1 - e^{-1.11 / T_{60}}) \tag{19.9}$$

$$e_\ell = (31200 \, T_{60} / V) \, e^{-0.04 \, r / T_{60}} \, (e^{-1.11 / T_{60}}) \tag{19.10}$$

Note that the revised reverberant-energy levels decrease linearly with distance, resulting in a 3 dB reduction at 40 m from the source. The general behavior is given in Fig. 19.7.

Figure 19.8 shows measurements by Bradley (1991) of the room gain in three unoccupied concert halls, Concertgebouw in Amsterdam, Musikvereinssaal in Vienna, and Symphony Hall in Boston, which are regarded as among the best in the world. The three relationships fit the measured data much better than the traditional two-field theory although there are some interesting variations. For Boston the theory underpredicts G at the nearer locations and overpredicts the level at the more distant locations.

FIGURE 19.7 Theoretical Behavior of Various Temporal Components of the Sound Energy (Barron and Lee, 1988)
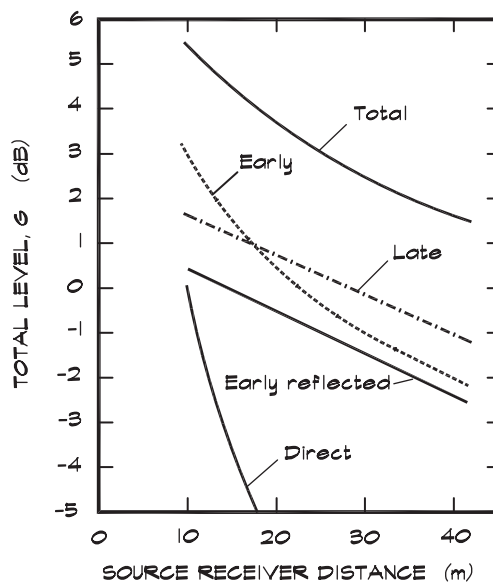
Early Reflections, Intimacy, and Clarity

The importance of early reflections has been recognized for some time. Vitruvius (1960), the Roman architect, extolled the value of what the Greeks called consonant sound or sound that is supported and strengthened by reflections from the stage and other nearby surfaces. Sabine (1964) referenced Vitruvius and also spoke of the need for reflections from surfaces that do not have too great a path length difference at the receiver. Beranek (1962) defined the initial time delay of the first reflection, t_I, as the property he calls intimacy. Barron (1993) gave a slightly different definition, which is the sense that music is being played in a small room. In his 1996 work, Beranek changed his definition, saying that it is the sensation that sound is being played in an appropriately sized room, which he characterizes primarily in terms of initial delay gap, but which also relates to loudness.

The initial delay time is the difference in milliseconds between the arrival time of the strongest reflection, minus the arrival time of the direct sound, at the center of the audience seating area. In 1962 Beranek considered this to be the most important factor in concert hall quality, assigning a maximum of 40 points to halls having an initial time delay of 20 msec or less, reducing credit linearly to zero when the gap is above 70 msec. In his later (1996) study this was reduced to 10 points maximum. He still maintained 20 msec as the threshold but held that beyond 35 msec quality suffered substantially. Ando's concert hall studies confirmed the importance of early reflections, although his test reflection was from the side, positioned at an angle about 36° from the centerline in the horizontal plane. Ando also found that the preferred initial delay time was just under 20 msec.

Barron (1993) reasons that intimacy is not precisely the same as early delay time. The sense that one is in a small room with the musicians is experienced by sitting near the players, irrespective of the delay. Indeed the gap is often greatest at locations closest to the orchestra.

FIGURE 19.8 Comparison of Measured 1-kHz G Values vs Source-Receiver Distance in Amsterdam, Vienna, and Boston (Bradley, 1991)

Open circles are on the main floor. Closed in the balcony.
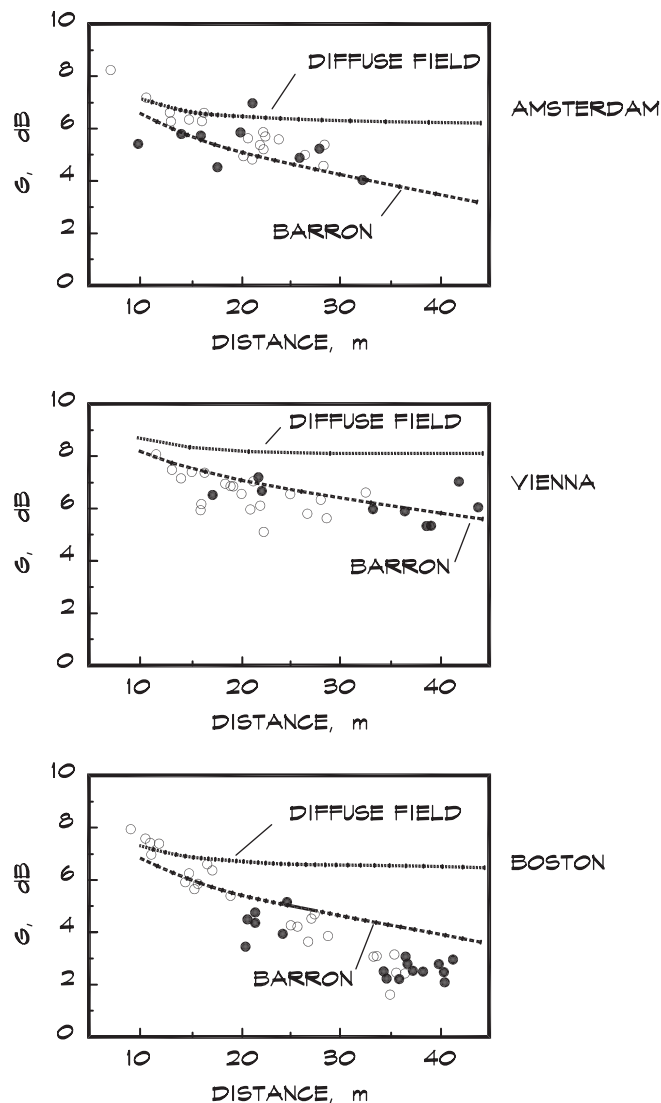
If intimacy were only dependent on the delay gap, he argues, the sound should always be more intimate at the rear of a hall, where the time gap is the smallest. Subjective surveys by Hawkes and Douglas (1971) and Barron (1988) have shown the opposite to be the case. Since the value of t_I depends on where the listener is seated, Barron also asks if it is appropriate to use a single number to characterize an entire concert hall. The difference here is primarily one of definition, since Beranek (1962) and Ando (1985) define intimacy as initial delay time, and Barron as the sense that one is in a small room.

The early-to-late signal-to-noise ratio, C_{80}, which was given in Eq. 17.40 in the chapter on speech intelligibility, is also used in musical acoustics. Called the clarity factor in concert

hall analysis, it is the ratio of the sound energy arriving before, to that arriving after, the first 80 milliseconds from the arrival of the direct sound, expressed as a level. It is measured in an unoccupied room and contains more information than the initial time delay, which does not account for the strength of the early reflections.

Using the three-segment model of Barron and Lee the C_{80} can be written as

$$C_{80} = 10 \log \left[(e_d + e_e) / e_\ell \right] \qquad (19.11)$$

Just as with speech intelligibility, a high signal-to-noise ratio, which results from strong early reflections, yields musical clarity. Values of the C_{80}, which can range from small positive numbers, implying a dead room, to small negative values for very reverberant spaces, fall into the ± 4 dB range. The preferred values of C_{80} are between 0 and -4 dB. Several highly successful halls: Boston, Amsterdam, and Vienna, have C_{80} (3) values (Beranek, 1996) that are between -2.7 and -3.7 dB. The (3) means that three C_{80} values, those in the 500, 1k, and 2k Hz octave bands, are averaged. Bradley (1991) has calculated occupied C_{80} values, which are reproduced in Fig. 19.9 for the three halls. The calculated values are based on measured unoccupied numbers in accordance with the relationship.

$$C_{80-o} = C_{80} + 13 \log \left[T_{60} / T_{60-o} \right] \qquad (19.12)$$

It is interesting to note how close the values are to one another.

Early reflections are important to the appreciation of rapid musical passages and passages played by the quieter instruments such as the harpsichord, recorder, and guitar. Convex surfaces are placed above the orchestra, at a height of around 20 feet, to provide reflections back to the musicians and the audience seated on the main floor. These surfaces should be arranged in the same plane to avoid Bragg scattering, discussed in Chapt. 7. For reinforcement over a wide frequency range, the individual panels should be relatively large, at least 6 feet (1.8 m) long, and arrayed across the entire width of the orchestra. A slight

FIGURE 19.9 Average of Measured C_{80} Values in Three Halls (Bradley, 1991)
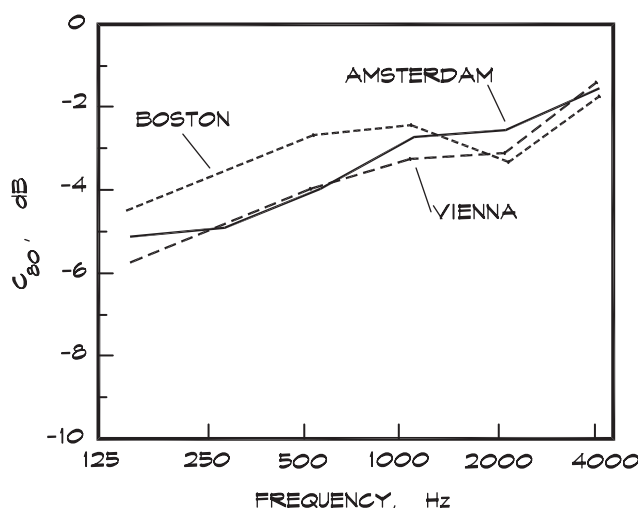
lateral convexity helps to fill in the gaps left by the space between panels. Longitudinal convexity compensates for changes in instrument or performer location. Cremer and Muller (1982) recommend a minimum open area of about 70%, with many small clouds being preferred to a few large reflectors, to insure coupling between the upper and lower volumes of the hall.

Sidewalls provide the necessary early reflections for the audience seated toward the rear of the concert hall. In rectangular rooms these are parallel. In surround halls local reflecting surfaces must be carefully crafted to fill in the needed reflections. The high ceiling is designed to be diffuse and thus is not particularly useful for this task.

Liveness, Reverberation Time, and Early Decay Time

Liveness or reverberation is the most recognizable acoustical parameter associated with concert halls. The reverberation time has been a useful metric since its discovery by Sabine. Although it is defined as the time required for the reverberant sound to decay 60 dB below the maximum, it is measured over a range of levels between -5 and -35 dB and then doubled. If it were measured over the full 60 dB range, the reverberant tail would run into the background noise and corrupt the measurement. In Table 19.5 liveness is assigned 15 points; in Table 19.6 it increases to 25 points. As we have discussed, liveness and clarity are not independent variables, which is why the latter was dropped in Ando's study of orthogonal preferences.

The early decay time is another measure of liveness. It is the reverberation time calculated from the initial portion of the room decay curve. Formally it is the time taken for the first 10 dB of level reduction multiplied by 6, making it comparable to the reverberation time. Early decay time varies less with occupancy than does the reverberation time and is measured without an audience. Beranek's (1996) data show a difference of about 0.3 seconds between the unoccupied T_E and the occupied T_{60} for the 52 halls surveyed

$$T_E \cong T_{60-o} + 0.3 \quad \text{(sec)} \tag{19.13}$$

although the differences in several of the best halls are larger. In both of Beranek's books the preferred reverberation times were 1.8 to 2.0 seconds for concert halls and 1.3 to 1.5 seconds for opera houses, although he notes that the range for successful opera houses extends as high as 1.7 seconds in Theatro Colon in Buenos Aires. Kuhl (1954) reported differences with the type of music: 1.54 sec for early classical music (Symphony No. 41 "Jupiter" by Mozart), 2.07 sec for romantic classical music (Symphony No. 4 by Brahms), and 1.48 sec for modern music ("Le Sacré du Printemps" by Stravinsky). Figure 17.10 gives general recommendations on reverberation times versus room volumes for various types of program material. Barron (1993) also lists a range of recommended reverberation times by type of music in Table 19.7.

Early decay time can be estimated from a closed formula such as the Sabine equation and Eq. 19.13; however, this does not separate the two. In concert hall design, early decay time is determined by measurements on models or by ray tracing. It depends primarily on the interactions with reflecting surfaces located near the orchestra. For Boston Symphony Hall, with 2600 seats, a volume of 662,000 cu ft (18,750 cu m), and a reverberation time of 1.85 seconds, the first 10 dB of reverberant room decay occurs in about 300 milliseconds. Equation 8.51 and rough dimensions, 172 ft (52 m) long × 76 ft (23 m) wide × 62 ft (19 m) high, allow the calculation of a gross surface area of 48,892 sq ft (4545 sq m) and a mean time between collisions of 48 msec. Thus in this room the early decay time is based only

TABLE 19.7   Recommended Occupied Reverberation Times (Barron, 1993)

Type of Music	Reverberation Time (sec)
Organ	> 2.5
Romantic classical	1.8 – 2.2
Early classical	1.6 – 1.8
Opera	1.3 – 1.8
Chamber	1.4 – 1.7
Drama (spoken word)	0.7 – 1.0

on the first six surface reflections for a given ray. Figure 19.10 gives examples of 1000 Hz early decay times measured at various positions in our three halls. It is interesting that in all three cases the measured values are lower close to the platform and increase with distance. Once the distance is greater than about 20 m the reverberation times flatten out and are constant.

Envelopment, Lateral Reflections, and Interaural Cross-correlation

Harold Marshall (1967) and Veneklasen and Hyde (1969) identified the importance of reflections that surround or envelop the listener with reverberant sound coming from the side. Later authors quantified these effects using the lateral energy fraction and the inter-aural cross-correlation coefficient (IACC). Strong side reflections are generated by narrow rectangular rooms and from surfaces placed close to the listener. Not surprisingly Ando's (1985) subjective preference studies showed a strong correlation between the IACC and room width.

The interaural cross-correlation is a measure of the similarity of sound arriving at two points—in this case, the two ears of the listener. Mathematically it is based on the interaural cross-correlation fraction defined as

$$IACF_t(\tau) = \frac{\int_{t_1}^{t_2} p_L(t)\, p_R(t + \tau)\, dt}{\left[\int_{t_1}^{t_2} p_L^2(t) \int_{t_1}^{t_2} p_R^2(t)\, dt\right]^{1/2}} \qquad (19.14)$$

where the L and R refer to the entrances to the left and right ear canals. The maximum possible value for $IACF_t$ is one, occurring when both signals are the same. The integration is done beginning from time t_1 measured from the arrival of the direct sound at one ear and ending at time t_2, which is selected arbitrarily depending on the period of interest. The variable τ accounts for the time difference between the two ears and is varied over a range from -1 to $+1$ msec from the first arrival. To obtain a single number the maximum value of Eq. 19.14 is taken

$$IACC_t = \left| IACF_t(\tau) \right|_{max} \qquad \text{for } -1 < \tau < +1 \qquad (19.15)$$

FIGURE 19.10   Measured 1 kHz T$_E$ Values vs Source Receiver Distance in Amsterdam, Vienna, and Boston (Bradley, 1991)
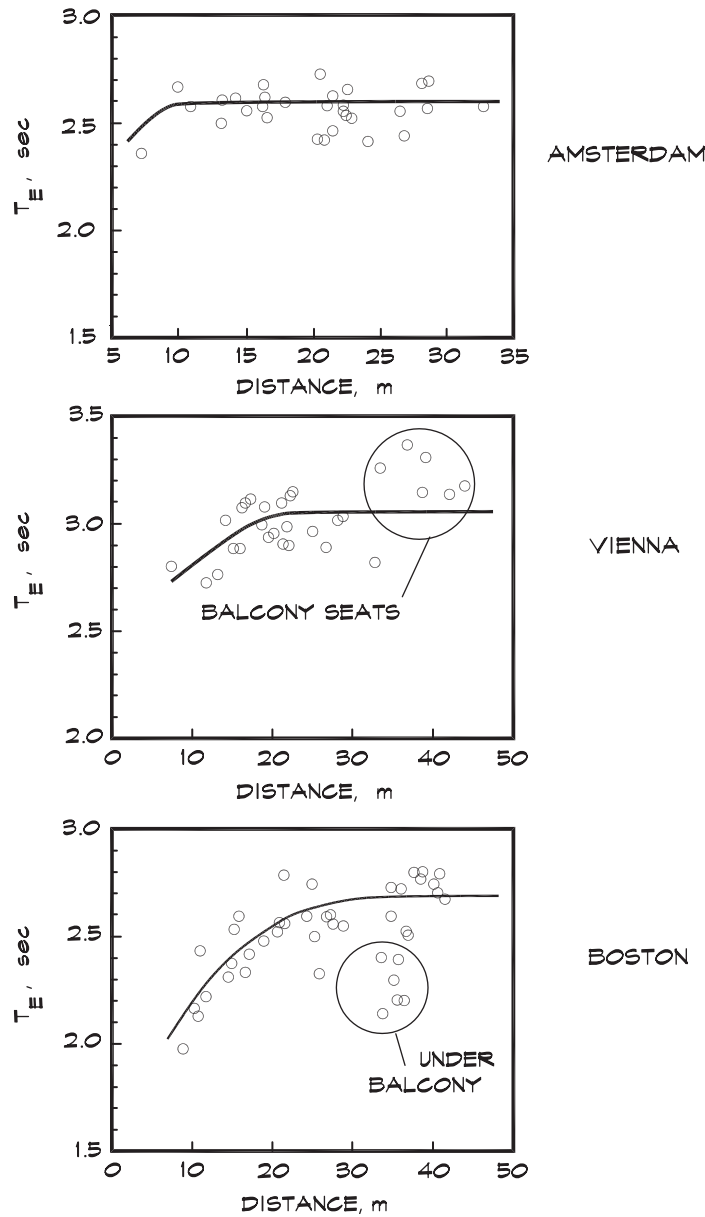
and is called the interaural cross-correlation coefficient. The integration time can be varied with different results. For $t_1 = 0$ and $t_2 = 1,000$ msec, the term is designated $IACC_A$. The early $IACC_E$ (0 to 80 msec) is a measure of the apparent source width (ASW) and the late $IACC_L$ (80 to 1,000 msec) is a measure of listener envelopment (Beranek, 1996).

Preferred values of the IACC are low, approaching 0.3, meaning that the sound arriving at each ear is only 30% correlated. The greater the difference, the higher the preference.

These coefficients are measured in the mid frequency octave bands (0.5, 1, and 2 kHz) and averaged. Data are often listed as (1 – IACC), for which higher numbers are better. Beranek (1996) lists data for 37 halls. The $(1 - IACC_{E3})$ numbers for three of the best are Boston Symphony Hall, 0.65, Amsterdam Concertgebouw, 0.62, and Vienna Gr. Musikvereinssaal, 0.71.

The strength of lateral reflections can be measured directly by using a second order bidirectional microphone, shown in Table 4.1, and then comparing it to an omnidirectional microphone. The figure-of-eight microphone, as it is called, is aligned so that its null direction points toward the source. The two signals are integrated out to 80 msec and compared

$$LF = \frac{\int_{.005}^{.08} p^2(t)\cos^2\theta\,dt}{\int_0^{.08} p^2(t)\,dt} \qquad (19.16)$$

The directional integration begins at 5 msec to insure that the direct sound is not included. The sound pressures are taken in the 125–1000 Hz frequency range. Okano, Beranek, and Hidaka (1998) have published a graph shown in Fig. 19.11 giving the relationship between IACC and the LF. Since they are highly correlated, one can be estimated from the other.

Lateral reflections and envelopment come about naturally from rectangular halls having widths on the order of 75 ft (23 m). A high degree of diffusion is particularly helpful, along with a shallow rake to the main floor seating area, which allows the sound to interact with the side walls in a plane above the audience. Deep overhanging balconies produce the opposite effect, cutting the audience off from the reverberant field in the rest of the room since the sound under the overhang only comes from the front.

FIGURE 19.11   Hall-Averaged Values of $(1-IACC_{E3})$ vs LF_{E3} as Determined in 28 Existing Concert Halls (Okano, Beranek, and Hidaka, 1998)
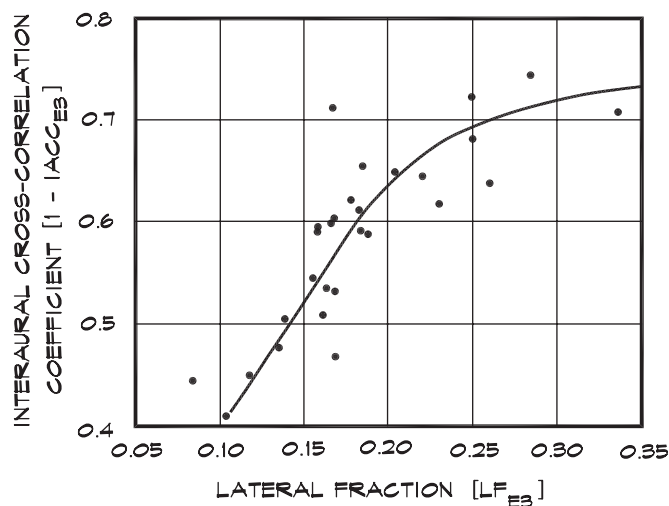
Loudness, G_{mid}, Volume, and Volume per Seat

The loudness of both the direct and the reverberant field sounds in a hall is quite important, especially in small recital halls where even a modestly sized orchestra can be overwhelming. Ando (1985), in his study of concert hall acoustics, identified loudness as one of the four orthogonal acoustical attributes. Listeners in that study preferred overall average maximum levels in the 77 to 79 dBA (slow) range for motif A and 79 to 80 dBA for motif B. Beranek (1996) recast this level preference in terms of the room gain, which is defined as the level of sound measured at any point in an empty hall due to an omnidirectional source located on stage, minus the free field (anechoic) level of the source at a distance of 10 m (33 ft).

$$G = 10 \log \frac{\int_0^{t_2} p^2(t)\, dt}{\int_0^{t_2} p_A^2(t)\, dt} \qquad (19.17)$$

where the subscript A indicates the anechoic or direct field. According to diffuse-field theory, the value of G_{mid} is proportional to the log of the total absorption in the space. Since the absorption is seldom measured directly, the room gain is computed from the ratio of the reverberation time to the room volume, both easily measured quantities. Figure 19.12 shows the relationship for a number of halls. This is written in terms of the Sabine equation for steady state ($t_2 = \infty$) condition in Eq. 19.6. When the room gain is averaged over the 500 and 1000 Hz octave-band values, it is known as G_{mid}. The average of the 250 and 125 Hz bands is G_{low}. Preferred values of G_{mid} are in the 5 ± 1 dB range. Above 5 dB halls can be overpowered by an orchestra, although two of the best halls, Concertgebouw (at 6.0), and Musikvereinssaal (at 7.0) have values above 5. Below 3.5 dB halls have too little gain.

Beranek (1996) argues that once the room gain and the reverberation time are chosen the volume is set through the relations given in Fig. 19.13, and the number of people by the absorption area from Fig. 19.14. To get to this point, Beranek assumes that the audience and orchestra represent 75% of the total absorption in a hall and that the average mid-frequency absorption coefficient is 0.85. The absorption area, S_T (sq m), is the combined area of the audience and the orchestra times a factor of 1.1 to account for the side absorption. The approximate formula (metric) for the occupied reverberation time using these assumptions is

$$T_{60-o} \cong 0.14\,(V / S_T) \qquad (19.18)$$

The need to control loudness is important and argues strongly for a volume per seat, which increases as the number of seats decreases. At low seating capacities a large volume per seat is necessary to control the loudness. At large capacities a low volume per seat is preferred to preserve precious acoustical energy.

Warmth and Bass Response

Bass reverberation, which is perceived as warmth, was one of the critical factors to come out of Beranek's 1962 book and was added to Ando's four orthogonal factors as part of his 1996 work. Beranek has quantified it in terms of the ratio between the average low-frequency reverberation times and those at the mid frequencies, a fraction that he defines

FIGURE 19.12   Measured Mid-Frequency Room Gain (Beranek, 1996)
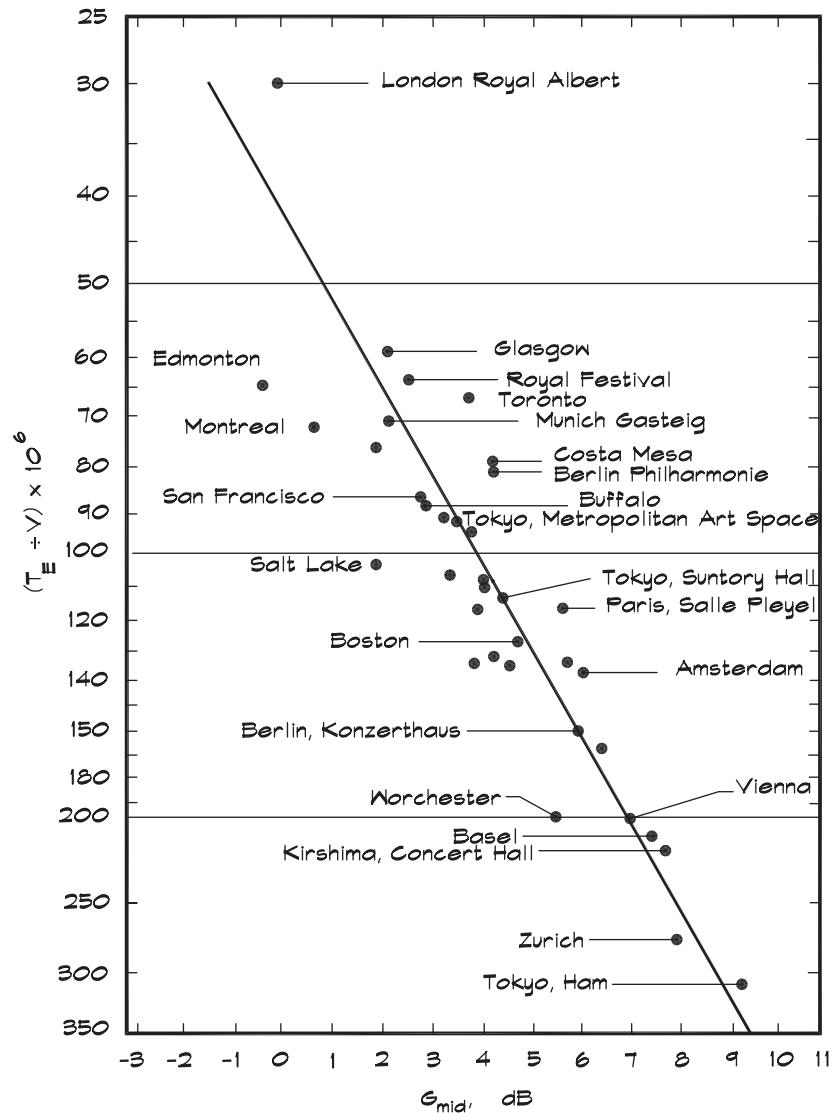
as the bass ratio

$$BR = \frac{T_{60}(125) + T_{60}(250)}{T_{60}(500) + T_{60}(1\,k)} \qquad (19.19)$$

Beranek (1996) cites bass ratios from 1.1 to 1.25 as being preferred for reverberation times of 2.2 seconds and ratios from 1.1 to 1.45 for reverberation times around 1.8 seconds. These generally are comparable to the curve given in Fig. 17.11. Occupied bass ratios for our three example concert halls are 1.09 (Amsterdam), 1.11 (Vienna), and 1.03 (Boston), which illustrate the difficulty in achieving high numbers. Vienna has large windows and both Amsterdam and Boston have wood floors over deep air spaces. In Amsterdam the orchestra

FIGURE 19.13 **Computational Chart for Determining the Volume of a Concert Hall (Beranek, 1996)**
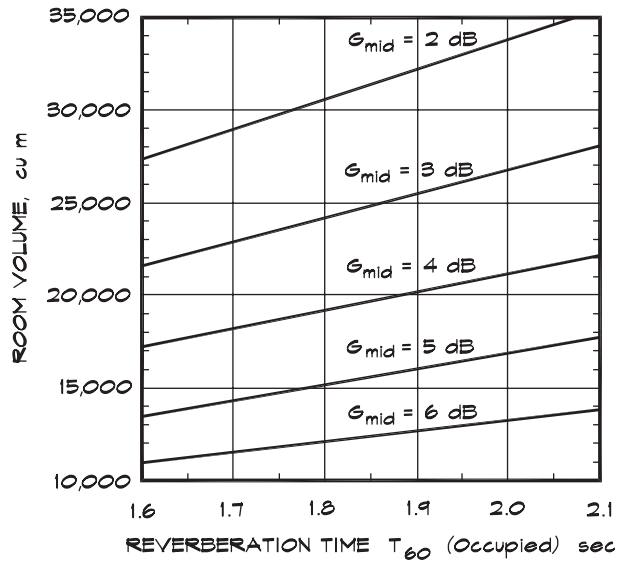
FIGURE 19.14 **Computational Chart for Determining the Acoustical Area of a Concert Hall (Beranek, 1996)**
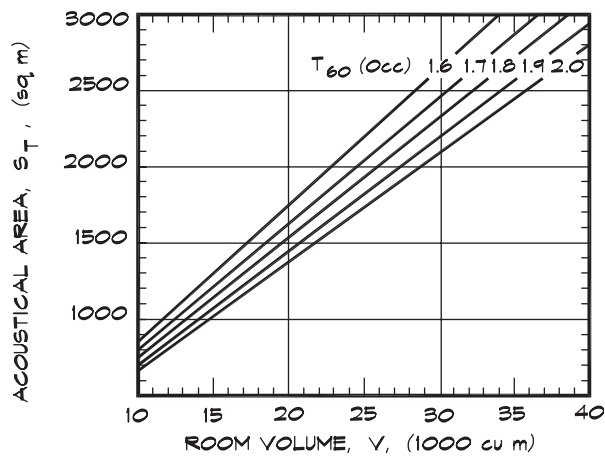
is placed atop a high (1.5 m) wood platform. In Boston the seating at the rear of the main floor is mounted on a removable floor of approximately 1" thick wood over an airspace about 2 meters deep. Each of these surfaces absorbs bass.

Bass reverberation is produced by very heavy materials such as 50 mm thick wood on a concrete or plaster backing, or a similar thickness of cement plaster. In halls such as McDermott in Dallas concrete reverberation chambers are used to augment the natural reverberation of the room. Thin surfaces of wood, drywall, and glass absorb low-frequency

energy and should be avoided. Where they are used as finish surfaces they should be glued directly to a backing of concrete or heavy plaster.

Diffusion, SDI

Diffusion, which is the scattering of sound in an omnidirectional rather than a specular pattern, is created by convex or irregular surfaces. The depth of the irregularity should be equal to or greater than a quarter of a wavelength to have appreciable effect at a given frequency. Diffusion contributes to envelopment, and the even distribution of reverberant sound. Beranek (1996) assigns 15 points to it in his rating scheme. Haan and Fricke (1997) relate hall quality, in part, to diffusivity based on a visual inspection. They assign a numerical value called the surface diffusivity index (SDI) to a surface as follows:

High Diffusivity (SDI = 1)

   Coffered ceiling with deep (> 100 mm or 4 in) recesses

   Random diffusing elements over the whole surface (> 50 mm or 2 in deep)

Medium Diffusivity (SDI = 0.5)

   Broken surfaces with shallow recesses (< 50 mm or 2 in deep)

   Flat surface behind a semitransparent hard screen

Low Diffusivity (SDI = 0)

   Smooth flat or curved surfaces

   Absorptive surface

Once the SDI has been established for a given surface the ratings for the whole auditorium are calculated based on a weighted average according to area.

   Although there is general agreement that diffusion is good, there is less certainty about the amount or type, and how to measure it. Researchers have struggled with the quantification problem, which is complicated since diffusion depends on the frequency and the angle of incidence of the incoming signal, and the receiver measurements must be performed at locations over the entire half-sphere surrounding the diffuser.

Ensemble, Blend, and Platform Acoustics

The supporting sound, that which returns to the orchestra, has been studied by Gade (1989a/b), Barron (1993), and others. Support is generated through reflections from nearby surfaces. The usual method of measurement is to use an omnidirectional source, located on the orchestra platform, and measure the return from reflecting surfaces with a microphone set at a distance of 1 m from the source. For an impulsive source such as a blank pistol shot, the energy will be returned as a series of scattered pulses. The ratio of the energy returned between 20 and 100 msec, compared to the initial level sampled between 0 and 10 msec (the direct level plus the reflection from the stage), is called the support factor (Beranek, 1996) and is a measure of the musician's ability to hear himself and others near him.

$$\text{ST1} = 10 \, \log \frac{\int_{.02}^{0.1} p^2(t) \, dt}{\int_{0}^{0.01} p^2(t) \, dt} \tag{19.20}$$

FIGURE 19.15 Support Factor Plotted against Platform Volume in 32 British Halls (Barron, 1993)
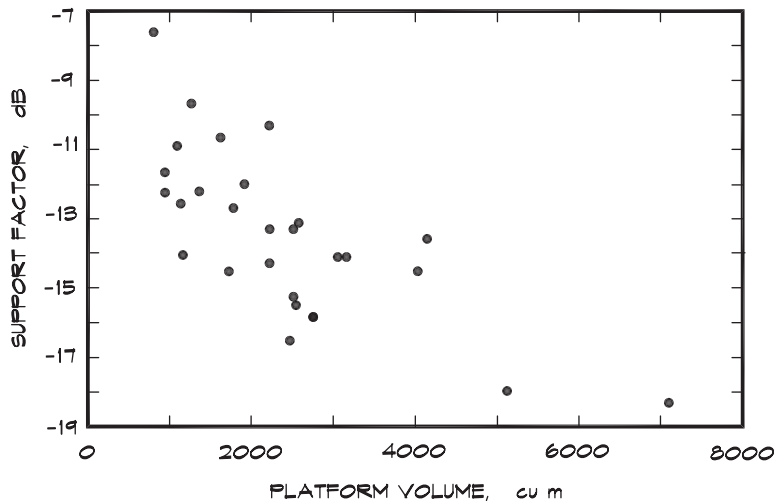
Gade (1989b) indicates that this parameter correlates well with the responses from musicians. Barron (1993) found that preferred values of the support factor range from -11 to -13 dB.

Gade (1989a) plotted objective support against platform volume (the platform area times the height to the ceiling or to suspended reflectors) in Fig. 19.15 for a number of British halls. The preferred volumes fall into the 1000 to 2000 cu m (35,000 to 70,000 cu ft) range, which gives us an idea of the reflector heights. Using diffraction theory it is straightforward to add the energies of each reflection within the time period to calculate ST1.

19.4   CONCERT HALLS

In his two comprehensive works, Beranek (1962 and 1996) compiled a substantial record of the design, materials, and statistics of concert and opera halls throughout the world. In 1993 Barron added a detailed survey of halls in Great Britain. Any designer can learn a great deal from a close examination of the drawings and photographs in these books. In this work we will examine a few examples, relying for the most part on data that Beranek compiled. From his definitions, in the following data tables L is the room length from the front of the platform to the average back wall position, D is the distance from the front of the platform to the most distant listener measured on or near centerline, W is the overall width, and H is the height from the lowest floor level to the ceiling above the audience.

Grosser Musikvereinssaal, Vienna, Austria

Generally considered the best in the world, the Viennese concert hall, which opened in 1870, is noted for its combination of low seating capacity and long reverberation time. Having a classic shoebox shape, shown in Fig. 19.16, its narrow width and ornate ceiling along with Oscar-like caryatids supporting the single balcony, provide an abundance of diffusing surfaces. Above the balcony are rows of highly decorated doors and deeply recessed windows that provide high-frequency scattering, along with the suspended crystal chandeliers.

FIGURE 19.16   Grosser Musikvereinssaal, Vienna, Austria (Beranek, 1996)
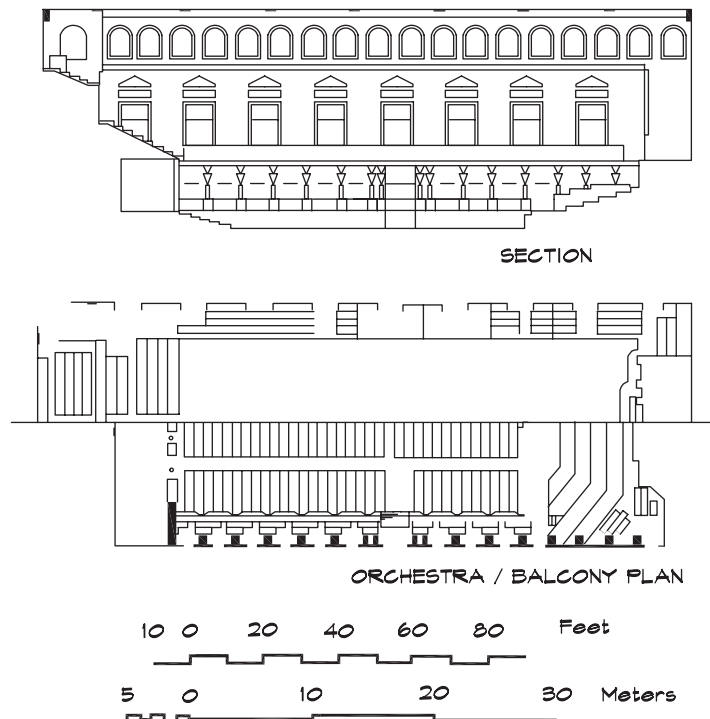
TABLE 19.8   Selected Technical Data for Grosser Musikvereinssaal (Beranek, 1996)

Attribute	Metric Units	FP Units
Volume (V)	15,000 cu m	530,000 cu ft
Dimensions (LWH)	35.7 m × 19.8 m × 17.4 m	117 ft × 65 ft × 57 ft
Furthest Seat (D)	40.2 m	132 ft
Seating Capacity (N)	1680	
Total Absorptive Area (S_T)	1,118 sq m	12,030 sq ft
V/N	8.93 cu m	315 cu ft
V/S_T	13.4 m	44 ft
T_{60} (Occ) = 2.0 s	T_E(Unocc) = 2.2 s	$(1 - IACC_{E3}) = 0.71$
t_I = 12 ms	G_{mid} = 7.1 dB	BR = 1.11
SDI = 1.0		
Architect: Theophil Ritter von Hansen		

The walls and ceiling are plaster, except around the stage, where the walls are wood. The side walls and balcony overhangs furnish early reflections to maintain clarity without suspended reflectors. Its low volume and minimal absorption yield the highest room gain of the three best halls.

Boston Symphony Hall, Boston, MA, USA

Boston Symphony Hall, shown in Fig. 19.17, was designed by Wallace Clement Sabine in the late nineteenth century, and opened in 1900. It has a classic shoebox shape, with a 54" (1.37 m) high raised platform, surrounded by a shallow shell at one end. The central feature of the orchestra enclosure are gilded organ pipes that span the rear wall of the shell and provide a reflecting shelf above the backs of the musicians. Around the sides and across the rear of the hall are two narrow balconies. Above the balconies on either side are niches

FIGURE 19.17   Symphony Hall, Boston, MA (Beranek, 1996)

SECTION

UPPER BALCONY PLAN

ORCHESTRA / LOWER BALCONY PLAN
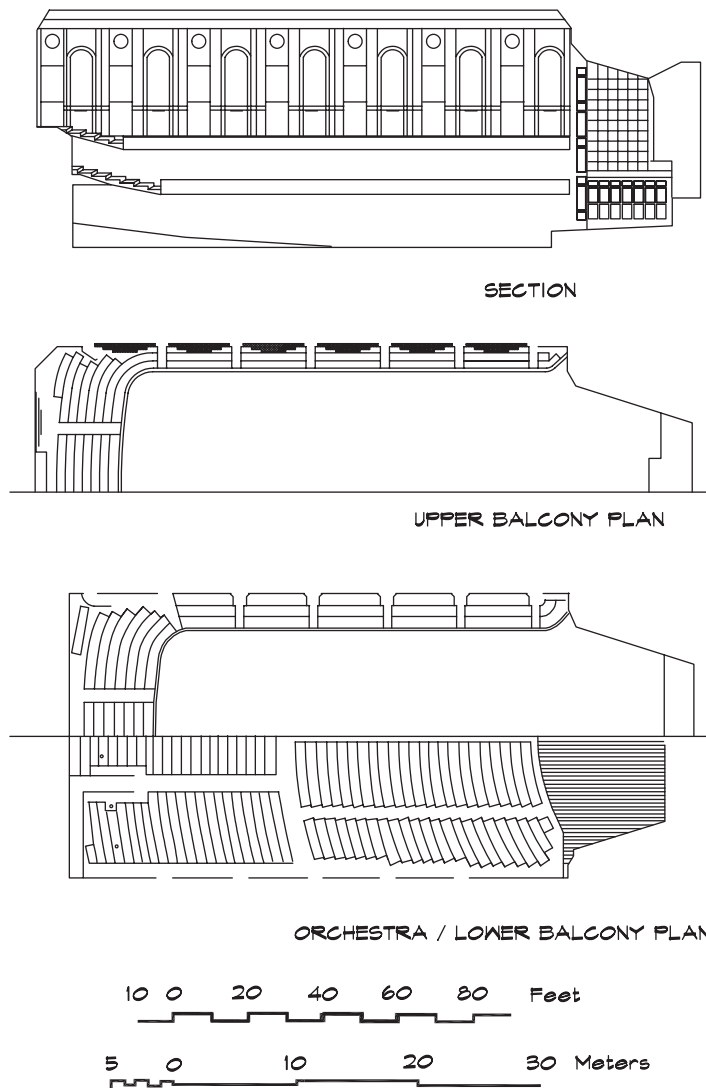
TABLE **19.9   Selected Technical Data for Boston Symphony Hall (Beranek, 1996)**

Attribute	Metric Units	FP Units
Volume (V)	**18,750 cu m**	**662,000 cu ft**
Dimensions (LWH)	**39 m × 23.6 m × 18.6 m**	**128 ft × 77 ft × 61 ft**
Furthest Seat (D)	**40.5 m**	**133 ft**
Seating (N)	**2625**	
Total Absorptive Area (S_T)	**1,522 sq m**	**16,385 sq ft**
V/N	**7.14 cu m**	**252 cu ft**
V/S_T	**12.3 m**	**40.4 ft**
T_{60} (Occ) = 1.85 sec	**T_E(Unocc) = 2.1 s**	**$(1 - IACC_{E3}) = 0.65$**
t_I = 15 msec	**G_{mid} = 4.7 dB**	**BR = 1.03**
SDI = 1.0		

Acoustician: Wallace C. Sabine   Architect: McKim, Mead, and White

supporting classical Greek and Roman statuary. The ceiling is built of 0.75" (19 mm) plaster formed into deeply coffered rectangles. The walls are mostly plaster on masonry (50%) or metal lath (30%) backing. The remainder, including the stage enclosure, are 0.5" (13 mm) to 1" (25 mm) wood. The floor is concrete with wood overlay, which rises gently at the rear to an elevation of 5' (1.5 m) above the slab. During the summer pops concerts are held and the sloped wooden floor is removed. Food is served and, in the tradition of the early Italian opera houses, conversations continue during the performances, which degrades the clarity in the rear of the main floor.

Boston is regarded as the finest concert hall in the United States. It has excellent clarity and loudness. Its balance is quite good and the bass is very good, particularly at the rear of the balcony. The orchestra platform is small, almost crowded, which helps the onstage ensemble. Its shallow depth improves the bass by encouraging the location of the double basses against the rear wall, under the organ pipes.

Concertgebouw, Amsterdam, Netherlands

Concertgebouw in Amsterdam, shown in Fig 19.18, opened in 1888. Like the two previous examples it has a shoebox shape, however it is much wider at 91 ft than either Vienna or Boston, and it has some seats behind the orchestra. There is no rake to the main floor but this is counterbalanced by a high platform (59 in / 1.5 m). The ceiling is coffered in the center portion with deep semicircular niches at the junction with the walls. These provide substantial diffusion over a wide range of frequencies.

The ceiling and walls are heavy (1.5 in / 4 cm) plaster applied on brick below the balconies. Floors are hardwood on 2 × 3 (5 × 7.5 cm) wood battens filled with 1.6 in (4 cm) of sand over a concrete slab. There is no orchestra enclosure or overhead reflectors, so the clarity is not quite as good as in Vienna and Boston. The sound is rich, full, and enveloping with good bass due to the heavy plaster surfaces.

FIGURE 19.18   Concertgebouw, Amsterdam, Netherlands (Beranek, 1996)

SECTION

ORCHESTRA / BALCONY PLAN
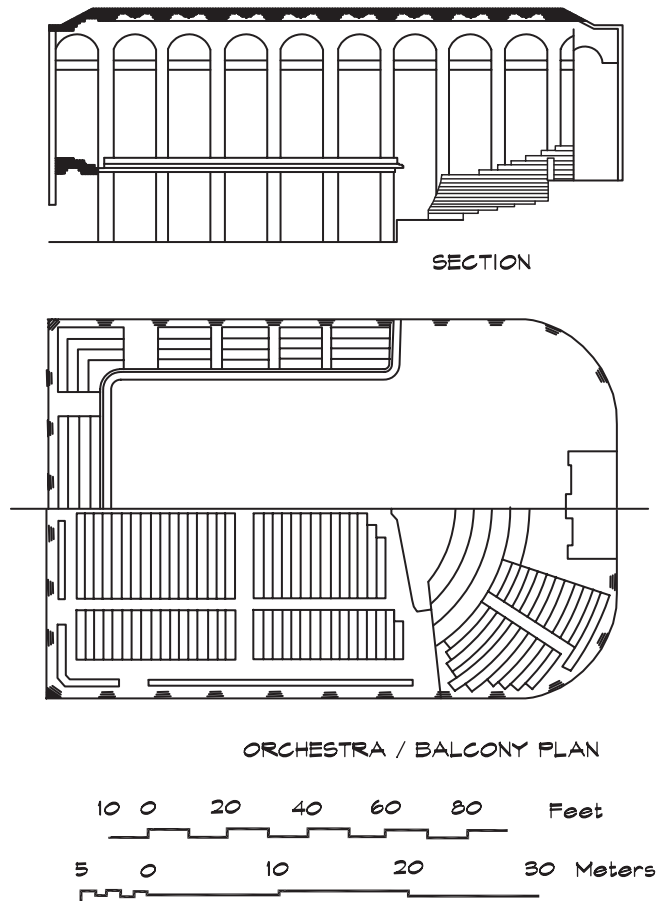
TABLE 19.10   Selected Technical Data for Concertgebouw (Beranek, 1996)

Attribute	Metric Units	FP Units
Volume (V)	18,780 cu m	663,000 cu ft
Dimensions (LWH)	26.2 m × 27.7 m × 17.1 m	86 ft × 91 ft × 56 ft
Furthest Seat (D)	25.6 m	84 ft
Seating (N)	2037	
Total Absorptive Area (S_T)	1,285 sq m	13,830 sq ft
V/N	9.2 cu m	325 cu ft
V/S_T	14.6 m	48 ft
T_{60} (Occ) = 2.0 s	T_E (Unocc) = 2.6 s	$(1 - IACC_{E3}) = 0.46$
$t_I = 21$ ms	$G_{mid} = 5.9$ dB	BR = 1.08
SDI = 1.0		
Architect: A. L. van Gendt		

Philharmonie Hall, Berlin, Germany

The Berlin Philharmonic Hall, which opened in 1963, was a dramatic departure from the traditional rectangular or fan-shaped configurations. The architect, Hans Scharoun, and the acousticians, Lothar Cremer with Joachim Nutsch, followed the design philosophy that the orchestra should be located near the middle of the room and be surrounded by the audience, generating the new type of classification—the surround hall. All surround halls sacrifice acoustical excellence mainly in the side and rear seating areas for audience proximity and visual stimulation. Figure 19.19 shows the plan and section of the Berlin hall, although a

FIGURE 19.19   Berlin Philharmonic Hall (Beranek, 1996)
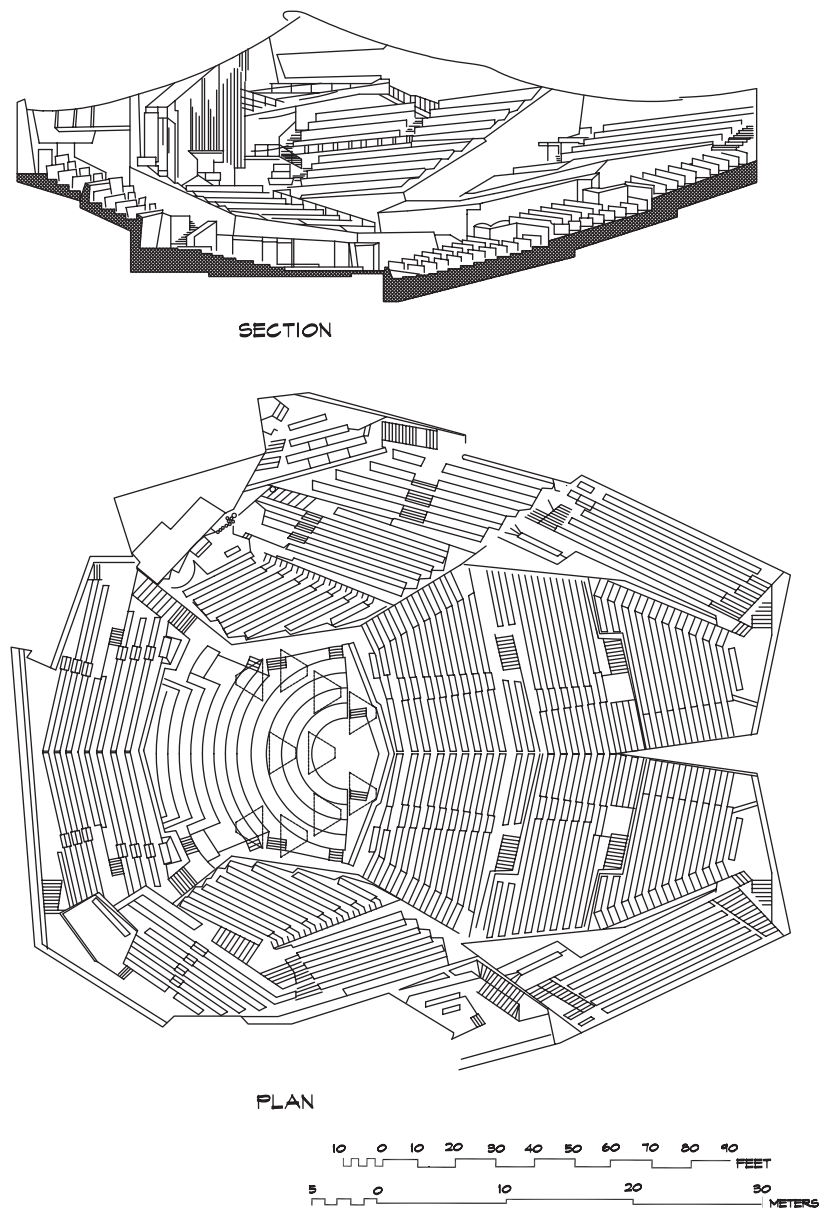
TABLE 19.11   **Selected Technical Data for Berlin Philharmonic Hall (Beranek, 1996)**

Attribute	Metric Units	FP Units
Volume (V)	21,000 cu m	741,300 cu ft
Dimensions (LWH)	29 m × 42.7 m × 12.8 m	95 ft × 140 ft × 42 ft
Furthest Seat (D)	30 m	98 ft
Seating (N)	2215	
Total Absorptive Area (S_T)	1,558 sq m	16,765 sq ft
V/N	9.0 cu m	317 cu ft
V/S_T	13.5 m	42.2 ft
$T_{60}(Occ) = 1.9$ s	$T_E(Unocc) = 2.1$ s	$(1 - IACC_{E3}) = 0.46$
$t_I = 21$ ms	$G_{mid} = 4.3$ dB	BR = 1.01
SDI = 0.8		

Acoustician: Lothar Cremer, Joachim Nutsch   Architect: Hans Scharoun

feeling for the dramatic three-dimensional layout is hard to get from these two dimensional renderings.

The continuous band of seating on the main floor steps up from the orchestra platform in terraces, which are separated by low chevron-shaped walls about 5 feet (1.5 m) high. These separate the seating areas visually and provide a break from the grazing wave reflected from the seats. The upper portion of the walls, which is frequently slanted down, sends sound back to the audience seated in front of them, providing additional early reflections.

Suspended overhead clouds help the musicians onstage and give high-frequency support to the nearest seats. The convex ceiling provides useful reflections in the rear of the hall. The division of the seats into terraced sections leaves each section with a nearby side wall, so useful for envelopment. A sharp vertical wedge bifurcates the rear section of seats providing another reflecting surface in that area. The result is a balanced clear lively sound in front of the orchestra.

On the sides and rear Barron (1993) notes that the character of the sound changes with the nearest instruments audible and those further away less so. Behind the orchestra this effect is less pronounced but the French horns are prominent and the piano and vocals are difficult to hear. The ceiling is treated with small pyramid-shaped Helmholtz resonator absorbers, designed to reduce the reverberation time in the lower registers so that the bass ratio is close to one. Beranek (1996) opines that this is somewhat overdone.

Eugene McDermott Concert Hall in the Morton H. Meyerson Symphony Center, Dallas, TX, USA

Dallas's McDermott Hall (Fig. 19.20) is a good example of a recent (1989) design approach incorporating a blend of the classic shoebox and opera-house forms with interesting technological innovations. The shape of the hall is nearly rectangular with a semicircular rear wall. Three shallow balconies ring the center seating area. The lowest is subdivided

FIGURE 19.20   McDermott Hall, Dallas, Texas, USA (Beranek, 1996)

ORGAN
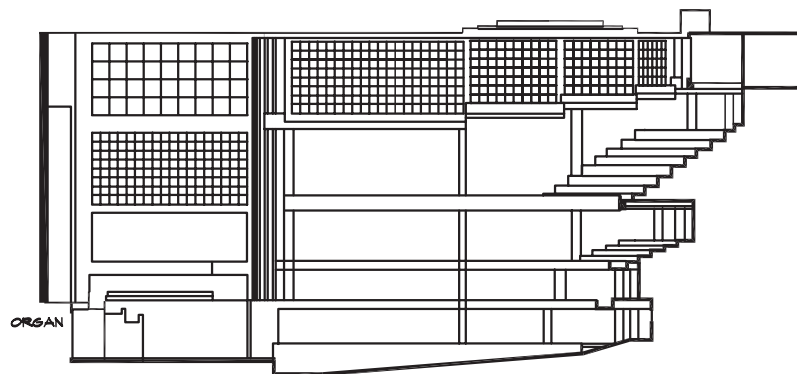
CENTERLINE SECTION
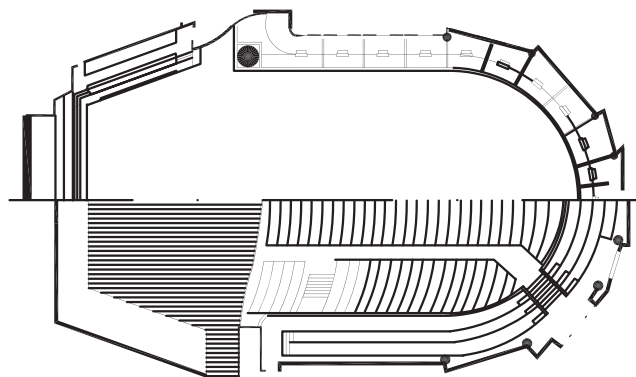
FIRST AND SECOND FLOOR
FLOOR PLANS

10 0   20   40   60   80   Feet

5   0   10   20   30 Meters

FIGURE 19.20   **(Continued)**

LATERAL SECTION

BALCONY PLANS
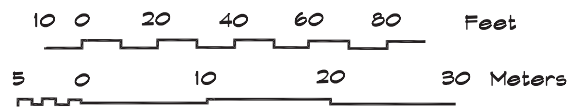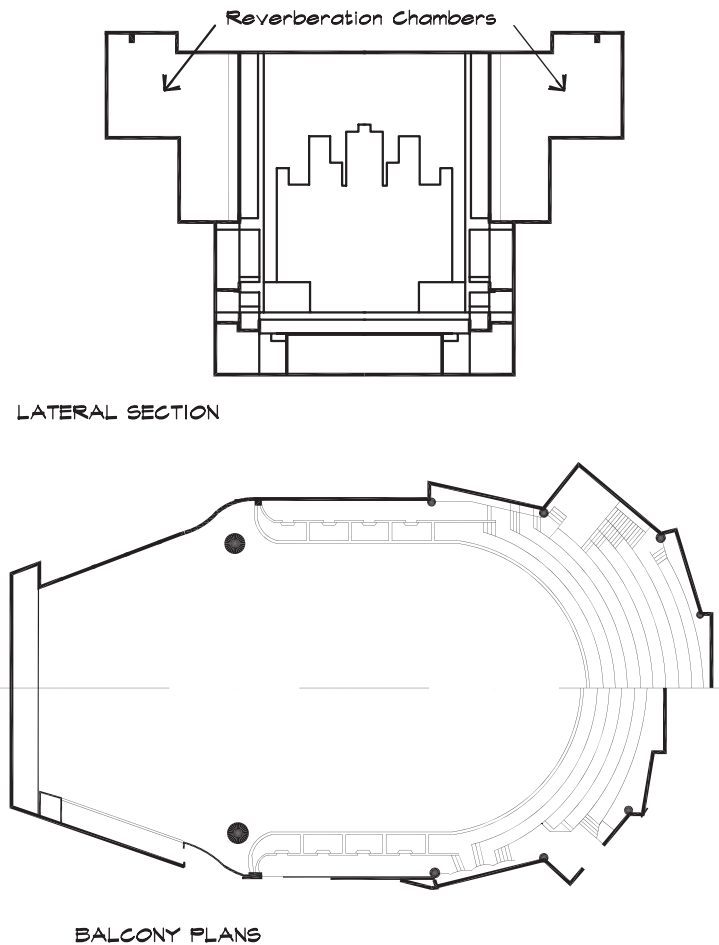
TABLE 19.12   Selected Technical Data for McDermott Hall (Beranek, 1996; Berkow, 2001)

Attribute	Metric Units	FP Units
Volume doors closed (V)	**23,900 cu m**	**844,000 cu ft**
Dimensions (LWH)	**30.8 m × 25.6 m × 26.2 m**	**101 ft × 84 ft × 86 ft**
Furthest Seat (D)	**40.5 m**	**133 ft**
Seating (N)	**2065**	
Total Absorptive Area (S_T)	**1,460 sq m**	**15,718 sq ft**
V/N	**11.6 cu m**	**409 cu ft**
V/S_T	**16.4 m**	**53.7 ft**
T_{60} (Occ) = 1.5 to 4.5 s	**T_E (Unocc) = 0.8 to 1.5 s**	

Acoustician: ARTEC Consultants;   Architect: Pei Cobb Freed & Partners

into boxes, while the highest rises upward from the center band of seats. The ceiling is very high at 86 feet (26.2 m) and nearly flat. For all its size, the hall seats just over two thousand people. The volume in the main hall is augmented by reverberation chambers, attached like mouse ears out of sight on the upper sides of the auditorium. These can add an additional 254,000 cu ft (7200 cu m), or 30%, to the room by opening up to 74, 4-inch (10 cm) thick mechanized concrete doors.

The main visible feature of the hall is a flying reflector suspended on cables above the orchestra platform, reminiscent of the Starship Enterprise. This serves to provide reflections back to the orchestra from a height that is adjustable, varying between 36 and 50 feet (11–15 m). For small groups, the intimacy can be increased by lowering the canopy. For organ music, where a highly reverberant sound is required, the canopy is raised, exposing the organ pipes behind. The moveable canopy has become a trademark solution to the overhead reflection problem developed by the acoustician Russell Johnson. It is so large that it subdivides the room into three volumes: below the canopy, the main space, and the reverberation chambers. This leaves the decay pattern a complicated merger of the three coupled spaces, but offers a promising solution to the problem of simultaneously achieving clarity and reverberation. The reverberation time can be varied over a wide range, but interestingly the early reverberation time is relatively short.

For all its technical innovation most of the hall's features are nicely blended into the architecture. The floor is terrazzo tile or painted concrete, while the ceiling is 5.5 in (14 cm) concrete. The walls are wood veneer on 0.5 in (13 mm) particle board bonded to 10 in (25 cm) masonry. The 4000 sq ft (372 sq m) canopy is built from 6 in (15 cm) laminated wood. Some of it is covered with 0.06 in (1.6 mm) felt to reduce glare. The stage is 0.5 in (13 mm) tongue and groove wood on wood boards on joists. The floor under the cellos and double basses is 2 in (5 cm) wood over a 3 ft (0.9 m) airspace.

Beranek (1996) found the balance, tone, and intimacy excellent nearly everywhere, best on the main floor and in the rear. The side balconies were less well balanced. He described the effect of the reverberation chambers as "not obvious," noticeable only after stop chords but not as running reverberance. All in all this is a very interesting hall.

19.5   OPERA HALLS

Opera halls and their history were discussed in detail by Forsyth (1985), and their acoustical attributes were surveyed and analyzed by Beranek (1962 and 1996) and Barron (1993). The following data are due primarily to the compilation of Beranek.

Theatro Colon, Buenos Aires, Argentina

Theatro Colon in Buenos Aires opened in 1908, as an opera house, but is also a highly rated concert hall. In his 1962 work Beranek found it to be in his top six concert halls. Its reverberation time is high for opera, at about 1.8 s (occupied), but quite appropriate for concerts. The shape is a classic horseshoe, seating 2487 people with six shallow balconies shown in Fig. 19.21.

As an opera house it is a favorite of singers because of the support they receive on stage. The side walls on either side of the forestage contribute early reflections as do the ceiling and vertical balcony facings. The pit is 3 m (10 ft) deep and so the best string sound is heard in

FIGURE 19.21 Theatro Colon, Buenos Aires, Argentina (Beranek, 1996)
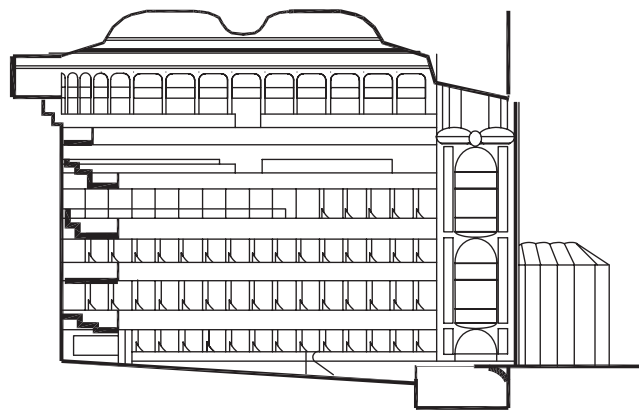
SECTION
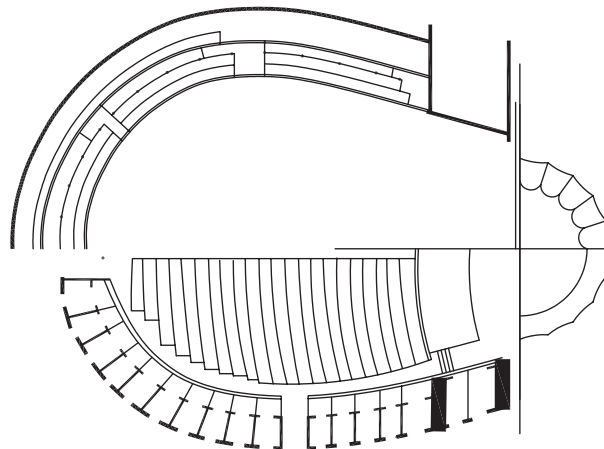
ORCHESTRA / BALCONY PLAN
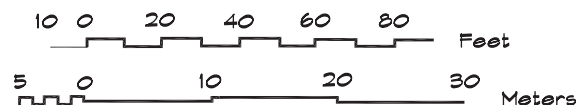
the upper balconies. In the concert mode the pit is covered and a semicircular shell formed of convex scallops is installed. The walls and ceiling are 1" (2.5 cm) plaster on wire lath. The floors are wood with carpet in the aisles.

Theatro Alla Scala, Milan, Italy

Theatro Alla Scala, shown in Fig. 19.22, opened in 1778 and since then has been the best known opera house in the world. Although it was nearly destroyed in World War II, it was

TABLE 19.13   Selected Technical Data for Theatro Colon (Beranek, 1996)

Attribute	Metric Units	FP Units
Opera		
Volume (V)	20,570 cu m	726,300 cu ft
Dimensions (LWH)	34.4 m × 24.4 m × 26.5 m	113 ft × 80 ft × 87 ft
Furthest Seat (D)	43 m	141 ft
Seating (N)	2487	
Total Absorptive Area (S_T)	2,144 sq m	23,077 sq ft
V/N	8.3 cu m	292 cu ft
V/S_T	9.6 m	31.5 ft
T_{60} (Occ) = 1.88 s (est)	t_1 = 19 ms	
Concerts		
Volume (V)	21,524 cu m	760,000 cu ft
Total Absorptive Area (S_T)	1,970 sq m	21,200 sq ft
V/N	8.67 cu m	306 cu ft
V/S_T	10.9 m	35.8 ft

Architect: Victor Meano

rebuilt to the same design and reopened in 1946 much as before. It has the classic horseshoe shape with six balconies, subdivided into boxes. Izenour (1977) describes it as the culmination of all that is good, and bad, in Baroque theaters—"a functioning museum." The ornate balcony fronts along with the compound curve of the ceiling provide strong reflections back to the singers on stage, which can be distracting to the audience sitting in the orchestra seats. The side wall balcony facings and narrow width provide a sense of intimacy and a sound that is "clear, warm, and brilliant" (Beranek, 1962) for those in the best seats.

The boxes and horseshoe seating arrangement were designed so that both the stage and the 20-seat royal box at the rear were visible. The front faces are about 56% open presenting bands, alternately reflective and absorbent, since the boxes are deep and well upholstered and little sound emerges. The result is a rich reverberant sound (Barron, 1993) in the center portion of the rear balconies, particularly in the front row. In the side balconies and in the rear of the boxes the sound is less accessible and the sight lines from the side particularly in the upper balconies are poor.

The pit is large and open, extending across the entire front of the stage. There is a little more than 2 m (6.6 ft) of stage overhang. The orchestra rail is slightly lower than the front of the stage, which slopes upward away from the audience. The coffered proscenium is nearly

FIGURE 19.22   Theatro Alla Scalla, Milan, Italy (Beranek, 1996)

SECTION

UPPER BALCONY PLAN

ORCHESTRA / FIRST TIER PLAN

| 10 0 | 20 | 40 | 60 | 80 | Feet |
| 5 | 0 | 10 | 20 | 30 | Meters |
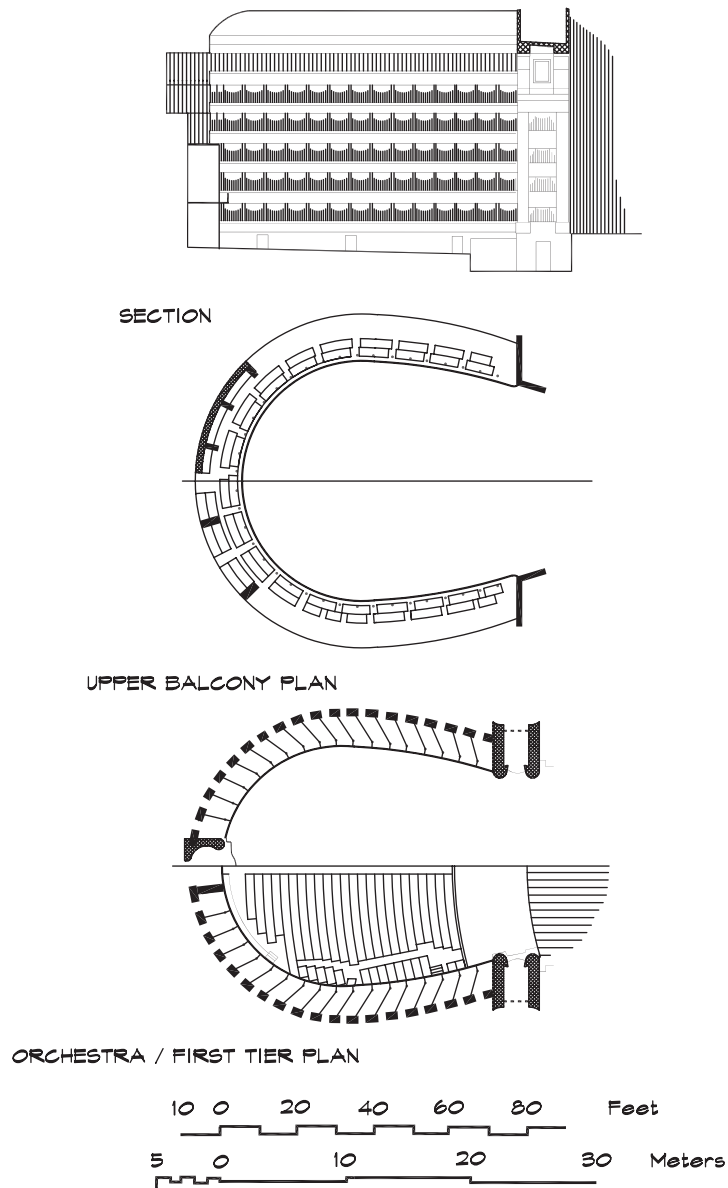
TABLE 19.14   Selected Technical Data for Theatro Alla Scala (Beranek, 1996)

Attribute	Metric Units	FP Units
Volume (V)	11,252 cu m	397,300 cu ft
Dimensions (LWH)	30.2 m × 20.1 m × 19.2 m	99 ft × 66 ft × 63 ft
Furthest Seat (D)	32 m	105 ft
Seating (N)	2289 (including 154 sight restricted seats)	
Total Absorptive Area (S_T)	1,635 sq m	17,600 sq ft
V/N	4.92 cu m	174 cu ft
V/S_T	6.9 m	22.6 ft
T_{60} (Occ) = 1.2 s	T_E (Unocc) = 1.2 s	$(1 - IACC_{E3}) = 0.48$
$t_I = 20$ ms	$G_{mid} = -1.4$ dB	BR = 1.21

Architect: Giuseppe Piermarini

horizontal above the orchestra, providing some additional support for the orchestra, though at a delay of more than 100 ms.

The walls and ceiling are plaster on wood frames. The vaulted ceiling is nearly flat with no diffusing elements. The floors are wood on a 3 ft (0.91 m) airspace on concrete and are carpeted. The stage and pit floor are wood.

This page intentionally left blank

20 DESIGN OF MULTIPURPOSE AUDITORIA AND SANCTUARIES

The acoustical properties that make a room good for speech are often the same as those that make it poor for music, and vise versa. For good speech intelligibility, room volumes and reverberation times should be low. The first reflections should be primarily from the ceiling, and there is little need for diffusion. Conversely, rooms designed for listening to unamplified music require longer reverberation times, higher volumes, lateral rather than overhead reflections, and high diffusion. Rooms designed for mixed uses require a judicious compromise between the needs of speech and music. Buildings of this type, including auditoria, theaters, churches, and synagogues, are among the most architecturally diverse of all spaces and the most challenging to design.

20.1 GENERAL DESIGN CONSIDERATIONS

Although there are design features unique to the type of room, there are also general guidelines for large mixed-use facilities that apply to all of these rooms.

1. The source should be elevated above the seated audience so that sight lines are clear of obstruction.

2. A sound system capable of reproducing the full program frequency range must be incorporated into the design. The loudspeaker layout should be arranged so that the talker is the perceived origination point.

3. Where unamplified music is a part of the program, the singers or musicians should be aided by nearby reflective surfaces both overhead and on either side. These can be integrated into the design of the structure, suspended above the players, or built into a moveable shell. Musical instruments supporting the singers should be located near them, so there is no great time difference between the two.

4. The floor should be raked to provide every other row sight lines of the APS.

5. The room volume and absorption should be controlled to achieve a reverberation time consistent with the program. Padded seating must be used to minimize the differences between the empty and occupied conditions. Room reverberation must be controlled to limit the loudness of large groups.

6. Background noise levels should be limited to NC 25 in small ($<$ 500 seats) auditoria and to NC 20 in opera houses and drama theaters. In large concert halls it should be limited to NC 15.

Program

Architectural designs begin with a program, listing the various uses contemplated for a space and the percentage distribution of each. Program definition allows the architect and acoustician to know whether to steer the design compromise toward a speech-like or music-like solution. Not infrequently, in the design of performance spaces, there may be disagreements as to the proper direction, not only within the design team, but also among the members of the client team. It is always best to sort this out in writing early in the process so that the direction is clear.

Changes to the program, particularly late in the process, can have profound consequences. Hidden agendas are difficult to uncover. This is particularly true when there is an expectation that the room will serve a purpose different from its stated use. For example, a church may be designed as a worship space, but may also be expected to serve as a theater, performing arts center, and television studio where there are significant additional lighting, rigging, audio, and HVAC requirements. A well-crafted program can allow these issues to be sorted out and can help establish a clear design direction.

Room Shape

Floor plans are laid out on the basis of the program, which drives the seating configuration, volume, sight lines, circulation, and aesthetics. In rooms designed for speech it is good practice to bring the audience close to the talker. A fan-shaped room, particularly one with balconies, allows a larger number of people to be close to the stage, than a rectangular room. For unamplified music, where strong side reflections are important, a narrow rectangular room with a high ceiling has traditionally yielded the best result. For rooms of mixed use a compromise between the speech and music requirements must be crafted.

Small general-purpose auditoria are typically rectangular, with the walls near the front of the room angled out from the stage. For lecture halls more of a fan shape is preferred, with the maximum angle between opposing walls no more than 140°. In the case of mixed use spaces the included angle falls between 40° and 80°, with smaller values being best for music. Examples are given in Fig. 20.1. The side walls at the rear of the room are either parallel or flared out at a shallower angle than in front. This scheme provides useful early reflections from the walls near the stage or platform, while allowing regular aisles and constant width seating sections at the rear.

In large multiuse theaters it becomes increasingly difficult to accommodate the audience with good sight lines. A fan shape is the usual choice, truncated on the sides, with one or more balconies. The distance to the farthest viewer depends on the type of performance. The human eye can perceive an object as small as one minute of arc (Burris-Meyer and Cole, 1975) or about 0.35" (9 mm) at 100 ft (30 m). As the last row is pushed back to 135 feet (41 m), the smallest resolvable dimension is increased to 0.5" (13 mm) and a raised eyebrow or small gesture is lost. Thus if the subtle facial expressions of a theatrical performance are to be appreciated, the farthest patron should be seated no more than about 80 feet away.

FIGURE 20.1 Side Wall Design Near the Stage
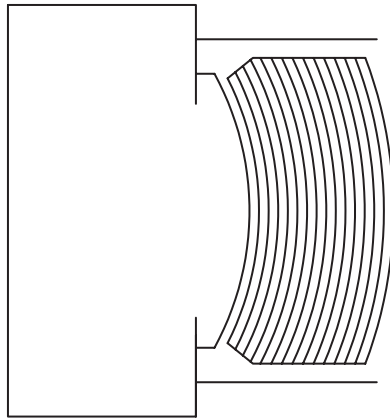
Rectangular seating plan – Poor side wall reflections
Potential flutter echo on the thrust stage
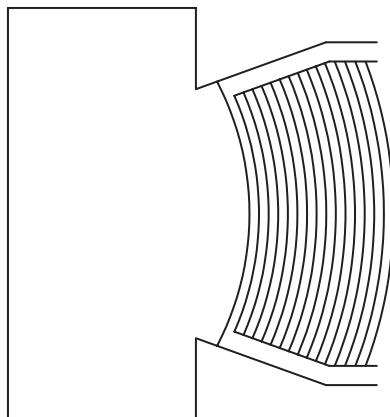
Angled seating plan – Better side wall reflections

This is a more restrictive requirement than seating for orchestral performances, and limits first floor seating to around 26 rows or 1100 seats for three banks of fourteen seats.

In very large spaces the seating fan is forced to a greater angle often with four seating banks with a center aisle or three banks with a half bank on each outside wall. In the Radio City Music Hall in New York for example there are five seating banks. The remainder of the audience is seated in the balconies, which must not cause shadowing through excessive overlap of the seats below. It is difficult to design auditoria for intimate theatrical productions larger than about 1500 seats. In large houses the types of performances must be adjusted to the scale of the space.

The shape of worship spaces is determined primarily by liturgical requirements. Churches require a focal point either at the front or in the center. A raised platform helps acoustics as well as sight lines, but if it is too high there may be unshielded sound paths to the

side or end walls, leading to long-delayed reflections and flutter echo. A cruciform shape may be highly desirable in some denominations. Medium-sized congregations, in the 500 to 1000 range, can be accommodated in a wide variety of room shapes, but care must be exercised not to let the room volumes get out of hand. Very large churches in the 2500 to 10,000 seat range are fan-shaped for the practical reason that this is the only way to accommodate the necessary seating. To maintain sight lines the included fan angle should not exceed 160°. These large venues rely on electronic sound reinforcement and video projection systems to transmit their message, so the sight lines to these sources are also important.

Religious and theatrical facilities are sometimes designed with circular or multifaceted hexagonal or octagonal floor plans. Such shapes should be avoided wherever possible since they focus sound and create localized regions of high level. Churches and theaters in the round, even with diffusive or absorptive walls, are also poor acoustical choices. At best they result in fair-to-mediocre sight and sound quality in spite of the expenditure of great effort and treasure.

Worship spaces have higher ceilings than auditoria and a stately architectural form, often with historical roots. Ceilings of religious structures can be dome-shaped, which generate focused reflections. When long delayed reflections arrive back at the talker at an elevated level, the effect can be particularly unpleasant. There is a combination of level and delay time (around 100–150 msec) so disconcerting to the talker, that, in the worst case, it can act as a severe impediment to normal speech. Large concave shapes should be avoided, particularly when the talker and listener are near the center of curvature. A calculation of the curvature gain can identify problem conditions. Curved walls can be treated with absorption, however since the normal-incidence absorption coefficients are lower than random-incidence values, there may still be reflected levels high enough to be of concern

Seating

Circulation and building code requirements influence the shape of the floor plan. In the conventional seating plan US building codes require that there be no more than 6 seats between a seated patron and an aisle, permitting a maximum of 14 seats in a section bounded by two aisles. Normal row-to-row spacing is 36 to 38" (0.92 to 0.97 m). In continental seating the larger distance between rows (40–42" or 1.01–1.07 m) allows them to be considered cross aisles and the six-seat limit no longer applies. Opera chairs are available in various widths ranging from 19 to 23" (0.48 to 0.58 m). Normal seats are about 22" wide (0.56 m) with some at 21" (0.53 m) to accommodate the stagger. A full 14-seat bank occupies 25.5 ft (7.8 m) plus the aisles.

The decision on whether to have a center aisle is influenced by the program. In religious structures a center aisle is the usual choice to provide for a processional march in traditional wedding ceremonies. In a theater the best seats are located in the center so an even number of aisles is a better alternative. Building codes in the United States specify minimum 36" (0.9 m) single-sided and 42" double-sided aisles, which widen 1.5" (38 mm) for every five feet of seating as they approach the nearest exit.

Handicapped seating requirements call for wheelchair spaces along with adjacent companion seats within the space. Recent changes to the Uniform Building Code to accommodate handicapped access can limit floor slopes to 1:12—less than ideal for every other row sight lines depending on the height of the APS. Requirements vary and enforcement of these codes differs. It is always best to get clear directions from the local building officials.

TABLE 20.1   Range of Volume per Seat by Type of Auditorium (Doelle, 1972)

Type of Auditorium	Volume per Seat cu ft (cu m)		
	Min	Mid	Max
Rooms for Speech	80 (2.3)	110 (3.1)	150 (4.3)
Concert Halls	220 (6.2)	275 (7.8)	380 (10.8)
Opera Houses	160 (4.5)	200 (5.7)	260 (7.4)
Churches/Synagogues	180 (5.1)	255 (7.2)	320 (9.1)
Multipurpose Auditoriums	180 (5.1)	250 (7.1)	300 (8.5)
Motion-picture Theaters	100 (2.8)	125 (3.5)	180 (5.1)

Room Volume

Room volumes are selected using the volume per seat as a guideline. Since the ideal reverberation time for speech is low, the preferred volume per seat for speech is also low, ranging from 80 to 150 cu ft (2.3 to 4.3 cu m), with smaller auditoria having the larger volume per seat. For unamplified music it can vary from 160 to 400 cu ft (4.5 to 11.3 cu m), again with smaller halls having the greater volume per seat. In rooms designed for mixed uses, the volumes fall between these values, 180 to 300 cu ft (5.1 to 8.5 cu m). Table 20.1 shows typical ranges by room use.

Reverberation Time

From the program, the designer can establish the reverberation time and a preferred volume per seat for the space. The seating capacity will then fix the overall volume of the room and the circulation and other functions will lead to a preliminary floor plan. Figure 17.10 shows reverberation time versus room volume values for various types of spaces. Figure 17.11 shows the preferred behavior of reverberation time with frequency for music. In small auditoria and churches the overall volumes are rarely high enough to raise the bass response to the level shown in this figure and the alternative, which is using heavy plaster or multiple layers of drywall, is cost prohibitive except in pure concert halls. As rooms grow larger a high volume can be used with applied absorption to control the mid-frequency reverberation. The reverberation time falls off naturally at high frequencies due to air absorption and thin absorbent materials. By using wood slats over absorptive panels it is possible to offset these effects and raise the high-frequency reverberation time. This provides a favorable frequency balance as long as the absorption is needed anyway at other frequencies.

Absorption

In large auditoria and religious structures the biggest absorbing surface is the seated audience. It provides about 85% of the total absorption in concert halls and somewhat less in auditoria where applied absorptive material may be used. Since it is desirable to maintain a consistent acoustical environment no matter the number of people, it is most important to use seats, whose absorption characteristics closely resemble that of a seated occupant. This requires that the chairs or pews have thick padding on both the seats and backs. Beranek (1996) observed that the absorptive properties of a given number of seats depends not on the number of seats,

but on the area they cover. Thus reverberation calculations should be based on an absorption coefficient per unit area of seating, not on the number of sabins per seat.

As sound propagates over the seats of a theater it is found that there is an extra attenuation above that expected from distance and grazing losses. This extra attenuation is centered on 125 Hz and appears as a deep dip in the attenuation vs frequency response curve. The phenomenon has been discussed in earlier chapters and measured data are shown in Fig. 7.44. Ando (1985) analyzed the effect and related it to the quarter-wave well impedance caused by the depth of the seats. He proposed various solutions including cavities in the floor and several geometrical alternatives. Unfortunately, there is little measured data available to determine the effectiveness of his suggestions.

When the natural acoustics of a room is augmented by a sound system and design constraints allow the use of absorbent surface materials, the room volume and surface orientations are less critical than in concert hall environments. In these cases absorptive materials can be added to control unwanted reflections and reverberation since the level generated by the sound system can make up for the energy lost through absorption. In rooms accommodating both music and speech, the ideal solution is to design to the reverberation time appropriate for the music, and to manage the intelligibility using the reinforcement system. Where unamplified speech must be supported, variable absorption can be a good alternative.

Balconies

Balconies allow more of the audience to be seated close to the stage and limit the slope of the orchestra seating. Balcony floors have steeper rakes than the orchestra floor, but the slope can be calculated using the same equations. The slope should not be greater than 30° (Ramsey and Sleeper, 1970) to 26° (Egan, 1988), and the top of the balcony should not be more than 65 feet above the stage to avoid vertigo (Egan, 1988). Figure 20.2 shows a typical balcony configuration.

Balcony overhangs must be controlled to allow the reverberant sound to reach the seats beneath them. Beranek suggests a depth-to-opening ratio of one for concert halls and two for opera houses. For speech, balcony overhangs can be deeper without undue degradation. A two-to-one depth-to-opening ratio is acceptable.

A slightly convex under-balcony ceiling can help redirect sound into the shielded area. Likewise a rising leading edge at the front of the balcony is also helpful. Where the

FIGURE 20.2 Balcony Design
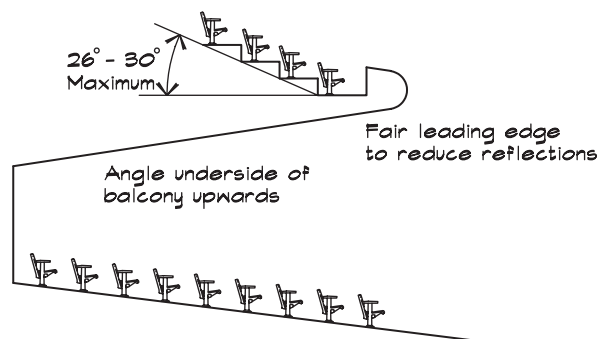
FIGURE 20.3 Flying Balcony Design
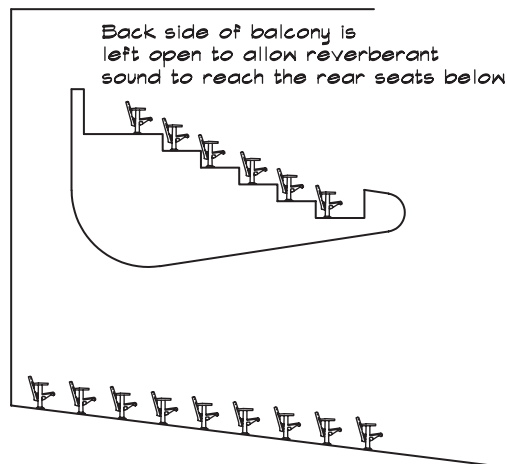
balcony overhang is very deep, both direct and reverberant sound have difficulty penetrating. A sound system can augment the direct sound, using loudspeakers located on the underside of the balcony. A concave or semicircular-ceiling cavity under the balcony can help generate a localized reverberant field to offset the effect of a deep overhang.

In rare instances, halls have been built with a flying balcony, separated from the rear wall of the room as in Fig. 20.3. This allows the sound to flow around the upper balcony to reach the rearmost under-balcony seats. It is an expensive solution, since it presents structural challenges, even when beams support the balcony from the rear.

Ceiling Design

The ceiling of an auditorium or theater is more complicated than those found in a lecture hall. When auditoria are designed for speech, strong overhead reflections are preferred, whereas for music, a ceiling that diffuses the sound and aids in the sense of envelopment, or feeling surrounded by the sound, is best. A flat ceiling can yield excellent results for speech if it is not too high and if the floor rake is sufficient. In auditoria and lecture halls, particularly when the floor is flat or slightly raked, a shaped ceiling is helpful. This type can be designed by dividing the surface into angled planes or separately supported reflectors, so that there is an even distribution of reflected sound over the audience.

The surface above the proscenium arch is particularly important. Figure 20.4 shows an example. The first reflecting surface should be convex and horizontal at the proscenium wall. Such a shape aides in the reflection of sound to the seats in the center of the orchestra section, which is the most difficult to cover. It is also more forgiving of changes in the source position than a sharply slanted reflector. By controlling the curvature the clusters, loudspeakers can be nested above the reflector where the shielding helps control feedback. One or more rows of theatrical lighting must be accommodated, located at 45° and 55° from a downstage actor. Consequently there is a scramble for the ceiling space in the third of the ceiling closest to the proscenium, which must include passive acoustical reflectors, loudspeakers, catwalks, and theatrical lighting.

FIGURE 20.4 Design of Proscenium Reflectors

Second reflector
may be angled slightly
depending on its height
above the stage and the
audience.

Loudspeakers

First reflector is horizontal
at the proscenium/rising towards
the audience. This supports the
singer and the orchestra both
onstage and in the pit.

AN EXAMPLE OF GOOD PROSCENIUM DESIGN

First reflector is angled
too much. No support
for singer or orchestra.

Second reflector
is angled too far down.
May cause an image shift
upwards or a long delayed
reflection.

Loudspeakers are located
too far back which will lead
to feedback problems on the
thrust stage.

AN EXAMPLE OF POOR PROSCENIUM DESIGN

Ceiling reflectors can be flat or convex shaped but are not concave or coffered. Some designers prefer to use individual panels, or clouds, since they are more easily adjusted after installation, and are in some cases less expensive. When this type of ceiling system is used, the reflectors should be arranged along a single planar or curved surface so that interference patterns due to Bragg imaging do not occur. Reflectors should be large enough that the frequencies of interest are scattered more or less specularly. Using a group or array

of reflecting panels can help offset this limitation and assure that low frequencies are also reflected (Leonard, Delsasso, and Knudsen, 1964). In Chapt. 7 we discussed the effects of reflector size on the frequency of the scattered sound. Where ceilings are very high or when there are ceilings at different heights, as is the case in some religious structures, the highest surfaces should be the first choice to receive absorptive treatment. These spaces sound best if the reverberation times are matched. Application of absorption to the whole area may not be required, but if some is treated the rest should maintain a consistent appearance whether treated or not. Where a highly diffuse ceiling is used, clarity is likely to suffer in the rear of the auditorium and in the balcony seats during unamplified use.

Audio Visual Considerations

As auditoria and religious structures become larger, they must rely on audio and video reinforcement systems to transmit the message to the audience. Floor layouts must accommodate sight lines, not only to the talker, but also to video screens and loudspeaker locations. If large loudspeakers are necessary to provide the directivity required for speech intelligibility, then the architectural real estate necessary to accommodate them must be included in the design. Loudspeakers should be arranged so that the source image is preserved, and frequently a central cluster above the proscenium is the best solution. When this does not match the visual expectation of the design team, enclosures can be incorporated to soften their visual impact.

If there are projected images in a theater, church, or lecture hall then the seating layout must accommodate the requirements of the screens. Figure 20.5 shows seating arrangements based on front and rear projection screens. The front row of seats should be no closer to the screen than one and one-half screen heights (1.5 H) or about one and one-eighth screen widths (1.125 D). The rearmost seat should be no more than 8H or 6D from the screen. In some cases screen sizes become very large and multiple screens must be used. This is particularly true in large fan-shaped churches where no single screen can be seen by the entire congregation.

FIGURE 20.5 Design of Projection Screens
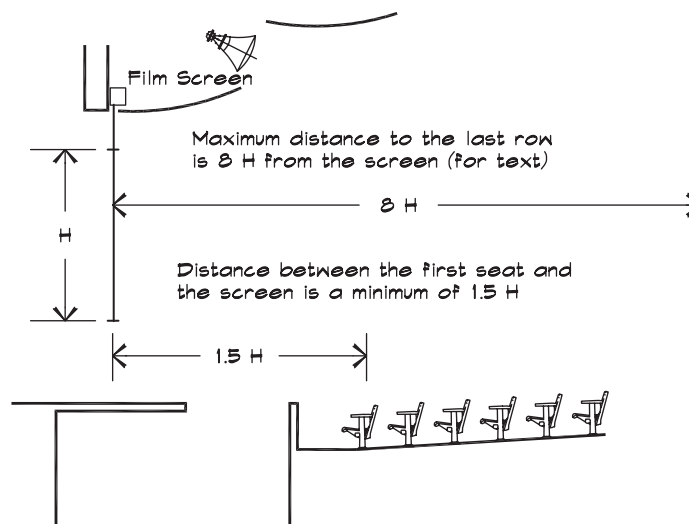
20.2   DESIGN OF SPECIFIC ROOM TYPES

Small Auditoria

The acoustical design of an auditorium is more complicated than that of a lecture hall, however the general principles are very similar. The variety of seating layouts, wall shapes, and ceiling designs is much greater in theaters than in lecture halls. Figure 20.6 shows several theater-seating arrangements, including the traditional proscenium stage, an open stage, thrust stage, and an arena stage. Of these, the proscenium stage arrangement is the most serviceable.

In a proscenium theater the audience views the actors on stage through the picture frame of the proscenium opening. In the United States a stage must be separated from the audience area by means of a fire curtain, which descends to cover the opening in case of a fire. Stage widths vary from about 40' to 50' (12 m to 15 m), with heights ranging from a minimum of 18' to about 30' (5.5 m to 9 m). A 2:1 width-to-height ratio is fairly typical. Very high proscenium openings are trimmed down with teaser curtains.

If the auditorium is to be used for orchestral or choral concerts, a shell is important, and the side walls of the room should merge smoothly with the walls of the shell. Where there is an orchestra pit, it should be convertible into a thrust stage or a place for additional seating. Every theater should be able to accommodate some kind of thrust stage or one will eventually be built over the seats.

Side wall designs in legitimate theaters are less critical than ceiling designs, particularly when the floor plan incorporates fan-shaped, black-box, or arena seating. In proscenium theaters, the lower side walls are left reflective, and the rear wall is treated with absorption. Upper side walls can also be treated, depending on the overall reverberation time requirements. It is useful to provide reflecting surfaces on the side walls close to the proscenium so

FIGURE 20.6 Basic Stage Forms Used in Theater Design

PROSCENIUM STAGE

ARENA STAGE

OPEN PROSCENIUM STAGE

OPEN STAGE
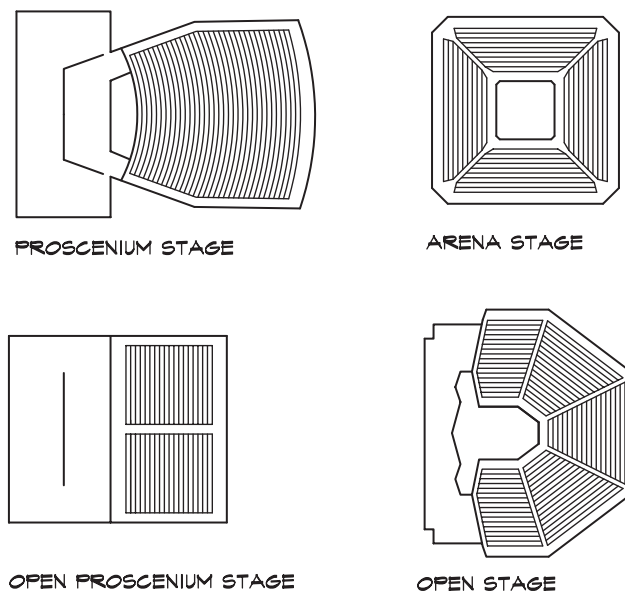
that when the actors face away from the audience, their voices are reflected back toward the seating area.

Rear walls in theaters and small auditoria are almost always absorptively treated. This is the case even with small recital halls, where high-reverberation times are desirable and difficult to obtain, since excessive loudness results from a hard back wall. Even if the program lists only small-group performances, eventually a small orchestra will be featured, which will overwhelm the space.

In virtually all theaters of more than 150 seats, a sound-reinforcement system is used. It is not uncommon to have radio mics on actors even in middle-school productions. Live theater is best served by a mixer located within the audience space. The front of the balcony or the rear of the orchestra seats are the preferred locations. Second best is a mixer located in a booth, with a minimum 6 ft (1.8 m) wide by 4 ft (1.2 m) high open window directly in front of him. For this width, double three-panel telescoping windows work well. In areas where security is a concern, a closeable window allows the technical booth to be locked.

Figure 20.7 shows a small auditorium at the Meadows School in Las Vegas, NV. Meadows combines a number of important features previously discussed. One unique element of the design is the cross aisle, which is at the same elevation as the stage. This is a convenient solution to the handicap-access problem both for the seating area and for the stage. It also allows flexibility in the staging of productions, graduations, and lectures. The walls are angled along the sides to merge with an orchestra shell and support wood diffusing elements.

The seating is easily accessible and provides excellent sight lines. The stage is relatively large with nearby access to the catwalks and the pit. Scenery is suspended from tracks running laterally across the stage. The lighting catwalks are convenient and do not require ladders for access, an important safety feature in school facilities. Side lighting platforms are positioned above the entry doors. Tracks for absorptive curtains run along the rear of each catwalk, above the audience, making the reverberation time somewhat variable. The pit is large enough to be used as a teaching and storage space and can be closed off to provide a thrust stage. An elevator is available for freight and passenger transportation to the pit. A two-tiered technical booth houses audio and lighting control on the lower level and follow spots on the upper level. The large technical-booth window is openable for mixing. Overhead panels give good support for early reflections and are coordinated with the design of the loudspeakers and catwalks. The rear wall is covered with 2" (50 mm) cloth-covered fiberglass panels.

Another interesting school auditorium, shown in Fig. 20.8, is Rugby Hall at Harvard-Westlake School in North Hollywood, CA. It is a small theater, which was remodeled from a flat-floored assembly room, originally at the level of the lobby, into a multipurpose auditorium. During the reconstruction the floor was dug out and the front lowered to provide a sloped-seating area and stage. The side walls were slanted in at the top and facets incorporated to provide early reflected sound. The ceiling was shaped for beneficial overhead reflections, while accommodating the existing steel beams and providing for an exposed lighting catwalk. The catwalk is sufficiently open that the sound system fires through it without noticeable loss, and is accessible from ladders on the sides.

Since this facility was built within an existing building shell, on a limited budget, there was no opportunity to include an orchestra pit. The orchestra is located either on the flat floor in front of the stage or on a temporary loft constructed about 15 ft (4.6 m) above the rear of the stage. This latter approach addresses the balance problem and provides reasonable blend,

FIGURE 20.7 Meadows School Auditorium, Las Vegas, NV, USA
(Acoustician: Marshall Long Acoustics)
(Architect: Killefer, Flammang, Purtil)

CENTERLINE SECTION

FLOOR PLAN

0   10   20   30   40   50

Scale (Feet)
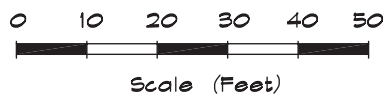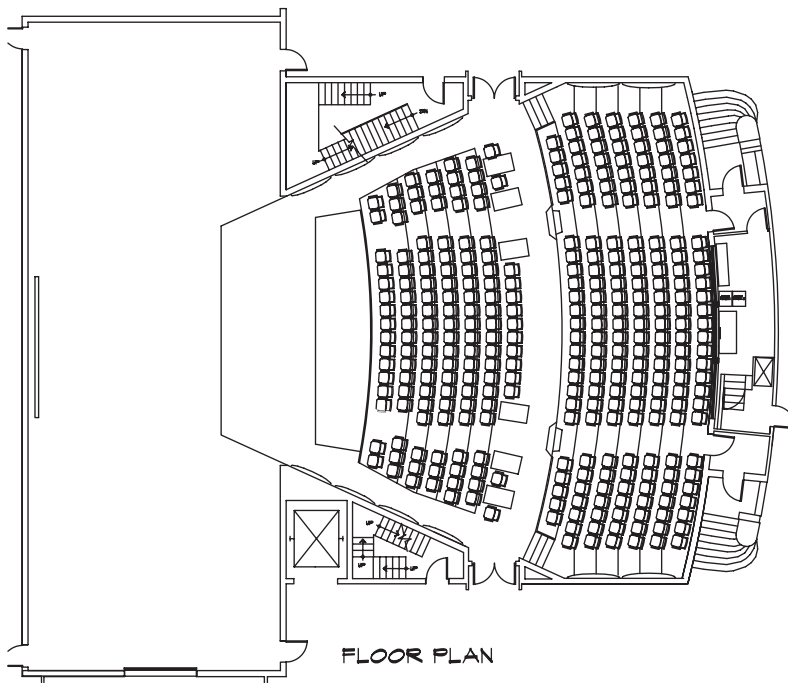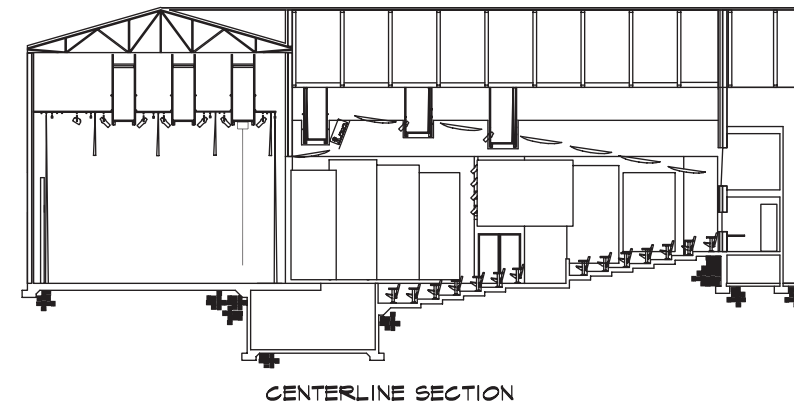
FIGURE 20.8 **Rugby Auditorium, Harvard Westlake School, North Hollywood, CA, USA**
(Acoustician: Marshall Long Acoustics)
(Architect: Johnson and Sylvestri)

LONGITUDINAL SECTION

LATERAL SECTION

FLOOR PLAN

Storage
Stagecraft
Storage

Foyer

Auditorium
Stepped Floor
For 386 Opera Chairs

Level
Floor
Orchestra

Platform

0   10   20   30   40   50

Scale (Feet)
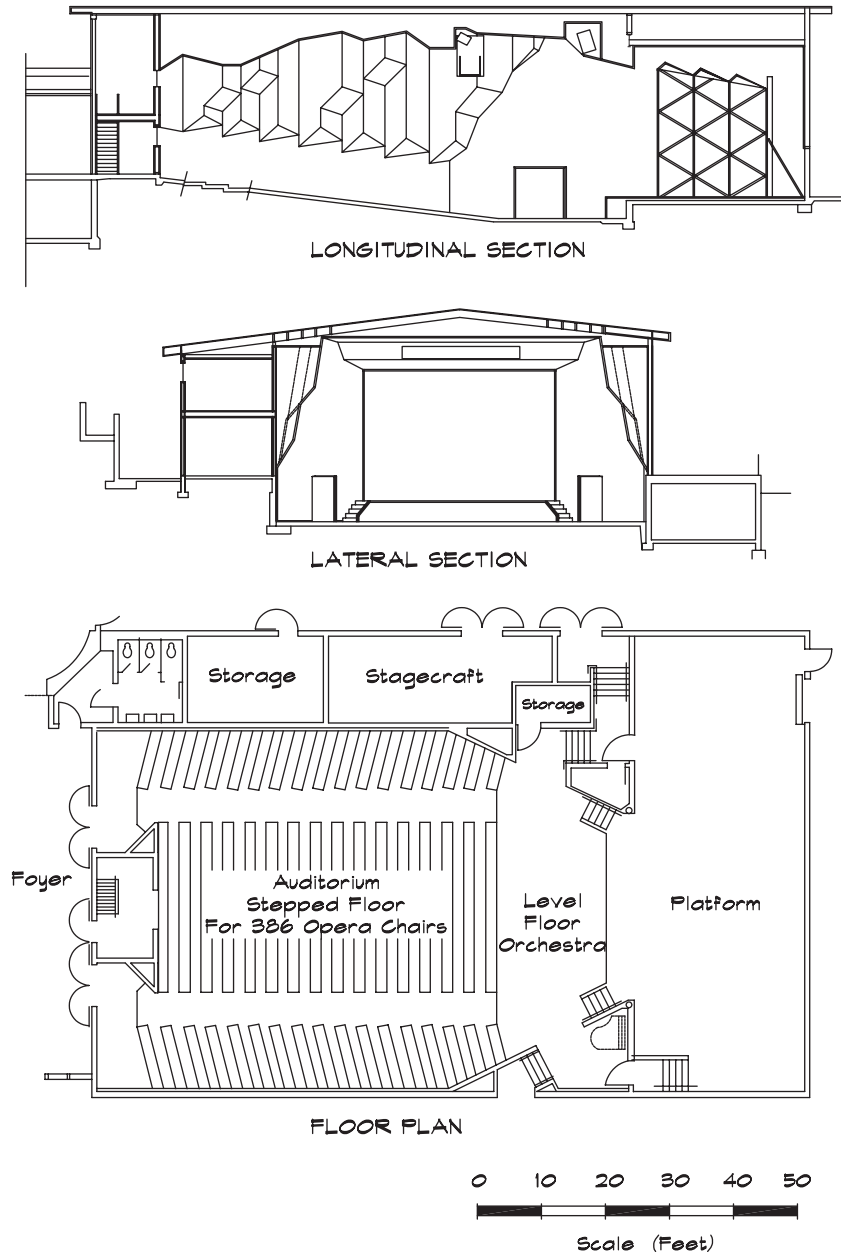
since the ceiling of the platform is close by. It removes some of the upstage area from use, so a thrust stage is built onto the flat floor area.

The design of the side walls is interesting. The bottom portion is flat and provides good support for speech. The lower wall facets are angled to give additional early reflections, while the upper walls are highly diffusive. The result is a dramatic jewel-like appearance, which was relatively easy to build in spite of its apparent complexity. The rear wall is made of wood slats over a cloth facing and a 1" (2.5 cm) fiberglass panel. The hall provides good support for both speech and musical performances.

Mid-Sized Theaters

An auditorium that serves a community as legitimate theater, lecture hall, and chamber orchestra hall, should accommodate the needs of both speech and music. Mid-sized auditoria follow many of the same design guidelines as small ones. With moderate seating requirements, these facilities can be designed to provide an excellent environment for both theater and orchestra. First-floor seating can be limited to 900 to 1000 seats, yielding very acceptable sight lines, with the remainder in the balcony. A good example is Ambassador Auditorium in Pasadena, CA, which seats 1250. It is a medium-sized hall, used for chamber orchestra, dance, small musical groups, and lectures. A plan and section are shown in Fig. 20.9. The design of the hall is subtle and interesting. The side walls fan outward in two steps and are faced with a beautiful wood finish. Above the lower walls is a large perforated metal enclosure on each side, overhanging the side aisles, painted in a textured wood finish. It houses large absorbing curtains, out of sight of the audience, to provide variable control of the reverberation. The rear wall is faced with the same perforated metal, over absorptive panels.

The visual ceiling is formed by gold anodized metal bars running along the length of the auditorium. It is transondent, but visually masks an upper ceiling formed from diffusive v-shaped plaster ridges running across the hall. The lighting catwalks and ductwork are exposed between the two ceilings but are painted black. Hanging below the lower ceiling are gold-colored reflective shields in rows across the hall. Two of these rows are located permanently above the audience. Two others are hung above the orchestra, forming a canopy that becomes the open roof of the orchestra shell. These large reflectors give the sound in the hall exceptional clarity, particularly in the orchestra seats. In the balcony the sound character is not as crisp, due to the oblique angle of incidence with the reflecting panels and the reflection from the stage floor, but is still quite clear.

The spacious pit floor, supported on a hydraulic lift, can be raised to form a thrust stage. When the pit floor is set to match the height of the audience floor, it can be used as an extra seating area. It can also be lowered to the normal pit level or still further to a storage level where it can serve as a large freight elevator.

The orchestra shell is constructed from wood panels, with coffered sections faced with wood dowels approximately 1.5" (38 mm) in diameter, spaced about 12" (0.3 m) apart. These do not add appreciably to the diffusion, because of their small size, but they break up the regularity of the coffers and create a pleasant sense of artistic balance. The reflectors above the shell are stored in the fly tower when not in use. They provide good high-frequency clarity on stage; however, since they are open to the space above they do not contain and project the bass. Lack of bass reverberation and envelopment are probably the only weaknesses of this space, which is the best chamber-music hall in Los Angeles and certainly the most beautiful.

FIGURE 20.9 **Ambassador College Auditorium, Pasadena, CA, USA**
(Acoustician: BBN; Architect: DMJM)

SECTION
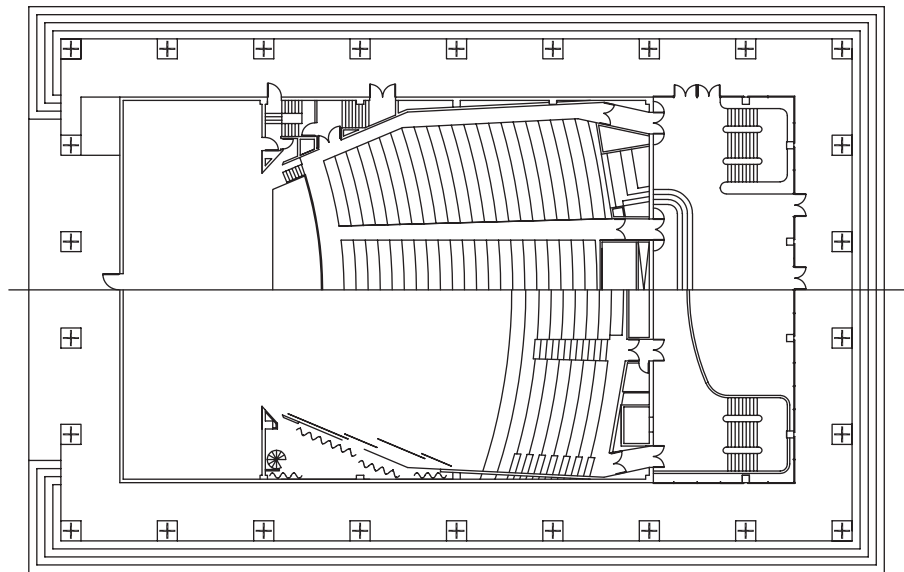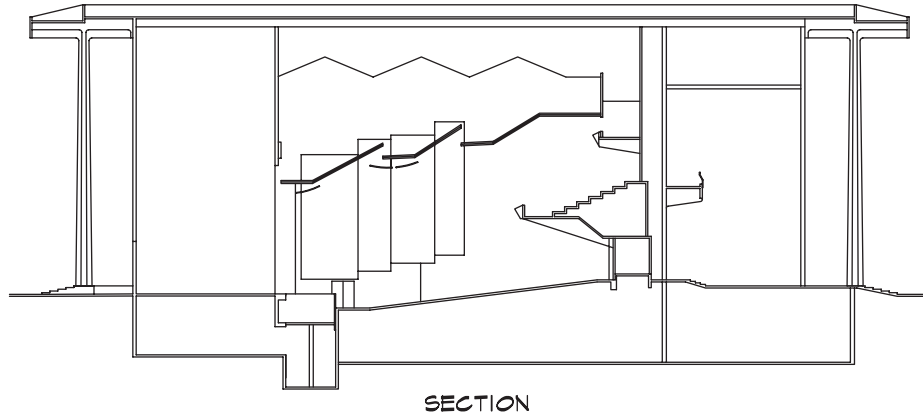
FIRST FLOOR PLAN – BALCONY PLAN

0   20   40   60   80   100

Large Auditoria

Large general-purpose auditoria in the 1500 to 2000 seat range must accommodate the full gamut of theatrical activities from orchestral performances to theater, ballet, lectures, and travelogues. The designers face a number of decisions about the shape, volume, reverberation time, clarity, and diffusion. Size magnifies any acoustical defects, so room volumes and reverberation times are best held to the low side of the concert hall range.

The stage should be big enough to handle a full theatrical performance with at least as much wing space as there is stage space. The width of the proscenium in a large theater can range from a minimum of 40 ft to as much as 60 or 65 feet and its height is about half its width. The full proscenium can be trimmed down with top (teaser) and side (tormentor) curtains. Ancillary rooms should include a large shop with easy access to the stage, orchestra and choir rehearsal spaces, and green and dressing rooms.

A fly tower above the stage is a necessity for legitimate theater. Fly towers are 2.5 times the proscenium opening in height so the line sets can be pulled out of sight. The scenery is raised and lowered from the side walls either at stage or catwalk level. The top of the fly tower must be accessible to service the loft blocks and gridiron. The stage catwalk system should be connected to the lighting catwalks located above the audience.

The orchestra pit can be open, if the hall is designed for opera, but is partially open in mixed-use facilities. The best pits have one or more hydraulic lifts to reconfigure the stage apron, and easy access from the practice and green rooms. The upstage edge of the pit opening must lie in front of the proscenium arch leaving four or five feet of space so that announcements and lectures can take place with the curtain drawn.

The auditorium must accommodate both theatrical and musical events with easy conversion between the two. The most common practice is to enclose the orchestra onstage within a shell either flown from the fly tower, stored in a dedicated room, or assembled from moveable towers. Another approach is to move the orchestra either partially or entirely in front of the proscenium and to close off the fly tower just behind the proscenium arch. This was the design concept used at Hamilton Place (Johnson, 2002) in Ontario, Canada. A 17,000 lb (7.7 m ton) cedar wall is lowered down to the stage floor, creating an orchestral platform in front of it, and neatly solving the acoustic problem of sealing off the fly tower. It also eliminates the need for back-stage storage of the shell and can serve as the fire curtain. The side and overhead reflectors can be designed for the same source locations irrespective of the performance configuration, and the overhead lighting requires little change. When the orchestra is on the thrust stage, the front seat wagons are lowered on the second lift and stored beneath the main floor seating area.

A sketch is given in Fig. 20.10. The flaring walls near the proscenium serve as acoustical reflectors for theater and as side walls of the orchestra shell. Simple hanging banners are used for variable absorption along the upper side walls. Both the upper and lower balconies float away from the side and rear walls, which increases the envelopment. The walls are highly diffuse and are displaced outward, a feature that increases the volume for music but still leaves space for the banners. It is a strong design, which is simple to convert from one form to another.

Traditional Churches

Church architecture has evolved out of a denomination-dependent historical context. Traditional Catholic churches look back to the cathedrals of the Middle Ages and often have high ceilings and the long reverberation times associated with Gregorian chant. Church design after Vatican II in 1969, when the saying of Mass in a language other than Latin was permitted, has moved toward an emphasis on speech and to breaking down the barriers between the laity and the clergy. Consequently, designs have tended toward lower reverberation times, smaller room volumes, padded pews, and more absorptive treatment.

**FIGURE 20.10   Hamilton Place, Hamilton, Ontario, Canada
(Acoustician: Russell Johnson; Architect: Trevor P. Garwood-Jones)**

SECTION

MAIN FLOOR AND FIRST BALCONY FLOOR PLANS

| 0 | 20 | 40 | 60 | 80 | 100 |

Scale (Feet)
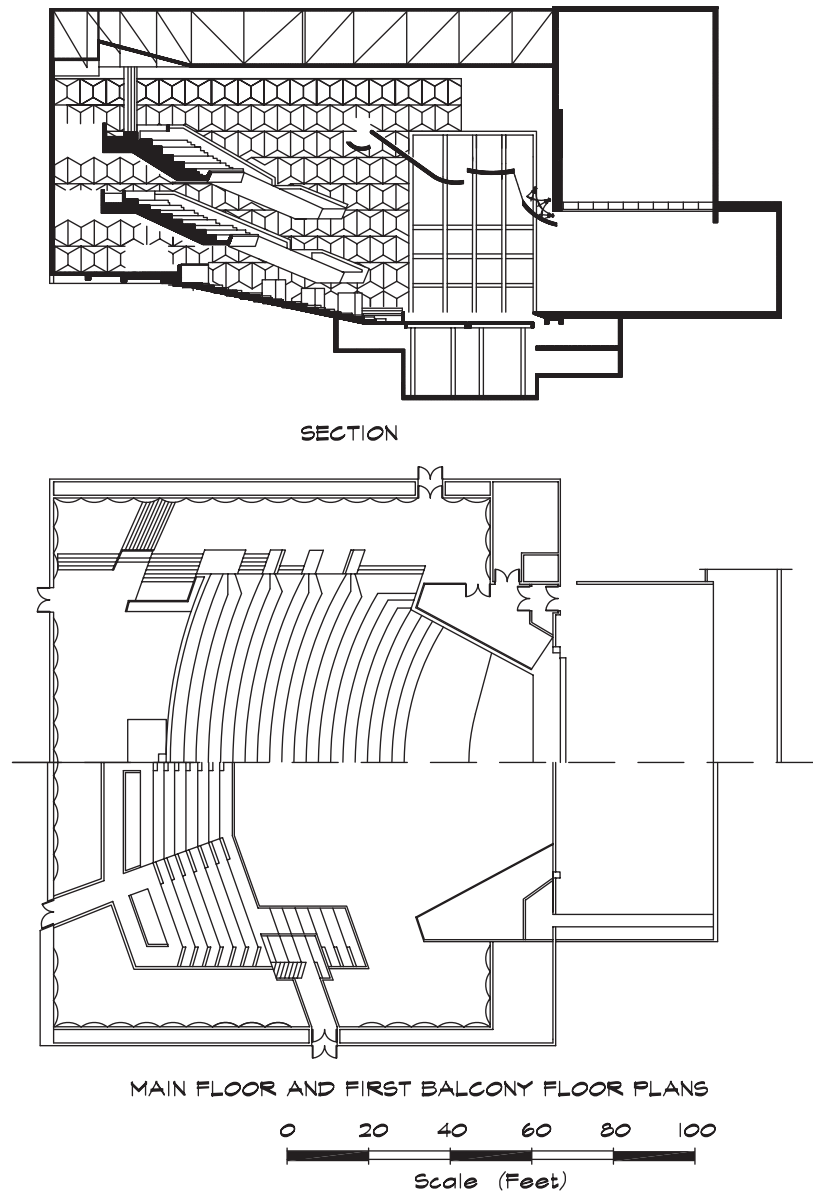
Episcopalian churches, reflecting their Anglican-Catholic heritage, are usually cruciform shaped, often with a double row of columns, reminiscent of the Roman basilicas. The pews are seldom padded but the room volumes tend to be lower than in Catholic churches. A raised pulpit, accessed by a steep wooden stairway, is a common feature. The choir is frequently located in a deep apse behind the altar. When monastic seating is used, choir voices do not project as well as when the choir is facing the congregation.

Other Protestant denominations place more emphasis on speech communications and have lower ceiling heights and padded pews. Their worship spaces, which evolved from

the northern European churches of the Reformation, can be rectangular-, cruciform-, or fan-shaped with a raised dais at the front. Electronic systems are becoming more central to the worship, particularly in the fundamentalist denominations. Many have multiple services on the same day, requiring different room configurations and musical setups. Since they support a variety of musical performances, stored presets for a given gain structure and a known group of microphones can save a good deal of time.

Today all religions need to preserve the dialogue between the congregation and the clergy so that speech intelligibility is critical. The overall shape of the room can assist with this. Churches in the round with the congregation surrounding a raised platform in the center of the room are difficult to design. The loudspeakers are ceiling mounted. Time delays are a challenge if there is more than one lectern position and the minister must turn his back on some of the congregation, or if the choir is located in a different part of the church. Worship spaces with both the dais and the choir at the front of the room sound much better.

Music is also important to worship, and the balance between speech and music is strongly influenced by the architecture. The choir should be located near the front, behind or on one side of the altar, so that the timing is consistent with the speech reinforcement system. Occasionally it is positioned at the rear on a dedicated balcony, in which case a separate dedicated sound system should be used. Accompanying instruments such as piano, organ, or instrumental groups should be located near the choir to help synchronize them with the singing. When there is an organ, its pipes should not be too far away from the singers or there will be a noticeable difference in the arrival time of the instrumental music and the singing. Churches having a pipe organ for instrumental concerts sometimes use a separate electronic synthesizer to support the choir.

Although there is no single best design for a worship space, several general design principles are helpful.

1. The chancel and pulpit should be elevated even if the loudspeaker is electronically reinforced.

2. Sections of the worship space that are acoustically separated should be designed to have acoustical properties similar to those in the main space. This may require the addition of absorptive treatment to high ceilings to balance out the reverberation times.

3. Solid walls or large ceiling beams should not separate seating areas, otherwise choral sound is not well distributed. Where large exposed structural members are necessary, they should be open trusses.

4. The choir should be located near the altar in an area that is open to the main part of the sanctuary, so that the singing can propagate freely throughout. The choir should be surrounded by reflective surfaces, to aid in distributing the sound to the remainder of the space. Choir enclosures should be free from flutter echoes, focusing, and long delayed reflections.

5. Pews or seats padded on the backs and sides are critical to minimize the difference between the empty and full condition.

6. An electronic reinforcement system, providing high intelligibility, even coverage, and the full range of frequencies without feedback, must be included. A mixer, located in the main space or in a nearby mix booth, should be used for singing.

7. Noise from both mechanical (interior) and environmental (exterior) sources must be controlled to a level consistent with the size of the space. Small churches are designed to an NC 30 (35 dBA) and large spaces to an NC 25 level (30 dBA).

One of the most difficult choices in church architecture is how reverberant to make the space when there is an emphasis on music. As a general rule, the reverberation time is designed to meet the musical needs of the space, and the intelligibility depends on the design of the sound system. In practice, however, the two must be designed together. If the sound system cannot overcome the reverberation, the signal-to-noise ratio must be increased either by adding absorption, by decreasing the loudspeaker-to-listener distance, or by increasing loudspeaker directivity. This does not mean that sound systems must be large and ugly to be intelligible. Intelligible sound systems can be designed without massive central clusters.

A good example of a reverberant church with excellent intelligibility is Saint Paul the Apostle Church in Chino Hills, CA, shown in Fig. 20.11. It has a high central roof supported by an intricate and beautiful truss structure. Fanning out from the raised roof area, at a lower elevation, is a semicircular roof, which drops from about 25 feet (7.6 m) to near 10 feet (3 m) at the outside walls. At the rear of the main sanctuary is a small mezzanine, where the mixer and audio equipment are located. The church seats about 1250 worshipers and was designed for both speech and music. The mid-frequency reverberation time is about 1.85 seconds even though nearly two-thirds of the high ceiling is absorbent.

The loudspeakers are integrated into the architecture of the space. In the low-ceiling area, there are ceiling-mounted 12" (0.3 m) diameter coaxial loudspeakers. The central seating section is covered by a pair of cabinet loudspeakers, built into the framing of the truss work. Large subwoofers are supported on the catwalks near the top of the center ceiling area. To preserve the source image, 5" (13 cm) loudspeakers are incorporated into the face of the steps around the dais. These are delayed so that they lag a natural sound coming from the altar, and all other loudspeakers are delayed in rings centered on this point. The result is a sound that is clear and intelligible and, from any point in the church, appears to be coming from the center.

Large Churches

Large churches, between 2500 to 5000 seats, are increasingly common, particularly in Baptist and fundamentalist denominations. Dependent on electronic audio reinforcement systems, they often feature video screens with projected images from television cameras or recorded sources. They are designed as both theatrical and religious spaces with complex sound, lighting, and video systems. Many services include entertainment in the form of high energy music, dance, folk singers or other musical groups, and prerecorded video images. The natural acoustics of the room itself does not add appreciably to the audience experience but can detract from it. Since rooms are large, the reverberation times should be modest and the ceiling should be designed to give support to congregational singing.

Reverberation times in the 1.5 second range are a good compromise value. Hard ceilings are preferred to absorptive ones both for singing and because high levels of amplified bass will cause the T-bar ceilings to buzz. A drywall ceiling also helps redirect sound from the loudspeakers toward the rear seats. Padded pews or opera chairs are very important, since most of the absorption comes from the seating area. Since worship services can last two hours or more, congregational comfort is important.

**FIGURE 20.11A   St. Paul the Apostle Church, Chino Hills, CA, USA
(Acoustician: Marshall Long Acoustics; Architect: WLC)**

SANCTUARY FLOOR PLAN

Scale (Feet)
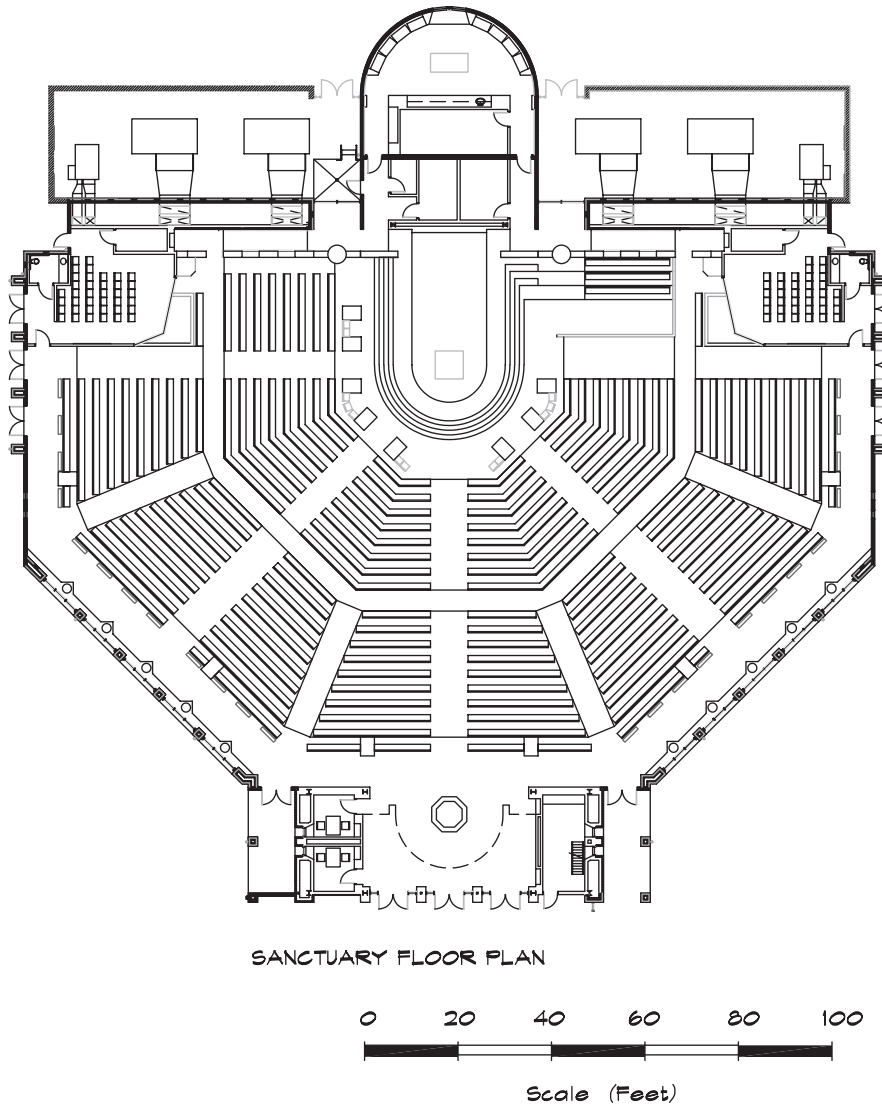
Because of the large scale, the seating arrangement is invariably fan-shaped and includes a substantial balcony. An included angle of no more than 160° is recommended due to sight line considerations. Since the rear walls are concave, a reflection from this surface can result in serious focusing, they are treated with at least 2" (52 mm) cloth-wrapped fiberglass panels. A calculation of the curvature gain for both the talker and loudspeaker positions can be undertaken to determine if absorptive treatment is necessary.

Balconies should be sufficiently stiff to withstand rhythmic movement by the congregation. The highest natural frequency of rhythmic jumping is about 1.75 Hz (Allen, 1997). The fundamental frequency of a church balcony should be designed above the third mode of the excitation frequency or about 6 Hz to minimize resonant vibration.

FIGURE 20.11B   St. Paul the Apostle Church, Chino Hills, CA, USA

LONGITUDINAL SECTION

LATERAL SECTION

Scale (Feet)
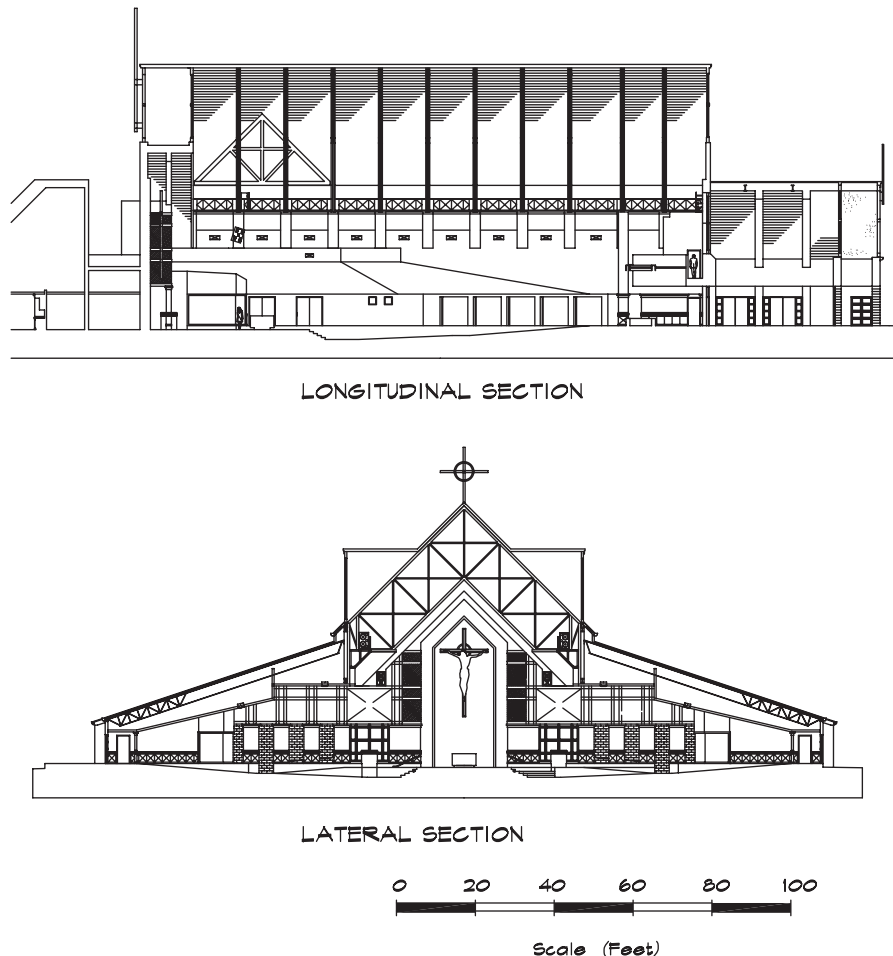
A canopy built above the platform housing the loudspeakers, video screens, and lighting instruments is the best choice. Since religious services can reach levels of 95 dBA or more, the sound system is large and requires a steel structure to provide support and access to the clusters. Amplifier racks should be located close to the loudspeakers to reduce the amount of heavy-gauge wire needed to be pulled. Ample power can be made available from nearby electrical rooms. Local step-down transformers must be vibrationally and acoustically isolated. In very large congregations (6,000 to 10,000 seats) multiple rings of loudspeakers are required to cover the whole seating area. Since clusters are more than 25 feet in the air, localizing loudspeakers around the platform are necessary to pull the image down. These can be built into the step riser using small horn or cone loudspeakers. Full-range loudspeakers are not necessary to give the illusion of direction, but the first-arriving sound must be within 10 to 12 dB of the cluster level.

A design sketch of the West Angeles Church, a large Pentecostal church in Los Angeles, is shown in Fig. 20.12. Seating 5000, its floor plan is fan-shaped with 60% of the seats in the balcony, including the long slanted areas along the side walls. The fan angle is 154°, but even at this angle there is some shielding of sight lines to choir area at the rear of the platform.

FIGURE 20.12   **West Angeles Cathedral, Los Angeles, CA, USA (Acoustician: Marshall Long Acoustics; Architect: Langdon and Wilson)**

0   20   40   60   80   100

Scale (Feet)

SECTION

BALCONY FLOOR PLAN
SHOWING CANOPY
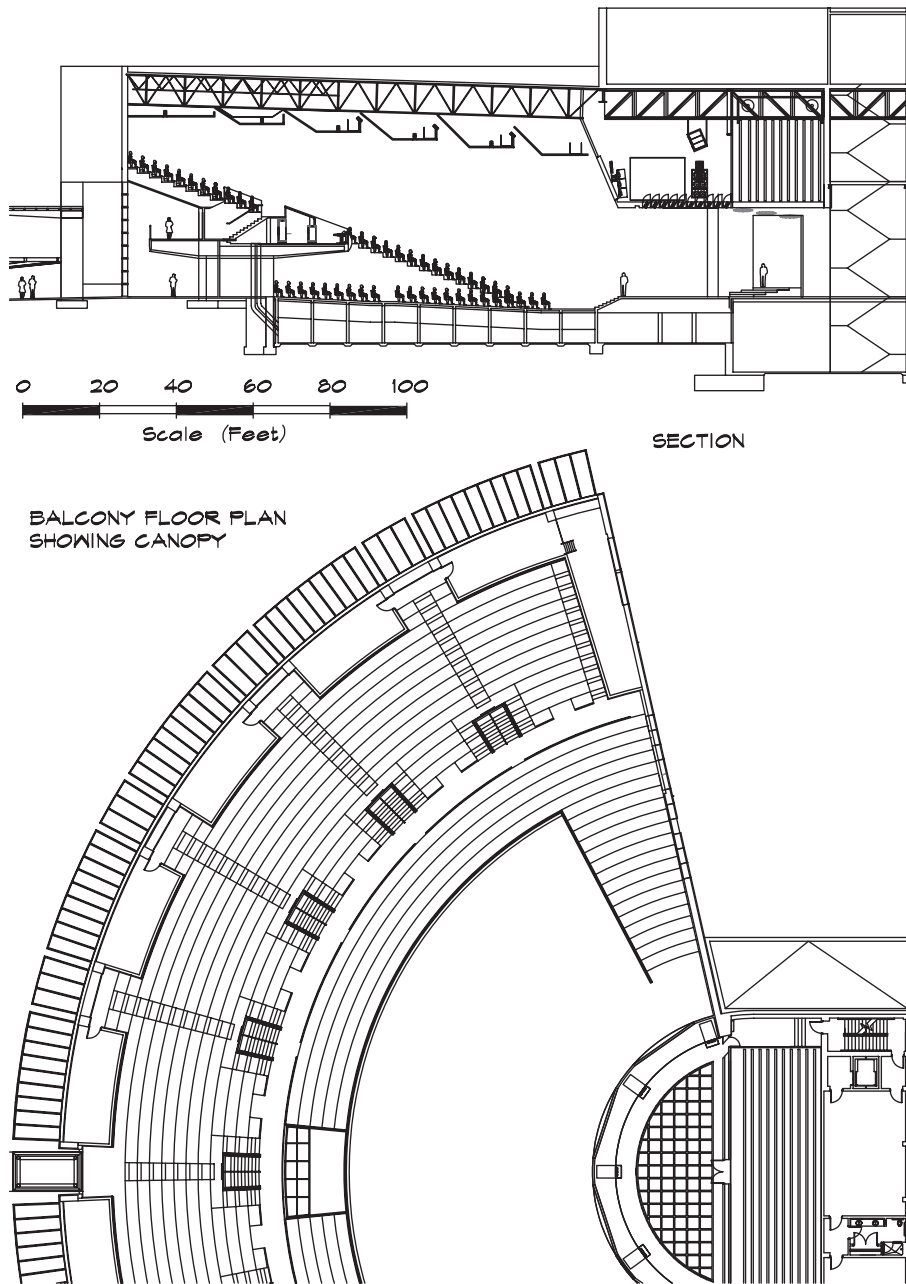
The front of the platform that projects out from the front wall, is clearly visible, and can support a wide variety of performances. A canopy was designed to house the loudspeaker clusters, rear-projection video screens, and lighting fixtures, making for easy access and good coverage angles. Lighting catwalks ring the ceiling and help define its shape. The sharply defined corner of the ceiling in front of each catwalk keeps the theatrical lighting from shining on the video screens—an important concern in spaces with live TV coverage, where light levels must be kept high. The underside of the canopy is about 23 feet (7 m) high. This is high enough to get a sense of space above the platform but low enough to provide good acoustical support for the choir. The underside of the canopy is diffusive to avoid an echo return from overhead. Unfortunately the canopy was eliminated by the client in the final design.

Dedicated audio and lighting control positions are located in an open mix booth on the front edge of the balcony with an enclosed equipment booth behind. The patchbays and outboard equipment racks are in back of the mixer position. The wall above these low racks is glazed, allowing the technical director (TD) a clear view of the platform from within an acoustically isolated space. Since the congregation must be able to see over the booth, its ceiling is slanted down toward the platform. Video switching for the projection screens occurs just behind the TD position. Mixing for audio and video recording takes place in a separate studio. Audio and video recordings of the service are made available as part of the outreach ministry.

Large churches such as this one are totally dependent on electronic technology to distribute their message. Visual contact with the minister is enhanced through live television pickup of the service and projection on large video screens. Multiple video screens located in a canopy are ideal since they can be located between the loudspeaker clusters, giving good sight lines to most congregants. Screens located on either side of the choir are also a feasible alternative, however the seating fan angle has to be lower than about 130° for this to work well. Rear-projection screens are preferred to front-projection screens, since they can be angled down and they do not wash out under high background-light levels.

Synagogues

A synagogue is designed acoustically like other religious spaces emphasizing speech. Music is sung by a cantor, who is sometimes electronically reinforced but often not. There is usually a social hall adjacent to the sanctuary, separated by large doors or moveable partitions, which can be opened to combine the spaces. The social hall can serve as an extension of the main sanctuary during holidays so the audio systems must be linked. Social halls are designed primarily for speech intelligibility. Occasionally churches and synagogues will share a facility, which is used as a synagogue on Friday and Saturday and a church on Sunday, so the room must accommodate the needs of both congregations.

Orthodox synagogues have separate seating areas for men and women, divided by a freestanding wall or curtain. Orthodox Jews are proscribed from working and from doing a number of other things on the Sabbath, beginning Friday night at sundown and continuing until sundown Saturday. There is, for example, a prohibition against the lighting or extinguishing of fire, although an existing fire may be used for cooking. This teaching affects the use of electronic sound reinforcement. Each local rabbi makes his own decision on the exact interpretation and some congregations prohibit amplified sound, where there is a voltage zero crossing that is considered a lighting (or extinguishing) of fire. Others forbid the use of a dynamic microphone that initially creates the positive and negative voltage, but allow capacitive microphones because they modulate a DC voltage by varying the capacitance.

In the case of a prohibition of a zero crossing, a battery can create a voltage offset. This reduces the power output of the amplifier since the signal can only swing from zero to the positive rail, but the design complies with the teaching. David Klepper (1999) has written an interesting article on the subject.

20.3   SPECIALIZED DESIGN PROBLEMS

Once the seating capacity and floor plan layout have been established, multipurpose auditoria still have a common set of specialized design problems to be solved. These include the shape and structure of the side walls and ceiling surfaces, the configuration of the orchestra shell and how it is stored, the layout of the pit and access to it, the accommodation of variable-acoustic elements including room volume, absorption and diffusion, and the inclusion of audio/visual elements.

Wall and Ceiling Design

Side wall and ceilings should provide useful reflections to the orchestra level seating, while angling outward to accommodate fan-shaped seating layout. One approach is shown in Fig. 20.13, a design study for a large multipurpose auditorium. An interesting feature of this design is the compound-arc shape of the ceiling and wall sections. When designing for speech intelligibility, a slightly curved convex shape is ideal, whereas for high diffusion a low-radius curve is preferred. The walls and ceiling in this example are formed in a convex shape, which appears nearly flat for sound coming from the stage, but is diffuse for sound returning from the rear and sides. It provides good intelligibility, based on the first reflection, and gives good diffusion on subsequent reflections. Consequently it acts like an acoustical diode, whose properties depend on the direction of sound incidence. The side walls are angled to give good support for actors and singers onstage as well as reasonable envelopment from side reflections. When an auditorium is designed with a highly diffuse ceiling, the clarity of both speech and music can suffer in the balcony, particularly when the side walls are far apart. Both Davies Hall in San Francisco and Royce Hall at UCLA in Los Angeles share this problem.

Note that in the Fig. 20.13 design a second group of loudspeakers is used to cover the balcony seats. Delayed clusters of this type should employ drivers having similar characteristics to those used for the main cluster. They should be located in front of the seating section they are covering, so an appropriate delay time may be selected. See Chapt. 18 for a discussion of this topic.

Shell Design

The design of shells and platforms is a subject meriting close attention. The general principles have been previously discussed; however, certain details are important to review. In multipurpose halls, shells are temporary structures, stored out of sight when not in use. In a concert hall the shell is a permanent construction and merges with the proscenium arch. In surround halls shells are formed from the partial-height walls around the orchestra platform.

A shell serves several functions:

1. It provides early reflections so that orchestra members can hear themselves and each other.

2. It separates the orchestra from the unfavorable acoustical environment in the fly tower and backstage.

FIGURE 20.13 **Freedman Forum (Design Study)**
(Acoustician: Marshall Long Acoustics)

SECTION

ORCHESTRA AND BALCONY FLOOR PLANS

Scale (Feet)
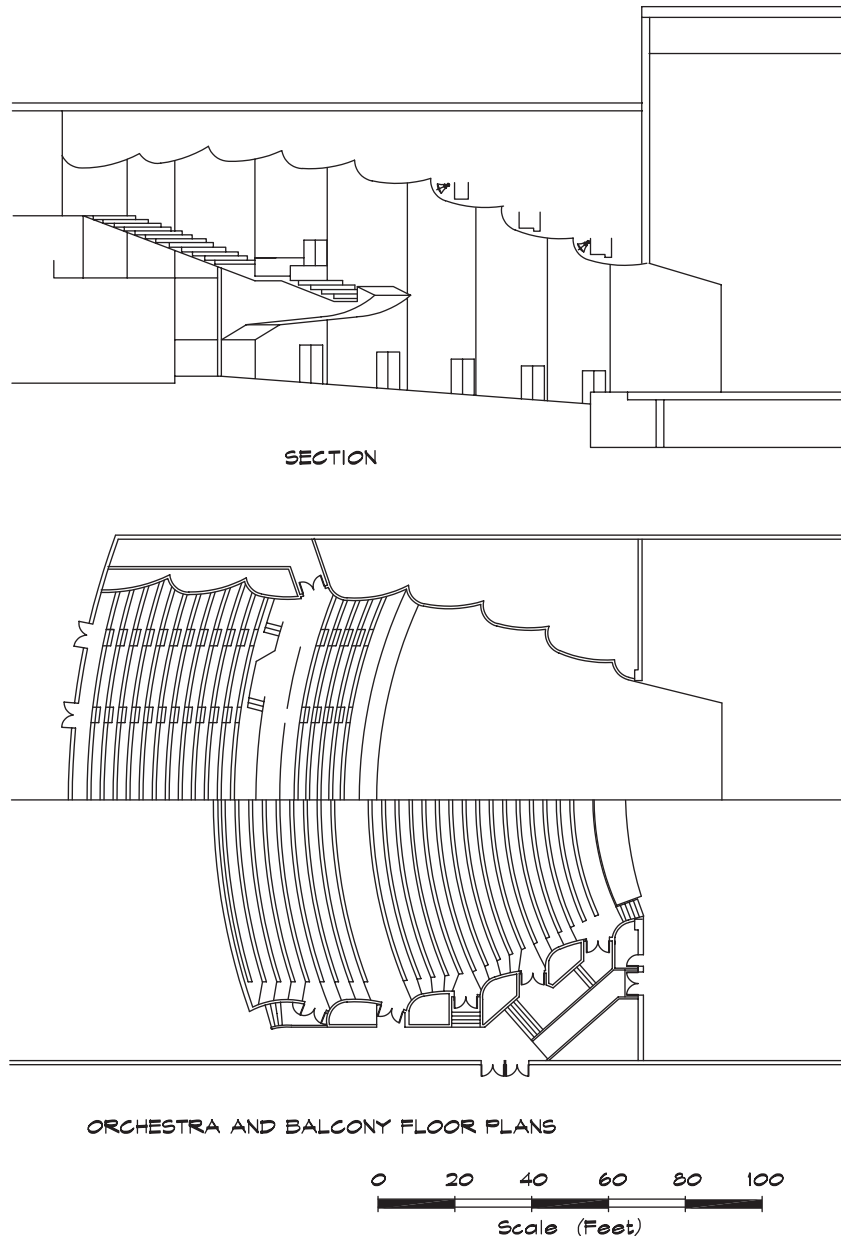
3. It helps reflect sound, primarily bass, to the audience.

4. It creates a local reverberant (diffuse) environment for the musicians.

5. It forms an attractive architectural backdrop for the orchestra, consistent with the design of the remainder of the auditorium.

6. If it is modular in construction, it can be stored efficiently when not in use.

Following these design goals we can attempt to find a Goldilocks solution—neither too deep, too high, nor too wide—just right. Depth is particularly critical. A shell should not be more than 30 to 40 feet deep from the front edge of the stage to the face of the rear wall. Boston Symphony Hall, a very good design, is about 35 ft (10.7 m) deep. Vienna is just over 30 ft (9.2 m). A shallow depth is particularly important for the reinforcement of the double basses, which should be arrayed along the rear wall of the enclosure. Not only does this arrangement benefit from a reflecting surface close by, it also forces the row of instruments to become a line source, when their notes are coherent, whose output is maximized in the direction of the audience. An overly deep enclosure allows the orchestra to move away from the rear surface, thereby giving up low-frequency gain. An overhang at the rear of the shell is also helpful. Both Boston and Vienna have excellent examples of this feature.

The orchestra enclosure should be narrower at the back and the shell walls should merge smoothly with the auditorium walls. The width of the platform and shell should average no more than 50 to 60 feet (15 to 18 m) at its midpoint, yielding the 2000 sq ft (186 sq m) or so of floor area recommended by Barron (1993) and Beranek (1996) for a full orchestra. When the orchestra is widely dispersed, the communication between the players is reduced. Gade (1989) found that beyond a distance of 26 ft (8 m) the delay in the direct sound can reduce the ease of ensemble playing. It is difficult to keep an orchestra this close together. Nearby reflectors either overhead or behind the orchestra can help offset distance effects.

Using Barron's (1993) recommendations for concert halls in Fig. 19.15, a platform volume of just under 70,000 cu ft (2000 cu m) yields a shell height of 35 to 45 ft (10.7 to 13.7 m). Boston's height is in this range at 43 ft (13 m). Amsterdam and Vienna have no shell. Carnegie Hall's shell is on the high side at 47 ft (14.3 m). In smaller auditoria this dimension can be reduced since proscenium heights are often no more than 20 ft (6 m). The front of the shell should match the proscenium when it is below 45 ft (13.7 m). It is also important that the ceiling of the enclosure not be too low. Low ceilings produce a sound on stage that is overly loud, and divide the hall into separate spaces with different reverberant characteristics. Barron (1993) recommends that the early decay time onstage be no less than 70% of that in the main hall.

The orientation of the shell ceiling is also important. A reasonable fraction of the energy impacting the ceiling should return to the orchestra. For an ST1 of -11 to -13 dB at a position in the center of the platform, energy must be returned from the ceiling as well as the rear and side walls. If the rear wall is 20 ft (6 m) away and perfectly reflective, it will contribute -15.7 dB (re 1 m), leaving an equal amount to be contributed from the ceiling and two side walls. If they are each 30 feet (9 m) away, at least 70% of the energy would have to be returned to the platform by a single reflection. Since this is impractical, a local reverberant field must be developed onstage to give the orchestra a sense of envelopment and balance. A combination of direct reflections and diffusive elements can be employed to keep a portion of the sound within the enclosure. Protruding elements can be used on the side walls of the shell to give additional reflecting surfaces.

An example, shown in Fig. 20.14, is a small hall in the John Arin Center at Sir Wilfrid Laurier University in Ontario, Canada, designed for recitals and lectures. The sketch is based on the author's original design. The size of the side-wall reflectors was reduced 60% by the architect in the final configuration. The shell is constructed in panels, supported by overhead rails. Each panel has a lower portion that can be swiveled about its vertical centerline to expose either its reflective or absorptive side. The angle of the side walls is set so that the panels can be shunted onto a second track to form a rear wall, positioned farther back, to accommodate a modestly sized orchestra. The panels have diffusing elements in the form of

FIGURE 20.14   Recital Hall, Wilfrid Laurier University, Ontario, Canada
(Acousticians: Marshall Long Acoustics – Theater
Vibron Ltd. – Mechanical Systems)
(Architect: Lingwood Dubeje)

SECTION

FLOOR PLAN

```
0    10   20   30   40   50
```
Scale (Feet)
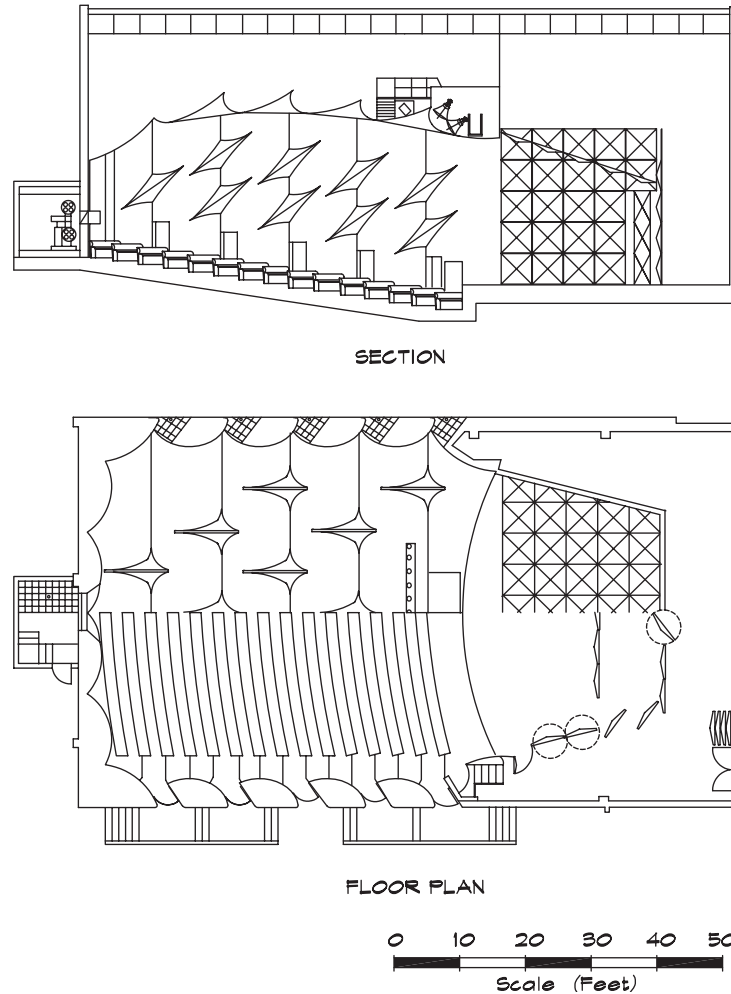
pyramids, angled so that one side is parallel to the stage floor. This provides high-frequency reflections back to the musicians.

In multipurpose auditoria the orchestra enclosure must be removable for theatrical performances. The shell ceiling can be designed to be flown from the rigging when there is a fly tower. If individually suspended clouds are used above the orchestra, bass energy will be lost into the absorptive fly tower and orchestral balance will suffer. Consequently a continuous roof is preferable to a series of open reflectors.

Modular side and rear panels can be rolled away on wheels or air casters to a storage area. There is a trade-off between ease of handling and bass absorption—lightweight materials being easier to move but more absorptive of bass. Barron (1993) recommends a material with a surface mass density of no less than 4 lbs/sq ft (20 kg/sq m), corresponding to 1" (25 mm)

FIGURE 20.15   **Ordway Hall, Saint Paul, MN, USA**
                (Acoustician: R. Lawrence Kirkegaard)
                (Architect: Benjamin Thompson)
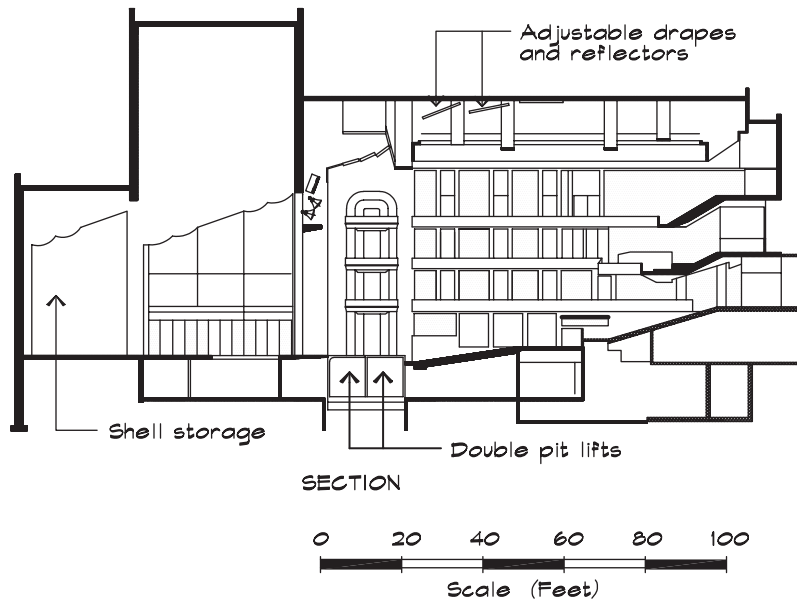
gypsum board or 1 3/8" (35 mm) plywood. These widths are feasible in fixed enclosures but difficult in a modular shell, which is constrained by weight to a maximum thickness of 5/8" (16 mm). Where thin wood is used, it can be shaped into a convex curve and backed with closely spaced structural stiffeners to reduce diaphragmatic absorption. Curves are constructed by laminating several thin sheets together. Heavy shells can be accommodated using air castors or rails. Figure 20.15 shows the orchestra shell of the Ordway Theater in Minneapolis, stored in its own room adjacent to the stage.

Platform Risers

Orchestra platforms are nearly always constructed of wood over an airspace, a configuration highly favored by musicians for the warmth of its sound. Askenfeld (1986) found that wood floors provide both beneficial support as a sounding board in the low registers, as well as low-frequency absorption for airborne sound. The flooring should be sufficiently light that it responds to vibrations generated by the cellos and double basses, and provides tactile feedback to the musicians, but not so light that it absorbs significant energy. Barron (1993) suggests 7/8" (22 mm) thick wood on sleepers spaced 24" (600 mm) apart to allow for some movement, while still maintaining structural support for heavy pianos or dance troupes. The depth of the airspace below the floor varies, but a cavity of more than a few inches is not recommended.

Portable stage risers are quite helpful for projection of sound, both as a local radiator and as a way of elevating the orchestra so that the players do not shield one another. Risers also form reflecting surfaces to contribute both diffusion and early reflected energy to the audience. Since they are modular and have a relatively short structural span, they can be

constructed of lighter wood than the main floor, but should not be less than 5/8" (16 mm) thick.

A riser system should be flexible enough to accommodate a choir located behind the orchestra. When the choir is not present it should be possible to move the orchestra back against the rear wall of the shell. A permanent seating area behind and above the orchestra is useful in concert halls and there are excellent examples in Vienna and Amsterdam. These seats can be used for the audience when there is no choir, although at a sacrifice in sound quality and balance for patrons seated there.

Pit Design

Pits in auditoria and multipurpose halls are designed in much the same way as in opera houses, with some exceptions. Stage overhangs in these facilities tend to be greater than in opera houses since the singers are not as powerful and orchestras need to be muted. Multipurpose auditoria rely on electronic reinforcement for individual singers and even for the orchestra. The audience seating area, which must be sacrificed to obtain an open pit, is so valuable that it is rarely worth giving up. It is critical to be able to raise the pit floor to the level of the stage either with a hydraulic lift or by installing a pit cover to provide for a thrust stage. The open portion of the pit can serve as an extra seating area when small musical groups are performing.

In musical theater, such as that found on Broadway, the pit band almost always is amplified, and sometimes a great effort must be expended by the sound designers to overcome the "natural" acoustics of the pit. Individual and sometimes multiple microphones are used for each section. A drum set, for example, might have five microphones to itself. Each of the feeds from an instrument section should be clean—that is, it should only include signal from the source being miked. In these instances absorptive panels are hung on the walls and gobos are used to separate sections of the orchestra so that they are isolated from one another. The best design approach in these cases is to allow extra space for absorptive or diffusive panels and provide plenty of microphone jacks—at least 24 and often as many as 48 are necessary.

Since access to the pit must be provided both for freight and the handicapped, an elevator is required. Figure 20.7 shows a good example of how this can be accomplished in a small high school auditorium. Even though an elevator is more expensive than a lift its flexibility and convenience pays for itself over the long term. Flexibility in the pit acoustics is also helpful. Removable diffusive and absorptive panels can be used to vary the local reverberation in different areas of the pit according to the seating arrangement of the orchestra.

Diffusion

Adequate diffusion is critical for obtaining an even distribution of reverberant sound in a listening space. Diffusion helps absorptive materials be more effective, by scattering sound so that it is more likely to encounter these surfaces. Where there is inadequate diffusion, acoustical defects such as flutter echo or coplanar reflection patterns can develop. Lack of diffusion can produce irregularities in the slope of the reverberant decay in a room. In concert halls and other critical listening environments the listener gains a sense of envelopment, of being surrounded by the sound, from reflections that come from the side. Lateral reflections are enhanced by materials or objects that increase diffusion.

Diffusion reduces the glare caused by reflections from flat or slightly curved panels. Too much high-frequency energy reflected from walls can produce an annoying brightness or,

in the case of parallel panels, a flutter echo. This condition can be treated by roughening a surface with irregularities on the order of 2.5 cm (1 in) deep or by adding a thin, 5 mm (3/16"), layer of absorptive felt or fabric curtain. Flutter also can be treated by angling a wall about 1:12 with respect to the opposite face.

The quantification of diffusion is a subject of some theoretical interest. Several methods available to model its effects in ray tracing programs are discussed in Chapt. 22. Two separate technical problems exist—first, how to characterize the interaction of a sound wave with a surface, and second, how to incorporate this characterization into the calculation of room acoustics. In the simplest case, illustrated by a numerical measure such as SDI, a single number rating is assigned, based on visual inspection of the room surfaces (Haan and Fricke, 1997). This, however, does not provide a clear method for the calculation of the level of a reflected sound wave, let alone the more complicated metrics such as interaural cross-correlation coefficient or lateral energy fraction.

Figure 20.16 shows several examples of diffusing surfaces. Ornamentation such as columns, statuary, caryatids, railings, balustrades, steps, organ pipes, and chandeliers can all help. Prefabricated diffusing materials are becoming available in wood, FRP, and masonry units, which have the advantage of providing a predictable behavior. Diffusion should be used in areas where specular reflections are not helpful. Although this sounds obvious, it helps identify surfaces where the application of diffusion may be relatively benign. In an auditorium, likely areas include ceilings above reflective panels, the upper portion of a side

FIGURE 20.16   Examples of Diffusing Surfaces
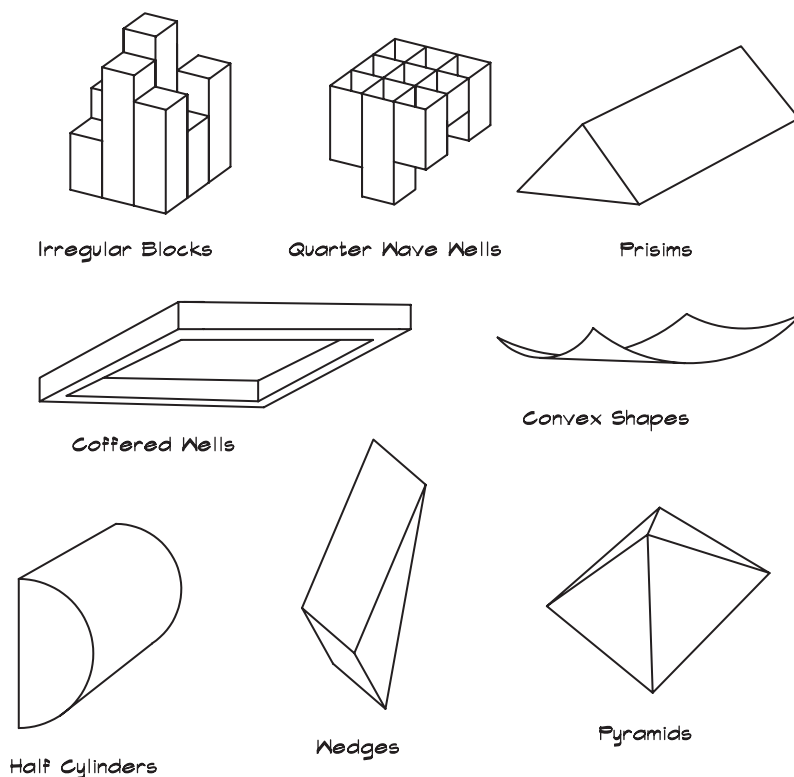
or rear wall, or on either side of the stage. Diffusion can also be helpful in orchestra pits, shell enclosures, practice rooms, and other small spaces.

Diffusing elements can include columns, statuary, and exposed structural members such as those in St. Paul the Apostle Church (Fig. 20.11B). Structural elements such as trusses or catwalks, as well as chandeliers and lighting instruments, projecting down from the ceiling, allow sound to pass beyond them and can yield excellent results. Figure 20.17 illustrates the design tradeoffs with lateral beams. If a deep beam or archway supports the ceiling, it can divide the room into separate acoustic spaces, since sound will be reflected back toward the platform and not propagate out. The combination of beam depth and ceiling height must be such that a significant fraction of the reflected energy continues to flow toward the audience.

FIGURE 20.17   Design of Coffered Ceilings
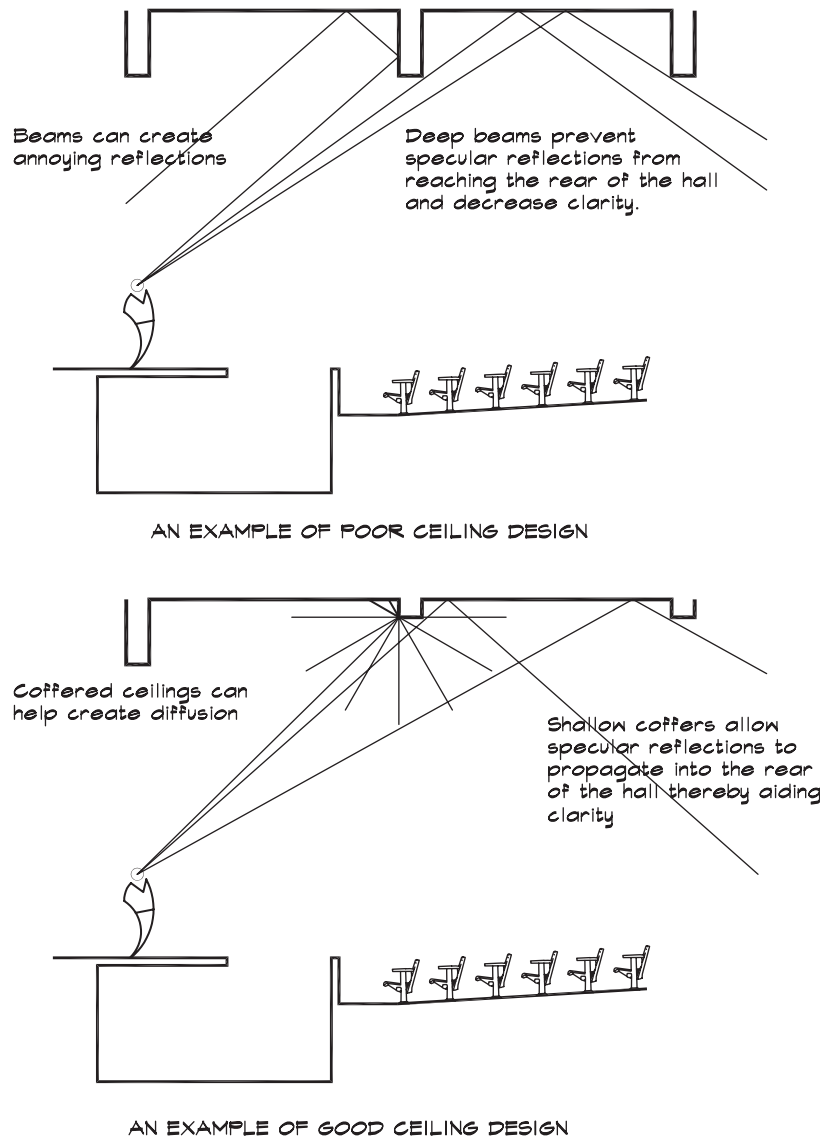
Shallow beams, on the order of one quarter wavelength deep, still help diffuse sound while allowing specular reflections from the flat surfaces to pass by. With high ceilings, deeper beams may be used since the approach angles are more acute.

The ideal tradeoff between diffuse and specular reflection is one of the more interesting design problems. Too little diffusion can result in inadequate envelopment, glare, and other undesirable characteristics. Excessive diffusion can also a pose a problem. A highly diffuse ceiling in a concert hall may reduce the clarity in the balcony if the specular reflections from the side walls are insufficient to compensate. Too much diffusion is also expensive and may not work well with the desired architecture. Surfaces providing both specular and diffuse reflections are ideal. Both Boston and Vienna are excellent examples of this characteristic. Their coffered ceilings are nearly flat, between the dividing beams, and are relatively shallow. The flat portions allow specular reflections to continue on toward the rear seats, while a portion of the sound is scattered off the beams.

Variable Absorption

In multipurpose auditoria and even in dedicated concert halls, there are occasions when the rooms will be used for speech or when the addition of absorption to reduce reverberation is appropriate. There are many complicated ways of doing this including rotating triangular absorbers, barn door panels, and sliding mechanisms. The simplest methods feature fabric curtains or banners hung from tracks that can be trundled or lowered into place either mechanically or by hand. Large areas of curtain are required to make substantial changes in the reverberation time. For example if a 2-second reverberation time is to be changed into 1.5 seconds using absorptive material, an area equal to about one-third the audience area must be added. This could require 4000 sq ft (370 sq m) of highly absorptive material in a 2000 seat hall, a substantial amount, given the fact that it must be stored away out of sight when not in use. Absorption is most often added using heavy (doubled 20 oz/sq yard) fabric banners that are lowered through slots in the ceiling, directly into the auditorium, or behind transondent perforated metal screens. Where there is space behind a balcony, or a side seating area, banners can cover a substantial area. Curtains should be positioned so that there are several inches of airspace behind them to maintain their effectiveness at low frequencies.

Beranek (1949) published data on absorptive curtains, given in Table 7.1. Gathered curtains are difficult to store unless they are supported on horizontal tracks or large rollers. The folds help improve the low-frequency absorption mainly by increasing the thickness. The amount of gather is expressed as a percentage of the total length of the curtain divided by its finished length. Curtain absorption is a strong function of the percentage of gather as shown in Fig. 20.18.

When absorptive banners cover portions of the lower side walls, they can absorb early reflections and detract from the clarity of speech. Therefore they should not be installed immediately adjacent to seating areas where they can reduce useful reflections. If absorptive treatment is placed on side walls near listeners, local overhead reflectors extending out from the walls can be helpful in adding back early reflections to side and rear balconies, since they will not be covered by a banner.

The more difficult it is to vary the absorption, the less likely it will be done. In small auditoria curtains can be hung from the ceiling adjacent to catwalks from which they can be slid into position by hand. The range of reverberation times available through this type of adjustment is limited, but a variation on the order of 0.3 seconds in small halls is possible and

FIGURE 20.18   The Effect of Draping on the Sound Absorption of Curtains (Mankovsky, 1971)
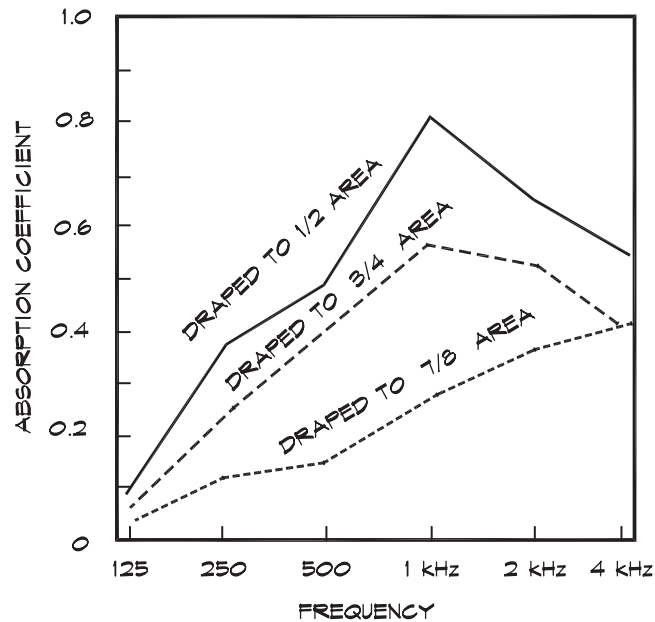
can be helpful. In large auditoria, curtains are motorized and preprogrammed presets can be used to automatically adjust the amount of exposed surface. One of the most flexible acoustic spaces is at the Institut de Recherche et Coordination Acoustique/Musique (IRCAM) in Paris. The room is used for recording, acoustic research, and as a small auditorium seating about 400. Both the volume and the absorption can be varied—the volume by raising or lowering the three-part ceiling and the absorption by rotating three-sided prisms to expose surfaces in several orientations, drawn in Fig. 20.19. It is highly flexible but not a good model for a general performance space due to its complexity.

Variable Volume

Since the reverberation time can be varied by changing either the absorption or the volume, it seems inevitable that variable volume halls would appear. Early examples include a number on which CRS Sirrine was the architect and George Izenour the theater consultant, including Jesse Jones Hall in Houston, Texas (BBN acousticians) and Edwin Thomas in Akron, Ohio (V. O. Knudsen acoustician). The method employed was to suspend ceiling panels from cables, which in the case of Jesse Jones were individual reflectors; in Edwin Thomas, the design used the catenary curve formed by the cables. The rear portion of a suspended ceiling could be lowered to the front of the balcony to reduce the volume and seating area of the space. The hardware required to carry out this transformation was substantial, and these designs have not been widely emulated. Detailed illustrations have been shown by Izenour (1977).

Another interesting design concept, first used in the Derngate Centre, Northampton, England and later in the Cerritos Performing Arts Center in California, employs mobile seating towers, supported on air castors capable of being moved about. A sketch of the

FIGURE 20.19 IRCAM Rotating Wall Prisms

A) Specularly Reflecting

B) Diffusing

C) Absorbing

D) Highly Diffusing
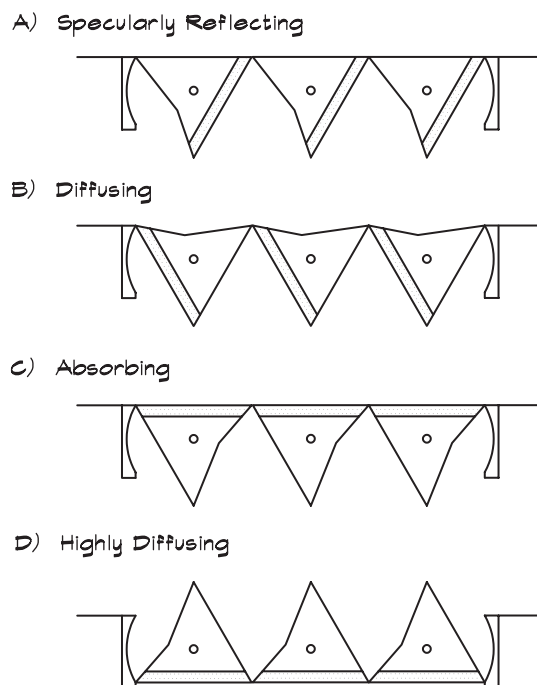
seating arrangements in the Cerritos Center is given in Fig. 20.20. The rear walls of the towers are constructed of perforated metal so that absorptive banners can be lowered behind them. The envelopment in these spaces is not high, since perforated metal does not give much reflective support (Barron, 1998). The design is very flexible, however, and a clever way of allowing the rearrangement of the space into multiple configurations.

A mechanically adjustable ceiling is the most straightforward way to change room volume. A vertically adjustable ceiling has been recently installed in the Sala Sao Paulo, Sao Paulo Brazil. This space was built by converting a large outdoor courtyard, formerly a waiting area for an administration building adjacent to the railroad station, into a concert hall. The open-air plaza was bordered by two rows of columns that formed the sides of the new hall. A coffered ceiling, consisting of 30 separate sections hung from cables, can be raised and lowered to adjust the volume according to the type of music being played. A sketch of the hall is shown in Fig. 20.21.

An increase in room volume lengthens the reverberation time of a space uniformly over the entire frequency range. It is unlikely to introduce coloration in the form of normal modes associated with resonant cavities. The increased reverberation is available to the listeners immediately as running reverberance, which means that it could negatively affect clarity, but also that it provides a greater sense of diffuse envelopment.

Coupled Chambers

Another method of raising the reverberation time in a hall is by increasing the room volume using coupled chambers, located adjacent to the main space, and accessed through openable doors or moveable wall sections. A reverberation characteristic results, which is somewhat

FIGURE 20.20A   Cerritos Center for the Performing Arts-Seating Configurations
(Acoustician: Lawrence Kirkegaard and Associates)
(Architect: Barton Meyers and Associates)

Concert Seating   Cabaret Seating   Arena Seating
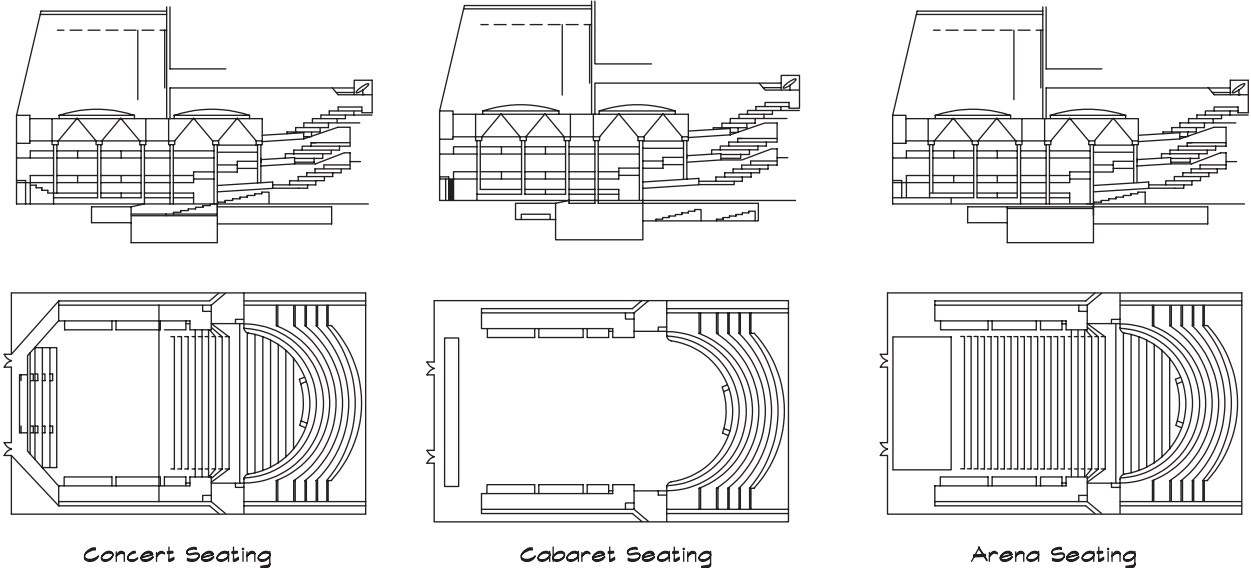
FIGURE 20.20B   Cerritos Center for the Performing Arts-Seating Configurations

Lyric Seating   Drama Seating   In the Round Seating
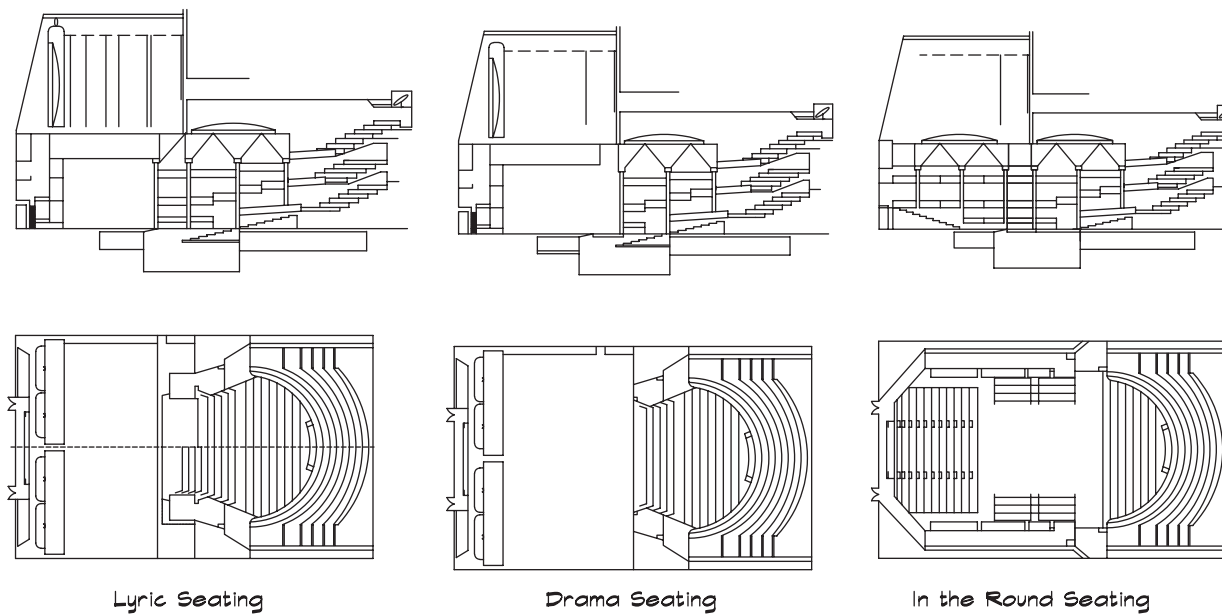
**FIGURE 20.21   Sala Sao Paolo, Sao Paolo, Brazil – Longitudinal Section
(Acoustician: ARTEC, Drawing reproduced with permission)**
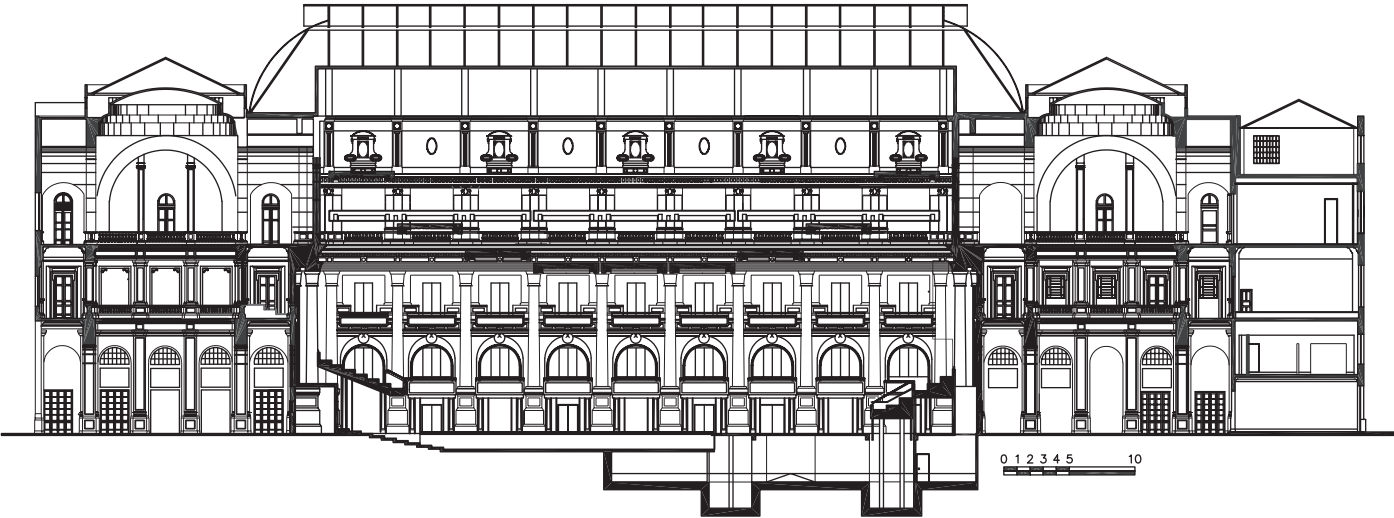
Figure 20.22 Dual Slope Reverberant Decay
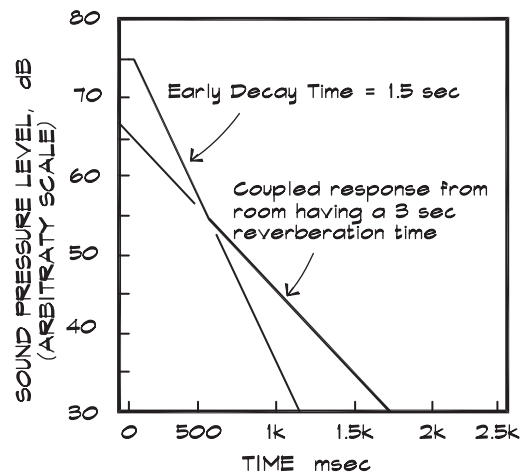
different than that obtained by simply increasing the volume in the main hall by raising the ceiling. Coupled volumes remove some of the energy from the primary hall and return it at a later time and at a lower level yielding a segmented energy-decay slope such as that shown in Fig. 20.22. This is perceived as a reverberant tail after a stop chord rather than as running reverberance (Beranek, 1996) audible during the music.

Separate hard-surfaced rooms, serving as reverberation chambers, can have characteristic resonant frequencies. A resonant device preferentially absorbs energy from the driving mechanism and returns it at a later time. Where there are characteristic modes of vibration in a coupled space these will persist longer than other frequencies. One hall, Sala Nezahualcoyotl built in Mexico City in 1970, has a concrete pit below the orchestra. Resonant chambers located directly under the orchestra are probably not a good idea since they absorb acoustic energy and in time become general storage areas. It is arguable that the energy would be more useful if it were available to the audience with the original sound rather than being banked for later distribution to the orchestra. When coupled chambers are located in the upper reaches of the auditorium the sound must first pass through the hall before entering them and is thus available to the audience. The Mexico City experiment has not been repeated.

Recently a number of halls designed by Artec in New York have included large reverberant chambers that are accessed through heavy openable doors or moveable sections of wall. The McDermott Hall in Dallas shown in Fig. 19.20 is a good example. The design maintains clarity from early reflections off the canopy, while giving reverberance to the space. The reverberation is not as strong as that associated with the classic rectangular halls such as Boston and Vienna but adds some liveness. Coupled chambers have primarily been included in orchestral halls rather than multipurpose auditoria.

Sound System Integration

When the sound system for a multipurpose hall is designed the loudspeaker layout is first modeled along the lines set forth in Chapt. 18. The most common methodology is to use a computer program to predict the loudspeaker coverage. Calculations must be undertaken in the 500, 1k, and 2kHz octave bands at a minimum to assure flat frequency response, feedback

FIGURE 20.23   Proscenium Loudspeaker Alignment
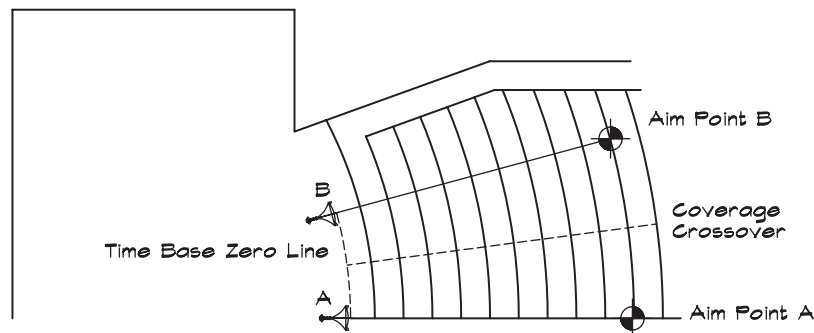
resistance, and adequate signal-to-noise ratio in the speech bands. Although equalization can be used to correct some of these problems, if the off-axis behavior of the loudspeakers is frequency dependent equalization may not produce an equal response at all locations.

In most multipurpose auditoria and churches, particularly those adopting fan-shaped seating layouts, the loudspeaker arrays required to cover the seating area include multiple horn and midrange cabinets, which are arranged across the front of the room. Since they are distributed in space there will be overlapping areas of coverage where care must be exercised in blending the sound fields from several sources. At receiver locations covered by more than one loudspeaker the arrival time from each source should be approximately the same so the transition between loudspeakers is smooth. The physical alignment of the loudspeakers is important, particularly at the overlap point. Figure 20.23 illustrates the concept. This loudspeaker arrangement is preferable to a central cluster such as that shown in Fig. 18.3. It yields better coverage and preserves the perceived source direction.

Since the directivity of high- and mid-range devices is not always the same, the number of the sources necessary to cover the audience is not always equal. For example, three horns may be required in an area that two mid-range cabinets can cover. In this case it is logical to place the mid-range cabinets between the horns. The faces of the loudspeakers should be arranged along an arc and time delays used to match the arrival time of each device. This matches the signals both in level and in time in the areas where the coverage of more than one loudspeaker occurs.

Cabinet loudspeakers are designed to match component directivity over the speech frequency range. Small horns maintain reasonable cabinet dimensions, but the directivity at the mid frequencies afforded by large horns cannot be duplicated in small boxes. Consequently cabinet loudspeakers are directional only above 2 kHz, particularly in the vertical plane. Loudspeaker manufacturers suggest that cabinets be arrayed to increase (or decrease) directivity, however an array such as that shown in Fig. 18.3 increases lateral high-frequency coverage but can decrease low-frequency coverage due to interference between the low-frequency sound fields in the horizontal plane. It may be preferable to match the directivities by using separate large-mouth horns and dual midrange boxes as shown in Fig. 18.2.

Where possible loudspeakers should be placed in a drywall enclosure, which protects the stage and provides some barrier shielding against feedback. Architectural design elements can be built around the enclosure. When a thrust stage is used, the extra shielding can be very helpful. The upper drawing in Fig. 20.4 gives a good example.

In large auditoria, a mixer should be located in the audience area, ideally on the center-line. The front of the balcony is probably the best location for a mix booth since the acoustic signal path is unobstructed. The FOH (front of house) mixer is seated at a mixing console with a clear view of the stage and with low-profile equipment racks located directly behind him. These racks house the sound sources necessary for the effects along with the wireless microphone receivers and jack bays necessary for the real-time control of the system. Amplifier racks and fixed audio processing and distribution equipment are remotely located since they do not require immediate adjustment.

In smaller facilities such as high school auditoria, where security is a concern, audio equipment is located in a lockable room or tech booth with an openable window separating the booth from the seating area. The window opening should be large enough, at least 4 ft (1.2 m) high by 6 ft (1.8 m) wide, to minimize low-frequency attenuation and give the operator a sense of the room. Eighteen-inch telescoping window panels allow a 6 ft opening in a 9 ft (2.7 m) total width. Mixing while listening to the sound using loudspeakers within a closed booth is not effective, although dummy heads with ear microphones have been used.

Electronic Augmentation

In spaces where there is insufficient natural reverberation, it is possible to introduce rever-beration electronically. The idea has a long history dating back to publications by Vermuelen (1958) and Olson (1959), who each proposed room-enhancement systems using microphones, delay lines, and loudspeakers. A number of commercial systems have subsequently been developed, which fall into two groups: direct field systems and, reverberant field systems. Both types sample the natural sound in the hall and use electronic processors to increase the reverberation time and occasionally the early reflections by reintroducing the signal through loudspeakers. The first group uses microphones close to the source, within one or two times the critical distance, and feeds the signal though processors and out to loudspeakers close to the stage as well as others located in the reverberant field. The second group uses microphones and loudspeakers located in the reverberant field. These cannot generate early reflected sounds.

The earliest systems consisted of a microphone, amplifier, and loudspeaker with either a single or multi-tapped delay line. A representative block diagram is in Fig. 20.24. In its simplest form a single microphone picks up the sound in the auditorium, delays it, and returns it back to the room via loudspeakers. Just as was the case in a reinforcement system this process generates a feedback loop characterized by a loop gain. The loop gain is defined as

$$\text{Loop Gain} = \mu = \frac{\text{Ave Mic Output from Loudspeakers}}{\text{Ave Mic Output from Source}} \qquad (20.1)$$

The system concept is the same as that shown in Fig. 18.13, except the microphones are not located as close to the talker and the feedback loop between the loudspeakers and the microphone is via the reverberant field. The loop gain is not constant with frequency. It has many bumps and dips, and varies with the position and orientation of the microphone. Clearly when the loop gain equals one we have sustained feedback and, in fact, the value must be much less than one.

The maximum value depends on the reverberation time of the room and the band-width of the system. For a broadband system and a 2-second room, the maximum loop gain before the onset of ringing is about -12 dB (Griesinger, 1991). In artificial reverberation

FIGURE 20.24 Single Channel Artificial Reverberator (Griesinger, 1991)

Simple Reverberator Made From a Comb Filter

0.10 D_e for an omnidirectional microphone
D_e = enhancement critical distance
= distance where the source level and the enhancement
system level are the same
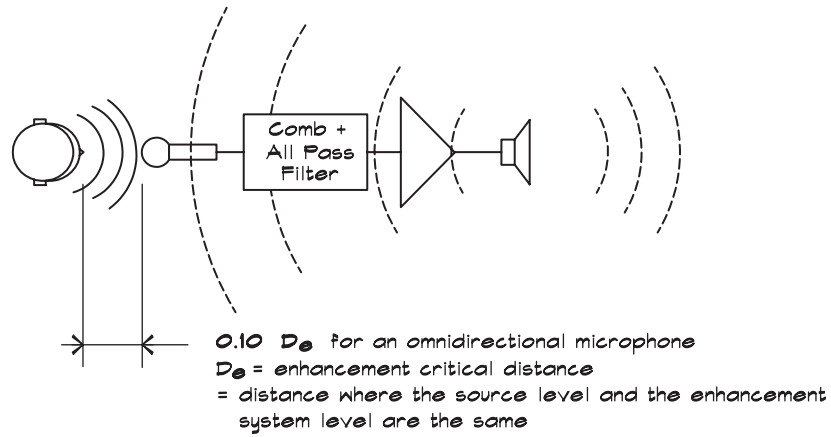
systems the loop gain should be another 8 dB lower or −20 dB to avoid coloration (Krokstad, 1991). This places rather severe constraints on the loudness of the system.

To overcome the feedback limitations the single microphone systems locate the pickup point close to the source. To meet the −20 dB limit, the ratio of the mic distance to the critical distance must be less then 1/10. In many halls the critical distance is on the order of 7 m (23 ft) (Griesinger, 1991) so an omnidirectional mic must be placed no more than 70 cm (2.3 ft) from the source. Although better for feedback, this close miking technique does not yield a representative sample of the sound in the room.

Directional mics can give some additional gain. A cardioid mic has about a factor of $\sqrt{3}$ (4.8 dB) increase in distance for the same feedback. For hypercardioids the factor is 2 (6 dB). But at 1.4 m (4.6 ft) you cannot single-mic an orchestra. Using multiple mics close to the sources overcomes some of this problem at a cost of reduced gain and considerable inconvenience. If the mics are mixed before processing as in Fig. 20.25, the nom correction reduces the minimum distance by $\sqrt{\text{nom}}$.

FIGURE 20.25 Microphone Mixing before Processing Increases Feedback Stability (Griesinger, 1991)

$\dfrac{0.174\ D_e}{\sqrt{NOM}}$ for cardioid microphones
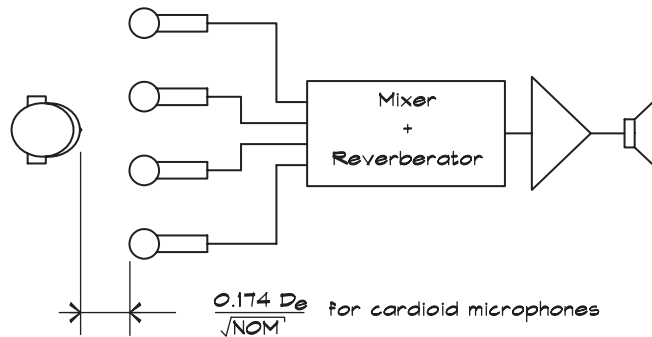
In an effort to achieve greater gain stability, systems with separate channels of reverberation, illustrated in Fig. 20.26, have been developed. If individual microphones and loudspeakers are separated so they do not influence each other, and if each channel meets the -20 dB gain limit, a channel will not be driven into an unstable feedback condition by the addition of another. Even if a single microphone is used to feed multiple reverberators before mixing, the same effect can be achieved. The overall reverberant level in the room and the reverberation time can be increased by 10 log (number of reverberators) and the source to microphone distance can be increased by a factor equal to the square root of that number. In practice each channel can increase the reverberation time by about 1% (Krokstad, 1991), so the total number of reverberators and loudspeakers needed may range from 50 to 100 in a typical system without additional processing.

Further improvements are possible through processing. The RODS (Reverberation on Demand System) system developed by Acoustic Management Systems uses a sophisticated gating arrangement pictured in Fig. 20.27. The logic module senses whether the sound in the room is rising or falling with time. The input to the delay is gated on when the room level is rising or constant and the output from the delay is connected to the loudspeakers only when

FIGURE 20.26 Multichannel Artificial Reverberation System (Griesinger, 1991)

Up to 50 or More Separate Channels
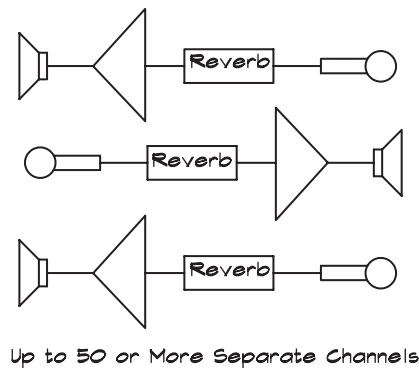
FIGURE 20.27 Reverberation on Demand System (Griesinger, 1991)
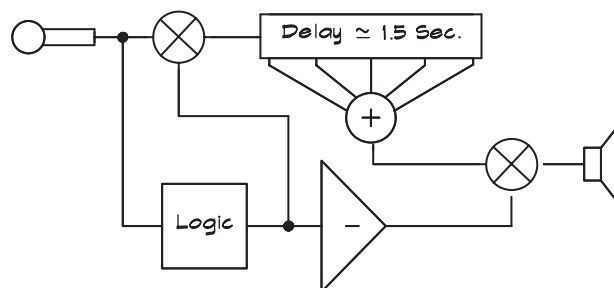
**FIGURE 20.28   LARES Reverberation System
(Griesinger, 1991)**
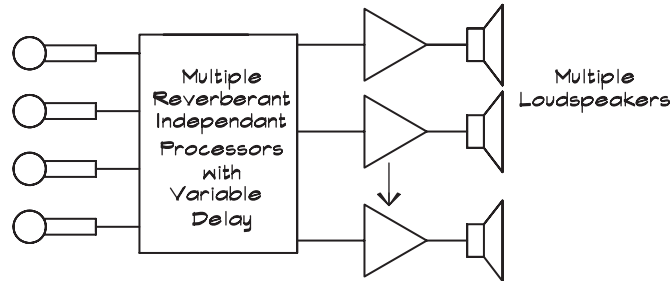
the level is falling. Feedback is reduced in this manner. Lateral energy is not augmented during continuous music but only during the times when the sound is decaying.

The LARES (Lexicon Acoustic Reinforcement and Enhancement System) system developed by David Griesinger (1991) uses multiple reverberators, shown in Fig. 20.28, which change their properties as a function of time. This is done by modulating the delay lengths in the reverberation algorithm (Frenette, 2000). Griesinger notes that a delay modulation results in a pitch shift so that the modulating source must be chosen carefully. For example, if random number generators were the source of the modulation it would be possible for all reverberators to go in the same direction at the same time, producing a noticeable pitch shift in the reverberation. A traffic cop in the software can sort this out. The variation must be sufficiently rapid that the autocorrelation function is zero for any two reverberators or for an individual reverberator with itself for a delay greater than 1 second. The randomization of the reverberator behavior allows the signal from a few (2–6) microphones to feed a large number (16–64) of processors and an even larger number of loudspeakers (up to 300+). Processing in the reverberation chain yields impressive increases in gain and the microphones can be moved back to 12 m (40 ft) from the source and still provide a substantial increase in reverberation time.

The overall loop gain follows the relationship

$$G_\mu \leq -12 \text{ dB (stability)} + 4.8 \text{ dB (cardioid microphones)}$$
$$-6 \text{ dB (safety factor)} + 6 \text{ dB (time variance)} \qquad (20.2)$$
$$+ 10 \log \text{ (number of reverberators)}$$

Even for a modest number of reverberators the system loop gain can be positive and the reverberation time, which follows the loop gain

$$G_\mu = 10 \log \frac{T_{60} \text{(enhanced)}}{T_{60} \text{(natural)}} \qquad (20.3)$$

increases accordingly.

Reinforcement systems can also control the time at which the energy is released. In rooms designed for speech sounds arriving at the listener earlier than 50 ms after the direct sound are useful for intelligibility particularly if they are in the median plane. Reflections arriving in the 50 to 150 ms range are not helpful for speech intelligibility and do not

contribute significantly to envelopment. In rooms designed for music it is desirable to be enveloped or surrounded by the sound field, particularly at frequencies below 300 Hz with sound arriving after 150 ms. In electronic enhancement systems low pass filtering can be helpful. Much of the positive effects fall into the frequency range below the 500 Hz, so more energy can be added to a space without increasing gain. A typical system attenuates signals above 500 Hz by 6 dB.

Some concert halls such as Boston enjoy early reflections from the shell or stage house, whereas others like Amsterdam have few reflections in this time period. Concertgebow is nevertheless highly intelligible since it has little masking in the middle time range, while enjoying excellent envelopment from late arriving reverberation. By using electronic enhancement, the sound energy in the time period beyond 150 ms can be altered without adding excessive energy to the 50 ms to 150 ms time period so that the extra reverberation will not degrade clarity.

21 DESIGN OF STUDIOS AND LISTENING ROOMS

21.1 SOUND RECORDING

Early Sound Recording

From the time of Thomas Edison's phonograph in 1877, up until about 1947 when practical tape recorders became available, recordings were made in real time as a single channel directly to the storage medium. The original Edison system employed a stylus attached to a diaphragm that scribed a grove into aluminum foil wrapped around a rotating cylinder. Later models used a wax cylinder, which could more easily be duplicated and stored. In 1887 Emil Berliner invented flat-disk recording that allowed straightforward manufacturing, although the initial quality was poor. Before 1925 all recording was done mechanically, with vertical hill and dale cuts in the surface. Interestingly, stereo recording was invented in 1929 by Arthur Keller of Bell Labs and later formulated by Blumlein in 1931 in its current 45°/45° groove modulation format (Alexandrovich, 1987), but the first commercial stereo recordings did not appear until 1957.

The early flat records rotated at a rate of 78 revolutions per minute (rpm), with information impressed, first on one and later on both sides of the disk. The record players were entirely mechanical. A sharpened needle stylus was attached to the center of a diaphragm, which was coupled to an expanding horn megaphone. A crank handle that wound a coiled spring provided motive power. Speed was controlled by a mechanical governor. In console units, openable doors at the end of the horn controlled the level. Since the first engineers had no temporary storage capability, there was no ability to manipulate or playback music for post production and thus no need for post-production facilities. Recordings were made with the duplicating equipment in the same room as the musicians. The sound level during a recording session was controlled by positioning a ball of yarn in a large megaphone used to concentrate the sound energy onto the pickup diaphragm (Alexandrovich, 1987).

With the invention of the audion (vacuum) tube by Lee De Forest in 1907, the audio amplifier by Harold D. Arnold in 1912, and the condenser microphone by E. C. Wente in 1917, sound could be converted to electrical signals, and used to drive a groove-cutting lathe to make a master disk from which duplicates could be pressed. Bell Telephone Laboratories

carried out experiments in "auditory perspective" and demonstrated three-channel stereo transmission on telephone lines in 1933 (SMPTE, 2001).

Sound for motion pictures had many originators. W. K. L. Dickson, working in Thomas Edison's laboratory, invented one of the early recording systems in 1895. It was offered to the public in the spring of 1895 as the Kinetophone and consisted of a recording on an Edison wax cylinder along with the Kinetoscope, a box housing a rotating strip of photographs that were observed through a peep hole. The sound was transmitted to the viewer via two rubber ear tubes.

In the silent film era of the 1910s, orchestras or theater organs played a musical score accompanying the film. Loudspeakers were later placed in the orchestra pit to replicate the musicians and still later added behind the screen for dialog—a system that required manual switching between the two by the projectionist. The vitaphone, a system of multiple long-playing (33.3 rpm) records, was introduced in 1926 as a way of recording music, but not dialog, for film. The first motion picture with dialog was *The Jazz Singer* in 1927. In 1928, Disney's *Steamboat Willie* appeared, featuring the first soundtrack created in post production including music, dialog, and sound effects.

Walt Disney's 1940 film *Fantasia* (Garity and Hawkins, 1941) was a giant technical leap forward, employing four channels of recorded information, three separate audio channels, and a tone control channel using a variable-density optical system printed on 35 mm film. The system used two linked projectors, one for the film and one for the sound. The film included an optical mono mix of the soundtrack as a backup, a scheme that is still in use today. It introduced several other innovations for the first time including multichannel surround, the pan-pot, overdubbing of orchestral parts, simultaneous multitrack recording, and three directivity-aligned loudspeakers located behind the screen (SMPTE, 2001).

The Disney engineers also originated many new techniques including the use of multiple optical recorders called dubbers (short for doublers) to do mixing. Musicians were seated in a large stage and played the score while the film was being screened, a technique that is still used today. The conductor watched the film listening to timing cues, called a click track, through a single headphone. Sound effects, later nicknamed "Foley" after Jack Foley, a sound editor at Universal Studios, were produced using walking surfaces and clever devices manipulated by hand. Dialog was recorded separately and added in post production, a process called automatic (sometimes automated) dialog replacement (ADR). The three components of film sound—music, effects, and dialog—were combined in a large dubbing theater with mixing consoles located near the middle of the room.

With the development of magnetic tape in Germany in the 1940s, recorded sounds could be played back and manipulated after the performance. Multitrack tape recorders became available in the 1950s and artists such as Les Paul raised looping or overlaying of recorded material to a fine art. With the ability to record and erase, the need arose to listen to the material during the post-production process and the room became part of the audio chain. This led to the development of studios specifically dedicated to sound recording and playback.

Recording Process

The goal of recording and subsequent playback is to deliver an experience that accurately recreates the original performance. Although this is still the object of most recordings, some performances are never heard by an audience in their original form and exist only as electronic

FIGURE 21.1 Types of Sound Studios
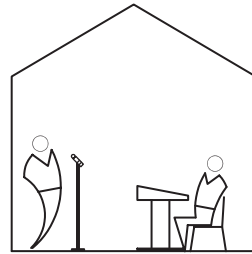
Home or Project Studio
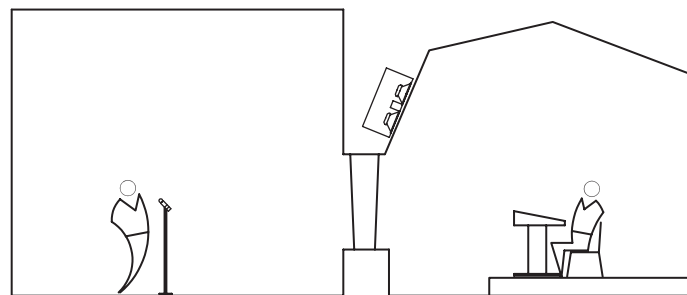
Separate Studio and Control Room
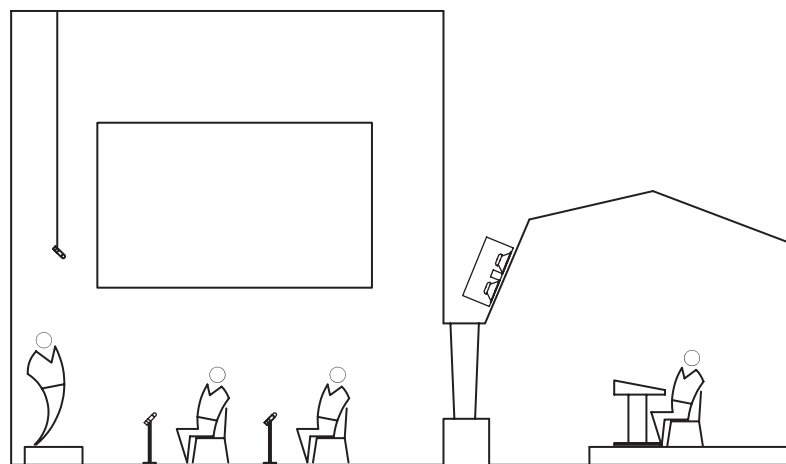
Scoring Stage and Control Room

signals. Their sole interaction with the architectural environment comes on playback in a listening room, and even this can be bypassed through the use of headphones. Most commercial recordings of music are done in rooms designed specifically for that purpose, carefully crafted to contribute positively to the process. Recording studios vary with the type of music; a simplified overview is given in Fig. 21.1.

In the simplest case, the performance and the recording both take place in one room. An instrument, such as a keyboard, is used to create the sounds that are monitored, either

on loudspeakers or headphones, and recorded through a small mixing console by a storage device. In this example the recorded sound never passes through a microphone and its only interaction with a room is during monitoring.

At a medium scale, studio musicians might play on acoustic (an unfortunate use of the term, which has become part of the culture) or electronic instruments, which are recorded using separate microphones or transducers built into the instrument. A recording might be made with all the musicians present at the same time, or with musicians playing their parts in separate studios, sometimes continents and weeks apart. When musicians play together, particularly loud instruments such as drum sets should be isolated in separate dedicated rooms so that their sounds do not bleed into the other microphones. Vocalists or sources needing a special environment, such as pianos, can also be placed in separate spaces.

A large symphony orchestra is recorded in a hall or scoring stage, using separate microphones for each section, plus a stereo pair on the centerline of the room, plus several more distributed throughout the room. Groups of players can be separated by portable barriers called gobos, but this affects the overall orchestral balance. Most mixers prefer to balance the orchestra using instrument placement and microphone location without resorting to isolating barriers (Murphy, 2001).

Recording Formats

The stereo format has dominated the recording industry since its commercial introduction in 1957. Since we have two ears in the horizontal plane, a pair of loudspeakers in the same plane can provide critical lateral cues for source localization. Recording techniques have improved to the extent that a phantom image can be reliably produced between or even outside the two loudspeakers. In the best combinations of recording and playback, a soundstage is created with depth as well as width, in which the listener can hear the instruments in their original positions.

Traditional film audio used right-center-left loudspeakers located behind the screen. Dialog was placed in the center and music could be distributed right and left. In 1973 a low-frequency effect called SenSurround was introduced for the Universal Studios' film Earthquake. In the earliest versions the signal was produced by a low-frequency noise generator and later by a recording on the film. At first there was a concern that this high-energy effect would damage theaters. The solution was to play the film 10 dB louder than the actual show levels, without an audience present, and see what shook loose (Stern, 1980). If nothing did, the theater was approved for showing.

Themed entertainment venues have been able to feature custom theaters with unique multitrack shows. In theme park attractions, audio animatronic (AA) characters, so named because the movements were controlled by audio tones, were designed with individual point sources for each figure. Loudspeakers were built into props and set pieces, or if the character is large enough as in the case of King Kong, into the figure itself. Multiple loudspeakers could be located throughout a theater or ride and the sound mixed down by engineers within the actual venue. Motion could be simulated using voltage controlled attenuators (VCA) under the control of a show control computer (Long, 2001). In the Sanrio Puroland Theme Park in Tokyo, Japan, a system designed by the author in the 1980s for the Time Machine of Dreams Theater utilized three loudspeaker clusters located behind the film screen with eight side and three rear loudspeakers each under individual computer control. Multiple overhead loudspeakers also were included. This system made complex motion simulation

possible, while allowing different films to be screened by changing the computer control software.

Recently the film industry has adopted a standard 5.1 system utilizing left, center, right, left surround, and right surround audio tracks (5) with a low frequency/effects (LFE) embedded bass track (.1). This is a simpler version of the multitrack formats used in theme parks and has the advantage of not requiring computer control. The sound is recorded onto the film or onto a digital disk and played by an outboard processor. Several competing systems are available. With the advent of digital projection equipment, both audio and video software in the future will be sent directly to theaters or the home via cable or wireless transmission. The 5.1 system or another similar multichannel surround system will probably become standardized for home use. There are a number of other combinations in service including five loudspeakers behind the screen, separate side and rear surrounds, one separate or two embedded bass tracks, but these have not found as wide an acceptance.

21.2   PRINCIPLES OF ROOM DESIGN

Rooms for sound recording and playback are used for three basic functions: listening, recording, and mixing. Rooms serving each function require a somewhat different environment, although there are many overlapping design considerations. All must be designed with a knowledge of the effects of scale based on the frequencies of interest. The smaller the room the greater the importance of low-frequency phenomena such as standing waves.

Standing Waves

The primary difference between the design of studios and listening rooms and that of auditoria and concert halls is in the control of standing waves. There are normal modes in all enclosed spaces but those in small rooms fall into the range that we can hear. From Chapt. 8 we recall that resonances in a closed-closed tube occur because the sound pressure is forced to a maximum at the ends, resulting in a pressure minimum in the center. The natural frequencies for the axial modes in one dimension are given by

$$f_n = \frac{n\,c}{2\,\ell} \tag{21.1}$$

where n = 1, 2, 3, ... In a room such as an auditorium, perhaps 60 feet (18.3 m) wide, the first mode (n = 1) will occur at about 9 Hz, well below our range of hearing. In a small studio, 15 feet (4.6 m) long, the first mode occurs at about 38 Hz, well within the audible range.

In a rectangular room the natural frequencies of the room modes were given in Eq. 8.43 and are repeated here:

$$f_{l\,m\,n} = \frac{c_0}{2} \left[\left(\frac{l}{\ell_x}\right)^2 + \left(\frac{m}{\ell_y}\right)^2 + \left(\frac{n}{\ell_z}\right)^2 \right]^{\frac{1}{2}} \tag{21.2}$$

where the l, m, and n are integers (0, 1, 2, . . .). To calculate every possible frequency it is necessary to work through all combinations of the integers. In practice however, only the lowest few really matter since most of the energy ends up there.

When two integers are zero, the wave form, which is called an axial mode, is a one-dimensional standing wave between two parallel surfaces. When only one index is zero the wave pattern is called a tangential mode, and includes reflections from the four surfaces in a plane parallel to the remaining two. When all indices are nonzero, the mode is oblique and includes reflections from all surfaces. In practice axial modes are the most important, followed by tangential. Oblique modes are seldom highly energized.

If the room is open on one side it can be modeled as a closed-open pipe. In this case the sound pressure has a maximum at the closed end and a minimum at the open end so there is no pressure extreme in the center of the room. The resonant frequencies are given by

$$f_n = \frac{(2n - 1)\, c_0}{4\, \ell} \tag{21.3}$$

where n is an integer 1, 2, 3, . . . and so forth. Our 15 ft (4.6 m) room now has a fundamental frequency of 19 Hz, half of what we had with the closed-closed condition. The second mode is at 56 Hz as shown in Fig. 8.3, and the null is displaced away from the center. In practice, of course, we do not leave one end of the room open but we can approach this boundary condition by making the wall very absorptive at low frequencies.

This simple calculation illustrates several important points. First, if we want to avoid a low-frequency null in the center of our room, we do not build our room out of a material such as concrete, which is highly reflective at low frequencies. Second, low-frequency absorptive treatment applied to one end of a room makes the room appear acoustically longer by lowering the first-mode frequency, and moves the first node away from the center of the room. This is a good thing for a control room since the mixer sits near the middle and does not want to experience so called "bass suckout."

When the room has the same dimensions in two orthogonal directions the pressure nulls will occur at the same frequencies and in the same place in the room, that is, the center. If room dimensions are even multiples of each other, then overlapping nulls also occur in the center. For the simple example of a 2:1 length ratio, the second mode of the longer dimension coincides with the fundamental of the short dimension. Although it is unusual to have room lengths of this ratio, it is not uncommon to have a length-to-height ratio on this order of magnitude. Thus we try to select room dimensions that are not integer multiples of each other. Several authors have suggested preferred ratios, which are given in Fig. 8.9.

Axial modes are not the only ones of concern. Figure 21.2 shows the three types of modes that can be self reinforcing, axial, tangential, and oblique. We need to be particularly cognizant of the possibility of room modes, especially when pressure maxima or minima coincide with the loudspeaker or listener position.

Bass Control

The control of low-frequency energy in small rooms is a matter of some delicacy. There are several main techniques that are used:

1. Overall control through low-frequency panel absorbers principally on the rear and side walls

2. Application of deep layers of absorptive material sometimes used in conjunction with panel absorbers

3. Construction of Helmholtz resonator cavities

FIGURE 21.2 Visualization of Room Modes Using Rays (Everest, 1994)
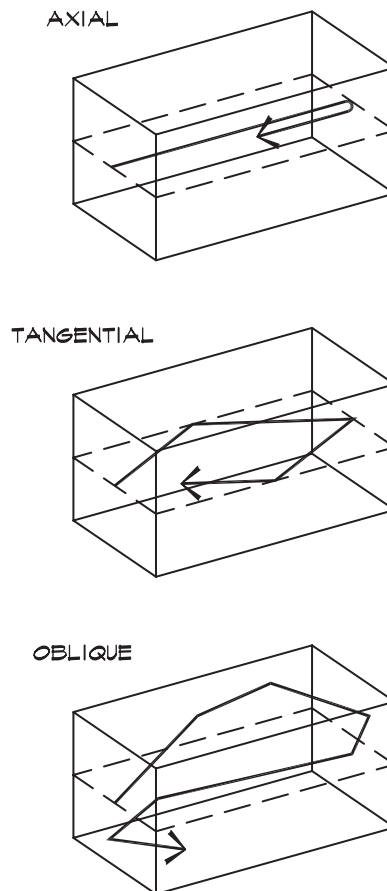
4. Locating the bass loudspeakers so that they do not excite the principal modes

5. Locating the main listener position so that it does not coincide with a major low-frequency node

These techniques, which can provide low-frequency control, reveal those steps that do not. Equalization, for example, can be used to raise or lower the overall level but cannot prevent the occurrence nor shift the location of nulls and interference patterns. Diffusion has little effect on low-frequency room modes. Small free-standing absorbers or localized patches of absorbent material have a minimal effect.

A drywall partition is an effective low-frequency panel absorber, as long as the surface is not built out of too many layers. Figure 7.41 gives examples of their properties. Even walls having two layers of drywall can be absorptive below 100 Hz. Panel absorbers can be tuned to the first axial mode of the room using Eq. 7.105. Table 21.1 shows combinations of possible materials and depths based on this equation.

Broadband absorbers can be constructed by layering pressed fiberglass boards over panel absorbers or by using very deep layers of fiberglass absorption. In cases where there is sufficient depth, wedge-shaped absorbers are employed to ease the transition between the air and fiberglass. The design of wedges for anechoic chambers is discussed in detail

TABLE **21.1**   **Resonant Frequencies of Panel Absorbers (Hz)**

Number of Layers	Depth of the Airspace with Fiberglass Batt (inches)					
(1/2" Drywall)	2	4	6	8	10	12
1	71	50	41	35	32	29
2	50	35	29	25	23	20
(1/4" Plywood)						
1	121	86	74	61	54	52

by Beranek and Sleeper (Beranek, 1946). Tapered fiberglass wedges are 99.9% (-30 dB) absorptive down to a frequency where the wedge depth is equal to a quarter wavelength of the incident sound. Most studios and listening rooms do not have sufficient depth to allow for this type of treatment but where there is the space, a deep absorber can yield impressive results (Sanicola, 1997).

Bass trapping using Helmholtz resonators can also be effective. The resonant frequency of a Helmholtz resonator, which is an enclosed volume with an open neck having a definable area and length, is calculated using Eq. 7.115. Since bass modes have pressure maxima at reflecting surfaces, where the particle velocity goes to zero, the cavity openings are most effective when located at these points—that is, at the edges and corners of a room. Volumes lined with batt insulation have a lower quality factor in their response curve and provide more broadband absorption than unlined spaces. Naturally occurring cavity spaces such as video monitor enclosures, return air plenums, soffits, raised floor platforms, and equipment enclosures can readily serve as absorptive cavities without the need for dedicated areas. Several examples are shown in Fig. 21.3.

The position of the subwoofers is another way of controlling bass buildup in a room. Subwoofers should be separated from the main LCR or stereo loudspeakers and there should be at least two of them, even if they are driven with the same signal. There are several considerations in woofer placement, some of which are conflicting. First loudspeakers located

FIGURE 21.3 Found Space Bass Traps
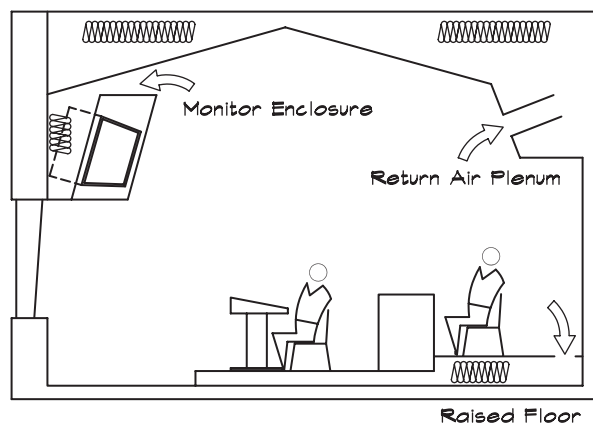
FIGURE 21.4 An Elevation View of the NRC/IEC Listening Room Showing Possible Listener and Woofer Locations (Toole, 1990)
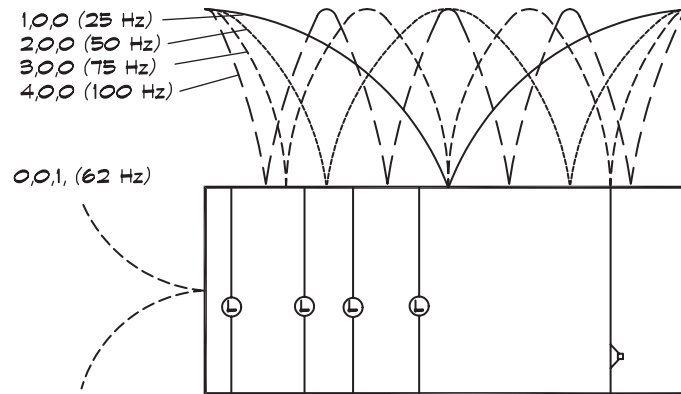
close (within 1/6 wavelength) to a hard reflecting surface will be more efficient, because the geometrical directivity due to the reflections from the nearby surfaces increases the power output for the same voltage input. Single-layer drywall partitions do not provide much increase in sound pressure but solid floors can be helpful. Woofers placed in the corners of a rectangular room will excite the greatest number of room modes since they all have pressure maxima there. However it may not be desirable to drive all the modes, since the listener may be sitting at a major node. In this case, it may be better to position the subwoofers at an intermediate point along the floor-wall junction to avoid pouring energy into the fundamental axial modes. By using two (or more) loudspeakers that can be moved around, optimum positions may be determined experimentally. The listener position can be controlled with a knowledge of the locations of the bass nodes. Figure 21.4 gives an example of possible loudspeaker and listener positions in a rectangular room relative to the locations of the low-frequency maxima and minima.

Audible Reflections

One design objective in recording and listening spaces is to minimize the negative effects of the room on the acoustic environment. In an ideal listening room the sound is transmitted from the loudspeaker to the listener with little or no coloration. Similarly, in a studio the sound of the performer should be clearly transmitted to the microphones. Since room reflections are unavoidable, experiments have been undertaken to determine the audibility of an individual reflection. Early experiments by Haas (1951) used two loudspeakers in front of the listener at an included angle of 45° with speech as the test signal. One loudspeaker was delayed with respect to the other and the listener was instructed to adjust the level of the reference loudspeaker until the two sources were perceived to be of equal loudness. The upper curve shown in Fig. 21.5 (Toole, 1990) was the result.

Figure 21.6 contains the results of later experiments that reexamined human reaction to a combination of delay and level, again using speech as the input signal. These yielded a variety of results, indeed a nearly continuous range of reactions, including equal-loudness lines significantly different from that found by Haas. Based on these experiments it can be said that there is no one single point at which the two signals were perceived as unified, since even when the second signal was 20 dB below the first it was still perceptible. As a

FIGURE 21.5 **Various Measures of Significance of a Lateral Reflection (Toole, 1990)**
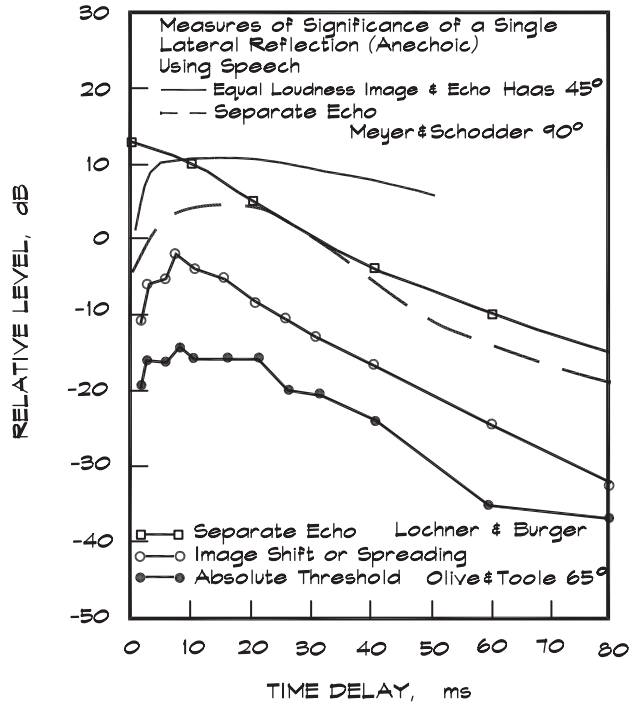
FIGURE 21.6 **Absolute Thresholds for a Single Lateral Anechoic Reflection (Olive and Toole, 1989)**
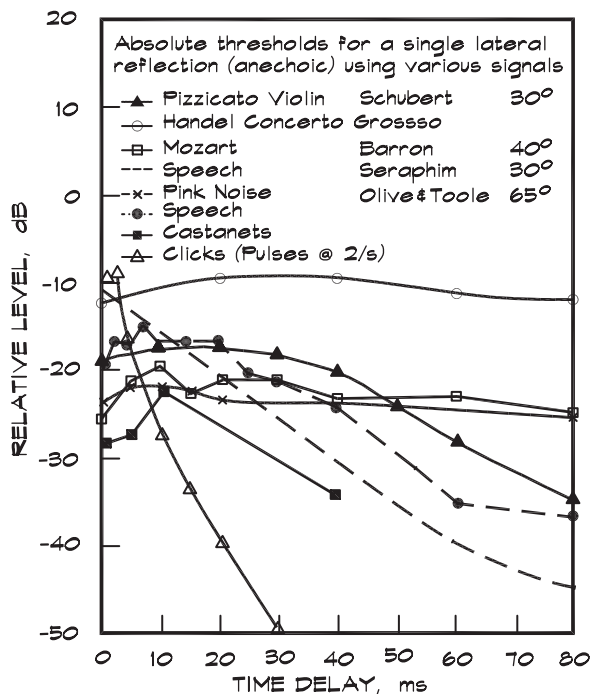
consequence Toole argues that the masking of a late reflection by a series of early reflections has probably been overemphasized in small listening rooms.

These results do not negate the effectiveness of delayed loudspeakers in sound reinforcement systems. Because they are A-B comparison tests, a shift in image can trigger a noticeable response. In a delayed loudspeaker system a change in image direction is one of the design objectives. Fixed installations do not feature A-B comparisons except during setup. Second, these tests were done in the horizontal plane where we are most sensitive to perceived direction. Time delays and level changes from loudspeakers located in the medial plane are less perceptible.

Separate experiments by Olive and Toole (1989) tested the influence of the source material as well as the level and delay. It was found that the audibility of reflections using short-duration signals varied greatly from those obtained with music and speech. Figure 21.7 illustrates the differences; although there was forward temporal masking, the nearly horizontal shift in level with delay time measured by Haas was observed only in the case of music. Speech thresholds dropped linearly with delay time and short-duration signals provided very little masking.

The audibility of reflections is also dependent on the reverberation time. Figure 21.8 shows the results of psychoacoustic studies by Nickson, Muncey, and Dubout, (1954). Here the source was speech and the "echo" signal was electronically delayed and presented through the same loudspeaker as the original. Note that the lower line representing 20% disturbed follows the reverberation time line quite closely. These straight lines are drawn based on the assumption of an exponential decay in the room. A reverberation time of 0.5 sec is equivalent to a 10 dB decrease in $(0.5/6 = 0.083$ sec). This is plotted as the top curve (Everest, 1994). The upshot is that the deader the room, the more noticeable are the individual reflections.

FIGURE 21.7   The Results of Two Psychoacoustical Listening Tests (Nickson, Muncey, and Dubout, 1954)
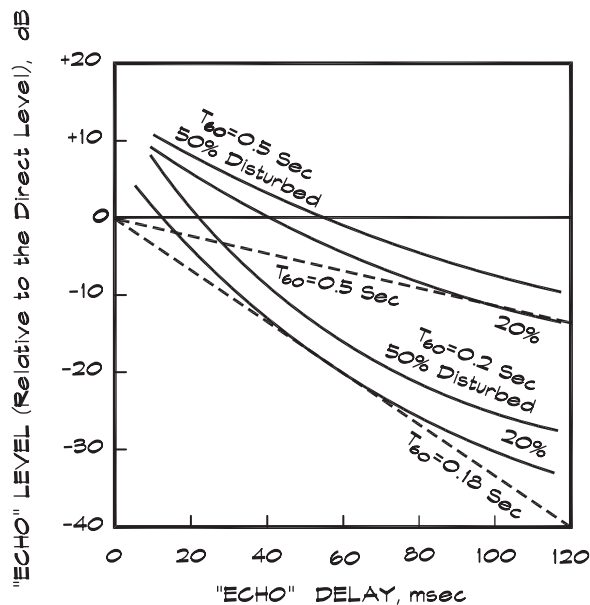
FIGURE 21.8 Configurations that Generate Flutter Echo Reverberation
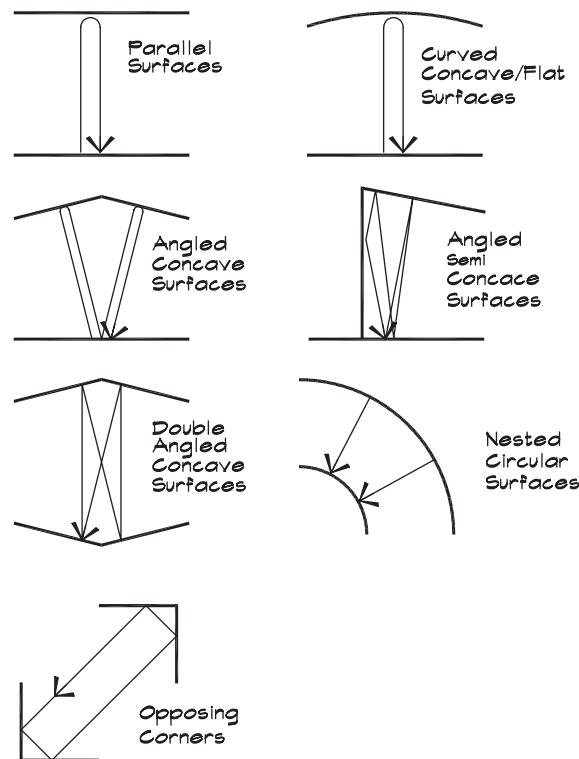
Everest (1994) divides the reaction to a reflection into four regions according to the time delay. Region 1, where directional cues are determined, is less than 1 ms; Region 2 is up to about 50 ms, where the integrating effects of the ear occur; Region 3 is an intermediate zone, which depends mostly on reverberation time, and Region 4 is that of a long-delayed reflection where the curves in Fig. 21.6 flatten out and approach the horizontal.

Clark (1983) performed an interesting series of studies to measure the effects of the audibility of time delays, phase shifts, and frequency shifts in listening rooms having a stereo pair of loudspeakers at 10' (3 m) distance and 60° included angle. This standard stereo configuration, even when a monaural signal is fed to both loudspeakers, is preferred by most listeners who describe the sound as "fuller, more solid, or having depth" in spite of the fact that the arrangement produces significant comb filtering at the listener's ear. Clark then used a single loudspeaker with a 24" × 30" reflecting surface to recreate the comb filter effect of two loudspeakers. In this case, when the reflecting surface was in the "wall" orientation little audible effect resulted, much less than the stereo loudspeaker arrangement with a monaural signal. With the reflector in the "table-top" orientation the effect was more noticeable but still small. A third experiment was done wherein an electronic filter was used to generate a comb filter, fed to one loudspeaker. Here the result was very noticeable and degrading, giving a nasal quality to voice reproduction.

In an extension of this work, Clark (1983) used electronic manipulation to introduce phase shift, time delay, and frequency shift into the signal path. Phase shifts of up to 2700° were inaudible as were time delays up to 10 msec. He speculated that time delays of up to 30 msec would also be inaudible but did not test in this range. Where all three effects are present,

FIGURE 21.9 Suggested Reverberation Times for Control Rooms (Fierstein, 1979)
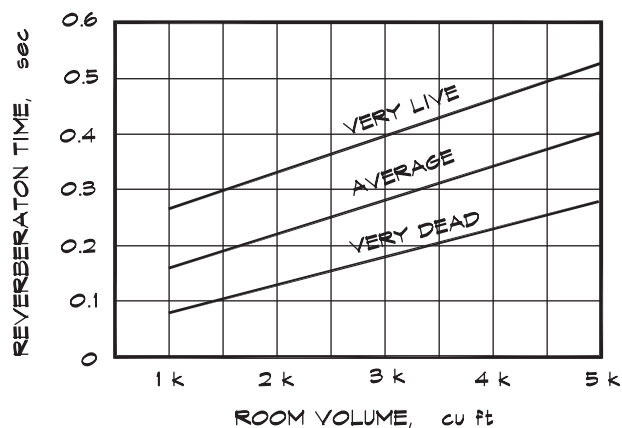
he judged that frequency shifts were the most audible. Stereo reproduction was preferred to single loudspeaker, even when a wall reflector was present. This likely is due to the fact that side-wall reflections help fill in the stereo comb filtering.

It is good practice, in control room design, to minimize the energy scattered to the mix position from surfaces immediately adjacent to the main loudspeakers. Likewise, it a good idea to provide a series of reflections that transition smoothly into a reverberant decay. This can be done using diffusion, surface orientation, and absorptive treatment to avoid high-energy reflections. In most rooms the side walls and ceiling are flared outward to direct the first reflection away from the mixer position. Rear walls are treated with absorption, diffusion, or a combination of the two.

Flutter Echo

In a music practice room or recording studio, where the source and receiver are close together, repeated multipath reflections known as flutter echo can be disturbing. The most commonly encountered example is between two parallel walls, but there are numerous geometric combinations capable of producing this phenomenon. Several examples are shown in Fig. 21.8 but these are not all-inclusive. Flutter can be treated with absorbing material, diffusing elements, staggered reflectors, or by canting the reflecting surfaces. The latter approach is not always effective since a third surface may complete the flutter loop. In the design of small rooms closed reflection loops of this type can be expected and treated with surface applied materials. A surface canted 1:12 suffices to eliminate the problem as long as the loop is not closed by other surfaces.

Reverberation

The reverberation time in small rooms is still an important design parameter. Figure 21.9 shows recommended values of the reverberation time for control rooms. The use of these data should be based on the program material to be played in the space. Rooms designed for the playback or broadcast of speech should be very dead; those for music may be somewhat more reverberant.

For average control room volumes preferred reverberation times fall into the 0.3 to 0.4 second range. In recording studios the reverberation times are variable, and range

**FIGURE 21.10   Reverberation Times for Studios in the 500–1000 Hz Range
(Doelle, 1972)**
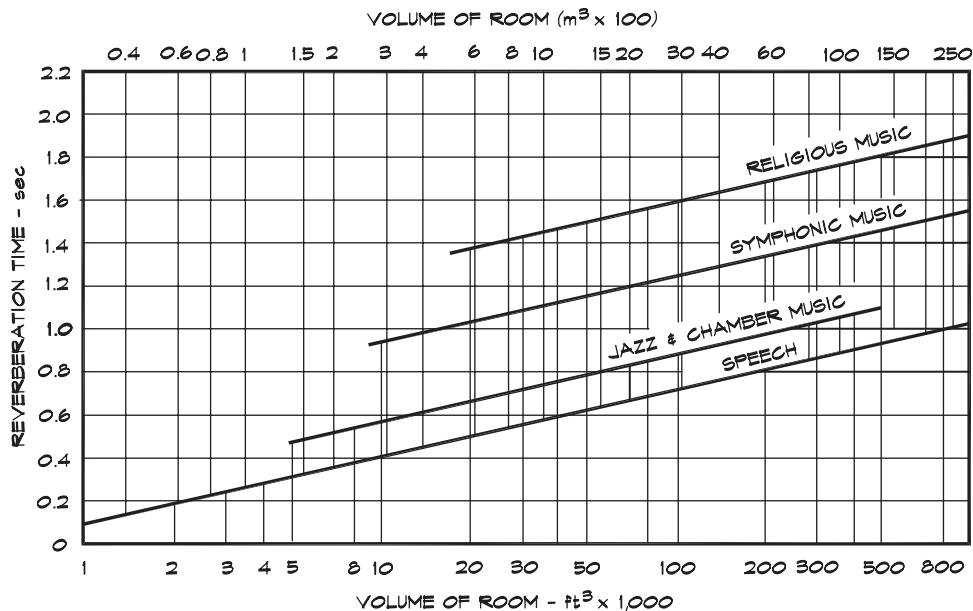
between 0.8 and 1.5 seconds, depending on the size of the room. Figure 21.10 gives a number of values based on room volume and the type of music. For small studios and control rooms, the preferred shape of the reverberation-time-versus-frequency curve is flat.

Scoring stages, designed for orchestral music, are like concert halls with reverberation times in the 1.7 to 2.2 second range, but can be furnished with heavy drapes or other variable absorption elements to reduce the reverberation as needed. In scoring stages a reverberation time that rises at low frequencies is desirable; however, too much low-frequency reverberation can reduce the clarity. Increases below 1 kHz (about half of those shown in Fig. 17.11) are appropriate.

Diffusion

A diffusive surface reflects incident sound in several directions rather than principally in one. Its reflections are termed nonspecular as contrasted to the specular or mirror-like reflections produced by a smooth flat surface. Reflectors such as cylinders can be diffusive in one plane and specular in another. Quadratic residue or quarter-wave slot diffusers can also behave in this way. Multifaceted reflectors can generate specular reflections in several directions and contribute to diffusion in a room although their behavior is not perfectly diffuse.

Figure 21.11 shows in a qualitative way the characterization of a sound interaction with a surface. The components of the process are described using absorption, transmission, and diffusion coefficients represented here by single-number values all less than one. This is a great simplification of the actual behavior, since there is a complicated relationship that depends on the type of incident wave, its angle (both incident and reflected), frequency, and the size of the reflecting surface.

Figure 21.12 illustrates more details of the interaction process. In a specular reflection from a hard surface, most of the energy rebounds at an angle centered on the angle

FIGURE 21.11   Sound Interaction with a Rough Surface
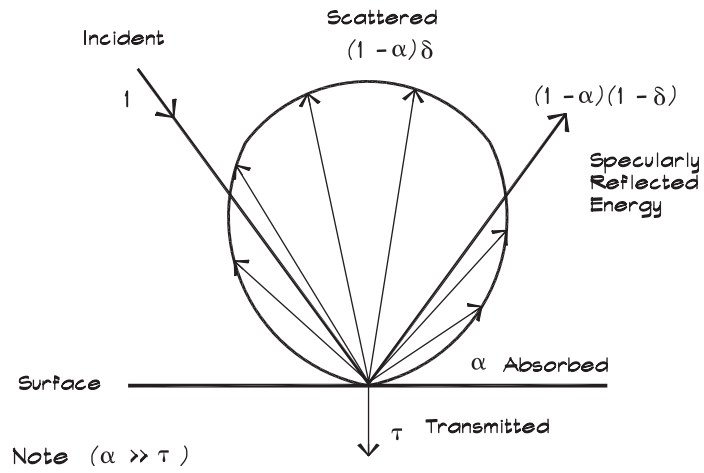
FIGURE 21.12   Comparison of the Spatio-Temporal Properties of Acoustical Interactions (D'Antonio, 1987)
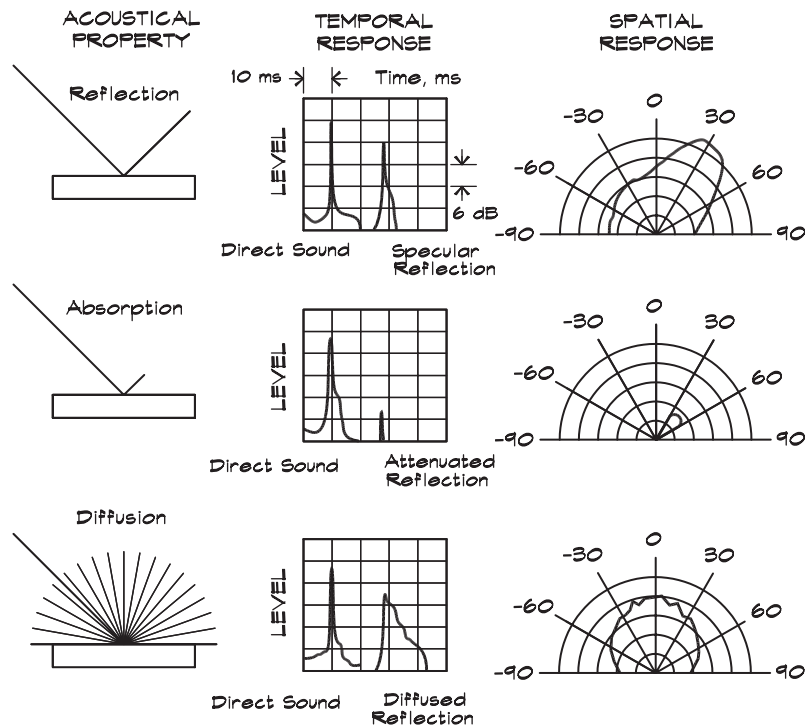
of incidence. The temporal response is constrained to a narrow band determined by the path length. Some temporal smearing is present due to the after vibration of the reflecting surface and the diffuse behavior of the material.

A reflection by a purely absorptive material is also specular, however the amplitude is decreased by an amount characterized by the absorption coefficient. The temporal behavior is narrowed since there is less reradiation by a porous absorber. The behavior of panel absorbers can be expected to show more temporal smearing.

The pattern generated by an ideal diffuser is spatially uniform. There also can be temporal spreading depending on the type of process. For example with quarter-wave tube diffusers, energy is stored in the wells and released over time. A diffuser such as a half cylinder or pyramid would produce a temporal pattern much like that of a specular reflector.

Diffusion in listening rooms and studios can be helpful by contributing to a sense of spaciousness and envelopment. It can help fill in the gaps between specular reflections. Where there are flutter echo problems a diffusive surface can be used to break up the flutter loop without adding excessive absorption. Diffusion can also make absorptive materials more effective by creating a reverberant field, which assures that the acoustic energy will interact with the absorbers. Diffusers do not need to be perfect scatterers to be effective.

Imaging

Imaging refers to the preservation of the spatial relationship in the original sound field perceived by the listener. In home listening rooms, designed for high-end audio, the stereo format with a subwoofer is the most common. Stereo loudspeakers are arranged at an included angle slightly greater than 60°, and the listener is about 10 to 12 ft (3 to 3.5 m) away, slightly closer than the separation distance between the loudspeakers. Many loudspeakers are very sensitive to placement, especially separation distance and toe-in angle. By varying these parameters one can often increase definition and detail in listening rooms. Space around the loudspeakers can be helpful in contributing to the soundstage. Where the dimensions allow it, loudspeakers should be placed at least 1.5 m (5 ft) from any walls. Reflections from a nearby wall can color the sound, particularly in the lower registers. Patches of absorptive material on side and rear walls help control rogue reflections. Transondent wall finishes such as wood slats are common in control rooms where cloth-covered panels can be located.

The design of professional listening rooms tends to be format driven. A sampling of possible loudspeaker arrangements is given in Fig. 12.13. Clearly there are so many possible arrangements that not all can be accommodated in a single room. A working room is designed for one principal format, with 5.1 being the most common for film and stereo the most common for TV and recorded music. The number and position of the surround loudspeakers is not always fixed but is fitted to the size and arrangement of the seating in the room.

The arrangement of a listening room can influence the audio image. Reflections from the side walls tend to broaden the phantom stereo image. Conversely side-wall absorption narrows it. Diffusion behind and to the side of the listener increases the sense of spaciousness. Too much diffusion behind the listener has been found to generate an acoustical fog or clutter (Toole, 1998).

Experiments were carried out in Japan by Kishinaga et al. (1979) to assess the best listening environment in which to evaluate home audio products. Four audio professionals did these experiments at Nippon-Gakki (Musical Instruments of Japan) for four different

FIGURE 21.13   Standards for Loudspeaker Placement in Studios, Listening Rooms, and Theaters

Classic Stereo   4 ch "Quadrophonic"   Dolby Stereo 3/1

60°   90°   45° 45°

Mono Surround

5 Channel 3/2   5.1 Dolby Surround   Dolby EX 6.1

Sub   Sub   Sub

L Surround   R Surround

Single or Multiple Surrounds   L Surround   R Surround   Rear Surround

Sony 7.1 (SDDS)   5.1 Dubbing Stage   ITU.R 3/2

Sub   Sub   Sub

60°   110° ±10°

45° Max

L Surround   R Surround   L Surround   R Surround
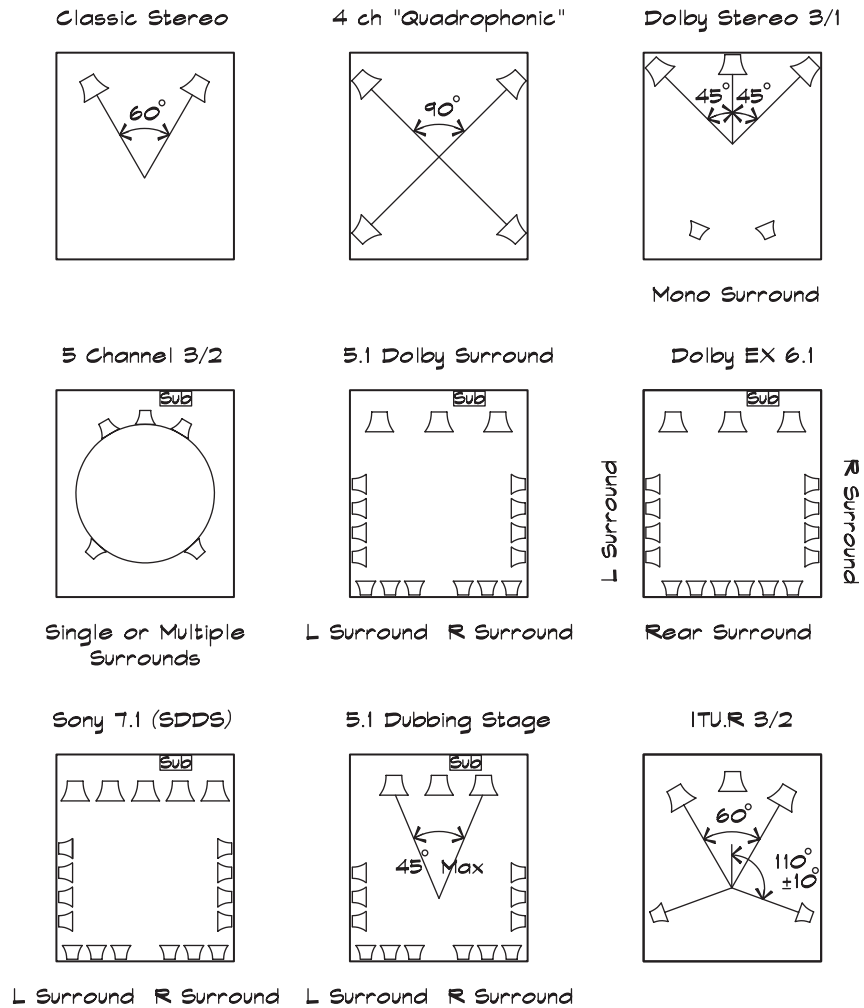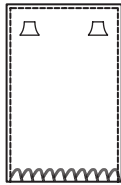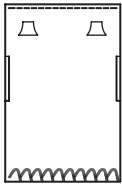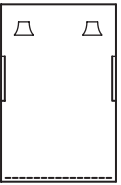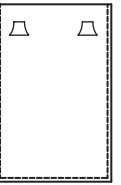
arrangements of absorption in a room. The test room had a hardwood floor and an absorptive ceiling, not a typical home environment. Since these data are over 20 years old, no diffusers were included in the mix of materials. The parameters used for judgment were:

1. Localization of the stereo image

2. Presence of coloration

3. Loudness

4. Broadening of the image

5. Perspective (probably quality of the soundstage)

   (Everest, 1994)

The results are summarized in Fig. 21.14. No one arrangement of materials yielded "good" results for all parameters. The sketches in this paper do not show sufficient detail to judge what other factors may have been important. Loudspeaker type, position, as well as

FIGURE 21.14 Summary of the Results of the Nippon Gakki Listening Tests (Kishinaga et al., 1979)

listener position could have contributed to the overall impression. However, based on this study, the highly absorptive configurations seemed to generate the most favorable responses.

Imaging in theater systems, using a left-center-right loudspeaker configuration, is less complicated than in stereo systems. Ideally the three front loudspeakers are located behind a perforated screen about 5/8 of the screen height up from the bottom. The two outside loudspeakers are placed close to the outside edges of the screen. When the screen is not perforated the loudspeakers can be positioned below the screen. This is preferable to two on the side and one beneath. The arrangement of surround loudspeakers is less critical. These are placed to the side and slightly behind the listener.

Noise Control

Background-noise levels in critical listening environments must be kept very low. In studio and listening rooms background levels are a matter of personal taste, ranging from an NC 30 to the threshold of hearing. Table 21.2 gives a starting point. Levels are listed in

TABLE 21.2   Background-Noise Levels in Studios and Listening Rooms

Room Type	Noise Level
Living Room	NC 25-30
Music Practice Rooms	NC 30–35
Band/Orchestra/Choral Room	NC 25–30
Video Post Production	NC 25–30
Listening Room/Home Theater	NC 20–25
Project Studio	NC 25–30
Sound Stage (film)	NC 20–25
Dubbing Stage	NC 20–25
Control Room	NC 15–20
Recording Studio	NC 10–15
Scoring Stage	NC 10–15
Foley Stage	< NC 10

terms of the NC level. A-weighted levels are about 5 dB higher for HVAC-generated noise. Although NC 10 is not formally defined, it is taken to be approximately 4 dB below NC 15 from 63 Hz to 500 Hz and 5 dB below NC 15 at 1000 Hz and above. Note that the higher background levels in music practice rooms are desirable due to the masking they provide.

Low background-noise levels are most critical when there are microphones in use in the room. A project studio often is used to put musical ideas together and to do scratch tracks and so is less sensitive, particularly if monitoring is done on headphones. The noise requirements can also vary with the use of the room. If a final recording secession is done in a project studio it could have the same requirements as a recording studio.

The low background necessary for Foley are due to the practice of mixing at levels well above that at which the original sound was recorded. Background levels are elevated accordingly and can become noticeable unless they are carefully controlled.

Noise Isolation

Klepper, Cavanaugh, and Marshall (1980) wrote an important paper on the design of music teaching facilities. In it, they pointed out that basic planning could help avoid many of the most common problems. Most critical areas should be separated by dead spaces such as corridors, storage rooms, and other buffers. Single-story construction avoids the floor separation problem. By grouping the noisy spaces together, costs can be reduced since the expensive high TL wall does double duty.

Noise isolation between rooms in music rooms and studios can be rather complex. Airborne noise can travel through partitions, HVAC systems, conduits, doors, and windows. Structure borne noise can be carried in common slabs, structural members, piping, and rigid conduit. Footfall noise can be transmitted laterally as well as vertically, particularly when the slab is above grade. A concrete corridor on an above-grade slab, 20 feet (6 m) away from an improperly isolated studio, can render it unusable.

Klepper et al. (1980) included a table showing recommendations on a single-number degree of isolation between music rooms, reproduced as Fig. 21.15. Also included are assumptions on background noise and source level. The table is based on a single-number approximation to the detailed calculation, done by subtracting the A-weighted background-noise level in the receiving room from the C-weighted peak-noise levels in the source room. Note that the difference between the NC levels and the A-weighted background levels given by these authors is based on the assumption that the background-noise spectrum has exactly the same shape as the NC curve. This seldom occurs in practice. More often there is about a 5 dB difference between the NC level and the A-weighted level. Although there is no source spectrum presented, the authors recommend that heavy materials such as grouted concrete blocks be used as a component of the wall material to obtain the necessary low-frequency isolation. Geerdes, Watters, and Hirtle (1971) developed a chart of isolation requirements in terms of octave-band noise reduction plus background-noise levels in the receiving room for practice and teaching rooms. Figure 21.16 gives their results.

Single-number ratings such as those given in Fig. 21.15 are useful for cost estimation and preliminary guidelines, but should not replace careful engineering computations. In professional studios isolation of adjacent studios must often exceed these values, and the transmission loss requirements must be calculated using the actual source spectrum and receiver background levels.

Specific construction details for the separation of music rooms were also published by Klepper et al. (1980). They show three levels of construction, illustrated in Fig. 21.17.

FIGURE 21.15   Acoustical Privacy Criteria for Music Buildings (Klepper, Cavanaugh, and Marshall, 1980)

	Recommended Minimum Receiving Room Background NC	dB(A)	Band Room	Orches-tral Room	Choral Room	Organ Practice	Music Class-room	Music Listen-ing	Practice Room	En-semble Room	Elec-tronic Music	Faculty Studio	dB(C)
Band Room	25	36	65	65	65	62	65	65	57	61	62	61	103
Orchestral Room	25	36		62	62	62	62	62	56	59	62	62	100
Choral Room	25	36			59	62	59	59	56	59	62	62	97
Organ Practice	35	44				54	62	62	54	58	58	58	100
Music Classroom	25	36					59	59	56	59	62	56	97
Music Listening	25	36						59	56	59	62	56	97
Practice Room	35	44							48	52	54	52	94
Ensemble Room	30	40								55	58	55	97
Electronic Music	30	40									58	58	100
Faculty Studio	30	40										52	94

RECOMMENDED MINIMUM NOISE INSULATION CLASS (NIC)* BETWEEN MUSIC ROOMS

Assumed Maximum Source Room Levels**

*Laboratory-derived sound transmission class (STC) values may be used with appropriate corrections (see text).

**Maximum levels as read on the C-scale of a sound level meter, exceeded only by 5% of peak readings, from several sources.

FIGURE 21.16   Music Privacy for Practice and Teaching Rooms (Geerdes, Watters and Hirtle, 1971)
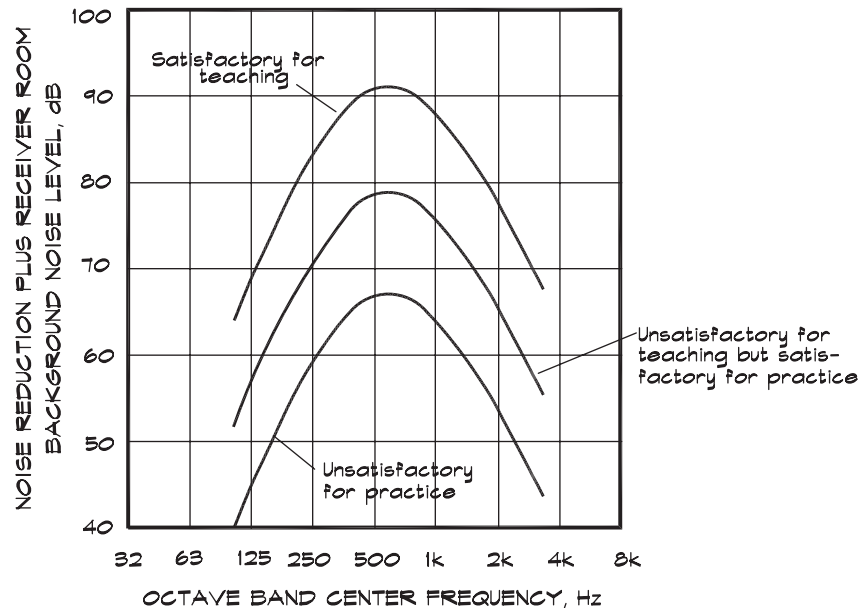
Construction A rates an NIC 65 and is a completely isolated room-within-a-room construction, which could be used for back-to-back band rooms or similar occupancies. Construction B is similar to A, but the floating floors are replaced with wood floating floors of double 1.5" (38 mm) plywood on 2" (50 mm) fiberglass board, unless the slab is on grade. The drywall on one side is removed. This rates an NIC of approximately 57. Construction C yields an NIC 48 using painted grouted CMU blocks and the same wood floating floors, which can be omitted when the slab is on grade.

Flanking

Flanking can significantly degrade carefully designed separations between studios and listening rooms. When a large conduit, duct, or plumbing pipe penetrates a sound-rated wall, as is often the case in TV studios, there can be significant sound transmission through the opening. Small openings can also make a significant difference and should be closed off.

Since there are large bundles of heavy wire in studios and since changes must be made to the cabling, a permanent seal is not possible. In permanent installations the opening is closed off with drywall and plastic pipe packed full depth with fiberglass or safing, and the cracks sealed with caulk on both sides. In flexible installations closed cell foam, fire stop compound, or other malleable materials can be used to seal the ends of a pipe. In some cases commercial isolation clamps are built into the common wall.

Where pipes, ducts, and conduits penetrate separated walls they must not form a bridge between the isolated structures. A structural break is required in these elements, particularly when studios utilize floating construction. Piping can be isolated using flexible no-hub connectors. Flexible conduit can be used and ductwork can include flexible connections.

Occasionally there are cases where a wire way is used to carry cabling between critical spaces. In these cases, it may be possible to fill the cavity with fiberglass batt or safing and

FIGURE 21.17   Separation Walls for Music Spaces to Provide a Given Noise Reduction between Adjacent Rooms (Klepper, Cavanaugh and Marshall, 1980)

Construction A – NIC 65

Double layer drywall on resilient spring hangers

Double layer drywall on metal studs

Fiberglass in air space

8" (200 mm) ASTM C145, normal weight grouted CMU (along corridor, 6" – 150mm)

Concrete slab on unit isolators (May be replaced with slab perimeter isolation joint on-grade if water table conditions permit)
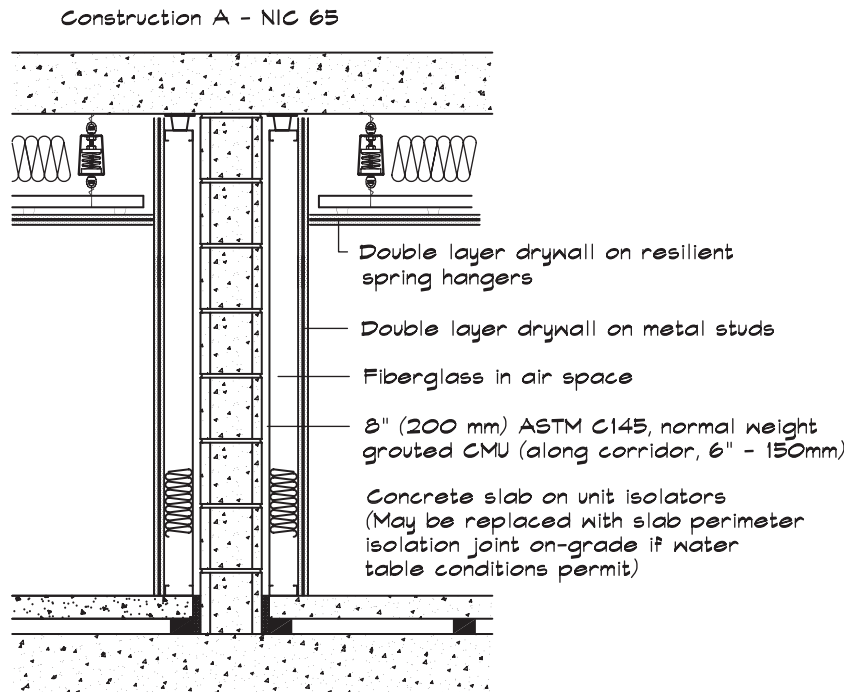
Construction B – NIC 57
Remove drywall on one side. Replace floating slabs with two layers of 1 1/2" (38 mm) wood flooring on 2" (50 mm) thick 6 lb/cu ft (100 kg/cu m) pressed fiberglass board. This can usually be omitted when the slab is on grade.

Construction C – NIC 48
Remove drywall on both sides. Replace floating slabs with two layers of 1 1/2" (38 mm) wood flooring on 2" (50 mm) thick 6 lb/cu ft (100 kg/cu m) pressed fiberglass board. This can usually be omitted when the slab is on grade.

cover it with a heavy lid that can be removed to access the wire. The object of any filler material is to block off the air passage between the two spaces or to provide a long path with a high attenuation.

HVAC Noise

HVAC units are a major source of noise in studios and listening rooms. For low-background levels flow-generated noise is particularly important to control. Terminal devices with adjustable dampers should be avoided. Volume control units should be located well upstream of the termination. Klepper et al. (1980) recommend that for an NC 20, dampers be located at least 15 ft (4.5 m) upstream; for an NC 35, the minimum distance is 5 ft (1.5 m). This assumes flexible duct or sheet metal duct with a minimum 1" (25 mm) liner between the device and the termination.

Both supplies and returns must be ducted. The final run to the terminal unit should be made with flexible duct that is not kinked or severely bent. Lining is required but may not be necessary for the entire length of the duct. The added duct area gained by removing duct liner near the terminal can be more important than the attenuation the liner provides. Silencers, preferably low-frequency traps, are almost always necessary near the mechanical units.

Packaged HVAC units, fan coils, and condensers should not be located directly above studios and sensitive listening rooms. In large studios and dubbing facilities this may require a separate structural support system for the equipment. In small studios it may be sufficient to locate fan coils over nonsensitive spaces such as bathrooms or closets with vibration isolation and silencers as required. Even when packaged rooftop units are remotely located there is still a possibility that low-frequency rumble can be transmitted into the roof via the ductwork. Duct runs, particularly those supported on lightweight roofs, should be vibration isolated. Even when there is a flexible connection between the ducts and the fan, low-frequency rumble in the air stream can be transmitted into the duct walls and down through the supports. Vibration isolators, having a deflection equal to that of the fan, are prudent for the first three points of support and half that thereafter. Detailed recommendations were discussed in Chapt. 11. Silencers placed at the roof penetration serve to counteract exterior noise breaking into the ducts from aircraft or other sources. Down shot units should be avoided unless there is sufficient room underneath to locate silencers and construct breakout enclosures.

Ductwork can transmit noise between rooms. HVAC ducts serving adjacent spaces must be routed so that they provide noise isolation equal to that of the other paths. Figure 21.18 gives an example of a duct layout for contiguous music practice rooms. The ducts here are assumed to be lined with 1" (25 mm) duct liner. In critical installations silencers also may be required between rooms.

FIGURE 21.18 Examples of Good and Bad Practice in Air Distribution Systems (Klepper, Cavanaugh, and Marshall, 1980)

Poorly Planned Duct System for Music Rooms

Well Planned Duct System for Music Rooms
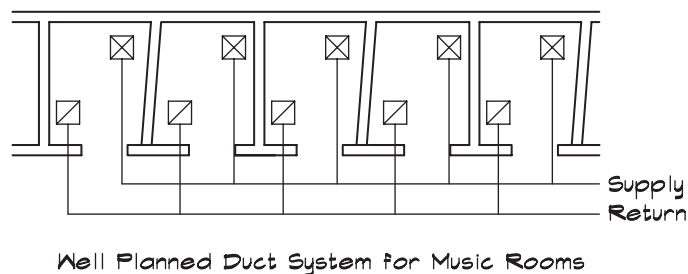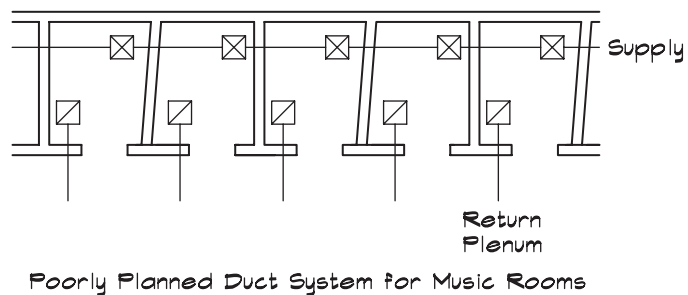
21.3   ROOMS FOR LISTENING

Music Practice Rooms

Music practice rooms range in size from single occupant spaces to rooms designed to accommodate a full orchestra. The use of a practice room differs from that of a performance space in that the sound needs to be heard only by the players and the teacher or conductor. The design objective in a practice room is not to mimic the acoustical characteristics of a performance space, but to allow musicians to play comfortably at their normal level. To the extent that a generalization can be made, the primary concern in these spaces is excessive loudness. This is certainly the most prevalent problem in band and choral practice rooms. In individual practice rooms, which can be quite small, coloration and flutter are also important factors.

Loudness is controlled by increasing the room volume and by adding absorption, on the ceiling. Room volumes of 550 to 700 cu ft (15.6 to 21.8 cu m) per instrumentalist and 350 to 500 cu ft (10.9 to 14.2 cu m) per vocalist are appropriate with ceiling heights of 18' to 22' (5.5 m–6.7 m) for instrumental and 16' to 20' (5 m to 6 m) choral spaces (Wenger, 1999). Ceilings should be 1" thick fiberglass acoustical tile. Prefabricated diffusers or inverted convex plastic skylights can be helpful, but they should cover less than about 20% of the ceiling. Wall absorption is beneficial in band rooms to address both flutter and reverberation. Barrel absorbers placed high on the walls are good for controlling excessive low-frequency reverberation. Floors are by and large hard surfaces, such as vinyl on concrete. An example of a high school practice room is shown in Fig. 21.19.

FIGURE 21.19   Design of a Band Practice Room
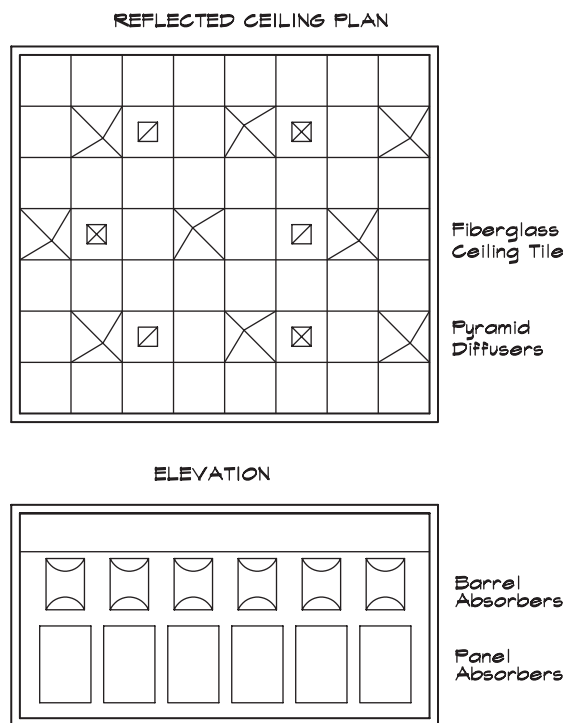
Small practice rooms can be designed with angled walls to help with flutter. Absorptive panels placed on contiguous walls are also helpful since repeated reflections can occur in a horizontal plane even if the bounding walls are not parallel. Where there is a hard angled ceiling it may not always eliminate flutter, so local surface-applied diffusers are appropriate. Absorptive panels are most effective when placed near the center of a wall since particle velocities are higher here than in the corners.

Listening Rooms

Listening rooms can be quite elaborate, sometimes rivaling a professional mastering or screening facility. These rooms tend to fall into three categories: pure listening rooms with stereo loudspeakers, video rooms with small monitor loudspeakers, and home theaters with surrounds.

Listening rooms are often very personal and their design can revolve around the type of loudspeaker and the individual preferences of the user. The stereo format demands axial symmetry with the listener located on-axis. The so-called sweet spot, where the stereo sound-stage is maintained, may be limited to a very few listeners. Traditional stereo loudspeaker placement starts with an included angle of a little more than 60°. The loudspeakers are placed about 10 to 12 feet (3 to 3.7 m) apart and the listener is slightly closer to the loudspeakers than their separation distance. The loudspeaker aim point is about 2 feet (0.6 m) behind the listener. There is some flexibility in loudspeaker positioning and manufacturers can recommend included angles as high as 100°. The high-frequency loudspeaker elements should be located in a single horizontal plane, preferably that of the listener's ears. Small differences in separation distance and toe-in angle can yield startling improvements in clarity so experimentation is encouraged.

To allow freedom of movement, the room must be designed with ample space around the loudspeakers. Accordingly the width of a dedicated listening room should be at least 16 to 18 feet (4.9 to 5.5 m) wide, leaving 3 to 4 feet (0.9 to 1.2 m) minimum between the loudspeaker and the side wall. At least one manufacturer (Dunlavy, 2001) recommends placing loudspeakers along the long wall; however, it has been the author's experience that placement along the short wall yields less low-frequency coloration and a more realistic bass response. The room depth should be on the order of 19 to 22 feet (5.8 to 6.7 m) with additional space so that some low-frequency absorption can be built into the rear walls. Ceilings should be high enough, perhaps 10 feet (3 m), that an absorbing or diffusing element can be placed at the specular reflection point without being visually oppressive.

Absorptive treatment can also be applied to the walls. If the loudspeakers are electro-static, absorptive panels are necessary on the walls behind the loudspeakers. Some absorption, including low-frequency treatment, is recommended behind the listener and it should be in the same horizontal plane as the listener. Toole (1998) recommends some, but not continuous, diffusion on the back wall.

Where a listening room includes a video projection system in combination with the stereo audio system, the screen can be located on the front wall between and behind the loudspeakers. The two need not be coplanar. The video projector may be mounted in the ceiling, in a separate projection room, or in a wall or floor-mounted cabinet. The same design principles apply to video rooms but they are not as critical as stereo listening rooms since the quality of the soundstage is not as good as with stereo music. An example of a home listening room design is given in Fig. 21.20. This was based on a stereo audio system. The loudspeakers were electrostatic so absorption on the front walls was particularly important.

FIGURE 21.20 An Example of a Home Listening System
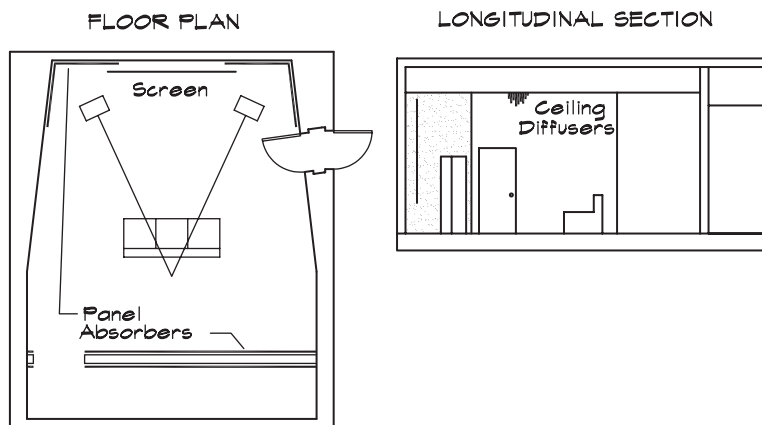
The storage room at the rear also helped provide bass absorption since the wall was covered with fiberglass panels over a diaphragmatic absorber.

Home theaters have become an entire industry, with publications dedicated to their design and construction. They mirror commercial theaters in that they support the 5.1 audio format as well as standard stereo format. The three front loudspeakers are best located behind a perforated projection screen with the surrounds mounted on the side walls slightly behind the listener position. If the display system is not transondent, the loudspeakers may be placed on either side and beneath the video surface. Ideally the high-frequency transducers should lie in the same horizontal plane. There is some flexibility in the placement of surrounds. When rooms can accommodate several occupants, surround loudspeakers are arranged in pairs along the side walls.

The left-center-right audio format is not as dependent on seating position to maintain the spatial relationship between the listener and the projection screen as the stereo format. Thus the area where a reasonable soundstage is maintained is larger than with simple stereo. Consequently there is a range of good seating locations. Since the seating area is larger, there are multiple specular reflection points on the side walls and a need for more absorptive material area. Home theaters, where seating capacities may vary from four to twenty, have absorptive side and rear walls that may be broken up with reflective vertical strips such as columns, lighting sconces, or other diffusive elements.

Bass buildup and rear-wall reflections should be controlled in home theaters just as it was in pure listening rooms. If loudspeakers are located behind a front-wall projection screen, the cavity can provide a space for bass absorption. Since home theaters are often located in living rooms, rather than in a dedicated space, bass trapping is more difficult and may depend on heavily upholstered furniture, thin glazing, HVAC ducts, and cabinetry.

Screening Rooms

Screening rooms are like home theaters but larger, and have the capability of film as well as video projection. Their capacity varies but falls into the 10 to 100 seat range. Since film projectors make noise, they are located in a separate booth, designed to isolate them from the theater. The level of projector noise depends on the film speed and width. Measured levels from film projectors are given in Fig. 21.21. Data are shown for both 35 and 70 mm projectors

FIGURE 21.21   Film Projector Noise at Two Feet
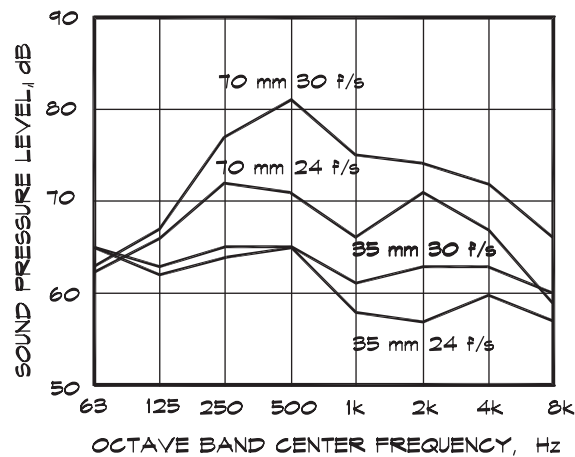
at 24 and 30 frames per second. Noise isolation design is straightforward. For 35 mm 24 f/s projectors the projection port can be double glazed 1/4" lam + 3" AS + 1/4" with at least one pane tilted away from vertical, not so much for sound isolation, but to prevent multiple reflected images on the screen. Laminated glass can be used in a projection port without degrading the image quality.

Loudspeakers located behind the projection screen can be mounted in a baffle wall or be freely suspended. Horns should be placed close to the screen to minimize back reflection and increase coupling. When a baffle wall is used, it should be at least double 5/8" (16 mm) drywall with 2" black fiberglass board on the screen side and R-11 batt in the cavity behind it. Where the loudspeakers penetrate the baffle wall, the openings must be sealed airtight so that the cavity does not become a mid-frequency Helmholtz resonator, which can color the sound.

The baffle wall cavity is a convenient location for return air HVAC ducts. If the return air grille is positioned below the screen across the front of the room it can be fashioned into a low-frequency Helmholtz resonator bass trap. An example of a professional screening room, designed for a video effects company, is given in Fig. 21.22. It can accommodate both film and video with a somewhat unusual dual three-beam video projector configuration mounted in the ceiling. In this project the surround loudspeakers were independently supported on steel columns located within the side walls to reduce vibrational transmission through the wall structure. The walls of the screening room were treated with 1" (25 mm) and the rear wall with 2" (52 mm) fiberglass panels. The cavity under the seating risers was filled with batt insulation and the front surfaces of the risers were left open, protected by a return air diffuser grille. The air was returned beneath the screen and the supply ducts were built into ceiling soffits on either side.

Video Post Production

Video post production facilities have rather modest acoustical requirements. Video post production takes place in a small office environment. Most of the audio work is done by monitoring on a pair of near-field loudspeakers placed on a desk, wall, or on stands a few feet from the listener. Soundstage and control of early reflections are not of particular concern.
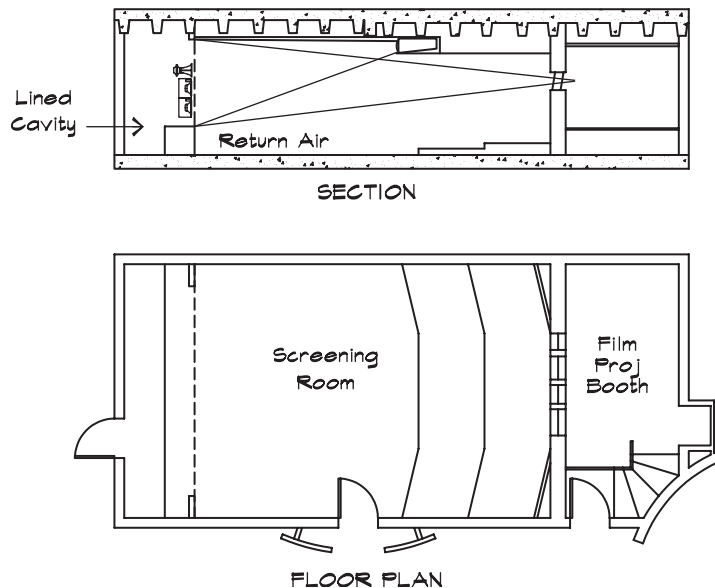
Work spaces tend to be small, with acoustical tile ceilings and absorptive walls. Floors are not carpeted to allow rolling chairs to move about freely.

21.4   ROOMS FOR RECORDING

Home Studios

Home studios, sometimes known as project studios, are increasingly common as high quality recording equipment becomes smaller and more affordable. The sophistication of this electronic gear has a direct influence on the proliferation of small studios since excellent recordings can now be made in a low-cost environment. The result has been a reaction from commercial studios trying to limit their number through land-use regulations. Under pressure from the commercial studios, cities such as Los Angeles have prohibited people from using their homes to make commercial recordings. Thus the home studio builder should check local ordinances and enforcement before beginning.

The second problem confronting a home studio user is that regulations in residential neighborhoods restrict noise levels at neighboring properties. These property-line ordinances typically limit nighttime noise levels to 45 dBA or 5 dB over the existing ambient, whichever is higher, within residential properties. Property line ordinances can limit the level at which a musician can play or require substantial construction to meet the local codes. A review of the local noise ordinance is therefore prudent.

Picking a location that provides natural sound isolation is a good start. If a basement is available, it is probably the best choice; or a separate structure can be used. Probably the most common choice, and one of the most difficult, is a garage. A two-car garage is about 24 feet square, enough for a one-room studio. Garages are lightly constructed and must be heavily reinforced to achieve adequate isolation. Exterior surfaces of plaster, brick, or

FIGURE 21.23   An Example of a Garage Studio

PLAN   SECTION
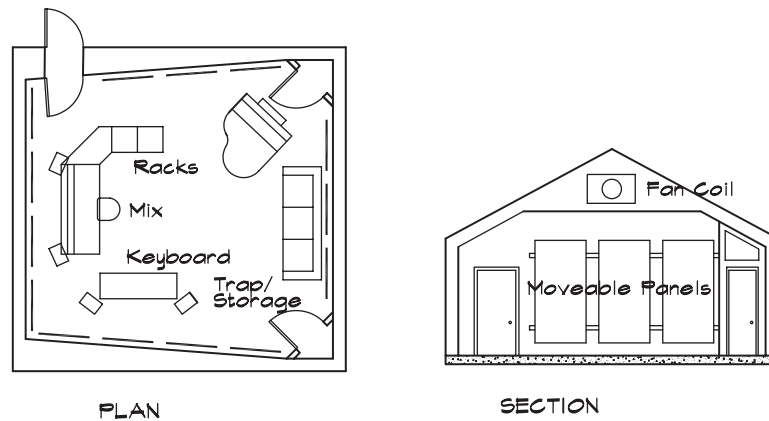
cement board, having a surface mass density of 10 lbs/sq ft (49 kg/sq m) or greater, can be used on the exterior with double drywall interior surfaces supported on a separate framing system or resilient isolators. In most cases the garage door must be removed, although it can be retained as an applied decorative element over the exterior wall.

A garage ceiling is too low and raising it requires added structural framing and review by a structural engineer. It should be double-drywall resiliently supported. The fan coil unit can be located above the ceiling with an access panel for service or a package unit outside the building can be employed. Careful calculations are necessary to insure isolation of the fan coil supply and return from the studio. Silencers or snaked flexible duct buried in batt insulation can help provide the necessary attenuation.

Figure 21.23 gives an example of a design for a personal studio built into a freestanding garage structure. It illustrates some of the difficulties in making a successful conversion. The layout of a successful project studio is quite personal and reflects the working habits of the user. In this example, the operator can mix and compose on a midi controller linked to a computer. A small number of musicians can be accommodated for a recording secession. Movable wall panels provide absorption and can be replaced with diffusive elements or simply removed. Storage closets double as bass traps. The floors are hardwood with throw rugs for added absorption.

Sound Stages

Sound stages are large open rooms used for indoor movie production. Acoustically they are designed to be dead with all surfaces except the floors covered with 4 to 6 inch (100 to 150 mm) deep blankets of absorptive material. The floors are smooth and flat so that cameras can be dollied. The exposed wall surfaces can be faced with commercial quilted blankets covered with hardware cloth below an elevation of 10 ft (3 m). The best rooms are built with isolated construction, floated floors, double-studded walls, and separately suspended gypboard ceilings. Access is provided via sound rated doors, which can be quite large. Some facilities have control rooms adjacent to the stage for mixing and recording.

The most difficult aspect of sound stage design is noise control. Isolation from exterior noise is a challenge because many stages are built in converted warehouses with lightweight roofs and little thought to the isolation of traffic and aircraft noise. Large air conditioning

FIGURE 21.24   Abbey Road Studio One, London, England (Abbey Road Studios, 2001)
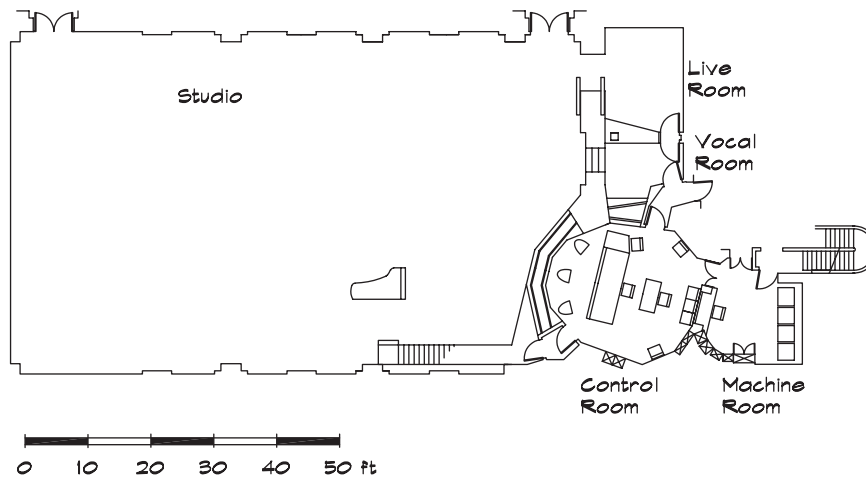
units are required to cool the stage lighting fixtures and this equipment is often located on the roof, where it is difficult to control. It is much preferable to separately support air handlers on grade or on an elevated steel platform dedicated to that purpose. Ductwork should be isolated from the structural framework either by resilient suspension or by a separate support system. Silencers located at a roof or wall penetration provide exterior as well as equipment noise control.

Scoring Stages

Scoring stages are rooms in which the music for a film is recorded. The orchestra conductor, who is the composer, faces both the musicians and a large screen on which the film is projected. As he conducts, he may listen through a single headphone to a click track, which aids in synchronization of the film and the score. Visual cues are also projected onto the screen in the form of streamers that progress from left to right across the screen to mark the beginning of a transition or effect when they reach the right-hand side.

A scoring stage is large, almost the size of a concert hall. Like concert halls, the best ones are shoebox-shaped with high ceilings and irregularly shaped diffusers on the walls and ceiling. A very good one, Studio 1 at Abbey Road Studios in London, is shown in Fig 21.24. Its dimensions are 92.6 ft × 59.7 ft × 39.4 ft high (28.2 m × 16.1 m × 12.2 m) and its total volume of 218,000 cu ft (6172 cu m) is about one-third that of Boston Symphony Hall. On one end there is a large (44 ft or 13.4 m wide) projection screen with the control room in an opposite corner.

Scoring stages are designed much like concert halls but without the requirements for an audience. The floors are flat and the walls and ceiling surfaces feature irregular shapes for diffusion. Reverberation times can be changed using moveable curtains or panels. For film, from 5 to 8 mics are used for the right-center-left and surround signals, and another 30 to 35 mics for individual instrument groups. The high ceilings sometimes make it difficult for the musicians to hear each other so 12 to 18 foldback channels are provided from the mix board to individual players through headphones. The orchestra can be seated on risers for visual cohesion and arranged to achieve a balanced sound.

Since sound stages are smaller than concert halls the orchestra cannot play quite as loudly as they would under performance conditions. When they do, the reverberation in the room, particularly the bass, can overwhelm the direct sound and yield a muddy recording. If the balance is correct and the control room is set up properly, the recording engineer can do a live mix including surrounds if necessary, however, the recorded tracks can be remixed at a later time.

The reverberation characteristics of a scoring stage are much the same as a concert hall. Abbey Road has a mid frequency reverberation time of about 2.2 seconds, rising slightly at lower frequencies and remaining fairly constant at high frequencies. The lack of audience and seat absorption limits the falloff of the high frequencies to that due to curtains, musicians, and air absorption so these rooms can be somewhat brighter than a performance hall.

The recording of symphonic music can also be done in an empty concert hall. In these cases the room is often extensively modified to accommodate this use. For example, when Royce Hall at UCLA is used for recording, a wooden platform for the musicians is constructed over a portion of the seating area and the opera chairs in the orchestra section are covered with 3/4" (19 mm) plywood over visqueen sheets to decrease high-frequency absorption (Murphy, 2001).

Recording Studios

Recording studios consist of one or more rooms where music is played and recorded. The musicians may all be present at the same time or they may never see one another. With the ability to move recorded music from place to place electronically, musicians may perform in rooms a continent away and days or weeks apart. When musicians are playing simultaneously, separate rooms are desirable to isolate the instruments so that they do not bleed into other microphones. These isolation booths also can be helpful in generating different acoustic environments.

A good studio must incorporate several acoustical factors:

1. Quiet—on the order of NC 10 to 15

2. Noise isolation from other areas (including footfall)

3. Freedom from acoustical defects such as flutter

4. Adequate absorption (often variable)

5. Reasonable diffusion

6. Isolated areas for recording individual instruments

7. Visual communication between the control room and the studios

8. Control of bass reverberation and modal buildup

Studios can be generic or highly personal, based on the working preferences of an individual user. A good example of the latter is Hum Studio in Santa Monica, CA, designed for Jeff Koz, a well-known composer. Figure 21.25 shows the floor plan for the main studio and control booth. Since most of the composition work is done at a keyboard with small digital mix boards, the traditional control room layout was not used. Instead, three work stations, each with a mix board, were arrayed along the front and side walls. Each could be used simultaneously during recording and mixing sessions. The main composing station was designed around the users' equipment. Since listening is done via small near-field loud-speakers, there was no need for large stereo monitors and no need for a large loudspeaker

FIGURE 21.25 Hum Studio A, Santa Monica, CA, USA
(Acoustician: Marshall Long Acoustics)
(Architect: Walter Meyer Associates)

FLOOR PLAN

LONGITUDINAL SECTION
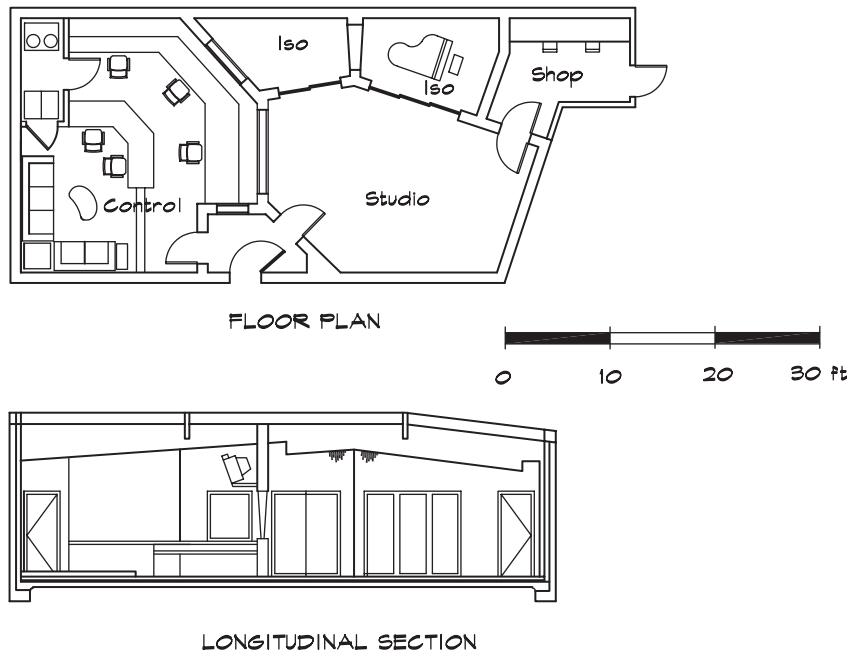
bridge above the main window. This arrangement freed up the center of the room for a client couch and social area instead of being dominated by a massive mixing console.

The studio consists of three rooms accessed from a small foyer separating the studio from the control room. Foyers can sometimes be used as isolation rooms particularly if there is a need for feedback such as with an electric guitar. Two isolation booths, with sliding glass doors, are available for individual instruments such as a piano or vocals. The walls and ceiling are constructed of multiple layers of drywall with a wood panel finish on the ceiling. Quilted absorbers are hung from hooks on the walls and can be removed or folded to reduce their area. The mid-frequency reverberation time is about 1.2 sec and flat with frequency. Bass trapping is done using the return-air plenum built above the ceiling. The segmented ceiling requires surface-applied wood diffusers to control flutter echo.

The control room is designed to be much deader, about 0.5 sec at mid-frequencies. The walls are faced with 2" (52 mm) cloth-wrapped fiberglass panels. The ceiling is hard—two layers of 5/8" drywall hung from springs. Bass traps are built into the space above the equipment closet and into the video monitor enclosure. Windows are arranged so that there is visual contact between the control room and any point in the studio, including the isolation booths.

Foley and ADR

Foley stages, where sound effects are generated by physical manipulation of devices, are often indistinguishable from landfills, due to the general clutter. A typical Foley stage consists of a dead room with walls and ceiling covered in broadband absorption and a hard-surface floor

FIGURE 21.26   Foley Stage
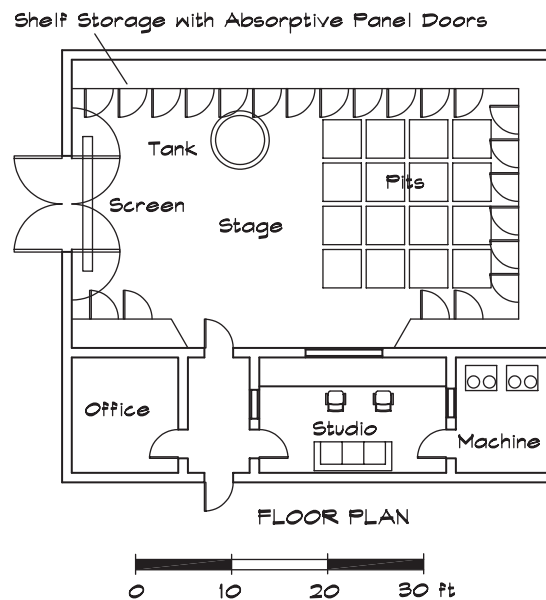
having multiple pits each 3 to 4 feet square, in which different walking surface materials are contained. The Foley artists watch the film, projected on a screen against one wall, while making the sound effects with their hands and feet and an assortment of mechanical gadgets. For example, if the film requires the sound of running along a sidewalk, the artist runs in place on a concrete slab in time with the film actor's steps, with a microphone suspended nearby. Gravel, wood, or sand may each have a separate pit. Water effects are created in a basin or large trough.

Since space is expensive, Foley pits sometimes are built into a traditional studio. This is less desirable than a dedicated space since recording studios are more reverberant than Foley stages and water is seldom available. Foley is messy and dirty and requires space around the pits for microphones and props. One approach is to build prop storage areas on the walls with absorptive panels mounted as doors. The airspace behind the panels improves bass absorption and the props are close by. Figure 21.26 gives an example of a Foley stage design based on this concept.

ADR or automatic (sometimes automated) dialog replacement is a technique using voice over, or the recording of dialog after the film has been shot. Whenever possible, film makers like to use the original sound recorded during filming but background noise or technical problems can make this impossible. In ADR the actors rerecord their parts in sync with the film. ADR stages are small, sometimes no bigger than a bathroom, and relatively dead. Low-frequency reverberation is a concern. Most have at least 2" (52 mm) thick panels on the walls. Since dialog replacement includes singing, ADR artists prefer rooms that are not completely dead (Farmer, 2001) and have a bit of volume, on the order of 8' × 12' × 9' (2.4 m × 3.7 m × 2.7 m). Larger stages can be used for recording voice over by adding absorptive panels around the actors. Flutter echo is particularly important to control so at least two nonparallel wall surfaces require treatment. ADR rooms should have a flat reverberation time versus frequency characteristic. Diffusion can be helpful and throw rugs are used to vary the room characteristics.

With animated films the dialog is recorded first and the animation created later to fit the sound. With film, the actors must watch the film and synchronize their voices to the picture. Video monitors are built into voice-over booths for this purpose. A communication system including a window between the booth and the studio and an intercom is a necessary part of the design.

21.5   ROOMS FOR MIXING

Dubbing Stages

Dubbing stages are large screening rooms, about the size of a commercial movie theater, with a full-sized projection screen and a single floor of opera chair seating. In the center of the seating is an area for three sound mixing consoles, one each for dialog, music, and effects, arrayed in a line across the theater. The film is projected on the screen using a projector fed by dubbers, which historically were mechanical transports that could be played forward or backward in synchronization with the picture. All the film sounds are combined into the final five channels that are ultimately transferred onto a CD and onto the film as a backup. Early films such as Fantasia used multiple film dubbers as storage devices for the audio tracks, which led to the current use of the word dub, meaning the replacement or recording of audio onto a film.

A dubbing stage should sound like a very good movie theater since that is where the final product will be displayed. The reverberation times given in Fig. 17.10 can be used as a guide. Side and rear walls are absorptive, occasionally broken up with reflective surfaces. The ceiling is black acoustical tile. Opera chairs are padded and the aisles are carpeted. The floor behind the mixing consoles is wood or vinyl to allow the chairs to roll easily. A series of technical racks are built into a long pedestal behind the mixers to house outboard processing gear. Producers and other executives frequently sit behind this console.

Control Rooms

Control rooms house the recording and electronic processing equipment necessary for mixing sound. The main component is the mixing console, the switchyard where the audio tracks are assembled onto a master recording device. The control room functions as a working space for mixing, as well as the social center of the studio, and the main client presentation area. Thus it must perform several different functions.

In its capacity as a stereo or multichannel mixing room the control room should incorporate a number of design features:

1. Quiet—on the order of NC 15 to 20
2. High noise isolation from the studio and machine rooms
3. Axial symmetry about the longitudinal centerline
4. Adequate absorption and reverberation control
5. Loudspeaker placement in accordance with the formats to be mixed
6. Deflection of first reflected sound away from the mix position
7. Control of bass via diaphragmatic absorbers or Helmholtz resonator trapping and loudspeaker placement
8. Convenient access to wiring and equipment racks for maintenance and setup of electronics

9.   Good visual communication with the studio spaces

10.   Some side wall and/or rear wall diffusion

11.   Video monitor for coordination of audio with video playback

12.   The ability to route audio and video between studios and control rooms and central storage areas

13.   Storage media that do not generate noise or undue thermal loads

As a client presentation and social center it should also have:

1.   Comfortable seating and good viewing angles for clients and visitors

2.   Speech isolation from the main studio

3.   Electronics interfaces including Internet or other high speed computer connections

4.   A flat workspace such as a table or desk

5.   Separate telephone room(s) for private conversations.

Figure 21.27 shows Studio A at Paisley Park Studio in Chanhassen, Minnesota. It consists of a series of recording rooms and a main control room fitted into a rectangular area 75 × 44 feet (22.9 × 13.4 m). It has a traditional design with the mixing console facing the window into the studio, flanked by stereo loudspeakers. One unique feature is the separating wall, which was cast as a monolithic concrete beam to provide structural support as well as isolation. Separate machine rooms for tape recorders and amplifiers are located on either side of the mix position. The rear wall includes a convex v-shape to direct first reflected sound away from the console with a projecting soffit above. Recently the design trend has been to lower the center window to accommodate a middle loudspeaker for mixing film or to rotate the control room so that the window is on the side. The best control rooms are relatively large, at least 20 to 25 feet (6.1 × 7.6 m) in each direction. Some designers prefer a room that is wider than it is deep as is the case at Paisley Park. With the introduction of digital consoles the space requirement for the mix board has been reduced, but most still retain at least 48 active faders. Tape machines are being replaced by digital storage units, which require less

Figure 21.27   Paisley Park Studio, Chanhassen, MN, USA
             (Acoustician: Marshall Long Acoustics)
             (Architect: Boto Design Associates)
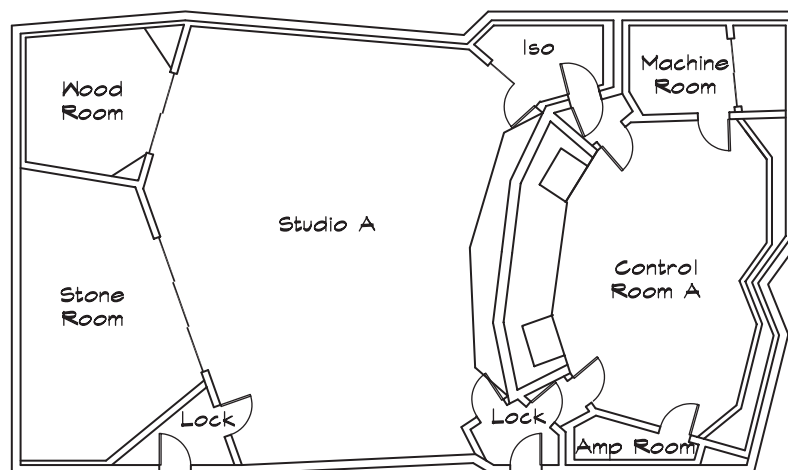
space but more cooling. The cooling fans for digital storage are rack mounted and generate enough noise to require location in a remote room behind double sets of heavy glazed doors.

21.6   DESIGN DETAILS IN STUDIOS

Noise Isolation

For the best noise isolation, studios and control rooms are built as room-within-a-room structures, floated on an isolated concrete slab, with separately supported walls and ceiling. Floor slabs should be point mounted on neoprene isolators having a deflection of at least 0.25 to 0.4 in (6 to 10 mm). Continuous floor support systems using cork, neoprene, mineral fiber, or fiberglass sheets are much less effective since the floor load is distributed and the deflections are small.

Walls and ceilings are double (or triple) constructed on separate supports with the interior walls standing on the floated slab and the top of the studs stabilized with isolating sway braces. Ceilings are hung from spring isolators to complete the box. Penetrations of the ceiling cavity for return air openings can utilize lined sections of duct to close off the hole. Recall that there is considerable low-frequency loss due to the end effect at the opening. Figure 21.28 gives an example from the Hum Studio main control room.

FIGURE 21.28   Isolation Details from Hum Studio
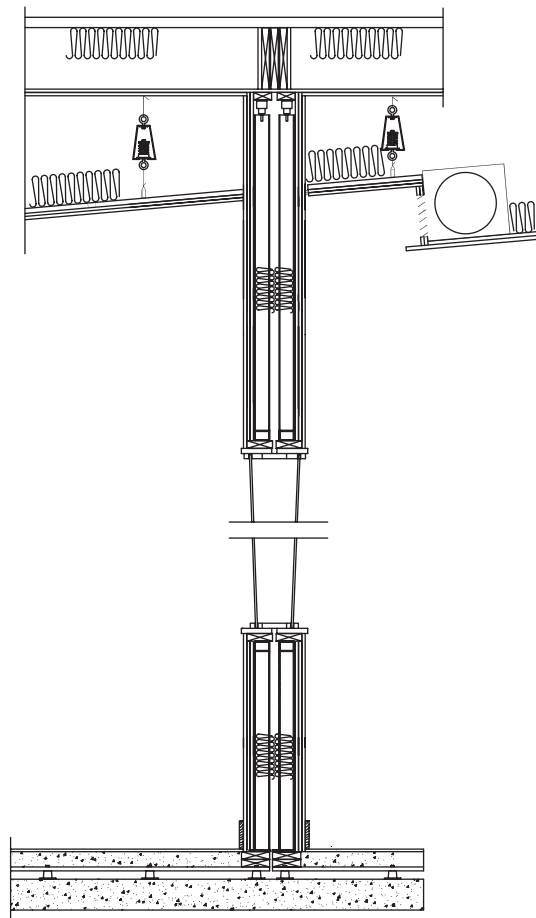
Symmetry

Control rooms should be symmetric about the line through the mixer position to retain stereo imaging. The side walls and ceiling are flared out to direct the first reflection around the mix position. At one time ceilings were angled toward the mix position to "compress" the bass, in part to try to offset the null of the fundamental mode in the center of the room. This design proved difficult to control since only some frequencies had their pressure maxima there and the effect was highly dependent on the receiver position. Now most ceilings are either flat or flare away from the mix position. They can be treated with absorption or diffusion near the specular reflection points.

Loudspeaker Placement

The traditional placement of stereo loudspeakers in a control room is at an included angle of around 60° at a distance of 11 to 12 ft. (3.4 to 3.7 m) from the mixer. Loudspeakers are aimed at a point about 2 ft (0.6 m) behind the mixer's head to give a wider sweet spot. They can be built into the front wall of the studio with either a baffle wall or just a simple enclosure or can be left free standing. If a baffle wall is used it should be wrapped around the loudspeaker using a heavy material, drywall but sometimes concrete, to minimize back transmission into the studio. In some cases, free-standing loudspeakers are placed on pedestals in front of the mixing console.

In surround systems three loudspeakers are located in front, two at or slightly outside the normal stereo position. It is important that these be in the same horizontal plane, with the loudspeakers oriented so that the high-frequency drivers are closest to the horizontal plane of the mixer.

Separate moveable subwoofers can be used for bass control. They are placed on the floor, against a wall near the null point of one of the fundamental modes. Some mixers prefer full-range loudspeakers to help control room modes, particularly when they also are used for the surrounds.

The location of surrounds is less critical than the LCR loudspeakers although they should be positioned to the side and slightly behind the mixer. The ITU-R BS775 standard calls for the placement of the front left and right loudspeakers from 2 to 4 m (6.5 to 13 ft) apart at an included angle of 60°. The rear surrounds are to be located 110° to 120° off the centerline although some mixers prefer angles as high as 125° (Mitchell, 2002). When they are located directly to the side, the directional localization is very poor and the envelopment is less effective.

Bass Control

Bass control is essential in studio and control room design. In control rooms the mixer must be confident that what he is hearing is on the audio track and not a construct of the room itself. Otherwise he cannot be assured of the accuracy of the recording and its repeatability in other rooms. In recording studios excessive bass can artificially lengthen the reverberation time in certain frequencies, causing reverberant bleed from track to track, coloration, and lack of clarity in the natural sound of the instruments.

Three physical methods are employed to achieve low-frequency absorption: 1) deep resistive materials such as fiberglass boards or batts, 2) diaphragmatic absorbers such as lightweight drywall or plywood panels, and 3) Helmholtz resonator cavities containing fiberglass batts for damping. Each of these has been discussed previously. Of the three,

FIGURE 21.29   Highly Absorptive Rear Wall

A   Structural wall

B   3.5" (90 mm) Fiberglass batt insulation

C   1/2" (13 mm) Sound deadening board on 2x4

D   3 1/2" (90 mm) Fiberglass batt insulation

E   1/2" (13 mm) Pressed fiberglass sheets (3 lb/cu ft)

F   1" (25 mm) Quilt batting

G   Stretched cloth surface
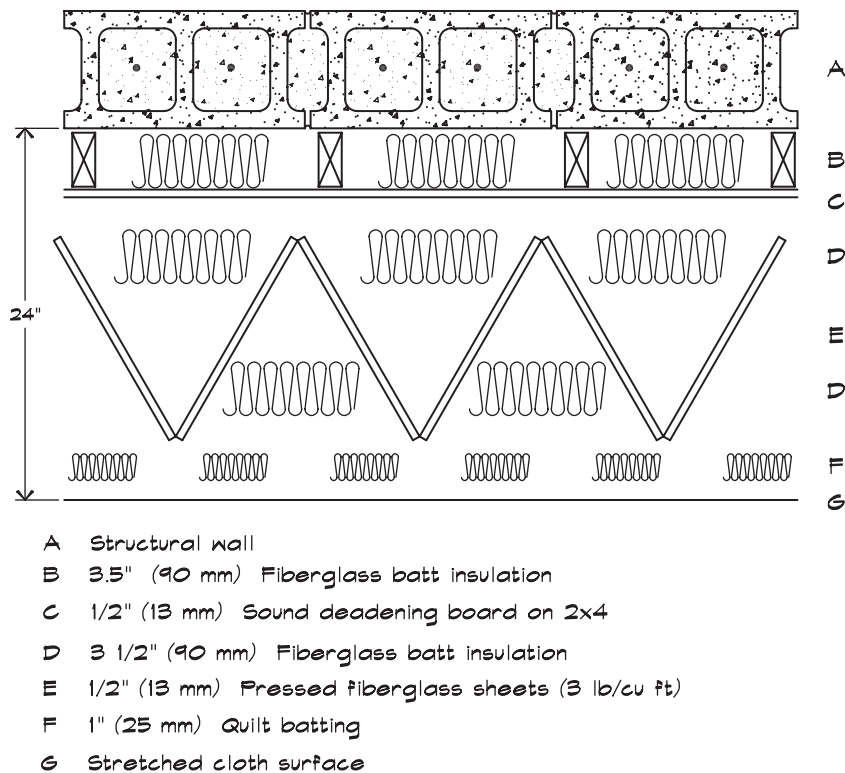
a deep layer of batting gives the best broadband response, but takes up considerable space. Figure 21.29 shows an example of a deep rear-wall absorber.

Helmholtz resonators are frequently used, but often misunderstood, bass absorbers. Their openings should be positioned at a pressure maximum such as along a surface edge or corner. Distributed openings are also effective and can be combined with a return air plenum by installing a short run of lined sheet-metal duct to act as the resonator neck. Resonator openings can be located behind porous absorbers since the fiberglass boards do not impede the flow of low-frequency energy. Cavities should be distributed around the room and filled with batt insulation to widen their bandwidth.

Studio Window Design

Large windows separating the control room from the studio are designed to provide clear visual communication between rooms while maintaining acoustical isolation. The degree of separation required is not as great as one might think since it is rare that a different musical track is being played in the control room, while mics are live in the studio. When live monitoring takes place, it is of the same material as that being recorded, so isolation is not as critical. Low-frequency separation helps keep the signal-to-noise ratio of the recorded material high. Voice privacy between the control room and the studio is critical.

An example of window design is given in Fig. 21.30. It is double-glazed construction, preferred because of its superior low-frequency performance. The edges of the cavity between the panes are lined with open cell neoprene foam or fiberglass boards, wrapped in cloth, to

FIGURE 21.30   Studio Window Detail
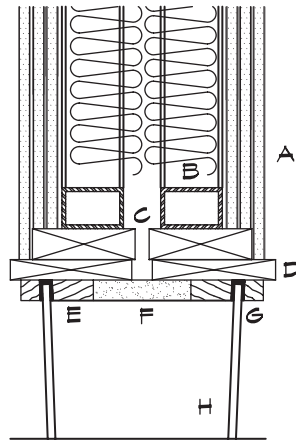
A   Separately supported isolation wall
B   Structural support frame with 2 x 3 1/2" (90 mm) batt insulation
C   Open slot between 2 x nailers
D   Finish wood window frame
E   1" (25 mm) Thick wood stops
F   1" (25 mm) Open cell foam or cloth wrapped fiberglass board
G   3/16" (5 mm) Rubber gasketing
H   Heavy window glazing – 1/2' + 3/8" thick

provide edge absorption. The cavity between the walls can be used as a Helmholtz resonator tuned to the window mass-air-mass resonance. Each pane should be supported separately on its own stud system and isolated floor slab. Window panes are angled, not so much for acoustic reasons, but to reduce light reflection and to provide space for the monitor enclosures above.

If structural supports are necessary, they can be included via pipe columns or a bearing wall between the two studio walls. Triple-panel construction is better for high frequencies but can be worse for low frequencies. Where a triple panel is used, a high-mass bearing wall such as grouted concrete block along with heavy glass in the center can offset some of the disadvantages and provides insurance against transmission through openings. If triple-panel construction is employed there must be adequate air gaps to reduce the lower limiting frequency.

The openings for the monitors should not degrade the wall performance or color the monitor performance. It is better to extend the separation wall up past the monitors to the resilient ceiling closure rather than to try to build an enclosure around the rear of the monitors.

Diffusion

The degree to which diffusion contributes to the sound quality in studios and control rooms is a subject of some debate. In scoring stages where stereo mics are positioned to capture the overall sound of an orchestra, diffusion is important since it enhances the orchestral blend. Studio 1 at Abbey Road, for example, uses diffusive shapes on most of the wall surfaces. When separate mics are used to isolate instruments, diffusion is less critical since it contributes to reverberant bleed, although it is still helpful for breaking up flutter echoes.

In control rooms some diffusion on the side and rear walls can help with the sense of envelopment and a widening of the stereo image.

There is at present no accepted method of quantifying the proper amount of diffusion in a simple way as there is with absorption. Davis and Davis (1979) suggest that control rooms be designed with a highly diffuse rear wall (live end) and absorptive surfaces around the monitors (dead end). Toole (1990) counters that a totally diffuse rear wall creates a fog of confusing reflections and that a smaller center-section of absorption in the rear wall is preferred. The advent of surround loudspeakers, particularly when they are as large and powerful as the front ones, means that rooms have to be designed with evenly distributed absorptive and diffusive elements.

ACOUSTIC
MODELING,
RAY TRACING,
AND
AURALIZATION

It is highly desirable to ascertain the acoustical characteristics of a performance space before time, treasure, and emotion are expended on its construction. In spite of this fact, the ability to make even the most rudimentary predictions a priori about the acoustical behavior of spaces dates only from the work of Sabine in the early twentieth century. Before this time concert halls were designed and built empirically based on previous examples or, as in the case of Garnier, based on pure chance.

In spite of the lack of technical guidelines, some of the finest halls were constructed before the study of room acoustics was subjected to the rigors of scientific analysis. Musikvereinssaal in Austria, a hall that still ranks among the best in the world, dates from the eighteenth century. Boston Symphony Hall, which benefited from Sabine's reverberation experiments, was designed without model testing or advanced analytical techniques.

The development of small computers in the late twentieth century gave us the ability to create mathematical models of acoustical spaces and to reproduce the sound of a room before it is constructed. We must be careful, however, that we do not fool ourselves into believing that these models are perfect representations of reality. The simplifications necessary to be able to carry out the calculations in a reasonable time still leave us with an imperfect picture, but as technical sophistication and computing ability increase, the models are improving.

22.1 ACOUSTIC MODELING

Early twentieth century investigators built physical scale models to test acoustical design ideas. Several techniques were employed to construct the interior of a room and generate the sound signal. One simple method was to use a two-dimensional wave table consisting of a flat, water-filled trough into which the plan or section of a hall could be inserted. This technique has been known at least as far back as the mid nineteenth century. Davis (1926) reviewed its history and described the work that he and Kaye did at the National Physical Laboratory. Water ripples were generated using a small oscillating paddle. The interaction with the interior room surfaces was studied by observing wave patterns that formed in the tank. A light could be projected through the bottom of the tank and onto

a screen for observation. The technique was limited to long wavelengths by the speed of the driving mechanism.

W. C. Sabine (1964) adapted spark photography to study the propagation of waves in the design of several theaters on which he consulted after the construction of Boston Symphony Hall. In 1928 Knudsen and Delsasso (Knudsen, 1932) used a similar but improved technique to investigate two-dimensional plan and section models of Royce Hall at UCLA.

Vermeulen and DeBoer (1936) developed a simple method of optical model testing used by Delsasso in his work on Schoenberg Hall at UCLA. To do a reflection study, small light bulbs partially covered with tape to create directivity were used as sources. Model surfaces were constructed from thin brass sheets bent into the shapes of the walls or ceiling and then chrome-plated to act as mirrors. Opaque sheets of glass were used as receivers to study the distribution of reflections by observing the brightness patterns formed by the scattered light (Delsasso, 1967). Walls and ceilings could be shaped to yield an even intensity of reflected light, and reflection patterns from individual surfaces could be studied using this technique. Light models are a high-frequency, short-wavelength system, which may not accurately portray low-frequency phenomena such as refraction. This method has its primary application in the study of early reflections.

Testing Scale Models

Spandock (1934) reported using 1:5 scale models of rooms for acoustical testing. He ensonified them at 2500 and 4000 Hz, which corresponds to 500 and 800 Hz in the full-size rooms. He and his followers later extended their work to 1:10 scale models using tape recordings of speech, played back at ten times the recording speed (Knudsen, 1970) in the model space. A small receiver microphone was used to collect sounds in the model and convert them back to the original frequency range.

In scale modeling, material properties must also be scaled. Yamamoto and Wakuri (1968) used 1 mm (0.04") thick Plexiglas plates, backed with 10 to 15 mm (3/8–5/8") air spaces, for reflective surfaces in their models. For absorption they used 2.9 mm (0.11") thick polyurethane foam sheets or 25 mm (1") thick mineral wool boards. In some cases, the polyurethane was 50% covered with 18 mm (3/4") wide strips of 0.07 mm (0.003") thick cellophane tape. In other instances the absorptive sheets were faced with suitably dimensioned spaced wood slats.

Air absorption in scale model testing presents another interesting problem. Since tests are conducted at frequencies as high as 100,000 Hz, its effects can be substantial. Experimenters (Yamamoto and Wakuri, 1968) use very low-humidity air (1.5% relative humidity) furnished by drying equipment. Other researchers use pure nitrogen, which has lower high-frequency absorption properties than air. Because most of the interest in building models is to check on the pattern of early reflections, air absorption is often less important than one would think. A 1:10 model of a two-second hall has a scaled reverberation time of 200 ms and the critical early reflections occur in about a tenth of that time. Thus the first 20 feet of sound travel in model space is of the most interest (Grozier, 2002).

Spark Testing

Model testing requires both small sources and small receivers. In a 1:10 model an eighth-inch microphone is small enough. At 1:20 it is equivalent to a 2.5" (64 mm) diameter mic capsule, which would be a problem above 1000 Hz. For impulse testing, a spark generator is used to

produce a small, short duration sound. The time history of a received signal can be plotted or used to determine properties of materials or the impulse response of a space. Figure 22.1 shows an experimental setup to measure the absorption coefficient of a material.

A perfectly reflecting surface is used as a standard of comparison and the direct sound level is the reference calibration. By matching the direct-field levels and comparing two graphs, the difference in the reflected levels will give the specular absorption coefficient for a given angle. Figure 22.2 illustrates a result obtained from a single reflection.

A difference in level will occur even for a perfectly reflecting surface due to the path length difference. When there is more than one surface, multiple reflections can occur. Figure 22.3 shows the effect of reflections from a floor and a wall. Multiple surfaces produce more complicated patterns that mimic the behavior of a real room.

Spark testing can also be used to measure the diffusive properties of a material. Small-scale aggregate such as that used for model railroad ballast can be scattered over a flat reflective sheet. For a diffuse material the specular reflection amplitude is much reduced but lateral reflections from reflectors on either side of the specular path scatter sound toward the microphone, albeit at a later time. Figure 22.4 illustrates the effect.

FIGURE 22.1 Setup for Measuring Sound Absorption of a Flat Sheet (Grozier, 2002)
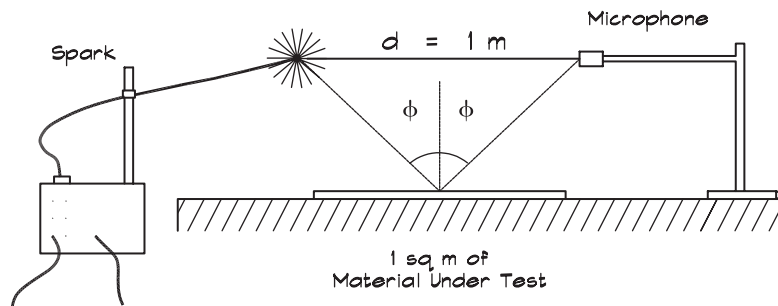
FIGURE 22.2 Reflections with the Source and Microphone over a Hard Floor (Grozier, 2002)
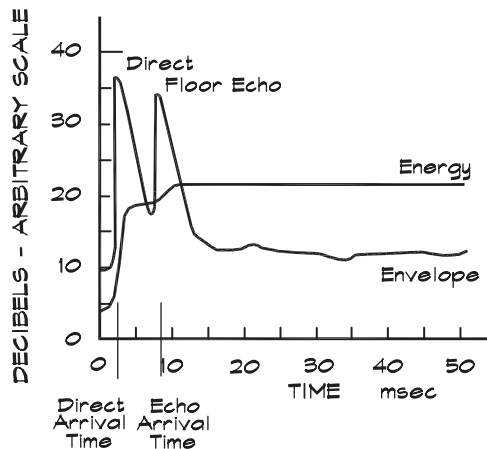
FIGURE 22.3 **End Wall Added to Floor (Grozier, 2002)**
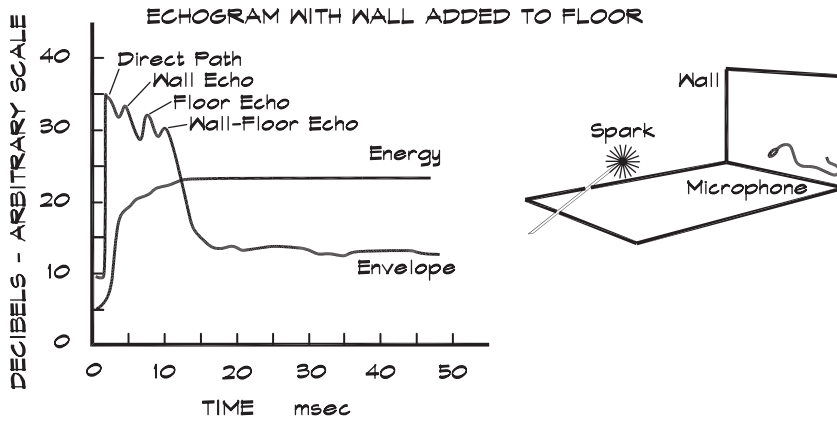
FIGURE 22.4 **Comparison between Reflections from Smooth and Rough Surfaces (Grozier, 2002)**
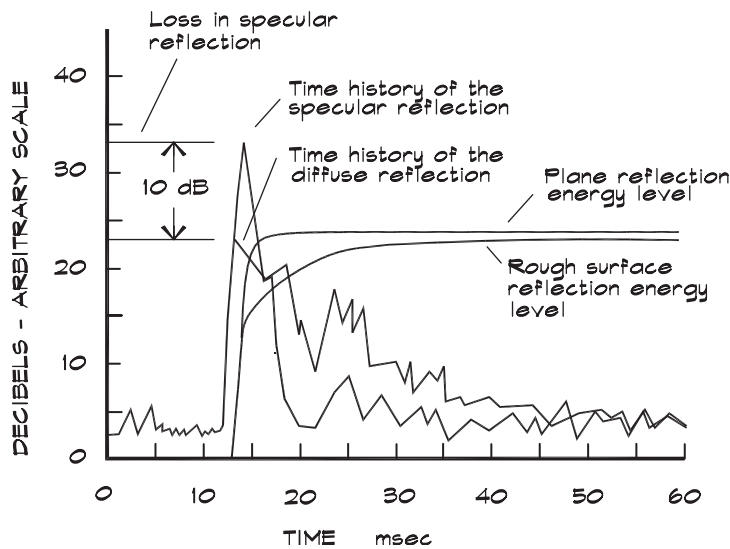
The art of model testing is unfortunately becoming lost as computer programs become more accurate. Three-dimensional physical models still serve as an important reality check on mathematical modeling. They are relatively inexpensive to build and test since they need not be as detailed as a visual model.

Ray Casting

Computers have become sufficiently powerful that mathematical modeling of three-dimensional spaces is now practical. The normal methodology is to create a surface model of an enclosed space using polygons or other easily represented surfaces. A mesh of contiguous polygons is formed and each is described by a list of vertices, connected by edges. A surface is characterized by its edges, vertices, a normal, and material properties such as absorption and diffusion coefficients.

FIGURE 22.5 Subdivision of the Source's Surface into Triangular Beams (Farina, 2002)
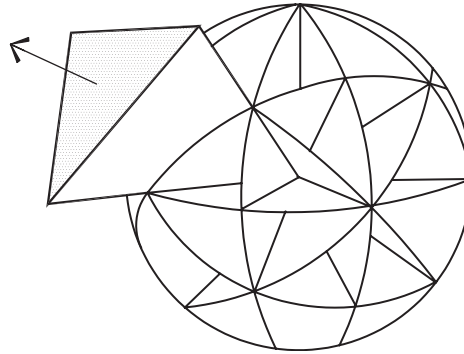
Rays are cast mathematically from a source and have retained properties including the original source strength and location, directivity, direction, and total distance from the source, amplitude, and bounds. Since a finite number of rays is cast, each ray actually represents a cone or pyramid-shaped beam of energy, radiating out from the source. The geometry is given in Fig. 22.5. Ray directions can be selected by using a uniform, random, or directed distribution, however a uniform pattern in which the center of each beam surface is chosen as an initial aim point is most common.

The question of how many rays to cast then arises. It is important that each room boundary be found by some ray, and that ray-surface strikes are not double counted. A ray is likely to find a surface having area S in a time t if the area of the ray wavefront is not greater than S/2. This leads to a minimum number of rays (Rindel, 2000) necessary to find a surface

$$N \geq \frac{8 \pi c^2}{S} t^2 \qquad (22.1)$$

For a hypothetical surface having a one square meter area and a propagation time of one second, the required number of rays is about 3×10^6. Thus, brute force ray tracing requires considerable computer time.

A receiver can be modeled as a point or sphere in space. In simple ray tracing a receiver hit occurs when a ray passes within a given radius of a listener. In beam tracing a hit is registered when the receiver falls within the pyramid beam triangle. If no receiver hit occurs, the ray is followed until it encounters a surface. When there is a surface hit, reflection calculations are performed based on the impact point using the surface normal, area, and material properties.

The output of a ray-tracing program includes the room's impulse response at a given receiver from which a number of metrics of interest can be calculated. When a receiver hit occurs, the arrival time, direction, and amplitude of the ray as a function of frequency are stored. Angles of incidence and amplitudes for each received ray allow an accurate reproduction of the sound (an auralization) of the space. Due to limits in computational capacity as well as human reaction to late arrivals, time limits are set on the propagation of rays. After a given time (or distance) a ray's remaining energy is given over to the reverberant field or simply abandoned.

FIGURE 22.6 Method of Images for a Rectangular Room
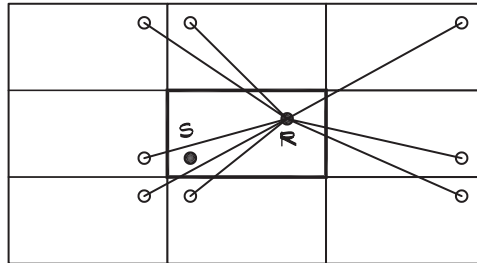
Image Source Method

The image source calculation method uses the mirror image of the source as the origination point for a new ray, drawn through the intersection point on the struck surface. Images of images are drawn until the desired order of reflection is achieved. The construction is straightforward for a simple rectangular enclosure but it becomes quite complicated if the room shape is complex. An example is given in Fig. 22.6. The number of image sources in a room of volume V for a radius $c\,t$ is (Rindel, 2000)

$$N_{refl} \geq \frac{4\,\pi\,c^3}{3\,V}\,t^3$$

(22.2)

This is approximately the number of specular reflections arriving at the receiver up to a time t after the initial sound emission.

    The method is quite accurate since no surfaces are missed, but the number of calculations required is very large. For n surfaces there are n first-order images, each of which can have $n-1$ second order images and so forth. For a reflection order i, the total number of sources is (Rindel, 2000)

$$N_{sou} = 1 + \frac{n}{(n-2)}\,((n-1)^i - 1) \cong (n-1)^i$$

(22.3)

Using Eq. 8.49, the mean free path in a room of 15,000 cu m (530,000 cu ft) is about 16 m (52 ft). In 600 ms about 13 reflections occur for a given ray path. Assuming a hall with 30 surfaces, the total number of image sources is $N_{sou} = 29^{13} \cong 10^{19}$, or more than we can comfortably accommodate. The procedure is also very inefficient since according to Eq. 22.2 only about 2500 of the images are valid for a given receiver.

    Image-source reflection models must validate the accuracy and uniqueness of a ray path. This can be done by confirming the visibility by back tracing a ray path from the receiver to the source to make sure that the sequence of surfaces is the reverse of the original path. To avoid duplication an image tree list of the early reflection images is maintained (Rindel, 2000).

Hybrid Models

A hybrid model divides the room's time history into an early period where individual reflections are computed, and a late period where only the statistical reverberant tail remains. The division can be based on a user selection of the reflection order, after which reflections

become diffuse, or on the use of a diffusion coefficient, or both. In a diffuse reflection the impacted surface becomes a new source rather than a reflector of sound. The surface element is assumed to radiate into the hemisphere in front of it. The intensity of the scattered sound can be based on an assumed directivity pattern such as Lambert's cosine law (Rindel, 2000), where the intensity of the scattered energy is proportional to the cosine of the angle between the incoming ray and the vector to the receiver, or it can simply be uniformly distributed (Farina, 2000). Visibility of the receiver must also be checked for diffuse reflections.

The optimum transition between the specular and diffuse reflections would at first appear to be at as high a reflection order as possible. Interestingly this turns out not to be the case. The probability that an image is visible from a receiver is proportional to the size of the surface. At higher reflection orders, missed images are more likely. With more missed images the accuracy of the program decreases. As the order of reflection increases, the ratio of the cone or beam area to the reflecting surface area increases, which overstates the specular energy contribution. Rindel (2000) argues that in a hybrid model a low reflection order (2 to 3) and a relatively small number of rays (500 to 1000) should be sufficient to characterize a typical auditorium.

22.2   RAY TRACING

In a ray-tracing calculation the sound energy is assumed to travel from the source to the receiver like a beam or ray of light. Reflections from each surface are taken to be specular. Figure 17.8 shows a simple example done in a two-dimensional CAD drawing. A source is positioned in the space and sound rays are drawn at equal intervals (usually 5°–10°) originating from the source point. When a ray intersects a surface the reflected ray is constructed and followed until it hits the receiver. By altering the reflecting surfaces, different shapes and orientations can be tried until the rays are evenly distributed throughout the audience. At this point the surface orientation is acceptable for one source location. The process is repeated for a number of possible source locations until the design has been completed. When modeling reflections from isolated free-hanging panels, reflection points closer than a quarter wavelength from the edge of the panel should not be assumed to produce specular reflections. Two-dimensional ray tracing, even when it is done manually, can be an effective tool for designing small rooms.

Rays

The mathematical modeling of ray tracing has undergone rapid development in the last 30 years through the work of computer graphics programmers. Excellent references by Glassner (1989), Hill (1990), Shirley (2000), and Haines (2002) are available, which treat the subject in considerable detail. All these authors present treatments similar to that shown here. One must exercise care however since different authors use somewhat different (row or column) matrix formulations, and not all of the matrices in these references are directly interchangeable.

When modeling sound propagation in a three-dimensional room we begin with a default frame of reference consisting of three orthogonal basis vectors ($\mathbf{x}$, $\mathbf{y}$, $\mathbf{z}$). All rays and surfaces are described mathematically relative to this coordinate system. Points are four-dimensional column vectors. Coordinate transformations are performed using 4×4 translation and rotation matrices, which were treated in Chapt. 18. Ray tracing deals with the interaction between rays and surfaces, either plane or curved. A ray is a line, most conveniently described in

FIGURE 22.7 Definition of a Ray
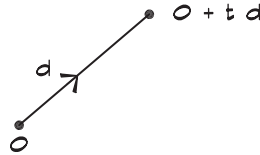
parametric form, using an origin (**o**), a direction vector (**d**), and a parameter (t) denoting the distance along the direction vector. Figure 22.7 gives an example.

$$\mathbf{p}(t) = \mathbf{o} + t\,\mathbf{d} \tag{22.4}$$

For example the line segment between points **a** and **b** is

$$\mathbf{p}(t) = \mathbf{a} + t\,(\mathbf{b} - \mathbf{a}) \tag{22.5}$$

where t is defined over the interval $t \in [t_a, t_b]$, and in this case, $t \in [0, 1]$. The direction vector is normalized to 1, and t can range to infinity. Equation 22.4 is an explicit or parametric form of the ray equation since any point on the ray can be determined simply by varying t.

Surfaces and Intersections

Surfaces are an infinite collection of points. Many of the simplest shapes can be modeled by using an implicit equation, which returns a zero value when a point (x,y,z) is on the surface (Shirley, 2000)

$$f(x, y, z) = 0 \tag{22.6}$$

If a point is not on the surface, a nonzero value is returned. The function is called implicit because it allows a given point to be tested but does not allow the explicit calculation of a set of points. For a surface of points $\mathbf{p} = (x, y, z)$ there is an implicit function

$$f(\mathbf{p}) = 0 \tag{22.7}$$

which is satisfied for all points on the surface. If the value of the function is greater than zero, the point is "outside" the surface, and if less than zero it is "inside" the surface. For spheres and cylinders the definition of inside and outside is obvious, but for planes the definition depends on the problem context.

The intersection of a ray and a surface occurs when the equation for the ray satisfies the implicit function for the surface

$$f(\mathbf{p}(t)) = 0 \tag{22.8}$$

or

$$f(\mathbf{o} + t\,\mathbf{d}) = 0 \tag{22.9}$$

The normal to the surface at the point of intersection, which is needed to calculate the reflected ray, is the gradient of the implicit function

$$\mathbf{n} = \nabla f(\mathbf{p}) = \left(\frac{\partial f(\mathbf{p})}{\partial x}, \frac{\partial f(\mathbf{p})}{\partial y}, \frac{\partial f(\mathbf{p})}{\partial z} \right) \tag{22.10}$$

FIGURE 22.8 Definition of a Plane
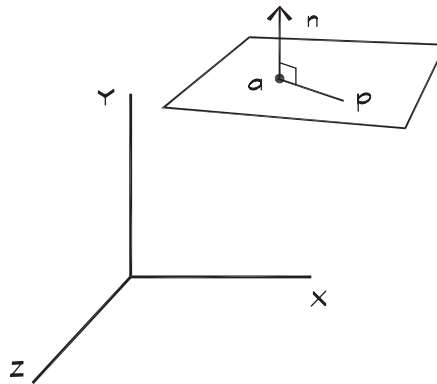
Planar Surfaces

To define the implicit function for an infinite plane containing point **a** and having normal **n**, as in Fig. 22.8, we write

$$(\mathbf{p} - \mathbf{a}) \cdot \mathrm{n} = 0 \tag{22.11}$$

Here **a** and **n** are known, and **p** is a sample point. When **p** lies in the plane defined by **n**, the vector drawn between **a** and **p** is normal to **n** if their dot product is zero.

Ray-Plane Intersection

The intersection of a ray with a plane, shown in Fig. 22.9, is obtained by substituting Eq. 22.4 into Eq. 22.11

$$(\mathbf{o} + t\,\mathbf{d} - \mathbf{a}) \cdot \mathbf{n} = 0 \tag{22.12}$$

and solving for t , the only unknown

$$t = \frac{-(\mathbf{o} - \mathbf{a}) \cdot \mathbf{n}}{\mathbf{d} \cdot \mathbf{n}} \tag{22.13}$$

FIGURE 22.9 Ray-Plane Intersection
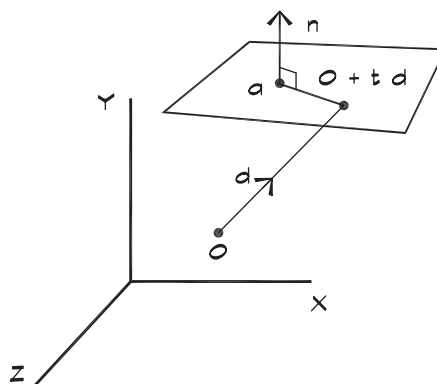
If the denominator is zero, the ray is parallel to the plane. If both the numerator and the denominator are zero, the ray lies in the plane.

In terms of the coefficients, a plane is defined by

$$a\,x + b\,y + c\,z + d = 0 \qquad (22.14)$$

and the intersection is (Glassner, 1989)

$$t = \frac{-(a\,x_0 + b\,y_0 + c\,z_0 + d)}{a\,x_1 + b\,y_1 + c\,z_1} \qquad (22.15)$$

where we have assumed that the scaling parameter is 1 in the four-element matrices, and the subscripts 0 and 1 refer to the values of the coefficients for **o** and **d**, respectively. The coefficient d is the shortest distance between the plane and the origin.

Ray-Polygon Intersections

Having determined the intersection point of a ray and an infinite plane we must see whether it lies within a polygon of interest. There are a number of techniques used to make this determination both for polygons of arbitrary shape and for the special case of triangles. The one shown here is from Haines (1989).

A polygon is defined by a list of vertices connected by edges. To see if a point on a plane lies within a polygon, an inside-outside test (known as the Jordan Curve Theorem) is performed by casting a ray, lying in the plane, in an arbitrary direction from the intersection point and counting the number of edge crossings. If the number is odd, the point is inside the polygon; otherwise it is outside. Figure 22.10 shows an example of a five-pointed star with a hollow center, and shows several scenarios. In this case horizontal rays are used to test the polygon.

The test is complicated for a plane in three-dimensional space. Fortunately it also works for the projection of the polygon onto an arbitrary two-dimensional surface. If one component of each point is removed, the remaining coordinates give the projection of the polygon onto a new **u-v** plane. The polygon can be translated so that the intersection coincides with the

FIGURE 22.10 Inside-Outside Crossing Test (Haines, 1989)
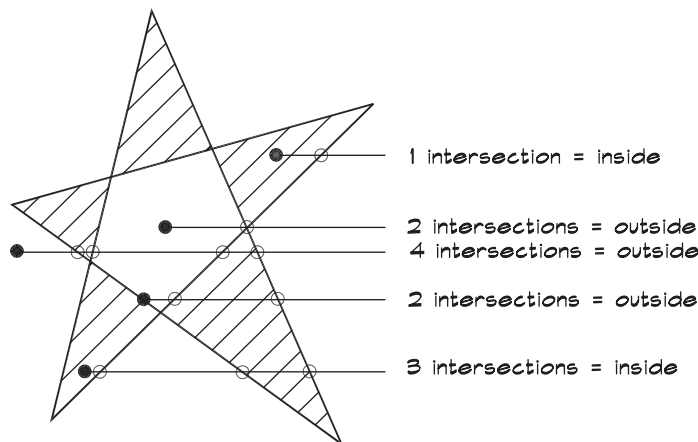
FIGURE 22.11   Polygon Crossing Test (Haines, 1989)
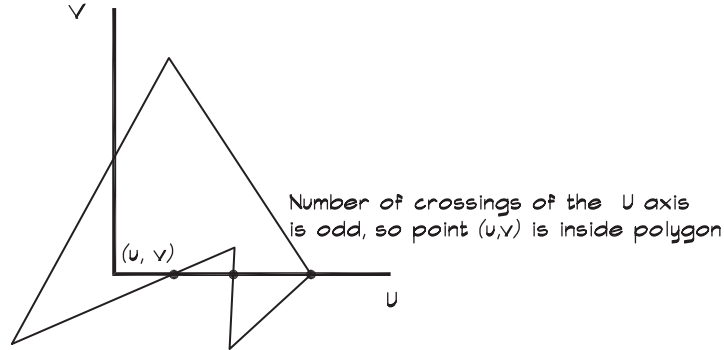
u-v origin. The intersection test then is performed using a ray aligned with the **u** axis as in Fig. 22.11.

If the plane of the polygon is normal to a basis vector, then the components in that direction are removed. Special care must be taken to address unique cases such as a vertex, which lies on the test ray axis. This can be done by defining a ray as incrementally above the **u** axis so that it does not coincide with the vertex (Berlin, 1985).

Ray-Sphere Intersection

A sphere, having a center $\mathbf{c} = (c_x, c_y, c_z)$ and radius R, is characterized by the second-degree polynomial (Shirley, 2000)

$$(x - c_x)^2 + (y - c_y)^2 + (z - c_z)^2 - R^2 = 0 \tag{22.16}$$

which in vector form is

$$(\mathbf{p} - \mathbf{c}) \cdot (\mathbf{p} - \mathbf{c}) - R^2 = 0 \tag{22.17}$$

The ray-sphere intersection is determined by plugging the ray formula into the sphere equation

$$(\mathbf{o} - t\mathbf{d} - \mathbf{c}) \cdot (\mathbf{o} - t\mathbf{d} - \mathbf{c}) - R^2 = 0 \tag{22.18}$$

By rearranging terms we obtain the solution in quadratic form

$$(\mathbf{d} \cdot \mathbf{d}) t^2 + 2\,\mathbf{d} \cdot (\mathbf{o} - \mathbf{c})\,t + (\mathbf{o} - \mathbf{c}) \cdot (\mathbf{o} - \mathbf{c}) - R^2 = 0 \tag{22.19}$$

The equation for a sphere located at the origin is

$$x^2 + y^2 + z^2 - R^2 = 0 \tag{22.20}$$

and the point of intersection is

$$t^2 (x_1^2 + y_1^2 + z_1^2) + 2\,t\,(x_0 x_1 + y_0 y_1 + z_0 z_1) \\ + (x_0^2 + y_0^2 + z_0^2) - R^2 = 0 \tag{22.21}$$

where the subscripts 0 and 1 again refer to the values of the coefficients for **o** and **d**, respectively. Note that the ray origin can be translated to maintain this location.

Equation 22.21 has the classic quadratic form

$$A t^2 + B t + C = 0 \qquad (22.22)$$

that can be solved using

$$t = \frac{-B \pm \sqrt{B^2 - 4AC}}{2A} \qquad (22.23)$$

Here the term under the radical, called the *discriminant,* tells how many real solutions there are. If positive, there are two intersections, one where the ray enters and the other where it leaves the sphere. If it is negative there are no intersections, and if zero the line is tangent to the sphere. It saves computing time to first check the discriminant to see if a solution exists. The general solution for t is

$$t = \frac{-\mathbf{d} \cdot (\mathbf{o} - \mathbf{c}) \pm \sqrt{(\mathbf{d} \cdot (\mathbf{o} - \mathbf{c}))^2 - (\mathbf{d} \cdot \mathbf{d})((\mathbf{o} - \mathbf{c}) \cdot (\mathbf{o} - \mathbf{c}) - R^2)}}{(\mathbf{d} \cdot \mathbf{d})} \qquad (22.24)$$

and the intersection point can be calculated by plugging the value of t into Eq. 22.1. If the sphere has been translated to the origin, **c** is set to zero.

The normal at the point of intersection is the gradient of Eq. 22.17

$$\mathbf{n} = 2 \, (\mathbf{p} - \mathbf{c}) \qquad (22.25)$$

and the unit normal is

$$\mathbf{n} = (\mathbf{p} - \mathbf{c}) \, / \, R \qquad (22.26)$$

Where there are two intersection points, the one having the smaller absolute value of t gives the nearer point. If the ray originates inside the sphere, the normal should be given a negative value.

Ray-Cylinder Intersection

The case of an infinite cylinder is similar to that of a sphere. A unit cylinder is formed by rotating the line x = 1 in the x-z plane about the z axis. For a cylinder of arbitrary radius having its center at the origin and its axis aligned with the z direction, the implicit function is

$$x^2 + y^2 - R^2 = 0 \qquad (22.27)$$

and the ray intersection is given by

$$t^2 \, (x_1^2 + y_1^2) + 2 \, t \, (x_0 x_1 + y_0 y_1) + (x_0^2 + y_0^2) - R^2 = 0 \qquad (22.28)$$

For a cylinder at an arbitrary location and orientation, the translation and rotation matrices necessary to move its center to the origin and to align its axis with the z coordinate are applied to the ray to maintain the proper relationship before solving for t. Once the value of t has been determined, it is substituted into Eq. 22.4 along with its direction vector to obtain the intersection point.

FIGURE 22.12   Quadric Surfaces

Ellipsoid   Paraboloid   Hyperbolic paraboloid

Hyperboloid
of one sheet

Hyperboloid
of two sheets

Cone

Sphere

Cylinder
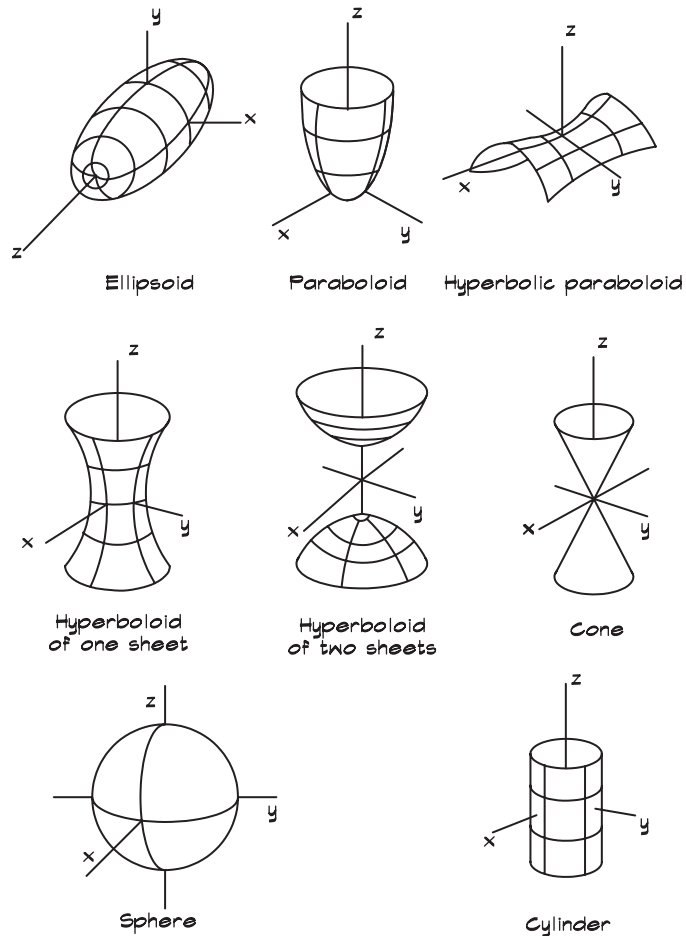
Ray-Quadric Intersections

Algebraic surfaces are implicit formulas of polynomials having the general form (Hanrahan, 1989)

$$\mathbf{p}\,(\text{x, y, z}) = \sum_{i=0}^{l} \sum_{j=0}^{m} \sum_{k=0}^{n} a_{ijk} x^{i}\, y^{j}\, z^{k} \qquad (22.29)$$

The degree of the surface is given by the maximum value of the coordinates $d = \max$ (l, m, n), and the number of terms in the equation describing a surface of degree d is $(d + 1)$ $(d + 2)(d + 3)/6$. A group of surfaces known as quadrics, consisting of polynomials having degree 2, are shown in Fig. 22.12. The generalized implicit equation for a quadric surface has ten terms and is given by

$$ax^{2} + 2bxy + 2cxz + 2dxw + ey^{2} + 2fyz$$
$$+ 2gyw + hz^{2} + 2izw + jw^{2} = 0 \qquad (22.30)$$

This can be written in matrix form as

$$\mathbf{x}^t \, \mathbf{Q} \, \mathbf{x} = 0 \tag{22.31}$$

where Q is a symmetric 4×4 matrix

$$\mathbf{Q} = \begin{bmatrix} a & b & c & d \\ b & e & f & g \\ c & f & h & i \\ d & g & i & j \end{bmatrix} \tag{22.32}$$

and $\mathbf{x}$ is a column vector and its transpose $\mathbf{x}^t$ is a row vector. The general solution for the intersection point is determined by substituting in the ray equation (Eq. 22.4). We then obtain a general equation

$$a_2 \, t^2 + a_1 \, t + a_0 = 0 \tag{22.33}$$

where

$$\begin{aligned} a_2 &= \mathbf{x}_1^t \, \mathbf{Q} \, \mathbf{x}_1 \\ a_1 &= 2\mathbf{x}_1^t \, \mathbf{Q} \, \mathbf{x}_0 \\ a_0 &= \mathbf{x}_0^t \, \mathbf{Q} \, \mathbf{x}_0 \end{aligned} \tag{22.34}$$

which can be solved using the quadratic equation. The subscripts 0 and 1 refer to the values for $\mathbf{o}$ and $\mathbf{d}$, respectively.

The **Q** matrix can be diagonalized so that only the terms along its diagonal are nonzero. This is known as its canonical form since the principal axes of the surface are aligned with the canonical basis vectors (x, y, z), and its center is at the origin.

Ray-Cone Intersection

When a cone is in canonical coordinates its implicit equation is (Hanrahan, 1989)

$$x^2 + y^2 - z^2 = 0 \tag{22.35}$$

and the ray intersection is determined by solving

$$t^2 \, (x_1^2 + y_1^2 - z_1^2) + 2 \, t \, (x_0 x_1 + y_0 y_1 - z_0 z_1) \\ + (x_0^2 + y_0^2 - z_0^2) = 0 \tag{22.36}$$

Ray-Paraboloid Intersection

The canonical equation of a paraboloid is (Hanrahan, 1989)

$$x^2 + y^2 + z = 0 \tag{22.37}$$

and

$$t^2 \, (x_1^2 + y_1^2) + 2 \, t \, (x_0 x_1 + y_0 y_1 - z_1) \\ + (x_0^2 + y_0^2 - z_0) = 0 \tag{22.38}$$

Although more complicated shapes are seldom necessary in acoustical ray tracing their implicit functions can be found in computer graphics texts such as Glassner (1989) or Hill (1990). Both quadric and superquadric shapes are also addressed in Ray Tracing News (RTNews), a web site maintained by Eric Haines.

22.3   SPECULAR REFLECTION OF RAYS FROM SURFACES

The mathematical characterization of reflections from surfaces is undergoing considerable research. The standard approach is to group the energy transfer into four components: specularly reflected, diffusely reflected, transmitted, and absorbed. Figure 21.13 shows the relationships between the components, which are characterized in terms of their coefficients. For room acoustics problems the transmitted energy is bundled with the absorbed energy and lumped into the absorption coefficient since it does not return to the originating space. In these formulas we seek useful and intuitive algorithms, which do not require massive computing power to utilize.

Specular Reflections

A specular or mirror-like reflection is pictured in Fig. 22.14. The reflected ray is given by (Shirley, 2000)

$$\mathbf{r} = \mathbf{d} + 2\,\mathbf{a} = \mathbf{d} + 2\,\frac{\mathbf{d}\cdot\mathbf{n}}{|\mathbf{n}|^2}\,\mathbf{n} \tag{22.39}$$

FIGURE 22.13   Reflection from a Surface
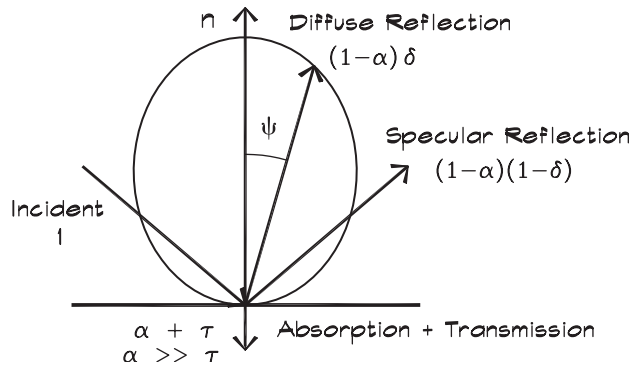
FIGURE 22.14   Specular Reflection from a Surface
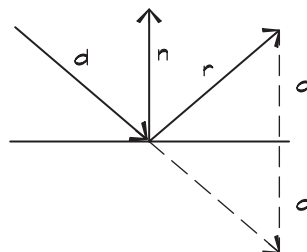
If the normal vector of the reflecting plane is itself normalized, the denominator in Eq. 22.39 becomes one. Once the new ray direction has been established it can be traced until it triggers a level limit.

Specular Reflections with Absorption

The direct-field intensity at a receiver following a single specular reflection from a large absorptive surface is given by (Farina, 2000)

$$I_{spec} = \frac{W \, Q_\phi}{4 \, \pi \, (r_1 + r_2)^2} \, (1 - \alpha) \, e^{-\gamma (r_1 + r_2)} \qquad (22.40)$$

where W = sound power of the source (W)

Q_ϕ = source directivity for a given angle ϕ

α = absorption coefficient (usually diffuse field)

γ = air absorption coefficient $\cong \dfrac{1.7 \cdot 10^{-8} \, f^2}{\varphi}$

r_1 = distance between the source and the surface (m)

r_2 = distance between the surface and the receiver (m)

φ = relative humidity (%)

The amplitude of specularly reflected rays is calculated using the absorption coefficient of the reflecting surface. Either the diffuse field absorption coefficient or a specular coefficient derived from it is used in most computer models. The standard reverberant measurement method smoothes out some of the variation and produces repeatable results. Diffuse absorption coefficients have the advantage of availability and convenience even though they only account for the angle of incidence in a statistical way.

Ideally a specular absorption coefficient, that accounts for the angle of incidence of the incoming ray, should be used, but these are rarely available from direct measurements and must be estimated from impedance data or from the diffuse coefficients. With impedance data the angular behavior of the specular absorption coefficient can be calculated from Eq. 7.63. One cannot, however, calculate the impedance from the diffuse-field absorption coefficient simply since there are an infinite number of combinations of real and imaginary parts that would give the same result.

Rindel (1993) suggested a method for estimating the angular dependence of the absorption coefficient by neglecting the imaginary part of the impedance and assuming the real part to be independent of angle of incidence; that is, the surface is locally reacting. The real part of the surface impedance is based on the diffuse-field absorption coefficient for a standard test surface of 11 sq m, assuming an angle of incidence around $55° - 60°$ and $\alpha_{60} \cong \alpha$.

$$r_{60} \cong \pm \sqrt{1 - \alpha} \qquad (22.41)$$

where r can be positive or negative. The relation for the pressure reflection factor is

$$r_\theta = \frac{Z_a - Z_f(\theta)}{Z_a + Z_f(\theta)} \qquad (22.42)$$

where Z_a = surface impedance, which depends on the material properties
   $Z_f(\theta)$ = field impedance, which depends on the angle of incidence
            and the panel size
   α = diffuse field absorption coefficient
   α_{60} = absorption coefficient at about a 60° angle of incidence
   r_θ = reflection coefficient for a given angle

When the sample size is infinite the field impedance is $Z_f(\theta) \rightarrow \rho c / \cos\theta$ and is real. For a finite area it is complex. Rindel (1993) has suggested an empirical relationship for its real part

$$Z_f(\theta) \cong \rho c \left[\left(\cos^2\theta - 0.6 \frac{2\pi}{k\,e} \right)^2 + \pi \left(0.6 \frac{2\pi}{k\,e} \right)^2 + \left(\frac{2\pi}{(k\,e)^2} \right)^4 \right]^{-1/4} \quad (22.43)$$

where k = wave number = $\dfrac{2\pi f}{c}$ (m^{-1})

   $e = \dfrac{4S}{P}$ = characteristic dimension of the test sample (m)

   S = surface area of the test sample (m^2)
   P = perimeter of the test sample (m)
   f = frequency (Hz)
   c = velocity of sound in the surface material (m/s)
   ρ = density of the surface material (kg/cu m)

Values of the equivalent field impedance, Z_f^*, measured under diffuse field conditions, suggested by Rindel (1993) for a test area of 11 sq m, are given in Table 22.1. The angle used in calculating the factor varies with frequency, approaching 52.5°, above 1000 Hz.

   An equivalent real part of the material impedance can be calculated using Eq. 22.41 and 22.42

$$Z_a = Z_f^* \frac{1 + r_\theta}{1 - r_\theta} = Z_f^* \frac{1 \pm \sqrt{1 - \alpha}}{1 \mp \sqrt{1 - \alpha}} \quad (22.44)$$

The sign of the radical is chosen according to the material in use. If the material is hard such as concrete, drywall, or wood, the upper sign is selected. If it is soft, having an impedance less than $2\,\rho_o\,c_o$, then the lower signs should be used. Using Eq. 22.43 and 22.44 in Eq. 22.42 we obtain an expression for the angular dependence of the absorption coefficient in terms of the diffuse field coefficients and the size of the reflecting surface.

Specular Absorption by Seats

Nishihara et al. (2001) published measurements of the absorption of a seated audience in chairs with differing thicknesses of padding at varying angles of incidence. They suggest

TABLE 22.1   Suggested Field Impedance for an 11 sq m Sample (Rindel, 1993)

Frequency (Hz)	125	250	500	1k	2k	4k
$Z_f^* / \rho c$	1.04	1.35	1.53	1.62	1.64	1.64

Figure 22.15 Oblique Absorption Coefficients at the Hypothetical Plane of a Seated Audience (Nishihara et al., 2001)
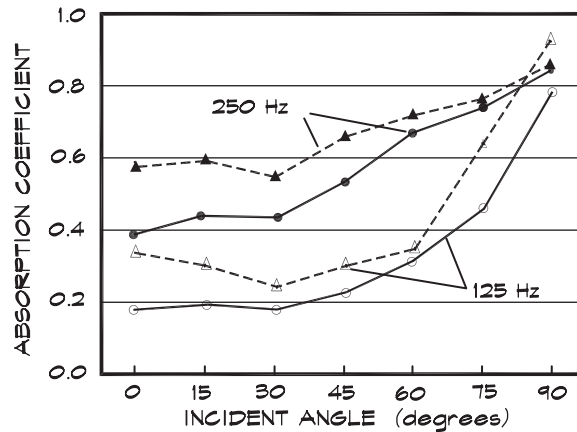
Calculations based on measurements at Musikvereinssaal (solid line) and Burgtheater (dotted line).

that the use of this type of data is more accurate because the distribution of the angle of incidence in a concert hall is not truly uniform. Often these numbers are dependent on surface irregularities, edge conditions, sample size and orientation, and other details of the measurement methodology. The measured angular behavior of low-frequency absorption they found is shown in Fig. 22.15. Note the increase in the absorption coefficient at angles approaching 90°.

22.4 DIFFUSE REFLECTION OF RAYS FROM SURFACES

The characterization of diffusion is currently undergoing considerable study. It has been assumed that a diffusing surface can be characterized by means of a coefficient, similar to the Sabine absorption coefficient, that varies between 0 (specular reflection) and 1 (complete diffusion), which can be measured in a standard way. Just as was the case with absorption, there may be different formulations depending on whether we are in a free field, having a given angle of incidence, or a diffuse field, with a random angle of incidence. To characterize the surface diffusion a scattering coefficient and measurement methodology were proposed by Mommentz and Vorlander, (1995)

$$\delta = \frac{E_{diff}}{E_{tot}} = \frac{E_{diff}}{E_{spec} + E_{diff}} \tag{22.45}$$

The scattering coefficient is the ratio between the diffusely reflected energy and the total reflected energy. Here a diffuse reflection is defined as any nonspecular reflection, even though a perfect diffuser will radiate a portion of the incident energy in the specular direction and even though a redirection rather than perfect diffusion of the energy may be what is occurring.

Measurement of the Scattering Coefficient

The measurement of all the diffuse energy is difficult so most methods measure the specularly reflected energy and use the diffuse absorption coefficient to calculate it

$$\delta = \frac{E_{diff}}{E_{tot}} = 1 - \frac{E_{spec}}{E_{tot}} \tag{22.46}$$

where $E_{spec}/E_{inc} = 1 - \alpha_{spec} = $ normalized specularly reflected energy

$\quad\quad\quad E_{tot}/E_{inc} = 1 - \alpha = $ normalized total reflected energy

so,

$$\delta = \frac{\alpha_{spec} - \alpha}{1 - \alpha} \tag{22.47}$$

which gives us a way of measuring the diffusion coefficient, δ.

Farina (2000) has suggested the technique pictured in Fig. 22.16, using a microphone 2 m above the floor that is dollied past a diffusing surface suspended 3.65 m above a loudspeaker flush mounted into the floor. Impulse response data are recorded at regular (28 mm) microphone intervals. Time windowing filters out the direct sound so that the impulse response of the reflection from the panel under test is obtained. The results from various panels are given in Fig. 22.17. Although this method yields consistent results, the technique has not been accepted as a standard. Some (e.g., D'Antonio, 1995) prefer a diffusion coefficient that characterizes the evenness of the diffused energy, based on the standard deviation of the measurements around a test surface. This approach is helpful for a comparison of products but not, as yet, particularly useful for modeling applications.

Diffuse Reflections

When a sound ray impacts a surface some of the energy is reflected specularly and some is diffused. The portion of the energy reflected specularly creates an intensity at a receiver (Naylor, 1993)

$$I_{spec} = \frac{W\,Q_\phi}{4\,\pi\,(r_1 + r_2)^2}\,(1 - \alpha)(1 - \delta)\,e^{-\gamma\,(r_1 + r_2)} \tag{22.48}$$

FIGURE 22.16 Measurement Methodology for the Specular Absorption Coefficient (Farina, 2000)
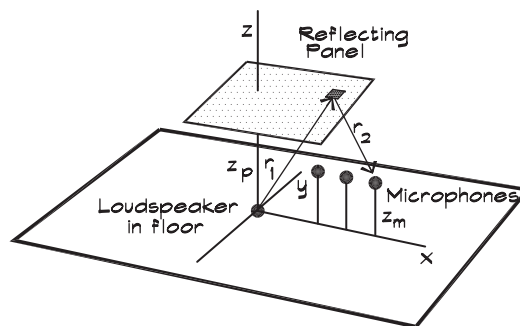
FIGURE 22.17   Comparison of Measured and Predicted Specularly Reflected Intensities (Farina, 2000)
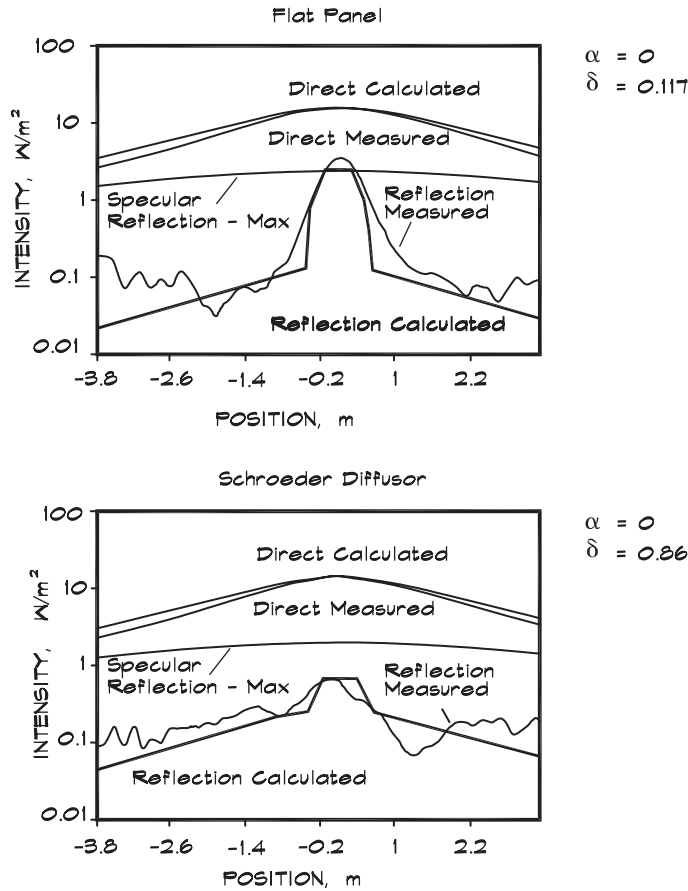
The remaining unabsorbed energy is assumed to be scattered. Most models treat the reflecting surface as a new sound source, radiating the diffuse portion of the energy into the hemisphere in front of it. In the simplest condition, where the beam area associated with an individual ray is smaller than the area of the impacted surface, as in Fig. 22.18, the diffuse

FIGURE 22.18   Pyramid Beam Impacting a Large Surface
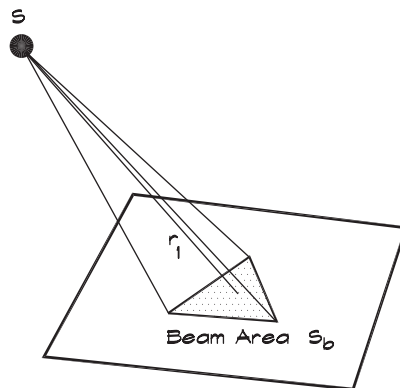
energy radiating from the surface is

$$W_{diff} = \frac{W Q_\phi}{N_r} \delta (1 - \alpha) e^{-\gamma\, r_1} \tag{22.49}$$

where N_r = number of equally spaced rays. Using Eq. 2.90 the intensity from a diffuse reflection at a receiver within the hemisphere is

$$I_{diff} = \frac{W Q_\phi Q_S \delta (1 - \alpha) e^{-\gamma\, (r_1 + r_2)}}{4 \pi N_r \left[r_2 + (Q_s S_b / 4 \pi)^{1/2} \right]^2} \tag{22.50}$$

where $\quad S_b = \dfrac{4 \pi r_1^2}{N_r} =$ beam area at a distance r_1 from the source

$\quad Q_s =$ directivity of the reflecting surface

$\qquad = 2$ for an omnidirectional hemisphere

$\qquad = 2 \cos \psi$ for Lambert's cosine law

$\quad \psi =$ angle between the scattering surface normal and
the outgoing ray

Some programs (e.g., ODEON) use directional scattering of the diffuse energy according to Lambert's cosine law, which is introduced using the surface directivity Q_s, and others (e.g., RAMSETE) use omnidirectional scattering.

Multiple Reflections

When a ray undergoes multiple reflections the effect of each successive surface's absorption and diffusion coefficients must be considered. Accordingly the surface absorption coefficient and the air absorption term for a single reflection are replaced by a product

$$(1 - \alpha) e^{-\gamma\, (r_1 + r_2)} \Rightarrow \prod_{i=1}^{n} (1 - \alpha_i) e^{-\gamma (r_{tot} + r_2)} \tag{22.51}$$

The total diffuse scattering coefficient represents the diminution in the intensity due to a succession of diffuse reflections, each of which removes some of the energy from the specular component. It is defined as

$$\delta_{tot} = \delta_{tot-1} + (1 - \delta_{tot-1}) \delta_n \tag{22.52}$$

The total diffusion coefficient increases slightly with each reflection until it approaches 1. At this point all reflections are diffuse and the sound field is totally reverberant.

A given receiver is illuminated by both specular and diffuse reflections. Figure 22.19 shows two hypothetical receivers. If a receiver lies within the specularly reflected pyramid beam, it receives both the specular and diffusely reflected intensities. If it is outside the beam it receives only the diffuse intensity, but these reflections come from every surface having a diffusion coefficient greater than zero. After each reflection the intensity of the remaining direct sound field is reduced by the amount absorbed and by the amount diffused.

FIGURE 22.19   **Pyramid Beam Impacting a Surface (Farina, 2000)**
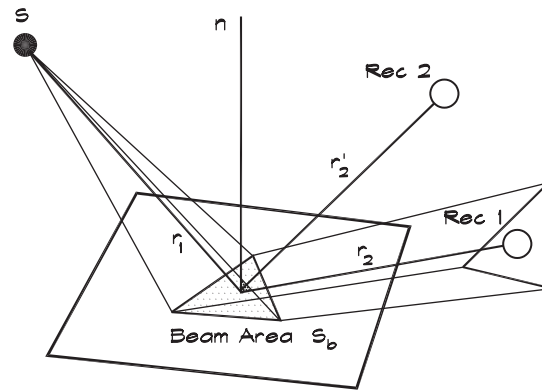
When there are multiple specular reflections from a series of surfaces the received intensity after the nth reflection is (Farina, 2000)

$$I_{spec,n} = \frac{W\,Q_\phi}{4\,\pi\,(r_{tot} + r_{n+1})^2}\left[\prod_{i=1}^{n}(1-\alpha_i)\right](1-\delta_{tot})\,e^{-\gamma\,(r_{tot} + r_{n+1})} \tag{22.53}$$

where r_{tot} = total distance (including reflections) between the source and
the current surface (m)
r_{n+1} = distance between the current surface and the receiver (m)

and the diffuse intensity from a large scattering surface after a series of reflections is

$$I_{diff,n} = \frac{W\,Q_\phi\,Q_s\left[\prod_{i=1}^{n}(1-\alpha_i)\right]\delta_{tot}\,e^{-\gamma\,(r_{tot} + r_{n+1})}}{4\,\pi\,N_r\left[r_{n+1} + (Q_s\,S_{tot}/4\,\pi)^{1/2}\right]^2} \tag{22.54}$$

where $S_{tot} = \dfrac{4\,\pi\,r_{tot}^2}{N_r}$ = beam area at a distance r_{tot} from the source

Edge Effects

As the ray-panel intersection point approaches a panel edge, purely specular scattering no longer occurs. Farina (2000) has suggested that edge and size effects be accounted for by using a linear interpolation of the diffusion coefficient between the edge of a panel and a point, which is a half wavelength from the edge; at this point the panel is assumed to be characterized by the full value of the coefficient. Figure 22.20 shows an example. Between the two points a local diffusion coefficient is assumed to be in effect (Farina, 2000)

$$\delta_{loc} = \delta_0 + (1-\delta_0)\left(1 - \frac{d}{\lambda/2}\right) \tag{22.55}$$

FIGURE 22.20   Local Value of the Scattering Coefficient (Farina, 2000)
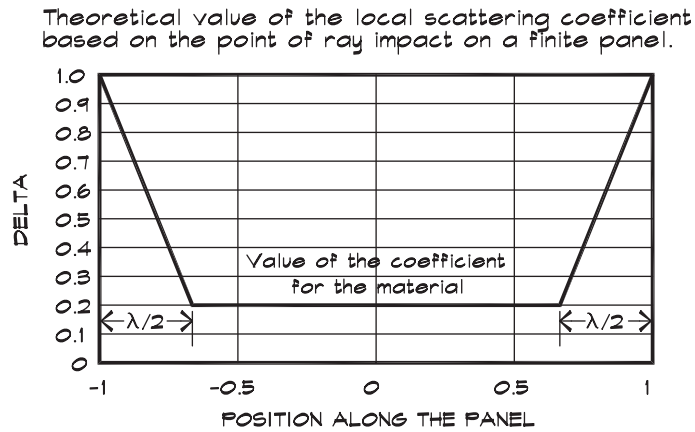
where   d = distance from the edge of the surface (m or ft) d ∈ [0, λ / 2]
       λ = wavelength of the incident sound (m or ft)
       δ_0 = value of the scattering coefficient characteristic of the material

Note that even when there is a flat reflector, with a surface diffusion coefficient of 0, the diffusion due to the edge effect is addressed in Eq. 22.55. The inclusion of edge effects in this manner helps account for diffraction near the end of a freely supported reflector, but overestimates the diffuse energy when there are adjacent reflecting surfaces whose normals are close together.

Hybrid Models and the Reverberant Tail

Every ray tracer has to deal with the transition between the early direct reflections, and the late reverberant field, and the limits imposed by computation time. Some programs (e.g., ODEON; Rindel, 2000), called hybrid models, use scattering coefficients in the normal way for the first two or three reflections, after which they abandon specular reflections and treat subsequent impacts as diffuse. The direction of the diffuse reflection can be selected at random by choosing an angle whose probability is based on Lambert's cosine law. This simplifies the calculations required and saves time but can miss multiple reflections.

Other programs (e.g., RAMSETE; Farina, 2000) remove a portion of the diffuse energy at each reflection, calculate its contribution at the receiver, and follow it no further. This simplification underestimates the diffuse-field energy, which might partake in multiple reflections after the initial one, but offsets the overestimation from the edge calculation. In this system all the energy remaining in a beam pyramid is assumed to be reflected specularly from the surface struck by the center ray even when the area of the beam pyramid is much greater than the reflecting area. The error introduced by this assumption overestimates the amount of specular energy reflected, but significantly reduces the computation time.

When the beam area is larger than the reflecting surface as in Fig. 22.21, not all the energy associated with a ray hits the surface, and a decision must be made as to how to treat the reflection. One approach is to clip the beam using the edges of the area struck, generating new beams, which continue on (Funkhouser et al., 1996). This approach is quite accurate but requires more computing power. Another approach is to reduce the specular energy by the ratio of the struck surface area to the beam area (when the beam area exceeds

FIGURE 22.21 **Pyramid Beam Impacting a Small Surface**
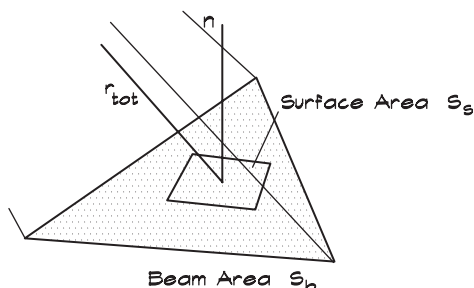
the surface area). The struck surface area would replace the beam area in Eq. 22.54 for the diffuse scattering component from the surface. The energy not striking the surface would be considered diffuse and could continue on a random or a diffused path. This would limit the specularly reflected energy to that actually hitting the surface.

The computation problem is a difficult one and is a topic of considerable interest. It may be possible some day to solve the room modeling problem exactly, but in the meantime clever models can give useful results with relatively simple approximations.

22.5 AURALIZATION

One product of a ray tracing model is the directional impulse response of a receiver in the space under study. This can be represented as a simple two-dimensional energy-time plot, which can serve as a basis for additional calculations such as reverberation time or other metrics discussed in Chapt. 19. In a more complicated form it includes directional information about each ray as well. An example based on Boston Symphony Hall is shown in Fig. 22.22. The y axis of the vertical distribution is based on the terms under the integral in the Paris equation where the probability of a ray coming from a given direction, $P(\theta)$, has replaced the diffuse-field probability, $\sin \theta$. Impulse response data can be obtained from scale model measurements as well as measurements taken in full-sized auditoria. In this manner models can be checked against actual field measurements.

Convolution

When the room response has been determined for a source and receiver location and orientation, the resulting impulse response can be convolved with a dry (anechoic) audio signal to obtain calculated results of playing sound in the room, a process called auralization. The theory is based on the Duhamel or convolution integral, which was discussed in Chapt. 11. For a linear system there is a transfer function that yields the system output for a given input (stimulus).

$$y(t) = \int_0^{t_p} f(\tau)\, h(t - \tau)\, d\tau \tag{22.56}$$

where $y(t)$ = output response of the room
$h(t - \tau)$ = impulse response of the room
$f(\tau)$ = forcing (input) function of the system
t_p = time period of interest

FIGURE 22.22   Directional Ray Arrival Distribution for a Model of Boston Symphony Hall (Nishihara et al., 2001)

The source position is 3 m from the edge of the stage on centerline and 1.5 m high. The receiver is near the center of the main floor but shifted to the side by a few meters.
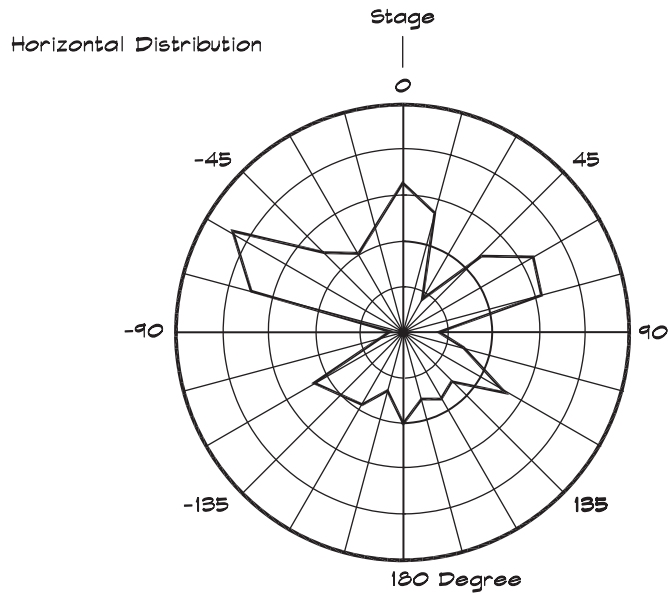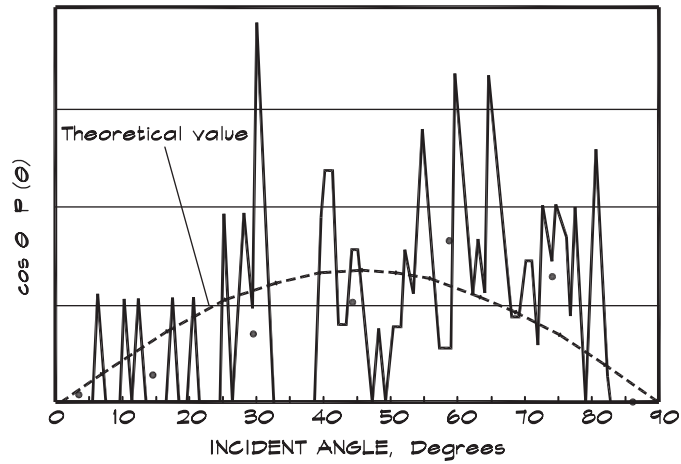
When the forcing function is a delta function, the system output is its impulse response

$$y(t) = \int_0^{t_p} \delta(\tau)\ h(t-\tau)\, d\tau = h(t) \tag{22.57}$$

Once the system response to a unit impulse (delta function) is known then the response to an arbitrary stimulus can be calculated.

FIGURE 22.23 Example of a Convolution Integral (Cheever, 2000)
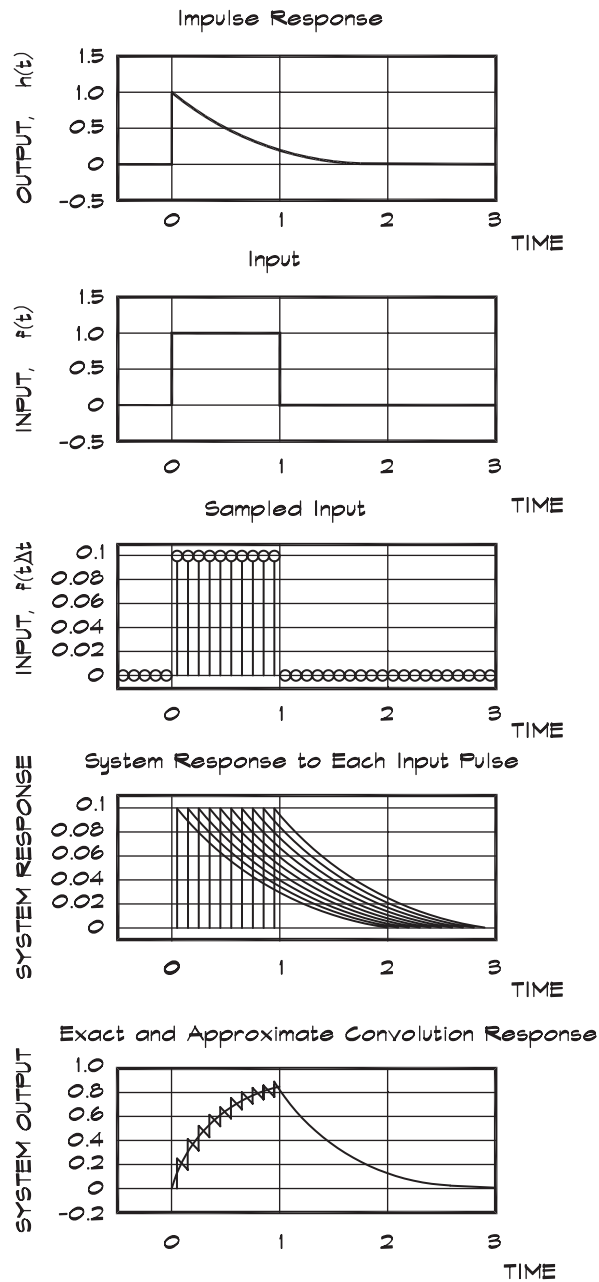
We can take an example by assuming that a room can be characterized by an impulse response

$$h(t) = e^{-t/\tau_0} \tag{22.58}$$

where τ_0 = characteristic decay time. For an arbitrary value of $\tau_0 = 0.5$ s, we can calculate the system behavior for $h(t) = e^{-2t}$ and a square-wave input. Figure 22.23 shows a plot

of this system's behavior with time. The overall response is obtained from a summation of the responses from individual impulses. In practice the convolution of the signal with the room impulse function is done digitally by a series of multiply and add functions in a computer. The result in this simple example yields the room response on onset of the stimulus

$$I(t) = I_0 \ (1 - e^{-t/\tau_0}) \tag{22.59}$$

and decay after its removal

$$I(t) = I_0 \ e^{-t/\tau_0} \tag{22.60}$$

The information contained in the output of the ray tracer is not only the energy-time behavior for the space, but also the direction of the incoming reflections. A receiver is characterized by a hedgehog of rays representing specular or diffuse reflections from a scattering surface. For every ray arriving at the listener there is a delay time, a frequency-related attenuation, and a direction to be applied to the original signal.

Directional Sound Perception

The recreation of a three-dimensional sound field relies on our ability to fool the listener into believing that the sound origination point is where we desire it to be. Accordingly we must examine the directional cues that furnish us with the information necessary to determine direction.

Rayleigh (1896) proposed a duplex theory for the perception of azimuthal sound direction. Two components were involved, the interaural time difference (ITD) and the interaural level difference (ILD) between the two ears. The ITD has a geometrical explanation, which is most simply understood by assuming a spherical shape to the head shown in Fig. 22.24.

The ITD can be calculated using this geometry for plane waves (Woodworth et al., 1954)

$$ITD = \frac{a}{c_0} \ (\theta + \sin\theta), \quad -\pi/2 \le \theta \le \pi/2 \tag{22.61}$$

FIGURE 22.24   Geometry of the Head for Azimuthal Direction Cues
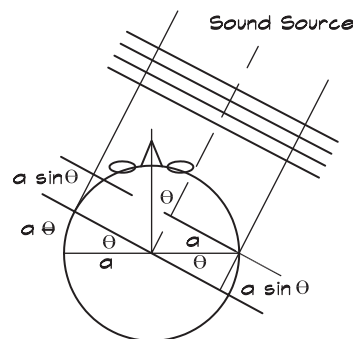
When the angle of incidence is zero—that is, when the source is in the medial plane of the listener—the IDT is zero. When the source is to the side, the value of the IDT has a maximum value

$$\text{ITD}_{\text{max}} = \frac{a}{c_0} \left(\pi / 2 + 1 \right) \tag{22.62}$$

The measured value for a typical subject is around 0.7 ms. At high frequencies, above about 1.5 kHz, there is an aliasing problem in determining the time delay. Using the level difference resolves the ambiguity.

   The second part of Raleigh's theory is due to the diffraction of the sound by the head, which reduces the sound level at the ear on the shielded side. Following the geometry in Fig. 22.24, the path-length difference for parallel sound incidence is (Blauert, 1983)

$$\Delta r = a \, \theta \tag{22.63}$$

and for a point source near the head assuming one unshielded ear

$$\Delta r = a \left[\left(n + \frac{1}{2} \right) \cos \varepsilon + \frac{1}{2} \left(\theta + \varepsilon \right) \right. $$
$$\left. - \sqrt{n^2 + n + \frac{1}{2} - \left(n + \frac{1}{2} \right) \sin \theta} \right] \tag{22.64}$$

where $n = \dfrac{r - a/2}{a}$ and $\varepsilon = \arcsin (a/2r) = \arcsin \left(\dfrac{1}{1 + 2n} \right)$.

   The shielding is then calculated using Eq. 5.11. At high frequencies the shielding may be as much as 20 dB; at low frequencies there is little level change and we rely on the time difference.

   Elevation cues come from reflections from the pinna or outer ear (CIPIC, 2001). The frequency response of the ear is directional as shown in Fig. 22.25. The cues to an overhead source stem from the fact that the pinna acts like a focusing device whose frequency response is directionally dependent. The reflection from the pinna produces a second path to the ear canal and the possibility of destructive interference. The greatest effect occurs at the half-wavelength path difference, which produces a pinna notch in the 6 to 16 kHz range. Both the notch frequency and depth change with source elevation, the depth being much more pronounced for sounds coming from the front.

   The perception of range is less well understood (CIPIC, 2001). It is influenced by the level of the direct sound, motion parallax, the direct-to-reverberant ratio in enclosed spaces and for sources quite close to the ear, a high degree of ILD. Motion parallax is the change in the azimuthal angle as the receiver moves, which is range dependent. The direct-to-reverberant ratio varies with the distance between the source and receiver.

Directional Reproduction

The simplest directional reproduction is accomplished by locating a loudspeaker at the desired source position or, short of that, in the source direction. This is a commonly employed

FIGURE 22.25 Elevation Cues from Pinna Reflections (CIPIC, 2001)
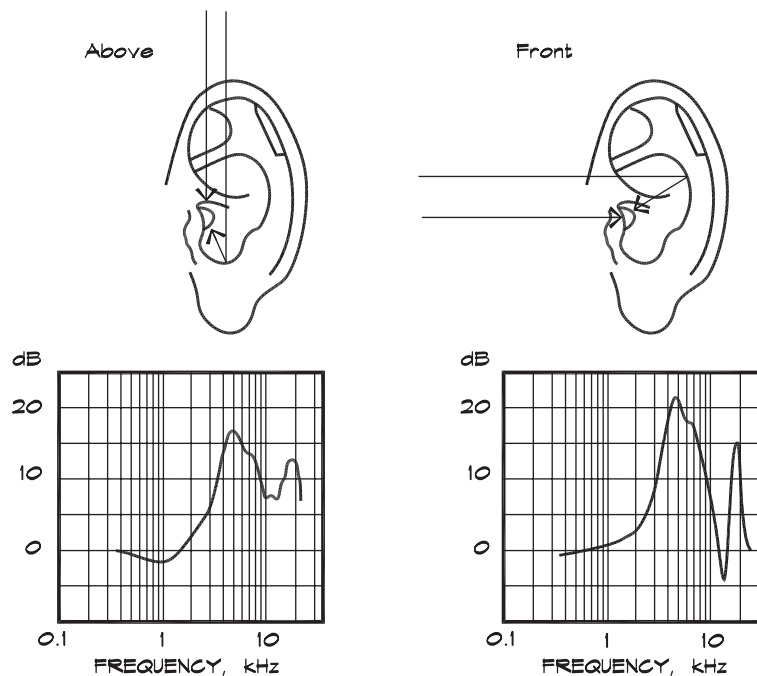
technique in theme park audio design where effects or dialog loudspeakers are located in props or set pieces constructed of perforated metal or other transondent materials. If there is more than one loudspeaker such as a central cluster with additional overhead loudspeakers, the earliest arrival time determines the perceived direction.

Stereo loudspeakers are the most commonly encountered reproduction configuration. In stereo reproduction, a phantom image can be positioned between the loudspeakers by panning or adjusting the volume of the signal sent to each one. There is a relatively small area near the centerline between the loudspeakers where an accurate stereo image is perceived. In careful recordings a sense of depth as well as width is apparent. Multichannel surround sound systems feature a series of loudspeakers in the azimuthal plane, which can act as groups of stereo pairs so that the apparent source direction can be set by panning between them.

Headphones can also be used to reproduce a stereo signal although most listeners prefer loudspeakers. Headphones interact with the pinna and alter the spatial relationships so elevation effects are not reliably reproduced (CIPIC, 2001). In a special case known as binaural recording, microphones are placed in the ear canals of a specially fitted mannequin so the listener is presented, through headphones, with the sound "heard" by the mannequin. The effect of binaural recording is startlingly real for certain source positions, mainly behind and to the side of the listener. Sources in front are difficult to localize and appear closer than they actually are. In many cases, frontal sounds appear to be located inside the listener's head.

Binaural sound can also be delivered to the listener from loudspeakers using a technique called cross-talk-canceled stereo. To do this we need to measure the effect the head has on sound coming from a given direction. Figure 22.26 illustrates the basic geometry. We measure the impulse response, h(t), of each ear for a given source position. This is called

FIGURE 22.26   Head-Related-Transfer-Function Measurements (CIPIC, 2001)

$$X_L(t) = \int h_L(\tau) \times (t-\tau) \, d\tau \qquad X_R(t) = \int h_R(\tau) \times (t-\tau) \, d\tau$$
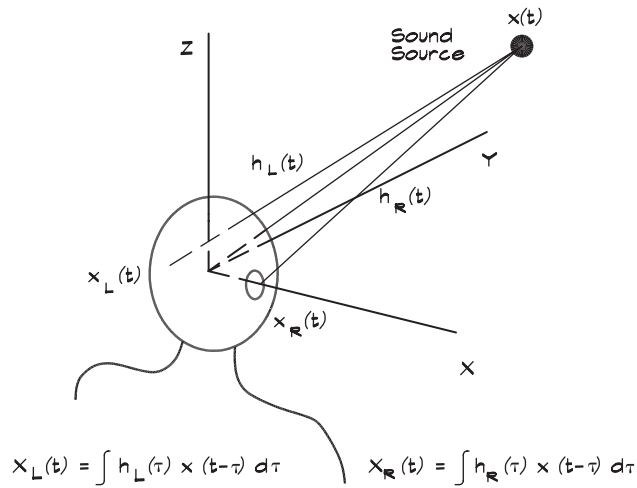
the Head-Related-Impulse-Response (HRIR) and its Fourier transform, H(f), is the Head-Related-Transfer-Function (HRTF). Once the HRTF is known for each ear we can reproduce a binaural signal from a monaural signal.

The HRTF are pairs of equalization curves (one for each ear) for every position in space. To simplify the measurement the source is positioned in the far field so the functional dependence reduces to azimuth, elevation, and frequency. Another approach is to model the HRTF based on the geometrical considerations previously discussed. A few examples are given in Fig. 22.27 and others are available online at CIPIC.com. These can be convolved with a dry signal using a special processor and presented to the listener by means of headphones or loudspeakers. Some systems also include a head tracker to account for the motion of the listener's head, to provide additional realism to the experience.

The recreation of three-dimensional cues from stereo loudspeakers, suggested by Schroeder and Atal (1963), is illustrated in Fig. 22.28. Ideally we want the left loudspeaker to deliver its signal only to the left ear and the right loudspeaker to the right ear. When a pair of loudspeakers is used, each source will deliver signal to both ears. Expressed mathematically the signal Y_1 reaching the left ear is a mixture of the pure signal S_1 and the crosstalk from S_2. In terms of the transfer functions

$$Y_1 = H_{11} \, S_1 + H_{12} \, S_2 \tag{22.65}$$

where H_{11} = HRTF between the left loudspeaker and the left ear
$\quad\quad\;\; H_{12}$ = HRTF between the right loudspeaker and the left ear
and for the right ear

$$Y_2 = H_{21} \, S_1 + H_{22} \, S_2 \tag{22.66}$$

In matrix form the signals are

$$\begin{bmatrix} Y_1 \\ Y_2 \end{bmatrix} = \begin{bmatrix} H_{11} & H_{12} \\ H_{21} & H_{22} \end{bmatrix} \begin{bmatrix} S_1 \\ S_2 \end{bmatrix} \tag{22.67}$$

FIGURE 22.27   Selected Head Related Transfer Functions (CIPIC, 2001)

Azimuthal Angle = 0°

Azimuthal Angle = 30°

Azimuthal Angle = 90°

Azimuthal Angle = 0° – Elevation Angle = 40°
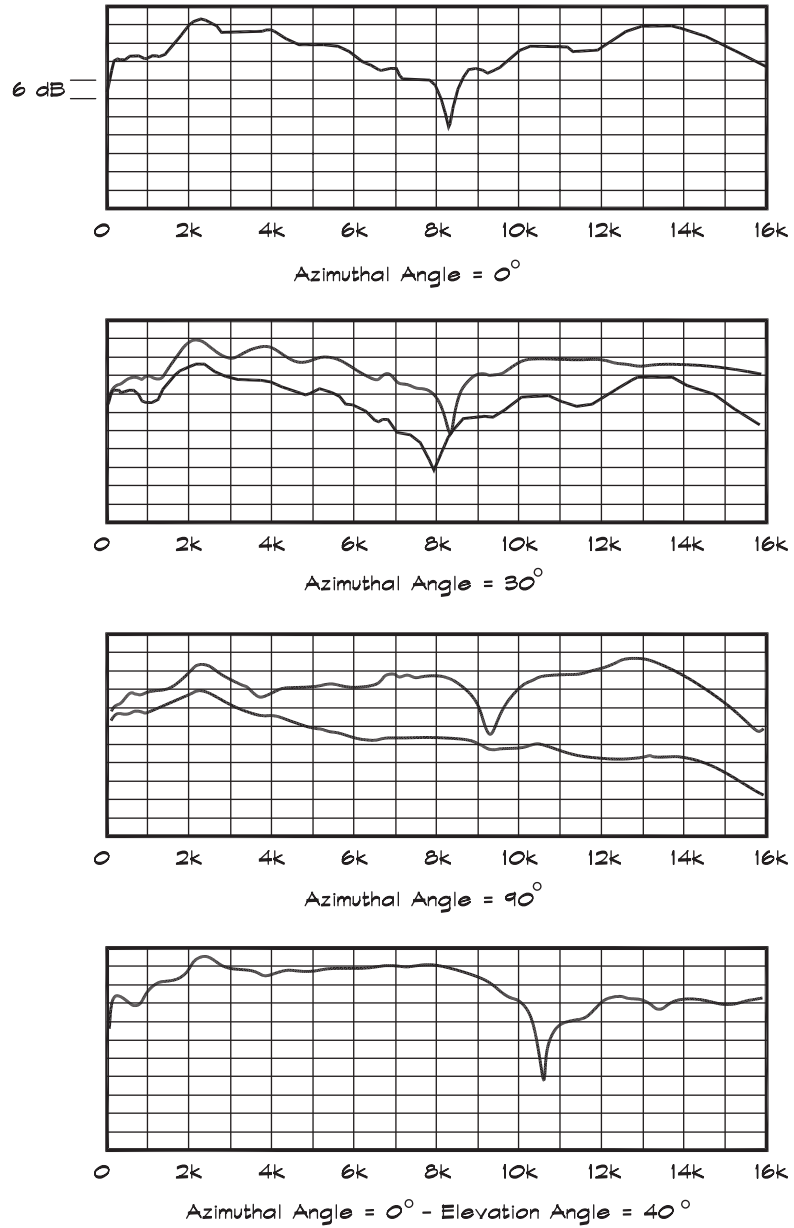
FIGURE 22.28 Binaural Reproduction Using Stereo Loudspeakers (Schroeder and Atal, 1963)
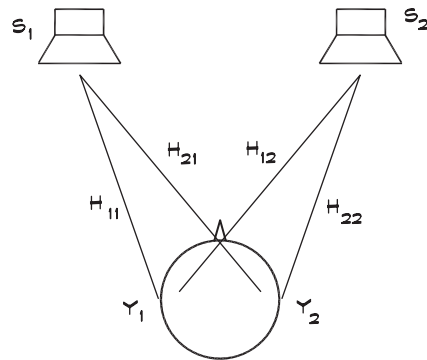
To find the proper signals we must invert the matrix

$$\begin{bmatrix} S_1 \\ S_2 \end{bmatrix} = \begin{bmatrix} H_{11} & H_{12} \\ H_{21} & H_{22} \end{bmatrix}^{-1} \begin{bmatrix} Y_1 \\ Y_2 \end{bmatrix} \tag{22.68}$$

which is not trivial. As the source receiver distance increases the impulse response becomes quite long. The signals are unique to the source and listener position. In practice if the listener turns his head by more than about 10° to 15°, the effect is lost.

REFERENCES

Abby Road Studios (2002). Private communication, plan reproduced with permission, 2002.

Adams, (2002). Dave L. Adams, "Firelight Lodge Sound Tests," (DLAA Project 6459). Denver, CO: Dave L. Adams Associates, 2002.

Alexandrovich (1987). George Alexandrovich, "Disk Recording and Playback," Handbook for Sound Engineers, The New Audio Cyclopedia, Glen Ballou, ed. © 1987 Indianapolis, IN: Howard W. Sams

Algazi et al. (2001). V.R. Algzi, R.O. Duda, D.M. Thompson, and C. Avendano, "The CIPIC HRTF Database." Proc. 2001 IEEE Workshop on Applications of Signal Processing to Audio and Electroacoustics, pp. 99–102.", New Paltz, NY: Mohonk Mountain House, Oct. 2001.

Allen (1974). D.L. Allen, "Vibrational Behaviour of Long-Span Floor Slabs." Canada: J. Civ. Eng., vol. 1, no. 1, 1974.

Allen (1997). D. Allen. Private Communication, 1997.

Allen (1976). D.E. Allen and J.H. Rainer, "Vibration Criteria for Long-Span Floors," Canada: Canadian Journal of Civil Engineering, vol. 3, no. 2, June 1976.

Allen (1975). D.L. Allen and John C. Swallow, "Annoying Floor Vibrations—Diagnosis and Therapy." Bay Village, OH: Sound and Vibration Magazine, 1975.

Anderson, et al. (1973). G.S. Anderson, L.N. Miller, and J.R. Shadley, "Fundamentals and Abatement of Highway Traffic Noise." Office of Environmental Policy, Federal Highway Administration, U.S. Department of Transportation, Bolt Beranek & Newman, June 1973.

Ando (1985). Y. Ando, Concert Hall Acoustics. New York, NY: Springer-Verlag, 1985.

Andree (1932). C.A. Andree, "The Effect of Position on the Absorption of Materials for the Case of a Cubical Room." from J. Acoust. Soc. Am. 3: 535–551, © 1932, Acoustical Society of America: Melville, NY.

ANSI (1971). ANSI S1.4, American National Standard Specification for Sound Level Meters. New York, NY: American National Standards Institute, 1971.

ANSI (1969). Excerpted from ANSI S3.5-1969 American National Standard Methods for the Calculation of the Articulation Index, © ANSI. This Standard has been withdrawn and replaced by, ANSI S3.5-1997 American National Standard Methods for Calculation of the Speech Intelligibility Index, which is available from the Acoustical Society of America, 3 Pinelawn Road, Suite 114E, Melville, NY 11747 <http://asa.aip.org>.

ANSI (1997). ANSI S3.5, Adapted from "ANSI S3.5-1997 American National Standard Methods for Calculation of the Speech Intelligibility Index." © 1998, with the permission of the Acoustical Society of America, 35 Pinelawn Road, Suite 114E, Melville, NY 11747.

ANSI (2002). ANSI S12.60, American National Standard Acoustical Performance Criteria, Design Requirements, and Guidlines for Schools, © 2002, with the permission of the Acoustical Society of America, 35 Pinelawn Road, Suite 114E, Melville, NY 11747

ASHRAE (1980). ASHRAE Handbook & Product Directory 1980 Systems. © 1980 Atlanta, GA: American Society of Heating, Refrigerating and Air-Conditioning Engineers, Inc., www.ashrae.org.

ASHRAE (1987). 1987 ASHRAE Handbook - HVAC Systems and Applications. © Atlanta, GA: American Society of Heating, Refrigerating and Air-Conditioning Engineers, www.ashrae.org.

ASHRAE (1995). 1995 ASHRAE Handbook, HVAC Applications. © 1995 Atlanta, GA: American Society of Heating, Refrigerating and Air-Conditioning Engineers, Inc., www.ashrae.org.

Askenfeld (1986). A. Askenfeld, "Stage floors and risers–supporting resonant bodies or sound traps?," Acoustics for Choir and Orchestra, Stockholm, Sweden: Royal Academy of Music.

ASTM (1997). E336-97. Standard Recommended Practice for Measurement of Airborne Sound Insulation in Buildings, 1997.

ASTM (1999). E413-87. Standard classification for rating sound insulation, 1999.

ASTM (1997). E1007-97. Standard test method for field measurement of tapping machine impact sound transmission through floor-ceiling assemblies and associated support structures, 1997.

ASTM (1966). Annual Book of ASTM Standards C423, Sound Absorption of Acoustical Materials in Reverberation Rooms. Philadelphia, PA: American Society for Testing and Materials, 1966.

ASTM (1970). Annual Book of ASTM Standards E90, Standard Method for Laboratory Measurement of Airborne Sound Transmission Loss of Building Partitions. Philadelphia, PA: American Society for Testing and Materials, 1970.

ASTM (1971). Annual Book of ASTM Standards E336, Measurement of Airborne Sound Insulation in Buildings. Philadelphia, PA: American Society for Testing and Materials, 1971.

ASTM (1973). Annual Book of ASTM Standards E492, Laboratory Measurement of Impact Sound Transmission Through Floor Ceiling Assemblies Using the Tapping Machine. Philadelphia, PA: American Society for Testing and Materials, 1973.

ASTM (1986). E1110-86. "Standard Classification for Determination of Articulation Class." Philadelphia, PA: American Society for Testing and Materials, 1986.

ASTM (1989). Annual Book of ASTM Standards E989, "Standard Classification for Determining Impact Insulation Class (IIC)." Philadelphia, PA: American Society for Testing and Materials, 1989.

ASTM (2000). E1408-91. Standard test method for laboratory measurement of the sound transmission loss of door panels and door systems, 2000.

Bagenal (1930). Hope Bagenal, "Bach's Music and Church Acoustics," Journal of the Royal Institute of British Architects 37, no. 5, Jan. 1930.

Bagenal (1931). H. Bagenal and A. Wood, Planning for Good Acoustics. Methuen, London, 1931.

Baker (1970). Optica Acta 18, (2) (1971). Special Issue of Image Evaluation by Means of Optical Transfer Functions, 1970.

Ballou (1987). Glen Ballou, ed. Handbook for Sound Engineers, The New Audio Cyclopedia. Indianapolis, IN: Howard W. Sams, 1987.

Barron (1988). M. Barron, "Subjective study of British symphony concert halls." Acustica. 66, 1988.

Barron (1993). M. Barron, "The acoustic survey of British auditoria." Reprinted with permission from J. Acoust. Soc. Am. 93, 2265 (A). © 1993, Acoustical Society of America: Melville, NY.

Barron (1995). M. Barron, "Balconies in Concert Halls." Trondheim, Norway: 15th International Congress on Acoustics, June, 1995.

Barron (1993). Michael Barron, Auditorium Acoustics and Architectural Design. London: Spon Press. Routledge, reprinted 1998.

Barron (1988). M. Barron and L.J. Lee, "Energy Relations in Concert Auditoria. I." Reprinted with permission from J. Acoust. Soc. Am., 84. © 1988, Acoustical Society of America: Melville, NY.

Barry (1978). T.M. Barry and J.A. Reagan, FHWA Highway Noise Prediction Model. U.S. Department of Transportation, Report No. FHWA-RD-77-108, 1978.

Benedetto (1985). , Giuliana Benedetto and Renato Spagnolo, "Reverberation time in enclosures: The surface reflection law and the dependence of the absorption coefficient on the angle of incidence." Reprinted with permission from J. Acoust. Soc. Am., 77(4), © 1985, Acoustical Society of America: Melville, NY.

Beranek (1947). L.L. Beranek, "The design of speech communication systems." Proceedings of the Institute of Radio Engineers, vol. 35, 1947.

Beranek (1949). L.L. Beranek, Acoustic Measurements. New York, NY: John Wiley & Sons, 1949.

Beranek (1954). Leo L. Beranek, Acoustics. New York, NY: McGraw-Hill. Reprinted (1954) New York, NY: American Institute of Physics. Courtesy Leo L. Beranek.

Beranek (1957). Leo L. Beranek, "Revised criteria for noise in buildings." Noise Control, Jan. 1957.

Beranek (1962). Leo L. Beranek, Music, Acoustics & Architecture. Original Edition, Cambridge, MA: Courtesy Leo L. Beranek, 1962.

Beranek (1971). L.L Beranek, ed., Noise and Vibration Control. Cambridge, MA: Courtesy Leo L. Beranek, 1971.

Beranek (1979) (Original Edition 1962). Leo L. Beranek, Music, Acoustics & Architecture. Cambridge, MA: Courtesy Leo L. Beranek, 1979.

Beranek (1989). Leo L. Beranek, "Balanced noise-criterion (NCB) curves." Reprinted with permission from J. Acoust. Soc. Am. vol. 86, No. 2, © 1986, Acoustical Society of America: Melville, NY, Aug. 1989.

Beranek (1992). Leo L. Beranek, "Concert Hall Acoustics." Reprinted with permission from J. Acoust. Soc. Am. vol. 92, No. 1, © 1992, Acoustical Society of America: Melville, NY, July 1992.

Beranek (1994). L.L. Beranek, "The acoustical design of concert halls." Reprinted with permission from J. Acoust. Soc. Am., 1(1), © 1994, Acoustical Society of America: Melville, NY.

Beranek (1996). Leo Beranek, How They Sound, Concert and Opera Halls. © 1996, Woodbury, NY: Acoustical Society of America.

Beranek (1998). Leo L. Beranek and Takayuki Hidaka, "Sound absorption in concert halls by seats, occupied and unoccupied, and by the hall's interior surfaces." Reprinted with permission from J. Acoust. Soc. Am., vol. 104, no. 6. © 1998, Acoustical Society of America: Melville, NY, Dec. 1998.

Beranek (1946). Leo L. Beranek and Harvey P. Sleeper, "The Design and Construction of Anechoic Sound Chambers," J. Acoust. Soc. Am., vol. 18, no. 1, pp. 140–150. © 1998, Acoustical Society of America: Melville, NY.

Beranek (1992). Leo L. Beranek and István L. Vér, Noise and Vibration Control Engineering Principles and Applications. © 1992, New York, NY: this material is used by permission of John Wiley & Sons, Inc.

Berkow (2001). Sam Berkow, Private communication, 2001.

Berlin (1985). E.P. Berlin, Jr., "Efficiency Considerations in Image Synthesis," Siggraph Course Notes, vol. 11, July 1985.

Biering (1983). H. Biering and O.Z. Pedersen, Technical Review, No. 1. System Analysis and Time Delay Spectrometry (Part 1). Marlborough, MA: Bruel & Kjaer Instruments, 1983.

Bistafa (2000). Sylvio R. Bistafa and John S. Bradley. "Reverberation time and maximum background-noise level for classrooms from a comparative study of speech intelligibility metrics." J. Acoust. Soc. Am., vol. 107, no. 2, © 2000, Acoustical Society of America: Melville, NY, Feb. 2000.

Bistafa (2000). Sylvio R. Bistafa and John S. Bradley, "Revisiting Algorihms for Predicing the Articulation Loss of Consonants Al_{cons}," Journal of the Audio Engineering Society, vol. 48, No. 6, Fig. 2, p. 537, and Figure 4, p. 539. New York, NY: Audio Engineering Society, June 2000.

Blauert (1983). Jens Blauert, Spatial Hearing, The Psychophysics of Human Sound Localization. Cambridge, MA: The MIT Press, 1983.

Blazier (1980). W.E. Blazier, Jr., "Revised Noise Criteria for Application in the Acoustical Design and Rating of HVAC Systems," Noise Control Engineering Journal, 16, 64–73.

Blazier (1981). W.E. Blazier, Jr., ed, "Noise Rating of Variable Air-Volume Terminal Devices." ASHRAE Transactions 87(1), Pt. 1, 1981.

Blazier (1994). Warren E. Blazier and Russell B. DuPree, "Investigation of low-frequency footfall noise in wood-frame, multifamily building construction." Reprinted with permission from J. Acoust. Soc. Am., vol. 96, no. 3, © 1994, Acoustical Society of America: Melville, NY, Sept. 1994.

Bolt (1946). R.H. Bolt, "Note on Normal Frequency Statistics for Rectangular Rooms." Reprinted with permission from J. Acoust. Soc. Am., Vol. XIX, no. 1, p. 130, © 1946, Acoustical Society of America: Melville, NY, July 1946.

Bradley (1986). J.S. Bradley, "Predictors of speech intelligibility in rooms." Reprinted with permission from J. Acoust. Soc. Am., 80(3), © 1986, Acoustical Society of America: Melville, NY, Sept. 1986.

Bradley (1991). J.S. Bradley, "A comparison of three classical concert halls." Reprinted with permission from J. Acoust. Soc. Am., 89, No. 3, © Mar. 1991, Acoustical Society of America: Melville, NY, Mar. 1991.

Bradley (1991). J.S. Bradley, "Some further investigations of the seat dip effect." Reprinted with permission from J. Acoust. Soc. Am., 90, © 1991, Acoustical Society of America: Melville, NY.

Bradley (1997). J.S. Bradley, "Sound Absorption of Gypsum Board Cavity Walls." New York, NY: Journal of the Audio Engineering Society, vol. 45, No. 4, Figure 1, p. 255. New York, NY: Audio Engineering Society, Apr. 1997.

Bradley (1998). J.S. Bradley, "Relationships amoung measures of speech intelligibility in rooms." Journal of the Audio Engineering Society, vol. 46. New York, NY: Audio Engineering Society, 1998.

Breton (1989). Gaelle Breton, Theaters. New York, NY: Princeton Architectural Press, Paris, France: Editions du Moniteur, 1989.

Bronsdon (1999). R.L. Bronsdon and H. Forschner, "A Propagation Model Based on Gaussian Beams that Account for Wind and Temperature Inversions," J. Noise Control Eng, 47(5) Sept.-Oct., 1999.

Brüel and Kjaer (1974). Instructions and Applications, 1974. "One-Inch Condenser Microphone Types 4144, 4545, 4146, 4161." Norcross, GA: Brüel and Kjaer, 1974.

Brüel and Kjaer (1978). Technical Review No. 4, "Reverberation Process at Low Frequencies," by Holger Larsen. Norcross, GA: Bruel and Kjaer.

Brüel and Kjaer (1979). J.R.Hassall and K. Zaveri, Acoustic Noise Measurements. 4th ed. Naerum, Denmark: Brüel & Kjaer Instruments, Jan. 1979.

Brüel and Kjaer (1986). Instruction Manual, Modular Precision Sound Level Meter, "Modular Precision Sound Level Meter Type 2231 plus Integrating SLM Module BZ 7100." Norcross, GA: Brüel and Kjaer, Feb. 1986.

Burkat (1998). Jacket notes from a classical CD.

Burris-Meyer (1975). Harold Burris-Meyer and Edward C. Cole, Theatres and Auditoriums. Huntington, NY: Robert E. Krieger Publishing Co., 1975.

Burroughs (1974). Lou Burroughs, Microphones: Design and Application, First Edition. Champaign, IL: Sagamore Publishing Co, 1974.

Cahill (1995). Thomas Cahill, How the Irish Saved Civilization: The Untold Story of Ireland's Heroic Role from the Fall of Rome to the Rise of Medieval Europe (Hinges of History, vol. 1) Anchor, 1995.

California Heat Pump (1982). Water Source Heat Pumps, CHP-A-059-82. Santa Monica, CA: California Heat Pump Co, 1982.

California, State of (1974). "California Noise Insulation Standards," California Administrative Code, Title 25, Chapter 1, Subchapter 1. © 1974 by The Bureau of National Affairs.

California, State of (1990). California Noise Insulation Standards, State Building Code (Part 2, Title 24, CCR), Appendix Chapter 35, Sound Transmission Control, 1990.

California, State of (1981). Office of Noise Control, Catalog of STC and IIC Ratings for Wall and Floor/Ceiling Assemblies. Berkeley, CA: Dept. of Health Services. Office of Noise Control, 1981.

Chanaud (1983). Robert C. Chanaud, Sound Conditioning Manual for Facilities Managers, Architects, & Design Professionals. Norcross, GA: Dyna-systems, 1983.

Chanaud (2000). Robert C. Chanaud, Private communication, 2000.

Chanaud (2002). Robert C. Chanaud. Sound Conditioning Manual, Designing Good Acoustics into the Office. Dynasound, Inc, 2002.

Cheever (2000). E. Cheever, Swarthmore College Internet. Swarthmore, PA, 2000.

Chu (2002). W.T. Chu and A.C.C. Warnock, IRC Research Report 104, "Detailed Directivity of Sound Fields around Human Talkers." Ontario, Canada: National Research Council Canada, Dec. 2002.

CIPIC (2001). "Spatial Sound: An Introduction." Center for Image Processing and Integrated Computing (CIPIC), University of California, Davis Interface Laboratory. http://interface.cipic.ucdavis.edu/CIL_tutorial/3D_psych/elev.htm, 2001.

Clark (1983). David Clark, "Measuring Audible Effects of Time Delays in Listening Rooms." AES, 74th Convention, New York, NY: AES, Oct. 1983.

Colloms (1980). Martin Colloms, High Performance Loudspeakers. © 1980, New York, NY: this material is used by permission of John Wiley & Sons, Inc.

Community (1991). Todd Rockwell, "To Smooth or Not to Smooth," Community Data Library, Volume One. Chester, PA: Community Professional Loudspeakers:

CONC (1981). California of STC and IIC Ratings for Wall and Floor/Ceiling Assemblies, Office of Noise Control, California Dept. of Health Services, 1981.

Craik (1996). R.J.M. Craik, Sound Transmission Through Buildings Using Statistical Energy Analysis. United Kingdom: Gower, Aldershot, 1996.

Craik et al. (1997). R.J.M. Craik, T.R.T. Nightingale and J.A. Steel, "Sound transmission through a double leaf partition with edge flanking." Reprinted with permission from National Research Council of Canada, Ontario, Canada and J. Acoust. Soc. Am., 101(2). © 1997, Acoustical Society of America: Melville, NY, Feb. 1997.

Cremer (1942). Theorie der Schalldämmung dünner Wände bei Schrägen einfall. Akust. Ztg, 1942.

Cremer (1952). L. Cremer, "Theorie des Klopfshalles bei Decken mit Schwimmenden Estrick." Acustica, 2, 1952.

Cremer et al. (1973). L. Cremer, M. Heckl, and E.E Ungar, Structure-Borne Sound, p. 244, Fig. IV/2 and p. 302, Fig. IV/20. © 1973, Berlin ·Heidelberg: Springer-Verlag.

Cremer (1982). Lothar Cremer and Helmut A. Müller, Principles and Applications of Room Acoustics, vol. 1. English translation with additions by T.J. Schultz, New York, NY: New York, NY: Applied Science Publishers, 1982.

Cremer (1982). Lothar Cremer and Helmut A. Müller, Principles and Applications of Room Acoustics, vol. 2. New York, NY: Applied Science Publishers, 1982.

Crown (1993). Macro-Tech 5000VZ Professional Power Amplifier Owner's Manual. © 1993, Elkhart, IN: Crown International.

Crown (1995) Micro-Tech 600/1200/2400 Professional Power Amplifiers Owner's Manual. © 1995, Elkhart, IN: Crown International.

D'Antonio (1987). Peter D'Antonio, Expand Your Acoustical Palette with the RPG Diffusor System. RPG brochure, © 1987. Marlboro, MD: RPG Diffusor Systems, Inc.

D'Antonio (1995). P. D'Antonio, "Two Decades of Diffusor Design and Development," 99th AES Convention, Invited Lecture, Preprint 4114 (P-1), New York, NY: Audio Engineering Society, Oct. 1995.

Davis (1926). A.H. Davis, Phys. Soc. Proc. 38, 1926.

Davis (1979). C. Davis and D. Davis. "(LEDE^{TM}) Live End-Dead End Control Room Acoustics . . . (TDS) Time Delay Spectrometry . . . (PZM^{TM}) Pressure Zone Microphones," Record./Eng. Prod, 1979.

Davis (1957). D.D. Davis, Jr. "Acoustical Filters and Mufflers," in C.M. Harris (ed.), Handbook of Noise Control, Chap. 21, McGraw-Hill, 1957.

Davis (1969). D. Davis, "Analyzing Loudspeaker Locations for Sound Reinforcement Systems." Journal of the Audio Engineering Society, vol. 17. New York, NY: Audio Engineering Society, Dec. 1969.

Davis (1978). Don Davis and Carolyn Davis. Sound System Engineering.First Edition, Fourth Printing, Indianapolis, IN: Howard W. Sams, 1978.

Davis (1987). Don Davis and Carolyn Davis, Sound System Engineering. 2nd ed. Indianapolis, IN: Howard W. Sams, 1987.

Davis et al. (1954). D.D. Davis, G.M. Stokes, D. Moore, and G.L. Stevens, "Theoretical and Experimental Investigation of Mufflers with Comments on Engine-Exhaust Muffler Design," Nat. Advis. Comm. Aeronaut. Rep. 1192, Washington, D.C, 1954.

de Boer (1940a). K. de Boer, Stereofonische Geluidsweergave (Stereophonic sound reproduction). Dissertation, Institute of Technology, Delf, 1940.

de Boer (1940b). K. de Boer, Plastische Klangwiedergabe (Three-dimensional sound reproduction). Philips Tech. Rev. 5, 1940.

Delany (1969). M.E. Delany and E.N. Bazley, "Acoustical properties of fibrous absorbent materials." Applied Acoustics, 3, 1969.

Delsasso (1967). Leo Delsasso, Private Communication, 1967.

DeVac Corp. (1997). "DeVAC: Master Sound Test Loss Recap Chart, 1-97." Carmichael, CA: DeVAC of California, 1997.

Dimarogonas (1990). A.D. Dimarogonas, "The Origins of Vibration Theory." Journal of Sound and Vibration, 140(2). New York, NY: Academic Press Limited, 1990.

Doelle (1972). Leslie L. Doelle, Environmental Acoustics. © 1972, New York, NY: Reprinted with permission from McGraw-Hill Book Company.

Dunlavy (2001). Internet www.soundstage.com/rev.equip/dunlavy_sciva.htm, 2001.

Egan (1988). M. David Egan, Architectural Acoustics. © 1988, New York, NY: Reprinted with permission from McGraw-Hill Book Company.

Electrovoice (1970). D.B. (Don) Keele, Jr., John Gilliom, and Ray Newman, ca. 1973, see also prosoundweb.com Jim Long interview 2004.

EPA (1974). Information on Levels of Environmental Noise Requisite to Protect Public Health and Welfare with an Adequate Margin of Safety, 550/9-74-004. Washington, D.C.: U.S. Environmental Protection Agency, Office of Noise Abatement and Control, March 1974.

Evans (1972). L.B. Evans, H.E. Bass, and L.C. Sutherland, "Atmospheric Absorption of Sound: Theoretical Predictions," J. Acoust. Soc. Am. 51 © 1972,: Melville, NY, Acoustical Society of America.

Everest (1994). F. Alton Everest, The Master Handbook of Acoustics. 3rd ed. © 1994, New York, NY: Reprinted with permission from McGraw-Hill Book Company.

Eyring (1930). Carl F. Eyring, "Reverberation Time in 'Dead' Rooms." Reprinted with permission from J. Acoust. Soc. Am. © 1930, Acoustical Society of America: Melville, NY, Jan. 1930.

Fahy (1985). Frank Fahy, Sound and Structural Vibration, Radiation, Transmission and Response. London, England: Academic Press an imprint of Elsevier Science, 1985.

Farina (2000). Angelo Farina, "Measurement of the surface scattering coefficient: comparison of the Mommertz/Vorlander approach with the new Wave Field Synthesis method." Liverpool (GB): International Symposium on Surface Diffusion in Room Acoustics, 16 April 2000.

Farina (2000). Angelo Farina, "Validation of the numerical simulation of the scattered sound field with a geometrical pyramid tracing approach." Liverpool (GB): ACOUSTICS 2000 IOA Conference, 17–18 April 2000.

Farina (2002). Angelo Farina, "Verification of the Accuracy of the Pyramid Tracing Algorithm by Comparison with Experimental Measurements of Objective Acoustic Parameters." Trondheim, Norway, ICA95 (International Conference on Acoustics), 26–30 June 1995.

Feynman (1989). Richard Feynman, Robert B. Leighton, and Matthew L. Sands, The Feynman Lectures on Physics: Commemorative Issue, Vol. 1, © 1989 California Institute of Technology, Reading, MA: Addison-Wesley Publishing.

Farmer (2001). William Farmer, Private Communication, 2001.

Fierstein (1979). Alan Fierstein, "Optimizing Control Room Reverberation," Recording Engineer/Producer Magazine, Aug. 1979.

Finne (1987). P. Finne, "Beregningsmodel for diffraktion. Akustiske anvendelser af Fresnel-Kirchhoffs approksimation." Msc thesis, The Acoustics Laboratory, Lyngby, 1987.

Flanagan (1972). J.L. Flanagan, Speech Analysis, Synthesis and Perception, 2nd ed. New York, NY: Springer-Verlag, 1972.

Fletcher (1963). Banister Fletcher, A History of Architecture on the Comparative Method. 17th ed. New York, NY: Charles Scribner's Sons, 1963.

Fletcher (1921). Harvey Fletcher, "An empirical theory of telephone quality." AT&T Internal Memorandum, 101(6). Case 211031, Report 21839, Oct 1921. Provo , UT: Brigham Young University, 1921.

Fletcher (1953). Harvey Fletcher, Speech and Hearing in Communication. ed. Jont B. Allen , 1995. Woodbury, NY: Acoustical Society of America: Melville, NY, 1953.

Fletcher (1950). H. Fletcher and R.H. Galt, "The perception of speech and its relation to telephony." Reprinted with permission from J. Acoust. Soc. Am. 22, © 1950, Acoustical Society of America: Melville, NY.

Fletcher (1933). Harvey Fletcher and W.A. Munson, "Loudness, Its Definition, Measurement and Calculation." Reprinted with permission from J. Acoust. Soc. Am. Vol. 5, © 1933, Acoustical Society of America: Melville, NY, Oct. 1933.

Fletcher (1937). Harvey Fletcher and W.A. Munson, "Relation between loudness and masking." J. Acoust. Soc. Am., 9, © 1937, Reprinted with permission from Acoustical Society of America: Melville, NY.

Foreman (1987). Chris Foreman, Handbook for Sound Engineers, The New Audio Cyclopedia edited by Glen Ballou. Indianapolis, IN: Howard W. Sams, 1987.

Forsyth (1985). Michael Forsyth, Buildings for Music. Cambridge, MA: MIT Press, 1985.

Forsyth (1987). Michael Forsyth, Auditoria. © 1987 Michael Forsyth, New York, NY: Van Nostrand Reinhold Co.

Franzoni (2001). Linda P. Franzoni, "A power conservation approach to predict the spatial variation of the cross-sectionally averaged mean-square pressure in reverberant enclosures." Reprinted with permission from J. Acoust. Soc. Am., 110 (6). © 2001, Acoustical Society of America: Melville, NY, Dec. 2001.

Franzoni (1999). Linda P. Franzoni and D.S. Labrozzi, "A study of damping effects on spatial distribution and level of reverberant sound in a rectangular acoustic cavity." J. Acoust. Soc. Am., 106(2). © 1999, Acoustical Society of America: Melville, NY.

French (1947). N.R. French and J.C. Steinberg. "Factors governing the intelligibility of speech sounds." J. Acoust. Soc. Am., 19, 90–119 © 1947, Acoustical Society of America: Melville, NY.

Frenette (2000). Jasmin Frenette, "Reducing Artificial Reverberation Algorithm Requirements Using Time-Variant Feedback Delay Networks," a research project, Dec. 2000, Music Engineering Technology. Coral Gables, FL: University of Miami, 2000.

Fry (1988). Alan Fry (ed.) Noise Control in Building Services. Pergamon Press. Sudbury, Suffolk, UK: Reprinted with permission from Sound Research Laboratories Ltd, 1988.

Funkhouser et al. (1996). Thomas Funkhouser, Ingrid Carlbom, Gary Elko, Gopal Pingalli, Mohan Sondhi, and Jim West, Bell Laboratories, "A Beam Tracing Approach to Acoustic Modeling for Interactive Virtual Environments," http://www.cs.princeton.edu/%7Efunkacoustics.html, 1996.

Gade (1989). A.C. Gade, "Investigations of Musicians' Room Acoustic Conditions in Concert Halls. II: Field Experiments and Synthesis of Results." Acustica, 69, 1989a/b.

Gade (1982). S. Gade, Technical Review, No. 3, Sound Intensity (Theory). Marlborough, MA: Brüel & Kjaer Instruments, 1982.

Garity (1941). Wm. E. Garity and J.N.A. Hawkins, "Fantasound." Journal of the Society of Motion Picture Engineers, Aug. 1941.

Garnier (1880). C. Garnier, Le nouveau Opéra de Paris, 2 vols. Ducher et Cie, Paris, 1876–1880.

Geerdes et al. (1971). H.P. Geerdes, B.G. Watters and P.W. Hirtle, "Sound Isolation for Music Activities." Washington DC: oral paper at 81st meeting of the Acoustical Society of America. Reprinted with permission from J. Acoust. Soc. Am. © 1971, Acoustical Society of America: Melville, NY, 21 April 1971.

Gibbs (1989). B.M. Gibbs and Y. Balilah, "The Measurement of Sound Transmission and Directivity of Holes by an Impulse Method." Reprinted from Journal of Sound and Vibration, Vol. 133(1), pp. 151–162. © 1989, New York, NY: Academic Press Limited with permission from Elsevier Science.

Ginn (1978). K.B. Ginn, Architectural Acoustics. Indianapolis, IN: B & K Instruments, 1978.

Glassner (1989). Andrew S. Glassner, ed., An Introduction to Ray Tracing. San Diego, CA: Academic Press, 1989.

Gordon (1978) J.E. Gordon, Structures. New York, NY & London, England: Plenum Press, 1978.

Graham (1975). J.B. Graham, "Fan Selection and Installation." ASHRAE Symposium Paper as given in ASHRAE, 1987. Atlanta, GA: American Society of Heating, Refrigerating and Air-Conditioning Engineers, June 1975.

Green (1982). David W. Green and Cameron W. Sherry, "Sound transmission loss of gypsum wallboard partitions, Report #1, Unfilled steel stud partitions." Reprinted with permission from J. Acoust. Soc. Am., 71(1), © 1982, Acoustical Society of America: Mellville, NY, Jan. 1982.

Griesinger (1991). David Griesinger, "Improving Room Acoustics Through Time-Variant Synthetic Reverberation," 90th Convention of the AES, Paris, 1991."

Grout (1996). Donald Jay Grout and Claude V. Palisca, A History of Western Music, 5th ed. © 1996, New York, NY: W.W. Norton & Co., Inc., 1996.

Grozier (2002). http://www.grozier.com/scattering.htm, 2002.

Guillen (1995). Michael Guillen, Five Equations that Changed the World: The Power and Poetry of Mathematics. Hyperion. ISBM 078 688 1879.

Gutenberg (1942). B. Gutenberg, "Propagation of Sound Waves in the Atmosphere," J. Acoust. Soc. Am., 14, © 1942, Acoustical Society of America: Melville, NY.

Haan (1995). C. H. Haan and F.R. Fricke. "Musician and music critic responses to concert hall acoustics." Proceedings of 15th International Congress on Acoustics, Trondheim, Norway, June 1995.

Haan (1997). C. Haan and F.R. Fricke. "An evaluation of the importance of surface diffusivity in concert halls," Applied Acoustics, vol. 51, no. 1, 1997.

Haas (1951). Helmut Haas. "The influence of a single echo on the audibility of speech," Journal of the Audio Engineering Society, 20, 2 (1972). (This is an English translation from the German by Dr. Ingr. K.P.R. Ehrenberg of Haas' original paper in Acustica, 1.2 (1951).

Haines (1989). Eric Haines, "Essential Ray Tracing Algorithms." Chapter 2 of An Introduction to Ray Tracing. ed. Andrew S. Glassner. San Diego, CA: Academic Press, 1989.

Haines (2002) Eric Haines, Ray Tracing News (RTNews) web site, 2002.

Halliday (1966). David Halliday and Robert Resnick, Physics Part I. © 1966, New York, NY: this material is used by permission of John Wiley & Sons, Inc.

Hamet (1996). J.F. Hamet, Personal Communication, 1996.

Hamet (1997). J.F. Hamet, INRETS. Cedex, France: unpublished, 1997.

Hanrahan (1989). Pat Hanrahan, "A Survey of Ray-Surface Intersection Algorithms," An Introduction to Ray Tracing. © 1989. San Diego, CA: Academic Press.

Harris (1957). Cyril M. Harris (ed.), Handbook of Noise Control. © 1957, Reprinted with permission from McGraw-Hill Book Company.

Harris (1966). C.M. Harris, "Absorption of Sound in Air versus Humidity and Temperature." Reprinted with permission from J. Acoust. Soc. Am., 40, © 1966, Acoustical Society of America: Melville, NY.

Harris (1991). C.M. Harris, ed., Handbook of Acoustical Measurements and Noise Control. 3rd ed. © 1991, New York, NY: Reprinted with permission from McGraw-Hill Book Company.

Harris (1994). Cyril M. Harris, Noise Control in Buildings, A Practical Guide for Architects and Engineers. © 1994, New York, NY: McGraw-Hill Book Company.

Harris (1961). Cyril M. Harris and Charles E. Crede. Shock & Vibration Handbook. 2nd ed. © 1961, New York, NY: Reprinted with permission from McGraw-Hill Book Company.

Harris (1992). D.A. Harris, "Quiet Lightweight Floor Systems," Bay Village, OH: Sound and Vibration Magazine, July 1992.

Hassall (1979). J.R.Hassall and K. Zaveri, Acoustic Noise Measurements. 4th ed. Naerum, Denmark: Brüel & Kjaer Instruments, Jan. 1979.

Hawkes (1971). R.J. Hawkes and H. Douglas, "Subjective acoustic experience in concert auditoria." Acustica, 24, 1971.

Hayashi et al. (1978). C. Hayashi, S. Kondo, and H. Kodama, "Psychological Assessment of Aircraft Noise Index." Reprinted with permission from J. Acoust. Soc. Am., 63, © 1978, Acoustical Society of America: Melville, NY.

Helmholtz (1877). H.L.F. Helmholtz, Lehre von den Tonempfindungen. Braunschweig: Vieweg.

Hemming (1988). Roy Hemming, Discovering Great Music. New York, NY: Newmarket Press, 1988.

Henricksen (1980). Cliff Henricksen, Technical Letter No. 237, "Directivity Response of Single Direct-Radiator Loudspeakers in Enclosures." Oklahoma City, OK: Altec Lansing Corp. Reprinted with permission from Telex Communications, 1980.

Hessler (1992). George F. Hessler, Jr. and Ben H. Sharp, "Predicting Sound Pressure Levels in the Near and Far Field from Radiating Partitions." Invited Paper. New Orleans, LA: Acoustical Society of America

Conference. Reprinted with permission from Acoustical Society of America: © 1992, Melville, NY, Nov. 1992.

Hill (1990). F.S. Hill, Jr.. Computer Graphics. © 1990, New York, NY: Macmillan Publishing Co.

Hindley (1965). Goeffrey Hindley, Larousse Encyclopedia of Music. Englewood Cliffs, NJ: Prentice Hall, 1965.

Hodgson (1998). M.R. Hodgson, "Experimental evaluation of simplified methods for predicting sound propagation in industrial workrooms," J. Acoust. Soc. Am. 103(4), 1998.

Hoover (1961). R.M. Hoover, "Tree Zones as Barriers for the Control of Noise due to Aircraft Operations," Bolt Beranek and Newman Inc. Rept. 844, February, 1961.

Hopkins (1948). Hopkins and Stryker, "A Proposed Loudness-Efficiency Rating for Loudspeakers and the Determination of System Power Requirements for Enclosures." reprinted from the March 1948 Edition of the Proceedings of the I.R.E., 1948.

Houtgast (1973). T.Houtgast and H.J.M. Steeneken, "The Modulation Transfer Function in Room Acoustics as a Predictor of Speech Intelligibility." Acustica 28, 66–73, 1973.

Houtgast et al. (1980). T. Houtgast and H.J.M. Steeneken, "A Physical Method for Measuring Speech Transmission Quality." Journal of the Audio Engineering Society, vol. 67, no. 1. New York, NY: Audio Engineering Society, 1980.

Houtgast (1983). T. Houtgast and H.J.M. Steeneken, "The Temporal Envelope Spectrum of Speech and it Significance in Room Acoustics." Proceedings of the Eleventh International Congress on Acoustics. vol. 7. GALF, Paris, France, 1983.

Houtgast (1985). T. Houtgast and H.J.M. Steeneken, Technical Review No. 3, The Modulation Transfer Function in Room Acoustics. Marlborough, MA: Brüel & Kjaer Instruments, 1985.

Houtgast (1980). T. Houtgast, H.J.M. Steeneken, and R. Plomp, "Predicting Speech Intelligibility in Rooms from the Modulation Transfer Function." Acustica, 11, 195–200, 1980.

HUD (1979). 24 CFR 51B - Environmental Criteria and Standards, U.S. Department of Housing and Urban Development, 1979.

Hudspeth (1994). A.J. Hudspeth and Vladislav S. Markin, "The Ear's Gears: Mechanoelectrical Transduction by Hair Cells." Reprinted with permission from Physics Today, © 1994, Woodbury, NY: American Institute of Physics.

Hunt (1964). Frederick V. Hunt, "Introduction to Dover Edition," Collected Papers on Acoustics by Wallace Clement Sabine. © 1964, New York, NY: Dover Publications.

Hunt (1978). F.V. Hunt, Origins in Acoustics. New Haven, CT & London, England: Yale University Press, 1978.

IAC Corp. (1989). Engineered Noise Control for Air-Handling Systems, Duct Silencers, Bulletin 1.0301.4, Applications Manual. Bronx, NY: © 1989, Industrial Acoustics Company.

Ingard (1994). K.U. Ingard, Notes on Sound Absorption Technology. ver. 94–2, © 1994, Kittery Point, ME: K.U. Ingard, 1994.

ISO (1999). 3741. "Acoustics: determination of sound power levels of noise sources. Precision methods for reverberation rooms." International Organization for Standardization (ISO), 1999.

ISO (1970). 140/III, Field and Laboratory Measurements of Airborne and Impact Sound Transmission. 3rd printing. Genève, Switzerland: International Organization for Standardization (ISO), 1970.

ISO (1998). ISO 140/IV. "Acoustics: measurement of sound insulation in buildings and of building elements. Part IV: Field measurements of airborne sound insulation between rooms. International Organization for Standardization (ISO), 1998.

ISO (1982, 1996). ISO/R 717. "Acoustics: rating of sound insulation in buildings and of building elements. Part 1: Airborne sound insulation in buildings and of interior building elements. Part 2: Impact sound insulation. Part 3: Airborne sound insulation of facade elements and facades." International Organization for Standardization (ISO), 1982, 1996.

ISO (1988). DIS 7779 (S12), "Acoustic measurement of airborne noise emitted by computer and business equipment." International Organization for Standardization (ISO), 1988.

ISO (1990). DIS 9613-1, "Acoustics - Attenuation of sound during propagation outdoors - Part 1: Method of calculation of the attenuation of sound by atmospheric absorption." Draft International Standard, International Organization for Standardization (ISO), 1990.

ISO (1994). 9613-2.2, "Acoustics - Attenuation of sound during propagation outdoors. Part 2: General method of calculation." Draft International Standard, International Organization for Standardization (ISO), 1994.

ISO (1998). 140/6. "Acoustics: measurement of sound insulation in buildings and of building elements. Part 6: Laboratory measurements of impact sound insulation of floors." International Organization for Standardization (ISO), 1998.

ISO (1998). 140/7. "Acoustics: measurement of sound insulaton in buildings and of building elements. Part 7: Field measurements of impact sound insulation of floors." International Organization for Standardization (ISO), 1998.

Izenour (1977). George C. Izenour, Theater Design. New York, NY: McGraw-Hill. The George C. Izenour Archive at Penn State University, 1977.

Jacob (1985). K.D. Jacob, "Subjective and Predictive Measures of Speech Intelligibility - The Role of Loudspeaker Directivity." Journal of the Audio Engineering Society, vol. 33. New York, NY: Audio Engineering Society, Dec. 1985.

JBL (1998). "JBL 2360A, 2365A, 2366A Bi-Radial® Constant Coverage Horns." Northridge, CA: JBL Professional, Jan. 1998.

JBL Professional (1997). Catalog cut "4895 Three-Way High Directivity Horn Loaded Positionable Array Element." Northridge, CA JBL Professional, Sept. 1997.

JBL Professional (2000). "Speech intelligibility - A JBL Professional Technical Note." Technical Notes, Vol 1, No 26. Northridge, CA: JBL Professional, Aug. 2000.

JBL (1988) JBL and Marshall Long, "JBL and the Los Angeles Sports Arena," A JBL Installation, Northridge, CA: JBL Incorporated, Sept. 1988.

Johnson (2002). Russell Johnson, ARTEC, Private Communication, 2002.

Jones (1984). R.S. Jones, Noise and Vibration Control in Buildings. © 1984, New York, NY: Reprinted with permission from McGraw-Hill Book Company.

Josse (1964). R. Josse and C. Lamure, Acustica 14, 266–280, 1964.

Josse (1969). R. Josse and C. Drouin, "Etude des impacts lourds a l'interieur des bâtiments d'habitation," Rapport de fin d'étude, Centre Scientifique et Technique du Bâtiment, Paris, February 1, 1969, DS No. 1, 1.24.69.

Junger (1972). Miguel C. Junger and David Feit, Sound, Structures, and Their Interaction. 2nd ed. Cambridge, MA: MIT Press, 1972.

Keele (1983). Don Keele, Private communication, 1983.

Kinetics (1990). ELIM Shores, "Report of: Field - Impact Insulation Class (F-IIC)." St. Paul, MN: Twin City Testing. Kinetics Corporation Test Data, Dublin, OH, 1990.

Kinetics (1996) Testing performed at the National Research Council Canada, Ottawa, Ontario. Kinetics Corporation Test Data, Dublin, OH, 1996.

Kinsler (1962). L.E. Kinsler and A.R. Frey, Fundamentals of Acoustics, 2nd ed. copyright © 1962, New York, NY: this material is used by permission of John Wiley & Sons, Inc.

Kinsler et al. (1982). L.E. Kinsler, A.R. Frey, A.B. Coppens, and J.V. Sanders Fundamentals of Acoustics, 3rd ed. copyright © 1982, New York, NY: this material is used by permission of John Wiley & Sons, Inc.

Kishinaga et al. (1979). Shinji Kishinaga, Yashushi Shimizu, Shigeo Ando, and Kiminori Yamaguchi, "On The Room Acoustic Design of Listening Rooms." Audio Eng. Soc 64th Convention, Preprint #1524. New York, NY: Audio Engineering Society, Nov. 1979.

Klark-Teknik. The Audio System Designer Technical Reference . © Klark-Teknik. Buchanan, MI: Mark IV Pro Audio Group.

Klein (1971). W. Klein, "Articulation loss of consonants as a basis for the design and judgment of sound reinforcement systems." Cologne: AES 1st European Convention, 1971.

Klepper (1999). David L. Klepper, "A different angle." S&VC , vol. 17, no. 1, Emeryville, CA, Jan. 1999.

Klepper et al. (1980). David L. Klepper, William J. Cavanaugh, and L. Gerald Marshall, "Noise Control in Music Teaching Facilities." Noise Control Engineering Journal, Vol. 15 No. 2, Sept/Oct 1980.

Knudsen (1932). V.O. Knudsen, Architectural Acoustics. © 1932, New York, NY: this material is used by permission of John Wiley & Sons, Inc.

Knudsen (1970). Vern O. Knudsen, "Model Testing of Auditoriums," S.1. J. Acoust. Soc. Am. vol. 47, no. 2 (part 1), February 1970. Acoustical Society of America: Melville, NY, 1970.

Knudsen (1965). V.O. Knudsen and L.P. Delsasso, "Acoustics of the Grady Gammage Auditorium, Arizona State University." 5th Congres International D'Acoustique, Liege 7–14 Septembre 1965.

Knudsen (1950). V.O. Knudsen and C. Harris, Acoustical Designing in Architecture. © 1950, New York, NY: this material is used by permission of John Wiley & Sons, Inc., 190.

Kopec (1990). John Kopec, Private communication, 1990.

Krokstad (1991). A. Krokstad, "Electroacoustic Means of Controlling Auditorium Acoustics." University of Trondheim report number 408507, The Norwegian Institute of Technology Division of Telecommunications O.S. Bragstads plass 4, N7034 Trondheim-nth, Norway, presented at the 90th Convention, 1991 February 1922, Paris, Audio Engineering Society. (AES), 1991.

Kryter (1970). Karl D. Kryter, The Effects of Noise on Man. Burlington, MA: Academic Press, 1970.

Kryter (1963 & 1964). K.D.Kryter and K.S. Pearsons, "Some effects of spectral content and duration on perceived noise level." Reprinted with permission from J. Acoust. Soc. Am. © 1963 & 1964, Acoustical Society of America: Melville, NY.

Kuhl (1954). W. Kuhl, Acustica, 4, 618–634.

Kurze (1971). U.J. Kurze and G.S. Anderson, "Sound Attenuation by Barriers." Applied Acoustics. vol. 4, 1971.

Kuttruff (1973). Heinrich Kuttruff, Room Acoustics. © Heinrich Kuttruff. London, England: Applied Science Publishers, 1973.

Landon (1995). H.C. Robbins Landon, Haydn in England 1791–1795. London: Thames and Hudson.

Lange (1953). T.H. Lange, Acustica 3, 1953.

Larsen (1978). Holger Larsen, Technical Review No. 4. "Reverberation Process at Low Frequencies." Naerum, Denmark: Brüel & Kjaer, 1978.

Leissa (1969). A.W. Leissa, "Vibration of Plates," NASA SP-160. Washington, D.C.: National Aeronautics and Space Administration, 1969.

Leizer (1966). I.G. Leizer, "Applicability of the Methods of Geometric Acoustics for the Calculation of Sound Reflection from Plane Surfaces." Soviet Physics–Acoustics, Vol. 12, No. 2, Oct.–Dec., 1966. Translated from Akusticheskii Zhurnal, vol. 12, no. 2, April–June, 1966.

Lenzen (1966). K.H. Lenzen, "Vibration of Steel Joist-Concrete Slab Floors." AISC, Engineering Journal, vol. 3, no. 1. Ames, IA: Iowa State University, 1966.

Leonard et al. (1964). R.W. Leonard, L.P. Delsasso, and V.O. Knudsen, "Diffraction of Sound by an Array of Rectangular Reflective Panels." Reprinted with permission from J. Acoust. Soc. Am., vol. 36, no. 12, © 1964, Acoustical Society of America: Melville, NY.

Levine (1948). H. Levine and J. Schwinger, "On the theory of diffraction by an aperture in an infinite screen." Physic. Rev. 74, 1948.

Lindsay (1966). Bruce Lindsay, "The Story of Acoustics." Reprinted with permission from J. Acoust. Soc. Am., 39(4), © 1966, Acoustical Society of America: Melville, NY.

Lochner (1964). J.P.A. Lochner and J.F. Berger, "The Influence of Reflections on Auditorium Acoustics." Journal of Sound and Vibration, 1, 1964.

London (1950). A. London, "Transmission of Reverberant Sound through Double Walls." Reprinted with permission from J. Acoust. Soc. Am., vol. 44, © 1950, Acoustical Society of America: Melville, NY, 1950.

Long (1980). "Design of Housing for Aircraft Noise," Presented to the 100th meeting of the Acoustical Society of America, Los Angeles, CA, 1980.

Long (1983). Marshall Long, "Constant Directivity Horns.": Sound and Video Contractor, Overland Park, KS, 1983.

Long (1987). Marshall Long, "Sound Transmission through Partitions." New York, NY: AES Journal, Jul/Aug. 1987.

Long (1993). Marshall Long, "Acoustical Ray Tracing, " National Science Foundation Phase I Final Report. Arlington, VA: National Science Foundation, 1993.

Long (1999). Marshall Long, "Getting the Message." S&VC, vol. 17, no. 1, Emeryville, CA, Sound & Video Contractor, Jan. 1999.

Long (2000). Marshall Long, "Architectural Acoustics: Theme Park Acoustics, Creativity in Theme Park Acoustics," Newport Beach, CA: Acoustical Society of America, Session 4aAA, Dec. 7, 2000.

Lukas (1975). J.S. Lukas, "Noise and Sleep." Reprinted with permission from J. Acoust. Soc. Am., 58, © 1975, Acoustical Society of America: Melville, NY.

Madsen (1970). E.R Madsen, "The Disclosure of Hidden Information in Sound Recording," a lecture given May 1970, and referenced in The Science of Sound, 2nd ed., 1990, p. 500, Fig. 25.2, written by Thomas D. Rossing. Glenview, IL: Addison-Wesley Publishing, May 1970.

Maekawa (1965). Z. Maekawa, "Noise Reduction by Screens." Memoirs of Faculty of Eng., Kobe, Japan: Kobe Univ., 1965.

Maekawa (1966). Z. Maekawa, "Noise Reduction by Screens of Finite Size." Memoirs of Faculty of Eng., Kobe, Japan: Kobe Univ., 1966.

Maekawa (1977). Z. Maekawa, "Shielding Highway Noise." Noise Control Engineering Journal. Ames, IA: Iowa State University, July–Aug. 1977.

Mankovsky (1971). V.S. Mankovsky, from Acoustics of Studios and Auditoria. by V.S. Mankovsky. Reprinted by permission of Elsevier Ltd, Oxford, UK, 1971.

Marshall (1967). A. Harold Marshall, "A note on the importance of room cross-section in concert halls." Journal of Sound and Vibration. 5, 1967.

Mason Industries (1968). Noise and Vibration Problems and Solutions, Condensed and published in Air Conditioning, Heating & Refrigeration News, 1-29-68. Hauppauge, NY: Mason Industries, 1968.

Mason Industries (1998). "Complete Seismic HVAC Engineering Specifications," SVCS Part 2, SVCS-110-3 Bulletin. Hauppauge, NY: Mason Industries, Sept. 1998.

Maxfield (1947). Maxfield and Albersheim, Bell Laboratories, 1947.

McLachlan (1934). N.W. McLachlan, Loudspeakers. New York, NY: Oxford Press, 1934.

Mechel (1992). Fridolin P. Mechel and István L. Vér, Chapter 8, "Sound-absorbing Materials and Sound Absorbers," Noise and Vibration Control Engineering Principles and Applications by Leo L. Beranek and István L. Vér, © 1980, New York, NY: this material is used by permission of John Wiley & Sons, Inc.

Meyer (1978). J. Meyer, Acoustics and the Performance of Music. Frankfurt/Main: Verlag Dis Musikinstrument, 1978.

Meyer (1952). E. Meyer and G.R. Schodder, Nachr. Akad. Wissensch. Göttingen, Math.-Phys. Kl., No. 6, 31, 1952.

Miller et al. (1951). G. A. Miller, G.A. Heise, and W. Lichten, "The intelligibility of speech as a function of the context of the test materials," J. Exp. Psychol. 41, 1951.

Miller (1968). Laymon Miller, Dept. of the Army Technical Manual, TM 5-805-9. "Power Plant Acoustics." Washington, D.C.: Headquarters, Department of the Army, 1968.

Miller (1980). Laymon N. Miller, "Noise and Vibration Control for Mechanical Equipment," Bolt Beranek and Newman, Inc. Report 4131, Project No. 08804. Huntsville, AL: Department of the Army Corps of Engineers, Jan. 1980.

Millington (1932). G. Millington, J. Acoust. Soc. Am., 4, 160, 1932.

Mindlin (1951). R.D. Mindlin, "Influence of Rotary Inertia and Shear on Flexural Motion of Elastic Plates," J. Appl. Mech., vol. 18, 1951.

Mitchell (2002). Doug Mitchell, "Surround Setup Scenarios," Nashville, TN: Audio Media Magazine, issue 49, Feb. 2002.

Moderow (1970). R.R. Moderow, "Vibration Characteristics of Steel Joist-Concrete Slab Floor Systems." M. Sc. Thesis, Dept. Civ. Eng., Lawrence, KS: Univ. Kansas, unpublished, 1970.

Mommentz (1995). E. Mommentz and M. Vorlander, "Measurement of scattering coefficients of surfaces in the reverberation chamber and in the free field," Proc. 15th Internat. Congress on Acoustics, Trondheim, Norway, 1995.

Monsanto Corp (1995). "Glass Sound Transmission Loss Data," Saflex, www.saflex.com/Acoustic/31atable.htm, 1995.

Morse (1948). Philip M. Morse, Vibration and Sound. New York, NY: McGraw-Hill. Reprinted (1981) Melville, NY: Acoustical Society of America, 1948.

Morse (1968). Philip M. Morse and K. Uno Ingard Theoretical Acoustics. New York, NY: McGraw-Hill. © 1968, New York, NY: Reprinted with permission from McGraw-Hill Book Company.

Murphy (2001). Shawn Murphy, Private Communication, 2001.

Nagata (1997). Minoru Nagata, Private Communication, 1997.

National Bureau of Standards (1975). Acoustical and Thermal Performance of Exterior Residential Walls, Doors and Windows, NBS Building Science Series 77. Washington D.C.: U.S. Depart. of Commerce, National Bureau of Standards, 1975.

National Research Council Canada (1966). "Sound transmission loss of a Q-Floor assembly with floor tile and fireproofing only." rpt. 433-PY, Ottawa, CA: National Research Council, Nov. 1966.

National Research Council Canada (1966). "Sound transmission loss of a Q-Floor assembly with floor tile, fireproofing and suspended ceiling system." rpt. 434-PY, Ottawa, CA: National Research Council, Nov. 1966.

Naylor (1993). G.M. Naylor, "ODEON - Another hybrid room acoustical model." Applied Acoustics, vol. 38 nos. 2–4, 1993.

Nickson et al. (1954). A.F.B. Nickson, R.W. Muncey, and P. Dubout, "The Acceptablity of Artificial Echoes With Reverberant Speech and Music." Acustica, Vol. 4, pp. 515–518. Oldenberg, Germany, 1954.

Nightingale (July 1998). T.R.T. Nightingale and J.D. Quirt, "Effect of electrical outlet boxes on sound insulation of a cavity wall." Reprinted with permission from J. Acoust. Soc. Am., 104(1), © 1998, Acoustical Society of America: Melville, NY, July 1998.

Nishihara et al. (2001). Noriko Nishihara, Takayuki Hidaka, and Leo L. Beranik, "Mechanism of sound absorption by seated audience in halls." Reprinted with permission from J. Acoust. Soc. Am., 110(5), Pt. 1, © 2001, Acoustical Society of America: Melville, NY, Nov. 2001.

Ogawa (1965). cited in Davis and Davis. Sound System Engineering. 1975, Fig. 4-21, Indianapolis, IN: Howard W. Sams, 1965.

Okano (1998). T. Okano, L. Beranek, and T. Hidaka, "Relations among interaural cross-correlation coefficient (IACC$_E$), lateral fraction (LF$_E$), and apparent source width (ASW) in concert halls," Reprinted with permission from J. Acoust. Soc. Am. 104 (1). © 1998, Acoustical Society of America: Melville, NY, July 1998.

Olive (1989). Sean E. Olive and Floyd E. Toole, "The Detection of Reflections in Typical Rooms." J. Audio Eng. Soc. 37 (7/8). New York, NY: Audio Engineering Society, July/Aug. 1989.

Ollerhead (1968). J.B. Ollerhead, "Subjective Evaluation of General Aircraft Noise," Tech. Rept. 68-35. Contract, FA67WA-1731. Washington, D.C.: Wyle Laboratories, Federal Aviation Administration, 1968.

Olson (1957). Harry F. Olson, Elements of Acoustical Engineering. New York, NY: Van Nostrand Reinhold, 1957.

Olson (1959). H.F. Olson, "Acoustoelectronic auditorium," J. Acoust. Soc. Am., vol. 31, no. 7, Melville, NY, 1959.

Olson (1991). Harry F. Olson, Acoustical Engineering. Philadelphia, PA: Professional Audio Journals, Inc., 1991.

Owens-Corning Fiberglas Corp. (1970). "Wood Stud Gypsum Board Drywalls Sound Transmission Tests." Product Testing Laboratories Report No. 32491. Toledo, OH: Owens Corning World Headquarters, Feb. 1970.

Owens-Corning Fiberglas Corp. (1971). "Sound Attenuation of Steel Stud Drywall Partitions." Toledo, OH: Owens Corning World Headquarters, May 1971.

PAC International (2001). RSIC-1 pamphlet. Tualatin, OR, 2001.

Palmer (1961). R.R. Palmer, A History of the Modern World, 2nd ed. New York, NY: Alfred A. Knopf, 1961.

Paris (1928). E.T. Paris, "On the Coefficient of Sound-Absorption Measured by the Reverberation Method," Phil. Mag., (7)5:489–497, 1928.

PCI Industries (1999). "E477-96 Silencer Test Report." Fort Worth, TX: PCI Industries Sound Testing Laboratory, 1999.

Pearsons et al. (May 1977). K.S. Pearsons, R.L. Bennett, and S. Fidell, "Speech Levels in Various Noise Environments." Report EPA-600/1-77-025, Washington, D.C.: U.S. Environmental Protection Agency, May 1977.

Peterson (1974). Arnold P.G. Peterson and Ervin E. Gross, Jr., Handbook of Noise Measurement. 7th ed. Concord, MA: General Radio, 1974.

Peutz (1971) V.M.A. Peutz, "Articulation loss of consonants as a criterion for speech transmission in a room." J. Audio Eng. Soc. 19 (11). New York, NY: Audio Engineering Society, 1971.

Peutz (1974). V.M.A. Peutz, "Designing Sound Systems for Speech Intelligibility, presented at the 48th Convention of the Audio Engineering Society," AES Journal, (Abstracts) vol. 22 (June 1974), preprint 967, New York, NY, 1974.

Peutz (1974). V.M.A. Peutz and W. Klein, "Articulation Loss of Consonants Influenced by Noise, Reverberation and Echo," (in Dutch), Acoust. Soc. Netherlands, vol. 28, 1974.

Peutz (1984). V.M.A. Peutz and B.H.M. Kok, "Speech Intelligibility," presented at the 75th Convention of the Audio Engineering Society, AES Journal, (Abstracts) vol. 32 (June 1984), preprint 2089, New York, NY, 1984.

Pierce,. (1981). Allan D. Pierce, Acoustics: An Introduction to Its Physical Principles and Applications.. © 1981, Allan D. Pierce. New York, NY: Reprinted with permission from McGraw-Hill Book Company.

Pierce (1983). John R. Pierce, from The Science of Musical Sound by John R. Pierce © 1983 by Scientific American Books. Used with permission by W.H. Freeman and Company.

Piercy (1971). J.E. Piercy, "Comparison of Standard Methods of Calculating the Attenuation of Sound in Air with Laboratory Measurements," presented orally to 82nd Meet. Acoust. Soc. Am., Denver, CO, 1971.

Pinnington (1988). R.J. Pinnington, "Approximate Mobilities of Builtup Structures," Report No. 162, Southampton, England: Institute of Sound and Vibration Research, 1988.

Plomp (1965). R. Plomp and W.J.M. Levelt, "Tonal Consonance and Critical Bandwidth," J. Acoust. Soc. Am., 38, © 1965, Acoustical Society of America: Melville, NY.

Quirt (1982). J.D. Quirt, "Sound transmission through windows I. Single and doubling glazing." Reprinted with permission from J. Acoust. Soc. Am., 72(3), © 1982, Acoustical Society of America: Melville, NY.

Ramsey (1986). Charles G. Ramsey and Harold R. Sleeper, Architectural Graphic Standards. © 1970, New York, NY: John Wiley & Sons.

Rausch (1943). E. Rausch, Maschinenfundamene und andere dynamische Bauaufgaben, Vertrieb VDI Verlag G.M.B.H. (Berlin).

Rayleigh (1894–1896). Baron Rayleigh (John William Strutt), The Theory of Sound. Vol. 1 and 2, orginally published in 1894 and 1896. Republished by Dover Publications in 1945, New York, NY.

Reif (1965). F. Reif, Fundamentals of statistical and thermal physics. New York, NY: McGraw-Hill Book Company 1965.

Reiher (1931). H. Reiher and F.J. Meister, "The Effects of Vibration on People." (in German) Forschung auf dem Gebiete des Ingenieurwesens, V.2 II, 1931. (Translation: Report No. F-TS-616-RE H.Q. Air Materials Coimmand, Wright Field, OH, 1949).

Reynolds (1981). D.D. Reynolds, Engineering Principles of Acoustics. Saddle River, NJ: © (1981) Reprinted by permission of Pearson Education, Inc.

Reynolds (1990). D.D. Reynolds, HVAC Systems Duct Design, 3rd ed., "Noise Control, Circular Ducts." Chantilly, VA: SMACNA, 1990.

Richart et al. (1970). F.E. Richart, Jr., J.R. Hall, Jr., and R.D.Woods, Vibrations of Soils and Foundations. © 1970, Reprinted by permission of Prentice-Hall, Upper Saddle River, NJ.

Rindel (1985). J.H. Rindel, "Attenuation of sound reflections from curved surfaces," in Proceedings of 24th Conference on Acoustics, The High Tatras, Czechoslovakia, October 1985.

Rindel (1986). J.H. Rindel, "Attenuation of Sound Reflections Due to Diffraction.".Nordic Acoustical Meeting, 20–22 August, 1986, Aalborg University. Aalborg, Denmark, 1986.

Rindel (1990). J.H. Rindel, "Attenuation of Sound Reflections from an Array of Reflectors." 29th Conference on Acoustics, Oct. 2–5, 1990. Strbske Pleso, 1990

Rindel (1993). J.H. Rindel, "Modelling the Angle-Dependent Pressure Reflection Factor." Applied Acoustics. England: Elsevier Science Publishers Ltd., 1993.

Rindel (2000). J.H. Rindel, "The Use of Computer Modeling in Room Acoustics." Journal of VibroEngineering, no. 3(4) /Index 41-72 Paper of the International Conference BALTIC-ACOUSTIC 2000/ISSN 1392-8716, 2000.

Rindel (2002). Jens Holger Rindel, "Computer Simulation Techniques for Acoustical Design of Rooms - How to Treat Reflections in Sound Field Simulation." proceedings, ASVA, Tokyo, 2–4 April 1997.

Roark (1975). Raymond J. Roark and Warren C. Young, Formulas for Stress and Strain, 5th ed., © 1975 by McGraw-Hill, New York, NY: McGraw-Hill.

Robinson (1956). D.W. Robinson and R.S. Dadson, "A re-determination of the equal-loudness relations for pure tones," *Br J. Appl. Phys.* 7 166–181, 1956.

Robinson (1964). D.W. Robinson and L.S. Whittle, "The loudness of octave-bands of noise." Acustica 14, 1964.

Rolland et al. (1948). Romain Rolland, Pierre Lalo, Vincent d'Indy, Pietro Mascagni, Henry T. Finck, Horatio Parker, and others. The International Library of Music for Home and Studio, vol. II. © 1948, The University Society.

Roozen et al. (1998). N.B. Roozen, M. Bockholts, P. Van Eck, and A. Hirschberg, "Vortex sound in bass-reflex ports of loudspeakers. Part I. Observation of response to harmonic excitation and remedial measures." Reprinted with permission from the author and J. Acoust. Soc. Am., vol. 104, no. 4, © 1998, Acoustical Society of America: Melville, NY, Oct. 1998.

Rosenblith (1953). W.A. Rosenblith, K.N. Stephens, and staff of Bolt Beranek and Newman, Inc., "Handbook of Acoustical Noise Control. II. Noise and Man." Rept. WADC TR 52-204. U.S. Air Force Aerospace Medical Laboratory, Wright-Patterson Air Force Base, Ohio, 1953.

Rossing (1990). T.D. Rossing, The Science of Sound. 2nd ed. Reading, MA: Addison Wesley, 1990.

Rossing (1995). Thomas D. Rossing and Neville H. Fletcher, Principles of Vibration and Sound. Reprinted with permission from the author and Springer-Verlag. © 1995, New York, NY: Springer-Verlag.

Ruzicka (July 1971). Jerome E. Ruzicka, "Fundamental Concepts of Vibration Control." Bay Village, OH: Sound and Vibration Magazine, July 1971.

Sabine (1900). Wallace Clement Sabine, "Reverberation," Chapter 1, The American Architect and The Engineering Record, from the Collected Papers on Acoustics, Wallace Clement Sabine. © 1964, New York, NY: Dover Publications, reprinted.

Sabine (1922, 1964). Wallace Clement Sabine, Collected Papers on Acoustics. New York, NY: Dover Publications, reprinted, 1964.

Sabine et al. (1975). Hale Sabine , Myron B. Lacher, Daniel R. Flynn, and Thomas L. Quindry, Acoustical and Thermal Performance of Exterior Residential Walls, Doors and Windows. National Bureau of Standards, Washington D.C, 1975.

Sandars (1968). N.K. Sandars, Prehistoric Art in Europe. London: Penguin.

Sanicola (1997). Henry Sanicola, Private Communication, 1997.

Sauter (1970). August Sauter, Jr. and Walter W. Soroka, "Sound Transmission through Rectangular Slots of Finite Depth between Reverberant Rooms," J. Acoust. Soc. Am., vol. 47, no. 1 (part 1), © 1970, Acoustical Society of America: Melville, NY.

Schaffer (1991). Mark E. Schaffer, A Practical Guide to Noise and Vibration Control for HVAC Systems. Atlanta, GA: ASHRAE, 1991.

Scharf (1970). B. Scharf, "Critical Bands," in Foundations of Modern Auditory Theory, ed. by J.V. Tobias. Burlington, MA: Academic Press, 1970.

Schneider et al. (1970). E.J. Schneider, J.E. Mutchler, H.R. Hoyle, E.H. Ode, and B.B. Holder, "The Progression of Hearing Loss from Industrial Noise Exposures." Am. Ind. Hygiene Assoc. Jour. 31: 368: Fairfax, VA, 1970.

Schroeder (1954). M.R. Schroeder, "Die statistischen Parameter der Frequenzkurven von großen Räumen," Acustica 4, 1954.

Schroeder (1979). Manfred R. Schroeder, "Binaural dissimilarity and optimum ceilings for concert halls: More lateral sound diffusion." Reprinted with permission from J. Acoust. Soc. Am., 65, 958–963, © 1979, Acoustical Society of America: Melville, NY, 1979.

Schroeder (1981). M.R. Schroeder, "Modulation transfer functions: Definition and measurement." Acustica 49, 1981.

Schroeder (May 1996). Manfred R. Schroeder, "The Schroeder frequency revisited." Physics Today. Woodbury, NY: American Institute of Physics, May 1996.

Schroeder (1963). M.R. Schroeder and B.S. Atal, "Computer simulation of sound transmission in rooms." In IEEE International Convention Record (7). New York, NY: IEEE Press, 1963.

Schuller et al. (1995). Willem M. Schuller, Fokke D. van der Ploeg, and Peter Bouter, Noise Control Engineering Journal,. "Impact of diversity in aircraft noise ratings," Ames, IA: Iowa State University, Nov–Dec 1995.

Schultz (1964). T.J. Schultz and B.G. Watters, "Propagation of sound across audience seating." Reprinted with permission from J. Acoust. Soc. Am., © 1964, Acoustical Society of America: Melville, NY, 1964.

Seraphim (1961). H.P. Seraphim, "Uber die wahrnehmbarkeir mehrerer Ruckwurfe von Sprachschall." Acustica II, 81, 1961.

Seto (1971). William W. Seto, Schaum's Outline of Theory and Problems of Acoustics. © 1971, New York, NY: Reprinted with permission from McGraw-Hill Book Company, 1971.

Sette (1933). W.J. Sette, J. Acoust. Soc. Am. 4, 160, 1933.

Sharp (1973). Ben H. Sharp, A Study of Techniques to Increase the Sound Insulation of Building Elements. WR 73-5. El Segundo, CA: Wyle Laboratories, June, 1973.

Shirley (2000). Peter Shirley, Realistic Ray Tracing. Natick, MA: A K Peters, 2000.

Shure, Inc. (2002). "Microphone directivity patterns." Evanston, IL: Shure, Incorporated, 2002.

Skudrzyk (1954). Eugen Skudrzyk, Die Grundlagen der Akustik. Wien: Springer-Verlag, 1954.

SMACNA (1990). HVAC Systems Duct Design, 3rd Edition. Chantilly, VA: © 1990, Sheet Metal and Air Conditioning Contractors' National Association, 1990.

Small (1973). Richard H. Small, "Vented-Box Loudspeaker Systems Part I, II, III & IV," New York, NY: Journal of the AES, vol. 21, no. 5, 6, 7, and 8, June, July, August, and September 1973.

SMPTE (1989). SMPTE Engineering Guideline, EG 19. "Design of Effective Cine Theaters." © 1989, White Plains, NY: Society of Motion Picture and Television Engineers.

SMPTE (2001). "Film Sound History - 30's," created by Jonathan Kay, Kimber Ghent, Brian Chumney, and Erik Lutkins. http://www.mtsu.edu/~smpte/thirties.html, 2001.

Snow (1955). William B. Snow, "Frequency Characteristics of a Sound Reinforcing System." AES Journal. New York, NY: Audio Engineering Society, Apr. 1955.

Spandock (1934). F. Spandock, "Akustische Modellversuche," Ann, der Physic, 20, 1934.

Steele (1996). James Steele, Theatre Builders. London, England: Academy Editions, 1996.

Steinberg (1929). John C. Steinberg, "Effects of Distortion Upon the Recognition of Speech Sounds." Reprinted with permission from J. Acoust. Soc. Am., © 1929, Acoustical Society of America: Melville, NY, Oct. 1929.

Stern (1980). Richard Stern, Private Communication, 1980.

Stevens (1972). J. Acoust. Soc. Am., 51, 575. © 1972, Acoustical Society of America: Melville, NY, 1972.

Stevens (1961). S.S. Stevens, "Procedure for calculating loudness." Mark IV, J. Acoust. Soc. Am., 33, © 1961, Acoustical Society of America: Melville, NY, 1961.

Stevens (1969). S.S. Stevens, "Assessment of Noise: Calculation Procedure Mark VII." Paper 355-128. Cambridge, MA: Laboratory of Psychophysics, Harvard University, December 1969.

Strayer (1955). Joseph R. Strayer, Western Europe in the Middle Ages, a Short History. New York, NY: Appleton-Century-Crofts, Inc, 1955.

Swing (1973). Jack W Swing and Donald B.Pies, Assessment of Noise Environments Around Railroad Operations. El Segundo, CA: Wyle Labs, July 1973.

Thiele (1971). A.N. Thiele, "Loudspeakers in Vented Boxes: Part I & II," New York, NY: Journal of the AES, vol. 19, no. 5 & 6, May & June 1971.

Thiele (1953). R. Thiele, "Directional Distribution and Time Sequence of Return of Sound in Rooms." Acoustica, vol. 3, no. 2, 1953.

Thiessen (1978). G.J. Thiessen, "Disturbance of Sleep by Noise." Reprinted with permission from J. Acoust. Soc. Am., 64, © 1978, Acoustical Society of America: Melville, NY.

Thiessen (1968). G.J. Thiessen and N. Olson, "Community Noise - SurfaceTransportation." Bay Village, OH: Sound and Vibration Magazine 2(4): 10, 1968.

Thomson (1965). William T. Thomson, Vibration Theory and Applications. © 1965, Reprinted by permission of Pearson Education, Inc., Upper Saddle River, NY, 1965.

TNM (1998). FHWA Traffic Noise Model Technical Manual, ver. 1.0. U.S. Dept. of Transportation, Federal Highway Administration, Office of Environment and Planning, Washington, DC, 1998.

Toole (1990). Floyd E. Toole, "Loudspeakers and Rooms for Stereophonic Sound Reproduction." AES 8th International Conference Proceedings, National Research Council of Canada Ottawa, Ont.. New York, NY: Audio Engineering Society, 1990.

Toole (2002). Floyd E. Toole, "Loudspeakers and Rooms for Multichannel Audio Reproduction, Part One: How many loudspeakers? What kind? Where do we put them?" www.harman.com 02/12/2002.

US EPA (1973). Model Noise Ordinance. U.S. Environmental Protection Agency, Washington, D.C, 1973.

Ungar (1979). Eric E. Ungar and Robert W.White, "Footfall-Induced Vibrations of Floors Supporting Sensitive Equipment." Bay Village, OH: Sound and Vibration Magazine, 1979.

Uniform Building Code (1982). Appendix, Chapter 35. © 1982, Whittier, CA: International Conference of Building Officials, 1982.

Uris et al. (2000). Antonion Uris, Ana Liopis, and Jaime Lin, "Sound Transmission Loss." Sound Solutions Magazine, July–Dec. 2000.

Van Houten (1979). J.J. Van Houten, "Test Report No. 802-79 for Speciality Products Co.." Orange, CA: J.J. Van Houten & Associates, 1979.

Veneklasen (1996). Paul Veneklasen, Private Communication, 1996.

Veneklasen (1969). P.S. Veneklasen and J.R. Hyde, "Auditorium Synthesis - Early Results of Listener Preference." Reprinted with permission from J. Acoust. Soc. Am., 46 97, © 1969, Acoustical Society of America: Melville, NY.

Vér (1971). István Vér, "Impact Noise Isolation of Composite Floors." Reprinted with permission from J. Acoust. Soc. Am., © 1971, Acoustical Society of America: Melville, NY, 1971.

Ver (1983). Istvàn Vér, "Prediction of Sound Transmission Through Duct Walls; Breakout and Pickup," Report No. 5116, ASHRAE TRP-319, American Society of Heating, Refrigeration, and Air Conditioning Engineers.

Ver (1984b). I. Ver, "Prediction of sound transmission through duct walls: Breakout and pickup." ASHRAE Transactions 90(2A), 1984b, 1984.

Ver (1971). Istvàn Vér and Curtis I. Holmer, "Interaction of Sound Waves with Solid Structures," Noise and Vibration Control, edited by Leo L. Beranek, © 1971, New York, NY: McGraw-Hill Book Co.

Ver (1983). Istvàn L. Vér, Prediction of Sound Transmission Through Duct Walls; Breakout and Pickup, Report 5116, Prepared for American Society of Heating, Refrigeration, and Air Conditioning Engineers, 1983.

Ver (1992). Leo L. Beranek and István L. Vér, Noise and Vibration Control Engineering Principles and Applications, Ch. 9, "Interaction of Sound Waves with Solid Structures." © 1992, New York, NY: this material is used by permission of John Wiley & Sons, Inc.

Vermuelen (1958). R. Vermuelen, "Stereo-Reverberation," J. Audio Eng. Soc., vol. 6, no. 2, April 1958.

Vermeulen (1936). R. Vermeulen and J. De Boer, Philips Tech Rev., 1, 46.

Vibron (1989). "Vibration Isolation Selection Guide, Heating/Ventilating and Air Conditioning Equipment," Don Allen. Mississauga, Ontario Canada: Vibron, 1989.

Vinokur (1996). Roman Y. Vinokur, "Evaluating Sound-Transmission Effects in Multi-Layer Partitions." Bay Village, OH: Sound and Vibration Magazine, July 1996.

Vitruvius (1960). Vitruvius, the Ten Books on Architecture. translated by Morris Hicky Morgan. New York, NY: Dover Publications, 1960.

von Bekesy (1960). G. von Bekesy, Experiments in Hearing. © 1960, New York, NY: Reprinted with permission from McGraw-Hill Book Company.

von Gierke (1973). H. von Gierke, Impact Characterization of Noise Including Implications of Identifying and Achieving Levels of Cumulative Noise Exposure. Environmental Protection Agency, 1973.

Waterhouse (1955). Richard V. Waterhouse, "Interference Patterns in Reverberant Sound Fields." Reprinted with permission from J. Acoust. Soc. Am.,27(2), © 1955, Acoustical Society of America: Melville, NY, Mar. 1955.

Watters et al. (1963). B.G. Watters, L.L. Beranek, F.R. Johnson, and I. Dyer, "Reflectivity of panel arrays in concert halls," SOUND 2, 1963.

Webster (1969). John C. Webster, Effects of Noise on Speech Intelligibility. Proc. of Conference, Noise as a Public Health Hazard, Washington D.C., June 13–14, 1968, A.S.H.A. Reports 4. Washington D.C.: The American Speech and Hearing Association, 1969.

Wegel (1924). R.L. Wegel and C.E. Lane, "Auditory masking of one pure tone by another and its possible relation to the dynamics of the inner ear." Phys. Rev. 23, 1924.

Wells (1958). R.J. Wells, "Acoustical Plenum Chambers." Noise Control, July 1958.

Wells (1967). R.J. Wells, Recent research relative to perceived noise level. (A) J. Acoust. Soc. Am., 42, © 1967, Acoustical Society of America: Melville, NY.

Wendt (1963). K. Wendt, Das Richtungshören bei der überlagerung zweier Schallfelder bei Intensitäts-und Laufzeitstereophonie (Directional hearing with two superimposed sound fields in intensity-and delay-difference stereophony). Dissertation, Technische Hochschule, Aachen, 1963.

Wenger (1999). Wenger Corporation, Planning Guide for Secondary School Music Facilities. © 1999, Owatonna, MN: Wenger Corporation, 1999.

Wilhelmi Corp Data (2000). based on Riverbank Acoustical Laboratories test RAL-A85-116, 2000.

Wilkens (1974). Wilkens and Plenge, Auditorium Acoustics, ed. Robin Mackenzie, "The Correlation between Subjective and Objective Data of Concert Halls." New York, NY: John Wiley & Sons.

Wilson (1965). G.P. Wilson and W.W. Soroka, "Approximation to the diffraction of sound by a circular aperture in a rigid wall of finite aperture." Reprinted with permission from J. Acoust. Soc. Am., 37, © 1965, Acoustical Society of America: Melville, NY, Feb. 1965.

Wilson (1976). "Architectural Acoustics Design and Noise Control in Army Medical Facilities." Technical Background Report for Appendix V - "Acoustical Control" to DOA Technical Manual 5-838-2, Medical Facilities Design - Army. Oakland, CA: Wilson, Ihrig & Associates, Jan. 1976.

Woodworth et al. (1954). R.S. Woodworth and H. Schlosberg. Experimental Psychology. New York, NY: Holt, 1954.

Wyle Laboratories (1971). Transportation Noise and Noise from Equipment Powered by Internal Combustion Engines. NTID300.13. El Segundo, CA: Wyle Laboratories, Dec. 1971.

Yamamoto (1968). T. Yamamoto and T. Wakuri, "Equipment and Materials Used in Scale NHK Laboratories Note," No. 77, 1.

INDEX